British Journal of Pharmacology

July 1995

Volume 115 Number 6 pages 869 – 1126

Dr S J Coker
Department of Pharmacology
University of Liverpool
P.O. Box 147
LIVERPOOL L69 3BX

British Journal of Pharmacology (1995) 115, 869-870 © 1995 Stockton Press All rights reserved 0007-1188/95 $12.00

SPECIAL REPORT

Prevention by the cannabinoid antagonist, SR141716A, of cannabinoid-mediated blockade of long-term potentiation in the rat hippocampal slice

Dawn R. Collins, Roger G. Pertwee & [1] Stephen N. Davies

Department of Biomedical Sciences, Marischal College, University of Aberdeen, Aberdeen, AB9 1AS

Incubation of rat hippocampal slices in the presence of the synthetic cannabinoid (–)-11-OH-Δ^8-dimethylheptyl tetrahydrocannabinol (HU-210) (100 nM) prevented the induction of long-term potentiation (LTP). Slices co-incubated with both HU-210 (100 nM) and the cannabinoid antagonist, SR141716A (100 nM), exhibited tetanically induced LTP, comparable to control slices. Intriguingly, co-incubation with HU-210 and SR141716A prevented the induction of the early, short-term phase of LTP.

Keywords: Cannabinoid; long-term potentiation; hippocampus; SR141716A

Introduction Long-term potentiation (LTP) describes a form of use-dependent synaptic plasticity that is a proposed model for learning and memory formation (Bliss & Collingridge, 1993). High affinity cannabinoid receptor binding sites are found in those brain regions, i.e. hippocampus and cortex, which exhibit LTP (Herkenham *et al.*, 1991). The memory deficits induced by cannabinoid administration have been recognised for many years (Miller & Braconnier, 1983) and application of Δ^9-tetrahydrocannabinol, the major component of marihuana has also been shown to prevent induction of LTP (Nowicky *et al.*, 1987). We have previously shown that application of the psychoactive synthetic cannabinoid, (–)-11-OH-Δ^8-dimethylheptyl-tetrahydrocannabinol (HU-210) prevents the formation of tetanically induced LTP in a stereospecific manner (Collins *et al.*, 1994). Here we have investigated the effect of SR141716A (N-(piperidin-1-yl)-5-(-4-chlorophenyl)-1-(2,4-dichlorophenyl)-4-methyl-1H-pyrazole-3-carboxamide hydrochloride), a highly selective and a competitive ligand for CB_1 cannabinoid receptors (Rinaldi-Carmona *et al.*, 1994), on the blockade of LTP by HU-210.

Methods For all experiments the drugs were mixed with two parts of Tween 80 by weight and then dispersed in standard perfusion medium. Transverse rat hippocampal slices (400 μm thick) were prepared and pre-incubated for 60–90 min with 100 nM HU-210, with 100 nM SR141716A, with 100 nM SR141716A plus 100 nM HU-210, or with normal medium containing an equivalent concentration of Tween 80. The concentration of SR141716A used was selected as 100 nM since this is in excess of concentrations shown to displace and reverse the effects of cannabinoids in rat brain synaptosomal membrane preparations (Rinaldi-Carmona *et al.*, 1994). The CA3 region was removed and the slices transferred to a standard interface chamber where they were constantly perfused (1 ml min^{-1}) with standard medium at 30°C (Collins *et al.*, 1994).

The Schaffer collateral commissural fibre pathway was stimulated at a frequency of 0.033 Hz and extracellular field excitatory postsynaptic potentials (field e.p.s.ps) were recorded from the CA1 region. Synaptic LTP was induced by the application of 1 or 2 bursts of high frequency stimuli (tetani) at a frequency of 100 Hz for 500 ms at 3 times the test stimulus strength.

Comparison of pre- and post-tetanic field e.p.s.p. amplitudes were made by Student's two-tailed, paired *t* test. *P* values of less than 0.05 were regarded as significant.

[1] Author for correspondence.

Results Tetanic stimulation of slices incubated in control medium evoked a rapidly forming and long-lasting potentiation of the synaptic response (mean field e.p.s.p. amplitude ± standard error was 187 ± 16% of control at 10 min post tetanus, 158 ± 18% at 50 min post tetanus, $P < 0.001$, $n = 6$, see Figure 1).

As previously reported (Collins *et al.*, 1994), incubation in the presence of 100 nM HU-210 prevented the formation of tetanically induced LTP, the field e.p.s.p. amplitude returning to baseline levels within approximately 10 min after tetanus application (mean field e.p.s.p. amplitude was 103 ± 17% at 10 min, 75 ± 21% at 50 min post tetanus, not significant, $n = 5$, see Figure 1).

In slices incubated in the presence of the cannabinoid receptor antagonist, SR141716A, the pre-tetanus responses were generally smaller than those recorded in control conditions and were more excitable, readily generating population spikes and taking a greater time to stabilise prior to tetanus application. In all 5 slices tetanic stimulation evoked robust LTP with a comparable time course to that recorded in control slices, although the magnitude of the potentiation was slightly reduced (mean field e.p.s.p. amplitude was 137 ± 9% at 10 min, 140 ± 5% at 50 min post tetanus, $P < 0.01$, $n = 5$, data not shown).

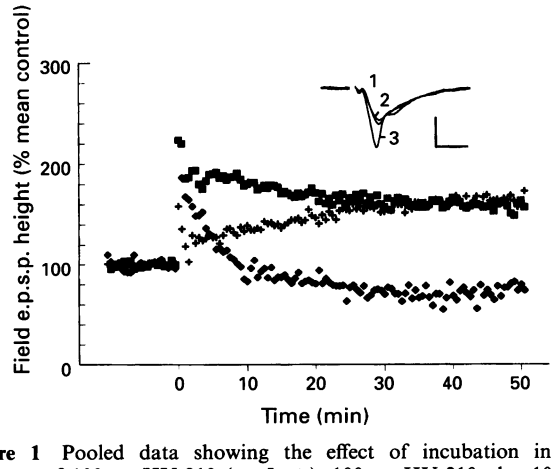

Figure 1 Pooled data showing the effect of incubation in the presence of 100 nM HU-210 ($n = 5$, ◆), 100 nM HU-210 plus 100 nM SR141716A ($n = 5$, +) or control medium ($n = 6$, ■). Tetanic stimulation was delivered to all slices at time 0. The inset traces illustrate responses from a representative slice incubated in HU-210 plus SR141716A showing control responses (1) and responses taken 10 min (2, the slightly larger response) and 50 min (3) after tetanic stimulation. The scale bar represents 1 mV by 10 ms.

When slices were co-incubated with HU-210 (100 nM) and SR141716A (100 nM) we found that HU-210-induced inhibition of LTP no longer occurred. Interestingly, in 5 out of the 6 trials, there was a marked loss of short-term potentiation (STP) so that following a brief, presumed post-tetanic, potentiation the response returned to control size and then gradually potentiated over the trial period (mean field e.p.s.p. amplitude was $131 \pm 6\%$ at 10 min, $163 \pm 8\%$ at 50 min post tetanus, $P = 0.001$, $n = 5$, see Figure 1).

Discussion The results show that the cannabinoid receptor antagonist SR141716A can prevent the effects of the synthetic psychoactive cannabinoid, HU-210, on LTP. Intriguingly though, a phase of short-term potentiation lasting up to 20 min after the tetanus remained blocked.

This is, to our knowledge, the first instance of tetanic stimulation (as opposed to drug perfusion) evoking a late phase of LTP in the absence of STP. Blockade of STP does not seem to be caused by an action of the antagonist alone, since although slices incubated in SR141716A exhibited a smaller and more excitable pre-tetanus response, they still showed robust synaptic potentiation (STP and LTP) which displayed a comparable time course to that evoked in slices incubated in Tween 80 alone.

The actions of SR141716A (and HU-210) on specific components of the synaptic response clearly need to be elucidated, but the observation that effects of HU-210 are both stereoselective (Collins *et al.*, 1994) and prevented by a known CB_1 cannabinoid receptor antagonist, strengthen the conclusion that HU-210 inhibits LTP via an action at a specific cannabinoid receptor.

We thank Professor R. Mechoulam (University of Jerusalem) for the gift of HU-210 and Sanofi Winthrop for SR141716A.

References

BLISS, T.V.P. & COLLINGRIDGE, G.L. (1993). A synaptic model of memory: long-term potentiation in the hippocampus. *Nature*, **361,** 31–39.

COLLINS, D.R., PERTWEE, R.G. & DAVIES, S.N. (1994). The action of synthetic cannabinoids on the induction of long-term potentiation in the rat hippocampal slice. *Eur. J. Pharmacol.*, **259,** R7–R8.

HERKENHAM, M., LYNN, A.B., JOHNSON, M.R., MELVIN, L.S., DE COSTA, B.R. & RICE, K.C. (1991). Characterization and localisation of cannabinoid receptors in rat brain: a quantitative in vitro autoradiographic study. *J. Neurosci.*, **11,** 563–583.

MILLER, L.L. & BRACONNIER, R.J. (1983). Cannabis: effects on memory and the cholinergic limbic system. *Psychol. Bull.*, **93,** 441–456.

NOWICKY, A.V., TEYLER, T.J. & VARDARIS, R.M. (1987). The modulation of long-term potentiation by Δ^9-tetrahydrocannabinol in the rat hippocampus in vitro. *Brain. Res. Bull.*, **19,** 663–672.

RINALDI-CARMONA, M., BARTH, F., HÉAULME, M., SHIRE, D., CALANDRA, B., CONGY, C., MARTINEZ, S., MARUANI, J., NÉLIAT, G., CAPUT, D., FERRARA, P., SOUBRIÉ, P., BRELIÈRE, J.C. & LE FUR, G. (1994). SR141716A, a potent and selective antagonist of the brain cannabinoid receptor. *FEBS Lett.*, **350,** 240–244.

(Received April 28, 1995
Accepted May 17, 1995)

British Journal of Pharmacology (1995) 115, 871-874 © 1995 Stockton Press All rights reserved 0007-1188/95 $12.00

Effect of illuminated nifedipine, a potent antioxidant, on intestinal and vascular smooth muscles

[1]V. Bauer, *V.V. Rekalov, I. Juránek, D. Gergel & P. Bohov

Institute of Experimental Pharmacology, Slovak Academy of Sciences, Bratislava, Slovak Republic and *Bogomoletz Institute of Physiology, Academy of Sciences of Ukraine, Kiev, Ukraine

1 The effects of nifedipine (Nif) and its illuminated nitroso product nitrosopine (NTP) were investigated on lipid peroxidation, KCl elevated smooth muscle tension, and ionic currents of single smooth muscle cells.

2 Illumination of Nif at 400-700 nm within 24-48 h changed it completely to a potent antioxidant, NTP.

3 Nif relaxed the KCl-induced contractions of guinea-pig taenia caeci and rat aorta and reduced the amplitude of the evoked inward Ca^{2+} current of taenia caeci cells in a concentration-dependent manner. NTP (up to 100 μM) was ineffective in this respect. Pretreatment by NTP (10 μM) did not affect the actions of Nif.

4 The evidence suggests that NTP, generated by day-light illumination from Nif, exerts antioxidant activity but is devoid of voltage-dependent Ca^{2+} channel (VDC) blocking property and does not interfere with the action of Nif on the smooth muscle cell membrane VDC.

Keywords: Illuminated nifedipine; smooth muscle; calcium current; antioxidant

Introduction

Ca^{2+} channel blockers (CCB) are widely used in treatment of smooth muscle disorders (e.g. ischaemic heart disease, Follath, 1989). Their beneficial effect is ascribed to inhibition of Ca^{2+} influx into the smooth muscle cells (Godfraind *et al.*, 1986; Speralakis *et al.*, 1992). It has been shown that some of the CCB also possess a free-radical scavenging or antioxidant activity (Mak & Weglicki, 1990). Nifedipine (Nif; 1,4-dihydro-2,6-dimethyl-4-(2-nitrophenyl)-3,5-pyridinedicarboxylic acid dimethyl ester) exposed to daylight converts to the nitroso-compound nitrosopine (NTP; 2,6-dimethyl-4-(2-nitroso-phenyl)-3,5-pyridinedicarboxylic acid dimethyl ester, Majeed *et al.*, 1987).

NTP was recently described as a potent free radical scavenger with the ability to inhibit lipid peroxidation (Mišík *et al.*, 1991). The aim of this study was therefore to prepare a constantly illuminated and chemically pure NTP and compare its action on smooth muscle tension, membrane currents and lipid peroxidation with that of Nif.

Methods

Guinea-pigs (weighing 400-600 g) and rats (weighing 200-300 g) were killed by cervical dislocation and exsanguination. Taenia of the guinea-pig caecum and rat aortae were isolated. Longitudinal muscle strips of the taenia caeci, 20 mm in length (Kadlec & Bauer, 1974) and rings of the aorta, 3 mm wide (Biamino & Knuckenberg, 1969) were used for isometric recording of the muscle tension. After 60 min stabilization, the experiments were carried out under an initial tension of 10 mN and at 37°C.

For membrane current recording, the smooth muscle cells of the taenia caeci were isolated enzymatically according to Soloviev *et al.* (1991) using a mixture of 2 mg collagenase and 3 mg bovine serum albumin in 1 ml of nominally Ca^{2+}-free external solution. Otherwise the procedure was similar to that described earlier (Bauer & Ito, 1991; Bauer *et al.*, 1994). The ionic currents were recorded with glass capillary microelectrodes (resistance of 3-5 MΩ) at room temperature using a patch clamp amplifier (Axopatch-1D) under whole-cell voltage clamp configuration (Hamill *et al.*, 1981).

To study the effects of the drugs on lipid peroxidation (LPO), egg phosphatidyl choline (PC) liposomes were used; 20 μl of egg yolk PC (10 mg ml^{-1} ethanol) was evaporated under a stream of N_2 followed by 30 min evaporation in a vacuum ($\leqslant 10^{-2}$ Pa). The dried samples were hydrated with 240 μl of the buffer (in mM): NaCl 150, Tris 5, pH 7.4 (HCl). The LPO was elicited by addition of 5 μl of 2 mM $FeSO_4$ and 5 μl of 1 mM H_2O_2 to these samples. The relative LPO was assessed by measuring the formation of 2-thiobarbituric acid reactive (TBA) products, mainly of the TBA-malondialdehyde complex according to a slightly modified (Ondriaš *et al.*, 1989) method of Haenen & Bast (1983). After 60 min incubation of the samples at 37°C, 150 μl of butylated hydroxytoluene (BHT) (75 mg BHT 50 ml^{-1} ethanol) was added to prevent further LPO. Then 1.5 ml of TBA solution (2.1 g TBA, 84 g trichloracetic acid, 3.57 ml of 37% HCl diluted with H_2O to 500 ml) was added and the samples were incubated for 20 min at 80°C. The samples were then cooled at 10°C in water bath and centrifuged at 1600 *g* 5 min. The supernatant was analyzed spectroscopically, where the absorption at [534 nm-(500 nm-576 nm)/2] was taken as a relative value of LPO.

Solutions

The bathing solutions were (in mM): NaCl 117, KCl 5, $CaCl_2$ 2.5, $MgSO_4$ 1.2, NaH_2PO_4 1.2, $NaHCO_3$ 25, glucose 11, pH 7.4, for mechanical recording and NaCl 135, KCl 6, $CaCl_2$ 2.5, $MgCl_2$ 1.2, NaH_2PO_4 1.0, $NaHCO_3$ 10, HEPES 10, glucose 5.4, pH 7.4 (NaOH) for patch clamp recording. The bathing solutions were gassed with 95% O_2 and 5% CO_2. The storage solution for isolated cells contained only 0.3 mM $CaCl_2$. The pipette solution for measuring the Ca^{2+} current contained (in mM): CsCl 140, $MgCl_2$ 2.5, HEPES 10, ATP 2, EGTA 1, pH 7.2 (NaOH). In potassium depolarizing solution 100 mM KCl was substituted for NaCl.

[1] Author for correspondence.

Chemicals

NTP was prepared from dissolved Nif (10 mM) in ethanol (u.v.-spectroscopy purity, Lachema) by daylight illumination in a glass tube (wall thickness of 1 mm) using a fluorescent lamp at a wave length corresponding to daylight (400–700 nm) at a distance of 10 cm for different periods of time.

The conversion of Nif (Bayer) to NTP and its purity were determined by gas chromatography mass spectrometry (GC-MS) using the HP 5890A gas chromatograph of Hewlett-Packard, equipped with an HP 5791A mass selective detector and HP 7673A autosampler. Quantification of Nif and NTP in the samples was made by means of the internal standard (darodipine, Sandoz) as well as by addition of known amounts of Nif or NTP to the samples. The lowest amounts detectable by the method used were 10 pg Nif 100 μl^{-1} injection and 50 pg NTP 100 μl^{-1} injection. In control experiments an appropriate amount of the solvent was added to the bathing solution. TBA was purchased from Fluka and BHT from Sigma.

Statistics

Results are expressed as means ± s.e.mean. Data were analyzed according to Student's *t* test. Probability levels of less than 0.05 were taken as indicating significant differences between means. The pD_2 ($-\log EC_{50}$) values were calculated according to Arunlakshana & Schild (1959). Acquisition and calculation of patch clamp data were performed by pCLAMP software (Axon Instruments).

Results

Determination of purity by GC-MS showed that the original batches of Nif contained less than 0.05% of NTP. Daylight illumination lasting 24 h resulted in an almost complete conversion of Nif to NTP. To reach full conversion (reduction of Nif concentration by at least 10^5 times) illumination lasting for 48 h was needed. After 48 h there were no traces of Nif in the NTP spectra at maximal gain (10 pg 100 μl^{-1}). The resulting NTP remained unchanged during the following 8 days (Figure 1). Such NTP was used in further experiments.

The lipid peroxidation measured as MDA production under the control conditions was 0.033 ± 0.004. Nif (25 μM) did not affect (reduction was to 0.028 ± 0.005) significantly ($P<0.26$) this MDA production while NTP (25 μM) significantly ($P<0.0001$) reduced it to 0.0034 ± 0.0003.

In contrast to Nif which relaxed the KCl (100 mM) precontracted guinea-pig taenia caeci ($pD_2 = 8.64 \pm 0.5$) and rat aorta ($pD_2 = 8.53 \pm 0.2$) with a threshold in the nanomolar concentration range, NTP in concentrations up to 10 μM (when the applied samples contained less than picomolar concentrations of Nif) did not affect the smooth muscle tension elevated by KCl in the guinea-pig taenia caeci ($n=9$) and rat aorta ($n=7$). Pretreatment with NTP (10 μM) for 10 min and in the continued presence of NTP in the bathing fluid did not change significantly the concentration-response curve of Nif. The pD_2 values of Nif in these conditions were 8.97 ± 0.6 (taenia caeci, $n=7$) and 8.74 ± 0.3 (aorta, $n=5$).

Depolarization of the membrane of isolated single smooth muscle cells of the taenia caeci under whole cell configuration

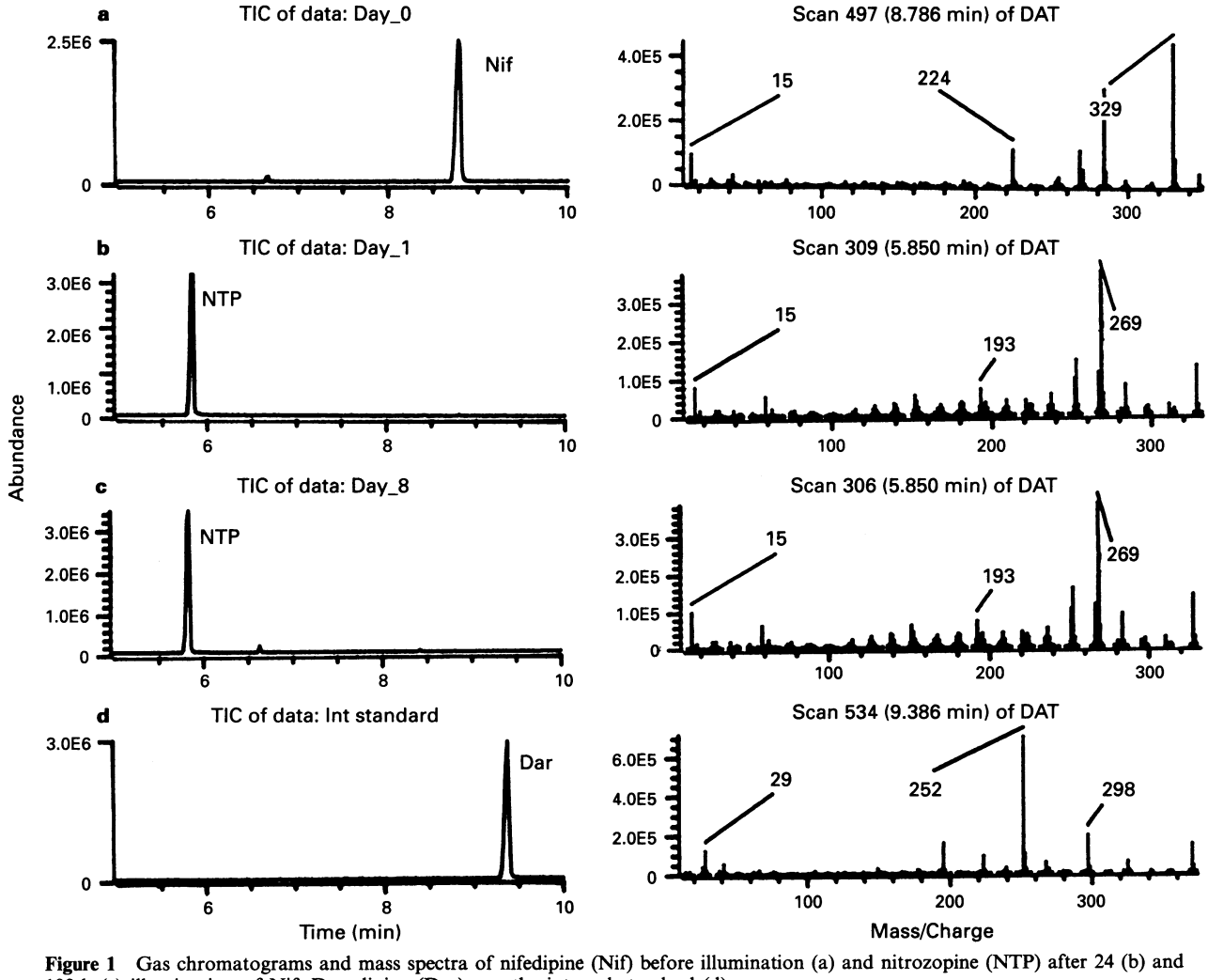

Figure 1 Gas chromatograms and mass spectra of nifedipine (Nif) before illumination (a) and nitrozopine (NTP) after 24 (b) and 192 h (c) illumination of Nif. Darodipine (Dar) was the internal standard (d).

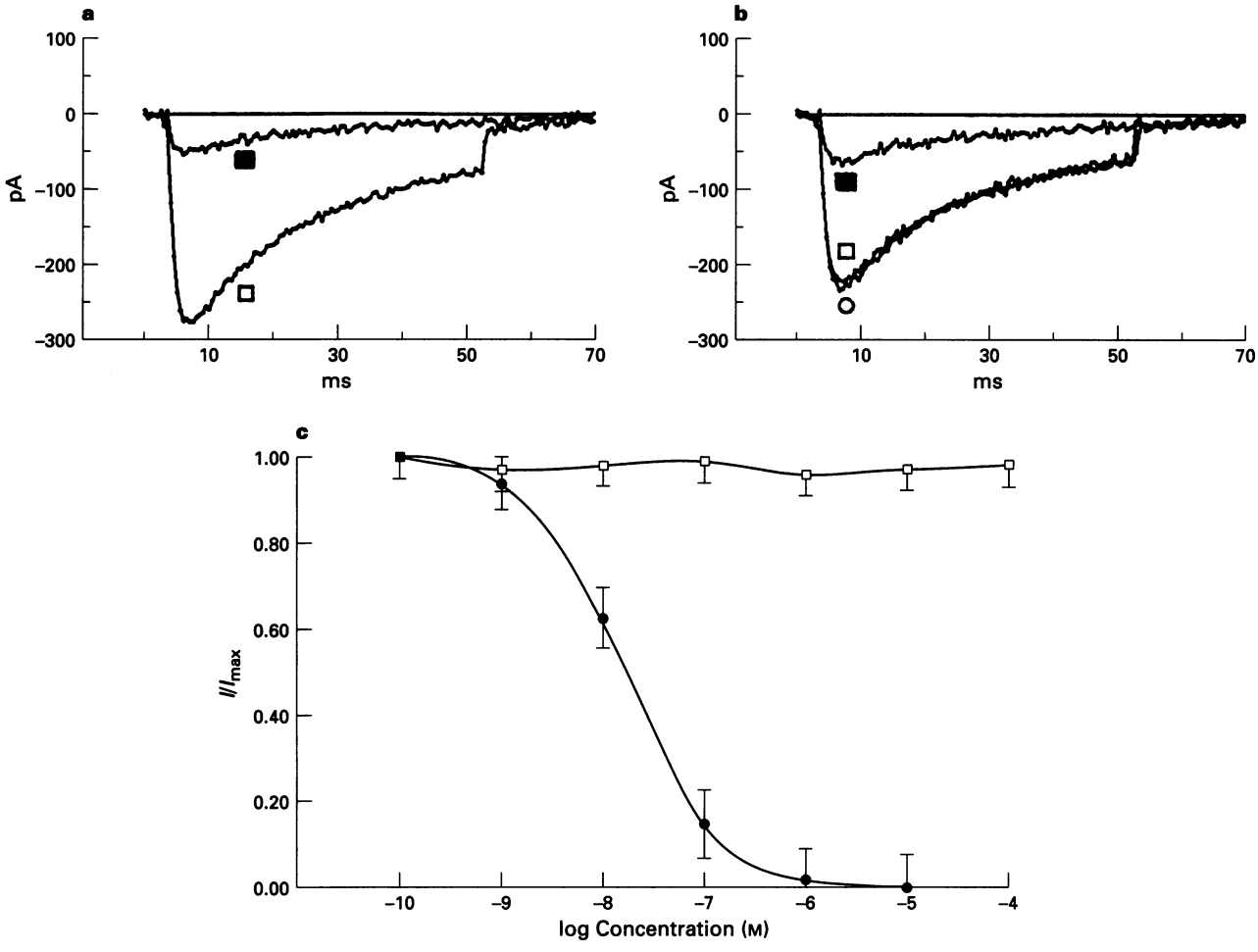

Figure 2 Effect of nifedipine (Nif, 0.1 μM) and its nitroso-product nitrosopine (NTP, 10 μM) on inward calcium current (I_{Ca}) in smooth muscle cells isolated from guinea-pig taenia caeci. Depolarization steps from −60 mV to 0 mV of 50 ms duration were applied. The pipette solution contained 1 mM EGTA. (□) Control response; (■) response in the presence of Nif (a); or NTP and Nif (b); (○) response in the presence of NTP. Concentration-dependent effect of Nif (●) and NTP (□) on peak I_{Ca} is shown in (c). Each point represents the mean with s.e.mean of at least six determinations.

from the holding potential (HP) of −60 mV to 0 mV for 50 ms, induced an inward current followed by an outward one. When CsCl replaced KCl in the pipette solution, only inward current was recorded. Ethanol, used as a solvent in our experiments, even at its highest final concentration (0.5 mM) in the bathing fluid did not alter the spontaneous and evoked mechanical and membrane responses ($n=4$).

Neither Nif nor NTP, in the concentration-range from 0.1 nM to 10 μM, influenced the holding membrane current ($n=5$). Nif (0.1 nM−10 μM) decreased the evoked inward calcium current induced by membrane depolarization (Figure 2a) in a concentration-dependent manner with $pD_2=7.82 \pm 0.11$ (Figure 2c). In contrast, NTP did not affect significantly the inward Ca^{2+} current up to a concentration of 0.1 mM (Figure 2b,c). Pretreatment with NTP for 10 min and its presence in the bathing fluid at a concentration of 10 μM, which did not alter the inward calcium current significantly ($103.9 \pm 2.3\%$ in its presence, $n=7$) had no significant effect on the action of Nif (0.1 μM) (Figure 2b). Nif reduced the inward calcium current to $18.9 \pm 1.8\%$ ($n=7$) in the absence and to $23.1 \pm 1.9\%$ ($n=7$) of the control values in the presence of NTP.

Discussion

In agreement with the results of Majeed *et al.* (1987) the nitro-group on the aromatic ring of Nif is converted to nitroso-group forming NTP under the illumination at $\lambda=400-700$ nm. To reach full conversion (reduction of Nif concentration by at least 10^5 times) under our conditions, illumination lasting from 24 to 48 h was needed. The resulting NTP possesses roughly 10 times higher antioxidative activity than unchanged Nif.

Nif as described earlier (Sperelakis *et al.*, 1992) decreased the muscle tension and the inward Ca^{2+} current. In contrast to the increased antioxidative activity, illumination of Nif led to gradual loss of its ability to relax the precontracted smooth muscles (guinea-pig taenia caeci, rat aorta) and to reduce the inward Ca^{2+} current of isolated smooth muscle cells. Since after pretreatment with NTP and even in its presence in high concentration in the bathing fluid, NTP did not influence the action of Nif on muscle strips and isolated cells, we might conclude that NTP does not bind to the binding site for Nif in the calcium channel of the smooth muscle membrane. Thus conversion of a part of the administered dose of Nif to NTP does not interfere with the action of its unaltered molecules.

Reactive oxygen species contribute to the tissue damage caused by atherogenesis and ischaemia/reperfusion. The possible role of an antiperoxidative action of calcium channel blockers in suppression of the atherogenesis has recently been suggested (Henry, 1991). Thus the molecules of Nif converted into NTP might also have been involved in such effect.

The authors are grateful to the Slovak Grant Agency for Science (grant No. 288 and 1017) for partially supporting this work.

References

ARUNLAKSHANA, O. & SCHILD, H.O. (1959). Some quantitative uses of drug antagonists. *Br. J. Pharmacol. Chemother.*, **14**, 48–58.

BAUER, V. & ITO, Y. (1991). Effect of potassium channel blocking agents on the actions of phenylephrine in rabbit tacnia caeci. *Gen. Physiol. Biophys.*, **10**, 111–124.

BAUER, V., REKALOV, V. & ITO, Y. (1994). Effects of phenylephrine on membrane currents in single smooth muscle cells of taenia caeci. *Methods Find. Exp. Clin. Pharmacol.*, **16**, 337–346.

BIAMINO, G. & KNUCKEMBERG, P. (1969). Synchronization and conduction of excitation in the rat aorta. *Am. J. Physiol.*, **217**, 376–382.

FOLLATH, F. (1989). The role of calcium antagonists in the treatment of myocardial ischemia. *Am. Heart J.*, **118**, 1093–1096.

GODFRAIND, T., EGLEME, C. & WIBO, M. (1986). Effect of dihydropyridines on human and animal isolated vessels. In Cardiovascular Effect of Dihydropyridine type calcium antagonists and agonists. *Proceedings of Bayer Symposia*, vol. IX., pp. 309–325. ed. Fleckenstein, A. & Van Breemen, C. Berlin: Springer Verlag.

HAENEN, G.R.M.M. & BAST, A. (1983). Protection against lipid peroxidation by a microsomal glutathione-dependent labile factor. *FEBS Lett.*, **159**, 24–28.

HAMILL, O.P., MARTY, A., NEHER, E., SAKMANN, B. & SIGWORTH, F.J. (1981). Improved patch clamp techniques for high resolution current recording from cells and cell-free membrane patches. *Pflügers Arch.*, **391**, 85–100.

HENRY, P. (1991). Antiperoxidative actions of calcium antagonists and atherogenesis. *J. Cardiovasc. Pharmacol.*, **18** (Suppl. 1), S6–S10.

KADLEC, O. & BAUER, V. (1971). Papaverine blockade of calcium action in depolarized taenia coli of the guinea-pig. *Experientia*, **27**, 815–816.

MAJEED, I.A., MURRAY, W.J., NEWTON, D.W., OTHMAN, S. & AL-TURK, W.A. (1987). Spectrophotometric study of the photodecomposition kinetics of nifedipine. *J. Pharm. Pharmacol.*, **39**, 1044–1046.

MAK, I.T. & WEGLICKI, W.B. (1990). Comparative antioxidant activities of propranolol, nifedipine, verapamil, and diltiazem against sarcolemmal membrane lipid peroxidation. *Circ. Res.*, **66**, 1449–1452.

MIŠÍK, V., STAŠKO, A., GERGEL, D. & ONDRIAŠ, K. (1991). Spin-trapping and antioxidant properties of illuminated and non-illuminated nifedipine and nimodipine in heart homogenate and model system. *Mol. Pharmacol.*, **40**, 435–439.

ONDRIAŠ, K., MIŠÍK, V., GERGEL, D. & STAŠKO, A. (1989). Lipid peroxidation of phosphatidylcholine liposomes depressed by the calcium channel blockers nifedipine and verapamil and by the antiarrhythmic–antihypoxic drug stobadine. *Biochim. Biophys. Acta.*, **1003**, 238–245.

SOLOVIEV, A.I., REKALOV, V.V., SHUBA, M.F., SAGAH, V.F., ZUGORKA, A.M. & BRAQUET, P. (1991). Influence of platelet-activating factor on outward potassium currents in Taenia coli single smooth muscle cells. *Biol. Membranes*, **8**, 736–742.

SPERELAKIS, N., INOUE, Y. & OHYA, Y. (1992). Fast Na^+ channels and slow Ca^{2+} current in smooth muscle from pregnant rat uterus. *Jpn. J. Pharmacol.*, **58** (Suppl. II) 96P–106P.

(Received January 24, 1995
Revised March 14, 1995
Accepted March 21, 1995)

British Journal of Pharmacology (1995) 115, 875-882 © 1995 Stockton Press All rights reserved 0007-1188/95 $12.00

Activation of the micturition reflex by NK_2 receptor stimulation in the anaesthetized guinea-pig

[1]Mark Bushfield, Maria Metcalfe & Alasdair M. Naylor

Department of Discovery Biology, Pfizer Central Research, Sandwich, Kent CT13 9NJ

1 The mechanisms underlying stimulation of bladder contractions and bronchoconstriction by the selective NK_2 receptor agonist, [β-Ala^8]NKA(4-10), were examined in the anaesthetized guinea-pig.

2 Atropine, α,β-methylene-ATP and ganglion blocking agents were used to examine the contribution of reflex arc activation and/or potentiation of efferent mechanisms to the NK_2 receptor-mediated responses seen in these two tissues.

3 [β-Ala^8]NKA(4-10)-induced bronchoconstriction was immediate, dose-dependent and was unaffected by pretreatment with ganglion blockers (hexamethonium or chlorisondamine), blockade of muscarinic receptors by atropine, or desensitization of P_2 purinoceptors by α,β-methylene-ATP.

4 At doses of 5 $\mu g\ kg^{-1}$ and above, [β-Ala^8]NKA(4-10) induced bladder contractions that appeared to be of an 'all-or-nothing' nature. These contractions occurred after a delay of 10 to 30 s and were often biphasic, comprised of an initial rapid component followed by a slower tonic component.

5 Pretreatment of the animals with either atropine or the desensitizing purinoceptor agonist α,β-methylene-ATP, resulted in partial inhibition of bladder contractile responses to [β-Ala^8]NKA(4-10). The combination of atropine and α,β-methylene-ATP pretreatment resulted in additive inhibition leading to complete blockade of the response.

6 The bladder responses to [β-Ala^8]NKA(4-10) (5 $\mu g\ kg^{-1}$) were inhibited by pretreatment with the ganglion blockers, hexamethonium and chlorisondamine, indicating a preganglionic mechanism of action.

7 These findings demonstrate the indirect nature of the bladder contractions induced by activation of NK_2 receptors in the anaesthetized guinea-pig. Contractions occur secondary to the release of endogenous cholinergic and NANC transmitters by activation of neuronal NK_2 receptors located at a preganglionic site, possibly on capsaicin-sensitive sensory afferent nerves, where NK_2 sites have been demonstrated autoradiographically. In contrast, [β-Ala^8]NKA(4-10)-induced bronchoconstriction in the anaesthetized guinea-pig is a direct smooth muscle contractile response that is unaffected by ganglion blockade or blockade of muscarinic receptors.

Keywords: Tachykinins: NK_2 receptors; [β-Ala^8]NKA(4-10); guinea-pig urinary bladder; guinea-pig airways; micturition reflex; sensory nerves

Introduction

Mammalian airways and bladder are richly innervated by capsaicin-sensitive primary afferent neurones (Holzer *et al.*, 1982; Polak & Bloom, 1982; Lundberg *et al.*, 1984; Su *et al.*, 1986) that are characterized by high levels of tachykinin immunoreactivity (Holzer *et al.*, 1982; Lundberg & Saria, 1986). The endogenous tachykinins, substance P (SP), neurokinin A (NKA) and NKB, are potent contractile agents in bladder (Falconieri-Erspamer *et al.*, 1973; Maggi *et al.*, 1988; Giuliani *et al.*, 1993) and airways (Devillier *et al.*, 1988; Frossard *et al.*, 1989; Frossard & Advenier, 1991) from various species. These effects are mediated by activation of tachykinin NK_1 (SP-preferring) and NK_2 (NKA-preferring) receptors (Frossard & Advenier, 1991; Maggi *et al.*, 1991d; Hall *et al.*, 1992; Longmore & Hill, 1992; Giuliani *et al.*, 1993).

The main functional roles of NK_1 and NK_2 receptors in airways and bladder vary, depending upon the species under examination. NK_2 receptors, predominantly, mediate direct contractile effects of tachykinins in guinea-pig and human trachea and bronchi preparations (Dion *et al.*, 1990; Frossard & Advenier, 1991; Maggi *et al.*, 1991c). However, NK_1 receptors also have a direct smooth muscle contractile role in guinea-pig, but not human, airways (Dion *et al.*, 1990; Frossard & Advenier, 1991; Ireland *et al.*, 1991; Maggi *et al.*, 1991c). NK_1 receptors, predominantly, mediate tachykinin-induced airway mucosecretion, vasodilatation, microvascular leakage and inflammatory cell activation (Rogers *et al.*, 1988; Joos & Pauwels, 1990; Frossard & Advenier, 1991). This has led to the suggestion that NK_1 receptors play a major role in neurogenic inflammation and that selective NK_1 and/or NK_2 antagonists, respectively, may be useful for the treatment of airway hyperresponsiveness and bronchoconstriction associated with asthma (Barnes, 1986; Manzini, 1993).

Tachykinin-induced contractions of rat, guinea-pig and hamster bladder preparations are mediated by both NK_1 and NK_2 receptors (Falconieri-Erspamer *et al.*, 1973; Maggi *et al.*, 1991a; Hall *et al.*, 1992), while human bladder contracts in response to activation of NK_2 but not NK_1 receptors (Dion *et al.*, 1990; Giuliani *et al.*, 1993). NK_1 receptors mediate SP-induced microvascular leakage and contribute to inflammatory responses in the bladder (Abelli *et al.*, 1989). Several *in vivo* studies have demonstrated contractile effects of NK_2 agonists on the bladder and airways in anaesthetized rats (Joos *et al.*, 1986; Maggi *et al.*, 1991a; Palea *et al.*, 1993; Lecci *et al.*, 1993) and guinea-pigs (Maggi *et al.*, 1991b; Buckner *et al.*, 1993; Belvisi *et al.*, 1994). The presence of NK_2 receptors on both smooth muscle and sensory neuronal sites in the bladder (Burcher & Buck, 1986; Carstairs *et al.*, 1993) indicates that the effects of NK_2 agonists in the bladder may be either direct, via smooth muscle contraction, and/or indirect, via activation of the afferent limb of the micturition reflex. In the present study we have compared the *in vivo* bronchoconstriction and bladder contractile responses induced by the selective NK_2 receptor

[1] Author for correspondence.

agonist, [β-Ala^8]NKA(4–10) (Rovero *et al.*, 1989), in the anaesthetized guinea-pig. In particular, we have used ganglion blocking and antimuscarinic agents, as well as α,β-methylene-ATP ([α,β-Me]ATP) (Kasakov & Burnstock, 1983), to examine the contribution of reflex arc activation and/or potentiation of efferent mechanisms to the NK_2 responses seen in these two tissues. Our results indicate that in the guinea-pig bladder, unlike the airways, [β-Ala^8]NKA(4–10)-induced contractions are indirect and result from NK_2-dependent activation of the micturition reflex. Some of this work has been presented in preliminary form to the British Pharmacological Society (Metcalfe *et al.*, 1994).

Methods

Animals

Female Dunkin Hartley guinea-pigs (350–450 g) were obtained from Charles River, UK, and were anaesthetized with urethane (1.2 g kg^{-1}, i.p.) and placed on a heating pad to maintain body temperature at 37°C. The carotid artery was cannulated (Portex Luer IV cannula) for blood pressure recording (Druck pressure transducer) and the left jugular vein cannulated for i.v. drug administration. After tying off the external urethra, a catheter was inserted via the dome into the bladder and connected via a three-way tap to a Millar microtip catheter (model MPC500) and transducer control unit (TCB500) for intraluminal pressure recording. The guinea-pigs were artificially ventilated (60 strokes min^{-1}; 10 ml kg^{-1}) with a Harvard small animal respirator (model 683) and the tracheal insufflation pressure recorded. Data were recorded and analysed with a Macintosh Maclab/8 data recording system controlled by a Macintosh IIci computer with Chart software. Animals were allowed to stabilize for 15 to 20 min after surgery before drug additions.

Drugs used in the study

Hexamethonium and [α,β-Me]ATP were obtained from Sigma (UK) and atropine was from Research Biochemicals Inc (UK). [β-Ala^8]NKA(4–10) was purchased from Bachem, U.K., Ltd. (±)-SR48968 (N-methyl-N[4-(4-acetyamino-4-phenylpiperidino)-2-(3,4-dichlorophenyl)butyl] benzamidine) (Emonds-Alt *et al.*, 1992) and (±)-SR140333 (1-{2-[3-(3,4,-

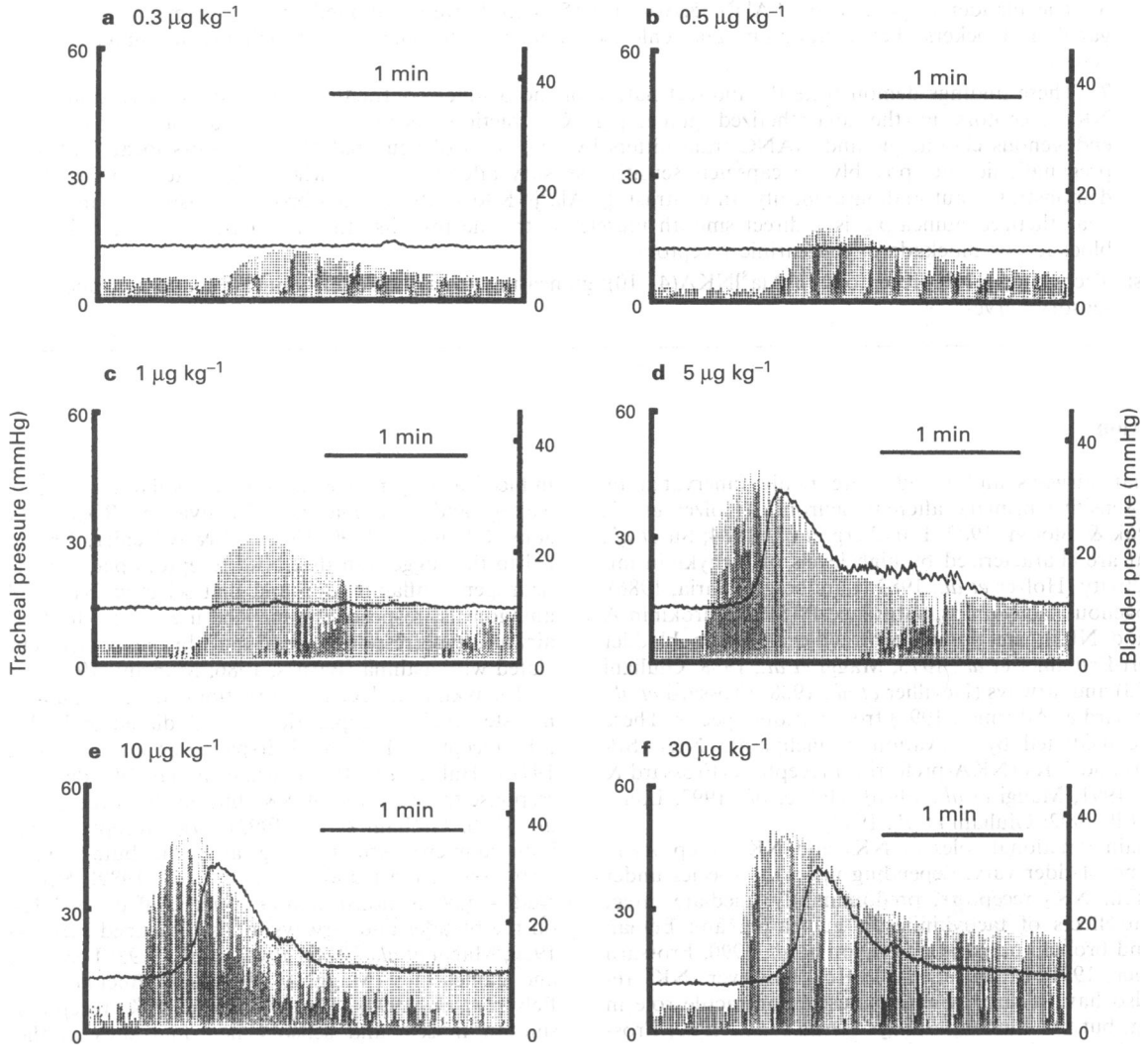

Figure 1 Traces illustrating the effects of [β-Ala^8]NKA(4–10) on bladder pressure and tracheal insufflation pressure in the anaesthetized guinea-pig. Intravenous administration of the indicated doses of [β-Ala^8]NKA(4–10) resulted in immediate and dose-related increases in tracheal insufflation pressure while delayed all-or-nothing bladder contractions were induced by doses of 5 μg kg^{-1} and above. All doses of [β-Ala^8]NKA(4–10) induced transient and variable increases (2 to 30 mmHg) in blood pressure that returned to baseline levels within 5 min. The traces shown are representative of 5 experiments in different animals. Bladder pressure, continuous line trace; tracheal pressure, shaded trace.

dichlorophenyl)-1-(3-isopropoxyphenylacetyl)piperidin-3-yl]-ethyl}-4-phenyl-1-azoniabicyclo[2.2.2]octane) (Emonds-Alt *et al.*, 1993) were synthesized by Mike Stace and Chris Burns, Discovery Chemistry Department, Pfizer Central Research, Sandwich. All other drugs and chemicals were obtained from Aldrich (U.K.) or BDH (U.K.) and were of the highest grade available. All drugs were dissolved in de-ionised water apart from [β-Ala^8]NKA(4–10) and (±)-SR140333 which were dissolved at 1 mg ml^{-1} in 100% and 50% dimethylsulphoxide (DMSO), respectively, and further dilutions were made in de-ionised water. All drugs were administered intravenously in a volume of 1 ml kg^{-1}.

Results

Airway and bladder responses to [β-Ala^8]NKA(4–10)

Administration of the NK_2 receptor agonist, [β-Ala^8]NKA(4–10) (5 μg kg^{-1}, i.v.) caused a contraction of the bladder and an increase in tracheal insufflation pressure. The bladder response to [β-Ala^8]NKA(4–10) occurred after a variable lag period of 10 to 30 s and displayed at least two distinct phases: an initial fast component and a slower tonic component. In some cases, the tonic phase of the contraction was accompanied by a series of transient rhythmic contractions. Dose-response studies showed the bladder contraction to be of an 'all or nothing' nature, with the threshold dose being between 1 and 5 μg kg^{-1} (Figure 1). In contrast, the tracheal response to [β-Ala^8]NKA(4–10) was immediate and dose-dependent (Figure 1) and displayed an ED_{50} of 0.63 μg kg^{-1} (geometric mean, range = 0.34–1.29, n = 5). The maximal response was achieved with between 5 and 10 μg kg^{-1}.

Effects of NK_1 and NK_2 antagonists on responses to [β-Ala^8]NKA(4–10)

In order to confirm the NK_2 receptor involvement in the responses of the anaesthetized guinea-pig to [β-Ala^8]NKA(4–10), we examined the effects of pretreatment with selective NK_1 and NK_2 receptor antagonists. The NK_2 receptor-selective (Emonds-Alt *et al.*, 1992) antagonist, (±)-SR48968 (1–300 μg kg^{-1}), abolished the bladder contraction in response to a threshold dose of [β-Ala^8]NKA(4–10) (5 μg kg^{-1}, i.v.) at doses of 30 μg kg^{-1} and above (Figure 2). (±)-SR48968 inhibited the [β-Ala^8]NKA(4–10) (5 μg kg^{-1}, i.v.)-induced increase in tracheal insufflation pressure in a dose-dependent manner (Figure 2), with an ED_{50} of 75.0 μg kg^{-1} (geometric mean, range = 35.5–1.29, n = 6). The tracheal response to a submaximal dose of [β-Ala^8]NKA(4–10) (1 μg kg^{-1}, i.v.) was inhibited with an ED_{50} of 25.4 μg kg^{-1} (geometric mean, range = 18.0–38.5, n = 4). In contrast, the

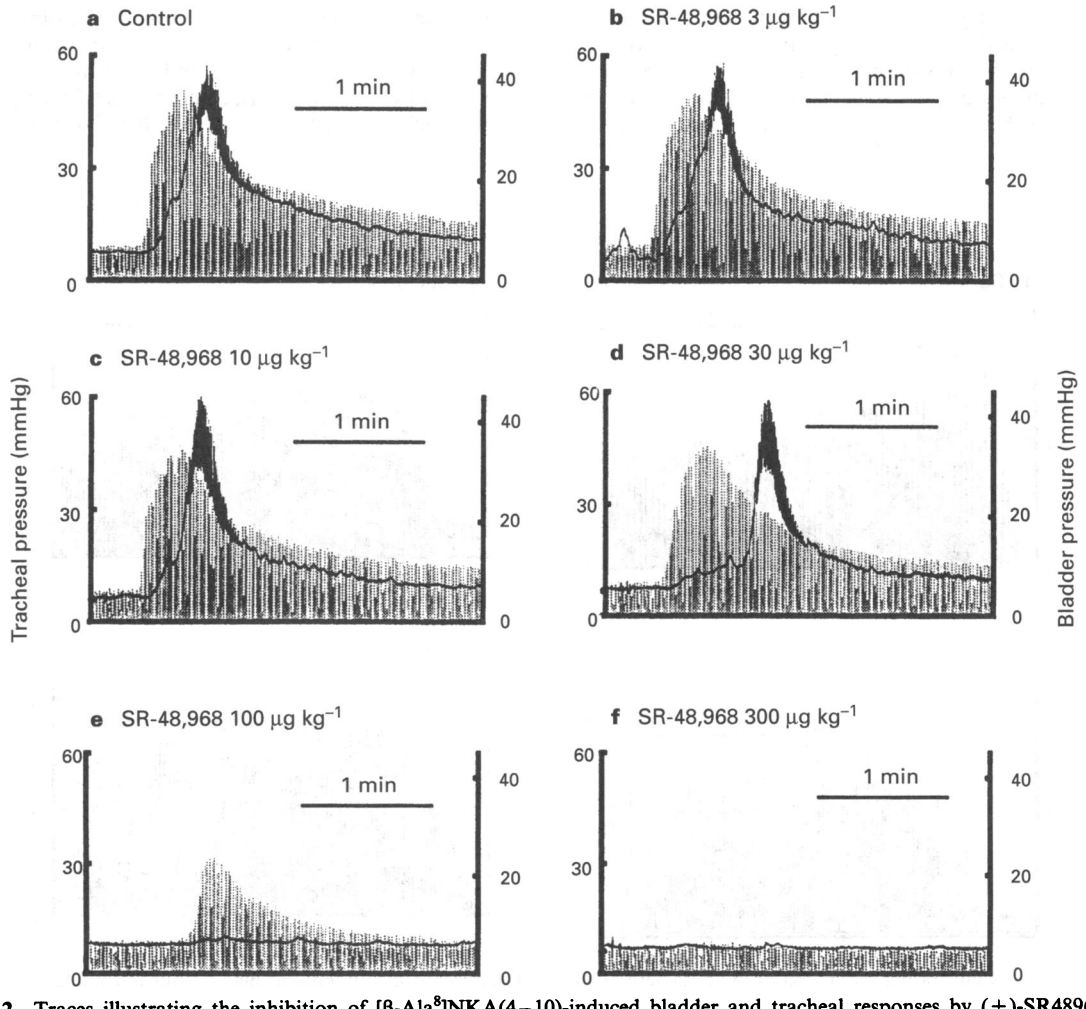

Figure 2 Traces illustrating the inhibition of [β-Ala^8]NKA(4–10)-induced bladder and tracheal responses by (±)-SR48968 was administered at the indicated doses 5 min prior to injection of [β-Ala^8]NKA(4–10) (5 μg kg^{-1}). Agonist-induced increases in tracheal insufflation pressure were inhibited in a dose-dependent manner while doses of 1 μg kg^{-1} and above of [β-Ala^8]NKA(4–10) were required to abolish the tracheal response. Traces shown are representative of 6 experiments in different animals. Bladder pressure, continuous line trace; tracheal pressure, shaded trace.

NK_1-selective (Emonds-Alt *et al.*, 1993) antagonist, (±)-SR-140333, at doses (10–1000 μg kg^{-1}) more than twenty fold higher than those necessary to inhibit SP-induced bronchoconstriction (Edmonds-Alt *et al.*, 1993), had no effect on [β-Ala^8]NKA(4–10) (5 μg kg^{-1}, i.v.)-induced bladder on tracheal responses (not shown).

Effects of ganglion blockade and inhibition of cholinoceptors and purinoceptors

Hexamethonium (0.1 to 30 mg kg^{-1}, i.v.) treatment 5 min prior to [β-Ala^8]NKA(4–10) had no effect on the increase in tracheal pressure. However, there was a dose-dependent inhibition of the bladder response (Figure 3), giving a maximal degree of inhibition of 80±6% (mean±s.e.mean, $n=7$). Similar results were seen with chlorisondamine (1–1000 μg kg^{-1}, i.v.) treatment which produced dose-dependent inhibition of [β-Ala^8]NKA(4–10) (5 μg kg^{-1}, i.v.) induced bladder (ED_{50} = 56.9 g kg^{-1}, geometric mean, range = 36.2–128, $n=4$) but not tracheal responses (Figure 4).

Injection of atropine (1 to 1000 μg kg^{-1}, i.v.) 5 min prior to [β-Ala^8]NKA(4–10) resulted in a dose-dependent partial inhibition of the bladder contraction. A maximum reduction of 63.2±6.7% (mean±s.e.mean, $n=5$) was achieved at the highest dose (Figure 5). The desensitising purinoceptor agonist, [α,β-Me]ATP (1–300 μg kg^{-1}) induced a direct stimulation of bladder smooth muscle contraction and inhibited the response to subsequent administration of [β-Ala^8]NKA(4–10). The direct bladder contractions in response to [α,β-Me]ATP were dose-related (Figure 6), unlike the all-or-nothing responses to [β-Ala^8]NKA(4–10). Pretreatment with [α,β-Me]ATP (1–300 μg kg^{-1}) 3 min prior to the NK_2 agonist, resulted in dose-dependent inhibition of the bladder contraction (Figure 7) with a maximum inhibition of 34.8±6.7% (mean±s.e.mean, $n=5$). Atropine pretreatment had no significant effect on the direct bladder smooth muscle contractile effect of [α,β-Me]ATP. However, the combination of atropine (300 μg kg^{-1}) and [α,β-Me]ATP (300 μg kg^{-1}) completely abolished the NK_2 agonist-induced bladder contraction (Figure 8). Neither atropine nor [α,β-Me]ATP modified the [β-Ala^8]NKA(4–10) (5 μg kg^{-1}) induced increase in tracheal insufflation pressure (Figure 8).

Discussion

The results of this study indicate that NK_2 receptor-dependent bronchoconstriction *in vivo* is mediated by a direct contractile effect on airway smooth muscle that is independent of cholinergic neurotransmission. These findings are in agreement with *in vitro* studies that have identified only direct smooth muscle contractile effects of NK_2 receptors in guinea-pig trachea (Devillier *et al.*, 1988; Frossard & Advenier, 1991). Tachykinin-induced enhancement of cholinergic neurotransmission has been demonstrated in guinea-pig airways. However, this effect was shown to be mediated by activation of NK_1 but not NK_2 receptors (Hall *et al.*, 1989; Watson *et al.*, 1993; Belvisi *et al.*, 1994).

In contrast to the direct bronchoconstrictor effect of [β-Ala^8]NKA(4–10) in the anaesthetized guinea-pig, the results of this study indicate that the *in vivo* bladder responses to NK_2 receptor activation are indirect. The NK_2 agonist-induced response was shown to be of an 'all-or-nothing' nature and occurred after a distinct lag period following injection of [β-Ala^8]NKA(4–10), indicative of an indirect mechanism of action, possibly via activation of a reflex arc. This possibility was further explored by use of blocking drugs to interfere with the post-junctional action of the main neurotransmitters implicated in micturition contractions. Activation of micturition contractions in the guinea-pig and other mammalian species is mediated by both cholinergic and purinergic neurotransmitters (Burnstock *et al.*, 1972; Fujii, 1988; Brading & Williams, 1990).

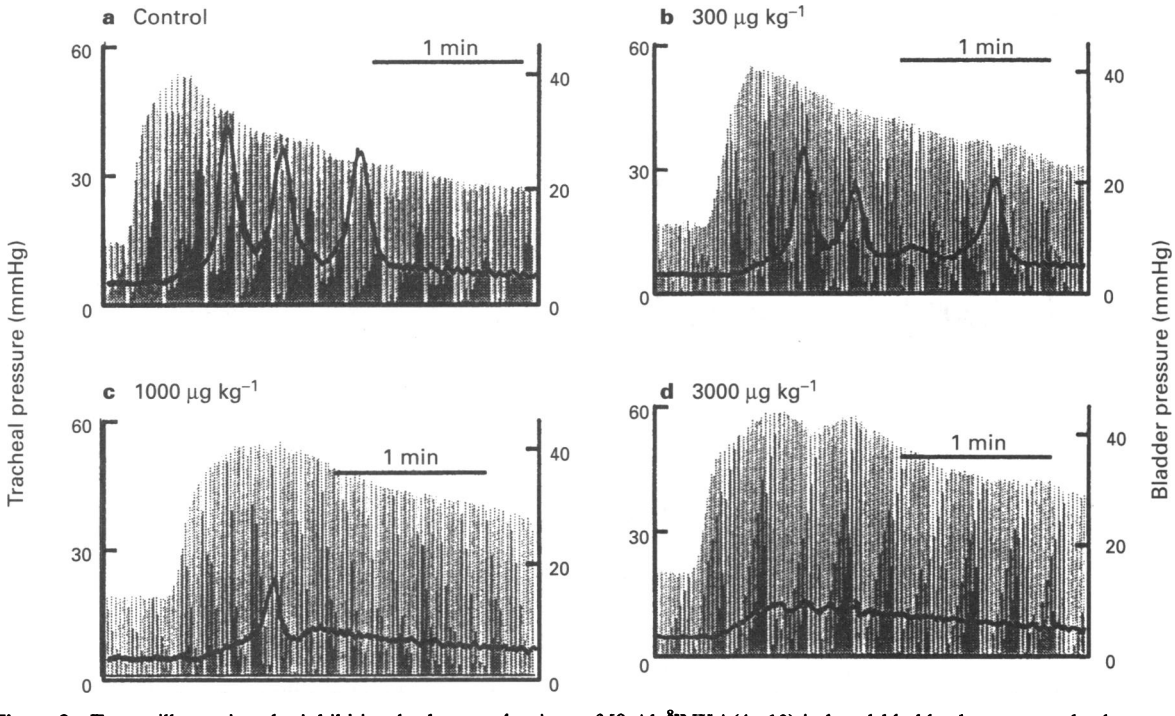

Figure 3 Traces illustrating the inhibition by hexamethonium of [β-Ala^8]NKA(4–10)-induced bladder but not tracheal responses. Animals were pretreated for 5 min with the indicated doses of hexamethonium prior to dosing with [β-Ala^8]NKA(4–10) (5 μg kg^{-1}). Agonist-induced bladder responses were inhibited by hexamethonium but tracheal responses were not significantly changed. Mean arterial blood pressure, before addition of hexamethonium, was 58.4±2.4 mmHg (mean±s.e.mean, $n=4$). Hexamethonium produced a dose-dependent depression in blood pressure that reached 38±5.3% of control at the highest dose tested. Traces shown are representative of 4 experiments in different animals. Bladder pressure, continuous line trace; tracheal pressure, shaded trace.

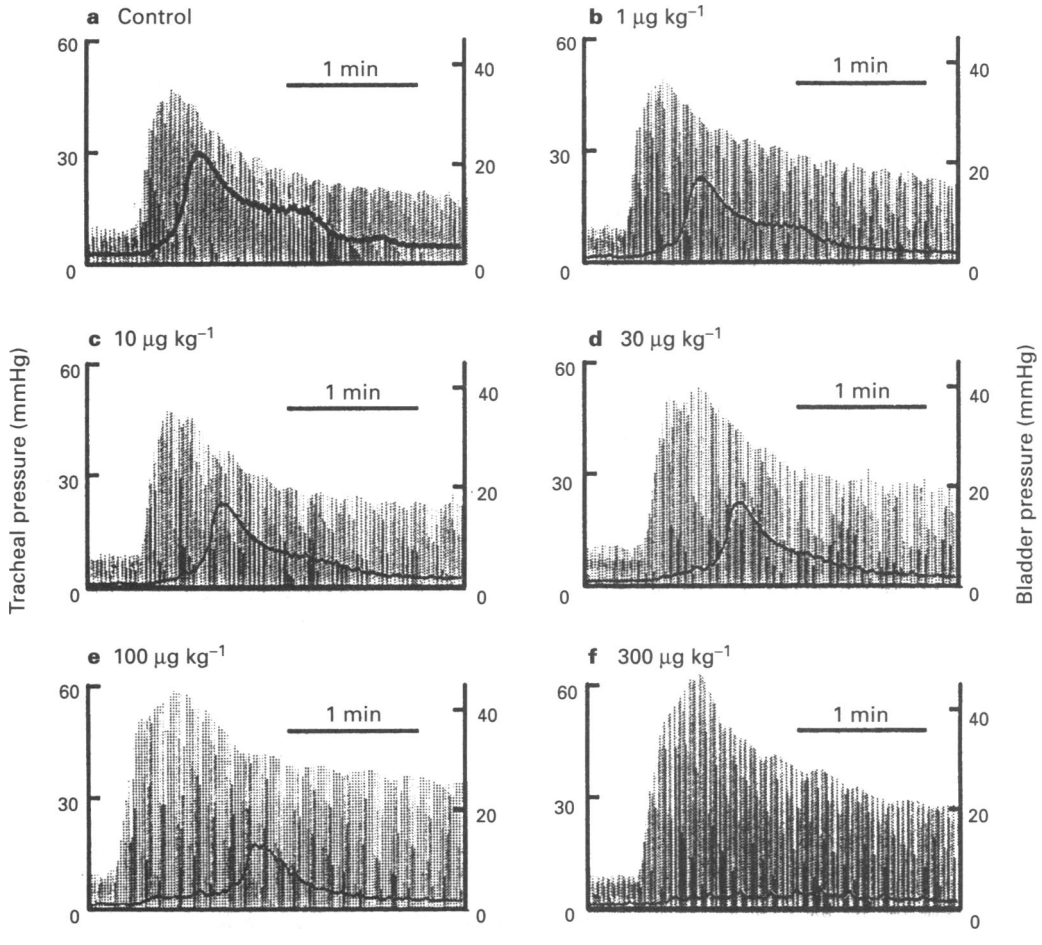

Figure 4 Traces illustrating the inhibition by chlorisondamine of [β-Ala^8]NKA(4–10)-induced bladder but not tracheal responses. Animals were pretreated for 5 min with the indicated doses of chlorisondamine prior to injection of [β-Ala^8]NKA(4–10) (5 μg kg^{-1}). Agonist-induced bladder responses were inhibited by chlorisondamine but tracheal responses were not significantly changed. Mean arterial blood pressure, before addition of chlorisondamine, was 70.2±5.2 mmHg (mean±s.e.mean, n=4). Chlorisondamine produced a dose-dependent depression in blood pressure that reached 53.3±5.5% of control at the highest dose tested. Traces shown are representative of 4 experiments in different animals. Bladder pressure, continuous line trace; tracheal pressure, shaded trace.

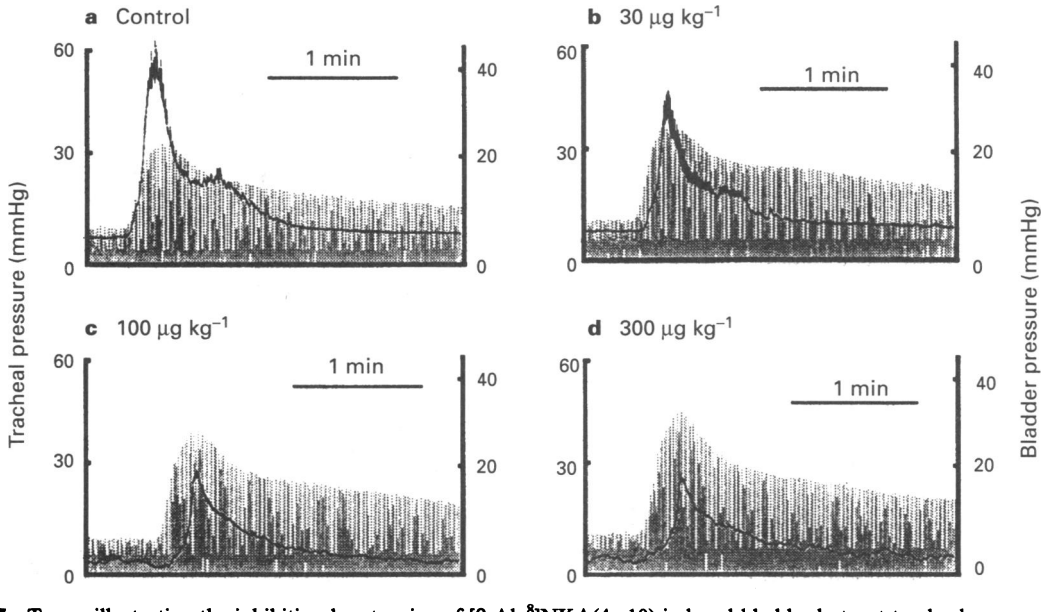

Figure 5 Traces illustrating the inhibition by atropine of [β-Ala^8]NKA(4–10)-induced bladder but not tracheal responses. Animals were pretreated for 5 min with the indicated doses of atropine prior to injection of [β-Ala^8]NKA(4–10) (5 μg kg^{-1}). Agonist-induced bladder responses were partially inhibited by atropine but tracheal responses were not significantly changed. Traces shown are representative of 5 experiments in different animals. Bladder pressure, continuous line trace; tracheal pressure, shaded trace.

Inhibition of these cholinergic and purinergic components by atropine and [α,β-Me]ATP, respectively, was shown to produce additive inhibition of [β-Ala^8]NKA(4–10) induced bladder contractions, indicating a prejunctional site of action of [β-Ala^8]NKA(4–10) *in vivo*. This effect could be mediated either by direct enhancement of efferent transmitter release or via activation of a reflex arc.

NK_2 receptor-dependent activation of the micturition reflex arc was confirmed by use of the ganglion blockers, hexamethonium and chlorisondamine, which both caused almost complete blockade of the [β-Ala^8]NKA(4–10) response. Taken together, these results indicate that i.v. administration of [β-Ala^8]NKA(4–10) induced reflex bladder contractions by an action on preganglionic efferent or afferent NK_2 receptors. Autoradiographic studies with [^{125}I]-NKA in rat and guinea-pig tissues have localized bladder NK_2 receptor sites to both smooth muscle and epithelia (Burcher & Buck, 1986; Carstairs *et al.*, 1993). Epithelial binding of [^{125}I]-NKA was absent in

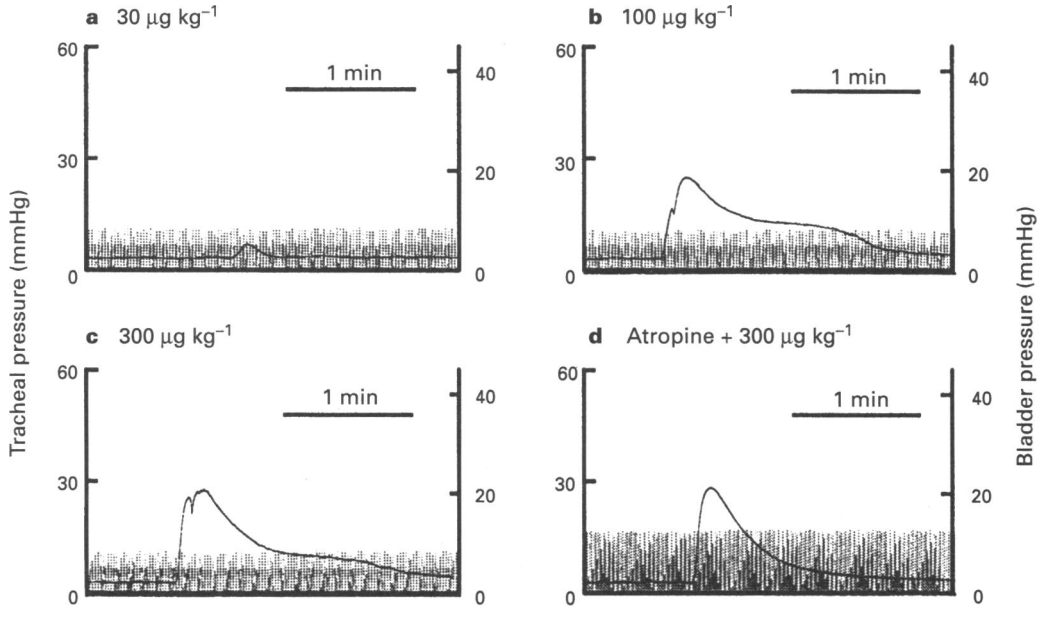

Figure 6 Traces illustrating the effects of [α,β-Me]ATP on bladder pressure in the anaesthetized guinea-pig. Intravenous administration of the indicated doses of [α,β-Me]ATP resulted in immediate dose-related transient increases in bladder pressure but had no effect on tracheal insufflation pressure. In one example (d), the animal had been pretreated with atropine (300 μg kg^{-1}, i.v.) 15 min prior to the administration of [α,β-Me]ATP. The traces shown are representative of 5 experiments in different animals. Bladder pressure, continuous line trace; tracheal pressure, shaded trace.

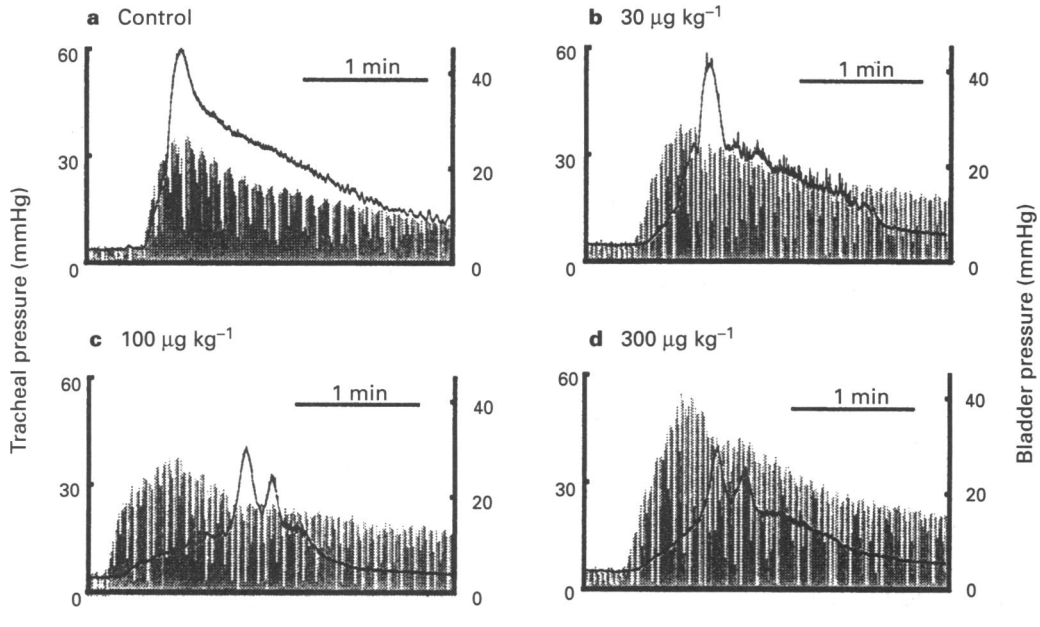

Figure 7 Traces illustrating the inhibition by [α,β-Me]ATP of [β-Ala^8]NKA(4–10)-induced bladder but not tracheal responses. Animals were pretreated for 3 min with the indicated doses of [α,β-Me]ATP prior to injection of [β-Ala^8]NKA(4–10) (5 μg kg^{-1}). [β-Ala^8]NKA(4–10)-induced bladder responses were partially inhibited by [α,β-Me]ATP pretreatment but tracheal responses were not significantly changed. Traces shown are representative of 5 experiments in different animals. Bladder pressure, continuous line trace; tracheal pressure, shaded trace.

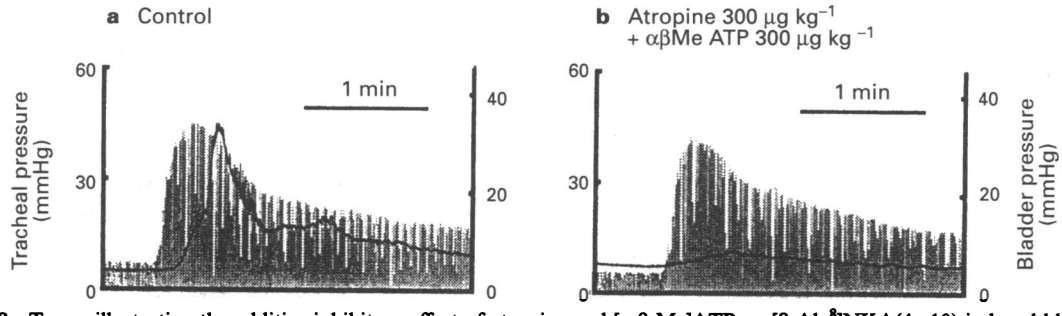

Figure 8 Traces illustrating the additive inhibitory effect of atropine and [α,β-Me]ATP on [β-Ala^8]NKA(4–10)-induced bladder but not tracheal responses. Animals were pretreated for 5 min with atropine (300 μg kg^{-1}) and for 3 min with [α,β-Me]ATP (300 μg kg^{-1}) prior to dosing with [β-Ala^8]NKA(4–10) (5 μg kg^{-1}). [β-Ala^8]NKA(4–10)-induced bladder responses were abolished by pretreatment with the combination of atropine and [α,β-Me]ATP but tracheal responses were not significantly changed. Traces shown are representative of 5 experiments in different animals. Bladder pressure, continuous line trace; tracheal pressure, shaded trace.

bladder from rats that had been treated with capsaicin as neonates (Carstairs *et al.*, 1993), indicating a possible location on capsaicin-sensitive afferent nerve terminals. Activation of these neuronal NK_2 receptors *in vivo* may underlie the stimulation of the micturition reflex by [β-Ala^8]NKA(4–10) seen in this study.

In a previous study, Maggi and co-workers demonstrated facilitation of reflex micturition by intravesical administration of [β-Ala^8]NKA(4–10), indicating a peripheral site of action (Maggi *et al.*, 1991b). These results were interpreted as reflecting a direct smooth muscle contraction by [β-Ala^8]NKA(4–10) leading to increased afferent discharge by bladder mechanoreceptors. However, a direct stimulant action on capsaicin-sensitive bladder afferent nerves could not be ruled out from this work or in related studies in guinea-pig and rat (Maggi *et al.*, 1987; 1991d; Lecci *et al.*, 1994). Indeed, results with [α,β-Me]ATP, in the present study, indicate that it is possible to induce large amplitude bladder contractions without activating the micturition reflex. Therefore, it is likey that NK_2 receptor-dependent activation of the micturition reflex is not merely a result of bladder smooth muscle contraction but involves an additional site of action. *In vivo* electrophysiological studies will be required to determine whether NK_2 receptor agonists can directly stimulate bladder afferent nerve firing, in the absence of detrusor contraction.

The existence of NKA in capsaicin-sensitive bladder afferent nerves, as well as the presence of receptors for this peptide on the same nerve terminals, raises the possibility of a role for endogenous NKA and NK_2 receptors in the control of reflex micturition. The stimulatory effect of exogenous NK_2 receptor agonists on bladder reflexes suggests that these receptors may play a positive feedback role in the regulation of micturition frequency. In a study in rats, using the selective NK_2 antagonist, SR48968, Lecci and co-workers presented evidence against a role for peripheral NK_2 receptors in the normal control of micturition (Lecci *et al.*, 1993). However, there is evidence from rat studies for a role of NK_2 receptors in bladder hypersensitivity induced by irritants such as xylene (Maggi *et al.*, 1991a; Pietra *et al.*, 1992). Whether the contribution of NK_2 receptors to the control of micturition in guinea-pigs is also restricted to conditions of irritation or inflammation remains to be determined. However, we have found that there are marked species differences in *in vivo* bladder sensitivity to neurokinins, with guinea-pigs more sensitive than rats to [β-Ala^8]NKA(4–10)-induced stimulation of the micturition reflex (unpublished observations). Autoradiographic studies in human bladder indicate the presence of submucosal (presumably neuronal) NK_2 receptors, in addition to those receptor sites located on detrusor smooth muscle (Nimmo *et al.*, 1993). As with rats and guinea-pigs, these receptors may contribute to sensitization of the micturition reflex in conditions of ongoing irritation and may contribute to the pathophysiology of diseases such as cystitis or urinary urge incontinence.

References

ABELLI, L., SOMMA, V,. MAGGI, C.A., REGOLI, D., ASTOLFI, M., PARLANI, M., ROVERO, P., CONTE, B. & MELI, A. (1989). Effects of tachykinins and selective tachykinin antagonists on vascular permeability in the rat lower urinary tract: evidence for involvement of NK_1 receptors. *J. Autonom. Pharmacol.*, **9**, 253–63.

BARNES, P.J. (1986). Asthma as an axon reflex. *Lancet*, **I**, 242–5.

BELVISI, M.G., PATACCHINI, R., BARNES, P.J. & MAGGI, C.A. (1994). Facilitatory effects of selective agonists for tachykinin receptors on cholinergic neurotransmission: evidence for species differences. *Br. J. Pharmacol.*, **111**, 103–110.

BRADING, A.F. & WILLIAMS, J.H. (1990). Contractile responses of smooth muscle strips from rat and guinea-pig urinary bladder to transmural stimulation: effects of atropine and α,β-methylene-ATP. *Br. J. Pharmacol.*, **99**, 493–498.

BUCKNER, C.K., LIBERATI, N., DEA, D., LENGEL, D., STINSON-FISHER, C., CAMPBELL, J., MILLER, S., SHENVI, A. & KRELL, R.D. (1993). Differential Blockade by tachykinin NK_1 and NK_2 receptor antagonists of bronchoconstriction induced by direct-acting agonists and the indirect-acting mimetics capsaicin, serotonin and 2-methyl-serotonin in the anaesthetised guinea-pig. *J. Pharmacol. Exp. Ther.*, **267**, 1168–75.

BURCHER, E. & BUCK, S.B. (1986). Multiple tachykinin binding sites in hamster, rat and guinea-pig urinary bladder. *Eur. J. Pharmacol.*, **128**, 165–177.

BURNSTOCK, G., DUMSDAY, B. & SMYTHE, A. (1972). Atropine-resistant excitation of the urinary bladder: the possibility of transmission via nerves releasing a purine nucleotide. *Br. J. Pharmacol.*, **44**, 451–461.

CARSTAIRS, J.R., MAGGI, C.A., ANDERSSON, P.O. & NIMMO, A.J. (1993). A novel tachykinin NK_2 receptor associated with capsaicin-sensitive afferent nerves in rat bladder. *Neuropeptides*, **24**, 200.

DEVILLIER, P., ADVENIER, L., DRAPEAU, G., MARSAC, J. & REGOLI, D. (1988). Comparison of the effects of epithelium removal and of an enkephalinase inhibitor on the neurokinin-induced contractions of the guinea-pig isolated trachea. *Br. J. Pharmacol.*, **94**, 675–684.

DION, S., ROUISSI, N., NANTEL, G., DRAPEAU, G., REGOLI, D., NALINE, E. & ADVENIER, C. (1990). Receptors for neurokinins in human bronchus and urinary bladder are of the NK_2 type. *Eur. J. Pharmacol.*, **178**, 215–219.

EMONDS-ALT, X., DOUTREMEPUICH, J.-D., HEAULME, M., NELIAT, G., SANTUCCI, V., STEINBERG, R., VILAIN, P., BICHON, D., DUCOUX, J.-P., PROIETTO, V., VAN BROECK, D., SOUBRIE, P., LE FUR, G. & BRELIERE, J.-C. (1993). In vitro and in vivo biological activities of SR140333, a novel potent non-peptide tachykinin NK_1 receptor antagonist. *Eur. J. Pharmacol.*, **250**, 403–413.

EMONDS-ALT, X., VILAIN, P., GOULAOUIC, P., PROIETTO, D., VAN BROECK, D., ADVENIER, C., NALINE, E., NELIAT, G., LE FUR, G. & BRELIERE, J.-C. (1992). A potent and selective antagonist of the neurokinin A (NK_2) receptor. *Life Sci.*, **50**, PL101–106.

FALCONIERI-ERSPAMER, G.L., NEGRI, L. & PICCINELLI, D. (1973). The use of preparations of urinary bladder smooth muscle for bioassay of and discrimination between polypeptides. *Naunyn-Schmied. Arch. Pharmacol.*, **279**, 61–74.

FROSSARD, N. & ADVENIER, C. (1991). Tachykinin receptors and the airways. *Life Sci.*, **49**, 1941–1953.

FROSSARD, N., RHODEN, K.J. & BARNES, P.J. (1989). The influence of epithelium in the guinea-pig airway response to tachykinins: role of endopeptidase and cyclooxygenase. *J. Pharmacol. Exp. Ther.*, **248**, 292–298.

FUJII, K. (1988). Evidence for ATP as an excitatory transmitter in guinea-pig, rabbit and pig urinary bladder. *J. Physiol.*, **404**, 39–52.

GIULIANI, S., PATACCHINI, R., BARBANTI, G., TURINI, D., ROVERO, P., QUARTARA, L., GIACHETTI, A. & MAGGI, C.A. (1993). Characteristics of the tachykinin NK_2 receptor in the human urinary bladder by means of selective neurokinin antagonists and peptidase inhibitors. *J. Pharmacol. Exp. Ther.*, **267**, 590–595.

HALL, A.K., BARNES, P.J., MELDRUM, L.A. & MACLAGAN, J. (1989). Facilitation by tachykinins of neurotransmission in guinea-pig pulmonary nerves. *Br. J. Pharmacol.*, **97**, 274–280.

HALL, J.M., FLOWERS, J.M. & MORTON, I.K.M. (1992). A pharmacological study of NK_1 and NK_2 tachykinin receptor characteristics in the rat isolated urinary bladder. *Br. J. Pharmacol.*, **107**, 777–784.

HOLZER, P., BUCSICS, A. & LEMBECK, F. (1982). Distribution of capsaicin-sensitive nerve fibres containing immunoreactcive substance P in cutaneous and visceral tissues of the rat. *Neurosci. Lett.*, **31**, 253–257.

IRELAND, S.J., BAILEY, F., COOK, A., HAGAN, R.M., JORDAN, C.C. & STEPHANS-SMITH, M.L. (1991). Receptors mediating tachykinin-induced contractile responses in the guinea-pig trachea. *Br. J. Pharmacol.*, **103**, 1463–1469.

JOOS, G.F., KIPS, J., PAUWELS, R. & VAN DER STRAETEN, M. (1986). The effect of tachykinins on the conducting airways of the rat. *Arch. Int. Pharmacodyn.*, **280**, suppl, 176–190.

JOOS, G.F. & PAUWELS, R.A. (1990). Mechanisms involved in neurokinin-induced bronchoconstriction. *Arch. Int. Pharmacodyn.*, **303**, 132–146.

KASAKOV, L. & BURNSTOCK, G. (1983). The use of the slowly degrading analogue α,β-methylene ATP to produce desensitisation of the P_2-purinoreceptor: effect on non-adrenergic non-cholinergic responses of the guinea-pig urinary bladder. *Eur. J. Pharmacol.*, **86**, 291–294.

LECCI, A., GIULIANI, S., MEINI, S. & MAGGI, C.A. (1994). In vivo effects of neurokinin B on rat urinary bladder motility: involvement of tachykinin NK_1 and NK_2 receptors. *Neuropeptides*, **27**, 53–62.

LECCI, A., GIULIANI, S., PATACCHINI, R. & MAGGI, C.A. (1993). Evidence against a peripheral role of tachykinins in the initiation of micturition reflex in rats. *J. Pharmacol. Exp. Ther.*, **264**, 1327–1332.

LONGMORE, J. & HILL, R.G. (1992). Characterisation of NK receptors in guinea-pig urinary bladder smooth muscle: use of selective antagonists. *Eur. J. Pharmacol.*, **222**, 167–170.

LUNDBERG, J.M., HOKFELT, T., MARTLING, C.R., SARIA, A. & CUELLO, C. (1984). Substance P-immunoreactive sensory nerves in the lower respiratory tract of various mammals including man. *Cell Tissue Res.*, **235**, 251–261.

LUNDBERG, J.M. & SARIA, A. (1986). Polypeptide-containing neurones in airway smooth muscle. *Annu. Rev. Pharmacol.*, **49**, 557–572.

MAGGI, C.A., GIULIANI, S., BALLATI, R., LECCI, A., MANZINI, S., PATACCHINI, R., RENZETTI, A.R., ROVERO, P., QUARTARA, L. & GIACHETTI, A. (1991a). In vivo evidence for tachykinergic transmission using a new NK_2 receptor-selective antagonist MEN-10376. *J. Pharmacol. Exp. Ther.*, **257**, 1172–1178.

MAGGI, C.A., GIULIANI, S,. SANTICIOLI, P., ABELLI, L. & GIACHETTI, A. (1991b). Facilitation of reflex micturition by intravesical administration of [β-Ala^8]NKA(4–10), a selective NK_2 tachykinin receptor agonist. *J. Urol.*, **145**, 184–187.

MAGGI, C.A., GIULIANI, S., SANTICIOLI, P., ABELLI, L., REGOLI, D. & MELI, A. (1987). Further studies on the mechanism responsible for the tachykinin-induced activation of reflex micturition: evidence for the involvement of the capsaicin-sensitive bladder mechanoreceptors. *Eur. J. Pharmacol.*, **136**, 189–205.

MAGGI, C.A., PARLANI, M., ASTOLFI, M., SANTICIOLI, P., ROVERO, P., ABELLI, L., SOMMA, V., GIULIANI, S., REGOLI, D., PATACCHINI, R. & MELLI, A. (1988). Neurokinin receptors in rat lower urinary tract. *J. Pharmacol. Exp. Ther.*, **246**, 308–315.

MAGGI, C.A., PATACCHINI, R., QUARTARA, L., ROVERO, P. & SANTICIOLI, P. (1991c). Tachykinin receptors in the guinea-pig isolated bronchi. *Eur. J. Pharmacol.*, **197**, 167–174.

MAGGI, C.A., PATACCHINI, R., SANTICIOLI, P. & GIULIANI, S. (1991d). Tachykinin antagonists and capsaicin-induced contraction of the rat isolated urinary bladder: evidence for tachykinin-mediated cotransmission. *Br. J. Pharmacol.*, **103**, 1535–1541.

MANZINI, S. (1993). Antagonists of NK_2 tachykinin receptors as a potential new class of antibronchospastic agents. *Gen. Pharmacol.*, **25**, 1–6.

METCALFE, M., BUSHFIELD, M., NAYLOR, A.M. & TEMPLETON, D. (1994). Tachykinin-activated bladder contractions in the anaesthetised guinea-pig. *Br. J. Pharmacol.*, **112**, 563P.

NIMMO, A.J., ANDERSSON, P.O., CHAPPLE, C.R. & CARSTAIRS, J.R. (1993). The autoradiographic localisation of neurokinin binding sites in human urinary bladder. *Neuropeptides*, **24**, 237.

PALEA, S., DALFORNO, G., GAVIRAGHI, G., HAGAN, R.M., TRIST, D.G. & PIETRA, C. (1993). Further studies on the effects of selective neurokinin agonists upon the activation of micturition reflex in rats. Evidence for a dual NK_1 receptor mediated excitatory and inhibitory activity. *Neuropeptides*, **24**, 285–291.

PIETRA, C., BETTELINI, L., HAGAN, R.M., WARD, P., MCELROY, A. & TRIST, D.G. (1992). Effects of selective antagonists as tachykinin NK_1 and NK_2 receptors on xylene-induced cystitis in rats. *Neuropeptides*, **22**, 52.

POLAK, J.M. & BLOOM, S.R. (1982). Regulatory peptides and neurone-specific enolase in the respiratory tract of man and other mammals. *Exp. Lung Res.*, **3**, 313–328.

ROGERS, D.F., BELVISI, M.G., AURSUDKIJ, B., EVANS, T.W. & BARNES, P.J. (1988). Effects and interactions of sensory neuropeptides on airway microvascular leakage in guinea-pigs. *Br. J. Pharmacol.*, **95**, 1109–1116.

ROVERO, P., PESTELLINI, V., RHALEB, N.-E., DION, S., ROUISSI, N., TOUSIGNANT, C., TELEMAQUE, S., DRAPEAU, G. & REGOLI, D. (1989). Structure-activity studies of neurokinin A. *Neuropeptides*, **13**, 263–270.

SU, H.C., WHARTON, J., POLAK, J.M., MULDERRY, P.K., GHATEI, M.A., GIBSON, G., TERENGHI, G., MORRISON, J.F.B., BALLESTA, J. & BLOOM, S.R. (1986). Calcitonin gene-related peptide immunoreactivity in afferent neurones supplying the urinary tract: combined retrograde tracing and immunochemistry. *Neurosci.*, **18**, 727–747.

WATSON, N., MACLAGAN, J. & BARNES, P.J. (1993). Endogenous tachykinins facilitate transmission through parasympathetic ganglia in guinea-pig trachea. *Br. J. Pharmacol.*, **109**, 751–759.

(Received January 12, 1995
Revised March 2, 1995
Accepted March 22, 1995)

British Journal of Pharmacology (1995) 115, 883-888 © 1995 Stockton Press All rights reserved 0007-1188/95 $12.00

Pharmacological activity of the C-terminal and N-terminal domains of secretory leukoprotease inhibitor *in vitro*

[1]Ken-ichi Masuda, Takashi Kamimura, Kunihito Watanabe, Tetsuya Suga, Masaharu Kanesaki, Akiko Takeuchi, Atsushi Imaizumi & Yoji Suzuki

Institute for Biomedical Research, Teijin Limited, 4-3-2 Asahi-ga-oka, Hino, Tokyo 191, Japan

1 In order to characterize the physiological functions of the domain structure of secretory leukoprotease inhibitor (SLPI), the biological capacities of half-length SLPIs, (Ser1-Pro54)SLPI and (Asn55-Ala107)SLPI, were investigated and compared with those of full-length SLPI.

2 The activities of these inhibitors against several serine proteases were determined using synthetic chromogenic substrates. The inhibitory capacity of the C-terminal domain, (Asn55-Ala107)SLPI, was as strong as that of full-length SLPI against human neutrophil elastase (NE), cathepsin G and chymotrypsin. It possessed less trypsin inhibitory activity than intact SLPI. For the N-terminal domain of SLPI, (Ser1-Pro54)SLPI, no inhibitory activity could be detected against the serine proteases tested in this study.

3 The inhibitory activity of (Asn55-Ala107)SLPI against the proteolysis of the natural substrates elastin and collagen by NE was comparable with that of full-SLPI (elastin, $IC_{50}=907\pm31$ nM for SLPI, 767 ± 33 nM for (Asn55-Ala107)SLPI; collagen, $IC_{50}=862\pm36$ nM for SLPI, 727 ± 47 nM for (Asn55-Ala107)SLPI).

4 The binding affinities of full- and half-length SLPIs for heparin were measured by affinity column chromatography. Full-length SLPI showed high affinity for heparin while the binding capacities of both half-length SLPIs were lower. (Concentration of NaCl for elution, 0.45 M for SLPI, 0.24 M for (Ser1-Pro54)SLPI, 0.27 M for (Asn55-Ala107)SLPI).

5 The effects of full-SLPI and (Asn55-Ala107)SLPI on blood coagulation were measured using the activated partial thromboplastin time (APTT). Full-length SLPI prolonged clotting time dose-dependently (1.25, 2.5 and 5.0 μM), whereas (Asn55-Ala107)SLPI had no effect even at the highest concentration.

6 In conclusion, the C-terminal domain of SLPI is a promising candidate for the treatment of inflammatory diseases in which participation of neutrophil proteases has been suggested.

Keywords: Secretory leukoprotease inhibitor (SLPI); domain structure; neutrophil protease; anti-protease; respiratory disease

Introduction

An imbalance between neutrophil proteases and anti-proteases is a possible mechanism for the origin of destructive lung diseases (Cohen *et al.*, 1983; Janoff, 1985). Neutrophil elastase (NE) is a lysosomal serine protease which is thought to be responsible for lung tissue degradation (Campbell *et al.*, 1987). NE attacks the extracellular matrix of the respiratory tract and degrades elastin (Boudier *et al.*, 1981), collagen (Mainardi *et al.*, 1980), fibronectin (McDonald *et al.*, 1980) and proteoglycans (Keiser *et al.*, 1976). Studies of the role of proteases in pulmonary diseases such as emphysema and cystic fibrosis have focused on NE (Snider *et al.*, 1984; Meyer *et al.*, 1991). The possible participation of cathepsin G in inflammation has also been reported. Cathepsin G enhances the activity of NE (Boudier *et al.*, 1981) and degrades cartilage matrix proteoglycan (Janusz & Doherty, 1991). Human plasma α_1-proteinase inhibitor, also known as α_1-antitrypsin, is a physiological inhibitor of these proteases (Beatty *et al.*, 1980) and its exogenous administration has been proposed as a therapeutic weapon to arrest or delay tissue destruction (Wewers *et al.*, 1987; Crystal *et al.*, 1989).

Secretory leukoprotease inhibitor (SLPI), also known as antileukoprotease, is another promising candidate for the treatment of diseases in which NE and cathepsin G could be involved (Travis & Fritz, 1991). It is a 107-residue, non-glycosylated serine protease inhibitor which inhibits a wide-range of proteases including NE, cathepsin G, chymotrypsin and trypsin (Smith & Johnson, 1985; Thompson & Ohlson, 1986). It has been reported to be widely distributed in submucosal glands (Franken *et al.*, 1989). In the respiratory tract, SLPI is produced by serous glandular cells in the central airways and by clara and goblet cells in the peripheral airways (Kramps *et al.*, 1981; De Water *et al.*, 1986). Recent studies have also demonstrated secretion of SLPI by type II pneumocyte cell lines (Sallenave *et al.*, 1993). The exact physiological function of SLPI is not clear, but its major role is thought to be protection of the airway epithelial surface from attack by neutrophil proteases (Vogelmeier *et al.*, 1991; Piccioni *et al.*, 1992). X-ray crystallographic analysis has shown that SLPI comprises two separate domains of similar architecture (Grütter *et al.*, 1988). Investigations into the relationship between the anti-protease activity of SLPI and its domain structures have demonstrated that inhibitory activity against NE, chymotrypsin and trypsin is located in the C-terminal domain (Stetler *et al.*, 1989; Meckelein *et al.*, 1990; Kramps *et al.*, 1990). We have also found recently that a recombinant half-sized SLPI containing the C-terminal domain, (Asn55-Ala107)SLPI, is as active an inhibitor as full-length SLPI against NE and cathepsin G (Masuda *et al.*, 1992; Renesto *et al.*, 1993). However, the inhibitory activity of the N-terminal domain has not been investigated quantitatively and the exact functions of the two domains have yet to be fully elucidated. It would be interesting to determine the physiological role of each domain.

In this study, we first investigated the inhibitory activities of (Ser1-Pro54)SLPI, (Asn55-Ala107)SLPI and full-length SLPI against several serine proteases using various synthetic chromogenic substrates. The inhibitory capacity of the activity-

[1] Author for correspondence.

retaining half-length SLPI, (Asn55-Ala107)SLPI, against the proteolysis of natural substrates by NE was further tested and compared with that of full-length SLPI. We then investigated the heparin-binding affinities of these inhibitors and examined the effects of (Asn55-Ala107)SLPI and intact SLPI on blood coagulation *in vitro* in order to explore the possibility of intravenous administration.

Methods

Enzymes and substrates

Human neutrophil elastase (NE) and cathepsin G were purchased from Elastin Products Co. (Owensville, MO, U.S.A.). Bovine pancreatic trypsin and chymotrypsin, as well as human plasma thrombin and plasmin, were from Sigma Chemical Co. (St Louis, MO, U.S.A.). Human plasma kallikrein was obtained from Protogen AG (Laufelfingen, Switzerland) and bovine factor Xa (FXa) was purchased from New England Biolabs Inc. (Beverly, MA, U.S.A.). The following synthetic substrates were used: methoxy succinyl-Ala-Ala-Pro-Val-4-nitroanilide (MeO-Suc-Ala-Ala-Pro-Val-pNA) for NE, benzoyl-Arg-4-nitroanilide (Bz-Arg-pNA) for trypsin, succinyl-Ala-Ala-Pro-Phe-4-nitroanilide (Suc-Ala-Ala-Pro-Phe-pNA) for chymotrypsin and succinyl-Phe-Pro-Phe-4-nitroanilide (Suc-Phe-Pro-Phe-pNA) for cathepsin G were obtained from Bachem Feinchemikalien AG (Bubendorf, Switzerland), while D-Phe-pipecolyl-Arg-4-nitroanilide (D-Phe-Pip-Arg-pNA) for thrombin, D-Val-Leu-Lys-4-nitroanilide (D-Val-Leu-Lys-pNA) for plasmin, D-Pro-Phe-Arg-4-nitroanilide (D-Pro-Phe-Arg-pNA) for kallikrein and benzoyl-Ile-Glu-Gly-Arg-4-nitroanilide (Bz-Ile-Glu-Gly-Arg-pNA) for FXa were purchased from Kabi Vitrum (Stockholm, Sweden).

Production of recombinant full- and half-length SLPIs

DNA fragments encoding the amino acids 1-107, 1-54 and 55-107 of SLPI (Thompson & Ohlson, 1986) were synthesized chemically using appropriate codons from *E.coli*. The human growth hormone gene was fused to the genes for full- and half-length SLPIs to optimize the expression size via a DNA sequence encoding Leu-Val-Pro-Arg, which can be cleaved by thrombin (Ikehara *et al.*, 1984; Masuda *et al.*, 1992). The expression vectors were constructed and introduced into *E. coli* HB101, the transformed cells were selected by ampicillin and cultured; then the fusion proteins were obtained as inclusion bodies. The fusion proteins were dissolved and cleaved with thrombin, and the full- and half-length SLPIs were purified by chromatography after refolding.

Inhibition assay using synthetic chromogenic substrates

(1) *Fifty percent inhibitory concentration* (IC_{50}). The reaction buffer used throughout this experiment was 0.1 M HEPES (pH 7.5), containing 0.5 M NaCl. The required inhibitor solution was preincubated for 10 min at 37°C in a total volume of 160 µl with appropriate amounts of the required enzyme. The reaction was started by adding 20 µl substrate and carried out for 20 min at 37°C. The light absorbance of the reaction mixture at 405 nm was measured. Residual enzyme activities were plotted for various concentrations of inhibitor and the IC_{50} was determined.

(2) *Inhibition constants* (K_i values). The substrates were 0.3 mM MeO-Suc-Ala-Ala-Pro-Val-pNA for NE and 1.0 mM Bz-Arg-pNA for bovine pancreatic trypsin, and the reaction buffer used for both enzymes was 0.1 M HEPES, containing 1.0 M NaCl, 0.1% (w/v) PEG-6000, pH 7.5. The required inhibitor solution was preincubated for 1 h at 25°C (total volume 160 µl) with appropriate amounts of the required enzyme, 20 nM elastase and 200 nM trypsin. The reactions were started by adding 20 µl substrate and carried out for 20 min at 25°C. The absorbance of the reaction mixture at 405 nm was recorded and the inhibition constants were determined (Henderson, 1972).

Proteolysis of elastin

Elastolysis was monitored by measuring the absorbance at 280 nm. The absorption of the soluble peptides resulting from the enzymatic digestion of elastin is due to desmosin and isodesmosin (Boudier *et al.*, 1981). The required inhibitor solution (0.9 ml) in 50 mM Tris buffer, pH 8.0, was added to 3.0 mg bovine ligament elastin (Sigma Chemical Company, St Louis, Missouri, U.S.A.). Elastolysis was started by adding 100 µl NE (final concentration, 0.5 µM) and the suspension was incubated for 2 h at 37°C; 400 µl of the continuously stirred suspension was removed and added to 15 µl 3 M acetate buffer, pH 4.5, in order to stop the reaction. After centrifuging at 4000 *g* for 15 min, the absorbances of the supernatants were read at 280 nm. Results were expressed as the percentage of enzymatic activity in controls without inhibitor.

Proteolysis of collagen

The required inhibitor solution (180 µl) in 50 mM Tris buffer, pH 7.5, containing 100 mM NaCl and 2.5 mM $CaCl_2$, was added to 50 µg bovine type I collagen labelled with fluorescein 5-isothiocyanate (FITC) (COSMO BIO Corp., Tokyo, Japan). The degradation of collagen was started by adding 20 µl NE (final concentration, 1 µM) and the reaction mixture was incubated for 3 h at 37°C; 200 µl of 50 mM Tris buffer, pH 9.5, containing 50% (v/v) ethanol was added in order to stop the reaction and precipitate intact collagen. After centrifugation at 4000 *g* for 15 min, the fluorescence of the supernatants, including denatured collagen, was detected with emission at 520 nm and excitation at 495 nm. Results were expressed as the percentage of enzymatic activity in controls without inhibitor.

Heparin-affinity chromatography

A mixture of full- and half-length SLPIs (20 µg) dissolved in 20 mM Tris buffer (pH 7.5) was applied to a TSK-gel Heparin-5PW column (7.5 mm × 7.5 cm, TOSOH Corp., Tokyo, Japan) and elution was carried out over 30 min with a gradient of 0–0.7 M NaCl in 20 mM Tris buffer, pH 7.5, at a flow rate of 1.0 ml min^{-1}. The effluent was monitored by measuring the absorbance at 215 nm.

Blood coagulation assay

Blood coagulation was assayed by a modification of the activated partial thromboplastin time (APTT) test (Fulcher & Zimmerman, 1982). The required inhibitor solution (20 µl) was preincubated with 100 µl activated partial thromboplastin (Sysmex SAP-20,Toa Medical Electronics Co., Kobe, Japan), 100 µl normal plasma and 100 µl FVIII-deficient plasma (George King Bio-Medical, Overland Park, KS, U.S.A.) for 2 min at 37°C. The coagulation assay was started by adding 100 µl 20 mM $CaCl_2$. The final concentrations of inhibitors were 1.25, 2.5 and 5.0 µM. The time required for clot formation was recorded using a blood coagulation analyser (Sysmex CA-100, Toa Medical Electronics Co., Kobe, Japan).

Results

Inhibition of enzymatic activity of serine proteases

We first evaluated the capacity of half-length SLPIs to inhibit the enzymatic activities of purified serine proteases, using synthetic chromogenic substrates. The inhibitory activity (IC_{50}) of (Asn55-Ala107)SLPI against elastase, cathepsin G and chymotrypsin was as strong as that of intact SLPI, but it

Table 1 Fifty percent inhibitory concentrations (IC_{50}) of SLPI and (Asn55-Ala107)SLPI against serine proteases

Enzyme (concentration; M)	*50% inhibitory concentration (M)* SLPI	(Asn55-Ala107)SLPI
NE (2.0×10^{-8})	1.0×10^{-8}	1.1×10^{-8}
Human cathepsin G (2.0×10^{-8})	5.5×10^{-9}	7.2×10^{-9}
Bovine pancreatic chymotrypsin (1.0×10^{-8})	1.0×10^{-8}	1.2×10^{-8}
Bovine pancreatic trypsin (2.0×10^{-7})	3.3×10^{-7}	2.3×10^{-6}
Human plasma thrombin (3.0×10^{-9})	$> 1.0 \times 10^{-5}$	$> 1.0 \times 10^{-5}$
Human plasma plasmin (1.0×10^{-7})	$> 1.0 \times 10^{-5}$	$> 1.0 \times 10^{-5}$
Human plasma kallikrein (1.0×10^{-8})	$> 1.0 \times 10^{-5}$	$> 1.0 \times 10^{-5}$
Bovine plasma FXa (1.0×10^{-8})	$> 1.0 \times 10^{-5}$	$> 1.0 \times 10^{-5}$

Assay conditions; 0.1 M HEPES (pH 7.5), 0.5 M NaCl, 37°C
Chromogenic substrates: NE, 0.3 mM MeO-Suc-Ala-Ala-Pro-Val-pNA; cathepsin G, 1.0 mM Suc-Phe-Pro-Phe-pNA; chymotrypsin, 1.0 mM Suc-Ala-Ala-Pro-Phe-pNA; trypsin, 1.0 mM Bz-Arg-pNA; thrombin, 0.2 mM D-Phe-Pip-Arg-pNA; plasmin, 0.8 mM D-Val-Leu-Lys-pNA; kallikrein, 2.0 mM D-Pro-Phe-Arg-pNA; FXa, 0.5 mM Bz-Ile-Glu-Gly-Arg-pNA.

Table 2 Inhibition constants (K_i values) of SLPI and (Asn55-Ala107)SLPI against neutrophil elastase (NE) and bovine pancreatic trypsin

Enzyme	K_i *value (M)* SLPI	(Asn55-Ala107)SLPI
NE	0.8×10^{-10}	1.2×10^{-10}
Bovine pancreatic trypsin	3.3×10^{-8}	1.0×10^{-6}

Assay conditions; 0.1 M HEPES (pH 7.5), 1.0 M NaCl, 0.1% (w/v) PEG-6000, 25°C
Chromogenic substrates: NE, 0.3 mM MeO-Suc-Ala-Ala-Pro-Val-pNA; trypsin, 1.0 mM Bz-Arg-pNA.

possessed less trypsin inhibitory activity than intact SLPI, and neither of the inhibitors showed any inhibitory activity against thrombin, plasmin, kallikrein or FXa (Table 1). No inhibitory activity of the N-terminal domain, (Serl-Pro54)SLPI (final concentration, 10 μM), could be detected against the serine proteases shown in Table 1. The inhibition constants (K_i values) of (Asn55-Ala107)SLPI and SLPI against NE and bovine pancreatic trypsin were determined. The K_i value of (Asn55-Ala107)SLPI for NE was comparable with that of intact SLPI but its trypsin inhibitory activity was reduced (Table 2). The C-terminal domain was more specific for NE than trypsin, compared with SLPI itself.

Inhibition of the proteolysis of elastin and collagen by NE

Since (Serl-Pro54)SLPI did not inhibit enzymatic activity, we investigated only the effects of SLPI and (Asn55-Ala107)SLPI on the proteolysis of the natural substrates, bovine elastin and type I collagen. All experiments were carried out without preincubation of NE and the inhibitors. Proteolysis was started by adding NE to the mixture of inhibitor and substrate described in Methods. SLPI effectively inhibited the degradation of elastin (Figure 1a) and collagen (Figure 2a), the active concentrations ranged from 0.5–2.0 μM. The IC_{50} of SLPI was 907±31 nM for elastin and 862±36 nM for collagen. The same effect was obtained with (Asn55-Ala107)SLPI, which inhibited the proteolysis of elastin (Figure 1b) and collagen (Figure 2b), IC_{50} values being 767±33 nM and 727±47 nM, respectively. The C-terminal domain of SLPI was therefore as active in inhibiting the proteolysis of natural substrates as the parent SLPI.

Heparin-binding affinities of full- and half-length SLPIs

The binding capacities of full- and half-length SLPIs for heparin were investigated by heparin-conjugate affinity chromatography, and the elution pattern of the inhibitors is shown in Figure 3. This chromatography showed that (Serl-Pro54)SLPI, (Asn55-Ala107)SLPI and SLPI bind to the matrix in 20 mM Tris buffer, pH 7.5, and elute with 0.24, 0.27 and 0.45 M NaCl, respectively. SLPI showed high affinity for heparin as has been

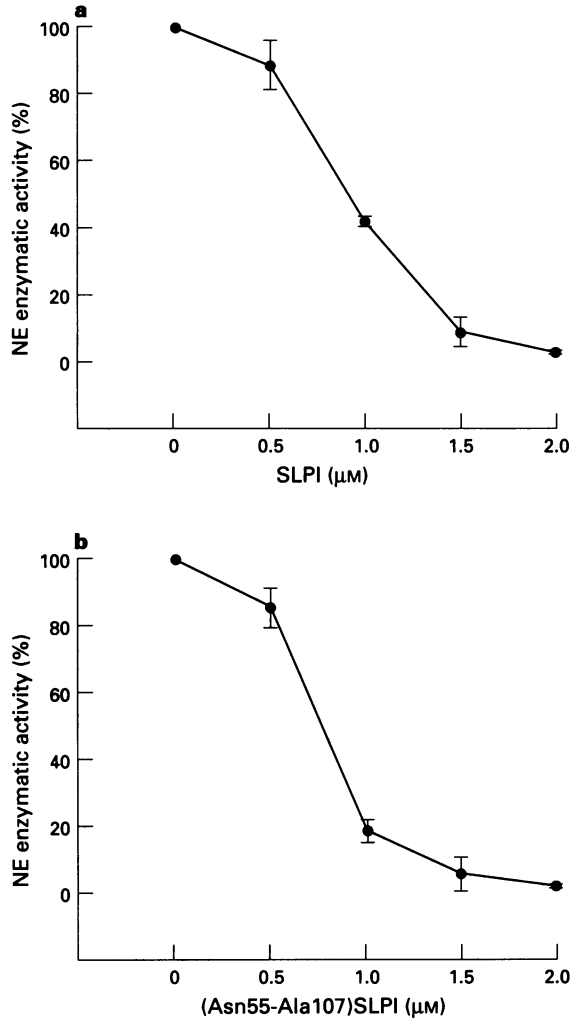

Figure 1 Inhibition of the proteolysis of bovine ligament elastin by SLPI (a) and (Asn55-Ala107)SLPI (b). Increasing concentrations of inhibitors were incubated for 2 h at 37°C in 50 mM Tris buffer (pH 8.0) in the presence of elastin (3 mg) and 0.5 μM neutrophil elastase (NE). Enzymatic activity was measured by reading the absorbance of the supernatant at 280 nm. Results are expressed as the percentage activity compared with controls without inhibitor. Each point is the mean±s.d. of 3 separate experiments.

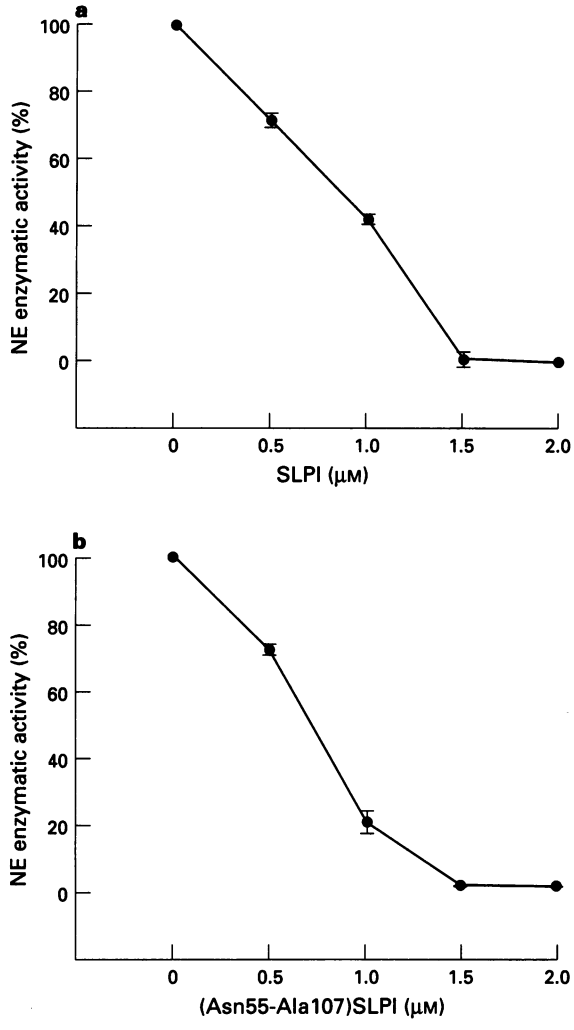

Figure 2 Inhibition of the proteolysis of bovine type I collagen by SLPI (a) and (Asn55-Ala107)SLPI (b). Increasing concentrations of inhibitors were incubated for 3 h at 37°C in 50 mM Tris buffer (pH 7.5) in the presence of FITC-labelled collagen (50 μg) and 1.0 μM neutrophil elastase (NE). Enzymatic activity was measured by reading the fluorescence of the supernatant with emission at 520 nm and excitation at 495 nm. Results are expressed as the percentage activity compared with controls without inhibitor. Each point is the mean ± s.d. of 3 separate experiments.

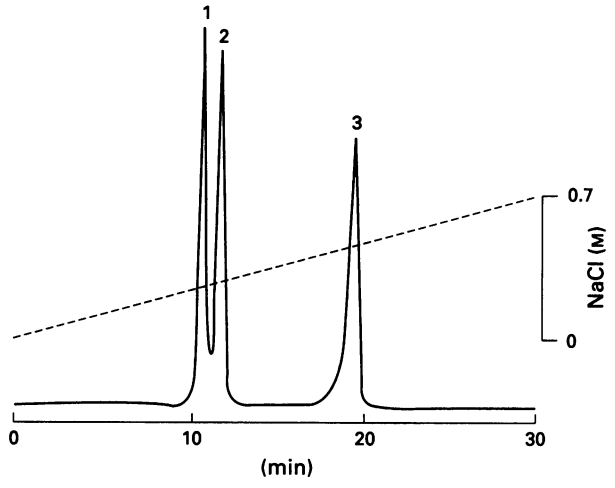

Figure 3 Heparin-affinity chromatography of full- and half-length SLPIs. A mixture of inhibitors dissolved in 20 mM Tris buffer (pH 7.5) was loaded onto a TSK-gel Heparin-5PW column. Elution was carried out over 30 min with a gradient of 0–0.7 M NaCl in 20 mM Tris buffer (pH 7.5) and the effluent was monitored at 215 nm. Peaks 1, 2 and 3 correspond to (Serl-Pro54)SLPI, (Asn55-Ala107)SLPI and SLPI, respectively.

Table 3 Effects of SLPI and (Asn55-Ala107)SLPI on blood coagulation

	APTT (s)
Control (no inhibitor)	105.1 ± 1.0
SLPI (1.25 μM)	162.0 ± 10.0*
SLPI (2.5 μM)	220.2 ± 10.4*
SLPI (5.0 μM)	361.7 ± 80.2*
(Asn55-Ala107)SLPI (1.25 μM)	102.9 ± 1.3
(Asn55-Ala107)SLPI (2.5 μM)	103.3 ± 3.4
(Asn55-Ala107)SLPI (5.0 μM)	107.7 ± 4.2

Inhibitors were preincubated for 2 min at 37°C with activated partial thromboplastin and human plasma (total volume 320 μl). The clotting time was measured after adding 100 μl 20 mM $CaCl_2$. Results are expressed as means ± s.d. of 3 distinct experiments. *$P < 0.05$ significant versus control.

previously described (Faller *et al.*, 1992). Both half-length SLPIs had reduced binding affinity for heparin compared with intact SLPI.

Effects of (Asn55-Ala107)SLPI and SLPI on blood coagulation

The effects of (Asn55-Ala107)SLPI and SLPI on blood coagulation were measured by the APTT test and the results are shown in Table 3. A dose-dependent inhibitory effect on coagulation was observed and APTT was significantly prolonged with 1.25, 2.5 and 5.0 μM SLPI (final concentrations). On the other hand, (Asn55-Ala107)SLPI showed no effect on APTT under the same conditions.

Discussion

SLPI is generally considered to play a defensive role at the respiratory epithelial surface and has a variety of physiological functions that protect the respiratory tissue matrix. These include: (a) inhibitory activity against a wide range of proteases (Smith & Johnson, 1985; Thompson & Ohlsson, 1986); (b) association with elastin fibres in the extracellular matrix of the human lung (Kramps *et al.*, 1989) and inhibition of proteolysis of elastin and fibronectin at the neutrophil-matrix interface (Rice & Weiss, 1990); (c) augmentation of glutathione, a major component of anti-oxidants, in lung epithelial lining fluid (Gillissen *et al.*, 1993) and (d) heparin-induced activation (Faller *et al.*, 1992). It is interesting to speculate upon the relationships between these biological functions and domain structure; however, little is known about the exact roles of the N-and C-terminal domains.

It has been postulated, in view of sequence similarities with the active site of Kazal inhibitors, that the N-terminal domain is active against trypsin whereas the C-terminal domain is active against elastase (Thompson & Ohlsson, 1986). However, further investigations into the relationship between SLPI's domain structure and its anti-protease activity have demonstrated that the inhibitory activities against NE, chymotrypsin and trypsin are all located in the C-terminal domain (Stetler *et al.*, 1989; Kramps *et al.*, 1990). Only weak activity against trypsin has been reported for the recombinant N-terminal domain, which was not completely purified (Meckelein *et al.*, 1990), but its activity has not been studied quantitatively. Our results demonstrate that the C-terminal domain, (Asn55-Ala107)SLPI, is as active in inhibiting NE, cathepsin G and chymotrypsin as the parent SLPI, and shows less trypsin inhibitory activity than intact SLPI. Indeed, the inhibitory ca-

pacity of (Asn55-Ala107)SLPI against the proteolysis of the natural substrates elastin and collagen by NE was as strong as that of full-SLPI. No inhibitory activity of the N-terminal domain, (Serl-Pro54)SLPI, could be detected even at concentrations 100 times greater than those of the proteases. These data suggest that all active inhibitory sites are located in the C-terminal domain and that the N-terminal domain plays only a co-operative role in inhibiting trypsin.

The binding capacity of SLPI for elastin and heparin is important for physiological and therapeutic reasons, but the binding region has not been clearly defined. We have demonstrated that the heparin-binding affinities of both the half-sized SLPIs, (Serl-Pro54)SLPI and (Asn55-Ala107)SLPI, are reduced compared with intact SLPI. We therefore speculate that the three-dimensional structure is critical in conferring high affinity for heparin and this finding may suggest considerations for the pharmacokinetics of SLPI derivatives.

Recombinant SLPI is being tested as a potential anti-elastase drug for the treatment of destructive lung diseases (Lucey *et al.*, 1990; Rudolphus *et al.*, 1991). It has been reported that aerosol administration of SLPI to sheep enhances the anti-NE capacity of the lung (Vogelmeier *et al.*, 1990). However, intravenous administration of the anti-protease might be more effective than inhalation for the treatment of severe destructive lung diseases in which airway obstruction occurs. In such patients, hypersecretion of mucus containing an increased number of neutrophils is observed. We have demonstrated that full-length SLPI prolongs blood coagulation *in vitro*, whereas (Asn55-Ala107)SLPI produced no effect on clotting time under the same conditions. We speculate that SLPI might have effects against trypsin-like proteases which function in the coagulation cascade although it is unclear which plasma protease is inhibited by SLPI. Our results suggest that (Asn55-Ala107)SLPI has no effect on APTT in this study because it has less trypsin inhibitory activity than intact SLPI. We suggest on the basis of these results that the C-terminal domain might be more desirable than SLPI for intravenous administration as an anti-elastase therapy.

In conclusion, (Asn55-Ala107)SLPI is a more specific inhibitor of NE and cathepsin G than of trypsin, compared with SLPI, and is as active in inhibiting the proteolysis of elastin and collagen by NE as intact SLPI. Furthermore, (Asn55-Ala107)SLPI had no effect on clotting time while SLPI inhibits blood coagulation. Thus, the C-terminal domain of SLPI could be a promising candidate, and could be administered via a variety of routes, for the treatment of conditions in which neutrophil proteases are involved.

References

BEATTY, K., BIETH, J. & TRAVIS, J. (1980). Kinetics of association of serine proteinases with native and oxidized alpha$_1$-proteinase inhibitor and alpha$_1$-antichymotrypsin. *J. Biol. Chem.*, **255**, 3931–3934.

BOUDIER, C., HOLLE, C. & BIETH, J.G. (1981). Stimulation of the elastinolytic activity of leukocyte elastase by leukocyte cathepsin G. *J. Biol. Chem.*, **256**, 10256–10258.

CAMPBELL, E.J., SENIOR, R.M. & WELGUS, H.G. (1987). Extracellular matrix injury during lung inflammation. *Chest*, **92**, 161–167.

COHEN, A.B. (1983). Supplement: protease and antiproteases in the lung. *Am. Rev. Respir. Dis.*, **127** (part 2), S2–S58.

CRYSTAL, R.G., BRANTLY, M.L., HUBBARD, R.C., CURIEL, D.T., STATES, D.J. & HOLMES, M.D. (1989). The alpha$_1$-antitrypsin gene and its mutations. Clinical consequences and strategies for therapy. *Chest*, **95**, 196–208.

DE WATER, R., WILLEMS, L.N.A., VAN MUIJEN, G.N.P., FRANKEN, C., FRANSEN, J.A.M., DIJKMAN, J.H. & KRAMPS, J.A. (1986). Ultrastructural localization of bronchial antileukoprotease in central and peripheral human airways by a gold-labeling technique using monoclonal antibodies. *Am. Rev. Respir. Dis.*, **133**, 882–890.

FALLER, B., MELY, Y., GERARD, D. & BIETH, J.G. (1992). Heparin-induced conformational change and activation of mucus proteinase inhibitor. *Biochemistry*, **31**, 8285–8290.

FRANKEN, C., MEIJER, C.J.L.M. & DIJKMAN, J.H. (1989). Tissue distribution of antileukoprotease and lysozyme in humans. *J. Histochem. Cytochem.*, **37**, 493–498.

FULCHER, C.A. & ZIMMERMAN, T.S. (1982). Characterization of the human factor VIII procoagulant protein with a heterologous precipitating antibody. *Proc. Natl. Acad. Sci. U.S.A.*, **79**, 1648–1652.

GILLISSEN, A., BIRRER, P., MCELVANEY, N.G., BUHL, R., VOGELMEIER, C., HOYT, R.F., HUBBARD, R.C. & CRYSTAL, R.G. (1993). Recombinant secretory leukoprotease inhibitor augments glutathione levels in lung epithelial lining fluid. *J. Appl. Physiol.*, **75**, 825–832.

GRÜTTER, M.G., FENDRICH, G., HUBER, R. & BODE, W. (1988). The 2.5 Å X-ray crystal structure of the acid-stable proteinase inhibitor from human mucous secretions analysed in its complex with bovine chymotrypsin. *EMBO J.*, **7**, 345–351.

HENDERSON, P.J.F. (1972). A linear equation that describes the steady-state kinetics of enzymes and subcellular particles interacting with tightly bound inhibitors. *Biochem. J.*, **127**, 321–333.

IKEHARA, M., OHTSUKA, E., TOKUNAGA, T., TANIYAMA, Y., IWAI, S., KITANO, K., MIYAMOTO, S., OHGI, T., SAKURAGAWA, Y., FUJIYAMA, K., IKARI, T., KOBAYASHI, M., MIYAKE, T., SHIBAHARA, S., ONO, A., UEDA, T., TANAKA, T., BABA, H., MIKI, T., SAKURAI, A., OISHI, T., CHISAKA, O. & MATSUBARA, K. (1984). Synthesis of a gene for human growth hormone and its expression in *Escherichia coli*. *Proc. Natl. Acad. Sci. U.S.A.*, **81**, 5956–5960.

JANOFF, A. (1985). Elastases and emphysema. Current assessment of the protease-antiproteases hypothesis. *Am. Rev. Respir. Dis.*, **132**, 417–433.

JANUSZ, M.J. & DOHERTY, N.S. (1991). Degradation of cartilage matrix proteoglycan by human neutrophils involves both elastase and cathepsin G. *J. Immunol.*, **146**, 3922–3928.

KEISER, H., GREENWALD, R.A., FEINSTEIN, G. & JANOFF, A. (1976). Degradation of cartilage proteoglycan by human leukocyte granule neutral protease. A model of joint injury. II. Degradation of isolated bovine nasal cartilage proteoglycan. *J. Clin. Invest.*, **57**, 625–632.

KRAMPS, J.A., FRANKEN, C., MEIJER, C.J.L.M. & DIJKMAN, J.H. (1981). Localization of low molecular weight protease inhibitor in serous secretory cells of the respiratory tract. *J. Histochem. Cytochem.*, **29**, 712–719.

KRAMPS, J.A., TE BOEKHORST, A.H.T., FRANSEN, J.A.M., GINSEL, L.A. & DIJKMAN, J.H. (1989). Antileukoprotease is associated with elastin fibers in the extracellular matrix of the human lung. An immunoelectron microscopic study. *Am. Rev. Respir. Dis.*, **140**, 471–476.

KRAMPS, J.A., VAN TWISK, C., APPELHANS, H., MECKELEIN, B., NIKIFOROV, T. & DIJKMAN, J.H. (1990). Proteinase inhibitory activities of antileukoprotease are represented by its second COOH-terminal domain. *Biochim. Biophys. Acta*, **1038**, 178–185.

LUCEY, E.C., STONE, P.J., CICCOLELLA, D.E., BREUER, R., CHRISTENSEN, T.G., THOMPSON, R.C. & SNIDER, G.L. (1990). Recombinant human secretory leukocyte-protease inhibitor: *in vitro* properties, and amelioration of human neutrophil elastase-induced emphysema and secretory cell metaplasia in the hamster. *J. Lab. Clin. Med.*, **115**, 224–232.

MAINARDI, C.L., HASTY, D.L., SEYER, J.M. & KANG, A.H. (1980). Specific cleavage of human type III collagen by human polymorphonuclear leukocyte elastase. *J. Biol. Chem.*, **255**, 12006–12010.

MASUDA, K., IMAIZUMI, A., KAMIMURA, T., WATANABE, K., SUGIYAMA, T., SUZUKI, Y. & OHTSUKA, E. (1992). Expression of the C-terminal domain of secretory leukoprotease inhibitor in *E. coli* as a thrombin-cleavable fusion protein. *Am. Rev. Respir. Dis.*, **145**, A-200.

MCDONALD, J.A. & KELLEY, D.G. (1980). Degradation of fibronectin by human leukocyte elastase. Release of biologically active fragments. *J. Biol. Chem.*, **255**, 8848–8858.

MECKELEIN, B., NIKIFOROV, T., CLEMEN, A. & APPELHANS, H. (1990). The location of inhibitory specificities in human mucus proteinase inhibitor (MPI): separate expression of the COOH-terminal domain yields an active inhibitor of three different proteinases. *Prot. Engineering*, **3**, 215–220.

MEYER, K.C., LEWANDOSKI, J.R., ZIMMERMAN, J.J., NUNLEY, D., CALHOUN, W.J. & DOPICO, G.A. (1991). Human neutrophil elastase and elastase/alpha$_1$-antiprotease complex in cystic fibrosis. *Am. Rev. Respir. Dis.*, **144**, 580–585.

PICCIONI, P.D., KRAMPS, J.A., RUDOLPHUS, A., BULGHERONI, A. & LUISETTI, M. (1992). Proteinase/proteinase inhibitor imbalance in sputum sol phases from patients with chronic obstructive pulmonary disease. Suggestions for a key role played by antileukoprotease. *Chest*, **102**, 1470–1476.

RENESTO, P., BALLOY, V., KAMIMURA, T., MASUDA, K., IMAIZUMI, A. & CHIGNARD, M. (1993). Inhibition by recombinant SLPI and half-SLPI (Asn55-Ala107) of elastase and cathepsin G activities: consequence for neutrophil-platelet cooperation. *Br. J. Pharmacol.*, **108**, 1100–1106.

RICE, W.G. & WEISS, S.J. (1990). Regulation of proteolysis at the neutrophil-substrate interface by secretory leukoprotease inhibitor. *Science*, **249**, 178–181.

RUDOLPHUS, A., KRAMPS, J.A. & DIJKMAN, J.H. (1991). Effect of human antileukoprotease on experimental emphysema. *Eur. Respir. J.*, **4**, 31–39.

SALLENAVE, J.M., SILVA, A., MARSDEN, E. & RYLE, A.P. (1993). Secretion of mucus proteinase inhibitor and elafin by Clara cell and type II pneumocyte cell lines. *Am. J. Respir. Cell Mol. Biol.*, **8**, 126–133.

SMITH, C.E. & JOHNSON, D.A. (1985). Human bronchial leukocyte protease inhibitor. *Biochem. J.*, **225**, 463–472.

SNIDER, G.L., LUCEY, E.C., CHRISTENSEN, T.G., STONE, P.J., CALORE, J.D., CATANESE, A. & FRANZBLAU, C. (1984). Emphysema and bronchial secretory cell metaplasia induced in hamsters by human neutrophil products. *Am. Rev. Respir. Dis.*, **129**, 155–160.

STETLER, G.L., FORSYTH, C., GLEASON, T., WILSON, J. & THOMPSON, R.C. (1989). Secretion of active, full- and half-length human secretory leukocyte protease inhibitor by *Saccharomyces cerevisiae*. *Biotechnology*, **7**, 55–60.

THOMPSON, R.C. & OHLSSON, K. (1986). Isolation, properties, and complete amino acid sequence of human secretory leukocyte protease inhibitor, a potent inhibitor of leukocyte elastase. *Proc. Natl. Acad. Sci. U.S.A.*, **83**, 6692–6696.

TRAVIS, J. & FRITZ, H. (1991). Potential problems in designing elastase inhibitors for therapy. *Am. Rev. Respir. Dis.*, **143**, 1412–1415.

VOGELMEIER, C., BUHL, R., HOYT, R.F., WILSON, E., FELLS, G.A., HUBBARD, R.C., SCHNEBLI, H.-P., THOMPSON, R.C. & CRYSTAL, R.G. (1990). Aerosolization of recombinant SLPI to augment antineutrophil elastase protection of pulmonary epithelium. *J. Appl. Physiol.*, **69**, 1843–1848.

VOGELMEIER, C., HUBBARD, R.C., FELLS, G.A., SCHNEBLI, H.-P., THOMPSON, R.C., FRITZ, H. & CRYSTAL, R.G. (1991). Antineutrophil elastase defense of the normal human respiratory epithelial surface provided by the secretory leukoprotease inhibitor. *J. Clin. Invest.*, **87**, 482–488.

WEWERS, M.D., CASOLARO, M.A., SELLER, S.E., SWAYZE, S.C., MCPHAUL, K.M., WITTES, J.T. & CRYSTAL, R.G. (1987). Replacement therapy for alpha$_1$-antitrypsin deficiency associated with emphysema. *N. Engl. J. Med.*, **316**, 1055–1062.

(Received January 20, 1995
Revised March 20, 1995
Accepted March 23, 1995)

British Journal of Pharmacology (1995) 115, 889–894 © 1995 Stockton Press All rights reserved 0007–1188/95 $12.00

Substance P-induced relaxation and hyperpolarization in human cerebral arteries

Jesper Petersson, [1]*Peter M. Zygmunt, †Lennart Brandt & *Edward D. Högestätt

Department of Neurology, Malmö General Hospital, Malmö, and Departments of *Clinical Pharmacology and †Neurosurgery, Lund University Hospital, S-22185 Lund, Sweden

1 Vascular effects of substance P were studied in human isolated pial arteries removed from 14 patients undergoing cerebral cortical resection.

2 Substance P induced a concentration-dependent relaxation in the presence of indomethacin. No relaxation was seen in arteries where the endothelium had been removed.

3 N^{ω}-nitro-L-arginine (L-NOARG, 0.3 mM) abolished the relaxation in arteries from six patients. The relaxation was only partially inhibited in the remaining eight patients, the reduction of the maximum relaxation being less than 50% in each patient.

4 The L-NOARG-resistant relaxation was abolished when the external K^+ concentration was raised above 30 mM.

5 Substance P caused a smooth muscle hyperpolarization (in the presence of L-NOARG and indomethacin), but only when the artery showed an L-NOARG-resistant relaxation.

6 The results indicate that nitric oxide is an important mediator of endothelium-dependent relaxation in human cerebral arteries. Furthermore, another endothelium-dependent pathway, causing hyperpolarization and vasodilatation, was identified in arteries from more than half the population of patients.

Keywords: Cerebral arteries; hyperpolarization; nitric oxide; relaxation; substance P; vascular endothelium

Introduction

Endothelium-dependent vascular relaxation was first reported more than a decade ago (Furchgott & Zawadzki, 1980). This phenomenon has later been demonstrated in a variety of animal blood vessels (for review, see Angus & Cocks, 1989). Depending on the animal species, vascular bed and stimulus used, different endothelium-dependent mechanisms may account for the relaxation. Nitric oxide (NO) or a NO-containing compound and prostacyclin are established endothelium-derived relaxing factors (Palmer *et al.*, 1987; de Nucci *et al.*, 1988; Myers *et al.*, 1990). The formation of NO from L-arginine by NO-synthase can be blocked by some analogues of L-arginine, such as N^{ω}-nitro-L-arginine (L-NOARG; Mülsch & Busse, 1990), and inhibitors of cyclo-oxygenase can be used to prevent the formation of vasoactive prostanoids. Recently, the existence of a third endothelium-dependent relaxant pathway has been proposed. This is based on observations in different isolated blood vessels of an endothelium-dependent smooth muscle hyperpolarization and relaxation resistant to inhibitors of NO-synthase and cyclo-oxygenase (Nagao & Vanhoutte, 1993).

The L-arginine-NO pathway and endothelium-dependent hyperpolarization have been demonstrated in cerebral arteries from different animals, and may act in concert to reinforce vascular relaxation (Faraci, 1992). Whereas nitric oxide appears to be an important regulator of the cerebral circulation (Faraci, 1993; Iadecola *et al.*, 1994), the role of endothelium-dependent hyperpolarization is unknown. Endothelium dysfunction has been implicated in several cerebrovascular disorders (Faraci, 1993), suggesting that both these systems may be affected by disease.

Endothelium-dependent relaxation has been demonstrated in both peripheral and cerebral arteries from man (see Lüscher & Vanhoutte, 1988; Faraci, 1992). However, only limited information is available regarding the role of NO and smooth muscle hyperpolarization in these responses. In human isolated coronary arteries, it has been suggested that both NO and smooth muscle hyperpolarization contribute to the endothelium-dependent relaxation (Chester *et al.*, 1990; Nakashima *et al.*, 1993). However, no such studies have been performed on cerebral arteries from man. The present study was therefore undertaken to examine the presence of different endothelium-dependent pathways in human pial arteries. In preliminary experiments, substance P (SP) was found to induce a consistent endothelium-dependent relaxation in this artery. Hence, SP was used to elicit endothelial cell activation in the present study.

Methods

Experimental procedure

Pieces of cerebral cortex with adjacent pial arteries were removed *en bloc* from 13 patients with brain tumours undergoing decompressive lobectomy and in one case partial cortical excision due to intractable epilepsy. Electrocoagulation was avoided in the vicinity of the excised vessels. Patient data and the location of the excised arteries are listed in Table 1. All patients were on medication with steroids prior to operation except for patient L (Table 1). The tissue samples were placed in cold Na^+ Krebs solution (for composition, see below) immediately after excision. On arrival at the laboratory, the arteries were dissected and cut into 1–2 mm long ring segments (diameter = 0.4–0.8 mm). The arterial segments were mounted between two parallel steel pins (diameter = 0.1 mm) in 2.5 ml organ baths (Model 5 A, Vågen, Sweden), containing Na^+ Krebs solution of the following composition (mM): NaCl 119, $NaHCO_3$ 15, KCl 4.6, NaH_2PO_4 1.2, $MgCl_2$ 1.2, $CaCl_2$ 1.5 and glucose 11. One of the pins was connected to a displacement device and the other one to a Grass Instruments FT03C force-displacement transducer (Högestätt *et al.*, 1983). The 'isometric wall tension' was recorded on a Grass Instruments model 7 D polygraph (U.S.A.). In the electrophysiological experiments, the vessel segment was mounted in a single-vessel

[1] Author for correspondence.

Table 1 Patient data and location of excised arteries

Patient	*Age*	*Sex*	*Clinical condition*	*Location of tissue (lobe)*
A	73	f	astrocytoma gr. III-IV	occipital right
B	69	f	meningioma	temporal right
C	73	m	astrocytoma gr. III-IV	occipital right
D	55	m	lymfoma	frontal left
E	62	f	astrocytoma gr. III	frontal right
F	76	f	astrocytoma gr. II-III	temporal left
G	69	m	astrocytoma gr. III	frontal right
H	61	m	astrocytoma gr. III-IV	temporal right
I	70	m	astrocytoma gr. III	frontal right
J	42	f	astrocytoma gr. IV	frontal left
K	59	m	astrocytoma gr. III	temporal left
L	30	m	epilepsy	temporal right
M	72	m	metastasis, carcinoma of lung	occipital right
N	67	m	metastasis, adenocarcinoma	parietal left

myograph (Model 400 A, J.P. Trading, Denmark), connected to a superfusion system (see Mulvany & Halpern, 1977). All solutions were continuously bubbled with carbogen (5% CO_2, 95% O_2) at a temperature of 37°C, resulting in a pH of 7.4. During an equilibration period of about 1 h, the vessels were repeatedly stretched until a stable resting tension of 2 mN mm^{-1} vessel length was obtained. Each segment was initially contracted by an isotonic 60 mM K^+ solution (containing the same constituents as the Na^+ Krebs solution except for an equimolar replacement of NaCl with KCl). The endothelium was removed by insufflating carbogen (0.2 l min^{-1}) through the vessel lumen for 2–4 min (Petersson *et al.*, 1993). Relaxant responses were studied in preparations contracted by the thromboxane A_2 receptor agonist, U46619. The concentration of U46619 was titrated for each vascular segment to achieve a similar contraction level in the absence and presence of 0.3 mM L-NOARG (i.e. 70–90% of the initial response to 60 mM K^+). Indomethacin (10 μM) was present in all experiments unless specified otherwise. The incubation period with L-NOARG and indomethacin was at least 40 min.

Recordings of the membrane potential were made in non-activated preparations with glass microelectrodes filled with 0.5 M KCl (tip resistance 85–155 MΩ). A computerized puller (Model BB-CH-PC, Mecanex S.A., Switzerland) was used to prepare the microelectrodes from borosilicate glass capillaries (1.5 mm o.d., 0.86 mm i.d.; Clark Electromedical Instruments, England). The microelectrode was advanced from the adventitial side of the artery by means of a Burleigh Inchworm motor driven micromanipulator (Burleigh Instruments, U.S.A.). A silver-silver chloride pellet immersed in the bath solution was used as reference electrode. The microelectrode was connected to an Axoprobe - 1A amplifier (Axon Instruments, U.S.A.) and the membrane potential was displayed on a pen recorder (Model BD 41 Kipp & Zonen, Holland) and oscilloscope (Model 5040 Kikusui, Japan). Successful impalements were characterized by a sudden negative shift in voltage followed by a stable negative potential for 5 min. The experiments were performed in the presence of indomethacin (10 μM), L-NOARG (0.3 mM) and nimodipine (0.1 μM), the latter in order to prevent spontaneous oscillations in tension.

Calculations and statistics

Responses are expressed as a percentage of the contraction before addition of SP. The negative logarithm of the SP concentration eliciting half maximum relaxation (pRC_{50}) was determined by linear regression analysis using the values immediately above and below half maximum response; R_{max} refers to the maximum relaxation obtained. Data are presented as mean ± s.e.mean, and *n* indicates the number of experiments (patients) performed. Groups of data were compared by Student's *t* test (two-tailed). Statistical significance was accepted when $P < 0.05$.

Drugs

U46619 (9,11-dideoxy-11α,9α,epoxymethano-prostaglandin $F_{2\alpha}$; Upjohn, Kalamazoo, MI, U.S.A.); substance P, N^{ω}-nitro-L-arginine (Sigma, St Louis, MO, U.S.A.); indomethacin (Confortid, Dumex, Copenhagen, Denmark); nimodipine (Nimotop, Bayer, Leverkusen, Germany); levcromakalim (SmithKline Beecham, Brentford, U.K.). Levcromakalim was dissolved in 70% ethanol. All other drugs were dissolved in distilled water. Stock solutions of the substances were stored at –70°C.

Results

The effect of SP was examined in pial arteries from 14 patients (Table 1). The majority of arteries developed spontaneous oscillations in tension, which were abolished by nimodipine (0.1 μM) or after replacement of the bath solution with 'Ca^{2+}-free' (0.1 mM EGTA) Krebs solution. SP induced a concentration-dependent relaxation in U46619-contracted arteries from all patients. Relaxation did not occur in preparations where the endothelium had been removed ($n = 11$). The SP-induced relaxation in intact arteries was completely abolished by 0.3 mM L-NOARG in six patients (patients A–F, Figure 1), whereas levcromakalim (1 μM) was still able to produce a complete relaxation ($n = 3$, data not shown). In arteries from the remaining eight patients (patients G–N, Table 1), the relaxation was only partially inhibited ($pRC_{50} = 9.3 \pm 0.1$ and $R_{max} = 62 \pm 7\%$ vs control $pRC_{50} = 9.8 \pm 0.2$ and $R_{max} = 89 \pm 5\%$, $P < 0.05$); in no case did L-NOARG reduce the maximum relaxation by more than 50% (Figure 2). The SP potency and maximum relaxation in the absence of L-NOARG did not differ significantly between arteries from patients A–F ($pRC_{50} = 9.6 \pm 0.1$, $R_{max} = 97 \pm 1\%$) and patients G–N ($pRC_{50} = 9.8 \pm 0.2$, $R_{max} = 89 \pm 5\%$). The L-NOARG-resistant relaxation was inhibited when the external K^+ concentration was increased to 30 or 60 mM (Figure 3).

The membrane potential was measured in vessel segments from four patients. The 'resting' membrane potential in the presence of L-NOARG, indomethacin and nimodipine was -38 ± 2 mV (9 impalements in 4 vessels, patients E, F, M and N). The effect of SP on the membrane potential in a vessel segment from patient N, in which L-NOARG only slightly inhibited the SP-induced relaxation (Figure 2), is shown in Figure 4a. As can be seen, SP hyperpolarized the membrane by 30 mV. However, SP was unable to elicit a hyperpolarization, as opposed to levcromakalim, in a vessel segment from patient F (Figure 4b), in which no relaxation was obtained in the presence of L-NOARG.

Indomethacin (10 μM) was present in all experiments described above. To investigate whether the formation of vasoactive prostanoids influences the SP-induced relaxation,

indomethacin was omitted in five experiments. These experiments were all performed on arterial segments from patients, displaying an L-NOARG-resistant relaxation (patients G–K, Table 1). As shown in Figure 5, the relaxation was more pronounced in the absence than in the presence of indomethacin.

Discussion

The results of the present study indicate that different mechanisms may contribute to endothelium-dependent relaxation in human pial arteries. The SP-induced relaxation was abolished by the NO synthase inhibitor L-NOARG in six out of 14 patients, and partially inhibited in the remaining eight patients. This suggests that the endothelium-dependent relaxation was mediated at least in part by NO or a NO-containing compound. The L-arginine-NO pathway has been demonstrated in cerebral arteries from different animal species (for review, see Faraci, 1992). Although endothelium-dependent relaxation has been observed in human basilar (Whalley *et al.*, 1987; Kanamaru *et al.*, 1989; Hatake *et al.*, 1990), middle cerebral (Martín de Aguilera *et al.*, 1990; Toda, 1990; Conde *et al.*, 1991; Akopov *et al.*, 1992) and pial (Hardebo *et al.*, 1987; Szabó *et al.*, 1992) arteries, the existence of an L-arginine-NO pathway in human isolated cerebral arteries has not been established previously.

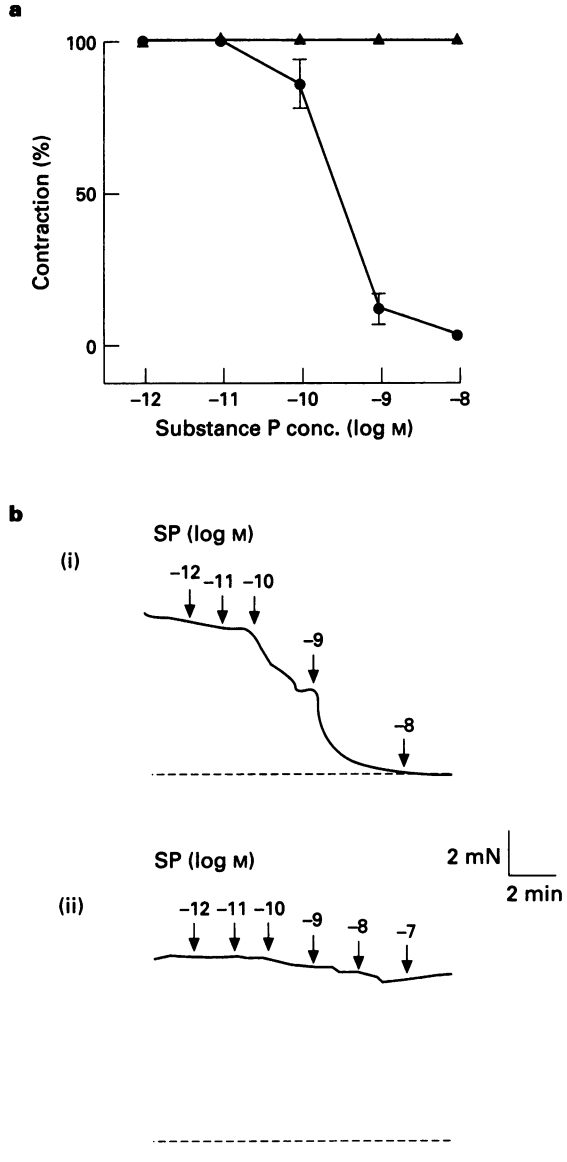

Figure 1 In arteries from six patients (patients A–F, Table 1), substance P (SP) evoked an endothelium-dependent relaxation, which was abolished by 0.3 mM N^{ω}-nitro-L-arginine (L-NOARG). (**a**) Concentration-response curves to SP in the absence (●) and presence (▲) of L-NOARG. Indomethacin (10 μM) was present throughout. Responses are expressed as a percentage of the contraction induced by U46619 before addition of SP. Data are presented as mean ± s.e.mean of six experiments. The contraction induced by U46619 before addition of SP was 4.2 ± 0.8 mN in the absence and 5.0 ± 1.0 mN in the presence of L-NOARG. (**b**) Two separate ring segments of the same artery from patient D were contracted by U46619: (i) shows the relaxation induced by SP; (ii) shows the effect of SP in the presence of 0.3 mM L-NOARG. Broken lines indicate the baseline tension before the contraction.

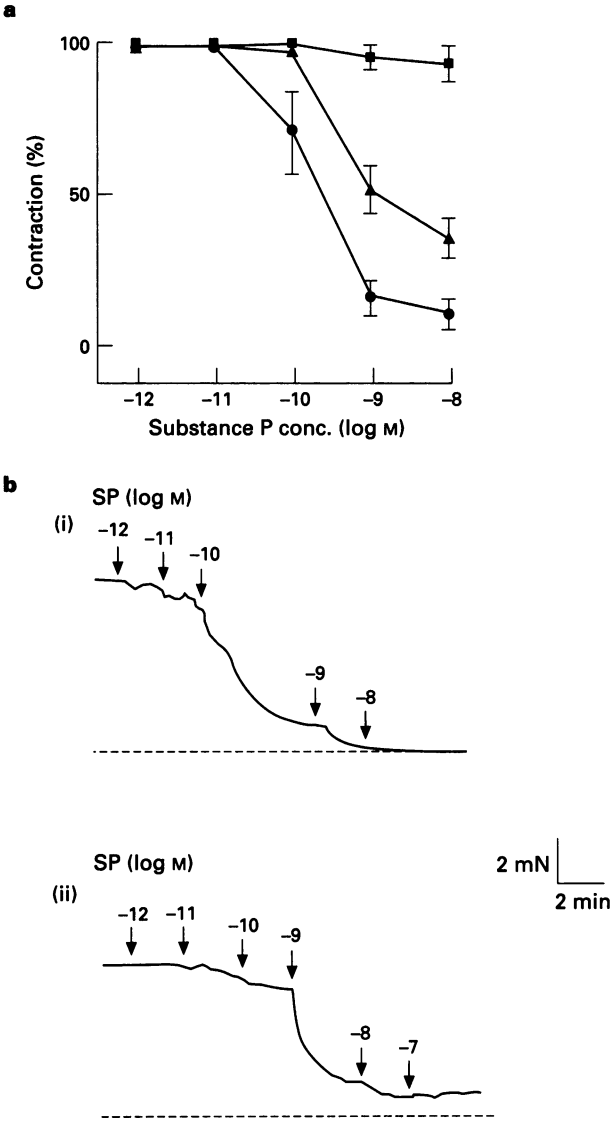

Figure 2 In arteries from eight patients (patients G–N, Table 1), substance P (SP) evoked an endothelium-dependent relaxation, which was partially resistant to 0.3 mM N^{ω}-nitro-L-arginine (L-NOARG). (**a**) Concentration-response curves to SP in the absence (●) and presence (▲) of L-NOARG, and in arterial segments without endothelium (■). Indomethacin (10 μM) was present throughout. Responses are expressed as a percentage of the contraction induced by U46619 before addition of SP. Data are presented as mean ± s.e.mean of five to eight experiments. The contraction induced by U46619 before addition of SP was 4.0 ± 0.8 mN in the absence and 5.6 ± 0.8 mN in the presence of L-NOARG, and 3.7 ± 1.0 mN in arteries without endothelium. (**b**) Two separate ring segments of the same artery from patient N were contracted by U46619: (i) shows the relaxation induced by SP; (ii) shows the effect of SP in the presence of 0.3 mM L-NOARG. Broken lines indicate the baseline tension before the contraction.

An L-NOARG-resistant relaxation was observed in eight out of 14 patients. This relaxation was not mediated by prostanoids, since the experiments were performed in the presence of indomethacin. An incomplete inhibition of NO-synthase by L-NOARG seems unlikely. First, L-NOARG abolished the SP-induced relaxation in K^+-depolarized arteries, suggesting that the formation of NO was indeed completely inhibited. Second, we used an L-NOARG concentration, which has previously been shown to abolish the cyclic GMP increase induced by acetylcholine in the rat aorta and hepatic artery (Zygmunt *et al.*, 1994a).

The SP-induced relaxation in the presence of L-NOARG was abolished when the K^+ concentration was raised above 30 mM, an approach previously used by others to differentiate between endothelium-dependent relaxation mediated by NO and hyperpolarization (Nagao & Vanhoutte, 1991; 1992; Adeagbo & Triggle, 1993; Cowan *et al.*, 1993; Zygmunt *et al.*, 1994a,b). Measurement of the membrane potential demonstrated an L-NOARG-resistant hyperpolarization, which in one vessel segment was accompanied by a relaxation. Fur-

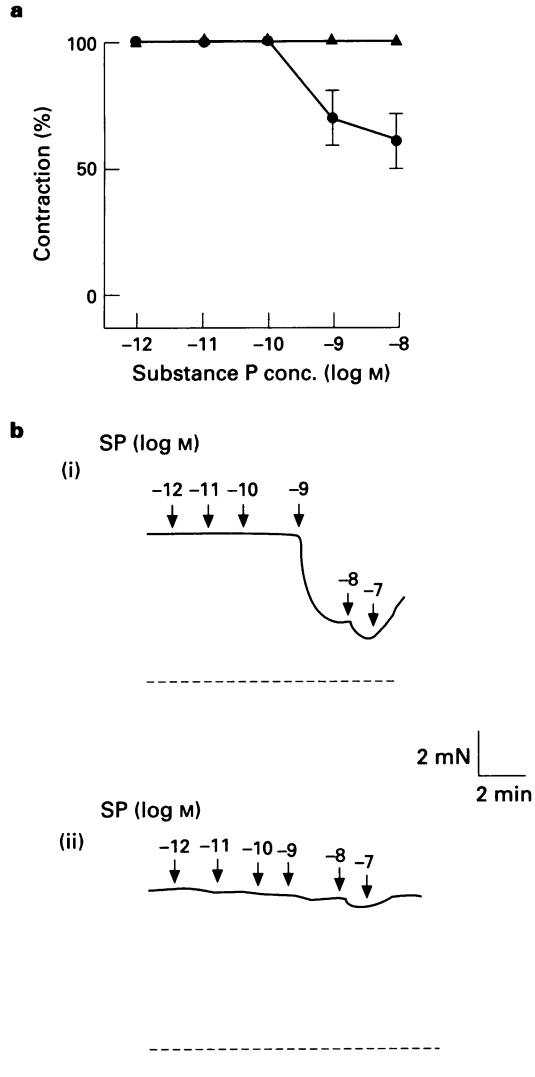

Figure 3 (a) Concentration-response curves for substance P (SP) in the absence (●) and presence (▲) of 0.3 mM N^{ω}-nitro-L-arginine (L-NOARG) in arteries contracted by a 60 mM K^+ solution. SP could not elicit an L-NOARG-resistant relaxation in this solution. Indomethacin (10 μM) was present throughout. Responses are expressed as a percentage of the contraction before addition of SP. Data are presented as mean ± s.e.mean of four experiments (patients H, J, L and N, Table 1). The contraction induced by the 60 mM K^+ solution before addition of SP was 5.7 ± 1.1 mN in the absence and 7.1 ± 1.2 mN in the presence of L-NOARG. (b) Exposure to a 30 mM K^+ solution inhibited the L-NOARG/indomethacin-resistant relaxation. The solution was prepared by adding 25.6 mM KCl to the Na^+ Krebs solution. Two separate ring segments of the same artery obtained from patient N (Table 1) were contracted by U46619 in the presence of 30 mM K^+ and indomethacin (10 μM): (i) shows the effect of SP in the absence of L-NOARG; (ii) shows the effect of SP in the presence of 0.3 mM L-NOARG. Broken lines indicate the baseline tension before the contraction.

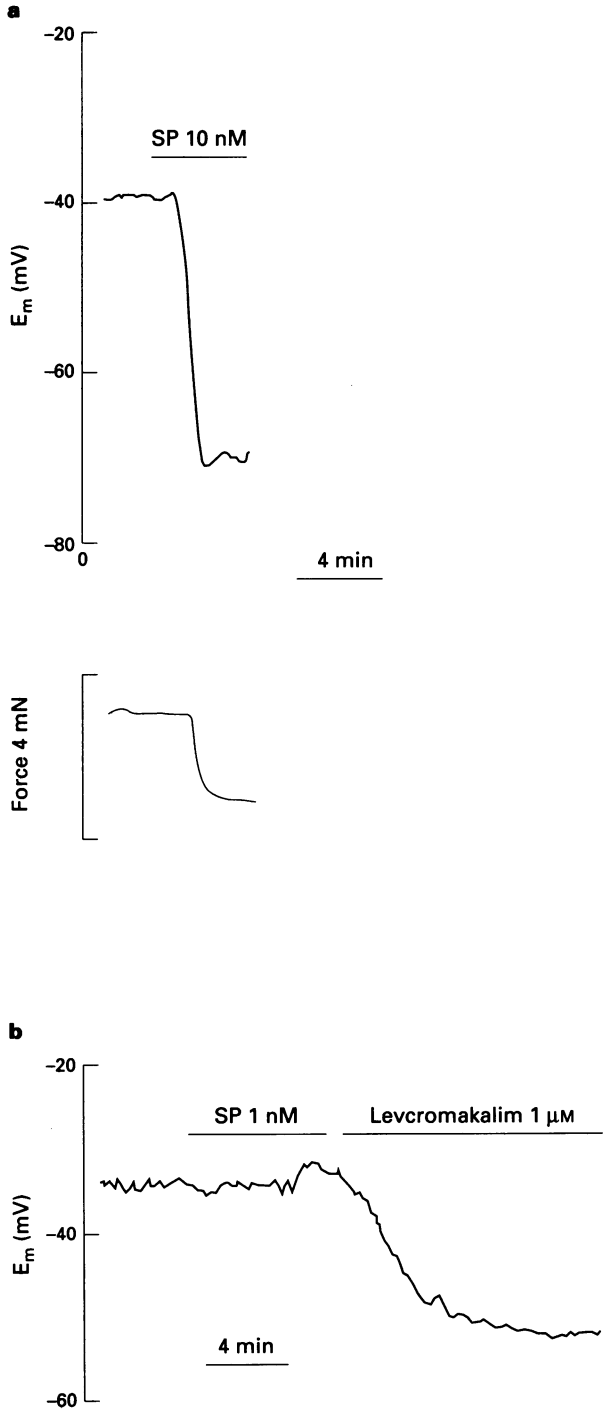

Figure 4 (a) Effect of substance P (SP) on the membrane potential and tension measured simultaneously in a vessel segment from patient N (Table 1). (b) Substance P (SP) did not cause a hyperpolarization in a vessel segment from patient F (Table 1). Hyperpolarization was, however, induced by levcromakalim. The experiments were performed in the presence of 0.3 mM N^{ω}-nitro-L-arginine, 10 μM indomethacin and 0.1 μM nimodipine.

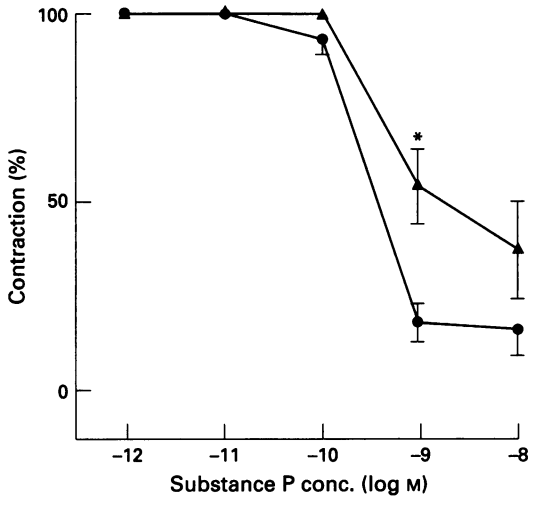

Figure 5 Concentration-response curves for substance P (SP) in the absence (●) and presence (▲) of 10 μM indomethacin in arteries contracted by U46619. N^{ω}-nitro-L-arginine (L-NOARG) (0.3 mM) was present throughout. Indomethacin was able to produce a small inhibition of the L-NOARG-resistant relaxation. Responses are expressed as a percentage of the U46619-induced contraction before addition of SP. The asterisk denotes a significant difference ($P < 0.05$) from experiments performed in the absence of indomethacin. Data are presented as mean ± s.e.mean of five experiments (patients G–K, Table 1). The contraction induced by U46619 before addition of SP was 4.4 ± 0.8 mN in the absence and 5.6 ± 1.0 mN in the presence of indomethacin.

thermore, SP was unable to induce a hyperpolarization unless the artery displayed an L-NOARG-resistant relaxation. These findings suggest that the L-NOARG-resistant hyperpolarization and relaxation are causally related to each other. Further studies are required to explore the cellular mechanism behind the endothelium-dependent hyperpolarization. However, ATP-sensitive potassium channels do not appear to be involved, since SP also elicited a hyperpolarization and relaxation in the presence of glibenclamide (unpublished observation).

To our knowledge a NO-independent hyperpolarization and relaxation mediated by the endothelium has not been shown before in human cerebral arteries, whereas such responses have been observed in feline middle, guinea-pig basilar and rabbit middle cerebral arteries (Brayden & Wellman, 1989; Nishiye *et al.*, 1989; Brayden, 1990). We have found only one study, using isolated coronary arteries, which has demonstrated an endothelium-dependent hyperpolarization in man (Nakashima *et al.*, 1993). Endothelium-dependent hyperpolarization may, thus, be an important mechanism for regulation of vascular tone not only in animals but also in man.

Arteries from six out of 14 patients lacked an L-NOARG-resistant relaxation. This subgroup of patients did not differ from the other patients with regard to age, sex, diagnosis, medication or the region where the tissue sample was taken. The total number of patients was, however, too small to discover such differences even if existent. Paramalignant phenomena or direct tumour infiltration are other possible confounding factors, but there was one case without malignancy in both subgroups of patients (patients B and L, Table 1). Interindividual differences in the responsiveness of human cerebral arteries have been recognized previously, e.g., with regard to the effects of different vasoconstrictor agents (Brandt *et al.*, 1981).

Cyclo-oxygenase activity has been demonstrated in both the endothelium and vascular smooth muscle (Moncada, 1982; de Nucci *et al.*, 1988). As shown in the present study, indomethacin produced a small inhibition of the SP-induced relaxation in the presence of L-NOARG. However, this does not necessarily mean that vasodilator prostanoids (e.g. prostacyclin) are produced by the endothelium in response to SP, since inhibition of cyclo-oxygenase might have changed the balance between different vasoactive arachidonic acid metabolites in a way that negatively affected the relaxant response to endothelium-dependent hyperpolarization.

The 'resting' membrane potential was –38 mV in human pial arteries. This is less negative than that recorded in animal cerebral arteries (Harder, 1980; Edwards *et al.*, 1988; Brayden & Wellman, 1989; Nishiye *et al.*, 1989; Plane & Garland, 1993), but similar to that observed in human coronary arteries (Nakashima *et al.*, 1993). The membrane potential measured in the present study might have been affected by the presence of L-NOARG, indomethacin and nimodipine. However, a similar resting membrane potential (–35 mV, average mean of two impalements) was recorded in one arterial segment in the absence of these drugs. Although unlikely, it cannot be excluded that the vessels were damaged during the surgical procedures. As demonstrated in patch clamp studies, the activation range for L-type voltage-dependent calcium channels is -40 to +10 mV (Reuter, 1983). Thus, activation of voltage-dependent calcium channels could explain the nimodipine-sensitive spontaneous contractile activity frequently observed in the present study. These properties might contribute to the tendency of cerebral arteries to develop vasospasm after subarachnoid haemorrhage.

This study demonstrates the presence of two different endothelium-dependent relaxant pathways in human cerebral arteries, one mediated by NO and the other by smooth muscle hyperpolarization. Both pathways may be important for the regulation of vascular tone in the cerebral circulation in man.

This work was supported by grants from the Medical Faculty at the Lund University, Thelma Zoégas, Greta and Johan Kocks and Elsa Schmitz' foundations.

References

ADEAGBO, A.S.O. & TRIGGLE, C.R. (1993). Varying extracellular $[K^+]$: a functional approach to separating EDHF- and EDNO-related mechanisms in perfused rat mesenteric arterial bed. *J. Cardiovasc. Pharmacol.*, **21**, 423–429.

AKOPOV, S.E., GRIGORIAN, M.R. & GABRIELIAN, E.S. (1992). The endothelium-dependent relaxation of human middle cerebral artery: effects of activated neutrophils. *Experientia*, **48**, 34–36.

ANGUS, J.A. & COCKS, T.M. (1989). Endothelium-derived relaxing factor. *Pharmacol. Ther.*, **41**, 303–352.

BRANDT, L., LJUNGGREN, B., ANDERSSON, K.-E. & HINDFELT, B. (1981). Individual variations in response of human cerebral arterioles to vasoactive substances, human plasma, and CSF from patients with aneurysmal SAH. *J. Neurosurg.*, **55**, 431–437.

BRAYDEN, J.E. (1990). Membrane hyperpolarization is a mechanism of endothelium-dependent cerebral vasodilation. *Am. J. Physiol.*, **259**, H668–H673.

BRAYDEN, J.E. & WELLMAN, G.C. (1989). Endothelium-dependent dilation of feline cerebral arteries: role of membrane potential and cyclic nucleotides. *J. Cereb. Blood Flow Metab.*, **9**, 256–263.

CHESTER, A.H., O'NEIL, G.S., TADJKARIMI, S., PALMER, R.M.J., MONCADA, S. & YACOUB, M.H. (1990). The role of nitric oxide in mediating endothelium dependent relaxations in the human epicardial coronary artery. *Int. J. Cardiol.*, **29**, 305–309.

CONDE, V.M., MARCO, E.J., FRAILE, L.M., BENITO, M.J., MORENO, J.M., SANZ, L.M. & LÓPEZ DE PABLO, A.L. (1991). Different influence of endothelium in the mechanical responses of human and cat isolated cerebral arteries to several agents. *J. Pharm. Pharmacol.*, **43**, 255–261.

COWAN, C.L., PALACINO, J.J., NAJIBI, S. & COHEN, R.A. (1993). Potassium channel-mediated relaxation to acetylcholine in rabbit arteries. *J. Pharmacol. Exp. Ther.*, **266**, 1482–1489.

DE NUCCI, G., GRYGLEWSKI, R.J., WARNER, T.D. & VANE, J.R. (1988). Receptor-mediated release of endothelium-derived relaxing factor and prostacyclin from bovine aortic endothelial cells is coupled. *Proc. Natl. Acad. Sci. U.S.A.*, **85**, 2334–2338.

EDWARDS, F.R., HIRST, G.D.S. & SILVERBERG, G.D. (1988). Inward rectification in rat cerebral arterioles; involvement of potassium ions in autoregulation. *J. Physiol.*, **404**, 455–466.

FARACI, F.M. (1992). Regulation of the cerebral circulation by endothelium. *Pharmacol. Ther.*, **56**, 1–22.

FARACI, F.M. (1993). Endothelium-derived vasoactive factors and regulation of the cerebral circulation. *Neurosurgery*, **33**, 648–659.

FURCHGOTT, R.F. & ZAWADZKI, J.V. (1980). The obligatory role of endothelial cells in the relaxation of arterial smooth muscle by acetylcholine. *Nature*, **288**, 373–376.

HARDEBO, J.E., KÅHRSTRÖM, J., OWMAN, C. & SALFORD, L.G. (1987). Endothelium-dependent relaxation by uridine tri- and diphosphate in isolated human pial vessels. *Blood Vessels*, **24**, 150–155.

HARDER, D.R. (1980). Comparison of electrical properties of middle cerebral and mesenteric artery in cat. *Am. J. Physiol.*, **239**, C23–C26.

HATAKE, K., KAKISHITA, E., WAKABAYASHI, I., SAKIYAMA, N. & HISHIDA, S. (1990). Effect of aging on endothelium-dependent vascular relaxation of isolated human basilar artery to thrombin and bradykinin. *Stroke*, **21**, 1039–1043.

HÖGESTÄTT, E.D., ANDERSSON, K.-E. & EDVINSSON, L. (1983). Mechanical properties of rat cerebral arteries as studied by a sensitive device for recording of mechanical activity in isolated small blood vessels. *Acta Physiol. Scand.*, **117**, 49–61.

IADECOLA, C., PELLIGRINO, D.A., MOSKOWITZ, M.A. & LASSEN, N.A. (1994). Nitric oxide synthase inhibition and cerebrovascular regulation. *J. Cereb. Blood Flow Metab.*, **14**, 175–192.

KANAMARU, K., WAGA, S., FUJIMOTO, K., ITOH, H. & KUBO, Y. (1989). Endothelium-dependent relaxation of human basilar arteries. *Stroke*, **20**, 1208–1211.

LÜSCHER, T.F. & VANHOUTTE, P.M. (1988). Endothelium-dependent responses in human blood vessels. *Trends Pharmacol. Sci.*, **9**, 181–184.

MARTIN DE AGUILERA, E., VILA, J.M., IRURZUN, A., MARTINEZ, M.C., MARTINEZ CUESTA, M.A. & LLUCH, S. (1990). Endothelium-independent contractions of human cerebral arteries in response to vasopressin. *Stroke*, **21**, 1689–1693.

MONCADA, S. (1982). Biological importance of prostacyclin. *Br. J. Pharmacol.*, **76**, 3–31.

MÜLSCH, A. & BUSSE, R. (1990). N^G-nitro-L-arginine (N^5-[imino(nitroamino)methyl]-L-ornithine) impairs endothelium-dependent dilations by inhibiting cytosolic nitric oxide synthesis from L-arginine. *Naunyn Schmied. Arch. Pharmacol.*, **341**, 143–147.

MULVANY, M.J. & HALPERN, W. (1977). Contractile properties of small arterial resistance vessels in spontaneously hypertensive and normotensive rats. *Circ. Res.*, **41**, 19–26.

MYERS, P.R., MINOR, R.L., JR., GUERRA, R., JR., BATES, J.N. & HARRISON, D.G. (1990). Vasorelaxant properties of the endothelium-derived relaxing factor more closely resemble S-nitrosocysteine than nitric oxide. *Nature*, **345**, 161–163.

NAGAO, T. & VANHOUTTE, P.M. (1991). Hyperpolarization contributes to endothelium-dependent relaxations to acetylcholine in femoral veins of rats. *Am. J. Physiol.*, **261**, H1034–H1037.

NAGAO, T. & VANHOUTTE, P.M. (1992). Hyperpolarization as a mechanism for endothelium-dependent relaxations in the porcine coronary artery. *J. Physiol.*, **445**, 355–367.

NAGAO, T. & VANHOUTTE, P.M. (1993). Endothelium-derived hyperpolarizing factor and endothelium-dependent relaxations. *Am. J. Respir. Cell Mol. Biol.*, **8**, 1–6.

NAKASHIMA, M., MOMBOULI, J.-V., TAYLOR, A.A. & VANHOUTTE, P.M. (1993). Endothelium-dependent hyperpolarization caused by bradykinin in human coronary arteries. *J. Clin. Invest.*, **92**, 2867–2871.

NISHIYE, E., NAKAO, K., ITOH, T. & KURIYAMA, H. (1989). Factors inducing endothelium-dependent relaxation in the guinea-pig basilar artery as estimated from the actions of haemoglobin. *Br. J. Pharmacol.*, **96**, 645–655.

PALMER, R.M.J., FERRIGE, A.G. & MONCADA, S. (1987). Nitric oxide release accounts for the biological activity of endothelium-derived relaxing factor. *Nature*, **327**, 524–526.

PETERSSON, J., RYMAN, T. & HÖGESTÄTT, E.D. (1993). Enhancement of depolarization-induced contractions after endothelium denudation is not related to an impaired production of nitric oxide or prostacyclin in the rabbit basilar artery. *Acta Physiol. Scand.*, **149**, 467–474.

PLANE, F. & GARLAND, C.J. (1993). Differential effects of acetylcholine, nitric oxide and levcromakalim on smooth muscle membrane potential and tone in the rabbit basilar artery. *Br. J. Pharmacol.*, **110**, 651–656.

REUTER, H. (1983). Calcium channel modulation by neurotransmitters, enzymes and drugs. *Nature*, **301**, 569–574.

SZABÓ, C., HARDEBO, J.-E. & SALFORD, L.G. (1992). Role of endothelium in the responses of human intracranial arteries to a slight reduction of extracellular magnesium. *Exp. Physiol.*, **77**, 209–211.

TODA, N. (1990). Mechanism underlying responses to histamine of isolated monkey and human cerebral arteries. *Am. J. Physiol.*, **258**, H311–H317.

WHALLEY, E.T., AMURE, Y.O. & LYE, R.H. (1987). Analysis of the mechanism of action of bradykinin on human basilar artery in vitro. *Naunyn Schmied. Arch. Pharmacol.*, **335**, 433–437.

ZYGMUNT, P.M., GRUNDEMAR, L. & HÖGESTÄTT, E.D. (1994a). Endothelium-dependent relaxation resistant to Nω-nitro-L-arginine in the rat hepatic artery and aorta. *Acta Physiol. Scand.*, **152**, 107–114.

ZYGMUNT, P.M., WALDECK, K. & HÖGESTÄTT, E.D. (1994b). The endothelium mediates a nitric oxide-independent hyperpolarization and relaxation in the rat hepatic artery. *Acta Physiol. Scand.*, **152**, 375–384.

(Received October 24, 1994
Revised February 17, 1995
Accepted March 24, 1995)

British Journal of Pharmacology (1995) 115, 895-902 © 1995 Stockton Press All rights reserved 0007-1188/95 $12.00

A novel receptor for diadenosine polyphosphates coupled to calcium increase in rat midbrain synaptosomes

[1,*]Jesús Pintor & M. Teresa Miras-Portugal

Departmento de Bioquimica and *E.U. Optica, Fac. Veterinaria, Universidad Complutense 28040 Madrid, Spain

1 Diadenosine polyphosphates, Ap_4A and Ap_5A, as well as ATP, α,β-MeATP and ADP-β-S, were able to elicit variable intrasynaptosomal Ca^{2+} increases in rat midbrain synaptic terminals. The origin of the Ca^{2+} increment was the extrasynaptosomal space since the elimination of extracellular Ca^{2+} abolished the effect of all the agonists.

2 The P_2-purinoceptor antagonist, suramin, did not affect the Ca^{2+}-increase evoked by diadenosine polyphosphates but dramatically blocked the Ca^{2+} entry induced by ATP and its synthetic analogues.

3 The actions of Ap_5A and ATP on the intrasynaptosomal Ca^{2+} increase did not cross-desensitize.

4 Concentration-response studies for diadenosine polyphosphates showed pD_2 values of 54.5 ± 4.2 μM and 55.6 ± 3.8 μM for Ap_4A and Ap_5A, respectively.

5 The entry of calcium induced by diadenosine polyphosphates could be separated into two components. The first represented a selective voltage-independent Ca^{2+} entry; the second, a sustained phase which was voltage-dependent.

6 Studies on the voltage-dependent Ca^{2+}-channels involved in the effects of the diadenosine polyphosphates, demonstrated that ω-conotoxin G-VI-A inhibited the sustained Ca^{2+}-entry, suggesting the participation of an N-type Ca^{2+}-channel. This toxin was unable to abolish the initial cation entry induced by Ap_4A or Ap_5A. ω-Agatoxin IV-A, tetrodotoxin, or nifedipine did not inhibit the effects of the diadenosine polyphosphates.

7 The effect of ATP on Ca^{2+}-entry was abolished by nifedipine and ω-conotoxin G-VI-A, suggesting the participation of L- and N-type Ca^{2+}-channels in the response to ATP.

8 These data suggest that Ap_4A, Ap_5A and ATP activate the same intracellular Ca^{2+} signal through different receptors and different mechanisms. Ap_4A and Ap_5A induce a more selective Ca^{2+}-entry in a voltage-independent process. This is the first time that a selective action of diadenosine polyphosphate through receptors other than P_1 and P_2-purinoceptors has been described.

Keywords: Ap_4A; Ap_5A; calcium channels; channel toxins; diadenosine polyphosphates; P_2-purinoceptors; synaptic terminal

Introduction

Purinoceptors are responsible for the actions of adenosine as well as adenine nucleotides in many tissues. Receptors for adenosine 5'-triphosphate (ATP), termed P_2-purinoceptors, have been widely studied in neural and non-neural tissues (Burnstock, 1990; 1992). P_2-purinoceptors were initially divided into P_{2X} and P_{2Y} subtypes in accordance with the potency order of ATP and synthetic analogues and their differential sensitivity to tachyphylaxis (Burnstock & Kennedy, 1985). In platelets, as well as in macrophages, purinoceptors were termed P_{2T} and P_{2Z}, (Gordon, 1986) respectively, and both possess characteristic agonist and antagonist profiles (Cockcroft & Gomperts, 1979; Colman, 1990; Hoyle, 1992). Although ATP has been considered the main agonist, other nucleotides can exert actions via P_2-purinoceptors. UTP and α,ω-adenine dinucleotides are the most recent active nucleotidic substances with actions that have been demonstrated in epithelia and central nervous system (O'Connor *et al.*, 1991; Klishin *et al.*, 1994). Both UTP and diadenosine polyphosphates activate recently defined P_2-purinoceptors named P_{2U} and P_{2D}, respectively (O'Connor, 1992; Pintor *et al.*, 1993a). The broad group of P_2-purinoceptors can be classified into two families: ionotropic channels activated by ATP (Benham & Tsien, 1987), and metabotropic receptors which are coupled to G proteins (Harden *et al.*, 1990; Zimmermann, 1994).

Although it has been demonstrated that ATP is stored in synaptic vesicles and that it is exocytotically released, it is only recently that the role of ATP as a neurotransmitter in the central nervous system has been determined (White, 1977; Potter & White, 1980). Since then ATP has been shown to activate ionic currents in central neurones (Ueno *et al.*, 1992; Shen & North, 1993; Illes & Norenberg, 1993); only by means of the trypanocide, suramin, a P_2-purinoceptor antagonist (Hoyle, 1990), was it possible to demonstrate that central synapses use ATP as a fast excitatory neurotransmitter (Edwards *et al.*, 1992). Together with ATP, two diadenosine polyphosphates, Ap_4A and Ap_5A, have been identified in the synaptic terminals from rat brain. These dinucleotides, as well as ATP, are released, in a Ca^{2+}-dependent process, by the action of depolarizing agents (Pintor *et al.*, 1992a). Both diadenosine polyphosphates, Ap_4A and Ap_5A, exert an inhibitory effect on synaptic transmission in the hippocampus (Klishin *et al.*, 1994), this effect probably being mediated by a xanthine-sensitive purinoceptor through protein kinase C (PKC) activation (Pintor & Miras-Portugal, 1994).

In several tissues, it has been demonstrated that ATP and diadenosine polyphosphates can activate the same purinoceptor subtypes (MacKenzie *et al.*, 1988; Hoyle *et al.*, 1989; Pintor & Miras-Portugal, 1994; Ralevic *et al.*, 1994). In the vas deferens and urinary bladder their actions are through a P_{2X}-purinoceptor (MacKenzie *et al.*, 1988; Hoyle *et al.*, 1989; 1990); in bovine adrenal gland endothelial and chromaffin cells as well as in the rat mesenteric vascular bed the effects of Ap_4A and Ap_5A are mediated by P_{2U}, P_{2X} and P_{2Y}-purinoceptors, respectively (Pintor *et al.*, 1991; Castro *et al.*, 1994; Ralevic *et*

[1] Author for correspondence at present address: Dept. Anatomy and Developmental Biology, University College London, Gower Street, London WC1E 6BT.

al., 1994). The recent discovery of the P_{2D}-purinoceptor (Pintor *et al.*, 1993a), highly specific for diadenosine polyphosphates in synaptic terminals, reinforced the theory of the existence of different purinoceptors for nucleotides and dinucleotides (Stone & Perkins, 1981; Hoyle, 1990).

The aim of the present study was to determine whether or not the diadenosine polyphosphates, Ap_4A and Ap_5A, can act on rat isolated brain synaptic terminals, and if so through which receptor.

Methods

Synaptosomal preparation

Synaptosomes were prepared from middle brain of male Wistar rats that had been cervically dislocated and decapitated (Pintor *et al.*, 1992a). Synaptosomal pellets containing 1 mg of protein were resuspended in 1 ml incubation medium (composition mM: NaCl 122, KCl 3.1, KH_2PO_4 0.4, $NaHCO_3$ 5, $MgSO_4$ 1.2, glucose 10 and TES buffer 20, pH 7.4).

Calcium concentration measurements

The cytosolic free calcium concentration was determined with fura-2 as described by Grynkiewicz *et al.* (1985). Five minutes after resuspension $CaCl_2$ (1.33 mM) and fura-2-acetoxymethyl ester (5 μM) were added. Following incubation for 35 min the synaptosomes were pelleted (centrifuged at 800 r.p.m. for 1 min), washed twice and resuspended into fresh medium containing $CaCl_2$ (1.33 mM). Fluorescence was measured in a Perkin Elmer Spectrofluorimeter LS-50B, and monitored at 340 nm (excitation wavelength) and 510 nm (emission wavelength). Data were collected at 0.5 s intervals. Free calcium measurements were carried out with a mixture formed of 50 μM EGTA and 38 μM $CaCl_2$ as described by Verhage *et al.* (1989) and Carbone & Swandulla (1989).

Nucleotides and dinucleotides were tested at a final concentration of 100 μM. The adenosine receptor antagonist DPCPX, was used at a concentration of 250 nM. In the cross-desensitization studies the nucleotides (also at 100 μM) were preincubated for 3 min before the application of the corresponding agonist. Suramin was applied at a concentration of 100 μM, 1 min before application of the nucleotides.

Membrane potential measurements

Synaptosomal plasma membrane potential was monitored with a potential-sensitive cationic cyanide dye, 3,3-diethylthiadicarbocyanide iodine ($DiSC_2(5)$) as described by Simms *et al.* (1974). Synaptosomes were preincubated at 37°C for 1 h, then pelleted and resuspended (1 mg ml^{-1}) in incubation medium containing $DiSC_2(5)$ (5 μM) and $CaCl_2$ (1.33 mM). After 5 min equilibration, the nucleotide and dinucleotide compounds were added at a concentration of 100 μM. Fluorescence was determined at 643 and 680 nm. Data were collected at 2 s intervals.

Intrasynaptosomal sodium measurements

Synaptosomal sodium increments were performed with SBFI dye (Minta & Tsien, 1989) and following the same protocol as described for fura-2. Fluorescence was monitored at the same excitation and emission wavelength as for the fura assay (340 nm and 510 nm, respectively). Data were collected at 2 s intervals.

Toxins

Tetrodotoxin (TTX, 5 μM), ω-conotoxin G-VI-A (ω-CgTx, 5 μM), ω-agatoxin IV-A (ω-Aga, 5 μM) and nifedipine (200 nM) were incubated with synaptosomes 30 min before the application of the agonists.

Nucleotide stability

To assess the stability of nucleotides and dinucleotides, their purity was determined before the experimental studies were carried out, by using high performance liquid chromatography (h.p.l.c.). Chromatographic analysis was also performed at the end of the experiments to verify that they had not been degraded. The chromatographic system was equilibrated with the following mobile phase: 0.1 mM KH_2PO_4, 2 mM tetrabutyl ammonium and 15% acetonitrile pH 7.4, as described by Pintor *et al.* (1992b). Detection was monitored at 260 nm wavelength.

Ap_6A, diadenosine hexaphosphate, was not assayed because of its poor stability (Pintor *et al.*, 1992b).

Drugs used

ATP, synthetic analogues as well as diadenosine polyphosphates were from Sigma (St. Louis, MO, U.S.A.), except Ap_5A which was purchased from Boehringer (Mannheim, Germany). Suramin was kindly provided by Dr A. Ijzerman. Fura-2 as well as $DiSC_2(5)$ and SBFI were obtained from Molecular Probes (U.S.A.). Tetrodotoxin and nifedipine were purchased from Sigma (St. Louis, U.S.A.), ω-Conotoxin G-

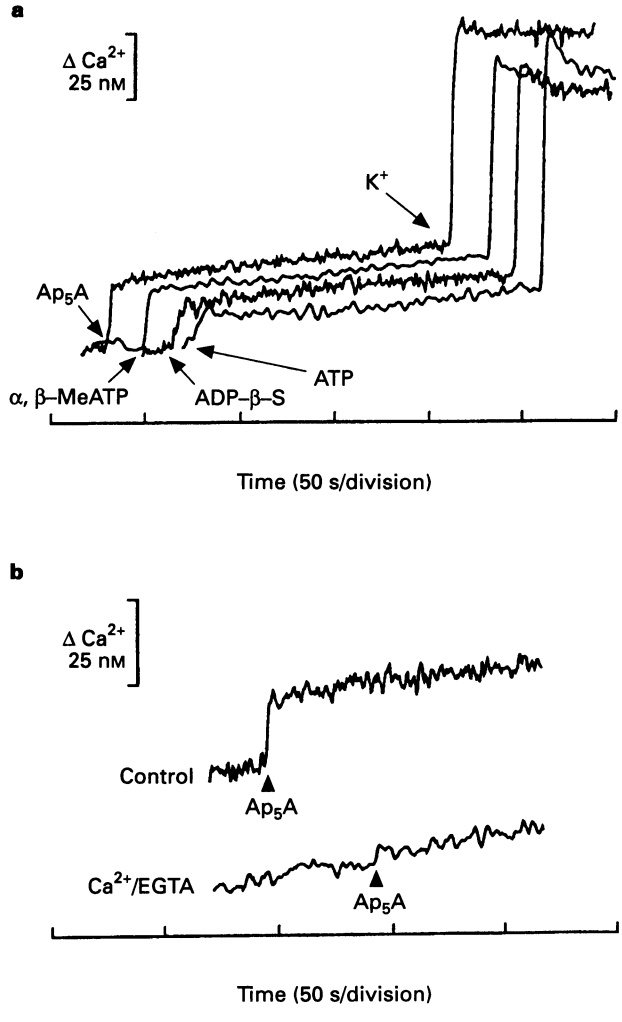

Figure 1 Effect of mono- and dinucleotides on rat brain intrasynaptosomal calcium levels: (a) different P_2-purinoceptor agonists induced an increase in intrasynaptosomal Ca^{2+} when applied at a final concentation of 100 μM. K^+ (30 nM) was used as a control of the synaptosomal functional response. (b) Response to diadenosine pentaphosphate (Ap_5A) in the presence of 1.33 mM extracellular Ca^{2+} and in the absence of extracellular Ca^{2+}. Traces are overlaid examples from different synaptosomal preparations.

VI-A and DPCPX were obtained from RBI (U.S.A.), ω-agatoxin IV-A from Alomone labs (Israel). Other reagents were analytical grade purchased from Merck (Darmstadt, Germany).

Statistical analysis

Data are presented as mean ± s.e.mean of at least four determinations in duplicate and in different synaptosomal preparations. Significant differences were determined by Student's two-tailed *t* test. When appropriate, single experimental traces are represented in the Figures; they are representative of at least four determinations in duplicate with equivalent results. Traces shown in figures are overlaid examples from different synaptosomal preparations.

Results

Effect of diadenosine polyphosphates and nucleotides on synaptosomal Ca^{2+} levels

The application of diadenosine polyphosphates, Ap_4A and Ap_5A, at final concentrations of 100 μM to synaptosomal preparations containing 1 mg protein ml^{-1}, induced an increase in cytosolic Ca^{2+} of 15 ± 1.4 nM and 26 ± 1.8 nM respectively.

ATP, as well as its synthetic analogues were able to induce the rise of intrasynaptosomal calcium levels. The amounts of calcium differed slightly among ATP and its analogues, the values being 18.1 ± 2.7 nM for ATP, 20.0 ± 2.4 nM for ADP-β-S and 23.7 ± 2.1 nM for α, β-MeATP ($P < 0.01$) (Figure 1a).

In the absence of extrasynaptosomal Ca^{2+}, Ap_5A was unable to induce any increase of the cytosolic calcium signal (Figure 1b). Ap_4A, as well as ATP and the synthetic analogues, behaved in a similar manner (data not shown). All the experiments were performed four times in duplicate.

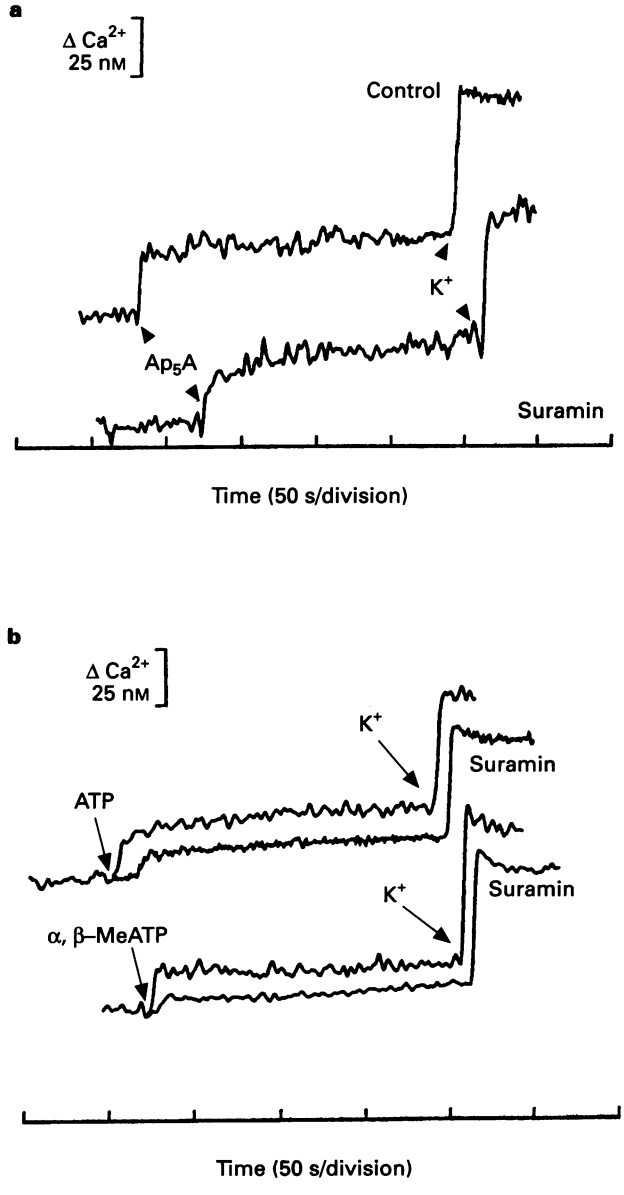

Figure 2 Effects of suramin on calcium entry into rat brain synaptosomes evoked by mono- and dinucleotides: (a) effect of diadenosine pentaphosphate (100 μM) on the intrasynaptomal calcium levels. The upper trace represents the effect in the absence of the P_2-purinoceptor antagonist, suramin. The lower record shows the effect in the presence of suramin (100 μM), under the conditions described in methods. (b) The effects of ATP (100 μM) and α,β-MeATP (100 μM), were blocked by preincubating synaptosomal preparations with suramin (100 μM). Traces are overlaid examples from different synaptosomal preparations.

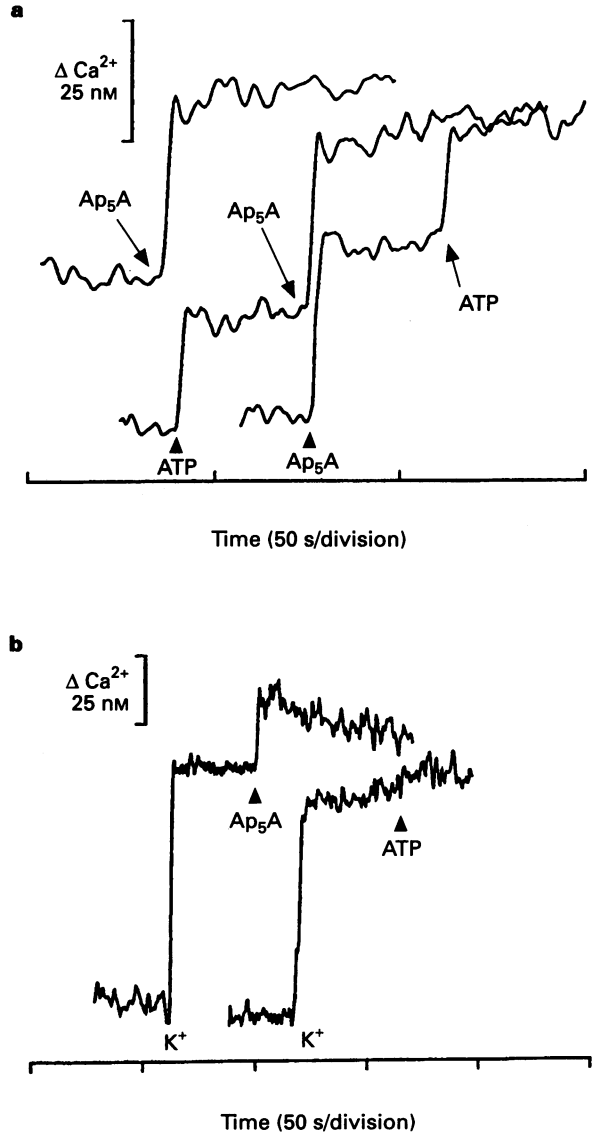

Figure 3 Cross-desensitization study between Ap_5A and ATP responses and effects of K^+ in rat brain synaptic terminals: (a) in the upper trace, Ap_5A (100 μM) was applied as control; application of ATP (100 μM) followed by Ap_5A (100 μM) (middle trace); application of Ap_5A (100 μM) and a further application of ATP (100 μM) (lower trace). (b) Effects of Ap_5A and ATP (both 100 μM) after application of K^+ (30 mM). Traces are overlaid examples from different synaptosomal preparations.

Pharmacology of the dinucleotide/nucleotide receptor action on Ca^{2+} influx

Preincubation of synaptosomal preparations with suramin (100 μM), a P_2-purinoceptor antagonist, did not affect the Ca^{2+}-transients evoked by Ap_5A (Figure 2a). In contrast, the Ca^{2+} transients elicited by ATP and its non-hydrolyzable analogues, were decreased to 9.5 ± 1.9 nM for ATP and 9.5 ± 1.7 nM for α,β-MeATP, when suramin (100 μM) was applied under the same conditions ($P<0.01$). (Figure 2b).

Prior application of ATP, did not alter the Ca^{2+} increase induced by Ap_5A, nor was there any change in the Ca^{2+} signal evoked by ATP when synaptosomal samples were pretreated with Ap_5A (Figure 3a). These results could suggest that the receptors subserving the effects of ATP and Ap_5A are different. To develop this possibility further and to determine the role played by the membrane potential in signalling, both substances were assayed after applications of K^+. As shown in Figure 3b, ATP did not induce a further increase in intrasynaptosomal Ca^{2+} but Ap_5A did, although a decay in the Ca^{2+} signal induced by Ap_5A could be observed. These experiments also suggested the existence of two purinoceptors with differential selectivity for diadenosine polyphosphates and ATP.

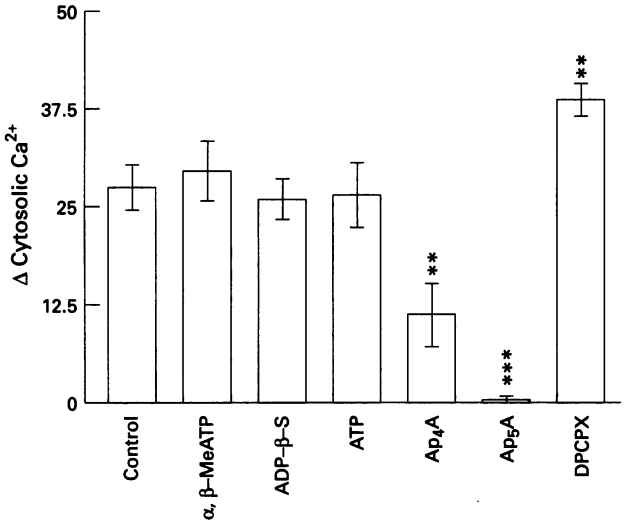

Figure 4 Desensitization studies with different mono- and dinucleotides in rat brain synaptic terminals: Effect of α,β-MeATP, ADP-β-S, ATP, Ap_4A and Ap_5A, preincubated in a final concentration of 100 μM, on the intrasynaptosomal Ca^{2+} increase induced by 100 μM Ap_5A. Data are means ± s.e.mean of four experiments in duplicate. $^{**}P<0.01$, $^{***}P<0.001$ vs control.

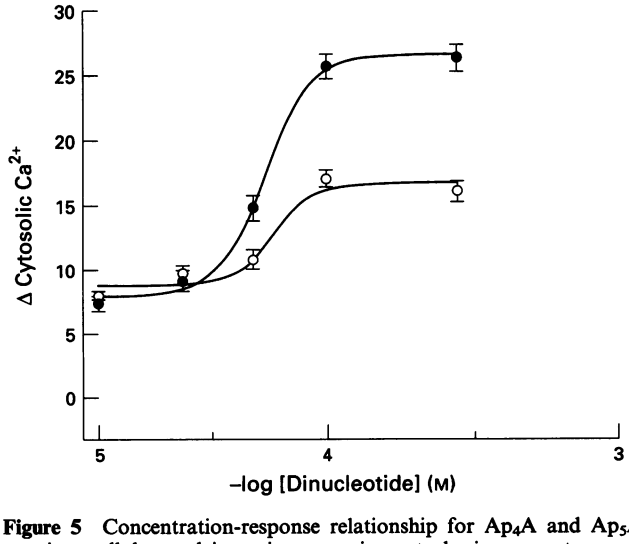

Figure 5 Concentration-response relationship for Ap_4A and Ap_5A on intracellular calcium increase in rat brain synaptosomes: concentration-dependence of Ap_4A (○) and Ap_5A (●) on the intrasynaptosomal Ca^{2+} levels. Data represent mean (± s.e.mean) maximal increase in Ca^{2+} levels (four experiments in duplicate).

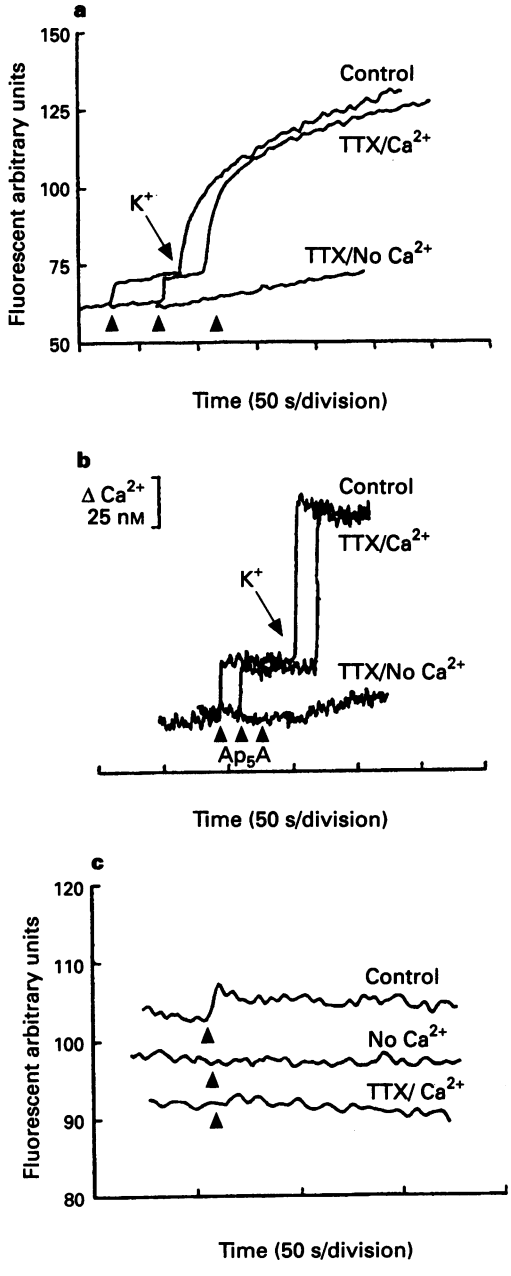

Figure 6 Effects of tetrodotoxin (TTX) on changes in membrane potential and intrasynaptosomal Ca^{2+} and Na^+ in rat brain synaptic terminals: (a) diadenosine pentaphosphate, 100 μM, induced depolarization in the presence and in the absence of 5 μM TTX (applications of the dinucleotide are indicated by the arrows). (b) TTX had no effect on the Ca^{2+}-signal evoked by Ap_5A. (c) Synaptosomal Na^+ increase induced by diadenosine pentaphosphate (indicated by the arrow). All the experiments are means of four experiments in duplicate. Traces are overlaid examples from different synaptosomal preparations.

Table 1 Effects of Ap_5A and ATP on intrasynaptosomal calcium signal, membrane potential, and sodium signals

	ΔCa^{2+} signal			$\Delta\Psi$			ΔNa^+ signal		
	Control	*Ca^{2+} free*	*+ TTX*	*Control*	*$-Ca^{2+}$*	*+ TTX*	*Control*	*$-Ca^{2+}$*	*+ TTX*
Ap_5A (100 μM)	26.0±1.8	0	25.3±2.2	7.5±1.1	0	7.2±1.4	4.6±1.0	0	0
ATP (100 μM)	18.1±2.7	0	10.8±1.2	4.5±0.8	0	3.7±0.9	5.0±1.2	3.6±0.7	2.7±0.5

ΔCa^{2+}, change in the intrasynaptosomal calcium signal expressed in nM; $\Delta\Psi$, change in the synaptosomal membrane potential expressed in arbitrary units; ΔNa^+, change in the intrasynaptosomal sodium signal expressed in arbitrary units. All values are mean ± s.e.mean of four experiments in duplicate.

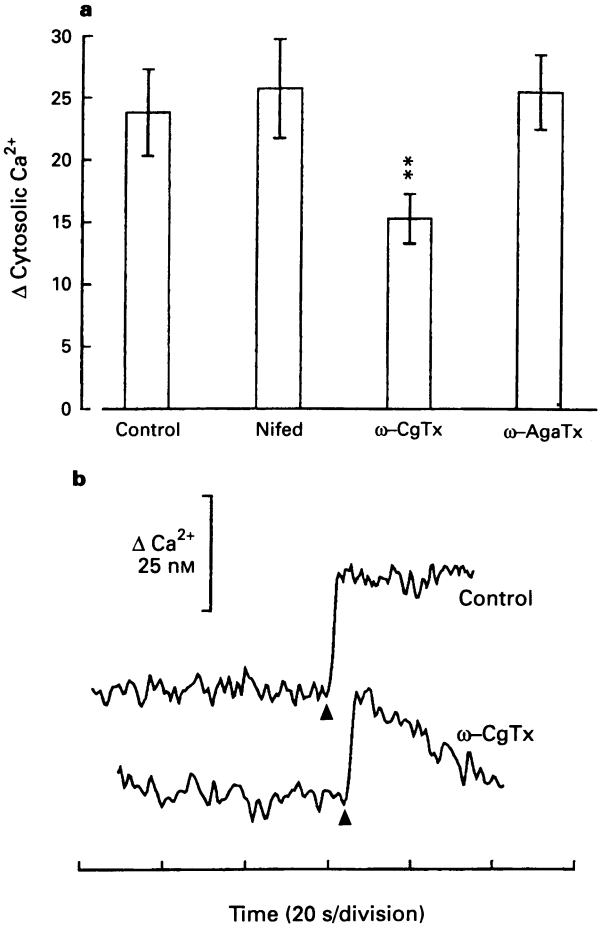

Figure 7 Effects of Ca^{2+}-channel antagonists on Ca^{2+}-signal evoked by Ap_5A in rat brain synaptic terminals: (a) effect of different calcium channel blockers on Ap_5A calcium signal. Nifedipine (Nifed), ω-conotoxin G-VI-A (ω-CgTx), ω-agatoxin IVA (ω-AgaTx) were preincubated for 30 min before the dinucleotide application. Results are means ± s.e.mean. All the experiments represent means of four different experiments in duplicate. $^{**}P<0.01$ vs control. (b) Differential kinetic response on Ca^{2+} sustained component to Ap_5A in the absence (control) and in the presence of ω-conotoxin G-VI-A. Arrows represent the application of the dinucleotide. These results are the means of four experiments in duplicate. Traces are overlaid examples from different synaptosomal preparations.

When synaptosomes were pre-incubated with ATP, ADP-β-S, α,β-MeATP, Ap_4A or Ap_5A, prior to application of Ap_5A, no inhibition of its effect was observed except in the cases of Ap_4A, which reduced the Ap_5A signal to 11.2±4.0 nM and Ap_5A which reduced it to 1.2±0.5 nM (Figure 4). The absence of cross-desensitization agrees with different purinoceptors for nucleotides and dinucleotides, their actions being independent and additive in the synaptosomal preparation.

To test whether diadenosine polyphosphates act through A_1-purinoceptors the synaptic terminals were pre-incubated with the A_1-purinoceptor antagonist, 8-cyclopentyl-1,3-dipropylxanthine (DPCPX, 250 nM). In the presence of this compound Ap_5A produced a greater increase in the Ca^{2+}-signal than in its absence (Figure 4), excluding an action through A_1 receptors. All the experiments were performed four times in duplicate.

Concentration-response relationship for diadenosine polyphosphates

The concentration-dependency of the diadenosine polyphosphate purinoceptor was studied for both Ap_4A and Ap_5A. The pD_2 values were 54.5±4.2 μM and 55.6±3.8 μM respectively (Figure 5). It is noteworthy that although both dinucleotides have approximately the same pD_2, Ap_4A elicited a smaller maximum response than did Ap_5A. All the experiments were performed four times in duplicate.

Effects of TTX and Ca^{2+}-channel blockers

The diadenosine polyphosphates evoked depolarization of the membrane potential as shown in Figure 6a. This response was completely abolished in the absence of Ca^{2+} (Table 1, Figure 6a), but it was apparently unaffected by the presence of the voltage-dependent Na^+ blocker, tetrodotoxin, (TTX, 5 μM); nor did TTX modify the Ca^{2+}-signal (Figure 6b). The same experiments were performed by measuring the changes in the intrasynaptosomal Na^+-levels. Ap_5A in the presence of Ca^{2+} induced an increase in synaptosomal Na^+ which was abolished by either the absence of Ca^{2+} or the presence of TTX (Figure 6c). These results excluded the initial membrane depolarization via entry of Na^+ and Ca^{2+} through a non-specific receptor-operated cation channel, and agree with a more selective Ca^{2+} entry (Table 1).

To study whether voltage-dependent Ca^{2+} channels (VDCC) are involved in the action of diadenosine polyphosphate, different Ca^{2+} channel blockers were examined, as shown in Figure 7a. The channel blockers nifedipine (200 nM) and ω-agatoxin IVA (5 μM), specific for L- and P-types of Ca^{2+}-channels respectively (Catteral & Striessnig, 1992; Mintz *et al.*, 1992), did not modify the Ca^{2+} entry induced by diadenosine polyphosphates. ω-Conotoxin G-VI-A (5 μM), which blocks the N-type Ca^{2+}-channel (Miller & Fox, 1990; Tsien & Tsien, 1990), inhibited the Ca^{2+} influx evoked by Ap_4A and Ap_5A at 100 μM by 40% (Figure 7b). The results are summarized in Table 2.

The possible involvement of T-channels in the Ap_5A response was excluded since this type of channel is rapidly inactivated by a potential-dependent process (Carbone & Swandulla, 1989). After depolarization with K^+ there is still Ca^{2+} entry, excluding the participation of this channel (Figure 3b). In the presence of Ni^{2+} (40 μM) there was no change in the Ca^{2+} signal evoked by the diadenosine polyphosphates (Table 2). All the experiments were performed four times in duplicate.

ATP (100 μM) also modified the membrane potential but to a lesser extent than did Ap_5A at the same concentration (Figure 8a). The presence of TTX decreased both the membrane depolarization (Figure 8a) and the Ca^{2+} entry induced by ATP (Table 1, Figure 8b), but not the increase in intrasynaptosomal Na^+ (Figure 8c). These results suggest that ATP opened a non-specific cation channel. ATP calcium in-

Table 2 Effects of calcium antagonists on the intrasynaptosmal calcium levels in response to Ap_5A and ATP

	Control	*ω-Conotoxin G-VI-A*	*ω-Agatoxin IV-A*	*Nifedipine*	Ni^{2+}
Ap_5A (100 μM)	26.0±1.8	15.1±1.8	25.1±3.0	25.4±3.9	25.7±2.8
ATP (100 μM)	18.1±2.7	12.0±3.6	20.4±3.2	2.7±1.3	19.4±2.9

Intrasynaptosomal calcium levels are expressed in nM.
All values are mean±s.e.mean of four experiments in duplicate.

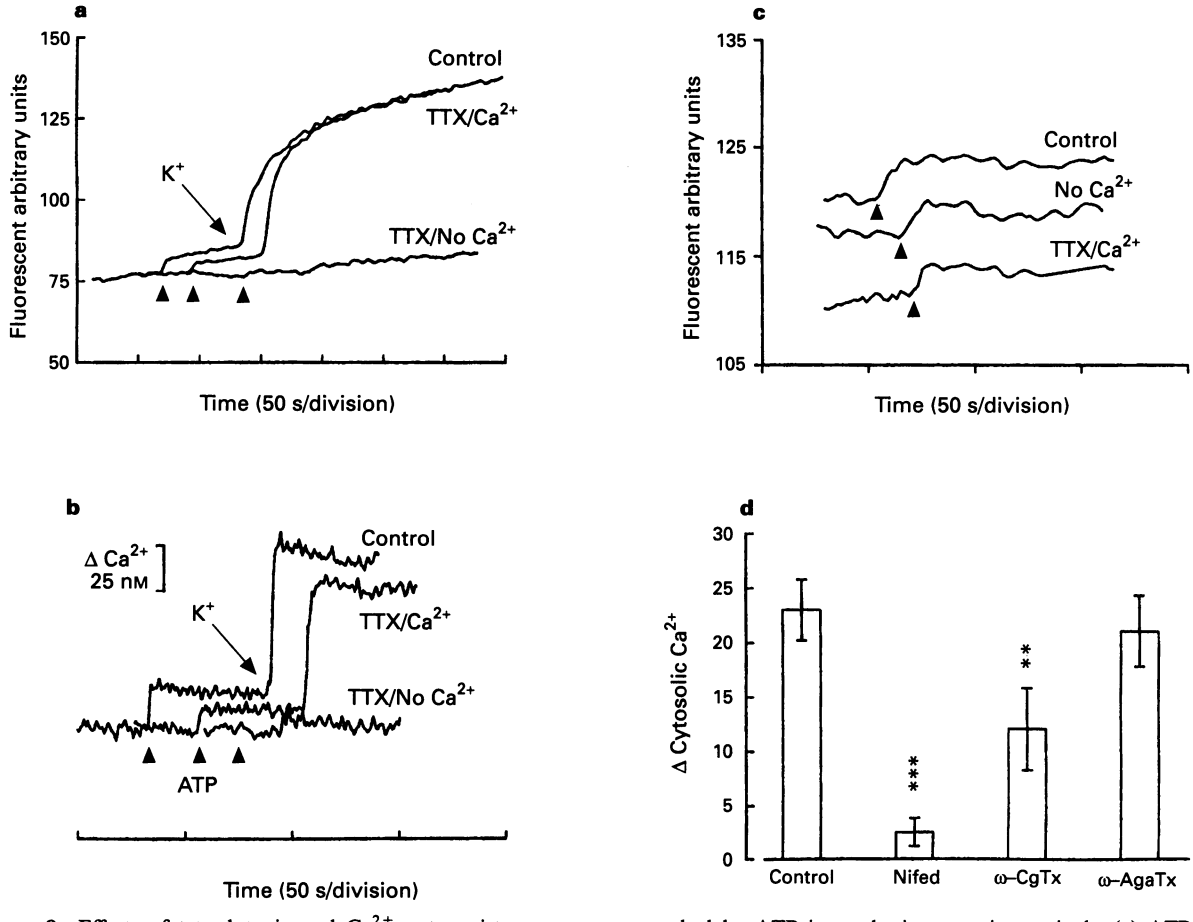

Figure 8 Effects of tetrodotoxin and Ca^{2+} antagonists on responses evoked by ATP in rat brain synaptic terminals: (a) ATP 100 μM induced depolarization which was partially sensitive to 5 μM TTX. (b) The Ca^{2+} influx induced by ATP was also partially inhibited by TTX. (c) Effect of 100 μM ATP on cytosolic Na^+ levels. (d) Ca^{2+} channel blockers, nifedipine, ω-conotoxin G-VI-A and ω-agatoxin IVA, were assayed under the conditions described in Methods. All the experiments represent means of four different experiments in duplicate. $^{**}P<0.01$, $^{***}P<0.001$ vs control. Arrows indicate when ATP was applied. Traces are overlaid examples from different synaptosomal preparations.

crements were nevertheless abolished by nifedipine and by ω-conotoxin G-VI-A (Figure 8d). In conclusion, part of the ATP effects are probably mediated by L and N voltage-dependent calcium channels. The results are summarized in Table 2. All the experiments were performed four times in duplicate.

Discussion

The results described here, concerning the Ca^{2+} signalling, indicate that the diadenosine polyphosphates, Ap_4A and Ap_5A, act via different mechanisms and different receptors, from ATP in synaptosomal preparations of rat midbrain.

The first evidence suggesting the existence of an independent receptor for the dinucleotides from that of ATP is the lack of inhibition of responses to the dinucleotides by suramin. In contrast, the effects of ATP and its analogues were markedly inhibited by this compound. Although this is not a good antagonist for differentiating subtypes of P_2-purinoceptors, it is a useful tool for studying whether or not the effects of diadenosine polyphosphates are mediated by P_2-purinoceptors. Clearly suramin is useful in demonstrating distinct receptors for ATP and diadenosine polyphosphates.

The inability to cross-desensitize the diadenosine polyphosphate responses with ATP or its non-hydrolyzable analogues, together with their additive responses in the intrasynaptosomal Ca^{2+} increase is further evidence for separate receptor populations. The lack of cross-desensitization in rat midbrain synaptosomes, concerning Ca^{2+} signalling, deserves special comment, because the receptors so far described which mediate the actions of diadenosine polyphosphates have also been described as ATP receptors. The effects of Ap_nA compounds in the central nervous system have been described in cortical neurones (Stone & Perkins, 1981), in nodose ganglia neurones (Krishtal *et al.*, 1988) and in rat hippocampal neurones (Klishin *et al.*, 1994). In all these cases the actions described

were probably through P_2-purinoceptors which means they are activated not only by diadeosine polyphosphates but also by ATP. The actions of both compounds in the hippocampus appear to be mediated by PKC activation, implying a metabotropic receptor (Klishin *et al.*, 1994). In the peripheral nervous system, both P_{2X} and P_{2Y} subtypes are stimulated by adenine dinucleotides as well as the P_{2U} receptor present in blood vessel endothelial cells (MacKenzie *et al.*, 1988; Marchenko *et al.*, 1988; Hoyle, 1990; Castro *et al.*, 1994; Pintor & Miras-Portugal, 1994).

The Ca^{2+} signal induced by diadenosine polyphosphates mediated via the purinoceptor present in midbrain synaptic terminals is dependent on extracellular Ca^{2+} levels. Ca^{2+} entry can be split into two components. The first, is a rapid and voltage-independent process, which takes place by the direct action of the dinucleotide on the novel purinoceptor; the second component is sustained and voltage-sensitive. Two facts corroborate this. On the one hand, application of K^+ before an application of Ap_5A abolishes the sustained component but does not affect the initial transient indicating the loss of a voltage-sensitive component. On the other hand, treatment with ω-conotoxin G-VI-A, which blocks the N-type voltage-dependent Ca^{2+} channel (Miller & Fox, 1990; Tsien & Tsien, 1990), mimicks the effect produced by K^+, confirming the voltage-dependency of this second, sustained component.

The initial Ca^{2+} entry induces a depolarization inside the synaptic terminal which opens a voltage-dependent sodium channel as demonstrated by the experiments performed with the sodium fluorophore SBFI dye (Minta & Tsien, 1989). However, the blockade of this voltage-dependent Na^+ channel by tetrodotoxin did not affect either the initial or the sustained voltage-dependent Ca^{2+} entry, indicating the bypassing of this channel when TTX is present in the incubation medium. Thus, the initial Ca^{2+} entry induced by diadenosine polyphosphates is sufficient to activate the ω-CgTx-sensitive N-type Ca^{2+} channel although under normal conditions the voltage-dependent Na^+ channel is also activated. The N-type VDCC, appears to be playing a role in the sustained Ca^{2+} entry after diadenosine polyphosphate stimulation; however the L, P and T types were excluded because of the lack of effects of nifedipine, ω-agatoxin IV-A and Ni^{2+}, respectively (Carbone & Swandulla, 1989; Catteral & Striessnig, 1992; Mintz *et al.*, 1992). This is not the case for ATP, which induced Ca^{2+} entry that could be inhibited by ω-conotoxin G-VI-A and nifedipine. The differential action of calcium channel blockers in the ATP and diadenosine polyphosphate responses represent an additional support for the existence of different receptor populations mediating their responses.

Adenosine, a well known modulator of excitatory neurotransmission in the central nervous system (Barrie & Nicholls, 1993), was able, through A_1 receptors, to modulate the response to diadenosine polyphosphates. Moreover, the experiments carried out in the presence of DPCPX, a well known A_1 antagonist, showed a significant increase in the intrasynaptosomal Ca^{2+} signalling. These results exclude the action of the adenine dinucleotides through A_1 receptors. Although this is only a preliminary result, a careful study of the relationship between neurotransmission and neuromodulation by dinucleotides and nucleotides needs to be carried out.

The existence of a specific receptor for diadenosine polyphosphates in rat brain synaptic terminals supports the putative neurotransmitter role of these substances in the central nervous system. The possible physiological relevance of Ap_nA compounds is beginning to be elucidated both *in vitro* and *in vivo*. Experiments carried out *in vitro* with synaptosomes have demonstrated the presence and release of adenine dinucleotides after stimulation with depolarizing agents (Pintor *et al.*, 1992a). More recently, it has been possible to describe the release of diadenosine polyphosphates *in vivo* induced by amphetamine sulphate (Pintor *et al.*, 1993b). The levels found in the perfusates were 64.5 nM for Ap_4A and 57.5 nM for Ap_5A in the perfusion media. Due to the presence of ecto-enzymes degrading these compounds and their own polyanionic structure, the presence of concentrations several orders of magnitude higher can be assumed at the synaptic cleft (Pintor *et al.*, 1994). In a peripheral model such as chromaffin cells, an extracellular concentration for Ap_4A, Ap_5A and Ap_6A close to 30 μM, for each one, was estimated after stimulation (Pintor *et al.*, 1991; 1992b).

Diadenosine tetraphosphate shows a maximal Ca^{2+} increase, roughly half of that obtained with diadenosine pentaphosphate although in terms of dose-response, the pD_2 values were extremely close, perhaps acting as a partial agonist in this system. On the basis of the binding and displacement studies with labelled Ap_4A, the presence of high and medium affinity binding sites with K_d values in the nM and in the μM range have been described in several neural preparations (Pintor *et al.*, 1991; 1993a). These receptors were termed P_{2D} on the basis of non-agreement of the displacement order with that reported in the literature for the formerly characterized ATP receptors (Pintor *et al.*, 1993a). Nevertheless, on a functional basis, studying the Ca^{2+} response in the midbrain synaptic terminals there appears to be a clear difference between diadenosine polyphosphate- and ATP-mediated actions. The potential for purinergic transmission is in this way significantly increased.

In conclusion, the results reported here show that diadenosine polyphosphates induce Ca^{2+} entry in two ways: firstly, a sharp increase which is voltage-independent and secondly a sustained entry via N-type, voltage-dependent Ca^{2+} channels. The voltage-independent Ca^{2+} entry can be explained either by a receptor-operated calcium channel or through a G protein coupled to a Ca^{2+} channel. Due to the differences with respect to the action of ATP, the novel P-purinoceptor does not appear to be a member of the P_2-purinoceptor family. However, although we believe that the receptor for dinucleotides is different from that for ATP in this preparation, we do not have enough evidence to propose a new name. Ideally we must await the development of a specific or selective antagonist before a firm proposal can be made.

We would like to thank Dr Charles Hoyle for his helpful comments and kind criticism and Miss Jacqueline Rafia and Mr Erik Lundin for their help in the preparation of this manuscript. This work has been supported by a research grant of Dirección General de Investigación Cientifica y Tecnológica (DGICYT) number of PB 92 0230, the Areces Neuroscience programme, 1994 and INTAS no. 822 of the EU. J.P. is a Ramon Areces Foundation fellowship holder.

References

BARRIE, A.P. & NICHOLLS, D.G. (1993). Adenosine A_1 receptor inhibition of glutamate exocytosis and protein kinase C-mediated decoupling. *J. Neurochem.*, **60**, 1081–1086.

BENHAM, C.D. & TSIEN, R.W. (1987). A novel receptor-operated Ca^{2+} permeable channel activated by ATP in smooth muscle. *Nature*, **328**, 275–278.

BURNSTOCK, G. (1990). Noradrenaline and ATP as cotransmitters in sympathetic nerves. *Neurochem. Int.*, **17**, 357–368.

BURNSTOCK, G. (1992). Physiological and pathological roles of purines: an update. *Drug Dev. Res.*, **28**, 195–206.

BURNSTOCK, G. & KENNEDY, C. (1985). Is there a basis for distinguishing two types of purinoceptors? *Gen. Pharmacol.*, **16**, 433–440.

CARBONE, E. & SWANDULLA, D. (1989). Neuronal calcium channels: kinetics, blockade and modulation. *Prog. Biophys. Mol. Biol.*, **54**, 31–58.

CASTRO, E., TOMÉ, A.J.R., MIRAS-PORTUGAL, M.T. & ROSARIO, L.M. (1994). Single cell fura-2 spectrofluoremetry reveals different purinoceptor subtypes coupled to Ca^{2+} influx and intracellular Ca^{2+} release in bovine adrenal chromaffin and endothelial cells. *Pflügers Arch.*, **426,** 524–533.

CATTERAL, W. & STRIESSNIG, J. (1992). Receptor sites for calcium antagonists. *Trends Pharmacol. Sci.*, **13,** 256–262.

COCKCROFT, S. & GOMPERTS, B.D. (1979). ATP induces nucleotide permeability in rat mast cells. *Nature*, **279,** 541–542.

COLMAN, R.W. (1990). ADP receptors in platelets. *Ann. N.Y. Acad. Sci.*, **603,** 198–210.

EDWARDS, F.A., GIBB, A.J. & COLQUHOUN, D. (1992). ATP receptor-mediated currents in the central nervous system. *Nature*, **359,** 144–147.

FORSYTH, K.M., SHINOZUKA, K., BJUR, R.A. & WESTFALL, D.P. (1990). Purine modulation of the norepinephrine release in the rat vas deferens. *Ann. N.Y. Acad. Sci.*, **603,** 507–509.

GORDON, J.L. (1986). Extracellular ATP: effect, sources and fate. *Biochem. J.*, **261,** 309–319.

GRYNKIEWICZ, G., PONIE, M. & TSIEN, R.Y. (1985). A new generation of Ca^{2+} indicators with greatly improved fluorescence properties. *J. Biol. Chem.*, **260,** 3440–3450.

HARDEN, T.K., BOYER, J.L., BROWN, H.A., COOPER, C.L., JEFFS, R.A. & MARTIN, M.W. (1990). Biochemical properties of a P_{2Y}-purinergic receptor. *Ann. N.Y. Acad. Sci.*, **603,** 256–266.

HOYLE, C.H.V. (1990). Pharmacological activity of adenine dinucleotides in the periphery possible receptor classes and transmitter function. *Gen. Pharmacol.*, **21,** 827–831.

HOYLE, C.H.V. (1992). Transmission: purines. In *Autonomic Neuroeffector Mechanisms*. ed. Burnstock, G. & Hoyle, C.H.V., pp. 387–498. Chur, Switzerland: Harwood Academic Press.

HOYLE, C.H.V., CHAPPLE, C. & BURNSTOCK, G. (1989). Isolated human bladder: evidence for an adenine dinucleotide acting on P_{2X}-purinoceptors and for purinergic transmission. *Eur. J. Pharmacol.*, **174,** 115–118.

HOYLE, C.H.V., KNIGHT, G.E. & BURNSTOCK, G. (1990). Suramin antagonizes responses to P_2-purinoceptors agonists and purinergic nerve stimulation in the guinea-pig urinary bladder and taenia coli. *Br. J. Pharmacol.*, **99,** 617–621.

ILLES, P. & NORENBERG, W. (1993). Neuronal ATP receptors and their mechanism of action. *Trends Pharmacol. Sci.*, **14,** 50–54.

KLISHIN, A., LOZOVAYA, N., PINTOR, J., MIRAS-PORTUGAL, M.T. & KRISHTAL, O. (1994). Possible functional role of diadenosine polyphosphates: negative feedback for excitation in hippocampus. *Neuroscience*, **58,** 235–236.

KRISHTAL, O.A., MARCHENKO, S.M., OBUKHOV, A.G. & VOLKOVA, T.M. (1988). Receptors for ATP in rat sensory neurones: the structure-function relationship for ligands. *Br. J. Pharmacol.*, **95,** 1057–1062.

MACKENZIE, I., KIRKPATRICK, K.A. & BURNSTOCK, G. (1988). Comparative study of the action of Ap_5A and α,β-methylene ATP on non-adrenergic, non-cholinergic neurogenic excitation in the guinea pig vas deferens. *Br. J. Phramacol.*, **94,** 699–706.

MARCHENKO, S.M., OBUKHOV, A.G., VOLKOVA, T.M. & TARUSOVA, N.B. (1988). Bis(5'adenosyl)tetraphosphate a partial agonist of the ATP receptors on sensory neurones of the rat. *Neirofiziologia*, **20,** 427–431.

MILLER, R.J. & FOX, A.P. (1990). Voltage-sensitive calcium channels. In *Intracellular Calcium Regulation*. ed. Bronner, F. pp. 97–138. New York: Wiley-Liss.

MINTA, A. & TSIEN, R.W. (1989). Fluorescent indicators for cytosolic sodium. *J. Biol. Chem.*, **264,** 19449–19457.

MINTZ, I., VENEMA, V., SWIDEREK, K., LEE, T., BEAN, B. & ADAMS, M. (1992). P-type calcium channels blocked by the spider toxin ω-Aga-IVA. *Nature*, **355,** 827–829.

O'CONNOR, S.E. (1992). Recent developments in the classification and functional significance of receptors of ATP and UTP. Evidence for nucleotide receptors. *Life Sci.*, **50,** 1657–1664.

O'CONNOR, S.E., DAINTY, I.A. & LEFF, P. (1991). Further classification of ATP receptors based on agonist studies. *Trends Pharmacol. Sci.*, **12,** 137–141.

PINTOR, J. & MIRAS-PORTUGAL, M.T. (1994). P_2 purinoceptors for diadenosine polyphosphates in the nervous system. *Gen. Pharmacol.*, **26,** 229–235.

PINTOR, J., DIAZ-REY, M.A. & MIRAS-PORTUGAL, M.T. (1993a). Ap_4A and ADP-β-S binding to P_2 purinoceptors present on rat brain synaptic terminals. *Br. J. Pharmacol.*, **108,** 1094–1099.

PINTOR, J., DIAZ-REY, M.A., TORRES, M. & MIRAS-PORTUGAL, M.T. (1992a). Presence of diadenosine polyphosphates - Ap_4A and Ap_5A - in rat brain synaptic terminals. Ca^{2+} dependent release evoked by 4-aminopyridine and veratridine. *Neurosci. Lett.*, **136,** 141–144.

PINTOR, J., PORRAS, A., MORA, F. & MIRAS-PORTUGAL, M.T. (1993b). In vivo induced release of diadenosine polyphosphates - Ap_4A and Ap_5A - from basal ganglia of concious rat after amphetamine adminstration. *Neurosci. Lett.*, **150,** 13–16.

PINTOR, J., PORRAS, A., MORA, F. & MIRAS-PORTUGAL, M.T. (1994). Dopamine receptor blockade inhibits the amphetamine induced release of diadenosine polyphosphates - Ap_4A and Ap_5A - from neostriatum of the conscious rat. *J. Neurochem.*, **64,** 670–676.

PINTOR, J., ROTLLÁN, P., TORRES, M. & MIRAS-PORTUGAL, M.T. (1992b). Characterization and quantification of diadenosine hexaphosphate in chromaffin cells: granular storage and secretagogue-induced release. *Anal. Biochem.*, **200,** 296–300.

PINTOR, J., TORRES, M., CASTRO, E. & MIRAS-PORTUGAL, M.T. (1991). Characterization of diadenosine tetraphosphate (Ap_4A) binding sites in cultured chromaffin cells: evidence for a P_{2Y} site. *Br. J. Pharmacol.*, **103,** 1980–1984.

POTTER, P.E. & WHITE, T.D. (1980). Release of adenine 5'-triphosphate from synaptosomes from different regions of rat brain. *Neuroscience*, **5,** 1351–1356.

RALEVIC, V., HOYLE, C.H.V. & BURNSTOCK, G. (1995). Pivotal role of phosphate chain length in vasoconstrictor versus vasodilator action of adenine dinucleotides. *J. Physiol.*, **483,** 703–713.

SHEN, K.Z. & NORTH, R.A. (1993). Excitation of rat locus coeruleus neurons by adenosine 5'-triphosphate: ionic mechanism and receptor characterization. *J. Neurosci.*, **13,** 894–899.

SIMMS, P.J., WAGGONER, A.S., WANG, C.H. & HOFFMAN, J.F. (1974). Studies on the mechanisms by which cyanine dyes measure membrane potential in blood cells and phosphatidylcholine vesicles. *Biochem.*, **13,** 3315–3330.

STONE, T.W. & PERKINS, M.N. (1981). Adenine dinucleotide effect on rat cortical neurones. *Brain Res.*, **229,** 241–245.

TSIEN, R.W. & TSIEN, R.Y. (1990). Calcium channels, stores and oscillations. *Annu. Rev. Cell. Biol.*, **6,** 715–760.

UENO, S., HARATA, N., INOUE, K. & AKAIKE, N. (1992). ATP-gated current in dissociated rat nucleus solitarii neurones. *J. Neurophysiol.*, **68,** 778–785.

VERHAGE, M., BESSELSEN, E., LOPES DA SILVA, F. & GHIJSEN, E. (1989). Ca^{2+} dependent regulation of presynaptic stimulus secretion coupling. *J. Neurochem.*, **53,** 1188–1194.

WHITE, T.D. (1977). Direct detection of depolarization-induced release from a synaptosomal preparation. *Nature*, **267,** 67–68.

ZIMMERMAN, H. (1994). Signaling via ATP in the nervous system. *Trends Pharmacol. Sci.*, **17,** 420–426.

(Received August 8, 1994
Received March 3, 1995
Accepted March 27, 1995)

British Journal of Pharmacology (1995) 115, 903-908 © 1995 Stockton Press All rights reserved 0007-1188/95 $12.00

Mode of action of thrombin in the rabbit aorta

Denis Godin, Francis Rioux, François Marceau & [1]Guy Drapeau

Centre de recherche (Université Laval), Hôtel-Dieu de Québec, 11 Côte du Palais, Québec (Québec), Canada G1R 2J6

1 Thrombin is a vasoactive protease that elicits the contraction of the rabbit aorta by activating a G-protein coupled receptor through cleavage of its N-terminal extracellular domain. Synthetic peptides corresponding to the newly exposed N-terminus, following thrombin cleavage, have been shown to reproduce some of the activities of thrombin in the rabbit aorta.

2 Intracellular pathways involved in the contractile response of the rabbit aorta to thrombin and synthetic peptides were examined by use of a series of inhibitors. A similar method was applied to characterize the mitogenic effect of thrombin on cultured smooth muscle cells (SMCs) derived from the same tissue.

3 Results from this study indicate that the contractile response of the rabbit aorta to thrombin is dependent on the activation of protein kinase C (PKC) and independent of extracellular calcium. The contractile response to thrombin can be fully reproduced by peptide agonists related to the N-terminal receptor sequence. However, subtle differences seem to exist between the mechanism of the contractile effect of thrombin and of the synthetic peptides, as both PKC activation and extracellular calcium were found to participate in the contractile effect of the synthetic peptides.

4 In cultured SMCs, both thrombin and the synthetic peptides increased inositol phosphate turnover; however, only thrombin elicited a mitogenic effect, which occurs at thrombin concentrations well below those needed to increase inositol phosphate turnover significantly. Activation of a tyrosine kinase pathway is involved in the mitogenic effect of thrombin on aortic SMCs.

5 Altogether these results suggest the existence of subtle differences between the mode of action of thrombin and of synthetic peptides related to the N-terminal thrombin receptor sequence, in the rabbit aorta.

Keywords: Thrombin; thrombin cleavable receptor; smooth muscle cells; rabbit aorta

Introduction

α-Thrombin is a key enzyme involved in blood coagulation and although its activity on soluble substrates in the circulation has been extensively studied, thrombin also exhibits hormone-like activity in many cell types (for review see Fenton, 1988 and Coughlin *et al.*, 1992). The cloning of a receptor mediating some of these activities has revealed a new class of G-protein coupled receptors that are activated by limited proteolysis of the N-terminal extracellular domain (Vu *et al.*, 1991); a second receptor that is activated in a similar way has recently been described (Nystedt *et al.*, 1994). These receptors can be activated by synthetic peptides, as short as five or six amino acids, such as Ser-Phe-Leu-Leu-Arg-Asn-NH_2 (NAT_6-NH_2) for the thrombin receptor (Hui *et al.*, 1992), corresponding to the newly generated aminoterminus receptor sequence following proteolytic cleavage.

Thrombin is a modulator of vessel tone that can act by either endothelium-dependent or -independent mechanism and the relaxation or contraction induced by thrombin can be reproduced by synthetic agonists of the cleavable receptor. In the intact rat aorta peptide agonists are relaxing agents (Yang *et al.*, 1992); however, contractile responses are observed when the endothelium is removed (Antonaccio *et al.*, 1993). Stimulation of the dog coronary arteries by an agonist of the thrombin cleavable receptor also produces an endothelium-dependent relaxation that is transformed into a contractile response in the absence of endothelium (Ku & Zaleski, 1993). In the rabbit aorta thrombin, NAT_6-NH_2 and an aminopeptidase resistant analogue, [Sar[1]]NAT_6-NH_2 (Godin *et al.*, 1994), produce a dose-dependent contraction suggesting that the cleavable receptor is involved in this activity.

Thrombin has also been found to exert mitogenic activity in several cell types (Fenton, 1988). However, intracellular signals generated by peptide agonists of the cleavable receptor seem insufficient to induce mitosis in hamster fibroblasts (Vouret-Craviari *et al.*, 1992). In an effort to characterize further the second messengers involved in the contractile response of the rabbit aorta, following stimulation by either thrombin or agonist peptides, we have evaluated the effect of different inhibitors in the presence of these contractile agents. We have also used these inhibitors to characterize second messengers activated following stimulation by thrombin or agonist peptides of cultured vascular smooth muscle cells (SMCs) derived from the rabbit aorta. Our results reveal a difference in the way contractile responses are obtained through activation by thrombin or peptide agonists and that a proliferative response of SMCs derived from the aorta is obtained only by stimulation with thrombin.

Methods

Organ bath pharmacology

The thoracic aorta was isolated from New Zealand White rabbits of either sex (1.5-2 kg). The vessels were cut into rings (2-3 mm width), suspended between a metal hook and a thread loop under a basal tension of 2 g in 5 ml organ chambers containing oxygenated (95% O_2:5% CO_2) and warmed (37°C) Krebs solution (Marceau *et al.*, 1991). Their responses to agents were recorded isometrically as described previously (Bouthillier *et al.*, 1987).

The mechanism of the contractile effect of the thrombin receptor agonist, [Sar[1]]NAT_6-NH_2 was analysed by applying a submaximal concentration (40 μM) of this peptide to the tissues after an equilibration period of 2 h. The concentration-effect relationship for this agent can be found elsewhere (Godin *et al.*, 1994). Inhibitory drugs were applied 30 min before each agonist and paired control tissues were used to

[1] Author for correspondence.

evaluate the effect, if any, of the drug vehicle. The same tissues were also challenged at 4 and 6 h by thrombin (60 nM) and KCl (20 mM), respectively, for purposes of comparison. The drugs used in this study were nifedipine, an L-type Ca^{2+} channel blocker (Murad, 1990), H-7, a protein kinase inhibitor (Hidata *et al.*, 1984), diclofenac, a cyclo-oxygenase inhibitor (Lewis & Furst, 1987), erbstatin, a tyrosine kinase inhibitor (Imoto *et al.*, 1987) and D-Phe-Pro-Arg-CH_2Cl (PPACK), an irreversible inhibitor of the catalytic activity of thrombin (Kettner & Shaw, 1979). The concentrations of the drugs were chosen according to their reported activity in various *in vitro* systems (Levesque *et al.*, 1993). The effect of the kinase inhibitor, H-7, was further documented over a wide range of concentrations of the thrombin receptor agonists; cumulative concentration-effect curves for [Sar^1]NAT_6-NH_2 and thrombin were constructed. In order to evaluate the contribution of the endothelium in the contractile response to each agent, the endothelium was carefully removed by rubbing with a metal spatula. The tissues were controlled by assessing the loss of the relaxant effect of acetylcholine (Furchgott & Zawadzki, 1980). We also replaced the Krebs solution by a calcium-free form to evaluate the contribution of extracellular calcium to the contractile effect of each agent. The Krebs solution was replaced by the calcium-free form 10 min before each contractile stimulation and the tissue preparation was maintained in normal Krebs solution between tests to avoid depletion of intracellular Ca^{2+} pools.

Cell culture

Several distinct lines of rabbit SMCs were established from rabbit aorta aseptically removed from freshly killed animals. The tissues (approximate weight 200 mg) were incubated at 37°C for 1.5 h in medium 199 (Gibco) supplemented with 10% foetal bovine serum (FBS; Gibco), antibiotics (streptomycin, 50 $\mu g\ ml^{-1}$, and penicillin 50 u ml^{-1}; Gibco), bacterial collagenase (type IA, 3 $mg\ ml^{-1}$) and elastase (type III, 1 $mg\ ml^{-1}$); all enzymes were obtained from Sigma (St-Louis, MO, U.S.A.). Dispersed cells and partly digested tissue fragments were centrifuged and resuspended in medium 199 supplemented with 10% FBS and antibiotics. This suspension was seeded directly in 25 cm^2 flasks coated with 0.2% gelatin. Cells were passaged on gelatin-coated surfaces at confluency with a brief trypsin (0.05%)/EDTA (0.53 mM) treatment. The cells were studied at passages 3 to 7 only.

[^{3}H]-thymidine incorporation

Cells, in Medium 199 containing 10% FBS, were plated at an initial density of 3×10^4 cells per well in gelatin-coated 12-well disposable plastic plates (Costar). The cells were growth-arrested, by incubation for 72 h in medium 199 containing 0.4% FBS, before being exposed to thrombin, NAT_6-NH_2, [Sar^1]-NAT_6-NH_2, FBS or to various drugs for 48 h. Enhanced thymidine incorporation was assessed after a 24 h exposure to [^{3}H]-thymidine (Dupont, Mississauga, Ont. Canada; 0.1 $\mu Ci\ ml^{-1}$; specific activity 84 Ci $mmol^{-1}$). The cells were then washed twice with saline, harvested with trypsin (0.05%)/EDTA (0.53 mM) and collected in borosilicate test tubes. The wells were rinsed once with 1 ml Triton X-100 1%/saline and nucleic acids precipitated with 1 ml trichloroacetic acid 40%/water. After a 20 min centrifugation at 2,700 *g*, the supernatant was withdrawn and the pellet resuspended in 1 ml distilled water, placed into scintillation vials containing 10 ml Ecolite + scintillation fluid (ICN Biomedicals, Irvine CA, U.S.A.) and counted in a liquid scintillation counter (Beckman LS 8000).

Inositol phosphate production

Labelling and stimulation of rabbit aorta SMCs were carried out according to Balla *et al.* (1988) with some modifications. Briefly, cells in medium 199 supplemented with 10% FBS and antibiotics, were seeded at a density of 2.5×10^5 in 2 cm^2 wells and cultured for 24 h. The cells were then washed three times with serum-free medium. The incorporation medium (500 μl) consisted of medium 199 containing 20 $\mu Ci\ ml^{-1}$ of *myo*-[^{3}H]-inositol (Amersham, specific activity 82 Ci $mmol^{-1}$), was added to the wells for a labelling period of 16–20 h. After incubation at 37°C in a humidified atmosphere containing 5% CO_2, each well was washed twice with Earle's balanced salt solution (EBSS). The cells were further incubated for 20 min in EBSS with 10 mM LiCl then challenged with thrombin or NAT_6-NH_2 at different concentrations for exactly 5 min. Stimulation was terminated by the addition of perchloric acid (final concentration 5%).

Inositol phosphates were extracted and separated as previously described (Guillemette *et al.*, 1989). At the end of the experiment, the cells were kept on ice for 30 min and then scraped from the wells and transferred into tubes. The wells were rinsed with additional perchloric acid (5% W/V) and the resulting media was centrifuged at 10,000 *g* for 5 min. Perchloric acid was extracted from the supernatant with a 1 : 1 mixture of Freon and tri-n-octylamine (Downes *et al.*, 1986; reagents from Sigma). After neutralization, the samples were applied to anion exchange resin (Dowex AG 1-X8 formate, 200–400 mesh, Bio-Rad No. 140-1450) columns (1 ml bed volume) for the separation of the inositol phosphates according to Berridge *et al.* (1983). The inositol phosphates were sequentially eluted with 3 × 5 ml of distilled water (free inositol), 3 × 5 ml of 0.2 M ammonium formate/0.1 M formic acid (inositol monophosphates, IP_1), 3 × 5 ml of 0.5 M am-

Table 1 Pharmacological analysis of the mode of action of thrombin and the thrombin receptor agonist [Sar^1]NAT_6-NH_2 in the rabbit aortic preparation

		Contractile responses (g)		
Treatment	n	*[Sar^1]NAT_6-NH_2* (40 μM)	*Thrombin* (60 μM)	*KCl* (20 μM)
Intimal damage	6	2.21 ± 0.12	1.69 ± 0.35	2.34 ± 0.58
Control	6	1.81 ± 0.19	1.64 ± 0.46	2.59 ± 0.53
Nifedipine 100 nM	8	1.12 ± 0.09*[a]	0.77 ± 0.09	0.31 ± 0.05***
Vehicle (Ethanol)	8	1.59 ± 0.13	0.75 ± 0.09	2.74 ± 0.31
Calcium-free Krebs	6	1.16 ± 0.19*	0.91 ± 0.24	0.51 ± 0.13***
Control	6	1.75 ± 0.10	0.97 ± 0.14	2.92 ± 0.24
Diclofenac 0.5 μM	8	1.63 ± 0.14*	0.64 ± 0.03	2.55 ± 0.28
Vehicle (Na_2CO_3)	8	1.41 ± 0.13	0.67 ± 0.05	2.42 ± 0.24
Erbstatin analogue	4	2.19 ± 0.31	1.75 ± 0.36	3.41 ± 0.42
Vehicle (DMSO)	4	2.28 ± 0.24	1.80 ± 0.47	3.34 ± 0.20
PPACK 1 μM	8	1.51 ± 0.28	0.03 ± 0.02*	1.25 ± 0.17
Vehicle (saline)	8	1.11 ± 0.23	1.30 ± 0.41	1.22 ± 0.18

[a] Values in each treated group were compared to controls from the same animals by Student's *t* test for paired samples: *$P < 0.05$; **$P < 0.01$; ***$P < 0.001$.

monium formate/0.1 M formic acid (inositol biphosphates, IP_2), 3 × 5 ml of 0.8 M ammonium formate/0.1 M formic acid (inositol trisphosphates, IP_3) and 3 × 5 ml of 1.0 M ammonium formate/0.1 M formic acid (inositol tetrakisphosphates, IP_4). The fractions were collected, mixed with Ecolite + scintillation fluid and counted for radioactivity in a liquid scintillation counter.

Reagents

The following drugs were purchased from Sigma (St-Louis MO, U.S.A.): nifedipine, diclofenac, PPACK, PGE_2 (prostaglandin E_2) and PMA (phorbol 12-myristate 13-acetate). Erbstatin analogue and H-7 (1-(5-isoquinolinesulphonyl)-2-methylpiperazine) were purchased from Biomol Res. Lab. Inc. (Plymouth Meeting PA, U.S.A.) Wortmannin was from Calbiochem (San Diego, CA, U.S.A.), iloprost from Berlex Canada Inc. (Lachine QC, Canada) and Thrombostat (bovine thrombin) from Parke-Davis (Scarborough ON, Canada). NAT_6-NH_2 and [Sar^1]NAT_6-NH_2 were synthesized in our laboratory by solid phase peptide synthesis methods. Their homogeneity was assessed by high performance liquid chromatography and their identity confirmed by mass spectrometry.

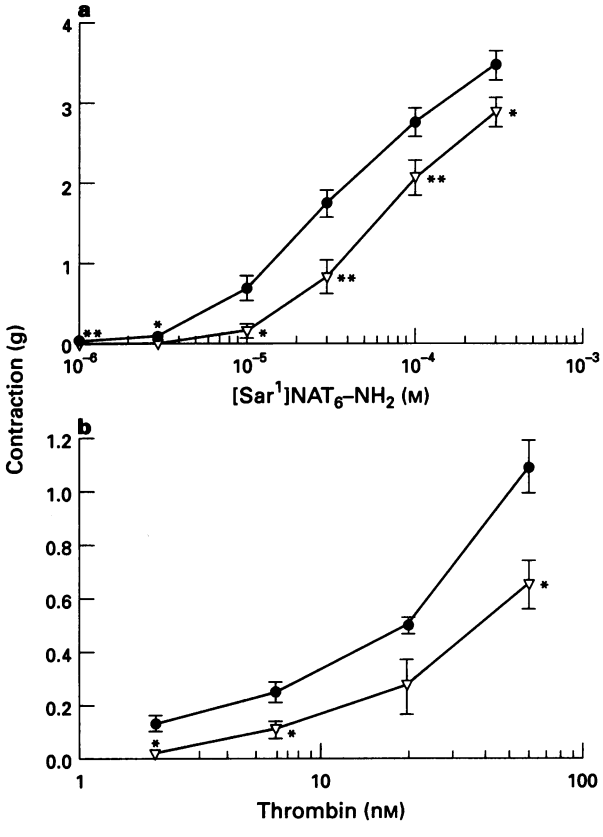

Figure 1 Effect of H-7 (▽ 10 μM) on the cumulative dose-response curve for [Sar^1]NAT_6-NH_2 (a) and thrombin (b). The results are expressed in g of developed contraction. Values are the mean ± s.e.mean of at least 6 determinations. Statistical analysis by Student's *t* test for paired samples: $*P<0.05$; $**P<0.001$ (● control responses).

Results

Contractility studies

A series of experiments using rabbit aortic rings was carried out to compare the mode of action of thrombin with an aminopeptidase resistant agonist of the thrombin cleavable receptor, [Sar^1]NAT_6-NH_2 (Godin *et al.*, 1994), and KCl used as a control agonist. Submaximal concentrations of these agonists were chosen based on previous experiments (Godin *et al.*, 1994; Levesque *et al.*, 1993). In order to avoid any tachyphylaxis, [Sar^1]NAT_6-NH_2 was always the first agonist injected after an equilibration period of 2 h, followed by thrombin and KCl successively with an interval of 2 h between agonists. Paired controls were used to evaluate the effect of solvents. All inhibitory drugs were applied 30 min before recording the response to each agonist.

As shown in Table 1, intimal damage did not modify the response to these agonists while it completely blocked the relaxation induced by acetylcholine, used as a control, of tissues pre-contracted with phenylephrine (data not shown). Nifedipine, the voltage-operated calcium channel blocker, was inactive against the thrombin-induced contraction of the rabbit aorta whereas a partial inhibition of the contraction induced by [Sar^1]NAT_6-NH_2 was observed. Extensive inhibition of the depolarizing agent KCl occurred in the same tissues, thus providing an internal control for the effectiveness of the drug in our assay. The contraction induced by KCl was profoundly affected in the presence of a Krebs solution devoid of calcium while the contraction induced by [Sar^1]NAT_6-NH_2 was reduced to 2/3 of the control and the effect of thrombin was left unchanged by calcium removal.

Diclofenac, an inhibitor of fatty acid cyclo-oxygenase, and the erbstatin analogue, an inhibitor of tyrosine kinases, did not have any depressant effect on the contraction induced by the three agonists presented in Table 1. An inhibitor of the catalytic activity of thrombin, PPACK, completely prevented the

Table 2 Inositol phosphates measurements in rabbit aortic smooth muscle cells 5 min after exposure to different concentrations of thrombin or NAT_6-NH_2[a]

	Inositol phosphates (c.p.m. per well)			
Stimulus	IP_1	IP_2	IP_3	IP_4
Control	6995 ± 1381	765 ± 140	328 ± 21	308 ± 66
Thrombin 10 nM	8277 ± 1743	929 ± 97	473 ± 32**	273 ± 24
Thrombin 100 nM	6038 ± 1547	1377 ± 371	509 ± 79	236 ± 39
Thrombin 1000 nM	11077 ± 1552	3074 ± 372**	1263 ± 104***	393 ± 41
NAT_6-NH_2 10 μM	6691 ± 1579	1714 ± 318*	684 ± 124*	271 ± 38
NAT_6-NH_2 100 μM	13504 ± 2531*	4351 ± 636***	1694 ± 145***	392 ± 24
Analysis of variance[b]	NS	$P<0.0001$	$P<0.0001$	$P<0.05$

[a] Smooth muscle cells from 3 different cell lines were used at passage 4 or 5 (values are the means ± s.e.mean of 9 experiments composed of triplicate determinations). The results have been normalized as c.p.m. of IP per 100,000 c.p.m. of the remaining cell-associated *myo*-inositol in each cell well.

[b] One-way analysis of variance was performed on each column (NS, not significant). Mann-Whitney's test was then applied to compare the effect of each treatment with the control cells: $*P<0.05$; $**P<0.01$; $***P<0.001$.

contraction of the rabbit aorta by thrombin at a concentration of 1 μM. The activities of the peptide agonist and of KCl were not influenced by this inhibitor.

Following the observation that single doses of thrombin or [Sar^1]NAT$_6$-NH$_2$ were affected by the protein kinase inhibitor H-7, full cumulative concentration-effect curves for these agonists were established in the presence of this inhibitor. As shown in Figure 1, H-7 (10 μM) significantly depressed all concentrations of thrombin and [Sar^1]NAT$_6$-NH$_2$. Previous experiments on the same tissue have also shown that H-7 significantly reduced the contraction to PMA while it affected only minimally contractions induced by KCl (Levesque *et al.*, 1993).

Cellular model of vascular effects

Evidence was obtained that cultured SMCs derived from the rabbit aorta respond to thrombin and NAT$_6$-NH$_2$ by inducing inositol phosphate (IP) turnover (Table 2). Significant increases in the production of IP$_2$ and IP$_3$ were observed in cells stimulated with thrombin. Although a dose-dependent effect is observed for thrombin, significant values were obtained only at concentrations of 10 and 1000 nM for IP$_3$ formation and 1000 nM for IP$_2$. NAT$_6$-NH$_2$ increased IP$_1$, IP$_2$ and IP$_3$ formation with a significant dose-dependent relation for both IP$_2$ and IP$_3$. Thrombin, NAT$_6$-NH$_2$ and [Sar^1]NAT$_6$-NH$_2$ were also tested for their ability to induce the incorporation of [^{3}H]-thymidine in quiescent cells of the same origin that were maintained in 0.4% FBS. Thrombin stimulated the incorporation of thymidine in these cells in a dose-related manner (Figure 2), with maximum incorporation attained at a dose of 10 nM while NAT$_6$-NH$_2$ and [Sar^1]NAT$_6$-NH$_2$ at doses in excess of 100 μM failed to produce any significant thymidine incorporation in these cells. Several inhibitors were tested for their ability to modulate the thrombin-induced DNA synthesis into rabbit cultured aortic SMCs (Table 3). Previous experiments had shown that diclofenac, an inhibitor of fatty acid cyclo-oxygenase, was useful in revealing agonist-induced thymidine incorporation in this model (Levesque *et al.*, 1993). As shown in Table 3 diclofenac (0.5 μM) revealed maximum expression of thymidine incorporation following stimulation with thrombin. In the presence of diclofenac, PGE$_2$ and iloprost (a PGI$_2$ analogue) produced a partial inhibition of DNA synthesis in cells stimulated by thrombin. Nifedipine produced a significant increase of thymidine incorporation in both control and thrombin-stimulated cells. A slight increase was also observed with PMA while wortmannin, a phospholipase D inhibitor, did not produce any significant inhibition of thrombin-stimulated thymidine incorporation. At a dose of 10 μM the PKC inhibitor, H-7, was without effect on either control or thrombin-stimulated cells, however, H-7, at a higher dose (30 μM) and the erbstatin analogue (a tyrosine kinase inhibitor) reduced the effect of thrombin to baseline values. At the same dose, H-7 also reduced DNA synthesis in control cells.

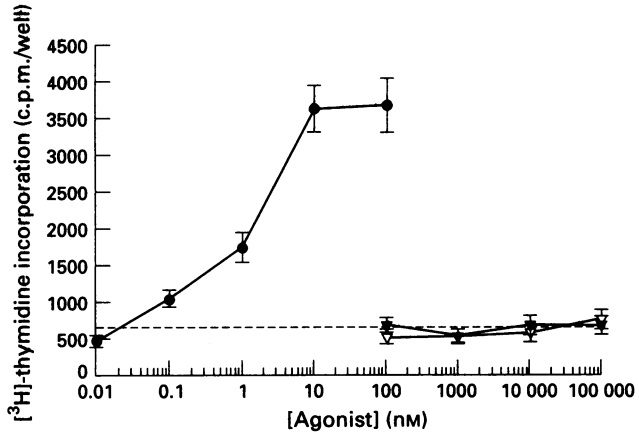

Figure 2 Effect of thrombin (●), NAT$_6$-NH$_2$ (▽) and [Sar^1]-NAT$_6$-NH$_2$ (▼) on the synthesis of DNA in cultured rabbit vascular smooth muscle cells. Data presented are the mean ± s.e. of several experiments involving triplicate determinations. Dashed line represents basal incorporation (0.4% FBS).

Table 3 [^{3}H]-thymidine incorporation by rabbit aortic smooth muscle cells[a]

Treatment	*Control*	*Thrombin stim. cells* (1 nM)
Control	661 ± 112	1891 ± 237
Diclofenac 0.5 μM	709 ± 112	2367 ± 301
+ PGE$_2$ 0.3 μM	666 ± 81	1371 ± 130
+ Iloprost 0.3 μM	525 ± 55	1451 ± 195
+ Nifedipine 0.1 μM	871 ± 101*	2995 ± 325**
+ Wortmannin 10^{-7} M	685 ± 90	2162 ± 228
+ PMA 1 μg ml^{-1}	798 ± 74*	NT
+ H-7 10 μM	808 ± 123	2633 ± 432
+ H-7 30 μM	360 ± 66**	676 ± 187***
+ Erbstatin analogue 10 μM	484 ± 147	705 ± 127*
ANOVA	$P < 0.0001$	$P < 0.0001$

[a] Values are the mean ± s.e.mean of at least 12 determinations from 4 separate experiments with different cell lines at passages 4 and 5 (NT: not tested). One-way analysis of variance was performed on each column. Mann-Whitney's test was then applied in each column to compare the effect of each treatment with the baseline or the thrombin-stimulated thymidine incorporation respectively (first line; *$P < 0.05$; **$P < 0.01$; ***$P < 0.001$). The effect of thrombin treatment alone within each treated group was assessed by Student's t test and was significant ($P < 0.0001$) for all groups except H-7 (30 μM) and erbstatin analogue-treated groups.

Discussion

The comparative mode of action of thrombin and a synthetic agonist of the cleavable receptor for thrombin, either NAT$_6$-NH$_2$ or [Sar^1]NAT$_6$-NH$_2$ was investigated using a fresh rabbit aortic preparation (contractility assay) and cultured SMCs derived from the same tissue (IP turnover, mitosis). Vascular responses to thrombin seem to vary according to species; some vascular beds, such as pig and dog coronary arteries or dog saphenous veins respond to thrombin, or an agonist peptide of the cleavable receptor, with an endothelium-dependent relaxation that is mediated by the release of nitric oxide and a endothelium-indendent contraction (Tesfamariam *et al.*, 1993; Ku & Zaleski, 1993). The contractile response of the rabbit isolated aorta to thrombin and [Sar^1]NAT$_6$-NH$_2$ is mediated by smooth muscle since mechanical removal of the endothelium did not affect the response to either agonists or to KCl used as a control agonist (Table 1).

As the contractile response of the rat aorta has been shown to be dependent on extracellular calcium, we investigated whether the rabbit aorta operates in a similar manner. A sustained contraction was observed with thrombin in the absence of extracellular calcium in the bathing fluid, while the contraction to KCl, a depolarizing stimulus dependent on extracellular Ca^{2+} (Cauvin *et al.*, 1983), was inhibited by almost 90% on calcium removal. In the same conditions a modest inhibition of the contraction to the agonist peptide, [Sar^1] NAT$_6$-NH$_2$ was observed. The partial inhibition of the contractile activity of this peptide by calcium removal was also in the same order as that produced by the calcium channel blocker nifedipine. While nifedipine had no effect on the contraction to thrombin, it abolished the KCl-induced contraction, which is consistent with the inhibitory effect of this drug on the voltage-operated calcium channel (Murad, 1990). It is worth noting that the responses to thrombin and agonists of the cleavable receptor of the rabbit and rat aorta differ in

several respects. First of all, human or rat thrombin have no effect on the rat aorta, which on the other hand responds to synthetic agonists of the thrombin cleavable receptor (Antonaccio *et al.*, 1993). Aside from showing an endothelium-dependent relaxation, which is not observed in the rabbit aorta, contractile responses of the rat aorta to peptide agonists rely on extracellular Ca^{2+} while in the rabbit preparation the effect of thrombin is independent of extracellular Ca^{2+} and the contraction to [Sar^1]NAT_6-NH_2 is only partially affected by Ca^{2+} removal or blockade of Ca^{2+} channels by nifedipine. The partial inhibition of [Sar^1]-NAT_6-NH_2-induced contractile responses by Ca^{2+} removal or nifedipine in the rabbit aorta may indicate that receptor activation by the peptide agonist, which does not involve proteolysis, may be more dependent on extracellular Ca^{2+} than activation following cleavage of the receptor by thrombin. It may also be due to the activation of another receptor that is insensitive to the proteolytic action of thrombin. A second G-protein coupled receptor that is proteolitically activated has recently been cloned from a mouse genomic library (Nystedt *et al.*, 1994). Although the endogenous protease that presumably activates this receptor has not been identified, this receptor is insensitive to thrombin but may be activated by trypsin. Like the thrombin receptor, it is also activated by a synthetic hexapeptide, Ser-Leu-Ile-Gly-Arg-Leu corresponding to the newly exposed N-terminus following proteolytic cleavage. Also structure-activity studies on rat and guinea-pig tissues using a series of peptide analogues suggest the existence of thrombin receptor subtypes for peptides related to NAT_6-NH_2 (Hollenberg *et al.*, 1993).

Data obtained in rabbit aortic rings also suggest the involvement of protein kinase(s) in the contractions provoked by thrombin or [Sar^1]NAT_6-NH_2. Protein kinase C is inhibited by H-7 (Hidata *et al.*, 1984), and accordingly has been shown to reduce the contractile effect of PMA, a direct activator of protein kinase C, in aortic rings (Levesque *et al.*, 1993). H-7, in the same assay, also shifted the concentration-response curve to both [Sar^1]NAT_6-NH_2 and thrombin (Figure 1). However, the use of H-7 as a protein kinase C inhibitor has some limitations owing to other inhibitory effects of this drug, as for example, on cyclic nucleotide-dependent protein kinases (Hidata *et al.*, 1984). While the contractile response of the rabbit aorta to thrombin has been shown to act synergistically with that of EGF the receptor for which is a tyrosine kinase (Deblois *et al.*, 1992), erbstatin, an inhibitor of this type of receptor did not block the responses of any of the agonists in Table 1. As previously observed (Deblois *et al.*, 1992), PPACK, in accordance with its inhibition of the catalytic site of thrombin, did block the contractile effect of the latter while it had no effect on [Sar^1]NAT_6-NH_2-induced contraction.

SMCs derived from the rabbit aorta and cultured over weeks retained the capacity to respond to both the agonist of the cleavable receptor, in this case NAT_6-NH_2, and to thrombin by the generation of phosphoinositides. The increased IP concentration after 5 min exposure to either agonist, evidence of the activation of phospholipase C, was obtained at concentrations comparable to those used for the contractile response of isolated tissues (Table 1; Godin *et al.*, 1994). The activation of phospholipase C following stimulation of the cleavable receptor by NAT_6-NH_2 is consistent with the participation of diacylglycerol-regulated protein kinase C in the contractile effect of this peptide and of thrombin as referred to above with the use of the protein kinase inhibitor H-7 (Figure 1). Significant increases in IP_2 and IP_3 occurred at both concentrations of NAT_6-NH_2 tested and a graded response is observed. A dose-dependent IP production was also observed in cells stimulated with thrombin although significant only for IP_3. Here also the doses used to obtain this response are similar to those necessary to contract the rabbit aorta (Godin *et al.*, 1994).

Although the response of cultured rabbit SMCs to thrombin and NAT_6-NH_2 is similar, with regard to IP breakdown, only thrombin could induce DNA synthesis in these cells (Figure 2). NAT_6-NH_2 or [Sar^1]NAT_6-NH_2 at doses up to 100 μM did not provoke any significant [^{3}H]-thymidine incorporation whereas with thrombin, a full concentration-effect curve was obtained with a threshold dose as small as 0.1 nM while a full effect was obtained at 10 nM. Interestingly the concentrations of thrombin needed to produce the incorporation of thymidine seem well below those needed to induce IP breakdown or contraction of the isolated aorta (Table 2; Godin *et al.*, 1994). There are also other indications that the intracellular pathways involved in DNA synthesis in rabbit SMCs are at least partly different from those mediating the contractile response to thrombin. DNA synthesis was blocked by the erbstatin analogue while this tyrosine kinase inhibitor had no effect on the contractile response. H-7, at a concentration of 10 μM, can shift the contractile dose-response curve to both [Sar^1]NAT_6-NH_2 and thrombin but does not affect DNA synthesis. At 30 μM the effect of H-7 on thymidine incorporation is probably of a toxic nature as control cells were also affected.

Within the limitations of our pharmacological approach, the contractile response of the rabbit aorta to thrombin seems to be mediated by the activation of PKC and can be reproduced with synthetic agonists. However mitogenic responses to thrombin, of cultured vascular SMCs derived from this tissue, require a tyrosine kinase signal that is not generated by stimulation of the cleavable receptor with peptide agonists. These findings agree with observations in hamster fibroblasts where peptide agonists of the thrombin receptor do not reproduce the mitogenic effect of thrombin (Vouret-Craviari *et al.*, 1993). The inhibition of the mitogenic effect of thrombin in our cultured cells by erbstatin indicates that a tyrosine kinase signal is essential for cell proliferation in this model. Tyrosine kinase activity is also required for the mitogenic activity of thrombin on neonatal rat vascular SMCs but is not needed for intracellular calcium release (Weiss & Nuccitelli, 1992). How this signal is generated in rabbit vascular SMCs whether through another type of receptor or through the autocrine release of a growth factor (Weiss & Maduri, 1993) remains to be established.

Supported by the Medical Research Council of Canada (grant MT-12570) and by the Québec Heart Foundation. F.M. and G.D. are Scholars of the 'Fonds de la recherche en Santé du Québec' and D.G. is a recipient of a Studentship from the same agency.

References

ANTONACCIO, M.J., NORMANDIN, D., SERAFINO, R. & MORELAND, S. (1993). Effects of thrombin and thrombin receptor activating peptides on rat aortic vascular smooth muscle. *J. Pharmacol. Exp. Ther.*, **266**, 125–132.

BALLA, T., BAUKAL, A.J., GUILLEMETTE, G. & CATT, K.J. (1988). Multiple pathways of inositol polyphosphate metabolism in angiotensin-stimulated adrenal glomerulosa cells. *J. Biol. Chem.*, **263**, 4083–4091.

BERRIDGE, M.J., DAWSON, R.M.C., DOWNES, C.P., HESLOP, J.P. & IRVINE, R.F. (1983). Changes in the levels of inositol phosphates after agonist-dependent hydrolysis of membrane phosphoinositides. *Biochem. J.*, **212**, 473–482.

BOUTHILLIER, J., DEBLOIS, D. & MARCEAU, F. (1987). Studies on the induction of pharmacological responses to des-Arg^9-bradykinin *in vitro* and *in vivo*. *Br. J. Pharmacol.*, **92**, 257–264.

CAUVIN, C., LOUTZENHISER, R. & VAN BREEMEN, C. (1983). Mechanisms of calcium-antagonist-induced vasodilation. *Annu. Rev. Pharmacol. Toxicol.*, **23**, 373–396.

COUGHLIN, S.R., T-KH., VU, D.T., HUNG, & WHEATON, V.I. (1992). Characterization of the cloned platelet thrombin receptor: issues and opportunities. *J. Clin. Invest.*, **89**, 351–355.

DEBLOIS, D., DRAPEAU, G., PETITCLERC, E. & MARCEAU, F. (1992). Synergism between the contractile effect of epidermal growth factor and that of des-Arg^9-bradykinin or of α-thrombin in rabbit aortic rings. *Br. J. Pharmacol.*, **105**, 939–967.

DOWNES, C.P., HAWKINS, P.T. & IRVINE, R.F. (1986). Inositol 1,3,4,5-tetrakiphosphate and not phosphatidylinositol 3,4-biphosphate is the probable precursor of inositol 1,3,4-trisphosphate in agonist-stimulated parotid gland. *Biochem. J.*, **258**, 501–506.

FENTON II, J.W. (1988). Regulation of thrombin generation and function. *Semin. Thromb. Hemost.*, **14**, 234–240.

FURCHGOTT, R.F. & ZAWADZKI, J.V. (1980). The obligatory role of endothelial cells in the relaxation of arterial smooth muscle by acetylcholine. *Nature*, **288**, 373–376.

GODIN, D., MARCEAU, F., BEAULÉ, C., RIOUX, F. & DRAPEAU, G. (1994). Aminopeptidase modulation of the pharmacological responses to synthetic thrombin antagonists. *Eur. J. Pharmacol.*, **253**, 225–230.

GUILLEMETTE, G., LAMONTAGNE, S., BOULAY, G. & MOUILLAC, B. (1989). Differential effects of heparin on inositol 1,4,5-triphosphate binding, metabolism and calcium release activity in the bovine adrenal cortex. *Mol. Pharmacol.*, **35**, 339–344.

HIDATA, H., INAGAKI, M., KAWAMOTO, S. & SASAKI, Y. (1984). Isoquinolinesulfonamides, novel and potent inhibitors of cyclic nucleotide dependent protein kinases and protein kinase C. *Biochemistry*, **23**, 5036–5041.

HOLLENBERG, M.D., ADEBAYO, A., LANIYONU, M.S. & MOORE, G.J. (1993). Role of the amino- and carboxyl-terminal domains of thrombin receptor-derived polypeptides in biological activity in vascular endothelium and gastric smooth muscle: evidence for receptor subtypes. *Mol. Pharmacol.*, **43**, 921–930.

HUI, K.Y., JAKUBOWSKI, J.A., WYSS, V.L. & ANGLETON, E.L. (1992). Minimal sequence requirement of thrombin receptor agonist peptide. *Biochem. Biophys. Res. Commun.*, **184**, 790–796.

IMOTO, M., UMEZAWA, K., ISSHIKI, K., KUNIMOTO, S., SAWA, T., TAKEUCHI, T. & UMEZAWA, H. (1987). Kinetic studies of tyrosine kinase inhibition by erbstatin. *J. Antibiot.*, **40**, 1417–1473.

KETTNER, C. & SHAW, E. (1979). D-Phe-Pro-ArgCH_2Cl–A selective affinity label for thrombin. *Thromb. Res.*, **14**, 969–973.

KU, D.D. & ZALESKI, J.K. (1993). Receptor mechanism of thrombin-induced endothelium-dependent and endothelium-independent coronary vascular effects in dogs. *J. Cardiovasc. Pharmacol.*, **22**, 609–616.

LEVESQUE, L., DRAPEAU, G., GROSE, J.H., RIOUX, F. & MARCEAU, F. (1993). Vascular mode of action of kinin B_1 receptors and development of a cellular model for the investigation of these receptors. *Br. J. Pharmacol.*, **109**, 1254–1262.

LEWIS, A.J. & FURST, D.W. (1987). *Nonsteroidal Anti-inflammatory Drugs: Mechanisms and Clinical Use*. New-York: Marcel Dekker.

MARCEAU, F., PETITCLERC, E., DEBLOIS, D., PRADELLES, P. & POUBELLE, P.E. (1991). Human interleukin-1 induces a rapid relaxtion of the rabbit isolated mesenteric artery. *Br. J. Pharmacol.*, **103**, 1367–1372.

MURAD, F. (1990). Drugs used for the treatment of angina: organic nitrates, calcium-channel blockers and β-adrenergic antagonists. In *The Pharmacological Basis of Therapeutics*. ed. Gilman, A.G., Rall, T.W., Nies, A.S. & Taylor, P. pp. 764–783. New-York: Pergamon Press.

NYSTEDT, S., EMILSSON, K., WAHLESTEDT, C. & SUNDELIN, J. (1994). Molecular cloning of a potential proteinase activated receptor. *Proc. Natl. Acad. Sci. U.S.A.*, **91**, 9208–9212.

TESFAMARIAM, B., ALLEN, G.T., NORMANDIN, D. & ANTONACCIO, M.J. (1993). Involvement of the 'tethered ligand' receptor in thrombin-induced endothelium-mediated relaxations. *Am. J. Physiol.*, **265**, H1744–9.

VOURET-CRAVIARI, V., VAN OBBERGHEN-SCHILLING, E., RASMUSSEN, U.B., LECOCQ, A. & POUYSSEGUR, J. (1992). Synthetic α-thrombin receptor peptides activate G protein-coupled signaling pathways but are unable to induce mitogenesis. *Mol. Biol. Cell*, **3**, 95–102.

VU, T.K-H., HUNG, D.T., WHEATIN, V.I. & COUGHLIN, S.R. (1991). Molecular cloning of a functional thrombin receptor reveals a novel proteolytic mechanism of receptor activation. *Cell*, **64**, 1057–1068.

WEISS, R.H. & MADURI, M. (1993). The mitogenic effect of thrombin in vascular smooth muscle cells is largely due to basic fibroblast growth factor. *J. Biol. Chem.*, **268**, 5724–5727.

WEISS, R.H. & NUCCITELLI, R. (1992). Inhibition of tyrosine phosphorylation prevents thrombin-induced mitogenesis, but not intracellular free calcium release, in vascular smooth muscle cells. *J. Biol. Chem.*, **267**, 5608–5613.

YANG, S.G., LANIYONU, A., SAIFEDDINE, M., MOORE, G.J. & HOLLENBERG, M.D. (1992). Actions of thrombin and thrombin receptor peptide analogues in gastric and aortic smooth muscle: development of bioassays for structure-activity studies. *Life Sci.*, **51**, 1325–1332.

(Received February 22, 1995
Accepted March 27, 1995)

British Journal of Pharmacology (1995) 115, 909-912 © 1995 Stockton Press All rights reserved 0007-1188/95 $12.00

Actions of the insecticide fipronil, on dieldrin-sensitive and -resistant GABA receptors of *Drosophila melanogaster*

Alastair M. Hosie, Howard A. Baylis, Steven D. Buckingham & [1]David B. Sattelle

The Babraham Institute Laboratory of Molecular Signalling, Department of Zoology, Downing Street, Cambridge, CB2 3EJ

1 Blocking actions of the novel insecticide, fipronil, were examined on GABA responses recorded from *Xenopus* oocytes expressing either wild type (dieldrin-sensitive) or mutant (dieldrin-resistant) forms of the *Drosphila melanogaster* GABA-gated chloride channel homo-oligomer, RDL (the product of the *resistance to dieldrin* locus: *Rdl*).

2 In the case of the wild type receptor, fipronil blocked GABA-induced currents inducing both a shift to the right in the GABA dose-response curve and depressing the maximum amplitude of responses to GABA. The potency of fipronil was dependent on the GABA concentration but was unaffected by membrane potential.

3 Mutant RDL GABA-receptors, which have a naturally occurring amino acid substitution ($A^{302}\rightarrow S$) in the putative ion-channel lining region, conferring resistance to dieldrin and picrotoxinin, were markedly less sensitive to fipronil than the wild-type receptors.

4 Fipronil antagonism is qualitatively similar to that produced by the structurally distinct compound, picrotoxinin. As the mutation $A^{302}\rightarrow S$ reduces the potency of both fipronil and picrotoxinin, homo-oligomeric RDL receptors should facilitate detailed studies of the molecular basis of convulsant/insecticide antagonist actions on GABA receptors.

Keywords: GABA receptor; *Drosophila metalogaster*; *Rdl* gene; insecticide; convulsant antagonist; fipronil; picrotoxinin

Introduction

Insect γ-aminobutyric acid (GABA) receptors are the targets of a number of important classes of insecticides and convulsants. These include cyclodienes (e.g. dieldrin), trioxabicyclooctanes (e.g. *t*-butylbicyclophosphorothionate: TBPS), picrotoxinin (PTX), lindane, toxaphenes, silatranes, dithianes, bicyclo-orthobenzoates (e.g. ethynylbicyclo-orthobenzoate: EBOB) and avermectins (Sattelle, 1990; Anthony *et al.*, 1993; Deng *et al.*, 1993).

The optimization of phenylpyrazole compounds for insecticidal activity has led to the development of fipronil (Hatton *et al.*, 1988). Scatchard analysis of radioligand binding studies showed that fipronil displaced, non-competitively, the binding of the GABA-receptor antagonist [^{3}H]-EBOB to membranes prepared from the heads of the house fly, *Musca domestica* (Cole *et al.*, 1993), suggesting that this compound acts upon insect GABA receptors.

The recent cloning of a *Drosophila melanogaster* GABA-gated chloride-channel subunit (RDL) has led to the elucidation of a molecular basis for cyclodiene resistance (ffrench-Constant *et al.*, 1991). When expressed in *Xenopus* oocytes, the RDL polypeptide forms functional, presumably homo-oligomeric receptors (ffrench-Constant *et al.*, 1993a). The known agonist and convulsant antagonist pharmacology of these expressed receptors (Buckingham *et al.*, 1994) resembles that demonstrated for several *in situ* insect GABA receptors (Sattelle, 1990). A naturally occurring alanine to serine substitution at residue 302 ($A^{302}\rightarrow S$), in the proposed channel-lining domain (M2), confers resistance to dieldrin and PTX both in heterologously expressed homo-oligomeric RDL GABA receptors and *in situ* GABA receptors of *D. melanogaster* (ffrench-Constant *et al.*, 1993a; Zhang *et al.*, 1994). Furthermore, mutation of this amino acid is implicated in the cyclodiene resistance of at least 60 strains of *D. melanogaster* and *D. simulans* collected from around the world (ffrench-Constant *et al.*, 1993b) and a range of other insect pest species (Thomson *et al.*, 1993). Consequently, the subunit and gene locus are here referred to respectively as RDL and *Rdl* (*resistance to dieldrin*). We have shown that the GABA response of wild type RDL homo-oligomers expressed in *Xenopus* oocytes is also blocked by fipronil (Buckingham *et al.*, 1994).

This paper details the nature of fipronil antagonism and provides the first direct comparison of the blocking actions of this phenylpyrazole on dieldrin-sensitive and dieldrin-resistant forms of the RDL GABA-gated chloride-channel expressed in *Xenopus* oocytes.

Methods

cRNA synthesis

The cloning of the cDNA encoding the wild type form of RDL has been described elsewhere (ffrench-Constant *et al.*, 1991). Plasmid pNB14.1, a gift from Dr R. T. Roush (Cornell), containing the wild type cDNA was linearised with the restriction endonuclease *Not*I. m^7G (5′)PPP(5′)G capped cRNA was synthesized with SP6 RNA-polymerase (Promega) using a standard protocol (Sambrook *et al.*, 1989).

The plasmid pW8/6 (a gift from Dr R. T. Roush) consisted of a cDNA encoding the dieldrin-resistant form of RDL ($A^{302}\rightarrow S$) in the vector pW8. The insert was excised from pW8 using *Not*I and subcloned with T4 DNA ligase (Promega) into the *Not*I site of pALTER-*Ex*1 (Promega) creating plasmid pARRT. Using pARRT as a template, capped cRNA was synthesised with T7 RNA-polymerase (Promega). As pARRT has a T7 RNA-polymerase termination sequence 3′ to the insert, it was not linearised.

Oocyte preparation and cRNA injection

Stage V and VI oocytes were removed from mature *Xenopus laevis* and manually defolliculated after a 40 min incubation with collagenase type IA (2 mg ml^{-1}) in a low-calcium version of standard oocyte saline, (standard saline composition (mM): NaCl 100, KCl 2, $CaCl_2$ 1.8, $MgCl_2$ 1, HEPES 5, pH 7.6). Each oocyte was injected with 40-50 ng of cRNA in 25-50 nl and

[1] Author for correspondence.

incubated at 17–18°C in saline supplemented with penicillin (100 units ml^{-1}), streptomycin (100 $\mu g\ ml^{-1}$), gentamycin (50 $\mu g\ ml^{-1}$) and 2.5 mM sodium pyruvate. Electrophysiological examination was performed 18–72 h after injection.

Electrophysiological investigation

Oocytes were secured in a 90 μl Perspex recording chamber and continuously perfused with saline (5 ml min^{-1}). All drugs were applied dissolved in the perfusate. Drugs initially were dissolved in dimethyl sulphoxide (PTX) or acetone (fipronil) at concentrations which ensured that the final concentration of solvent in the perfusate never exceeded 1% v/v. The concentrations of solvent used had no effect on the current required to clamp the membrane at −60 mV. Membrane currents were monitored under two-electrode voltage-clamp using 1 M KCl filled electrodes (3–10 MΩ) and an Axoclamp 2A amplifier (Axon Instruments). Signals were displayed on an oscilloscope (Trio) and recorded on a chart recorder (Tektronix).

Only oocytes which yielded stable responses to at least three control doses of GABA, applied at approximately 2 min intervals were used. In all experiments the antagonists were added to the perfusate at the peak of the response to the final control application of GABA. The oocytes were continually exposed to antagonist thereafter. This was found to produce a more consistent percentage blockade than when fipronil was co-applied with GABA. Experiments were conducted at a clamped membrane potential of −60 mV. The voltage-dependence of fipronil block was determined by subtracting the clamp current observed in saline from that observed with 50 μM GABA (a non-desensitizing concentration) in the absence and presence of 50 nM fipronil during brief excursions of the clamped potential from −60 mV to a range of potentials between −90 mV and −10 mV. All averaged data are presented as the mean ± the standard deviation (s.d.).

All reagents for RNA synthesis were purchased from Promega (U.K.) except for $m^7G(5')ppp(5')G$ cap analogue, which was obtained from NEB (U.K.). Collagenase type IA, GABA and PTX were obtained from Sigma (U.K.). Fipronil was synthesized by the method of Hatton *et al.* (1988).

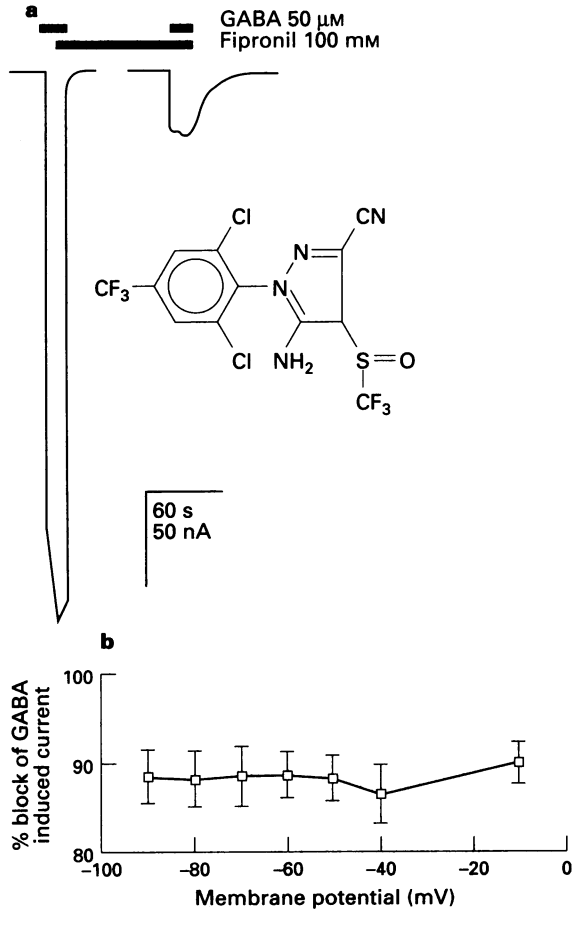

Figure 1 (a) Blockade of the response to 50 μM GABA by 0.1 μM fipronil in *Xenopus* oocytes pre-injected with cRNA encoding the wild-type RDL subunit and voltage clamped at −60 mV. GABA was applied in the perfusate for 15 s to obtain the control response. Fipronil was added at the end of the GABA application. After 2 min of incubation in fipronil, GABA was co-applied with the antagonist for 15 s. These data are typical of 20 separate experiments. The chemical structure of fipronil is shown (inset). (b) Block by fipronil of GABA-induced currents is independent of membrane potential between −90 mV and −10 mV. Each point is the mean ± s.d. of the responses seen in four oocytes.

Results

Antagonism of GABA-induced currents by fipronil

The application of GABA (in the range 1 μM to 1 mM) resulted in rapid, dose-dependent inward currents in *Xenopus* oocytes injected with either wild type or dieldrin-resistant RDL cRNA and voltage-clamped at −60 mV. When fipronil was applied alone at 1 mM it had no effect on the oocyte membrane current (data not shown) but at 10 nM–1 μM it reduced the response of wild-type RDL homo-oligomers to GABA (Figure 1a). Recovery from fipronil blockade was slow and incomplete after washing for 10 min in normal saline. The blockade by fipronil (50 nM) of the response to 50 μM GABA was independent of membrane potential between −90 mV and −10 mV (Figure 1b). Fipronil effected a shift to the right in the GABA dose-response curve to wild-type homo-oligomers and also decreased the amplitude of the maximum GABA response in a concentration-dependent manner. The reduction in the maximum response to GABA could not be overcome

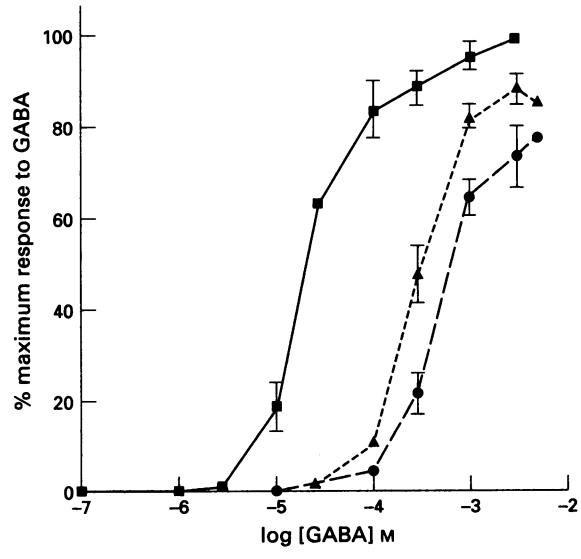

Figure 2 GABA dose-response data obtained in the absence (■, $n=6$) and presence of 0.1 μM fipronil (▲, $n=3$) and 1 μM fipronil (●, $n=3-6$). GABA was applied for 15 s at increasing concentrations, 2–3 min being allowed between each successive challenge to minimize the possible effects of desensitization. The experiments were repeated with fipronil present in the perfusate. Data from each oocyte were normalized to the amplitude of the response to 3 mM GABA. Note the increase in the concentration of GABA required to elicit a half maximal response and the insurmountable depression of that maximum.

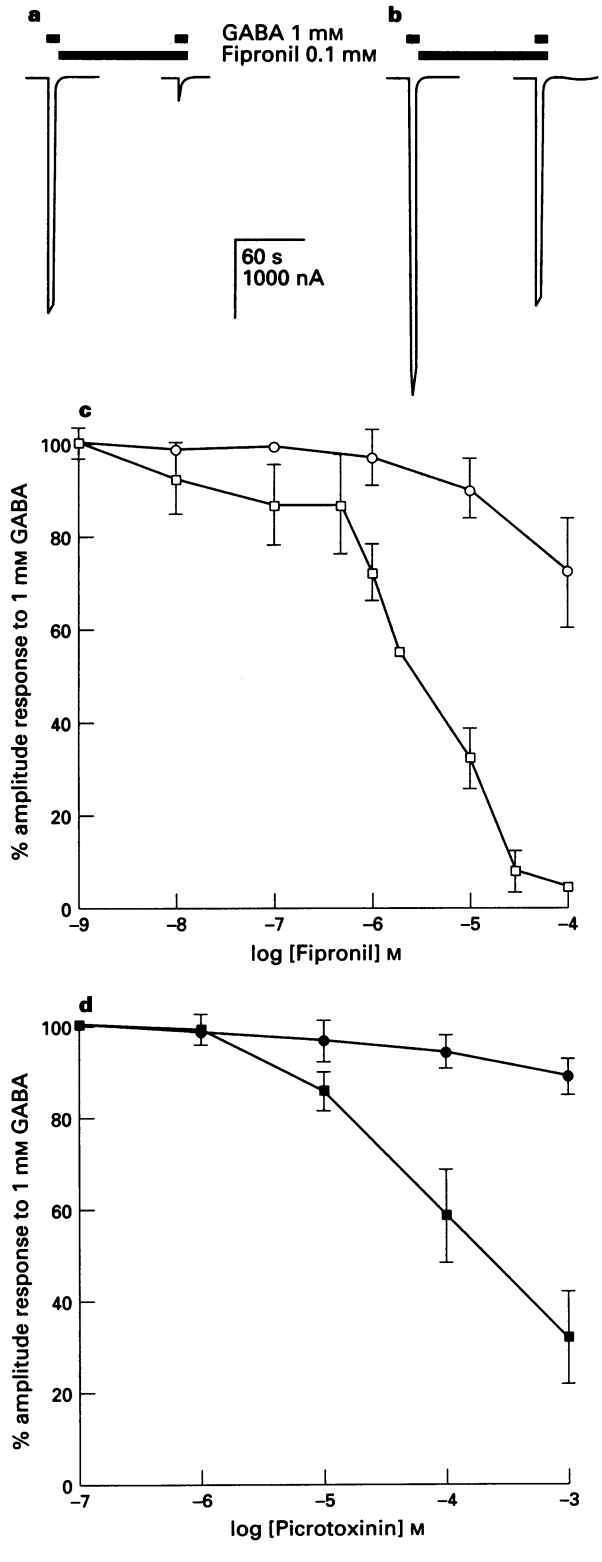

Figure 3 Blockade by 100 μM fipronil of the responses of wild-type (a) and mutant (b) RDL homo-oligomers to 1 mM GABA. The A^{302}→S mutation greatly decreased the potency of fipronil. The dose-inhibition relationship for fipronil (c) and picrotoxinin (PTX) (d) on the responses to 1 mM GABA of wild type (□,■) and dieldrin-resistant RDL (○,●) homo-oligomers. In each case the data were normalized to the amplitude of the response to 1 mM GABA. Each point represents the mean amplitude of the responses recorded in six separate oocytes. Fipronil is a more potent antagonist of GABA-induced currents than PTX. However, the potency of both compounds is markedly reduced by the A^{302}→S mutation in the putative second transmembrane region of the RDL polypeptide.

with higher concentrations of agonist (Figure 2a). The percentage block effected by fipronil was dependent on the GABA concentration, with maximal inhibition being observed at low agonist concentrations.

Action of fipronil on the dieldrin-resistant form of RDL

Fipronil also reduced the amplitude of GABA responses of *Xenopus* oocytes expressing the dieldrin-resistant form of RDL (Figure 3a and b). However, the point mutation (A^{302}→S) of the proposed channel lining region greatly reduced the potency of both fipronil and PTX (Figure 3c and d). Whereas in wild-type RDL receptors, 20 μM fipronil and 200 μM PTX effected approximately a 50% reduction in the amplitude of the response to 1 mM GABA, such a reduction could not be achieved for dieldrin-resistant receptors with 5 fold higher concentrations of either fipronil or PTX. The low solubility of the antagonists prevented quantification of the effect of higher concentrations of antagonist.

Discussion

This study demonstrates for the first time that the mutation (A^{302}→S) in the putative channel lining region of the RDL subunit which confers cyclodiene and PTX resistance also reduces the potency of the phenylpyrazole insecticide, fipronil.

Studies on wild-type RDL homo-oligomers show that fipronil is neither a purely competitive, nor purely non-competitive GABA antagonist. A similar mixed, or complex, antagonist action has been described for PTX block of the GABA response of lobster muscle (Smart & Constanti, 1986). PTX block of crustacean muscle GABA receptors, like that of fipronil on expressed *D. melanogaster* wild-type RDL homo-oligomeric receptors, was dependent upon agonist concentration and yet was insurmountable. Indeed, the percentage block effected by a given dose of PTX at an equipotent agonist concentration was dependent upon the agonist compound used (e.g. GABA, β-hydroxybutric acid and guanidoacetic acid). The best fits of the crustacean agonist dose-response data in the presence of PTX were achieved when it was assumed that the binding of PTX favoured the receptor entering an agonist bound closed-state, for example a desensitized state, rather than blocking the channel directly. Under whole-cell clamp, PTX was observed to bind preferentially to an agonist bound state of GABA receptors of rat sympathetic neurones, the rate at which a steady-state blockade was achieved being enhanced by brief, repetitive application of GABA (Newland & Cull-Candy, 1992). Again it was concluded that PTX binds preferentially to an agonist bound form of the receptor whereby the convulsant stabilizes a closed form of the receptor channel although the authors did not discount the possibility that PTX could also block the channel allosterically. Like the fipronil block described here, PTX antagonism of GABA responses in the rat was independent of membrane potential, and therefore neither compound is acting as a voltage-dependent channel blocker.

In *M. domestica*, phenyl pyrazole compounds such as fipronil, which are structurally distinct from cyclodienes and PTX, are non-competitive inhibitors of [^{3}H]-EBOB binding, whereas cyclodienes and PTX displace [^{3}H]-EBOB competitively (Deng *et al.*, 1991; 1993). Therefore it is of interest that the mutation in M2 which results in resistance to picrotoxin and dieldrin and alters the rate of receptor desensitization (ffrench-Constant *et al.*, 1993a; Zhang *et al.*, 1994) should also reduce the potency of fipronil. The A^{302}→S point mutation must alter, either directly or allosterically, the binding sites for both PTX and fipronil and/or the mechanism(s) which both compounds use to reduce GABA-induced currents. Indeed, Zhang *et al.* (1994) suggest that the A^{302}→S substitution has such a dual effect on the interactions between PTX and wild-type and mutant *Drosophila* GABA receptors *in situ*. Given the similarity between the block by fipronil and PTX of GABA

receptors it will be of interest to examine further if fipronil and PTX utilize a common mechanism, such as increasing the rate of receptor desensitization, to antagonise GABA responses.

The results of this study lead to the prediction that cyclodiene-resistant *D. melanogaster* expressing the mutant RDL polypeptide will exhibit cross resistance to fipronil, underscoring the potential usefulness of expression studies in anticipating pre-existing resistance to candidate novel insecticides. Weak cross-resistance to fipronil has been reported in dieldrin-resistant *M. domestica* (Colliot *et al.*, 1992; Cole *et al.*, 1993), however, the molecular basis for this resistance is as yet unknown.

The fact that RDL subunits for functional homo-oligomers both when expressed transiently in *Xenopus* oocytes and stably in *Drosophila* S2 cells (Millar *et al.*, 1994) could be of great value in elucidating the mechanism(s) by which insecticidal and convulsant compounds block the GABA receptor.

Note added in proof

Two recent studies have demonstrated a dramatic decrease in the binding of [^{3}H]-EBOB to *Drosophila* with alleles for mutant *Rdl* relative to wild type (Cole *et al.*, 1995; Lee *et al.*, 1995). Furthermore, fipronil was a less potent displacer of [^{3}H]-EBOB bound to membranes prepared from mutant flies. Thus it appears that the $A^{302}\rightarrow S$ substitution may affect both the binding and effector mechanisms of convulsant ligands.

We are grateful to R.T. Roush, J. Lis, D. Nero, M. Barr, M. Kwan, M. Robinson and R. MacIntyre who helped prepare pW8/6. A.M.H. is supported by a Medical Research Council research studentship and H.A.B. by the BBSRC Intracellular Signalling Programme.

References

ANTHONY, N.M., HARRISON, J.B. & SATTELLE, D.B. (1993). GABA receptor molecules of insects. In *Comparative Molecular Neurobiology*. ed. Pichon, Y. pp. 172–209. Basel: Birkhauser Verlag.

BUCKINGHAM, S.D., HOSIE, A.M., ROUSH, R.T. & SATTELLE, D.B. (1994). Actions of agonists and convulsant antagonists on a *Drosophila melanogaster* GABA receptor (Rdl) homo-oligomer expressed in *Xenopus* oocytes. *Neurosci. Letts.*, **181,** 137–140.

COLE, L.M., NICHOLSON, R.A. & CASIDA, J.E. (1993). Action of phenylpyrazole insecticides at the GABA-gated chloride channel. *Pestic. Biochem. Physiol.*, **46,** 47–54.

COLE, L.M., ROUSH, R.T. & CASIDA, J.E. (1995). *Drosophila* GABA-gated chloride channel: Modified [^{3}H]EBOB binding site associated with Ala→Ser or Gly mutants of *Rdl* subunit. *Life Sci.*, **56,** 757–767.

COLLIOT, F., KUKOROWSKI, K.A., HAWKINS, D.W. & ROBERTS, D.A. (1992). Fipronil: a new soil and foliar broad spectrum insecticide. In abstracts of *Brighton Crop Protection Conference: Pests and Diseases*, Vol.3 (177), pp. 29.34. London: British Crop Protection Council.

DENG, Y., PALMER, C.J. & CASIDA, J.E. (1991). House fly brain γ-aminobutyric acid-gated chloride channel: target for multiple classes of insecticide. *Pestic. Biochem. Physiol.*, **41,** 60–65.

DENG, Y., PALMER, C.J. & CASIDA, J.E. (1993). House fly head GABA-gated chloride channel: four putative insecticide binding sites differentiated by [^{3}H]-EBOB and [^{35}S]-TBPS. *Pestic. Biochem. Physiol.*, **47,** 98–112.

FFRENCH-CONSTANT, R.H., MORTLOCK, D.P., SCHAFFER, C.D., MACINTYRE, R.J. & ROUSH, R.T. (1991). Molecular cloning and transformation of cyclodiene resistance in *Drosophila*: an invertebrate γ-aminobutyric acid subtype A receptor locus. *Proc. Natl. Acad. Sci. U.S.A.*, **88,** 7209–7213.

FFRENCH-CONSTANT, R.H., ROCHELEAU, T.A., STEICHEN, J.C. & CHALMERS, A.E. (1993a). A point mutation in a *Drosophila* GABA receptor confers insecticide resistance. *Nature*, **363,** 449–451.

FFRENCH-CONSTANT, R.H., STEICHEN, J.C., ROCHELEAU, T.A., ARONSTEIN, K. & ROUSH, R.T. (1993b). A single-amino acid substitution in a γ-aminobutyric acid subtype A receptor locus is associated with cyclodiene insecticide resistance in *Drosophila* populations. *Proc. Natl. Acad. Sci. U.S.A.*, **90,** 1957–1961.

HATTON, L.R., HAWKINS, D.W., PEARSON, C.J. & ROBERTS, D.A. (1988). Derivatives of N-phenylpyrazoles. *Eur. Pat.*, **295,** 117.

LEE, H.-J., ZHANG, H.-G., JACKSON, M.B. & FFRENCH-CONSTANT, R.H. (1995). Binding and physiology of 4′-ethynyl-4-n-propylbicycloorthobenzoate (EBOB) in cyclodiene resistant *Drosophila*. *Pestic. Insect Physiol.*, **51,** 30–37.

MILLAR, N.S., BUCKINGHAM, S.D. & SATTELLE, D.B. (1994). Stable expression of a functional *Drosophila* GABA-gated chloride channel in a *Drosophila* cell line. *Proc. R. Soc. B.*, **258,** 307–314.

NEWLAND, C.F. & CULL-CANDY, S.G. (1992). On the mechanism of action of picrotoxin on GABA receptor channels in dissociated sympathetic neurones of the rat. *J. Physiol.*, **447,** 191–213.

SAMBROOK, J., FRITSCH, E.F. & MANIATIS, T. (1989). *Molecular Cloning: A Laboratory Manual*, pp. 10.32–10.33. Cold Spring Harbour, NY: Cold Spring Harbour Lab.

SATTELLE, D.B. (1990). GABA receptors of insects. *Adv. Insect. Physiol.*, **22,** 1–113.

SMART, T.G. & CONSTANTI, A. (1986). Studies on the mechanism of action of picrotoxin and other convulsants at the crustacean muscle GABA receptor. *Proc. R. Soc. B.*, **227,** 191–216.

THOMSON, M., STEICHEN, J.C. & FFRENCH-CONSTANT, R.H. (1993). Conservation of cyclodiene insecticide resistance associated mutations in insets. *Insect Mol. Biol.*, **2,** 149–154.

ZHANG, H.-G., FFRENCH-CONSTANT, R.H. & JACKSON, M.B. (1994). A unique amino acid of the *Drosophila* GABA receptor with influence on drug sensitivity by two mechanisms. *J. Physiol.*, **479,** 65–75

(Received January 12, 1995
Revised March 23, 1995
Accepted March 28, 1995)

British Journal of Pharmacology (1995) 115, 913-916 © 1995 Stockton Press All rights reserved 0007-1188/95 $12.00

Inhibition of bronchoconstriction by pituitary adenylate cyclase activating polypeptide (PACAP 1-27) in guinea-pigs *in vivo*

Anders Lindén, Shigemi Yoshihara, Brendan Chan & [1]Jay A. Nadel

Cardiovascular Research Institute and Department of Medicine, University of California San Francisco, 505 Parnassus Avenue, San Francisco, California 94143-0130, U.S.A.

1 We studied the inhibitory effect of pituitary adenylate cyclase activating polypeptide (PACAP 1-27) on the increase in total pulmonary resistance (R_L) caused either by allergen or histamine in anaesthetized, ventilated guinea-pigs.

2 PACAP 1-27 given via i.v. infusion (0.045–4.5 nmol kg^{-1} min^{-1}) dose-dependently reduced the increase in R_L caused by inhaled ovalbumin and histamine. At the highest dose, PACAP 1-27 prevented the increase in R_L caused by ovalbumin and histamine completely. Infusion of PACAP 1-27 and the β_2-adrenoceptor agonist, salbutamol (0.045–4.5 nmol kg^{-1} min^{-1}) inhibited the increase in R_L similarly, but salbutamol increased the heart rate more than PACAP 1-27.

3 PACAP 1-27 and salbutamol given via inhaled aerosol (0.1 mM, 20 breaths) significantly reduced the increase in R_L caused by histamine infused i.v., whereas aerosolised sterile saline did not. Both PACAP 1-27 and salbutamol caused bronchodilator effects within 1 min of drug inhalation and these effects remained throughout the 20 min of study.

4 Because PACAP 1-27 produced significant bronchodilatation and rapid onset of sustained action *in vivo* and without pronounced cardiovascular side effects, we conclude that this peptide may have therapeutic potential as a bronchodilator.

Keywords: Bronchodilator; histamine; inhalation; intravenous infusion; ovalbumin; PACAP; pulmonary resistance; salbutamol

Introduction

Immunoreactivity for pituitary adenylate cyclase activating polypeptide (PACAP) is present in airway smooth muscle of guinea-pigs and man (Cardell *et al.*, 1991; Luts *et al.*, 1993). *In vitro*, PACAP 1-38 relaxes guinea-pig and rabbit tracheal smooth muscle precontracted by histamine and by acetylcholine (Cardell *et al.*, 1991; Kanemura *et al.*, 1993). PACAP 1-38 also increases adenosine 3':5'-cyclic monophosphate (cyclic AMP) in tracheal smooth muscle, providing a possible mechanism for the relaxant effect of PACAP 1-38 (Kanemura *et al.*, 1993). However, the extent to which PACAP 1-27, the N-terminal residue of PACAP 1-38, relaxes airway smooth muscle is unknown and the PACAPs have not been tested against bronchoconstriction *in vivo*.

We assessed PACAP 1-27 as a bronchodilator and compared it with a β_2-adrenoceptor agonist, salbutamol, in anaesthetized, ventilated guinea-pigs. The two bronchodilators were administered both by i.v. infusion and by inhaled aerosol. Increase in total pulmonary resistance (R_L) was induced by ovalbumin inhalation and by histamine both by inhalation and i.v. infusion. Heart rate was monitored as an indicator of cardiovascular side effects during i.v. infusion of the bronchodilators.

Methods

Animals

Eighty-two male Hartley guinea-pigs (Simonsen Lab. Inc., Gilroy, CA, U.S.A.) were maintained pathogen-free (mean ± s.d. weight: 420 ± 54 g) in a temperature-controlled environment with sterile laboratory food and water freely available.

Sensitization procedure

For ovalbumin challenge, animals were sensitized by intraperitoneal injection of ovalbumin (70 mg) dissolved in sterile saline (1.5 ml) (Bertrand *et al.*, 1993). This injection was given twice, at one week intervals, and the animals were challenged two weeks after the second injection.

Measurement of R_L

Animals were initially anaesthetized with pentobarbitone (45 mg kg^{-1}, i.p.) and then ventilated (85 × 3 ml min^{-1}) via a tracheal cannula connected to a constant-volume ventilator (model 683 Harvard Aparatus, South Natick, MA, U.S.A.). As previously described (Bertrand *et al.*, 1993), airflow was monitored continuously with a pneumotachygraph (A. Fleisch Medical, Richmond, VA, U.S.A.) connected to a differential pressure transducer (model DP45; Validyne Engineering, Northridge, CA, U.S.A.). A fluid-filled catheter was introduced into the oesophagus to measure local pressure as an approximation of pleural pressure. Intratracheal pressure was measured with another catheter connecting the tracheal tube to the pneumotachygraph. Transpulmonary pressure was measured with a differential pressure transducer (model DP7; Validyne Engineering, Northridge, CA). Output signals representing transpulmonary pressure and airflow were amplified (model CD19; Validyne Engineering, Northridge, CA) and recorded on a polygraph recorder (model 1508 B Visicorder; Honeywell, Denver, CO). R_L was calculated as previously described (Dusser *et al.*, 1988). Heart rate was monitored via an electrocardiogram recorded on the polygraph recorder. A catheter (22 GA 1IN Angiocath; Becton Dickinson Vascular Access, Sandy, UT, U.S.A.) was inserted in the right jugular vein for delivery of drugs. Finally, a supplemental dose of pentobarbitone (10 mg kg^{-1}, i.v.) was followed by hyperinflation of the lungs.

Protocol for bronchodilators via i.v. infusion

In experiments with histamine, the muscarinic antagonist, atropine (1 mg kg^{-1}, i.v.) was given to inhibit cholinergic neural reflexes. Twenty min later, either ovalbumin (10 mg ml^{-1}, 5 breaths) or histamine (3.1 mg ml^{-1}, 5 breaths) was given by aerosol (0.12 ml min^{-1}) using an ultrasonic nebuliser

[1]Author for correspondence.

(Pulmo-Sonic model 25; DeVillbiss, Somerset, PA, U.S.A.). These R_L responses reached 90% of maximum R_L caused by histamine given as a bolus i.v. (3.1 mg kg^{-1}). In experiments with histamine alone, histamine challenges were administered twice at the same dose. One hundred min after the first challenge, which served as a reference, pentobarbitone (3 mg kg^{-1}, i.v.) and atropine (1 mg kg^{-1}, i.v.) were given, followed by lung hyperinflation; 20 min later, a second challenge was given.

PACAP-27 (0.045 to 4.5 nmol kg^{-1} min^{-1}), salbutamol (0.045 to 4.5 nmol kg^{-1} min^{-1}) or sterile saline was given i.v. (1.0 ml) via an infusion pump (model 600-000; Harvard Apparatus), starting 5 min before and continuing 10 min after airway challenge. In experiments using histamine aerosol, i.v. infusion was given during the second aerosol challenge.

Pretreatment with pyrilamine (10 mg kg^{-1}, i.p.) and cimetidine (10 mg kg^{-1}, i.p.), a histamine H_1- and H_2-antagonist, respectively, reduced the ovalbumin-induced increase in R_L from 0.92 ± 0.07 cmH_2O ml^{-1} s^{-1} in control animals to 0.03 ± 0.02 cmH_2O ml^{-1} s^{-1} in pretreated animals ($P < 0.0001$, $n = 4-5$). After pretreatment with atropine alone, the corresponding increase in R_L was 0.91 ± 0.03 cmH_2O ml^{-1} s^{-1} ($P = 0.98$, $n = 3-5$), thereby confirming the dominant role of histamine in the responses to ovalbumin (Barnes *et al.*, 1988).

Protocol for bronchodilators via inhaled aerosol

As in the experiments on brochodilators delivered i.v., atropine was given initially. Twenty min later, an increase in R_L was established by infusion of histamine i.v. (20 μg kg^{-1} min^{-1}) during 30 min (2.0 ml), producing an R_L response reaching 30% of maximum R_L caused by histamine given as a bolus i.v. (3.1 mg kg^{-1}). When the R_L increase stabilized after an additional 7 min, either PACAP 1-27 salbutamol (0.1 mM, 20 breaths) or sterile saline was given by aerosol inhalation. R_L was then recorded for another 20 min.

Drugs

Atropine sulphate, histamine diphosphate, chicken egg albumin (grade V, ovalbumin), pyrilamine maleate salt and salbutamol hemisulphate were purchased from Sigma, St. Louis, MO, U.S.A. Pituitary adenylate cyclase-activating peptide (PACAP 1-27) was provided by American Peptide Co, Sunnyvale, CA, U.S.A. Sodium pentobarbitone was obtained from Anthony Products Co., Arcadia, CA, U.S.A. and cimetidine hydrochloride was purchased from SmithKline Beecham Pharmaceuticals, Philadelphia, PA, U.S.A. Pentobarbitone and cimetidine were used as commercially available buffer solutions; all other drugs were dissolved and diluted in sterile saline (NaCl 0.9%).

Statistics

Correlation factors were evaluated by Spearman's non-parametric rank correlation. Slopes of dose-response data were compared by multiple linear regression. Single measure points were compared by Student's two-tailed t test (Colton, 1974).

Results

Bronchodilators via i.v. infusion

Ovalbumin challenge PACAP 1-27 prevented the peak increase in R_L caused by inhaled ovalbumin in a dose-dependent fashion ($r = -0.87$, $P < 0.0001$, $n = 21$) (Figure 1). The highest dose of PACAP 1-27 completely abolished the increase in R_L caused by inhaled ovalbumin (Figures 1 and 2). The two highest doses of PACAP 1-27 produced sustained and significant inhibition during the 20 min of observation that followed after the i.v. infusion of PACAP 1-27 was completed (Figure 2). Baseline R_L values were similar in all groups compared (data not shown).

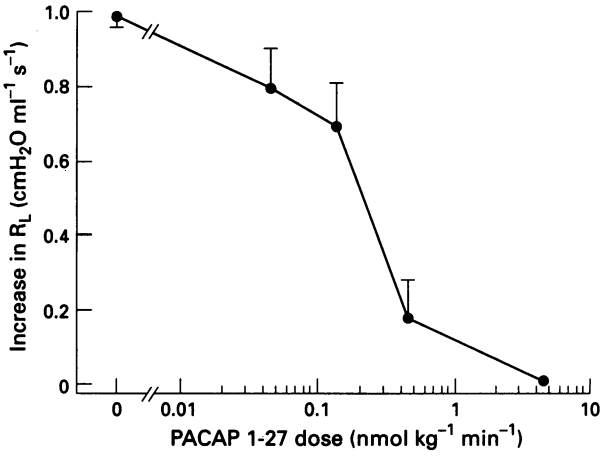

Figure 1 Inhibitory effect of PACAP 1-27 (15 min infusion i.v.) on the peak increase in total pulmonary resistance (R_L) induced by inhaled ovalbumin (10 mg ml^{-1}, 5 breaths) in sensitized guinea-pigs. Mean values with s.e.mean ($n = 4-5$).

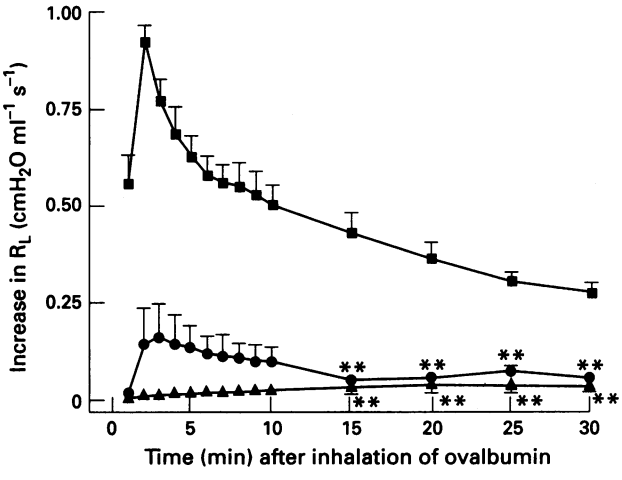

Figure 2 Time course for the inhibitory effect of PACAP 1-27 (15 min infusion, i.v.) on increase in total pulmonary resistance (R_L) induced by inhaled ovalbumin (10 mg ml^{-1}, 5 breaths) in sensitized guinea-pigs. PACAP 1-27 was given in 0.45 (●) or 4.5 (▲) nmol kg^{-1} min^{-1} and was compared with saline (■). Mean values with s.e.mean. $^{**}P \leq 0.01$ compared with saline (Student's t test, $n = 4$).

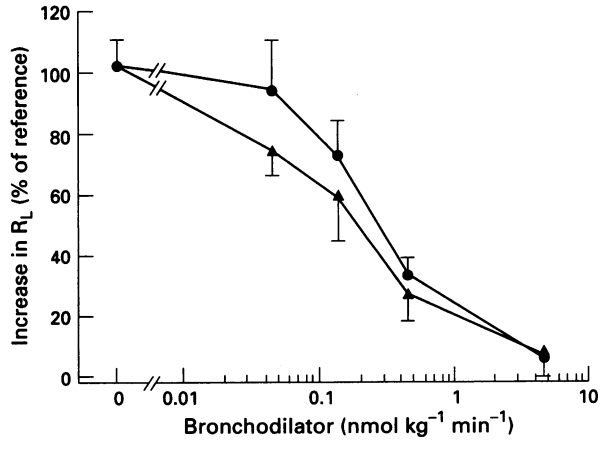

Figure 3 Inhibitory effect of PACAP 1-27 (●) or salbutamol (▲) (15 min infusion, i.v.) on the peak increase in total pulmonary resistance (R_L) induced by inhaled histamine (3.1 mg ml^{-1}, 5 breaths) in guinea-pigs. The histamine-induced increase in R_L is presented as a percentage (% of reference) of a preceding reference response to inhaled histamine (3.1 mg ml^{-1}, 5 breaths), given prior to the bronchodilator. Mean values with s.e.mean ($n = 4-5$).

Table 1 Baseline levels (mean ± s.d.) of total pulmonary resistance (R_L: $cmH_2O\,ml^{-1}\,s^{-1}$) and heart rate (HR: beats min^{-1})

Route of delivery		*Drug*	
Infusion i.v.	*PACAP 1-27*	*Salbutamol*	*Saline*
R_L	0.17 ± 0.03	0.16 ± 0.02	0.16 ± 0.02
HR	189 ± 11	186 ± 20	188 ± 7
n	17*	17*	5
Inhalation			
R_L	0.16 ± 0.01	0.16 ± 0.01	0.16 ± 0.02
n	5	5	5

*Each value represents the average of all doses given of this drug ($n = 4-5$ at each dose).

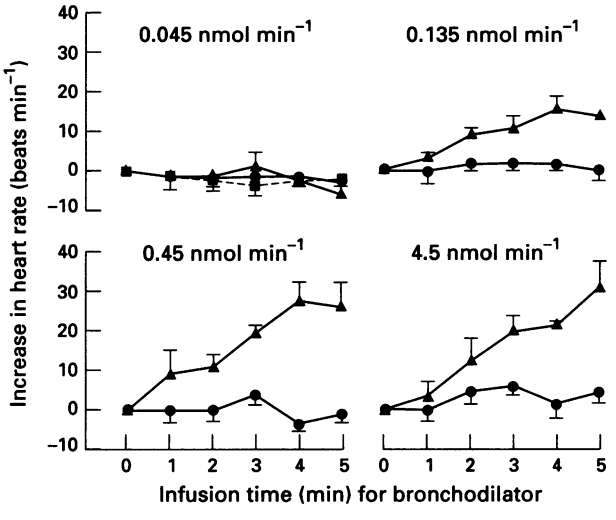

Figure 4 Effect of PACAP 1-27 (●), salbutamol (▲) or saline (■) on heart rate during the first 5 min of bronchodilator infusion i.v. in guinea-pigs. Mean values with s.e.mean ($n = 3-5$).

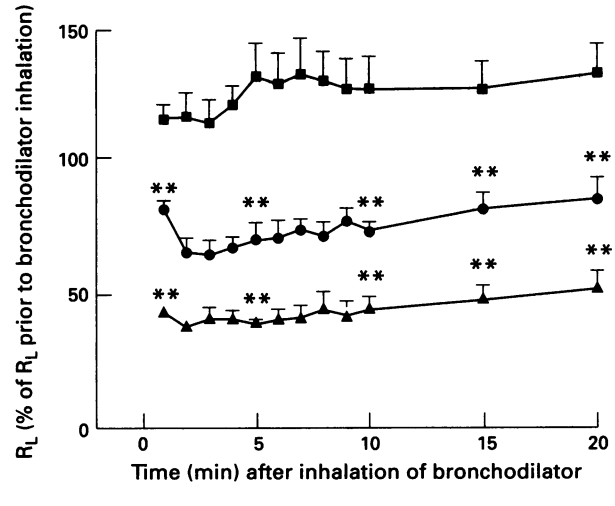

Figure 5 Effect of inhaled PACAP 1-27 (●) or salbutamol (▲) (0.1 mM) given by aerosol ($85 \times 3\,ml\,min^{-1}$, 20 breaths) on histamine-induced ($20\,\mu g\,kg^{-1}\,min^{-1}$, i.v.) increase in total pulmonary resistance (R_L) in anaesthetized guinea-pigs. The effect of inhaled saline (■) is also presented. The data are presented as percentages of the histamine-induced increase in R_L immediately prior to the inhalation of aerosol. Mean values with s.e.mean. $^{**}P \leq 0.01$ compared with saline (Student's *t* test, $n = 4-5$).

Histamine challenge Both PACAP 1-27 ($r = -0.87$, $P < 0.0001$, $n = 22$) and salbutamol ($r = -0.88$, $P < 0.0001$, $n = 22$) prevented the peak increase in R_L caused by inhaled histamine dose-dependently (Figure 3). Multiple linear regression analysis showed no statistically significant difference in the slopes of the dose-response curves for PACAP 1-27 and salbutamol ($P = 0.61$, $n = 17$). The highest dose of PACAP 1-27 and salbutamol completely abolished the increase in R_L caused by inhaled histamine (Figure 3). However, the histamine response during saline infusion lasted only 10 min, and therefore it was not possible to determine the duration of inhibitory action for PACAP 1-27 and salbutamol (data not shown).

The increase in R_L caused by the histamine reference challenge was 0.77 ± 0.05 and 0.75 ± 0.03 $cmH_2O\,ml^{-1}\,s^{-1}$ (mean ± s.e.mean), in the PACAP 1-27 and salbutamol groups respectively, and were not significantly different ($P = 0.82$, $n = 17$). Baseline R_L values were similar in all groups (Table 1).

Salbutamol ($r = 0.84$, $P = 0.0002$, $n = 21$) but not PACAP 1-27 ($r = 0.40$, $P = 0.07$, $n = 22$) increased heart rate (HR) dose-dependently during the first 5 min of i.v. infusion (Figure 4). Multiple linear regression analysis proved the difference between the slopes of the dose-response curves to be statistically significant ($P = 0.03$, $n = 16-17$). Baseline HR values were similar in all groups (Table 1).

Bronchodilators via inhaled aerosol

When PACAP 1-27 or salbutamol was given by inhalation they inhibited increase in R_L caused by histamine infused i.v., with a peak inhibitory effect (% of histamine-induced R_L) of 39 ± 6% and 66 ± 3% (mean ± s.e.mean) respectively. The corresponding peak effect of inhaled saline (control) was −3 ± 7% which was significantly different from the effect of either PACAP 1-27 ($P = 0.002$, $n = 5$) or salbutamol ($P < 0.0001$, $n = 5$). The time from drug delivery until peak drug response was 3.6 ± 1.1 and 5.4 ± 1.3 min (mean ± s.e.mean), for PACAP 1-27 and salbutamol, respectively; this difference was not statistically significant ($P = 0.32$, $n = 5$). Both PACAP 1-27 and salbutamol produced a significant inhibitory effect 1 min after drug delivery, and this effect was sustained throughout the 20 min of R_L recording (Figure 5).

The level of histamine-induced R_L immediately before drug inhalation was 0.24 ± 0.01 and 0.23 ± 0.03 $cmH_2O\,ml^{-1}\,s^{-1}$ (mean ± s.e.mean) in the PACAP 1-27 and salbutamol groups respectively and were not significantly different ($P = 0.72$, $n = 5$). Baseline R_L values were similar in all groups (Table 1).

Discussion

PACAP 1-27 given by i.v. infusion abolished the increase in R_L caused by inhaled ovalbumin and histamine in guinea-pigs *in vivo* without any significant increase in heart rate. When given by inhalation, PACAP 1-27 inhibited the increase in R_L caused by histamine infused i.v.

Intravenous delivery of PACAP 1-27 and salbutamol inhibited a nearly maximum increase in R_L caused by inhaled

histamine dose-dependently. There was no significant difference in this relaxant effect between PACAP 1-27 and the β_2-adrenoceptor agonist, salbutamol. Because salbutamol effectively inhibits bronchoconstriction clinically (Wallin *et al.*, 1993), our findings suggest that PACAP 1-27 given systemically has a significant potency and efficacy as a bronchodilator. This idea is also supported by our experiments with ovalbumin-induced increase in R_L because PACAP 1–27 given i.v. also dose-dependently inhibited this near maximum increase in R_L. Although the effects on R_L were similar, salbutamol increased heart rate dose-dependently, while PACAP 1-27 did not.

Inhaled aerosols of PACAP 1-27 and salbutamol also inhibited the increase in R_L caused by histamine. This suggests that PACAP 1-27 may be effective as a bronchodilator not only for systemic treatment but also for inhalation. Vasoactive intestinal polypeptide (VIP) is structurally similar to PACAP 1-27 and acts via the same receptor (Arimura, 1992). However, in contrast to our findings with PACAP 1-27, inhaled VIP is reported to have no bronchodilator effect on bronchoconstriction in guinea-pigs *in vitro* (O'Donnell *et al.*, 1994). Furthermore, inhaled VIP has only a weak bronchodilator effect in asthmatic subjects (Barnes & Dixon, 1984). It is possible that VIP is more easily cleaved in the airways by local peptidases such as neutral endopeptidase (Nadel, 1992). The fact that bronchodilatation with PACAP 1–27 lasted throughout the 20 min of study also suggests that this peptide is not susceptible to local peptidases.

In separate experiments, we confirmed a direct, potent relaxant effect of PACAP 1–27 on primate bronchial smooth muscle precontracted by carbachol *in vitro*, comparable to the effect of salbutamol (data not shown). Furthermore, our *in vivo* data indicated inhibition of bronchoconstrictor responses caused by histamine directly and those caused by antigen (ovalbumin). Thus, PACAP 1-27 exerts functional antagonism of histamine at the level of smooth muscle but additional pathways of action, such as inhibition of histamine release from mast cells, may also play a role in allergic bronchoconstriction.

In conclusion, this study indicates that PACAP 1-27 produces significant and sustained bronchodilatation *in vivo*, both when given i.v. and by inhalation. PACAP 1-27 does not cause pronounced cardiovascular side effects when given i.v. and it has a rapid onset of action when given by inhalation. PACAP 1-27, or its structural analogues, may therefore have therapeutic potential as bronchodilator drugs.

Supported in part by NIH PPG Grant HL-06285. A.L. was funded by the Sweden-America Foundation, the Swedish Heart Lung Fund, the Swedish Institute and the Swedish Medical Research Council.

References

ARIMURA, A. (1992). Pituitary adenylate cyclase activating polypeptide (PACAP): discovery and current status of research. *Regul. Pept.*, **37**, 287–303.

BARNES, P., CHUNG, K.F. & PAGE, C.F. (1988). Inflammatory mediators and asthma. *Pharmacol. Rev.*, **40**, 49–84.

BARNES, P. & DIXON, C.M. (1984). The effect of inhaled vasoactive intestinal polypeptide on bronchial reactivity to histamine in humans. *Am. Rev. Respir. Dis.*, **130**, 162–166.

BERTRAND, C., NADEL, J.A., GRAF, P. & GEPPETTI, P. (1993). Capsaicin increases airflow resistance in guinea-pigs *in vivo* by activating both NK2 and NK1 tachykinin receptors. *Am. Rev. Respir. Dis.*, **148**, 909–914.

CARDELL, L.-O., UDDMAN, R., LUTS, A. & SUNDLER, F. (1991). Pituitary adenylate-cylcase activating peptide (PACAP) in guinea pig lung: distribution and dilatory effects. *Regul. Pept.*, **36**, 379–390.

COLTON, T. (1974). *Statistics in Medicine*. 1st Edition. Boston, MA, U.S.A.: Little, Brown & Co.

DUSSER, D.J., UMENO, E., GRAF, P.D., DJOKIC, T.D., BORSON, D.B. & NADEL, J.A. (1988). Airway neutral endopeptidase-like enzymes modulate tachykinin-induced bronchoconstriction *in vivo*. *J. Appl. Physiol.*, **65**, 2585–2591.

KANEMURA, T., TAMAOKI, J., CHIYOTANI, A., TAKEYAMA, K., SAKAI, N., TAGAYA, E. & KONNO, K. (1993). Role of Na^+-K^+-ATPase in airway smooth muscle relaxation by vasoactive intestinal peptide and pituitary adenylate cyclase activating peptide. *Res. Commun. Chem. Pathol. Pharmacol.*, **79**, 11–22.

LUTS, A., UDDMAN, R., ALM, P., BASTERRA, J. & SUNDLER, F. (1993). Peptide-containing nerve fibers in human airways: distribution and coexistence pattern. *Int. Arch. Allergy Immunol.*, **101**, 52–60.

NADEL, J.A. (1992). Neurogenic inflammation in airways and its modulation by peptidases. *Ann. N.Y. Acad. Sci.*, **664**, 408–414.

O'DONNELL, M., GARIPPA, R.J., RINALDI, N., SELIG, W.M., TOCKER, J.E., TANNU, S.A., WASSERMAN, M.A., WELTON, A. & BOLIN, D.R. (1994). Ro-25-1553: a novel, long-acting vasoactive intestinal peptide agonist. Part II: Effect on *in vitro* and *in vivo* models of pulmonary anaphylaxis. *J Pharmacol. Exp. Ther.*, **270**, 1289–1294.

WALLIN, A., SANDSTROM, T., ROSENHALL, L. & MELANDER, B. (1993). Time course and duration of bronchodilatation with formoterol dry powder in patients with stable asthma. *Thorax*, **48**, 611–614.

(Received January 23, 1995
Accepted March 28, 1995)

British Journal of Pharmacology (1995) 115, 917-924 © 1995 Stockton Press All rights reserved 0007-1188/95 $12.00

Attenuation of adrenomedullin-induced renal vasodilatation by N^G-nitro L-arginine but not glibenclamide

[1]Katsuyuki Miura, Tsuneyuki Ebara, Michiaki Okumura, Takeshi Matsuura, Shokei Kim, Tokihito Yukimura & Hiroshi Iwao

Department of Pharmacology, Osaka City University Medical School, Osaka 545, Japan

1 The present study was conducted in order to elucidate the *in vivo* contribution of nitric oxide (NO) and the glibenclamide-sensitive potassium channel in the renal action of adrenomedullin in anaesthetized dogs.

2 Intrarenal arterial infusion of adrenomedullin (20 ng kg^{-1} min^{-1}) elicited a pronounced increase in renal blood flow with no changes in systemic blood pressure. The renal vasodilator action of adrenomedullin was markedly attenuated by pretreatment with N^G-nitro L-arginine (L-NOARG), but this was reversed by continuous infusion of L-arginine.

3 Pretreatment with glibenclamide almost completely blocked the renal vasodilatation induced by lemakalim, but had no effect on the renal vasodilator and diuretic action of adrenomedullin.

4 Intrarenal arterial infusion of adrenomedullin induced diuresis and natriuresis. Diuretic and natriuretic action of adrenomedullin was also attenuated by L-NOARG. L-Arginine partly reversed the effect of L-NOARG and adrenomedullin-induced diuresis and natriuresis.

5 These data indicate that the *in vivo* renal vasodilator action of adrenomedullin is mediated by the release of NO. The glibenclamide-sensitive potassium channel is not involved in the renal action of adrenomedullin, at least, not in anaesthetized dogs. Since the inhibition of L-NOARG of adrenomedullin-induced diuresis occurred concomitantly with the attenuation of the renal vasodilator action of adrenomedullin, direct involvement of NO in adrenomedullin-induced diuresis remains to be established.

Keywords: Adrenomedullin; nitric oxide; glibenclamide; N^G-nitro L-arginine; EDRF

Introduction

Adrenomedullin is a potent vasodilator peptide first found in human phaeochromocytoma (Kitamura *et al.*, 1993a). Adrenomedullin exists not only in naive adrenal medulla, but also in circulating blood and in the kidney (Kitamura *et al.*, 1993a). Messenger RNA of adrenomedullin is expressed in the kidney (Kitamura *et al.*, 1993b; Sakata *et al.*, 1993). We have shown that adrenomedullin is a potent renal vasodilator with a diuretic action (Ebara *et al.*, 1994). These data imply a possible role of adrenomedullin in the regulation of renal function. However, the mechanism(s) of action of adrenomedullin has not been elucidated. The structure of adrenomedullin has homology with those of calcitonin gene-related peptide (CGRP) and amylin, sharing a six-residue ring structure formed by a disulphide bond and the C-terminal amide structure (Kitamura *et al.*, 1993a). In addition, adrenomedullin and CGRP may share, at least in part, a common receptor, since the vasodilator action of adrenomedullin was attenuated in the presence of CGRP[8-37], an antagonist of the CGRP receptor (Nuki *et al.*, 1993). Since both adrenomedullin and CGRP elevate adenosine 3':5'-cyclic monophosphate (cyclic AMP) in cultured vascular smooth muscle cells (Kubota *et al.*, 1985; Eguchi *et al.*, 1994; Ishizaka *et al.*, 1994), it was speculated that adrenomedullin and CGRP act directly on vascular smooth muscle and elicit vasorelaxation via the accumulation of cyclic AMP. In contrast, endothelium-dependence (Brain *et al.*, 1985; Prieto *et al.*, 1991; Gray & Marshall, 1992a,b) and the possible implication of the glibenclamide-sensitive potassium channel (Nelson *et al.*, 1990) in the vasodepressor action of CGRP have been reported. Therefore, the present study was performed to elucidate the *in vivo* role of NO and the glibenclamide-sensitive potassium channel in the renal action of adrenomedullin.

Methods

Animal preparation

Mongrel dogs of either sex weighing 8 to 19 kg were anaesthetized with sodium pentobarbitone (30 mg kg^{-1}, i.v.). The anaesthetic was supplemented as required to maintain surgical anaesthesia. The dogs were ventilated artificially by use of a constant volume respirator (model 607, Harvard). The right brachial artery and vein were cannulated for blood sampling and an infusion of inulin solution (100 mg kg^{-1} bolus followed by 100 mg kg^{-1} h^{-1} in saline, 0.2 ml kg^{-1} min^{-1}), respectively. Another catheter was placed in the abdominal aorta via the right femoral artery and systemic blood pressure was monitored continuously with a pressure transducer (400T, Nihon Kohden). The left kidney was exposed through a retroperitoneal flank incision as described previously (Okumura *et al.*, 1992). All visible renal nerves were cut and 10% phenol in 70% ethanol was applied around the renal artery to facilitate observation of the direct effects of the peptide on the renal vasculature and tubular function, without the influence of changes in activity of the renal nerves. Renal blood flow was measured by an electromagnetic flow meter (MFV-1200, Nihon Kohden). A 23-gauge needle was inserted into the left renal artery proximal to the flow probe for infusion of saline or adrenomedullin solution, at the rate of 0.3 ml min^{-1}. A polyethylene catheter was inserted into the left ureter for urine collection. After the completion of surgery, the dogs were left for 60 to 90 min to allow stabilization of systemic blood pressure, renal blood flow and urine flow.

[1] Author for correspondence.

Protocols

Effects of L-NOARG on renal responses to adrenomedullin The dogs were divided into three groups.

Group I (adrenomedullin alone) After two consecutive timed urine collections with midpoint arterial blood collections (3 ml each), adrenomedullin was infused for 25 min into the renal artery, at the rate of 20 ng kg^{-1} min^{-1} in 6 dogs; 5, 10 and 20 min after the start of the peptide infusion, blood samples were obtained with timed urine collections. Additional blood samples with timed urine collections were taken at 10, 30 and 60 min after the cessation of peptide infusion.

Group II (adrenomedullin with L-NOARG) Five dogs were given L-NOARG into the renal artery at the rate of 80 μg kg^{-1} min^{-1} for 25 min. Ten min later, control blood samplings with timed urine collection were started. The remainder of the experiment was essentially the same as for group I. Our previous study has shown that renal blood flow decreased following intrarenal arterial infusion of L-NOARG at the rate of 80 μg kg^{-1} min^{-1} for 25 min and remained depressed for more than 1 h after the cessation of infusion (Yukimura *et al.*, 1992).

Group III (adrenomedullin with L-NOARG and L-arginine) Four dogs received intrarenal arterial infusion of L-arginine hydrochloride at the rate of 2 mg kg^{-1} min^{-1} during the entire period of the experiments. Thirty min after the start of L-arginine infusion, the same protocol was adopted as that used for group II.

In an additional group of experiments, the effectiveness and specificity of L-NOARG were assessed in 5 dogs. For this purpose, bolus injections of acetylcholine (20 ng kg^{-1}) and nitroglycerin (1 μg kg^{-1}) into the renal artery was made before and 30–60 min after the cessation of intrarenal arterial infusion of L-NOARG (80 μg kg^{-1} min^{-1} for 25 min). The increase in renal blood flow was assessed by comparison of the maximal increase and the area under the response curve for the renal blood flow. The latter was performed on a Macintosh IIsi computer using public domain NIH Image programme.

Effects of glibenclamide on renal vascular responses to adrenomedullin To elucidate the role of the glibenclamide-sensitive potassium channel in the renal vascular action of adrenomedullin, glibenclamide (3 mg kg^{-1}) was administered intravenously to 4 dogs. After 30 min, adrenomedullin was infused into the renal artery at the rate of 20 ng kg^{-1} min^{-1} in 4 dogs. As a corresponding control group, 4 additional dogs were given the vehicle, dimethylformamide (40 μl kg^{-1}) instead of glibenclamide, after which adrenomedullin was administered.

In a separate group of experiments ($n=3$), effective blockade of the renal vasodilator action of lemakalim by glibenclamide was assessed. Intrarenal arterial injection of lemakalim (1 μg kg^{-1}) was conducted after administration of vehicle (40 μl kg^{-1}, i.v.) and glibenclamide (3 mg kg^{-1}, i.v.), respectively.

Analytical procedures

Inulin was determined by colorimetry, as described by Walser *et al.* (1955) and glomerular filtration rate (GFR) was estimated by the inulin clearance. Urinary and plasma concentrations of sodium and potassium were measured by flame photometry (205D, Hitachi, Tokyo, Japan).

Statistical analysis

Results presented in the paper are shown as means ± s.e.mean. Intergroup differences in the data were analysed either by Student's t test or one-way analysis of variance (ANOVA). Data within the groups were analysed by a complete randomized block ANOVA. Following ANOVA, individual statistical differences were determined by Duncan's multiple range comparison test (SuperANOVA, Abacus Concepts., Berkeley, U.S.A.). When data appeared heteroscedastic, logarithmic transformation was performed before data analysis (Zar, 1984).

Drugs

The drugs used were: acetylcholine chloride, L-arginine hydrochloride (Ishizu Pharmaceutical, Osaka), nitroglycerin (Millisrol inj., Nippon Kayaku, Tokyo), sodium pentobarbitone (Tokyo Chemical Industry, Tokyo), glibenclamide, inulin (Sigma, St. Louis, U.S.A.). Human adrenomedullin and N^G-nitro L-arginine were purchased from Peptide Institute (Osaka). Lemakalim was a kind gift from SmithKline Beecham Seiyaku (Tokyo).

Results

Effects of L-NOARG on renal responses to adrenomedullin

Figure 1 shows the effects of L-NOARG and L-arginine on the renal action of adrenomedullin. As previously reported (Ebara *et al.*, 1994), intrarenal arterial infusion of adrenomedullin at the rate of 20 ng kg^{-1} min^{-1} elicited a marked increase in renal blood flow from 4.0 ± 0.3 to 5.9 ± 0.4 ml g^{-1} min^{-1} at 20 min without any changes in systemic blood pressure. GFR tended to increase from 0.97 ± 0.06 to 1.05 ± 0.05 ml g^{-1} min^{-1} at 10 min, but this change was not statistically significant. As a result, filtration fractions were decreased from 38.3 ± 3.1% to 26.7 ± 1.2% with adrenomedullin alone ($P<0.01$). Adrenomedullin increased urine flow and urinary excretion of sodium and potassium approximately two-fold.

The pre-infusion value of renal blood flow was significantly lower in group II (2.5 ± 0.2 ml g^{-1} min^{-1}) than in group I (4.0 ± 0.3 ml g^{-1} min^{-1}). This value in group III was 3.6 ± 0.6 ml g^{-1} min^{-1}, which was not statistically different either from that in group I or in group II. Following L-NOARG treatment, adrenomedullin increased renal blood flow significantly from 2.5 ± 0.2 to 3.0 ± 0.2 ml g^{-1} min^{-1} at 20 min, but the magnitude of the increase was apparently less than that observed in the absence of L-NOARG. Figure 2 summarizes the magnitude of the increases in renal blood flow elicited by adrenomedullin. Adrenomedullin alone increased renal blood flow by 1.87 ± 0.14 ml g^{-1} min^{-1} (by 48.2 ± 5.3%) at 20 min. In dogs pretreated with L-NOARG (group II), this increase in renal blood flow at 20 min after the start of adrenomedullin infusion was 0.46 ± 0.10 ml g^{-1} min^{-1} (by 18.5 ± 3.8%) which was significantly smaller than that seen with adrenomedullin alone. When dogs were given L-arginine during the entire period of the experiment, L-NOARG failed to attenuate the elevation of renal blood flow elicited by adrenomedullin (Figures 1, 2). Under this condition, adrenomedullin increased renal blood flow by 1.73 ± 0.40 ml g^{-1} min^{-1} (by 47.2 ± 7.9%) which was not statistically different from that with adrenomedullin alone.

Pre-infusion values of GFR were 0.97 ± 0.06 ml g^{-1} min^{-1} in group I 0.65 ± 0.06 ml g^{-1} min^{-1} in group II and 0.83 ± 0.11 ml g^{-1} min^{-1} in group III, respectively. There was a statistically significant difference only between those of group I and group II ($P<0.05$). Adrenomedullin did not affect the course of GFR following either L-NOARG or L-NOARG in combination with L-arginine (Figure 1). Pretreatment with L-NOARG attenuated adrenomedullin-induced reduction in filtration fraction (37.6 ± 4.8% during control and 33.6 ± 4.5% at 20 min after the start of adrenomedullin infusion, $P>0.05$). When L-arginine was given with L-NOARG, adrenomedullin elicited a reduction in filtration fraction from 38.0 ± 4.8% to 28.0 ± 3.7% ($P<0.05$).

Pre-infusion values of urine flow and urinary excretion of

sodium and potassium were significantly lower in group II (adrenomedullin with L-NOARG) and group III (adrenomedullin with L-NOARG and L-arginine) compared to group I (adrenomedullin alone) (Figure 1). Adrenomedullin alone significantly increased urine flow and urinary sodium excretion from 22.8 ± 4.3 to 52.0 ± 7.9 $\mu l\ g^{-1}\ min^{-1}$ and from 5.2 ± 1.0 to 9.6 ± 1.3 $\mu Eq\ g^{-1}\ min^{-1}$, respectively. Similarly, adrenomedullin significantly increased urine flow and urinary electrolytes excretion following treatment with L-NOARG irrespective of co-administration of L-arginine. The percentage increases in urine flow elicited by adrenomedullin were $166 \pm 63\%$ in group I (adrenomedullin alone) which was not statistically different from those in the L-NOARG group (group II, $140 \pm 56\%$) or those in the L-NOARG and L-arginine-treated group (group III, $147 \pm 52\%$). Urinary excretion of sodium increased by $111 \pm 23\%$ with adrenomedullin alone, which was statistically the same as group II ($200 \pm 106\%$) and group III ($185 \pm 30\%$). Similarly, there was no statistically significant difference in the percentage increases in urinary potassium excretion among these groups (group I, $77 \pm 23\%$, group II $85 \pm 39\%$, group III, $85 \pm 13\%$). Fractional excretion of sodium increased significantly ($P < 0.01$) in all groups from $3.4 \pm 0.6\%$ to $6.0 \pm 0.8\%$ (group I), from $1.3 \pm 0.5\%$ to $2.6 \pm 0.7\%$ (group II) and from $1.3 \pm 0.3\%$ to $3.3 \pm 0.9\%$

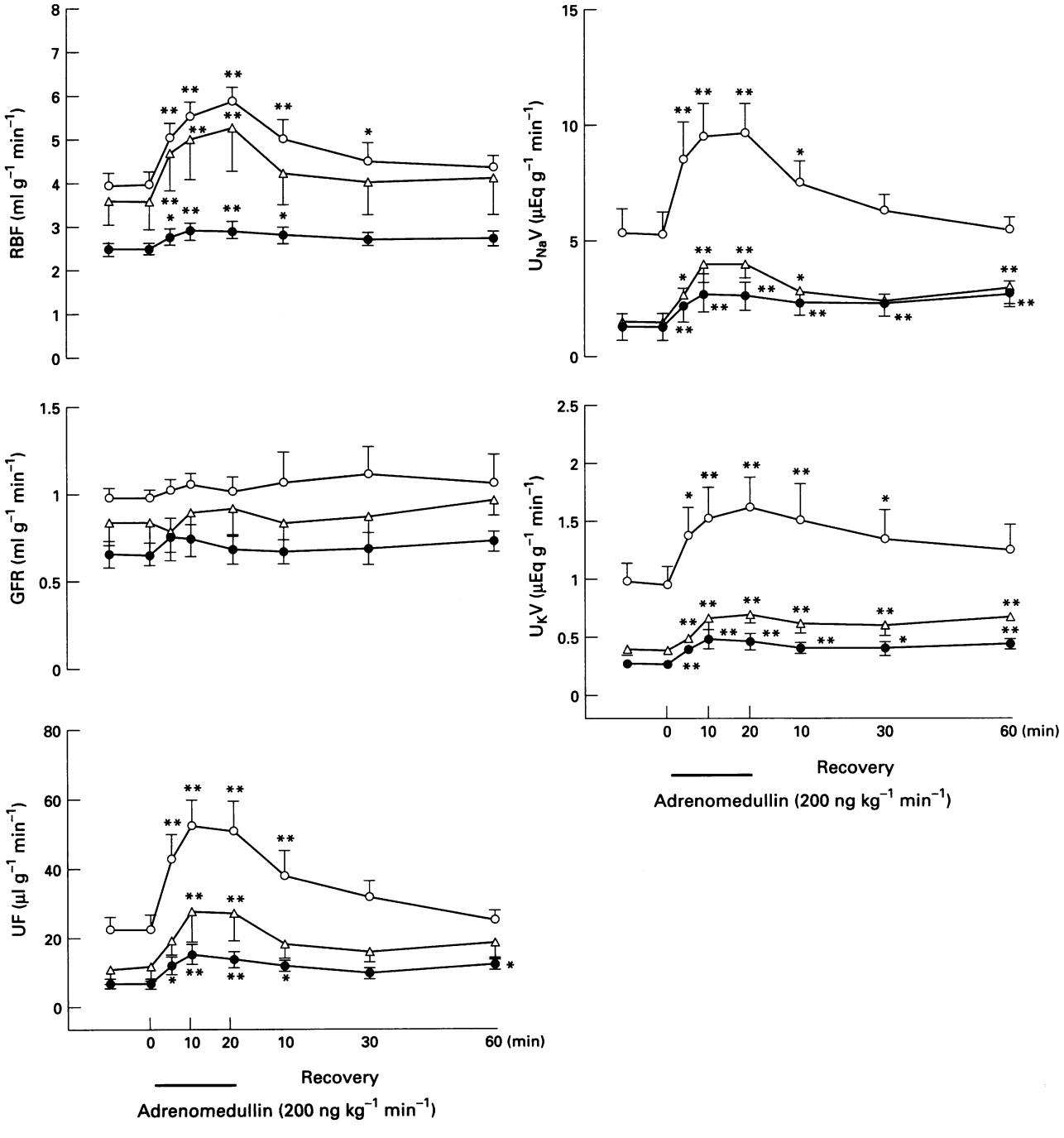

Figure 1 Effects of N^G-nitro L-arginine (L-NOARG) on the renal action of adrenomedullin. Adrenomedullin was infused into the renal artery for 25 min at the rate of 20 ng kg^{-1} min^{-1}. Symbols represent the following: (○), group I (adrenomedullin alone); (●) group II (adrenomedullin with L-NOARG); (△) group III (adrenomedullin with L-NOARG and L-arginine); RBF, renal blood flow; GFR, glomerular filtration rate; UF, urine flow; $U_{Na}V$, urinary excretion of sodium; U_KV, urinary excretion of potassium. Data were corrected for the kidney weight. $^*P < 0.05$ and $^{**}P < 0.01$ compared to the pre-infusion values.

(group III) after 20 min of adrenomedullin infusion, respectively. However, since basal output of fluid and electrolytes from the kidney was reduced by L-NOARG (Figure 1), pretreatment with L-NOARG significantly attenuated adrenomedullin-induced increase in urine flow and urinary excretion of sodium when increases were compared in terms of absolute value (Figure 2). The increases in urine flow and urinary sodium excretion in group II (adrenomedullin following L-NOARG treatment) were 6.9 ± 1.9 μl g^{-1} min^{-1} and 1.3 ± 0.4 μEq g^{-1} min^{-1} which were significantly lower than those with adrenomedullin alone (group I, 28.5 ± 6.4 μl g^{-1} min^{-1}, 4.5 ± 1.0 μEq g^{-1} min^{-1}). Even when L-arginine was given with L-NOARG treatment, basal output of fluid and electrolytes remained depressed (Figure 1). The increases in urine flow and urinary excretion of sodium during adrenomedullin administration in group III (adrenomedullin treatment together with L-arginine and L-NOARG) were 16.1 ± 6.3 μl g^{-1} min^{-1} and 2.6 ± 0.4 μEq g^{-1} min^{-1}, respectively. The magnitude of the adrenomedullin-induced increase in urine flow and urinary sodium excretion in group III ranged between those in group I and group II and these values were not statistically different from those in group I or group III.

As described above, basal urine flow and urinary excretion of sodium were lower in group II and group III compared to those in group I, which may suggest L-NOARG-decreased urine flow and urinary excretion of sodium was not reversed by administration of L-arginine. However, we have data showing that reduced output of fluid and sodium by L-NOARG at a

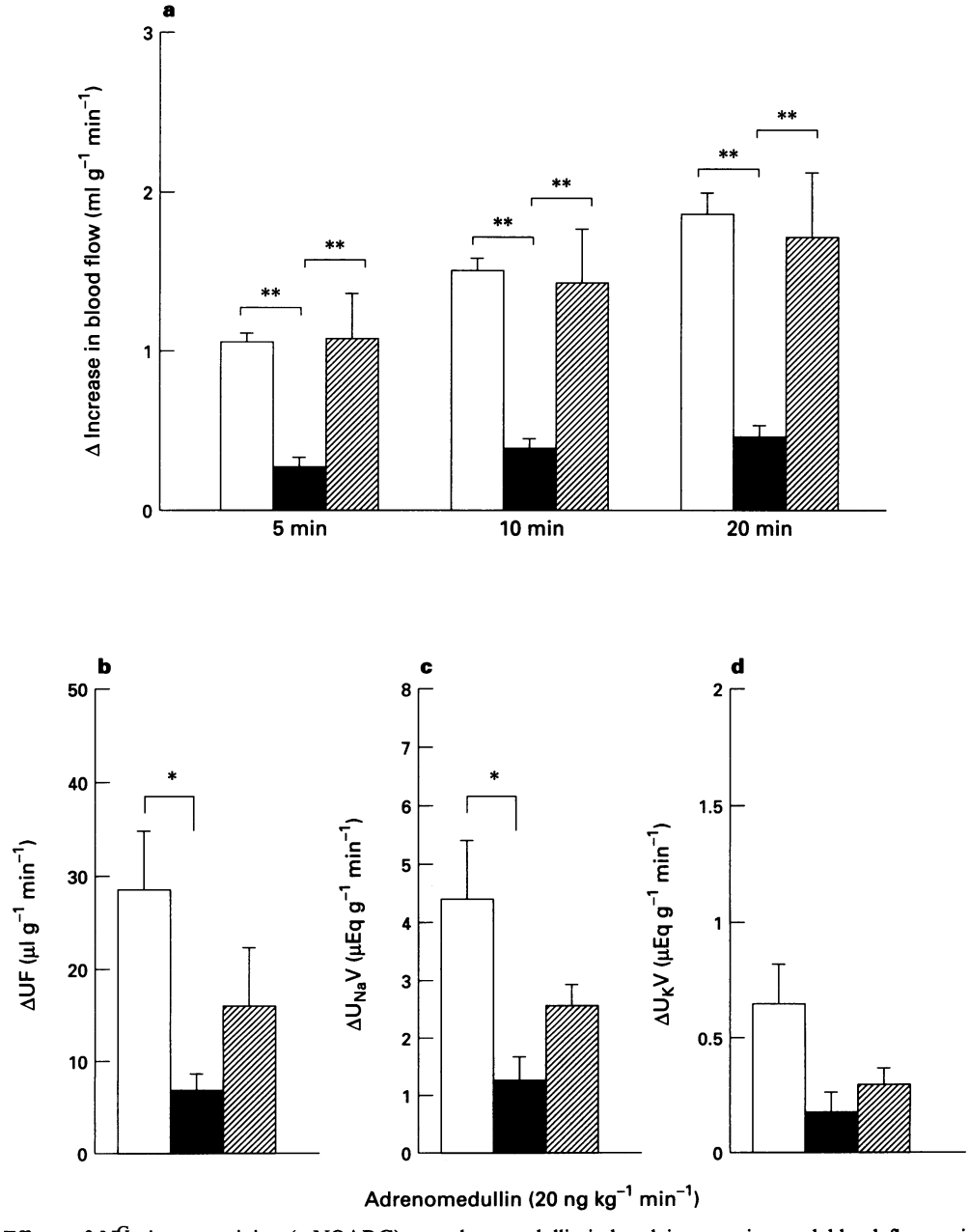

Figure 2 Effects of N^G-nitro L-arginine (L-NOARG) on adrenomedullin-induced increase in renal blood flow, urine flow and urinary electrolytes excretion. (a) Increase in renal blood flow from the level just before adrenomedullin infusion. Abscissa scale shows the time after the start of adrenomedullin infusion. Lower panels: increase from the level just before adrenomedullin infusion in urine flow (UF, b), urinary excretion of sodium ($U_{Na}V$, c) and urinary excretion of potassium (U_KV, d) at 20 min after the start of adrenomedullin infusion. Open column, group I (adrenomedullin alone); solid column, group II (adrenomedullin with L-NOARG); hatched column, group III (adrenomedullin with L-NOARG and L-arginine). $^*P < 0.05$ and $^{**}P < 0.01$ between the indicated groups.

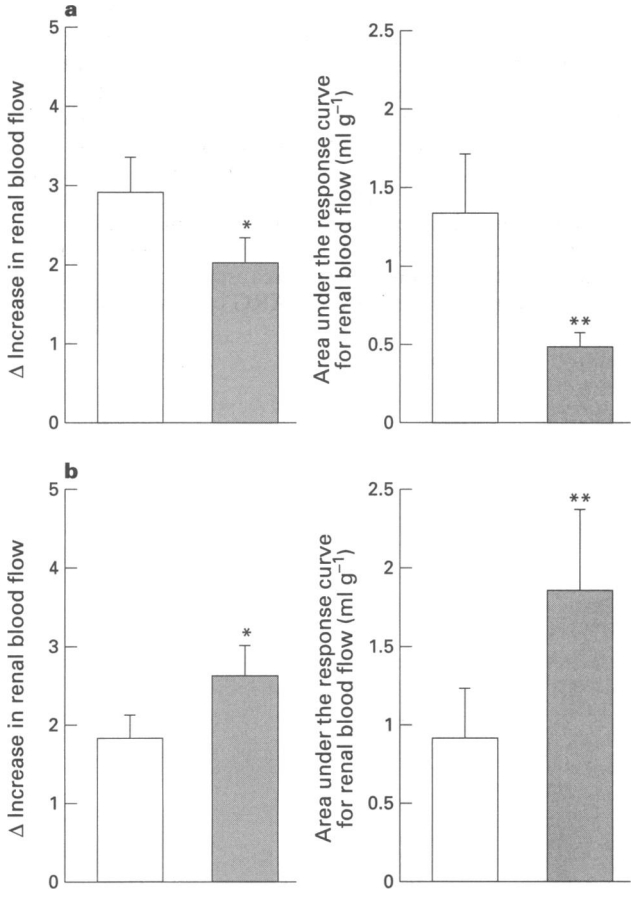

Figure 3 Effects of N^G-nitro L-arginine (L-NOARG) on the renal blood flow increase induced by intrarenal arterial injection of (a) acetylcholine and (b) nitroglycerin. Open column indicates the renal blood flow increase before L-NOARG; hatched column following L-NOARG administration. Left panel shows the increase in renal blood flow. Right panel indicates the area under the response curve for the renal blood flow. $^*P<0.05$ and $^{**}P<0.01$ compared to the values before L-NOARG administration.

dose used in the present experiments was reversed by subsequent infusion of L-arginine. Intrarenal arterial infusion of L-NOARG for 30 min at a rate of 80 μg kg^{-1} min^{-1} decreased urine flow and urinary excretion of sodium from 25.2 ± 10.0 to 8.0 ± 2.4 μl g^{-1} min^{-1} and from 3.1 ± 0.8 to 1.1 ± 0.3 μEq g^{-1} min^{-1}, respectively; these values reverted to 34.9 ± 10.2 μl g^{-1} min^{-1} and 4.7 ± 1.2 μEq g^{-1} min^{-1} as a result of subsequent infusion of L-arginine at a rate of 2 mg kg^{-1} min^{-1} ($n=5$, unpublished observation).

Figure 3 shows the effective blockade by L-NOARG of the vasodilator action of acetylcholine (ACh), a typical endothelium-dependent vasodilator. Bolus injection of ACh into the renal artery increased renal blood flow by 2.9 ± 0.5 ml g^{-1} min^{-1}. Following L-NOARG, ACh increased renal blood flow by 2.0 ± 0.3 ml g^{-1} min^{-1}, which was significantly lower than ACh alone. Increase by ACh of the area under the response curve for renal blood flow was 1.3 ± 0.4 ml g^{-1} before L-NOARG, and this was significantly attenuated following L-NOARG (0.5 ± 0.1 ml g^{-1}). In contrast, the renal vasodilator action of nitroglycerin was markedly potentiated by L-NOARG. Nitroglycerin increased renal blood flow by 1.8 ± 0.3 ml g^{-1} min^{-1} before L-NOARG, and this was significantly increased by L-NOARG treatment (2.6 ± 0.4 ml g^{-1} min^{-1}). The area under the response curve with nitroglycerin was also increased from 0.9 ± 0.3 to 1.9 ± 0.5 ml g^{-1} following L-NOARG treatment.

Effects of glibenclamide on renal vascular responses to adrenomedullin

Following vehicle (dimethylformamide) administration, intrarenal arterial injection of lemakalim increased renal blood flow by 0.77 ± 0.12 ml g^{-1} min^{-1}, which was almost completely blocked by glibenclamide administration (by 0.04 ± 0.02 ml g^{-1} min^{-1}) (Figure 4). In contrast, glibenclamide did not affect the adrenomedullin-induced increase in renal blood flow (Figure 4). In addition, adrenomedullin-induced diuresis and natriuresis were not affected by glibenclamide (Figure 4).

Discussion

The main finding of the present study was that L-NOARG markedly attenuated the renal vasodilator action of adrenomedullin. Intrarenal arterial infusion of adrenomedullin at a rate of 20 ng kg^{-1} min^{-1} induced a marked increase in renal blood flow without changes in blood pressure, indicating renal vasodilatation elicited by adrenomedullin. We previously reported that there was a dose-dependent increase in renal blood flow by adrenomedullin including the dose used in the present study (Ebara *et al.*, 1994). Following L-NOARG treatment, this renal vasodilatation was significantly attenuated. L-NOARG is a potent inhibitor of NO synthase (NOS) (Dubbin *et al.*, 1990) and endothelium-dependent vasodilatation (Moore *et al.*, 1990; Yamashita *et al.*, 1991; Okumura *et al.*, 1992). In fact, L-NOARG markedly attenuated the renal vasodilator action of ACh, a typical endothelium-dependent vasodilator, but not that of nitroglycerin (Figure 3). Furthermore, L-NOARG-induced attenuation of the renal vasodilator action of adrenomedullin was largely reversed by sustained administration of L-arginine. These data strongly suggest that arginine-derived NO is involved in the mechanism of adrenomedullin-induced renal vasodilatation. As the magnitude of the increase in renal blood flow induced by nitroglycerin was potentiated by L-NOARG, it is unlikely that L-NOARG suppressed the vasodilator action of vasoactive substances in a non-specific manner.

Eguchi *et al.* (1994) reported that specific adrenomedullin receptors exist and functionally couple to adenylate cyclase in rat cultured vascular smooth muscle cells. As cyclic AMP is an intracellular mediator of vasodilatation, they proposed that the vasorelaxant effect of adrenomedullin is mediated by the accumulation of cyclic AMP in vascular smooth muscle cells. This mechanism of vasodilator action may also function, at least in part, in the renal vasodilator action of adrenomedullin that remains following L-NOARG. Recently, it was shown that cyclic AMP induces NOS and enhances NO production in rat vascular smooth muscle cells (Imai *et al.*, 1994). However, it is unlikely that the cyclic AMP-inducible NOS is involved in the renal vasodilator action of adrenomedullin, for NOS induction requires at least 60 min (Szabo *et al.*, 1993) whereas the renal vasodilator action of adrenomedullin became manifest immediately after the start of administration.

It was shown that specific binding sites of adrenomedullin in cultured vascular smooth muscle cells also interact with CGRP (Eguchi *et al.*, 1994). CGRP[8-37], an antagonist for CGRP receptor, blocked adrenomedullin-induced cyclic AMP formation in cultured vascular smooth muscle cells (Eguchi *et al.*, 1994) and antagonized the vasodilator effect of adrenomedullin in the rat perfused mesenteric vascular bed (Nuki *et al.*, 1993). Therefore, it was speculated that adrenomedullin and CGRP may interact with the same receptor. Although CGRP also stimulates adenylate cyclase it was shown that endothelium-derived NO is involved in the vasorelaxation of isolated vascular strips (Gray & Marshall, 1992a,b). Our finding that L-NOARG attenuated the renal vasodilator action of adrenomedullin may be consistent with the hypothesis that adrenomedullin interacts with the CGRP receptor.The vasodilator action of adrenomedullin was accompanied by a sig-

nificant increase in urine flow and the urinary excretion of sodium and potassium in all groups. Since basal output of fluid and electrolytes with L-NOARG even in the presence of L-arginine (groups II and III) was lower than that in control group (group I), the interpretation of the effects of L-NOARG on adrenomedullin-induced diuresis is difficult. When adrenomedullin-induced increases in urine flow and urinary electrolytes excretion were expressed as percentage increases, there are no statistically significant effects of L-NOARG and/or L-arginine. However, significant attenuation of adrenomedullin-induced diuresis and natriuresis were found with L-NOARG treatment when increases were compared in terms of absolute change. When L-arginine was given with L-NOARG, adrenomedullin-induced increases in urine flow and urinary excretion of sodium were not statistically different from those observed with adrenomedullin alone. Therefore, it is suggested that L-arginine, partially reversed the attenuation by L-NOARG of adrenomedullin-induced diuresis and natriuresis. It is well known that NO stimulates cyclic GMP production. Atrial natriuretic peptide enhances cyclic GMP production and inhibits sodium and water transport in the tubular cells (Zeidel *et al.*, 1987). We previously mentioned that NO may be involved in the regulation of renal tubular reabsorption of sodium and water, since a small dose of L-NOARG causes antidiuresis and

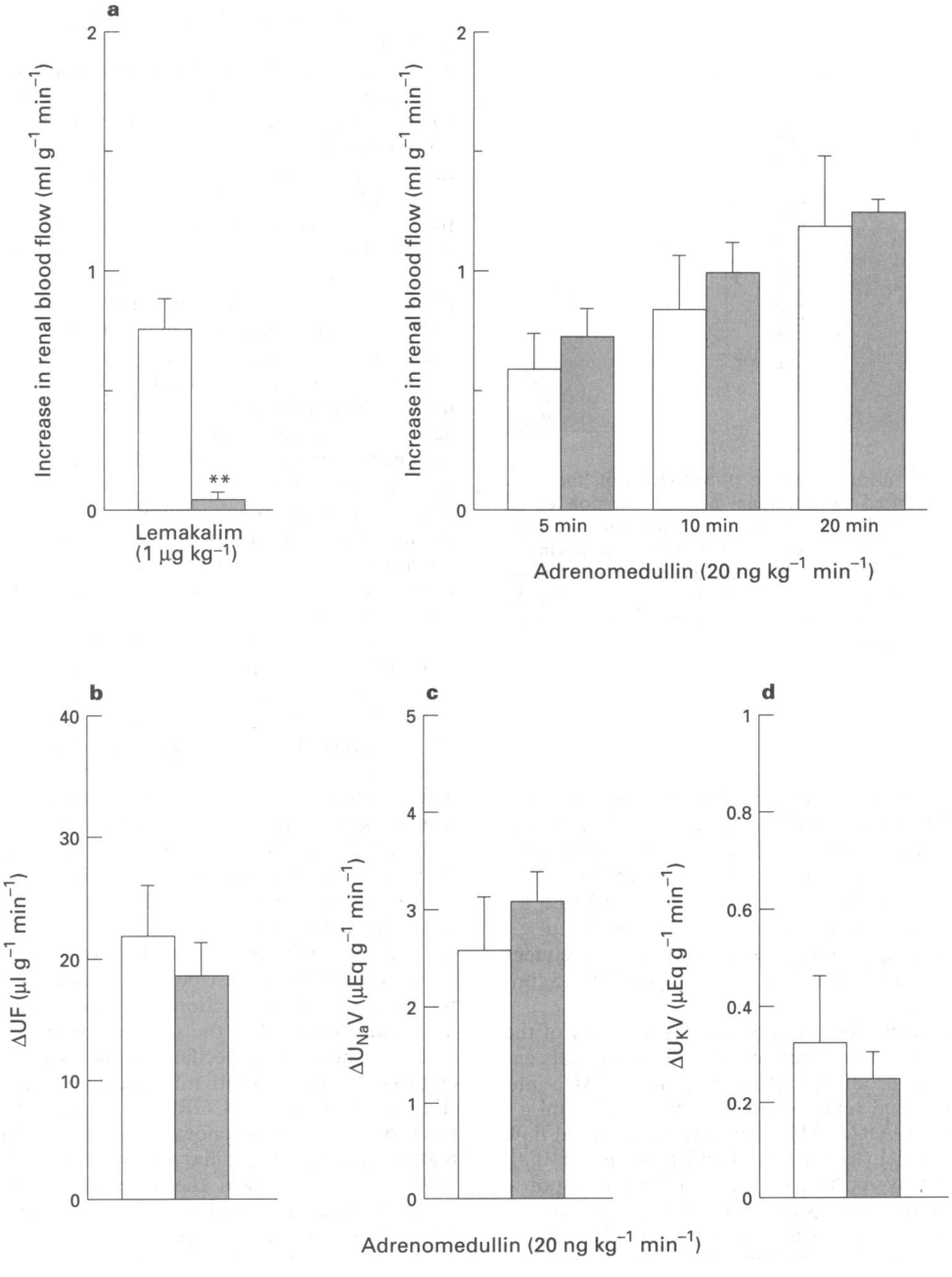

Figure 4 Effects of glibenclamide on increases in renal blood flow, urine flow and urinary excretion of electrolytes induced by intrarenal infusion of lemakalim and adrenomedullin. (a) Increase in renal blood flow by lemakalim (left panel) and by adrenomedullin. Abscissa scale shows the time after the start of adrenomedullin infusion. Lower panels: increase from the level just before adrenomedullin infusion in urine flow (UF, b), urinary excretion of sodium ($U_{Na}V$, c) and urinary excretion of potassium (U_KV, d) at 20 min after the start of adrenomedullin infusion. Open column indicates the renal blood flow increase after vehicle (dimethylformamide) administration; stippled column following glibenclamide administration. $^{**}P < 0.01$ compared to the values after vehicle administration.

antinatriuresis without affecting renal blood flow, glomerular filtration rate or systemic blood pressure (Yukimura *et al.*, 1992). Our present results together with these findings may suggest that adrenomedullin causes diuresis and natriuresis, at least in part, through enhanced production of NO.

However, there are limitations in elucidating the mechanism(s) of the diuretic action of adrenomedullin. First, the reduced basal output of fluid and electrolytes elicited by L-NOARG was not apparently reversed by L-arginine. Although we do not know the reason, we have data showing that antidiuretic action of L-NOARG could be reversed by L-arginine (for details, see results). Nevertheless, this may suggest that L-NOARG has a non-specific action in altering the intrarenal regulatory mechanisms, particularly the process of renal tubular reabsorption. Previous reports on the effects of NOS inhibition by arginine analogues gave controversial results. In dogs, NOS inhibitors caused antidiuresis (Yukimura *et al.*, 1992; Majid *et al.*, 1993). Radermacher *et al.* (1992), on the contrary, reported that inhibition of NOS resulted in attenuation of sodium reabsorption in rat isolated perfused kidney. Thus, the role of NO in the renal tubular function remains to be established. Second, whether the diuretic action of adrenomedullin is a result of direct action of adrenomedullin on the tubules is unknown at present. The diuretic action is always associated with renal haemodynamic changes (Ebara *et al.*, 1994). If the diuretic action of adrenomedullin is secondary to the haemodynamic change, attenuation of adrenomedullin-induced renal vasodilatation by L-NOARG would have resulted in blocking of the diuretic action of adrenomedullin. In this respect, it is of note that the filtration fraction was decreased with adrenomedullin alone and a reduced filtration fraction would decrease postglomerular oncotic pressure, which may lead to the inhibition of proximal tubular transport (Baylis *et al.*, 1976). Since L-NOARG blocked adrenomedullin-induced reduction in the filtration fraction, inhibition by L-NOARG of adrenomedullin-induced diuresis may be solely a result of blockade of the NO-mediated haemodynamic changes elicited by adrenomedullin. Therefore, following pretreatment with L-NOARG and L-arginine, adrenomedullin again elicited a reduction in filtration fraction and adrenomedullin-induced diuresis was recovered at least in part. Finally, in order to clarify the mechanism of action of adrenomedullin on urine formation, a more precise study, such as microperfusion of the tubular segment *in vitro* would be required.

Nelson demonstrated that activation of the potassium channel of vascular smooth muscle cells by CGRP leads to a relaxation of rabbit mesenteric artery which is blocked by glibenclamide. This fact, together with the notion of the similarity of receptors for adrenomedullin and CGRP, led us to test whether activation of the glibenclamide-sensitive potassium channel is involved in the renal action of adrenomedullin. Glibenclamide effectively blocked the renal vasodilator action of lemakalim, a typical ATP-sensitive potassium channel opener. However, glibenclamide had no effect on the adrenomedullin-induced increase in renal blood flow, urine flow and urinary excretion of electrolytes. These data indicate that the *in vivo* renal vasodilator action and diuretic action of adrenomedullin in dogs are not related to activation of the glibenclamide-sensitive K channel.

In summary, our observations suggest that adrenomedullin has an arginine-derived NO-mediated renal vasodilator action in anaesthetized dogs. The glibenclamide-sensitive potassium channel is not involved in the renal action of adrenomedullin.

This work was partly supported by a Grant-in-Aid for Scientific Research from the Ministry of Education, Science and Culture.

References

BRAIN, S.D., WILLIAMS, T.J., TIPPINS, J.R., MORRIS, H.R. & MACINTYRE, I. (1985). Calcitonin gene-related peptide is a potent vasodilator. *Nature*, **313**, 54–56.

BAYLIS, C., DEEN, W.M., MYERS, B.D. & BARRY, M. (1976). Effects of some vasodilator drugs on transcapillary fluid exchange in renal cortex. *Am. J. Physiol.*, **230**, 1148–1158.

DUBBIN, P.N., ZAMBETIS, M. & DUSTING, G.J. (1990). Inhibition of endothelial nitric oxide biosynthesis by N-nitro-L-arginine. *Clin. Exp. Pharmacol. Physiol.*, **17**, 281–286.

EBARA, T., MIURA, K., OKUMURA, M., MATSUURA, T., KIM, S., YUKIMURA, T. & IWAO, H. (1994). Effect of adrenomedullin on renal hemodynamics and functions in dogs. *Eur. J. Pharmacol.*, **263**, 69–73.

EGUCHI, S., HIRATA, Y., KANO, H., SATO, K., WATANABE, Y., WATANABE, T.X., NAKAJIMA, K., SAKAKIBARA, S. & MARUMO, F. (1994). Specific receptors for adrenomedullin in cultured rat vascular smooth muscle cells. *FEBS Lett.*, **340**, 226–230.

GRAY, D.W. & MARSHALL, I. (1992a). Human alpha-calcitonin gene-related peptide stimulates adenylate cyclase and guanylate cyclase and relaxes rat thoracic aorta by releasing nitric oxide. *Br. J. Pharmacol.*, **107**, 691–696.

GRAY, D.W. & MARSHALL, I. (1992b). Nitric oxide synthesis inhibitors attenuate calcitonin gene-related peptide endothelium-dependent vasorelaxation in rat aorta. *Eur. J. Pharmacol.*, **212**, 37–42.

IMAI, T., HIRATA, Y., KANNO, K. & MARUMO, F. (1994). Induction of nitric oxide synthase by cyclic AMP in rat vascular smooth muscle cells. *J. Clin. Invest.*, **93**, 543–549.

ISHIZAKA, Y., ISHIZAKA, Y., TANAKA, M., KITAMURA, K., KANGAWA, K., MINAMINO, N., MATSUO, H. & ETO, T. (1994). Adrenomedullin stimulates cyclic AMP formation in rat vascular smooth muscle cells. *Biochem. Biophys. Res. Commun.*, **200**, 642–646.

KITAMURA, K., KANGAWA, K., KAWAMOTO, M., ICHIKI, Y., NAKAMURA, S., MATSUO, H. & ETO, T. (1993a). Adrenomedullin: a novel hypotensive peptide isolated from human pheochromocytoma. *Biochem. Biophys. Res. Commun.*, **192**, 553–560.

KITAMURA, K., SAKATA, J., KANGAWA, K., KOJIMA, M., MATSUO, H. & ETO, T. (1993b). Cloning and characterization of cDNA encoding a precursor for human adrenomedullin. *Biochem. Biophys. Res. Commun.*, **194**, 720–725.

KUBOTA, M., MOSELEY, J.M., BUTERA, L., DUSTING, G.J., MACDONALD, P.S. & MARTIN, T.J. (1985). Calcitonin gene-related peptide stimulates cyclic AMP formation in rat aortic smooth muscle cells. *Biochem. Biophys. Res. Commun.*, **132**, 88–94.

MAJID, D.S., WILLIAMS, A. & NAVAR, L.G. (1993). Inhibition of nitric oxide synthesis attenuates pressure-induced natriuretic responses in anaesthetized dogs. *Am. J. Physiol.*, **264**, F79–F87.

MOORE, P.K., AL-SWAYEH, O.A., CHONG, N.W., EVANS, R.A. & GIBSON, A. (1990). L-N^G-nitro arginine (L-NOARG), a novel, L-arginine-reversible inhibitor of endothelium-dependent vasodilatation *in vitro*. *Br. J. Pharmacol.*, **99**, 408–412.

NELSON, M.T., HUANG, Y., BRAYDEN, J.E., HESCHELER, J. & STANDEN, N.B. (1990). Arterial dilations in response to calcitonin gene-related peptide involve activation of K^+ channels. *Nature*, **344**, 770–773.

NUKI, C., KAWASAKI, H., KITAMURA, K., TAKENAGA, M., KANAGAWA, K., ETO, T. & WADA, A. (1993). Vasodilator effect of adrenomedullin and calcitonin gene-related peptide receptors in rat mesenteric vascular beds. *Biochem. Biophys. Res. Commun.*, **196**, 245–251.

OKUMURA, M., MIURA, K., YAMASHITA, Y., YUKIMURA, T. & YAMAMOTO, K. (1992). Role of endothelium-derived relaxing factor in the *in vivo* renal vascular action of adenosine in dogs. *J. Pharmacol. Exp. Ther.*, **260**, 1262–1267.

PRIETO, D., BENEDITO, S. & NYBORG, N.C (1991). Heterogeneous involvement of endothelium in calcitonin gene-related peptide-induced relaxation in coronary arteries from rat. *Br. J. Pharmacol.*, **103**, 1764–1768.

RADERMACHER, J., KLANKE, B., SCHUREK, H.-J., STOLTE, H.F. & FRÖLICH, J.C. (1992). Importance of NO/EDRF for glomerular and tubular function: Studies in the isolated perfused rat kidney. *Kidney Int.*, **41**, 1549–1559.

SAKATA, J., SHIMOKUBO, T., KITAMURA, K., NAKAMURA, S., KANGAWA, K., MATSUO, H. & ETO, T. (1993). Molecular cloning and biological activities of rat adrenomedullin, a hypotensive peptide. *Biochem. Biophys. Res. Commun.*, **195,** 921–927.

SZABO, C., MITCHELL, J.A., THIEMERMANN, C. & VANE, J.R. (1993). Nitric oxide-mediated hyporeactivity to noradrenaline precedes the induction of nitric oxide synthase in endotoxin shock. *Br. J. Pharmacol.*, **108,** 786–792.

WALSER, M., DAVIDSON, D.G. & ORLOFF, J. (1955). The renal clearance of alkali-stable inulin. *J. Clin. Invest.*, **34,** 1520–1523.

YAMASHITA, Y., YUKIMURA, T., MIURA, K., OKUMURA, M., YAMANAKA, S. & YAMAMOTO, K. (1991). Effects of N^G-nitro-L-arginine on renal hemodynamic responses to endothelin-3 in anaesthetized dogs. *J. Cardiovasc. Pharmacol.*, **17,** S332–S334.

YUKIMURA, T., YAMASHITA, Y., MIURA, K., OKUMURA, M., YAMANAKA, S. & YAMAMOTO, K. (1992). Renal effects of nitric oxide synthase inhibitor, L-N^G-nitro arginine in dogs. *Am. J. Hypertens.*, **5,** 484–487.

ZAR, J.H. (1984). *Biostatistical Analysis* 2nd edition, New Jersey: Prentice-Hall, Inc.

ZEIDEL, M.L., SILVA, P., BRENNER, B.M. & SEIFTER, J.L. (1987). cGMP mediates effects of atrial peptide on medullary collecting duct cells. *Am. J. Physiol.*, **252,** F551–F559.

(Received July 26, 1994
Revised December 30, 1994
Accepted March 30, 1995)

British Journal of Pharmacology (1995) 115, 925-932 © 1995 Stockton Press All rights reserved 0007-1188/95 $12.00

Characterization of acute homologous desensitization of μ-opioid receptor-induced currents in locus coeruleus neurones

*P.B. Osborne & [1]J.T. Williams

Vollum Institute, Oregon Health Sciences University, Portland OR97201, U.S.A. and *Department of Pharmacology D06, University of Sydney, NSW 2006, Australia

1 Acute homologous desensitization of μ-opioid receptor-induced currents was pharmacologically characterized in locus coeruleus (LC) neurones by use of intracellular and whole cell recording in superfused brain slices.

2 Following desensitization of opioid receptors by perfusion with a high concentration of [Met^5] enkephalin (ME) for 5 min, there was a reduction in the maximum response and a rightward shift of the concentration-response curves for ME, [D-Ala^2, *N*-MePhe^4, Gly-ol]enkephalin (DAMGO) and normorphine.

3 By simultaneously fitting the operational model to the paired pre- and post-desensitization concentration-response data for each agonist, estimates of the level of desensitization were obtained. The values obtained for the three agonists (between 88% and 96%) were similar and did not vary according to the efficacy of the agonist used.

4 Use of whole cell patch recording techniques caused a slow rundown in the amplitude of ME currents (approx. 40% reduction over 60 min) but did not greatly affect the expression of acute desensitization of opioid currents.

5 When included in the patch recording solution, the phosphatase inhibitors, microcystin (50 nM–4 μM) and okadaic acid (1 μM) had no effect on the induction of desensitization or the normal ability of opioid or α_2-adrenoceptors to produce currents. Microcystin decreased the rate of recovery of the ME (300 nM) currents following desensitization; however, okadaic acid had little effect on the rate of recovery from desensitization.

6 Strong calcium buffering with BAPTA (10–20 mM) had no effect on desensitization or the recovery from desensitization.

7 These results suggest that acute homologous desensitization of μ-opioid receptors in LC neurones entails a rapid loss of responsiveness that involves a majority of the receptor population. The mechanism by which desensitization is reversed may involve a non-calcium-dependent protein phosphatase but the processess that cause desensitization remain unclear.

Keywords: Locus coeruleus; receptors; opioid; phosphoprotein phosphatase; drug tolerance

Introduction

Desensitization of receptors exposed to continual or excessive stimulation is a widespread biological phenomenon. In the case of receptors that couple to G proteins three basic mechanisms underlying desensitization have been defined (reviewed by Huganir & Greengard 1990; Lefkowitz *et al.*, 1990; Dohlman *et al.*, 1991; Palczewski & Benovic, 1991): (1) *Receptor uncoupling*, where interference in the ability of the receptor to associate with G proteins occurs, resulting in an interruption of the transduction pathway to the effector. Uncoupling is often initiated by receptor phosphorylation. (2) *Sequestration*, where the receptor enters a compartment which is not accessible to agonists. (3) *Receptor downregulation*, which involves internalization of the receptors and their probable subsequent destruction. Both uncoupling and sequestration can take place rapidly, within minutes or seconds, and are potentially reversible processes. Downregulation is normally a slower process that takes place over many minutes, or more commonly hours, the reversal of which requires synthesis of new receptors.

Models of the molecular mechanisms by which G-protein coupled receptors desensitize have come mainly from studies of the rhodopsin- and β_2-adrenoceptors. The extent to which these models apply to desensitization of other receptor types remains to be established. Desensitization of opioid receptors has been demonstrated under both *in vitro* and *in vivo* conditions (reviewed by Johnson & Fleming, 1989). Biochemical studies of cloned cell lines have shown that prolonged exposure to agonists causes uncoupling of μ- and δ-opioid receptors that is followed later by receptor downregulation (Puttfarken *et al.*, 1988; Law *et al.*, 1983; Vachon *et al.*, 1987). At present little is known about the mechanisms that cause uncoupling of opioid receptors, although studies using cell free membrane preparations have shown that phosphorylation of μ-opioid receptors by cAMP-dependent protein kinase can prevent coupling by G_i (Harada *et al.*, 1989), and that acid phosphatase treatment of δ-opioid receptors from NG108 cells can decrease agonist-induced inhibition of adenylyl cyclase (Louie *et al.*, 1988).

Studies of LC neurones in brain slice preparations have shown that μ-opioid receptors (which open potassium channels when activated) can be rapidly desensitized by short term exposure to high concentrations of opioid agonist (Harris & Williams, 1991). This 'acute desensitization' develops rapidly within a few minutes and can recover within a slightly longer period. Induction requires concentrations of agonist that are maximally effective at activating currents, while full agonists cause greater desensitization than partial agonists. The development of desensitization is independent of receptor number, as there was no change after the receptor population had been reduced with β-chlornaltrexamine, an irreversible opioid receptor antagonist (Harris & Williams, 1991). A notable feature of the process is that it is *homologous* for opioid receptors as there is little cross-desensitization with α_2-adrenoceptors,

[1] Author for correspondence.

which in LC neurones couple to the same conductance as opioid receptors (Andrade & Aghajanian, 1985; North *et al.*, 1985). A small but significant reduction in the amount of desensitization and a decrease in the time taken to recover was seen following treatment with either staurosporine, a non-specific kinase inhibitor, or forskolin, an adenylyl cyclase activator. While the full meaning of these last seemingly conflicting observations is not clear, they do suggest that protein kinase activation may have some role in the desensitization process.

In the present study we have quantified the effect of acute desensitization on the dose-response relationships of both full- and partial-opioid receptor agonists. We have also investigated further the possible involvement of kinase activation as a mechanism of desensitization by examining the effects of inhibitors of protein phosphatases introduced intracellularly by use of patch recording electrodes.

Methods

Male Wistar rats were used for all experiments and housed according to NIH guidelines. Rats weighed 150–200 g and were a minimum of 6 weeks of age.

Exact details of the method of tissue preparation used have been published previously (Williams *et al.*, 1982; 1988). Briefly, rats were anaesthetized with halothane and killed. Horizontal slices, 250–300 μm in thickness, containing the LC were cut with a vibratome and stored in an oxygenated chamber at 35°C. For recording, a hemisected slice was submerged in a tissue bath (0.5 ml volume) and superfused with artificial cerebrospinal fluid (ACSF; 1.5 ml min^{-1}) at 35°C. The solution was equilibrated with 95% O_2/5% CO_2 and contained (mM): NaCl 126, KCl 2.5, NaH_2PO_4 1.4, $MgCl_2$ 1.2, $CaCl_2$ 2.4, glucose 11, $NaHCO_3$ 25.

For intracellular recording, microelectrodes were filled with 2M KCl and had resistances of 28–40 MΩ. Measurement of current and voltage were made with an Axoclamp 2A amplifier. Membrane currents were recorded in discontinuous voltage-clamp mode with a switching frequency of 4–5.2 kHz. The potential at the headstage of the amplifier was monitored at all times with a separate oscilloscope. Experiments were carried out only when the potential at the headstage was flat for at least 20% of the cycle prior to sampling.

Patch clamp recordings were made in the whole cell configuration without visualization of the cells or cleaning of the slice surface. Measurement of current was made with an Axopatch-1D amplifier. Patch pipettes were made from borosilicate micropipette glass (World Precision Instruments) and had resistances of 2–3 MΩ. The pipette solution contained (mM): K gluconate 125, NaCl 15, $MgCl_2$ 2, EGTA 11, HEPES 10, MgATP 2, NaGTP 0.25, and was adjusted to a pH of 7.3 with KOH and an osmolarity of 280–290 mOsmol. Other compounds were added to this solution where specified. Junction potentials of approximately -10 mV were not corrected for. Series resistance was measured directly in current clamp and was then monitored throughout each experiment using test pulses. Data were used only when the total series resistance was maintained below 10 MΩ throughout the experiment. Data were digitized and then acquired and stored on a computer using PClamp or Axotape software (Axon Instruments, CA, U.S.A.).

Analysis of data

To construct concentration-response curves for opioid agonists, currents were standardized against the maximal response to UK14304 (10 μM) (an α_2-adrenoceptor agonist). Harris & Williams (1991) have demonstrated previously that the amplitude of adrenergic currents is not significantly affected by opioid receptor desensitization. The mean data for each agonist was first fitted to a logistic function of the form:

$$E = M\frac{[A]^n}{[A]^n + k^n}$$

in which E and [A] are the pharmacological effect and concentration of agonist respectively, M is the maximum response, k is the EC_{50} and n is the slope parameter. Next, an analysis was performed for each agonist in which paired sets of data obtained pre- and post-desensitization were simultaneously fitted to the equation:

$$E = \frac{E_m T^n [A]^n}{(K_a + [A])^n + T^n [A]^n}$$

where the effect E is expressed in terms of the concentration of agonist A, the theoretical maximal effect E_m (i.e. effect if all receptors are fully occupied), the Hill coefficient n, the dissociation constant K_a, and the 'transducer ratio' T. The latter ratio relates the total receptor concentration (R_T) to the concentration of receptor-ligand complexes that are required to produce a half maximal effect (K_E), so that $T = R_T/K_E$. From the fit, two values of T were estimated that represent the change in the transducer ratio that is caused by desensitization; single values of the remaining parameters were obtained. The model was developed by Black and colleagues (1985) and is known as the 'operational model of agonism'. It was adapted for analysis of the effects of desensitization by Lohse (1990) who estimated the amount of desensitization in the manner:

$$\% \text{ desensitization} = (1 - T_{\text{desensitized}}/T_{\text{non-desensitized}}) \times 100$$

Curve fitting was performed using a simplex optimization algorithm implemented using Axograph (for simultaneous fitting to paired data sets) or Kaleidagraph software.

Statistics

Means are given with s.e.means. Paired groups were compared by a Mann-Whitney U test. Multiple treatment groups were compared against a control group using a Kruskal-Wallace test in combination with Dunn's test (Glantz, 1992).

Drugs used

Stock solutions of bestatin (Peninsula), DAMGO (D-Ala^2,*N*-MePhe^4,Gly-ol] enkephalin; Sigma), [Met^5] enkephalin (Sigma), thiorphan (Peninsula) and UK 14304 (5-bromo-N-(4,5-dihydro-1H-imidazol-2-yl)-6-quinoxdlinamine; Research Biochemicals) were made in distilled water and stored at 4°C. Stock solutions of microcystin (Biomol) were made using in dimethylsulphoxide (DMSO) and stored at 4°C. BAPTA (Sigma) was dissolved directly in the internal recording solution. [Met^5]enkephalin was perfused together with the peptidase inhibitors bestatin (20 μM) and thiorphan (2 μM) (Williams *et al.*, 1987).

Results

Effects of acute desensitization on agonist concentration-response curves

The effect of acute desensitization on the concentration-response relationship of 3 opioid agonists (ME, DAMGO and normorphine) was examined on LC neurones that were voltage-clamped ($V_{hold} = -60$ mV) using intracellular microelectrodes. Opioid receptors were desensitized by perfusing slices with ME (30 μM) for a period of 5 min (Figure 1a). As described previously (Harris & Williams, 1991) ME (30 μM), a supramaximally effective concentration, caused a response which peaked at (524±41 pA, $n = 19$) and then decayed to 334±29 pA (63±1.6% of control). Single test concentrations of agonist were applied immediately after desensitizing concentrations of ME were washed from the bath. Concentration-response relationships for ME, DAMGO and normorphine were measured under both control and desensitized conditions. A logistic function (equation 1) was fitted to each

curve to obtain the location parameters (maximum response, EC_{50} and slope) which are summarized in Table 1. The maximum response obtained with normorphine was less than the maxima achieved with ME and DAMGO, which is consistent with a previous study in which normorphine was shown to act as a partial agonist on LC neurones (Christie *et al.*, 1987). For each agonist, desensitization caused both a depression of the amplitude of the maximal response (normorphine > ME > DAMGO) and a rightward shift of the curve (DAMGO > normorphine > ME). The dose-ratios calculated from the EC_{50} concentrations (desensitized: control) were 15.6 (DAMGO), 3.9 (ME) and 7.6 (normorphine).

The data were analysed further by the method of Lohse *et al.* (1990) in which the entire curves are used (rather than only the change in the maximal response) to provide an estimate of the amount of desensitization produced (see Discussion). For each agonist equation (2) was simultaneously fitted to the data obtained pre- and post-desensitization (comprising a pair of concentration-response relationships). From each fit, two values of the 'transducer ratio' T were obtained (T_0 = control data; T_1 = desensitized data) which were then used to calculate '% desensitization' which was equal to $(1-T_1/T_0)$ x 100. The curve of best fit to the mean data for each agonist is plotted in Figure 1b and the estimates for each parameter are presented in Table 2. From the estimates of T_0 and T_1 the amount of desensitization was determined as 88% for ME, 96% for DAMGO and 91% for normorphine. The values of the dissociation constant estimated for DAMGO, ME and normorphine were 2.9 μM, 5.2 μM and 9 μM respectively; the latter values are close to previous estimates of 2 μM for ME and 9–

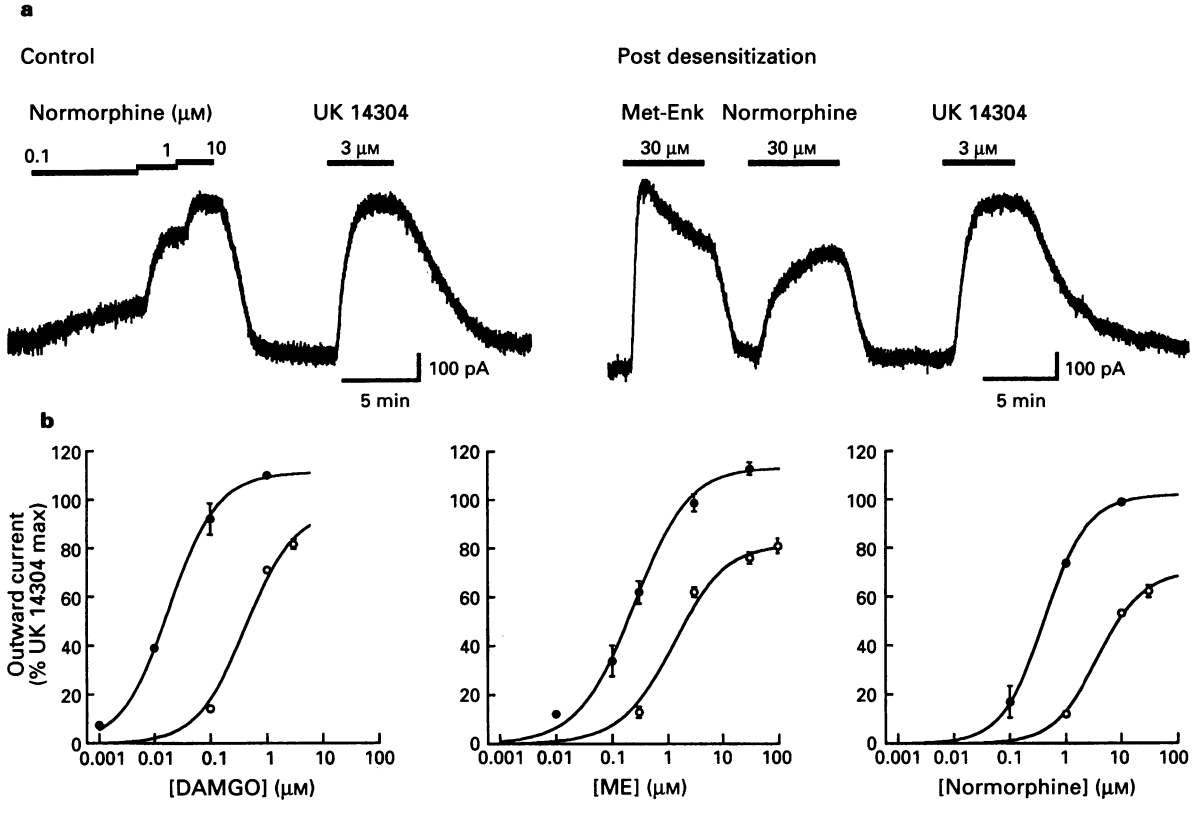

Figure 1 Desensitization of opioid currents measured with different opioid agonists. In (a) in the left panel is shown a control experiment in which cumulative application of 3 concentrations of normorphine (0.1, 1 and 10 μM) at the bars caused outward currents of increasing amplitude. The normorphine current was reversed by perfusion with naloxone (1 μM) after which UK-14304 (3 μM) was applied. In the right panel Met-Enk (30 μM) was applied for 5 min during which desensitization was produced as indicated by the decline in the current amplitude. After washout of the high concentration of Met-Enk (ME) normorphine (30 μM) was applied at the bar causing an outward current; this was reversed with naloxone and UK-14304 (3 μM) was then applied. Note that the current produced post-desensitization by 30 μM normorphine is smaller in amplitude than the currents produced by normophine using lower concentrations of 1 and 10 μM in control conditions. In (b) concentration-response curves for DAMGO, ME and normorphine were constructed under control conditions (●) and immediately following washout of a desensitizing concentration (30 μM, 5 min) of ME (○). The lines drawn through the data are the results of operational model-fitting (equation 2). For each agonist only T varied between curves, a single value of n, E_m, K_a being estimated, these values are presented in Table 2. In these and other recordings LC neurones were voltage clamped to a potential of −60 mV. The rapid deflections in the current trace represent synaptic currents.

Table 1 Logistic fitting of agonist concentration-response curves

	Control			*Desensitized*		
Agonist	EC_{50}(nM)	*Maximum*(%)	*Slope*	EC_{50}(nM)	*Maximum*(%)	*Slope*
DAMGO	20	113	0.90	311	85	1.40
ME	283	117	0.72	1100	79	1.24
Normorphine	426	102	1.11	3250	66	1.27

Estimates of parameters obtained from fits of a logistic function to individual agonist concentration-response data obtained under control conditions, and following desensitization induced by ME (30 μM, 5 min). Responses are expressed as percentages of the current produced by a maximally effective concentration of UK14304 (1 μM). For abbreviations, see text.

16 μM for normorphine obtained in LC neurones from experiments in which the irreversible antagonist β-funaltrexamine was used (Williams & North, 1984).

Table 2 Operational model fitting of paired pre- and post-desensitization agonist concentration-response curves

Agonist	E_m(%)	K_a(μM)	n	T_0	T_1
DAMGO	111	2.9	1	155	5.9
ME	123	5.2	.85	18	2.2
Normorphine	105	9.0	1.2	21	1.9

Estimates of parameters obtained from simultaneous fits to the operational model function of paired sets of agonist concentration-response data obtained under control conditions and following desensitization induced by ME (30 μM, 5 min). The parameters are the maximal effect, Em; the agonist dissociation, K_a; the Hill coefficient, n; and the transducer ratios under control, T_0, and desensitized, T_1, conditions. Responses are expressed as percentages of the current produced by a maximally effective concentration of UK14304 (1 μM). For abbreviations, see text.

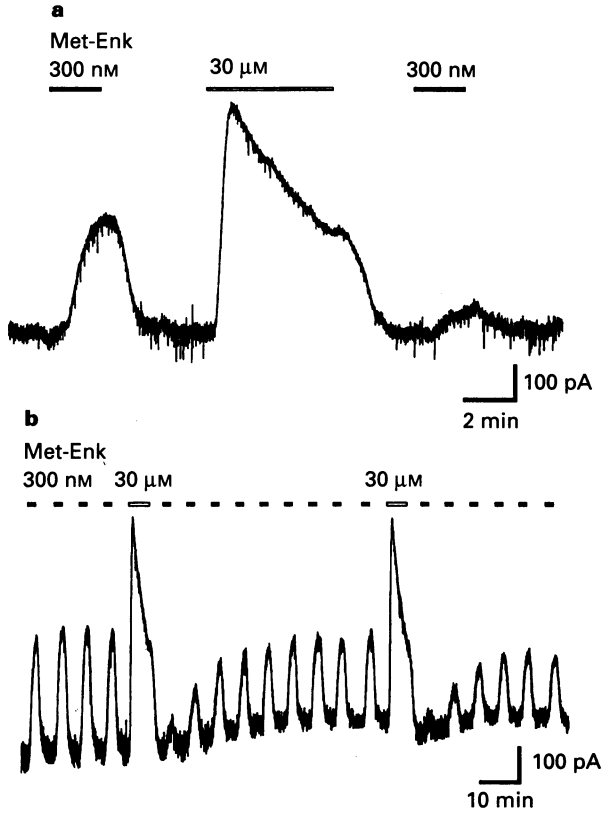

Figure 2 Whole-cell recordings of acute desensitization. Recordings from LC neurones recorded by the whole-cell patch clamp technique. In (a) application of Met-Enk (300 nM) at the bar caused an outward current that reversed upon washout. Met-Enk (30 μM) caused a larger current that peaked and then declined in amplitude over a 5 min period in the continued presence of agonist. After washout of the high concentration of Met-Enk, reapplication of the low concentration caused a current that was reduced in amplitude. In (b) another cell is shown over a longer time period. Desensitizing concentrations of Met-Enk (30 μM) were applied over two 5 min intervals and in each case the current peaked and then declined in amplitude. After these applications, currents activated by the low concentration were reduced in amplitude initially but then progressively increased in size. Note that the amplitude of the opioid current was reduced progressively during the course of the experiment, and that full recovery of the agonist current following desensitization was never achieved.

'Whole-cell' patch recording of acute opioid receptor desensitization

Patch clamp recording in the whole-cell configuration was used to enable chemical inhibitors to be introduced intracellularly. Under voltage clamp conditions between −200 to −50 pA of current was required to hold cells to a potential of −60 mV. Perfusion of slices with ME caused outward currents that were no different in appearance from those recorded with intracellular microelectrodes (Figure 2a). The peak amplitude of currents produced using 300 nM and 30 μM concentrations of ME was 306±35 pA ($n=5$) and 460±41 pA ($n=11$) respectively. In comparison with intracellular recording however, the amplitude of opioid

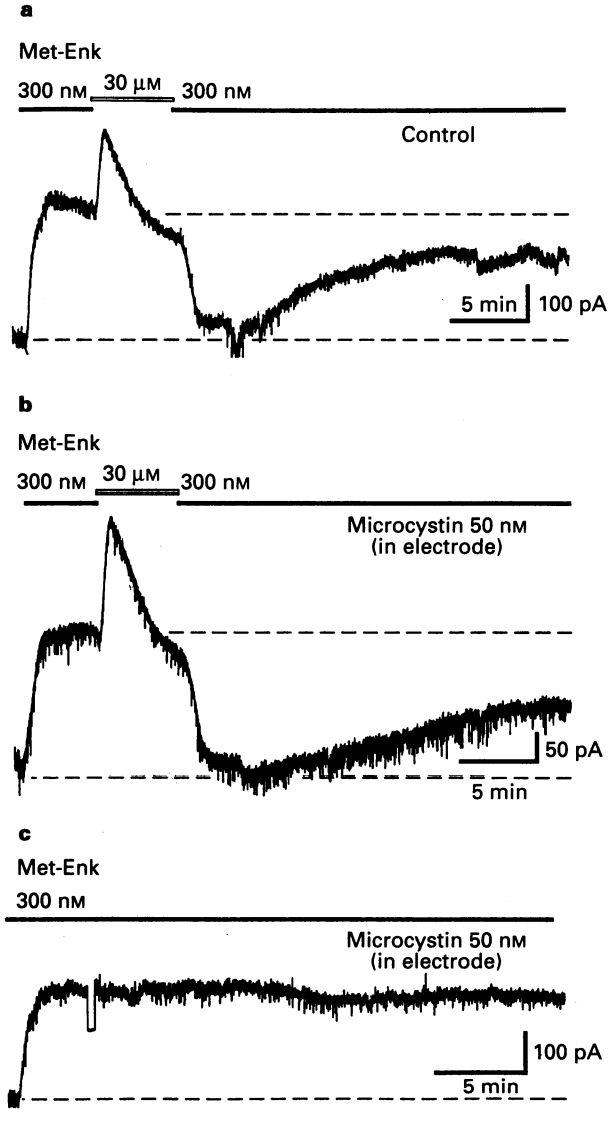

Figure 3 Microcystin prolongs μ-opioid receptor desensitization. Three experiments in which a low (300 nM) concentration of Met-Enk was applied for a 45 min period as shown by the bars. (a) Shows a control experiment. Perfusion of the low Met-Enk concentration was interrupted by an application of a desensitizing concentration of Met-Enk (30 μM, 5 min), after which the current produced by the low concentration was reduced in amplitude and then recovered. In (b) the same experiment has been repeated but with microcystin (50 nM) included in the recording electrode. Note the prolongation of the time course of recovery of the current following desensitization. In (c) microcystin (50 nM) was included in the recording electrode but the desensitizing concentration of Met-Enk was not applied. The rundown of the control current does not appear sufficient to account for the effect of microcystin following opioid receptor desensitization.

currents was not as well maintained but slowly decreased over time (Figure 2b). This 'run-down' was not specific to opioid currents since α_2-adrenoceptor currents were affected in a similar manner.

Acute desensitization of opioid receptors could still be produced when patch recording was used. As illustrated in Figures 2a and b, during a 5 min application of ME (30 μM) the current peaked and then sagged by 50.1±2.2% ($n=11$) during the period. Immediately after washout of the desensitizing concentration, application of ME (300 nM) caused a response that was 18±3% ($n=5$) of control currents measured prior to desensitization. With repeated application of ME (300 nM) the currents progressively recovered in amplitude over a 30 min period. Recovery beyond 70% of the pre-desensitization control value was never observed, presumably due to the rundown referred to above. An acute desensitization/recovery cycle could be produced more than once in a single cell (Figure 2b). In order to minimize the effect of run-down when comparing experiments performed on different cells, a standard protocol was used (Figure 3a). Once electrical access had been establishd, drug applications were made at 5 min intervals. During the initial 15 min period, 1 or 2 control responses to a 300 nM concentration of ME were obtained, and then a 30 μM desensitizing concentration was perfused for 5 min. This was then washed out and the low (300 nM) concentration was again repeatedly applied. In a variation of this experiment, ME (300 nM) was applied continuously for a 45 min period with the exposure to the 30 μM concentration made after the first 5 min (Figure 3b).

Effects of intracellularly applied inhibitors on acute desensitization

In three experiments the Ser/Thr protein phosphatase inhibitor, okadaic acid (1 μM), was included in the recording solution. The amplitude and kinetics of agonist currents were not affected by this treatment, but it was noted that there was a trend in these cells towards a prolongation of recovery from desensitization (Figure 4a). Okadaic acid can permeate cell membranes, which may limit the effective concentration that can be achieved intracellularly, particularly at distal regions of the neurone. Therefore we made use of another phosphatase inhibitor, microcystin, which is not membrane permeable. When microcystin (50 nM and 4 μM; $n=8$) was included in the recording solution there was a prolongation of the time course of the recovery from desensitization of opioid currents (Figures 3b and 4a). The amplitude of ME (300 nM) currents measured during recovery were fit with a single exponential and time constants of recovery were obtained of 3.5 min under control conditions (8 cells), 6.7 min with okadaic acid (3 cells) and 36.7 min with microcystin (8 cells). To confirm that microcystin was indeed causing a long lasting prolongation of opioid receptor desensitization, a comparison was made of responses to 30 μM ME reapplied 30–40 min after the first application of this concentration (Figure 4c). In control cells the response to a second application of ME (30 μM) was reduced in amplitude by 12.9±0.07% ($n=3$) due to the rundown described previously. In the microcystin-treated cells there was a reduction of 27.3±7% ($n=5$) which was significantly different from the control value ($P<0.05$, Dunn's test). This result suggests that there was incomplete recovery from desensitization in the microcystin cells even some 30 min after desensitization was produced.

To demonstrate that the actions of microcystin were specific for the opioid receptor, UK14304, an α_2-adrenoceptor agonist was also applied 30–40 min after desensitization had been produced. Currents produced by a maximally effective concentration of the agonist UK14304 (1 μM) were measured in control ($n=3$) and microcystin-treated cells ($n=5$), and there was no significant difference in amplitude ($P>0.05$). This result suggests that the ion channels that are the common effector for both opioid- and α_2-adrenoceptors in LC neurones (Andrade & Aghajanian, 1985; North & Williams, 1985) are not affected by microcystin treatment.

Recovery from desensitization was the only parameter that was affected by microcystin treatment. The amplitude of ME currents in control and microcystin cells measured with 300 nM ME were 295±23 pA ($n=8$) and 231±24 pA ($n=8$) respectively, and with 30 μM ME were 441±44 ($n=8$) and 371±40 ($n=8$). The effect of microcystin on the induction of desensitization was assessed by measuring the decrease in the current produced by 30 μM ME over a 5 min period and the time constant of the decay. The percentage decreases in current amplitude in control and microcystin cells were 51.7±1.6% ($n=9$) and 55.2±1.6% (8) respectively, while the time constant of decay was 3.52±0.73 min ($n=5$) and 3.22±0.23 min

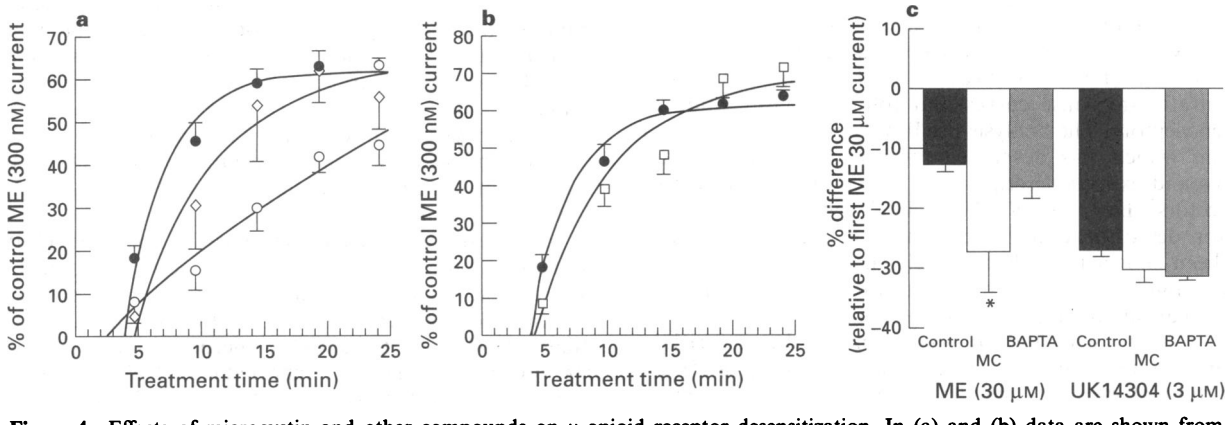

Figure 4 Effects of microcystin and other compounds on μ-opioid receptor desensitization. In (a) and (b) data are shown from experiments in which opioid receptors were desensitized with Met-Enk (ME 30 μM, 5 min), after which the amplitude of currents produced by 300 nM ME were measured at 5 min intervals. The data have been expressed as a percentage of the amplitude of 300 nM ME currents measured prior to desensitization. The data from control experiments (8 cells; ●) which have been plotted in (a) and (b) was fitted by a single exponential (solid line) with a time constant of 3.5 min. In (a) is shown data from experiments in which okadaic acid (1 μM, 3 cells; ◇) or microcystin (50 nM - 4 μM, 8 cells; ○) were included in the electrode solution. The respective time constants of recovery for these experiments was 6.7 and 36.7 min. In (b) data are shown from a similar experiment where BAPTA (10–20 mM, 4 cells; □) was used. In (c) are plotted the mean amplitudes of ME (30 μM) or UK14,304 (3 μM) activated currents recorded with control internal solution or with microcystin (MC, 4 μM) or BAPTA (10–20 mM) added. Currents were measured 30–50 min after washout of the desensitizing concentration of ME (for measurement of both ME and UK 14,304 currents, $n=3,5,3$ respectively for control, microcystin and BAPTA experiments). The ME activated current in the presence of microcystin is significantly different from the control ($P<0.005$).

($n=5$). No significant differences were found in any of these comparisons (Mann-Whitney U, $P>0.05$). The lack of effect of microcystin on rundown of the opioid current is illustrated by the cell shown in Figure 3c.

Calcium is not a requirement for acute desensitization

Microcystin is an ineffective inhibitor of calcium-dependent phosphatases (MacKintosh *et al.*, 1990). To test for the possibility of a calcium-dependent process involved in desensitization, the calcium chelator BAPTA (10–20 mM) was added to the electrode solution in 4 experiments. BAPTA at these concentrations (10–20 mM) would be expected to lower the intracellular calcium concentration, as well as provide strong buffering against transient concentration changes (e.g. see Beech *et al.*, 1991). BAPTA had no effect on the control currents nor on the induction of desensitization. Following desensitization, BAPTA appeared to delay the onset of recovery, although recovery to a level equivalent to control experiments was achieved within a comparable time period (Figure 4b). Peak currents produced following recovery from desensitization by a second application of ME (30 μM) or UK14304 in the BAPTA-treated cells were not significantly different from control currents ($P>0.05$; Figure 4c).

Discussion

In this study, electrophysiological techniques have been used to record from rat locus coeruleus neurones and to characterize further the acute homologous desensitization of μ-opioid receptor-induced currents described by Harris & Williams (1991). Two major observations have been made. Firstly, when the effect of acute desensitization on the concentration-response relationships of three opioid agonists was quantitatively measured, a profound loss of receptor responsiveness was seen. Secondly, intracellular application of a phosphatase inhibitor prolonged the time required for desensitization to reverse, but had no effect on either the induction of desensitization or the normal ability of opioids to produce currents.

A quantitative comparison was made of the effects of μ-receptor desensitization on responses to three opioid agonists. Christie *et al.* (1987) have established previously in experiments using LC neurones that ME and DAMGO act as full receptor agonists, and normorphine as a partial agonist. Acute desensitization caused a shift to the right and a reduction in the maximum response of the concentration-response relationship of all three agonists. An analytical method was applied which has been utilized previously by Lohse *et al.* (1990) to measure changes in isoprenaline concentration-response curves that follow desensitization of β-adrenoceptors. The analysis used the 'operational model of agonism' which was developed to provide a generally applicable and explicit description of the coupling of receptors to effectors (Black *et al.*, 1985; Leff, 1988). Estimates of receptor desensitization made using the operational model have been shown to be linearly related to changes in signal transduction efficacy, unlike estimates derived from changes in maximal stimulation (see Lohse *et al.*, 1990, for discussion). In the present study it was estimated that the reduction in the percentage of receptors induced by a 5 min application of ME was similar for each of three agonists, falling in a range from 88% to 96%. This measure of desensitization is derived from the ratio of the two estimates of the model parameter T, which in this case represents the efficacy of signal transduction achieved by receptors in a non-desensitized and desensitized state respectively. The transducer ratio, or T, is defined in the model as being equal to the total receptor number divided by the concentration of agonist that gives a half-maximal effect. This means that in functional terms, a loss of receptor responsiveness can be attributed to either:–(1) a removal of receptors (i.e. receptor sequestration or downregulation); or (2) a reduction in the coupling efficiency between receptors and the effector system (i.e. receptor uncoupling). Although chronic opiate treatment can cause a limited loss of opioid receptors from membranes prepared from brain (Bhargava & Gulati, 1990), the extent of such changes varies considerably and does not correlate well with loss of opioid receptor function. These and other observations have led workers to propose that receptor uncoupling is the major mechanism underlying μ-opioid receptor tolerance (for examples see Christie *et al.*, 1987; Puttfarken *et al.*, 1988; Werling *et al.*, 1989; Kennedy & Henderson, 1991).

Christie *et al.* (1987) found that following *chronic* exposure of LC neurones to morphine, less tolerance was measured with DAMGO than with normorphine. While the concentration-response relationship for DAMGO was shifted twofold to the right with no change in the maximum, there was a 40% reduction of the maximum of the curve obtained for normorphine. Furchgott analysis of the normorphine data estimated that the change was equivalent to a 70–80% loss in receptor numbers. From those observations it was concluded that the intrinsic efficacy of an opioid determines the degree of tolerance observed. In the present study, acute desensitization to ME caused a loss of receptors that when analysed using the operational model was independent of the intrinsic efficacy of the test agonist used. The results from both studies are consistent. In the present study desensitization with ME caused a greater loss of receptors than in chronic morphine treatment; however, the shift in the morphine concentration-response curve was greater than for either ME or DAMGO.

As yet it is not known if desensitization of opioid receptors participates in the tolerance to opiate agonists that develops with chronic exposure when opioids are abused or taken therapeutically (reviewed by Johnson & Fleming, 1989). However, Harris & Williams (1991) have shown that opioid receptors in LC neurones desensitize less in brain slices taken from chronically morphine-treated rats. This observation suggests that some link may exist between desensitization induced with acute exposure and the tolerance induced by chronic treatment.

In the present study the effects of inhibitors of protein phosphatases on acute opioid receptor desensitization were also examined. Inclusion of microcystin in the recording solution consistently slowed the rate at which the amplitude of ME currents recovered following desensitization. The decay of the current produced by the high (30 μM) concentration of ME was not affected by microcystin, which indicates that the induction of desensitization was unchanged. Also microcystin did not affect the coupling of non-desensitized opioid receptors as there was no change in the amplitude of currents induced by low (300 nM) concentrations of ME. Furthermore, the ion channels underlying the agonist current were also unaffected, since microcystin did not cause a change in the amplitude of currents induced by α_2-adrenoceptors which couple to the same channels as μ-opioid receptors (Andrade & Aghajanian, 1985; North *et al.*, 1985).

Microcystin was used at concentrations between 50 nM and 4 μM. In another recent study, 10 μM microcystin added to the recording solutions was found to alter excitatory postsynaptic currents recorded from hippocampal CA1 neurones (Wylie & Nicoll, 1994). The K_i value for microcystin measured in cell-free preparations has been reported (MacKintosh *et al.*, 1990) as 0.1 nM against phosphatase types 1 and 2A, and around 100 nM for phosphatase 2B (calcineurin). The lack of an effect of BAPTA in the present study argues against the participation of calcium-dependent mechanisms in opioid receptor desensitization, and therefore would exclude calcineurin. In two experiments concentrations of microcystin as low as 50 nM continued to be effective which is consistent with the high potency of the drug against phosphatase type 1 and 2A. Another phosphatase inhibitor, okadaic acid, was also used but in only three experiments due to variation in the results obtained. Unlike microcystin, okadaic acid is more selective for phosphatase type 2A than for type 1 (Cohen *et al.*, 1990) which

might account for the variability seen. Okadaic acid is also membrane-permeable and may diffuse out of the cytoplasm before an effective concentration at receptor sites can be achieved.

The effects of microcystin suggest that dephosphorylation is necessary for recovery from desensitization. As yet, the molecular mechanism by which G-protein coupled receptors undergo homologous desensitization has been well-defined only for rhodopsin- and β-adrenoceptors. The process, which is similar for both receptor types, is initiated by rhodopsin- or β-adrenoceptor-kinases phosphorylating agonist-bound receptors; cytoplasmic arrestin proteins can then bind to the phosphorylated receptor which interferes with receptor-G protein coupling. The recovery phase has been shown to involve dephosphorylation of the desensitized receptors by Ser/Thr protein phosphatases (Fowles & Akhtar, 1989; Palczewski *et al.*, 1989). Binding of arrestin has the slowest kinetics; therefore if dephosphorylation does not occur recovery is greatly prolonged as arrestin will continue to reassociate with the receptor when it unbinds. The extent to which such mechanisms underlie homologous desensitization of other G-protein-coupled receptors remains to be demonstrated but there is a superficial similarity between homologous desensitization of opioid receptors in LC neurones and of β-adrenoceptors (see also Harris & Williams, 1991).

A biochemical study has demonstrated that phosphorylation of μ-opioid receptors by cyclic AMP-dependent protein kinase interferes with coupling of the receptors to G-proteins (G_i) (Harada *et al.*, 1989). In the predicted amino acid sequence of the μ-opioid receptor which has recently been cloned (Chen *et al.*, 1993; Thompson *et al.*, 1993), there are consensus recognition sites for protein kinase C and cyclic AMP-dependent protein kinase phosphorylation. One of these sites (Thr^{279}) corresponds to a site in the β-adrenoceptor thought to participate in *heterologous* desensitization of the receptor caused by PKA activity (Clark *et al.*, 1989; Hausdorff *et al.*, 1989). In LC neurones however, Harris & Williams (1991) found that only a small amount of the desensitization produced was heterologous. Furthermore, only very limited effects on desensitization were observed following treatment with a non-specific kinase inhibitor (staurosporine) or stimulators of cyclic AMP metabolism (forskolin and phosphodiesterase inhibitors). Recent experiments carried out in our laboratory have shown that, in fact, forskolin treatment can result in an increase in the amplitude of opioid-induced currents (Osborne & Williams, unpublished observations). Therefore it would appear that in LC neurones cyclic AMP-dependent mechanisms are not involved in homologous desensitization of opioid receptors and also do not contribute to any significant level of heterologous desensitization. It remains to be determined whether stimulation of receptor types other than α_2-adrenoceptors can result in cross-desensitization with opioid receptors.

The loss of responsiveness of μ-receptors following short term opioid exposure has been noted but not been widely studied. It is difficult to assess the prevalence of acute desensitization in other tissues. Fading of opioid inhibition of synaptic transmission has been noted in the dorsal horn (Dickenson & Sullivan, 1986), in hippocampus (Capogna *et al.*, 1993) and in the guinea-pig myenteric plexus (Cherubini *et al.*, 1985). However, acute desensitization of μ-opioid receptors does not occur invariably. For example in SH-SY5Y cells acute desensitization of μ-opioid receptors coupled to calcium channels was not observed, although tolerance following chronic exposure to opioids could be demonstrated (Kennedy & Henderson, 1991). It is not apparent if acute homologous desensitization of μ-opioid receptors would occur in central neurones under normal physiological conditions. However, in situations of chronic opioid use, sufficient levels of opioids in the brain may be achieved to produce acute desensitization (see Harris & Williams 1991, for discussion), although in LC neurones normorphine produced the least amount of desensitization of the agonists that were studied. The efficacy of opioid agonists *in vivo* may in part reflect the extent and time course to which they invoke desensitization of μ-opioid receptors. In the present study, acute desensitization in each case increased the slope of the concentration-response relationship; *in vivo* such a change would increase the steepness of the dose-response curve, reducing the concentration-range separating subthreshold and maximally effective doses.

The authors wish to thank Dr MacDonald Christie for reading the manuscript, Dr John Clements for writing the code module for Axograph which performed the simultaneous curve fitting, and Dr K.-Z. Shen for his valuable technical advice on the whole cell recording technique.

This research was supported by United States Public Health Service Grants DA08163 and DA00141 from the National Institute on Drug Abuse, and in part by a University of Sydney Medical Foundation Fellowship to P.B.O.

References

ANDRADE, R. & AGHAJANIAN, G.K. (1985). Opiate- and α_2-adrenoceptor-induced hyperpolarization of locus coeruleus neurons in brain slices: reversal by cyclic adenosine 3':5'-monophosphate analogues. *J. Neurosci.*, **5**, 2359–2364.

BEECH, D.J., BERNHEIM, L., MATHIE, A. & HILLE, B. (1990). Intracellular Ca^{2+} buffers disrupt muscarinic suppression of Ca^{2+} current and M current in rat sympathetic neurons. *Proc. Natl. Acad. Sci. U.S.A.*, **88**, 652–656.

BHARGAVA, J.W. & GULATI, A. (1990). Down-regulation of brain and spinal cord μ-opiate receptors in morphine tolerant-dependent rats. *Eur. J. Pharmacol.*, **190**, 305–311.

BLACK, J.W., LEFF, P., SHANKLEY, N.P. & WOOD, J. (1985). An operational model of pharmacological agonism: the effect of E/[A] curve shape on agonist dissociation constant estimation. *Br. J. Pharmacol.*, **84**, 561–571.

CAPOGNA, M., GÄHWILER, B.H. & THOMPSON, S.M. (1993). Mechanism of μ-opioid receptor-mediated presynaptic inhibition in the rat hippocampus *in vitro*. *J. Physiol.*, **470**, 539–558.

CHEN, Y., MESTEK, A., LIU, J., HURLEY, J.A. & YU, L. (1993). Molecular cloning and functional expression of a μ-opioid receptor from rat brain. *Mol. Pharmacol.*, **44**, 8–12.

CHERUBINI, E., MORITA, K. & NORTH, R.A. (1985). Opioid inhibition of synaptic transmission in the guinea pig myenteric plexus. *Br. J. Pharmacol.*, **85**, 805–817.

CHRISTIE, M.J., WILLIAMS, J.T. & NORTH, R.A.N. (1987). Cellular mechanisms of opioid tolerance: studies in single brain neurons. *Mol. Pharmacol.*, **32**, 633–638.

CLARK, R.B., FRIEDMAN, J., DIXON, R.A.F. & STRADER, C.D. (1989). Identification of a specific site required for rapid heterologous desensitization of the β-adrenergic receptor by cAMP-dependent protein kinase. *Mol. Pharmacol.*, **36**, 343–348.

COHEN, P., HOLMES, C.F.B. & TSUKITANI, Y. (1990). Okadaic acid: a new probe for the study of cellular regulation. *Trends Biochem. Sci.*, **15**, 98–102.

DICKENSON, A.H. & SULLIVAN, A.F. (1986). Electrophysiological studies on the effects of intrathecal morphine on nociceptive neurones in the rat dorsal horn. *Pain*, **24**, 211–222.

DOHLMAN, H.G., THORNER, J., CARON, M.G. & LEFKOWITZ, R.J. (1991). Model systems for the study of seven-transmembrane-segment receptors. *Annu. Rev. Biochemistry*, **60**, 653–88.

FOWLES, C. & AKHTAR, M. (1989). Interplay of phosphorylation and dephosphorylation in vision: protein phosphatases of bovine rod outer segments. *Biochem.*, **28**, 9385–9391.

GLANTZ, S.A. (1992). *Primer of Biostatistics*. New York: McGraw-Hill Inc.

HARADA, H., UEDA, H., WADA, Y., KATADA, T., UI, M. & SATOH, M. (1989). Phosphorylation of μ-opioid receptor – a putative mechanism of selective uncoupling of receptor-Gi interaction, measured with low K_m GTPase and nucleotide-sensitive agonist binding. *Neurosci. Lett.*, **100,** 221–226.

HARRIS, G.C. & WILLIAMS, J.T. (1991). Transient homologous mu-opioid receptor desensitization in rat locus coeruleus neurons. *J. Neurosci.*, **11,** 2574–81.

HAUSDORFF, W.P., BOUVIER, M., O'DOWD, B.F., IRONS, G.P., CARON, M.G. & LEFKOWITZ, R.J. (1989). Phosphorylation sites on two domains of the β_2-adrenergic receptor are involved in distinct pathways of receptor desensitization. *J. Biol. Chem.*, **264,** 12657–12655.

HUGANIR, R.L. & GREENGARD, P. (1990). Regulation of neurotransmitter receptor desensitization by protein phosphorylation. *Neuron*, **5,** 555–567.

JOHNSON, S.M. & FLEMING, W.W. (1989). Mechanisms of cellular adaptive sensitivity changes: applications to opioid tolerance and dependence. *Pharmacol. Rev.*, **41,** 435–488.

KENNEDY, C. & HENDERSON, G. (1991). μ-Opioid receptor inhibition of calcium current: development of homologous tolerance in single SH-SY5Y cells after chronic exposure to morphine *in vitro*. *Mol. Pharmacol.*, **40,** 1000–1005.

LAW, P.Y., HOM, D.S. & LOH, H.H. (1983). Opiate receptor down-regulation and desensitization in neuroblastoma x glioma NG108-15 cells are two separate cellular processes. *Mol. Pharmacol.*, **24,** 413–424.

LEFF, P. (1988). Analysis of agonist action using the operational model. *Trends Pharmacol. Sci.*, **9,** 395–398.

LEFKOWITZ, R.J., HAUSDORFF, W.P. & CARON, M.G. (1990). Role of phosphorylation in desensitization of the beta-adrenoceptor. *Trends Pharmacol. Sci.*, **11,** 190–4.

LOHSE, M.J., BENOVIC, J.L., CARON, M.G. & LEFKOWITZ, R.J. (1990). Multiple pathways of rapid β_2-adrenergic desensitization. Delineation with specific inhibitors. *J. Biol. Chem.*, **265,** 3202–3211.

LOUIE, A.K., ZHAN, J.Z. & BENOVIC, H.H. (1988). Modification of opioid receptor activity by acid phosphatase in neuroblastoma x glioma NG108-15 cells. *Biochem. Biophys. Res. Commun.*, **152,** 1369–1375.

MACKINTOSH, C., BEATTIE, K.A., KLUMPP, S., COHEN, P. & CODD, G.A. (1990). Cyanobacterial microcystin is a potent and specific inhibitor of protein phosphatases 1 and 2A from both mammals and higher plants. *FEBS Lett*, **264,** 187–192.

NORTH, R.A.N. & WILLIAMS, J.T. (1985). On the potassium conductance increased by opioids in rat locus coeruleus neurons. *J. Physiol.*, **364,** 265–280.

PALCZEWSKI, K. & BENOVIC, J.L. (1991). G-protein-coupled receptor kinases. *Trends Biochem. Sci.*, **16,** 387–341.

PALCZEWSKI, K., HARGRAVE, P.A., MCDOWELL, J.H. & INGEBRITSEN, T.S. (1989). The catalytic subunit of phosphatase 2A dephosphorylates phosphoopsin. *Biochem.*, **28,** 415–419.

PUTTFARKEN, P.S., WERLING, L.L. & COX, B.M. (1988). Effects of chronic morphine exposure on opioid inhibition of adenylyl cyclase in 7315c cell membranes: a useful model for the study of tolerance at μ opioid receptors. *Mol. Pharmacol.*, **33,** 520–527.

THOMPSON, R.C., MANSOUR, A., AKIL, H. & WATSON, S.J. (1993). Cloning and pharmacological characterization of a rat μ opioid receptor. *Neuron*, **11,** 903–913.

VACHON, L., COSTA, T. & HERZ, A. (1987). GTPase and adenylate cyclase desensitize at different rates in NG108-15 cells. *Mol. Pharmacol.*, **31,** 159–168.

WERLING, L.L., MCMAHON, P.N. & COX, B.M. (1989). Selective changes in μ opioid receptor properties induced by chronic morphine exposure. *Proc. Natl. Acad. Sci. U.S.A.*, **86,** 6393–6397.

WILLIAMS, J.T., CHRISTIE, M.J., NORTH, R.A. & ROQUES, B.P. (1987). Potentiation of enkephalin action by peptidase inhibitors in rat locus coeruleus *in vitro*. *J. Pharmacol. Exp. Ther.*, **243,** 397–401.

WILLIAMS, J.T., EGAN, T.M. & NORTH, R.A. (1982). Enkephalin opens potassium channels on mammalian central neurons. *Mol. Pharmacol.*, **26,** 489–497.

WILLIAMS, J.T. & NORTH, R.A. (1984). Opiate-receptor interactions on single locus coeruleus neurones. *Mol. Pharmacol.*, **26,** 489–497.

WILLIAMS, J.T., NORTH, R.A. & TOKIMASA, T. (1988). Inward rectification of resting and opiate-activated potassium currents in rat locus coeruleus neurons. *J. Neurosci.*, **8,** 4299–4306.

WYLIE, D.J.A. & NICOLL, R.A. (1994). A role for protein kinases and phosphatases in the Ca^{2+}-induced enhancement of hippocampal AMPA receptor mediated synaptic responses. *Neuron*, **13,** 635–643.

(Received January 20, 1995
Revised March 20, 1995
Accepted March 30, 1995)

British Journal of Pharmacology (1995) 115, 933-936 © 1995 Stockton Press All rights reserved 0007-1188/95 $12.00

Labelling with [^{125}I]-SB 207710 of a small 5-HT$_4$ receptor population in piglet right atrium: functional relevance

[1]Alberto J. Kaumann, James A. Lynham & *Anthony M. Brown

Human Pharmacology Laboratory, The Babraham Institute, Cambridge CB2 4AT and *SmithKline Beecham Pharmaceuticals, Department of Psychiatry Research, New Frontiers Science Park, Third Avenue, Harlow, Essex CM19 5AW

1 We investigated the affinity of SB 207710 for sinoatrial 5-HT$_4$ receptors and the density of right atrial 5-HT$_4$ receptors with [^{125}I]-SB 207710 in right atria of new-born piglets.

2 SB 207710 (1–100 nM) antagonized the 5-HT-evoked tachycardia surmountably with a pK_B of 9.8.

3 [^{125}I]-SB 207710 (5–1500 pM) labelled a small population of saturable binding sites with a pK_D of 10.1 and with 5-HT$_4$ receptor characteristics. The density of atrial binding sites with 5-HT$_4$ receptor characteristics was 174 and 22 times lower respectively than those of atrial β_1- and β_2-adrenoceptors, labelled with (–)-[^{125}I]-cyanopindolol.

4 We suggest that the small 5-HT$_4$ receptor population may in part explain why the maximal tachycardia caused by 5-HT is smaller than that caused by catecholamines.

Keywords: Piglet right atrium; 5-HT$_4$ receptor density; [^{125}I]-SB 207710; tachycardia; β_1 and β_2-adrenoceptor densities

Introduction

5-Hydroxytryptamine (5-HT) causes tachycardia through 5-HT$_4$ receptors in piglet right atria (Kaumann, 1990; Medhurst & Kaumann, 1993), in anaesthetized pigs (Villalon *et al.*, 1990) and plausibly in man (reviewed in Kaumann, 1994). The 5-HT-evoked tachycardia is less pronounced than that elicited by (–)-isoprenaline through β-adrenoceptors (Kaumann, 1990; Medhurst & Kaumann, 1993), suggesting that the 5-HT$_4$ receptor population is small compared to the β-adrenoceptor population. We have recently introduced [^{125}I]-SB 207710, a radioligand of high specific activity and selectivity for 5-HT$_4$ receptors (Brown *et al.*, 1993) and a potential tool for detecting small receptor populations. We therefore used [^{125}I]-SB 207710 and defined binding conditions which detected a small population of 5-HT$_4$ receptors in right atrial tissue from new-born piglets. For comparison, (–)-[^{125}I]-cyanopindolol was used to label β-adrenoceptors. We also investigated the potency of the non-radioactive form of SB 207710 as antagonist of the positive chronotropic effects of 5-HT.

Methods

Experiments on spontaneously beating atria

Seventy four Cambarough piglets (either sex, 2–5 days old) were used. Anaesthesia, dissection and setting up of right atria, as well as other conditions were those previously described (Kaumann, 1990; Medhurst & Kaumann, 1993). Spontaneously beating right atria were rapidly dissected in warm solution containing (mM): Na^+ 120, K^+ 5, Ca^{2+} 2.25, Mg^{2+} 0.5, Cl^- 98.5, SO_4^{2-} 0.5, HCO_3^- 34, HPO_4^{2-} 1, EDTA 0.04, deionised and twice distilled water, equilibrated with 95% O_2 and 5% CO_2. The atria were set up in pairs in a 50 ml organ bath at 37°C in the above solution supplemented with (mM): Na^+ 15, fumarate 5, pyruvate 5, L-glutamate 5 and glucose 10. A single concentration-effect curve, in the presence or absence of SB 207710 preincubated for 2 h, was determined on each atrium by sequential administration of 5-HT to the bath in amounts that increased the total concentration in steps of 0.5 log unit. All experiments were carried out in the presence of 400 nM (±)-propranolol, 6 μM cocaine and 200 μM ascorbate to reduce possible indirect β-adrenoceptor-mediated effects, capture of 5-HT and oxidation of 5-HT, respectively (Kaumann, 1990). The experiments were terminated by the addition of a saturating concentration of (–)-isoprenaline (200 μM) still in the presence of 5-HT or 5-HT plus SB 207710 to allow normalisation of responses in different preparations. The concentration of (–)-isoprenaline used was calculated to surmount completely the antagonism by (±)-propranolol. To exclude the possibility that SB 207710 could block β-adrenoceptors, we determined a single concentration-effect curve to (–)-isoprenaline, in the absence or presence of the highest concentration of SB 207710 (100 nM) used. The positive chronotropic effects of 5-HT were expressed as a percentage of the total increase in beating rate caused by 5-HT plus 200 μM (–)-isoprenaline (ΔHR % ΔIso). Simple competitive antagonism by SB 207710 of the effects of 5-HT was checked with a Schild-plot (Arunlakshana & Schild, 1959); the 95% confidence interval of the slope was estimated and pK_B calculated. The equilibrium dissociation constant K_B (–log K_B = pK_B) for the SB 207710-5-HT$_4$ receptor complex was estimated from

$$pK_B = \log(\text{5-HT concentration-ratio} - 1) - \log[\text{SB 207710}] \quad (1)$$

[^{125}I]-SB 207710 binding assays

Twenty five new-born piglets of either sex were killed on the day of birth. The heart was excised and immediately washed free of blood with the cold solution described above for dissection of right atria for chronotropic studies. All further procedures were carried out on ice. The right atrium was dissected. Atrial tissue (1.0 g) was reduced to a powder under liquid nitrogen and homogenized for 10 s in 1 ml of 50 mM Tris HCl and 1 mM EDTA, pH 7.0 at 20°C with a Polytron PT7 probe at speed setting 8, and diluted with a further 9 ml of the same buffer. The diluted homogenate was filtered through gauze and centrifuged for 10 min at 14000 *g*, 4°C. The pellet was resuspended in 10 ml buffer and centrifuged as before, then finally resuspended in binding buffer containing (mM): Tris HCl 50, EDTA 1, EGTA 5, $MgCl_2$ 2, ascorbate 1, phenyl methyl sulphonyl fluoride 0.5, and 0.5% bovine serum albumin, pH 7.4 at 37°C.

For 5-HT$_4$ receptor studies, binding assays were carried out in tubes containing 100 or 200 μl binding buffer with 200–600 μg protein. Saturation binding was carried out with [^{125}I]-SB 207710, 5–1500 pM, in the absence or presence of 5-HT,

[1] Author for correspondence.

100 μM. Specific binding was defined as the difference between total binding and binding in the presence of 5-HT 100 μM. For binding inhibition studies, around 50 pM [^{125}I]-SB 207710 was used in the absence and presence of 8–10 concentrations of competing ligand; the medium also contained 100 μM GTP. All assays were carried out in duplicate. After an incubation period of 60 min at 37°C, the contents were filtered on Whatman GF/C filters presoaked in 0.3% polyethyleneimine and 1 μM SB 207710 using a Brandel harvester and washed 3 times with 4 ml ice-cold solution containing 50 mM Tris HCl and 2 mM $MgCl_2$, pH 7.0 at 20°C. Filters were counted in a Packard γ-counter at 79% efficiency.

To assess the densities of β_1- and β_2-adrenoceptors, (–)-[^{125}I]-cyanopindolol, 1–300 pM, was used to assess saturation kinetics and around 50 pM for inhibition of binding by the β_1-selective antagonist, CGP 20712 A (0.1 nM–100 μM) (Kaumann & Lemoine, 1987). Binding removed by 200 μM (–)-isoprenaline was considered specific. After 2 h incubation at 37°C, 200 μl samples were diluted with ice cold buffer, filtered and counted as described above.

Protein was measured by the method of Bradford (1976) with bovine serum albumin used as standard.

Data from saturation binding and inhibition of binding by competing ligands were analysed by non-linear regression using GRAFIT (Leatherbarrow, 1992).

Drugs and materials

[^{125}I]-SB 207710 was obtained from Amersham (Buckinghamshire, UK) and (–)-[^{125}I]-cyanopindolol from NEN (Stevenage, UK). Bovine serum albumin (fraction V), GTP disodium salt, 5-hydroxytryptamine hydrochloride (5-HT), 5-methoxytryptamine hydrochloride (5 MeOT), (–)-isoprenaline hydrochloride and cocaine hydrochloride were purchased from Sigma (Poole, Dorset). Tropisetron was purchased from RBI (Natick, MA, U.S.A.). SB 207710 (1-butyl-4-piperidinyl)-methyl 8-amino-7-iodo-l, 4-benzodioxan-5-carboxylate), renzapride, 5-carboxyamidotryptamine (5-CT) and SB 203186 {(1-piperidinyl)ethyl lH-indole 3 carboxylate} were synthesized at SmithKline Beecham. Cisapride was a gift from Janssen (Beerse, Belguim). (±)-Propranolol hydrochloride was a gift from ICI Pharmaceuticals (Macclesfield, Cheshire). CGP 20712A 1-[2-{(3-carbamoyl 4-hydroxy)phenoxy} ethylamino]-3-{4-(1-methyl-4-trifluoromethyl-2-imidazolyl)phenoxy}-2-propanol methanesulphonate was a gift from CIBA-Geigy (Basle, Switzerland).

All stock solutions were made up in twice distilled water except tropisetron and cisapride (dimethylsulphoxide), 5-HT and (–)-isoprenaline (0.2 mM ascorbate).

Results

SB 207710 as competitive antagonist

SB 207710 (1–100 nM) did not affect atrial beating rate but caused a concentration-dependent and surmountable shift of the concentration-effect curve to 5-HT (Figure 1a). The slope of the Schild-plot did not differ from one (Figure 1b). The pK_B for SB 207710, calculated from individual EC_{50} concentration-ratios with respect to a mean EC_{50} (mol l^{-1}) value of 5-HT ($n=39$), was 9.83±0.13 (mean±s.e.mean).

SB 207710 failed to affect the tachycardia caused by (–)-isoprenaline ruling out affinity for β-adrenoceptors at the concentration (100 nM) used. The –logEC_{50} M values for (–)-isoprenaline were 8.98 and 8.84 for 2 atria in the absence of SB 207710 and 9.06 and 9.05 for another 2 atria in the presence of SB 207710.

Binding of [^{125}I]-SB 207710

Figure 2a shows that [^{125}I]-SB 207710 labelled a population of saturable binding sites as defined with 100 μM 5-HT. The estimated B_{max} was 0.34 fmol mg^{-1} protein with a K_D of 73 pM. The estimated concentration of saturable binding sites was 0.58±0.09 (range 0.34–1.1) fmol mg^{-1} protein in 9 independent assays. In this and 6 independent assays non-specific binding was 45±6% with approximately 50 pM [^{125}I]-SB 207710. The onset of binding, measured with 60 pM [^{125}I]-SB 207710, was fast with a $t_{\frac{1}{2}} \sim 100$ s. After 10 min incubation the dissociation of [^{125}I]-SB 207710 from the binding sites was measured with a saturating concentration (1 μM) of unlabelled SB 207710 and also found to be fast ($t_{\frac{1}{2}} \sim 100$ s).

The antagonists SB 207710 (this work), SB 203186 (Medhurst & Kaumann, 1993) and tropisetron (Kaumann, 1990) inhibited binding of [^{125}I]-SB 207710 (Figure 2b) with pK_i values of 9.5, 7.6 and 6.4 respectively. The partial agonists renzapride and cisapride (Kaumann, 1990) inhibited binding of [^{125}I]-SB 207710 with pK_i values of 7.1 and 4.2 respectively (Figure 2c). The agonists 5-HT, 5-MeOT and 5-CT (Kaumann, 1990; Medhurst & Kaumann, 1993) inhibited binding of [^{125}I]-SB 207710 (Figure 2d) with pK_i values of 6.6, 5.2 and 4.0 respectively. The standard errors on all pK_i values were consistently smaller than 0.2 log units.

Saturable binding of (–)-[^{125}I]-cyanopindolol

Saturation binding with (–)-[^{125}I]-cyanopindolol yielded a density of β-adrenoceptors of 114 fmol mg^{-1} protein of which 89±3% were β_1 and 11±3% β_2, as estimated from a biphasic binding inhibition curve of CGP 20712A.

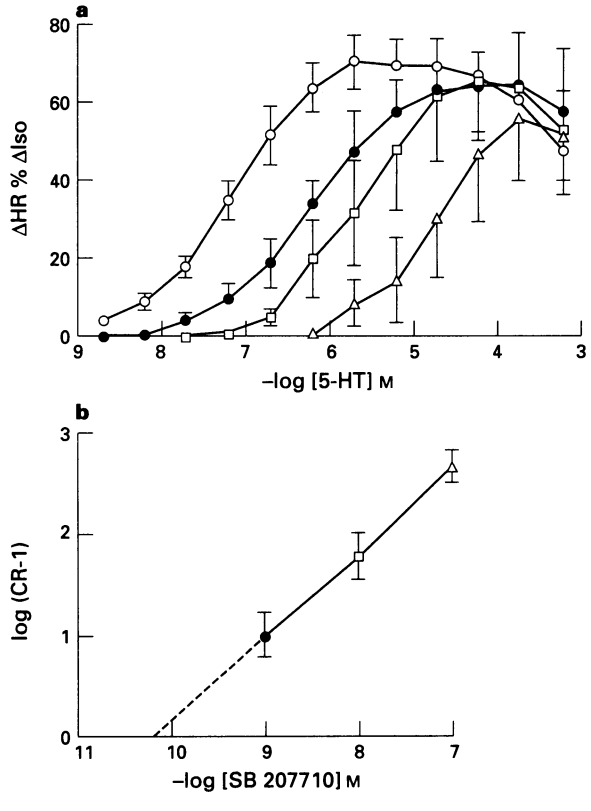

Figure 1 (a) Concentration-effect curves to 5-HT in the absence (○), ($n=39$) and presence of 1 (●, $n=6$), 10 (□, $n=4$) and 100 nM (△, $n=4$) SB 207710 in piglet right atrium; data are means ±s.e.mean. Chronotropic effects are expressed as a percentage of the increase in beating caused by agonist alone or in the presence of antagonist, plus 200 μM (–)-isoprenaline (ΔHR% ΔIso). (b) Double log plot for simple competitive inhibition by SB 207710; data from (a), calculated using equation (1); mean slope±0.95 confidence interval = 0.81±0.31.

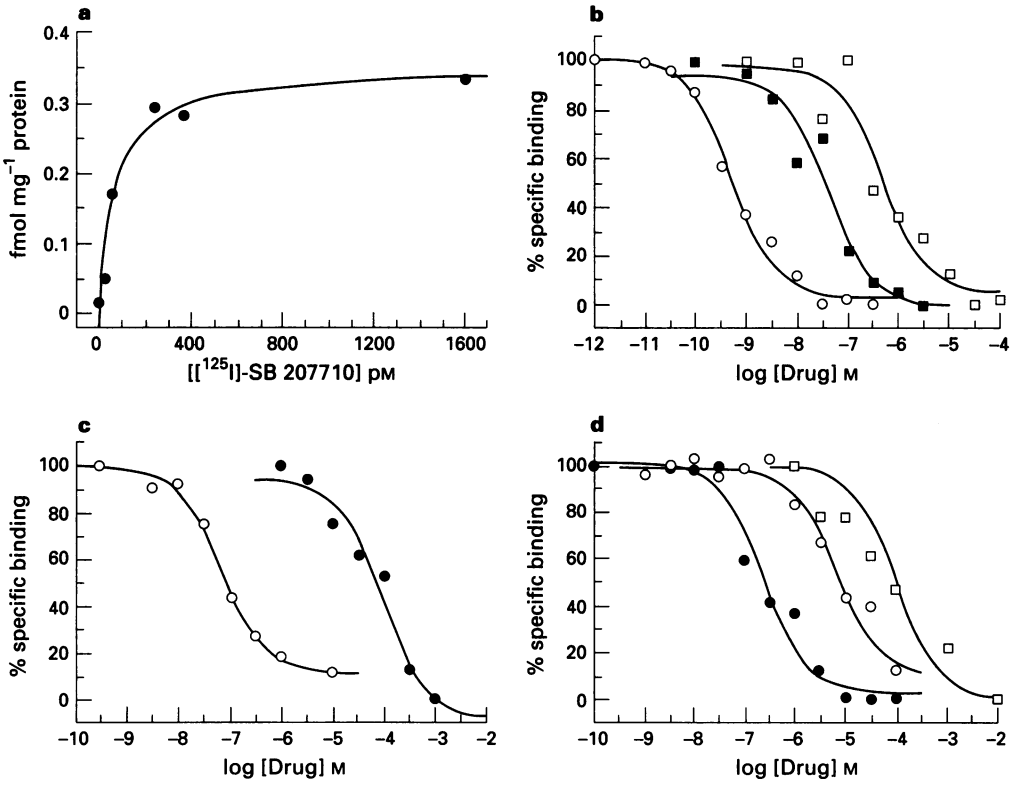

Figure 2 Specific binding of [^{125}I]-SB 207710 (a) and inhibition of binding by antagonists (b), partial agonists (c) and agonists (d). Antagonists (b) are SB 207710 (○), SB 203186 (■) and tropisetron (□). Partial agonists (c) are: renzapride (○) and cisapride (●). Agonists (d) are: 5-HT (●), 5-MeOT (○) and 5-CT (□). All data points are duplicates from 1 or 2 experiments.

Discussion

In piglet right atrium we detected a small population of saturable binding sites labelled with the 5-HT$_4$ receptor-selective ligand [^{125}I]-SB 207710. The non-radioactive form of SB 207710 also antagonized competitively the positive chronotropic effects of 5-HT in piglet right atrium ($pK_B = 9.8$, this work), in agreement with previous estimates of affinity for 5-HT$_4$ receptors in human atrium ($pK_B = 10.1$, Kaumann, 1994). The 5-HT$_4$ receptor nature of the saturable binding sites is supported by the close similarity of affinity values for SB 207710, estimated from binding of its radioiodinated form and from antagonism. Furthermore, the absolute values of the binding affinities of the antagonists, SB 207710, SB 203186 and tropisetron are in excellent agreement with the corresponding estimates of affinity from antagonism of the positive chronotropic effects of 5-HT in piglet atrium (this work; Kaumann, 1990; Medhurst & Kaumann, 1993) and positive inotropic effects in human atrium (Kaumann *et al.*, 1994; Kaumann, 1994). The 5-HT$_4$ receptor nature is also supported by the rank order of potencies, estimated from inhibition of [^{125}I]-SB 207710 binding, of agonists (5-HT > 5-MeOT > 5-CT) and partial agonists (renzapride > cisapride), which are similar to those found from functional studies in beating piglet right atrium (Kaumann, 1990; Medhurst & Kaumann, 1993) and human atrium (summarised in Kaumann, 1994).

The binding affinity of cisapride for 5-HT$_4$ receptors, estimated by us for piglet atrial membranes, was lower than the chronotropic potency estimated for cisapride on beating piglet atria (Medhurst & Kaumann, 1993). The reasons for this discrepancy are not yet known. In addition, a consistently higher affinity or stimulant potency of cisapride has been reported for cerebral 5-HT$_4$ receptors of several species (Dumuis *et al.*, 1989; Grossman *et al.*, 1993; Brown *et al.*, 1993) including man (Domenech *et al.*, 1993) than for both porcine (Kaumann, 1990; Medhurst & Kaumann, 1993; this work) and human (Kaumann *et al.*, 1991) atrial 5-HT$_4$ receptors, suggesting that cerebral and cardiac 5-HT$_4$ receptors may be different subtypes (Kaumann *et al.*, 1991). The recently cloned 5-HT$_4$ receptor has two splice variants, 5-HT$_{4S}$ and 5-HT$_{4L}$ for both rat and man receptor homologues, which differ in length and sequence of the carboxy tail (Gerald *et al.*, 1994). The affinities of cisapride for each of the two receptor forms have not yet been disclosed. It would be interesting to know whether these affinities differ and, whether the higher affinity form exists in the brain and the lower affinity form in the atrium.

A small discrepancy is the observation that in isolated atria of both piglet and man, 5-HT is more potent than renzapride whilst the opposite is seen in binding. This may relate to the observations that renzapride is a partial agonist whilst 5-HT is a full agonist for both piglet and human atria and would be explained if there were some receptor reserve for 5-HT ($pK_i = 6.6$ vs $-\log EC_{50} = 7.3$) but not for renzapride, at least in piglet right atrium.

The 5-HT$_4$ receptor population, detected in piglet atrium, was remarkably small compared to the β_1- and β_2-adrenoceptor populations, which were 174 times and 22 times more abundant, respectively. Despite this marked discrepancy in the measured receptor numbers the maximum 5-HT-induced tachycardia is only 20 to 30% smaller than that of a β-adrenoceptor-saturating concentration of (–)-isoprenaline (Figure 1a this work; Kaumann, 1990; Medhurst & Kaumann, 1993). Conceivably the 5-HT$_4$ receptor density of the small population of sinoatrial cells has been underestimated because membrane particles were prepared from the whole right atrium and our receptor density estimate represents an average of the 5-HT$_4$ receptors of both sinoatrial node cells and non-sinoatrial cells. A more precise assessment of the relationship between chronotropic efficacy of agonists and densities of β_1- and β_2-adrenoceptors, and 5-HT$_4$ receptors, must therefore await the quantitation of these receptor populations in the sinoatrial node with autoradiography. [^{125}I]-SB 207710 will be a useful tool for this purpose, as well as for the labelling of other peripheral 5-HT$_4$ receptors, including those of human atrium.

References

ARUNLAKSHANA, O. & SCHILD, H.O. (1959). Some quantitative uses of drug antagonism. *Br. J. Pharmacol. Chemother.*, **14**, 48–58.

BRADFORD, M. (1976). A rapid and sensitive method for the quantitation of microgram quantities of protein utilizing the principle of protein-dye binding. *Anal. Biochem.*, **72**, 248–254.

BROWN, A.M., YOUNG, T.J., PATCH, T.L., CHEUNG, C.W., KAUMANN, A.J., GASTER, L. & KING, F.D. (1993). [^{125}I] SB 207710, a potent, selective radioligand for 5-HT$_4$ receptors. *Br. J. Pharmacol.*, **110**, 10P.

DOMENECH, T., BELETA, J., FERNANDEZ, A.G., GRISTWOOD, R.W., CRUZ-SANCHEZ, F., TOLOSA, E. & PALACIOS, J.M. (1993). Identification and characterization of serotonin 5-HT$_4$ receptor binding sites in human brain: comparison with other mammalian species. *Mol. Brain Res.*, **21**, 176–180.

DUMUIS, A., SEBBEN, M. & BOCKAERT, J. (1989). The gastrokinetic prokinetic benzamide derivatives are agonists at the non-classical 5-HT receptor (5-HT$_4$) positively coupled to adenylate cyclase in neurons. *Naunyn-Schmied Arch. Pharmacol.*, **340**, 403–410.

GERALD, CH., HARTIG, P., BRANCHEK, T. & WEINSHANK, R.L. (1994). DNA encoding 5-HT$_4$ serotonin receptors and uses thereof. *International patent WO 94/14957.*

GROSSMAN, C.J., KILPATRICK, G.J. & BUNCE, K.T. (1993). Development of a radioligand binding assay for 5-HT$_4$ receptors in guinea-pig and rat brain. *Br. J. Pharmacol.*, **109**, 618–624.

KAUMANN, A.J. (1990). Piglet sinoatrial 5-HT receptors resemble human atrial 5-HT$_4$-like receptors. *Naunyn-Schmied Arch. Pharmacol.*, **342**, 619–622.

KAUMANN, A.J. (1994). Do human atrial 5-HT$_4$ receptors mediate arrhythmias? *Trends Pharmacol. Sci.*, **15**, 451–455.

KAUMANN, A.J., GASTER, L.M., KING, F.D. & BROWN, A.M. (1994). Blockade of human atrial 5-HT$_4$ receptors by SB 207710, a selective and high affinity 5-HT$_4$ receptor antagonist. *Naunyn-Schmied. Arch. Pharmacol.*, **349**, 546–548.

KAUMANN, A.J. & LEMOINE, H. (1987). β_2-Adrenoceptor-mediated positive inotropic effect of adrenaline in human ventricular myocardium: quantitative discrepancies with binding and adenylate cyclase stimulation. *Naunyn-Schmied. Arch. Pharmacol.*, **335**, 403–411.

KAUMANN, A.J., SANDERS, L., BROWN, A.M., MURRAY, K.J. & BROWN, M.J. (1991). A 5-HT$_4$-like receptor in human right atrium. *Naunyn-Schmied. Arch. Pharmacol.*, **344**, 150–159.

LEATHERBARROW, R.J. (1992). *GRAFIT VERSION 3.0.* Erithacus Software Ltd (Staines, UK).

MEDHURST, A.D. & KAUMANN, A.J. (1993). Characterization of the 5-HT$_4$ receptor mediating tachycardia in piglet isolated right atrium. *Br. J. Pharmacol.*, **110**, 1023–1030.

VILLALON, C.M., DEN BOER, M.O., HEILIGERS, J.A.C. & SAXENA, P.R. (1990). Mediation of 5-hydroxytryptamine-induced tachycardia in the pig by the putative 5-HT$_4$ receptor. *Br. J. Pharmacol.*, **102**, 107–112.

(Received February 27, 1995
Revised March 28, 1995
Accepted April 3, 1995)

British Journal of Pharmacology (1995) 115, 937-944 © 1995 Stockton Press All rights reserved 0007-1188/95 $12.00

Ca^{2+}-dependent and -independent mechanism of cyclic-AMP reduction: mediation by bradykinin B_2 receptors

[1]Henk Sipma, Adriaan den Hertog & Adriaan Nelemans

Groningen Institute for Drugs Studies (GIDS), Department of Clinical Pharmacology, University of Groningen, Bloemsingel 1, 9713 BZ Groningen, The Netherlands

1 Bradykinin caused a transient reduction of about 25% in the cyclic AMP level in forskolin prestimulated DDT_1 MF-2 smooth muscle cells (IC_{50}: 36.4±4.9 nM) and a pronounced, sustained inhibition (40%) of the isoprenaline-stimulated cyclic AMP level (IC_{50}: 37.5±1.1 nM).

2 The Ca^{2+} ionophore, ionomycin, mimicked both the bradykinin-induced transient reduction in the forskolin-stimulated cyclic AMP level and the sustained reduction in the isoprenaline-stimulated cyclic AMP level.

3 The Ca^{2+}-dependent effect on cyclic AMP induced by bradykinin was mediated solely by Ca^{2+} release from internal stores, since inhibition of Ca^{2+} entry with $LaCl_3$ did not reduce the response to bradykinin.

4 The involvement of calmodulin-dependent enzyme activities, protein kinase C or an inhibitory GTP binding protein in the bradykinin-induced responses was excluded since a calmodulin inhibitor, calmidazolium, a PKC inhibitor, staurosporine and pertussis toxin, respectively did not affect the decline in the cyclic AMP level.

5 Bradykinin enhanced the rate of cyclic AMP breakdown in intact cells, which effect was not mimicked by ionomycin. This suggested a Ca^{2+}-independent activation of phosphodiesterase activity by bradykinin in DDT_1 MF-2 cells.

6 The bradykinin B_1 receptor agonist, desArg^9-bradykinin, did not affect cyclic AMP formation in isoprenaline prestimulated cells, while the bradykinin B_2 receptor antagonists, Hoe 140 (D-Arg[Hyp^3, Thi^5, D-Tic^7, Oic^8]-BK) and D-Arg[Hyp^3, Thi^{5,8}, D-Phe^7]-BK completely abolished the bradykinin response in both forskolin and isoprenaline prestimulated cells.

7 Bradykinin caused an increase in intracellular Ca^{2+}, which was antagonized by the bradykinin B_2 receptor antagonists, Hoe 140 and D-Arg[Hyp^3, Thi^{5,8}, D-Phe^7]-BK. The bradykinin B_2 receptor agonist, desArg^9-bradykinin, did not evoke a rise in cytoplasmic Ca^{2+}.

8 It is concluded, that stimulation of bradykinin B_2 receptors causes a reduction in cellular cyclic AMP in DDT_1 MF-2 cells. This decline in cyclic AMP is partly mediated by a Ca^{2+}/calmodulin independent activation of phosphodiesterase activity. The increase in $[Ca^{2+}]_i$ mediated by bradykinin B_2 receptors inhibited forskolin- and isoprenaline-activated adenylyl cyclase differently, most likely by interfering with different components of the adenylyl cyclase signalling pathway.

Keywords: Cyclic AMP; Ca^{2+}; phosphodiesterase; bradykinin B_2 receptor; DDT_1 MF-2 cell

Introduction

Bradykinin is an important mediator of various biological processes, including regulation of blood pressure, neurotransmission and bronchoconstriction. The existence of bradykinin B_1 and B_2 receptors has been firmly established (Hall, 1992). Recently, a novel bradykinin B_3 receptor was proposed (Pyne & Pyne, 1993; 1994).

It was reported that bradykinin induces phospholipase C activation resulting in the formation of inositol 1,4,5-trisphosphate (Ins(1,4,5)P_3) and the accumulation of cytoplasmic Ca^{2+} in DDT_1 MF-2 smooth muscle cells (Gerwins & Fredholm, 1992; Dickenson & Hill, 1992). Besides activation of phospholipase C, bradykinin has been reported to affect the cellular adenosine 3': 5'-cyclic monophosphate (cyclic AMP) level. In cultured tracheal smooth muscle cells, bradykinin elicited accumulation of cyclic AMP (Stevens *et al.*, 1994). In contrast, bradykinin evoked inhibition of cyclic AMP accumulation was observed in D384-human astrocytoma cells (Balmforth *et al.*, 1992; Altiok & Fredholm, 1993) and in NCB-20 hybrid neuronal cells (Garritsen *et al.*, 1992b). These inhibitory actions were caused by a simultaneous increase in cytoplasmic Ca^{2+}. Recently, inhibition of adenylyl cyclase activity caused by an inhibitory GTP binding protein was reported on stimulation of P_{2U} purinoceptors in DDT_1 MF-2 cells (Sipma *et al.*, 1994).

In this study we describe a bradykinin-induced decrease in the cyclic AMP level in DDT_1 MF-2 cells. Depending on the agonist used to activate adenylyl cyclase, this decline in cyclic AMP was either transient or sustained in nature. Furthermore we classified the bradykinin receptor subtype mediating these responses and studied the mechanisms underlying the effect of bradykinin on the cyclic AMP level.

Methods

Cell culture

DDT_1 MF-2 cells, derived from a Syrian hamster vas deferens (Norris *et al.*, 1974) were cultured in Dulbecco's modified essential medium supplemented with 7 mM $NaHCO_3$, 10 mM HEPES at pH 7.2 (DMEM) and 10% foetal calf serum at 37°C in 5% CO_2 (Molleman *et al.*, 1989).

[1] Author for correspondence.

Experimental design and sample preparation

DDT_1 MF-2 cells were growm in monolayers in 9.6 cm^2 plastic wells as described earlier (Hoiting *et al.*, 1990). The medium was replaced by 2 ml DMEM at 20°C, 30 min before starting the experiment by adding agonists. Before adding bradykinin some cell preparations were pre-exposed to forskolin (1 μM) for 10 min or to isoprenaline (10 μM, 10 min). Antagonists were added 2 min before exposure to bradykinin.

Cyclic AMP phosphodiesterase activity in intact cells was measured as previously described by Garritsen *et al.* (1992a). Isoprenaline pretreated (1 μM, 10 min) cells were quickly washed 3 times by aspiration and addition of new solution supplemented with the β_2-adrenoceptor antagonist, propranolol (100 nM). Under these conditions *de novo* synthesis of cyclic AMP was abolished.

Reactions were stopped by removal of the medium and addition of 400 μl 5% trichloroacetic acid (TCA). Samples were placed on ice for at least 45 min and subsequently washed 3 times with 800 μl water-saturated diethylether and neutralised with KOH (25 μl, 0.2 mM).

Measurements of cyclic AMP

A radioligand binding assay was used to determine cyclic AMP concentrations, using a standard curve of cyclic AMP in ether-extracted trichloroacetic acid solution (Brown *et al.*, 1971). To reach equilibrium, 50 μl sample was incubated with a buffer composed of 50 mM Tris-HCl (pH 7.4), 4 mM EDTA, 20 μg cyclic AMP binding protein, 200 μg bovine serum albumin and 10 μl [^{3}H]-cyclic AMP (190 nM, 40 Ci $mmol^{-1}$) to a total volume of 160 μl at 4°C for at least 2 h. The reaction was terminated by adding 500 μl of a charcoal suspension (Norit A special, 3.5 g l^{-1}) followed by centrifugation to remove the excess [^{3}H]-cyclic AMP. Radioactivity in the supernatant was measured by scintillation counting.

Measurements of intracellular calcium

Cells (10^6 cells ml^{-1}) were washed with and resuspended in a buffer solution containing (mM): NaCl 145, KCl 5, $MgSO_4$ 0.5, $CaCl_2$ 1, glucose 10, bovine serum albumin 2% and HEPES 10, (pH 7.4) (Hesketh *et al.*, 1983) and were loaded with Fura-2 AM (3 μM) for 45 min at 37°C. The cells were collected by centrifugation (20 s, 1000 *g*) and washed two times before the fluorescence measurement with buffer without bovine serum albumin. Calcium-free solution contained Mg^{2+} (6.2 mM) to prevent membrane leakage and EGTA (0.4 mM) to remove extracellular Ca^{2+} (Den Hertog, 1981). Fura-2 fluorescence of the cells (excitation: 340 nM and 380 nM; emission 510 nm) was measured at 22°C. The cell suspension was continuously magnetically stirred. The internal calcium concentration was calculated (Hesketh *et al.*, 1983) using 0.015% of Triton X-100 as permeabilizing agent.

Data analysis

Data are presented as mean ± s.e.mean and were considered significantly different from control values at $P<0.05$ using Student's unpaired *t* test. A Sigma plot logistic curve fitting programme (Jandel Scientific, U.S.A.) was used to determine EC_{50} and IC_{50} values and to analyse binding parameters obtained from the respective radioligand binding assays.

Chemicals

Adenosine 3':5'-cyclic monophosphate (cyclic AMP) was from Boehringer (Germany). Forskolin, isoprenaline, bradykinin, desArg^9-bradykinin, pertussis toxin, 3-isobutyl-1-methyl-xanthine and staurosporine were purchased from Sigma, (U.S.A.). D-Arg[Hyp^3, Thi^{5,8}, D-Phe^7]-BK was from Hoechst AG (Germany). D-Arg[Hyp^3, Thi^5, D-Tic^7, Oic^8]-BK (Hoe 140) was from Peninsula Laboratories Inc. (U.S.A.). Calmidazolium chloride was obtained from Biomol (U.S.A.). [2,8-^{3}H]-adenosine 3':5'-cyclic monophosphate was obtained from Du Pont-New England Nuclear (U.S.A.). $LaCl_3$ and all other chemicals were from Merck (Germany).

Results

Forskolin and isoprenaline induced cyclic AMP accumulation

Stimulation of DDT_1 MF-2 cells with forskolin (1 μM) resulted in an increase in basal cellular cyclic AMP from 2.1 ± 0.2 pmol/10^6 cells to 8.6 ± 0.3 pmol/10^6 cells. In the presence of the β-adrenoceptor agonist, isoprenaline (1 μM), intracellular cyclic AMP reached a maximum of 65.6 ± 3.5 pmol/10^6 cells. Both forskolin and isoprenaline induced cyclic AMP formation were maximal after 10 min of exposure to the agonists and remained stable for at least 10 min afterwards as described in detail elsewhere (Sipma *et al.*, 1995).

Bradykinin and cyclic AMP

Stimulation of DDT_1 MF-2 cells with bradykinin (1 μM, 2 min) did not affect the basal cyclic AMP level (not shown). Bradykinin evoked a transient decline in cellular cyclic AMP in forskolin (1 μM, 10 min) pretreated cells (Figure 1a). The cellular cyclic AMP level showed a minimum between 0.5 and 2 min and returned to its original value after 5 min of exposure to bradykinin. This action of bradykinin on forskolin pretreated cells was concentration-dependent (Figure 2a, IC_{50}: 36.4 ± 4.9 nM). Bradykinin induced a pronounced, sustained decrease in the cyclic AMP level in isoprenaline (1 μM, 10 min) pretreated cells (Figure 1b). Bradykinin also elicited a pronounced response when cells were pretreated with a lower concentration of isoprenaline (10 nM), resulting in a similar rise in cyclic AMP concentration as seen with forskolin (Figure 1c). The reduction of isoprenaline (1 μM)-induced cyclic AMP exhibited a similar concentration-dependency on bradykinin (Figure 2b, IC_{50}: 37.5 ± 1.1 nM) as observed for forskolin pretreated cells. Exposure of DDT_1 MF-2 cells to bradykinin has previously been shown to elicit Ca^{2+} release from Ins(1,4,5)P_3-sensitive internal stores and to provoke Ca^{2+}-entry (Gerwins & Fredholm, 1992; Dickenson & Hill, 1992). Exposure of cells to forskolin or isoprenaline did not change the basal cytoplasmic Ca^{2+} concentration ($[Ca^{2+}]_i$) or the bradykinin-induced increase in $[Ca^{2+}]_i$ (Table 1).

Involvement of an inhibitory G-protein

The involvement of inhibitory GTP binding proteins (G_i) in the effects of bradykinin on cyclic AMP was studied by use of pertussis toxin (PTX). Pretreatment of DDT_1 MF-2 cells with PTX (100 ng ml^{-1}, 24 h) neither affected the forskolin induced formation of cyclic AMP nor reduced the bradykinin-induced decline in the forskolin-stimulated cyclic AMP level (Figure 3a). Remarkably, the isoprenaline-induced formation of cyclic AMP was reduced after pre-exposure of cells to PTX. Under these experimental conditions, bradykinin still decreased the isoprenaline-stimulated cyclic AMP level (Figure 3b).

Ionomycin and cyclic AMP

In order to investigate the contribution of cytoplasmic Ca^{2+} to the effects observed, ionomycin (5 μM) was used to permeabilize plasma membranes and to deplete internal Ca^{2+} stores. In the presence of extracellular Ca^{2+} this treatment resulted in a transient decline in the forskolin-induced cyclic AMP level and a maintained decrease in the isoprenaline-induced cyclic AMP level (Figure 4). The characteristics of the cyclic AMP response in the presence of ionomycin were similar to those obtained with bradykinin (Figure 1).

Contribution of Ca^{2+}-entry

In order to estimate the relative contribution of Ca^{2+} entry and Ca^{2+} mobilization from internal stores to the bradykinin induced decline in cyclic AMP levels, Ca^{2+} entry was blocked with lanthanum ions ($LaCl_3$). The bradykinin-induced maximal increase in $[Ca^{2+}]_i$ was reduced to about 65% of the control response (Figure 5, Table 1) in the presence of $LaCl_3$ (50 μM). Moreover, the slowly declining phase of the Ca^{2+} response, representing Ca^{2+}-entry, was completely abolished by $LaCl_3$ (Figure 5). Inhibition of Ca^{2+} entry with $LaCl_3$ (50 μM) did not change the forskolin or isoprenaline-stimulated cyclic AMP level and did not affect the bradykinin induced decline in the forskolin- or isoprenaline-induced cyclic AMP level (Table 2).

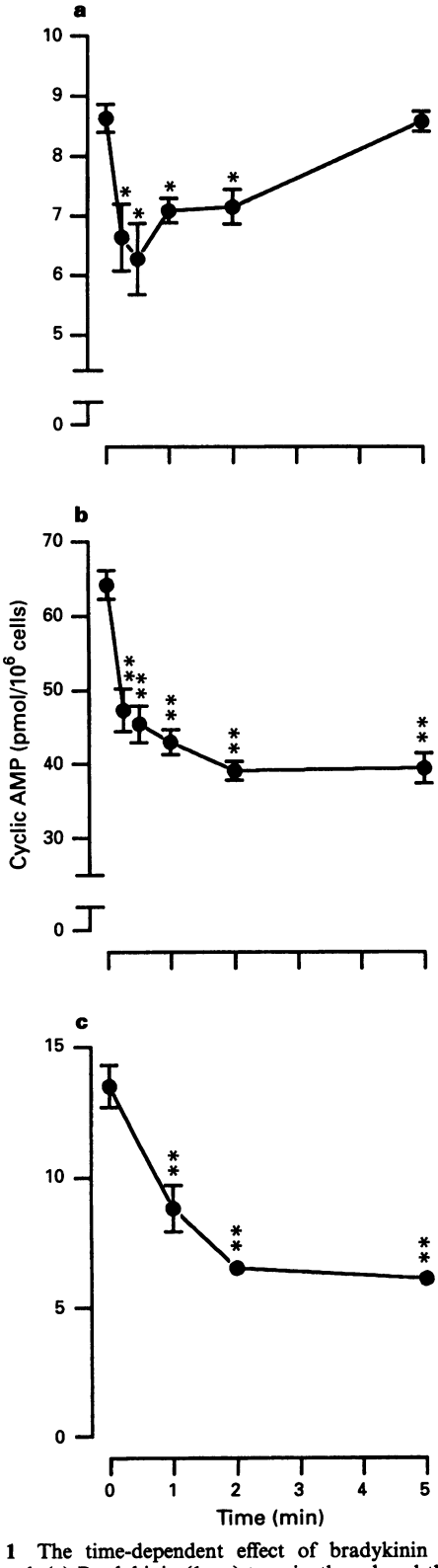

Figure 1 The time-dependent effect of bradykinin on the cyclic AMP level. (a) Bradykinin (1 μM) transiently reduced the cyclic AMP level in forskolin (1 μM, 10 min) prestimulated cells. (b) The bradykinin (1 μM)-induced reduction of cyclic AMP accumulation in isoprenaline (1 μM, 10 min) prestimulated cells is sustained. (c) The effect of bradykinin on cellular cyclic AMP after pretreatment of the cells with a low concentration of isoprenaline (10 nM, 10 min). *Different from values obtained in the absence of bradykinin, $P<0.05$; **$P<0.01$. Each point represents the mean ± s.e.mean of at least 5 experiments.

Involvement of protein kinase C and calmodulin dependent enzymes

Pretreatment of cells with the protein kinase C inhibitor, staurosporine (0.5 μM, 5 min), did not change the basal level of forskolin- or isoprenaline-induced cyclic AMP and did not affect the bradykinin-induced decline in the forskolin- and isoprenaline-stimulated cyclic AMP level (Table 3).

A calmodulin inhibitor was used to determine whether the inhibitory effect of Ca^{2+} on cyclic AMP levels was mediated by Ca^{2+}/calmodulin-dependent enzymes. Calmidazolium is known to inhibit calmodulin-dependent enzymes with high potency (Gietzen, 1983). Pre-exposure of cells to calmidazo-

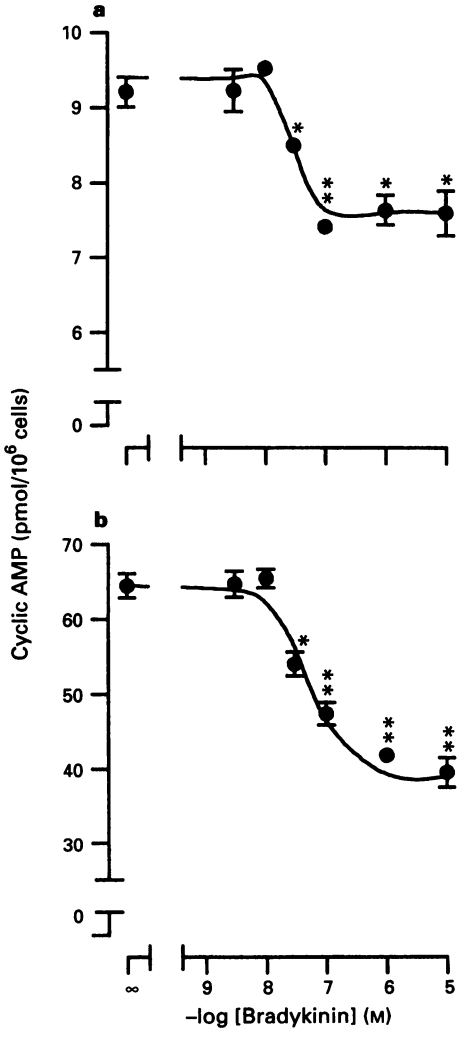

Figure 2 The concentration-dependent effect of bradykinin on the cyclic AMP level. (a) The bradykinin-induced reduction of cyclic AMP accumulation after 2 min in forskolin (1 μM, 10 min) pretreated cells. (b) The reduction in the cyclic AMP level in isoprenaline (1 μM, 10 min) pretreated cells. *Different from values obtained in the absence of bradykinin, $P<0.05$; **$P<0.01$. Each point represents the mean ± s.e.mean of at least 5 experiments.

Table 1 Bradykinin-induced increases in cytoplasmic Ca^{2+} in DTT_1 MF-2 cells

Treatment	*Basal* $[Ca^{2+}]_i$ *(nM)*	*Bradykinin induced increase in* $[Ca^{2+}]_i$ *(nM)*
None	153±9	155±22
Forskolin	160±12	154±24
Isoprenaline	156±14	158±30
$LaCl_3$	165±12	103±15*
Hoe 140	163±15	2.1±1.1*
D-Arg[Hyp^3, Thi^{5,8}, D-Phe^7]-BK	156±11	10±2.9*

Pretreatment of cells with forskolin (1 μM, 10 min) or isoprenaline (1 μM, 10 min) did not affect bradykinin (1 μM)-induced Ca^{2+} metabolism. Blocking Ca^{2+} entry by pretreatment of cells with $LaCl_3$ (50 μM, 2 min) reduced the bradykinin-induced evoked rise in $[Ca^{2+}]_i$. The bradykinin-induced maximal increase in cytoplasmic Ca^{2+} ($[Ca^{2+}]_i$) was abolished by the bradykinin B_2 receptor antagonist Hoe 140 (D-Arg[Hyp^3, Thi^5, D-Tic^7, Oic^8]-BK, 1 μM, 2 min) and D-Arg[Hyp^3, Thi^{5,8}, D-Phe^7]-BK (10 μM, 2 min). *Different from stimulation with bradykinin, $P<0.01$. Data are presented as mean ± s.e.mean of at least 4 experiments.

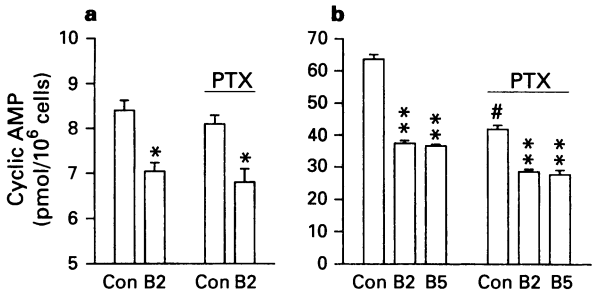

Figure 3 The effect of pertussis toxin on the bradykinin induced decline in cyclic AMP. Cells were treated in the presence or absence of pertussis toxin (PTX, 100 ng ml^{-1}, 24 h, horizontal bar). (a) The bradykinin (B2, 1 μM, 2 min)-induced reduction in forskolin pretreated (1 μM, 10 min) cells. (b) The bradykinin (1 μM, B2:2 min, B5:5 min)-induced reduction in isoprenaline pretreated (1 μM, 10 min) cells. *Different from respective control stimulation in the absence of bradykinin, $P<0.05$; **$P<0.01$. #Different from values obtained in the absence of PTX, $P<0.01$. Data are expressed as mean ± s.e.mean of 8 experiments.

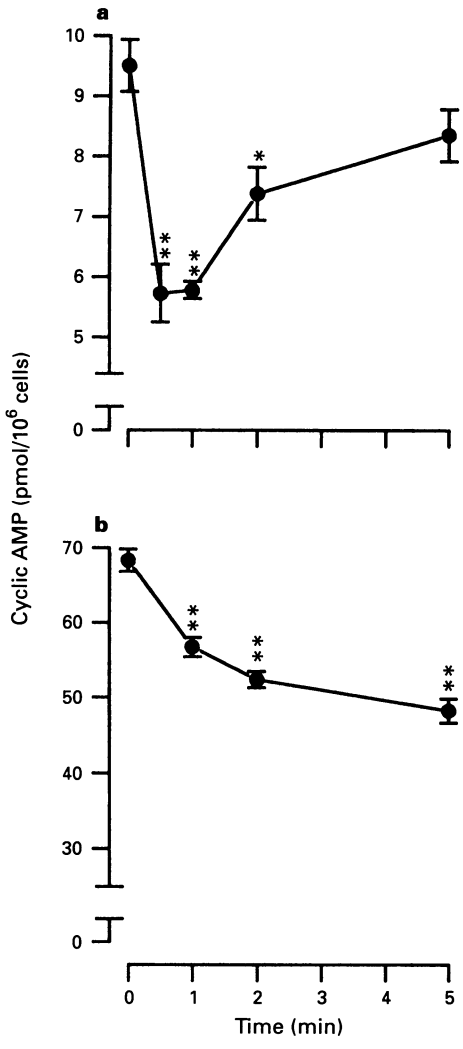

Figure 4 The effects of ionomycin on prestimulated cyclic AMP levels. (a) Ionomycin (5 μM) caused a transient decline in the forskolin (1 μM, 10 min) induced cyclic AMP level and (b) a sustained reduction in the isoprenaline (1 μM, 10 min)-enhanced cyclic AMP level in Ca^{2+} (1.8 mM) containing buffer. *Different from values obtained in the absence of ionomycin, $P<0.05$; **$P<0.01$. Each point represents the mean ± s.e.mean of 4 experiments.

lium (10 μM, 10 min) did not affect the forskolin- or isoprenaline-induced cyclic AMP level. Furthermore, the bradykinin-induced reduction in the forskolin and isoprenaline-stimulated cyclic AMP level was not affected by calmidazolium (Table 4).

The effect of bradykinin on cyclic AMP-phosphodiesterase activity

Cyclic AMP phosphodiesterase activity was measured after inhibition of *de novo* synthesis of cyclic AMP. The cyclic AMP level of unstimulated cells decreased time-dependently under these conditions (Figure 6). This decrease in the cyclic AMP level was completely inhibited in the presense of the non-specific phosphodiesterase inhibitor 3-isobutyl-1-methyl xanthine (IBMX, 200 μM), which showed that the reduction in the cyclic AMP level was completely due to cyclic AMP phosphodiesterase activity. Bradykinin (1 μM), added immediately after removal of isoprenaline, enhanced the rate of cyclic AMP breakdown, an effect which was also completely inhibited by IBMX. Ionomycin (5 μM) did not mimic the effect of bradykinin on phosphodiesterase activity (not shown).

Bradykinin receptor subtype

The bradykinin B_1 receptor agonist, des-Arg^9-bradykinin did not affect isoprenaline induced cyclic AMP formation (Table 5). The bradykinin B_2 receptor antagonist, D-Arg[Hyp^3, Thi^5, D-Tic^7, Oic^8]-BK (Hoe 140) completely blocked the bradykinin-induced reduction of the cyclic AMP level in forskolin and isoprenaline prestimulated cells. Hoe 140 concentration-dependently blocked the inhibitory response of bradykinin (1 μM) on isoprenaline-stimulated cyclic AMP accumulation (IC_{50} value: 34.0±1.5 nM, Figure 7). The bradykinin B_2 receptor antagonist, D-Arg[Hyp^3, Thi^{5,8}, D-Phe^7]-BK, likewise abolished the effect of bradykinin on the isoprenaline-induced cyclic AMP level (Table 5).

The bradykinin (1 μM)-induced rise in $[Ca^{2+}]_i$ was completely abolished by Hoe 140 (1 μM) and for 93% by D-Arg-[Hyp^3, Thi^{5,8}, D-Phe^7]-BK (10 μM) (Table 1). Exposure of cells to desArg^9-bradykinin (0.3 μM) did not affect $[Ca^{2+}]_i$ (increase $[Ca^{2+}]_i$: 1.3±1.1 nM, $n=4$).

Discussion

This study shows that bradykinin caused a transient or sustained reduction in prestimulated cellular cyclic AMP levels in

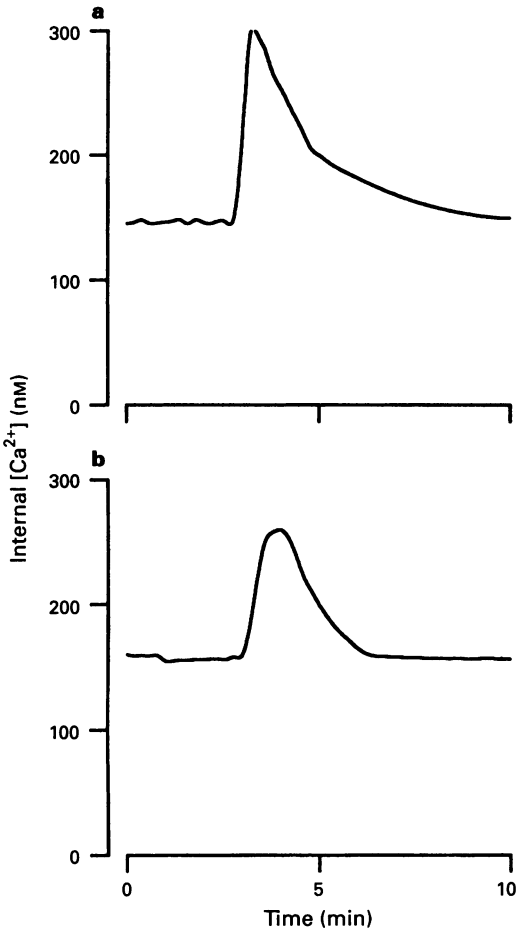

Figure 5 The effect of inhibition of Ca^{2+} entry on the bradykinin-induced increase in $[Ca^{2+}]_i$. (a) The bradykinin (1 μM)-induced rise in $[Ca^{2+}]_i$ in Ca^{2+} containing buffer. (b) $LaCl_3$ (50 μM) added 2 min in advance reduced the bradykinin-evoked maximal increase in $[Ca^{2+}]_i$ and completely inhibited the slowly declining phase of $[Ca^{2+}]_i$ representing Ca^{2+} entry. Each tracing is representative of at least 4 experiments.

DDT_1 MF-2 smooth muscle cells. A transient decline in the cyclic AMP level was observed after stimulation of the catalytic subunit of adenylyl cyclase with forskolin. After stimulation of β-adrenoceptors with isoprenaline, the bradykinin-induced reduction in the cyclic AMP level was pronounced and sustained in nature. These different characteristics of the response to bradykinin cannot be explained by a difference in the cyclic AMP level elicited by forskolin and isoprenaline, since the bradykinin-induced reduction in the cyclic AMP level was also pronounced and sustained in cells pretreated with a low concentration of isoprenaline.

Bradykinin activates phospholipase C, resulting in formation of Ins(1,4,5)P_3, mobilization of Ca^{2+} from internal stores and Ca^{2+} entry across the plasma membrane (Gerwins & Fredholm, 1992; Dickenson & Hill, 1992; this paper). We showed that an increase in $[Ca^{2+}]_i$ evoked by ionomycin mimicked the effects of bradykinin on the forskolin- and isoprenaline-induced cyclic AMP level. These observations demonstrate, that an increase in intracellular Ca^{2+} is probably involved in the bradykinin-induced reduction of cellular cyclic AMP in DDT_1 MF-2 cells. Since the bradykinin-induced increase in $[Ca^{2+}]_i$ is not changed by either forskolin or isoprenaline, the differential effect of bradykinin on cyclic AMP cannot be explained by discrete regulation of bradykinin-induced Ca^{2+} metabolism. Bradykinin and P_{2U} purinoceptor-mediated transient inhibition of prostaglandin E_1-induced cyclic AMP formation in NCB-20 hybrid neuronal cells has been reported previously (Garritsen *et al.*, 1992a,b). Likewise,

Table 2 Ca^{2+} entry and the bradykinin induced reduction in cellular cyclic AMP

	Cyclic AMP (pmol/10^6 cells)	
Treatment	*Isoprenaline*	*Forskolin*
None	64.9 ± 1.0	9.3 ± 0.5
Bradykinin (2 min)	42.7 ± 0.9**	7.2 ± 0.3*
Bradykinin (5 min)	41.2 ± 1.2**	
$LaCl_3$	66.2 ± 1.8	9.1 ± 0.6
$LaCl_3$, bradykinin (2 min)	46.4 ± 0.7**	7.2 ± 0.4*
$LaCl_3$, bradykinin (5 min)	46.3 ± 1.0**	

Inhibition of Ca^{2+}-entry by pre-exposure of cells to $LaCl_3$ (50 μM, 2 min) did not affect the bradykinin (1 μM)-induced reduction in the forskolin (1 μM, 10 min) or isoprenaline (1 μM, 10 min)-stimulated cyclic AMP level. *Different from values obtained in the absence of bradykinin $P<0.05$; **$P<0.01$. Data are expressed as mean ± s.e.mean of 6 experiments.

Table 3 Protein kinase C and the bradykinin induced reduction in the cyclic AMP level

	Cyclic AMP (pmol/10^6 cells)	
Treatment	*Isoprenaline*	*Forskolin*
None	64.4 ± 2.5	9.3 ± 0.5
Bradykinin (2 min)	44.9 ± 2.6**	7.2 ± 0.3*
Bradykinin (5 min)	43.3 ± 0.7**	
Staurosporine	68.7 ± 2.0	9.6 ± 0.9
Staurosporine, bradykinin (2 min)	46.1 ± 0.9**	7.5 ± 0.4*
Staurosporine, bradykinin (5 min)	48.4 ± 1.3**	

The bradykinin (1 μM)-evoked decline in the forskolin (1 μM, 10 min) and isoprenaline (1 μM, 10 min)-stimulated cyclic AMP level was not affected by pretreatment of cells with staurosporine (0.5 μM, 5 min). *Different from values obtained in the absence of bradykinin $P<0.05$, **$P<0.01$. Data are expressed as mean ± s.e.mean of 6 experiments.

Table 4 Calmodulin and the bradykinin induced reduction in the cyclic AMP level

	Cyclic AMP (pmol/10^6 cells)	
Treatment	*Isoprenaline*	*Forskolin*
None	63.7 ± 1.8	9.1 ± 0.4
Bradykinin (2 min)	36.0 ± 1.6**	6.5 ± 1.7*
Bradykinin (5 min)	41.0 ± 1.4**	
Calmidazolium	62.0 ± 1.6	9.0 ± 0.3
Calmidazolium, bradykinin (2 min)	41.1 ± 1.9**	6.6 ± 0.4*
Calmidazolium, bradykinin (5 min)	40.9 ± 1.1**	

Pretreatment of cells with the calmodulin antagonist, calmidazolium (10 μM, 10 min), did not influence the bradykinin (1 μM)-evoked decline in the forskolin (1 μM, 10 min) or isoprenaline (1 μM, 10 min)-stimulated cyclic AMP level. *Different from values obtained in the absence of bradykinin $P<0.05$, **$P<0.01$. Data are expressed as mean ± s.e.mean of 4 experiments.

sustained inhibition of agonist-induced cyclic AMP elevation caused by stimulation of endogenous bradykinin receptors and stably transfected substance K receptors was observed in C6-2B rat glioma cells (Debernardi *et al.*, 1991). Release of Ca^{2+} from internal stores was supposed to be responsible for the

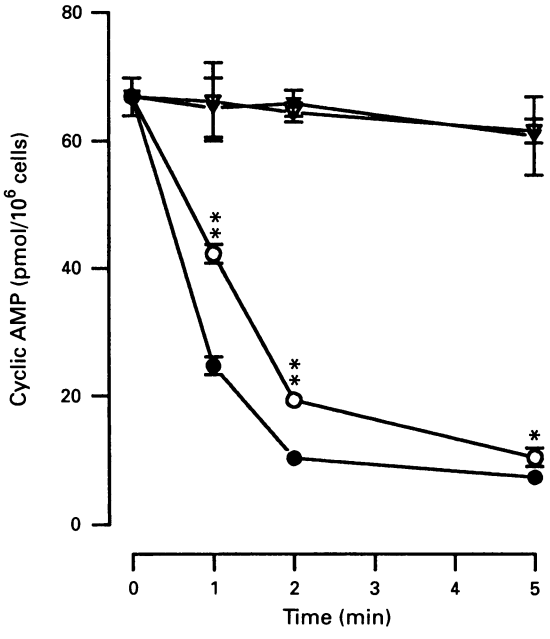

Figure 6 Bradykinin enhanced the rate of cyclic AMP breakdown. DDT_1 MF-2 cells were pretreated with isoprenaline (1 μM, 10 min) and after removal of isoprenaline, cyclic AMP was measured. Control (○); in the presence of isobutyl methylxanthine (▽, IBMX, 200 μM); bradykinin (●, 1 μM); or IBMX and bradykinin (▼). *Different from cyclic AMP level in the presence of bradykinin, $P<0.05$; **$P<0.01$. Data are expressed as mean ± s.e.mean of 5 experiments.

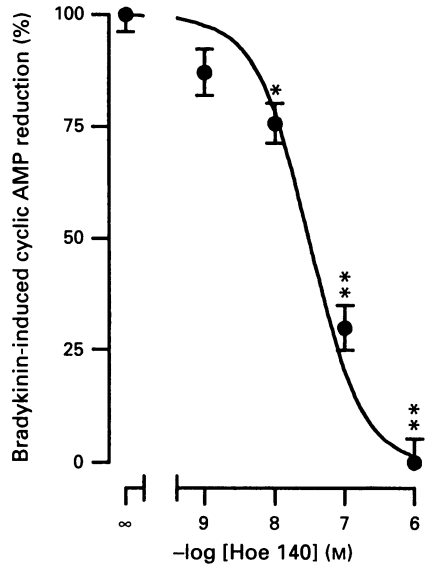

Figure 7 Inhibition of bradykinin-induced reduction of the cyclic AMP level by Hoe 140. The B_2 receptor antagonist, Hoe 140 (D-Arg[Hyp^3, Thi^5, D-Tic^7, Oic^8]-BK), added to the cells 2 min in advance, concentration-dependently inhibited the bradykinin (1 μM, 2 min)-induced reduction of the cyclic AMP level in isoprenaline (1 μM, 10 min) prestimulated cells. The control levels of isoprenaline enhanced cyclic AMP and of isoprenaline given together with Hoe 140 (1 μM, 2 min) were 64.5 ± 2.8 and 68.9 ± 1.9 pmol/10^6 cells, respectively. *Different from values obtained in the absence of Hoe 140, $P<0.05$; **$P<0.01$. Each point represents the mean ± s.e.mean of 4 experiments.

Table 5 The effect of bradykinin receptor agonists and antagonists on cellular cyclic AMP in DDT_1 MF-2 cells

	Cyclic AMP (pmol/10^6 cells)	
Treatment	*Isoprenaline*	*Forskolin*
None	64.5 ± 2.0	8.7 ± 0.2
Bradykinin	40.9 ± 0.4**	7.1 ± 0.3*
desArg^9-bradykinin (0.3 μM)	69.6 ± 1.7	
Hoe 140	65.0 ± 1.8	8.8 ± 0.2
Hoe 140 + bradykinin	69.1 ± 1.1	8.3 ± 0.3
Hoe 140 + bradykinin (5 min)	61.1 ± 1.7	
D-Arg[Hyp^3, Thi^{5,8}, D-Phe^7]-BK	62.1 ± 4.0	
D-Arg[Hyp^3, Thi^{5,8}, D-Phe^7]-BK + bradykinin	63.0 ± 1.5	

Bradykinin (1 μM, 2 min, unless otherwise stated) was used to decrease the prestimulated cyclic AMP level. Enhanced cyclic AMP levels were obtained by pretreatment of cells with isoprenaline (1 μM, 10 min) or forskolin (1 μM, 10 min). Concentrations used of Hoe 140 (D-Arg[Hyp^3, Thi^{5,8}, D-Tic^7, Oic^8]-BK) and D-Arg[Hyp^3, Thi^{5,8}, D-Phe^7]-BK were 1 μM and 10, respectively. *Different from values obtained in the absence of bradykinin $P<0.05$; **$P<0.01$. Data are expressed as mean ± s.e.mean of at least 4 experiments.

inhibitory action on adenylyl cyclase under these conditions. The bradykinin-evoked slowly declining phase of the Ca^{2+} response is caused by Ca^{2+} entry from the extracellular environment in DDT_1 MF-2 cells. Our results showed that inhibition of Ca^{2+} entry by $LaCl_3$ did not affect the bradykinin-induced decline in the cyclic AMP level. Therefore, Ca^{2+} entry does not play a substantial role in the effect of bradykinin on cyclic AMP formation. Thus, the bradykinin-induced response is solely mediated by Ca^{2+} release from internal compartments. In contrast, it was reported that inhibition of the forskolin, dopamine and 5'-N-ethyl-carboxamidoadenosine-induced cyclic AMP level by bradykinin as observed in D384-human astrocytoma cells was dependent on Ca^{2+} entry (Balmforth *et al.*, 1992; Altiok & Fredholm, 1993).

Reduction in cyclic AMP levels by the activation of protein kinase C was reported previously (Fleming *et al.*, 1992; Bascands *et al.*, 1993). Recently, Assender *et al.* (1994), reported the presence of 3 protein kinase C isoenzymes, among which was the Ca^{2+}-dependent α-isoform, in DDT_1 MF-2 cells. The bradykinin-induced response in DDT_1 MF-2 cells was not affected by the protein kinase C inhibitor, staurosporine, a feature also observed after stimulation of P_{2U} purinoceptors in DDT_1 MF-2 cells (Sipma *et al.*, 1994). Moreover, it was shown that the protein kinase C activator, phorbol 12-myristate 13-acetate, did not inhibit cyclic AMP formation (Sipma *et al.*, 1994). Thus, protein kinase C does not play a role in the regulation of bradykinin-evoked cyclic AMP metabolism in DDT_1 MF-2 cells.

The calmodulin inhibitor, calmidazolium, did not affect the bradykinin-induced reduction in the forskolin and isoprenaline-enhanced cyclic AMP level, which showed that calmodulin-dependent enzymes, like protein kinases and phosphodiesterases were not involved in the response. Moreover, it has been shown that Ca^{2+} ions directly inhibited adenylyl cyclase activity in a biphasic and cooperative manner in membrane preparations of D384-human astrocytoma cells (Altiok & Fredholm, 1993), NCB-20 hybrid neuroblastoma cells (Boyanjian *et al.*, 1991), platelets and GH_3 pituitary derived cells (Caldwell *et al.*, 1992) and of cardiac cells (Colvin *et al.*, 1991). These observations strongly suggest that Ca^{2+} ions exert a direct effect on the mechanism leading to adenylyl cyclase stimulation in DDT_1 MF-2 cells.

Besides the Ca^{2+}-dependent mechanism of cyclic AMP reduction, bradykinin was found to enhance the rate of cyclic AMP breakdown in a protocol where *de novo* synthesis of cyclic AMP was prevented. Activation of the phosphodiesterase activity by bradykinin was not dependent on Ca^{2+} since ionomycin did not mimic the effect of bradykinin. Increased phosphodiesterase activity was found after stimulation of

muscarinic receptors in 1321N1 human astrocytoma cells (Tanner *et al.*, 1986) and in the pregnant-rat myometrium (Goureau *et al.*, 1990). However, these activations appeared to be secondary to the simultaneous increase in $[Ca^{2+}]_i$.

The bradykinin-induced reduction in cyclic AMP levels was not inhibited by PTX, which demonstrated that an inhibitory G-protein was not involved. In contrast, stimulation of P_{2U} purinoceptors in DDT_1 MF-2 cells (Sipma *et al.*, 1994) and stimulation of P_2 purinoceptors in rat hepatocytes (Okajima *et al.*, 1987) caused inhibition of adenylyl cyclase via a G_i protein. Remarkably, PTX decreased the isoprenaline-induced formation of cyclic AMP. How PTX induced this effect remains to be established.

Three mechanisms of cyclic AMP reduction have been identified in DDT_1 MF-2 cells. Stimulation of P_{2U} purinoceptors leads to activation of a G_1 protein and effects a pronounced reduction in cyclic AMP levels. This response is sustained in nature in both forskolin and isoprenaline pretreated cells (Sipma *et al.*, 1994). Two other processes thought to decrease cellular cyclic AMP are described in this paper and concern bradykinin-induced activation of a cyclic AMP phosphodiesterase in a Ca^{2+}/calmodulin-independent manner and a Ca^{2+}-dependent mechanism. The obtained transient reduction in the forskolin-elevated cyclic AMP level implies that both the activation of the phosphodiesterase and the Ca^{2+}-dependent inhibition of adenylyl cyclase catalytic activity are short-lived. Since a sustained inhibition of the cyclic AMP level was observed in isoprenaline pretreated cells, this effect was most likely mediated by Ca^{2+} acting at the level of the β-adrenoceptor and/or the stimulatory G-protein. The results obtained with $LaCl_3$ showed that a transient increase in $[Ca^{2+}]_i$ apparently can induce events leading to a sustained inhibition of adenylyl cyclase as suggested previously by DeBernardi *et al.* (1991). Histamine H_1 receptors were also reported to mediate a modest transient reduction in cyclic AMP in DDT_1 MF-2 cells. This effect was most probably due to a histamine-induced increase in $[Ca^{2+}]_i$ (Sipma *et al.*, 1994). Pretreatment of DDT_1 MF-2 cells with cyclic AMP-enhancing agents reduced the histamine H_1 receptor-mediated formation of inositol phosphates and the release of Ca^{2+} from internal stores (Dickenson *et al.*, 1993; Sipma *et al.*, 1995) but not the rise in $[Ca^{2+}]_i$ induced by bradykinin. This may explain that bradykinin is more effective in reducing cellular cyclic AMP than histamine.

The effect of bradykinin on the cellular cyclic AMP level and the increase in $[Ca^{2+}]_i$ was abolished in the presence of the bradykinin B_2 receptor antagonists, Hoe 140 and D-Arg[Hyp^3, Thi^{5,8}, D-Phe^7]-BK in DDT_1 MF-2 cells. It was reported that D-Arg[Hyp^3, Thi^{5,8}, D-Phe^7]-BK antagonized bradykinin B_2 receptor-mediated total inositol phosphate formation in canine tracheal smooth muscle cells (Yang *et al.*, 1994) and Ins(1,4,5)P_3 formation in guinea-pig cultured tracheal smooth muscle (Pyne & Pyne, 1993). Hoe 140 has been identified as a highly potent B_2 receptor antagonist (Lembeck *et al.*, 1991), with IC_{50} values from 0.1 nM–40 nM for several contractile responses. The IC_{50} value (34 nM) found by us for reduction of the cyclic AMP level is in the same range. It is proposed that bradykinin B_3 receptors are insensitive to bradykinin B_2 receptor antagonists (Pyne & Pyne, 1993; 1994). Thus, since both the Ca^{2+}-dependent and Ca^{2+}-independent mechanism resulting in the bradykinin-induced decline in the cyclic AMP level as well as activation of the phospholipase C pathway were blocked by bradykinin B_2 receptor antagonists and not elicited by a bradykinin B_1 receptor agonist, desArg^9-bradykinin, the responses described are mediated by bradykinin B_2 receptors.

In summary, bradykinin B_2 receptors mediate a reduction in the prestimulated cyclic AMP level in DDT_1 MF-2 cells. Besides activation of a Ca^{2+}/calmodulin-independent phosphodiesterase, the effect of bradykinin on cyclic AMP was mediated by Ca^{2+} acting on different components of the adenylyl cyclase signal transduction pathway.

References

ALTIOK, N. & FREDHOLM, B.B. (1993). Bradykinin inhibits cyclic AMP accumulation in D384-human astrocytoma cells via calcium-dependent inhibition of adenylyl cyclase. *Cell. Signal.*, **5**, 279–288.

ASSENDER, J.W., KONTY, E. & FREDHOLM, B.B. (1994). Expression of protein kinase C isoforms in smooth muscle cells in various states of differentiation. *FEBS Lett.*, **342**, 76–80.

BASCANDS, J.L., PECHER, C. & GIROLAMI, J.P. (1993). Indirect inhibition by bradykinin of cyclic AMP generation in isolated rat glomeruli and mesangial cells. *Mol. Pharmacol.*, **44**, 818–826.

BALMFORTH, A.J., PARKINSON, F.E., ALTIOK, N. & FREDHOLM, B.B. (1992). Identification of a B_2-bradykinin receptor linked to phospholipase C and inhibition of dopamine stimulated cyclic AMP accumulation in the human astrocytoma cell line D384. *Naunyn-Schmied. Arch. Pharmacol.*, **346**, 303–310.

BOYANJIAN, C.L., GARRITSEN, A. & COOPER, D.M.F. (1991). Bradykinin stimulates $[Ca^{2+}]$-mobilization in NCB-20 cells leading to direct inhibition of adenylyl cyclase; a novel mechanism for inhibition of cAMP production. *J. Biol. Chem.*, **166**, 4995–5003.

BROWN, B.L., ALBANO, J.D.M., EKINS, R.P., SGHERZI, A.M. & TAMPION, W. (1971). A single and sensitive saturation assay method for the measurement of adenosine-3′,5′-cyclic monophosphate. *Biochem. J.*, **121**, 561–562.

CALDWELL, K.K., BOYAJIAN, C.L. & COOPER, D.M.F. (1992). The effects of Ca^{2+} and calmodulin on adenylyl cyclase activity in plasma membranes derived from neural and non-neural cells. *Cell Calcium.*, **13**, 107–121.

COLVIN, R.A., OIBO, J.A. & ALLEN, R.A. (1991). Calcium inhibition of cardiac adenylyl cyclase. Evidence for two distinct sites of inhibition. *Cell Calcium.*, **12**, 19–27.

DEBERNARDI, M.A., TAKASHI, S. & BROOKER, G. (1991). Inhibition of cAMP accumulation by intracellular calcium mobilization in C6-2B cells stably transfected with substance K receptor cDNA. *Proc. Natl. Acad. Sci. U.S.A.*, **88**, 9257–9261.

DEN HERTOG, A. (1981). Calcium and the α-action of catecholamines on guinea-pig taenia caeci. *J. Physiol.*, **316**, 109–125.

DICKENSON, J.M. & HILL, S.J. (1992). Histamine H_1-receptor-mediated calcium influx in DDT_1 MF-2 cells. *Biochem. J.*, **284**, 425–431.

DICKENSON, J.M., WHITE, T. & HILL, S.J. (1993). The effects of elevated cyclic AMP levels on histamine H_1-receptor-stimulated inositol phospholipid hydrolysis and calcium mobilization in the smooth muscle cell line DDT_1 MF-2. *Biochem. J.*, **292**, 409–417.

FLEMING, N., MELLOW, L. & BHULLAR, D. (1992). Regulation of the cAMP signal transduction pathway by protein kinase C in rat submandibular cells. *Eur. J. Physiol.*, **421**, 82–89.

GARRITSEN, A., ZHANG, Y. & COOPER, D.M.F. (1992a). Purinergic receptor regulation of signal transduction in NCB-20 cells. *Mol. Pharmacol.*, **41**, 743–749.

GARRITSEN, A., ZHANG, Y., FIRESTONE, J.A., BROWNING, M.D. & COOPER, D.M.F. (1992b). Inhibition of cyclic AMP accumulation in intact NCB-20 cell as a direct result of elevation of cytosolic Ca^{2+}. *J. Neurochem.*, **59**, 1630–1639.

GERWINS, P. & FREDHOLM, B.B. (1992). Stimulation of adenosine A_1 receptors and bradykinin receptors, which act via different G proteins, synergistically raises inositol 1,4,5-trisphosphate and intracellular free calcium in DDT_1 MF-2 smooth muscle cells. *Proc. Natl. Acad. Sci. U.S.A.*, **89**, 7330–7334.

GIETZEN, K. (1983). Comparison of the calmodulin antagonist compound 48/80 and calmidazolium. *Biochem. J.*, **216**, 611–616.

GOUREAU, O., TANFIN, Z. & HARBON, S. (1990). Prostaglandins and muscarinic agonists induce cyclic AMP attenuation by two distinct mechanisms in the pregnant-rat myometrium. *Biochem. J.*, **271**, 667–673.

HALL, J.M. (1992). Bradykinin receptors: pharmacological properties and biological roles. *Pharmacol. Ther.*, **56**, 131–190.

HESKETH, T.R., SMITH, G.A., MOORE, J.P., TAYLOR, M.V. & METCALFE, J.C. (1983). Free cytoplasmic calcium concentration and mitogenic stimulation of lymphocytes. *J. Biol. Chem.*, **258,** 4876–4882.

HOITING, B., MOLLEMAN, A., DUIN, M., DEN HERTOG, A. & NELEMANS, A. (1990). The P_2-purinoceptor mediated inositol phosphate formation in relation to cytoplasmic calcium in DDT_1 MF-2 smooth muscle cells. *Eur. J. Pharmacol.*, **189,** 31–39.

LEMBECK, F., GRIESBACHER, T., ECKHARDT, M., HENKE, S., BREIPOHL, G. & KNOLLE, J. (1991). New, long-acting, potent bradykinin antagonists. *Br. J. Pharmacol.*, **102,** 297–304.

MOLLEMAN, A., NELEMANS, A. & DEN HERTOG, A. (1989). P_2 purinoceptor-mediated membrane currents in DDT_1 MF-2 smooth muscle cells. *Eur. J. Pharmacol.*, **169,** 167–174.

NORRIS, J.S., GORSKI, J. & KOHLER, P.O. (1974). Androgen receptors in a syrian hamster ductus deferens tumour cell line. *Nature*, **248,** 422–424.

OKAJIMA, F., TOKUMITSU, Y., KONDO, Y. & UI, M. (1987). P_2 purinergic receptors are coupled to two signal transduction systems leading to inhibition of cAMP generation and to production of inositol trisphosphate in rat hepatocytes. *J. Biol. Chem.*, **262,** 13483–13490.

PYNE, S. & PYNE, N.J. (1993). Differential effects of B_2 receptor antagonists upon bradykinin-stimulated phospholipase C and D in guinea-pig cultured tracheal smooth muscle. *Br. J. Pharmacol.*, **110,** 477–481.

PYNE, S. & PYNE, N.J. (1994). Bradykinin-stimulated phosphatidate and 1,2-diacylgylcerol accumulation in guinea-pig airway smooth muscle: evidence for regulation 'down-stream' of phospholipases. *Cell. Signal.*, **6,** 269–277.

SIPMA, H., DEN HERTOG, A. & NELEMANS, A. (1994). The phospholipase C activating P_{2U} purinoceptor also inhibits cAMP formation in DDT_1 MF-2 cells. *Eur. J. Pharmacol.*, **268,** 431–437.

SIPMA, H., DUIN, M., HOITING, B., DEN HERTOG, A. & NELEMANS, A. (1995). Regulation of histamine and UTP induced increases in $Ins(1,4,5)P_3$, $Ins(1,3,4,5)P_4$ and Ca^{2+} by cAMP in DDT_1 MF-2 cells. *Br. J. Pharmacol.*, **114,** 383–390.

STEVENS, P.A., PYNE, S., GRADY, M. & PYNE, N.J. (1994). Bradykinin-dependent activation of adenylate cyclase activity and cyclic AMP accumulation in tracheal smooth muscle occurs via protein kinase C-dependent and -independent pathways. *Biochem. J.*, **297,** 233–239.

TANNER, L.I., HARDEN, T.K., WELLS, J.N. & MARTIN, M.W. (1986). Identification of the phosphodiesterase regulated by muscarinic cholinergic receptors of 1321N1 human astrocytoma cells. *Mol. Pharmacol.*, **29,** 455–460.

YANG, C.M., HSIA, H.C., CHOU, S.P., ONG, R., HSIEH, J.T. & LUO, S.F. (1994). Bradykinin-stimulated phosphoinositide metabolism in cultured canine tracheal smooth muscle cells. *Br. J. Pharmacol.*, **111,** 21–28.

(Received November 7, 1994
Revised March 1, 1995
Accepted April 3, 1995)

British Journal of Pharmacology (1995) 115, 945-952 © 1995 Stockton Press All rights reserved 0007-1188/95 $12.00

A role for mast cells in adenosine A_3 receptor-mediated hypotension in the rat

J.P. Hannon, H.J. Pfannkuche & [1]J.R. Fozard

Preclinical Research, Sandoz Pharma Ltd., CH-4002 Basel, Switzerland

1 The adenosine A_3 receptor agonist, N^6-2-(4-aminophenyl)ethyladenosine (APNEA) induces hypotension in the anaesthetized rat. The present experiments were carried out to explore the role of mast cells in the response.

2 Intravenous injection of APNEA (1-30 $\mu g\ kg^{-1}$ to rats in which the A_3 receptor-mediated response had been isolated by pretreatment with 8-(*p*-sulphophenyl) theophylline (8-SPT)), induced dose-related falls in blood pressure accompanied at higher doses by small falls in heart rate. Responses to the mast cell degranulating agent, compound 48/80 (10-300 $\mu g\ kg^{-1}$, i.v.) were qualitatively similar to those to APNEA.

3 Pretreatment with sodium cromoglycate (0.25-20 $mg\ kg^{-1}$, i.v.) induced dose-related, although incomplete, blockade of the hypotensive responses to APNEA. At 20 $mg\ kg^{-1}$, sodium cromoglycate also inhibited the cardiovascular response to compound 48/80 but had no effects on those to the selective A_1 receptor agonist, N^6-cyclopentyladenosine (CPA) or the selective A_{2A} receptor agonist, 2-[*p*-(2-carboxyethyl)phenylamino]-5'-N-ethylcarboxamidoadenosine (CGS 21680). Lodoxamide (0.01-20 $mg\ kg^{-1}$) also blocked selectively but incompletely the response to APNEA.

4 The cardiovascular responses to compound 48/80 (10-300 $\mu g\ kg^{-1}$, i.v.) were markedly suppressed in animals which had received repeated doses of the compound by the intraperitoneal route. Similarly APNEA was essentially devoid of cardiovascular activity in such preparations. In contrast, responses to CPA were similar in animals treated repeatedly with compound 48/80 to those obtained in control animals.

5 Plasma and serum histamine concentrations were markedly increased associated with the pronounced hypotensive responses induced by intravenous injections of APNEA (30 or 100 $\mu g\ kg^{-1}$) in the presence of 8-SPT, or compound 48/80 (300 $\mu g\ kg^{-1}$).

6 Taken together the data implicate the mast cell in a key role in adenosine A_3 receptor-mediated hypotension in the anaesthetized rat.

Keywords: Adenosine A_3 receptor; APNEA; compound 48/80; mast cell degranulation; hypotension; histamine

Introduction

The adenosine A_3 receptor agonist, N^6-2-(4-aminophenyl)-ethyladenosine (APNEA) induces dose-related hypotensive responses in both anaesthetized rats (Carruthers & Fozard, 1993a; Fozard & Hannon, 1994) and in pithed preparations with blood pressure raised to normal with a variety of different pressor agents (Fozard & Carruthers, 1993a; Carruthers & Fozard, 1993b). Significantly, the response shows the major features of the recently cloned rat A_3 receptor (Zhou *et al.*, 1992) both with respect to agonist and antagonist pharmacology (Carruthers & Fozard, 1993b; Fozard & Carruthers, 1993a,b; Fozard & Hannon, 1994) and in being suppressed in animals pretreated with pertussis toxin (Carruthers & Fozard, 1993a).

Although both a fall in systemic vascular resistance and a decrease in cardiac output contribute to the hypotension induced in the rat by activation of adenosine A_3 receptors (Salzmann & Fozard, 1994), the actual target cell(s) involved have not been determined. Indeed, it is unknown whether APNEA acts directly on elements of the cardiovascular system or indirectly by inducing transmitter or mediator release. With respect to the latter, a plausible candidate for an intermediary role is the mast cell, which has been shown to express the A_3 receptor (Ali *et al.*, 1990; 1991; Ramkumar *et al.*, 1993) and to be activated by ligands with A_3 receptor agonist properties (Ramkumar *et al.*, 1993). Significantly, both the biochemical events and facilitation of mediator release induced by A_3 receptor-mediated activation of mast cells are pertussis toxin-sensitive (Ali *et al.*, 1990; Qian & McCloskey, 1993). The present experiments were designed to explore the role of mast cells in the hypotensive responses induced by A_3 receptor activation in the rat.

A preliminary account of part of this work has been presented to the British Pharmacological Society (Hannon & Fozard, 1994).

Methods

Animals

Male Sprague-Dawley rats weighing 210-510 g were used throughout. They were supplied by Biological Research Laboratories (Füllinsdorf, Switzerland) and kept under normal laboratory conditions.

Cardiovascular studies

Animals were anaesthetized with pentobarbitone sodium, 60 $mg\ kg^{-1}$, i.p. and set up for recording blood pressure and heart rate and for intrajugular venous administration of drugs as previously described (Carruthers & Fozard, 1993a). After a stabilization period of approximately 15 min, dose-response curves to APNEA, the adenosine A_1 receptor selective agonist, N^6-cyclopentyladenosine (CPA), the adenosine A_{2A} receptor selective agonist, 2-[*p*-(2-carboxyethyl)phenylamino]-5'-N-ethylcarboxamidoadenosine (CGS 21680) or the mast cell degranulating agent, compound 48/80, were established by cumulative bolus injection; the intervals between doses were sufficient to allow a plateau response to develop. In the case of

[1] Author for correspondence.

APNEA, the A_1/A_2 receptor antagonist, 8-(*p*-sulphophenyl)theophylline (8-SPT) was injected intravenously at a dose of 40 mg kg^{-1} 5 min prior to establishing the agonist dose-response curve in order to 'isolate' the A_3 receptor-mediated component of the response to APNEA (see Carruthers & Fozard, 1993a; Fozard & Carruthers, 1993a; Fozard & Hannon, 1994). Only one agonist dose-response curve was generated per animal.

Sodium cromoglycate or lodoxamide were injected intravenously 3 min before establishing the dose-response curves to the adenosine agonists or compound 48/80. Animals were 'desensitized' to the effects of compound 48/80 by injecting 1 mg kg^{-1}, i.p., four times at 3 h intervals on the day before the experiment and 3 mg kg^{-1}, i.p., 2–3 h prior to anaesthesia on the experimental day. In selected cases, the peritoneal cavities were lavaged with 10 ml of normal saline and microscopical analysis of the numbers of intact granulated mast cells carried out following differential staining with Diff-Quick (Baxter Dade, Switzerland).

Mean values (± s.e.mean) from *n* individual experiments are presented.

Measurement of histamine concentrations in serum and plasma

Rats were anaesthetized and prepared for intrajugular venous administration of drugs as described under *Cardiovascular studies* above. A cannula was placed in one common carotid artery for collection of blood. After a stabilization period of approximately 15 min, 19 animals were allocated randomly into 5 groups: Group 1 received 8-SPT (40 mg kg^{-1}, i.v.) 5 min prior to a single i.v. injection of APNEA (30 $\mu g\ kg^{-1}$), group 2 received 8-SPT (40 mg kg^{-1}, i.v.) 5 min prior to an i.v. injection of APNEA, (100 $\mu g\ kg^{-1}$); group 3 received the vehicle for 8-SPT i.v. 5 min prior to an i.v. injection of APNEA (100 $\mu g\ kg^{-1}$); group 4 received 8-SPT 5 min prior to i.v. injection of the vehicle for APNEA; group 5 received vehicle for 8-SPT i.v. 5 min prior to an i.v. injection of vehicle for APNEA. In a second experiment, 8 animals were allocated randomly into two groups: Group 1 received compound 48/80 (300 $\mu g\ kg^{-1}$, i.v.); group 2 received an equivalent volume of vehicle. Two min after drug or vehicle administration, blood was collected for a period of approximately 10 min by allowing it to drip into potassium EDTA-coated or Eppendorff tubes for the preparation of plasma of serum samples, respectively. Samples were stored at −20°C until required for assay.

For assay of histamine, samples were thawed and diluted with Krebs solution (composition in mM: NaCl 118, KCl 4.7, $CaCl_2$ 2.5, KH_2PO_4 1.2, $MgSO_4$ 1.2 $NaHCO_3$ 25, dextrose 10; pH 7.4) supplemented with 10 mM HEPES. Histamine concentrations were measured in duplicate for each sample with a commercially available ELISA test system based on avidine-biotin interactions (IBL, Hamburg, Germany). The limit of detection was 0.25 ng ml^{-1} and cross-reactivity to 5-hydroxytryptamine was less than 0.005%.

Measurement of lung function

The method is similar to that described in detail for the guinea-pig by Chapman *et al.* (1992). In brief, rats were anaesthetized with pentobarbitone sodium (60 mg kg^{-1}, i.p.) and given gallamine triethiodide (10 mg kg^{-1}, i.m.) to suppress spontaneous respiration. Preparations were maintained at 37°C with a heated pad controlled by a rectal thermistor, and ventilated (8 ml kg^{-1}, 1 Hz) via a tracheal cannula with a mixture of air and oxygen (50:50, v/v). Ventilation was monitored at the trachea by a pneumotachograph (Fleisch 0000, Zabona, Switzerland) connected to a differential pressure transducer (MP 4514871, Validyne, U.S.A.). Coincident pressure changes within the thorax were measured via an intrathoracic cannula, using a differential pressure transducer (MP 4524, Validyne, U.S.A.); blood pressure and heart rate were recorded from the carotid artery with a pressure transducer (P23Dd, Gould, U.S.A.). From measurements of air-flow and transpulmonary pressure, airway resistance (R_L, $cmH_2O\ l^{-1}\ s^{-1}$) was calculated after each respiratory cycle by use of a digital electronic pulmonary monitoring system (PMS, Mumed, London, U.K.). Agonists were injected i.v. as described above.

Compounds used

Pentobarbitone sodium was obtained from Sanofi Santé Animale (Libourne, France). Compound 48/80 (condensation product of N-methyl-*p*-methoxyphenylethylamine with formaldehyde), histamine dihydrochloride, 5-hydroxytryptamine creatinine sulphate, gallamine triethiodide, and sodium cromoglycate were obtained from Sigma, Buchs, Switzerland. Lodoxamide (tromethamine) was a gift from the Upjohn Company, Kalamazoo, Mich. U.S.A. N^6-2-(4-aminophenyl) ethyladenosine (APNEA); N^6-cyclopentyladenosine (CPA), 2-[*p*-(2-carboxyethyl)phenylamino]-5′-N-ethylcarboxamidoadenosine (CGS 21680) and 8-(*p*-sulphophenyl)theophylline dihydrate (8-SPT) were synthetized at Sandoz, Basel, Switzerland by Dr Fulvio Gadient. The adenosine agonists were dissolved in 50% dimethylsulphoxide in distilled water and diluted immediately before use in 0.9% w/v NaCl. 8-SPT (40 mg) was dissolved in 0.2 ml 0.4 N NaOH and diluted with distilled water to 20 mg ml^{-1}. All other compounds were made up in 0.9% w/v NaCl.

Results

The cardiovascular responses to CPA, CGS 21680, APNEA and compound 48/80: effects of sodium cromoglycate and lodoxamide

The prototype adenosine A_1 receptor agonist, CPA (0.3–10 $\mu g\ kg^{-1}$), induced potent and pronounced hypotensive and bradycardic effects when injected intravenously into anaesthetized rats (Figure 1a). The selective A_{2A} receptor agonist, CGS 21680 (0.3–30 $\mu g\ kg^{-1}$, i.v.), also induced dose-related hypotensive responses which were not accompanied by significant changes in heart rate (Figure 1b). Intravenous injection of APNEA (1–30 $\mu g\ kg^{-1}$) to rats in which the A_3 receptor-mediated response had been 'isolated' by pretreatment with 8-SPT (40 mg kg^{-1}) induced dose-related falls in blood pressure accompanied at higher doses by small falls in heart rate (Figure 1c). Responses to the mast cell degranulating agent, compound 48/80 (10–300 $\mu g\ kg^{-1}$, i.v.), were qualitatively similar to those of APNEA (Figures 1d, 4 and 5).

Pretreatment with sodium cromoglycate, 0.25–20 mg kg^{-1}, i.v. induced dose-related, although incomplete, blockade of the hypotensive responses to APNEA (Figure 1c). The doses of APNEA which reduced blood pressure by 30 mmHg (ED_{30}) were 7.1 ± 0.8 ($n=4$), 9.0 ± 0.5 ($n=4$), 17.2 ± 0.4 ($n=3$), 27.8 ± 0.2 ($n=3$), 35.0 ± 5.7 ($n=6$) $\mu g\ kg^{-1}$ for the animals given vehicle or 0.25, 1.25, 5 and 20 mg kg^{-1} of sodium cromoglycate respectively (Figure 1c); a dose of 60 mg kg^{-1} gave no further blockade (ED_{30} 37.8 ± 6.9 $\mu g\ kg^{-1}$, $n=4$). SCG at 20 mg kg^{-1} had no significant effects on the cardiovascular responses induced by CPA (Figure 1a) or CGS 21680 (Figure 1b) but suppressed significantly the response to compound 48/80 at 100 $\mu g\ kg^{-1}$ (Figure 1d).

Lodoxamide, 0.01–20 mg kg^{-1}, i.v. also blocked progressively, but incompletely, the responses to APNEA (Figure 2). The doses of APNEA which reduced blood pressure by 30 mmHg (ED_{30}) were 7.1 ± 0.8 ($n=4$), 12.9 ± 2.3 ($n=5$), 23.9 ± 3.6 ($n=4$), 16.3 ± 2.3 ($n=4$), 23.0 ± 2.2 ($n=4$), 24.8 ± 0.8 ($n=3$), 46.2 ± 3.9 ($n=4$) for the animals given vehicle or 0.01, 0.05, 0.25, 1.25, 5 or 20 mg kg^{-1} of lodoxamide, respectively (Figure 2). Lodoxamide, 20 mg kg^{-1} also inhibited responses to compound 48/80 (Figure 1d) but had no effects on the cardiovascular response to CPA (Figure 1a).

Neither sodium cromoglycate nor lodoxamide induced any changes in blood pressure or heart rate *per se*.

Effects of pretreatment with compound 48/80 on the cardiovascular responses to compound 48/80, APNEA and CPA

Rats were given compound 48/80 i.p. at a dose of 1 mg kg^{-1} four times at 3 h intervals on the day before the experiment and at 3 mg kg^{-1} 2–3 h prior to anaesthesia on the experimental day. Mild scratching was evident following the lower dose of compound 48/80; scratching was more pronounced following the higher dose and the animals appeared sedated. In agreement with the literature (Enerbäck & Svensson, 1980), microscopical analysis of the cells obtained following peritoneal lavage of control animals revealed 4.0 ± 0.3% (n = 4) of the total cell population to be intact granulated mast cells. In

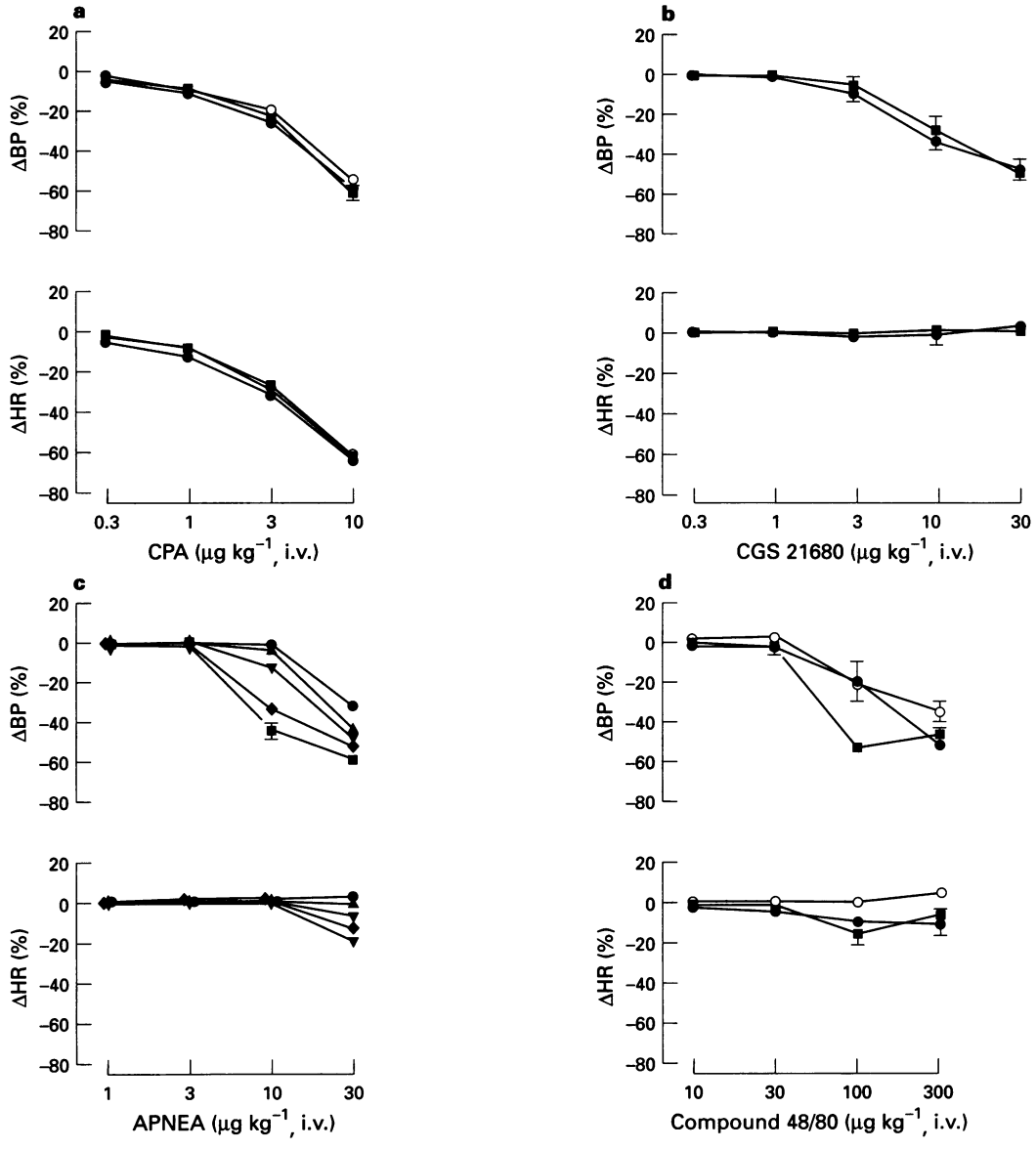

Figure 1 Effects of mast cell stabilizing agents on the cardiovascular responses to N^6-cyclopentyladenosine (CPA) (a), 2-[*p*-(2-carboxyethyl)phenylamino]-5′-N-ethylcarboxamidoadenosine (CGS 21680) (b), N^6-2-(4-aminophenyl)ethyladenosine (APNEA) (c) and compound 48/80 (d) in anaesthetized rats. (■) Vehicle-pretreated controls; (◆), (▼), (▲), (●) animals pretreated with 0.25, 1.25, 5 or 20 mg kg^{-1} sodium cromoglycate (SCG); (○) animals pretreated with 20 mg kg^{-1} lodoxamide (Lod). Points represent mean values (± s.e.mean where these exceed the size of the point) of the number of animals shown in parentheses below. The baseline mean arterial blood pressure (BP) and heart rate (HR) values just prior to starting the agonist injection sequences were:

CPA (vehicle)	134 ± 10 mmHg	446 ± 22 b min^{-1}	(4)
CPA (SCG, 20)	140 ± 4 mmHg	432 ± 7 b min^{-1}	(4)
CPA (Lod, 20)	144 ± 9 mmHg	437 ± 14 b min^{-1}	(4)
CGS 21680 (vehicle)	120 ± 6 mmHg	429 ± 12 b min^{-1}	(6)
CGS 21680 (SCG, 20)	124 ± 6 mmHg	421 ± 27 b min^{-1}	(3)
APNEA (vehicle)	133 ± 5 mmHg	417 ± 11 b min^{-1}	(4)
APNEA (SCG, 0.25)	146 ± 10 mmHg	447 ± 9 b min^{-1}	(4)
APNEA (SCG, 1.25)	152 ± 4 mmHg	430 ± 24 b min^{-1}	(3)
APNEA (SCG, 5)	137 ± 7 mmHg	423 ± 27 b min^{-1}	(3)
APNEA (SCG, 20)	133 ± 3 mmHg	398 ± 22 b min^{-1}	(6)
Co. 48/80 (vehicle)	134 ± 7 mmHg	422 ± 22 b min^{-1}	(4)
Co. 48/80 (SCG, 20)	135 ± 6 mmHg	412 ± 16 b min^{-1}	(4)
Co. 48/80 (Lod, 20)	129 ± 7 mmHg	410 ± 18 b min^{-1}	(5)

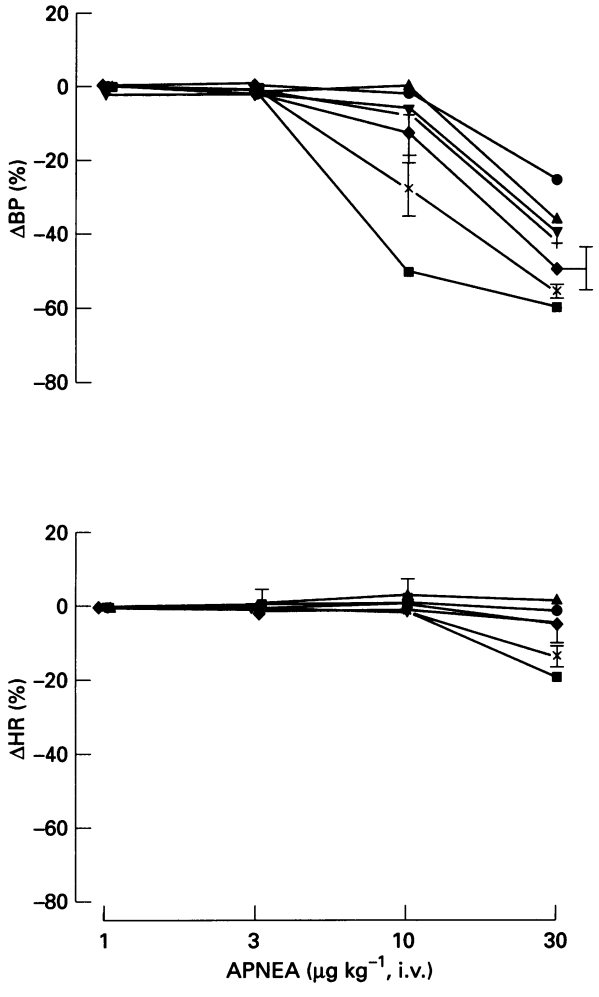

Figure 2 Effects of lodoxamide on the cardiovascular responses to N^6-2-(4-aminophenyl)ethyladenosine (APNEA) in anaesthetized rats. (■) Vehicle-pretreated controls; (X), (▼), (◆), (+), (▲) and (●); animals pretreated with 0.01, 0.05, 0.25, 1.25, 5 or 20 mg kg^{-1} lodoxamide (Lod). Points represent mean values (±s.e.mean where these exceed the size of the point) of the number of animals shown in parentheses below. The baseline mean arterial blood pressure (BP) and heart rate (HR) values just prior to starting the agonist injection sequences were:

APNEA (vehicle)	133±5 mmHg	417±11 b min^{-1}	(4)
APNEA (Lod, 0.01)	148±3 mmHg	444±15 b min^{-1}	(5)
APNEA (Lod, 0.05)	145±9 mmHg	429±21 b min^{-1}	(4)
APNEA (Lod, 0.25)	134±27 mmHg	408±10 b min^{-1}	(4)
APNEA (Lod, 1.25)	133±7 mmHg	381±21 b min^{-1}	(4)
APNEA (Lod, 5)	137±4 mmHg	413±4 b min^{-1}	(3)
APNEA (Lod, 20)	139±2 mmHg	425±22 b min^{-1}	(4)

contrast, no intact granulated mast cells were observed in peritoneal fluid samples from animals treated with compound 48/80. The cardiovascular response to *intravenously* injected compound 48/80 was markedly suppressed in animals which had received repeated doses of the compound by the *intraperitoneal* route (Figure 3a). Similarly, APNEA was essentially devoid of cardiovascular activity in such preparations (Figure 3b). In contrast, the response to CPA did not differ significantly from that obtained in control animals (Figure 3c).

Plasma and serum histamine concentrations following APNEA and compound 48/80

The doses of APNEA (30 and 100 μg kg^{-1}, i.v.) and compound 48/80 (300 μg kg^{-1}, i.v.) chosen for these experiments were expected to give long-lasting (>30 min) falls in blood pressure (see Figures 1, 4 and 5), and this was confirmed in studies in two separate animals with each agent at the doses indicated (data not illustrated). The data are presented in Table 1. The concentrations of histamine measured in plasma and serum in vehicle-treated animals were close to the standard values reported earlier for these tissues by several authors (see review by Tasaka, 1991). The plasma and serum histamine concentrations were not altered following 8-SPT, 40 mg kg^{-1}, i.v. They were, however, in each case, markedly and dose-dependently increased following both APNEA, 30 μg kg^{-1} (75 and 13 fold of the control values, respectively) and APNEA, 100 μg kg^{-1} (158 and 28 fold of the control values, respectively) in the presence of 8-SPT. In animals not treated with 8-SPT, the increase in plasma and serum histamine concentrations induced by APNEA, 100 μg kg^{-1} were not significantly different from those seen in the 8-SPT-treated animals. In a second experiment, compound 48/80, 300 μg kg^{-1} induced a marked and significant ($P<0.01$) increase in the plasma and serum histamine concentrations (2013±116 and 2342±507 ng ml^{-1}, respectively, $n=4$) relative to vehicle-treated control animals (14.5±2.1 and 42.9±1.6 ng ml^{-1}, respectively, $n=4$).

Effects of APNEA and compound 48/80 on lung function

The cardiovascular effects of APNEA, 1–30 μg kg^{-1}, i.v., (injected after 8-SPT, 40 mg kg^{-1}, i.v.), and compound 48/80, 0.1–1 mg kg^{-1}, i.v., were similar in animals instrumented for recording lung function to those seen in experiments where only the cardiovascular effects were monitored (compare Figures 4 and 5 with Figures 1c and 1d). The prominent hypotensive responses to APNEA were not accompanied by changes in airway resistance and this was true irrespective of whether the animals had received prior injections of 5-hydroxytryptamine (5-HT). In contrast, bolus injections of 5-HT induced dose-related increases in airway resistance associated with short-lived hypotensive responses (Figure 4). Compound 48/80 routinely at lower doses (<0.1 mg kg^{-1}, i.v.) induced falls in blood pressure with no accompanying change in airway resistance; at higher doses (>0.3 mg kg^{-1}, i.v.) compound 48/80 induced increases in airway resistance which, however, were not associated with more pronounced falls in blood pressure (Figure 5). Intravenous bolus injections of histamine, 10–100 μg kg^{-1}, induced short-lived falls in blood pressure but had no effects on airway resistance (Figure 5).

Discussion

In the present study, APNEA was used to induce A_3 receptor-mediated hypotensive responses in the anaesthetized rat. Since APNEA is relatively non-selective (Fozard & Carruthers, 1993a), the A_3 receptor component of the cardiovascular response was effectively 'isolated' by pretreatment of animals with the broad spectrum adenosine receptor antagonist, 8-SPT, at a dose well in excess of those required to antagonize A_1, A_{2A} and A_{2B} receptors in this preparation (Fozard & Carruthers, 1993a,b; see also Fozard & Hannon, 1994). The data generated provide strong evidence that the hypotensive response to adenosine A_3 receptor activation in the rat is largely, if not exclusively, a consequence of mediator release from mast cells.

Blockade of the response to APNEA by sodium cromoglycate and lodoxamide

Sodium cromoglycate and lodoxamide are chemically quite distinct yet have in common the property of inhibiting the release of mediators from mast cells in response to antigen challenge or compound 48/80; lodoxamide is significantly more potent (≤100 fold) than sodium cromoglycate in this respect (Brogden *et al.*, 1974; Johnson *et al.*, 1978). Dose-dependent blockade of the response to APNEA by both com-

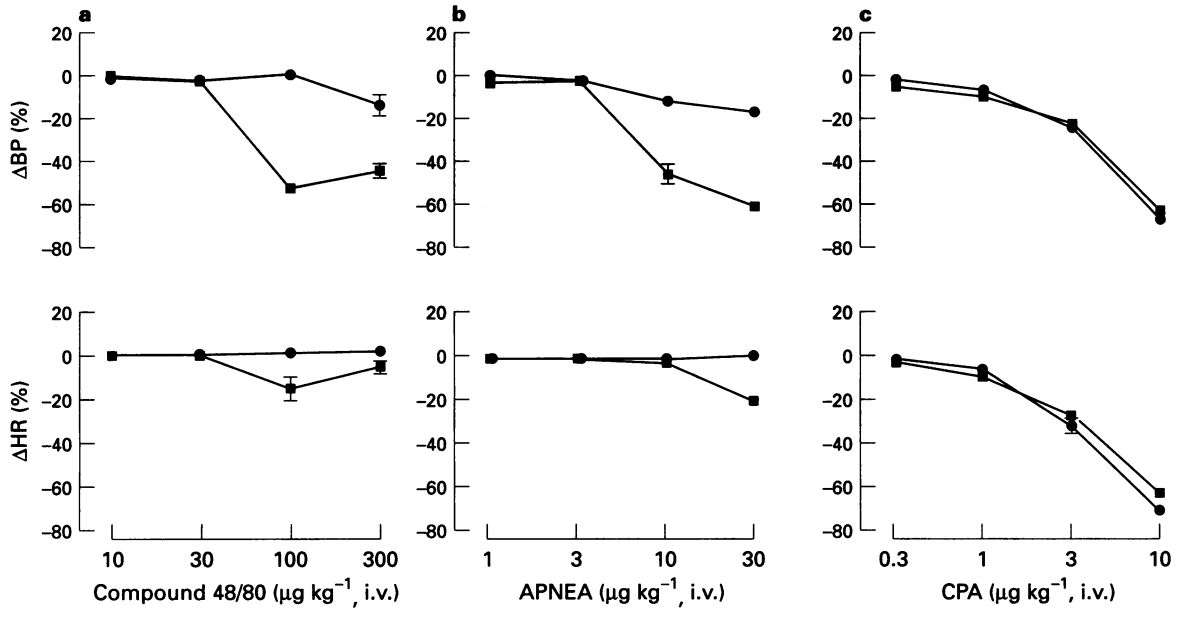

Figure 3 The effects of repeated pretreatment with compound 48/80 on the cardiovascular responses to compound 48/80 (a), N^6-2-(4-aminophenyl)ethyl adenosine (APNEA) (b) and N^6-cyclopentyladenosine (CPA) (c). (■) Controls; |(●), animals pretreated with compound 48/80, 1 mg kg^{-1}, i.p. four times at 3 h intervals on the day before the experiment and 3 mg kg^{-1}, i.p. 2–3 h prior to anaesthesia on the experimental day. Points represent mean values (± s.e.mean where these exceed the size of the point) of the number of animals shown in parentheses below. The baseline mean arterial blood pressure (BP) and heart rate (HR) values just prior to starting the injection sequences were:

48/80 (control)	134 ± 7 mmHg	422 ± 22 b min^{-1}	(4)
48/80 (48/80 - pretreated)	122 ± 8 mmHg	468 ± 4 b min^{-1}	(5)
APNEA (control)	133 ± 5 mmHg	417 ± 11 b min^{-1}	(4)
APNEA (48/80 - pretreated)	128 ± 4 mmHg	444 ± 9 b min^{-1}	(4)
CPA (control)	134 ± 10 mmHg	446 ± 22 b min^{-1}	(4)
CPA (48/80 - pretreated)	136 ± 8 mmHg	445 ± 20 b min^{-1}	(4)

Table 1 Rat plasma and serum histamine concentrations following 8-SPT and/or APNEA

	Vehicle I[a] + *vehicle II*[b]	*8-SPT 40*[c] + *vehicle II*[b]	*8-SPT 40*[c] + *APNEA 30*[d]	*8-SPT 40*[c] + *APNEA 100*[d]	*Vehicle I*[a] + *APNEA 100*[d]
Plasma (ng ml^{-1})	19.7 ± 2.1 (3)	14.3 ± 2.5 (4)	1073 ± 131* (4)	2253 ± 311* (4)	1803 ± 301* (4)
Serum (ng mg^{-1})	59.5 ± 11.6 (3)	67.9 ± 16.7 (4)	910 ± 168* (4)	1870 ± 249* (4)	1754 ± 54* (4)

Values are means (± s.e.mean) with number of experiments indicated in parentheses.
[a]Vehicle for 8-SPT; [b]vehicle for APNEA; [c]8-SPT 40 mg kg^{-1} given i.v. 5 min prior to APNEA or vehicle for APNEA; [d]APNEA 30 or 100 μg kg^{-1} given 5 min after 8-SPT or vehicle for 8-SPT.
Plasma was prepared from blood collected for approximately 10 min starting 2 min following vehicle II or APNEA administration.
*Significantly different from respective control value, $P < 0.05$ (Bonferroni-Holm multiple comparison test).
For abbreviations, see text.

pounds with lodoxamide being clearly the more potent would thus be consistent with a role for mast cells in the response to APNEA. The interpretation would be supported by the fact that sodium cromoglycate and lodoxamide also block the hypotensive response to compound 48/80, a recognised activator of mediator release from mast cells (Paton, 1951; Moran *et al.*, 1962). Of the other possible explanations, non-specific cardiovascular suppression can be ruled out since responses to the selective A_1 receptor agonist, CPA, and the selective A_{2A} receptor agonist, CGS 21680, were unaffected following an optimal dose of sodium cromoglycate. Sodium cromoglycate has been reported to interfere with adenosine binding to rat serosal mast cell membranes (Marquardt & Wasserman, 1985) raising the possibility of a direct interaction with the A_3 receptor. This seems unlikely, however, since blockade by sodium cromoglycate is incomplete and less than that which can be achieved with the surmountable A_3 receptor antagonist, BW-A522 (Fozard & Hannon, 1994). Moreover, when tested in a radioligand binding assay for the cloned rat A_3 receptor, neither sodium cromoglycate nor lodoxamide induced significant displacement at 0.1 mM (K. Jacobson, personal communication; for methodology, see Gallo-Rodriguez *et al.*, 1994). The incomplete blockade of APNEA by sodium cromoglycate and lodoxamide remains to be explained. It is, however, entirely consistent with *in vitro* findings where mediator release inhibition is often incomplete and may show a bell-shaped dose-response relationship (Johnson *et al.*, 1978; Tanizaki *et al.*, 1992).

Blockade of the response to APNEA in animals treated repeatedly with compound 48/80

Repeated treatment with compound 48/80 to achieve depletion of mast cell-derived mediators has been a successful strategy in

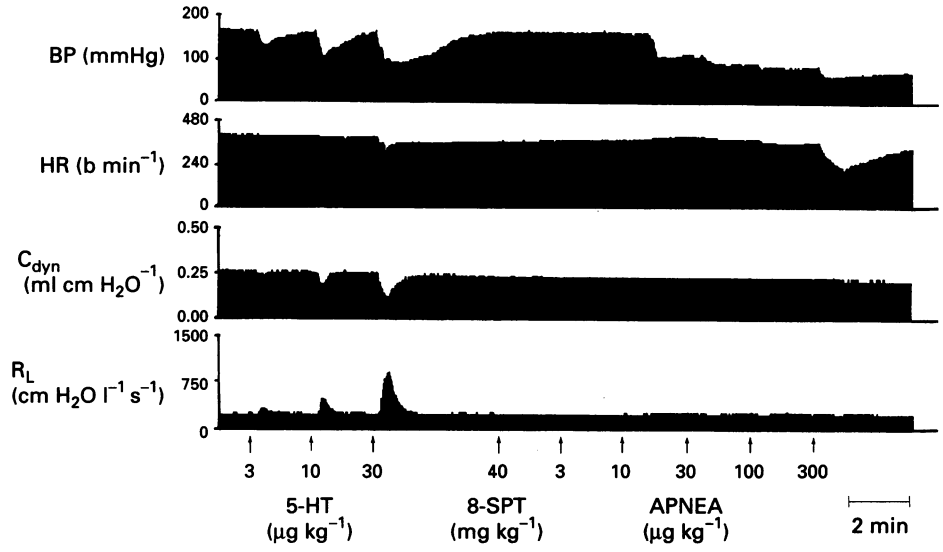

Figure 4 Effects of 5-hydroxytryptamine (5-HT) and N^6-(2-(4-aminophenyl)ethyl adenosine (APNEA) administered after 8-(*p*-sulphophenyl)theophylline (8-SPT) on mean arterial blood pressure (BP), heart rate (HR) and airways compliance (C_{dyn}) and resistance (R_L) in an anaesthetized rat. The record is representative of 4 similar experiments.

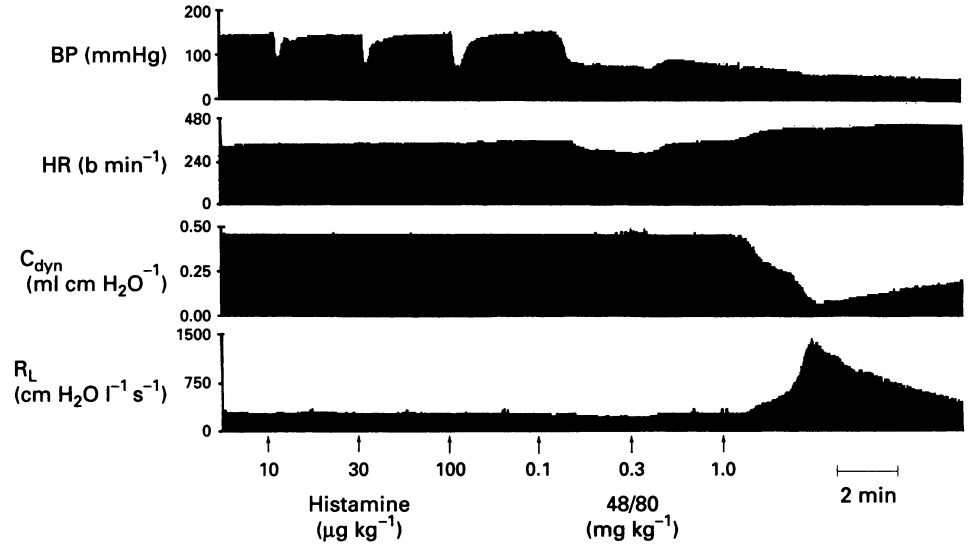

Figure 5 Effects of histamine and compound 40/80 (48/80) on mean arterial blood pressure (BP), heart rate (HR) and airways compliance (C_{dyn}) and resistance (R_L) in an anaesthetized rat. The record is representative of 4 similar experiments.

defining the role of the mast cell in a variety of experimental circumstances (see, for example, Di Rosa *et al.*, 1971; Banks *et al.*, 1990). The pretreatment paradigm used in the present experiments (1 mg kg^{-1}, i.p. four times at 3 h intervals on the day before the experiment and 3 mg kg^{-1}, i.p. 2–3 h prior to anaesthesia on the experimental day) was based on these earlier studies and was clearly effective. Thus, evidence of mast cell degranulation was seen *during* treatment in the form of scratching and elimination of the response to intravenously administered compound 48/80 *after* treatment indicates an eventual extensive depletion of mast cell-derived mediators. Moreover, microscopical analysis of peritoneal lavage fluid revealed a complete absence of intact granulated mast cells following the desensitization protocol with compound 48/80. It bears emphasis that baseline blood pressures and heart rate were within the normal range in the compound 48/80 pretreated animals and the sensitivity to CPA in these animals was unchanged. Hence, suppression of the effect of compound 48/80 in the pretreated animals cannot be attributed to non-specific depression of cardiovascular sensitivity. The fact that under these circumstances, responses to APNEA were suppressed to a similar extent to those to compound 48/80 provides strong evidence of a key role for mast cells in A_3 receptor-mediated hypotension in rats.

Direct evidence for the involvement of mast cells in the cardiovascular responses to APNEA and compound 48/80 in rats

If, in fact, mast cells do play a key role in the cardiovascular responses to APNEA and compound 48/80, then it should be possible to detect evidence of mediator release following administration of these agents. In practice, substantial and dose-related increases in the concentration of the mast cell mediator, histamine, were observed in plasma and serum associated with the sustained hypotensive responses to single doses of 30 and 100 μg kg^{-1} APNEA; at the highest dose the release of histamine following APNEA was similar to that seen following

compound 48/80, 300 $\mu g\ kg^{-1}$. Since, 8-SPT, used to 'isolate' the A_3 receptor-mediated component of the response to APNEA, neither increased histamine levels *per se* nor modified the response to APNEA, mediator release can be unequivocally attributed to the effects of APNEA.

It bears emphasis that the implication from these *in vivo* studies is that A_3 receptor activation is *per se* sufficient to activate powerfully mast cell mediator release whereas from *in vitro* studies the predominant effect is to augment mediator release induced by stimuli such as allergen and compound 48/80 (Marquardt *et al.*, 1978; Ali *et al.*, 1990; Ramkumar *et al.*, 1993). The reason for this difference remains to be clarified. Nevertheless, there are several examples of mast cell-dependent functional responses to adenosine receptor ligands apparently acting independently of a second activating stimulus, including bronchoconstriction in rats (Pauwels & Van Der Straeten, 1987) and contraction of human bronchi (Björk *et al.*, 1992) and constriction of arterioles from the hamster cheek pouch (Doyle *et al.*, 1994) *in vitro*.

General similarity between responses to APNEA and compound 48/80

The overall similarity in the cardiovascular and histamine releasing profiles of APNEA and compound 48/80 is striking and clearly consistent with a common underlying mechanism of action. To extend the comparison of the properties of APNEA and compound 48/80, we investigated if changes in lung function accompanied the cardiovascular changes. Both similarities and differences between the two compounds were evident. Thus, both APNEA and compound 48/80 produced maximal hypotensive effects at doses which did not alter airways resistance or compliance. However, higher doses of compound 48/80 induced marked bronchoconstriction whereas no effects on pulmonary function were seen with APNEA even at doses 30 times those producing a prominent fall in blood pressure. In the context of an intermediary role for the mast cell it would appear that the mediator(s) released show selectivity for the cardiovascular system over the airways. This may reflect a primary contribution of histamine which in the same model induces prominent hypotensive effects without causing bronchoconstriction. The fact that APNEA has a far more prolonged effect on blood pressure than does histamine alone may simply reflect the quantity and/or time course of histamine released by APNEA. Alternatively, the finding may reflect the concomitant release of other mediators such as the leukotrienes. Studies are currently in progress to define the relative contribution of the different candidate mediators to the cardiovascular response to A_3 receptor activation in the rat. The reason for the difference between APNEA and compound 48/80 in that the latter induces bronchoconstriction at higher doses remains to be determined. The finding does not, of course, preclude a common mechanism (or site) of action at the lower doses and may simply reflect differences in the overall efficacy of the stimulus to mast cell mediator release.

Conclusion

The findings presented in this paper shed new light on the mechanisms underlying adenosine A_3 receptor-mediated hypotensive responses in the anaesthetized rat. Such responses are mimicked closely by the mast cell mediator releasing agent, compound 48/80, and suppressed selectively by sodium cromoglycate and lodoxamide which have mast cell stabilizing properties. Moreover, in rats depleted of mast cell mediators by repeated exposure to compound 48/80 responses to APNEA are selectively suppressed. Finally, hypotensive responses to both APNEA and compound 48/80 are associated with substantial increases in plasma histamine. Taken together, the data implicate the mast cell in a key role in A_3 receptor-mediated hypotension and are entirely consistent with the fact that rat mast cells express the A_3 receptor and are activated by ligands with A_3 receptor agonist properties *in vitro* (Ali *et al.*, 1990; 1991; Ramkumar *et al.*, 1993).

It is a pleasure to thank Dr Fulvio Gadient for synthesizing APNEA, CPA, CGS 21680 and 8-SPT and Dr K. Jacobson for permission to quote his unpublished data obtained with sodium cromoglycate and lodoxamide in the cloned rat A3 receptor binding assay.

References

ALI, H., CUNHA-MELO, J.R., SAUL, W.F. & BEAVEN, M.A. (1990). Activation of phospholipase C via adenosine receptors provides synergistic signals for secretion in antigen-stimulated RBL-2H3 cells. *J. Biol. Chem.*, **265**, 745–753.

ALI, H., MÜLLER, C.E., DALY, J.W. & BEAVEN, M.A. (1991). Methylxanthines block antigen-induced responses in RBL-2H3 cells independently of adenosine receptors or cyclic AMP: evidence for inhibition of antigen binding to IgE. *J. Pharmacol. Exp. Ther.*, **258**, 954.

BANKS, B.E.C., DEMPSEY, C.E., VERNON, C.A., WARNER, J.A. & YAMEY, J. (1990). Anti-inflammatory activity of bee venom peptide 401 (mast cell degranulating peptide) and compound 48/80 results from mast cell degranulation *in vivo*. *Br. J. Pharmacol.*, **99**, 350–354.

BJÖRK, T., GUSTAFSSON, L.E. & DAHLÉN, S.E. (1992). Isolated bronchi from asthmatics are hyperresponsive to adenosine which apparently acts indirectly by liberation of leukotrienes and histamine. *Am. Rev. Resp. Dis.*, **145**, 1087–1091.

BROGDEN, R.N., SPEIGHT, T.M. & AVERY, G.S. (1974). Sodium cromoglycate (cromolyn sodium): A review of its mode of action, pharmacology, therapeutic efficacy and use. *Drugs*, **7**, 164–282.

CARRUTHERS, A.M. & FOZARD, J.R. (1993a). Effect of pertussis toxin treatment on the putative adenosine A_3 receptor-mediated hypotensive responses in the rat. *Eur. J. Pharmacol.*, **250**, 185–188.

CARRUTHERS, A.M. & FOZARD, J.R. (1993b). Hypotensive responses to the putative adenosine A_3 receptor agonist N^6-2-(4-aminophenyl)ethyl adenosine in the rat. *Drug Dev. Res.*, **30**, 147–152.

CHAPMAN, I.D., KRISTERSSON, A., MATHELIN, G., SCHÄUBLIN, E., MAZZONI, L., BOUBEKEUR, K., MURPHY, N. & MORLEY, J. (1992). Effects of potassium channel opener (SDZ PCO 400) on guinea-pig and human pulmonary airways. *Br. J. Pharmacol.*, **106**, 423–429.

DI ROSA, M., GIROUD, J.P. & WILLOUGHBY, D.A. (1971). Studies of the mediators of the acute inflammatory response induced in rats in different sites by carrageenin and turpentine. *J. Pathol.*, **104**, 15–29.

DOYLE, M.P., LINDEN, J. & DULING, B.R. (1993). Nucleoside-induced arteriolar constriction: a mast cell-dependent response. *Am. J. Physiol.*, **266**, H2042–H2050.

ENERBÄCK, L. & SVENSSON, I. (1980). Isolation of peritoneal mast cells by centrifugation on density gradients of Percoll. *J. Immunol. Methods*, **39**, 135–145.

FOZARD, J.R. & CARRUTHERS, A.M. (1993a). Adenosine A_3 receptors mediate hypotension in the angiotensin II-supported circulation of the pithed rat. *Br. J. Pharmacol.*, **109**, 3–5.

FOZARD, J.R. & CARRUTHERS, A.M. (1993b). The cardiovascular effects of selective adenosine A_1 and A_2 receptor agonists in the pithed rat: no role for glibenclamide-sensitive potassium channels. *Naunyn-Schmied. Arch. Pharmacol.*, **347**, 192–196.

FOZARD, J.R. & HANNON, J.P. (1994). BW-A522 blocks adenosine A_3 receptor-mediated hypotensive responses in the rat. *Eur. J. Pharmacol.*, **252**, R5–R6.

GALLO-RODRIGUEZ, C., JI, X., MELMAN, N., SIEGMAN, B.D., SANDERS, L.H., ORLINA, J., FISCHER, B., PU, Q., OLAH, M.E., VAN GALEN, P.J.M., STILES, G.L. & JACOBSON, K.A. (1994). Structure-activity relationships of N^6-benzyladenosine-5'-uronamides as A_3-selective adenosine agonists. *J. Med. Chem.*, **37**, 636–646.

HANNON, J.P. & FOZARD, J.R. (1994). A role for mast cells in adenosine A_3 receptor-mediated hypotension in the anaesthetized rat. *Br. J. Pharmacol.*, **113**, 113P.

JOHNSON, H.G., VAN HOUT, C.A. & WRIGHT, J.B. (1978). Inhibition of allergic reactions by cromoglycate and by a new anti-allergy drug U-42,585E. *Int. Archs Allergy Appl. Immun.*, **56**, 416–423.

MARQUARDT, D.L., PARKER, C.W. & SULLIVAN, T.J. (1978). Potentiation of mast cell mediator release by adenosine. *J. Immunol.*, **120**, 871–878.

MARQUARDT, D.L. & WASSERMAN, S.I. (1985). [^{3}H]Adenosine binding to rat mast cells–pharmacologic and functional characterization. *Agents Actions*, **6**, 453–461.

MORAN, N.C., UVNAS, B. & WESTERHOLM, B. (1962). Release of 5-hydroxytrptamine and histamine from rat mast cells. *Acta Physiol. Scand.*, **56**, 26–41.

PATON, W.D.M. (1951). Compound 48/80: a potent histamine liberator. *Br. J. Pharmacol. Chemother.*, **6**, 499–508.

PAUWELS, R.A. & VAN DER STRAETEN, M.E. (1987). An animal model for adenosine-induced bronchoconstriction. *Am. Rev. Resp. Dis.*, **136**, 374–378.

QIAN, Y.X. & MCCLOSKEY, M.A. (1993). Activation of mast cell K^+ channels through multiple G protein-linked receptors. *Proc. Natl. Acad. Sci. U.S.A.*, **90**, 7844–7848.

RAMKUMAR, V., STILES, G.L., BEAVEN, M.A. & ALI, H. (1993). The A_3 adenosine receptor is the unique adenosine receptor which facilitates release of allergic mediators in mast cells. *J. Biol. Chem.*, **268**, 16887–16890.

SALZMANN, R. & FOZARD, J.R. (1994). The haemodynamic basis of the hypotensive response to the putative adenosine A_3 receptor agonist, N^6-2-(4-aminophenyl)ethyl adenosine (APNEA) in the rat. *Drug Dev. Res.*, **31**, 270.

TANIZAKI, Y., OHTANI, J. & KIMURA, I. (1992). Actions and cross-reactivity of antiallergic agents and a calcium channel antagonist on rat peritoneal mast cells. Difference in the action mechanisms and cross-reactivity among the agents. *Agents Actions*, **37**, 8–15.

TASAKA, K. (1991). Histamine and the blood. In *Handbook of Experimental Pharmacology*, Vol. 97, *Histamine and Histamine Antagonists*. ed. Uvnäs, B., pp. 473–510. Berlin: Springer Verlag.

ZHOU, Q.Y., LI, C., OLAH, M.E., JOHNSON, R.A., STILES, G.L. & CIVELLI, O. (1992). Molecular cloning and characterization of an adenosine receptor: the A_3 adenosine receptor. *Proc. Natl. Acad. Sci. U.S.A.*, **89**, 7432–7436.

(Received November 15, 1994
Revised March 15, 1995
Accepted April 3, 1995)

British Journal of Pharmacology (1995) 115, 953-960 © 1995 Stockton Press All rights reserved 0007-1188/95 $12.00

Potentiation, activation and blockade of $GABA_A$ receptors of clonal murine hypothalamic GT1-7 neurones by propofol

Snehal Adodra & [1]Tim G. Hales

Department of Anesthesiology, Brain Research Institute, UCLA Medical Center, Los Angeles, CA 90024, U.S.A.

1 The actions of GABA and the intravenous general anaesthetic propofol (2,6-diisopropylphenol) on $GABA_A$ receptors of self-replicating GT1-7 hypothalamic neurones were investigated by the patch clamp technique.

2 GABA (1 μM - 1 mM) dose-dependently activated inward currents with an EC_{50} of 27 μM, recorded from whole cells voltage-clamped at -60 mV. GABA (100 μM)-activated currents reversed at the Cl^- equilibrium potential.

3 Propofol (0.1 - 100 μM) dose-dependently potentiated GABA (100 μM)-evoked currents with an EC_{50} of 5 μM.

4 In the absence of GABA, propofol (10 μM - 1 mM) activated small inward currents with a reversal potential similar to the Cl^- equilibrium potential. The peak current amplitudes activated by propofol were only 31% of those activated by GABA in the same cells.

5 Like GABA (100 μM)-activated currents, propofol (100 μM)-activated currents were inhibited by the $GABA_A$ receptor antagonist, bicuculline (10 μM) and were abolished by Zn^{2+} (100 μM).

6 Propofol (10, 30 and 100 μM) dose-dependently activated currents in the absence of GABA. However, the peak amplitude of currents activated by propofol declined with concentrations >100 μM. The cessation of application of a high dose of propofol (1 mM) was associated with a current 'surge'.

7 The surge current, seen after application of propofol (1 mM), had a reversal potential similar to the Cl^- equilibrium potential. The ratio between peak current amplitude in the presence of propofol (1 mM) and surge current amplitude after propofol application, were not dependent on holding potential. Thus, it is unlikely that the surge current represents reversal of a voltage-dependent block of $GABA_A$ receptors by propofol.

8 The amplitude of the surge current exceeded the amplitude of the initial propofol (1 mM)-evoked current following brief applications, but declined after prolonged applications of the drug.

9 The observed modulatory actions of propofol may be due to separate potentiation, activation and inhibitory sites for this anaesthetic agent on GT1-7 cell $GABA_A$ receptors.

Keywords: Propofol; general anaesthetics; $GABA_A$ receptors; GT1-7 cells; hypothalamic neurones; patch clamp

Introduction

γ-Aminobutyric acid type A ($GABA_A$) receptors are widely distributed throughout the brain and periphery. Mammalian bicuculline-sensitive $GABA_A$ receptors are modulated by several therapeutic agents with anticonvulsant, anxiolytic, and anaesthetic properties, such as benzodiazepines, anaesthetic barbiturates, anaesthetic steroids, volatile agents, chlormethiazole, etomidate, propanidid, and propofol (see Franks & Lieb, 1994; Hales & Olsen, 1994). $GABA_A$ receptor-chloride-ion channels are thought to comprise five subunits (Olsen & Tobin, 1990). There have been multiple subunits cloned, including α1-6, β1-3, γ1-3 and δ (Burt & Kamatchi, 1991). These subunits are differentially expressed throughout the nervous system (Wisden *et al.*, 1992; Laurie *et al.*, 1992) and can combine to form bicuculline-sensitive $GABA_A$ receptors with varying biophysical and pharmacological properties (Pritchett *et al.*, 1989; Draguhn *et al.*, 1990; Smart *et al.*, 1991; Wafford *et al.*, 1991; Angelotti & Macdonald, 1993; Verdoorn, 1994).

$GABA_A$ receptor subunits are not only differentially distributed between brain regions, (Wisden *et al.*, 1992; Laurie *et al.*, 1992), but are also known to vary within neurones at different developmental stages (Shivers *et al.*, 1989; Smart & Constanti, 1990). This regional and developmental heterogeneity may explain reports of variable $GABA_A$ receptor modulation by some agents (Pritchett & Seeburg, 1990; Smart & Constanti, 1990; Wafford *et al.*, 1991). Clonal cell lines provide a less heterogeneous system for the study of receptor expression and properties. However, although many cell lines express $GABA_A$ receptor mRNAs, few have functional receptors (Hales *et al.*, 1992; Noble *et al.*, 1993; Hales & Tyndale, 1994; Tyndale *et al.*, 1994).

In this study the modulation by the widely used general anaesthetic, propofol, of functional $GABA_A$ receptors in self-replicating GnRH-secreting hypothalamic GT1-7 neurones (Mellon *et al.*, 1990), was investigated. $GABA_A$ receptors of GT1-7 cells have previously been characterized by use of molecular and electrophysiological techniques (Hales *et al.*, 1992; 1994). The clonal nature of these cells, and their stable expression of $GABA_A$ receptors, has allowed a detailed investigation of the modulatory actions of propofol using the whole cell configuration of the patch clamp technique. A preliminary account of a part of this work has appeared in abstract form (Adodra & Hales, 1994).

Methods

Cell culture

Self-replicating hypothalamic GT1-7 neurones were maintained in culture as described previously (Hales *et al.*, 1992; 1994). Cells were grown in Dulbecco's Modified Eagles Medium (DMEM) supplemented with calf serum 5% (v/v), horse serum 5%, penicillin (50 iu ml^{-1}) and streptomycin (0.05 mg ml^{-1}), at 37°C in 95% air/5% CO_2 and 100% relative

[1] Author for correspondence.

humidity (reagents from Gibco). Cells were used for electrophysiological recordings 3–14 days after subculturing into 35 mm culture dishes (Costar). Experiments were performed at room temperature (22–25°C).

Electrophysiology

The whole cell configuration of the patch clamp technique was used to record GABA- and propofol-evoked currents from single GT1-7 cells voltage-clamped at −60 mV (unless otherwise stated). The recording chamber was continuously and rapidly (20 ml min^{-1}) perfused by gravity feed with an extracellular solution of the following composition (in mM): NaCl 140, KCl 2.8, $MgCl_2$ 2.0, $CaCl_2$ 1.0, glucose 6.0 and HEPES-NaOH (pH 7.2). Recording electrodes contained CsCl 140, $MgCl_2$ 2.0, $CaCl_2$ 0.1, ATP (Mg salt) 3, EGTA 1.1, and HEPES-CsOH (pH 7.2). Membrane currents were monitored with an Axopatch-1A (Axon Instruments Inc.) patch clamp amplifier. Currents were low-pass filtered at a cutoff frequency of 2 kHz (Bessel characteristics), digitized with a digital audio processor (Sony PCM-501ES) and recorded onto VCR tapes for subsequent analysis.

In experiments examining activation of GABA$_A$ receptors, GABA or propofol was applied locally by pressure ejection (General Valve Picospritzer II) at a pressure of 70 kPa, from glass micropipettes positioned approximately 50 μm from the cell under investigation. Cells were continuously and rapidly superfused with recording solution to help prevent GABA$_A$ receptor desensitization. In dose-response experiments randomized doses of GABA or propofol were applied via different pipettes with similar resistances positioned in the same location (with the aid of an eye piece graticule). During concentration-response experiments, agonists were applied for prolonged periods (≥1 s) in order to achieve equilibrium concentrations. However, it is likely that dilution occurs at some receptor sites therefore concentrations represent maximum estimates of the true agonist concentrations. A period of at least 4 min wash was allowed between each application to prevent desensitization. All other drugs were bath-applied, as was propofol in experiments investigating its GABA-potentiating effect.

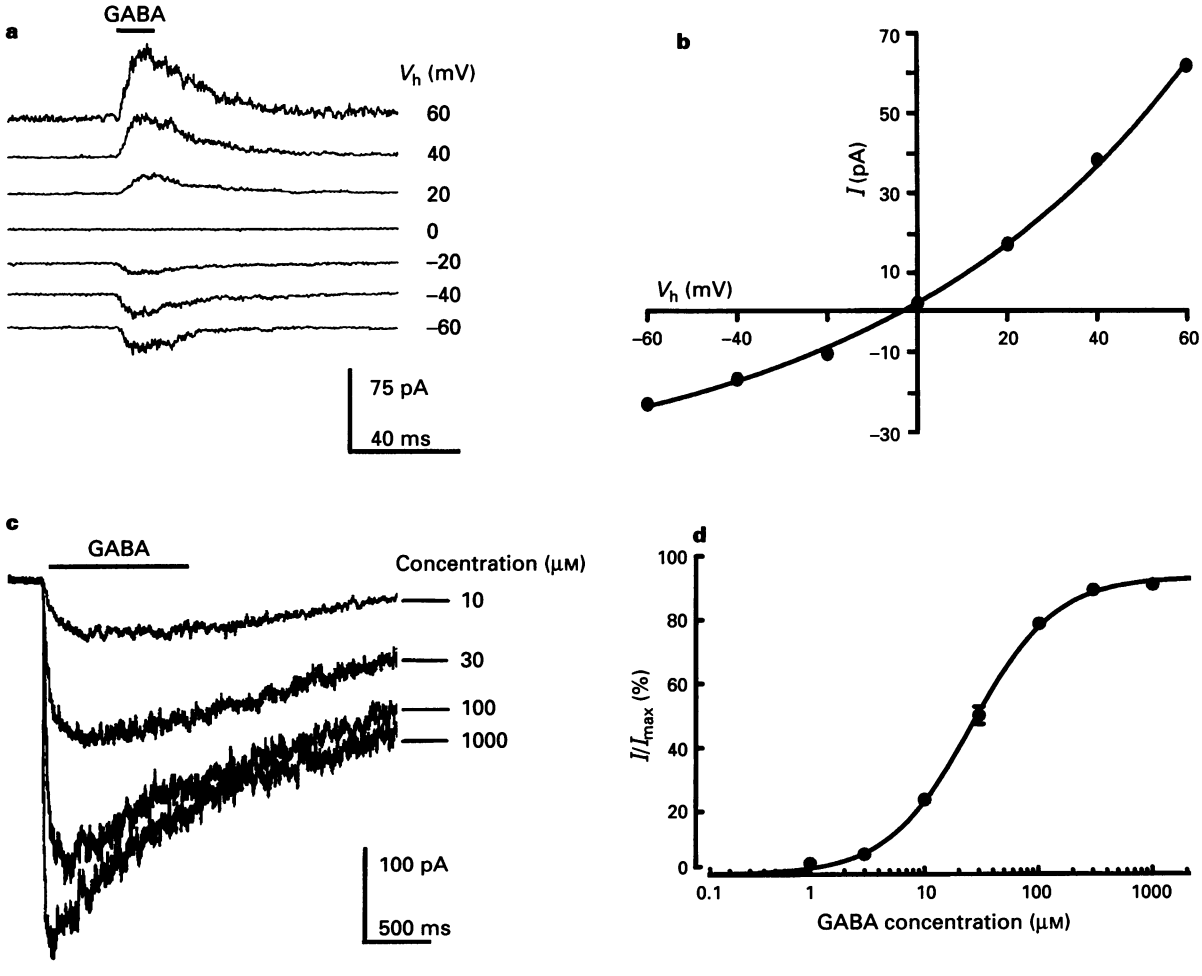

Figure 1 GABA-evoked currents recorded from GT1-7 cells. (a) Traces illustrating whole cell currents evoked by locally applied GABA (100 μM, for 10 ms at 70 kPa) at holding potentials (V_h) from −60 mV to 60 mV. Traces are averages of two currents at each potential. (b) The relationship between holding potential and amplitude of the currents in (a) is shown graphically, and indicates that GABA-induced currents have a reversal potential of approximately 0 mV with 144 mM and 148 mM Cl^- inside and outside the cell, respectively. (c) Dose-dependent activation of GABA$_A$ receptors by GABA. Prolonged local applications (1 s) of GABA (10 μM–1 mM) to a cell voltage-clamped at −60 mV activate Cl^- currents in a dose-dependent manner. (d) A graph of the mean amplitude of the GABA-induced currents is plotted against the concentration of GABA (on a logarithmic scale). Peak current amplitudes were measured and expressed as a percentage of the highest amplitude current recorded from individual cells. The points are mean dose-response data from six cells. Where bigger than the data points, s.e.means are shown. The curve was fitted to a logistics equation (see Methods) and provides an EC_{50} value of 26.6 μM, and a Hill coefficient of 1.6.

Data analysis

Propofol and GABA-evoked whole cell currents were replayed onto a chart recorder (Gould Brush 2400) for manual analysis, or digitized (Digidata 1200 interface, Axon Instruments Inc.) at a frequency of 10 kHz onto the hard drive of an IBM PC and analysed with pCLAMP software (Axon Instruments Inc.). Illustrations of raw data were produced either by reproduction of chart recordings or by retrieval of digitized information from the IBM PC onto a laser printer. GABA and propofol concentration-response curves were compiled and then best fitted using the logistic equation:

$$I = I_{max}/(1 + (EC_{50}/C)^{n_H})$$

Where I is the agonist activated current amplitude (as % of maximum current observed), I_{max} the maximum current (as % maximum observed), EC_{50} the concentration of agonist eliciting a half maximal response, C the agonist concentration and n_H the Hill coefficient. When fitting propofol potentiation dose-response curves the equation was modified to:

$$I = 100 + I_{max}/(1 + (EC_{50}/C)^{n_H})$$

Where I is the amplitude of the GABA-activated current (expressed as % control), I_{max} is the maximum propofol-potentiated current (as % control), EC_{50} is the concentration of propofol eliciting a half maximal potentiation, C the propofol concentration and n_H the Hill coefficient.

All quantitiative results are expressed as the arithmetic mean ± s.e.mean.

Drugs used

Drugs used in this study were: γ-aminobutyric acid (GABA), bicuculline methiodide (both from Sigma) and 2,6-diisopropylphenol (propofol, from Aldrich). Stock solutions of propofol were made up at 100 mM in ethanol. In potentiation

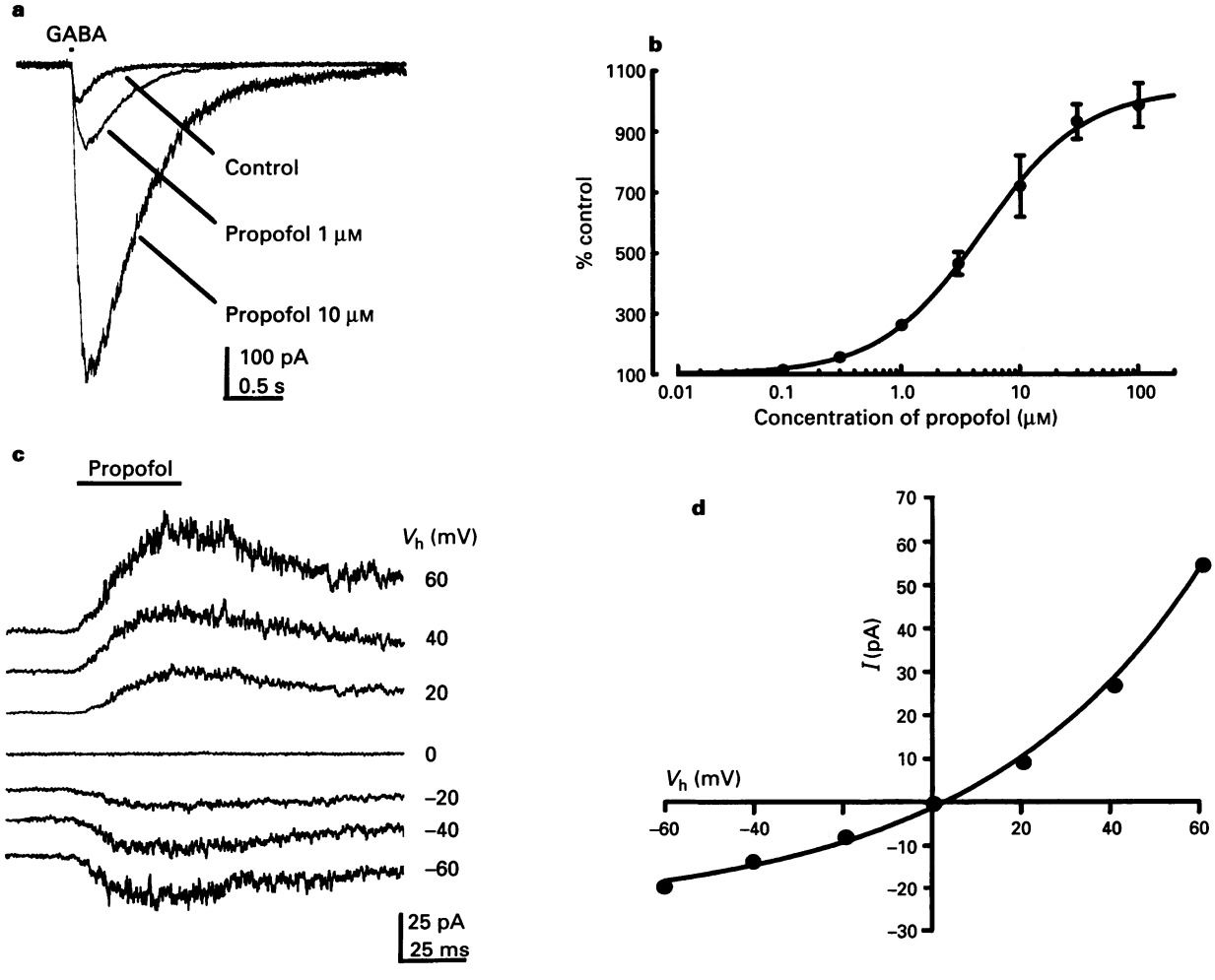

Figure 2 Potentiation of GABA-evoked currents and activation of GABA$_A$ receptors by propofol. (a) Traces illustrating potentiation of GABA-evoked currents by propofol (1–10 μM) recorded from a cell voltage-clamped at −60 mV. GABA (100 μM) was pressure-applied (70 kPa for 10 ms) and propofol was bath-applied at the indicated doses. Propofol-evoked potentiations were reversed on wash out of the drug. Superimposed traces are averages of three currents under each condition. (b) A graph illustrating the cumulative dose-response relationship for propofol-evoked potentiation of GABA-activated currents. Each data point represents the mean potentiation (expressed as a percentage of control GABA response amplitude) induced by propofol in 4–10 separate cells. Propofol concentrations are plotted on a logarithmic scale, and s.e.means are shown. The fitted logistic curve provides an EC_{50} value of 4.8 μM, and a Hill coefficient of 1.0. (c) Pressure applied (45 ms at 70 kPa) propofol (100 μM) directly activated small currents in the absence of GABA, recorded from a cell with 144 mM and 148 mM Cl^- inside and outside the cell, respectively. Currents were recorded from the same cell, with varying holding potentials from −60 mV to 60 mV. Traces represent averages of two currents recorded at each potential. (d) A graph of the relationship between the peak response amplitude and the holding potential, for the currents in (c). The equilibrium potential for propofol-evoked currents in this case was 0 mV, similar to the equilibrium potential for GABA-activated currents (see Figure 1). The mean equilibrium potential for propofol-activated currents was calculated to be 0.2 ± 0.1 mV (n = 4).

experiments the final concentration of ethanol did not exceed 0.1% (v/v). This concentration of ethanol has no effect on GABA-evoked currents recorded from GT1-7 cells (Hales *et al.*, 1992). In experiments examining the direct activation of $GABA_A$ receptors by propofol, concentrations of the drug up to 1 mM were tested, necessitating a maximum final ethanol concentration of 1%. While this concentration of ethanol has small potentiating effects on GABA-evoked currents there are no direct actions of ethanol (1%) in GT1-7 cells (Hales *et al.*, 1992).

Results

Activation of $GABA_A$ receptors by GABA

Self-replicating hypothalamic GT1-7 neurones have been reported to express functional $GABA_A$ receptors (Hales *et al.*, 1992). In confirmation of this previous report all GT1-7 cells tested ($n>100$) responded to locally applied GABA (100 μM) with inward whole cell currents recorded at a holding potential of -60 mV (Figure 1). From the current-voltage relationship it was determined that GABA-activated currents exhibited outward rectification and reversed close to the Cl^- equilibrium potential of ~ 0 mV with approximately equal concentrations of the ion on both sides of the GT1-7 cell membrane (Hales *et al.*, 1992; Figure 1a and b).

GABA (1 μM – 1 mM), pressure applied for 1 s, dose-dependently activated currents recorded from GT1-7 cells voltage-clamped at -60 mV (Figure 1c and d). The threshold for activation was around 1 μM GABA with an EC_{50} of 26.6 μM. Peak currents were activated by 300 μM GABA ($n=6$).

Potentiation of GABA-evoked currents by propofol

GABA-evoked currents recorded from GT1-7 cells are modulated by the anaesthetic barbiturate, pentobarbitone and the anaesthetic steroid, 5α-pregnan-3α-ol-20-one, but are insensitive to the benzodiazepine, diazepam (Hales *et al.*, 1992). In this study, currents activated by brief (10 ms) applications of GABA (100 μM), were dramatically and dose-dependently potentiated by propofol (0.3 – 100 μM), when the general anaesthetic was bath applied (Figure 2a and b). Propofol-evoked potentiations were fully reversed upon washing out the drug. The threshold concentration of propofol for potentiation of GABA-evoked currents was approximately 300 nM and the EC_{50} was 4.8 μM. Propofol at concentrations >10 μM generally caused transient potentiations of GABA-evoked currents even in the continued presence of the drug (data not shown). This phenomemon could be due to desensitization and/or block of $GABA_A$ receptors by propofol (see Figures 4 and 5). In order to minimize the effect of desensitization and/or block, in such cases the peak amplitude of the current in the presence of propofol was used to calculate the degree of po-

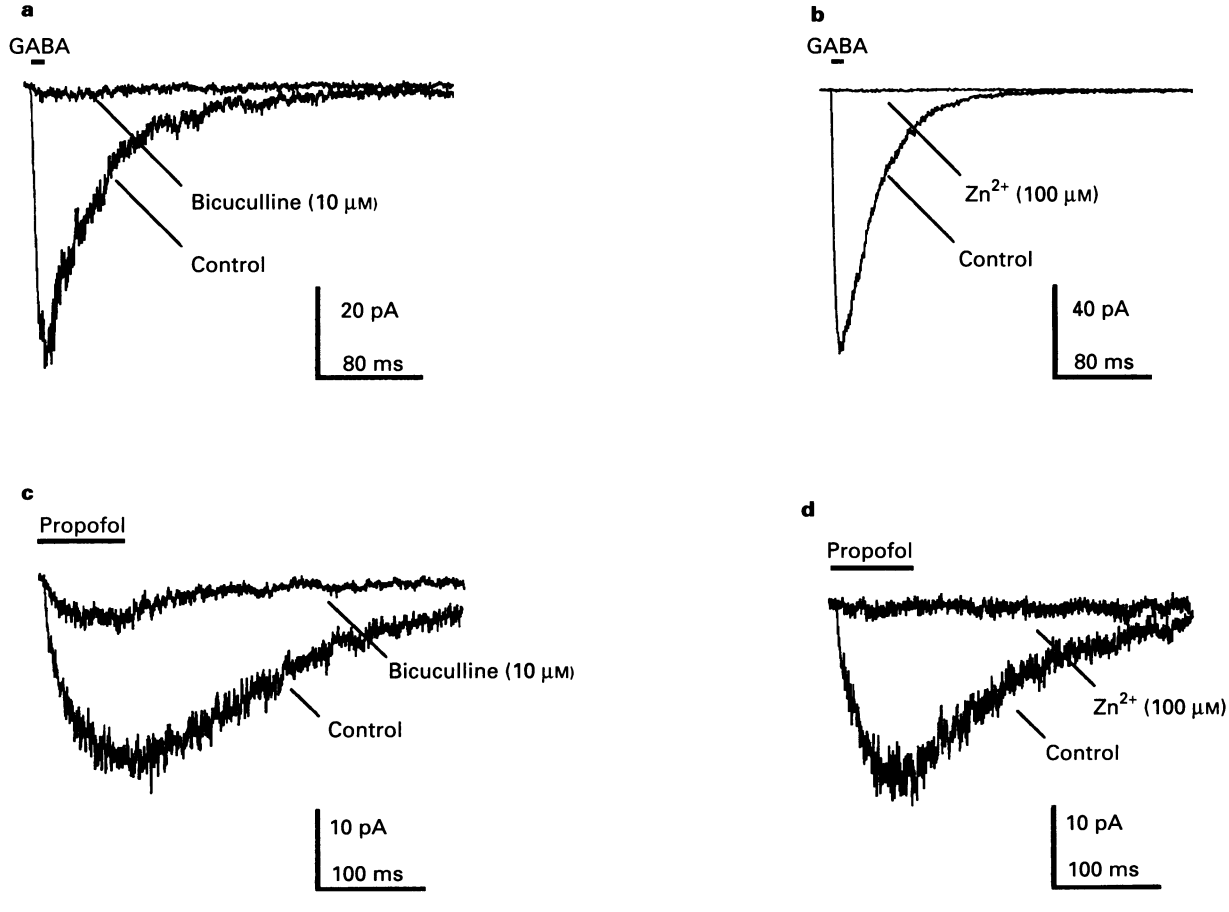

Figure 3 Bicuculline methiodide and Zn^{2+} inhibit both GABA- and propofol-evoked currents. (a) Bicuculline methiodide (10 μM) inhibited currents evoked by GABA (100 μM). (b) Zn^{2+} (100 μM) abolished currents evoked by GABA (100 μM). In (a) and (b), GABA was applied locally (for 6.5 ms at 70 kPa). Bicuculline methiodide and Zn^{2+} were bath applied. (c) Bicuculline methiodide (10 μM) reduced the amplitude of currents evoked by propofol (100 μM), to $31 \pm 2.4\%$ of control ($n=6$). (d) Zn^{2+} (100 μM) abolished ($n=6$) currents activated by local application of propofol (100 μM). For both (c) and (d), propofol was applied locally (for 80 ms at 70 kPa). Zn^{2+} and bicuculline methiodide were bath-applied. All currents were recorded at -60 mV, and superimposed traces represent the average of three currents.

tentiation. Maximum potentiation was achieved with 100 μM propofol, which increased GABA-evoked responses to 988 ± 73% (n = 6) of control current amplitude.

Activation of GABA$_A$ receptors by propofol

Propofol has been reported to activate directly GABA$_A$ receptors of adrenomedullary chromaffin cells (Hales & Lambert, 1991) and hippocampal neurones (Hara *et al.*, 1993; Orser *et al.*, 1994) in the absence of GABA. Pressure application of propofol (100 μM, for 45 ms) to GT1-7 cells activated small inward currents at negative potentials which became outward when cells were clamped at potentials above 0 mV (Figure 2c and d). The reversal potential of propofol-evoked currents with approximately equal Cl^- on both sides of the cell membrane, was 0.2 ± 0.1 mV (n = 4), similar to the theoretical reversal potential of ~0 mV. Like GABA-evoked currents recorded from GT1-7 cells, propofol-activated currents also exhibited outward rectification (n = 4).

Currents recorded from GT1-7 cells, activated by brief applications of GABA (100 μM) were inhibited when the GABA$_A$ receptor selective antagonist, bicuculline methiodide (10 μM), was applied via the superfusate (n = 5; Figure 3a). GABA-evoked currents were also abolished by Zn^{2+} (100 μM, n = 6; Figure 3b). Low concentrations of Zn^{2+} are thought to inhibit GABA$_A$ receptors in GT1-7 cells due to the absence of γ subunits (Hales *et al.*, 1992). In support of propofol (100 μM) activating GABA$_A$ receptors in GT1-7 cells lacking γ subunits, propofol-evoked currents were also inhibited by bicuculline methiodide (10 μM, n = 4) and blocked by Zn^{2+} (100 μM, n = 4; Figure 3c and d).

In order to characterize the dose-dependence of the activation of GT1-7 cell GABA$_A$ receptors by propofol, the anaesthetic was pressure-applied for prolonged periods at different concentrations, from micropipettes situated adjacent to cells voltage-clamped at −60 mV. Propofol (10, 30 and 100 μM) dose-dependently activated whole cell currents (Figure 4a and b). However, current amplitudes declined when the propofol concentration exceeded 100 μM. This hindrance of propofol-activated current was associated with a 'surge' current seen on cessation of application of high concentrations of propofol (300 μM and 1 mM; Figures 4 and 5). When peak GABA- and propofol-activated current amplitudes were compared in the same cells the latter were found to be only 31 ± 3% of the former (n = 9).

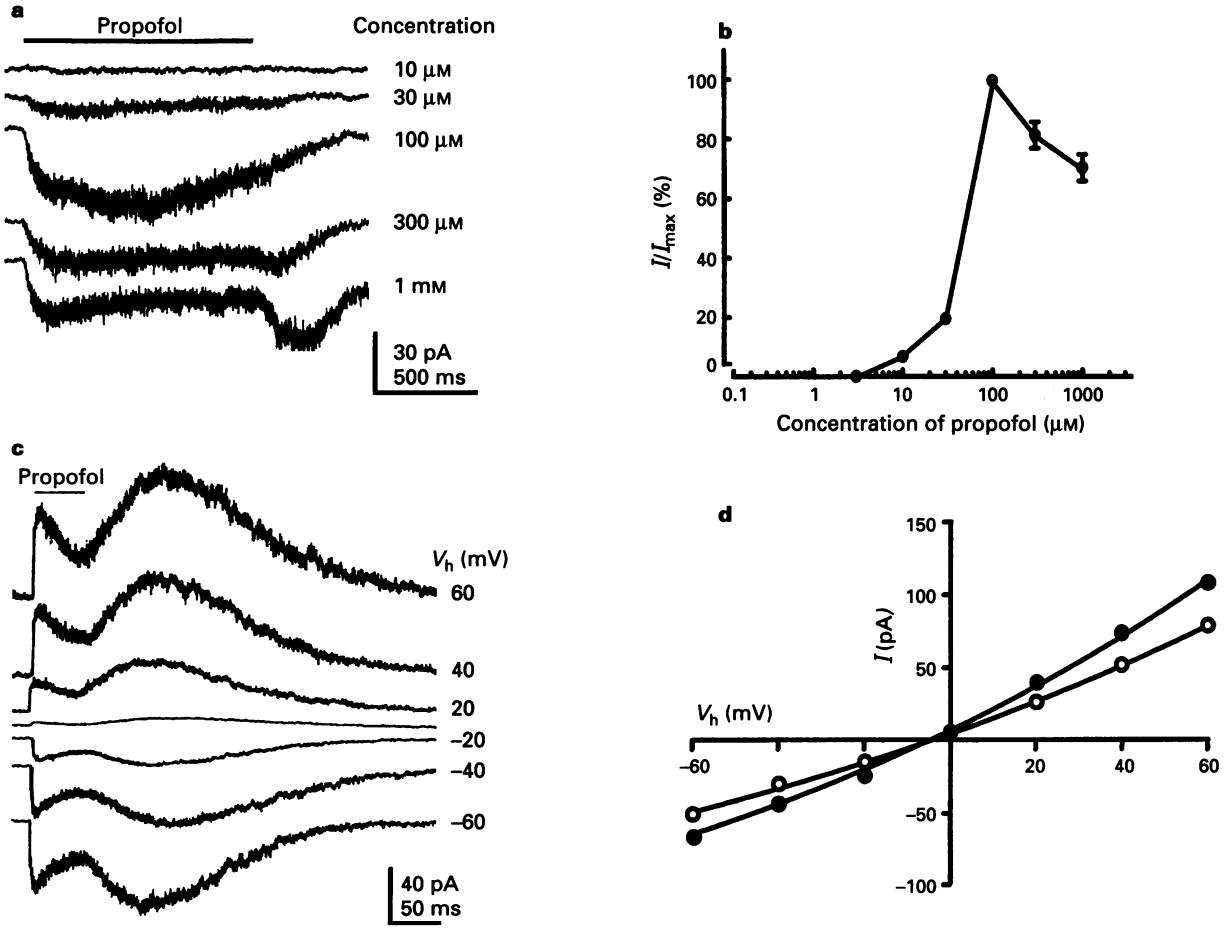

Figure 4 Dose-dependent activation and block of GABA$_A$ receptors by propofol. (a) Traces illustrating dose-dependent activation of GT1-7 cell GABA$_A$ receptors by propofol (10 μM − 1 mM). Cessation of application of propofol concentrations of greater than 100 μM (300 μM and 1 mM) caused a 'surge' current. (b) Log concentration-response curve for currents activated by propofol (3 μM − 1 mM). The threshold for activation of propofol was approximately 10 μM. Current amplitudes are expressed as a percentage of the highest amplitude response evoked on each cell. Each point represents mean data from six cells. A logistics curve could not be fitted to the data points due to the reduction in current amplitude caused by propofol concentrations greater than 100 μM. However, it is estimated from the graph that the half-maximal current would occur with approximately 50 μM propofol. (c) Propofol (1 mM)-activated currents recorded from a GT1-7 cell clamped at potentials between −60 and 60 mV. (d) A graph of the current-voltage relationship for the currents illustrated in (c): (○) represent peak current amplitudes in the presence of propofol; (●) peak amplitudes of surge currents appearing on cessation of propofol application. Both peak and surge currents reversed at approximately the Cl^- equilibration potential of ~0 mV (with 144 mM and 148 mM Cl^- inside and outside the cell, respectively). Additionally, the ratios between the peak and surge currents did not appear to vary with voltage.

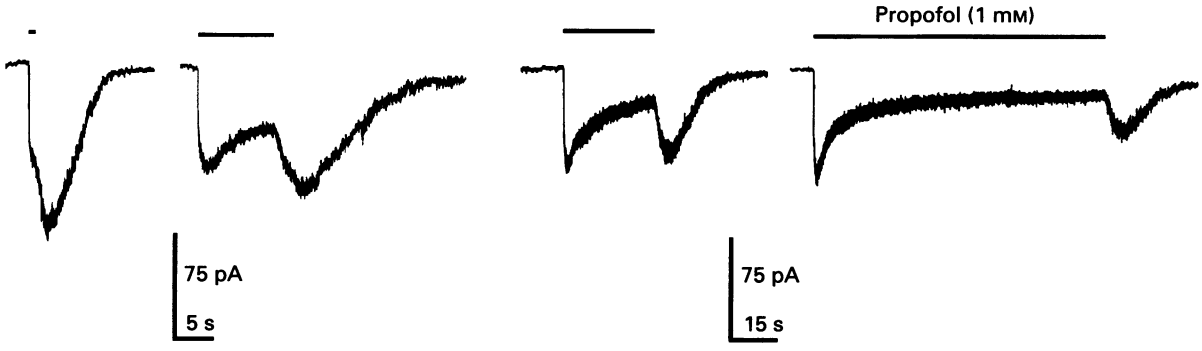

Figure 5 The relationship between duration of propofol application and surge current amplitude. Currents recorded from the same cell activated by propofol (1 mM) applied for 1, 10, 30 and 100 s. The current amplitude declined in the continued presence of propofol, but rebounded on cessation of the application. The amplitude of the surge current seen following 1 and 10 s propofol applications was greater than that of the peak current in the presence of the drug. However, the amplitude of the surge current declined with the duration of propofol application.

Propofol block of $GABA_A$ receptors

The post-propofol (1 mM) surge current could be caused by rapid recovery from: (i) blockade of $GABA_A$ receptor-Cl^--ion channels; (ii) desensitization; or (iii) allosteric inhibition of $GABA_A$ receptor-Cl^- channel gating. To test whether the surge current was caused by reversal of propofol-induced voltage-dependent block of $GABA_A$ receptor-Cl^--ion channels, the relationship between the holding potential and surge current amplitude was investigated (Figure 4c and d). Both the transient current in the presence of propofol (1 mM) and the surge current following application of the drug reversed at 0 mV (Figure 4c and d). The ratio between the two currents showed no dependence on holding potential and their current-voltage relationships resembled that seen for the lower concentration of propofol (100 μM). Taken together, these data suggest that neither the propofol-evoked hindrance, nor the reversal of this phenomenon (seen as a current surge) show voltage-dependence.

The possible role of desensitization in the hindrance of the propofol (1 mM)-evoked current and subsequent surge current was investigated by examining the surge current amplitude after drug applications of different durations (Figure 5). This protocol revealed that the surge current amplitude declined as the length of propofol application was increased (Figure 5). This is unlikely to occur if the surge current represents rapid recovery from desensitization since there would be more recovery (and hence a bigger surge) following protocols which caused greater desensitization. It is likely that the decline in the surge amplitude with prolongation of propofol application represents the relatively slow onset of desensitization (Figure 5).

Discussion

The results of this study support and extend previous reports of functional $GABA_A$ receptors on self-replicating GnRH-secreting hypothalamic GT1-7 neurones (Hales *et al.*, 1992; 1994; Bosma, 1993). This clonal cell line was further exploited here to investigate the actions of the widely used intravenous general anaesthetic, propofol, on $GABA_A$ receptors.

Low concentrations of propofol potentiate GABA-evoked currents recorded from bovine chromaffin cells, rodent and murine hippocampal neurones (Hales & Lambert, 1991; Hara *et al.*, 1994; Orser *et al.*, 1994), and GT1-7 cells. In addition, the general anaesthetic directly activates $GABA_A$ receptors at higher concentrations, relevant to total intravenous anaesthesia (Hales & Lambert, 1991; Hara *et al.*, 1993; Orser *et al.*, 1994). Numerous other compounds with general anaesthetic properties potentiate the actions of GABA and at higher doses directly activate $GABA_A$ receptors. These agents include anaesthetic barbiturates (Macdonald *et al.*, 1986), anaesthetic steroids (Cottrell *et al.*, 1987; Harrison *et al.*, 1987), etomidate (Robertson, 1989), chlormethiazole (Hales & Lambert, 1992) and volatile agents (Jones *et al.*, 1992; Yang *et al.*, 1992). The anticonvulsant and anxiolytic benzodiazepines are also potent potentiators of GABA-evoked responses, but are unable to activate directly $GABA_A$ receptors in the absence of GABA. It has been suggested that this difference in the action of general anaesthetics and the benzodiazepines on the $GABA_A$ receptor may underlie their different therapeutic properties (Schulz & Macdonald, 1981).

GT1-7 cell $GABA_A$ receptors are insensitive to the anxiolytic benzodiazepine, diazepam and membranes from these cells do not bind [^{3}H]-flunitrazepam (Hales *et al.*, 1992). It is thought that this lack of benzodiazepine modulation is caused by the absence of a γ subunit from the functional receptors. It is known from recombinant $GABA_A$ receptor studies, that the γ subunit is a prerequisite for benzodiazepine modulation of the $GABA_A$ receptor and that the selectivity of benzodiazepines in this respect is influenced by the identity of the α subunit (Pritchett *et al.*, 1989; Ymer *et al.*, 1990; Puia *et al.*, 1991). The long form of the alternatively spliced γ2 subunit has also been implicated in the actions of relatively low concentrations of ethanol (20 mM) on $GABA_A$ receptors (Wafford *et al.*, 1991). Ethanol, at this concentration, has no effect on GABA-evoked currents recorded from GT1-7 cells (Hales *et al.*, 1992). To add to the evidence for a lack of γ subunits in GT1-7 cell $GABA_A$ receptors, GABA-evoked currents recorded from these cells are blocked potently by Zn^{2+} (Hales *et al.*, 1991); Zn^{2+} is less potent as an inhibitor of GABA responses recorded from cells expressing γ subunits (Draguhn *et al.*, 1990; Smart *et al.*, 1991).

Unlike benzodiazepines and ethanol, low propofol concentrations cause profound potentiation of GABA-activated currents recorded from GT1-7 cells. The anaesthetic steroid, 5α-pregnan-3α-ol-20-one and the anaesthetic barbiturate, pentobarbitone, also potentiated GABA-activated currents recorded from these cells (Hales *et al.*, 1992). These data suggest that the γ subunit is not required for potentiation of GABA-evoked currents by these general anaesthetics. Studies of recombinant receptors lacking γ subunits have also demonstrated that this subunit is not required for the GABA potentiating actions of anaesthetic barbiturates and steroids (Puia *et al.*, 1990; Horne *et al.*, 1993). In fact, of all the mammalian receptor subunit combinations tested to date, only homomeric ρ GABA receptors localized in the retina have been reported to mediate GABA-evoked currents which are not potentiated by anaesthetic barbiturates and steroids (Shimada *et al.*, 1992; Woodward *et al.*, 1992; Hales & Olsen, 1994). However, these receptors are also unusual in that their activation by GABA is not blocked by the selective $GABA_A$ receptor antagonist, bicuculline (Shimada *et al.*, 1992).

Unlike low concentrations of propofol which potentiate GABA responses, in the absence of GABA high concentrations of the drug were required to cause discernible direct activation of Cl^- currents. Consistent with previous reports of propofol activation of GABA$_A$ receptors (Hales & Lambert, 1992; Hara *et al.*, 1993; Orser *et al.*, 1994), propofol-evoked currents recorded from GT1-7 cells were blocked by bicuculline methiodide. Propofol-activated currents were also blocked by Zn^{2+} suggesting that these, like GABA-evoked currents, are mediated by activation of GABA$_A$ receptors lacking γ subunits in this cell line. Propofol concentrations required for activation of GT1-7 GABA$_A$ receptors were higher than those reported for GABA$_A$ receptor activation in bovine chromaffin cells (Hales & Lambert, 1991) and rodent hippocampal neurones (Hara *et al.*, 1993).

The large separation between the threshold for potentiation and activation of GABA$_A$ receptors in GT1-7 cells may be a feature of their subunit combination(s). It is possible that the absence of the γ subunit contributes to this difference in the potency of propofol as a potentiator and an activator. Potentiation and activation by propofol may require different subunits and hence some receptor combinations may be more sensitive to one action of the anaesthetic than the other. Interestingly, Orser and colleagues (1994) reported a high threshold of propofol activation of GABA$_A$ receptors in embryonic murine hippocampal neurones. The dose-response relationship for this action of propofol in their preparation looks strikingly similar to that reported here. It may be significant that GABA-responses recorded from embryonic neurones tend to be more sensitive to Zn^{2+} (Smart & Constanti, 1990) and this has been explained by a lack of γ subunits (Draguhn *et al.*, 1990; Smart *et al.*, 1991). Hence the absence of a γ subunit from the GABA$_A$ receptor may make propofol less potent and/or efficacious as an activator in GT1-7 cells and embryonic neuronal preparations. Rigorous pharmacological comparisons of various subunit combinations of recombinant GABA$_A$ receptors will be required to investigate this and other possibilities further.

There is little known about the actions of propofol on GABA$_A$ receptors of different subunit combinations. Both propofol and pentobarbitone directly activate homomeric human $\beta1$ GABA$_A$ receptors expressed in *Xenopus* oocytes (Sanna *et al.*, 1995). The same study demonstrated that a dose of propofol which directly activated recombinant $\alpha1\beta1\gamma2$ receptors eliciting large currents, activated barely detectable currents when applied to oocytes expressing $\alpha1\beta1$ receptors. Recent studies of $\alpha2\beta1$ and $\alpha2\beta1\gamma2$ receptors expressed in human embryonic kidney cells also suggest that smaller currents are activated by propofol relative to GABA in cells lacking the γ subunit (Jones *et al.*, 1995). These observations support the hypothesis that the presence of the γ subunit increases the potency and/or efficacy of propofol as an activator of GABA$_A$ receptors.

In addition to potentiation and activation, propofol also inhibits current through GT1-7 cell GABA$_A$ receptor Cl^- ion channels at high concentrations. The inhibitory action of propofol is exposed by the surge current associated with the termination of application of high concentrations of the drug. A similar phenomenon has been seen in experiments on chromaffin cells (Peters *et al.*, 1989) and dorsal root ganglion neurones (Robertson, 1989) with pentobarbitone and etomidate. More recently it has also been observed in experiments involving high concentrations of propofol in embryonic murine hippocampal neurones (Orser *et al.*, 1994).

In all these cases the blocking action of these drugs is manifested as a surge current following their application at relatively high concentrations. The present study suggests that the blocking effect of propofol is independent of voltage. GABA$_A$ receptor block by pentobarbitone also appears to be independent of voltage (Robertson, 1989). Taken together, these observations suggest that GABA$_A$ receptor inhibition by these anaesthetics is not due to a channel block similar to that seen at the N-methyl-D-aspartate receptor with charged blocking compounds such as the dissociative anaesthetic, ketamine (Halliwell *et al.*, 1989).

The onset of block and the appearance of the surge current are probably too rapid to represent the onset and recovery from propofol-evoked desensitization (Orser *et al.*, 1994). The suggestion that this phenomenon is not related to desensitization is supported by the observation of smaller surge currents following longer, desensitizing applications of propofol. The most likely explanation would seem to be a low-affinity propofol site on the GABA$_A$ receptor through which the agent allosterically inhibits channel gating. This site is presumably only accessed at high concentrations and rapidly left during wash, resulting in the appearance of a surge current caused by propofol still bound at its agonist site.

Thus propofol may have three modulatory sites on the GT1-7 cell GABA$_A$ receptor for potentiation, activation and inhibition. These sites may all have different subunit specificities, but do not appear to require the γ subunit. The prevalence of agonist and inhibitory sites on different receptor subtypes may influence the apparent efficacy of propofol as a GABA$_A$ receptor activator and perhaps also as a general anaesthetic.

This work was supported by a grant to T.G.H. from The National Institute of General Medical Sciences, U.S.A. (GM48456).

References

ADODRA, S. & HALES, T.G. (1994). Propofol: A low efficacy activator of GABA$_A$ receptors in GT1-7 cells. *Soc. Neurosci. Abst.*, **20**, 511.

ANGELOTTI, T.P. & MACDONALD, R.L. (1993). Assembly of GABA$_A$ receptor subunits: $\alpha1\beta1$ and $\alpha1\beta\gamma2S$ subunits produce unique ion channels with dissimilar single-channel properties. *J. Neurosci.*, **13**, 1429–1440.

BOSMA, M.M. (1993). Ion channel properties and episodic activity in isolated immortalized gonadotropin-releasing hormone (GnRH) neurons. *J. Memb. Biol.*, **136**, 85–96.

BURT, D.R. & KAMATCHI, G.L. (1991). GABA$_A$ receptor subtypes: from pharmacology to molecular biology. *FASEB J.*, **5**, 2916–2923.

COTTRELL, G.A., LAMBERT, J.J. & PETERS, J.A. (1987). Modulation of GABA$_A$ receptor activity by alphaxalone. *Br. J. Pharmacol.*, **90**, 491–500.

DRAGUHN, A., VERDORN, T.A., EWERT, M., SEEBURG, P.H. & SAKMANN, B. (1990). Functional and molecular distinction between recombinant rat GABA$_A$ receptor subtypes by Zn^{2+}. *Neuron*, **5**, 781–788.

FRANKS, N.P. & LIEB, W.R. (1994). Molecular and cellular mechanisms of general anaesthesia. *Nature*, **367**, 607–614.

HALES, T.G., KIM, H., LONGONI, B., OLSEN, R.W. & TOBIN, A.J. (1992). Immortalized hypothalamic GT1-7 neurons express functional γ-aminobutyric acid type A receptors. *Mol. Pharmacol.*, **42**, 197–202.

HALES, T.G. & LAMBERT, J.J. (1991). The actions of propofol on inhibitory amino acid receptors of bovine adrenomedullary chromaffin cells and rodent central neurones. *Br. J. Pharmacol.*, **104**, 619–628.

HALES, T.G. & LAMBERT, J.J. (1992). Modulation of GABA$_A$ and glycine receptors by chlormethiazole. *Eur. J. Pharmacol.*, **210**, 239–246.

HALES, T.G. & OLSEN, R.W. (1994). Basic pharmacology of intravenous induction agents. In *The Pharmacological Basis of Anesthesiology: Basic Science and Clinical Applications* ed. Bowdle, T.A., Horita, A.H., Karasch, E.D. pp. 295–306. Chichester: Churchill Livingstone Inc.

HALES, T.G., SANDERSON, M.J. & CHARLES, A.C. (1994). GABA has excitatory actions on GnRH-secreting immortalized hypothalamic (GT1-7) neurons. *Neuroendocrinol.*, **59**, 297–308.

HALES, T.G. & TYNDALE, R.F. (1994). Few cell lines with GABA$_A$ mRNAs have functional receptors. *J. Neurosci.*, **14**, 5429–5436.

HALLIWELL, R.F., PETERS, J.A. & LAMBERT, J.J. (1989). The mechanism of action and pharmacological specificity of the anticonvulsant NMDA antagonist MK-801: a voltage clamp study on neuronal cells in culture. *Br. J. Pharmacol.*, **96**, 480–494.

HARA, M., KAI, Y. & IKEMOTO, Y. (1993). Propofol activates GABA$_A$ receptor-chloride ionophore complex in dissociated hippocampal pyramidal neurons of the rat. *Anesthesiol.*, **79**, 781–788.

HARA, M., KAI, Y. & IKEMOTO, Y. (1994). Enhancement by propofol of the γ-animobutyric acidA response in dissociated hippocampal pyramidal neurons of the rat. *Anesthesiol.*, **81**, 988–994.

HARRISON, N.L., MAJEWSKA., M.D., HARRINGTON, J.W. & BARKER, J.L. (1987). Structure-activity relationships for steroid interaction with the γ-aminobutyric acidA receptor complex. *J. Pharmacol. Exp. Ther.*, **241**, 346–353.

HORNE, A.L., HARKNESS, P.C., HADINGHAM, K.L., WHITING, P. & KEMP, J.A. (1993). The influence of the γ2L subunit on the modulation of responses to GABA$_A$ receptor activation. *Br. J. Pharmacol.*, **108**, 711–716.

JONES, M.V., BROOKS, P.A. & HARRISON, N.L. (1992). Enhancement of γ-aminobutyric acid-activated Cl^- currents in cultured rat hippocampal neurones by three volatile anaesthetics. *J. Physiol.*, **449**, 279–293.

JONES, M.V., HARRISON, N.L., PRITCHETT, D.B. & HALES, T.G. (1995). Modulation of the GABA$_A$ receptor by propofol is independent of the γ subunit. *J. Pharmacol. Exp. Ther.*, (in press).

LAURIE, D.J., SEEBURG, P.H. & WISDEN, W. (1992). The distribution of 13 GABA$_A$ receptor subunit mRNAs in the rat brain. II. Olfactory bulb and cerebellum. *J. Neurosci.*, **12**, 1063–1076.

MACDONALD, R.L., SKERRITT, J.H. & WERZ, M.A. (1986). Barbiturate and benzodiazepine actions on mouse neurons in cell culture. In *Molecular and Cellular Mechanisms of Anesthetics*. ed. Roth, S.S. & Miller, K.W. pp. 17–25. New York & London: Plenum Press.

MELLON, P.L., WINDLE, J.J., GOLDSMITH, P.C., PADULA, C.A., ROBERTS, J.L. & WEINER, R.I. (1990). Immortalization of hypothalamic GnRH neurons by genetically targeted tumorigenesis. *Neuron.*, **5**, 1–10.

NOBLE, P.J., ANDERSON, S.M., DE SOUZA, R.J., CROSS, A.J. & STEPHENSON, F.A. (1993). Identification of the GABA$_A$ receptor α3 subunit in the IMR-32 neuroblastoma cell line. *J. Neurochem.*, **61**, 752–755.

OLSEN, R.W. & TOBIN, A.J. (1990). Molecular biology of GABA$_A$ receptors. *FASEB J.*, **4**, 1469–1480.

ORSER, B.A., WANG, L.-Y., PENNEFATHER, P.S. & MACDONALD, J.F. (1994). Propofol modulates activation and desensitization of GABA$_A$ receptors in cultured murine hippocampal neurons. *Neurosci.*, **14**, 7747–7760.

PETERS, J.A., LAMBERT, J.J. & COTTRELL, G.A. (1989). An electrophysiological investigation of the characteristics and function of GABA$_A$ receptors on bovine adrenomedullary chromaffin cells. *Pflügers Arch.*, **415**, 95–103.

PRITCHETT, D.B. & SEEBURG, P.H. (1990). γ-Aminobutyric acidA receptor α5-subunit creates novel type II benzodiazepine receptor pharmacology. *J. Neurochem.*, **54**, 1802–1804.

PRITCHETT, D.B., SONTHEIMER, H., SHIVERS, B.D., YMER, S., KETTENMANN, H., SCHOFIELD, P.R. & SEEBURG, P.H. (1989). Importance of a novel GABA$_A$ receptor subunit for benzodiazepine pharmacology. *Nature*, **338**, 582–585.

PUIA, G., SANTI, M.R., VICINI, S., PRITCHETT, D.B., PURDY, R.H., PAUL, S.M., SEEBURG, P.H. & COSTA, E. (1990). Neurosteroids act on recombinant human GABA$_A$ receptors. *Neuron.*, **4**, 759–765.

PUIA, G., VICINI, S., SEEBURG, P.H. & COSTA, E. (1991). Influence of recombinant γ-aminobutyric acid-A receptor subunit composition on the action of allosteric modulators of γ-aminobutyric acid-gated Cl^- currents. *Mol. Pharmacol.*, **39**, 691–696.

ROBERTSON, B. (1989). Actions of anaesthetics and avermectin on GABA$_A$ chloride channels in mammalian dorsal root ganglion neurones. *Br. J. Pharmacol.*, **98**, 167–176.

SANNA, E., GARAU, F. & HARRIS, R.A. (1995). Novel properties of homomeric β1 γ-aminobutyric acid type A receptors: Actions of the anesthetics propofol and pentobarbital. *Mol. Pharmacol.*, **47**, 213–217.

SCHULZ, D.W. & MACDONALD, R.L. (1981). Barbiturate enhancement of GABA-mediated inhibition and activation of chloride ion conductance: correlation with anticonvulsant and anesthetic actions. *Brain Res.*, **209**, 177–188.

SHIMADA, S., CUTTING, G. & UHL, G.R. (1992). γ-Aminobutyric acid A or C receptor? γ-Aminobutyric acid rho 1 receptor RNA induces bicuculline-, barbiturate-, and benzodiazepine-insensitive γ-aminobutyric acid responses in *Xenopus* oocytes. *Mol. Pharmacol.*, **41**, 683–687.

SHIVERS, B.D., KILLISCH, I., SPRENGEL, R., SONTHEIMER, H., KOHLER, M., SCHOFIELD, P.R. & SEEBURG, P.H. (1989). Two novel GABA$_A$ receptor subunits exist in distinct neuronal subpopulations. *Neuron.*, **3**, 327–337.

SMART, T.G. & CONSTANTI, A. (1990). Differential effect of zinc on the vertebrate GABA$_A$-receptor complex. *Br. J. Pharmacol.*, **99**, 643–654.

SMART, T.G., MOSS, S.J., XIE, X. & HUGANIR, R.L. (1991). GABA$_A$ receptors are differentially sensitive to zinc: dependence on subunit composition. *Br. J. Pharmacol.*, **103**, 1837–1839.

TYNDALE, R.F., HALES, T.G., OLSEN, R.W. & TOBIN, A.J. (1994). Distinctive patterns of GABA$_A$ receptor subunit mRNAs in 13 cell lines. *J. Neurosci.*, **14**, 5417–5428.

VERDOORN, T.A. (1994). Formation of heteromeric γ-aminobutyric acid type A receptors containing two different α subunits. *Mol. Pharmacol.*, **45**, 475–480.

WAFFORD, K.A., BURNETT, D.M., LEIDENHEIMER, N.J., BURT, D.R., WANG, J.B., KOFUJI, P., DUNWIDDIE, T.V., HARRIS, R.A. & SIKELA, J.M. (1991). Ethanol sensitivity of the GABA$_A$ receptor expressed in Xenopus oocytes requires 8 amino acids contained in the γ2L subunit. *Neuron.*, **7**, 27–33.

WISDEN, W., LAURIE, D.J., MONYER, H. & SEEBURG, P.H. (1992). The distribution of 13 GABA$_A$ receptor subunit mRNAs in the rat brain. I. Telencephalon, diencephalon, mesencephalon. *J. Neurosci.*, **12**, 1040–1062.

WOODWARD, R.M., POLENZANI, L. & MILEDI, R. (1992). Effects of steroids on γ-aminobutyric acid receptors expressed in Xenopus oocytes by poly(A)$^+$ RNA from mammalian brain and retina. *Mol. Pharmacol.*, **41**, 89–103.

YANG, J., ISENBERG, K.E. & ZORUMSKI, C.F. (1992). Volatile anesthetics gate a chloride current in postnatal rat hippocampal neurons. *FASEB J.*, **6**, 914–918.

YMER, S., DRAGUHN, A., WISDEN, W., WERNER, P., KEINANEN, K., SCHOFIELD, P.R., SPRENGEL, R., PRITCHETT, D.B. & SEEBURG, P.H. (1990). Structural and functional characterization of the γ1 subunit of GABA$_A$/benzodiazepine receptors. *EMBO J.*, **9**, 3261–3267.

(Received January 3, 1995
Revised March 20, 1995
Accepted April 4, 1995)

British Journal of Pharmacology (1995) 115, 961-968 © 1995 Stockton Press All rights reserved 0007-1188/95 $12.00

Application of a model to explore interspecies differences in acetylcholine M-receptor-stimulated gastric acid secretion

[1]Nicola J. Welsh, [2]Nigel P. Shankley & James W. Black

Department of Analytical Pharmacology, King's College School of Medicine & Dentistry, The Rayne Institute, 123 Coldharbour Lane, London SE5 9NU

1 Concentration-effect curves were obtained, in the absence and presence of histamine H_2-receptor blockade, to 5-methylfurmethide (5-MeF) and McN-A 343, high efficacy and low efficacy acetylcholine (ACh) M-receptor agonists, respectively, in isolated stomach preparations from the mouse and immature rat and guinea-pig.

2 In the immature guinea-pig assay, the responses to 5-MeF and McN-A 343 were abolished by histamine H_2-receptor blockade suggesting that the responses were totally dependent upon gastric mucosal histamine. However, in the mouse and immature rat assays, although the histamine H_2-receptor antagonists produced small but significant rightward shifts and, in some cases, depression of the maximum of the agonist concentration-effect curves, a significant secretory response remained, presumed to be due to direct stimulation of oxyntic cells.

3 Previously, by assuming that the histamine H_2-receptor blockade alters the mode of agonist-stimulated acid secretion from mainly an indirect action mediated by histamine release to direct stimulation of the oxyntic cell, we applied an operational model of agonism to similar data obtained in the mouse preparation. In that study we were able to account for the behaviour of 5-MeF and McN-A 343 by assuming that the agonists expressed 6 fold higher efficacy, τ in the operational model of agonism, at ACh M-receptors on the histamine-releasing cells than on the oxyntic cells. In this study it was possible to account for the variation in the behaviour of the agonists both between and within assays by simply varying the efficacy expressed by the agonists at each of the cells in the model. The efficacy variation could be due to receptor concentration variation.

4 The data and analysis are discussed in terms of contemporary models for the role of histamine in the regulation of gastric acid secretion.

Keywords: Receptor, muscarinic; parasympathomimetics; gastric acid secretion; histamine

Introduction

Although when applied exogenously histamine is a powerful stimulant of gastric acid secretion, its physiological role in the gastric mucosa remains unclear. In particular, the question of how gastrin and acetylcholine (ACh) stimulate gastric acid secretion is unresolved. Do these agents release histamine locally or is a subthreshold background of histamine needed to potentiate their activity at the oxyntic cell? In previous publications, we developed the hypothesis that they act indirectly by releasing mucosal histamine (see Black & Shankley, 1987). In this study, we have investigated the histamine-dependence of the secretory response mediated by ACh M-receptors and have continued to use this hypothesis as an initial basis for interpretation. In a previous paper (Black & Shankley, 1986), we described a study of the neural regulation of gastric acid secretion in isolated, lumen-perfused, mouse stomach preparations. We concluded that the responses produced by electrical stimulation were mediated by ACh released by preganglionic nerve stimulation. The stimulation-frequency responses could be abolished by both histamine H_2-receptor antagonists and ACh M-receptor antagonists. However, it was still possible to obtain a response to the stable ACh muscarinic agonist, 5-methylfurmethide (5-MeF), in the presence of histamine H_2-receptor blockade (Black & Shankley, 1985a). Therefore, we concluded that the neurally-released ACh acted selectively on histamine-releasing cells whereas 5-MeF stimulated ACh M-receptors located on both histamine-releasing and oxyntic cells (Black & Shankley, 1987).

These studies have now been extended to the guinea-pig and rat (Welsh *et al.*, 1994) in an attempt to explore the generality of the model developed for the mouse. In the guinea-pig, as in the mouse, histamine H_2-receptor blockade abolished the vagal response. In the rat, however, the frequency-effect curves could not be abolished by either ACh M- or histamine H_2-receptor blockade alone but were abolished by a combination of the two. This suggested that there was direct cholinergic innervation of the oxyntic cell and a non-cholinergic innervation which either involved histaminergic nerves or nerves containing another transmitter which acted to release gastric mucosal histamine. However, we could not rule out that there was also an indirect cholinergic histamine release, as in the other species (Welsh *et al.*, 1994).

In the isolated mouse stomach assay, we found that the ACh M-receptor agonist, McN-A 343, expressed lower potency than 5-MeF which appeared to be due not only to lower receptor binding affinity, but also to lower intrinsic efficacy (Black & Shankley, 1985b). Subsequently, Eglen *et al.* (1987) also reached the conclusion that McN-A 343 behaves as a low efficacy agonist at ACh M-receptors. By simultaneously applying an operational model of agonism (Black & Leff, 1983) to the 5-MeF and McN-A 343 concentration-effect curve data obtained in the absence and presence of histamine H_2-receptor blockade, we were able to estimate the relative efficacy of the agonists at both the histamine-releasing and oxyntic cells. Using the model we were able to simulate the experimental data by assuming that there was a six fold higher expression of efficacy at ACh M-receptors on the histamine cell than at those on the oxyntic cell in the mouse stomach assay (Black & Shankley, 1985b). We now report the extension of this analysis to the immature guinea-pig and rat isolated stomach preparations, in particular to ask whether there is an ACh M-receptor-mediated release of histamine in the rat assay. As part of this study, we obtained a new data set on the mouse sto-

[1] Author for correspondence.
[2] Present address: James Black Foundation, 68 Half Moon Lane, London SE24 9JE.

mach assay under identical experimental conditions to those used in the original study. Both data sets are presented because the effects of histamine H_2-receptor antagonism appeared to be different.

Methods

Isolated, lumen-perfused, whole stomach preparations

Gastric acid secretion was measured in isolated, lumen-perfused, stomach preparations essentially as described previously for the mouse (Black & Shankley, 1985c). Young adult male mice (Charles River, 22–26 g, fasted 18 h with free access to water) and pre-weaned rat pups (Wistar, 32–38 g corresponding to an age range of 10–23 days) were killed by cervical dislocation. The abdomen was opened and the oesophagus ligated close to the stomach. A polythene cannula (2 mm internal diameter) was inserted into the pylorus via the duodenal bulb and a small incision made in the fundus through which the stomach contents were gently washed. A second cannula was tied into this incision. The stomachs were then transferred into 40 ml organ baths containing buffered serosal solution (mM: NaCl 118, KCl 4.8, $MgSO_4$ 1.2, KH_2PO_4 1.14, $NaHPO_4$ 15.9, $CaCl_2$ 0.65, glucose 31.6) maintained at 37°C and gassed with 95% O_2/5% CO_2. The lumen was perfused from the fundic to the pyloric cannulae with warmed unbuffered mucosal solution (mM: NaCl 118, KCl 4.8, $MgSO_4$ 1.2, $CaCl_2$ 0.65, glucose 31.6) gassed with 100% O_2, and the perfusate passed over a pH-electrode system adjusted for height to provide 12 cmH_2O intragastric pressure.

Guinea-pig mucosal sheet preparation

Immature, male guinea-pigs, weighing 180–220 g were killed by cervical dislocation, the abdomen was opened and the stomach removed. The dissection technique, employed previously for the mouse (Shankley *et al.*, 1988), was adapted from that described by Main & Pearce (1978) for the rat. In brief, the stomach was opened by an incision along the greater curvature and a piece of glandular mucosa gently tied to a Perspex tissue holder drilled to allow perfusion of the lumenal mucosal surface. After ligation to produce a watertight seal, the overlying muscle layer was removed from the mucosa by injecting saline between mucosal and muscle layers to create a blister so that the muscle layer could be safely excised. In all other respects the conditions were as for the whole stomach preparations except that the back pressure was reduced to 6 cmH_2O.

Experimental design

Six preparations were used simultaneously and, after a 60 min stabilization period, any not showing stable basal responses were rejected (less than 5%). Thereafter, drugs were added to the serosal solution according to individual experimental protocols. The total volume of vehicle did not exceed 1 ml and had no effect on basal gastric acid secretion in the assays.

A randomized block design was used throughout for allocation of experimental treatments such that, as far as possible, each organ bath received each treatment within the course of an experiment. The effects of histamine H_2-receptor blockade on the two agonists, 5-MeF and McN-A 343, were investigated within separate experiments except in the case of the guinea-pig mucosal sheet assay, when both agonists were studied within the same experimental protocol.

Acid secretory responses were expressed as ΔpH, that is the difference between basal pH, measured immediately prior to experimental intervention, and stimulated pH. This response metameter was chosen in preference to $[H^+]$ as a previous analysis has shown that pH values obtained under basal and stimulated conditions are normally-distributed (Shankley, 1985). Fully-defined agonist concentration-effect curves were obtained by cumulative dosing at 0.25 or 0.5 $\log_{10}$ unit intervals when stable response plateaux were achieved. In preliminary experiments, the validity of the cumulative dosing regimen was confirmed by comparing the curve maxima to the response to single, near-maximal, bolus doses (data not shown).

Data analysis

Where possible, the agonist concentration-effect curve data from individual preparations were fitted, using a computer programme based on the procedure described by Parker & Waud (1971), to a general logistic function to provide esti-

Table 1 Logistic curve-fitting parameters (±s.e.mean) for 5-methylfurmethide (5-MeF) and McN-A 343 concentration-effect curves obtained in the absence and presence of histamine H_2-receptor blockade (100 μM tiotidine or 20 μM famotidine for the guinea-pig assay) in isolated stomach preparations of mouse, and immature guinea-pig and rat

	n	$\log[A_{50}]$	p	$\alpha(\Delta pH)$
Mouse				
5-MeF	6	−7.67 ± 0.07	1.64 ± 0.09	0.54 ± 0.04
5-MeF (+H_2-block)	6	−7.40 ± 0.07	2.38 ± 0.25	0.36 ± 0.04
McN-A 343	6	−5.10 ± 0.10	1.00 ± 0.14	0.63 ± 0.10
McN-A 343 (+H_2-block)	6	−4.66 ± 0.11	2.11 ± 0.32	0.38 ± 0.09
Guinea-pig				
5-MeF	4	−7.23 ± 0.17	1.40 ± 0.36	0.55 ± 0.07
5-MeF (+H_2-block)	5		NF	−0.02 ± 0.08
McN-A 343	5	−4.78 ± 0.12	0.86 ± 0.19	0.34 ± 0.06
McN-A 343 (+H_2-block)	6		NF	0.00 ± 0.09
Rat				
5-MeF	8	−7.36 ± 0.02	3.92 ± 0.38	0.60 ± 0.06
5-MeF (+H_2-block)	8	−7.10 ± 0.05	2.80 ± 0.30	0.37 ± 0.03
McN-A 343	7		NF	0.13 ± 0.05
McN-A 343 (+H_2-block)	9		NF	0.12 ± 0.03

NF = not fitted.

mates of the midpoint location ($\log[A_{50}]$), midpoint slope parameter (p) and upper asymptote (α) as described previously (Black & Shankley, 1985c). For analysis and display purposes the individual computed parameter estimates for each treatment group were expressed as mean ± s.e.mean and single logistic curves simulated shown superimposed upon the experimental data. Computed logistic curve-fitting parameters were compared using Student's t test. Values of $P<0.05$ were considered significant.

Operational model of agonism

Previously, we were able to account quantitatively for the data obtained on the mouse stomach assay (Black & Shankley, 1985b) using an operational model of agonism (Black & Leff, 1983). In the present study, simulations were obtained using the following form of the model which describes agonist concentration-effect data in terms of four parameters,

$$E = \frac{E_m[A]^n\tau^n}{(K_A+[A])^n+[A]^n\tau^n},$$

where E is pharmacological effect, [A] is agonist concentration, K_A is the agonist equilibrium dissociation constant, n is the slope of the transducer function relating occupancy to effect and τ is the efficacy parameter or transducer ratio which is given by the ratio of the total receptor concentration ($[R_0]$) and the midpoint location parameter of the transducer function (K_E). E_m is the maximum pharmacological effect.

The goodness-of-fit of the model simulations to the experimental data was assessed using a chi-squared analysis where chi-squared was calculated by comparing the mean observed data points with the expected values obtained by model simulation using the following equation:

$$\chi^2=\sum\frac{(\text{observed-expected})^2}{\text{m.(expected}^2)+\text{c}},$$

where the denominator is a correction factor applied to account for the fact that an approximately linear relationship was found between the observed variance (σ^2) and the square of the observed effect values for the data from each assay and the values of c and m were estimated from a linear regression analysis of these data. In this way the chi-squared value was corrected to account for any differences in the amplitude of the 5-MeF and McN-A 343 concentration-effect curves within an assay.

Drugs

Tiotidine (a gift from Imperial Chemical Industries Ltd.) and famotidine (a gift from Merck, Sharp and Dohme Ltd.) were dissolved in dilute HCl to give 0.2 mM stock solutions. Nifedipine (Sigma Chemical Co. Ltd.) was dissolved in 100% ethanol to give a 20 mM stock solution; subsequent dilutions were made in distilled water. Isoprenaline hydrochloride (Sigma Chemical Co. Ltd.) was dissolved and diluted in stoichiometric aqueous ascorbic acid to prevent oxidation. All other compounds were dissolved in distilled water and sources were: atropine sulphate (Sigma Chemical Co. Ltd.); 5-methylfurmethide iodide (a gift from Wellcome Foundation Ltd.); McN-A 343 (4-(*m*-chlorophenylcarbamoyloxy)-2-butynyl-trimethylammonium chloride, (a gift from McNeil Laboratories U.S.A. Ltd.).

Results

Effect of histamine H_2-receptor blockade on 5-methylfurmethide and McN-A 343 concentration-effect curves in isolated stomach assays

Single concentrations of selective histamine H_2-receptor antagonists (100 μM tiotidine or 20 μM famotidine for the guinea-pig assay) were used to obtain H_2-receptor blockade. These concentrations were at least one thousand-fold greater than the K_B values estimated on the stomach assays when histamine was used as agonist (Black *et al.*, 1985a; Welsh *et al.*, 1992). These concentrations had no significant effect on basal acid secretion in any of the assays. We have assumed

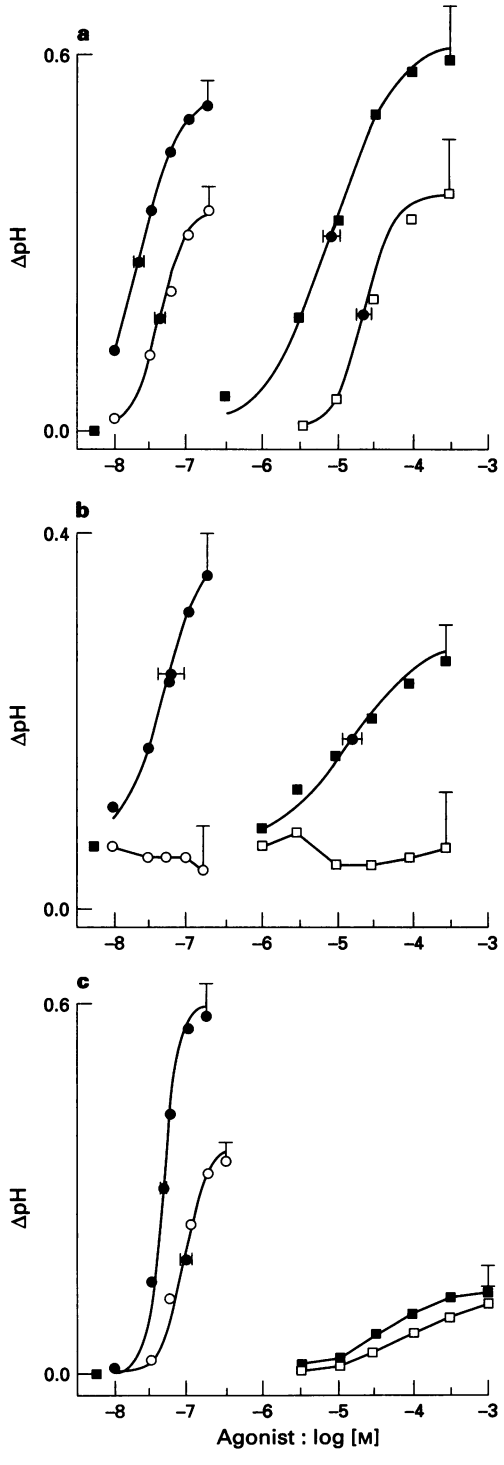

Figure 1 Agonist concentration-effect curves obtained with 5-methylfurmethide (●,○) and McN-A 343 (■,□) in the absence (closed symbols) and presence (open symbols) of histamine H_2-receptor block (100 μM tiotidine or 20 μM famotidine for the guinea-pig assay). Data are shown from (a) the current mouse stomach study, (b) immature guinea-pig and (c) immature rat. The curves shown superimposed on the mean experimental data points ($n=4/9$ ± s.e.mean) were obtained by logistic curve-fitting (for details see methods).

that these concentrations produced essentially the maximum achievable blockade of endogenous histamine. The receptor selectivity of the agents at these high concentrations was evaluated (data not shown) by investigating the effects of tiotidine and famotidine on 5-MeF curves obtained on an ACh M-receptor assay, the guinea-pig isolated gall bladder (Bishop *et al.*, 1992). Tiotidine (100 μM) had no significant effect. Famotidine (20 μM) produced a small, parallel shift (dose-ratio = 3.1) of the 5-MeF concentration-effect curve. However, famotidine was used only in the guinea-pig stomach preparation where its effect could not possibly be confused with this small shift (see below). The switch to famotidine for the guinea-pig assay experiments was made simply because our supply of tiotidine was exhausted.

Mouse stomach The effect of the histamine H_2-receptor antagonism was assessed by its effect on the concentration-effect logistic curve-fitting parameters (Table 1). In the mouse assay, tiotidine (100 μM) produced a small but significant rightward shift and steepening of both the 5-MeF and McN-A 343 concentration-effect curves. The upper asymptote (α) of the 5-MeF curve was significantly reduced by 33%. The mean value of the McN-A 343 curve maximum was also reduced by 40% but because of exceptionally large variances this difference was not statistically significant as tested at the 95% confidence level (Table 1, Figure 1a).

In the original mouse stomach study tiotidine (100 μM) produced a small, but significant, shift (dose-ratio $\sim$6) and significant steepening of the 5-MeF concentration-effect curve with no change in maximum asymptote (Black & Shankley, 1985a; Figure 2a). The McN-A 343 concentration-effect curve was both significantly shifted to the right and depressed by 85% in the presence of 30 μM tiotidine (Figure 2a). In the present study, the curves obtained in the mouse stomach assay were not as steep as their counterparts in the original study.

Immature guinea-pig 5-MeF did not produce consistent, concentration-dependent, acid secretory responses in the guinea-pig whole stomach assay which had been used in previous studies on vagal stimulation of gastric acid secretion (Welsh *et al.*, 1994). The problem was that powerful, 5-MeF-induced, contractions of the fundic smooth muscle interfered with the lumen perfusion. Attempts were made to antagonize functionally the muscle contraction with either the β-adrenoceptor agonist, isoprenaline (100 μM), or the calcium channel blocker, nifedipine (1 μM). Neither was found to improve the assay. Therefore, a mucosal sheet preparation was used in which the serosal muscle layer had been stripped away by the technique described by Main & Pearce (1978). The effect of preparing the mucosal sheet assay on the integrity of the gastric mucosa and, in particular, on the integrity of responses apparently mediated by histamine release, was assessed by comparing pentagastrin and histamine concentration-effect curves obtained on both the sheet and intact stomach assays. We have shown previously that the pentagastrin response is abolished by histamine H_2-receptor blockade in the immature guinea-pig isolated stomach preparation (Shankley *et al.*, 1992). The pentagastrin and histamine concentration-effect curves obtained on the sheet and intact stomach assay apparently differed only in amplitude. Both agonists had a smaller maximum response (α) in the sheet assay as might be expected for a smaller secretory surface area (Table 2).

In the gastric mucosal sheet assay, 5-MeF and McN-A 343, like histamine and pentagastrin, produced concentration-dependent acid secretion. The upper asymptote of the McN-A 343 curve was significantly lower than that obtained with 5-MeF (Table 1) and the responses to both agonists were totally abolished by histamine H_2-receptor blockade (20 μM famotidine, Figure 1b).

Immature rat In the rat assay, the control 5-MeF curve was approximately twice as steep as those obtained in the mouse and guinea-pig assays although 5-MeF was approximately equipotent in the three assays (Table 1, Figure 1c). In the presence of tiotidine (100 μM) the 5-MeF-curve was shifted to the right (dose-ratio $\sim$2) and depressed but, in contrast to the result in the mouse stomach, the curve was significantly flattened. McN-A 343 behaved as a partial agonist with respect to 5-MeF in the absence and presence of histamine H_2-receptor blockade. It was not possible to fit the McN-A 343 data to the logistic function due to the poor definition of some of the individual curves. However, inspection of the mean data (Figure 1c), suggests that histamine H_2-receptor blockade did not produce a large change in the shape or location of the curves.

Application of an operational model of agonism

As in our previous analysis (Black & Shankley, 1985b), it was assumed that histamine H_2-receptor blockade converted ACh M-receptor agonist activity by an indirect action due to histamine release to a direct muscarinic action on the oxyntic cells. For simplicity and in the absence of information to the contrary, the ACh M-receptors were assumed to be identical in all species and on both the histamine-releasing and oxyntic cells. Therefore, the same K_A values were used to stimulate each 5-MeF and McN-A 343 curve. The K_A values for 5-MeF (2.4 μM) and McN-A 343 (15 μM) were fixed at those values estimated by Leff *et al.* (1985) on guinea-pig trachea and Van Rossum (1962) on the rat intestine, respectively. The [A_{50}] values of the 5-MeF concentration-effect curves (Table 1) were all at least 30 fold lower than the K_A value so that, according to the model of agonism, 5-MeF could be considered to behave as a high efficacy agonist in all assays in both the absence and presence of histamine H_2-receptor blockade. Previously, it has been shown that the transducer slope parameter, n, and the maximum effect, E_m, in the operational model of agonism are indistinguishable from the slope (p) and upper asymptote (α), respectively, of the concentration-effect curves obtained with high efficacy agonists (Black *et al.*, 1985b). Therefore, out of necessity, the values of n and E_m were fixed at the values of p and α, respectively, estimated for the 5-MeF curves obtained in

Table 2 Logistic curve-fitting parameters (± s.e.mean) for histamine and pentagastrin curves obtained on immature guinea-pig gastric sheet and whole stomach assays

	n	$log[A_{50}]$	p	$\alpha(\Delta pH)$
Mucosal sheet				
Histamine	5	−5.48 ± 0.22	1.38 ± 0.23	0.54 ± 0.05
Pentagastrin*	6	−8.20	0.76	0.10
Whole stomach				
Histamine	8	−5.67 ± 0.12	1.40 ± 0.19	0.66 ± 0.02
Pentagastrin	7	−8.29 ± 0.08	0.96 ± 0.11	0.36 ± 0.07

* Due to the small responses in some preparations it was not possible to fit all the data. Therefore the parameters shown were obtained by logistic curve-fitting the mean data.

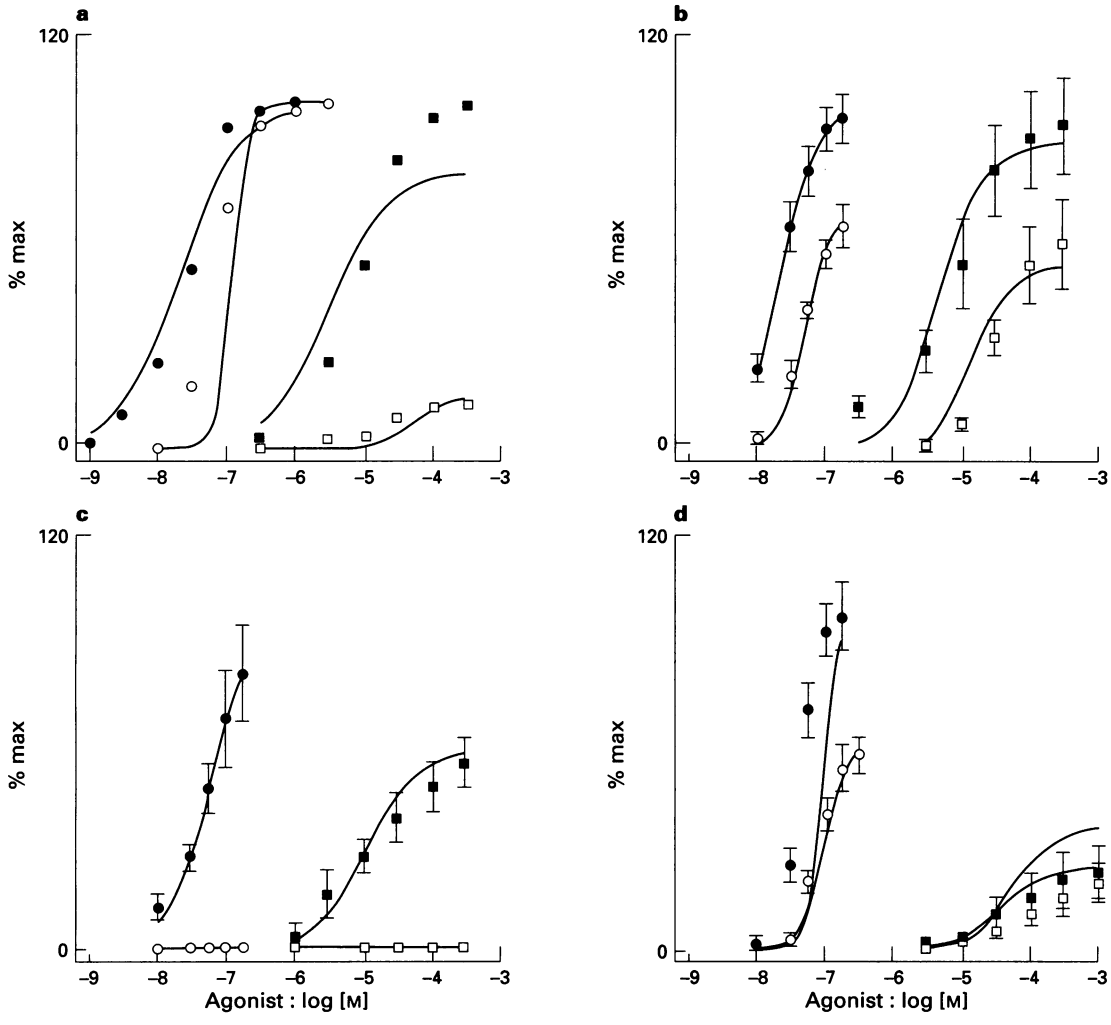

Figure 2 5-Methylfurmethide (5-MeF, ●,○) and McN-A 343 (■,□) experimental concentration-effect curve data obtained in the absence (closed symbols) and presence (open symbols) of histamine H_2-receptor blockade using concentrations of the antagonists tiotidine or famotidine equivalent to at least 300 fold their K_B values. Panels show data from (a) the original mouse stomach study (redrawn from Black & Shankley, 1985b), (b) the current mouse stomach study, (c) immature guinea-pig and (d) immature rat. The curves shown superimposed on the mean experimental data points ($n=4/9 \pm$ s.e.mean) were obtained using an operational model of agonism (see methods). The 5-MeF and McN-A 343 K_A values were fixed at 2.4 and 15 μM, respectively and the following additional parameter values were used in the simulations:

	E_M	n	τ
(a) Original mouse			
5-MeF	100	1.0	120
5-MeF (+100 μM tiotidine)	100	3.8	20
McN-A 343	100	1.0	4
McN-A 343(+30 μM tiotidine)	100	3.8	0.67
(b) Mouse			
5-MeF	100	1.6	110
5-MeF (+100 μM tiotidine)	70	2.4	50
McN-A 343	100	1.6	3.7
McN-A 343(+100 μM tiotidine)	70	2.4	1.7
(c) Immature guinea-pig			
5-MeF	100	1.4	39
5-MeF (+20 μM famotidine)*	0	–	–
McN-A 343	100	1.4	1.3
McN-A 343(+20 μM famotidine)*	0	–	–
(d) Immature rat			
5-MeF	100	3.9	27
5-MeF (+100 μM tiotidine)	60	2.8	27
McN-A 343	100	3.9	0.9
McN-A 343(+100 μM tiotidine)	60	2.8	0.9

* The response obtained in the presence of histamine H_2-receptor blockade was not significantly different from zero and was therefore assumed to be zero for simulation purposes.

the absence and presence of histamine H_2-receptor blockade (Table 1). To facilitate the simulation and comparison of the data obtained across species, the effect data with both agonists were normalized to these E_m values. Furthermore, when there was no significant difference between the control maximum effect obtained with 5-MeF and McN-A 343 both were considered to be equal to 100%. Thus, the constraints introduced by making the assumption that 5-MeF was a high efficacy agonist had the effect of leaving only the efficacy parameter, τ, in the model to account for the variation in the behaviour of the agonists in the absence and presence of H_2-receptor blockade both between and within species. Therefore, values of τ were determined maintaining a constant ratio between the 5-MeF and McN-A 343 values in all experimental data sets as would be expected for a pair of agonists acting at the same class of receptor. The τ ratio was fixed at 30 which was the value previously estimated in the mouse stomach.

The simulations and parameter values determined, including the original mouse stomach assay data and model simulation (Black & Shankley, 1985b), are presented in Figure 2. Chi-squared analysis indicated that there were no significant differences ($P>0.05$) between the observed and expected values for the model simulations of the guinea-pig ($\chi^2=8.96$; d.f. = 6) and new mouse stomach data ($\chi^2=17.58$; d.f. = 12). In contrast, according to the analysis, the model did not provide an adequate description of the data obtained in the rat assay ($\chi^2=255.2$; d.f. = 14; $P>0.05$). For reasons discussed below, the rat stomach data were resimulated with the constraint of the τ ratio between 5-MeF and McN-A 343 removed in the absence of histamine H_2-receptor blockade (Figure 3). By increasing the τ ratio from 30 to 75 we were able to obtain a reasonable description of the data ($\chi^2=15.39$; d.f. = 14; $P<0.05$).

Discussion

Our original hypothesis, which evolved to account for the differential effects of histamine H_2-receptor blockade on 5-MeF and McN-A 343 concentration-effect curves obtained in the mouse stomach preparation, was that ACh M-receptors were present on both histamine-releasing and oxyntic cells in the gastric mucosa. Accordingly, histamine H_2-receptor blockade was assumed to switch ACh M-receptor agonist activity due to an indirect action mediated by histamine release to a direct muscarinic action on the oxyntic cells. The ACh M-receptors on the histamine-releasing and the oxyntic cells were judged to be identical and probably of the M_2- or M_3-receptor subtype because the pK_B estimates (~6.8) made for pirenzepine, the selective ACh M-receptor antagonist, were indistinguishable in the absence and presence of histamine H_2-receptor blockade when 5-MeF was used as agonist and when McN-A 343 was used as agonist in the absence of histamine H_2-receptor blockade (Black & Shankley, 1985a,b). Although we cannot apply the more rigorous methods of simulation and significance testing applied to the current data, nevertheless, at that time we believed that we were able to account for the data using an operational model of agonism (Black & Leff, 1983). In the model we assumed that the agonists expressed 6 fold higher efficacy at ACh M-receptors located on the histamine-releasing cells than at those receptors on the oxyntic cells. In model terms, 5-MeF behaved as a high efficacy agonist at both cells whereas McN-A 343, expressing lower efficacy, behaved as a partial agonist (see Figure 2a) with a τ ratio of 30.

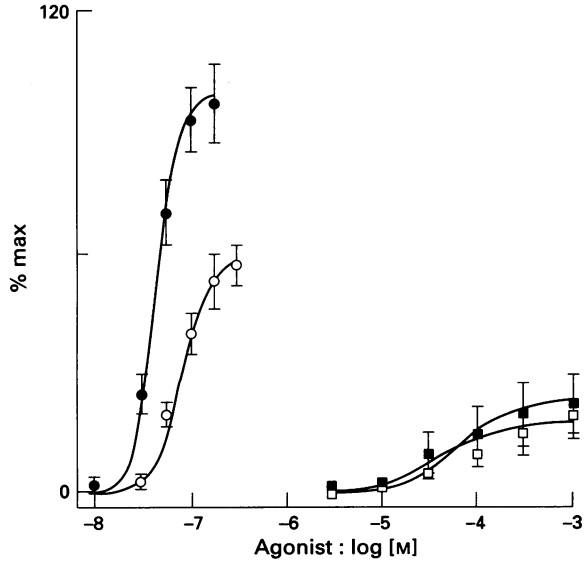

Figure 3 5-Methylfurmethide (5-MeF, ●,○) and McN-A 343 (■,□) experimental concentration-effect curve data obtained in the absence (closed symbols) and presence (open symbols) of histamine H_2-receptor block (100 μM tiotidine) obtained on the immature rat stomach. The curves shown superimposed on the mean experimental data points ($n=7/9\pm$s.e.mean) were obtained using an operational model of agonism (Black & Leff, 1983) as described in the text. In contrast to the simulations shown in Figure 2d, the τ values of the agonists were as follows: 5-MeF, 55; 5-MeF (+H_2-block), 27; McN-A 343, 0.75; McN-A 343 (+H_2-block), 0.9.

In this study, the logistic curve-fitting procedure allowed the comparison of the agonist concentration-effect curves obtained within and between the different experiments (Figure 1 and Table 1). Evidently, there was considerable variation in the data obtained between the species and also, perhaps unexpectedly, between the original and current mouse stomach assay data (Figure 2). The operational model of agonism (Black & Leff, 1983) was applied to determine whether the within and between assay variation in the mouse could be accounted for by the original hypothesis. According to the model, the values of the tissue-dependent parameters (E_m and n) were dictated by the behaviour of the high efficacy agonist, 5-MeF, and values of the agonist equilibrium dissociation constants (K_A) were held fixed at the values used in the original analysis as though the agonists could not discriminate between any of the ACh M-receptors expressed in the assays. Despite the fact that the model simulation presented in the original study was not a particularly good fit, we decided to accept initially the constraint of the τ ratio of 30 chosen in that analysis because a constant ratio across all the data sets is needed to satisfy the hypothesis. The only available variable was the absolute value for τ for the agonists in each tissue. With these constraints, it was possible to simulate the new mouse data by assuming simply that the τ values of 5-MeF ($\tau=50$) and McN-A 343 ($\tau=1.7$) at the oxyntic cell receptor had increased from the original values by 2.5 fold and, in fact, a much better fit was obtained with this new data set (Figure 2).

In the model, τ is defined by $[R_0]/K_E$ and we cannot determine from these data whether the change was due to an increase in ACh M-receptor concentration and/or an increase in the efficiency of receptor-effector coupling. The increase in agonist efficacy between the two mouse stomach experiments is equivalent to a 0.4 log unit leftward shift of a high efficacy agonist concentration-effect curve according to the operational model of agonism. In our experience, this degree of shift in agonist potency is often encountered within the range of replicate $[A_{50}]$ estimates even in the most robust of isolated tissue bioassays. Previously, we expressed a preference for receptor concentration as the source of variation in the action of 5-MeF and McN-A 343 between histamine-releasing and oxyntic cells (Black & Shankley, 1985a,b) on the basis that receptor concentration is the simplest choice in model terms and is being increasingly recognised as a biological variable. We are still not aware of any reported variation in the number of ACh M-receptors on these cells. However, such variation has been reported for other gastrointestinal hormone receptors, for example, Rubin *et al.* (1988) found that rats, both fed and

starved, exhibited a four fold circadian variation in fundic mucosal gastrin receptor concentration expressed in terms of number of binding sites per mg protein.

In the guinea-pig stomach preparation histamine H_2-receptor blockade abolished the effects of both the agonists (Figure 1b). Therefore, it was possible to simulate the data using the model of agonism simply by assuming that the value of τ at the oxyntic cell ACh M-receptors in the model was too low for the expression of agonism (Figure 2c). The response to electrical field stimulation of the vagus, which could be abolished by atropine, was also abolished by histamine H_2-receptor blockade in this species (Welsh *et al.*, 1994). Previously, we have argued (Black & Shankley, 1987) that, in the mouse, ACh was restricted to the region of the histamine-releasing cells by neural configuration and by acetylcholinesterase (AChE) activity. This view was confirmed by the finding that, following inhibition of AChE, frequency-effect curves were still obtained in the presence of histamine H_2-receptor blockade as though ACh could now diffuse to the oxyntic cells (Black & Shankley, 1987). Unfortunately, we were unable to perform a similar test in the guinea-pig preparation because the AChE inhibitor, physostigmine, produced powerful contractions of the guinea-pig fundic smooth muscle which interfered with the lumen-perfusion of the preparation (Welsh *et al.*, 1994). This has still to be examined in the guinea-pig, isolated, gastric mucosal sheet preparation.

In the current data set, the poorest model simulations were obtained with the immature rat stomach assay data (Figure 2d). Evidently, the simple model could not describe the data. Nevertheless, the elements of the simple model must still apply to the rat. The effects of 5-MeF are partially removed by histamine H_2-receptor blockade indicating, presumably, the presence of ACh M-receptors on histamine-releasing cells. The remainder of the 5-MeF-induced secretion is assumed to be due to direct activation of ACh M-receptors on oxyntic cells. If the model is still applicable qualitatively but fails quantitatively, the failure must be due to application of inappropriate assumption-led constraints. For example, the model assumption that the ACh M-receptors are homogeneous across the species with respect to McN-A 343 and 5-MeF could be flawed. This would allow for variation in the values of the model parameters τ and K_A for each agonist. Clearly, this degree of parameter value flexibility would greatly reduce the analytical value of the model. However, we are not aware of any compelling evidence for different ACh M-receptors on oxyntic and histamine-secreting cells within or between species.

We also explored the validity of the primary assumption that histamine H_2-receptor blockade simply converted ACh M-receptor stimulation from a single action on histamine-releasing cells to a single action on oxyntic cells. Inspection of the 5-MeF curves obtained in the rat in the absence and presence of histamine H_2-receptor blockade (Figure 1) reveals that the location of the curves overlap to some extent so that the control curve may have an additional component due to direct oxyntic cell activation. The fact that the simple model provided a reasonable description of the mouse and guinea-pig data suggests that if there was an interaction between the direct and indirect pathways in the control curves then it was not very large. In contrast, there were features of the data obtained in the rat which suggested that the 5-MeF control concentration-effect curve could be the product of a potentiating interaction between released histamine and 5-MeF. First, the curve was approximately twice as steep as that obtained in the mouse and guinea-pig assays (Table 1). Second, the curve slope parameter was reduced in the presence of histamine H_2-receptor blockade whereas in the mouse and guinea-pig the slope increased. In agreement with this observation, we have previously found that histamine H_2-receptor blockade decreased the slope of a frequency-effect curve obtained by electrical stimulation of the vagus nerve in the rat assay (Welsh *et al.*, 1994).

Potentiating interactions at the level of the oxyntic cell were originally conceived by Grossman & Konturek (1974) and subsequently demonstrated directly by Soll (1978). A formal model and, hence mathematical description, of the oxyntic cell potentiating interactions has not been reported. However, intuitively, steep concentration-effect curves might be expected if the stimuli produced by the activation of the two oxyntic cell receptors interacted in a super-additive manner. In terms of the operational model of agonism applied in this study, this would lead to 5-MeF expressing apparently higher efficacy than expected if it was acting solely by the release of histamine. The 5-MeF and McN-A 343 curves obtained in the presence of histamine H_2-receptor blockade would not be expected to be confounded by potentiation because any such interaction was blocked. Indeed, examination of the model simulation (Figure 2d) suggested that the τ ratio of 30 could be maintained for this pair of curves if they were simulated in isolation. A much improved fit was obtained when the data were re-simulated with the τ ratio only allowed to vary for the 5-MeF and McN-A 343 curves obtained in the absence of histamine H_2-receptor blockade (Figure 3). The increase in τ ratio between 5-MeF and McN-A 343 required to account for the data indicates that the degree of potentiation is proportional to the agonist intrinsic efficacy as expected. Thus, it was necessary to increase the absolute values of τ for 5-MeF but not McN-A 343.

In conclusion, the acid secretory response to ACh M-receptor stimulation and the interaction with histamine H_2-receptor antagonists are significantly different between the guinea-pig, mouse and rat preparations. As in previous publications we have interpreted the effects of H_2-receptor blockade in terms of histamine-secreting cells being functionally-coupled to oxyntic cells. The application of the model of agonism to the data suggests that the differences could be due simply to variations in the efficacy of the agonist expressed at ACh M-receptors on histamine-secreting and oxyntic cells and between species. The ability of the model of agonism to account for the data obtained between and within tissues by varying the efficacy (τ) but not the affinity (K_A) parameter values suggests that efficacy and affinity can be treated, in this instance at least, as independent parameters, an assumption which has been challenged (Colquhoun, 1987). In the guinea-pig, the density of ACh M-receptors on the oxyntic cell may be insufficient to enable a direct secretory response to cholinergic stimulation, whereas in the mouse, although vagal stimulation acted only via histamine release, stable ACh M-receptor agonists may act directly on the oxyntic cell to stimulate acid secretion. In the rat, where we have previously shown that there is a non-cholinergic neuronal component which is either histaminergic or acts via release of histamine (Welsh *et al.*, 1994), the current analysis has exposed a significant ACh M-receptor mediated histamine release in this species which may act synergistically with ACh at the level of the oxyntic cell. The modelling-led conclusion is that it appears that both hypotheses for the regulation of gastric acid secretion described in the introduction need to be invoked. Interestingly, we have previously found a potentiating interaction between vagal nerve and pentagastrin stimulation of gastric acid secretion in the immature rat stomach preparation (Shankley *et al.*, 1992).

The authors would like to thank Zeneca PLC for financial support and Dr J Wood for statistical advice.

References

BISHOP, L.A., GERSKOWITCH, V.P., HULL, R.A.D., SHANKLEY, N.P. & BLACK, J.W. (1992). Combined dose-ratio analysis of cholecystokinin-receptor antagonists, devazepide, lorglumide and loxiglumide in the guinea-pig gall bladder. *Br. J. Pharmacol.*, **106**, 61–66.

BLACK, J.W. & LEFF, P. (1983). Operational models of pharmacological agonism. *Proc. R. Soc. B.*, **220**, 141–162.

BLACK, J.W. & SHANKLEY, N.P. (1985a). Pharmacological analysis of the muscarinic receptors coupled to oxyntic cell secretion in the mouse stomach. *Br. J. Pharmacol.*, **86**, 601–607.

BLACK, J.W. & SHANKLEY, N.P. (1985b). Pharmacological analysis of the muscarinic receptors involved when McN-A 343 stimulates acid secretion in the mouse isolated stomach. *Br. J. Pharmacol.*, **86**, 609–617.

BLACK, J.W. & SHANKLEY, N.P. (1985c). The isolated mouse stomach preparation of the mouse: a physiological unit for pharmacological analysis. *Br. J. Pharmacol.*, **86**, 571–579.

BLACK, J.W. & SHANKLEY, N.P. (1986). Pharmacological analysis of the inhibition by pirenzepine and atropine of vagal-stimulated acid secretion in the isolated stomach of the mouse. *Br. J. Pharmacol.*, **88**, 291–297.

BLACK, J.W. & SHANKLEY, N.P. (1987). How does gastrin act to stimulate oxyntic cell secretion? *Trends Pharmacol. Sci.*, **8**, 486–490.

BLACK, J.W., LEFF, P. & SHANKLEY, N.P. (1985a). Further analysis of anomalous pK_B values for histamine H_2-receptor antagonists on the mouse isolated stomach assay. *Br. J. Pharmacol.*, **86**, 581–587.

BLACK, J.W., LEFF, P. & SHANKLEY, N.P. (1985b). An operational model of pharmacological agonism: the effect of curve shape on agonist dissociation constant estimation. *Br. J. Pharmacol.*, **84**, 561–571.

COLQUHOUN, D. (1987). Affinity, efficacy and receptor classification: is the classical theory still useful? In *Perspectives on Receptor Classification*. ed. Black, J.W., Jenkinson, D.H. & Gerskowitch, V.P. pp. 103–114. New York: A.R. Liss. Inc.

EGLEN, R.M., KENNY, B.A., MICHEL, A.D. & WHITING, R.L. (1987). Muscarinic activity of McN-A-343 and its value in muscarinic receptor classification. *Br. J. Pharmacol.*, **90**, 693–700.

GROSSMAN, M.I. & KONTUREK, S.J. (1974). Inhibition of acid secretion in dog by metiamide, a histamine antagonist acting at H_2 receptors. *Gastroenterol.*, **66**, 517–521.

LEFF, P., MARTIN, G.R. & MORSE, J.M. (1985). Application of the operational model of agonism to establish conditions when functional antagonism may be used to estimate agonist dissociation constants. *Br. J. Pharmacol.*, **85**, 655–665.

MAIN, I.H.M. & PEARCE, J.B. (1978). A rat isolated mucosal sheet preparation for studying the pharmacology of gastric secretion and the synthesis or release of endogenous substances. *J. Pharmacol. Methods*, **1**, 27–38.

PARKER, R.B. & WAUD, D.R. (1971). Pharmacological estimation of drug-receptor dissociation constants. Statistical evaluation. *J. Pharmacol. Exp. Ther.*, **177**, 1–24.

RUBIN, N.H., SINGH, P., ALINDER, G., GREELEY, G.H., RAYFORD, P.L., RIETVELD, W.J. & THOMPSON, J.C. (1988). Circadian rhythms in gastrin receptors in rat fundic stomach. *Dig. Dis. Sci.*, **33**, 931–937.

SHANKLEY, N.P. (1985). Pharmacological analysis of the regulators of gastric acid secretion. *University of London, Ph.D. thesis.*

SHANKLEY, N.P., BLACK, J.W., GANELLIN, C.R. & MITCHELL, R.C. (1988). Correlation between log P (oct/H_2O) and pK_B estimates for a series of muscarinic and histamine H_2-receptor antagonists on the mouse isolated stomach assay. *Br. J. Pharmacol.*, **86**, 581–587.

SHANKLEY, N.P., WELSH, N.J. & BLACK, J.W. (1992). Histamine dependence of pentagastrin-stimulated gastric acid secretion in rats. *Yale J. Biol. Med.*, **65**, 613–619.

SOLL, A.H. (1978). The interaction of histamine with gastrin and carbamylcholine on oxygen uptake by isolated mammalian parietal cells. *J. Clin. Invest.*, **61**, 381–389.

VAN ROSSUM, J.M. (1962). Classification and molecular pharmacology of ganglionic blocking agents. *Int. J. Neuropharmacol.*, **2**, 97–110.

WELSH, N.J., SHANKLEY, N.P. & BLACK, J.W. (1992). Comparison of antagonist pK_B estimates in lumen-perfused stomach assays from guinea-pig, rat and mouse. *Br. J. Pharmacol.*, **106**, 98P.

WELSH, N.J., SHANKLEY, N.P. & BLACK, J.W. (1994). Comparative analysis of the vagal stimulation of gastric acid secretion in rodent isolated stomach preparations. *Br. J. Pharmacol.*, **112**, 93–96.

(Received December 1, 1994
Revised March 24, 1995
Accepted April 5, 1995)

British Journal of Pharmacology (1995) 115, 969-974 © 1995 Stockton Press All rights reserved 0007-1188/95 $12.00

Selective inhibition by barbiturates of the synthesis of endothelium-derived hyperpolarizing factor in the rabbit carotid artery

*Volker Lischke, Rudi Busse & [1]Markus Hecker

Centre of Physiology and *Department of Anaesthesiology, Johann Wolfgang Goethe University Clinic, Theodor-Stern-Kai 7, D-60590 Frankfurt am Main, Germany

1 Several lines of evidence suggest that both volatile and intravenous anaesthetics may interfere with the synthesis and release of endothelium-derived vasoactive factors. We have investigated the effects of three different barbiturates on the release of nitric oxide (NO) and endothelium-derived hyperpolarizing factor (EDHF) in phenylephrine (1 μM)-preconstricted, endothelium-intact ring segments of the rabbit carotid artery. The segments were pretreated with the cyclo-oxygenase inhibitor, diclofenac (1 μM), to prevent the formation of vasoactive prostanoids, such as prostacyclin (PGI_2).

2 Acetylcholine (ACh) elicited a concentration-dependent relaxation (EC_{50} 0.15 μM) in control segments which was not significantly different from the relaxant responses of segments pretreated with methohexitone (0.03-0.3 mM), phenobarbitone (0.1-0.3 mM) or thiopentone (0.1-0.3 mM).

3 Inhibition of NO synthesis with N^G-nitro-L-arginine (0.1 mM) significantly reduced the maximum relaxant response to ACh from 96 to 40%. This NO/PGI_2-independent relaxation appeared to be mediated by the release of EDHF, since it was strongly diminished in the presence of the K^+_{Ca} inhibitors, tetrabutylammonium (1-3 mM) and charybdotoxin (10 nM), following preconstriction with potassium calcium (40 mM) or removal of the endothelium. Thiopentone or methohexitone markedly attenuated the EDHF-mediated relaxant response to ACh, while phenobarbitone had no effect. The endothelium-independent relaxation elicited by sodium nitroprusside (0.01-10 μM), on the other hand, was only marginally affected by these anaesthetics.

4 The cytochrome P450 inhibitor, clotrimazole (3-100 μM), mimicked the inhibitory effect of thiopentone and methohexitone on the NO/PGI_2-independent relaxant response to ACh. Moreover the cytochrome P450-catalyzed *O*-dealkylation of 7-ethoxycoumarin by rabbit liver microsomes was inhibited in the presence of thiopentone or methohexitone (0.3-1 mM), while phenobarbitone was without effect.

5 These findings suggest that thiopentone and methohexitone selectively attenuate the EDHF-mediated relaxant response to ACh in the rabbit carotid artery, presumably by interfering with its synthesis from arachidonic acid via the cytochrome P450 epoxygenase pathway.

Keywords: Endothelium-derived hyperpolarizing factor; nitric oxide; acetylcholine; barbiturates; carotid artery; cytochrome P450

Introduction

The vascular endothelium appears to play a pivotal role in mediating some of the haemodynamic effects of anaesthetics (Johns, 1993). Previous investigations have focussed primarily on the interaction of anaesthetics with the synthesis of nitric oxide (NO) by the endothelium and/or its effect on vascular smooth muscle. From these studies it would appear that volatile anaesthetics are potent inhibitors of the NO-dependent vasodilatation at clinically relevant concentrations (Uggeri *et al.*, 1992). Moreover intravenous anaesthetics, such as barbiturates, have been shown to inhibit the endothelium-dependent dilator response to acetylcholine in certain vascular beds (Gerkens, 1987; Terasako *et al.*, 1994). It remains to be elucidated how this barbiturate effect is brought about.

In principle the vascular endothelium is capable of releasing at least three different vasoactive autacoids in response to receptor-dependent agonists: NO, prostacyclin (PGI_2), and an endothelium-derived hyperpolarizing factor (EDHF). By opening K^+_{Ca} channels this factor hyperpolarizes the underlying smooth muscle cells, hence causing a relaxation of the entire vessel wall (Chen *et al.*, 1991; Cowan & Cohen, 1991; Holzmann *et al.*, 1994; Nakashima *et al.*, 1993; Suzuki *et al.*, 1992). Moreover recent experimental evidence suggests that EDHF is a cytochrome P450-derived arachidonic acid metabolite, presumably an epoxide or a mixture thereof (Hu & Kim, 1993; Rosolowsky & Campbell, 1993; Bauersachs *et al.*, 1994; Hecker *et al.*, 1994a; Fulton *et al.*, 1995).

The aim of the present study was to identify the mechanism by which barbiturates interfere with the release of NO and EDHF in isolated segments of the rabbit carotid artery as a vascular model.

Methods

Organ bath studies

New Zealand White rabbits of either sex (1.4-3.2 kg body weight) were anaesthetized with pentobarbitone sodium (Nembutal, Sanofi, 60 mg kg^{-1}, i.v.) and exsanginuated by cutting through both the aorta and vena cava. The left and right carotid artery were dissected, cleaned of adventitial adipose and connective tissue, and cut into rings of 3-4 mm width which were mounted between K30 force transducers (Hugo Sachs Elektronik, March, Germany) and a rigid support for measurement of isometric force. Four rings were simultaneously incubated in 10 ml-organ baths (kindly made available by Hugo Sachs Elektronik), containing warmed (37°C), oxygenated (95% O_2/5% CO_2) Krebs-Henseleit solu-

[1] Author for correspondence.

tion, pH 7.4 (composition in mM: Na^+ 144.0; K^+ 5.9; Cl^- 126.9; Ca^{2+} 1.6; Mg^{2+} 1.2; $H_2PO_4^-$ 1.2; SO_4^{2-} 1.2; HCO_3^- 25.0; D-glucose 11.1) to which the cyclo-oxygenase inhibitor, diclofenac, was added at a concentration of 1 μM. Passive tension was adjusted over a 30 min equilibration period to 2 g, and the Krebs-Henseleit solution exchanged in 10 min intervals. Thereafter the segments were preconstricted with phenylephrine (1 μM) to ~2 g, and the integrity of the endothelium was tested by briefly applying 1 μM acetylcholine; segments showing <60% relaxation were discarded.

Experimental protocol

After washout of phenylephrine and acetylcholine, the rings were allowed to equilibrate for 20 min and then preconstricted again with phenylephrine (1 μM). When a stable constriction was obtained, the barbiturates or other test compounds were administered to three rings for 15 min, and a cumulative concentration-response curve to acetylcholine (0.03–10 μM) was established in the presence of the barbiturates followed by a washout period of 30 min. One segment received no barbiturate, but was exposed to acetylcholine at the same time as the other three rings (time control).

To study the effects of the anaesthetics on the NO/PGI_2-independent relaxant response to acetylcholine, in addition to diclofenac the segments were treated with the NO synthase inhibitor, N^G-nitro-L-arginine (0.1 mM), for 30 min followed by the same experimental protocol as described before (i.e. three rings received the test compounds, the fourth segment did not). After another 30 min washout period, the segments were again constricted with phenylephrine, and the effects of the test compounds on the endothelium-independent relaxation induced by sodium nitroprusside (SNP, 0.01–10 μM) were investigated in the same manner.

Despite the repeated exposure to acetylcholine no tachyphylaxis was observed in any of the control segments throughout the study ($n=59$).

Cytochrome P450 assay

To elucidate the potential cytochrome P450-inhibitory effect of the barbiturates, a sensitive spectrofluorometric assay was employed in which the *O*-dealkylation of 7-ethoxycoumarin to the highly fluorescent 7-hydroxycoumarin (umbelliferon) is monitored over time (Ullrich & Weber, 1972; Prough *et al.*, 1978). As a source of cytochrome P450 the microsomal fraction from the liver of non-induced New Zealand White rabbits was prepared essentially as previously described for NO synthase (Hecker *et al.*, 1994b). An aliquot of the microsomal protein (0.5 mg) was stirred in a quartz glass cuvette with 0.1 M Tris-HCl buffer (pH 7.6), containing 20 μM 7-ethoxycoumarin. After 2 min equilibration at 37°C, in the presence or absence of the anaesthetics, the reaction was initiated by the addition of NADPH (0.1 mM) and monitored over a period of 10 min in a dual wavelength spectrofluorometer (PTI, Wedel, Germany) with the excitation and emission wavelengths set to 370 and 455 nm respectively. Calibration of the assay was performed by adding known concentrations of umbelliferon (0.1–10 μM) to a cuvette containing heat-denatured microsomal protein. The specificity of the fluorimetric assay was confirmed by using the cytochrome P450 inhibitor, metyrapone (1 mM), which almost completely abrogated the microsomal de-ethylase activity (93.3 ± 1.4% inhibition, $n=6$).

Statistics

Unless indicated otherwise, all data in the figures and text are expressed as means ± s.e.mean of n observations with ring segments from different arteries. Statistical evaluation was performed by two-sided Fischer-Pitman analysis followed by a Bonferroni post test for multiple comparisons with a P-value <0.05 considered statistically significant.

Materials

Diclofenac (Voltaren) was obtained from Ciba-Geigy (Wehr, Germany); apamin and charybdotoxin from Alomone Laboratories (Jerusalem, Israel); N^G-nitro-L-arginine (free acid) from Serva (Heidelberg, Germany); acetylcholine, clotrimazole, 7-ethoxycoumarin, NADPH, metyrapone (2-methyl-1,2-di-3-pyridyl-1-propanone), phenylephrine, sodium nitroprusside and umbelliferon from Sigma (Deisenhofen, Germany); methohexitone sodium (Brevimytal) from Lilly (Bad Homburg, Germany); phenobarbitone sodium (Luminal) from Bayer (Leverkusen, Germany); and thiopentone sodium (Trapanal) from Byk Gulden (Konstanz, Germany).

Results

Acetylcholine-induced NO-dependent relaxation

Exposure of endothelium-intact carotid artery segments to a half-maximally effective concentration of phenylephrine (1 μM) produced an active tension of 2.4 ± 0.1 g ($n=47$). The subsequent addition of acetylcholine resulted in a concentration-dependent relaxation in endothelium-intact (Figures 1–3), but not in endothelium-denuded rings ($n=4$). In the presence of phenobarbitone (Figure 1a), methohexitone (Figure 2a) or thiopentone (Figure 3a) at concentrations up to 0.3 mM, neither the level of preconstriction (Table 1) nor the relaxant response to acetylcholine was significantly different from the corresponding control segments, suggesting that the barbiturates did not affect basal or agonist-stimulated NO release. In agreement with this finding, all three barbiturates (0.01–1 mM) failed to affect the activity of a semi-purified constitutive NO synthase preparation from rabbit brain and freshly isolated porcine aortic endothelial cells ($n=6-8$), as determined by monitoring the N^G-nitro-L-arginine-sensitive conversion of radiolabelled L-arginine to L-citrulline (Hecker *et al.*, 1994b).

Acetylcholine-induced EDHF-mediated relaxation

After incubation of the segments with N^G-nitro-L-arginine for 30 min, the vasoconstrictor effect of phenylephrine was significantly enhanced (3.9 ± 0.1 g, $n=59$, $P<0.01$; cf. Table 1), indicative of a loss of basal NO release. The concentration-response curve to acetylcholine was significantly shifted to the right (from 0.15 ± 0.03 to 0.45 ± 0.07 μM, $n=47-59$, $P<0.01$), while its maximum relaxant effect was reduced from 95.5 ± 0.4 to 40.0 ± 4.8% ($P<0.01$).

This NO/PGI_2-independent relaxation was markedly attenuated when the segments were preconstricted with potassium chloride (40 mM, Figure 4a) to the same level of tone as attained with phenylephrine and N^G-nitro-L-arginine (Table 2). The non-selective K^+_{Ca} channel inhibitor tetrabutylammonium (1–3 mM, Figure 4b) and charybdotoxin

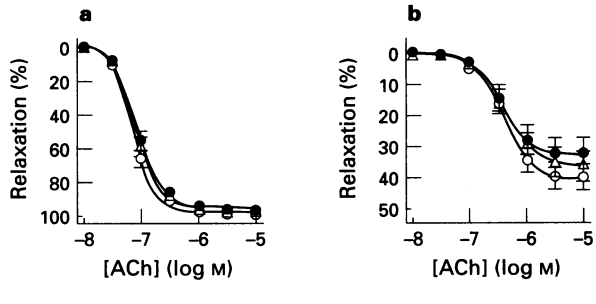

Figure 1 Effects of phenobarbitone (○, 0.1 mM; △, 0.3 mM) on the relaxant response to acetylcholine (●) in the absence (**a**) and presence (**b**) of N^G-nitro-L-arginine ($n=8-11$).

Table 1 Effects of phenobarbitone, methohexitone and thiopentone on contractions to phenylephrine (1 μM) in the absence (untreated) and presence (treated) of 0.1 mM N^G-nitro-L-arginine

Compound	Concentration (mM)	Force (g) Untreated	Treated	n
	0	2.4±0.2	3.8±0.2**	11
Phenobarbitone	0.1	2.4±0.2	3.7±0.2**	11
	0.3	2.3±0.1	3.7±0.2**	10
	0	3.2±0.2	5.1±0.3**	14
Methohexitone	0.03	2.5±0.2•	3.3±0.1*,•	7
	0.1	2.8±0.2	4.1±0.2**,•	11
	0	2.4±0.3	3.6±0.3*	8
Thiopentone	0.1	2.4±0.2	3.4±0.2**	12
	0.3	2.3±0.2	3.0±0.2*	13

*$P<0.05$, **$P<0.01$ vs. untreated; •$P<0.05$ vs. time control, i.e. 0 mM methohexitone.

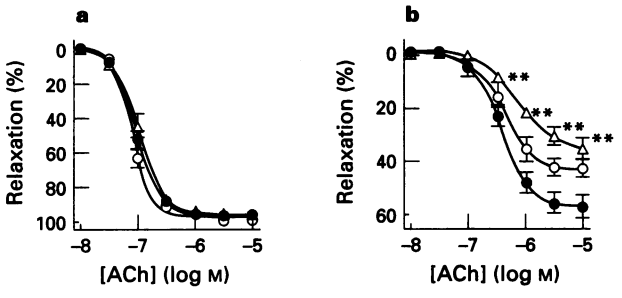

Figure 2 Effects of methohexitone (○, 0.03 mM; △, 0.1 mM) on the relaxant response to acetylcholine (●) in the absence (**a**) and presence (**b**) of N^G-nitro-L-arginine ($n=7-14$, **$P<0.01$ vs. segments not exposed to methohexitone).

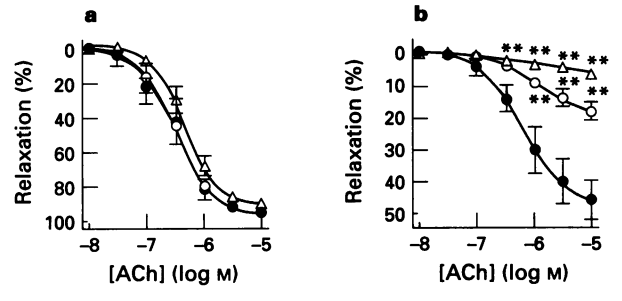

Figure 3 Effects of thiopentone (○, 0.1 mM; △, 0.3 mM) on the relaxant response to acetylcholine (●) in the absence (**a**) and presence (**b**) of N^G-nitro-L-arginine ($n=8-13$, **$P<0.01$ vs. segments not exposed to thiopentone).

(10 nM, Figure 4c), a specific inhibitor of large conductance (35–250 pS) K^+_{Ca} channels (Miller *et al.*, 1985), also strongly diminished the relaxant response to acetylcholine in segments pretreated with N^G-nitro-L-arginine, while apamin (1 μM), a specific inhibitor of small conductance (6–14 pS) K^+_{Ca} channels (Blatz & Magleby, 1986), had no effect (Figure 4d). Similarly, the K^+_{ATP} channel inhibitor, glibenclamide (3 μM; Cowen & Cohen, 1991) did not attenuate the N^G-nitro-L-arginine-resistant relaxant response to acetylcholine ($n=4$), suggesting that this NO/PGI_2-independent relaxation was mediated by the release of EDHF from the endothelium and the activation of medium to high conductance K^+_{Ca} channels in the smooth muscle.

Phenobarbitone in concentrations up to 0.3 mM failed to affect the acetylcholine-induced EDHF-mediated relaxation (Figure 1b) which, on the other hand, was significantly attenuated by 0.1 mM methohexitone (Figure 2b). At 0.3 mM the inhibitory effect of methohexitone was virtually identical ($n=9$), suggesting that 0.1 mM represents the maximally effective concentration of this barbiturate. In the presence of thiopentone, the NO/PGI_2-independent relaxant response to acetylcholine was strongly reduced at 0.1 mM and abolished at 0.3 mM (Figure 3b). Moreover pentobarbitone, which was used to anaesthetize the rabbits before the removal of the carotid arteries, had no significant effect on the acetylcholine-induced release of NO or EDHF in concentrations up to 0.3 mM ($n=6$).

Role of cytochrome P450

The inhibitory effect of methohexitone and thiopentone on the EDHF-mediated acetylcholine-induced relaxation was mimicked by the cytochrome P450 inhibitor, clotrimazole, with an IC_{50}- value of ~5 μM (Figure 5a). Clotrimazole on the other hand did not affect the endothelium-dependent relaxant response to acetylcholine in the absence of N^G-nitro-L-arginine ($n=6-9$).

In a separate series of experiments, clotrimazole also potently (IC_{50}~10 μM) inhibited the cytochrome P450 activity present in rabbit liver microsomes which was determined by monitoring the *O*-dealkylation of 7-ethoxycoumarin to umbelliferon (Figure 5b). In this assay system, phenobarbitone was virtually inactive and methohexitone produced only a moderate inhibitory effect, while thiopentone was as effective as, but less potent than clotrimazole in attenuating the microsomal cytochrome P450 activity (Figure 5c).

Sodium nitroprusside-induced relaxation

Phenobarbitone had no inhibitory effect on the endothelium-independent relaxant response to sodium nitroprusside which on the other hand was slightly enhanced by methohexitone and modestly attenuated by thiopentone (Figure 6a). Similar findings were obtained at a barbiturate concentration of 0.3 mM ($n=5-32$). Moreover phenobarbitone and thiopentone (0.3 mM) did not significantly affect the stimulation by sodium nitroprusside of a purified soluble guanylyl cyclase preparation isolated from bovine lung ($n=3$), as determined by monitoring the conversion of radiolabelled GTP to cyclic GMP (Hecker *et al.*, 1994b). Clotrimazole did not alter the relaxant response to sodium nitroprusside (Figure 6b).

Discussion

The present findings demonstrate that in the carotid artery of the rabbit barbiturates, such as phenobarbitone, pentobarbitone, methohexitone or thiopentone, have no significant effect on the acetylcholine-induced release of NO from the en-

Table 2 Effects of high K^+ (isotonic replacement of Na^+ by K^+), the K^+_{Ca} channel antagonists and clotrimazole (treated) on contractions to phenylephrine (1 μM) in the presence of 0.1 mM N^G-nitro-L-arginine

Compound	Concentration	Force (g) Untreated	Treated	n
K^+	40 mM	3.5±0.3	3.5±0.1	6
Apamin	1 μM	4.0±0.2	4.9±0.6	4
Charybdotoxin	10 nM	4.0±0.2	4.5±0.2	4
Tetrabutylammonium	1 mM	3.7±0.8	4.3±0.6	6
	3 mM		3.2±0.5	7
Clotrimazole	3 μM	4.1±0.2	3.5±0.2	17
	10 μM		4.5±0.2	9
	100 μM		3.3±0.3*	9

*$P<0.05$ vs. N^G-nitro-L-arginine alone, i.e. untreated.

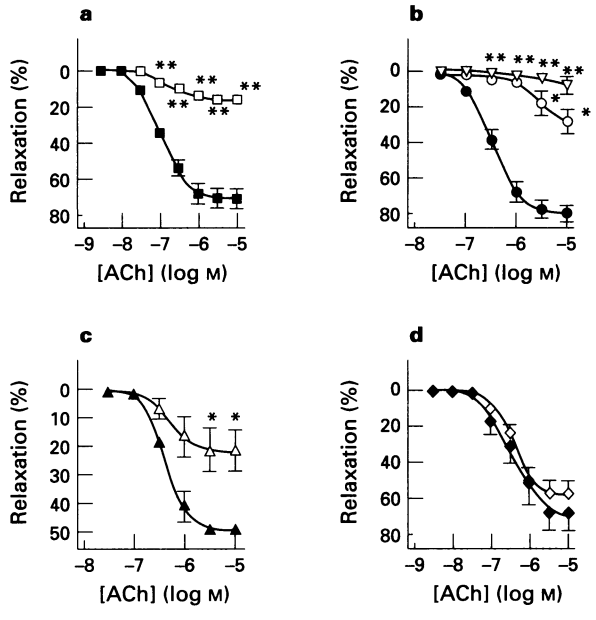

Figure 4 Effects of (**a**) preconstriction with potassium chloride (□, 40 mM), and exposure to (**b**) tetrabutylammonium (○, 1 mM; ▽, 3 mM), (**c**) charybdotoxin (△, 10 nM) or (**d**) apamin (◇, 1 μM) on the relaxant response to acetylcholine in the presence of N^G-nitro-L-arginine ($n=4-7$; *$P<0.05$, **$P<0.01$, vs. segments not exposed to high K^+ (■) or the K^+_{Ca} inhibitors; ●, ▲, ◆).

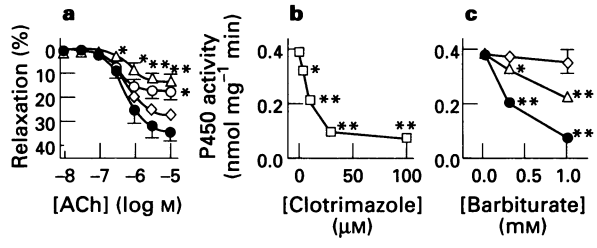

Figure 5 (**a**) Effects of clotrimazole (◇, 3 μM, ○, 10 μM, △, 100 μM) on the relaxant response to acetylcholine in the presence of N^G-nitro-L-arginine ($n=6-9$; *$P<0.05$, **$P<0.01$ vs. segments not exposed to the cytochrome P450 inhibitor, ●). (**b,c**) Effects of (**b**) clotrimazole (□) and (**c**) phenobarbitone (◇), methohexitone (△) or thiopentone (●) on the *O*-dealkylation of 7-ethoxycoumarin by rabbit liver microsomes ($n=3-5$; *$P<0.05$, **$P<0.01$ vs. control). Where no error bar is shown, s.e.mean falls within the dimensions of the symbol.

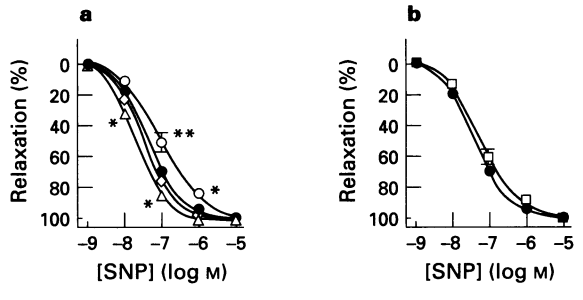

Figure 6 Effects of (**a**) phenobarbitone (◇, 0.1 mM), methohexitone (△, 0.1 mM) and thiopentone (○, 0.1 mM; $n=9-32$) or (**b**) clotrimazole (□, 0.1 mM, $n=9$) on the endothelium-independent relaxant response to sodium nitroprusside (SNP; *$P<0.05$, **$P<0.01$ vs. segments not exposed to the barbiturates or the cytochrome P450 inhibitor, ●).

dothelium and/or its effect on soluble guanylyl cyclase in the smooth muscle. In contrast two of these anaesthetics, methohexitone and thiopentone, markedly attenuated the NO/PGI_2-independent relaxant response to acetylcholine which was mediated by the release of EDHF, as shown by the lack of effect of acetylcholine on N^G-nitro-L-arginine-treated segments in the presence of depolarizing concentrations of K^+ or after K^+_{Ca} channel blockade. This effect of the two barbiturates was mimicked by the cytochrome P450 inhibitor, clotrimazole, reinforcing the notion that EDHF is a cytochrome P450-derived arachidonic acid metabolite (Pinto *et al.*, 1987; Bauersachs *et al.*, 1994; Hecker *et al.*, 1994a; Fulton *et al.*, 1995). Moreover the finding that clotrimazole was a potent inhibitor of the NO/PGI_2-independent relaxant response to acetylcholine provides further indirect evidence that EDHF is an arachidonic acid epoxide (Hu & Kim, 1993; Rosolowsky & Campbell, 1993; Hecker *et al.*, 1994a), since this cytochrome P450 inhibitor is thought to block specifically the epoxygenase pathway of arachidonic acid metabolism (Capdevilla *et al.*, 1988; Fulton *et al.*, 1995).

Although barbiturates are well known for their stimulatory effect on cytochrome P450 gene expression, information concerning their effect on cytochrome P450 activity is rather scarce. Unfortunately the amount of cytochrome P450 present in the endothelium of the rabbit carotid artery is too small to allow a determination of its activity by conventional fluorimetric methods. We have therefore investigated the potential cytochrome P450-inhibitory effect of the barbiturates by monitoring the *O*-dealkylation of 7-ethoxycoumarin to umbelliferon in rabbit liver microsomes. Thiopentone and methohexitone, but not phenobarbitone inhibited this cytochrome P450-dependent de-ethylase reaction, suggesting that in principle these anaesthetics can interfere with the cytochrome P450-dependent synthesis of EDHF rather than with its effect on smooth muscle K^+_{Ca} channel activity. This hypothesis was strengthened by the relative inhibitory potency of the two

barbiturates in the cytochrome P450 assay which matched the extent of their inhibitory effect on the acetylcholine-induced release of EDHF. In this context, however, it is important to note that the de-ethylase reaction in the microsomes and the epoxygenase-like formation of EDHF are likely to be catalyzed by two very different cytochrome P450 isoenzymes.

Thiopentone, but not pentobarbitone, causes a moderate inhibition of the endothelium-dependent relaxant response to acetylcholine in the canine coronary artery and in the rat aorta, and this effect has been attributed to an interaction of the anaesthetic with the release and/or effect of NO (Terasako *et al.*, 1994). However at 0.3 mM thiopentone had no significant effect on the acetylcholine-induced increase in intravascular cyclic GMP (an index of NO release), while at this concentration the barbiturate clearly attenuated the acetylcholine-induced relaxation. Moreover the relaxant response to acetylcholine in these arteries is known to involve the release of EDHF (Pinto *et al.*, 1987; Chen *et al.*, 1991; Suzuki *et al.*, 1992). The findings of Terasako *et al.* (1994) may therefore be interpreted similarly to ours as an inhibition by thiopentone of the acetylcholine-induced EDHF release.

The lack of effect of the barbiturates on the NO-mediated relaxant response to acetylcholine was substantiated by the finding that these anaesthetics have no direct inhibitory effect on endothelial NO synthase activity. Moreover their marginal effect on the endothelium-independent relaxation elicited by sodium nitroprusside as well as their lack of effect on the stimulation of purified soluble guanylyl cyclase by this NO donor suggest that they do not interfere with the NO-induced formation of cyclic GMP in the vascular smooth muscle at concentrations which markedly attenuate the acetylcholine-induced synthesis of EDHF.

When compared to NO, the physiological importance of EDHF release, e.g. in isolated coronary (Holzmann *et al.*, 1994) and carotid arteries (this study) where 40–60% of the relaxant response to bradykinin or acetylcholine is resistant to inhibition of either NO or PGI_2 formation, may have been overlooked. In the coronary microcirculation of the rat heart only the duration, but not amplitude, of the dilator response to bradykinin is affected by the combined treatment with an inhibitor of NO synthase and cyclo-oxygenase (Bauersachs *et al.*, 1994; Fulton *et al.*, 1995). Similarly, the duration, but not amplitude, of the systemic hypotensive response to acetylcholine, ATP or bradykinin in the anaesthetized rat *in vivo* is reduced following application of an NO synthase inhibitor (O'Shaughnessy *et al.*, 1992). Taken together these findings imply that the release of EDHF may play an important role in the control of local vascular tone under physiological conditions.

Moreover it is conceivable that under conditions of reduced NO synthesis, i.e. in atherosclerosis, hypertension or ischaemia, the release of this autacoid represents a compensatory or reserve mechanism for the maintenance of vascular tone. Indeed, in the carotid artery of hypercholesteroleamic rabbits, the NO-independent, charybdotoxin-sensitive relaxant response to acetylcholine is preserved, while the acetylcholine-induced NO release is strongly impaired (Najibi *et al.*, 1994). The adverse effect of thiopentone and methohexitone on the synthesis of EDHF may therefore pose a haemodynamic problem during the induction of anaesthesia with these barbiturates in patients with atherosclerosis.

This work was supported by grants from the Deutsche Forschungsgemeinschaft (Bu 486/4-3, He 1587/5-1) and the European Commission (BMH1-CT92-1893). M.H. is the recipient of a Heisenberg fellowship from the Deutsche Forschungsgemeinschaft. We thank Dr Agnieszka T. Bara for her help with the organ bath studies and Gabriele Hoch for expert technical assistance.

References

BAUERSACHS, J., HECKER, M. & BUSSE, R. (1994). Display of the characteristics of endothelium-derived hyperpolarizing factor by a cytochrome P450-derived arachidonic acid metabolite in the coronary microcirculation. *Br. J. Pharmacol.*, **113**, 1548–1553.

BLATZ, A.L. & MAGLEBY, K.L. (1986). Single apamin-blocked Ca^{2+}-activated K^+ channels of small conductance in cultured rat skeletal muscle. *Nature*, **323**, 718–720.

CAPDEVILA, J., GIL, L., ORELLANA, M., MARNETT, L.J., MASON, J.I., YODAGIRI, P. & FALCK, J.R. (1988). Inhibitors of cytochrome P-450 dependent arachidonic acid metabolism. *Arch. Biochem. Biophys.*, **261**, 257–263.

CHEN, G.F., YAMAMOTO, Y., MIWA, K. & SUZUKI, H. (1991). Hyperpolarization of arterial smooth muscle induced by endothelial humoral substances. *Am. J. Physiol.*, **260**, H1888–H1892.

COWEN, C.L. & COHEN, R.A. (1991). Two mechanisms mediate the relaxation by bradykinin of pig coronary artery: NO-dependent and -independent responses. *Am. J. Physiol.*, **261**, H380–H385.

FULTON, D., MAHBOUBI, K., MCGIFF, J.C. & QUILLEY, J. (1995). Cytochrome P450-dependent effects of bradykinin in the rat heart. *Br. J. Pharmacol.*, **114**, 99–102.

GERKENS, J.F. (1987). Barbiturate inhibition of endothelium-dependent dilatation of blood- and Krebs-perfused rat tail arteries. *Eur. J. Pharmacol.*, **134**, 293–301.

HECKER, M., BARA, A.T., BAUERSACHS, J. & BUSSE, R. (1994a). Characterization of the endothelium-derived hyperpolarizing factor released from coronary arteries as a cytochrome P450-derived arachidonic acid metabolite. *J. Physiol.*, **481**, 407–414.

HECKER, M., MÜLSCH, A., BASSENGE, E., FÖSTERMANN, U. & BUSSE, R. (1994b). Subcellular localisation and characterization of nitric oxide synthase(s) in endothelial cells - physiologic implications. *Biochem. J.*, **299**, 247–252.

HOLZMANN, S., KUKOVETZ, W.R., WINDISCHHOFER, W., PASCHKE, E. & GRAIER, W.F. (1994). Pharmacologic differentiation between endothelium-dependent relaxations sensitive and resistant to nitro-L-arginine in coronary arteries. *J. Cardiovasc. Pharmacol.*, **23**, 747–756.

HU, S. & KIM, H.S. (1993). Activation of K^+ channel in vascular smooth muscles by cytochrome P450 metabolites of arachidonic acid. *Eur. J. Pharmacol.*, **230**, 215–221.

JOHNS, R.A. (1993). Endothelium, anaesthetics, and vascular control. *Anesthesiology*, **79**, 1381–1391.

MILLER, C., MOCZYDLOWSKI, E., LATORRE, R. & PHILLIPS, M. (1985). Charybdotoxin, a protein inhibitor of single Ca^{2+}-activated K^+ channels from mammalian skeletal muscle. *Nature*, **313**, 316–318.

NAJIBI, S., COWAN, C.L., PALACINO, J.J. & COHEN, R.A. (1994). Enhanced role of potassium channels in relaxations to acetylcholine in hypercholesterolemic rabbit carotid artery. *Am. J. Physiol.*, **266**, H2061–H2067.

NAKASHIMA, M., MOMBOULI, J.-V., TAYLOR, A.A. & VANHOUTTE, P.M. (1993). Endothelium-dependent hyperpolarization caused by bradykinin in human coronary arteries. *J. Clin. Invest.*, **92**, 2867–2871.

O'SHAUGHNESSY, K.O., NEWMAN, C.M. & WARREN, J.B. (1992). Inhibition in the rat of nitric oxide synthesis in vivo does not attenuate the hypotensive action of acetylcholine, ATP or bradykinin. *Exp. Physiol.*, **77**, 285–292.

PINTO, A., ABRAHAM, N.G. & MULLANE, K.M. (1987). Arachidonic acid-induced endothelial-dependent relaxations of canine coronary arteries: contribution of a cytochrome P-450-dependent pathway. *J. Pharmacol. Exp. Ther.*, **240**, 856–863.

PROUGH, R.A., BURKE, M.D. & MAYER, R.T. (1978). Direct fluorometric methods for measuring mixed-function oxidase activity. *Methods Enzymol.*, **52**, 372–377.

ROSOLOWSKY, M. & CAMPBELL, W.B. (1993). Role of PGI_2 and epoxyeicosatrienic acids in relaxation of bovine coronary arteries to arachidonic acid. *Am. J. Physiol.*, **264**, H327–H335.

SUZUKI, H., CHEN, G. & YAMAMOTO, Y. (1992). Endothelium-derived hyperpolarizing factor (EDHF). *Jpn. Circ. J.*, **56**, 170–174.

TERASAKO, K., NAKAMURA, K., TODA, H., KUKUYAMA, M., HATANO, Y. & MORI, K. (1993). Barbiturates inhibit both endothelium-dependent and independent relaxation mediated by cyclic GMP. *Anesth. Analg.*, **78**, 823–830.

UGGERI, M.J., PROCTOR, G.J. & JOHNS, R.A. (1992). Halothane, enflurane, and isoflurane attenuate both receptor and non-receptor mediated EDRF production in rat thoracic aorta. *Anesthesiology*, **76**, 1012–1017.

ULLRICH, V. & WEBER, P. (1972). The O-dealkylation of 7-ethoxycoumarin by liver microsomes. *Hoppe-Seyler's Z. Physiol. Chem.*, **353**, 1171–1177.

(Received February 9, 1995
Revised March 27, 1995
Accepted April 7, 1995)

British Journal of Pharmacology (1995) 115, 975-980 © 1995 Stockton Press All rights reserved 0007-1188/95 $12.00

Further evidence from functional studies for somatostatin receptor heterogeneity in guinea-pig isolated ileum, vas deferens and right atrium

[1]W. Feniuk, J. Dimech, E.M. Jarvie & P.P.A. Humphrey

Glaxo Institute of Applied Pharmacology, Department of Pharmacology, University of Cambridge, Tennis Court Road, Cambridge CB2 1QJ

1 Somatostatin (SRIF) causes a concentration-dependent inhibition of neurotransmission in guinea-pig ileum and vas deferens as well as negative inotropy in guinea-pig isolated right atrium. The SRIF receptors mediating these effects have now been further characterized by use of the peptides BIM-23027, BIM-23056 and L-362855, reported as selective for the recombinant SRIF receptor types, sst_2, sst_3 and sst_5, respectively.

2 BIM-23027 was a highly potent agonist at causing an inhibition of neurotransmission in the guinea-pig ileum (EC_{50} value 1.9 nM), being about 3 times more potent than SRIF (EC_{50} value 6.8 nM). In contrast, in both guinea-pig vas deferens and right atrial preparations, BIM-23027 was a relatively weak agonist being at least 30-100 times weaker than SRIF. In guinea-pig atria, BIM-23027 (3 μM) antagonized the negative inotropic action of $SRIF_{28}$ (apparent $pK_B = 5.9 \pm 0.1$) but had no effect on the negative inotropic action of cyclohexyladenosine.

3 The inhibitory effect of BIM-23027 in the guinea-pig ileum was readily desensitized. Prior exposure to BIM-23027 (0.3 μM) markedly attenuated the inhibitory effect of SRIF but had no effect on the inhibitory action of clonidine suggesting that BIM-23027 and SRIF act via a common receptor mechanism.

4 L-362855 caused a concentration-dependent inhibition of neurotransmission in both the guinea-pig ileum and vas deferens as well as causing negative inotropy in the guinea-pig atrium but was at least 30-100 times weaker than SRIF. In guinea-pig isolated atria, L-362855 (3 μM) did not antagonize the negative inotropic action of $SRIF_{28}$.

5 BIM-23056 in concentrations up to 1 μM was inactive as an agonist in guinea-pig isolated ileum, vas deferens and atrium and did not antagonize the inhibitory actions of SRIF in any of these preparations.

6 The results from this study support our previous contention that the sst_2 receptor type mediates inhibition of neurotransmission by SRIF in the guinea-pig ileum. The SRIF receptor type mediating inhibition of neurotransmission in the guinea-pig vas deferens appears different, but similar, to that mediating negative inotropy in the atrium. However the characteristics of these latter receptors appear different from that of the recombinant sst_2, sst_3 and sst_5 receptors for SRIF described for rat and man.

Keywords: Somatostatin; SRIF receptor agonists; BIM-23027; BIM-23056; L-362855

Introduction

Somatostatin (SRIF) produces its effect by interacting with specific receptors located on the cell membrane. It is evident that at least five different SRIF receptor genes exist, whose products (termed sst_1-sst_5) belong to the seven-transmembrane superfamily of G-protein coupled receptors (see Hoyer *et al.*, 1995). However, the functional consequences of activation or blockade of these receptors either *in vitro* or *in vivo* remains to a large extent unknown. We have previously provided evidence from *in vitro* studies that the SRIF receptors that mediate negative inotropy in the guinea-pig heart and that mediate an inhibition of neurogenically mediated contraction in the vas deferens are similar and that these receptors differ from the SRIF receptor mediating an inhibition of neurogenic contraction in the guinea-pig ileum (Feniuk *et al.*, 1993). This conclusion was largely based on the observed differences in the relative potencies of SRIF and the larger 28 amino acid peptide, $SRIF_{28}$, the latter being some 30 times more potent than SRIF in the heart and vas deferens, whilst in the ileum the two peptides are of similar potency.

Recently several peptides have been identified which on the basis of radioligand binding studies display a high degree of selectivity for certain of the recombinant SRIF receptors. Thus BIM-23027 and BIM-23056 display a high selectivity for sst_2 and sst_3 receptors, respectively (see Raynor *et al.*, 1993a,b), whilst L-362855 shows high selectivity for the SRIF receptor cloned by O'Carroll and colleagues (1992) and is now termed sst_5 by international agreement (see Hoyer *et al.*, 1995) to distinguish it from the distinct sst_4 receptor, cloned by Bruno and colleagues (1992). To date, few functional studies with these receptor selective peptides have been described.

In the present study we have compared the relative potencies of BIM-23027, BIM-23056 and L-362855 with SRIF in guinea-pig isolated atria, vas deferens and ileum in order to re-examine our proposal that the SRIF receptor type in the atrium and vas deferens differs from that in the ileum and also to determine whether the characteristics of these receptors resemble those of any of the recombinant SRIF receptors stably expressed in various cell lines. A preliminary account of these findings has been presented to the British Pharmacological Society (Feniuk *et al.*, 1994a).

Methods

Guinea-pig isolated ileum

Male Dunkin Hartley guinea-pigs (200-450 g) were humanely killed and lengths of distal ileum (approximately 15 cm from the ileo-caecal junction) were removed and placed in a mod-

[1] Author for correspondence.

ified Krebs solution of the following composition (mM): NaCl 118, $NaHCO_3$ 25, KCl 4.7, $MgSO_4.7H_2O$ 0.6, KH_2PO_4 1.2, D-glucose 11.1, $CaCl_2.6H_2O$ 1.3, at room temperature and gassed with 95% O_2/5% CO_2. Preparations (approximately 1.5 cm in length) were cleared of adhering connective tissue and mounted between a pair of parallel platinum electrodes in 4 ml organ baths for recording isometric tension changes with a Dynamometer UF1 force transducer from an initial resting tension of 0.5 g. Bath temperature was maintained at 37–38°C. Following an initial equilibration period of at least 30 min, transmural electrical field stimulation was applied (0.1 Hz, 0.1 ms continuously) at supramaximal currents of approximately 800 mA delivered from Digitimer D330 multistimulator. Control concentration-effect curves to SRIF on neurogenically mediated contractile responses were obtained by non-cumulative addition and each sequentially increasing drug concentration was washed from the bath once the inhibitory effect had reached a maximum. The preparations were then left for at least 30 min following which concentration-effect curves to SRIF were either repeated (time-matched controls) or concentration-effect curves to a test agonist determined. Agonist effects were measured as inhibition of the neurogenically mediated contraction and effects of test agonists were subsequently expressed as percentages of the SRIF maximum obtained in the same preparation.

Desensitization studies Desensitization was achieved by addition of BIM-23027 (0.3 μM) for 4 min followed by a 1 min washout period before administration of various concentrations of agonist. Concentration-effect curves to agonists were constructed before and following prior exposure to BIM-23027.

Guinea-pig vas deferens

Pairs of vasa deferentia were removed from male Dunkin Hartley guinea-pigs and prepared for recording isometric tension changes as described above. Preparations were stimulated electrically (5 Hz, 0.5 ms 1.5 s every 30 s) and concentration-effect curves to SRIF were obtained by non-cumulative addition (see above). These experiments were carried out in the continuous presence of phosphoramidon (1 μM) since we have previously shown that the effects of SRIF in the guinea-pig vas deferens are enhanced in the presence of peptidase inhibitors (Feniuk *et al.*, 1993). The potencies of test agonists was measured by use of a protocol identical to that described above. In the vas deferens, one of the pair of vasa deferentia always acted as a time-matched control in order to monitor spontaneous changes in agonist sensitivity. As in the case of the ileum studies, responses to the test agonist were normalized as a percentage of the SRIF maximum obtained in the same preparation. However, since SRIF abolished neurogenically mediated contractile response in all experiments, concentration-effect curves were identical regardless of whether responses were measured as % inhibition or % SRIF maximum.

Guinea-pig isolated right atria

Male Dunkin Hartley guinea-pigs (220–450 g) were humanely killed by cervical dislocation and the hearts rapidly removed. Spontaneously beating right atrial preparations were cleared of adherent ventricular tissue and mounted for recording of spontaneous isometric contractions at 32°C, as previously described in detail (Feniuk *et al.*, 1993). Cumulative concentration-effect curves for SRIF were obtained on each preparation, successive doses being added when the effect of the previous concentration had reached a plateau. Following a 60 min interval a second cumulative curve to the test agonist was obtained as described above. Using such a protocol, it has previously been shown that concentration-effect curves to SRIF are highly reproducible (Dimech *et al.*, 1993; Feniuk *et al.*, 1993).

In some studies, BIM-23027 and L-362855 were tested as SRIF receptor blocking drugs. The antagonist contact time was 30 min and the experimental protocol was identical to one previously described in detail (Dimech *et al.*, 1993). The antagonist effects of BIM-23027 and L-362855 were examined against $SRIF_{28}$-induced negative inotropic effects.

Statistical analyses

All values stated are the arithmetic mean ± s.e.mean of n observations except for EC_{50} values (agonist concentration producing 50% of its own maximal response) and concentration-ratios (ratio of equieffective agonist concentrations in presence and absence of antagonist derived from points on the linear and parallel parts of the concentration-effect curves) that are quoted as geometric mean (95% confidence limits). Where appropriate pK_B values were calculated according to the equation $pK_B = \log_{10}(CR-1) - \log_{10}(B)$ where CR is the ratio of equi-effective concentrations of the agonist in the presence and absence of a fixed antagonist concentration (B).

Drugs used

Somatostatin (SRIF) and $SRIF_{28}$ were from Peninsula. Clonidine hydrochloride and N-cyclohexyladenosine were purchased from Sigma. BIM-23027 (c[N-Me-Ala-Tyr-D-Trp-Lys-Abu-Phe]), BIM-23056 (D-Phe-Phe-Tyr-D-Trp-Lys-Val-Phe-D-Nal-NH_2) and L-362855 (c[Aha-Phe-Trp-D-Trp-Lys-Thr-Phe]), where Abu is aminobutyric acid and Aha is 7-aminoheptanoic acid, were synthesized by Dr J Kitchin's team in the Medicinal Chemistry Department, Glaxo Research and Development, Greenford.

All the peptides, with the exception of BIM-23056 were initially dissolved in distilled water to produce a concentration of 1 mM, then divided into aliquots and stored frozen. Dilutions were kept on ice during the course of an experiment. BIM-23056 was initially dissolved in 10% dimethylsulphoxide.

Results

Guinea-pig isolated ileum

Electrical field stimulation of guinea-pig isolated ileum caused neurogenically mediated contractile responses that could be inhibited by SRIF(1–100 nM) in a concentration-dependent manner. Concentration-effect curves to SRIF were reproducible in the time-matched control preparations. The EC_{50} values for first and second concentration-effect curves were 9.9(7.1–13.9) nM and 10.0(7.7–12.8) nM respectively with no difference in the maxima (49 ± 3 and 45 ± 2% inhibition, $n = 19$). Supramaximal concentrations of SRIF produced smaller inhibitory effects resulting in 'bell-shaped' concentration-effect curves (Figure 1).

In the test preparations ($n = 19$), a similar potency was observed for SRIF (EC_{50} 6.8(5.6–8.1) nM, maximum inhibition 54 ± 3%). BIM-23027 also caused a concentration-dependent inhibition of neurogenic contractions in the guinea-pig isolated ileum (EC_{50} 1.9(1.2–3.1)) but the maximum inhibition seen with BIM-23027 (39 ± 2%) was significantly less ($P < 0.05$, paired t test) than that observed with SRIF. As with SRIF, the concentration-effect curve for BIM-23027 was bell-shaped. On the basis of comparisons of the EC_{50} values, BIM-23027 was about three times more potent than SRIF (Figure 1).

L-362855 also caused a concentration-dependent inhibition of neurogenic contractions in the guinea-pig isolated ileum. The threshold concentration causing inhibition was 30 nM. At the highest concentration tested (1 μM), a maximum inhibitory effect was not reached. The inhibition seen with L-362855 (1 μM) was 60 ± 4% of the SRIF maximum effect (Figure 1).

BIM-23056 was devoid of agonist activity in the guinea-pig ileum in concentrations up to 1 μM ($n = 4$). At the end of two of these experiments, the effect of SRIF (0.1 μM) in the presence of BIM-23056 was examined. BIM-23056 (1 μM) had little effect on the inhibitory action of SRIF (0.1 μM) which pro-

duced a 47% inhibition of neurogenic contractions in the absence and a 41% inhibition in the presence of BIM-23056 (values are mean from 2 experiments).

Desensitization studies

Since the concentration-effect curve to BIM-23027 in the guinea-pig ileum was 'bell-shaped' and its effects subject to desensitization, BIM-23027 was used in cross-desensitization experiments with SRIF. Pre-exposure of the preparation to BIM-23027 (0.3 μM) for a 4 min period followed by washout, abolished the effect of subsequent dose of BIM-23027 (Figure 2) and markedly attenuated the inhibitory effect of SRIF. In marked contrast, pre-exposure to BIM-23027 had no effect on the inhibitory action of the α_2-adrenoceptor agonist, clonidine (Figure 2).

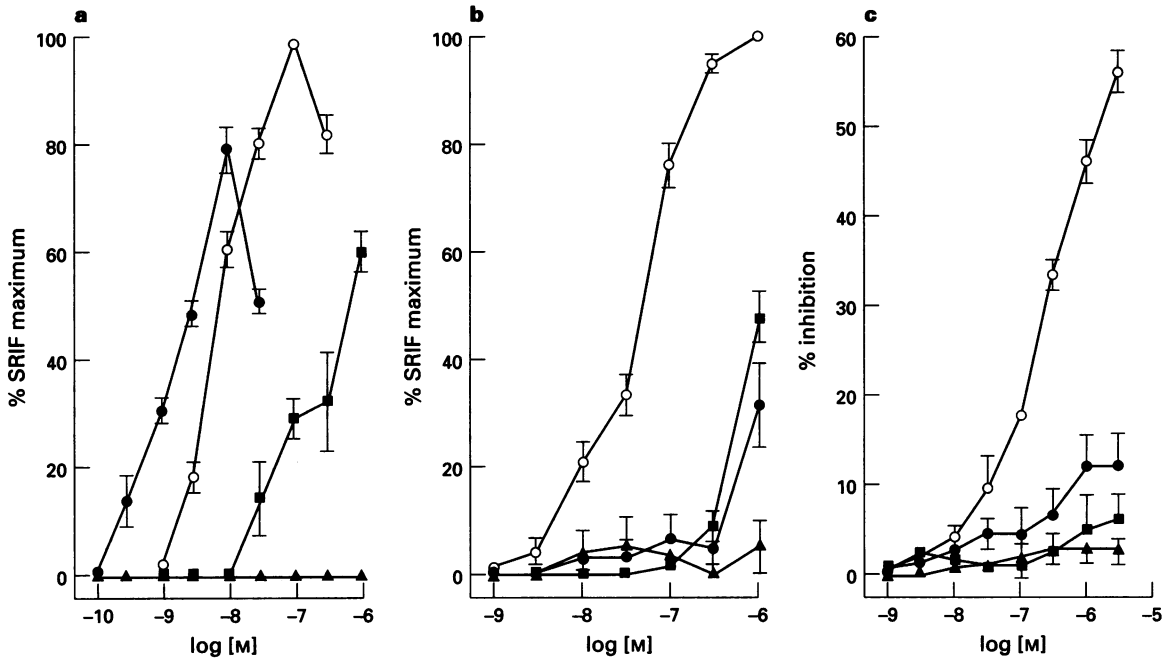

Figure 1 Inhibitory effects of somatostatin (SRIF) and some selective SRIF receptor ligands, (SRIF (○), BIM-23027 (●), L-362855 (■) and BIM-23056 (▲)) on (a) neurogenically mediated contractile responses of guinea-pig isolated ileum; (b) neurogenically mediated contractile responses of guinea-pig isolated vas deferens; (c) also shown are the negative inotropic effects of SRIF and selective SRIF receptor ligands in guinea-pig isolated right atrium. Values shown are mean ± s.e.mean from 4–20 experiments.

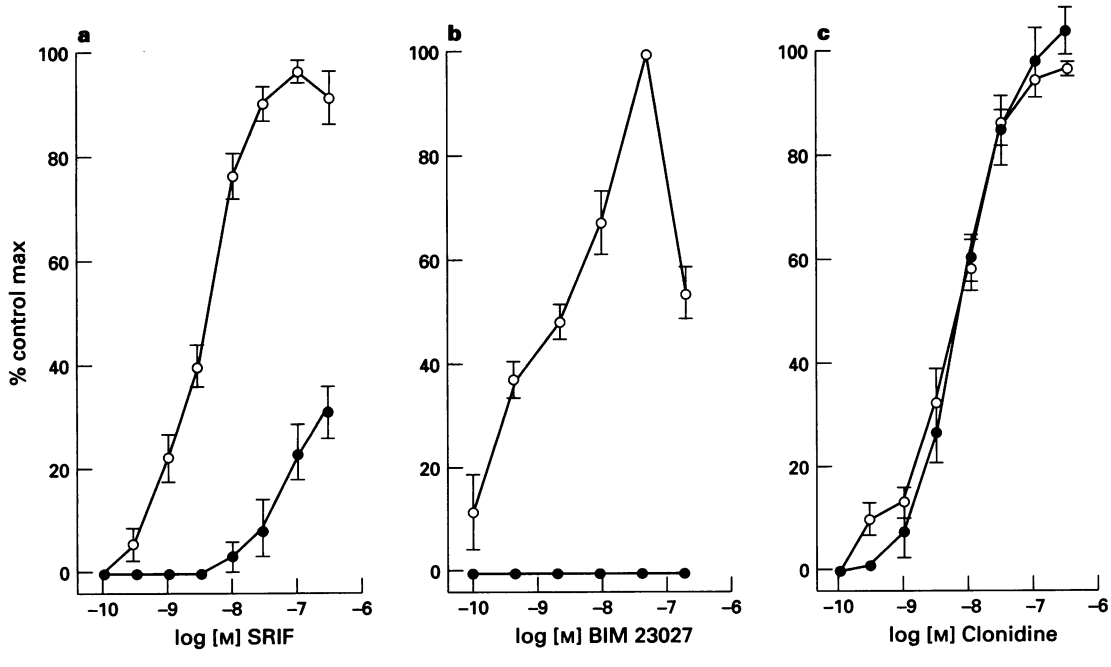

Figure 2 Effect of: (a) somatostatin (SRIF), (b) BIM-23027 and (c) clonidine on neurogenically mediated contractile responses of guinea-pig isolated ileum in the absence (○) and following a 4 min pretreatment with BIM-23027 (0.3 μM) with subsequent washout (●). BIM-23027 was applied before each concentration of test agonist. Values are the mean ± s.e.mean from 4 experiments. The ordinate shows responses expressed as a percentage of the maximum inhibition obtained to each agonist during the determination of the first concentration-effect curve.

Guinea-pig isolated vas deferens

SRIF caused a concentration-dependent inhibition of neurogenic contractions in the guinea-pig isolated vas deferens. In the time-matched control preparations the concentration-effect curves to SRIF were very reproducible (EC_{50} values of first and second concentration-effect curves were 50(35–71) nM and 92(67–127) nM, respectively). At the highest concentration tested (1 μM), neurogenically mediated contractile responses were abolished by SRIF.

In marked contrast to the findings in the guinea-pig isolated ileum, BIM-23027 was a much weaker agonist than SRIF in the vas deferens. BIM-23027 was virtually devoid of agonist activity in concentrations up to 300 nM and at 1 μM inhibited neurogenic contractions by only 32 ± 8% (Figure 1). L-362855 was of similar potency to BIM-23027 in the guinea-pig vas deferens causing a 48 ± 5% inhibition of neurogenic contractions at a concentration of 1 μM (Figure 1).

BIM-23056 was devoid of agonist activity in the vas deferens in concentrations up to 1 μM ($n=4$). At the end of two of these experiments, the effect of BIM-23056 (1 μM) on the inhibitory action of SRIF (1 μM) was examined. SRIF (1 μM) caused a 91% inhibition of neurogenic contractions in the absence and an 84% inhibition in the presence of BIM-23056 (values are mean from 2 experiments).

Guinea-pig isolated right atria

SRIF caused a concentration-dependent decrease in developed tension in guinea-pig isolated right atria. The profile of action of the agonists studied was very similar to that seen in the vas deferens. Both BIM-23027 and L-362855 were at least 30 times weaker than SRIF but neither of these agonists caused more than a 15% inhibition of developed tension (Figure 1). BIM-23056 was essentially devoid of agonist activity in concentrations up to 1 μM (Figure 1). Furthermore BIM-23056 (1 μM) did not modify the inhibitory action of SRIF (1 μM). SRIF caused a 42 ± 5% and a 45 ± 7% inhibition of developed tension in the absence and presence of BIM-23056 (1 μM) respectively ($n=4$ experiments).

Since both BIM-23027 and L-362855 displayed low intrinsic activity, their ability to antagonize $SRIF_{28}$-induced decreases in developed tension were also examined (Figure 3). BIM-23027 (3 μM) caused an approximate sixfold rightward displacement of the $SRIF_{28}$ concentration-effect curve (apparent $pK_B = 5.9 \pm 0.1$, $n=4$) whilst having no effect on the concentration-effect curve to cyclohexyladenosine (concentration-ratio = 0.73(0.39–1.38), $n=4$). L-362855 (3 μM) had little or no effect on the $SRIF_{28}$ concentration-effect curve (concentration-ratio = 1.6(1.2–2.0), $n=4$).

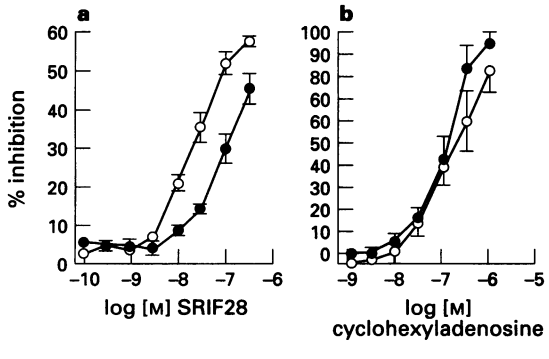

Figure 3 Negative inotropic effect of: (a) $SRIF_{28}$ and (b) cyclohexyladenosine in the absence (○) and presence (●) of BIM-23027 (3 μM). All values shown are mean ± s.e.mean from 4 experiments.

Discussion

Somatostatin (SRIF) produced a concentration-dependent inhibition of neurogenically mediated contractions in the guinea-pig isolated ileum and vas deferens as well as a negative inotropic action in the guinea-pig isolated right atrium confirming findings from our earlier studies (Dimech *et al.*, 1993; Feniuk *et al.*, 1993). We have previously suggested that the SRIF receptor type mediating inhibition in the ileum differs from that in the vas deferens and the atrium, a conclusion largely based on the observed differences in the relative potencies of the two naturally occurring forms of somatostatin, SRIF and $SRIF_{28}$. Furthermore we suggested that the SRIF receptor type mediating neurogenic inhibition in the ileum was similar to the recombinant sst_2 receptor, whilst that in the vas deferens and heart was similar to the recombinant SRIF receptor cloned by O'Carroll and co-workers (1992), now called sst_5 (see Introduction).

Recently some receptor-selective peptides have been identified from ligand binding studies using various recombinant SRIF receptor types stably transfected into different cell lines (Raynor *et al.*, 1993a,b). These peptides include BIM-23027, BIM-23056 and L-362855 which are respectively selective for recombinant sst_2, sst_3 and sst_5 receptors. However the functional effects of these peptides in either cells transfected with these recombinant receptors or in preparations naturally expressing SRIF receptors is largly unknown. We therefore investigated the effects of these peptides in the guinea-pig isolated ileum, vas deferens and right atrium not only to determine their functional activity but also to re-examine our original proposal of SRIF receptor heterogeneity in guinea-pig tissues.

The sst_2 receptor selective ligand, BIM-23027, was a highly potent agonist in the guinea-pig isolated ileum being at least three times more potent than SRIF, while producing a somewhat lower maximum effect. Both the sst_3 and sst_5 receptor-selective peptides (BIM-23056 and L-362855, respectively) were much weaker than SRIF and maximal inhibitory effects were not observed with concentrations of the peptides as high as 1 μM. The high agonist potency of BIM-23027 in causing inhibition of neurogenic contraction in the guinea-pig ileum is consistent with our previous conclusion that the SRIF receptor type mediating inhibition in the ileum is similar to the recombinant sst_2 receptor (Feniuk *et al.*, 1993). Although BIM-23027 also displays some affinity for the recombinant sst_3 receptor, the lack of effect of the putative sst_3 selective ligand, BIM-23056, either as an agonist or antagonist, would argue against an involvement of this receptor. The concentration-effect curve to BIM-23027 in the ileum was 'bell-shaped' suggesting that that activity of BIM-23027 might be susceptible to desensitization. Indeed, pre-exposure of the guinea-pig ileum to BIM-23027 with subsequent washout resulted in the abolition of the inhibitory effect of a second dose of BIM-23027 and a marked attenuation of the inhibitory action of SRIF, suggesting that both peptides act via a common receptor mechanism. However, it is unclear why there was still a residual response to SRIF, but not BIM-23027, following desensitization with BIM-23027. It is possible that SRIF mediates inhibition in the guinea-pig ileum by two distinct receptor mechanisms of which only one is prone to desensitization by BIM-23027. With this in mind, it is noteworthy that the inhibitory concentration-effect curve to L-362855 appeared biphasic in nature. Alternatively, it is possible that the quantitative differences in the profile of BIM-23027 and SRIF inhibitory effects seen following BIM-23027 desensitization relates to the difference in their maximum effects. Thus, if BIM-23027 has lower intrinsic efficacy than SRIF, it would be expected to be more affected by desensitization. Regardless, the selectivity of action of BIM-23027 in desensitizing responses both to itself and SRIF was clearly demonstrated by the inability of BIM-23027 to desensitize inhibitory responses to the α_2-adrenoceptor agonist, clonidine. In the context of desensitization, it is noteworthy that the recombinant sst_2 receptor can also be readily desensitized by prior exposure to

such agonists as seglitide (Rens-Domiano *et al.*, 1992) and that the contractile action of SRIF in the rat colon which also appears to be mediated via neuronal sst_2 receptors is desensitized by BIM-23027 (McKeen *et al.*, 1994).

BIM-23027 also discriminated between the SRIF receptors mediating inhibition of neurogenic contraction in the ileum and the SRIF receptors mediating inhibition in the vas deferens and negative inotropy in the guinea-pig right atrium. In marked contrast to findings in the ileum where BIM-23027 was more potent than SRIF, BIM-23027 was considerably weaker than SRIF in both the vas deferens and right atrium providing further evidence that the SRIF receptor type in the ileum is different from that in the latter tissues (see Feniuk *et al.*, 1993). Since BIM-23027 behaved as a low efficacy agonist in the guinea-pig atria, it was tested as a potential SRIF receptor antagonist. BIM-23027 antagonized the negative inotropic action of $SRIF_{28}$ whilst having no effect on that to cyclohexyladenosine. These findings demonstrate that BIM-23027, like its structural analogue, seglitide (Dimech *et al.*, 1993) is a specific, albeit, weak, SRIF receptor antagonist in the guinea-pig isolated right atrium. The higher efficacy of BIM-23027 in the guinea-pig vas deferens precluded attempts to use it as an antagonist. The usefulness of these cyclic hexapeptides as SRIF receptor antagonists in other tissues from different species remains to be determined.

The profile of action of the other two receptor-selective peptides, BIM-23056 and L-362855, in both the vas deferens and atria was similar, both being either weak or inactive as agonists or antagonists, which supports our previous contention that the SRIF receptors in these two preparations are of the same type. We previously speculated (Feniuk *et al.*, 1993) that the SRIF receptor type involved is similar to the recombinant sst_5 receptor cloned by O'Carroll *et al.* (1992) on the basis that $SRIF_{28}$ was considerably more potent than SRIF. The findings from this study would appear to indicate that neither sst_5 nor sst_3 receptors mediate inhibition in the vas deferens or negative inotropy in the atrium, since the respective receptor selective ligands, L-362855 and BIM-23056 were either weak, or in the case of BIM-23056 inactive, in these isolated tissue preparations. However, it is possible that the difference in the potency of L-362855 could be accounted for by a species difference, since to data no guinea-pig SRIF receptor genes have been cloned. Interestingly, comparisons of the affinities of several SRIF analogues for inhibition of [Tyr^{11}]-SRIF binding to human and rat sst_5 receptors showed marked differences (O'Carroll *et al.*, 1994; Patel & Srikant, 1994). It would be interesting to determine the potency of L-362855 as an inhibitor of insulin secretion from pancreatic β cells where at least in the rat, $SRIF_{28}$ has been shown to be a more potent agonist than SRIF in inhibiting insulin secretion (Mandarino *et al.*, 1981; Amherdt *et al.*, 1987). Such a profile is consistent with the characteristics of the sst_5 receptor, and in a recent study Rossowski & Coy (1993) provided evidence with selective agonists to claim that sst_5 receptors mediate SRIF-induced inhibition of insulin secretion. An alternative possibility is that SRIF receptor type mediating negative inotropy and inhibition of neurotransmission in the guinea-pig vas deferens represents a novel receptor which like sst_5 also shows selectivity for $SRIF_{28}$. Such a protein has been identified in mouse AtT-20 cells, which do not express mouse pituitary sst_5 mRNA (Patel *et al.*, 1994). The functional significance of other recombinant (sst_1 and sst_4) SRIF receptor types still remains unknown and selective pharmacological probes for those receptors are much needed. The relationship of the SRIF receptors present in the guinea-pig vas deferens and atria *vis-a-vis* the known recombinant SRIF receptors is at present unclear. An involvement of the recombinant sst_1 and sst_4 receptor in this study seems unlikely since we have previously shown that peptides such as angiopeptin (BIM-23014) and octreotide, which have low affinity for the recombinant sst_1 and sst_4 receptors (Raynor *et al.*, 1993a,b) are both potent in the vas deferens and atrial preparations, although in the latter they behave as low efficacy agonists (Feniuk *et al.*, 1993). Furthermore, the apparent dissociation constants for seglitide and angiopeptin in guinea-pig isolated atria (pK_B 6.5 and 7.4, respectively) are also inconsistent with an action at sst_1 and sst_4 receptors.

As well as studying the effect of SRIF and some selective SRIF receptor ligands in the preparations described here, additional functional studies have been carried out in rat isolated distal colon (McKeen *et al.*, 1994), mouse vas deferens (Feniuk & Humphrey, 1994) and rat isolated gastric mucosa (Feniuk *et al.*, 1994b). In the rat colon, SRIF causes neurogenic contractile responses whilst in the mouse vas deferens, SRIF inhibits neurogenic contraction and in the rat mucosa, it inhibits gastrin-induced acid secretion. By comparing the rank orders of agonist potencies in all of these preparations (see Table 1), it is evident that two very distinct agonist profiles exist. One profile is characterized by SRIF and $SRIF_{28}$ displaying similar potency and where BIM-23027 is more potent than SRIF (guinea-pig ileum, mouse vas deferens, rat colon, rat gastric mucosa). This contrasts dramatically with the profile observed in the guinea-pig atria and vas deferens (Feniuk *et al.*, 1993), where $SRIF_{28}$ is considerably more potent than SRIF and where BIM-23027 is a very weak agonist. The high agonist potency of BIM-23027 in the former group suggests a receptor resembling the recombinant sst_2 receptor mediates these effects. The first defined physiologically relevant action of SRIF, namely the inhibition of growth hormone release from anterior pituitary cells, also appears to be mediated via sst_2 receptors (Raynor *et al.*, 1993a,b). Although on the basis of current evidence sst_2 receptors appear to mediate a diverse range of actions of SRIF, it is noteworthy that the sst_2 transcripts can be alternatively spliced to form two closely related proteins (Vanetti *et al.*, 1992). Thus, it is possible that some of these actions are mediated via sst_{2a} receptors (369 amino acids) whilst others are mediated via sst_{2b} receptors (346 amino acids). However, agonists such as BIM-23027 do not display any selectivity for either receptor variant (Reisine *et al.*, 1993).

In summary the results from this functional study using some recently identified SRIF receptor selective ligands support the view that the SRIF receptor mediating an inhibition of neurogenic contraction in the guinea-pig ileum differs from that mediating inhibition in the guinea-pig vas deferens and causing negative inotropic effects in the atria. The two receptor types presumed to be involved can be distinguished by the relative potencies of the two naturally occurring forms of somatostatin, SRIF and $SRIF_{28}$ (Feniuk *et al.*, 1993) and by the relative potency of the sst_2 receptor-selective ligand, BIM-23027.

We acknowledge the skilled technical assistance of Helen Williams.

Table 1 Comparisons of agonist potency orders in isolated tissue preparations containing SRIF receptors

Preparation	*Response*	*Agonist potency order*	*Reference*
Guinea-pig ileum	Inhibition of neurogenic contraction	BIM-23027 > SRIF ≥ $SRIF_{28}$	Feniuk *et al.* (1993); this study
Rat gastric mucosa	Inhibition of [H^+] secretion	BIM-23027 ≥ SRIF = $SRIF_{28}$	Feniuk *et al.* (1994b)
Rat colon	Contraction	BIM-23027 > SRIF ≥ $SRIF_{28}$	McKeen *et al.* (1994)
Mouse vas deferens	Inhibition of neurogenic contraction	BIM-23027 > SRIF > $SRIF_{28}$	Feniuk & Humphrey, (1994); unpublished observations
Guinea-pig vas deferens	Inhibition of neurogenic contraction	$SRIF_{28}$ > SRIF > > BIM-23027	Feniuk *et al.* (1993); this study
Guinea-pig atrium	Negative inotropy	$SRIF_{28}$ > SRIF > > BIM-23027	Feniuk *et al.* (1993); this study

References

AMHERDT, M., PATEL, Y. & ORCI, L. (1987). Selective binding of somatostatin-14 and somatostatin-28 to islet cells revealed by electron microscopic autoradiography. *J. Clin. Invest.*, **80,** 1455–1458.

BRUNO, J.F., XU, J., SONG, J. & BERELOWITZ, M. (1992). Molecular cloning and functional expression of a brain-specific somatostatin receptor. *Proc. Natl. Acad. Sci. U.S.A.*, **89,** 11151–11155.

DIMECH, J., FENIUK, W. & HUMPHREY, P.P.A. (1993). Antagonist effects of seglitide (MK678) at somatostatin receptors in guinea-pig isolated right atria. *Br. J. Pharmacol.*, **109,** 898–899.

FENIUK, W., DIMECH, J. & HUMPHREY, P.P.A. (1993). Characterisation of somatostatin receptors in guinea-pig isolated ileum, vas deferens and right atrium. *Br. J. Pharmacol.*, **110,** 1156–1164.

FENIUK, W., DIMECH, J. & HUMPHREY, P.P.A. (1994a). Further evidence for somatostatin (SRIF) receptor heterogeneity from functional studies in guinea-pig isolated tissues. *Br. J. Pharmacol.*, **113,** 132P.

FENIUK, W. & HUMPHREY, P.P.A. (1994). Somatostatin-induced inhibition of neurotransmission in the mouse isolated vas deferens is resistant to pertussis toxin. *Eur. J. Pharmacol.*, **261,** 333–337.

FENIUK, W., JARVIE, E.M. & HUMPHREY, P.P.A. (1994b). Somatostain (SRIF)-induced inhibition of gastric acid secretion in the rat isolated gastric mucosa. *Br. J. Pharmacol.*, **113,** 43P.

HOYER, D., BELL, G.I., BERELOWITZ, M., EPELBAUM, J., FENIUK, W., HUMPHREY, P.P.A., O'CARROLL, A.-M., PATEL, Y.C., SCHONBRUNN, A., TAYLOR, J.E. & REISINE, T. (1995). An updated perspective on classification and nomenclature of somatostatin receptors. *Trends Pharmacol. Sci.*, **16,** 86–88.

MANDARINO, L., STENNER, D., BLANCHARD, W. *et al.* (1981). Selective effects of somatostatin-14, -25 and -28 on *in vitro* insulin and glucagon secretion. *Nature*, **291,** 76–78.

MCKEEN, E.S., FENIUK, W. & HUMPHREY, P.P.A. (1994). Mediation by $SRIF_1$ receptors of the contractile action of somatostatin in the rat isolated distal colon; studies using some novel SRIF analogues. *Br. J. Pharmacol.*, **113,** 628–634.

O'CARROLL, A.M., LOLAIT, S.J., KONIG, M. & MAHAN, L.C. (1992). Molecular cloning and expression of a pituitary somatostatin receptor with preferential affinity for somatostatin-28. *Mol. Pharmacol.*, **42,** 939–946.

O'CARROLL, A.M., RAYNOR, K., LOLAIT, S.J. & REISINE, T. (1994). Characterisation of cloned human somatostatin receptor SSTR5. *Mol. Pharmacol.*, **46,** 291–298.

PATEL, Y.C., PANETTA, R., ESCHER, E., GREENWOOD, M. & SRIKANT, C.B. (1994). Expression of multiple somatostatin receptor genes in AtT-20 cells. *J. Biol. Chem.*, **269,** 1506–1509.

PATEL, Y.C. & SRIKANT, C.B. (1994). Subtype selectivity of peptide analogues for all five cloned human somatostatin receptors (hsstr1-5). *Endocrinology*, **135,** 2814–2817.

RAYNOR, K., MURPHY, W.A., COY, D.H., TAYLOR, J.E., MOREAU, J.-P., YASUDA, K., BELL, G.I. & REISINE, T. (1993a). Cloned somatostatin receptors: Identification of subtype selective peptides and demonstration of high affinity binding of linear peptides. *Mol. Pharmacol.*, **43,** 838–844.

RAYNOR, K., O'CARROLL, A.M., KONG, H., YASUDA, K., MAHAN, L.C., BELL, G.I. & REISINE, T. (1993b). Characterisation of cloned somatostatin receptor subtypes $SSTR_4$ and $SSTR_5$. *Mol. Pharmacol.*, **44,** 385–392.

REISINE, T., KONG, H.Y., RAYNOR, K., YANO, H., TAKEDA, J., YASUDA, K. & BELL, G.I. (1993). Splice variant of the somatostatin receptor 2 subtype, somatostatin receptor 2B, couples to adenylyl cyclase. *Mol. Pharmacol.*, **44,** 1016–1020.

RENS-DOMIANO, S., LAW, S.F., YAMADA, Y., SEINO, S., BELL, G.I. & REISINE, T. (1992). Pharmacological properties of 2 cloned somatostatin receptors. *Mol. Pharmacol.*, **42,** 28–34.

ROSSOWSKI, W.J. & COY, D.H. (1993). Potent inhibitory effects of a type four receptor selective somatostatin analogue on rat insulin release. *Biochem. Biophys. Res. Commun.*, **197,** 366–371.

VANETTI, M., KOUBA, M., WANG, X., VOGT, G. & HÖLT, V. (1992). Cloning and expression of a novel mouse somatostatin receptor (SSTR2B). *FEBS Lett.*, **311,** 290–294.

(Received February 14, 1995
Revised March 24, 1995
Accepted April 14, 1995)

British Journal of Pharmacology (1995) 115, 981-986 © 1995 Stockton Press All rights reserved 0007-1188/95 $12.00

Characterization of an α_{1D}-adrenoceptor mediating the contractile response of rat aorta to noradrenaline

[1]B.A. Kenny, D.H. Chalmers, P.C. Philpott & A.M. Naylor

Department of Discovery Biology, Pfizer Central Research, Sandwich, Kent, CT13 9NJ

1 The affinities of a number of α_1-adrenoceptor antagonists were determined by displacement of [^{3}H]-prazosin binding from cloned human α_{1A}-adrenoceptors (previously designated cloned α_{1c} subtype), α_{1B} α_{1D} and rat α_{1D}-adrenoceptors, stably expressed in rat-1 fibroblasts. Functional affinity estimates for these compounds were also determined from noradrenaline-mediated contractions of rat aorta.

2 BMY 7378 displayed high affinity for cloned human α_{1D}-adrenoceptors ($pK_i = 8.2 \pm 0.10$) and was selective over α_{1A} ($pK_i = 6.2 \pm 0.10$) and α_{1B} subtypes (6.7 ± 0.11). WB 4101, benoxathian and phentolamine displayed high affinity for α_{1A} and α_{1D} adrenoceptors compared to the α_{1B} subtype. Spiperone displayed high affinity and selectivity for α_{1B} adrenoceptors (pK_i 8.8 ± 0.16). 5-Methyl-urapidil was selective for cloned α_{1A} adrenoceptors.

3 Comparative binding affinities (pK_i) for compounds at cloned human and rat$_{1D}$ adrenoceptors were almost identical ($r = 0.99$, slope $= 1.08$).

4 Prazosin, doxazosin and 5-methyl-urapidil were potent, competitive antagonists of noradrenaline-mediated contractions of rat aorta (pA_2 values of 9.8, 8.8 and 7.8 respectively). The selective α_{1D} antagonist BMY 7378 was also a potent antagonist on rat aorta ($pK_B = 8.3 \pm 0.1$) but the interaction of this compound was not consistent with competitive antagonism at a single population of receptors.

5 Functional affinities for compounds determined against noradrenaline-mediated contractions of rat aorta correlated well with binding affinities at cloned α_{1D}-adrenoceptors ($r = 0.96$), but not with α_{1A} ($r = 0.61$) or α_{1B} ($r = 0.46$) subtypes.

6 Noradrenaline-mediated contractions of rat aorta were sensitive to the alkylating effects of chlorethylclonidine (CEC). CEC (10 μM) caused a small rightward shift in the noradrenaline concentration-response curve. CEC at 100 μM caused a further shift and suppression of the maximum response to noradrenaline.

7 The results of this study suggest that noradrenaline predominantly, but not exclusively, mediates contraction of rat aorta through the activation of an α_{1D}-adrenoceptor.

Keywords: α_1-Adrenoceptors; [^{3}H]-prazosin binding; rat aorta; adrenoceptor antagonists

Introduction

Pharmacological studies have consistently demonstrated the existence of at least two different α_1-adrenoceptor subtypes, α_{1A} and α_{1B}, in a number of tissues. Molecular cloning studies have done much to support the existence of multiple α_1 subtypes and three cloned subtypes have been identified and designated $\alpha_{1a/d}$, α_{1b} and α_{1c} (Bylund *et al.*, 1994). However, whilst the properties of cloned and tissue α_{1B} adrenoceptors are clearly similar, the relationship between cloned $\alpha_{1a/d}$ and α_{1c} subtypes in relation to endogenous receptors has only recently become clear (Ford *et al.*, 1994). When appropropriately defined in tissues such as rat submaxillary gland (Michel *et al.*, 1989) the pharmacological properties of tissue α_{1A}-adrenoceptors have been shown to be consistent with the cloned α_{1c} subtype (Faure *et al.*, 1994). Therefore, to remove ambiguity, both the cloned and endogenous subtype are referred to as an α_{1A} adrenoceptor (Bylund *et al.*, 1995). Thus, current α_1 adrenoceptor classification recognises three native and cloned subtypes which have been designated α_{1A}, α_{1B} and α_{1D} (used throughout this paper), corresponding to cloned subtypes previously designated as α_{1c}, α_{1b} and $\alpha_{1a/d}$ (Hieble *et al.*, 1995). Tissue correlates of cloned α_{1A} adrenoceptors have been demonstrated in rat submaxillary gland, human prostate and rabbit liver (Taddei *et al.*, 1993; Faure *et al.*, 1994) and correlates of the cloned α_{1B} subtype have been shown in rat liver and spleen (Kenny *et al.*, 1994a). However, whilst the presence of α_{1D}-adrenoceptors has been suggested in heterogeneous tissue populations (Michel & Insel, 1994), unequivocal demonstration of this endogenous subtype has not been shown to date. This in part has been precluded by the lack of selective compounds for this subtype, although recent preliminary evidence has indicated that BMY 7378 may be selective for cloned α_{1D}-adrenoceptors over other α_1 subtypes (Saussy *et al.*, 1994).

In an attempt to characterize the α_1-adrenoceptor mediating the contractile response of the rat aorta, several studies have concluded that the receptor cannot be classified as either α_{1A} or α_{1B} (Oriowo & Ruffolo, 1992; Aboud *et al.*, 1994) although others have suggested that a number of different subtypes contribute to the contractile response (Piascik *et al.*, 1991; van der Graaf *et al.*, 1993). Rat aorta expresses α_{1D}-adrenoceptors at the mRNA level (Perez *et al.*, 1991) and Aboud *et al.* (1994) suggested that since the pharmacological profile of the response could not be reconciled with either an α_{1A} or α_{1B} subtype, this tissue may possess a functional α_{1D}-adrenoceptor. In the present study we have characterized the pharmacological properties of rat aorta in comparison to cloned α_1-adrenoceptor subtypes and our data suggest that the contractile response of the rat aorta to noradrenaline is predominantly, but not exclusively, mediated by an α_{1D}-adrenoceptor.

A preliminary account of some these data has been presented to the British Pharmacological Society (Kenny *et al.*, 1994b; 1995).

[1] Author for correspondence.

Methods

Radioligand binding studies of cloned α_1 adrenoceptors

Cloning of rat and human α_1 adrenoceptor cDNAs and stable transfection into rat-1 fibroblasts was carried out as previously described (Schwinn *et al.*, 1995). The cells were grown in Dulbecco's modified Eagle's medium (DMEM) supplemented with 10% foetal calf serum and 300 μg ml^{-1} G418 sulphate, a neomycin analogue. For subculturing, cell monolayers were washed with Hank's balanced salt solution and trypsinized briefly with 0.05% trypsin, 0.5 mM EDTA and divided 1 : 5 to 1 : 20 every 3–4 days. Radioligand binding experiments were performed with membranes prepared from rat 1 fibroblast cells expressing individual α_1 subtypes. Scraped cells were homogenized in ice cold 50 mM Tris buffer (pH 7.5) with a Polytron homogenizer (PT10, setting 6, 20 s). The membranes were washed three times by centrifugation (20 min at 48, 000 *g*) and resuspended in fresh buffer before storage at −70°C. Cell membranes were stored at 0.5 mg ml^{-1} protein. Binding of [^{3}H]-prazosin was measured in 400 μl aliquots of diluted membranes (2–10 μg fibroblast protein) in 50 mM Tris buffer (pH 7.5) in a final assay volume of 500 μl. Non specific binding was determined in the presence of 1 μM phentolamine. Saturation isotherms were constructed by sequential dilution from a top concentration of 8 nM [^{3}H]-prazosin. Assays were incubated at 25°C with [^{3}H]-prazosin for 30 min and terminated by the addition of ice cold Tris buffer and rapid cold filtration over Whatman GF/B filters under vacuum. Saturation and displacement binding data were analysed by iterative non-linear curve fitting programmes (Graph PAD software, San Diego, U.S.A.).

Contractile responses of the rat aorta

Rings of thoracic aorta (approx 3–5 mm in length) from male Sprague-Dawley rats (250–300 g) were denuded of endothelium by gentle rubbing and suspended in organ baths under a resting tension of 1 g in Krebs Ringer bicarbonate of the following composition (mM); NaCl 120, KCl 5.5, $CaCl_2$ 2.5, NaH_2PO_4 1.2, $MgCl_2$ 1.2, $NaHCO_3$ 20, glucose 11 and EDTA 0.03 and gassed with 95% O_2/5% CO_2. The solution also contained 10 μM cocaine, 10 μM corticosterone, 1 μM propranolol and 0.5 μM yohimbine. Tissues were exposed to a sensitizing dose of (−)-noradrenaline (100 μM) and washed over a 30 min period. Isometric contractions were obtained in response to cumulative additions of (−)-noradrenaline in the absence and presence of antagonists (incubated for 30 min). Antagonist pA_2 values were obtained from a plot of log (agonist DR-1) against log antagonist concentration where the slope was not different from unity (Arunlakshana & Schild, 1959). In other experiments, estimates of affinity were determined from the negative logarithm of the antagonist dissociation constant (K_B), determined from the equation $K_B = [A]/(DR-1)$ where the dose ratio (DR) was produced by a single concentration of antagonist [A].

In experiments with chloroethylclonidine (CEC), control concentration-response curves to noradrenaline were carried out and the tissues were then exposed to CEC (10 and 100 μM) for 30 min followed by a 60 min washout period, after which a second concentration-response curve to noradrenaline was carried out.

Drugs used in the study

The following drugs were used: [^{3}H]-prazosin from Amersham U.K.; noradrenaline, cocaine hydrochloride, and corticosterone (Sigma, U.K.); chlorethylclonidine, benoxathian, urapidil, 5-methyl-urapidil, WB-4101 (2-(2,6-dimethoxyphenoxyethyl) aminomethyl-1,4-benzodioxane hydrochloride), BMY 7378 (8-[2-[4-(2-methoxyphenyl)-1-piperazinyl] ethyl]-8-azaspiro [4, 5] decane-7,9-dione dihydrochloride), and spiperone (Research Biochemicals Inc., Semat, U.K.); phentolamine hydrochloride (Ciba-Geigy, Basle, Switzerland); prazosin, doxazosin, alfuzosin, indoramin and SNAP 1069 ([1-(3-benzoylpropyl)-4-benzamidopiperidine dihydrate] were synthesized in the Department of Discovery Chemistry, Pfizer Central Research (Sandwich, U.K.). All other drugs and chemicals were obtained from Sigma (U.K.) or B.D.H. (U.K.). Drugs were dissolved in distilled H_2O or DMSO at 1 mM and subsequent dilutions made in assay buffer.

Results

[^{3}H]-prazosin binding to cloned α_1 adrenoceptor subtypes

The pharmacological profile of cloned rat α_{1D} and human α_{1A}, α_{1B} and α_{1D}-adrenoceptors was assessed by displacement of [^{3}H]-prazosin binding from rat-1 fibroblasts, stably transfected with cDNA encoding each of the α_1 adrenoceptor subtypes. The expression levels of rat and human α_{1D} subtypes were similar (1 pmol mg^{-1}) but were higher for human α_{1A} and α_{1B} subtypes (4–6 pmol mg^{-1}). In each case, analysis of saturation data indicated a single class of high affinity sites. K_d values ($n = 5-6$) were 0.13±0.02 nM for rat α_{1D} and 0.34±0.05, 0.20±0.03 and 0.22±0.05 for human α_{1A}, α_{1B} and α_{1D}-adrenoceptors respectively.

The profile of competing compounds for [^{3}H]-prazosin binding at each α_1-adrenoceptor subtype was determined by displacement of 0.2 nM [^{3}H]-prazosin by at least 12 con-

Table 1 Binding affinities (pK_i) for compounds at cloned human (α_{1A}, α_{1B} and α_{1D}) and rat (α_{1D})-adrenoceptors

	pK_i			
Compound	*Human α_{1A}*	*Human α_{1B}*	*Human α_{1D}*	*Rat α_{1D}*
BMY 7378	6.2±0.10	6.7±0.11	8.2±.010	ND
Prazosin	9.7±0.20	9.6±0.14	9.5±0.10	9.7±0.03
Doxazosin	8.5±0.20	9.0±0.20	8.4±0.12	8.5±0.09
WB 4101	9.3±0.10	8.2±0.16	9.2±0.06	9.4±0.07
5-methyl-urapidil	8.5±0.09	6.8±0.13	7.8±0.09	7.6±0.09
Benoxathian	8.9±0.23	7.8±0.14	8.6±0.12	8.9±0.09
Phentolamine	8.1±0.09	7.1±0.15	7.8±0.03	8.0±0.15
SNAP 1069	7.8±0.19	7.6±0.18	6.8±0.20	ND
Indoramin	8.3±0.03	8.0±0.12	7.3±0.15	7.2±0.10
Alfuzosin	8.0±0.20	8.0±0.13	8.5±0.07	8.5±0.15
Spiperone	7.6±0.12	8.8±0.16	8.1±0.03	8.2±0.15
Urapidil	6.9±0.07	ND	6.9±0.19	6.8±0.03

Affinities were determined by displacement of 0.2 nM [^{3}H]-prazosin from rat-1 fibroblasts stably expressing cloned α_1-adrenoceptor subtypes by 12 concentrations of competing drug. Values represent mean±s.e.mean for 3–5 separate determinations. Hill slopes were not significantly different from unity (ND, not determined).

centrations of competing drug. Displacement affinities (pK_i) are shown in Table 1. Prazosin displayed high and similar affinities (pK_i 9.5–9.7) for all α_1 adrenoceptor subtypes. BMY displayed high affinity for cloned human α_{1D}-adrenoceptors (pK_i 8.2±0.10) and was selective over α_{1A} (pK_i 6.2±0.10) and α_{1B} (pK_i 6.7±0.11) subtypes. Other compounds examined displayed a selective profile for one or more of the receptors studied (Table 1). Consistent with a previous report (Michel *et al.*, 1989) spiperone showed moderate selectivity for α_{1B} over α_{1A} and α_{1D}-adrenoceptors. 5-Methyl-urapidil, WB 4101, benoxathian, and phentolamine were selective for α_{1A} over α_{1B}-adrenoceptors. 5-Methyl-urapidil, indoramin and SNAP 1069 exhibited selectivity for α_{1A} over α_{1D} subtypes.

Displacement affinities for compounds at cloned human and rat α_{1D}-adrenoceptors were very similar (Table 1). Correlation analysis (Figure 1; $r=0.99$, slope = 1.08) confirmed the identical pharmacological profile of compounds for the species homologues of the α_{1D} adrenoceptor.

Effect of competing antagonists

Noradrenaline caused concentration-dependent isometric contractions of rat aorta with a pD_2 of 7.88±0.08 ($n=8$) and a maximum contraction of 1.5–2.0 g. Prazosin, doxazosin and 5-methyl-urapadil shifted noradrenaline concentration-response curves (CRC) to the right and Schild analysis (Figure 2) yielded pA_2 estimates of 9.8±0.30, 8.8±0.08 and 7.8±0.19 respectively. Schild slopes (0.93, 1.02 and 1.04 respectively) were consistent with competitive antagonism. Comparison of the functional potencies for compounds on rat aorta (Table 2) with binding affinity at cloned human α_{1D}-adrenoceptors correlated well (Figure 3a; $r=0.95$). In contrast, functional affinity estimates compared poorly with binding affinities at cloned human α_{1B}-adrenoceptors (Figure 3b; $r=0.61$) and human α_{1A}-adrenoceptors (Figure 3c; $r=0.46$).

The selective α_{1D} antagonist, BMY 7378, also shifted noradrenaline CRC to the right, yielding an apparent pK_B of 8.3±0.1 at 0.03 μM. However, CRC to noradrenaline were not shifted proportionally relative to the increase in BMY 7378 concentration (0.03–1.0 μM). Thus, the slope of the Schild plot was significantly lower than unity (0.62, 95% confidence limits 0.45–0.80, $P<0.05$). Dose-ratios for BMY 7378 (Table 3) were not commensurate with increasing concentrations of antagonist employed and CRC in the presence of BMY 7378 were steeper than corresponding controls.

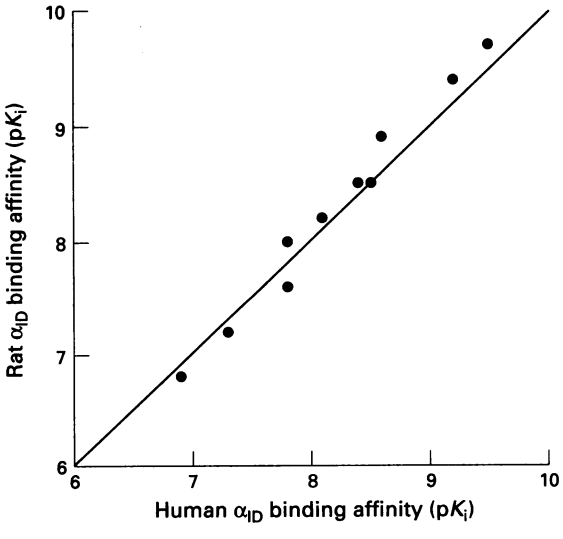

Figure 1 Comparative binding affinities at cloned human and rat α_{1D}-adrenoceptors. Data points are mean binding affinities for the compounds presented in Table 1. Regression analysis ($r=0.99$, slope = 1.1) indicates a very similar pharmacological profile of the two species homologues.

Effect of CEC

Exposure of rat aorta to 10 μM CEC caused a 3 fold dextral shift in the CRC to noradrenaline with no significant reduction in the maximum response. After exposure to 100 μM CEC, noradrenaline curves were shifted further to the right achieving 60% of the maximum response (Figure 4).

Combination experiments

Dose ratios (DR) were determined in the presence of 0.1 μM BMY 7378 and 3 μM indoramin alone or in combination to determine if the two antagonists inhibited noradrenaline-mediated contraction of rat aorta through an interaction at a common site or mutually independent sites (Paton & Rang, 1965). DR analysis (Table 4) indicated that the experimentally

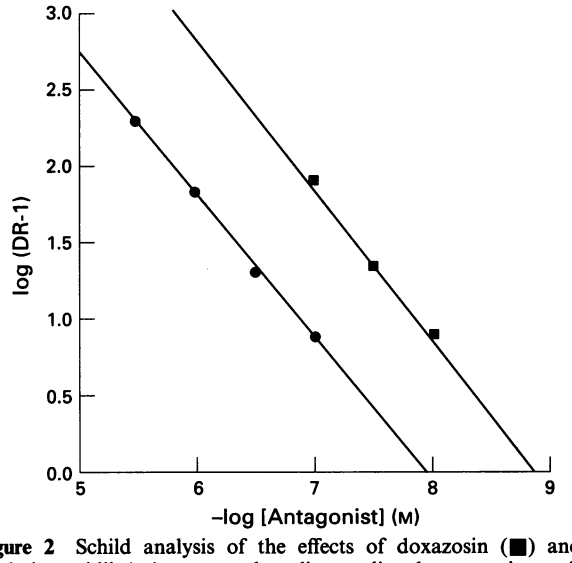

Figure 2 Schild analysis of the effects of doxazosin (■) and 5-methyl-urapidil (●) on noradrenaline-mediated contractions of rat aorta. Each data point represents a separate experiment.

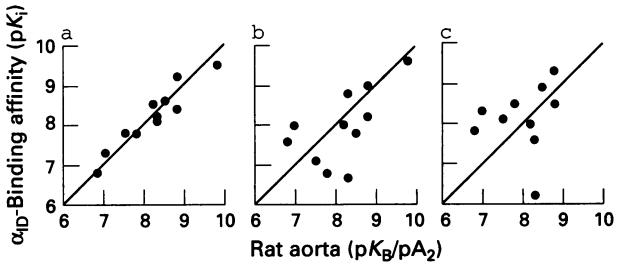

Figure 3 Comparative binding affinities (pK_i values, Table 1) at cloned human α_{1D} (Figure 3a), α_{1B} (Figure 3b), α_{1A} (Figure 3c) adrenoceptors and antagonist affinity estimates on rat aorta (pA_2/pK_B values, Table 3). In each case a theoretical line of equality is shown and regression analysis of the data is indicated in the text.

Table 2 Functional potency of BMY 7378 against noradrenaline-mediated contractions of rat aorta

Concentration of BMY 7378	*Dose-ratio*
0.03 μM	7.3±1.2
0.1 μM	16.7±4.0
0.3 μM	28.7±6.1
1.0 μM	56.9±8.6

Dose-ratios were determined from the shift in the noradrenaline CRC response curve in the presence of BMY 7378 compared to corresponding controls. Values represent the mean±s.e.mean for 4 determinations.

determined combination dose-ratio (38.5 ± 9) was very close to the predicted value from individual dose-ratios for the two antagonists acting at a single site (predicted value 37.5) rather than independent sites (predicted value 337).

Table 3 Functional potencies of antagonists (pA_2 or pK_B) against noradrenaline-mediated contractions of rat aorta

Compound	*pA_2 (slope)*
Prazosin	9.8 ± 0.30 (0.93)
Doxazosin	8.8 ± 0.08 (1.02)
5-methyl-urapidil	7.8 ± 0.19 (1.04)
	pK_B
WB 4101	8.8 ± 0.12
Indoramin	7.0 ± 0.10
Benoxathian	8.5 ± 0.06
Phentolamine	7.5 ± 0.05
Spiperone	8.3 ± 0.06
Alfuzosin	8.2 ± 0.20
SNAP 1069	6.8 ± 0.12

Antagonist potencies (mean ± s.e.mean for 3–4 experiments) were determined as described in methods. pK_B values were determined in the presence of a single concentration of antagonist.

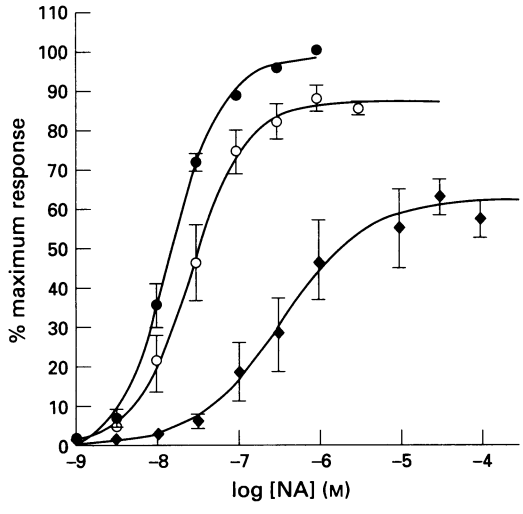

Figure 4 The effect of chlorethylclonidine (CEC) on noradrenaline-mediated contractions of rat aorta. Tissues were exposed to CEC at 10 μM (○) or 100 μM (◆) for 30 min followed by washout for 60 min. Responses are expressed as a percentage of the noradrenaline maximum obtained from the first control curve (●).

Table 4 Dose-ratio analysis of noradrenaline-mediated contractions of rat aorta with BMY 7378 and indoramin

Compound	*Mean dose-ratio*
BMY 7378 (0.1 μM)	12.9 ± 3.3
Indoramin (3 μM)	25.9 ± 6.3
BMY 7378 (0.1 μM) + 5-methyl-urapidil (3 μM)	38.5 ± 9.0
Predicted single site ($DR_1 + DR_2$)-1	37.8
Predicted independent site ($DR_1 \times DR_2$)	334.1

Dose-ratios were determined from 4–5 separate experiments, with all determinations carried out in parallel: means ± s.e.mean are given. Experimentally derived values are given in comparison to predicted values for the compounds acting at a single site or exclusively at independent sites.

Discussion

A number of different studies have attempted to characterize the α_1-adrenoceptor subtype(s) mediating the contractile response of the rat aorta, although several different conclusions have been reached. Some studies suggest that the α_1-adrenoceptor population is a homogeneous entity (Mir & Fozard, 1990; Eltze & Boer, 1992; Aboud *et al.*, 1993) which has been postulated to be either an α_{1B} subtype (Eltze & Boer, 1992) or a receptor which cannot be classified as either α_{1A} or α_{1B} (Mir & Fozard, 1990; Aboud *et al.*, 1993). Other studies have concluded that a number of different α_1 subtypes contribute to the response (Piascik *et al*, 1991; 1994; van der Graaf *et al.*, 1993). On the basis of the data presented in this paper, our results support the contention suggested in some of these studies (Mir & Fozard, 1990; Aboud *et al.*, 1993) that the contractile response to noradrenaline is mediated by a non α_{1A}, non α_{1B} subtype. Indeed, our data suggest that the contractile response to this agonist is predominantly mediated by an α_{1D}-adrenoceptor.

Functional affinity estimates on rat aorta determined with noradrenaline were highly correlated with binding affinities determined at the cloned α_{1D}-adrenoceptor. These data are consistent with the preliminary report of Saussy *et al.* (1994) using phenylephrine as an agonist. This conclusion could be drawn on the basis of binding data in the present study obtained with either cloned rat or human α_{1D}-adrenoceptors. Recently reported studies (Kenny *et al.*, 1994b; Schwinn *et al.*, 1995) show only minor differences between cloned α_1-adrenoceptors from different species. [+]-Niguldipine appears to be an exception having relatively high affinity for human and rat α_{1A}-adrenoceptors compared to the bovine homologue in some (Forray *et al.*, 1994b; Weinberg *et al.*, 1994) but not all (Schwinn *et al.*, 1995) studies. This has enabled reconciliation between the cloned and native α_{1A} subtype (Faure *et al.*, 1994; Ford *et al.*, 1994; Hieble *et al.*, 1995). In contrast to cloned α_{1D}-adrenoceptors, binding data with cloned α_{1A} and α_{1B} subtypes correlated poorly with functional affinity determinations on rat aorta. Indeed, compounds with varying degrees of subtype selectivity inhibited contractions of the aorta with binding affinities only consistent with those determined at the α_{1D} subtype (most notably with BMY 7378, indoramin, 5-methyl-urapidil and SNAP 1069).

It is difficult to compare binding data with cloned α_{1D}-adrenoceptors obtained in our study with the binding characteristics of a homogeneous population of native α_{1D}-adrenoceptors since this has not been described to date. The presence of α_{1D}-adrenoceptors has been suggested in some heterogeneous tissue populations such as rat kidney (Michel *et al.*, 1993). Some studies have suggested that following CEC treatment of rat cortex, the population of sites is characteristic of either α_{1D} (Kenny *et al.*, 1994a) or α_{1A}-adrenoceptors (Eltze & Boer, 1992), although it seems probable that the population of sites following CEC in this tissue is heterogeneous since discriminatary compounds such as (+)-niguldipine reveal multiple sites after CEC treatment (Han & Minneman, 1991; Ford *et al.*, 1994). Nevertheless, the pharmacological profile of cloned rat and human α_{1D}-adrenoceptors obtained in the present study clearly differs from the characteristics of α_{1A} and α_{1B}-adrenoceptors defined in tissues such as rat submaxillary gland and rat liver (Faure *et al.*, 1994).

Our data indicate that the contractile response of the rat aorta in response to noradrenaline is predominantly mediated by a single receptor, namely on α_{1D} subtype, and this is also supported by analysis of combination experiments with BMY 7378 and indoramin. We characterized the effect of BMY 7378 and indoramin in combination, using an indoramin concentration sufficiently high to antagonize any putative α_{1A} or α_{1B} adrenoceptors present. Dose-ratio analysis of the data for the antagonists alone and in combination was consistent with the presence of a single site for which both antagonists mutually competed. This approach was also taken by Eltze & Boer (1992) using WB-4101 and 5-methyl-urapidil,

and they also concluded that a single subtype mediated the response to noradrenaline. However, this finding may not hold at higher antagonist concentrations, typically evoking much larger agonist dose-ratios and may be limited by the relative contribution of different receptor subtypes. Alternatively, another site may be present which is not effectively antagonized by either BMY 7378 or indoramin.

It could be argued that the CEC sensitivity of the contractile response of rat aorta might be indicative of α_{1B}-adrenoceptors (Eltze & Boer, 1992); however, this conclusion is not supported by the pharmacological profile of any of the compounds examined. Both rat and human homologues of the cloned α_{1D}-adrenoceptor show a moderate degree of sensitivity to alkylation by CEC, greater than the α_{1A} subtype, but to a lesser extent than the α_{1B} subtype (Forray *et al.*, 1994a,b; Schwinn *et al.*, 1994). The effect of CEC on the rat aorta is consistent with the sensitivity of the cloned α_{1D}-adrenoceptor to CEC and contrasts with the reported insensitivity of the α_{1A} subtype in smooth muscle preparations (Bylund *et al.*, 1994). However, it is often difficult to reconcile findings with CEC as a means of differentiating between subtypes since alkylation by CEC is dependent on species, time of exposure and nature of the preparation which makes comparison of different experimental protocols difficult. Thus, the component of the noradrenaline response that was resistant to CEC in our studies could indicate incomplete alkylation of the α_{1D}-adrenoceptor or the presence of a CEC resistant subtype(s). Analysis of antagonist profiles following CEC treatment would provide some insight into the nature of any additional component. It is interesting to note that some α_1-adrenoceptor subtypes which cannot be reconciled with currently identified cloned adrenoceptors are relatively insensitive to CEC (α_{1L}-adrenoceptors; Muramatsu *et al.*, 1990).

The exclusive presence of mRNA for the α_{1D}-adrenoceptor has been suggested in rat aorta on the basis of Northern analysis (Lomasney *et al.*, 1991) although more recent *in situ* hybridization studies have indicated the presence of all three α_1 subtypes (Piascik *et al.*, 1994). Heterogeneity of α_1-adrenoceptors has also been claimed on the basis of [^{3}H]-prazosin binding to rat aorta membranes in which compounds such as WB 4101 and 5-methyl-urapidil exhibit two different binding affinities (Piasik *et al.*, 1994). Piascik *et al.* (1991) also reported that the concentration-response curve to phenylephrine following CEC treatment became biphasic, indicating the presence of two functional α_1-adrenoceptors, only one of which was CEC-sensitive. Further evidence for heterogeneity of α_1-adrenoceptors on rat aorta has also been claimed on the basis of other functional studies (van der Graaf *et al.*, 1994) in which noradrenaline concentration-response curves in the presence of several antagonists could not be accounted for by simple competitive antagonism at a single receptor (Schild slopes lower than unity and steepening of agonist concentration-response curve). Cellular signalling pathways have previously been used as an additional criterion for discriminating between subtypes and in rat aorta both dependence and independence of the α_1-mediated contractile response on extracellular Ca^{2+} has been demonstrated (Mir & Fozard, 1990; Oriowo *et al.*, 1990). However, differential coupling to signalling mechanisms cannot be reliably used to classify α_1-adrenoceptor subtypes (Minneman, 1988) and in rat aorta since antagonist potencies were unaffected by the presence of nifedipine, both intracellular Ca^{2+} increases and dihydropyridine-sensitive calcium entry can be attributed to activation of a single subtype (Mir & Fozard, 1990; Ruffolo *et al.*, 1991).

Thus, whilst in our studies evidence indicates that a single subtype predominantly mediates the contractile response to noradrenaline, we cannot preclude the existence of other subtypes. Using the selective α_{1D} antagonist BMY 7378, pA_2 determinations consistently yielded Schild slopes less than unity (slope = 0.62). Dose-ratios were not commensurate with increasing concentrations of BMY 7378 and noradrenaline curves were steepened in the presence of the antagonist. This finding is consistent with the contention that noradrenaline activates more than one receptor, although this profile was not exhibited by other antagonists in our and other studies (Eltze & Boer, 1992; Aboud *et al.*, 1993), nor is it supported by data derived from combination studies.

A number of studies with cloned human and other mammalian α_1-adrenoceptors indicate that noradrenaline has higher affinity for the cloned α_{1D} subtype in comparison to other subtypes (Perez *et al.*, 1991; Michel & Insel, 1994). Since noradrenaline displays high affinity on rat aorta (possibly reflecting a large receptor reserve), it may be possible that this agonist is relatively selective for α_{1D}-adrenoceptors under the conditions used in our study, to the extent that activation of other subtypes occurs only at much higher agonist concentrations. This could account for steepening of noradrenaline curves and low Schild slope with BMY 7378. Taken together, although our data suggest a predominant role for α_{1D}-adrenoceptors in the contractile response to noradrenaline, consistent with other reports suggesting that a single subtype mediates the contractile response, we cannot fully exclude the presence of other subtypes.

In summary, we have shown that the pharmacological profile of compounds at cloned human and rat α_{1D}-adrenoceptors is consistent with functional affinity estimates determined on rat aorta. The selective α_{1D} antagonist, BMY 7378, also antagonized noradrenaline-mediated contractions of rat aorta consistent with α_{1D} binding affinity although the profile of this compound did not suggest competitive antagonism at a single receptor. The data in our study suggests that noradrenaline predominantly contracts the rat aorta through an α_{1D}-adrenoceptor, but the involvement of other subtypes cannot be precluded at the present time.

References

ABOUD, R., SHAFII, M. & DOCHERTY, J.R. (1993). Investigation of the subtypes of α_1 adrenoceptor mediating contractions of rat aorta, vas deferens and spleen. *Br. J. Pharmacol.*, **109**, 80–87.

ARUNLAKSHANA, O. & SCHILD, H.O. (1959). Some quantitative uses of drug antagonists. *Br. J. Pharmacol. Chemother.*, **14**, 48–52.

BYLUND, D.B. (1992). Subtypes of α_1 and α_2 adrenergic receptors. *FASEB J.*, **6**, 832–840.

BYLUND, D.B., EIKENBURG, D.C., HIEBLE, J.P., LANGER, S.Z., LEFKOWITZ, R.J., MINNEMAN, K.P., RUFFOLO, R.R. & TRENDELENBERG, U. (1994). International Union of Pharmacology Nomenclature of Adrenoceptors. *Pharmacol. Rev.*, **46**, 121–136.

ELTZE, M. & BOER, R. (1992). The adrenoceptor agonist, SDZ NVI 085, discriminates between α_{1A} and α_{1B} adrenoceptor subtypes in vas deferens, kidney and aorta of the rat. *Eur. J. Pharmacol.*, **224**, 125–136.

FAURE, C., PIMOULE, C., ARBILLA, S., LANGER, S.Z. & GRAHAM, D. (1994). Expression of α_1 adrenoceptor subtypes in rat tissues: implications of α_1 adrenoceptor classification. *Eur. J. Pharmacol.*, **268**, 141–149.

FORD, A.P.D.W., WILLIAMS, T.J., BLUE, D.R. & CLARKE, D.E. (1994). α_1 Adrenoceptor classification: sharpening Occam's razor. *Trends Pharmacol. Sci.*, **15**, 167–170.

FORRAY, C., BARD, J.A., LAZ, T.M., SMITH, K.E., VAYAAS, P.J., WEINSHANK, R.L., GLUCHOWSKI, C. & BRANCHEK, T.A. (1994a). Comparison of the pharmacological properties of the cloned human and rat α_{1C} adrenergic receptors. *FASEB J.*, **8**, A353.

FORRAY, C., BARD, J.A., WETZEL, J.M., CHIU, G., SHAPIRO, E., TANG, R., LEPOR, H., HARTIG, P.R., WEINSHANK, R.L., BRANCHEK, T.A. & GLUCHOWSKI, C. (1994b). The α_1 adrenoceptor that mediates smooth muscle contraction in human prostate has the pharmacological properties of the cloned human α_{1C} subtype. *Mol. Pharmacol.*, **45**, 703–708.

HAN, C. & MINNEMAN, K.P. (1991). Interaction of subtype selective antagonists with α_1 adrenergic receptor binding sites in rat tissues. *Mol. Pharmacol.*, **40**, 531–538.

HIEBLE, J.P., BYLUND, D.B., CLARKE, D.E., EIKENBURG, D.C., LANGER, S.Z., LEFKOWITZ, R.J., MINNEMAN, K.P. & RUFFOLO, R.R. (1995). Recommendation for Nomenclature of α_1 Adrenoceptors: Consensus Update. *Pharmacol Rev.*, (in press).

KENNY, B.A., NAYLOR, A.M., GREENGRASS, P.M., RUSSELL, M.J., FRIEND, S.J., READ, A.M. & WYLLIE, M.G. (1994a). Pharmacological properties of the cloned $\alpha_{1A/D}$ adrenoceptor subtype are consistent with the α_{1A} adrenoceptor characterised in rat cerebral cortex and vas deferens. *Br. J. Pharmacol.*, **111**, 1003–1008.

KENNY, B.A., PHILPOTT, P.C., NAYLOR, A.M. & WYLLIE, M.G. (1994b). Comparative properties of cloned mammalian and human $\alpha_{1A/D}$ and α_{1C} adrenoceptors. *Br. J. Pharmacol.*, **113**, 98P.

KENNY, B.A., CHALMERS, D.H. & NAYLOR, A.M. (1995). Characterization of a functional α_{1D} adrenoceptor on rat aorta. *Br. J. Pharmacol.*, **114**, 25P.

LOMASNEY, J.W., COTECCIA, S., LORENZ, W., LEUNG, W.Y., SCHWINN, D.A., YANG-FENG, T.L., BROWNSTEIN, M., LEFKOWITZ, R.J. & CARON, M.G. (1991). Molecular cloning and expression of the cDNA for the α_{1A} adrenergic receptor. *J. Biol. Chem.*, **266**, 6356–6369.

MCGRATH, J.C., BROWN, C.M. & WILSON, V.G. (1989). Alpha adrenoceptors: a critical review. *Med. Res. Rev.*, **9**, 407–533.

MICHEL, A.D., LOURY, D.N. & WHITING, R.L.(1989). Identification of a single α_1 adrenoceptor corresponding to the α_{1A} subtype in rat submaxillary gland. *Br. J. Pharmacol.*, **98**, 883–889.

MICHEL, M.C., BUSHER, R., KERKER, J., KRANEIS, H., ERDBRUGGER, W. & BRODDE, E.E. (1993). α_1 Adrenoceptor subtype affinities of drugs for the treatment of prostatic hypertrophy. *Naunyn-Schmied Arch Pharmacol.*, **348**, 385–395.

MICHEL, M.C. & INSEL, P.A. (1994). Comparison of cloned and pharmacologically defined rat tissue α_1 adrenoceptor subtypes. *Naunyn-Schmied. Arch. Pharmacol.*, **350**, 136–142.

MINNEMAN, K.P. (1988). Alpha$_1$ adrenergic receptor subtypes, inositol phosphates, and sources of cell Ca^{2+}. *Pharmacological. Rev.*, **40**, 87–119.

MIR, A.K. & FOZARD, J.R. (1990). A single α_1 adrenoceptor, distinct from the α_{1A} and α_{1B} subtypes, may mediate contraction of rat aorta to phenylephrine. *Br. J. Pharmacol.*, **98**, 651P.

MURAMATSU, I., OHMURA, T., KIGOSHI, S., HASHIMOTO, S. & OSHITA, M. (1990). Pharmacological subclassification of α_1 adrenoceptors in vascular smooth muscle. *Br. J. Pharmacol.*, **99**, 197–201.

ORIOWO, M.A. & RUFFOLO, R.R. (1992). Heterogeneity of postjunctional α_1 adrenoceptors in mammalian aortae: subclassification based on chlorethylclonidine, WB 4101 and nifedipine. *J. Vasc. Res.*, **29**, 33–40.

PATON, W.D.M. & RANG, H.P. (1965). The uptake of atropine and related drugs by intestinal smooth muscle of the guinea-pig in relation to acetylcholine receptors. *Proc. R. Soc.*, **163**, 1–44.

PEREZ, D.M., PIASCIK, M.T. & GRAHAM, R.M. (1991). Solution-phase library screening for the identification of rare clones: isolation of an α_{1D} adrenergic receptor cDNA. *Mol. Pharmacol.*, **40**, 876–883.

PIASCIK, M.T., SPARKS, M.S., PRUITT, T.A. & SOLTIS, E.E. (1991). Evidence for a complex interaction between the subtypes of the α_1 adrenoceptor. *Eur. J. Pharmacol.*, **199**, 279–289.

PIASCIK, M.T., SMITH, M.S., SOLTIS, E.E. & PEREZ, D.M. (1994). Identification of the mRNA for the novel α_{1D} adrenoceptor and two other α_1 adrenoceptors in vascular smooth muscle. *Mol. Pharmacol.*, **46**, 30–40.

RUFFOLO, R.R., NICHOLS, A.J., STADEL, J.M. & HIEBLE, J.P. (1991). Structure and function of α adrenoceptors. *Pharmacol. Rev.*, **43**, 475–505.

SAUSSY, D.L., GOETZ, A.S., KING, H.K. & TRUE, T.A. (1994). BMY 7378 is a selective antagonist of α_{1D} adrenoceptors. *Can. J. Physiol. Pharmacol.*, **72**, A323.

SCHWINN, D.A., JOHNSTON, G.I., PAGE, S.O., MOSLEY, M.J., WILSON, K.H., WORMAN, N.P., CAMPBELL, S., FIDOCK, M.D., FURNESS, L.M., PARRY-SMITH, D.J., PETER, B. & BAILEY, D.S. (1995). Cloning and pharmacological characterisation of human α_1 adrenergic receptors: sequence corrections and direct comparison with other species homologs. *J. Pharmacol. Exp. Ther.*, **272**, 134–142.

TADDEI, C., POGGESI, E., LEONARDI, A. & TESTA, R. (1993). Affinity of different α_1 agonists and antagonists for the α_1 adrenoceptors of rabbit and rat liver membranes. *Life Sci.*, **53**, 177–181.

VAN DER GRAFF, P.H., WELSH, N.J., SHANKLEY, N.P. & BLACK, J.W. (1993). Evidence for heterogeneity of α_1 adrenoceptors in the rat aorta. *Br. J. Pharmacol.*, **110**, 124P.

WEINBERG, D.H., TRIVEDI, P., TAN, C.P., MITRA, S., PERKINS-BARROW, A., BORKOWSKI, D., STRADER, C.D. & BAYNE, M. (1994). Cloning expression and characterisation of human α_1 adrenergic receptors α_{1A}, α_{1B} and α_{1C}. *Biochem. Res. Commun.*, **201**, 1296–1304.

(Received January 9, 1995
Revised March 15, 1995
Accepted April 11, 1995)

British Journal of Pharmacology (1995) 115, 987-992 © 1995 Stockton Press All rights reserved 0007-1188/95 $12.00

Thapsigargin- and cyclopiazonic acid-induced endothelium-dependent hyperpolarization in rat mesenteric artery

[1]Mitsuhiro Fukao, Yuichi Hattori, Morio Kanno, *Ichiro Sakuma & *Akira Kitabatake

Departments of Pharmacology and *Cardiovascular Medicine, Hokkaido University School of Medicine, Sapporo 060, Japan

1 The present study was designed to determine whether putative, selective inhibitors of the Ca^{2+}-pump ATPase of endoplasmic reticulum, thapsigargin (TSG) and cyclopiazonic acid (CPA), induce endothelium-dependent hyperpolarization in the rat isolated mesenteric artery. The membrane potentials of smooth muscle cells of main superior mesenteric arteries were measured by the microelectrode technique.

2 In tissues with endothelium, TSG ($10^{-8}-10^{-5}$ M) caused sustained hyperpolarization in a concentration-dependent manner. In tissues without endothelium, TSG did not cause any change in membrane potential. CPA (10^{-5} M) also hyperpolarized the smooth muscle membrane, an effect that was endothelium-dependent and long-lasting.

3 The hyperpolarizing responses to these agents were not affected by indomethacin or N^G-nitro-L-arginine (L-NOARG).

4 In Ca^{2+}-free medium, neither TSG nor CPA elicited hyperpolarization, in contrast to acetylcholine which generated a transient hyperpolarizing response.

5 In rings of mesenteric artery precontracted with phenylephrine, TSG and CPA produced endothelium-dependent relaxations. L-NOARG significantly inhibited the relaxations to these agents, but about 40-60% of the total relaxation was resistant to L-NOARG. The L-NOARG-resistant relaxations were abolished by potassium depolarization.

6 These results indicate that TSG and CPA can cause endothelium-dependent hyperpolarization in rat mesenteric artery possibly by releasing endothelium-derived hyperpolarizing factor and that membrane hyperpolarization can contribute to the endothelium-dependent relaxations to these agents. The mechanism of hyperpolarization may be related to increased Ca^{2+} influx into endothelial cells triggered by depletion of intracellular Ca^{2+} stores due to inhibition of endoplasmic reticulum Ca^{2+}-pump ATPase activity.

Keywords: Thapsigargin; cyclopiazonic acid; acetylcholine; endothelium; hyperpolarization; vasorelaxation; vascular smooth muscle

Introduction

Endothelial cells modulate the tone of underlying vascular smooth muscle cells by releasing prostacyclin (Moncada *et al.*, 1977), endothelium-derived relaxing factor (EDRF) (Furchgott & Zawadzki, 1980) and contracting factors (Lüscher *et al.*, 1992). EDRF is now considered to be identical to nitric oxide (NO) (Palmer *et al.*, 1987) or to a related nitroso compound (Myers *et al.*, 1990). Endothelial cells also mediate hyperpolarization of smooth muscle cells in response to agents such as acetylcholine (Chen *et al.*, 1988; Feletou & Vanhoutte, 1988). Some electrophysiological studies have demonstrated that endothelium-dependent hyperpolarization does not appear to be mediated by NO (Bény & Brunet, 1988; Garland & McPherson, 1992), suggesting the existence of another biologically-active, endothelium-derived factor. The yet undefined factor causing membrane hyperpolarization has been named endothelium-derived hyperpolarizing factor (EDHF) (Taylor & Weston, 1988; Furchgott & Vanhoutte, 1989; Suzuki *et al.*, 1992).

Thapsigargin (TSG) is a tumour-promoting agent extracted from the umbelliferous plant *Thapsia garcanica* (Christensen *et al.*, 1981) which has been shown to inhibit selectively the Ca^{2+}-pump ATPase of endoplasmic reticulum in a variety of tissues (Thastrup *et al.*, 1990). TSG causes endothelium-dependent relaxation in rat aorta (Mikkelsen *et al.*, 1988; Zheng *et al.*, 1994) and in guinea-pig aorta (Matsuyama *et al.*, 1993). TSG elevates cytosolic Ca^{2+} concentration in endothelial cells (Gericke *et al.*, 1993) and the release of EDRF is dependent on intracellular Ca^{2+} (Singer & Peach, 1982). These findings suggest that the increase in cytosolic Ca^{2+} concentration in endothelial cells may be responsible for the TSG-induced endothelium-dependent relaxation.

Increased cytosolic Ca^{2+} concentration in endothelial cells has also been proposed as an obligatory step in the production and/or release of EDHF (Chen & Suzuki, 1990). Thus, TSG might induce endothelium-dependent hyperpolarization by releasing EDHF. To assess this possibility, the present study was designed to investigate the effect of TSG on the membrane potential of smooth muscle cells in rat isolated mesenteric arteries. We also examined the effect of cyclopiazonic acid (CPA), another selective inhibitor of endoplasmic reticulum Ca^{2+} pump ATPase (Seidler *et al.*, 1989; Georger *et al.*, 1988) in order to determine whether the observed electrical effect of TSG, if any, is attributed to the selective inhibition of the enzyme, and compared the effects of TSG and CPA with those of acetylcholine (Chen & Suzuki, 1990). We found that both TSG and CPA elicited endothelium-dependent hyperpolarization. Further experiments were carried out to assess the contribution of membrane hyperpolarization to endothelium-dependent relaxations induced by these agents.

Methods

Electrophysiological experiments

Male Wistar rats between 10 and 15 weeks old and weighing 250-340 g, were anaesthetized with diethyl ether. The main branch of the superior mesenteric arteries was excised carefully

[1] Author for correspondence.

and placed on a plate containing oxygenated physiological salt solution (PSS) at room temperature. The arteries were dissected free from surrounding tissues, cut into rings 3-mm in length, and opened longitudinally. Care was taken to ensure that the endothelial cell layer was not damaged during tissue preparation. Where indicated, the endothelial cells were removed by gently rubbing the intimal surface of the vessel with a moistened cotton ball. The tissue was pinned down, intimal side upward, on the bottom of an organ chamber (capacity 3 ml), and superfused at a constant flow rate of 7 ml min^{-1} with normal PSS aerated with 95% O_2 and 5% CO_2. The temperature of the perfusate was kept constant at 37°C. Normal PSS contained the following (mM); NaCl 118.2, KCl 4.7, $CaCl_2$ 2.5, $MgCl_2$ 1.2, KH_2PO_4 1.2, $NaHCO_3$ 25.0, and glucose 10.0. For Ca^{2+}-free PSS, Ca^{2+} was omitted and 0.2 mM EGTA was added. After the preprations were allowed to equilibrate for 60 min, glass microelectrodes filled with 3 M KCl (tip resistance 40–80 MΩ) were inserted into the smooth muscle cells from the intimal surface. Electrical signals were monitored continuously on an oscilloscope (Nihon Kohden, VC-10, Tokyo, Japan) and recorded on a chart recorder (Watanabe Sokki, WR3101, Tokyo, Japan). For data analysis we used only the experiments in which a single impalement was maintained.

Mechanical experiments

Rat mesenteric arterial rings were prepared as described above. Each ring was suspended by a pair of stainless steel hooks in a water-jacketed bath filled with 25 ml of normal PSS. The solution in the bath was gassed with 95% O_2 and 5% CO_2 and its temperature was maintained at 37°C. The rings were stretched until a resting tension of 1 g was reached and then allowed to equilibrate for 60 min. Force generation was monitored using an isometric transducer (Sanei-Sokki, 45196, Tokyo, Japan) and a carrier amplifier (Sanei-Sokki, 1236). The output of the force transducer was registered on a pen recorder (TOA Electronics, ERP-241A, Tokyo, Japan) through a polygraph recorder (Sanei-Sokki, 142-8).

After the equilibration period, the rings were exposed several times to high K^+ PSS (40 mM $[K^+]_0$) until reproducible contractile responses were obtained. High K^+ PSS was made by substituting NaCl with equimolar KCl. The vessels were then precontracted with 10^{-6} M phenylephrine. After the contraction had reached a plateau level, 10^{-6} M TSG or 10^{-5} M CPA was applied. When 3×10^{-5} M N^G-nitro-L-arginine (L-NOARG) was used in order to exclude the involvement of EDRF-NO in the responses to TSG and CPA, it was added 15 min before the addition of phenylephrine. Because pretreatment with L-NOARG markedly enhanced the phenylephrine-induced contractions, care was taken to match the contractions induced by phenylephrine in control and pretreated rings. Thus, in the experiments with L-NOARG, the tissues were precontracted with 10^{-7} M phenylephrine. Relaxations were expressed as a percentage of the height of the contraction induced by phenylephrine.

Drugs

The compounds used were as follows: TSG (Calbiochem-Novabiochem Corp., San Diego, CA, U.S.A.); CPA, L-NOARG, indomethacin and (−)-phenylephrine hydrochloride (Sigma Chemical Co., St. Louis, MO, U.S.A.); and acetylcholine chloride (Wako Pure Chemical Industries, Osaka, Japan). TSG was prepared as a stock solution (2×10^{-2} M) in dimethyl sulphoxide and diluted in ethanol. CPA was dissolved in dimethyl sulphoxide. L-NOARG and indomethacin were prepared in 0.2 N HCl and 50 mM Tris, respectively. Other chemicals were dissolved in distilled water. Further dilutions were made with PSS.

Statistical analysis

All values are presented in terms of the means ± s.e.mean. Analysis by Student's t test was performed for paired and unpaired observations. P values less than 0.05 were considered significant.

Results

Endothelium-dependent hyperpolarization by acetylcholine

The resting membrane potentials of vascular smooth muscle cells in preparations with endothelium averaged −55.5 ± 0.4 mV ($n=68$). Removal of the endothelium produced no significant change in the resting membrane potential (−56.0 ± 1.5 mV, $n=5$, $P>0.5$). When the preparations were exposed to Ca^{2+}-free PSS, the resting membrane potentials were gradually depolarized (see Figures 1b, 4b and 5b). The membrane potentials were depolarized by 8 ± 1 and 16 ± 2 mV ($n=10$, $P<0.001$) at 5 and 10 min after exposure to Ca^{2+}-free PSS, respectively.

In tissues with intact endothelium, application of 10^{-6} M acetylcholine promptly hyperpolarized the membrane potential (Figure 1a). The hyperpolarizing response to acetylcholine was composed of two components as previously reported (Chen & Suzuki, 1990); i.e., an initial transient and following sustained phase. The time required to reach the peak amplitude of the initial transient component was within 10 s. The sustained component reached maximum amplitudue at 20–60 s after the addition of acetylcholine, and decayed with a very slow time course. In Ca^{2+}-free PSS, acetylcholine produced only a transient hyperpolarizing effect (Figure 1b). After the endothelium was removed, acetylcholine no longer caused hyperpolarization (data not shown).

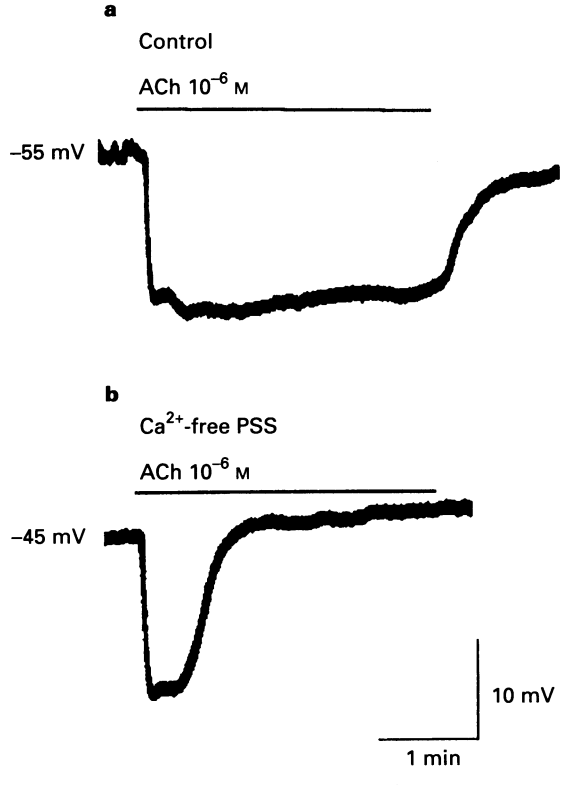

Figure 1 Effect of acetylcholine (ACh, 10^{-6} M) on cell membrane potential of rat mesenteric artery with endothelium in normal PSS (a) and in Ca^{2+}-free PSS (b). ACh was applied 5 min after exposure to Ca^{2+}-free PSS. Traces were recorded in different tissues.

Endothelium-dependent hyperpolarization of TSG and CPA

Figure 2 shows typical membrane potential changes elicited by TSG at different concentrations in the presence of endothelial cells. Application of TSG in concentrations less than 3×10^{-9} M caused no detectable change in the membrane potentials. At concentrations of 10^{-8} M or higher, TSG produced a gradual, progressive hyperpolarization of the membrane potential in a concentration-dependent manner. The time required to reach a peak effect after the addition of TSG was much longer than that after the addition of acetylcholine. Figure 3 summarizes the concentration-dependent hyperpolarizing effect of TSG on the membrane potential of smooth muscle cells of rat mesenteric arteries. TSG hyperpolarized by -18.3 ± 0.9 mV ($n=4$, $P<0.001$) at a concentration of 10^{-6} M, which was required to reach the maximum amplitude. In tissues without an endothelium, 10^{-6} M TSG produced no significant change in the membrane potential ($n=4$, Figure 4a). The hyperpolarizing effect of 10^{-6} M TSG was not observed in Ca^{2+}-free PSS even in endothelium-intact tissues ($n=4$, Figure 4b).

Figure 5 shows the typical membrane potential changes elicited by CPA. CPA also produced sustained membrane hyperpolarization of smooth muscle cells (Figure 5a), an effect not observed in tissues from which the endothelium had been removed ($n=4$). CPA at a concentration of 10^{-5} M hyperpolarized the membrane potential by -16.2 ± 1.2 mV ($n=5$, $P<0.001$). However, CPA caused no hyperpolarization in Ca^{2+}-free PSS even if the endothelium was intact ($n=4$, Figure 5b).

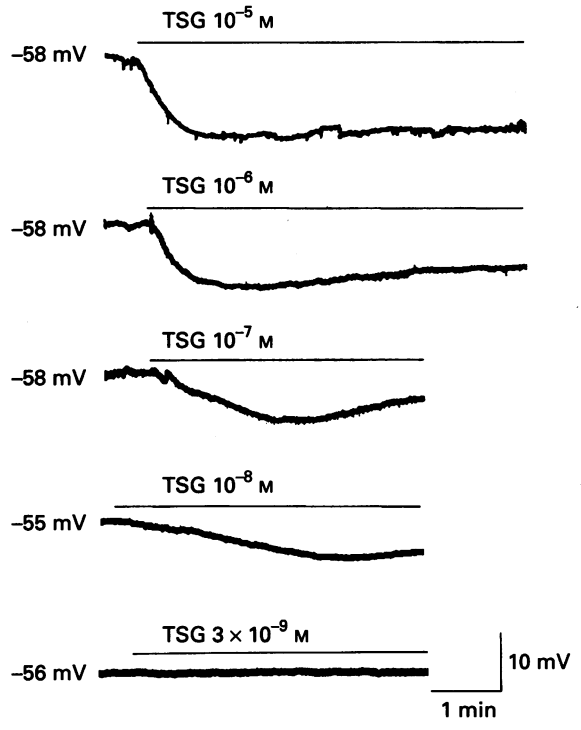

Figure 2 Effect of thapsigargin (TSG) at different concentrations on cell membrane potential of rat mesenteric artery with endothelium. Each trace is typical of the effect of that concentration of TSG.

Influence of L-NOARG and indomethacin on endothelium-dependent hyperpolarization

In order to assess the possible involvement of endogenous vasoactive prostanoids and EDRF-NO in the endothelium-dependent hyperpolarization, the influence of indomethacin and L-NOARG on the responses to acetylcholine, TSG and CPA was examined. Neither indomethacin nor L-NOARG affected the resting membrane potential. The maximal amplitude of the hyperpolarizing effect elicited by 10^{-6} M TSG was not affected by pretreatment of the tissues with either 10^{-5} M indomethacin or 3×10^{-5} M L-NOARG (Figure 6). Similarly, pretreatment with indomethacin or L-NOARG had no influence on the hyperpolarizing responses to 10^{-6} M acetylcholine and 10^{-5} M CPA ($n=4$, for each group).

Endothelium-dependent relaxation by TSG and CPA

As shown in Figure 7, 10^{-6} M TSG induced marked relaxation in the endothelium-intact arterial ring preparations which had been precontracted with phenylephrine. In the presence of 3×10^{-5} M L-NOARG, the relaxant response to TSG was significantly reduced (control $93 \pm 5\%$, and L-NOARG treated $53 \pm 4\%$; $P<0.001$). The intriguing finding was that even in the presence of L-NOARG, TSG produced transient relaxations (Figures 7 and 8a). In the arterial rings precontracted with phenylephrine after both high K^+ PSS (25 mM) and L-NOARG were applied, TSG no longer caused relaxations (Figure 8b). Removal of the endothelium virtually abolished the relaxant responses to TSG regardless of whether L-NOARG was present (Figure 8c). CPA at 10^{-5} M also caused endothelium-dependent relaxations of the phenylephrine-precontracted arterial rings (Figure 7). Pretreatment with L-NOARG attenuated the relaxant effect induced by CPA. However, a small but substantial relaxant response to CPA was still observed even in the presence of L-NOARG.

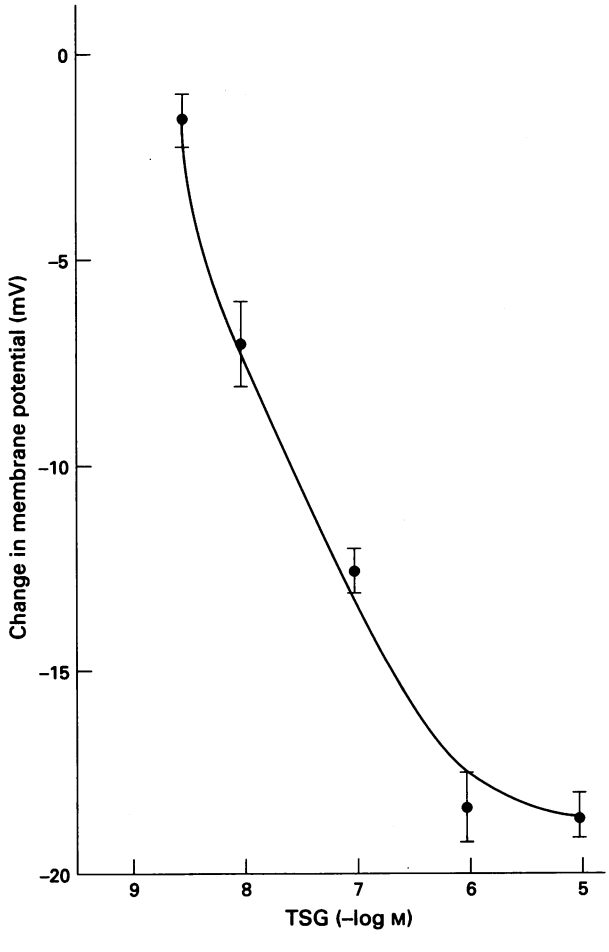

Figure 3 Concentration-response curve for the hyperpolarizing effect of thapsigargin (TSG) in rat mesenteric artery with endothelium. The points are the means ± s.e.mean of four to five experiments.

Discussion

The present study demonstrated that TSG and CPA each caused sustained endothelium-dependent hyperpolarization in rat mesenteric arteries. Recently, it has been shown that TSG releases NO from endothelial cells and thereby induces relaxation of guinea-pig aorta precontracted with phenylephrine (Matsuyama *et al.*, 1993). Exogenous NO produces membrane hyperpolarization of smooth muscle cells of rat small mesenteric artery (Garland & McPherson, 1992) and of guinea-pig uterine artery (Tare *et al.*, 1990), although the hyperpolarizing effect of NO could be blocked by prior depolarization (Garland & McPherson, 1992). In the present experiments, however, NO released by TSG and CPA seems an unlikely candidate to mediate endothelium-dependent hyperpolarization, because the hyperpolarizing responses to both agents were insensitive to L-NOARG, an inhibitor of NO synthase (Moore *et al.*, 1990). The production of vasoactive prostanoids is not likely to contribute to the endothelium-dependent hyperpolarizing responses. Although prostacyclin has been reported to produce hyperpolarization of smooth muscle cells in canine carotid artery (Siegel *et al.*, 1989), the magnitude and time course of hyperpolarization induced by TSG and CPA remained unchanged by pretreatment with indomethacin. Hence, another substance released from the endothelial cells, presumably EDHF, is likely to account for endothelium-dependent hyperpolarization elicited by TSG and CPA.

In rat mesenteric arterial rings precontracted with phenylephrine, TSG and CPA caused endothelium-dependent relaxations. The relaxant responses to these agents, which were observed in the presence of indomethacin, were significantly reduced by pretreatment with L-NOARG. It thus appears that EDRF-NO partly contributes to the endothelium-dependent relaxant responses to TSG and CPA. However, the major part of the vasorelaxant responses was resistant to L-NOARG. The possibility that the relaxation in the presence of L-NOARG was caused by residual NO, which was not blocked by L-NOARG at the concentration used in this study, is unlikely,

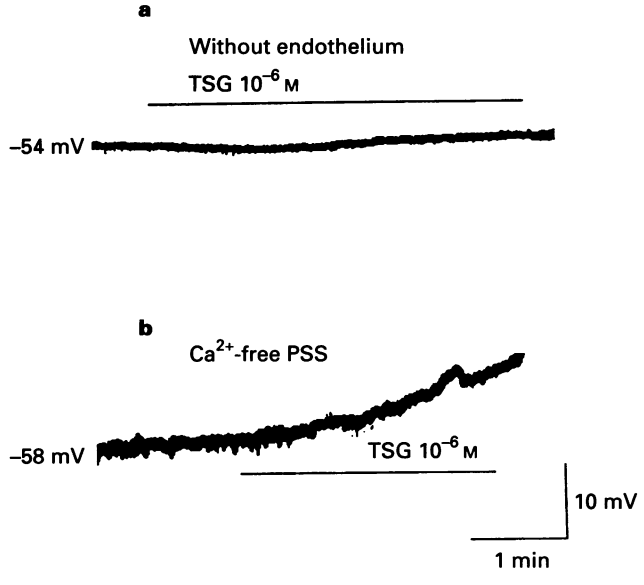

Figure 4 Influence of removal of endothelium (a) and exposure to Ca^{2+}-free PSS (b) on the effect of 10^{-6} M thapsigargin (TSG) on cell membrane potential of rat mesenteric artery. The experiment with Ca^{2+}-free PSS was performed using a tissue with endothelium intact. TSG was applied 5 min exposure to Ca^{2+}-free PSS.

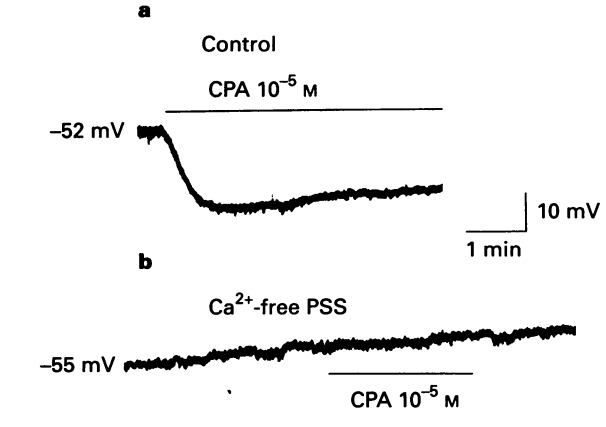

Figure 5 Effect of cyclopiazonic acid (CPA, 10^{-5} M) on cell membrane potential of rat mesenteric artery with endothelium in normal PSS (a) and in Ca^{2+}-free PSS (b). CPA was applied 5 min after exposure to Ca^{2+}-free PSS. Traces were recorded in two different tissues.

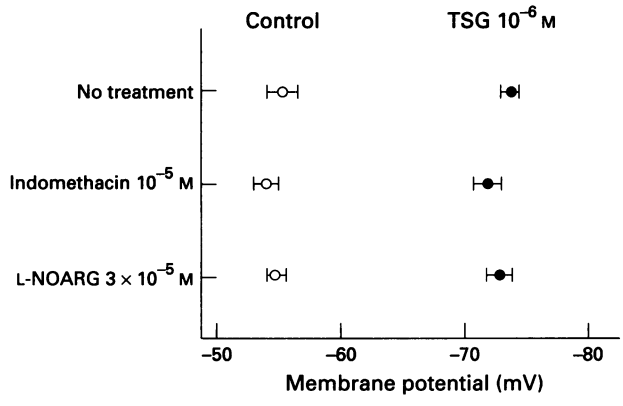

Figure 6 Influences of pretreatment with 10^{-5} M indomethacin or 3×10^{-5} M N^G-nitro-L-arginine (L-NOARG) on membrane hyperpolarization produced by 10^{-6} M thapsigargin (TSG) in rat mesenteric artery. TSG was applied 15–30 min after the addition of indomethacin or L-NOARG. Membrane potentials and peak amplitude of hyperpolarization are expressed as the mean ± s.e.mean of four experiments.

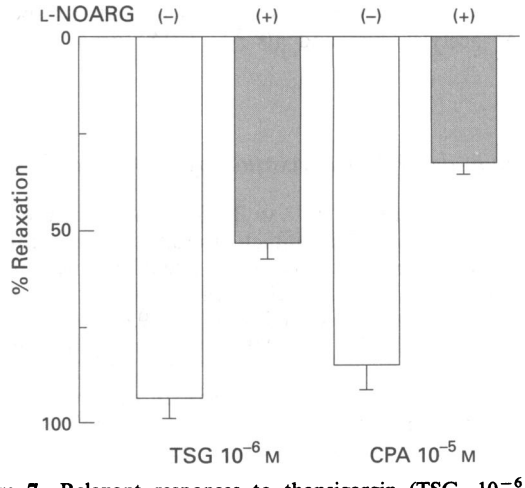

Figure 7 Relaxant responses to thapsigargin (TSG, 10^{-6} M) and cyclopiazonic acid (CPA, 10^{-5} M) in rat mesenteric artery with endothelium in the absence and presence of N^G-nitro-L-arginine (L-NOARG 3×10^{-5} M). The arterial rings were precontracted with phenylephrine at 10^{-7} M (with L-NOARG) or 10^{-6} M (without L-NOARG). L-NOARG was added to the bath 15 min before a precontraction was elicited. The values are shown as the means ± s.e.mean of four to six experiments. All experiments were performed in the presence of 10^{-5} M indomethacin.

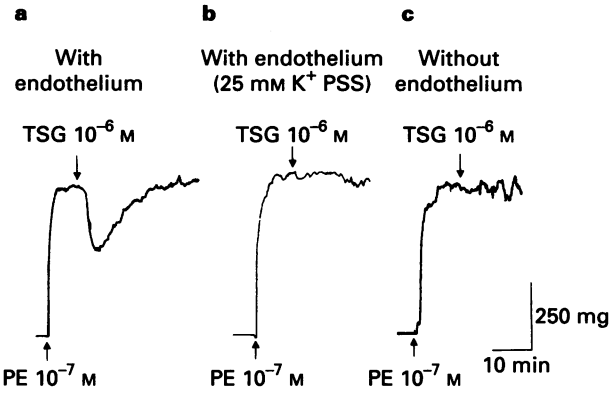

Figure 8 The vasorelaxant effect of thapsigargin (TSG, 10^{-6} M) in rat arterial rings precontracted with phenylephrine (PE, 10^{-7} M) in the presence of L-NOARG (3×10^{-5} M) and indomethacin (10^{-5} M). (a) Control; (b) rings depolarized with 25 mM K^+ PSS: note the disappearance of the vasorelaxant effect of TSG; (c) rings without endothelium.

because at this concentration L-NOARG has been reported to eliminate the production of EDRF-NO (Nagao & Vanhoutte, 1992; Fujii *et al.*, 1992). Furthermore, the relaxant response to TSG was abolished by the combined application of L-NOARG and high K^+ solution (25 mM). Endothelium-dependent hyperpolarization and the associated relaxation have been reported to be impaired by elevating the extracellular K^+ concentration (Chen & Suzuki, 1990; Nagao & Vanhoutte, 1992). Thus, it may be concluded that the relaxation of rat mesenteric artery evoked by TSG and CPA was caused in part by endothelium-dependent hyperpolarization of the smooth muscle cells in addition to the production of EDRF-NO. Interestingly, a recent report has shown that endothelium-dependent hyperpolarization can account for approximately 50% of the relaxation elicited by acetylcholine in the rat mesenteric artery (Waldron & Garland, 1994).

Contrary to the present findings in rat mesenteric artery, previous studies have demonstrated that pretreatment with the NO synthase inhibitors caused an almost complete inhibition of the relaxant responses to TSG and CPA in aortae from guinea-pigs and rats (Matsuyama *et al.*, 1993; Zheng *et al.*, 1994). Possible reasons for this discrepancy may be related to a difference in contribution of EDHF to relaxation between the two vessels. Nagao *et al.* (1992) have shown that in the presence of L-NOARG (3×10^{-5} M), acetylcholine caused about 70% relaxation in rat mesenteric artery but no longer caused relaxation in rat aorta.

The importance of the elevation of cytosolic Ca^{2+} concentration in the endothelial cells in the release of EDHF has been proposed (Chen & Suzuki, 1990). This hypothesis has been supported by the findings that A-23187 is capable of inducing endothelium-dependent hyperpolarization in several kinds of arteries including rat mesenteric artery (Chen & Suzuki, 1990; Nakashima & Vanhoutte, 1993). TSG has been shown to elevate the cytosolic Ca^{2+} concentration in a variety of cells including human umbilical vein endothelial cells (Takemura *et al.*, 1989; Thastrup *et al.*, 1990; Thastrup, 1990; Gericke *et al.*, 1993). CPA has been also reported to result in an increase in intracellular Ca^{2+} concentration in thyroid FRTL-5 cells (Tornquist, 1993) and in Friend erythroleukaemia cells (Schaefer *et al.*, 1994). Thus, the increased cytosolic Ca^{2+} concentration in endothelial cells with TSG and CPA may be responsible for the endothelium-dependent hyperpolarizing effects demonstrated in this study. The hyperpolarizing responses to TSG and CPA were not generated in Ca^{2+}-free solution, indicating that the responses are not due to release of Ca^{2+} from intracellular stores. In contrast, acetylcholine produced a transient hyperpolarizing effect in Ca^{2+}-free solution. In endothelial cells, the agonist-stimulated hydrolysis of membrane phosphatidylinositol results in a production of inositol polyphosphates (Derian & Moskowitz, 1986; Lambert *et al.*, 1986). Thus the acetylcholine-induced transient hyperpolarization is likely to be related to a mobilization of Ca^{2+} from endothelial intracellular stores by inositol 1,4,5-trisphosphate (Chen & Suzuki, 1990). Although TSG activates the release of Ca^{2+} from intracellular stores without generation of inositol polyphosphates in NG115-401L cells (Jackson *et al.*, 1988) and in parotid acinar cells (Takemura *et al.*, 1989), it has been shown in human umbilical vein endothelial cells that the increase in intracellular Ca^{2+} concentration induced by TSG depends on the extracellular Ca^{2+} concentration (Gericke *et al.*, 1993).

TSG and CPA can deplete the rapidly exchanging intracellular Ca^{2+} stores by blocking the refilling of Ca^{2+} stores, possibly due to inhibition of activity of the Ca^{2+}-pump ATPase located on the endoplasmic reticulum (Goerger *et al.*, 1988; Seidler *et al.*, 1989; Thastrup *et al.*, 1990). The depletion of intracellular Ca^{2+} stores has been proposed as the signal for Ca^{2+} entry (Putney, 1986). It has been recently suggested that a novel messenger named 'Ca^{2+}-influx factor' mediates Ca^{2+} influx triggered by emptying of intracellular Ca^{2+} stores (Randriamampita & Tsien, 1993). The possible pathway for Ca^{2+} entry into endothelial cells is thought to be nonspecific cation channels in human umbilical vein endothelial cells (Nilius, 1990). TSG and CPA activate a nonspecific cation channel in human umbilical vein endothelial cells (Gericke *et al.*, 1993; Zhang *et al.*, 1994). It thus seems likely that both TSG and CPA deplete intracellular Ca^{2+} stores in endothelial cells and the emptying of the Ca^{2+} stores generates an intracellular signal to trigger Ca^{2+} influx through a nonspecific cation channel. Opening of the nonspecific cation channel by these agents could supply sufficient Ca^{2+} into the endothelial cells to promote the production and release of EDHF. This intriguing proposal would best explain the present finding that the endothelium-dependent hyperpolarization elicited by TSG and CPA was exclusively dependent on the presence of extracellular Ca^{2+}.

As previously observed in rabbit carotid artery (Chen & Suzuki, 1990), acetylcholine generated sustained hyperpolarization following an initial transient hyperpolarization in rat mesenteric artery. The sustained hyperpolarizing response was sensitive to the extracellular Ca^{2+} concentration. Chen & Suzuki (1990) have shown that pretreatment with procaine can block preferentially the sustained component of the acetylcholine-induced hyperpolarization. This finding implies that inhibition by procaine of the Ca^{2+} release from intracellular stores (Itoh *et al.*, 1981) prevents the influx of Ca^{2+} from the extracellular medium. This is consistent with the idea that Ca^{2+} entry is initiated by the depletion of the intracellular Ca^{2+} stores. Thus, we assume that the mechanisms for activation of Ca^{2+} entry by acetylcholine and by TSG and CPA may be the same, although the time required to reach the peak amplitude of the sustained hyperpolarization by acetylcholine was somewhat shorter than that by TSG and CPA.

In conclusion, the present findings demonstrate that putative, selective inhibitors of endoplasmic reticulum Ca^{2+}-pump ATPase, TSG and CPA, cause endothelium-dependent hyperpolarization in rat mesenteric artery. The ability of these agents to produce hyperpolarizing effects, possibly *via* release of EDHF, may be mediated by the promotion of Ca^{2+} influx into endothelial cells that can be triggered by the emptying of intracellular Ca^{2+} stores. The results of the present study also indicate that the endothelium-dependent relaxation induced by TSG and CPA is mediated by both EDRF-NO and EDHF.

We would like to thank Prof. H. Suzuki for excellent technical advice, and Miss R. Yamazaki and Miss S. Yamada for secretarial assistance. This work was supported in part by a Grant-in-Aid for Science Research from the Ministry of Education, Science and Culture of Japan.

References

BÉNY, J.-L. & BRUNET, P.C. (1988). Neither nitric oxide nor nitroglycerin accounts for all the characteristics of endothelially mediated vasodilatation of pig coronary arteries. *Blood Vessels*, **25**, 308–311.

CHEN, G. & SUZUKI, H. (1990). Calcium dependency of the endothelium-dependent hyperpolarization in smooth muscle cells of the rabbit carotid artery. *J. Physiol.*, **421**, 521–534.

CHEN, G., SUZUKI, H. & WESTON, A.H. (1988). Acetylcholine releases endothelium-derived hyperpolarizing factor and EDRF from rat blood vessels. *Br. J. Pharmacol.*, **95**, 1165–1174.

CHRISTENSEN, S.B., LARSEN, I.K. & RASMUSSEN, U. (1981). Thapsigargin and thapsigargicin, two histamine-liberating sesquiterpene lactones from thapsia gargania. X-ray analysis of the 7,11-epoxide of thapsigargin. *J. Org. Chem.*, **47**, 649–652.

DERIAN, C.K. & MOSKOWITZ, M.A. (1986). Polyphosphoinositide hydrolysis in endothelial cells and carotid artery segments (bradykinin-2 receptor stimulation is calcium-dependent). *J. Biol. Chem.*, **261**, 3831–3837.

FELETOU, M. & VANHOUTTE, P.M. (1988). Endothelium-dependent hyperpolarization of canine coronary smooth muscle. *Br. J. Pharmacol.*, **93**, 515–524.

FUJII, K., TOMINAGA, M., OHMORI, S., KOBAYASHI, K., KOGA, T., TAKATA, Y. & FUJISHIMA, M. (1992). Decreased endothelium-dependent hyperpolarization to acetylcholine in smooth muscle of the mesenteric artery of spontaneously hypertensive rats. *Circ. Res.*, **70**, 660–669.

FURCHGOTT, R.F. & VANHOUTTE, P.M. (1989). Endothelium-derived relaxing and contracting factors. *FASEB J.*, **3**, 2007–2018.

FURCHGOTT, R.F. & ZAWADZKI, J.W. (1980). The obligatory role of endothelial cells in the relaxation of arterial smooth muscle by acetylcholine. *Nature*, **288**, 373–376.

GARLAND, C.J. & MCPHERSON, G.A. (1992). Evidence that nitric oxide does not mediate the hyperpolarization and relaxation to acetylcholine in the rat small mesenteric artery. *Br. J. Pharmacol.*, **105**, 429–435.

GERICKE, M., DROOGMANS, G. & NILIUS, B. (1993). Thapsigargin discharges intracellular calcium stores and induces transmembrane currents in human endothelial cells. *Pflügers Arch.*, **422**, 552–557.

GOERGER, D.E., RILEY, R.T., DORNER, J.W. & COLE, R.J. (1988). Cyclopiazonic acid inhibition of the Ca^{2+}-transport ATPase in rat skeletal muscle sarcoplasmic reticulum vesicles. *Biochem. Pharmacol.*, **37**, 978–981.

ITOH, T., KURIYAMA, H. & SUZUKI, H. (1981). Excitation-contraction coupling in smooth muscle cells of the guinea-pig mesenteric artery. *J. Physiol.*, **321**, 513–535.

JACKSON, T.R., PATTERSON, S.I., THASTRUP, O. & HANLEY, M.R. (1988). A novel tumor promoter, thapsigargin, transiently increases cytoplasmic free Ca^{2+} without generation of inositol phosphates in NG115-401L neuronal cells. *Biochem. J.*, **253**, 81–86.

LAMBERT, T.L., KENT, R.S. & WHORTON, A.R. (1986). Bradykinin stimulation of inositol polyphosphate production in porcine aortic endothelial cells. *J. Biol. Chem.*, **261**, 15228–15293.

LÜSCHER, T.F., BOULANGER, C.M., DOHI, Y. & YANG, Z. (1992). Endothelium-derived contracting factors. *Hypertension*, **19**, 117–130.

MATSUYAMA, S., SHUNTOH, H., KATAYAMA, S. & TANAKA, C. (1993). Thapsigargin induces an endothelium-dependent, intracellular calcium ion-dependent vasodilation in vitro. *Life Sci.*, **53**, 618–688.

MIKKELSEN, E.O., THASTRUP, O. & CHRISTENSEN, S.B. (1988). Effects of thapsigargin in isolated rat thoracic aorta. *Pharmacol. Toxicol.*, **62**, 7–11.

MONCADA, S., HERMAN, A.G., HIGGS, E.A. & VANE, J.R. (1977). Differential formation of prostacyclin (PGX or PGI_2) by layers of the arterial wall. An explanation for the anti-thrombotic properties of vascular endothelium. *Thromb. Res.*, **11**, 323–344.

MOORE, P.K., AL-SWAYEH, O.A., CHONG, N.W., EVANS, R.A. & GIBSON, A. (1990). L-N^G-nitro arginine (L-NOARG), a novel, L-arginine-reversible inhibitor of endothelium-dependent vasodilation *in vitro*. *Br. J. Pharmacol.*, **99**, 408–412.

MYERS, P.R., MINOR, R.L. JR., GUERRA, R. JR., BATES, J.N. & HARRISON, D.G. (1990). Vasorelaxant properties of the endothelium-derived relaxing factor more closely resemble *S*-nitrosocysteine than nitric oxide. *Nature*, **345**, 161–163.

NAGAO, T., ILLIANO, S. & VANHOUTTE, P.M. (1992). Heterogeneous distribution of endothelium-dependent relaxations resistant to N^G-nitro-L-arginine in rats. *Am. J. Physiol.*, **263**, H1090–H1094.

NAGAO, T. & VANHOUTTE, P.M. (1992). Hyperpolarization as a mechanism for endothelium-dependent relaxations in the porcine coronary artery. *J. Physiol.*, **445**, 355–367.

NAKASHIMA, M. & VANHOUTTE, P.M. (1993). Endothelin-1 and -3 cause endothelium-dependent hyperpolarization in the rat mesenteric artery. *Am. J. Physiol.*, **265**, H2137–H2141.

NILIUS, B. (1990). Permeation properties of a non-selective cation channel in human vascular endothelial cells. *Pflügers Arch.*, **416**, 609–611.

PALMER, R.M.J., FERRIGE, A.G. & MONCADA, S. (1987). Nitric oxide accounts for the biological activity of endothelium-derived relaxing factor. *Nature*, **327**, 524–526.

PUTNEY, J.W. JR. (1986). A model for receptor-regulated calcium entry. *Cell Calcium*, **7**, 1–12.

RANDRIAMAMPITA, C. & TSIEN, R.Y. (1993). Emptying of intracellular Ca^{2+} stores releases a novel small messenger that stimulates Ca^{2+} influx. *Nature*, **364**, 809–814.

SCHAEFER, A., MAGÓCSI, M., STÖCKER, U., KÓSA, F. & MARQUARDT, H. (1994). Early transient suppresion of *c-myb* mRNA levels and induction of differentiation in Friend erythroleukemia cells by the $[Ca^{2+}]_i$-increasing agents cyclopiazonic acid and thapsigargin. *J. Biol. Chem.*, **269**, 8786–8791.

SEIDLER, N.W., JONA, I., VEGH, M. & MARTONOSI, A. (1989). Cyclopiazonic acid is a specific inhibitor of the Ca^{2+}-ATPase of sarcoplasmic reticulum. *J. Biol. Chem.*, **264**, 17816–17823.

SIEGEL, G., CARL, A., ADLER, A. & STOCK, G. (1989). Effect of the prostacyclin analogue iloprost on K^+ permeability in the smooth muscle cells of the canine carotid artery. *Eicosanoids*, **2**, 213–222.

SINGER, H.A. & PEACH, M.J. (1982). Calcium- and endothelium-mediated smooth muscle relaxation in rabbit aorta. *Hypertension*, **4** (Suppl. II), II19–II25.

SUZUKI, H., CHEN, G. & YAMAMOTO, Y. (1992). Endothelium-derived hyperpolarizing factor (EDHF). *Jpn. Circ. J.*, **56**, 170–173.

TAKEMURA, H., HUGHES, A.R., THASTRUP, O. & PUTNEY, J.W. JR. (1989). Activation of calcium entry by the tumor promoter, thapsigargin, in parotid acinar cells. Evidence that an intracellular calcium pool, and not an inositol phosphate, regulates calcium fluxes at the plasma membrane. *J. Biol. Chem.*, **264**, 12266–12271.

TARE, M., PARKINGTON, H.C., COLEMAN, H.A., NEILD, T.O. & DUSTING, G.J. (1990). Hyperpolarization and relaxation of arterial smooth muscle caused by nitric oxide derived from the endothelium. *Nature*, **346**, 69–71.

TAYLOR, S.G. & WESTON, A.H. (1988). Endothelium-derived hyperpolarizing factor: a new endogenous inhibitor from the vascular endothelium. *Trends Pharmacol. Sci.*, **9**, 272–274.

THASTRUP, O. (1990). Role of Ca^{2+}-ATPase in regulation of cellular Ca^{2+} signalling, as studied with the selective microsomal Ca^{2+}-ATPase inhibitor, thapsigargin. *Agents Actions*, **29**, 8–15.

THASTRUP, O., CULLEN, P.J., DRØBAK, B.K., HANLEY, M.R. & DOWSON, A.P. (1990). Thapsigargin, a tumor promotor, discharges intracellular Ca^{2+} stores by specific inhibition of the endoplasmic reticulum Ca^{2+}-ATPase. *Proc. Natl. Acad. Sci. U.S.A.*, **87**, 2466–2470.

TORNQUIST, K. (1993). Activation of calcium entry by cyclopiazonic acid in thyroid FRTL-5 cells. *Cell Calcium*, **14**, 411–417.

WALDRON, G.J. & GARLAND, C.J. (1994). Contribution of both nitric oxide and a change in membrane potential to acetylcholine-induced relaxation in the rat small mesenteric artery. *Br. J. Pharmacol.*, **112**, 831–836.

ZHANG, H., INAZU, M., WEIR , B., BUCHANAN, M. & DANIEL, E. (1994). Cyclopiazonic acid stimulates Ca^{2+} influx through non-specific cation channels in endothelial cells. *Eur. J. Pharmacol.*, **251**, 119–125.

ZHENG, X.F., KWAN, C.Y. & DANIEL, E. (1994). Role of intracellular Ca^{2+} in EDRF release in rat aorta. *J. Vasc. Res.*, **31**, 18–24.

(Received November 14, 1994
Revised February 27, 1995
Accepted March 28, 1995)

British Journal of Pharmacology (1995) 115, 993-1000 © 1995 Stockton Press All rights reserved 0007-1188/95 $12.00

Differential sensitivity of basal and acetylcholine-stimulated activity of nitric oxide to destruction by superoxide anion in rat aorta

Kousar B. Mian & [1]William Martin

Clinical Research Initiative on Heart Failure, West Medical Building, University of Glasgow, Glasgow, G12 8QQ

1 In this study we compared the ability of superoxide anion to destroy the relaxant activity of basal and acetylcholine (ACh)-stimulated activity of NO in isolated rings of rat aorta.

2 Superoxide dismutase (SOD, 1-300 u ml^{-1}) induced a concentration-dependent relaxation of phenylephrine (PE)-induced tone in endothelium-containing rings which was blocked by N^G-nitro-L-arginine (L-NOARG, 30 μM), but had no effect on endothelium-denuded rings. It was likely therefore that the relaxant action of SOD resulted from protection of basally produced NO from destruction by superoxide anion, generated either within the tissue or in the oxygenated Krebs solution.

3 In contrast, a concentration of SOD (50 u ml^{-1}) which produced almost maximal enhancement of basal NO activity, had no effect on ACh (10 nM-3 μM)-induced relaxation.

4 In the presence of catalase (3000 u ml^{-1}) to prevent the actions of hydrogen peroxide, superoxide anion generation using hypoxanthine (HX, 0.1 mM)/xanthine oxidase (XO, 16 mu ml^{-1}) produced an augmentation of PE-induced tone in endothelium-containing but not endothelium-denuded rings. This was likely to have resulted from removal of the tonic vasodilator action of basally-produced NO by superoxide anion, since it was blocked in tissues treated with SOD (250 u ml^{-1}), N^G-monomethyl-L-arginine (L-NMMA, 30 μM) or L-NOARG (30 μM). Pyrogallol (0.1 mM) had a similar action to HX/XO, but produced an additional augmentation of tone by an endothelium-independent mechanism.

5 In contrast to their ability to destroy almost completely the basal activity of NO, HX (0.1 mM)/XO (16 mu ml^{-1}) and pyrogallol (0.1 mM) had no effect on ACh-induced relaxation at any concentration. An increase in the concentration of HX to 1 mM or pyrogallol to 0.3 mM did, however, lead to a profound decrease in the magnitude and time course of ACh-induced relaxation at all concentrations.

6 Treatment with diethyldithiocarbamate (DETCA, 0.1 mM, 1 h) to inhibit endogenous Cu-Zn SOD, augmented PE-induced tone in endothelium-containing rings and abolished the ability of HX (0.1 mM)/XO (16 mu ml^{-1}) and L-NMMA (30 μM) to augment tone. It was likely that DETCA had led to the destruction of basal NO activity by increasing superoxide anion levels since its actions were reversed by exogenous SOD (10-300 u ml^{-1}).

7 In contrast to its ability to destroy basal activity of NO completely, DETCA (0.1 mM) produced only a slight blockade of ACh-induced relaxation. However, if these tissues were subsequently treated with concentrations of HX (0.1 mM)/XO (16 mu ml^{-1}) or pyrogallol (0.1 mM), which had no effect by themselves on ACh-induced relaxation, a profound blockade was seen and this was reversed completely with SOD (250 u ml^{-1}).

8 The data suggest that basal activity of NO is more sensitive to inactivation by superoxide anion than ACh-stimulated activity and this probably results from differential protection by endogenous Cu-Zn SOD. It is possible therefore that endogenous SOD lowers superoxide anion levels to such an extent that only small amounts of NO, such as those produced under basal conditions, are destroyed. Following generation of superoxide anion with HX/XO or pyrogallol, or inhibition of Cu-Zn SOD with DETCA, levels of the free radical will increase such that greater amounts of NO, such as those produced following stimulation with ACh, will then be destroyed.

Keywords: Nitric oxide; superoxide anion; superoxide dismutase; diethyldithiocarbamate; vasodilatation; acetylcholine; EDRF

Introduction

Endothelium-derived relaxing factor (EDRF) is a potent vasodilator produced by vascular endothelial cells (Furchgott & Zawadzki, 1980) and has recently been characterized as nitric oxide (NO) or a chemically related species (Palmer *et al.*, 1987; Myers *et al.*, 1989; 1990). Recently, the interaction between NO and superoxide anion has received a great deal of attention. This interaction leads to destruction of the vasodilator actions of EDRF and authentic nitric oxide in cascade bioassay systems (Gryglewski *et al.*, 1986; Rubanyi & Vanhoutte, 1986a; Furchgott *et al.*, 1990), induction of endothelium-dependent vasoconstriction in arterial rings from loss of the dilator actions of basally produced nitric oxide (Katusic & Vanhoutte, 1989; Ohlstein & Nichols, 1989), and production of a cytotoxic oxidant, peroxynitrite (Beckman *et al.*, 1990). This widespread potential for loss of NO-induced vasodilatation and production of peroxynitrite following the reaction of NO with superoxide anion has led to the suggestion that this process contributes to a number of pathological situations such as hypertension (Wei *et al.*, 1985), ischaemia-reperfusion injury (Downey, 1990), hypercholesterolaemia/ atherosclerosis (Minor *et al.*, 1990), diabetes (Langenstroer & Pieper, 1992) and cytotoxic brain injury (Lipton *et al.*, 1993).

In vascular endothelium, the production of NO is subject to complex control; it is stimulated by a large number of biological mediators such as acetylcholine (ACh; Furchgott & Zawadzki, 1980) and by the physical shearing force of flowing

[1] Author for correspondence.

blood (Rubanyi *et al.*, 1986). In addition, there is a basal production of NO which exerts a tonic vasodilator action on endothelium-containing arterial rings (Eglème *et al.*, 1984; Martin *et al.*, 1986; Martin, 1988). Recent reports have suggested differences in the effects of drugs on basal and agonist-stimulated activity of NO. For example, in the perfused vascular bed of the rabbit ear, N^G-nitro-L-arginine methyl ester (L-NAME) inhibits both basal and ACh-induced activity of NO, but only in the former case is blockade reversed by L-arginine (Randall & Griffith, 1991). Furthermore, in the isolated coronary artery of the greyhound, the inhibitor of acetyl-coA lysolecithin acyltransferase, thimerosal, has a complex action, transiently producing endothelium-dependent relaxation and then blocking agonist-stimulated but not basal production of NO (Crack & Cocks, 1992). Furthermore, in the rat aorta N^G-monomethyl-L-arginine (L-NMMA) selectively inhibits basal but not agonist-stimulated production of NO (Frew *et al.*, 1993). The ability of superoxide dismutase (SOD) to potentiate the effects of basal NO in a cascade bioassay or arterial rings (Gryglewski *et al.*, 1986; Rubanyi & Vanhoutte, 1986a; Ohlstein & Nichols, 1989; Langenstroer & Pieper, 1992), but to have no effect on the relaxant actions of ACh in arterial rings (Abrahamsson *et al.*, 1992), suggests differential actions of superoxide anion on basal and agonist-stimulated activity of NO.

In this study, we wished to determine if basal and ACh-stimulated activity of NO in rat aorta were equally sensitive to destruction by superoxide anion. The effects of superoxide anion were assessed either by generating the free radical by use of the hypoxanthine/xanthine oxidase (HX/XO) system or the drug, pyrogallol, or by increasing the background level of the free radical by inhibiting the endogenous Cu-Zn form of SOD with diethyldithiocarbamate (DETCA; Heikkila *et al.*, 1976; Cocco *et al.*, 1981).

Methods

Preparations of aortic rings

Female Wistar rats of approximately 200–250 g were killed by stunning and exsanguination. The thoracic aorta was removed and cut into 2.5 mm wide transverse rings with a razor blade slicing device. In some experiments, the endothelium was removed by locating the aortic ring between two stainless steel hooks, placing a 2 g weight on the bottom hook and gently rubbing the intimal surface with a moist matchstick for 10–20 s. Endothelial denudation was deemed successful if no relaxation took place in response to ACh (1 μM).

Tension recording

The aortic rings were mounted under 1 g resting tension on stainless steel hooks in 20 ml organ baths maintained at 37°C containing Krebs solution (mM): NaCl 118, KCl 4.8, $CaCl_2$ 2.5, $MgSO_4$ 1.2, $NaHCO_3$ 24, and glucose 11 and gassed with 95% O_2 and 5% CO_2. Tension was recorded isometrically by means of Grass FT03C transducers and responses were displayed on a Grass polygraph model 7. Tissues were allowed to equilibrate for 90 min before experiments were carried out, during which time the resting tension was re-adjusted to 1 g, as required.

Experimental protocols

Basal activity of nitric oxide (NO) was assessed indirectly by measuring the endothelium-dependent depression of phenylephrine (PE)-induced vasoconstriction (Martin *et al.*, 1986). The rationale for these experiments is that basal production of NO in endothelium-containing rings of rat aorta exerts a tonic vasodilator action opposing the effects of vasoconstrictor agents. Consequently, this endothelium-dependent depression of vasoconstriction will be blocked or enhanced by agents which block or enhance the activity of NO, respectively. In these experiments, endothelium-containing rings were contracted with PE (20 nM) and when the contraction had stabilized, the effects of the superoxide anion generators, hypoxanthine (HX, 0.1 mM)/xanthine oxidase (16 mu ml^{-1}) and pyrogallol (0.1 mM), the superoxide anion scavenger, superoxide dismutase (SOD, 250 u ml^{-1}), or the inhibitors of NO synthase, N^G-monomethyl-L-arginine (L-NMMA, 30 μM) and N^G-nitro-L-arginine (L-NOARG, 30 μM), were examined on tone. In the early experiments with HX/XO, it was clear that a delayed relaxant effect was produced resulting from the generation of hydrogen peroxide. Consequently, where indicated in the results, experiments were performed in the presence of catalase (3000 u ml^{-1}) to prevent the accumulation of hydrogen peroxide. In certain experiments, the effects of inhibiting endogenous Cu-Zn SOD with the copper chelator, diethyldithiocarbamate (DETCA; Heikkila *et al.*, 1976; Cocco *et al.*, 1981) were also investigated on PE-induced tone. In these experiments, aortic rings were incubated for 1 h with DETCA (0.1 mM) before the contractile actions of PE (20 nM) were examined. Each of the above experiments was also conducted in endothelium-denuded rings but the concentration of PE used was lowered to 1–3 nM so as to attain a similar degree of tone to that obtained in endothelium-containing rings.

Agonist-stimulated activity of NO was determined by assessing ACh-induced relaxation. Cumulative concentration-response curves to ACh (10 nM–3 μM) were constructed in endothelium-containing rings following induction of submaximal PE (30–100 nM)-induced tone. The baths were washed out, and the tissues allowed to re-equilibrate. In experiments in which the effects of HX (0.1 or 1 mM)/XO (16 mu ml^{-1}) and pyrogallol (0.1 or 0.3 mM) were to be studied on ACh-induced relaxation, we ensured that the level of tone prior to inducing relaxation was similar to that of untreated preparations. In order to achieve this, tissues were initially precontracted with lower concentrations of PE (2–30 nM). Subsequent addition of the free radical generators produced a further elevation of tone in endothelium-containing tissues by destroying basal NO activity, and when the contraction had stabilized, a further cumulative concentration-response curve to ACh was obtained. In studies involving inhibition of endogenous Cu-Zn SOD, the rings were incubated with DETCA for 1 h. Various concentrations of DETCA were tested, and 0.1 mM was chosen for most experiments since it produced a sub-maximal (25–30%) inhibition of ACh-induced relaxation by itself. Cumulative concentration-response curves to ACh (10 nM–3 μM) in the

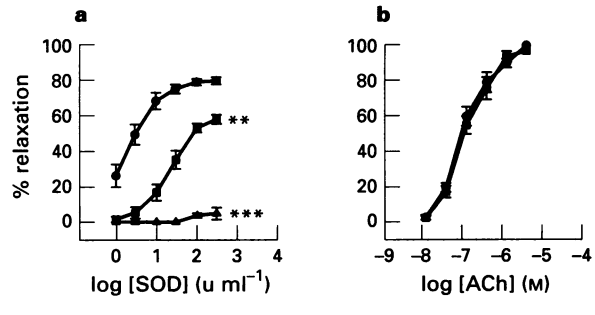

Figure 1 (a) Concentration-response curves showing relaxation to superoxide dismutase (SOD, 1–300 u ml^{-1}) on phenylephrine-contracted endothelium-containing (●) and endothelium-denuded (▲) rings of rat aorta and blockade of relaxation following inhibition of endogenous Cu-Zn SOD with diethyldithiocarbamate (DETCA, 0.1 mM, 1 h, ■). (b) Concentration-response curves showing relaxation to acetylcholine (ACh, ●) and the inability of SOD (50 u ml^{-1}, ■) to affect this relaxation. Each point is the mean ± s.e.mean of 6 observations. $^{**}P < 0.005$ and $^{***}P < 0.001$ indicate a significant difference from maximal relaxation in untreated endothelium-containing rings, respectively.

presence of HX (0.1 mM)/XO (16 mu ml^{-1}) and pyrogallol (0.1 mM) were also constructed in DETCA-treated rings. All experiments involving HX/XO, pyrogallol or DETCA were conducted in the presence of catalase (3000 u ml^{-1}), added as 5 min pretreatment to prevent accumulation of hydrogen peroxide. In some experiments, the ability of exogenously added SOD to protect against the inhibitory effects of HX/XO, pyrogallol or DETCA was studied and, in these, it was added as a 20 min pretreatment. Responses to ACh were expressed as a percentage (%) relaxation of the PE-induced tone.

Drugs

Acetylcholine chloride, catalase (bovine liver), diethyldithiocarbamate, N^G-nitro-L-arginine, phenylephrine hydrochloride, hypoxanthine, superoxide dismutase (bovine erythrocyte, Cu-Zn-containing) and xanthine oxidase (buttermilk) were obtained from Sigma (Poole, Dorset), whilst pyrogallol was obtained from BDH (Poole, Dorset). N^G-monomethyl-L-arginine was a gift from Wellcome Laboratories (Beckenham, Kent). All drugs were dissolved and dilutions made in saline (0.9%), except for hypoxanthine which was dissolved in 0.1% sodium hydroxide.

Statistical analysis

Results are expressed as the mean ± s.e.mean for n separate experiments and comparisons were made by one-way analysis of variance followed by Fisher's test. A probability of 0.05 or less was considered significant.

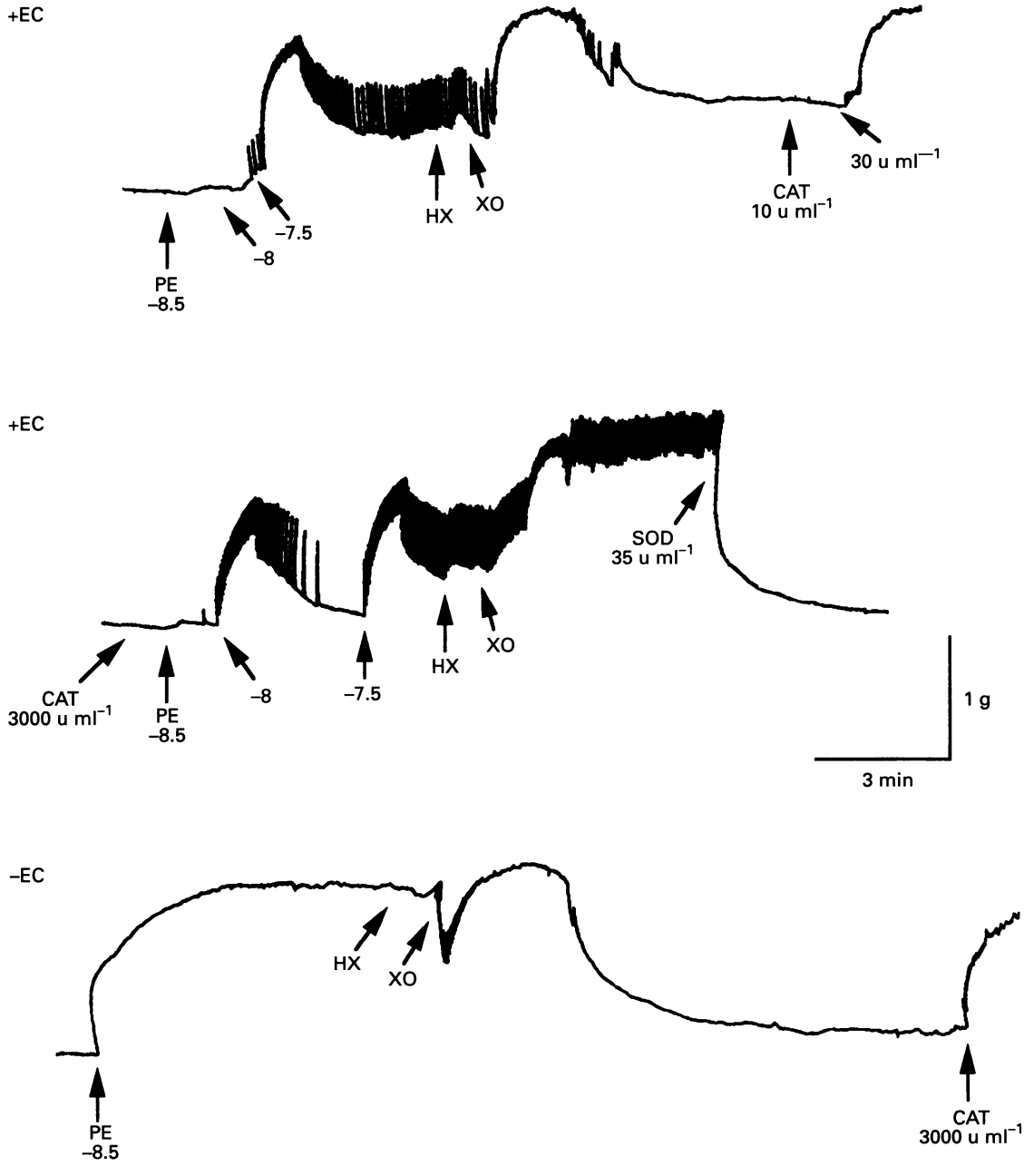

Figure 2 Individual experimental tracings showing two separate effects of hypoxanthine (HX, 0.1 mM)/xanthine oxidase (XO, 16 mu ml^{-1}) on rings of rat aorta; an immediate rise in phenylephrine (PE)-induced tone in endothelium-containing (+EC) but not endothelium-denuded (–EC) rings which was reversed by superoxide dismutase (SOD, 35 u ml^{-1}), and a delayed fall in tone in both endothelium-containing and endothelium-denuded rings which was inhibited by catalase (CAT, 30–3000 u ml^{-1}). Drug concentrations are expressed in log molar units and enzyme concentrations are in units ml^{-1}.

Results

Effects of superoxide dismutase on basal and ACh-stimulated activity of NO

Following induction of phenylephrine (PE, 30–100 nM)-induced tone (1.60±0.10 g, $n=8$) in endothelium-containing rings of rat aorta, superoxide dismutase (SOD, 1–300 u ml^{-1}) produced a powerful concentration-dependent relaxation (maximum relaxation 79.9±2.0%, Figure 1a, Figure 3a). In endothelium-denuded rings, lower concentrations of PE (3–10 nM) were required to induce a similar degree of tone (1.54±0.15 g, $n=6$) to endothelium-containing rings, but in these, SOD produced no relaxation. Pretreatment with L-NOARG (30 μM) for 10 min to inhibit basal NO synthesis blocked SOD-induced relaxation in endothelium-containing rings (data not shown). Treatment of endothelium-containing rings with DETCA (0.1 mM) for 1 h to inactivate endogenous Cu-Zn SOD led to a 30±1.4% reduction in the maximal relaxation induced by SOD (Figure 1a). In endothelium-containing rings pretreated with SOD (50 u ml^{-1}), higher concentrations of PE (100–300 nM) were required to induce a similar degree of tone (1.08±0.05 g, $n=6$) to untreated rings (1.12±0.08 g, $n=6$) contracted with PE (30–100 nM) but ACh (10 nM–3 μM)-induced relaxation was unaffected (Figure 1b).

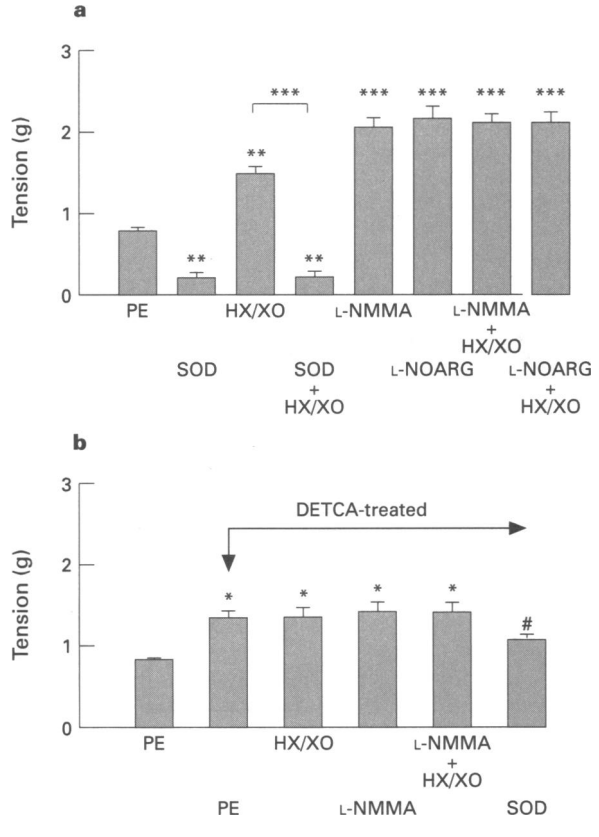

Figure 3 (a) Hypoxanthine (HX, 0.1 mM)/xanthine oxidase (XO, 16 mu ml^{-1}), N^G-monomethyl-L-arginine (L-NMMA, 30 μM) and N^G-nitro-L-arginine (L-NOARG, 30 μM) all potentiated phenylephrine (PE, 20 nM)-induced tone in endothelium-containing rings of rat aorta. Superoxide dismutase (SOD, 250 u ml^{-1}) relaxed PE-induced tone and prevented the potentiation induced by HX/XO. Furthermore, following treatment with L-NMMA or L-NOARG, subsequent treatment with HX/XO fail to enhance tone further. (b) Diethyldithiocarbamate (DETCA, 0.1 mM, 1 h) enhanced PE (20 nM)-induced tone in endothelium-containing rings of rat aorta and prevented the ability of HX (0.1 mM)/XO (16 mu ml^{-1}) and L-NMMA (30 μM) to potentiate tone. SOD (250 u ml^{-1}) produced only a slight relaxation of PE-induced tone in DETCA-treated endothelium-containing rings. All experiments were conducted in the presence of catalase (3000 u ml^{-1}) to prevent the relaxant effects of HX/XO. Each column is the mean±s.e.mean of 6 observations. $^*P<0.05$ $^{**}P<0.005$ and $^{***}P<0.001$ indicate a significant difference from rings receiving PE only. $^\#P<0.05$ indicates a significant difference from DETCA-treated endothelium-containing rings receiving PE only.

Effects of hypoxanthine/xanthine oxidase (HX/XO) on basal and ACh-stimulated activity of NO

HX (0.1 mM)/XO (16 mu ml^{-1}) produced two effects on rings of rat aorta; an immediate rise in PE-induced tone in endothelium-containing but not endothelium-denuded rings which was blocked by SOD (Figure 2, Figure 3a), and a delayed fall in both endothelium-containing and endothelium-denuded rings which was blocked by catalase (30–3000 u ml^{-1}, Figure 2). All subsequent experiments were conducted in the presence of catalase (3000 u ml^{-1}) to prevent the relaxant actions of HX/XO. Treatment of endothelium-containing rings with L-NMMA (30 μM) or L-NOARG (30 μM) to block basal NO synthesis potentiated PE-induced tone and blocked the ability of HX/XO to enhance tone (Figure 3a). Furthermore, treatment for 1 h with DETCA (0.1 mM) enhanced PE-induced tone in endothelium-containing rings (Figure 3b) and prevented the ability of HX/XO or L-NMMA to potentiate tone (Figure 3b). Treatment with HX/XO, L-NMMA, L-NOARG or DETCA had no effect on PE-induced tone in endothelium-denuded rings of rat aorta (data not shown).

In the presence of HX (0.1 mM)/XO (16 mu ml^{-1}), lower concentrations of PE (10–30 nM) were required to induce a similar degree of tone (1.35±0.08 g) to that of control rings (1.42±0.10 g) contracted with PE (30–100 nM). However, HX/XO had no effect on relaxations produced by ACh at any concentration in endothelium-containing rings (Figure 4, Figure 5a). Increasing the concentration of HX to 1 mM did, however, lead to a profound blockade of ACh-induced relaxation (Figure 4, Figure 5a). HX (1 mM)/XO (16 mu ml^{-1}) also reduced the duration of relaxation (Figure 4). Furthermore, treatment with DETCA (0.1 mM, 1 h) to inhibit endogenous Cu-Zn SOD led to a partial inhibition of ACh-induced relaxation by itself and potentiated the ability of HX (0.1 mM)/XO (16 mu ml^{-1}) to block ACh-induced relaxation (Figure 5b). The blockade of ACh-induced relaxation by HX (1 mM)/XO (16 mu ml^{-1}) alone or by HX (0.1 mM)/XO (16 mu ml^{-1}) in DETCA-treated tissues was prevented by pretreatment with exogenous SOD (250 u ml^{-1}). The ability of DETCA alone to inhibit ACh-induced relaxation was, however, only partially reversed by exogenous SOD (250 u ml^{-1}, data not shown).

Effects of pyrogallol on basal and ACh-stimulated activity of NO

Pyrogallol (0.1 mM) produced an immediate rise in PE-induced tone in both endothelium-containing and endothelium-denuded rings but the rise was significantly greater in the former (Figure 6). Pretreatment with SOD (250 u ml^{-1}) partially blocked the rise in tone induced by pyrogallol in endothelium-containing but had no effect in endothelium-denuded rings (Figure 6). Pyrogallol, like HX/XO, also produced a delayed fall in tone in both endothelium-containing and endothelium-denuded rings which was blocked by catalase (100–3000 u ml^{-1}). Consequently, all experiments with this agent were conducted in the presence of catalase (3000 u ml^{-1}).

In the presence of pyrogallol (0.1 mM), lower concentrations of PE (2–20 nM) were required to induce a similar degree of tone (1.49±0.08 g) to that of control rings (1.56±0.07 g) contracted with PE (30–100 nM). Pyrogallol had no effect, however, on relaxations produced by ACh at any concentration in endothelium-containing rings (Figure 7a). Increasing

the concentration of pyrogallol to 0.3 mM did, however, lead to a profound blockade of ACh-induced relaxation (Figure 7a) and this also reduced the duration of relaxation (not shown). Furthermore, treatment with DETCA (0.1 mM, 1 h) potentiated the ability of pyrogallol (0.1 mM) to block ACh-induced relaxation (Figure 7b). The blockade by pyrogallol (0.3 mM) alone or by pyrogallol (0.1 mM) in DETCA-treated tissues was prevented by pretreatment with exogenous SOD (250 u ml^{-1}).

Discussion

It is well established that exogenously added SOD potentiates both basal and agonist-stimulated activity of NO in cascade bioassay systems (Gryglewski *et al.*, 1986; Rubanyi & Vanhoutte, 1986a). In isolated arterial rings SOD also potentiates basal activity (Ohlstein & Nichols, 1989; Langenstroer & Pieper, 1992; this study) but, surprisingly, it has no effect on agonist-stimulated activity of NO (Abrahamsson *et al.*, 1992;

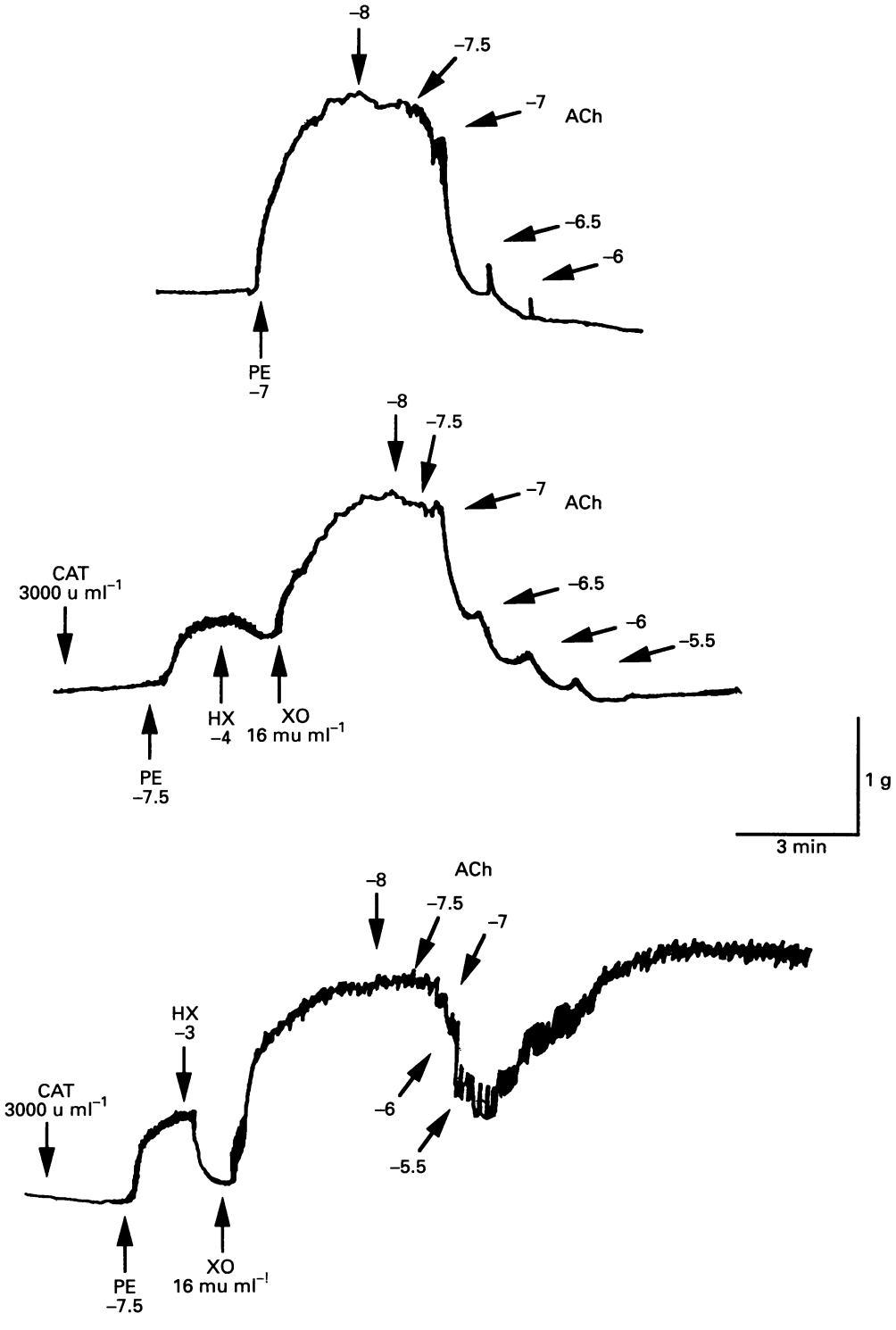

Figure 4 Individual experimental tracings showing the ability of hypoxanthine (HX, 0.1 mM and 1 mM)/xanthine oxidase (XO, 16 mu ml^{-1}) to inhibit acetylcholine (ACh)-induced relaxation in phenylephrine (PE)-contracted endothelium-containing rings of rat aorta. All experiments were conducted in the presence of catalase (CAT, 3000 u ml^{-1}) to prevent the relaxant effects of HX/XO. Drug concentrations are expressed in log molar units and enzyme concentrations are in units ml^{-1}.

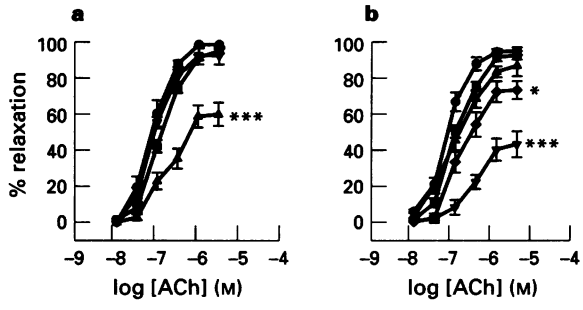

Figure 5 (a) Concentration-response curves showing relaxation to acetylcholine (ACh, ●) on phenylephrine (PE)-contracted endothelium-containing rings of rat aorta, blockade of relaxation by hypoxanthine (HX, 1 mM)/xanthine oxidase (XO, 16 u ml^{-1}, ▲) but no blockade by HX (0.1 mM)/XO (16 mu ml^{-1}, ■), and protection against blockade by the former by superoxide dismutase (250 u ml^{-1}, ▼). (b) Concentration-response curves to ACh (●) and the inability of HX (0.1 mM)/XO (16 m u ml^{-1}, ■) to block this relaxation. Following inhibition of endogenous Cu-Zn SOD with diethyldithiocarbamate (DETCA, 0.1 mM, 1 h, ◆) ACh-induced relaxation was partially inhibited and subsequent treatment with HX/XO (▼) now produced a profound blockade. Furthermore, this blockade was prevented by exogenous SOD (250 u ml^{-1}, ▲). All experiments were conducted in the presence of catalase (3000 u ml^{-1}) to prevent the relaxant effects of HX/XO. Each point is the mean ± s.e.mean of 5–12 observations. *$P<0.05$, and ***$P<0.001$ indicate a significant difference from maximal relaxation in untreated rings, respectively.

Figure 7 (a) Concentration-response curves showing relaxation to acetylcholine (ACh, ●) on phenylephrine (PE)-contracted endothelium-containing rings of rat aorta, blockade of relaxation by pyrogallol 0.3 mM (▲) but no blockade by 0.1 mM (■), and protection against blockade by the former by superoxide dismutase (250 u ml^{-1}, ▼). (b) Concentration-response curves to ACh (●) and the inability of pyrogallol (0.1 mM, ■) to block this relaxation. Following inhibition of endogenous Cu-Zn SOD with diethyldithiocarbamate (DETCA, 0.1 mM, 1 h, ▲) ACh-induced relaxation was partially inhibited and subsequent treatment with pyrogallol (▼) now produced a profound blockade. Furthermore, this blockade was prevented by exogenous SOD (250 u ml^{-1}, ◆). All experiments were conducted in the presence of catalase (3000 u ml^{-1}) to prevent the relaxant effects of pyrogallol. Each point is the mean ± s.e.mean of 6–12 observations. *$P<0.05$ and ***$P<0.001$ indicate a significant difference from maximal relaxation in untreated rings, respectively.

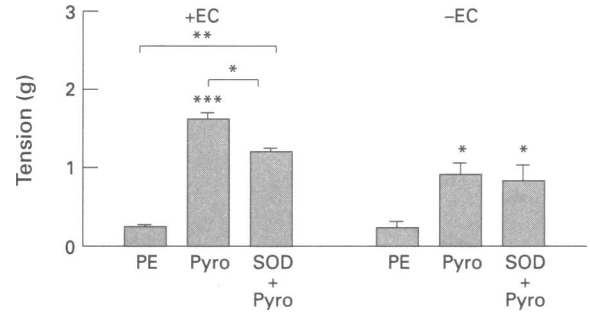

Figure 6 Augmentation of phenylephrine (PE)-induced tone by pyrogallol (Pyro, 0.1 mM) in endothelium-containing (+EC) and endothelium-denuded (–EC) rings of rat aorta and partial blockade of this in endothelium-containing but not endothelium-denuded rings by superoxide dismutase (SOD, 250 u ml^{-1}). All experiments were conducted in the presence of catalase (3000 u ml^{-1}) to prevent the relaxant effects of pyrogallol. The concentrations of PE in endothelium-containing (20 nM) and endothelium-denuded (1 nM) rings were chosen to produce equal levels of tone (0.26 ± 0.02 g and 0.26 ± 0.06 g, respectively). Each column is the mean ± s.e.mean of 6–9 observations. *$P<0.05$, **$P<0.005$ and ***$P<0.001$ indicate a significant difference from rings receiving PE only, or between groups joined by brackets.

this study). Clearly, the differential effects of SOD in cascade bioassay systems and arterial rings need to be explained. In the present study we attempted to determine if SOD and superoxide anion have differential effects on basal and agonist-stimulated activity of NO in rat aorta.

We found that SOD produced a powerful concentration-dependent relaxation of endothelium-containing rings of rat aorta but had no effect on endothelium-denuded rings. Relaxation appeared to be mediated by NO since it was blocked by L-NOARG, an inhibitor of NO synthesis (Moore *et al.*, 1990). The relaxant effects of SOD are therefore likely to have arisen from removal of superoxide anions, generated either within the tissue or in the oxygenated Krebs solution, which were destroying basally produced NO. Surprisingly, we found that a concentration of SOD (50 u ml^{-1}) which induced almost maximal potentiation of basal NO activity had absolutely no effect on ACh-induced relaxation. The background level of superoxide anion in the oxygenated tissue was therefore exerting a selective destructive action on basal but not agonist-stimulated activity of NO.

This selective action was investigated further by generating superoxide anion with HX/XO and pyrogallol. These experiments were complicated by the fact that superoxide anion-generating systems also give rise to other reactive oxygen species such as hydrogen peroxide (H_2O_2), hydroxyl radical and peroxynitrite which can damage the endothelium and thereby impair endothelium-dependent relaxations (Kvietys *et al.*, 1989; Beckman *et al.*, 1990; Todoki *et al.*, 1992; Dowell *et al.*, 1993). We wished to examine specifically the interaction between NO and superoxide anion and, consequently, catalase (3000 u ml^{-1}) was included in all experiments in order to remove H_2O_2. The use of catalase successfully prevented the occurrence of any damage to the endothelium as seen by our ability to generate reproducible concentration-response curves to ACh in the presence of HX/XO and pyrogallol. We also found that the delayed relaxant action of superoxide anion generators resulting from the production of H_2O_2, which both increases the liberation of NO (Rubanyi & Vanhoutte, 1986b) and mediates direct vascular muscle relaxation (Burke & Wolin, 1987; Zembowicz *et al.*, 1993), was also abolished by catalase. In the presence of catalase, HX (0.1 mM)/XO (16 mu ml^{-1}) produced an immediate and sustained increase in PE-induced tone in endothelium-containing but not endothelium-denuded rings. The increase in PE-induced tone was not seen if the tissues had been pretreated with SOD or the inhibitors of NO synthase, L-NMMA or L-NOARG, and is consistent with the previously reported endothelium-dependent vasoconstrictor action of superoxide anion (Ohlstein & Nichols, 1989; Katusic & Vanhoutte, 1989) through destruction of basal NO. Pyrogallol (0.1 mM), however, enhanced PE-induced tone in both endothelium-containing and endothelium-denuded rings, although that obtained in the former was greater. The endothelium-dependent component, as with HX/XO, was absent in tissues pretreated with SOD and is therefore also likely to have been due to destruction of basal NO by superoxide anion. The origin of the endothelium-independent augmentation of tone by pyrogallol is unclear, but it may be unrelated to the ability of the drug to generate superoxide anion since it was unaffected by SOD.

A major novel finding of this study, however, was that despite almost completely blocking basal NO activity, as indicated by the enhancement of PE-induced tone which was only further enhanced slightly by L-NMMA, HX (0.1 mM)/XO (16 mu ml^{-1}) and pyrogallol (0.1 mM) had no effect on ACh-induced relaxation. Thus, these experiments together with those demonstrating SOD-induced relaxation, clearly highlighted a greater sensitivity of basal than agonist-stimulated activity of NO to destruction by superoxide anion. What was less clear at this stage, however, was whether the data suggested a chemical difference between basal and agonist-stimulated NO. Indeed, some workers have proposed that basal EDRF is free NO, while that released in response to agonists comes from a pre-formed store (Ignarro, 1991; Cocks & Angus, 1991) of a stable NO-releasing molecule such as an S-nitrosothiol (Myers *et al.*, 1990).

Although our study indicated a difference in the susceptibility to destruction by superoxide anion, the difference was one of degree rather than being absolute since generating higher levels of superoxide anion by employing higher concentrations now led to the magnitude and duration of ACh-induced relaxation being greatly inhibited. As in previous studies (Wei *et al.*, 1985; Rubanyi & Vanhoutte, 1986b; Abrahamsson *et al.*, 1992), the inhibition was likely to have occurred as a consequence of destruction of agonist-stimulated NO by superoxide anion since it was blocked by SOD. Thus, it appeared that higher concentrations of superoxide anion were required to destroy agonist-stimulated than basal NO.

It was possible that the greater sensitivity of basal than agonist-stimulated NO to destruction might reflect differential protection by endogenous SOD and this was tested by inhibiting the enzyme. There are two major forms of this enzyme, a Cu-Zn-containing form which is located both extracellularly and intracellularly and a Mn-containing form which resides mainly in mitochondria (Hassan, 1988). The copper chelator, DETCA, inhibits the Cu-Zn-containing form of the enzyme both intracellularly and extracellularly (Kelner *et al.*, 1989), leading to increased levels of superoxide anion, as detected by lucigenin-elicited chemiluminescence (Cherry *et al.*, 1990; Omar *et al.*, 1991). Previous studies have shown that treatment of cultured endothelial cells in a cascade bioassay with DETCA led to loss of NO activity and this was likely to have resulted from destruction rather than reduced synthesis of NO since the release of total nitrogen oxides, as measured by chemiluminescence, was unaffected (Mügge *et al.*, 1991). We found that treatment with DETCA (0.1 mM) for 1 h enhanced the sensitivity of endothelium-containing but not endothelium-denuded rings to PE. This augmentation is likely to have occurred from the complete loss of basal activity of NO since HX/XO and L-NMMA subsequently failed to enhance PE-induced tone in these tissues. The restoration of basal NO activity following addition of SOD to DETCA-treated tissues, albeit reduced in comparison to control tissues, indicated that the loss had occurred as a consequence of destruction by the greater steady-state levels of superoxide anion. Furthermore, in these experiments where treatment with DETCA had led to a complete loss of basal activity of NO, ACh-induced relaxation was blocked only slightly, further strengthening the view that basal and agonist-stimulated activity are differentially sensitive to destruction. Others have reported that increasing the concentration of DETCA can lead to almost complete loss of ACh-induced relaxation (Mügge *et al.*, 1991; Omar *et al.*, 1991) and we have confirmed this, but such inhibition is only partially reversed by SOD so may be mainly due to destruction intracellularly in endothelial cells where exogenous SOD cannot penetrate. Consistent with this proposed intracellular site of action is the ability of DETCA to inhibit relaxation to nitrovasodilators, an effect reported to occur through destruction of NO by superoxide anion inside smooth muscle cells (Omar *et al.*, 1991). In our experiments we found that following pretreatment with a low concentration of DETCA (0.1 mM), subsequent treatment with concentrations of HX (0.1 mM)/XO (16 mu ml^{-1}) or pyrogallol (0.1 mM) that had little effect on ACh-induced relaxation themselves now produced a profound blockade and this was completely reversed upon addition of exogenous SOD. Clearly, therefore, endogenous Cu-Zn SOD protects agonist-induced NO from destruction by superoxide anion and this can be abolished following treatment with DETCA. It is likely therefore that the greater sensitivity of basal than agonist-stimulated activity of NO to destruction by superoxide anion is due to differential protection by Cu-Zn SOD rather than to differences in their chemical nature. Our proposed explanation for this is that under normal circumstances, endogenous Cu-Zn SOD activity lowers levels of superoxide anion, which may originate from endothelial cells or from the oxygenated Krebs solution, to such an extent that the low levels of NO produced under basal conditions can be destroyed but high levels produced following stimulation by ACh cannot. However, if levels of superoxide anion are increased further, either by generation of the free radical or by reducing its breakdown by inhibiting Cu-Zn SOD with DETCA, the higher levels of NO produced following agonist stimulation can now be destroyed. This explanation may also account for the inability of exogenous SOD to potentiate agonist-stimulated activity of NO in arterial rings (Abrahamsson *et al.*, 1992; this study), since there is already sufficient endogenous SOD present. In contrast, SOD is probably able to potentiate the activity of NO in a cascade bioassay system (Gryglewski *et al.*, 1986; Rubanyi & Vanhoutte, 1986a; Furchgott *et al.*, 1990) because there is no SOD in the intervening space to protect against the destructive action of superoxide anion.

In conclusion, our findings suggest that both basal and ACh-stimulated activity of NO can be destroyed by superoxide anion. The apparently greater sensitivity of the former may not necessarily indicate a chemical difference from agonist-stimulated NO but may simply reflect differential protection by endogenous Cu-Zn SOD.

K.B.M. is supported by a University of Glasgow Postgraduate Scholarship. We are grateful to the B.H.F. for financial support.

References

ABRAHAMSSON, T., BRANDT, U., MARKLUND, S.L. & SJÖQVIST, P.-O. (1992). Vascular bound recombinant extracellular superoxide dismutase type C protects against the detrimental effects of superoxide radicals on endothelium-dependent arterial relaxation. *Circ. Res.*, **70**, 264–271.

BECKMAN, J.S., BECKMAN, T.W., CHEN, J., MARSHALL, P.A. & FREEMAN, B.A. (1990). Apparent hydroxyl radical production by peroxynitrite: Implications for endothelial injury from nitric oxide and superoxide. *Proc. Natl. Acad. Sci. U.S.A.*, **87**, 1620–1624.

BURKE, T.M. & WOLIN, M.S. (1987). Hydrogen peroxide elicits pulmonary arterial relaxation and guanylate cyclase activation. *Am. J. Physiol.*, **252**, H721–H732.

CHERRY, P.D., OMAR, H.A., FARRELL, K.A., STUART, J.S. & WOLIN, M.S. (1990). Superoxide anion inhibits cGMP-associated bovine pulmonary arterial relaxation. *Am. J. Physiol.*, **259**, H1056–H1062.

COCCO, D., CALABRESE, L., RIGO, A., ARGESE, E. & ROTILIO, G. (1981). Re-examination of the reaction of diethyldithiocarbamate with the copper of superoxide dismutase. *J. Biol. Chem.*, **256**, 8983–8986.

COCKS, T.M. & ANGUS, J.A. (1991). Evidence that contractions of isolated arteries by L-NMMA and NOLA are not due to inhibition of basal EDRF release. *J. Cardiovasc. Pharmacol.*, **17** (Suppl. 3), S159–S164.

CRACK, P. & COCKS, T.M. (1992). Thimerosal blocks stimulated but not basal release of endothelium-derived relaxing factor (EDRF) in dog isolated coronary artery. *Br. J. Pharmacol.*, **107,** 566–572.

DOWELL, F.J., HAMILTON, C.A., MCMURRAY, J. & REID, J.L. (1993). Effects of a xanthine oxidase/hypoxanthine free radical and reactive oxygen species generating system on endothelial function in New Zealand white rabbit aortic rings. *J. Cardiovasc. Pharmacol.*, **22,** 792–797.

DOWNEY, J.M. (1990). Free radicals and their involvement during long-term myocardial ischemia and reperfusion. *Annu. Rev. Physiol.*, **52,** 487–504.

EGLÈME, C., GODFRAIND, T. & MILLER, R.C. (1984). Enhanced responsiveness of rat isolated aorta to clonidine after removal of the endothelial cells. *Br. J. Pharmacol.*, **81,** 16–18.

FREW, J.D., PAISLEY, K. & MARTIN, W. (1993). Selective inhibition of basal but not agonist-stimulated activity of nitric oxide in rat aorta by N^G-monomethyl-L-arginine. *Br. J. Pharmacol.*, **110,** 1003–1008.

FURCHGOTT, R.F., JOTHIANANDAN, D. & FREAY, D. (1990). Endothelium-derived relaxing factor: some old and new findings. In *Nitric Oxide from L-Arginine: a Bioregulatory System.* ed. Moncada, S. & Higgs, E.A. pp. 5–17. Amsterdam: Excerpta Medica.

FURCHGOTT, R.F. & ZAWADZKI, J.V. (1980). The obligatory role of endothelial cells in the relaxation of arterial smooth muscle by acetylcholine. *Nature*, **288,** 373–376.

GRYGLEWSKI, R.J., PALMER, R.M.J. & MONCADA, S. (1986). Superoxide anion is involved in the breakdown of endothelium-derived vascular relaxing factor. *Nature*, **320,** 454–456.

HASSAN, H.M. (1988). Biosynthesis and regulation of superoxide dismutase. *Free Radical Biol. Med.*, **5,** 377–385.

HEIKKILA, R.E., CABBAT, F.S. & COHEN, G. (1976). *In vivo* inhibition of superoxide dismutase in mice by diethyldithiocarbamate. *J. Biol. Chem.*, **251,** 2182–2185.

IGNARRO, L.J. (1991). Heme-dependent activation of guanylate cyclase and cyclic GMP formation by endogenous nitric oxide: a unique transduction mechanism for transcellular signalling. *Blood Vessels*, **28,** 67–73.

KATUSIC, Z.S. & VANHOUTTE, P.M. (1989). Superoxide anion is an endothelium-derived contracting factor. *Am. J. Physiol.*, **257,** H33–H37.

KELNER, M.J., BAGNELL, R., HALE, B. & ALEXANDER, N.M. (1989). Inactivation of intracellular copper-zinc superoxide dismutase by copper chelating agents without glutathione depletion and methemoglobin formation. *Free Radical Biol. Med.*, **6,** 355–360.

KVIETYS, P.R., INAUEN, W., BACON, B.R. & GRISHAM, M.B. (1989). Xanthine oxidase-induced injury to endothelium: role of intracellular iron and hydroxyl radical. *Am. J. Physiol.*, **257,** H1640–H1646.

LANGENSTROER, P. & PIEPER, G.M. (1992). Regulation of spontaneous EDRF release in diabetic rat aorta by oxygen free radicals. *Am. J. Physiol.*, **263,** H257–H265.

LIPTON, S.A., CHOI, Y.-H., PAN, Z.-H., LEI, S.Z., CHEN, H.-S.V., SUCHER, N.J., LOSCALZO, J., SINGEL, D.J. & STAMLER, J.S. (1993). A redox-based mechanism for the neuroprotective and neurodestructive effects of nitric oxide and related nitroso-compounds. *Nature*, **346,** 626–632.

MARTIN, W. (1988). Basal release of endothelium-derived relaxing factor. In *Relaxing and Contracting Factors.* ed. Vanhoutte, P.M. pp. 159–178. Clifton, N.J.: Humana Press.

MARTIN, W., FURCHGOTT, R.F., VILLANI, G.M. & JOTHIANANDAN, D. (1986). Depression of contractile responses in rat aorta by spontaneously released endothelium-derived relaxing factor. *J. Pharmacol. Exp. Ther.*, **237,** 529–538.

MINOR, R.L., MYERS, P.R., GUERRA, R., BATES, J.N. & HARRISON, D.G. (1990). Diet-induced atherosclerosis increases the release of nitrogen oxides from rabbit aorta. *J. Clin. Invest.*, **86,** 2109–2116.

MOORE, P.K., AL-SWAYEH, O.A., CHONG, N.W.S., EVANS, R. & GIBSON, A. (1990). N^G-nitro-L-arginine (L-NOARG) a novel, L-arginine-reversible inhibitor of endothelium-dependent vasodilatation *in vitro*. *Br. J. Pharmacol.*, **99,** 408–412.

MÜGGE, A., ELWELL, J.H., PETERSON, T.E. & HARRISON, D.G. (1991). Release of intact endothelium-derived relaxing factor depends on endothelial superoxide dismutase activity. *Am. J. Physiol.*, **260,** C219–C225.

MYERS, P.R., GUERRA, R. & HARRISON, D.G. (1989). Release of NO and EDRF from cultured bovine aortic endothelial cells. *Am. J. Physiol.*, **256,** H1030–H1037.

MYERS, P.R., MINOR, R.L., GUERRA, R., BATES, J.N. & HARRISON, D.G. (1990). Vasorelaxant properties of the endothelium-derived relaxing factor more closely resemble S-nitrosocysteine than nitric oxide. *Nature*, **345,** 161–163.

OHLSTEIN, E.H. & NICHOLS, A.J. (1989). Rabbit polymorphonuclear neutrophils elicit endothelium-dependent contraction in vascular smooth muscle. *Circ. Res.*, **65,** 917–924.

OMAR, H.A., CHERRY, P.D., MORTELLITI, M.P., BURKE-WOLIN, T. & WOLIN, M.S. (1991). Inhibition of coronary artery superoxide dismutase attenuates endothelium-dependent and -independent nitrovasodilator relaxation. *Circ. Res.*, **69,** 601–608.

PALMER, R.M.J., FERRIGE, A.G. & MONCADA, S. (1987). Nitric oxide release accounts for the biological activity of endothelium-derived relaxing factor. *Nature*, **327,** 524–526.

RANDALL, M.D. & GRIFFITH, T.M. (1991). Differential effects of L-arginine on the inhibition by N^G-nitroL-arginine methyl ester of basal and agonist-stimulated EDRF activity. *Br. J. Pharmacol.*, **104,** 743–749.

RUBANYI, G.M., ROMERO, J.C. & VANHOUTTE, P.M. (1986). Flow-induced release of endothelium-derived relaxing factor. *Am. J. Physiol.*, **250,** H1145–H1149.

RUBANYI, G.M. & VANHOUTTE, P.M. (1986a). Superoxide anions and hyperoxia inactivate endothelium-derived relaxing factor. *Am. J. Physiol.*, **250,** H822–H827.

RUBANYI, G.M. & VANHOUTTE, P.M. (1986b). Oxygen-derived free radicals, endothelium, and responsiveness of vascular smooth muscle. *Am. J. Physiol.*, **250,** H815–H821.

TODOKI, K., OKABE, E., KIYOSE, T., SEKISHITA, T. & ITO, H. (1992). Oxygen free radical-mediated selective endothelial dysfunction in isolated coronary artery. *Am. J. Physiol.*, **262,** H806–H812.

WEI, E.P., KONTOS, H.A., CHRISTMAN, C.W., DEWITT, D.S. & POVLISHOCK, J.T. (1985). Superoxide generation and reversal of acetylcholine-induced cerebral arteriolar dilation after acute hypertension. *Circ. Res.*, **57,** 781–787.

ZEMBOWICZ, A., HATCHETT, R.J., JAKUBOWSKI, A.M. & GRYGLEWSKI, R.J. (1993). Involvement of nitric oxide in the endothelium-dependent relaxation induced by hydrogen peroxide in the rabbit aorta. *Br. J. Pharmacol.*, **110,** 151–158.

(Received September 2, 1994
Revised January 25, 1995
Accepted May 1, 1995)

British Journal of Pharmacology (1995) 115, 1001-1004 © 1995 Stockton Press All rights reserved 0007-1188/95 $12.00

Accumulation of endogenous inhibitors for nitric oxide synthesis and decreased content of L-arginine in regenerated endothelial cells

[1]Hiroshi Azuma, Jun Sato, Hidehisa Hamasaki, Akiko Sugimoto, *Eiji Isotani & **Satoshi Obayashi

Department of Medicinal Chemistry, Institute for Medical and Dental Engineering, Departments of *Neurosurgery and **Gynecology and Obstetrics, Tokyo Medical and Dental University, 2-3-10 Surugadai, Kanda, Chiyoda-ku, Tokyo 101, Japan

1 We examined regeneration of endothelial cells (ECs), neointima formation, decreased endothelium-dependent relaxation (EDR) and changes in the contents of L-arginine, N^G-monomethyl-L-arginine (L-NMMA), asymmetrical N^G, N^G-dimethylarginine (ADMA) and symmetrical N^G,N'^G-dimethylarginine (SDMA) in the regnerated ECs, 6 weeks after balloon denudation of the rabbit carotid artery.

2 Regeneration of ECs was completed in 6 weeks and a significant neointima formation accompanied by the decreased EDR was observed.

3 L-NMMA and ADMA contents in the regenerated ECs (23.5 ± 4.3 and 21.2 ± 2.0 pmol mg^{-1} DNA, respectively) were significantly ($P < 0.05$ and $P < 0.01$) higher than those in the control ECs (8.8 ± 3.0 and 7.4 ± 1.9 pmol mg^{-1} DNA, respectively), whereas L-arginine was significantly ($P < 0.005$) decreased in the regenerated ECs ($31,470 \pm 1,050$ pmol mg^{-1} DNA) as compared to that in the control ECs ($47,870 \pm 1,890$ pmol mg^{-1} DNA). SDMA content was below the assay limits.

4 L-NMMA and ADMA, but not SDMA, inhibited the EDR induced by acetylcholine in a concentration-dependent manner. The inhibition with L-NMMA and ADMA was prevented by an addition of L-arginine, but not by D-arginine.

5 These results suggest that the accumulation of endogenous inhibitors for nitric oxide synthesis and decreased L-arginine content are associated with decreased NO production/release from regenerated ECs and neointima formation.

Keywords: Neointima formation; endogenous inhibitors for NO synthesis; balloon denudation; decreased endothelium-dependent relaxation; EDRF/NO

Introduction

As proposed by Ross & Glomset (1976a,b) and Ross (1986), denudation and nondenudation intimal injuries may play an important role in the development of atherosclerotic vascular disease (Ip *et al.*, 1990). We have reported that restoration of the endothelium after balloon denudation of the rabbit carotid artery was completed in 6 weeks and that regenerated ECs were less capable of producing/releasing the endothelium-derived relaxing factor (EDRF/nitric oxide: NO) (Azuma *et al.*, 1990; 1992; Niimi *et al.*, 1994). EDRF/NO inhibits platelet adhesion and aggregation (Azuma *et al.*, 1986; Radomski *et al.*, 1987), which is considered as an initiating event for neointima formation (Ross, 1986; Schwartz *et al.*, 1981). It has also been demonstrated that NO inhibits smooth muscle cell proliferation (Garg & Hassid, 1989).

These findings when considered together suggest that the neointima formation after endothelial removal might be caused at least partly through impairment of the ability of ECs to produce/release EDRF/NO. However, the mechanism by which the production/release of EDRF/NO is reduced remains unclear. Recently, Vallance *et al.* (1992) have obtained evidence N^G-monomethyl-L-arginine (L-NMMA) and asymmetrical N^G,N^G-dimethyl arginine (ADMA) play a role as endogenous inhibitors of NO synthesis. The present experiments were, therefore, designed to determine the regeneration of ECs, the neointima formation, the decreased EDR and the changes in content of L-arginine, L-NMMA, ADMA and symmetrical N^G,N'^G-dimethylarginine (SDMA) in the regenerated ECs after balloon denudation of the rabbit carotid artery.

[1] Author for correspondence.

Methods

Endothelial removal

Endothelial removal of the rabbit carotid artery was performed according to the method described previously (Azuma *et al.*, 1990). Briefly, the right common carotid artery of Japanese White male rabbit was exposed under anaesthesia with sodium pentobarbitone (25 mg kg^{-1}, i.v.) by aseptic surgery. An embolectomy catheter (12-040-3F/40 cm/3F, American Edwards Laboratories, Santa Ana, CA, U.S.A.) was then inserted into the proximal portion of the artery in retrograde fashion through a small nick made near the carotid bifurcation. The luminal surface of the artery from the origin to the balloon entrance was then gently rubbed back-and-forth with the balloon filled with 0.15 ml of air. This method of removal of ECs did not cause deep injury of the vascular wall (Azuma *et al.*, 1990; 1992; Niimi *et al.*, 1994). After the balloon was removed, the arterial incision was sutured with 10-0 nylon thread, keeping patency of the artery. The left carotid artery, underwent a sham operation and served as a control. At 6 weeks after the balloon denudation, animals were anaesthetized with sodium pentobarbitone and exsanguinated via the femoral arteries. This study complied with the Animal Welfare Regulations of Tokyo Medical and Dental University and the Guiding Principles for the Care and Use of Laboratory Animals approved by the Japanese Pharmacological Society.

Morphological examinations

Scanning electron microscopic examinations were performed on the previously denuded and sham-operated carotid arteries. The method of preparing the specimens is described elsewhere (Azuma *et al.*, 1990). The density of normal and regenerated

ECs was determined by scanning electron microscopy (ESM-3200, Elionics). To confirm the endothelial origin of the lining cells, vessels were stained with von Willebrand factor antibody (rabbit antihuman von Willebrand factor, Dako) using the labelled streptavidin-biotin staining technique (Dako LSAB kit) (Niimi *et al.*, 1994). Light microscopic observations were also made (Azuma *et al.*, 1990). To provide a semiquantitative parameter for assessing neointima formation, the intimal area and medial area were determined by means of an image analyzer (Quadra-950, Macintosh and Image scanner, Scanjet IIc, Hewlett Packard). The ratio (%) of the intimal area to the medial area was calculated.

Measurement of mechanical responses

Both common carotid arteries were isolated and immersed in cold modified Krebs solution. A transverse strip, 2 mm in width, was cut off with a razor blade and mounted vertically in an organ bath containing 5 ml modified Krebs solution continuously bubbled with 95% O_2 and 5% CO_2 at 37±0.5°C. Special care was taken to avoid unintentional rubbing of the intraluminal surface. The mechanical responses were determined according to the method described elsewhere (Azuma *et al.*, 1990). To compare the EDR to acetylcholine (ACh) between the previously denuded right and sham-operated left carotid artery strips, E_{max} (% maximum response) and –log ED_{50} (–log concentration producing 50% of the E_{max}) were obtained from the log concentration-relaxation curves to ACh. Relaxation induced by ACh was expressed as a percentage of the 10^{-6} M noradrenaline (NA)-induced contraction. Three different concentrations (3×10^{-5}, 10^{-4} and 3×10^{-4} M) of authentic L-NMMA (Sigma) and ADMA, and 3×10^{-4} M SDMA (Sigma) were tested against ACh-induced EDR. Potency of these inhibitors was compared as E_{max} of the ACh-induced EDR and –log ED_{50} values of ACh in the absence or presence of the inhibitors. ADMA was synthesized in our laboratory according to the method described by Kakimoto & Akazawa (1970).

Determination of L-arginine, L-NMMA, ADMA and SDMA

Contents of L-arginine, L-NMMA, ADMA and SDMA in the regenerated and control ECs were determined by means of automated high-performance liquid chromatography (h.p.l.c.) according to the method described by Villanueva *et al.* (1987) with minor modification. The automated analytical system was equipped with a solvent selection system (LV-980-03), 2 h.p.l.c. pumps (PU-980), an autosampler (AS-950), a column oven (CO-960), a fluorescence detector (FP-920) and an integrator (807-IT, all from Jasco, Tokyo). ECs were collected by gently rubbing the innermost surface of the previously denuded right and sham-operated left carotid arteries with a microspatula in 5 M ice-cold HEPES buffer (pH 7.4) and then sonicated at 20 W for 15 s (Sonifire 250, Branson), followed by an addition of trichloroacetic acid at a final concentration of 5%. Arterial strips from which endothelium had been deliberately removed were devoid of ECs on the intimal surface, and the intact subendothelial layer was identified by scanning electron microscopy. The homogenate was centrifuged at 1,300 *g* for 10 min. Supernatant was separated and 100 µl aliquot of the supernatant was applied for h.p.l.c. The composition of the eluting buffers and the elution time are shown in Table 1. The buffers were prepared from freshly distilled and deionized water, adjusted to the required pH and filtered through a Millipore filter (Type HA, 0.45 µm pore size; Millipore Waters). The flow-rates were 0.55 ml min^{-1} for the buffers and 0.33 ml min^{-1} for the orthophthalaldehyde fluorogenic reagent (Nakalai Chemicals Co., Kyoto, Japan). One column (AApak Li, 6.0mmIDx100mm, Jasco) temperature, 60°C, was used during the analyses. Regeneration of the column was achieved in 15 min with a solution of 0.6 M lithium hydroxide and re-equilibration was completed in 60 min with the first buffer (0.1 N lithium citrate, pH 6.06). The column back-pressure generated during analyses was 28 kg cm^{-2}. The chromatograms and retention times of the authentic L-arginine, ADMA, L-NMMA, SDMA and paraphenylenediamine dihydrochloride (Wako Pure Chemicals) used as an internal standard are shown in Figure 1a. The equations of relationships between the concentrations (Y) of authentic compounds and the ratio (X: response factor) of the fluorescence peak area of the authentic compounds to that of the internal standard were determined as follows: $Y = 59.38X - 0.515$ ($r = 0.9995$) for L-arginine, $Y = 71.26X - 0.437$ ($r = 0.9995$) for ADMA, $Y = 28.45X - 0.427$ ($r = 0.9996$) for L-NMMA, and $Y = 71.65X - 0.233$ ($r = 0.9998$) for SDMA. The concentration of each compound in the ECs was determined by the equation described above after estimating the response factor (X) of the peak corresponding to the retention time of authentic compounds.

Determination of DNA

The microassay of DNA was performed according to the fluorometric method described by Kissane & Robins (1958). Protein concentration was measured with bovine serum albumin as a standard by the method of Lowry *et al.* (1951).

Table1 Composition and conditions of eluting buffers

Buffer	*Lithium citrate* (N)	*pH*	*Elution time* (min)
1	0.1	6.06	8
2	0.6	6.85	8
3	1.1	7.00	25
4	1.4	7.05	70

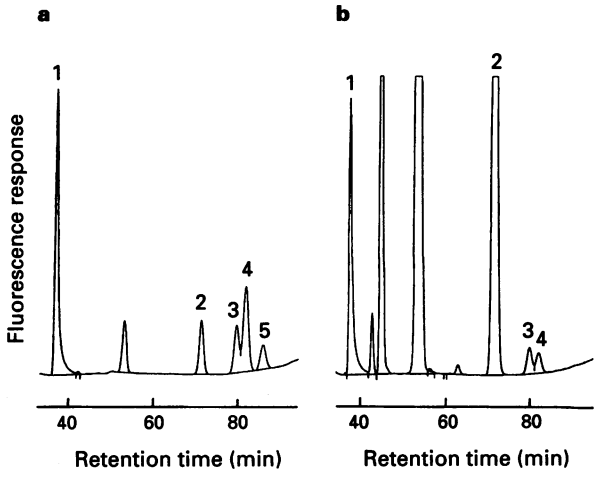

Figure 1 Chromatographic analysis of a standard mixture of L-arginine and its methylated derivatives (a) and crude extract of regenerated ECs (b). Retention time (RT) is given as mean±s.e.mean of 6 determinations on a mixture containing 200 pmol of each of the authentic compounds (a). Total of 6 determinations for the crude extract of the control ($n = 3$) and regenerated ECs ($n = 3$) were averaged (b). Paraphenylenediamine (11 nmol) was used as an internal standard (IS). The column and the elution programme employed gave a good overall resolution.

a *Peak*	*Compound*	*RT* (min)	*b* *Peak*	*RT* (min)
1	IS	37.7±0.12 (6)	1	37.7±0.13 (6)
2	L-Arginine	71.6±0.05 (6)	2	71.6±0.04 (6)
3	L-NMMA	80.1±0.04 (6)	3	80.1±0.04 (6)
4	ADMA	82.3±0.04 (6)	4	82.3±0.05 (6)
5	SDMA	86.6±0.03 (6)		

Statistical analysis

Values are expressed as mean ± s.e.mean. The statistical analysis was carried out by a two way analysis of variance (ANOVA). If the mean values were found to be different at $P < 0.05$ by means of ANOVA, either Scheffe or Student's t test was also applied.

Results

Morphological findings

In the sham-operated left carotid artery (under control conditions), scanning electron microscopy revealed that the luminal surface was completely covered with ECs, which were regularly arranged parallel to the direction of the blood stream. Six weeks after denudation, a full endothelial lining on the luminal surface was observed. However, the regenerated ECs were morphologically different from native ones; they were irregularly oriented. The density (cells mm^{-2}) of regenerated ECs was 9,540 ± 317 ($n = 5$), a value which was significantly ($P < 0.005$) different from 6,493 ± 248 ($n = 5$) in the control.

In the light microscopic observations of the cross sections of vascular wall, no noticeable changes could be detected in the control and the intima media^{-1} ratio (%) was estimated to be 4.8 ± 0.6 ($n = 5$). Six weeks after denudation, a marked neointima formation was detectable. The intima media^{-1} ratio was 38.7 ± 8.2% ($n = 5$), which was significantly ($P < 0.005$) different from the value in the control.

Endothelium-dependent relaxation (EDR) to ACh

ACh ($10^{-9} \sim 3 \times 10^{-6}$ M) produced a concentration-dependent relaxation during a contraction with 10^{-6} M NA. The ACh (10^{-6} M)-induced relaxation was abolished after the *in vitro* denudation of ECs and greatly inhibited by the pretreatment of strips with N^G-nitro-L-arginine (10^{-4} M) and methylene blue (3×10^{-5} M), but was unaffected by indomethacin (10^{-5} M), indicating that the relaxation might be dependent on the endothelium and mediated by EDRF/NO, but not by prostacyclin. Comparison of the E_{max} and $-\log ED_{50}$ values between the control left and the previously denuded right carotid arteries showed that the EDR was greatly reduced in the latter. The E_{max} and $-\log ED_{50}$ were determined to be 72.4 ± 7.8% ($n = 5$) and 7.38 ± 0.07 ($n = 5$), respectively, in the control, and 18.9 ± 2.6% ($P < 0.005$, *vs.* control, $n = 5$) and 5.78 ± 0.09 ($P < 0.005$ *vs.* control, $n = 5$), respectively, in the previously denuded artery. The magnitude of precontraction with 10^{-6} M NA was not significantly different between the two groups {854 ± 169 mg in the control ($n = 5$) and 826 ± 172 mg in the previously denuded artery ($n = 5$)}.

Contents of DNA, L-arginine, L-NMMA, ADMA and SDMA in ECs

The DNA content in the regenerated ECs (176.7 ± 4.7 μg mg^{-1} protein, $n = 3$) was significantly ($P < 0.005$) greater than that in the control (131.2 ± 4.8 μg mg^{-1} protein, $n = 3$). The changes in the L-arginine, L-NMMA, ADMA and SDMA contents are given in terms of pmol mg^{-1} DNA and shown in Table 2. L-NMMA and ADMA contents were significantly ($P < 0.05$ and $P < 0.01$) more increased in the regenerated ECs than in the control ECs. On the other hand, L-arginine contents showed a significantly ($P < 0.0005$) greater decrease in the regenerated ECs. The content of SDMA was below the assay limits.

Inhibitory activities of L-NMMA, ADMA and SDMA on the ACh-induced EDR

The inhibitory activities of L-NMMA, ADMA and SDMA are given in terms of E_{max} (%) and $-\log ED_{50}$ and shown in

Table 2 Comparison of L-arginine, N^G-monomethyl-L-arginine (L-NMMA), asymmetrical N^G, N^G-dimethylarginine (ADMA) and symmetrical N^G, N'^G-dimethylarginine (SDMA) contents in the endothelial cells (ECs)

	n	*Tissue content* (pmol mg^{-1} DNA) L-Arginine	*L-NMMA*	*ADMA*	*SDMA*
Control ECs	3	47,870 ± 1,890	8.8 ± 3.0	7.0 ± 1.9	–
Regenerated ECs	3	31,470 ± 1,050***	23.5 ± 4.3*	21.2 ± 2.0**	–

Results are given as mean ± s.e.mean. Significant difference vs. control at *$P < 0.05$, **$P < 0.01$ and ***$P < 0.005$. –: below the assay limitation by the h.p.l.c method.

Table 3 Inhibitory activities of N^G-monomethyl-L-arginine (L-NMMA), asymmetrical N^G, N^G-dimethylarginine (ADMA) and symmetrical N^G, N'^G-dimethylarginine (SDMA) on the acetylcholine (ACh)-induced endothelium-dependent relaxation (EDR) in the control carotid artery strips

Treatment	*Concentration* (M)	n	*ACh-induced EDR* Emax (%)	*–log ED50*
	–	5	76.9 ± 4.3	7.44 ± 0.13
	3×10^{-5}	5	51.6 ± 8.8*	7.05 ± 0.04*
L-NMMA	1×10^{-4}	5	40.7 ± 5.1***	7.00 ± 0.01**
	3×10^{-4}	5	34.3 ± 2.4***	6.97 ± 0.02**
	–	5	79.3 ± 3.7	7.45 ± 0.13
	3×10^{-5}	5	68.2 ± 5.1	7.22 ± 0.07
ADMA	1×10^{-4}	5	58.9 ± 7.3*	7.12 ± 0.06*
	3×10^{-4}	5	48.0 ± 7.2***	6.98 ± 0.01***
	–	5	77.6 ± 3.7	7.45 ± 0.19
SDMA	3×10^{-4}	5	77.9 ± 3.4	7.46 ± 0.21

Results are given as mean ± s.e.mean. As a result of ANOVA followed by Schaffe's test, $P < 0.01$ for control vs. 10^{-4} M L-NMMA and $P < 0.005$ for control vs. 3×10^{-4} M L-NMMA, $P < 0.05$ for control vs. 10^{-4} M ADMA and $P < 0.005$ for control vs. 3×10^{-4} M ADMA. Significant difference vs. corresponding control at *$P < 0.05$, **$P < 0.01$ and ***$P < 0.005$, respectively (Student's t test). Inhibitory potency was expressed as E_{max} of the ACh-induced EDR and $-\log ED_{50}$ of ACh in the absence or presence of authentic L-NMMA, ADMA or SDMA. -: No treatment with authentic compound.

Table 3. The ACh-induced EDR was inhibited by L-NMMA and ADMA in a concentration-dependent manner, but not by SDMA at the highest concentration of 3×10^{-4} M. The activity in the reduction of E_{max} and ED_{50} values with L-NMMA was slightly more potent than that with ADMA. L-NMMA (3×10^{-4} M) and ADMA (3×10^{-4} M) did not produce inhibition of ACh-induced EDR in the presence of 3×10^{-3} M L-arginine. D-Arginine (3×10^{-3} M) was without effect on the inhibitory activities of L-NMMA and ADMA.

Discussion

Six weeks after removal of the endothelium from the rabbit carotid artery, the endothelial lining was re-established with significantly increased density of the regenerated ECs. Significant impairment of the ACh-induced EDR was accompanied by a marked neointimal formation. All these findings were similar to those in our previous papers (Azuma *et al.*, 1990; 1992; Niimi *et al.*, 1994). We have demonstrated that the impairment of the ACh-induced EDR is due to reduction in the production/release of EDRF/NO by the regenerated ECs and that the capacity to produce/release EDRF/NO per cell greatly reduces since the cell density had significantly increased over the normal (Azuma *et al.*, 1990; Niimi *et al.*, 1994). However, the mechanism by which impairment of the production/release of EDRF/NO is caused remains unclear. In the present experiments, we discovered that contents of L-NMMA and ADMA, but not of SDMA, were significantly higher in the regenerated ECs. L-NMMA and ADMA, but not SDMA, inhibited the ACh-induced EDR. The inhibition of ACh-induced EDR with the two methylarginine derivatives was prevented by addition of L-arginine, but not by D-arginine. These results combined with the evidence demonstrating that L-NMMA and ADMA play a role as endogenous inhibitors of NO synthesis (Vallance *et al.*, 1992) suggest that the reduced production/release of EDRF/NO in the regenerated ECs is at least partly due to the accumulation of the endogenous inhibitors of NO synthesis. The content of L-arginine as a substrate for NO synthesis was significantly decreased in the regenerated ECs. This may partly account for the decreased production/release of NO in the regenerated ECs. It should be noted, however, that even in the regenerated ECs, the ratio of endogenous inhibitors to L-arginine was small. Therefore, it remains to be determined if these levels of L-NMMA and ADMA are able to inhibit NO synthesis in control cells and whether the degree of inhibition is enhanced in regeneratd ECs in which accumulated levels of the inhibitors increased. Further studies on this aspect are in progress in our laboratories.

It is well established that EDRF/NO is an anti-aggregating substance (Azuma *et al.*, 1986; Radomski *et al.*, 1987), which is considered as an initiating event for neointima formation (Schwartz *et al*,. 1981; Ross, 1986) and it has been suggested by Garg & Hassid (1989) that endogenous EDRF/NO may act as an inhibitory modulator of vascular smooth muscle cell mitogenesis. In addition, the increase in plasma endothelin-1, a potent mitogen (Hirata *et al.*, 1989), is thought to reflect a rise in vascular production of the peptide in response to the impaired release of EDRF/NO from ECs (Boulanger & Lüscher, 1990). We have reported that the increased level of endothelin-1 in the vascular wall accompanied by a decreased production/release of EDRF/NO would be involved in neointima formation (Niimi *et al.*, 1994; Azuma *et al.*, 1994). If these findings are considered together, they suggest that the accumulation of endogenous inhibitors for NO synthesis is associated with the decreased NO production/release from regenerated ECs and neointima formation after endothelial removal in the rabbit carotid artery.

This work was supported in part by Smoking Research Foundation (SRF) for Biomedical Research in Japan and Salt Science Research Foundation (SSRF) in Japan. The authors thank Dr A. Saito for preparation of histological specimens.

References

AZUMA, H., FUNAYAMA, N., KUBOTA, T. & ISHIKAWA, M. (1990). Regeneration of endothelial cells after balloon denudation of the rabbit carotid artery and changes in responsiveness. *Jpn. J. Pharmacol.*, **52,** 541–552.

AZUMA, H., HAMASAKI, H., NIIMI, Y., TERADA, T. & MATSUBARA, O. (1994). Role of endothelin-1 in neointima formation after endothelial removal in rabbit carotid arteries. *Am. J. Physiol.*, **267** (*Heart Circ. Physiol.*, **36**), H2259–H2267.

AZUMA, H., ISHIKAWA, M. & SEKIZAKI, S. (1986). Endothelium-dependent inhibition of platelet aggregation. *Br. J. Pharmacol.*, **88,** 411–415.

AZUMA, H., NIIMI, Y. & HAMASAKI, H. (1992). Prevention of intimal thickening after endothelial removal by a nonpeptide angiotensin II receptor antagonist, losartan. *Br. J. Pharmacol.*, **106,** 665–671.

BOULANGER, C & LÜSCHER, T.F. (1990). Release of endothelin from the porcine aorta, inhibition by endothelium-derived nitric oxide. *J. Clin. Invest.*, **85,** 587–590.

GARG, U.C. & HASSID, A. (1989). Nitric oxide-generating vasodilators and 8-bromo-cyclic guanosine monophosphate inhibit mitogenesis and proliferation of cultured rat vascular smooth muscle cells. *J. Clin. Invest.*, **83,** 1774–1777.

HIRATA, Y., TAKAGI, Y., FUKUDA, Y. & MARUMO, F. (1989). Endothelin is a potent mitogen for rat vascular smooth muscle cells. *Arteriosclerosis*, **78,** 225–228.

IP, J.H., FUSTER, V., BADIMON, L., BADIMON, J., TABMAN, M.B. & CHESEBRO, J.H. (1990). Syndromes of accelerated atherosclerosis. *Am. J. Coll. Cardiol.*, **15,** 1667–1687.

KAKIMOTO, Y. & AKAZAWA, S. (1970). Isolation and identification of N^G,N^G- and N^G,N'^G-dimethylarginine, N^ε-mono, di-, and trimethyllysine, and glucosylgalactosyl- and galactosyl-δ-hydroxylysine from human urine. *J. Biol. Chem.*, **245,** 5751–5758.

KISSANE, J.M. & ROBINS, E. (1958). The fluorometric measurement of deoxyribonucleic acid in animal tissue with special reference to the central nervous system. *J. Biol. Chem.*, **233,** 184–188.

LOWRY, O.H., ROSEBROUGH, N.J., FARR, A.L. & RANDALL, R.J. (1951). Protein measurement with the Folin phenol reagent. *J. Biol. Chem.*, **193,** 265–275.

NIIMI, Y., AZUMA, H. & HIRAKAWA, K. (1994). Repeated endothelial removal augments intimal thickening and attenuates EDRF release. *Am. J. Physiol.*, **266** (*Heart Circ. Physiol.*, **35**), H1348–H1356.

RADOMSKI, M.W., PALMER, R.M.J. & MONCADA, S. (1987). The antiaggregating properties of vascular endothelium: interaction between prostacyclin and nitric oxide. *Br. J. Pharmacol.*, **92,** 639–646.

ROSS, R. (1986). The pathogenesis of atherosclerosis - an update. *N. Engl. J. Med.*, **314,** 488–500.

ROSS, R. & GLOMSET, J.A. (1976a). The pathogenesis of atherosclerosis (first of two parts). *N. Engl. J. Med.*, **295,** 369–377.

ROSS, R. & GLOMSET, J.A. (1976b). The pathogenesis of atherosclerosis (second of two parts). *N. Engl. J. Med.*, **295,** 420–425.

SCHWARTZ, S.M., GAJDUSEK, C.M. & SELDEN, S.C. (1981). Vascular wall growth control: the role of the endothelium. *Arteriosclerosis*, **1,** 107–171.

VALLANCE, P., LEONE, A., CALVER, A., COLLIER, J. & MONCADA, S. (1992). Accumulation of an endogenous inhibitor of nitric oxide synthesis in chronic renal failure. *Lancet*, **339,** 572–575.

VILLANUEVA, V.R., MARDON, M., LE GOFF, M.Th. & MONCELON, F. (1987). Improved high-performance liquid chromatographic analysis of methylated amino acids and related compounds and its application to the analysis of samples of polluted healthy and damaged *Picea* needles without extract purification. *J. Chromatogr.*, **393,** 107–113.

(Received May 3, 1995
Accepted May 5, 1995)

British Journal of Pharmacology (1995) 115, 1005-1012 © 1995 Stockton Press All rights reserved 0007-1188/95 $12.00

Modulation of excitatory amino acid responses by tachykinins and selective tachykinin receptor agonists in the rat spinal cord

[1]Michael J. Cumberbatch, *Boris A. Chizh & [2]P. Max Headley

Department of Physiology, University of Bristol, School of Medical Sciences, University Walk, Bristol, BS8 1TD and *Department of Pharmacology, Moscow Sechenov Medical Academy, 2/6 B. Pirogovskaya St, Moscow 119881, Russia

1 The effects of tachykinins and agonists selective for the three subtypes of neurokinin (NK) receptor have been tested on spinal neuronal responses both to the excitatory amino acids (EAAs) NMDA, AMPA and kainate, and to noxious heat stimuli. The agonists were applied by microiontophoresis in *in vivo* experiments in α-chloralose-anaesthetized, spinalized rats.

2 The NK_1-selective agonist, GR 73632, enhanced responses to all three EAAs similarly, whilst the NK_2-selective agonist, GR64349, reduced responses to AMPA and kainate without affecting those to NMDA, and the NK_3 selective agonist, senktide, enhanced responses to AMPA and kainate.

3 The endogenous ligands substance P (SP) and neurokinin A (NKA) both enhanced responses to NMDA with little effect on responses to kainate, whereas neurokinin B (NKB) selectively enhanced responses to kainate without affecting those to NMDA.

4 The effects of GR73632 on EAA responses showed some differences between the dorsal and ventral horn, with more selectivity towards enhancement of NMDA responses in the ventral horn, but a smaller maximum effect.

5 Background activity was significantly enhanced by GR73632, GR64349, SP and NKA but not by senktide or NKB. GR73632 had the greatest effect on background firing, but this action was variable between cells and was related both to the location within the spinal cord and to the degree of spontaneous activity prior to GR73632 administration.

6 Responses to noxious heat were enhanced consistently only by NKA.

7 These data show that selective agonists for the tachykinin receptors are capable of modulating EAA responses differentially. SP, NKA and NKB appear to act via more than one receptor type when modulating EAA responses *in vivo*. This indicates that NK-EAA interactions can be more specific than suggested hitherto, with the combined actions at NK_1 and NK_2 receptors biasing EAA responsiveness towards NMDA receptor mediated functions, whereas NK_3 receptor activation would have the opposite effect. The physiological role of such interactions is likely to be complex.

Keywords: Tachykinins; NK_1 receptors; NK_2 receptors; NK_3 receptors; substance P; neurokinin A; neurokinin B; NMDA; AMPA; kainate; excitatory amino acids; nociceptive; spinal cord

Introduction

The neurokinins (NKs; or tachykinins) represent a family of neuropeptides that is thought to be important in the transmission of nociceptive information and the induction/mediation of hyperalgesic changes in the spinal dorsal horn. In previous studies, intrathecal substance P (SP) induced behavioural responses indicative of pain (Hylden & Wilcox, 1981) and reduced tail flick latencies to noxious stimuli (Cridland & Henry, 1986); more recently, similar results have been obtained with agonists selective for the NK_1 and NK_2 receptor subtypes (Picard *et al.*, 1993). These results are consistent with electrophysiological data, which show that SP and related NKs can excite spinal neurones both *in vitro* (Konishi & Otsuka, 1974; Fisher *et al.*, 1994) and *in vivo* (Henry *et al.*, 1975; Fleetwood-Walker *et al.*, 1990; 1993). Substance P and neurokinin A (NKA) have been found in the nerve terminals of primary afferent fibres (Dalsgaard *et al.*, 1985), and in many of these they are co-localized with excitatory amino acids (EAA) (De Biasi & Rustioni, 1988; Merighi *et al.*, 1991). Both NKs and EAAs can be released into the spinal cord following noxious peripheral stimulation (Duggan *et al.*, 1988; 1990; Skilling *et al.*, 1988).

Although there is no direct evidence for co-release of EAAs and NKs, there is considerable evidence for interactions between the two neurotransmitter systems. NKs have been shown to modulate both the release of endogenous EAAs (Kangrga *et al.*, 1990) and the postsynaptic responses to EAAs in spinal neurones *in vitro* (Randic *et al.*, 1990) and *in vivo* (Dougherty & Willis, 1990); SP can selectively enhance responses to N-methyl-D-aspartate (NMDA) (Dougherty & Willis, 1991; Rusin *et al.*, 1993). These various effects are however rather variable. Because this may relate to the lack of selectivity of the agonists used, we have now investigated the interaction between NK and EAA agonists on spinal neurones *in vivo*, and have compared the actions of selective and naturally occurring tachykinins. The effects of the various NKs on responses to nociceptive stimuli were tested in parallel. Some of these data have been presented previously in abstract form (Cumberbatch *et al.*, 1994a).

Methods

Animal preparation

Experiments were performed on 75 male rats (295-365 g). Anaesthesia was induced and maintained with halothane (1-2% in O_2 for maintenance) for the duration of the surgery. This involved cannulating the trachea, carotid artery and jugular vein, followed by a laminectomy from L2 to T8 and spinalization at T9 to T10. The animal was immobilised in a recording frame and was transferred to α-chloralose anaesthesia (50 mg kg^{-1} initially followed by an infusion at

[1]Present address: Merck Sharp & Dohme Research Laboratories, Neuroscience Research Centre, Terlings Park, Harlow, Essex, CM20 2QR.
[2]Author for correspondence.

approximately 10 mg kg^{-1} h^{-1}, i.v.). The animals usually breathed spontaneously (O_2 enriched air), but in some experiments they were ventilated after paralysis with pancuronium (1.5 mg kg^{-1} h^{-1}, i.v.). In these animals end tidal CO_2 was monitored and kept close to pre-paralysis levels; the adequacy of anaesthesia was ensured by maintaining the same anaesthetic regime and by monitoring the cardiovascular responses to noxious stimuli applied rostral to the level of spinalization. Fluid therapy (isotonic saline and/or Haemaccel, Hoechst) was given at a rate of approximately 3 ml kg^{-1} h^{-1}. Blood pressure was monitored throughout and systolic values remained above 90 mmHg. Core temperature was maintained close to 37°C (range 36.0–37.5°C).

Electrophysiology and drug administration

A seven barrelled micropipette was inserted into the spinal cord (L5–L6 segment) and the central barrel was used to record extracellularly from single dorsal or ventral horn neurones. Five of the outer barrels were used to administer drugs by microiontophoresis (Table 1). GR73632 and GR64349 (Hagan *et al.*, 1989) were gifts from Glaxo Research and Development; other NKs were obtained from Sigma and the EAAs from Tocris Neuramin. Retaining currents were applied to the outer barrels to prevent leakage of drug solutions; a standard 0.5V was used to compensate for variability in electrode barrel resistance. A sixth barrel (200 mM NaCl) was used for automated current balancing. Because of the limitation of 5 drug barrels, only 2 NKs could be tested on responses to all 3 EAAs, or alternatively, 3 NKs could be tested on responses to 2 EAAs; the 3×3 way comparison was not possible on individual cells.

NMDA, α-amino-3-hydroxy-5-methyl-4-isoxazolepropionate (AMPA) and kainate were ejected iontophoretically and all three excited the majority of neurones tested (Headley & Grillner, 1990). Neurones were selected that responded to all 3 agonists but that did not respond to Na^+ or Cl^- currents of at least 100 nA. NMDA, AMPA and kainate were then ejected in regular cycles of 4–5 min (mean ejection currents: NMDA 27 nA, AMPA 12nA, kainate 21 nA). The peak firing rates (25–75 spikes s^{-1}) were matched for each EAA on individual cells and were always submaximal. With some cells noxious heat was also applied to the hind paw receptive field using a contact heat device with a ramp (5 s) from 35°C to the test temperature of 45.2–49.9°C (held for 10–15 s). Extracellular action potentials were recorded and displayed both as spikes per second (spikes s^{-1}) and as counts over the stimulus application. Any discharge between stimulus applications was termed background activity; this background baseline was subsequently subtracted from all evoked responses.

Once a series of stable response cycles was obtained a NK agonist was ejected in a cumulative current-doubling regime (5–80 nA) until either a clear effect was seen or, if no effect, until the maximum current of 80 nA was reached. Each current was ejected over at least 2 stimulus cycles (i.e. at least 6–8 min) and drug effects were measured for all parameters within the same cycle. Drug effects were expressed either as percentages of control (where control was the mean of the last three pre-test responses, based on spike counts), or as the change in the number of EAA-evoked spikes. The time to half recovery ($t_{\frac{1}{2}}$) following the termination of the drug application was also calculated; since each stimulus was necessarily at a different point in the 3–4 min cycle, the resolution of these $t_{\frac{1}{2}}$ values is limited. Statistical analysis was performed on untransformed data using either the Wilcoxon matched pairs test or the Mann-Whitney U-test. Comparisons were made either between test and the three pre-test control counts (* in figures) or, between the effects of a NK on different EAA responses (#). A probability level of <0.05 was deemed significant.

Results

Effects of selective tachykinin receptor agonists on responses to excitatory amino acids

The NK_1 agonist, GR73632, was tested upon 61 neurones from the dorsal and ventral horns (5–80 nA, mean maximum current 14 nA). Figure 1a illustrates that with cells on which NMDA, AMPA and kainate were cycled together, GR 73632 enhanced responses to all three EAAs to a similar degree. This effect was consistent and, on the 11 cells that were tested with more than one ejection current, the effect was current-dependent. The population data (Figure 2a) show that responses to all three EAAs were enhanced significantly, although there was a significantly greater enhancement of responses to NMDA than of those to AMPA. There was no difference between the effects of GR73632 on responses to each EAA on dorsal *vs.* ventral horn neurones. However, in the ventral but not dorsal horn, there was a significantly greater enhancement of responses to NMDA relative to those to both AMPA or kainate (Figure 3a). The effects of GR73632 on EAA responses did not correlate with the change in the background activity. Responses remained enhanced for some time after cessation of ejection (mean time of half recovery ($t_{\frac{1}{2}}$) was 10 min, range 3–32 min).

The NK_2 agonist, GR64349, was tested on 51 neurones from the dorsal and ventral horns (5-80 nA, mean maximum 30 nA) and had effects markedly different from those of the NK_1 agonist. Figure 1b shows for one neurone that GR64349 significantly depressed responses to kainate more than AMPA, with little effect on responses to NMDA. This was consistent for all cells ($n=18$; Figure 2a), and was current-dependent on 16 of the 17 units tested. Responses recovered rapidly ($t_{\frac{1}{2}}$ mean 5 min, range 3–16 min). When analysed separately on dorsal and ventral horn neurones, GR64349 did not affect responses to NMDA on dorsal horn neurones, whereas these responses were slightly enhanced with ventral horn neurones (Figure 3b).

Table 1 The neurokinin and excitatory amino acid compounds used in this study

Drug	*Receptor*	(mM)	pH	*Ejected as*	*Full name*
GR73632	NK_1	1/50	4.5–5.0	cation	δ-Ava-Phe-Phe-Pro-Leu(Me)-Met.NH_2
Substance P	NK_1	1/50	4.5–5.0	cation	Arg-Pro-Lys-Pro-Gln-Glu-Phe-Phe-Gly-Leu-Met.NH_2
GR64349	NK_2	1/50	4.5–5.0	cation	Lys-Asp-Ser-Phe-Val-Rlactam-Met.NH_2
Neurokinin A	NK_2	1/50	4.5–5.0	cation	His-Lys-Thr-Asp-Ser-Phe-Val-Gly-Leu-Met.NH_2
Senktide	NK_3	1/50	8.0–8.5	anion	Succinyl-Asp-Phe-MePhe-Gly-Leu-Met.NH_2
Neurokinin B	NK_3	1/50	8.0–8.5	anion	Asp-Met-His-Asp-Phe-Phe-Val-Gly-Leu-Met.NH_2
NMDA	NMDA	100/100	7.5–8.0	anion	*N*-methyl-D-aspartic acid
AMPA	AMPA	5/200	7.5–8.0	anion	(**RS**)-α-amino-3-hydroxy-5-methyl-4-isoxazole-propionic acid
Kainic acid	Kainate	5/200	7.5–8.0	anion	Kainic acid

mM refers to the concentration of the drug in a solution of 50, 100 or 200 mM NaCl. The pH of solutions was adjusted with HCl or NaOH.

Responses to AMPA were affected variably on ventral horn neurones, whereas responses to kainate were reduced silmilarly with both cell groups.

The NK_3 agonist, senktide, was tested on 19 neurones from the dorsal horn (5–40 nA, mean maximum 16 nA) and had effects essentially opposite to those of the NK_2 agonist. Figure 1 illustrates the effect of senktide on the responses of one neurone. Responses to AMPA and kainate were selectively enhanced compared to those to NMDA. This effect was consistent as shown by the pooled data in Figure 2a. AMPA and kainate responses recovered rapidly ($t_{\frac{1}{2}}$ mean 1 min, maximum 4 min). Senktide was not tested on ventral horn neurones.

Effects of naturally occurring tachykinins on responses to NMDA and kainate

The NK_1 preferring tachykinin, substance P (SP), was tested upon 17 neurones from the dorsal and ventral horns (5–

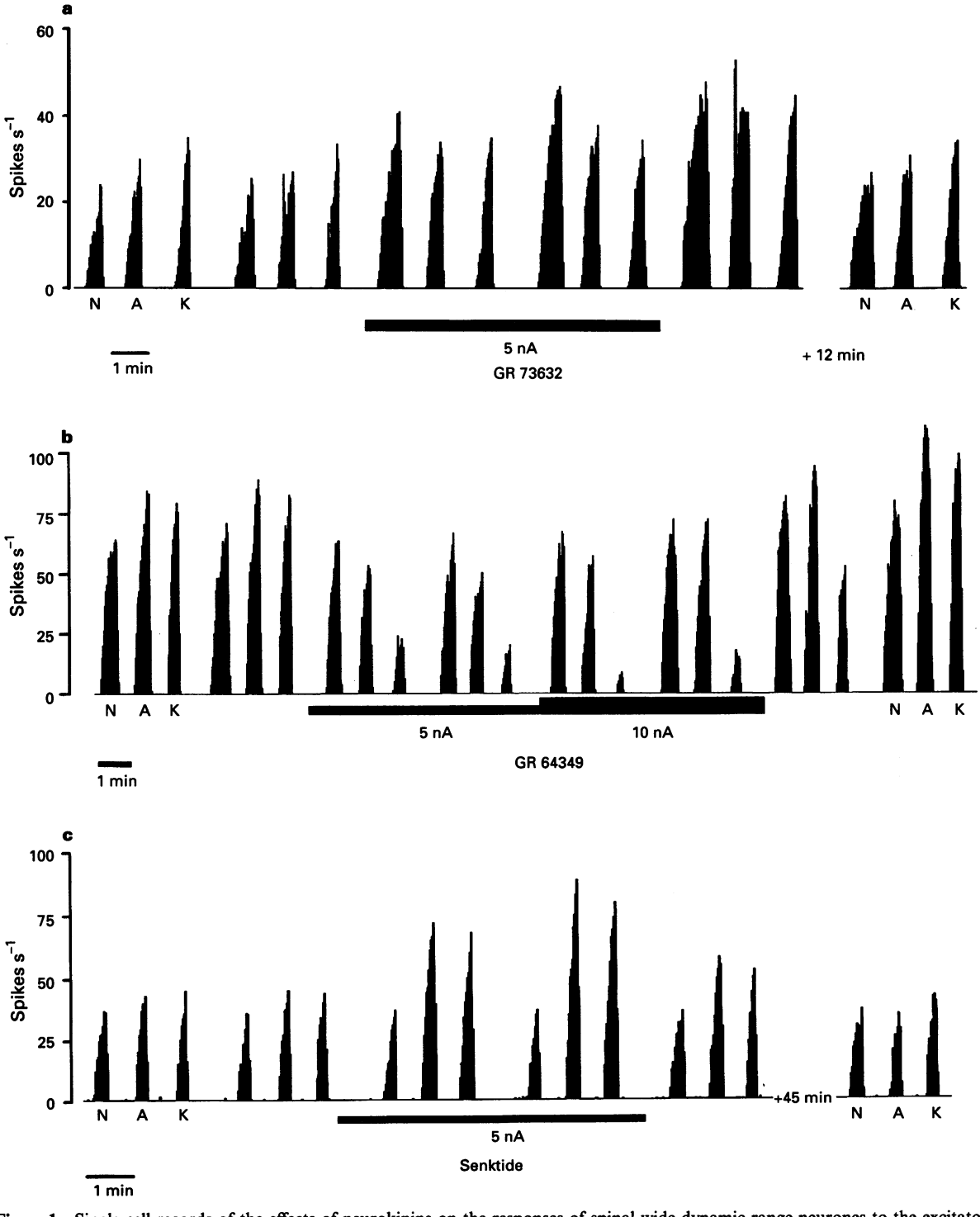

Figure 1 Single cell records of the effects of neurokinins on the responses of spinal wide dynamic range neurones to the excitatory amino acid agonists NMDA (N), AMPA (A) and kainate (K). The amino acids were ejected iontophoretically in regular cycles and ejection currents were adjusted to elicit similar amplitude, submaximal, responses. Thereafter a selective neurokinin (NK) agonist was ejected over 2 cycles at each current tested: (a) the NK_1 agonist, GR73632, (b) the NK_2 agonist, GR64349 and (c) the NK_3 agonist, senktide. Each NK agonist had a distinctive effect upon the excitatory amino acid responses. Data from 3 neurones in the ventral (a) or dorsal horns (b,c) of 3 α-chloralose-anaesthetized, spinalized rats.

40 nA, mean maximum 17 nA). With 11 of 17 cells, responses to NMDA were enhanced (to 146±7% control, mean±s.e.mean; $P<0.001$ *vs.* control) and with the remaining 6 cells were reduced (to 63±11% control; $P<0.05$); this variability did not correlate with either location in the spinal cord or background activity. The pooled data show no significant change in the NMDA response (Figure 2b). Responses returned to control values with a mean $t_{\frac{1}{2}}$ of 5 min (range 3–12 min). Responses to kainate were not affected significantly.

The NK_2 preferring tachykinin, neurokinin A (NKA, 5–20 nA, mean maximum 8 nA) had effects similar to SP, but was more consistent. When tested upon 10 neurones from the dorsal horn, responses to NMDA were enhanced significantly (Figure 2b), whilst responses to kainate were relatively unchanged; the difference between NMDA and kainate was significant. Responses to NMDA recovered rapidly ($t_{\frac{1}{2}}$ mean 1 min, maximum 4 min).

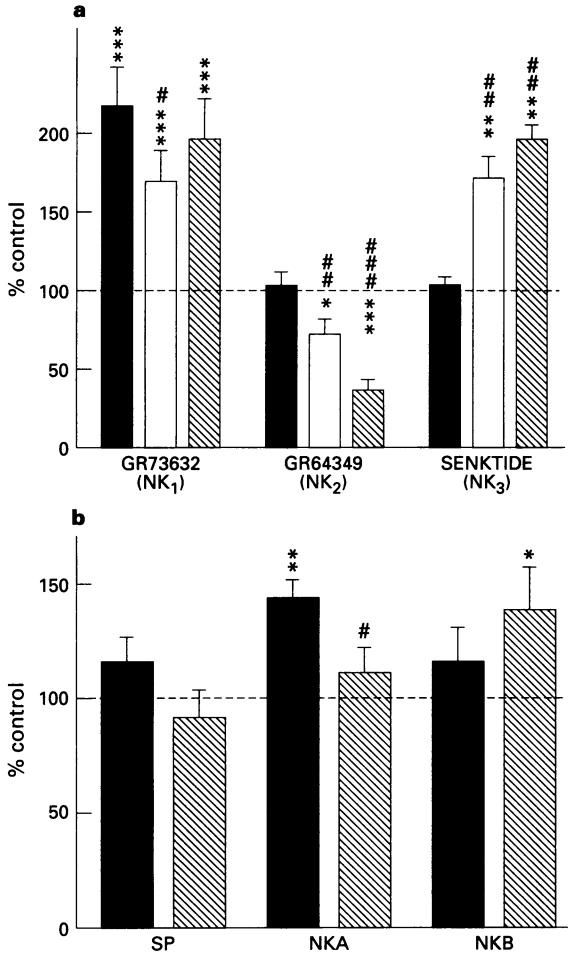

Figure 2 Population data of the effects of selective NK agonists (a) and endogenous neurokinins (b) upon the responses of spinal neurones to the excitatory amino acids NMDA (solid columns), AMPA (open columns) and kainate (hatched columns). Data are expressed as the percentages of the mean of three pre-test control responses, after correcting responses by subtracting background activity. (a) Effects of the NK_1 agonist, GR73632 (5-40, mean 9 nA, $n=28$), the NK_2 agonist, GR64349 (5-40, mean 14 nA, $n=18$) and the NK_3 agonist, senktide (5-20, mean 11 nA, $n=8$). (b) Effects of the three endogenous neurokinins, substance P (SP, 5-40, mean 15 nA, $n=17$), neurokinin A (NKA, 5-20, mean 8 nA, $n=9$) and neurokinin B (NKB, 5-40, mean 16 nA, $n=8$). A significant difference from control is indicated by $*P<0.05$, $**P<0.01$, $***P<0.005$, whilst a significant difference between the effects of a neurokinin on responses to AMPA or kainate *vs.* NMDA is indicated by $\#P<0.05$, $\#\#P<0.01$, $\#\#\#P<0.005$.

The NK_3 preferring tachykinin, neurokinin B (NKB) was tested upon 8 neurones from the dorsal horn (5–40 nA, mean maximum 16 nA) and had effects opposite to those of both SP and NKA; as with senktide, responses to kainate were enhanced significantly (Figure 2b), whilst those to NMDA were less affected. Responses recovered to control values with a mean $t_{\frac{1}{2}}$ of 5 min (range 3–20 min).

The effects of the tachykinins on background activity

The NK_1 and NK_2 agonists, GR73632, GR64349, SP and NKA all enhanced background activity significantly; conversely, the NK_3 agonists, senktide and NKB had little effect (Figure 4a). The selective NK_1 agonist, GR73632, had by far the greatest mean effect, although this hides considerable variability; some cells showed a large increase in the background activity (*e.g.* Figure 2a in Chizh *et al.*, 1995) whereas others remained quiescent even when the responses to the EAAs were much enhanced. There was some correlation ($r=0.34$; $P<0.05$) between GR73632-evoked activity and the depth of the neurone relative to the pial surface (Figure 4b); GR73632 evoked an increase of more than 5 spikes s^{-1} with 67% of 18 neurones in the ventral horn compared to only 40% of 43 neurones in the dorsal horn. There was a population of neurones in the deep dorsal horn (21 of the 43 cells, Figure 4b) with which there was little change in the background activity (<1 spike s^{-1}).

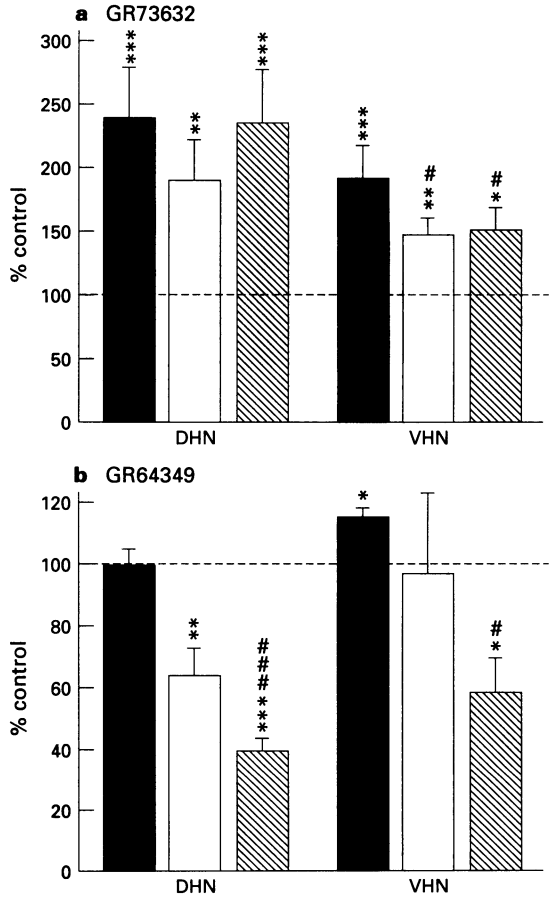

Figure 3 Comparison of the effects of the NK_1 agonist GR73632 (a) and the NK_2 agonist GR64349 (b) upon responses to NMDA (solid columns), AMPA (open columns) and kainate (hatched columns) on dorsal horn neurones (DHN; $n=15$ for GR73632, $n=14-44$ for GR64349) and on ventral horn neurones (VHN; $n=13$ for GR73632, $n=4-7$ for GR64349). A significant difference between control and test counts is indicated by $*P<0.05$, $**P<0.01$ and $***P<0.005$. A difference between the effects of the NK agonist on AMPA or kainate *vs* NMDA responses is shown by $\#P<0.05$, $\#\#\#P<0.005$.

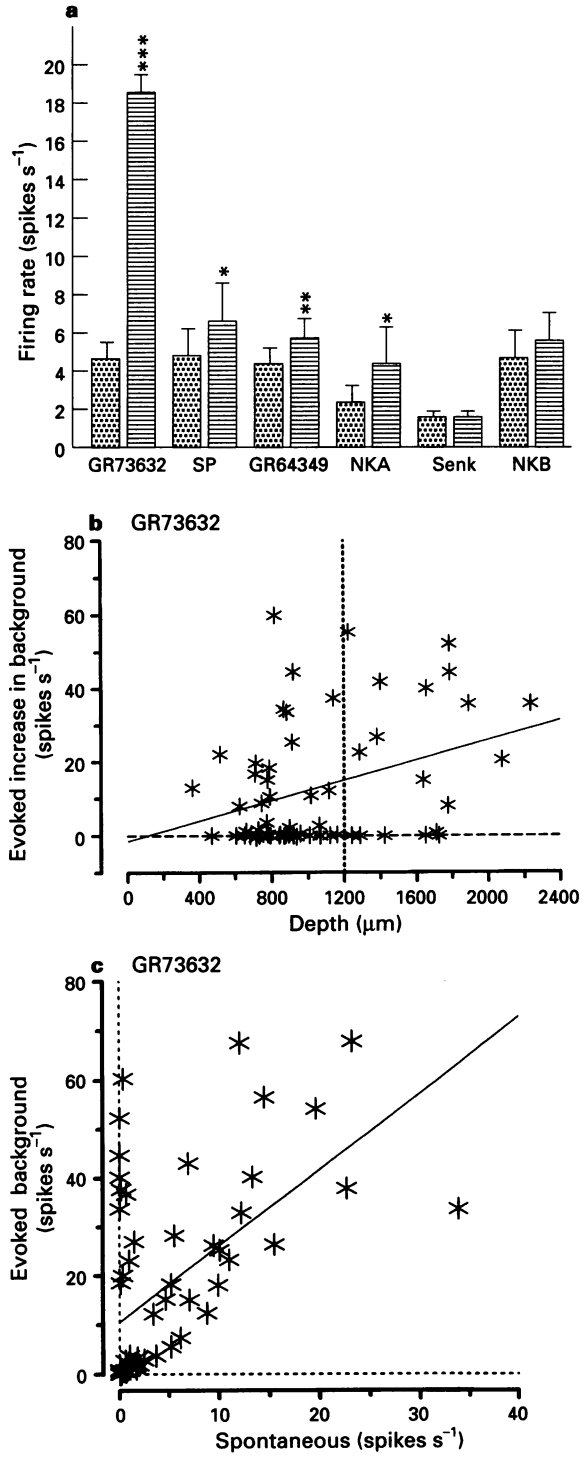

Figure 4 Effects of neurokinins on background activity of spinal neurones. (a) Spontaneous activity prior to drug administration (stippled columns) and neurokinin evoked activity (hatched columns). Data are presented as mean firing rate determined over a period of 60 s. GR73632 $n=61$, substance P (SP) $n=17$, GR64349 $n=50$, NKA $n=10$, senktide (Senk) $n=19$ and NKB $n=8$. A significant difference between spontaneous and test counts is indicated by $^{*}P<0.05$, $^{**}P<0.01$, $^{***}P<0.005$. (b) The effect of GR73632 on background activity was correlated with the depth of the electrode relative to the cord surface. To give a clear indication of the cells on which GR73632 did not alter spontaneous activity, data are expressed as a change in the mean firing rate above spontaneous levels (*ie.* evoked firing rate less control firing rate). The slope represents the linear regression ($r=0.34$; $P<0.05$). (c) GR73632 evoked activity related to the initial spontaneous activity. The slope indicates the linear regression ($r=0.55$; $P<0.001$).

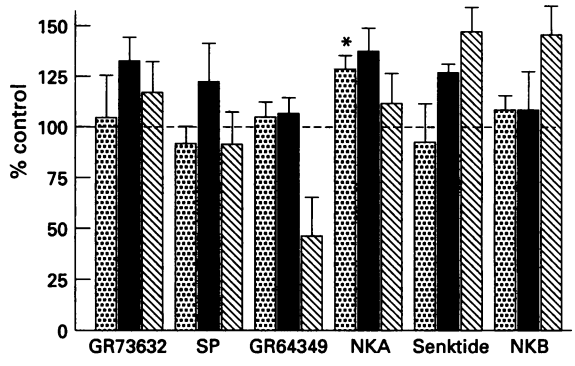

Figure 5 The effects of selective and endogenous neurokinin agonists on responses to noxious heat (stippled columns; 45.5–49.9°C; 15–20 s) on dorsal and ventral horn neurones. These responses were compared to those to NMDA (solid columns) and kainate (hatched columns) on the same neurones. Data are shown for the NK_1 agonist, GR73632 (5–10 nA, mean 6 nA, $n=9$); the endogenous NK_1 preferring agonist, substance P (SP; 5–20 nA, mean 9 nA, $n=9$); the NK_2 agonist, GR64349 (5–80 nA, mean 28 nA, $n=16$); the NK_2-preferring agonist, neurokinin A (NKA; 5–20 nA, mean 9 nA, $n=7$); the NK_3 agonist senktide (5–20 nA mean 11 nA, $n=6$) and the NK_3-preferring agonist, neurokinin B (NKB; 5–40 nA, mean 14 nA, $n=6$). A significant effect of a neurokinin on nociceptive responses, compared to pre-drug control, is indicated by $^{*}P<0.05$. See Figure 2 for the significance levels of the effects of the NK agonists on responses to amino acids.

The effect of GR73632 on background activity was also compared with the level of pre-drug spontaneous activity, an indicator of initial cell excitability. Figure 4c indicates that there was some correlation between the two ($r=0.55$; $P<0.001$). GR73632 increased the background activity of 76% of the 29 cells that had a level of spontaneous firing higher than 1 spike s^{-1}, but only of 38% of the 32 cells that had very low or no spontaneous activity (<1 spike s^{-1}).

With the NK_2 and NK_3 agonists there was no correlation between their effects on background activity and either depth or initial spontaneous activity.

The effects of the tachykinins on responses to noxious heat

Only NKA consistently affected responses to noxious heat, enhancing responses to 126±7% control ($n=7$, $P<0.05$, Figure 5). The other endogenous tachykinins and selective agonists had effects that were variable from cell to cell. There was no correlation between the effects of each agonist on heat responses when compared to depth in the cord, pre-agonist spontaneous activity or agonist-evoked background activity. Figure 5 summarizes these data and for comparison shows the effects of the NKs on the responses to NMDA and kainate tested on the same cells.

Discussion

The selective NK receptor agonists clearly caused diverse, receptor-specific modulations of EAA responses in the rat spinal cord, implying that NK receptors are differentially involved in the fine-tuning of EAA receptor-mediated neurotransmission.

Effects of the selective NK agonists on EAA responses

The NK_1 agonist, GR73632, enhanced responses to all three EAAs consistently and to similar degrees, and background activity was also enhanced with many cells. The non-selectivity of the enhancements suggests that they may have been secondary either to a direct depolarizing effect that would sum with other inward currents, or to an increase in membrane

resistance that would increase the effectiveness of such currents. The effects are likely to have been mediated via NK_1 receptors, both because this agonist has been shown to be highly selective (Hagan *et al.*, 1989) and because the effects were blocked by the NK_1 receptor antagonist, GR82334 (Chizh *et al.*, 1994; 1995). However, since the NK_1 and NK_2 agonists were ejected from acidified solutions, the possibility of effects being mediated by proton ejection needs to be considered. Ejection of protons can cause direct excitation, but this is only seen at pH values below about 3 (Curtis & Watkins, 1960) whereas in these experiments the NK_1 and NK_2 agonists were ejected from solutions of pH 4.5–5.0. Protons can also modulate EAA responses directly, preferentially decreasing NMDA responses (Vyklický *et al.*, 1990; Traynelis & Cull-Candy, 1991). Such effects of protons seem unlikely here, firstly because the similarly acidic NK solutions of GR73632 and GR64369 had differential effects on EAA responses, and secondly because the effects of GR73632 were prevented by ejection of an antagonist from a solution of similar pH (Chizh *et al.*, 1994; 1995).

The magnitude of the effect of GR73632 was variable between individual neurones, and one possibility is that this could relate to the distribution of NK_1 receptors in the spinal cord. Although they occur throughout the dorsal and ventral horns, they are concentrated in the superficial dorsal horn and on motoneurones (Yashpal *et al.*, 1988; Mantyh *et al.*, 1989; Brown *et al.*, 1993; Bleazard *et al.*, 1994). In the dorsal horn there is a relatively uniform distribution of NK_1 receptors over the soma and dendrites, indicating that there are extrasynaptic receptors (Liu *et al.*, 1994) but this is not necessarily the case in the ventral horn. Variable local concentrations of receptors may, therefore, have contributed to the inter-cell variability.

The hypothesis of a primary depolarizing effect of NK_1 agonists is consistent with numerous reports of excitation by substance P (SP). However, if NK_1 receptor activation causes depolarization, the question arises why GR73632 increased the spike firing rate with only about one third of the cells in the present experiments. The most likely explanation is that with many silent cells there was a depolarization that remained subthreshold for evoking spikes; this is consistent with the finding that background activity was enhanced with nearly all cells that were spontaneously active (Figure 4c). It remains possible that some NK_1 receptors did not induce depolarizing currents, which would be consistent with the report that SP can enhance responses to EAAs under voltage-clamp conditions (Randic *et al.*, 1990).

NK receptors have been linked to various second messenger systems. Intracellular Ca^{2+} levels can be enhanced by NKs (Womack *et al.*, 1988) via an inward Ca^{2+} current that may be linked to second messenger systems (Murase *et al.*, 1989). Moreover, SP can enhance responses to NMDA via a mechanism involving protein kinase C and cyclic AMP (Rusin *et al.*, 1992; 1993) and NK_1 receptor activation can selectively enhance inositol phosphate production in primary cultures of spinal cord neurones (Parsons *et al.*, 1993). NK_1 receptors may therefore mediate their effects on EAA responses via more than one mechanism, again contributing to the inter-cell variability.

The NK_2 receptor-selective agonist, GR64349, had effects on EAA responses that were consistently opposite to those of the NK_3 agonist, senktide. Neither agonist had a major effect on background activity, as in a previous study (Fleetwood-Walker *et al.*, 1993). This suggests that, unlike the NK_1 agonist effects, the changes in EAA responses were not secondary to changes in cell excitability, but the mechanism for the interactions cannot be predicted from these experiments. Since the effects reversed rapidly they are likely to involve a change in the EAA receptor or channel kinetics rather than receptor up/down-regulation.

Binding studies indicate that NK_2 and NK_3 receptors are preferentially localized to the superficial dorsal horn (Yashpal *et al.*, 1988; Mantyh *et al.*, 1989) yet the effects observed were consistent throughout the dorsal horn and, where tested, in the ventral horn. Since GR64349 and senktide had opposite effects, and as they were ejected with opposite polarities from solutions that were acidic and alkaline respectively, the possibility of current or proton artefacts must again be assessed. Firstly all cells were tested for resistance to current at 100 nA (see Methods). Secondly the actions of the NK_2 agonist are not consistent with proton effects (see above) and were in addition reversed on some cells by a NK_2 receptor antagonist (Chizh *et al.*, 1994; 1995). Thirdly the NK_3 solutions were within half a pH unit of extracellular values. These considerations indicate that it is unlikely that current or proton effects were responsible for the actions observed.

Effects of the naturally occurring tachykinins on EAA responses

The effects on EAA responses of the NK_1-preferring endogenous neurokinin, SP, were variable between cells, as reported previously (Dougherty & Willis, 1990; Randic *et al.*, 1990; Rusin *et al.*, 1993). Although SP and NKA are NK_1 and NK_2 receptor-preferring respectively, the selectivities of these agonists are poor compared to those of GR73632 and GR64349 (Hagan *et al.*, 1989). One might expect that, at the high localized concentrations that occur with iontophoresis, there will be little receptor selectivity between NK_1 and NK_2 receptors by either SP or NKA. The combination of an NK_1 mediated enhancement of responses to all three EAAs and an NK_2 mediated depression of kainate and AMPA responses could have resulted in a net selective enhancement of NMDA responses. This was just what was observed in the current experiments with NKA, although the SP effect was more variable and did not reach significance.

This greater variability with SP compared to either NKA or GR73632 could be related to a more rapid peptidase inactivation (Hooper *et al.*, 1985; Theodorsson-Norheim *et al.*, 1987; see also Duggan *et al.*, 1992). Moreover the N-terminal sequence of SP has been demonstrated to modulate responses to EAAs via a non-NK receptor mechanism (Larson & Sun, 1992; Budai *et al.*, 1992). Such non-NK effects were not responsible for the EAA effects of GR73632 since these effects were reversed by a NK_1 antagonist (Chizh *et al.*, 1994; 1995).

NKB had effects similar to those of the selective NK_3 agonist, senktide. However, the lower selectivity between kainate and NMDA responses with NKB *vs.* senktide suggests that the endogenous ligand was causing some NK_1-mediated effects.

The data therefore suggest that SP, NKA and NKB acted via more than one receptor type under these conditions. Given that the synaptic concentration of these agonists is likely to be high, endogenously released NKs may also have actions via more than one NK receptor. Moreover, NKA and SP are co-localized in some primary afferents (Dalsgaard *et al.*, 1985). Conversely, NKB is not found in primary afferent fibres but is localized instead in ascending fibres and interneurones (Ogawa *et al.*, 1985; Too & Maggio, 1991; Moussaoui *et al.*, 1992). The functional effects of these three endogenous tachykinins may therefore be anatomically related.

Effects of neurokinins on nociceptive responses

Enhancement of NMDA responses might be expected to promote nociceptive responses, since NMDA receptors have been linked with the generation and maintenance of pronociceptive states (review by Meller & Gebhart, 1993). On the other hand, AMPA/kainate receptors are involved in mediating both nociceptive and non-nociceptive responses (Dougherty *et al.*, 1992; Cumberbatch *et al.*, 1994b). Alteration of AMPA/kainate responsiveness would therefore be expected to alter both nociceptive and non-nociceptive transmission.

Selective NK_1 agonists administered intrathecally can indeed facilitate nociceptive reflexes in behavioural tests (Picard *et al.*, 1993), but, despite the increase of EAA responses, GR73632 did not enhance nociceptive responses in the spinal

neurones tested in this study. It is possible that intrathecal administration promotes a sufficiently widespread excitation to cause the release of other endogenous neurotransmitters that in turn modulate neurotransmission. Iontophoretic application of NK_1 agonists will have had a far more localized effect and may not even have reached the distal dendrites of the single neurone under study. Under these conditions the effects on synaptic responses may be expected to be much less than following intrathecal administration.

The selective NK_2 agonist, GR64349, depressed AMPA/kainate responses, so that one would predict that it would also have depressed synaptic responses. Previous studies have shown that higher ejection currents of GR64349 did depress responses to noxious heat, although at lower currents the responses were enhanced (Fleetwood-Walker *et al.*, 1993). We saw no evidence for such a bivalent action; GR64349 had no detectable effect on nociceptive responses. With NK_3 agonists, intrathecal administration can cause antinociception and motor flaccidity (Papir-Kricheli *et al.*, 1987). Here senktide enhanced AMPA/kainate responses, but failed to affect nociceptive responses; failure to reach synaptic sites could again underlie this lack of effect. It is therefore difficult to interpret the present findings on NK-AMPA/kainate receptor interactions with respect to physiological mechanisms.

Concerning the endogenous ligands, the preferential NK_2 agonist, NKA selectively enhanced NMDA responses, and also increased responses to noxious heat. These effects are consistent with behavioural experiments showing that intrathecal NKA was pro-nociceptive (Hylden & Wilcox, 1981; Cridland & Henry, 1986). The lack of effect of SP on nociceptive responses may be for the same reasons as its lesser effect on NMDA responses as discussed above. The absence of effect of NKB on nociceptive responses again correlates with its lack of effect on NMDA responses.

Conclusions

Agonists selective for the NK receptor sub-types are capable of modulating responses to EAAs differentially. Endogenous NKs appear to mediate their effects via more than one type of NK receptor, and possibly via other non-neurokinin mechanisms as well. Release of endogenous tachykinins may alter the balance of NMDA *vs.* AMPA/kainate receptor mediated transmission. Thus SP/NKA may shift glutamatergic transmission towards NMDA receptors, and this could selectively promote nociceptive responses. Conversely, endogenously released NKB may promote neurotransmission via AMPA/kainate receptors. The physiological relevance of the endogenous modulations of EAA responses and of glutamatergic neurotransmission can only be elucidated with selective NK antagonists. Such studies have been reported previously in brief (Chizh *et al.*, 1994) and are described in more detail in the following paper (Chizh *et al.*, 1995).

We thank the MRC, the Wellcome Trust and Glaxo Research and Development Ltd for financial support, Dr P.J. Birch, Glaxo, for the gift of neurokinin compounds and Mr Ivor Norman for technical assistance.

References

BLEAZARD, L., HILL, R.G. & MORRIS, R. (1994). A comparison of the distribution of NK-1 receptors in the dorsal horn of the spinal cord with that of neurones responsive to agonists acting at this receptor, in the rat. *J. Physiol.*, **476**, C42.

BROWN, J.L., JASMIN, L., MANTYH, P., VIGNA, S. & BASBAUM, A.I. (1993). Immunocytochemical localization of the NK_1 receptor in the spinal cord and brain of the rat. *Proc. IASP*, **7**, Abst 1270.

BUDAI, D., WILCOX, G.L. & LARSON, A.A. (1992). Modulation of N-methyl-D-aspartate and (RS)-α-amino-3-hydroxy-5-methylisoxazole-4-propionic acid (AMPA) responses of spinal nociceptive neurons by a N-terminal fragment of substance P. *Eur. J. Pharmacol.*, **216**, 441–444.

CHIZH, B.A., CUMBERBATCH, M.J., BIRCH, P.J. & HEADLEY, P.M. (1994). Neurokinins released tonically in the spinal cord of anaesthetized rats modulate excitatory amino acid efficacy. *Br. J. Pharmacol.*, **112**, 609P.

CHIZH, B.A., CUMBERBATCH, M.J., BIRCH, P.J. & HEADLEY, P.M. (1995). Tonic modulation of excitatory amino acid responses by tachykinin NK_1 and NK_2 receptors in the rat spinal cord. *Br. J. Pharmacol.*, **115**, 1013–1019.

CRIDLAND, R.A. & HENRY, J.L. (1986). Comparison of the effects of substance P, neurokinin A, physalaemin and eledoisin in facilitating a nociceptive reflex in the rat. *Brain Res.*, **381**, 93–99.

CUMBERBATCH, M.J., CHIZH, B.A., BIRCH, P.J. & HEADLEY, P.M. (1994a). Interactions between selective agonists of neurokinin NK_1 and NK_2 and excitatory amino acid receptors in the anaesthetized rat. *J. Physiol.*, **476**, 44P.

CUMBERBATCH, M.J., CHIZH, B.A. & HEADLEY, P.M. (1994b). AMPA receptors have an equal role in spinal nociceptive and non-nociceptive transmission. *NeuroReport*, **5**, 877–880.

CURTIS, D.R. & WATKINS, J.C. (1960). The excitation and depression of spinal neurones by structurally related amino acids. *J. Neurochem.*, **6**, 117–141.

DALSGAARD, C.-J., HAEGERTSTRAND, A., THEODORSSON-NORHEIM, E., BRODIN, E. & HOKFELT, T. (1985). Neurokinin A–like immunoreactivity in rat primary sensory neurones; coexistence with substance P. *Histochem.*, **83**, 37–39.

DE BIASI, S. & RUSTIONI, A. (1988). Glutamate and substance P coexist in primary afferent terminals in the superficial laminae of spinal cord. *Proc. Natl. Acad. Sci. U.S.A.*, **85**, 7820–7824.

DOUGHERTY, P.M., PALECEK, J., PALECKOVA, V., SORKIN, L.S. & WILLIS, W.D. (1992). The role of NMDA and non-NMDA excitatory amino acid receptors in the excitation of primate spinothalamic tract neurones by mechanical, chemical, thermal and electrical stimuli. *J. Neurosci.*, **12**, 3025–3041.

DOUGHERTY, P.M. & WILLIS, W.D. (1990). Long-lasting enhancement of excitability of spinothalamic neurones following combined application of excitatory amino acids and substance P in anaesthetized macaques. *J. Physiol.*, **425**, 38P.

DOUGHERTY, P.M. & WILLIS, W.D. (1991). Enhancement of spinothalamic neuron responses to chemical and mechanical stimuli following combined micro-iontophoretic application of *N*-methyl-D-aspartic acid and substance P. *Pain*, **47**, 85–93.

DUGGAN, A.W., HENDRY, I.A., MORTON, C.R., HUTCHISON, W.D. & ZHAO, Z.Q. (1988). Cutaneous stimuli releasing immunoreactive substance P in the dorsal horn of the cat. *Brain Res.*, **451**, 261–273.

DUGGAN, A.W., HOPE, P.J., JARROTT, B., SCHAIBLE, H.G. & FLEETWOOD-WALKER, S.M. (1990). Release, spread and persistence of immunoreactive neurokinin A in the dorsal horn of the cat following noxious cutaneous stimulation. Studies with antibody microprobes. *Neurosci.*, **35**, 195–202.

DUGGAN, A.W., SCHAIBLE, H.G., HOPE, P.J. & LANG, C.W. (1992). Effect of peptidase inhibition on the pattern of intraspinally released immunoreactive substance P detected with antibody microprobes. *Brain Res.*, **579**, 261–269.

FISHER, N.D., BARANAUSKAS, G. & NISTRI, A. (1994). Multiple types of tachykinin receptor mediate a slow excitation of rat spinal motoneurones *in vitro*. *Neurosci. Lett.*, **165**, 84–88.

FLEETWOOD-WALKER, S.M., MITCHELL, R., HOPE, P.J., EL-YASSIR, N., MOLONY, V. & BLADON, C.M. (1990). The involvement of neurokinin receptor subtypes in somatosensory processing in the superficial dorsal horn of the cat. *Brain Res.*, **519**, 169–182.

FLEETWOOD-WALKER, S.M., PARKER, R.M.C., MUNRO, F.E., YOUNG, R.Y., HOPE, P.J. & MITCHELL, R. (1993). Evidence for a role of tachykinin NK2 receptors in mediating brief nociceptive inputs to rat dorsal horn (laminae III-V) neurons. *Eur. J. Pharmacol.*, **242**, 173–181.

HAGAN, R.M., IRELAND, S.J., JORDAN, C.C., BERESFORD, I.J.M., DEAL, M.J. & WARD, P. (1991). Receptor-selective, peptidase resistant agonists at neurokinin NK_1 and NK_2 receptors: new tools for investigating neurokinin function. *Neuropept.*, **19,** 127–135.

HEADLEY, P.M. & GRILLNER, S. (1990). Excitatory amino acids and synaptic transmission: the evidence for a physiological function. *Trends Pharmacol. Sci.*, **11,** 205–211.

HENRY, J.L., KRNJEVIC, K. & MORRIS, M.E. (1975). Substance P and spinal neurones. *Can. J. Physiol. Pharmacol.*, **53,** 423–432.

HOOPER, N.M., KENNY, A.J. & TURNER, A.J. (1985). Neurokinin A (substance K) is a substrate for endopeptidase-24.11 but not for peptidyl dipeptidase A (angiotensin-converting enzyme). *Biochem. J.*, **231,** 356–361.

HYLDEN, J.L.K. & WILCOX, G.L. (1981). Intrathecal substance P elicits a caudally-directed biting and scratching behaviour in mice. *Brain Res.*, **217,** 212–215.

KANGRGA, I., LAREW, J.S.A. & RANDIC, M. (1990). The effects of substance P and calcitonin gene-related peptide on the efflux of endogenous glutamate and aspartate from the spinal dorsal horn *in vitro*. *Neurosci. Lett.*, **108,** 155–160.

KONISHI, S. & OTSUKA, M. (1974). Excitatory action of hypothalamic substance P on spinal motoneurones of newborn rats. *Nature*, **252,** 734–735.

LARSON, A.A. & SUN, X. (1992). Amino terminus of substance P potentiates kainic acid-induced activity in the mouse spinal cord. *J. Neurosci.*, **12,** 4905–4910.

LIU, H., BROWN, J.L., JASMIN, L., MAGGIO, J.E., VIGNA, S.R., MANTYH, P.W. & BASBAUM, A.I. (1994). Synaptic relationship between substance P and the substance P receptor: light and electron microscopic characterization of the mismatch between neuropeptides and their receptors. *Proc. Natl. Acad. Sci. U.S.A.*, **91,** 1009–1013.

MANTYH, P.W., GATES, T., MANTYH, C.R. & MAGGIO, J.E. (1989). Autoradiographic localization and characterization of tachykinin receptor binding sites in the rat brain and peripheral tissues. *J. Neurosci.*, **9,** 258–279.

MELLER, S.T. & GEBHART, G.F. (1993). Nitric oxide (NO) and nociceptive processing in the spinal cord. *Pain*, **52,** 127–136.

MERIGHI, A., POLAK, J.M. & THEODOSIS, D.T. (1991). Ultrastructural visualization of glutamate and aspartate immunoreactivities in the rat dorsal horn, with respect to the colocalization of glutamate, substance P and calcitonin-gene related peptide. *Neurosci.*, **40,** 67–80.

MOUSSAOUI, S.M., LE PRADO, N., BONICI, B., FAUCHER, D.C., CUINE, F., LADURON, P.M. & GARRET, C. (1992). Distribution of neurokinin B in rat spinal cord and peripheral tissues: comparison with neurokinin A and substance P and effects of neonatal capsaicin treatment. *Neurosci.*, **48,** 969–978.

MURASE, K., RYU, P.D. & RANDIC, M. (1989). Excitatory and inhibitory amino acids and peptide-induced responses in acutely isolated rat spinal dorsal horn neurons. *Neurosci. Lett.*, **103,** 56–63.

OGAWA, T., KANAZAWA, I. & KIMURA, S. (1985). Regional distribution of substance P, neurokinin-A and neurokinin-B in rat spinal cord, nerve roots and dorsal root ganglia, and the effects of dorsal root section or spinal transection. *Brain. Res.*, **359,** 152–157.

PAPIR-KRICHELI, D., FREY, J., LAUFER, R., GILON, C., CHOREV, M., SELINGER, Z. & DEVOR, M. (1987). Behavioural effects of receptor-specific substance P agonists. *Pain*, **31,** 263–276.

PARSONS, A.M., EL-FAKAHANY, E.E. & SEYBOLD, V.S. (1993). Tachykinin-induced formation of inositol phosphates in primary cultures of rat neonatal spinal neurons. *Soc. Neurosci. Abst.*, **19,** 298.11.

PICARD, P., BOUCHER, S., REGOLI, D., GITTER, B., HOWBERT, J.J. & COUTURE, R. (1993). Use of non-peptide tachykinin receptor antagonists to substantiate the involvement of NK_1 and NK_2 receptors in a spinal nociceptive reflex in the rat. *Eur. J. Pharmacol.*, **232,** 255–261.

RANDIC, M., HECIMOVIC, H. & RYU, P.D. (1990). Substance P modulates glutamate-induced currents in acutely isolated rat spinal dorsal horn neurones. *Neurosci. Lett.*, **117,** 74–80.

RUSIN, K.I., BLEAKMAN, D., CHARD, P.S., RANDIC, M. & MILLER, R.J. (1993). Tachykinins potentiate *N*-methyl-D-aspartate responses in acutely isolated neurons from the dorsal horn. *J. Neurochem.*, **60,** 952–960.

RUSIN, K.I., RYU, P.D. & RANDIC, M. (1992). Modulation of excitatory amino acid responses in rat dorsal horn neurons by tachykinins. *J. Neurophysiol.*, **68,** 265–286.

SKILLING, S.R., SMULLIN, D.H., BEITZ, A.J. & LARSON, A.A. (1988). Extracellular amino acid concentrations in the dorsal spinal cord of freely moving rats following veratridine and nociceptive stimulation. *J. Neurochem.*, **51,** 127–132.

THEODORSSON-NORHEIM, E., HEMSÉN, A., BRODIN, E. & LUNDBERG, J.M. (1987). Sample handling techniques when analyzing regulatory peptides. *Life Sci.*, **41,** 845–848.

TOO, H.P. & MAGGIO, J.E. (1991). Immunocytochemical localization of neuromedin K (neurokinin B) in rat spinal ganglia and cord. *Peptides*, **12,** 431–443.

TRAYNELIS, S.F. & CULL-CANDY, S.G. (1991). Pharmacological properties and H^+ sensitivity of excitatory amino acid receptor channels in rat cerebellar granule neurones. *J. Physiol.*, **433,** 727–763.

VYKLICKÝ, L., VLACHOVÁ, A. & KRUSEK, J. (1990). The effect of external pH changes on responses to excitatory amino acids in mouse hippocampal neurones. *J. Physiol.*, **430,** 497–517.

WOMACK, M.D., MACDERMOTT, A.B. & JESSELL, T.M. (1988). Sensory transmitters regulate intracellular calcium in dorsal horn neurons. *Nature*, **334,** 351–353.

YASHPAL, K., DAM, T.V. & QUIRION, R. (1988). Autoradiographic localization of neurokinin receptors in rat spinal cord. *Regul. Pept.*, **22,** 191.

(Received July 22, 1994
Revised March 22, 1995
Accepted April 6, 1995)

British Journal of Pharmacology (1995) 115, 1013–1019 © 1995 Stockton Press All rights reserved 0007–1188/95 $12.00

Endogenous modulation of excitatory amino acid responsiveness by tachykinin NK_1 and NK_2 receptors in the rat spinal cord

*Boris A. Chizh, [1]Michael J. Cumberbatch, †Philip J. Birch & [2]P. Max Headley

Department of Physiology, University of Bristol, School of Medical Sciences, University Walk, Bristol, BS8 1TD; *Department of Pharmacology, Moscow Sechenov Medical Academy, 2/6 B. Pirogovskaya St., Moscow 119881, Russia and †Pharmacology 1, Glaxo Research and Development Ltd., Park Road, Ware, Hertfordshire SG12 0DP

1 The effects of selective tachykinin (neurokinin, NK) NK_1 and NK_2 receptor antagonists have been examined on spinal neurones in α-chloralose anaesthetized, spinalized rats. They were tested for effects on responses both to excitatory amino acids (EAA) and to noxious heat stimuli. They were also tested for their ability to reverse the actions of selective NK agonists.

2 The NK_1-selective antagonists GR82334 (peptide) and CP-99,994 (non-peptide), when applied by microiontophoresis, both reduced responses to kainate > AMPA > NMDA. Intravenous CP-99,994 (3 mg kg^{-1}) also reduced responses to kainate but had inconsistent effects on nociceptive responses.

3 GR82334, applied microiontophoretically, reduced the enhancement by the selective NK_1 agonist, GR73632 of both responses to EAAs and background activity. Systemic CP-99,994 ($\leqslant$10 mg kg^{-1}) failed to reverse the effects of GR73632.

4 The selective peptide NK_2 antagonist, GR103537, had no consistent effects on responses to EAAs when applied by iontophoresis. In contrast, the non-peptide NK_2 antagonist, GR159897, administered systemically (0.5–2 mg kg^{-1}, i.v.) enhanced responses to kainate (but not NMDA); responses to noxious heat were enhanced only weakly.

5 Iontophoretically-administered GR103537 attenuated the effects of the NK_2 agonist GR64349, which selectively reduced responses to kainate compared to those to NMDA. Systemically administered GR159897 ($\leqslant$2 mg kg^{-1}, i.v.) caused little antagonism of the effects of GR64349.

6 The data indicate that under these conditions the non-peptide antagonists are not reliable at reversing the actions of selective NK agonists.

7 These results suggest that there is a tonic release of endogenous tachykinins that can modulate glutamatergic neurotransmission in the spinal cord. They provide further support for the hypothesis that release of endogenous NKs acting on NK_1 and NK_2 receptors can promote NMDA receptor mediated glutamatergic transmission.

Keywords: Excitatory amino acids; peptide tachykinin receptor antagonist; non-peptide tachykinin receptor antagonist; NK_1 receptors; NK_2 receptors; spinal cord; dorsal horn

Introduction

Substance P (SP) and neurokinin A (NKA) are tachykinins (or neurokinins, NKs) that are found in the nerve terminals of primary afferent fibres in the dorsal horn (Dalsgaard *et al.*, 1985), many of which also contain the excitatory amino acids (EAAs) glutamate or aspartate (De Biasi & Rustioni, 1988; Merighi *et al.*, 1991). Both these NKs as well as EAAs can be released following noxious peripheral stimulation (Duggan *et al.*, 1988; 1990; Skilling *et al.*, 1988) and there is considerable evidence for an interaction between the two neurotransmitter systems. SP and NKA selectively enhanced responses to N-methyl-D-aspartate (NMDA) in isolated dorsal horn neurones (Rusin *et al.*, 1992). However, SP has also been shown to enhance responses to α-amino-3-hydroxy-5-methyl-4-isoxazole propionate (AMPA), quisqualate and kainate to varying degrees when tested *in vivo* (Dougherty & Willis, 1990; 1991; Mjellem-Joly *et al.*, 1991). More recently we have shown that agonists that are selective for the NK receptor sub-types produce distinct and consistent effects on EAA responses; the naturally occurring tachykinins SP, NKA and NKB, which are less selective, had mixed NK receptor-mediated effects (see preceding paper, Cumberbatch *et al.*, 1995). Since these experiments involved exogenous application of agonists, it is difficult to interpret the physiological role of such NK-EAA interactions. It is necessary to examine the effects of NK antagonists on EAA and synaptic responses to assess the level of endogenous modulation.

Combined application of sub-threshold doses of NK and EAA antagonists have been reported to reduce wind-up and reflex facilitation in rats (Xu *et al.*, 1992) and responses in the formalin test in mice (Seguin & Millan, 1994). Furthermore, behavioural studies have shown that selective NK_1 antagonists blocked the pro-nociceptive effects of intrathecal EAAs (Mjellem-Joly *et al.*, 1991). However, since intrathecal application of EAAs is likely to excite a high proportion of neurones in the dorsal horn, many of the effects observed may have been via a secondary release of other endogenous neurotransmitters.

The present study was therefore designed to test for modulation of the responses of spinal neurones to NMDA, AMPA, kainate and noxious heat by endogenously released NKs, and to determine the relative roles of NK_1 and NK_2 receptors in this process. Some of the data have been published previously in abstract form (Chizh *et al.*, 1994).

Methods

Experiments were performed on 31 α-chloralose anaesthetized, spinalized male rats. The methods used for anaethesia, animal preparation, electrophysiological recording and data analysis have been described fully in the preceding papter (Cumberbatch *et al.*, 1995). The solutions used for the iontophoretic

[1] Present address: Merck Sharp & Dohme Research Labortatories, Neuroscience Research Centre, Terlings Park, Harlow, Essex CM20 2QR.
[2] Author for correspondence.

administration of EAA and NK agonists were also given. In the present study the following NK antagonist drugs were also used: the peptide NK_1 antagonist GR82334 (Hagan *et al.*, 1991); the non-peptide NK_1 antagonist CP-99,994 (McLean *et al.*, 1993); the peptide NK_2 antagonist GR103537 (Hagan *et al.*, 1993); and the non-peptide NK_2 antagonist GR159897 (Ball *et al.*, 1994). Details of structures and of the solutions used for microiontophoresis are shown in Table 1.

Mean iontophoretic ejection currents used to elicit similar amplitude and sub-maximal EAA responses were NMDA 27 nA, AMPA 12 nA, kainate 21 nA. Iontophoretic administrations of GR159897 were abandoned because of excessive effects on spike configuration. Nociceptive responses were not tested with iontophoretic administrations of NK antagonists because of the uncertainty of drug distribution to the relevant synapses. In some experiments the NK antagonists were tested upon the responses to iontophoretically applied NK_1 or NK_2 selective agonists; in these experiments the agonist was tested once in the absence of antagonist, and, following recovery, again during concurrent ejection of the antagonist.

For the tests with the non-peptide NK antagonists administered systemically, cells were also activated by noxious heat stimuli (45.2–49.9°C) applied to the hind paw receptive field with a contact heat device. Dose-ranges used were CP-99,994 1–3 mg kg^{-1}, and GR159897 0.5–2 mg kg^{-1}, i.v. In tests of the ability of these systemic antagonists to reverse the actions of NK agonists, the agonists were tested immediately after the last cumulative dose of i.v. antagonist.

Data are shown as means ± s.e.mean. Statistical analysis was performed using either the Wilcoxon matched pairs test or the Mann-Whitney U-test. A probability level of <0.05 was assumed to be significant.

Results

Forty five cells were examined in the dorsal horn of the spinal cord (depth from pial surface 360–1360 μm).

Effects of NK_1 receptor antagonists GR82334 and CP-99,994 on EAA and nociceptive responses

The peptide NK_1 antagonist, GR82334, was tested by iontophoresis (10–40 nA, mean 15 nA) with 16 cells from the dorsal horn (11 wide dynamic range (WDR), 3 low threshold mechanoreceptive (LTMR), 1 proprioceptive and 1 with no detectable receptive field). It was ejected during ongoing cycles of matched and submaximal responses to the selective EAA agonists NMDA, AMPA and kainate. Figure 1a illustrates the effects of this NK_1 antagonist on the responses of a single dorsal horn neurone; responses to all three EAAs were reduced, with those to kainate being most affected. The pooled data (Figure 1c) show that this greater reduction of responses to kainate was consistent; the order of reduction was kainate > AMPA > NMDA. The EAA responses recovered fully and approximately in parallel; for kainate the mean time to half recovery ($t_{\frac{1}{2}}$) was 6 min, with a range of 3–22 min. Background activity was not affected by GR82334; the mean spontaneous activity was 1.6 ± 1.5 spikes s^{-1} during control and 1.8 ± 1.5 spikes s^{-1} during ejection of GR82334.

The non-peptide NK_1 antagonist, CP-99,994, was tested by iontophoresis (10–20 nA, mean 11 nA) on 8 cells (7 WDR, 1 LTMR) and had effects very similar to those of GR82334. The example of Figure 1b is on the same cell as the GR82334 test of Figure 1a. These effects of CP-99,994 were consistent, with the order of reduction again being kainate > AMPA > NMDA (Figure 1c). As with GR82334, background activity was not affected by CP-99,994; mean values were 2.8 ± 2.7 spikes s^{-1} during the control period and 2.7 ± 2.5 spikes s^{-1} in the presence of CP-99,994. The $t_{\frac{1}{2}}$ recovery was 3–8 min.

CP-99,994 was also tested systemically (1–3 mg kg^{-1}, i.v.) on 10 cells (9 WDR, 1 high threshold mechanoreceptive; HTMR). Even high doses had only small effects, reducing responses to kainate at 3 mg kg^{-1} (to 85 ± 7% control; $P<0.05$) without affecting responses to NMDA (93 ± 7% control). It was not tested on responses to AMPA. Background activity was reduced slightly (from 3.1 ± 1.1 to 2.0 ± 0.7 spikes s^{-1}) but this was not significant. CP-99,994 was also tested on responses to noxious heat with 7 cells, but these responses were affected very variably (108 ± 17% control; range 52–190% control). The variability could not be correlated with receptive field properties or cell location.

Tests were also performed to assess the ability of the these NK_1 antagonists to reverse the actions of the selective NK_1 agonist, GR73632, which enhanced EAA responses non-selectively (Figure 2; see also preceding paper, Cumberbatch *et al.*, 1995). GR82334 blocked or attenuated this action of GR73632, as is shown for a single cell in Figure 2. Figure 2a shows the direct excitation and enhancement of EAA responses by GR73632 and Figure 2b shows that this effect was attenuated following pretreatment with an 8 min ejection of the antagonist. Note that the GR73632 ejection was twice as long as during the control test. This effect of the antagonist was consistent on 8 cells tested, as is shown in the pooled data of Figure 2c. Similar tests were attempted with CP-99,994, but were abandoned because the higher ejection currents required caused excessive attenuation of spikes.

To control for the possibility that the effects of GR82334 on EAA were due to antagonism of GR73632 that was leaking out of the micropipette (thereby enhancing EAA responses), GR73632 was excluded from the electrodes with 7 cells. GR82334 had the same effect on these cells as on those tested when GR73632 was in the pipette: responses to kainate were reduced to 26 ± 6% control, those to AMPA to 52 ± 6%, and those to NMDA to 74 ± 6% (all $P<0.05$ *vs.* control).

CP-99,994 was examined by systemic administration for its ability to antagonize the effects of GR73632. At the very high doses of 3–10 mg kg^{-1} ($n=5$) it did not antagonize the effects of GR73632, whether on background activity or on EAA enhancements.

Effects of the NK_2 receptor antagonists GR103537 and GR159897 on EAA and nociceptive responses

The peptide NK_2 antagonist GR103537 was tested by iontophoretic ejection (5–40 nA, mean 21 nA) upon responses to

Table 1 Structures of the neurokinin (NK) antagonists and solutions used for microiontophoresis

Drug	*Receptor*	*(mM)*	*pH*	*Ejected as*	*Full name*
GR82334	NK_1	1/50	4.5–5.0	cation	Trp-Leu-SLac-D-Pro-Asn-Lys-Phe-Tyr-Gly-Leu-Met.NH_2
CP-99,994	NK_1	20/20	4.5–5.0	cation	(+)-(2S,3S)-3-(2-methoxybenzylamino)-2-phenylpiperidine
GR103537	NK_2	1/50	4.5–5.0	cation	CyCO-Gly-Ala-D-Trp-PheRNMe_2
GR159897	NK_2	20/20	4.5–5.0	cation	(**R**)-1-[2-(5-fluoro-1H-indol-3-yl)ethyl]-4-methoxy-4-[(phenylsulphinyl) methyl]-piperidine

mM refers to the concentration of the NK in either 20 mM or 50 mM saline. Equivalent data for the NK and excitatory amino acid agonists used in this study are given in Table 1 of Cumberbatch *et al.*, 1995.

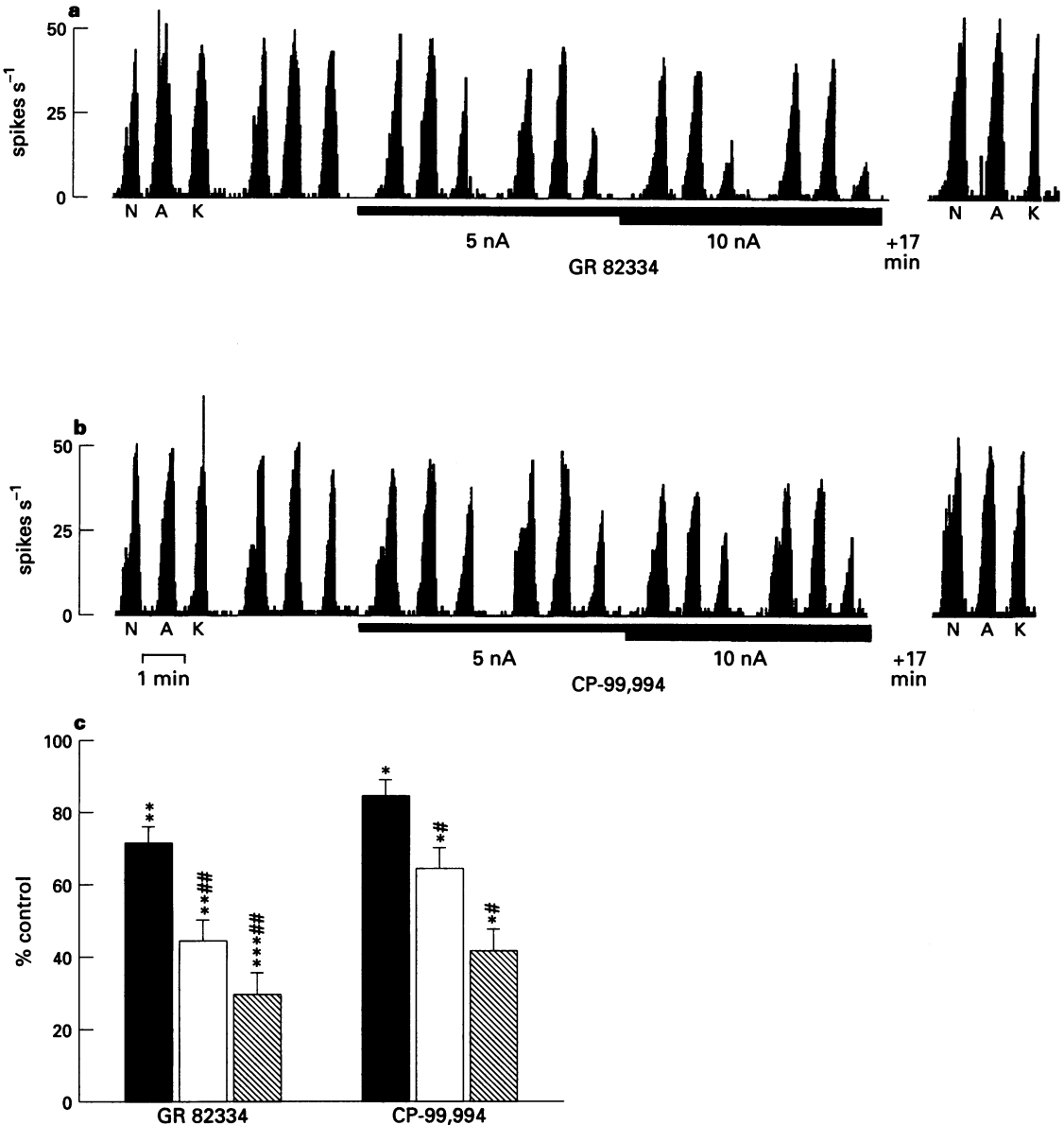

Figure 1 Microiontophoretic tests of the effects of two tachykinin NK_1 receptor antagonists, GR82334 and CP-99,994, on responses to the excitatory amino acids NMDA (N), AMPA (A) and kainate (K) on spinal neurones of α-chloralose anaesthetized, spinalized rats. (a) Original record of the effect of GR82334 on a single neurone. (b) Action of CP-99,994 on the same unit. (c) Pooled data of the actions of GR82334 ($n=11$) and CP-99,994 ($n=7$) on responses to NMDA (solid columns), AMPA (open columns) and kainate (hatched columns). Data are expressed as a percentage of the mean (with s.e.mean) of 3 pre-drug control responses. A significant difference from control is indicated by $*P<0.05$, $**P<0.01$, $***P<0.005$. A significant difference between the effects on AMPA/kainate *vs.* NMDA responses is indicated by $\#P<0.05$, $\#\#P<0.01$.

EAAs with 11 cells (6 WDR, 2 LTMR and 3 with no detectable receptive field). The effects were variable, with either increases or decreases of responses to all three EAAs; the pooled data show little change (Figure 3b). Background activity remained unchanged; mean values were 2.7 ± 1.9 spikes s^{-1} during the control period compared to 3.0 ± 2.2 spikes s^{-1} in the presence of GR103537.

The non-peptide NK_2 receptor antagonist, GR159897, was tested by i.v. administration (0.5–2 mg kg^{-1}) on 9 neurones (8 WDR, 1 with no receptive field) from the dorsal horn. Responses to kainate were selectively enhanced in a dose-dependent fashion, whilst responses to NMDA remained unchanged. An example on a single neurone is shown in Figure 3a, whilst the pooled data of Figure 3b demonstrate that this effect was consistent and reached significance at 2 mg kg^{-1} ($135\pm8\%$ control). Background activity remained unchanged, being 2.7 ± 1.1 spikes s^{-1} during the control period and 2.8 ± 1.2 spikes s^{-1} after 2 mg kg^{-1} GR159897. Responses to noxious heat were tested with 6 cells. Responses were increased by the 2 mg kg^{-1} dose with 5 cells (to a mean $138\pm21\%$ control, not significant; range 111–222%) but were depressed in the other cell (to 29% control) giving a mean non-significant increase for all 6 cells of $120\pm25\%$ control. EAA responses remained enhanced until the end of the experiment (up to 1 h after the last dose). This is presumably due to slow metabolism of this drug; the $t_{\frac{1}{2}}$ recovery was approximately 90 min in the guinea-pig (Ball *et al.*, 1994).

The NK_2 antagonists were examined over the same dose-range for their ability to antagonize the actions of the NK_2 agonist, GR64349. This agonist consistently reduced responses

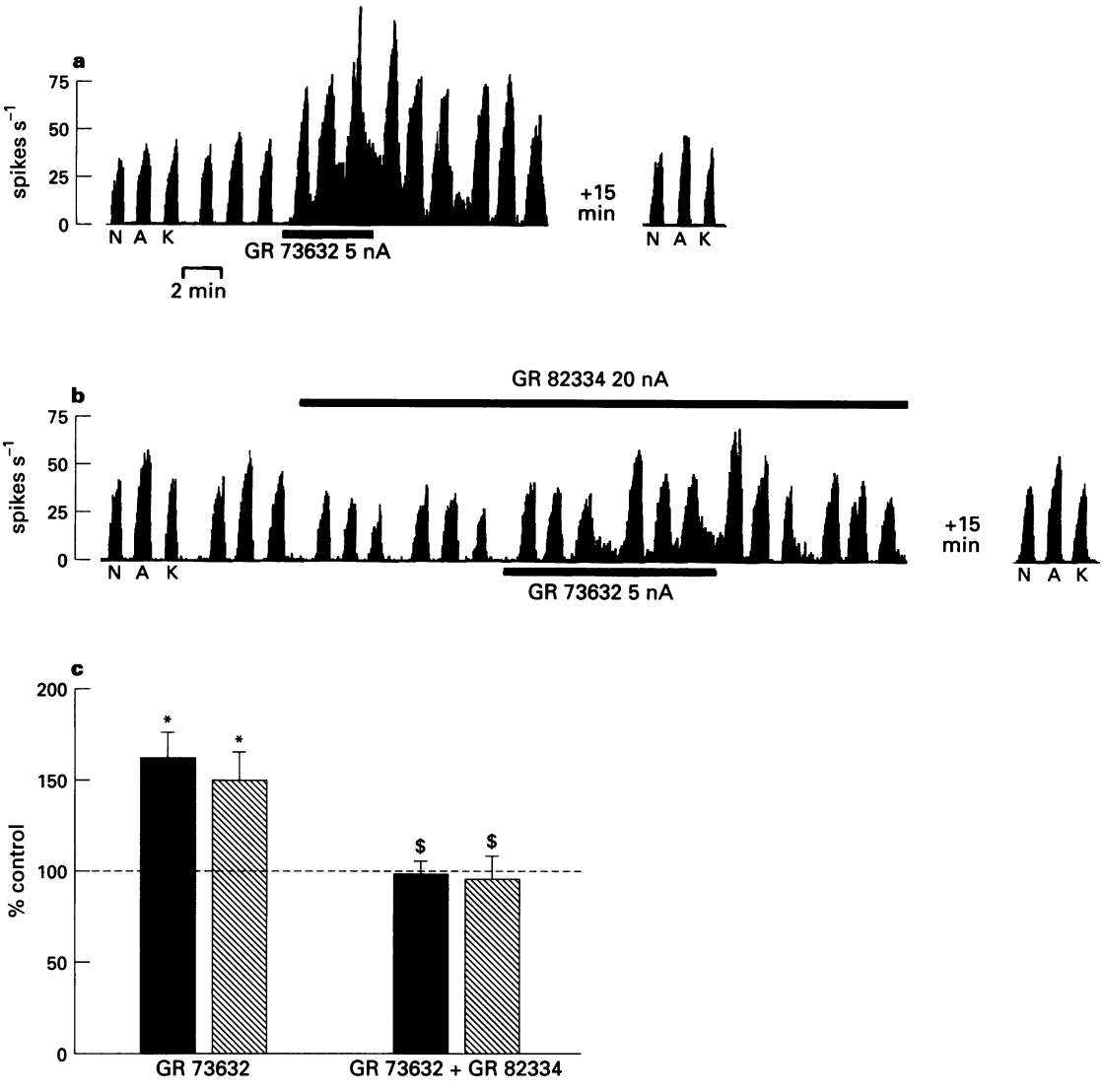

Figure 2 (a) The effects of the NK_1 agonist, GR73632, on the background discharge and on responses to NMDA (N), AMPA (A) and kainate (K) of a dorsal horn neurone. (b) Following recovery, a second ejection of GR73632 was made in the presence of the NK_1 antagonist, GR82334. Note that GR82334 ejection started 7 min before GR73632, and that the agonist ejection was twice as long as in (a). (c) Pooled data for the effects of the agonist on responses to NMDA (solid columns) and kainate (hatched columns) in the absence (left) and presence (right) of GR82334 ($n=8$). Control refers to the last three cycles prior to the first ejection of GR73632. A significant effect of the NK_1 agonist *vs.* control is shown by $^*P<0.05$; a significant difference from this effect in the presence of the antagonist is indicated by $\$P<0.05$.

to AMPA and kainate but not NMDA (Figure 4a; see also Cumberbatch *et al.*, 1995). The peptide antagonist GR103537 reduced the actions of GR64349 when tested by iontophoresis on 3 neurones. In the example of Figure 4a GR64349 depressed responses to kainate but not to NMDA and this effect was blocked following 7 min pretreatment with GR103537 (Figure 4b). In contrast, the non-peptide antagonist GR159897 administered systemically (0.5–2 mg kg^{-1} i.v., $n=7$) only weakly reversed the actions of GR64349 on EAA responses; kainate responses were 49±3% control with GR64349 alone and 64±7% control following the administration of GR159897 2 mg kg^{-1} (not significantly different).

Discussion

Effectiveness of antagonists at reversing agonist actions

In the preceding paper (Cumberbatch *et al.*, 1995) we showed that NK agonists had selective actions on responses to EAA. NK_1 agonists enhanced EAA responses non-selectively, NK_2 agonists reduced kainate and AMPA but not NMDA responses and NK_3 agonists increased responses to AMPA and kainate. In the present study we have tested the ability of peptide and non-peptide NK_1 and NK_2 antagonists to reverse these actions. NK_3 antagonists were not tested as there was none suitable at the time these experiments were performed. The peptide antagonists GR82334 (NK_1) and GR103537 (NK_2) were effective when administered iontophoretically. The non-peptide antagonists, CP-99,994 and GR159897, could not be tested successfully by iontophoresis because the high ejection currents required altered spike configuration. When given intravenously, they had only weak antagonist actions, even at high doses.

The results indicate that under these conditions the non-peptide antagonists used are not entirely suitable, at the doses tested, for assessing actions of endogenously-released neurokinin agonists. CP-99,994 has been shown to have variable effects *in vivo* (McLean *et al.*, 1993; Jackson *et al.*, 1994) and the non-peptide NK_1 antagonists in general tend to have non-specific effects on neurotransmission (Wang *et al.*, 1994). Concerning GR159897, other reports (Ball *et al.*, 1994;

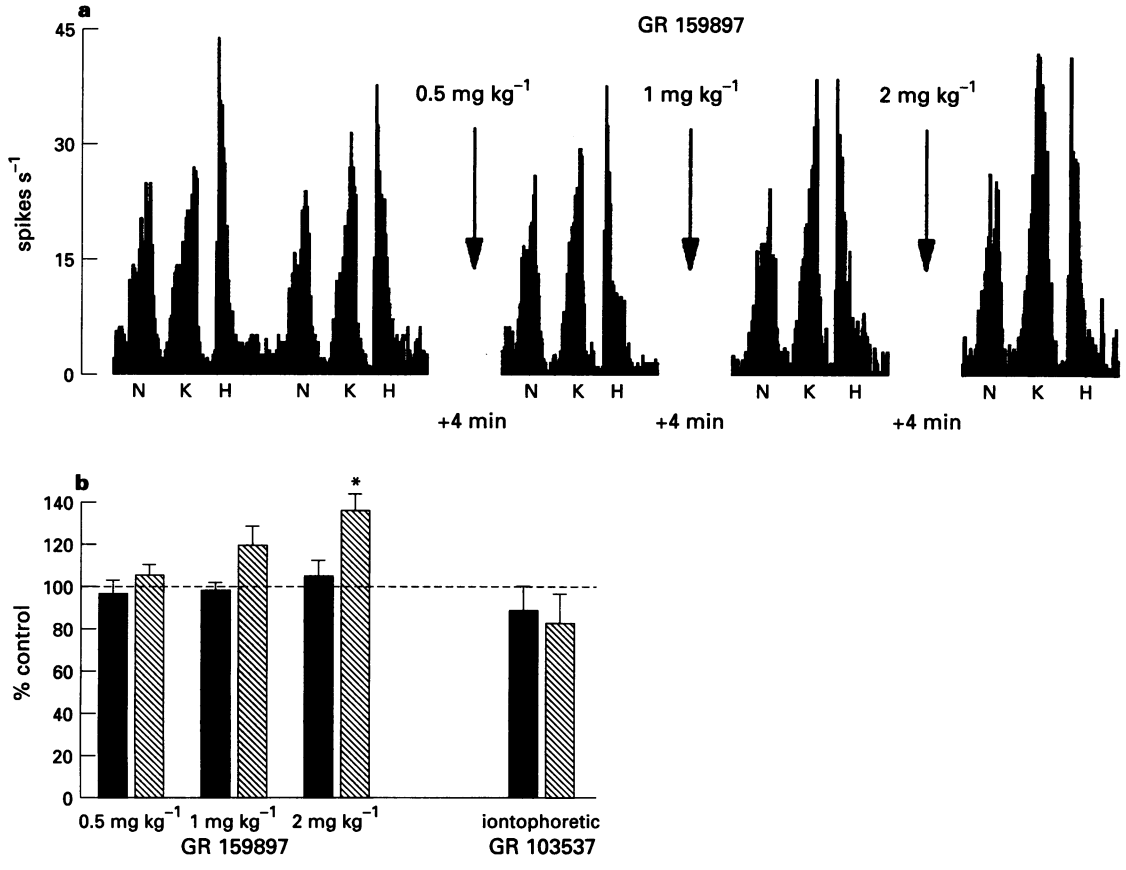

Figure 3 (a) Effects of cumulative intravenous doses of GR159897, a selective NK_2 receptor antagonist, on responses of a dorsal horn neurone to the excitatory amino acids NMDA (N) and kainate (K) and to noxious heat stimuli (H) applied to the receptive field on the paw. (b) Pooled data for the effects of the NK_2 antagonists, GR159897 and GR103537 on responses to NMDA (solid columns) and kainate (hatched columns). GR159897 was given intravenously (0.5 mg kg^{-1}, $n=6$; 1 mg kg^{-1}, $n=9$; 2 mg kg^{-1}, $n=7$). GR103537 was administered iontophoretically (5–40, mean 20 nA; $n=11$). A significant change from control is indicated by $^*P<0.05$.

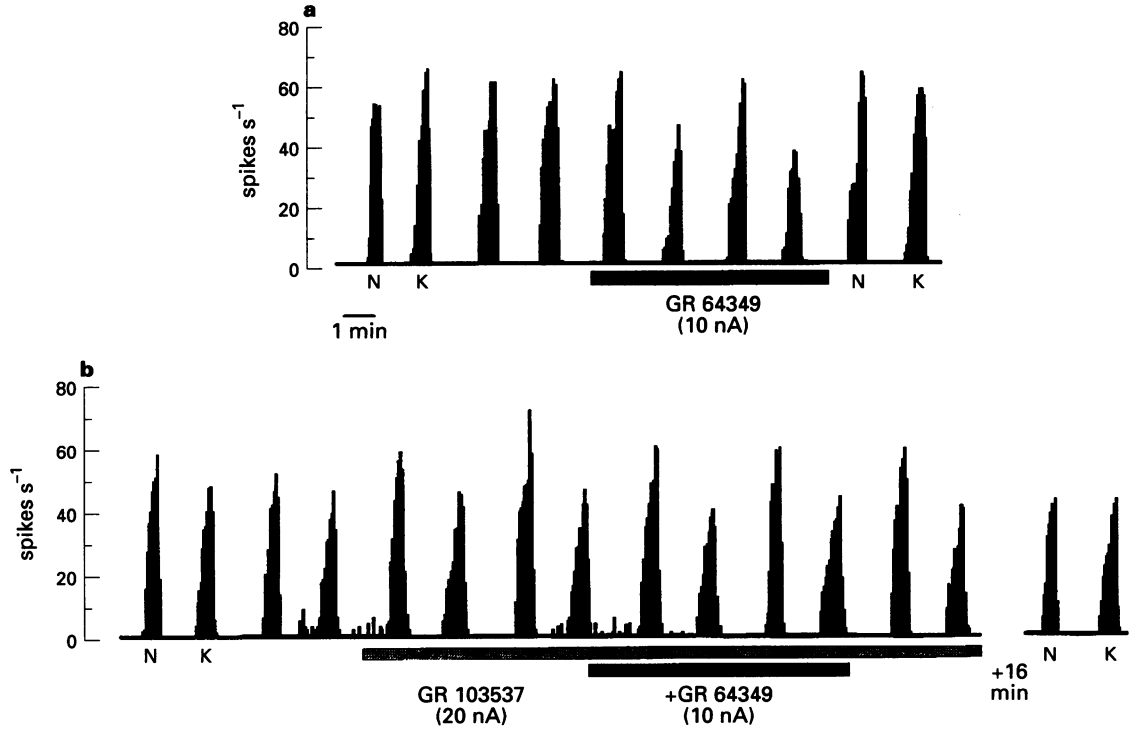

Figure 4 (a) Reduction by the NK_2 agonist, GR64349 of responses to kainate (K) but not NMDA (N) on a single spinal neurone. (b) Blockade of these effects, in a subsequent test on the same neurone, by iontophoretic co-ejection of the peptide NK_2 antagonist, GR103537.

Stratton *et al.*, 1994) do indicate that the systemic doses used in the present study should have been adequate for NK_2 antagonism. A likely explanation for the relative weakness of the systemically administered antagonists at reversing the effects of iontophoretically-administered NK agonists is that the focal concentrations of agonists are high relative to the (presumably lower and more uniform) concentration of systemically administered antagonists.

Actions of NK antagonists on responses to EAA

The NK_1 receptor antagonists reduced the responses to kainate > AMPA > NMDA when tested iontophoretically, and CP-99,994 reduced responses to kainate but not NMDA when tested i.v. The simplest explanation is that there was a tonic release of endogenous tachykinins that was facilitating the responses to EAA via an action at NK_1 receptors. Release of tachykinins in the dorsal horn under similar conditions has already been established (Duggan *et al.*, 1988; 1990). The effect was not an artefact due to leakage of GR73632 from the electrodes causing an artificial enhancement of the EAA responses, because when the agonist was omitted from the electrodes the two NK_1 antagonists were still effective. Since GR82334 and CP-99,994 are structurally quite different, and similar (albeit weak) effects were seen with systemic CP-99,994, the effects produced are unlikely to have been artefacts caused by non-NK receptor-mediated mechanisms (see also Cumberbatch *et al.*, 1995).

The NK_2 antagonist, GR159897, caused a small enhancement of kainate responses, an effect opposite to that of the NK_1 agonist, GR64349. This implies that there is also tonic release of endogenous tachykinin(s) acting at NK_2 receptors. The lack of effect of the peptide antagonist GR103537 on EAA responses is hard to explain.

The selective NK_1 agonist GR73632 caused a relatively non-selective enhancement of responses to all 3 EAAs (Cumberbatch *et al.*, 1995), whereas both NK_1 antagonists preferentially depressed responses to kainate. This implies that more than NK_1 receptor antagonism was occurring. Since the effects of the NK_1 antagonists were similar to those of the NK_2 agonist, GR64349 (compare Figures 1a and 4a) it is possible that the antagonism of the NK_1 mediated effects somehow altered the effectiveness of the tonic NK_2 receptor mediated component. There are two possible explanations. Firstly either the agonists or the antagonists may not be selective (but see Hagan *et al.*, 1991; McLean *et al.*, 1993). Secondly NK_1 receptors are more abundant in the dorsal horn than NK_2 receptors (Yashpal *et al.*, 1988; Mantyh *et al.*, 1989; Brown *et al.*, 1993; Bleazard *et al.*, 1994). Synaptically released SP and NKA (which are not particularly selective between NK_1 and NK_2 receptors) will therefore be more likely to act via the more abundant NK_1 receptors. Blocking this NK_1 effect could allow a weaker NK_2-mediated component to become more prominent. We consider this second possibility more likely.

These data therefore suggest a tonic release of tachykinins, and activation of NK_1 and NK_2 receptors, under these conditions. It is, however, possible that this does not reflect normal basal release. The surgery was distant from the receptive fields of the units studied, and there was no detectable inflammation within the receptive field, so that it is unlikely that NKs will have altered the synaptic input onto the neurones studied by peripheral mechanisms. The preparatory surgery is, however, likely to have enhanced general spinal excitability (see Hartell & Headley, 1991). By analogy with the finding that inflammation-induced spinal hyperexcitability can be blocked by NK antagonists (Birch *et al.*, 1992; Kellstein & Proffitt, 1992), it is likely that spinal release of tachykinins would be enhanced under the conditions of electrophysiological experiments such as these.

Relative lack of effectiveness of NK antagonists on synaptic transmission

Since the NK antagonists modulated EAA responses, one would predict that they would also modify synaptic transmission, whether spontaneous or evoked. Moreover both NK_1 and NK_2 agonists enhanced background activity (Cumberbatch *et al.*, 1995), and endogenously released tachykinins would be expected to have similar actions. The ineffectiveness of the NK antagonists at reducing background activity cannot be explained by a lack of tonic release of endogenous NKs, because EAA responses were clearly affected by the antagonists. It is therefore more likely that the NK antagonists did not reach sufficient concentrations at the active synapses to block transmission/modulation by endogenous NKs. This is entirely likely with iontophoretic applications, which cause only very focal concentrations close to the electrode, and which may therefore not reach the relevant synapses. Systemically administered NK antagonists, on the other hand, should achieve a uniform distribution. Nonetheless, neither i.v. CP-99,994 nor GR159897 significantly reduced background activity at the relatively high doses tested.

Iontophoretically-administered antagonists were not tested on nociceptive responses because of the technical limitations of access to the relevant synaptic sites. Systemically-administered antagonists were examined, but were relatively ineffective and/or inconsistent at altering nociceptive responses evoked by peripheral heat stimuli. CP-99,994 had extremely variable effects on nociceptive responses, with the mean effect being not significant; it was not possible to relate the variations to any experimental variable. GR159897 increased nociceptive responses with 5 of 6 units, consistent with its effect on EAA responses, but this effect did not reach statistical significance. These enhancements by GR159897 differ from the results of another study using NK_2 selective compounds, which indicated that spinal thermal nociceptive responses were depressed by NK_2 antagonists (Fleetwood-Walker *et al.*, 1993).

In conclusion, these data show that there is a tonic release of endogenous tachykinins under the conditions of these electrophysiological experiments. These tachykinins act via both NK_1 and NK_2 receptors to modulate neuronal responses to EAAs acting at kainate, AMPA and NMDA receptors, and these interactions are receptor specific. The data are consistent with the hypothesis, based on NK agonist action (Cumberbatch *et al.*, 1995), that NK_1 and NK_2 receptor activation by endogenous tachykinins will push glutamatergic neurotransmission towards NMDA receptor activity, an action that could promote nociception. Further experiments will be required to establish how this EAA modulation influences synaptic responses to nociceptive and non-nociceptive inputs, both in the normal state and during pathological conditions such as peripheral inflammation, when NK and EAA release may be enhanced.

We thank the MRC and the Wellcome Trust for financial support and Mr Ivor Norman for technical assistance.

References

BALL, D.I., BERESFORD, I.J.M., WREN, G.P.A., PENDRY, Y.D., SHELDRICK, R.L.G., WALSH, D.M., TURPIN, M.P. & HAGAN, R.M. (1994). *In vitro* and *in vivo* pharmacology of the non-peptide antagonist at tachykinin NK_2-receptors, GR159897. *Br. J. Pharmacol.*, **112**, 48P.

BIRCH, P.J., HARRISON, S.M., HAYES, A.G., ROGERS, H. & TYERS, M.B. (1992). The non-peptide NK_1 receptor antagonist, (±)-CP-96,345, produces antinociceptive and anti-oedema effects in the rat. *Br. J. Pharmacol.*, **105**, 508–510.

BLEAZARD, L., HILL, R.G. & MORRIS, R. (1994). A comparison of the distribution of NK_1 receptors in the dorsal horn of the spinal cord with that of neurones responsive to agonists acting at this receptor, in the rat. *J. Physiol.*, **476,** 43P.

BROWN, J.L., JASMIN, L., MANTYH, P., VIGNA, S. & BASBAUM, A.I. (1993). Immunocytochemical localization of the NK_1 receptor in the spinal cord and brain of the rat. *Proc. Int. Assn. Study Pain*, **7,** Abst. 1270.

CHIZH, B.A., CUMBERBATCH, M.J., BIRCH, P.J. & HEADLEY, P.M. (1994). Neurokinins released tonically in the spinal cord of anaesthetized rats modulate excitatory amino acid efficacy. *Br. J. Pharmacol.*, **112,** 609P.

CUMBERBATCH, M.J., CHIZH, B.A. & HEADLEY, R.M. (1995). Modulation of excitatory amino acid responses by tachykinins and selective tachykinin receptor agonists in the rat spinal cord. *Br. J. Pharmacol.*, **115,** 1005–1012.

DALSGAARD, C.-J., HAEGERTSTRAND, A., THEODORSSON-NORHEIM, E., BRODIN, E. & HÖKFELT, T. (1985). Neurokinin A-like immunoreactivity in rat primary sensory neurons; coexistence with substance P. *Histochem.*, **83,** 37–39.

DE BIASI, S. & RUSTIONI, A. (1988). Glutamate and substance P coexist in primary afferent terminals in the superficial laminae of spinal cord. *Proc. Natl. Acad. Sci. U.S.A.*, **85,** 7820–7824.

DOUGHERTY, P.M. & WILLIS, W.D. (1990). Long-lasting enhancement of excitability of spinothalamic tract neurones following combined application of excitatory amino acids and substance P in anaesthetized macaques. *J. Physiol.*, **425,** 38P.

DOUGHERTY, P.M. & WILLIS, W.D. (1991). Enhancement of spinothalamic neuron responses to chemical and mechanical stimuli following combined micro-iontophoretic application of *N*-methyl-D-aspartic acid and substance P. *Pain*, **47,** 85–93.

DUGGAN, A.W., HENDRY, I.A., MORTON, C.R., HUTCHISON, W.D. & ZHAO, Z.Q. (1988). Cutaneous stimuli releasing immunoreactive substance P in the dorsal horn of the cat. *Brain Res.*, **451,** 261–273.

DUGGAN, A.W., HOPE, P.J., JARROTT, B., SCHAIBLE, H.-G. & FLEETWOOD-WALKER, S.M. (1990). Release, spread and persistence of immunoreactive neurokinin A in the dorsal horn of the cat following noxious cutaneous stimulation. Studies with antibody microprobes. *Neuroscience*, **35,** 195–202.

FLEETWOOD-WALKER, S.M., PARKER, R.M.C., MUNRO, F.E., YOUNG, M.R., HOPE, P.J. & MITCHELL, R. (1993). Evidence for a role of tachykinin NK_2 receptors in mediating brief nociceptive inputs to rat dorsal horn (laminae III–V) neurons. *Eur. J. Pharmacol.*, **242,** 173–181.

HAGAN, R.M., BERESFORD, I.J.M., STABLES, J., DUPERE, J., STUBBS, C.M.M., ELLIOTT, P.J., SHELDRICK, R.L.G., CHOLLET, A., KAWASHIMA, E., MCELROY, A.B. & WARD, P. (1993). Characterization, CNS distribution and function of NK_2 receptors using potent NK_2 receptor antagonists. *Regul. Pept.*, **46,** 9–19.

HAGAN, R.M., IRELAND, S.J., BAILEY, F., MCBRIDE, C., JORDAN, C.C. & WARD, P. (1991). A spirolactam conformationally-constrained analogue of physalaemin which is a peptidase-resistant, selective neurokinin NK_1 receptor antagonist. *Br. J. Pharmacol.*, **102,** 168P.

HARTELL, N.A. & HEADLEY, P.M. (1991). Preparative surgery enhances the direct spinal actions of three injectable anaesthetics in the anaesthetized rat. *Pain*, **46,** 75–80.

JACKSON, A., RUPINIAK, N., PEARCE, D. & BOYCE, S. (1994). Specific and non-specific effects of the NK_1 receptor antagonist CP-99,994 on locomotor activity in guinea-pigs. *Br. J. Pharmacol.*, **112,** 51P.

KELLSTEIN, D.E. & PROFFITT, M.M. (1992). Electrophysiological evidence that peripheral NK_1 receptors mediate hyperalgesia in an acutely inflamed joint model of arthritis. *Soc. Neurosci. Abst.*, **18,** 292.3.

MANTYH, P.W., GATES, T., MANTYH, C.R. & MAGGIO, J.E. (1989). Autoradiographic localization and characterization of tachykinin receptor binding sites in the rat brain and peripheral tissues. *J. Neurosci.*, **9,** 258–279.

MCLEAN, S., GANONG, A., SEYMOUR, P.A., SNIDER, R.M., DESAI, M.C., ROSEN, T., BRYCE, D.K., LONGO, K.P., REYNOLDS, L.S., ROBINSON, G., SCHMIDT, A.W., SIOK, C. & HEYM, J. (1993). Pharmacology of CP-99,994; a non-peptide antagonist of the tachykinin neurokinin-1 receptor. *J. Pharmacol. Exp. Ther.*, **267,** 473–479.

MERIGHI, A., POLAK, J.M. & THEODOSIS, D.T. (1991). Ultrastructural visualization of glutamate and aspartate immunoreactivities in the rat dorsal horn, with respect to the co-localization of glutamate, substance P and calcitonin-gene related peptide. *Neuroscience*, **40,** 67–80.

MJELLEM-JOLY, N., LUND, A., BERGE, O.-G. & HOLE, K. (1991). Potentiation of a behavioural response in mice by spinal coadministration of substance P and excitatory amino acid agonists. *Neurosci. Lett.*, **133,** 121–124.

RUSIN, K.I., RYU, P.D. & RANDIC, M. (1992). Modulation of excitatory amino acid responses in rat dorsal horn neurons by tachykinins. *J. Neurophysiol.*, **68,** 265–286.

SEGUIN, L. & MILLAN, M.J. (1994). The glycine B receptor partial agonist, (+)-HA966, enhances induction of antinociception by neurokinin 1 antagonists. *Eur. J. Pharmacol.*, **253,** R1–R3.

SKILLING, S.R., SMULLIN, D.H., BEITZ, A.J. & LARSON, A.A. (1988). Extracellular amino acid concentrations in the dorsal spinal cord of freely moving rats following veratridine and nociceptive stimulation. *J. Neurochem.*, **51,** 127–132.

STRATTON, S.C., BERESFORD, I.J.M. & HAGAN, R.M. (1994). GR159897, a potent non-peptide tachykinin NK_2 receptor antagonist, releases suppressed behaviours in a novel aversive environment. *Br. J. Pharmacol.*, **112,** 49P.

WANG, Z.Y., TUNG, S.R., STRICHARTZ, G.R. & HÅKANASON, R. (1994). Non-specific actions of the non-peptide tachykinin receptor antagonists, CP-96,345, RP 67580 and SR48968, on neurotransmission. *Br. J. Pharmacol.*, **111,** 179–184.

XU, X.-J., DALSGAARD, C.-J. & WIESENFELD-HALLIN (1992). Spinal substance P and *N*-methyl-D-aspartate receptors are co-activated in the induction of central sensitization of the nociceptive flexor reflex. *Neuroscience*, **51,** 641–648.

YASHPAL, K., DAM, T.V. & QUIRION, R. (1988). Autoradiographic localization of neurokinin receptors in rat spinal cord. *Regul. Pept.*, **22,** 191.

(Received October 5, 1994
Revised March 22, 1995
Accepted April 5, 1995)

British Journal of Pharmacology (1995) 115, 1020-1026 © 1995 Stockton Press All rights reserved 0007-1188/95 $12.00

NANC neurotransmission in lamina propria of the rabbit urethra: regulation by different subsets of calcium channels

Pia K.E. Zygmunt, Peter M. Zygmunt, [1]Edward D. Högestätt & Karl-Erik Andersson

Department of Clinical Pharmacology, Lund University Hospital, S-22185 Lund, Sweden

1 Electrical field stimulation (EFS) of the rabbit urethral lamina propria elicited a frequency-dependent non-adrenergic, non-cholinergic (NANC) relaxation, which was abolished by N^{ω}-nitro-L-arginine (L-NOARG).

2 ω-Conotoxin GVIA, a selective blocker of N-type voltage-operated calcium channels (VOCCs), and ω-conotoxin MVIIC (blocker of N- and Q-type VOCCs) inhibited the NANC relaxation, and the inhibition was inversely related to the frequency of stimulation. Combined, the two toxins were more effective than ω-conotoxin GVIA alone.

3 The relaxation induced by the nitric oxide (NO) donor, 3-morpholino-sydnonimine (SIN-1) was not affected by ω-conotoxin MVIIC.

4 ω-Agatoxin IVA (blocker of P-type VOCCs) did not attenuate the NANC relaxation.

5 Reduction of the calcium concentration from 1.5 to 0.5 mM reduced the NANC relaxation at low but not at high frequencies of stimulation; the relaxation induced by SIN-1 was not affected.

6 EFS (20 Hz, 30 s) increased the cyclic GMP level 3 fold in normal Krebs solutions, but was unable to enhance significantly the cyclic GMP level after calcium omission. L-NOARG reduced the cyclic GMP content in 'calcium-free' medium, indicating an ongoing NO synthesis that was independent of extracellular calcium.

7 Caffeine, ryanodine and thapsigargin (inhibitors of sarcoplasmic calcium release), and CGP 37157 (inhibitor of mitochondrial sodium/calcium exchange) had no effect on the NANC relaxation.

8 It is suggested that nitrergic nerve activation in the rabbit urethral lamina propria is mediated in part by N-type (ω-conotoxin GVIA-sensitive) and in part by Q-type (ω-conotoxin MVIIC-sensitive) VOCCs. With high frequences of stimulation, another mechanism, possibly calcium-independent, appears to become operational.

Keywords: Calcium; calcium channels; NANC neurotransmission; nitric oxide; ω-conotoxins; rabbit urethra

Introduction

Nitric oxide (NO) has been suggested as the neuronal mediator of non-adrenergic, non-cholinergic (NANC) relaxation in several tissues, including the lower urinary tract (Sneddon & Graham, 1992; Andersson, 1993). Electrical field stimulation (EFS) of the rabbit urethral lamina propria elicits a tetrodotoxin-sensitive NANC relaxation (Zygmunt *et al.*, 1993a), which can be abolished by the NO synthase inhibitor N^{ω}-nitro-L-arginine (L-NOARG), suggesting that NO formation is a crucial step in the response (Zygmunt *et al.*, 1993a,b). Furthermore, NADPH diaphorase staining, presumably identifying NO synthase, has been localized to nerve fibres in rabbit urethral lamina propria, implying that activation of NO producing (nitrergic) nerves is responsible for the NANC relaxation (Zygmunt *et al.*, 1993a).

We have recently shown that ω-conotoxin GVIA (ω-CgTx GVIA), a blocker of N-type voltage-operated calcium channels (VOCCs), inhibits NANC relaxation in the rabbit urethra at low frequencies of stimulation (Zygmunt *et al.*, 1993b). However, a significant ω-conotoxin-resistant component was observed at stimulation frequencies higher than 2 Hz. The NANC relaxation was unaffected by inhibitors of L-type (nimodipine) and T-type (tetramethrin, Ni^{+}) VOCCs, which raised the possibility that the ω-conotoxin-resistant component was mediated by VOCCs distinct from the L- and T-type, or even by a calcium influx-independent mechanism. Release of VIP from the rat enteric nerves, and noradrenaline and GABA from rat brain slices have been shown to persist in 'calcium-free' medium, which could indicate that release of calcium from intracellular stores is sufficient to uphold transmitter release in some nerves (Minchin, 1980; Sandoval, 1980; Schoffelmeer & Mulder, 1983; Belai *et al.*, 1987).

To clarify further the role of calcium in NANC nerve activation, we examined the effects of ω-conotoxin MVIIC (ω-CgTx MVIIC), a neuronal VOCC blocker with a calcium channel selectivity distinct from that of ω-CgTx GVIA (Hillyard *et al.*, 1992; Randall *et al.*, 1993; Wheeler *et al.*, 1994), and the selective P channel blocker ω-agatoxin IVA (Mintz *et al.*, 1992) on NANC relaxation in the rabbit urethral lamina propria. The effects of lowering the extracellular calcium concentration and drugs interfering with endoplasmic and mitochondrial calcium transport were also studied.

Methods

Tissue preparation

Female rabbits (New Zealand White) with an average weight of 3 kg were stunned by a blow on the head and exsanguinated. The abdomen was opened and the bladder and urethra were removed and placed in ice-cold Krebs solution of the following composition (mM): NaCl 119, $NaHCO_3$ 15, KCl 4.6, NaH_2PO_4 1.2, $MgCl_2$ 1.2, $CaCl_2$ 1.5, and glucose 11. The bladder and urethra were opened longitudinally and separated by a transverse cut at the level of the bladder neck. The lamina propria of the urethra was separated from the smooth muscle layers under a microscope, and strip preparations (1 × 2 × 5 mm) were prepared as described previously (Zygmunt *et al.*, 1993a). The strips were suspended between two

[1] Author for correspondence.

metal pins by means of silk ligatures in organ baths (5 ml), containing Krebs solution. Vessel segments of the rabbit ear artery (REA) were suspended in the same organ baths (Zygmunt & Högestätt, 1993). The Krebs solution was continuously bubbled with a mixture of 95% O_2 and 5% CO_2 at 37°C, resulting in a pH of 7.4. One of the metal pins was connected to a movable unit allowing adjustment of tension, and the other to a Grass Instruments FT O3C force-displacement transducer. The 'isometric' tension was displayed on a Grass Instruments model 7 D polygraph. The resting tension of the preparations was adjusted to 4 mN during an equilibration period of 1 h.

Experimental procedure

EFS was achieved by two platinum wire electrodes placed parallel to the preparations in the organ bath. Square wave pulses with a duration of 0.3 ms were delivered at frequencies of 0.5–40 Hz. The polarity was changed after each pulse to reduce oxidation of the electrodes. In order to study relaxant responses, the preparations were contracted with 1 nM arginine vasopressin (AVP), which produced a long-lasting and stable contraction (Zygmunt *et al.*, 1993b). Phentolamine (1 μM) and propranolol (1 μM) were present in all these experiments. Initially in each experiment the preparations were stimulated electrically for 5 s (urethral lamina propria) or 10 s (REA) every second min with a stimulation frequency of 12 Hz (urethral lamina propria) or 10 Hz (REA). Optimum voltage was determined by increasing the voltage until a maximum response was obtained (this voltage was then used in all subsequent stimulations). This 'maximum response' served as a reference, and is hereafter referred to as the reference relaxation (urethral lamina propria). The reference relaxation in the urethral lamina propria was 68±4% (72 strips from 21 rabbits) of the AVP-induced contraction. Frequency-response relationships were studied by stepwise increasing the frequency of stimulation from 0.5 to 40 Hz, allowing a two-min interval between the frequency steps. The effects of the intracellular calcium modulators thapsigargin, ryanodine, caffeine and CGP 37157 on the NANC relaxation were studied at a single stimulation frequency of 12 Hz. The preparations were stimulated 'continuously' at each frequency until the response stabilized (usually 1–2 min) to obtain an estimate of the maximum response at that frequency. Each preparation was subjected to only one series of stimulation frequencies. Thus, no more than one concentration of VOCC blocker or extracellular calcium was tested in each preparation. A control group subjected to the same stimulation protocol was always run in parallel. The choice of incubation time for the ω-CgTxs was based on a series of initial experiments, where the effect of 0.1 μM ω-CgTx GVIA ($n=7$) or 1 μM ω-CgTx MVIIC ($n=2$) was studied on urethral lamina propria stimulated with 5 s trains of pulses (10 Hz) every second min. These experiments showed that a maximum inhibition was obtained after about 10 min. Thus, to assure a maximum blockade of the ω-CgTx-sensitive calcium channels, an incubation period of 20 min was used in the experiments. The preincubation period with the other drugs and in low calcium medium was also 20 min.

Cyclic GMP and cyclic AMP measurements

Lamina propria preparations were suspended in organ bath as described above. Cyclic nucleotides were measured in unstimulated preparations and in preparations subjected to 20 Hz EFS for 30 s in Krebs solution with and without calcium ($CaCl_2$ replaced by 0.1 mM EGTA). AVP (1 nM), phentolamine (1 μM) and propranol (1 μM) were present throughout. The preincubation period in 'calcium-free' Krebs solution was 10 min. The preparations were subsequently frozen in liquid nitrogen. The tissue was homogenized in 10% trichloroacetic acid (TCA) in water with a glass-glass homogenizer and centrifuged at 3000 r.p.m. (4°C) for 10 min. Protein content in the pellets was determined by the Coomassie Plus Protein Assay Reagent based on the Bradford method (Pierce, Rockford, ILL, U.S.A.). The supernatants were extracted 5 times with 5 ml of water-saturated diethyl ether. The aqueous phase was evaporated and the residue stored at −20°C. Residues were dissolved in 0.05 M sodium acetate and the amounts of guanosine 3′:5′-cyclic monophosphate (cyclic GMP) and cyclic AMP were quantified by use of [^{125}I]-cyclic GMP and [^{125}I]-cyclic AMP RIA kit (RIANEN, Du Pont, Wilmington, DE, U.S.A.). [^{3}H]-cyclic AMP recovery marker was added to the TCA tissue homogenate. Recovery was 77%.

Drugs

(±)-Noradrenaline hydrochloride, (±)-propranolol hydrochloride, N^{ω}-nitro-L-arginine, arginine vasopressin acetate, tetrodotoxin (TTX), ω-conotoxin GVIA, thapsigargin, ryanodine (all from Sigma, St. Louis, MO, U.S.A.), caffeine (ACO, Stockholm, Sweden), phentolamine methane sulphonate (Ciba-Geigy, Basel, Switzerland), 3-morpholino-sydnonimine hydrochloride (SIN-1; Casella AG, Frankfurt am Main, Germany), ω-conotoxin MVIIC and ω-agatoxin IVA (Alomone labs, Jerusalem, Israel) were dissolved in distilled water. (±)-Nimodipine (Bayer, Leverkusen, Germany) and CGP 37157 (Ciba-Geigy AG, Basel, Switzerland) were dissolved in absolute ethanol.

Calculations and statistics

Responses are expressed as a percentage of the initial reference response (see above). Nimodipine, caffeine and low calcium medium reduced the AVP-induced contraction. The AVP concentration was therefore increased in these cases to regain the initial tension. When the preparation failed to return to the initial tension, R/T values were used to calculate drug effects (Garcia-Pascual *et al.*, 1991). R/T values express the relaxation (R) as a percentage of the tension (T) recorded immediately before each train of stimulation. Results are expressed as mean values ± s.e.mean, and n denotes the number of experiments (animals) performed. Student's t test (two-tailed) for unpaired observations was used in the statistical analyses. Where appropriate, analysis of variance (ANOVA) followed by Bonferroni/Dunn's *post hoc* test (Statview 4.0) was used (Ludbrook, 1994). The results from the cyclic GMP measurements were subjected to logarithmic transformation before statistical analysis to adjust for intergroup differences in variance. Statistical significance was accepted when $P<0.05$.

Results

Effect of L-NOARG

EFS of the AVP-contracted rabbit urethral lamina propria elicited a frequency-dependent relaxation, which was abolished by 1 μM TTX (Figure 1). At high frequencies of stimulation (≥12 Hz), the response generally became 'biphasic' with an initial transient relaxation that stabilized at a lower level after 1–2 min (Figure 2). At 20 Hz stimulation the transient and stable component amounted to 108±4% and 93±5% ($n=10$) of the initial reference relaxation (elicited by 12 Hz stimulation), respectively. The NO synthase inhibitor L-NOARG (0.3 mM) abolished both components of the relaxation, and reversed the response to a contraction at stimulation frequencies ≥12 Hz (Figure 1). The EFS-induced contraction was partially TTX-sensitive at 40 Hz stimulation (Figure 1).

Effects of ω-CgTx MVIIC and ω-CgTx GVIA

ω-CgTx MVIIC (1 μM) and ω-CgTx GVIA (0.1 μM) both inhibited the NANC relaxation, and the effect was larger at low than at high frequencies of stimulation (Figure 3, Table 1). A

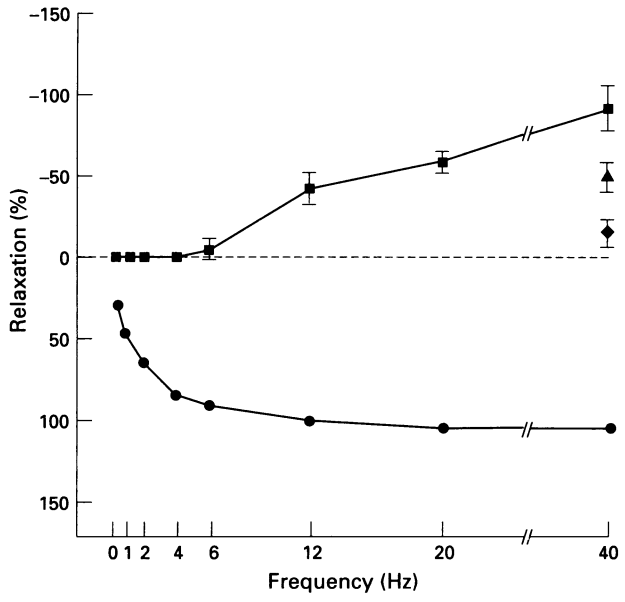

Figure 1 Responses to electrical field stimulation (frequency 0.5–40 Hz, pulse duration 0.3 ms, train duration 1–2 min, optimum voltage) in the urethral lamina propria incubated with 0.3 mM N^{ω}-nitro-L-arginine (■) or vehicle (●). The effects of 1 μM tetrodotoxin at 40 Hz stimulation in the absence (◆) and presence (▲) of N^{ω}-nitro-L-arginine are also shown. The preparations were contracted by arginine vasopressin (1 nM) before stimulation. Results are expressed as a percentage of the initial reference relaxation (see Methods), and are given as mean values ± s.e.mean ($n=4$).

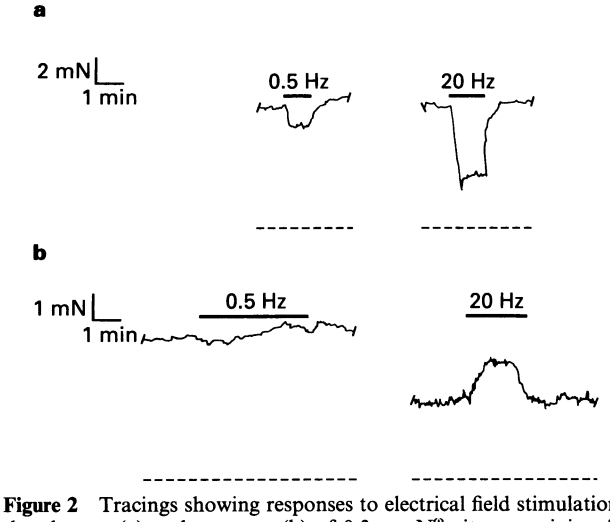

Figure 2 Tracings showing responses to electrical field stimulation in the absence (a) and presence (b) of 0.3 mM N^{ω}-nitro-L-arginine. The tracings in (a) and (b) were obtained from two separate urethral lamina propria preparations. Solid bars indicate the periods of electrical field stimulation. The preparations were contracted by arginine vasopressin (1 nM) before electrical field stimulation, and broken lines indicate the baseline tension before the contraction.

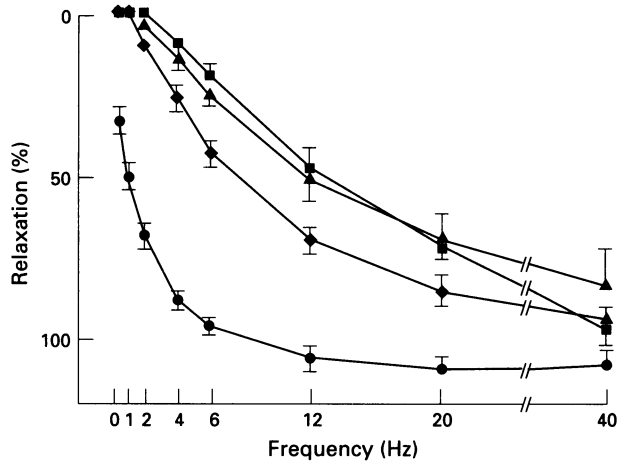

Figure 3 Frequency-response curves for the NANC relaxation in urethral lamina propria incubated with 0.1 μM ω-conotoxin GVIA (◆), 1 μM ω-conotoxin MVIIC (▲), 0.1 μM ω-conotoxin GVIA + 1 μM ω-conotoxin MVIIC (■) or vehicle (●). The preparations were contracted by arginine vasopressin (1 nM) before electrical field stimulation (stimulation parameters as in Figure 1). Results are expressed as a percentage of the initial reference relaxation (see Methods), and are given as mean values ± s.e.mean ($n=5-9$).

higher concentration of ω-CgTx MVIIC (3 μM, $n=2$) or ω-CgTx GVIA (1 μM, $n=7$) did not produce a further inhibition (tested only at 10 Hz stimulation). The NANC relaxation at 6 Hz stimulation was significantly smaller after incubation with ω-CgTx MVIIC than after incubation with ω-CgTx GVIA (Figure 3). The inhibition obtained by ω-CgTx MVIIC (1 μM) plus ω-CgTx GVIA (0.1 μM) was significantly larger than that obtained by ω-CgTx GVIA (0.1 μM) alone at 4, 6 and 12 Hz stimulation, but almost identical with that seen with ω-CgTx MVIIC (1 μM) alone (Figure 3, Table 1). ω-CgTx MVIIC (1 μM) did not affect the AVP-induced contraction or the relaxation induced by SIN-1. The pIC_{50} and I_{max} values for SIN-1 were 4.9 ± 0.1 and 77 ± 6% ($n=5$), and 5.0 ± 0.1 and 98 ± 8% ($n=5$) in the absence and presence of ω-CgTx MVIIC, respectively.

In order to mimic a physiological impulse pattern, i.e. fairly regular pulse-synchronous burst of impulses often occurring in short sequences separated by periods of neural silence (Wallin, 1981), some of the lamina propria preparations were subjected to 10 Hz EFS in 1 s trains at 10 s or 5 s intervals. Using these stimulation parameters, ω-conotoxin GVIA (0.1 μM) reduced the maximum relaxant response from 72 ± 6% to 30 ± 2% (10 s intervals, $n=4$) and from 88 ± 5% to 41 ± 2% (5 s intervals, $n=4$) of the initial reference relaxation.

The effects of ω-CgTx MVIIC and ω-CgTx GVIA on adrenergic contractions in the REA were also examined. As shown in Figure 4, the EFS-induced contractile responses were abolished by ω-CgTx MVIIC (1 μM) as well as by 0.1 μM

Table 1 Inhibitory effects of ω-conotoxins on electrically-induced non-adrenergic, non-cholinergic relaxation in the urethral lamina propria

Treatment	EF_{50}	E_{max}(%)	n
Control	$1.3 \pm 0.2^{a,b,c}$	110 ± 4	9
ω-Conotoxin GVIA 0.1 μM	$7.0 \pm 0.5^{a,d}$	99 ± 5	9
ω-Conotoxin MVIIC 1 μM	10 ± 1.3^{b}	83 ± 11	5
ω-Conotoxin GVIA 0.1 μM + ω-conotoxin MVIIC 1 μM	$13 \pm 1.3^{c,d}$	97 ± 5	7

The preparations were contracted by arginine vasopressin (1 nM) before electrical field stimulation. ^{a,b,c,d}Significant differences ($P<0.05$) between groups with identical letters according to analysis of variance (ANOVA) followed by Bonferroni/Dunn's *post hoc* test. EF_{50} denotes the frequency producing half maximum relaxation. E_{max} indicates the maximal relaxation obtained within the frequency interval tested (0.5–40 Hz), and is expressed as a percentage of the initial reference relaxation (see Methods). Results are expressed as mean values ± s.e.mean, where *n* indicates the number of preparations (animals) examined.

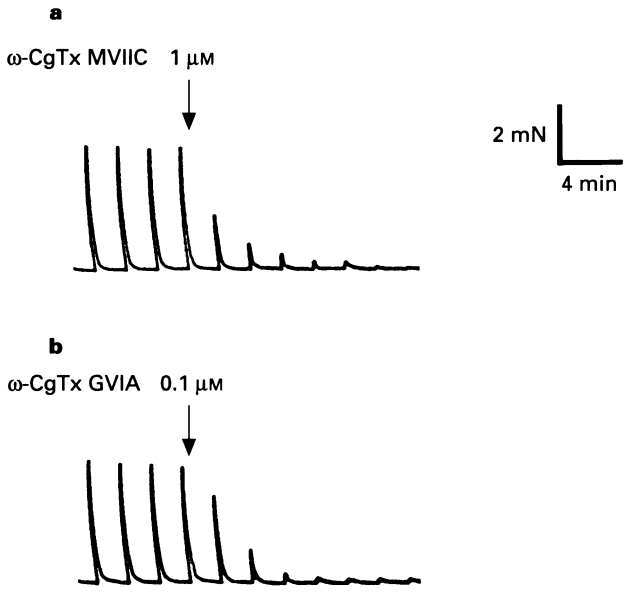

Figure 4 Tracings showing the effect of ω-conotoxin (ω-CgTx) MVIIC (a) and GVIA (b) on the contractile responses to electrical field stimulation (10 Hz for 10 s every second min, pulse duration 0.3 ms) in two segments of the rabbit ear artery.

ω-CgTx GVIA ($n=3$). The contractile response to exogenous noradrenaline (10 nM–0.1 mM) was, however, unaffected by the ω-CgTxs (data not shown).

Effects of ω-agatoxin IVA and nimodipine

ω-Agatoxin IVA (30 nM) and nimodipine (0.1 μM, $n=4$, data not shown) did not attenuate the electrically-induced NANC relaxation in the rabbit urethral lamina propria. However, at stimulation frequencies ≥ 4 Hz, ω-agatoxin IVA caused a small enhancement of the response (Figure 5). The SIN-1-induced relaxation was not affected by ω-agatoxin IVA and nimodipine (data not shown).

Effects of extracellular calcium

When the extracellular calcium concentration was reduced from 1.5 mM to 0.5 mM the maximum NANC relaxation in rabbit urethral lamina propria was significantly reduced at frequencies ≤ 4 Hz and increased at 40 Hz (Figure 6), whereas the relaxation induced by SIN-1 was unaffected ($n=3$). It was not possible to study the effect of nominally 'calcium-free' solution, since AVP failed to elicit a contraction in that medium.

Changes in cyclic nucleotides

In ordinary Krebs solution, EFS (20 Hz for 30 s) increased the cyclic GMP content from 1.4 ± 0.5 to 4.6 ± 1.3 pmol mg^{-1} protein ($n=6$). When calcium was omitted from the Krebs solution the basal cyclic GMP content increased 3 fold (Figure 7). EFS did not significantly enhance the cyclic GMP content in 'calcium-free' solution. However, the wide range of cyclic GMP levels measured at baseline (1.8 to 9.4 pmol mg^{-1} protein) and after EFS (1.7 to 20 pmol mg^{-1} protein) made it difficult to detect a statistically significant difference. Notably, pretreatment with L-NOARG (0.3 mM) in 'calcium-free' solution caused an 84% reduction of the cyclic GMP content after EFS (Figure 7). The cyclic AMP contents in Krebs solution were 46 ± 7 and 42 ± 7 pmol mg^{-1} protein ($n=6$) in unstimulated and stimulated preparations, respectively. The corresponding values in 'calcium-free' solution were 36 ± 2 and 36 ± 4 pmol mg^{-1} protein ($n=6$). These values did not differ significantly.

Effects of modulators of intracellular calcium release

Thapsigargin (1 μM), ryanodine (10 μM) and caffeine (1 mM), inhibitors of calcium release from different intracellular stores (Takemura *et al.*, 1989; Ehrlich *et al.*, 1994), and CGP 37157 (10 μM), which is an inhibitor of mitochondrial sodium/calcium exchange in heart (Cox *et al.*, 1993), had no effect on the NANC relaxation induced by 12 Hz stimulation in the lamina propria (Table 2).

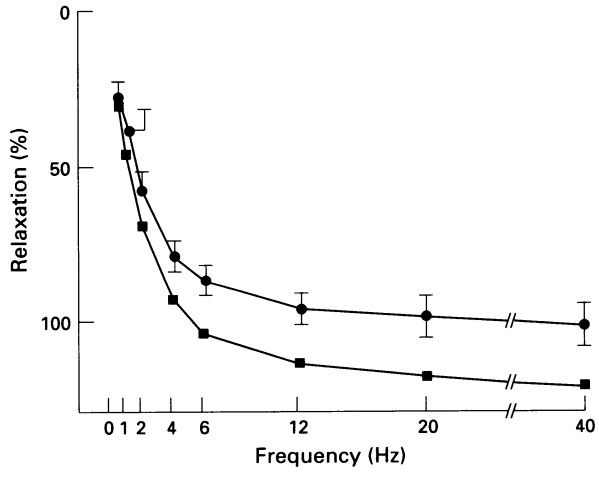

Figure 5 Frequency-response curves for the NANC relaxation in urethral lamina propria incubated with 30 nM ω-agatoxin IVA (■) or vehicle (●). The preparations were contracted by arginine vasopressin (1 nM) before electrical field stimulation (stimulation parameters as in Figure 1). Results are expressed as a percentage of the initial reference relaxation (see Methods), and are given as mean values ± s.e.mean ($n=4$).

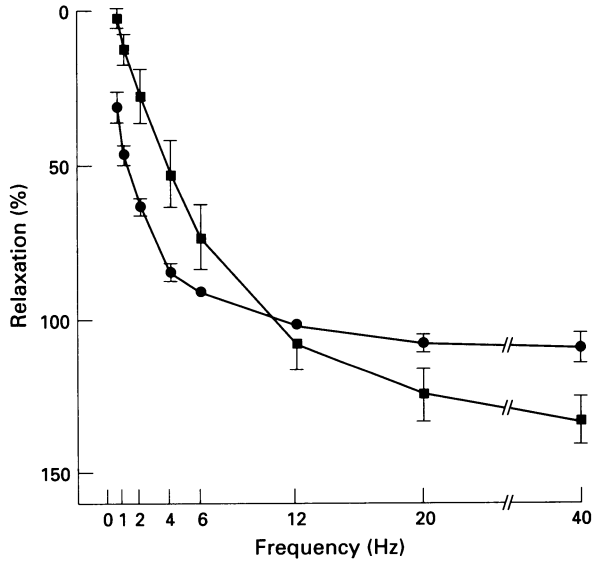

Figure 6 Effect of the extracellular calcium ion concentration on the NANC relaxation in the urethral lamina propria contracted by arginine vasopressin (1 nM) before electrical field stimulation (stimulation parameters as in Figure 1). Responses were recorded in Krebs solution, containing 1.5 mM (●) or 0.5 mM (■) calcium. Results are expressed as a percentage of the initial reference relaxation (see Methods), and are given as mean values ± s.e.mean ($n=5$).

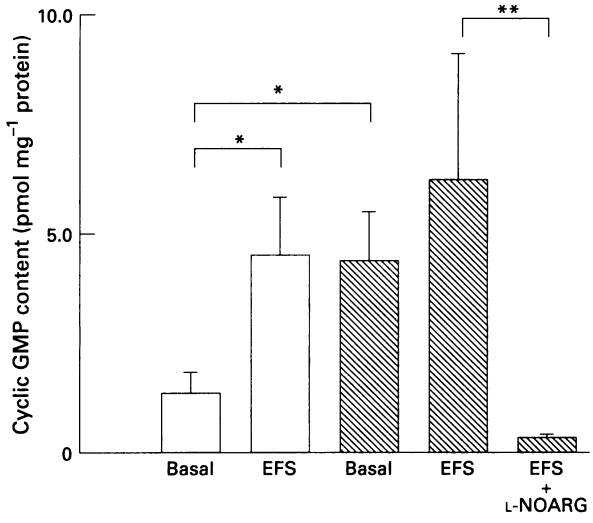

Figure 7 Effect of calcium omission on cyclic GMP accumulation after electrical field stimulation (EFS, 20 Hz for 30 s) in the urethral lamina propria. The strip preparations were suspended in organ baths and contracted by arginine vasopressin (1 nM). The cyclic GMP content was measured in 'normal' Krebs solution (1.5 mM calcium, open columns) or after a 10 min incubation period in nominally 'calcium-free' solution (0.1 mM EGTA, hatched columns). Basal refers to the cyclic GMP content in preparations not subjected to EFS. N^{ω}-nitro-L-arginine (L-NOARG, 0.3 mM) was present in the incubation medium in some experiments. The strips were quickly frozen in liquid nitrogen, and the cyclic GMP content determined by radioimmunoassay. Results are given as mean ± s.e.mean ($n = 5-6$). $^{*}P<0.05$, $^{**}P<0.01$.

Discussion

We have previously studied the frequency-dependence of the NANC relaxation in rabbit urethral lamina propria (Zygmunt *et al.*, 1993b). In that study, the stimulation period at each frequency was limited to 5 s, and hence the number of impulses delivered at each period increased the higher the frequency of stimulation (e.g. 5 pulses at 1 Hz and 100 pulses at 20 Hz). In order to obtain measurement of the maximum response at each frequency, the stimulation was continued for 1–2 min in the present study. Despite the difference in stimulation parameters the frequency-response curves turned out to be almost identical with that obtained previously. However, as evident from the individual tension tracings, a stimulation period of 30–60 s was often required to reach a maximum response at frequencies ≤2 Hz.

The NANC relaxation was completely inhibited by L-NOARG and accompanied by an increase of the cyclic GMP level, indicating that the response was mediated by NO. In the presence of L-NOARG, a contractile response was observed at high frequencies of stimulation (≥12 Hz). The contraction was partially sensitive to TTX (tested at 40 Hz stimulation), suggesting that the response was mediated in part by non-adrenergic nerves (resistant to phentolamine and propranolol) and in part by direct muscle stimulation. The NANC relaxation generally became 'biphasic' at high frequencies of stimulation (>12 Hz); after an initial peak the relaxation decreased before the tension stabilized. This response occurred at the same frequencies as did the L-NOARG-resistant contraction, suggesting that the reduction of the relaxation reflected the development of a contractile response superimposed on the NANC relaxation.

A 'biphasic' response to high frequency stimulation has also been demonstrated in pig and dog urethra (Hashimoto *et al.*, 1992; 1993; Bridgewater *et al.*, 1993). In pig urethra, EFS induced an initial transient relaxation, which at high frequencies (40–80 Hz) was followed by a prolonged second relaxation after cessation of stimulation (Bridgewater *et al.*, 1993). Both relaxation components were of NANC origin, but only the initial component was inhibited by L-NOARG. A similar 'biphasic' relaxant response was observed at stimulation frequencies ≥5 Hz in dog urethra (Hashimoto *et al.*, 1993). Again, the initial transient component was markedly reduced by L-NOARG, whereas the second slow component was unaffected. The neurotransmitter mediating the second relaxation component could not be identified in these studies. We found no evidence of a second component of relaxation produced by an additional neurotransmitter in rabbit urethral lamina propria.

In line with our previous study (Zygmunt *et al.*, 1993b), ω-CgTx GVIA inhibited the NANC relaxation in rabbit urethral lamina propria in a frequency-dependent manner, implying that activation of N-type VOCCs is an important step linking EFS to smooth muscle relaxation particularly at low frequencies of stimulation. The NANC relaxation does not seem to depend on L- and T-type VOCCs, since nimodipine (L channel blocker; present study), nickel and tetramethrin (T channel blockers) have been shown not to affect the response (Zygmunt *et al.*, 1993b). P-type VOCCs also do not seem to be involved, since the selective P channel blocker ω-agatoxin IVA (Mintz *et al.*, 1992) was unable to attenuate the NANC relaxation, but rather enhanced the response at high stimulation frequencies. We have no explanation for this enhancement, but the failure of ω-agatoxin IVA to affect the SIN-1-induced relaxation makes an interaction with the NO effector system unlikely.

ω-CgTx MVIIC, another Conus peptide isolated from the cone snail *Conus magus* (Hillyard *et al.*, 1992), induced a frequency-dependent inhibition of the NANC relaxation similar to that obtained with ω-CgTx GVIA. The ω-CgTx MVIIC concentration used in these experiments (1 μM) has been shown to inhibit $^{45}Ca^{2+}$ influx by approximately 70% in rat brain synaptosomes (Hillyard *et al.*, 1992). Incubation with both ω-CgTx GVIA and ω-CgTx MVIIC was more effective than treatment with ω-CgTx GVIA alone. The concentration of ω-CgTx GVIA used in these experiments was sufficient to elicit a maximum inhibition, since a 10 times higher con-

Table 2 Effects of modulators of intracellular calcium-release on the maximum NANC relaxation induced by electrical field stimulation (12 Hz for 1–2 min) in the urethral lamina propria

	Relaxation (%)		
Treatment	*Control*	*Treatment*	n
Thapsigargin 1 μM	101 ± 3	97 ± 3	4
Ryanodine 10 μM	102 ± 3	122 ± 12	6
Caffeine 1 μM	99 ± 3	93 ± 4	4
CGP 37157 10 μM	99 ± 3	102 ± 9	4

The preparations were contracted by arginine vasopressin (1 nM) before electrical field stimulation. Results are expressed as a percentage of the initial reference relaxation (see Methods), and are expressed as mean values ± s.e.mean, where *n* indicates the number of preparations (animals) examined.

centration had no further effect. These results suggest that ω-CgTx MVIIC has an additional effect, which is not shared with ω-CgTx GVIA. Clearly, this effect of ω-CgTx MVIIC was not postjuntional, since the relaxant response to the NO donor SIN-1 was unaffected. Hence, it is possible that yet another subtype of VOCC is involved in NANC neurotransmission in the rabbit urethral lamina propria.

ω-CgTx MVIIC has been shown to block P channel-mediated (ω-CgTx GVIA-resistant) synaptic transmission (Hillyard *et al.*, 1992). However, the effect of ω-CgTx MVIIC observed in the present study does not appear to be mediated by inhibition of P channels, since ω-agatoxin IVA was found to have no inhibitory effect. ω-CgTx MVIIC has recently been suggested to inhibit another type of neuronal VOCC termed Q channel (Hillyard *et al.*, 1992; Randall *et al.*, 1993; Wheeler *et al.*, 1994). This channel type may in addition to N channels mediate calcium influx in NANC nerves in the rabbit urethral lamina propria.

A combination of ω-CgTx MVIIC and ω-CgTx GVIA did not produce a larger inhibition of the NANC relaxation than did ω-CgTx MVIIC alone. This would indicate that ω-CgTx MVIIC also inhibits ω-CgTx GVIA-sensitive N-type VOCCs, a possibility previously suggested by Hillyard *et al.* (1992) and Grantham *et al.* (1994). To address this question further we studied the effect of ω-CgTx MVIIC on adrenergic contractions in the REA. Adrenergic neurotransmission in this artery has been suggested to depend on N-type VOCCs (Zygmunt & Högestätt, 1993). ω-CgTx MVIIC was able to inhibit this response completely. Since the contractile response to exogenous noradrenaline was unaffected by the ω-CgTxs, these findings provide additional evidence that ω-CgTx MVIIC can inhibit N-type VOCCs.

A significant ω-CgTx-resistant component of the NANC relaxation was observed at frequencies $\geqslant 2$ Hz. This component increased the higher the frequency of stimulation, and at 40 Hz stimulation the relaxation was almost completely resistant to the ω-CgTxs. It may be argued that the regular high frequency impulse pattern used in these experiments does not occur in intact animals, and consequently the ω-CgTx-resistant component may be physiologically irrelevant. To the best of our knowledge, the impulse pattern in NANC nerves has not been determined. However, impulse activity in sympathetic nerves has been recorded in man (Wallin, 1981). The activity consisted of high frequency bursts of impulses separated by silent intervals. In order to mimic this impulse pattern, the lamina propria was stimulated with 1 s trains of pulses (10 Hz) at 10 s or 5 s intervals. Again, ω-CgTx GVIA produced only a partial inhibition of the response, inferring that the mechanisms responsible for the ωCgTx-resistant component of the NANC relaxation may be of physiological importance.

To study whether the NANC relaxation is dependent on extracellular calcium the response to EFS was determined in a solution containing 0.5 mM calcium. At low stimulation frequencies ($\leqslant 4$ Hz) the relaxation was significantly reduced, but at 40 Hz the relaxation was significantly increased. Unfortunately, the effect of a nominally calcium-free solution could not be examined, because the preparation failed to contract in that medium. Instead, we measured the cyclic GMP level as an indirect measure of NANC nerve activation. If the ω-CgTx-resistant component of the NANC relaxation is independent of extracellular calcium, EFS should be able to increase the formation of cyclic GMP in 'calcium-free' medium. However, EFS at 20 Hz (mainly ω-CgTx-resistant) failed to increase the cyclic GMP level significantly in the absence of extracellular calcium, although the large variability of the data made it almost impossible to demonstrate a difference between the groups. Notably, L-NOARG significantly reduced the cyclic GMP level in 'calcium-free' medium. This would indicate that NO can be formed in the absence of extracellular calcium, indicating that activation of NO synthase may in part be independent of calcium influx in rabbit urethral lamina propria. However, the results do not allow us to speculate on the type or origin of the NO forming enzyme.

We have previously speculated that the ω-CgTx GVIA-resistant component of the NANC relaxation in the rabbit urethral lamina propria may be independent of calcium influx (Zygmunt *et al.*, 1993b). To study whether release of calcium from intracellular stores was involved in the NANC relaxation, the effects of drugs affecting this process were investigated. Caffeine has been shown to inhibit IP_3-induced calcium release, but it is also capable of activating the ryanodine receptor-calcium release channel (Ehrlich *et al.*, 1994). Ryanodine can inhibit stimulation-induced intracellular calcium release by binding to the ryanodine receptor on the sarcoplasmic reticulum (Ehrlich *et al.*, 1994). However, neither caffeine nor ryanodine had an effect on the NANC relaxation in the present study. Thapsigargin, which acts by depleting IP_3-sensitive intracellular calcium stores (Takemura *et al.*, 1989), also had no effect on the NANC relaxation. Finally, the NANC relaxation was unaffected by CGP 37157, which has been suggested to antagonize selectively mitochondrial sodium/calcium exchange (Cox *et al.*, 1993). It therefore seems unlikely that release of calcium from intracellular stores is involved in NANC neurotransmission in the rabbit urethral lamina propria. This raises the question whether neuronal NO synthase may in part be regulated in a calcium-indpendent manner, a possibility previously suggested by Kostka *et al.* (1993). An important distinction between NO and other neurotransmitters is that NO does not seem to be stored in vesicles, and therefore is not released by a calcium-activated exocytotic process. NO is rather thought to be produced on demand and to reach adjacent effector cells by passive diffusion (Snyder, 1992). Although the constitutive NO synthase present in neurones is a calcium/calmodulin-dependent enzyme (Bredt *et al.*, 1991; Murad *et al.*, 1992), the mechanisms regulating enzyme activity in the intact cell have not been delineated. Thus, the 'calcium hypothesis' for neurotransmitter release (Katz, 1969) may not be applicable to NO release from NANC nerves.

This work was supported by the Swedish Medical Research Council (no 06837), the Medical Faculty at Lund University and the Swedish Society for Medical Research.

References

ANDERSSON, K.-E. (1993). Pharmacology of lower urinary tract smooth muscles and penile erectile tissues. *Pharmacol. Rev.*, **45**, 253–308.

BELAI, A., RALEVIC, A. & BURNSTOCK, G. (1987). VIP release from enteric nerves is independent of extracellular calcium. *Regul. Pept.*, **19**, 79–89.

BREDT, D.S., HWANG, P.M., GLATT, C.E., LOWENSTEIN, C., REED, R.R. & SNYDER, S.H. (1991). Cloned and expressed nitric oxide synthase structurally resembles cytochrome P-450 reductase. *Nature*, **351**, 714–718.

BRIDGEWATER, M., MACNEIL, H.F. & BRADING, A.F. (1993). Regulation of tone in pig urethral smooth muscle. *J. Urol.*, **150**, 223–228.

COX, D.A., CONFORTI, L., SPERELAKIS, N. & MATLIB, M.A. (1993). Selectivity of inhibition of Na^+-Ca^{2+} exchange of heart mitochondria by benzothiazepine CGP-37157. *J. Cardiovasc. Pharmacol.*, **21**, 595–599.

EHRLICH, B.E., KAFTAN, E., BEZPROZVANNAYA, S. & BEZPROZVANNY, I. (1994). The pharmacology of intracellular Ca^{2+}-release channels. *Trends Pharmacol. Sci.*, **15**, 145–148.

GARCIA-PASCUAL, A., COSTA, G., GARCIA-SACRISTAN, A. & ANDERSSON, K.-E. (1991). Relaxation of sheep urethral muscle induced by electrical stimulation of nerves: involvement of nitric oxide. *Acta Physiol. Scand.*, **141,** 531–539.

GRANTHAM, C.J., BOWMAN, D., BATH, C.P., BELL, D.C. & BLEAKMAN, D. (1994). ω-Conotoxin MVIIC reversibly inhibits a human N-type calcium channel and calcium influx into chick synaptosomes. *Neuropharmacology*, **33,** 225–258.

HASHIMOTO, S., KIGOSHI, S. & MURAMATSU, I. (1992). Neurogenic responses of urethra isolated from the dog. *Eur. J. Pharmacol.*, **213,** 117–123.

HASHIMOTO, S., KIGOSHI, S. & MURAMATSU, I. (1993). Nitric oxide-dependent and -independent neurogenic relaxation of isolated dog urethra. *Eur. J. Pharmacol.*, **231,** 209–214.

HILLYARD, D.R., MONJE, V.D., MINTZ, I.M., BEAN, B.P., NADASDI, L., RAMACHANDRAN, J., MILJANICH, G., AZIMI-ZOONOOZ, A., MCINTOSH, J.M., CRUZ, L.J., IMPERIAL, J.S. & OLIVERA, B.M. (1992). A new conus peptide ligand for mammalian presynaptic Ca^{2+} channels. *Neuron*, **9,** 69–77.

KATZ, B. (1969). *The Release of Neurotransmitter Substances* (The Sherrington Lectures 10). Springfield, Illinois: Thomas.

KOSTKA, P., JANG, E., WATSON, E.G., STEWART, J.L. & DANIEL, E.E. (1993). Nitric oxide synthase in the autonomic nervous system of canine ileum. *J. Pharmacol. Exp. Ther.*, **264,** 234–239.

LUDBROOK, J. (1994). Repeated measurements and multiple comparisons in cardiovascular research. *Cardiovasc. Res.*, **28,** 303–311.

MINCHIN, M.C.W. (1980). The role of Ca^{2+} in the protoveratrine-induced release of γ-aminobutyrate from rat brain slices. *Biochem. J.*, **190,** 333–339.

MINTZ, I.M., VENEMA, V.J., SWIDEREK, K.M., LEE, T.D., BEAN, B.P. & ADAMS, M.E. (1992). P-type calcium channels blocked by the spider toxin ω-Aga-IVA. *Nature*, **355,** 827–829.

MURAD, F., FÖRSTERMANN, U., NAKANE, M., SCHMIDT, H., POLLOCK, J., SHENG, H., MATSUMOTO, T., WARNER, T., MITCHELL, J., TRACEY, R. & BUECHLER, W. (1992). The nitric oxide-cyclic GMP signal transduction pathway in vascular smooth muscle preparations and other tissues. *Jpn. J. Pharmacol.*, **58,** 150P–157P.

RANDALL, A.D., WENDLAND, B., SCHWEIZER, F., MILJANICH, G., ADAMS, M.E. & TSIEN, R.W. (1993). Five pharmacologically distinct high voltage-activated Ca^{2+} channels in cerebellar granule cells. *Soc. Neurosci. Abstr.*, **19,** 1478.

SANDOVAL, M.E. (1980). Sodium-dependent efflux of [^{3}H]GABA from synaptosomes probably related to mitochondrial calcium mobilization. *J. Neurochem.*, **35,** 915–921.

SCHOFFELMEER, A.N.M. & MULDER, A.H. (1983). [^{3}H]noradrenaline release from brain slices induced by an increase in the intracellular sodium concentration: role of intracellular calcium stores. *J. Neurochem.*, **40,** 615–621.

SNEDDON, P. & GRAHAM, A. (1992). Role of nitric oxide in the autonomic innervation of smooth muscle. *J. Auton. Pharmacol.*, **12,** 445–456.

SNYDER, S.H. (1992). Nitric oxide: first in a new class of neurotransmitters? *Science*, **257,** 494–496.

TAKEMURA, H., HUGHES, A.R., THASTRUP, O. & PUTNEY, J.W. JR. (1989). Activation of calcium entry by the tumor promoter thapsigargin in parotid acinar cells. *J. Biol. Chem.*, **264,** 12266–12271.

WALLIN, B.G. (1981). New aspects of sympathetic function in man. In *Butterworths International Medical Reviews. Neurology 1, Clinical Neurophysiology*. pp. 145–167. London: Butterworth.

WHEELER, D.B., RANDALL, A. & TSIEN, R.W. (1994). Roles of N-type and Q-type Ca^{2+} channels in supporting hippocampal synaptic transmission. *Science*, **264,** 107–111.

ZYGMUNT, P.K.E., PERSSON, K., ALM, P., LARSSON, B. & ANDERSSON, K.-E. (1993a). The L-arginine/nitric oxide pathway in the rabbit urethral lamina propria. *Acta Physiol. Scand.*, **148,** 431–439.

ZYGMUNT, P.M. & HÖGESTÄTT, E.D. (1993). Calcium channels at the adrenergic neuroeffector junction in the rabbit ear artery. *Naunyn Schmied. Arch. Pharmacol.*, **347,** 617–623.

ZYGMUNT, P.M., ZYGMUNT, P.K.E., HÖGESTÄTT, E.D. & ANDERSSON, K.-E. (1993b). Effects of ω-conotoxin on adrenergic, cholinergic and NANC neurotransmission in the rabbit urethra and detrusor. *Br. J. Pharmacol.*, **110,** 1285–1290.

(Received January 18, 1995
Revised March 13, 1995
Accepted March 20, 1995)

British Journal of Pharmacology (1995) 115, 1027–1037 © 1995 Stockton Press All rights reserved 0007–1188/95 $12.00

Effects of BRL55834 in rat portal vein and bovine trachea: evidence for the induction of a glibenclamide-resistant, ATP-sensitive potassium current

[1]G. Edwards, [2]J. Schneider, [2]A. Niederste-Hollenberg, *Th. Noack & A.H. Weston

School of Biological Sciences, G.38 Stopford Building, University of Manchester, Manchester M13 9PT, UK and *Department of Physiology, Philipps University, Deutschhausstrasse 2, 35033 Marburg, Germany

1 The effects of the benzopyran K-channel opener, BRL55834, on mechanical activity in bovine trachealis and rat portal vein were studied together with membrane currents in freshly-isolated single cells derived from these tissues.

2 BRL55834 (3 nM–1 μM) produced a concentration-dependent relaxation of bovine trachealis precontracted with 100 μM histamine and reduced the spontaneous mechanical activity of rat portal veins, effects which were antagonized by glibenclamide (1–10 μM) but were not reversible on washing. In contrast, charybdotoxin (250 nM) did not modify the spasmolytic effect of BRL55834 in bovine trachealis.

3 BRL55834 (10 nM–10 μM) did not relax segments of bovine trachealis precontracted with 80 mM KCl.

4 In some freshly-isolated single cells from bovine trachealis held at −10 mV, BRL55834 (3 μM) induced a time-independent outward K-current which was partially resistant to inhibition by glibenclamide (10 μM). In other cells, a very noisy, outwardly-rectifying and charybdotoxin-sensitive current developed in the presence of BRL55834 (3 μM) and in time-matched control cells.

5 In freshly-isolated single cells from rat portal vein held at −10 mV, BRL55834 (3 μM) induced a time- and calcium-independent outward K-current which was partially resistant (approximately 25% inhibition at +40 mV) to subsequent inhibition by glibenclamide (10 μM). In contrast, levcromakalim induced a time-independent outward K-current which was completely inhibited by glibenclamide 10 μM.

6 With the non-hydrolysable ATP analogue, AMP-PCP (5 mM), in the pipette, the ability of BRL55834 to induce a time-independent K-current in portal vein cells was markedly reduced (approximately 80% inhibition at +40 mV) whereas the effects of 10 μM levcromakalim were totally inhibited.

7 The glibenclamide-resistant current component induced by BRL55834 was totally inhibited by phentolamine (100 μM), a concentration that had no effect on the peak current ($I_{BK(Ca)}$) induced by NS1619 (33 μM).

8 Stationary fluctuation analysis of the noise associated with the glibenclamide-insensitive K-current induced by BRL55834 in rat portal vein cells indicated that the unitary current flowing through the underlying channels was 0.26 pA at −10 mV, a value inconsistent with the involvement of BK_{Ca}.

9 It is concluded that the relaxations of both bovine trachea and rat portal vein produced by BRL55834 are associated with the opening of K-channels. These are probably identical to the ATP-sensitive K-channel opened by levcromakalim, although the involvement of an additional K-channel cannot be excluded. The reduced sensitivity of the BRL55834-induced changes to glibenclamide and to AMP-PCP may result from avid binding of BRL55834 to its site of action.

Keywords: BRL55834; levcromakalim; K-currents; rat portal vein; bovine trachea; charybdotoxin; glibenclamide; phentolamine; AMP-PCP; K_{ATP}; BK_{Ca}

Introduction

With few exceptions, compounds which open the ATP-sensitive K-channel (K_{ATP}) are somewhat vascular-selective and higher concentrations of these agents are generally required to open this channel in non-vascular tissues and in cardiac and skeletal muscle than in vascular preparations (Edwards & Weston, 1993; 1995). Thus the therapeutic usefulness of substances like aprikalim and levcromakalim for conditions such as bronchial asthma may be limited by hypotensive side-effects, especially at high doses (see reviews by Edwards & Weston, 1993; Gopalakrishnan *et al.*, 1993; Hamilton *et al.*, 1993).

Recently, however, several compounds which open K_{ATP} but which do not show vascular selectivity have been described (Taylor *et al.*, 1992; Koga *et al.*, 1993; Pirotte *et al.*, 1993; Ishizawa *et al.*, 1994). One of these, the benzopyran derivative BRL55834, is a bronchodilator at doses which have relatively little effect on blood pressure when administered to animals either intravenously, intraduodenally or by inhalation (Bowring *et al.*, 1993; Arch *et al.*, 1994). The reason for the enhanced airway effects of BRL55834 is not known, although it is possible that it exerts smooth muscle relaxant actions which are additional to the opening of K_{ATP}. Indeed, Lawson *et al.* (1993) concluded that two mechanisms were involved in relaxations induced by BRL55834 in guinea-pig trachealis, since the effects of this benzopyran were only partially glibenclamide-sensitive.

In isolated patches from bovine trachealis, Ward *et al.* (1992) noted that BRL55834 could stimulate the opening of the large conductance, Ca^{2+}-sensitive K-channel (BK_{Ca}). Since this channel is thought to play an important role in determining the resting membrane potential in tracheal smooth muscle (reviewed by Small *et al.*, 1993), an action on BK_{Ca} could thus contribute to the observed tissue selectivity of BRL55834 *in vivo*.

[1] Author for correspondence.
[2] Present address: Department of Physiology, Philipps University, Deutschhausstrasse 2, 35033 Marburg, Germany.

The objective of the present investigation was to study further the *in vitro* effects of BRL55834 using strips of bovine trachealis and freshly-isolated single smooth muscle cells from this tissue. Comparative experiments were also performed on single cells and whole segments of rat portal vein, a well-characterized system which responds to a variety of K-channel modulators (see Edwards & Weston, 1993). Using this approach, together with the use of NS1619, an opener of BK_{Ca} (Edwards *et al.*, 1994), it was hoped to learn more about the possible basis of the reported selective bronchodilator effects of this agent (Bowring *et al.*, 1993). Preliminary accounts of some of these observations have been presented (Niederste-Hollenberg *et al.*, 1994; Edwards *et al.*, 1995).

Methods

Tissue bath experiments

Whole portal veins and segments of bovine trachea were each mounted under 10 mN tension for isometric recordings. The tissues were allowed to equilibrate in Krebs solution (see Drugs and solutions) for 1 h at 37°C before they were exposed at 20 min intervals to increasing concentrations of BRL55834 added cumulatively. In the case of the tracheal segments, tone was induced by the addition of histamine, 100 μM, to the Krebs solution. Antagonism by glibenclamide was studied by first incubating the tissues for 30 min with the appropriate concentration of this agent before the subsequent concentration-effect curve to BRL55834 was constructed in the continuing presence of glibenclamide. Bovine trachealis was incubated in the presence of charybdotoxin for 15 min before exposure to increasing concentrations of BRL55834 in the continuing presence of this inhibitor. Since charybdotoxin induces neurotransmitter release from cholinergic neurones (Tagaya *et al.*, 1994), the trachealis tissue-bath experiments involving this compound were performed in the presence of 100 nM atropine. The effect of BRL55834 was only very slowly reversible by washing and therefore only a single cumulative concentration-effect protocol was performed on each tissue in either the presence or absence of modifying agent.

Mechanical responses of the tissues were recorded with an Apple Macintosh Plus computer in conjunction with MacLab hardware (MacLab 8) and software (Chart, version 2.5) (Analog Digital Instruments).

Production of isolated cells

Tissues were placed in low-Ca^{2+} PSS and carefully cleaned of fat and connective tissue with fine scissors in conjunction with a dissecting microscope. Small strips of tracheal smooth muscle or intact portal veins were placed in an enzyme solution originally described by Klöckner & Isenberg (1985). The tissues were then agitated for 20 min in the enzyme solution at 37°C, washed in the same solution free of enzyme and cut into small segments. These were than triturated with a wide bore, smooth tipped pipette in Kraftbrühe (KB-medium; Klöckner & Isenberg, 1985). Cells were stored at 6°C in KB-medium and used within 9 h of separation.

Single-cell electrophysiology

The whole-cell configuration of the patch-clamp technique (Hamill *et al.*, 1981) was employed using an Axopatch-1C amplifier (Axon Instruments). The settling time of this system was less than 500 μs. Patch pipettes were pulled from Pyrex glass (H15/10, Jencons, U.K.) and had resistances of 3–4 MΩ when filled with the internal (intracellular) solution. Voltage commands and data acquisition were performed on-line with an AT-compatible computer equipped with an appropriate interface, the sampling frequency of which was 15 kHz (Axolab 1100 or Axon TL-1, Axon Instruments, U.S.A.). For cell stimulation and for recording and analysing data, the pCLAMP 5.5 programme was used (Axon Instruments). Data were stored on a digital audio tape recorder (Sony; cut-off frequency 20 kHz) and the evoked membrane currents were monitored on a Gould Windograf recorder (–3 dB cut-off frequency 460 Hz).

The effects of BRL55834 were investigated by adding the appropriate amount of this agent to the main reservoir containing the external solution to ensure that responses were obtained under steady-state conditions. The bath (volume: 1 ml) was continuously perfused (1 ml min^{-1}) with fresh external solution using a pump (Microperpex, Pharmacia LKB, Freiburg, Germany); a second identical pump was used to remove excess solution from the recording chamber. All experiments were performed at room temperature (24°C–26°C).

Drugs and solutions

The low-Ca^{2+} PSS used for tissue dissection comprised (mM): KOH 130, $CaCl_2$ 0.05, taurine 20, pyruvate 5, creatine 5, HEPES 10, buffered with methanesulphonic acid to pH 7.4. The enzyme solution for separation of portal vein cells had the same composition but also contained collagenase (Type VIII) 1 mg ml^{-1}, pronase (Calbiochem) 0.2 mg ml^{-1} and fatty acid-free albumin 1 mg ml^{-1}. For separation of tracheal cells, these enzyme concentrations were halved. KB-medium comprised (mM): KCl 85, KH_2PO_4 30, $MgSO_4$ 5, Na_2ATP 5, K-pyruvate 5, creatine 5, taurine 20, β-OH-butyrate 5, fatty acid-free

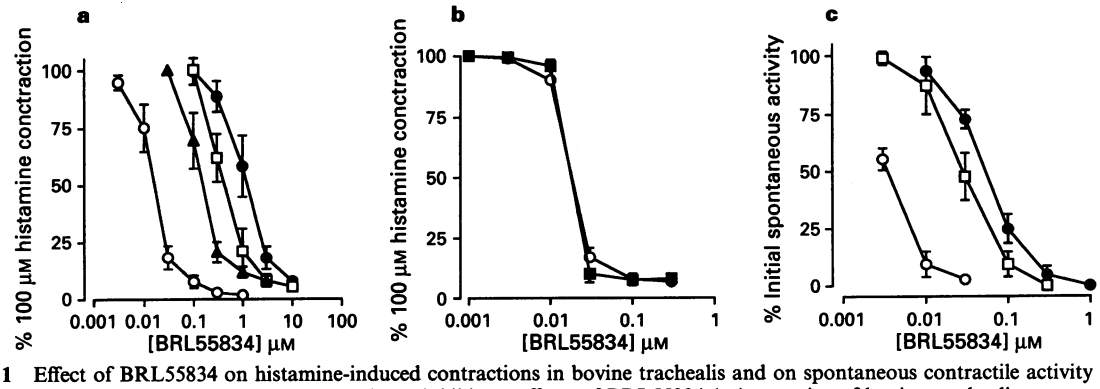

Figure 1 Effect of BRL55834 on histamine-induced contractions in bovine trachealis and on spontaneous contractile activity in rat portal veins. The concentration-dependent mechano-inhibitory effects of BRL55834 (○) on strips of bovine trachealis precontracted with 100 μM histamine (a) or on spontaneous activity in intact portal veins (c) were antagonized by glibenclamide (▲, 1 μM; □, 3 μM; ●, 10 μM). In contrast, charybdotoxin (250 nM, ■) did not modify the response of the histamine-precontracted bovine trachealis to BRL55834 (b). Each point represents the mean ± s.e.mean, $n = 3–4$.

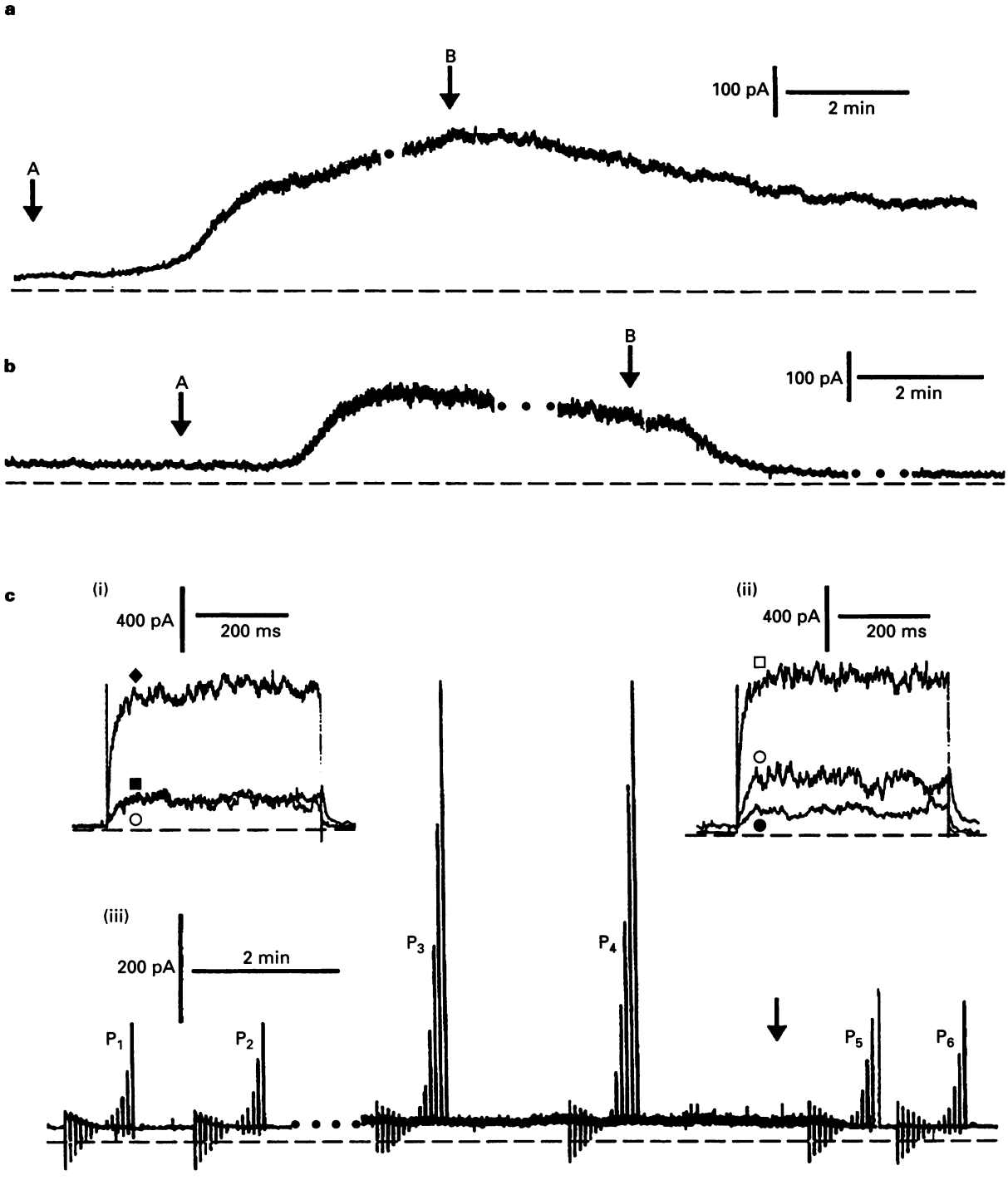

Figure 2 Effect of BRL55834 on whole-cell currents in bovine trachealis and rat portal vein cells under calcium-free conditions (Ca-free pipette solution, Ca-free PSS, see Methods). (a,b) Typical traces comparing the effect of 3 μM BRL55834 on a single cell isolated from bovine trachealis (a; holding potential 0 mV) with the effect of 10 μM levcromakalim on a rat portal vein cell (b; holding potential −10 mV). In the tracheal cell, BRL55834 (superfusion started at A) produced a marked increase in the outward current associated with an increase in current noise. Glibenclamide (10 μM, superfusion started at B) only partially inhibited the BRL55834-induced current. In contrast the current induced by levcromakalim in the portal vein cell (superfusion started at A) was fully inhibited by glibenclamide (10 μM, superfusion started at B). Gaps in the traces in (a) and (b) are to scale and represent periods in which the cell was stepped to different test potentials. (c(i), c(ii)) Tracheal cells were held at −10 mV to inactivate the time-dependent currents, $I_{K(A)}$ and $I_{K(V)}$, and then stepped for 500 ms to a test potential of +50 mV (○). (c(i)) After 25 min exposure to 3 μM BRL55834 there was a marked increase in the outward current at +50 mV (◆) which was inhibited by subsequent exposure to charybdotoxin (■). (c(ii)) In a time-matched control cell there was a similar increase in current over a 25 min period (□) which was also inhibited by 100 nM charybdotoxin (●). (c(iii)) Trace showing the development of an outwardly-rectifying, charybdotoxin-sensitive current with time in a single bovine trachealis cell. P indicates application of test protocols in which the cell was stepped from the holding potential (−10 mV) to a series of test potentials (from −80 mV to +50 mV in 10 mV increments). At P_1 and P_2 control currents were obtained within a few minutes of formation of the whole-cell recording configuration. P_3 and P_4 were applied approximately 21 min and 23 min after disruption of the membrane (dotted line indicates 20 min period). Note that the increase in current noise at the holding potential was not associated with the development of an outward current (unlike the trace shown in (a)) although there was a marked increase in outward current at the test potentials more positive than 0 mV. Charybdotoxin (100 nM; added at the arrow) rapidly inhibited both the noise at the holding potential and the time-induced outwardly-rectifying current (P_5, P_6). Individual traces were derived from different cells. The horizontal dashed line represents the zero current level.

albumin 1 mg ml^{-1}, pH adjusted to 7.20 at 6°C with KOH.

The composition of the calcium-free bath (external) solution (Ca-free PSS) was (mM): NaCl 125, KCl 4.8, $MgCl_2$ 3.7, KH_2PO_4 1.2, glucose 11, HEPES 10, EGTA 1.0. The bath solution containing calcium (Ca-PSS) consisted of (mM): NaCl 125, KCl 4.8, $MgCl_2$ 1.2, KH_2PO_4 1.2, $CaCl_2$ 2.5, glucose 11, HEPES 10. The bath solutions were buffered with NaOH to pH 7.30 and aerated with O_2. The Ca-free pipette (internal) solution comprised (mM): NaCl 5, KCl 120, $MgCl_2$ 1.2, K_2HPO_4 1.2, glucose 11, HEPES 10, EGTA 1.2, oxalacetic acid 5, sodium pyruvate 2, sodium succinate 5, buffered with KOH to pH 7.30 at 24°C. In those experiments in which cells were exposed to Ca-PSS, EGTA was omitted from the pipette solution. The Ca^{2+} concentration in the EGTA-free pipette solution (due to contamination of the constituent salts) was determined to be approximately 1 μM using fura-2 and atomic absorption spectrophotometry. However, assuming a contaminant concentration of 10 μM Ca^{2+} in the external and in the pipette solutions, the presence of 1 mM and 1.2 mM EGTA

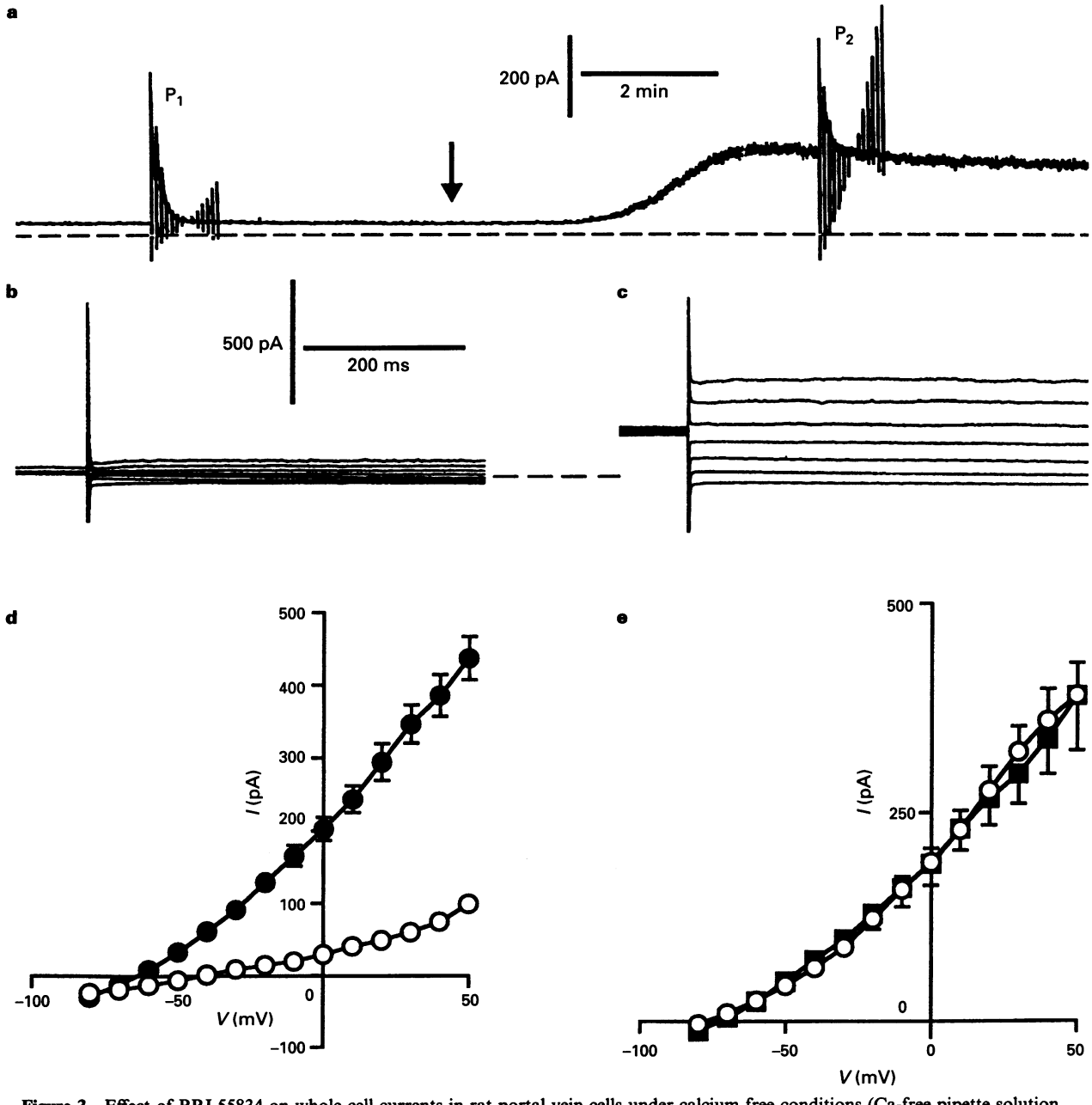

Figure 3 Effect of BRL55834 on whole-cell currents in rat portal vein cells under calcium-free conditions (Ca-free pipette solution, Ca-free PSS, see Methods). (a) Typical trace showing the increase in a noisy outward current induced by BRL55834 (3 μM; superfusion started at arrow) at a holding potential of −10 mV. P_1 and P_2 represent test protocols during which the cell was stepped from the holding potential (−10 mV) to a series of test potentials (from −80 mV to +50 mV in 10 mV increments). P_1 shows control currents obtained within a few minutes of formation of the whole-cell recording configuration; the resting membrane potential estimated from zero current crossover was between −50 and −40 mV. Note the marked increase in current at the test potentials after exposure to BRL55834 (P_2) and the membrane hyperpolarization to −60 mV. (b) and (c) represent computer-derived mean currents obtained in 5 cells during P_1 and P_2 before and after exposure to BRL55834, respectively. For clarity, only traces obtained at test potentials from −80 mV to +40 mV in 20 mV increments are presented. (d) *I-V* relationships derived from protocols P_1 (○) and P_2 (●). (e) The magnitude of the time-independent current induced by BRL55834 (derived by subtracting the control current at each test potential from the corresponding currents subsequently obtained in the same cells in presence of 3 μM BRL55834) was similar in the presence (■) or absence (○) of bath calcium. Each point represents the mean ± s.e.mean, $n = 5-7$.

(ethylene glycol-*bis* (β-aminoethyl ether) tetra-acetic acid) in the bath and pipette solutions, respectively, was calculated (Fabiato, 1988) to produce an average free calcium concentration in the 'Ca-free' solutions of less than 1 nM.

Krebs solution used for the tissue bath experiments had the following composition (mM): NaCl 118, KCl 4.8, $CaCl_2$ 2.5, $MgSO_4$ 1.2, KH_2PO_4 1.2, $NaHCO_3$ 25, glucose 11.1. This solution was gassed with a mixture of 95% O_2 and 5% CO_2 at 37°C.

Adenylyl-(β,γ-methylene)-diphosphonate (tetralithium salt; AMP-PCP; Calbiochem) was dissolved directly in pipette solution. BRL55834 (3S,4R)-3,4-dihydro-2,2-dimethyl-4-(2-oxopiperidin-1-yl)-6-pentafluoroethyl-2H-1-benzopyran-3-ol) and levcromakalim (SmithKline Beecham), NS1619 (1-(2'-hydroxy-5'-trifluoromethylphenyl)-5-trifluoromethyl-2(3*H*)benzimidazolone; NeuroSearch) and glibenclamide were each first dissolved in dimethyl sulphoxide (DMSO) to produce a concentrated stock solution (20 mM). Phentolamine hydrochloride, atropine sulphate and histamine dihydrochloride were prepared as stock solutions in distilled water. Dilutions of stock solutions were prepared with the appropriate bath solution immediately before they were required. Charybdotoxin (Latoxan) was dissolved directly into the Krebs or bath solutions and used immediately. Unless otherwise stated, all reagents and compounds were obtained from Sigma.

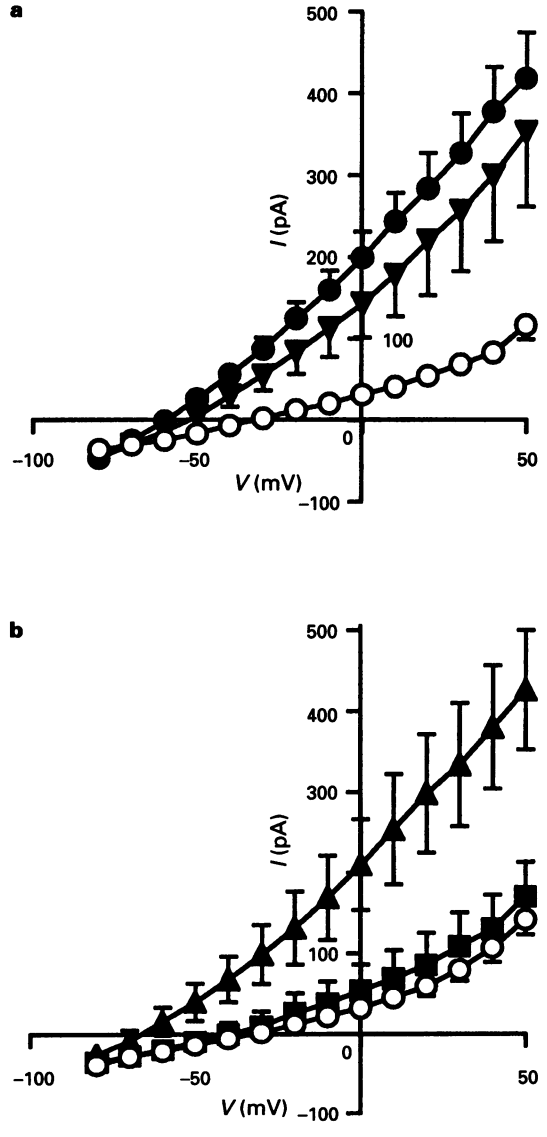

Figure 4 Effect of glibenclamide on the time-dependent current stimulated by BRL55834 or levcromakalim in rat portal vein cells. Under essentially calcium-free conditions (Ca-free pipette solution, Ca-free PSS, see Methods), both BRL55834 (1 μM; ●, a) and levcromakalim (10 μM; ▲, b) induced a voltage- and time-independent current on stepping from a holding potential of −10 mV to test potentials more positive than −60 mV. Subsequent exposure to glibenclamide (10 μM) for 10 min had little effect on the response to BRL55834 (▼, a) but completely inhibited the current induced by levcromakalim (■, b); (○) indicates control currents. Each point represents the mean + and/or − s.e.mean, n = 4–6.

Results

Mechano-inhibitory effects of BRL55834

BRL55834 relaxed strips of bovine trachealis precontracted with histamine, 100 μM. Using a cumulative protocol, the concentration-effect curve for BRL55834 was steep and its effects were very difficult to reverse by prolonged washing. It was thus impossible to determine the glibenclamide sensitivity of BRL55834-induced relaxation using repeated exposure to BRL55834 in the presence of successively increasing concentrations of glibenclamide. Cumulative dose-response experiments to BRL55834 were therefore conducted only once on each tracheal strip, in the presence or absence of glibenclamide. Using this approach, glibenclamide produced a competitive-like inhibition of the mechano-inhibitory effects of BRL55834 (Figure 1a).

To determine whether any component of the action of BRL55834 involved BK_{Ca}, similar experiments were performed in the presence of 250 nM charybdotoxin. To eliminate any charybdotoxin-induced functional antagonism of BRL55834 due to inhibition of BK_{Ca} on nerve terminals and consequent increased transmitter release, these experiments were carried out with 100 nM atropine in the PSS. Under these conditions, charybdotoxin (250 nM) produced a very small contractile effect in two out of four tissues and was without effect on the remaining two preparations. In no preparation was the concentration-effect relationship to BRL55834 significantly modified by charybdotoxin (Figure 1b).

When the trachealis was pre-contracted with 80 mM KCl-Krebs (prepared by isosmolar substitution of KCl for NaCl) the magnitude of the contraction oscillated slowly with time, but nevertheless remained relatively constant. BRL55834 had no effect on the 80 mM KCl-induced contraction. Thus, after 25 min exposure to 10 μM BRL55834 (at the end of an experiment in which BRL55834 10 nM–10 μM was added cumulatively in 10 fold increments at 20 min intervals) the mean contraction was 111.2±20.4% of the initial contraction (n=4) in comparison to the time-matched control (exposed to equivalent concentrations of vehicle) which was 104.1±26.9% of the initial contraction (n=4).

In spontaneously-contracting portal veins, low concentrations of BRL55834 (in the range 3–10 nM) reduced the size of the contractions without any reduction in their frequency. When the concentration of BRL55834 was further increased, contraction frequency was also reduced. As observed in bovine trachealis, these effects of BRL55834 were essentially irreversible even after 100 min of repeated washing and spontaneous contractions only returned to control levels after exposure to 1 μM glibenclamide. Cumulative dose-response experiments to BRL55834 were therefore conducted only once on each vein, in the presence or absence of glibenclamide. Under these conditions, the mechano-inhibitory effects of BRL55834 were antagonized in a competitive manner by pre-exposure to glibenclamide (Figure 1c).

Effect of BRL55834 on whole-cell currents in bovine trachealis cells

Bovine trachealis cells were initially held at 0 mV or −10 mV with Ca-free PSS in the bath and pipette. In the presence of 3 μM BRL55834, a slowly-developing outward current, the noise of which gradually increased, was observed in 5 out of 16 cells. The characteristics of this current (mean amplitude

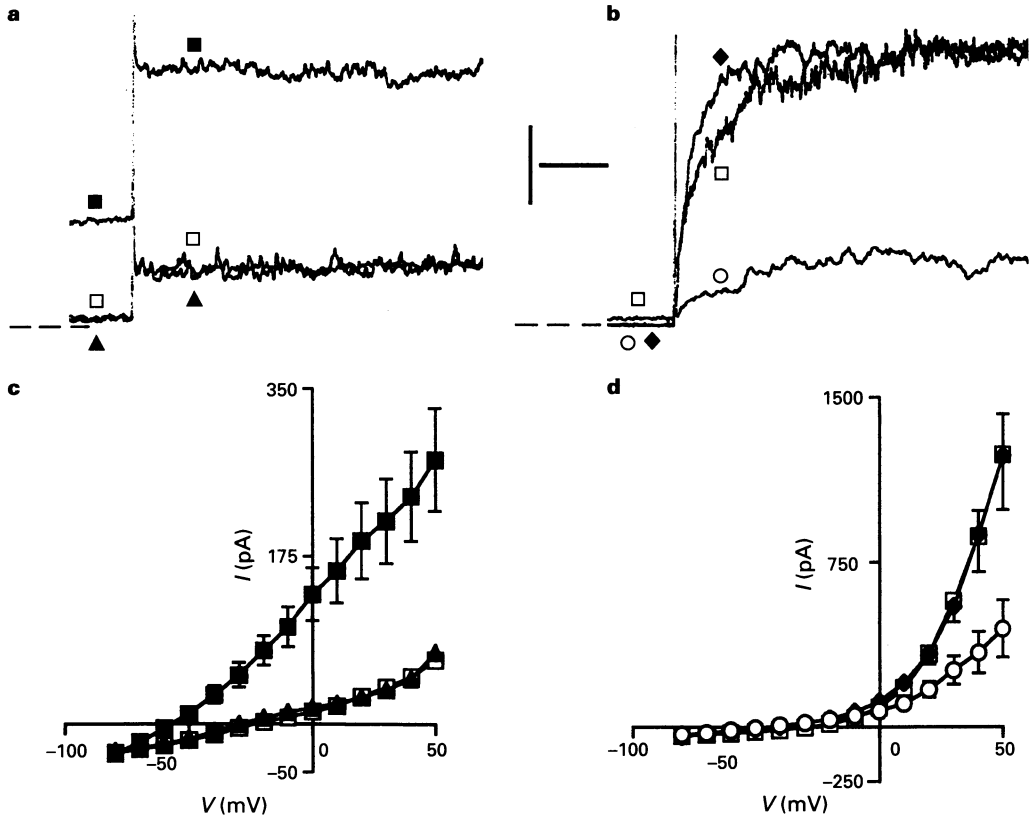

Figure 5 Effect of phentolamine on currents stimulated by BRL55834 or NS1619 in rat portal vein cells. (a), (c) Under essentially calcium-free conditions (Ca-free pipette solution, Ca-free PSS, see Methods) and in the presence of 10 μM glibenclamide, 3 μM BRL55834 (■) induced a voltage- and time-independent K-current which was evident on stepping from a holding potential of −10 mV to test potentials more positive than −70 mV (test potential in (a) was +50 mV). (▲) Represents the control current in the presence of glibenclamide. Subsequent exposure to phentolamine (100 μM; □) completely inhibited the glibenclamide-insensitive K-current induced by BRL55834 within 5 min. When calcium was included in the bath solution (Ca-PSS) and EGTA excluded from the pipette solution (b, d), the control current (○) (observed on stepping to test potentials from a holding current of −10 mV) comprised not only the time-independent current, but also a voltage-dependent current, $I_{BK(Ca)}$ (test potential in (b) was +50 mV). $I_{BK(Ca)}$ was enhanced by NS1619 (33 μM; ◆). In the continued presence of NS1619, phentolamine (100 μM; □) had no effect on the induced peak current. In (a) and (b), the zero current level is indicated by a dashed line. The horizontal calibration bar indicates 100 ms; the vertical bar represents 80 pA (a) or 400 pA (b). Each point in (c) and (d) represents the mean + and/or − s.e.mean, n = 4–6.

130±25 pA, $n=5$; compare Figures 2a and 2b) were similar to those of the glibenclamide-sensitive current induced by levcromakalim, aprikalim and P1060 in single cells from rat portal vein and previously identified as $I_{K(ATP)}$ (Noack *et al.*, 1992a; Edwards *et al.*, 1993; Ibbotson *et al.*, 1993). However, a substantial component (52–67%, $n=5$) of the current induced by 3 μM BRL55834 in bovine trachealis remained after exposure to glibenclamide (10 μM; Figure 2a). This residual current at −10 mV showed none of the characteristics of $I_{BK(Ca)}$ shown in Figure 2c (large amplitude noise and marked outward rectification in the potential range +10 to +50 mV). No increase in an $I_{K(ATP)}$-like current was seen in time-matched control cells ($n=6$).

In 5 (out of 10) tracheal cells held in the range 0 to −10 mV; however, no marked increase in outward current was seen in the presence of 3 μM BRL55834. Instead, after a period of 20–25 min there was an increase in noise at the holding potential (Figure 2c (iii)). Using voltage-step protocols the associated current was found to be outwardly-rectifying, non-inactivating and showed time-dependent activation from a threshold potential of approximately 0 mV (Figure 2c (i), 2c (iii)). It could be readily abolished by subsequent exposure to 100 nM charybdotoxin indicating that the underlying channel was BK_{Ca} (Figure 2c (iii)). When whole-cell currents were generated in time-matched control cells, a charybdotoxin-sensitive current was also induced (Figure 2c (ii)). Thus, although 3 μM BRL55834 appeared to induce $I_{BK(Ca)}$ in some cells tested, very similar increases in $I_{BK(Ca)}$ also occurred in four cells which were not exposed to this agent.

Characteristics of the time-dependent current induced by BRL55834 in portal vein cells

Because of the appearance of $I_{BK(Ca)}$ in the trachealis even in the absence of BRL55834, the effects of this agent were

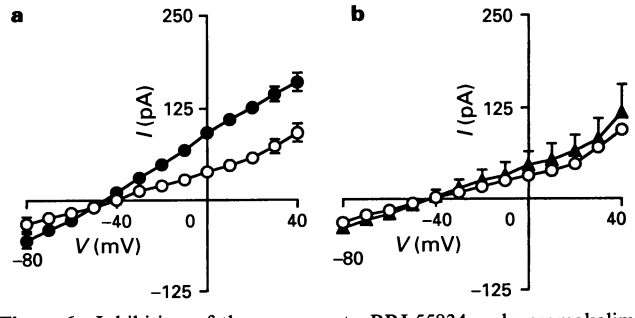

Figure 6 Inhibition of the response to BRL55834 or levcromakalim by AMP-PCP in the pipette solution. Holding potential −10 mV. Under calcium-free conditions (Ca-free pipette solution, Ca-free PSS, see Methods), 3 μM BRL55834 (●, $n=6$) stimulated a small voltage- and time-independent K-current (a). In contrast, 10 μM levcromakalim (▲, $n=3$) had no effect on voltage-independent currents under these conditions (b). (○) Represents control currents. Each point represents the mean + and/or − s.e.mean.

further examined in cells from rat portal vein held at −10 mV in Ca-free PSS. After 10 min exposure of these to 3 μM BRL55834, a slowly-developing outward current, the noise of which gradually increased, was always observed (Figure 3a). Voltage-step protocols showed that the magnitude of a time-independent current was markedly increased (Figure 3a–d). This current reversed at approximately −80 mV, indicating that it was carried by K^+ and its magnitude was not enhanced in the presence of Ca-PSS (Figure 3e).

Effect of glibenclamide As observed in bovine trachealis, the current induced by BRL55834 was only slightly inhibited by subsequent exposure to glibenclamide (Figure 4a), in contrast to the effects of levcromakalim which were abolished. The response to BRL55834 was more markedly reduced by glibenclamide ($P < 0.05$) if the cells were first exposed to this sulphonylurea (compare Figures 4a and 5c). Nevertheless, even after 10 min pre-exposure to glibenclamide (10 μM), BRL55834 (3 μM) was still capable of stimulating a sizeable time-independent K-current (Figure 5a,c). In contrast, the stimulation of $I_{K(ATP)}$ by levcromakalim (10 μM) was almost fully inhibited by 10 min pre-exposure to 10 μM glibenclamide (data not shown, see Edwards *et al.*, 1993).

Effects of AMP-PCP When the pipette solution contained the non-hydrolysable ATP analogue AMP-PCP (5 mM), 3 μM BRL55834 was capable of inducing a small, time-independent current, although under these conditions the response to BRL55834 (68 ± 28 pA at +40 mV, $n = 5$) was reduced compared with that seen in the absence of AMP-PCP (311 ± 28 pA at +40 mV, $n = 5$; see Figures 3d and 6a). In contrast, 10 μM levcromakalim had no effect on $I_{K(ATP)}$ when 5 mM AMP-PCP was present in the pipette (Figure 6b).

Effects of BRL55834 on $I_{BK(Ca)}$ in portal vein cells

The glibenclamide-resistant current induced by 3 μM BRL55834 in portal vein cells was not inhibited by charybdotoxin (up to 250 nM, data not shown). It was, however, completely abolished by phentolamine (100 μM; Figure 5a,c), a concentration which had no effect on the peak $I_{BK(Ca)}$ stimulated by NS1619, the opener of BK_{Ca}, (Figure 5b,d).

The use of NS1619 allowed important comparisons between the characteristics of $I_{BK(Ca)}$ and those of the glibenclamide-resistant current induced by BRL55834. The latter was quasi-instantaneous and voltage-independent (Figure 5a,c) whereas

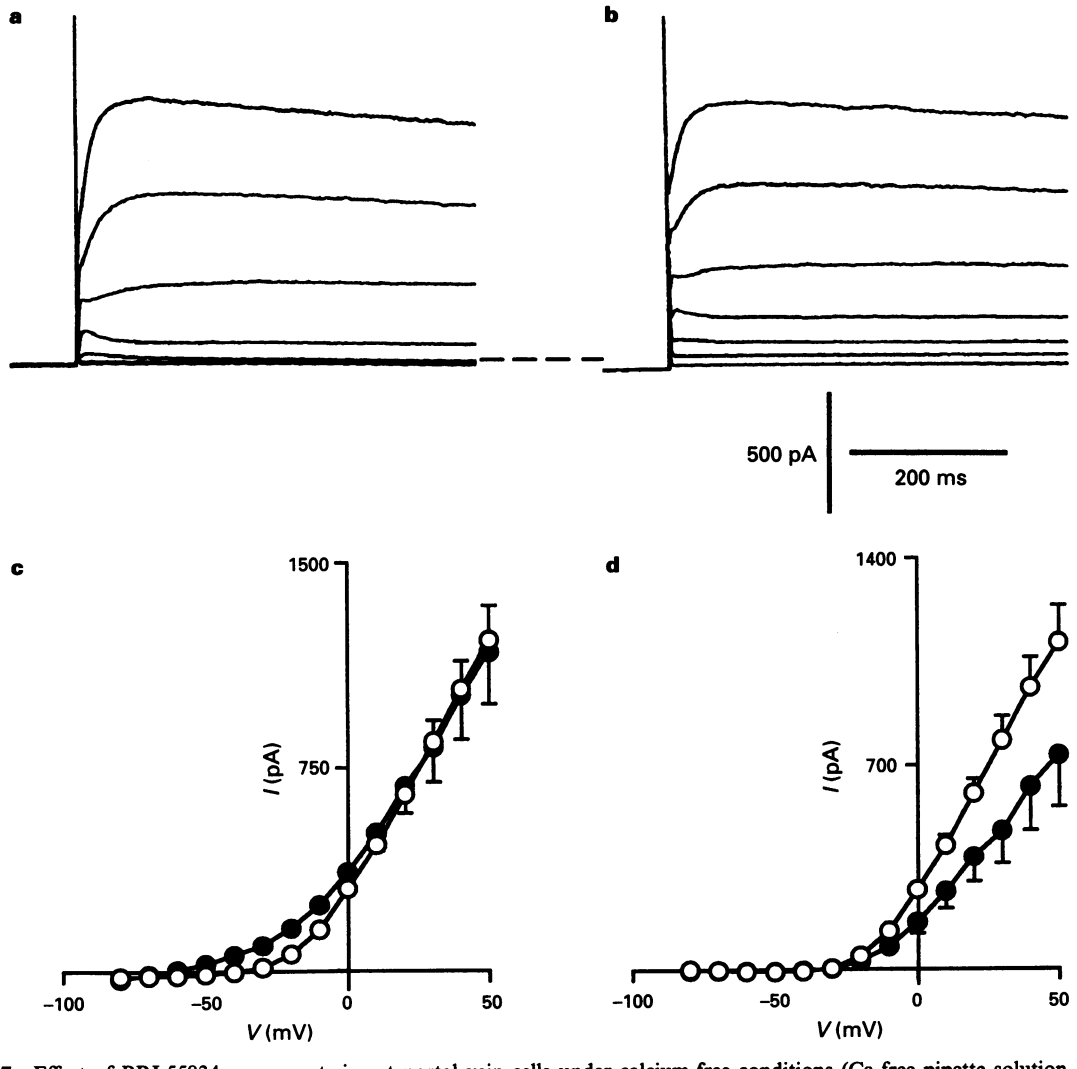

Figure 7 Effect of BRL55834 on currents in rat portal vein cells under calcium-free conditions (Ca-free pipette solution, Ca-free PSS, see Methods). On stepping to test potentials (−80 mV to +40 mV in 20 mV increments) from a holding potential of −90 mV the peak total outward current was similar before (a, ○ in c) or after 10 min exposure to 3 μM BRL55834 (b, ● in c). Each trace in (a) and (b) is the computer-derived average of currents observed in 5 cells from different animals. The horizontal dashed line represents the zero current level. (d) The reduction of $I_{K(V)}$ by BRL55834 ($I_{K(V)}$ was derived by subtracting the currents obtained at each test potential on stepping from −10 mV from the corresponding total currents at the same test potentials). (○) and (●) indicate the control current and current in the presence of BRL55834, respectively. Each point represents the mean ± s.e.mean, $n = 5$.

that stimulated by NS1619 showed time-dependent activation from potentials positive to approximately −10 mV (Figure 5b,d).

Unitary conductance of the time-independent current induced by BRL55834 in portal vein cells

The current induced by BRL55834 exhibited low frequency oscillations (1−5 min^{-1}), the amplitude of which was up to 20 pA at a holding potential of −10 mV. Similar oscillations were observed after presumed ATP depletion or run-down of K_{ATP} (Noack *et al.*, 1992b) and we initially assumed that they represented the opening of an additional K-channel (possibly BK_{Ca}) with a larger unitary conductance than K_{ATP} (Niederste-Hollenberg *et al.*, 1994). However, the voltage-dependencies of the BRL55834-induced current in the presence and absence of glibenclamide were essentially identical (Figure 4a) suggesting that perhaps only one K-channel was involved.

To clarify this, stationary fluctuation analysis of the noise associated with the BRL55834-induced current which remained in the presence of 10 μM glibenclamide at −10 mV was performed as previously described (Noack *et al.*, 1992a,b). Such analysis requires a high sampling rate (to record accurately high-frequency components) coupled with a time interval which is sufficiently long to ensure that the noise signal in the collection period is truly representative and to avoid the possibility of underestimating current variance (Silberberg & Magleby, 1993; Clapp *et al.*, 1994). To overcome limitations of the pClamp software which allowed only 2048 data points to be recorded, the current mean (μ) and variance (σ^2) for several (x) random samples each of 500 ms duration were determined and these values computed to provide the more accurate values, $\mu_{1\to x}$ and $(\sigma_{1\to x})^2$. The algorithms below were used to compute new equivalent values from 2 such samples.

$$\mu_{1\to 2} = (\mu_1 + \mu_2)/2$$

$$\text{and } (\sigma_{1\to 2})^2 = [\sigma_1^2 + \sigma_2^2 + 0.5\,(\mu_1^2) + 0.5\,(\mu_2^2) - \mu_1.\mu_2].0.5$$

The repetitive step-wise use of this procedure was carried out for up to 8 random samples from each of 3 cells to achieve improved accuracy.

These calculations yielded a unitary current value of approximately 0.26 pA which was somewhat smaller than, but still within the same range as, that reported previously by us and by others for $I_{K(ATP)}$ induced by levcromakalim (Noack *et al.*, 1992a; Clapp *et al.*, 1994; Criddle *et al.*, 1994) and substantially less than the NS1619-induced single channel current carried via BK_{Ca} in rat portal vein (Edwards *et al.*, 1994). These calculations provide no evidence for the involvement of BK_{Ca} but are consistent with the view that the glibenclamide-resistant component of the current induced by BRL55834 is carried by K_{ATP}.

Effects of BRL55834 on $I_{K(V)}$ in rat portal vein cells

When rat portal vein cells were held at −90 mV under essentially calcium-free conditions and stepped (in 10 mV increments) to a range of test potentials (−80 to +50 mV), the dominant current was the slowly-activating and -inactivating delayed rectifier K-current, $I_{K(V)}$, which activated at approximately −35 mV (Figure 7a,c; see also Noack *et al.*, 1992a; Edwards *et al.*, 1993). In the presence of BRL55834 3 μM, the total outward current (time-dependent and -independent currents; holding potential −90 mV) obtained on stepping to potentials more positive than +20 mV was unaffected (Figure 7b,c). This indicates that $I_{K(V)}$ must have been simultaneously reduced since BRL55834 markedly increased a time-independent current (see Figure 3). Subtraction of this component from the total current showed the extent to which $I_{K(V)}$ was inhibited by BRL55834 (Figure 7d). The increase in total current observed in the range −50 to 0 mV in the presence of BRL55834 (Figure 7a) was due to the stimulation of a time- and voltage-independent K-current.

Discussion

BRL55834-induced relaxation of bovine trachealis and rat portal vein: effects of glibenclamide

The ability of BRL55834 to relax histamine-contracted strips of bovine trachealis was more or less sensitive to inhibition by glibenclamide depending on the experimental protocol employed. If tissues were first exposed to BRL55834 to obtain a 'control' concentration-response relationship, it was almost impossible to reverse the relaxant effects of this agent by washing. Subsequent exposure to increasing concentrations of glibenclamide did antagonize the relaxant actions of BRL55834 but the extent to which the concentration-effect curve was further shifted to the right by glibenclamide decreased the longer the tissue was exposed to the benzopyran. Similar results were reported by Lawson *et al.* (1993). In contrast, if the tissues were exposed only once to BRL55834 in the presence or absence of glibenclamide, the resulting concentration-dependent relaxations to BRL55834 were antagonized by this sulphonylurea in a competitive-like manner typical of that described for other K-channel openers like levcromakalim (see Edwards & Weston, 1993). A similar, protocol-dependent inhibition of the effects of BRL55834 by glibenclamide was observed in portal vein.

Exposure to charybdotoxin completely failed to antagonise the relaxant actions of BRL55834 on the histamine-precontracted bovine trachealis, findings consistent with those of Lawson *et al.* (1993) on the BRL55834-induced inhibition of spontaneous tone in guinea-pig trachealis. Furthermore, BRL55834 was unable to relax strips of bovine trachealis which had been contracted with 80 mM KCl. Thus these whole tissue data collectively suggest a dominant role for K_{ATP} in the relaxations produced by BRL55834 in both tissues with no evidence of the involvement of BK_{Ca}.

Effects of BRL55834 on K-currents in bovine trachealis

Exposure of bovine isolated trachealis cells to BRL55834 only occasionally induced the typical non-inactivating K-current characteristic of a K-channel opener like levcromakalim. Instead, an outwardly-rectifying, non-inactivating current with a threshold activation potential of approximately −10 mV was more commonly observed. These characteristics, together with the full inhibition of this current by charybdotoxin, initially suggested that BRL55834 was capable of stimulating not only K_{ATP} but also BK_{Ca}. However, in control trachealis cells, $I_{BK(Ca)}$ also developed with time. Since the relaxation produced by BRL55834 in whole tissues was clearly glibenclamide-sensitive and unaffected by charybdotoxin, some change in the properties of the isolated trachealis cells and one which was induced by the enzymatic separation procedures seems likely.

In fact, these cells showed little tolerance to mechanical agitation during cell separation. In addition to long spindle-shaped smooth muscle cells, numerous smaller structures (possibly nuclei) were always apparent. It is thus possible that mechanical agitation damaged the cell membrane and modified ion channel properties in many of the trachealis cells used in the present study. It is therefore likely that the induction of $I_{BK(Ca)}$ by BRL55834 (present study) and the reported opening of BK_{Ca} (Ward *et al.*, 1992) in trachealis cells or patches may be related to some modification of ion channels during cell separation procedures.

Effects of BRL55834 on $I_{K(ATP)}$ and $I_{BK(Ca)}$ in rat portal vein

In view of the difficulties experienced in recording glibenclamide-sensitive currents from bovine trachealis, whole-cell clamp experiments were carried out in portal vein cells. These showed that both BRL55834 and levcromakalim stimulated a voltage-, time- and calcium-independent K-current. However, whereas the current induced by levcroma-

kalim could be almost totally inhibited by subsequent exposure to glibenclamide or by inclusion of the non-hydrolysable ATP analogue, AMP-PCP, in the pipette solution, these procedures were relatively poor inhibitors of the current stimulated by BRL55834. These observations are thus consistent with the findings of the present study and of Lawson *et al.* (1993) that the relaxation of guinea-pig trachealis by BRL55834 was partially glibenclamide-resistant, especially when tissues were exposed to BRL55834 prior to glibenclamide.

There was, however, a marked contrast between the glibenclamide-insensitive current induced by BRL55834 and that stimulated by NS1619, the opener of BK_{Ca} (Edwards *et al.*, 1994; Olesen *et al.*, 1994). $I_{BK(Ca)}$ induced by NS1619 had an activation threshold close to 0 mV and showed marked outward rectification whereas the *I-V* relationship for the glibenclamide-insensitive current produced by BRL55834 showed none of these characteristics and could be fitted by the Goldman-Hodgkin-Katz equation. Furthermore, the total BRL55834-induced current was completely inhibited by phentolamine, an inhibitor of $I_{K(ATP)}$ (Ibbotson *et al.*, 1993). In contrast, this agent had no effect on $I_{BK(Ca)}$ induced by NS1619, actions consistent with the findings of an earlier study in isolated patches from bovine trachealis (Berry *et al.*, 1991). Stationary fluctuation analysis of the noise associated with the current induced by BRL55834 in the presence of glibenclamide also failed to provide evidence for the possible involvement of a large-conductance K-channel in the response to this benzopyran derivative. Indeed, this analysis indicated than even the glibenclamide-resistant current induced by BRL55834 was indistinguishable from $I_{K(ATP)}$.

Why is a component of the BRL55834-induced current glibenclamide- and AMP-PCP-insensitive?

Inhibition by glibenclamide is a characteristic of the current induced by agents like levcromakalim and regarded by many as an indication that K_{ATP} is the ion channel involved (Edwards & Weston, 1993; 1994). Thus the partial glibenclamide-resistance of the K-current induced by BRL55834 could indicate that this compound stimulates the opening of more than one type of K-channel. However, the mechanism by which sulphonylureas inhibit K_{ATP} and antagonize the effects of K_{ATP}-channel openers is still unknown. In general, it is assumed that inhibition follows binding of the sulphonylurea to a plasma-membrane receptor site which is not on K_{ATP} but which is closely associated with the channel (Ashcroft & Ashcroft, 1992; Edwards & Weston, 1993; Ashford *et al.*, 1994). Thus glibenclamide-resistance may not necessarily exclude the possibility that the underlying channel is K_{ATP}. We therefore examined whether the current induced by BRL55834 was ATP-sensitive, an axiomatic feature of K_{ATP} (Ashcroft, 1988; Edwards & Weston, 1993).

We have previously demonstrated that the glibenclamide-sensitive current induced by the K-channel opener, P1060, is substantially inhibited by the inclusion of 5 mM MgATP in the pipette solution (Ibbotson *et al.*, 1993). However, the effects of K_{ATP}-channel openers such as levcromakalim are mimicked by procedures designed to reduce channel phosphorylation, suggesting that these compounds may effectively act as dephosphorylating agents (Edwards *et al.*, 1993). If this is so, then increasing $[ATP]_i$ could stimulate kinase activity and functionally antagonize the effects of the K_{ATP}-channel openers. Since K_{ATP} is inhibited not only by ATP but also by non-hydrolysable ATP analogues such as AMP-PCP (see Ashcroft, 1988), we used this analogue (which does not stimulate kinases) in preference to MgATP.

With AMP-PCP in the pipette, the response to BRL55834 was greatly inhibited and the degree of inhibition of the BRL55834-induced current was much greater than that produced by glibenclamide. Thus a substantial part of the glibenclamide-resistant current must be sensitive to AMP-PCP and, by definition, the underlying channel was presumably K_{ATP}.

A small but significant part of the current induced by BRL55834 was AMP-PCP-resistant which could indicate the involvement of a second K-channel in the action of this benzopyran derivative. However, noise analysis suggested that the glibenclamide-resistant component of the induced current was carried by a single population of channels with a relatively small unitary conductance. Furthermore, like K_{ATP}, the underlying channel showed no voltage-sensitivity and could be fully inhibited by phentolamine. These features, together with the monophasic concentration-relaxation curves to BRL55834 in both trachea and portal vein (which were shifted in a competitive manner by glibenclamide) collectively suggest that BRL55834 stimulates only $I_{K(ATP)}$ but in a manner which is partially glibenclamide-resistant. The involvement of a second channel cannot, however, be totally excluded.

The sulphonylurea receptor site is apparently allosterically linked to the site of action of the K_{ATP}-channel openers (Bray & Quast, 1992; Manley *et al.*, 1993). Thus, a contributory factor in the glibenclamide-resistant effects of BRL55834 (in contrast to those of levcromakalim) may relate to the apparently powerful binding of this agent to its site of action. Evidence for this was obtained in tissue bath experiments in which the mechano-inhibitory effects of this compound were not reversed even by frequent washing for periods of up to 100 min. Similarly, in the whole-cell clamp experiments, the effects of BRL55834 were difficult to reverse by washing, in contrast to those of levcromakalim.

Effect of BRL55834 on K_V

The inhibition of $I_{K(V)}$ by K-channel openers like levcromakalim and which was first highlighted by Noack *et al.* (1992a), was also a feature of the action of BRL55834 in the present study. In fact, the magnitude of the non-inactivating K-current induced by BRL55834 was similar to the absolute amount by which $I_{K(V)}$ was inhibited such that the total current seemed essentially unchanged even at potentials positive of +10 mV. At present, there is no definitive explanation for this phenomenon which has now been described by several workers using a variety of K-channel openers (Edwards *et al.*, 1993; Ibbotson *et al.*, 1993; Clapp *et al.*, 1994; McHugh & Beech, 1995). One possibility is that the 'openers' exert distinct opening and inhibitory effects on two distinct channels, K_V and K_{ATP} (Edwards *et al.*, 1993; Ibbotson *et al.*, 1993). Recently, however, McHugh & Beech (1995) have proposed that the efflux of K^+ through K_{ATP} in the presence of a K-channel opener is so large that the 'supply' of K^+ available to K_V is limited with consequent reduction in $I_{K(V)}$. An alternative explanation is that K_{ATP} is a voltage-insensitive state of K_V (Edwards *et al.*, 1993; Edwards & Weston, 1994). Although this proposition seems untenable for cardiac muscle in which the molecular structure of the first cloned ATP-sensitive K-channel (rcK_{ATP-1}) is very different from that of a typical delayed rectifier channel (Ashford *et al.*, 1994), the mRNA for rcK_{ATP-1} was not detected by these workers in either smooth or skeletal muscle. Further studies are in progress to clarify the mechanisms which underly the dual effects of BRL55834 and of the other K-channel openers on $I_{K(V)}$ and $I_{K(ATP)}$.

Conclusions

In intact trachealis, the relaxant effects of BRL55834 were inhibited by glibenclamide. Although both $I_{K(ATP)}$ and $I_{BK(Ca)}$ were stimulated by BRL55834 in isolated cells from this tissue, the latter, but not the former, developed spontaneously and its appearance was probably associated with changes which occurred during cell separation. In portal vein, the balance of the evidence favours the induction by BRL55834 of only $I_{K(ATP)}$, although the involvement of an additional K-channel which is not BK_{Ca} cannot be totally excluded.

In vitro, BRL55834 was more potent at inhibiting spontaneous contractions in the rat portal vein than in relaxing his-

tamine-precontracted bovine trachealis. Thus the previously-described *in vivo* selectivity of BRL55834 (Bowring *et al.*, 1993) was not reflected *in vitro*. This may result from the pharmacokinetic properties of BRL55834 and here the observed long-lasting effects of BRL55834 compared to those of levcromakalim may be significant. An additional factor is that BRL55834 may depress NANC excitatory neurotransmission in concentrations lower than those required to relax smooth muscle, an effect reported by Burka *et al.* (1991) using levcromakalim. The possibility that such an action of BRL55834 could account for its bronchodilator effects in the absence of the anticipated hypotensive effects (Arch *et al.*, 1994) cannot be excluded and forms the basis of a future study.

BRL55834 was generously supplied by Dr D.R. Buckle (SmithKline Beecham) and NS1619 was kindly donated by Dr S.P. Olesen (NeuroSearch). Helpful discussions with Dr O.B. McManus and with Dr D.J. Beech who also gave access to in press material are gratefully acknowledged. The study was supported by Pfizer Central Research, The Medical Research Council and the Royal Society.

References

ARCH, J.R.S., BOWRING, N.E. & BUCKLE, D.R. (1994). Evaluation of the novel potassium channel activator BRL 55834 as an inhaled bronchodilator in guinea-pig and rats – comparison with levcromakalim and salbutamol. *Pulm. Pharmacol.*, **7**, 121–128.

ASHCROFT, F.M. (1988). Adenosine 5'-triphosphate-sensitive potassium channels. *Annu. Rev. Neurosci.*, **11**, 97–118.

ASHCROFT, S.J.H. & ASHCROFT, F.M. (1992). The sulfonylurea receptor. *Biochim. Biophys. Acta*, **1175**, 45–49.

ASHFORD, M.L.J., BOND, C.T., BLAIR, T.A. & ADELMAN, J.P. (1994). Cloning and functional expression of a rat heart K_{ATP} channel. *Nature*, **370**, 456–459.

BERRY, J.L., ELLIOTT, K.R.F., FOSTER, R.W., GREEN, K.A., MURRAY, M.A. & SMALL, R.C. (1991). Mechanical, biochemical and electrophysiological studies of RP 49356 and cromakalim in guinea-pig and bovine trachealis muscle. *Pulm. Pharmacol.*, **4**, 91–98.

BOWRING, N.E., ARCH, J.R.S., BUCKLE, D.R. & TAYLOR, J.F. (1993). Comparison of the airways relaxant and hypotensive potencies of the potassium channel activators BRL 55834 and levcromakalim (BRL 38227) in vivo in guinea-pigs and rats. *Br. J. Pharmacol.*, **109**, 1133–1139.

BRAY, K.M. & QUAST, U. (1992). A specific binding site for K^+ channel openers in rat aorta. *J. Biol. Chem.*, **267**, 11689–11692.

BURKA, J.F., BERRY, J.L., FOSTER, R.W., SMALL, R.C. & WATT, A.J. (1991). Effects of cromakalim on neurally-mediated responses of guinea-pig tracheal smooth muscle. *Br. J. Pharmacol.*, **104**, 263–269.

CLAPP, L.H., GURNEY, A.M, STANDEN, N.B. & LANGTON, P.D. (1994). Properties of the ATP-sensitive K^+ current activated by levcromakalim in isolated pulmonary arterial myocytes. *J. Membr. Biol.*, **140**, 205–213.

CRIDDLE, D.N., GREENWOOD, I.A. & WESTON, A.H. (1994). Levcromakalim-induced modulation of membrane potassium currents, intracellular calcium and mechanical activity in rat mesenteric artery. *Naunyn Schmied. Arch. Pharmacol.*, **349**, 422–430.

EDWARDS, G., IBBOTSON, T. & WESTON, A.H. (1993). Levcromakalim may induce a voltage-independent K-current in rat portal veins by modifying the gating properties of the delayed rectifier. *Br. J. Pharmacol.*, **110**, 1037–1048.

EDWARDS, G., NIEDERSTE-HOLLENBERG, A., SCHNEIDER, J., NOACK, Th. & WESTON, A.H. (1994). Ion channel modulation by NS 1619, the putative BK_{Ca} channel opener, in vascular smooth muscle. *Br. J. Pharmacol.*, **113**, 1538–1547.

EDWARDS, G., NIEDERSTE-HOLLENBERG, A., SCHNEIDER, J., NOACK, Th. & WESTON, A.H. (1995). Comparison of the effects of levcromakalim and BRL55834 in rat portal vein. *Br. J. Pharmacol.*, **114**, 33p.

EDWARDS, G. & WESTON, A.H. (1993). The pharmacology of ATP-sensitive potassium channels. *Annu. Rev. Pharmacol. Toxicol.*, **33**, 597–637.

EDWARDS, G. & WESTON, A.H. (1994). Effect of potassium channel modulating drugs on isolated smooth muscle. In *Handbook of Experimental Pharmacology*, Volume 111. pp. 469–531. ed: Szerkeres, L. & Papp, J. Gy. Heidelberg: Springer.

EDWARDS, G. & WESTON, A.H. (1995). The pharmacology of the potassium channel openers. *Cardiovasc. Drugs Ther.*, (in press).

FABIATO, A. (1988). Computer programs for calculating total from specified free or free from specified total ionic concentrations in aqueous solutions containing multiple metals and ligands. *Methods Enzymol.*, **157**, 378–417.

GOPALAKRISHNAN, M., JANIS, R.A. & TRIGGLE, D.J. (1993). ATP-sensitive K^+ channels – pharmacologic properties, regulation, and therapeutic potential. *Drug Dev. Res.*, **28**, 95–127.

HAMILL, O.P., MARTY, A., NEHER, E., SAKMANN, B. & SIGWORTH, F.J. (1981). Improved patch clamp techniques for high-resolution current recording from cells and cell-free membrane patches. *Pflügers Arch.*, **391**, 85–100.

HAMILTON, T.C., BEERAHEE, A., MOEN, J.S., PRICE, R.K., RAMJI, J.V. & CLAPHAM, J.C. (1993). Levcromakalim. *Cardiovasc. Drug Rev.*, **11**, 199–222.

IBBOTSON, T., EDWARDS, G., NOACK, Th. & WESTON, A.H. (1993). Effects of P1060 and aprikalim on whole-cell currents in rat portal vein; inhibition by glibenclamide and phentolamine. *Br. J. Pharmacol.*, **108**, 991–998.

ISHIZAWA, T., KOGA, H., SATO, H., MAKINO, T., TAKA, N., TAKAHASHI, T., SATO, T. & NABATA, H. (1994). Substituent effects of benzopyran-4-(N-cyano)carboxamidine potassium channel openers for selectivity to guinea pig trachealis. *Bioorg. Med. Chem. Lett.*, **4**, 1995–1998.

KLÖCKER, U. & ISENBERG, G. (1985). Action potentials and net membrane currents of isolated smooth muscle cells (urinary bladder of the guinea-pig). *Pflügers Arch.*, **405**, 329–339.

KOGA, H., SATO, H., ISHIZAWA, T., KUROMARU, K., NABATA, H., IMAGAWA, J., YOSHIDA, S. & SUGO, I. (1993). N,N-Disubstituted benzopyran-4-(N'-cyano)carboxamidines, cromakalim analogs with selective activity for guinea pig trachealis. *Bioorg. Med. Chem. Lett.*, **3**, 1111–1114.

LAWSON, K., BARRAS, M., ARMSTRONG, J.M. & HICKS, P.E. (1993). Effects of glibenclamide and charybdotoxin on relaxations to the potassium channel activator BRL-55834 in guinea-pig trachea. *Br. J. Pharmacol.*, **110**, 23P.

MANLEY, P.W., QUAST, U., ANDRES, H. & BRAY, K. (1993). Synthesis of and radioligand binding studies with a tritiated pinacidil analogue – receptor interactions of structurally different classes of potassium channel openers and blockers. *J. Med. Chem.*, **36**, 2004–2010.

MCHUGH, D. & BEECH, D. (1995). Inhibition of delayed rectifier K-current by levcromakalim in single intestinal smooth muscle cells: effects of cations and dependence on K^+-flux. *Br. J. Pharmacol.*, **114**, 391–399.

NIEDERSTE-HOLLENBERG, A., SCHNEIDER, J., EDWARDS, G., NOACK, Th. & WESTON, A.H. (1994). Modulation of K-currents in rat portal vein by BRL55834. *Br. J. Pharmacol.*, **113**, 36P.

NOACK, Th., DEITMER, P., EDWARDS, G. & WESTON, A.H. (1992a). Characterization of potassium currents modulated by BRL-38227 in rat portal vein. *Br. J. Pharmacol.*, **106**, 717–726.

NOACK, Th., EDWARDS, G., DEITMER, P. & WESTON, A.H. (1992b). Potassium channel modulation by ATP depletion; a comparison with the effects of levcromakalim (BRL38227). *Br. J. Pharmacol.*, **107**, 945–955.

OLESEN, S.P., MUNCH, E., MOLDT, P. & DREJER, J. (1994). Selective activation of Ca^{2+}-dependent K^+ channels by novel benzimidazolone. *Eur. J. Pharmacol.*, **251**, 53–59.

PIROTTE, B., DETULLIO, P., LEBRUN, P., ANTOINE, M.H., FONTAINE, J., MASEREEL, B., SCHYNTS, M., DUPONT, L., HERCHUELZ, A. & DELARGE, J. (1993). 3-(Alkylamino)-4*H*-pyridol[4,3-e]-1,2,4-thiadiazine 1,1-dioxides as powerful inhibitors of insulin release from rat pancreatic β-cells – a new class of potassium channel openers? *J. Med. Chem.*, **36**, 3211–3213.

SILBERBERG, S.D. & MAGLEBY, K.L. (1993). Preventing errors when estimating single channel properties from the analysis of current fluctuations. *Biophys. J.*, **65**, 1570–1585.

SMALL, R.C., BERRY, J.L., COOK, S.J., FOSTER, R.W., GREEN, K.A. & MURRAY, M.A. (1993). Potassium channels in airways. In *Pharmacology of the Respiratory Tract: Experimental and Clinical Research*. ed. Chung, K.F. & Barnes, P.J. pp. 137–176. New York: Marcel Dekker, Inc.

TAGAYA, E., TAMAOKI, J., ISONO, K., TAKEYAMA, K., CHIYOTANI, A. & KONNO, K. (1994). Modulation of cholinergic neurotransmission by Ca^{2+}-activated K channel and Na^{+}-K^{+}-ATPase in canine airway smooth muscle. *Arerugi*, **43**, 62–67.

TAYLOR, S.G., BUCKLE, D.R., SHAW, D.J., WARD, J.S. & ARCH, J.R.S. (1992). An investigation of the selectivities of BRL 55834 and BRL 38227 as relaxants of guinea-pig tracheal spirals relative to portal vein. *Br. J. Pharmacol.*, **105**, 242P.

WARD, J.S., TAYLOR, S.G. & COLLIER, M.L. (1992). The novel benzopyranol potassium channel activator BRL55834 activates two potassium channels in bovine airway smooth muscle. *Br. J. Pharmacol.*, **107**, 49P.

(Received December 6, 1994
Revised March 13, 1995
Accepted March 20, 1995)

British Journal of Pharmacology (1995) 115, 1038–1042 © 1995 Stockton Press All rights reserved 0007–1188/95 $12.00

Endothelial modulation of vasoconstrictor responses to endothelin-1 in human placental stem villi small arteries

S. Sabry, *F. Mondon, M. Levy, *F. Ferré & [1]A.T. Dinh-Xuan

Laboratoire de Physiologie Respiratoire and Laboratoire de Biologie Cellulaire, CHU Cochin Port-royal, Université René Descartes–Paris V, 27 rue du faubourg Saint-Jacques, 75014 Paris and *INSERM U 361, Paris, France

1 The aim of this study was to assess the role of endothelial cells in the modulation of vasocontractile responses to endothelin-1 (ET-1) of human placental vasculature.

2 Isolated stem villi small arteries (diameter = 170–250 μm) were obtained from healthy parturients who underwent caesarean surgery during the 39th week of pregnancy for cephalo-pelvic disproportion. Isometric tension was measured in vascular rings mounted in a myograph system and challenged with ET-1 (10^{-12} to 10^{-6} M).

3 The vasocontractile response to ET-1 was significantly ($P<0.0001$) increased in endothelial-denuded (active tension = 1156 ± 214 mN mm^{-1}) as compared with endothelial-preserved vascular rings (active tension = 458 ± 48 mN mm^{-1}). This difference was significantly ($P<0.05$) but only partly abolished by the NO synthase inhibitor N^{ω}-nitro-L-arginine (L-NOARG, 10^{-4} M).

4 In endothelial-preserved rings submaximally precontracted with 5-hydroxytryptamine (10^{-6} M), ET-1 (10^{-12} to 10^{-9} M) induced dose-dependent relaxation (maximum relaxation = 70 ± 7%) at 10^{-9} M, which was followed, at higher doses (10^{-8} to 10^{-6} M), by a contraction. In contrast, no relaxation was seen in endothelial-denuded rings. The relaxation in rings with endothelium was significantly ($P<0.001$) reduced by L-NOARG (10^{-4} M). Moreover, it was totally abolished by combined pretreatment with L-NOARG (10^{-4} M) and the sulphonylurea glibenclamide (10^{-5} M).

5 In conclusion, endothelial cells modulate the vascular responses to ET-1 through the release of NO and a substance acting on the ATP-sensitive K^+ channel of smooth muscle of stem villi small arteries from healthy parturients.

Keywords: Nitric oxide; endothelium-derived hyperpolarizing factor; glibenclamide; ATP-sensitive K^+ channels

Introduction

Pharmacological responses of isolated blood vessels to various vasoactive agonists are modulated by endothelial cells which can release both dilator and constrictor substances. Dilator substances include nitric oxide (NO) and an unidentified endothelium-derived hyperpolarizing factor (EDHF). NO activates the soluble enzyme guanylate cyclase, whereas EDHF hyperpolarizes vascular smooth muscle by opening membrane K^+ channels (Taylor & Weston, 1988). Although recent evidence suggests that NO also causes hyperpolarization (Bolotina *et al.*, 1994), as does EDHF, it is still debated as to whether NO and EDHF are the same or two different compounds (Tare *et al.*, 1990).

Constrictor substances are mainly represented by a family of structurally related 21 amino-acid peptides, termed endothelin (ET) (Yanagisawa *et al.*, 1988), which includes three different isoforms, ET-1, ET-2 and ET-3 (Inoue *et al.*, 1989). The vasoactive properties of ET-1 are complex, depending in part on the dose and route of administration, initial blood pressure in the experimental animal used, and the type of vascular bed (De Nucci *et al.*, 1988; Lippton *et al.*, 1989). ET-1 produces potent and long-lasting vasoconstriction in a large variety of vascular beds from several species (Sakata *et al.*, 1989; Yanagisawa & Masaki, 1989), including man (Maggi *et al.*, 1989). In addition, ET-1 exerts potent mitogenic effects on vascular smooth muscle and mesangial cells (Komuro *et al.*, 1988; Simonson *et al.*, 1989). It is therefore suggested that ET-1 might be an important pathogenic factor for vascular remodelling and vasospasm (Lerman *et al.*, 1991). By contrast, ET-1 also causes vasorelaxation by inducing endothelial release of prostacyclin (De Nucci *et al.*, 1988), NO (Tod & Cassin, 1992; Warner *et al.*, 1989), and EDHF (Nakashima & Vanhoutte, 1993). It is also likely that part of the vasodilator effect of ET-1 is mediated by activation of K^+ channels on vascular smooth muscle, as these effects are inhibited by various K^+ channel blockers (Hasunuma *et al.*, 1990; Lippton *et al.*, 1991).

The foeto-placental vasculature is not innervated (Fox & Khong, 1990). Modulation of its tone thus relies entirely on local and/or circulating vasoactive factors. Specific and high affinity binding sites for ET-1 have been characterized on smooth muscle of foeto-placental vasculature (Robaut *et al.*, 1991; Mondon *et al.*, 1993). As ET-1 immunoreactivity is detected in endothelium of placental vessels and in villi syncytiotrophoblast (Ferré *et al.*, 1993), a paracrine and autocrine action of the peptide in placental physiology is likely. Whilst it is known that ET-1 exerts potent vasoconstrictor effects on foeto-placental blood vessels (Wilkes *et al.*, 1990; Gude *et al.*, 1991; MacLean *et al.*, 1992; Myatt *et al.*, 1992; Sabry *et al.*, 1995), the modulatory role of endothelial cells on ET-1-induced vasoconstriction in this particular vascular bed is as yet uncertain. As the placenta plays a pivotal role in nutrient transport and oxygen delivery from the mother to the foetus, it is important to know whether endothelial dysfunction leads to increased vasoconstriction of foeto-placental vessels to ET-1. We therefore examined the influence of the endothelium and, in particular two of its products, NO and EDHF, on the vascular responses to ET-1. We have chosen to test placental stem villi small arteries in this study as these vessels are believed to contribute to the establishment of the foeto-placental resistance in man (Kaufmann, 1982; Leiser *et al.*, 1991).

[1]Author for correspondence.

Methods

Tissue preparation

Placentae were collected immediately after elective caesarean section from healthy parturients in whom cephalopelvic disproportion had been diagnosed. The caesarean section was performed whilst the patients were under thiopentone sodium succinylcholine anaesthesia, and it took place during the 39th week of pregnancy, outside the labour period. No preoperative medication except for atropine was given. All parturients underwent normal pregnancy and non had evidence of pulmonary, renal or cardiovascular disorders.

Immediately after delivery, pieces of placenta were excised between the decidual and chorionic plates. The tissue was then immersed in a receptacle filled with preoxygenated Krebs solution and was transported to the laboratory for dissection. Stem villi small arteries were carefully isolated from placenta tissue, cleaned under the light microscope, and cut into rings 2 mm in length and 170–250 μm internal diameter. In some vascular rings, the endothelium was carefully removed by gently rubbing the intimal surface with a knotted human hair (Osol *et al.*, 1989). After dissection, placental stem villi small arteries were mounted under the microscope as vascular rings by threading the vessels onto two tungsten wires (25 μm diameter). The wires were secured to supports connected to a force transducer, on the one hand, and a micrometer on the other (Mulvany & Halpern, 1977). Dissection and mounting of the rings were performed in Krebs solution at room temperature. The composition of the Krebs solution was as follows (in mM: NaCl 118, $NaHCO_3$ 25.5, KCl 5.9, $NaHPO_4$ 1.2, $MgSO_4$ 1.2, $CaCl_2$ 2.5 and glucose 5.6). The buffered solution was bubbled with 95% O_2 and 5% CO_2 and maintained at 37°C by a recirculating heater system.

Once mounted, the vessels were warmed at 37°C and allowed to equilibrate in Krebs solution for 15 min, with an initial internal circumference set to give a slight wall tension of 0.2 mN mm^{-1}. The resting tension-internal circumference relationship was then determined. From this, we applied the Laplace law to calculate the effective pressure, i.e. the pressure necessary to extend the vessel to the measured internal circumference (Mulvany & Halpern, 1977):

$$\text{effective pressure} = \frac{\text{wall tension} \times 2\pi}{\text{internal circumference}}$$

The corresponding curve of effective pressure as a function of internal circumference was then constructed using a computer programme (Shart, AD Instruments Ltd, London). Then, the rings were set to an internal circumference equivalent to 90% of what they would have if relaxed *in situ* under transmural pressure of 80 mmHg. The latter was estimated as in the *in vivo* distension pressure of human stem villous arterioles (Wilkin, 1958). It is known that near-maximal active wall tension is developed when the ring is set at this internal circumference (Mulvany & Aalkjaer, 1990). After completion of the progressive stretching procedure to determine the normalized internal circumference, each individual ring was allowed to equilibrate for 1 h.

Experimental protocol

After an initial challenge with KCl (60 mM), all vessels were washed and allowed to rest until the tension again reached the baseline. Vasoconstrictor effects were tested by challenging rings, both with and without endothelium, with cumulative concentrations of ET-1 (10^{-2} to 10^{-6} M). Vasorelaxant effects of ET-1 (10^{-12} to 10^{-6} M) were tested in rings with endothelium submaximally precontracted with 5-HT (10^{-6} M), a potent vasoconstrictor agonist for the foeto-placental vasculature (Sabry *et al.*, 1995). Some vessels were incubated with N^{ω}-nitro-L-arginine (L-NOARG; 10^{-4} M) for 30 min to inhibit NO synthesis. Others were incubated with both L-NOARG and the sulphonylurea glibenclamide (10^{-5} M), for 20 min to inhibit both NO production and activity of the ATP-sensitive K^+ channel. All vessels were preincubated for 30 min with indomethacin (10^{-5} M) to inhibit synthesis of prostanoids. Relaxation with 10^{-6} M acetylcholine (ACh) was tested in all vascular preparations to assess the functional integrity of endothelium.

Different vascular segments were used at each time due to the long lasting effects of ET-1.

Drugs

ET-1 was obtained from Neosystem (Strasbourg, France), whereas ACh, indomethacin, L-NOARG and 5-HT were purchased from Sigma (St Louis, Missouri, U.S.A.). Glibenclamide was obtained from Hoechst (Paris, France). All drugs were freshly prepared before use. Dilution of all chemicals was carried out in distilled water except for indomethacin, which was dissolved in ethanol (final bath concentration 0.01%).

Statistical analysis

Results were expressed as active tension values (mN mm^{-1}) when comparisons were made between rings obtained from different placentae. For comparisons between rings obtained from the same placenta, results were expressed as % maximal contraction in response to ET-1 (10^{-6} M). ANOVA for repeated measurements was used to compare the effects of ET-1 in rings with and without endothelium, and to assess the effects of L-NOARG either alone or in combination with glibenclamide as compared with control rings. All data are expressed as mean ± s.e.mean. A P value of less than 0.05 was considered significant.

Results

The effects of ET-1 on the vasocontractile responses of rings with and without endothelium are illustrated in Figure 1. Removal of the endothelium resulted in a significantly greater vasoconstrictor response to ET-1, increasing the active tension from 458 ± 48 mN mm^{-1} in rings with endothelium ($n=9$) to 1156 ± 214 mN mm^{-1} in rings without endothelium ($n=7$) ($P<0.0001$) (Figure 1).

The role played by NO in modulation of the vasocontractile response to ET-1 was assessed in a separate set of experiments

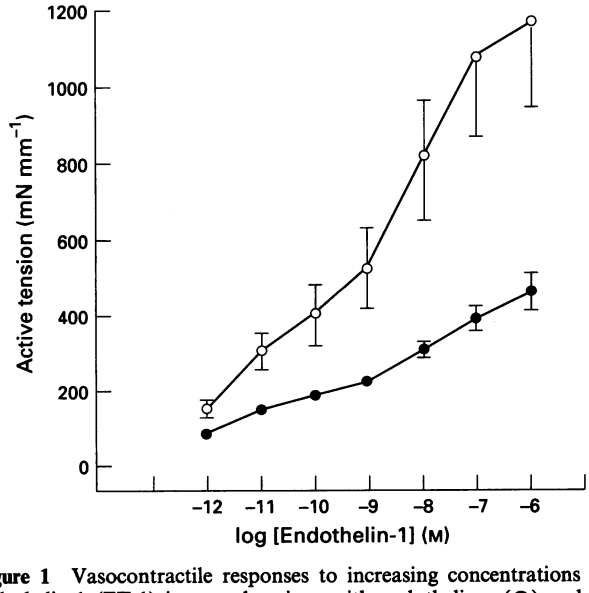

Figure 1 Vasocontractile responses to increasing concentrations of endothelin-1 (ET-1) in vascular rings with endothelium (●) and in rings where the endothelium had been removed (○). Results are expressed as means ± s.e.mean of 7 to 9 observations.

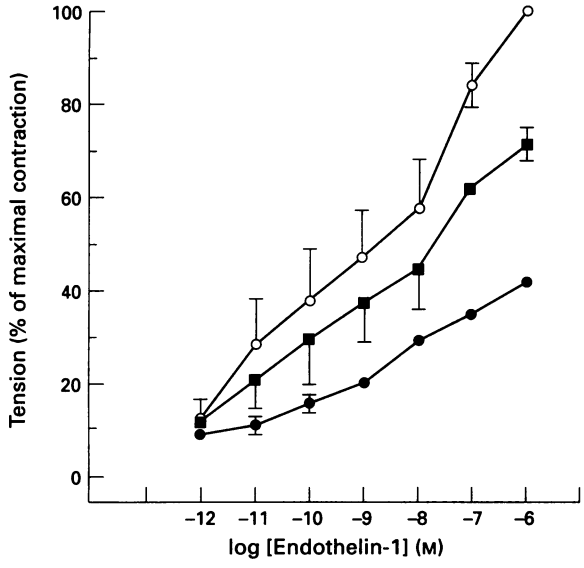

Figure 2 Vasocontractile responses to increasing concentrations of endothelin-1 (ET-1) in vascular rings with endothelium, either untreated (●) or preteated with N^{ω}-nitro-L-arginine (■), and in rings where the endothelium had been removed (○). Results are expressed as means ± s.e.mean of 3 observations.

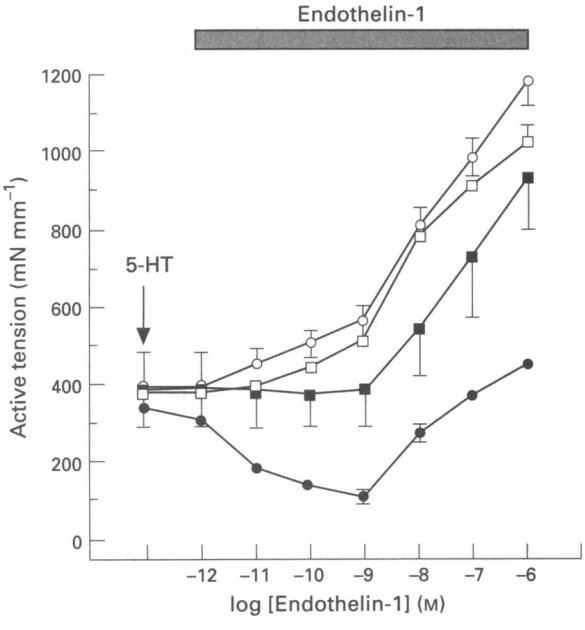

Figure 3 Effects of pretreatment with N^{ω}-nitro-L-arginine (L-NOARG) (■) and the combination of L-NOARG and glibenclamide (□) on responses to endothelin-1 in rings precontracted with 5-hydroxytryptamine (5-HT, 10^{-6} M). Pretreated rings with endothelium were compared with control rings with (●) and without (○) endothelium. Results are expressed as means ± s.e.mean of 4 observations.

where 3 rings obtained from the same placenta were tested at the same time (Figure 2). The first two rings either had their endothelium removed or left intact, whereas the third ring, in which the endothelium was preserved, was pretreated with L-NOARG (10^{-4} M). Thus, 9 rings obtained from 3 placentae were tested in this set of experiments. A significantly ($P<0.001$) greater vasocontractile response to ET-1 was again seen in rings without endothelium as compared with rings with endothelium (Figure 2). However pretreatment with L-NOARG (10^{-4} M) of rings with endothelium significantly ($P<0.05$), but incompletely, abolished the vasorelaxation (Figure 2).

In a last set of experiments, 4 rings obtained from the same placenta were studied at the same time (Figure 3). The first three rings underwent the same protocol as that previously described for Figure 2, whereas the fourth ring was pretreated with a combination of L-NOARG (10^{-4} M) and glibenclamide (10^{-5} M). Thus, 16 rings obtained from 4 placentae were tested in this set of experiments. To determine whether ET-1 had any vasorelaxant effects, increasing concentrations of ET-1 (10^{-12} to 10^{-6} M) were tested in rings submaximally precontracted with 5-HT (10^{-6} M). Rings with endothelium relaxed when low concentrations of ET-1 (10^{-12} to 10^{-9} M) were applied, eliciting maximum relaxation (70 ± 7%) at 10^{-9} M (Figure 3). This relaxation was endothelium-dependent as no relaxation was seen when the endothelium was removed. Moreover, removal of the endothelium caused a further contraction of the rings. The relaxation in rings with endothelium was partly abolished with L-NOARG (10^{-4} M) pretreatment, whereas it was totally abolished by combined pretreatment with L-NOARG (10^{-4} M) and glibenclamide (10^{-5} M) (Figure 3).

Discussion

The main results of this study indicate (i) that endothelial cells exert a modulatory effect on ET-1-induced vasoconstriction in small stem villi arteries from healthy term parturients, and (ii) that this modulatory effect is mediated by vasodilator substances which are released from endothelial cells upon ET-1 stimulation.

In a recent study, we have demonstrated that ET-1 is approximately 1,000 times more potent than 5-HT and phenylephrine in causing vasoconstriction of the stem villi small arteries (Sabry *et al.*, 1995). Data from the present study show that ET-1-induced vasoconstriction is even more accentuated when the endothelium is removed (Figure 1). This suggests that ET-1 stimulates the release of one (or several) vasodilator substances from the endothelium. These dilator substances act, in turn, by a braking mechanism to reduce the ET-1-induced contraction of smooth muscle of the stem villi arteries. This hypothesis is further supported by our findings that ET-1, at low concentrations (10^{-12} to 10^{-9} M), causes relaxation of vascular rings that had been submaximally precontracted with 5-HT. This relaxation is endothelium-dependent, as no relaxation was seen in rings where the endothelium had been mechanically removed. It is likely that at these relatively low concentrations, ET-1 acts mainly on endothelial cells by causing the release of endothelial vasodilator substances. Higher concentrations of ET-1 (10^{-8} to 10^{-6} M) cause vasoconstriction, probably as a result of a predominant effect of ET-1 on vascular smooth muscle.

To determine the nature of vasodilator substances which are released from endothelial cells upon ET-1 stimulation, we examined, in two separate sets of experiments, the influence of the NO synthase inhibitor L-NOARG (Ishii *et al.*, 1990; Moore *et al.*, 1990), and of the combination of L-NOARG and the ATP-sensitive K^+ channel blocker, glibenclamide. Vascular rings preincubated for 30 min with L-NOARG significantly lost their ability to relax with low concentrations of ET-1. This suggests that a major portion of relaxation induced by ET-1 was indeed mediated by NO. Our observation is consistent with reports from previous studies on the role of NO in the vasorelaxant effects of ET-1 in various vascular beds of several species (De Nucci *et al.*, 1988; Sakata *et al.*, 1989; Tod & Cassin, 1992) and extends these results to human foeto-placental vasculature.

The vasorelaxant response to ET-1 is, however, incompletely inhibited by L-NOARG, notwithstanding the fact that large amounts of this NO synthase inhibitor were used. Inefficiency of L-NOARG in completely inhibiting NO production might be one explanation. However, a more likely

explanation is that ET-1 induces the release of vasodilator substances different from NO. Several authors have suggested that EDHF could be one such substance (VanRenterghem, 1988; Brayden, 1990). The identity of EDHF remains elusive (Suzuki & Chen, 1990). However, compelling evidence suggests that this endothelial factor acts mainly on the ATP-sensitive K^+ channel (Standen *et al.*, 1989), which can be specifically blocked by agents such as the sulphonylurea glibenclamide (Quast & Cook, 1989). Because there is some evidence to suggest that NO also causes hyperpolarization of the vascular smooth muscle (Tare *et al.*, 1990), it is not clear whether EDHF can be identified with NO or whether they are two separate endothelial products. However, more recent evidence suggests that hyperpolarization of vascular smooth muscle caused by NO is mediated primarily by activation of a calcium-dependent channel (Archer *et al.*, 1994; Bolotina *et al.*, 1994), probably through an increase in guanosine 3':5'-cyclic monophosphate (cyclic GMP) and subsequent stimulation of cyclic GMP-dependent protein kinase (Archer *et al.*, 1994). It is, therefore, likely that NO and EDHF, which activate two different K^+ channels (i.e., the calcium-dependent K^+ channel and the ATP-sensitive K^+ channel, respectively), are two different compounds. Consistent with this hypothesis is our demonstration of complete inhibition of the vasodilator response to ET-1 by a combination of L-NOARG and glibenclamide. This suggests that the L-arginine-NO pathway on the one hand, and ATP-sensitive K^+ channel activation, on the other, account for all the vasodilator effects of ET-1 in human stem villi arteries.

Compelling evidence now suggests that ET-1 may play a role in the physiology and pathophysiology of the foeto-placental circulation in man. Indeed, plasma levels of ET-1 are elevated in preeclampsia as compared with normal pregnancy (Mastrogiannis *et al.*, 1991; Nova *et al.*, 1991; Clark *et al.*, 1992). Furthermore, high levels of ET-1 are closely related with biological markers of renal impairment in preeclampsia (Clark *et al.*, 1992). ET-1 levels also appear to rise late in gestation in normal pregnant women (Clark *et al.*, 1992). It is still uncertain as to whether increased ET-1 levels could indirectly (through the release of NO and EDHF) contribute to the decrease in vascular resistance, which normally occurs during late gestation (Greiss, 1966; Peeters *et al.*, 1980). Nevertheless, it is likely that functional integrity of the endothelium could affect in a critical manner the vascular responses to ET-1 in both healthy and high risk pregnancies (McQueen *et al.*, 1993).

This study was supported by grants from the Mutuelle Générale de l'Éducation Nationale and from the Délégation à la Recherche Clinique, Assistance Publique-Hôpitaux de Paris.

References

ARCHER, S.L., HUANG, J.M.C., HAMPL, V., NELSON, D.P., SHULTZ, P.J. & WEIR, E.K. (1994). Nitric oxide and cGMP cause vasorelaxation by activation of a charybdotoxin-sensitive K channel by cGMP-dependent protein kinase. *Proc. Natl. Acad. Sci. U.S.A.*, **91**, 7583–7587.

BOLOTINA, V.M., NAJIBI, S., PALACINO, J.J., PAGANO, P.J. & COHEN, R.A. (1994). Nitric oxide directly activates calcium-dependent potassium channels in vascular smooth muscle. *Nature*, **368**, 850–853.

BRAYDEN, J.E. (1990). Membrane hyperpolarization is a mechanism of endothelium-dependent cerebral vasodilatation. *Am. J. Physiol.*, **259**, H668–H673.

CLARK, B.A., HALVORSON, L., SACHS, B. & EPSTEIN, F.H. (1992). Plasma endothelin levels in preeclampsia: elevation and correlation with uric acid levels and renal impairment. *Am. J. Obstet. Gynecol.*, **166**, 962–968.

DE NUCCI, G., THOMAS, R., D'ORLEANS-JUSTE, P., ANTUNES, E., WALDER, C., WARNER, T.D. & VANE, J.R. (1988). Pressor effects of circulating endothelin are limited by its removal in the pulmonary circulation and by the release of prostacyclin and endothelium-derived relaxing factor. *Proc. Natl. Acad. Sci. U.S.A.*, **85**, 9797–9800.

FERRÉ, F., MONDON, F., MIGNOT, T.M., CRONIER, L., CAVERO, I., ROSTÈNE, W. & MALASSINÉ, A. (1993). Endothelin-1 binding sites and immunoreactivity in the cultured human placental trophoblast: evidence for an autocrine and paracrine role for endothelin-1. *J. Cardiovasc. Pharmacol.*, **22** (Suppl. 8), S214–S218.

FOX, S.B. & KHONG, T.Y. (1990). Lack of innervation of human umbilical cord: an immunohistological and histochemical study. *Placenta*, **11**, 59–62.

GREISS, Jr, F.C. (1966). Pressure-flow relationship in the gravid uterine vascular bed. *Am. J. Obstet. Gynecol.*, **96**, 41–47.

GUDE, N.M., KING, R.G. & BRENNECKE, S.P. (1991). Endothelin: release by and potent constrictor effect on the fetal vessels of human perfused placental lobules. *Reprod. Fertil. Dev.*, **3**, 495–500.

HASUNUMA, K., RODMAN, D.M., O'BRIEN, R.F. & MCMURTRY, I.F. (1990). Endothelin 1 causes pulmonary vasodilatation in rats. *Am. J. Physiol.*, **259**, H48–H54.

INOUE, A., YANAGISAWA, M., KIMURA, S., KASUYA, Y., MIYAUCHI, T., GOTO, K. & MASAKI, T. (1989). The human endothelin family: three structurally and pharmacologically distinct isopeptides predicted by three separate genes. *Proc. Natl. Acad. Sci. U.S.A.*, **86**, 2863–2867.

ISHII, K., CHANG, B., KERWIN, J.F., HUANG, Z.J. & MURAD, F. (1990). N^{ω}-nitro-L-arginine: a potent inhibitor of endothelium-derived relaxing factor formation. *Eur J. Pharmacol.*, **176**, 219–223.

KAUFMANN, P. (1982). Development and differentiation of the human placental villous tree. *Bibl. Anat.*, **22**, 29–39.

KOMURO, I., KURIHARA, H., SUGIYAMA, T., TAKAKU, F. & YAZAKI, Y. (1988). Endothelin stimulates c-fos and c-myc expression and proliferation of vascular smooth muscle cells. *FEBS Lett.*, **238**, 249–252.

LEISER, R., KOSANKE, G. & KAUFMANN, P. (1991). In *Placenta Basic Research for Clinical Application*. ed. Soma, H. Basel: Karger.

LERMAN, A., EDWARDS, B.S., HALLETT, J.W., HEUBLEIN, D.M., SANDBERG, S.M. & BURNETT, Jr, J.C. (1991). Circulating and tissue endothelin immunoreactivity in advanced atherosclerosis. *N. Engl. J. Med.*, **325**, 997–1001.

LIPPTON, H.L., COHEN, G.A., MCMURTRY, I.F. & HYMAN, A.L. (1991). Pulmonary vasodilatation to endothelin isopeptides *in vivo* is mediated by potassium channel activation. *J. Appl. Physiol.*, **70**, 947–952.

LIPPTON, H.L., HAUTH, T.A., SUMMER, W.R. & HYMAN, A.L. (1989). Endothelin produces pulmonary vasoconstriction and systemic vasodilation. *J. Appl. Physiol.*, **66**, 1008–1012.

MCLEAN, M.R., TEMPLETON, A.G.B. & MCGRATH, J.C. (1992). The influence of endothelin-1 on human foeto-placental blood vessels: a comparison with 5-hydroxytryptamine. *Br. J. Pharmacol.*, **106**, 937–941.

MAGGI, C.A., GIULIANI, S., PATACCHINI, R., ROVERO, P., GIACHETTI, A. & MELI, A. (1989). The activity of peptides of the endothelin family in various mammalian smooth muscle preparations. *Eur. J. Pharmacol.*, **174**, 23–31.

MASTROGIANNIS, D.S., O'BRIEN, W.F., KRAMMER, J. & BENOIT, R. (1991). Potential role of endothelin-1 in normal and hypertensive pregnancies. *Am. J. Obstet. Gynecol.*, **165**, 1711–1716.

MCQUEEN, J., KINGDOM, J.C.P., CONNELL, J.M.C. & WHITTLE, M.J. (1993). Fetal endothelin levels and placental vascular endothelin receptors in intrauterine growth retardation. *Obstet. Gynecol.*, **82**, 992–998.

MONDON, F., MALASSINÉ, A., ROBAUT, C., VIAL, M., BANDET, J., TANGUY, G., ROSTÈNE, W., CAVERO, I. & FERRÉ, F. (1993). Biochemical characterization and autoradiographic localization of [^{125}I]endothelin-1 binding sites on trophoblast and blood vessels of human placenta. *J. Clin. Endocrinol. Metab.*, **76**, 237–244.

MOORE, P.K., AL-SWAYEH, O.A., CHONG, N.W.S., EVANS, R.A. & GIBSON, A. (1990). L-N^G-nitro-arginine, (L-NOARG), a novel L-arginine-reversible inhibitor of endothelium-dependent vasodilatation *in vitro*. *Br. J. Pharmacol.*, **99,** 408–412.

MULVANY, M.J. & AALKJAER, C. (1990). Structure and function of small arteries. *Physiol. Rev.*, **70,** 921–961.

MULVANY, M.J. & HALPERN, W. (1977). Contractile properties of small arterial resistance vessels in spontaneously hypertensive and normotensive rats. *Circ. Res.*, **41,** 19–26.

MYATT, L., BREWER, A.S. & BROCKMAN, D.E. (1992). The comparative effects of big endothelin-1, endothelin-1, and endothelin-3 in the human fetal-placental circulation. *Am. J. Obstet. Gynecol.*, **167,** 1651–1656.

NAKASHIMA, M. & VANHOUTTE, P.M. (1993). Endothelin-1 and -3 cause endothelium-dependent hyperpolarization in the rat mesenteric artery. *Am. J. Physiol.*, **265,** H2137–H2141.

NOVA, A., SIBAI, B.M., BARTON, J.R., MERCER, B.M. & MITCHELL, M.D. (1991). Maternal plasma level of endothelin is increased in preeclampsia. *Am. J. Obstet. Gynecol.*, **165,** 724–727.

OSOL, G., CIPOLLA, M. & KNUTSON, S. (1989). A new method for mechanically denuding the endothelium of small (50–150 μm) arteries with a human hair. *Blood Vessels*, **26,** 320–324.

PEETERS, L.L., GRUTTERS, G. & MARTIN, C.B. (1980). Distribution of cardiac output in the unstressed pregnant guinea-pig. *Am. J. Obstet. Gynecol.*, **138,** 1177–1184.

QUAST, U. & COOK, N.S. (1989). Moving together: K^+ channel openers and ATP-sensitive K^+ channels. *Trends Pharmacol. Sci.*, **10,** 431–435.

ROBAUT, C., MONDON, F., BANDET, J., FERRÉ, F. & CAVERO, I. (1991). Regional distribution and pharmacological characterization of [^{125}I] endothelin-1 binding sites in human fetal placental vessels. *Placenta*, **12,** 55–67.

SABRY, S., MONDON, F., FERRÉ, F. & DINH-XUAN, A.T. (1995). *In vitro* contractile and relaxant responses of human resistance placental stem villi arteries of healthy parturients: role of endothelium. *Fund. Clin. Pharmacol.*, **9,** 46–51.

SAKATA, K., OZAKI, H., KWON, S.C. & KARAKI, H. (1989). Effects of endothelin on the mechanical activity and cytosolic calcium levels of various types of smooth muscle. *Br. J. Pharmacol.*, **98,** 483–492.

SIMONSON, M.S., WANN, S., MENÉ, P., DUBYAK, G.R., KESTER, M., NAKAZATO, Y., SEDOR, J.R. & DUNN, M.J. (1989). Endothelin stimulates phospholipase C, Na^+/H^+ exchange, c-fos expression, and mitogenesis in rat mesangial cells. *J. Clin. Invest.*, **83,** 708–712.

STANDEN, N.B., QUAYLE, J.M., DAVIES, N.W., BRAYDEN, J.E., HUANG, Y. & NELSON, M.T. (1989). Hyperpolarizing vasodilators activate ATP-sensitive K^+ channels in arterial smooth muscle. *Science*, **245,** 177–180.

SUZUKI, H. & CHEN, G. (1990). Endothelium-derived hyperpolarizing factor (EDHF): an endogenous potassium-channel activator. *News Physiol. Sci.*, **5,** 212–215.

TARE, M., PARKINGTON, H.C., COLEMAN, H.A., NEILD, T.O. & DUSTING, G.J. (1990). Hyperpolarization and relaxation of arterial smooth muscle caused by nitric oxide derived from the endothelium. *Nature*, **346,** 69–71.

TAYLOR, S.G. & WESTON, A.H. (1988). Endothelium-derived hyperpolarizing factor: a new endogenous inhibitor from the vascular endothelium. *Trends Pharmacol. Sci.*, **9,** 272–274.

TOD, M.L. & CASSIN, S. (1992). Endothelin-1-induced pulmonary arterial dilatation is reduced by N^{ω}-nitro-L-arginine in fetal lambs. *J. Appl. Physiol.*, **72,** 1730–1734.

VAN RENTERGHEM, C., VIGNE, P., BARHANIN, J., SCHMID-ALLIANA, A., FRELIN, C. & LAZDUNSKI, M. (1988). Molecular mechanism of action of the vasoconstrictor peptide endothelin. *Biochem. Biophys. Res. Commun.*, **157,** 977–985.

WARNER, T.D., DE NUCCI, G. & VANE, J.R. (1989). Rat endothelin is a vasodilator in the isolated perfused mesentery of the rat. *Eur. J. Pharmacol.*, **159,** 325–326.

WILKES, B.M., MENTO, P.F., HOLLANDER, A.M., MAITA, M.E., SUNG, S. & GIRARDI, E.P. (1990). Endothelin receptors in human placenta: relationship to vascular resistance and thromboxane release. *Am. J. Physiol.*, **258,** E864–E870.

WILKIN, P. (1958). Morphogénèse. In *Le Placenta Humain: Aspects Morphologiques et Fonctionnels*. ed. Snoeck, J. pp. 23–70. Paris: Masson.

YANAGISAWA, M., KURIHARA, H., KIMURA, S., TOMOBE, Y., KOBAYASHI, M., MITSUI, Y., YAZAKI, Y., GOTO, K. & MASAKI, T. (1988). A novel potent vasoconstrictor peptide produced by vascular endothelial cells. *Nature*, **332,** 411–415.

YANAGISAWA, M. & MASAKI, T. (1989). Endothelin, a novel endothelium-derived peptide: pharmacological activities, regulation and possible roles in cardiovascular control. *Biochem. Pharmacol.*, **38,** 1877–1883.

(Received January 3, 1995
Revised March 22, 1995
Accepted March 30, 1995)

British Journal of Pharmacology (1995) 115, 1043-1047 © 1995 Stockton Press All rights reserved 0007-1188/95 $12.00

Glucocorticoid-induced annexin 1 secretion by monocytes and peritoneal leukocytes

*†Christine Coméra & [1]*Françoise Russo-Marie

*INSERM U332, Institut Cochin de Génétique Moléculaire, 22 rue Méchain 75014 Paris, France and †INRA, Laboratoire de Pharmacologie et de Toxicologie, 180 chemin de Tournefeuille, 31931 Toulouse, France

1 We have studied the ability of the glucocorticoid, dexamethasone, to induce annexin 1 secretion by either human blood monocytes or rat peritoneal leukocytes.

2 The *in vivo* treatment of rats with dexamethasone (1.25 mg kg^{-1}) selectively induced secretion of annexin 1 by peritoneal leukocytes, as assessed by incubating these cells in culture medium. Annexin 1 secretion was also induced in human cultured monocytes, *in vitro*, by 10^{-6}M dexamethasone.

3 Annexin 1 secretion was inhibited in the presence of 20 mM NH_4Cl or by conducting the experiments at 18°C. In contrast, it was not inhibited by monensin, nocodazole or brefeldin A.

4 The time necessary for annexin 1 synthesis and secretion was less than 15 min.

5 These data indicate that glucocorticoids induce annexin 1 secretion by monocytes or peritoneal leukocytes. Because it is not inhibited by monensin, nocodazole or brefeldin A and it is rapid, annexin 1 secretion seems to occur by the secretory pathway similar to that used by several cytosolic proteins such as interleukin-1β.

Keywords: Annexin 1; lipocortin 1; glucocorticoids; secretion; monocytes; peritoneal leukocytes

Introduction

Annexins form a family of structurally homologous proteins that are synthesized in the cell cytosol and to which different biological functions have been attributed (reviewed in Flower & Rothwell, 1994; Raynal & Pollard, 1994). Among them, it has been suggested that annexin 1 (or lipocortin 1) is the messenger of part of the anti-inflammatory action of glucocorticoids. Indeed, mRNA and protein levels of annexin 1 can be increased by glucocorticoids (Wallner *et al.*, 1986, Goulding *et al.*, 1990; Browning *et al.*, 1990; Solito *et al.*, 1991; Ambrose *et al.*, 1992; Peers *et al.*, 1993; Flower & Rothwell, 1994; Raynal & Pollard, 1994). In addition, extracellular locations of annexin 1 were reported in body fluids, cell surfaces or cell supernatants, some of them being glucocorticoid-inducible (Goulding *et al.*, 1990; Browning *et al.*, 1990; Ambrose & Hunninghake, 1990; Smith *et al.*, 1990; Christmas *et al.*, 1991; Solito *et al.*, 1991; Peers *et al.*, 1993; Serres *et al.*, 1994; Flower & Rothwell, 1994; Raynal & Pollard, 1994). Finally, annexin 1 has extracellular anti-inflammatory properties which have been observed either *in vitro* or *in vivo* (Cirino *et al.*, 1987; 1989; Fradin *et al.*, 1988; Maridonneau-Parini *et al.*, 1989; Browning *et al.*, 1990; Flower & Rothwell, 1994; Raynal & Pollard, 1994). It reproduces several anti-inflammatory actions of glucocorticoids such as inhibition of cellular PLA_2 activity and neutrophil migration. However, this potential annexin 1 function has been the subject of controversy for several reasons. First, the glucocorticoid-induction of annexin 1 synthesis or release is restricted to certain cells or certain culture conditions (Northup *et al.*, 1988; Raynal & Pollard, 1994). Second, the physiological relevance of this extracellular function implies that annexin 1 is secreted. However, as opposed to most of the secreted proteins, annexin 1 is synthesized in the cytosol of cells and does not have the signal peptide that targets proteins to the endoplasmic reticulum and the classical secretory pathway (Raynal & Pollard, 1994). A newly discovered secretory route, exporting cytosolic proteins, has been reported and it was suggested this might be used by annexin 1 (Muesh *et al.*, 1990; Christmas *et al.*, 1991).

In order to assess the potential extracellular anti-inflammatory role of annexin 1 and its relation to glucocorticoids, we studied if the latter induced a physiological annexin 1 secretion in cells that are involved in inflammation. We show that glucocorticoids induce annexin 1 secretion in normal human blood monocytes or rat peritoneal leukocytes. The annexin 1 secretory pathway is characterized and shows close similarity with the one used by interleukin-1β (IL-1β).

[1] Author for correspondence.

Methods

Cell preparation

Mononuclear cells Peripheral blood mononuclear leukocytes (about 20% monocytes and 80% lymphocytes) from healthy donors were provided by the Blood Transfusion Centre of the Hôtel-Dieu (Paris). These cells were isolated by erythrocyte sedimentation using Dextran T500 (Pharmacia Biotech, Saint-Quentin, France) and mononuclear cells were separated from polymorphonuclear cells by centrifugation through Ficoll-Hypaque (Pharmacia Biotech) according to Britigan *et al.* (1988). The mononuclear leukocytes were washed three times in PBS (phosphate buffered saline, calcium- and magnesium-free) by 10 min centrifugation at 300 *g* and resuspended in RPMI 1640, medium (Flow Laboratories, Puteaux, France), containing 0.02% Ultroser (steroid-free, IBF, Villeneuve la Garenne, France), 1 mM L-glutamine, 100 u ml^{-1} of penicillin-streptomycin and 20 mM HEPES at 37°C. Monocytes were counted by non-specific esterase staining (Contreras *et al.*, 1980) and were dispensed at 2 to 5×10^6 monocytes/well in 12 or 24 well culture plates. They were allowed to adhere at 37°C with 5% CO_2 for 45 to 60 min and non-adherent cells were removed by three washes with PBS. Adherent monocytes were incubated in RPMI buffer at 37°C and 5% CO_2 in the presence or in the absence of 10^{-6} M dexamethasone (Sigma Chemical, Saint-Quentin-Fallavier, France).

Rat peritoneal cells: Male wistar rats (250 to 300 g) were treated for 2 or 24 h with an intraperitoneal injection of saline (0.9% NaCl) or 1.25 mg kg^{-1} phospho-dexamethasone (Merck Sharp & Dohme-Chibret, Paris, France) in saline (2 ml kg^{-1}). These conditions were used to study annexin 1 secretion because they were previously reported to induce up to 6 fold the

amount of annexin 1 mRNA in these cells (Wallner *et al.*, 1986). Rats were killed with ether and peritoneal cells were harvested by washing the cavity with 20 ml of PBS containing 1 mM final EDTA (ethylene diamine tetraacetic acid) to remove potential extracellular annexins, bound on cell surfaces. They were centrifuged for 10 min at 300 *g*, resuspended in RPMI buffer at 1 to 2×10^7 cells ml^{-1} and incubated for 30 min at 37°C.

Cell and supernatant treatment and analysis

At the end of the incubation periods, extracellular annexin 1 bound to the cell surface was washed off by adding 2 or 5 mM EDTA to the medium for a 2 min incubation period. Cells were separated from the medium by a short centrifugation of 20 s at 13,000 r.p.m. This centrifugation did not induce any cell lysis and allowed rapid separation of the cells from the medium. In experiments with adherent monocytes, cells and supernatants were separated by directly aspirating the medium. The latter was separated from any remaining cells by centrifugation at 13,000 r.p.m. for 20 s.

Analysis of annexin content by Western-Blot experiments

Cells were homogenized in 25 mM Tris/HCl, 0.25% Nonidet P-40 containing 1 μg ml^{-1} leupeptin, 1 μg ml^{-1} antipain, 1 μg ml^{-1} pepstatin A, 15 μg ml^{-1} benzamidine, 4 mM phenylmethyl-sulphonyl fluoride and 1000 iu ml^{-1} aprotinin followed by sonication. Aliquots of cell homogenates and supernatants were reserved for measuring the lactate dehydrogenase (LDH) activity. The remaining supernatant proteins were precipitated with 10% final of trichloroacetic acid and centrifuged for 10 min at 13,000 r.p.m. and 4°C. Cell homogenates and supernatant proteins were equilibrated in Laemmli's sample buffer, boiled for 5 min and subjected to SDS-PAGE (sodium dodecyl sulphate-polyacrylamide gel electrophoresis) and Western-blot analysis as previously described (Laemmli, 1970; Coméra *et al.*, 1989). Monospecific rabbit polyclonal antibodies directed against either annexin 1, 2 (a generous gift from J.C. Cavadore, INSERM U249, Montpellier), 5 or 6 were used. Some anti-annexin 1 antibodies were immunoaffinity purified with an annexin 1-sepharose 4B column that we made using 3.6 mg of human recombinant annexin 1 (kindly provided by Biogen, Boston, MA, U.S.A.) bound to 720 mg of CNBR-activated sepharose 4B, previously swollen and washed in HCl 1 mM, as described by the manufacturer (Pharmacia Biotech). Recombinant annexin 1 was allowed to bind to CNBR-activated sepharose 4B in buffer A ($NaHCO_3$ 0.1 M, pH 8.3, NaCl 0.5 M) for 16 h at 4°C, followed by an incubation period of 2 h at room temperature in blocking buffer (1 M ethanolamine, pH 8) and sequential washes in buffer A, buffer B (0.1 M acetate, pH 4, 0.5 M NaCl), then buffer A. Protein concentrations were determined as described by Bradford (1976).

Determination of cell viability

Cell viability was determined by trypan blue exclusion or by spectrophotometric measurement of LDH activity in both supernatants and cell homogenates, as described by the manufacturer (Boerhinger Mannheim, Meylan, France, kit: 1 087 592). The trypan blue exclusion method was used for peritoneal leukocyte samples which contained low numbers of cells. Peritoneal samples contained less than 3% dead cells as measured by trypan blue and less than 5% dead cells when measured by LDH activity.

Metabolic labelling of human monocytes and immunoprecipitation of annexin 1

Adherent monocytes, 4.5×10^6/well, were incubated overnight in RPMI buffer in the presence or absence of 10^{-6} M dexamethasone followed by 45 min incubation in the same conditions but in a medium devoid of methionine; 250 μCi/well of [^{35}S]-methionine (Amersham, Les Ulis, France) was then added for a further incubation of 15 or 30 min. Subsequently, 5 mM EDTA was added for 2 min and supernatants were isolated as previously described. Annexin 1 was immunoprecipitated from supernatants by incubation at 4°C with anti-annexin 1 antibodies for 2 h. After addition of 450 μg of protein-A sepharose (Phamacia Biotech, Saint-Quentin, France) and a 1 h-incubation, the mixtures were washed 6 times with 20 mM triethanolamine/HCl pH 7.4, 150 mM NaCl, 5 mM EDTA, 1% Triton X-100, 0.2% SDS buffer followed by centrifugation 5 min at 10,000 *g*. An additional wash was performed in the above buffer but in the absence of detergents. The samples were analysed by SDS-PAGE, protein fixation, a 30 min incubation in Amplify solution (Amersham), drying and autoradiography.

Results

Glucocorticoid-induced annexin 1 secretion

Dexamethasone-induced annexin 1 release was observed from either peritoneal leukocytes isolated from *in vivo* treated rats (Figure 1) or human cultured blood monocytes (Figure 2). However, dexamethasone did not change the intracellular annexin 1 content of peritoneal leukocytes (Figure 1b). In both cell types, the release of annexin 1 was inhibited in the presence of 20 mM NH_4Cl in the medium. Annexin 1 release by peritoneal leukocytes was very abundant: whereas cell death was very low (< 5%), 50% of the total annexin 1 amount had been

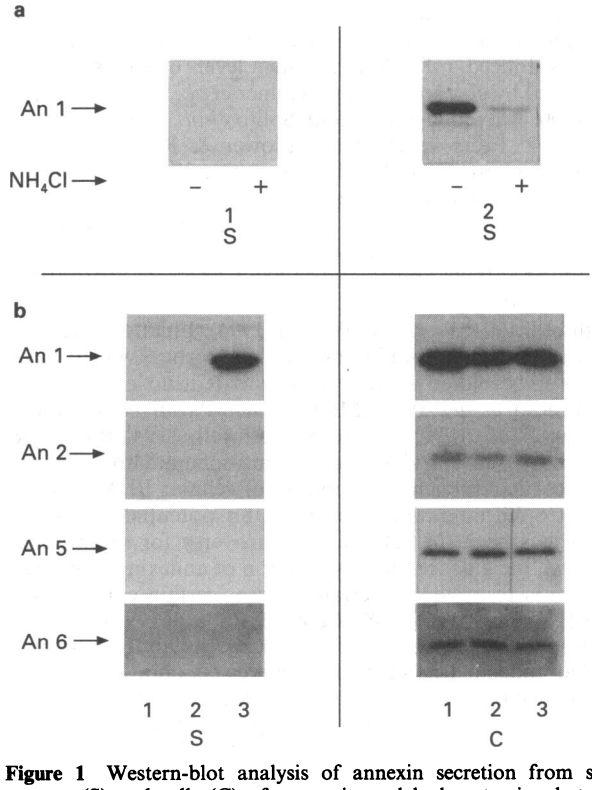

Figure 1 Western-blot analysis of annexin secretion from supernatants (S) and cells (C) of rat peritoneal leukocytes incubated for 30 min in RPMI medium. Rats were previously treated with saline for 2 h (1) or with 1.25 mg of dexamethasone for 2 h (2) or for 24 h (3). (a) Effect of the presence (+) or the absence (–) of 20 mM NH_4Cl in the incubation media on annexin 1 release in supernatants. (b) Analysis of the presence, in cells and supernatants, of annexin 1 (An 1), 2 (An 2), 5 (An 5) and 6 (An 6). Cell homogenates (30 μg proteins) and equivalent volumes of supernatant samples were loaded.

released from peritoneal cells during the 30 min incubation period (Figure 1b, quantified by densitometric scanning in two separate experiments). Peritoneal cells also expressed annexin 2, 5 and 6 but none of these proteins was detected in the medium (Figure 1b).

As shown previously (Browning *et al.*, 1990), the ability of dexamethasone to induce annexin 1 secretion was variable. It was observed in 8 out of 20 experiments for human blood monocytes and in 3 out of 12 experiments for rat peritoneal leukocytes. Moreover for both cell types, the time of dexamethasone treatment necessary to induce annexin 1 secretion was variable. For instance, in one experiment (Figure 1a) annexin 1 secretion by peritoneal leukocytes was induced 2 h after dexamethasone treatment of the rats while in another experiment (Figure 1b), no secretion was seen after 2 h but was seen 24 h after dexamethasone. In this latter study annexin 1 release was either very abundant or not detectable at all.

Modulation by chemicals or temperature of annexin 1 secretion by monocytes

This study was done on human cultured monocytes responding to *in vitro* dexamethasone induction that was performed for 3 or 16 h (Figure 2). Different chemicals were used that block the transport of proteins at different steps along the classical secretory pathway which secrete proteins with a signal peptide. This type of protein secretion is inhibited by (i) brefeldin A which prevents the egress from the endoplasmic reticulum (ER), (ii) the monovalent ionophore monensin which blocks the transport in the late Golgi, (iii) nocodazole which depolymerizes microtubules and inhibits the migration of vesicles and (iv) amines (ammonium chloride, methylamine or others) which stop vesicle or granule transport by increasing their intracellular pH (Tartakoff, 1983; Dean *et al.*, 1984; Klausner *et al.*, 1992). We also analysed the effect of incubation at 18°C which inhibits intracellular trafficking (Rubartelli *et al.*, 1990). NH_4Cl was used at 20 mM which is the suboptimal dose that does not induce cellular lysis and is consistent with the concentration of methylamine (10 mM) used to block interleukin-1β secretion (Rubartelli *et al.*, 1990). Monensin and brefeldin A were used at 10 μM and 0.5 μg ml^{-1} respectively, according to Rubbartelli *et al.* (1990) and nocodazole at 33 μM, the suboptimal dose to avoid cytotoxicity. This latter was reported to depolymerize monocyte microtubules and to induce interleukin-1β secretion when used at a concentration as low as 3.3 μM (Newton, 1990).

Cellular lysis was from 5 to 7% for every sample shown in Figure 2a and was from 8 to 10% except in the presence of monensin and brefeldin A where they were, 19 and 13%, respectively, for the samples shown in Figure 2b. Annexin 1 release was inhibited in the presence of 20 mM NH_4Cl and at 18°C. In contrast, this release was not inhibited but rather increased in the presence of either 10 μM monensin, 33 μM nocodazole or 0.5 μg ml^{-1} brefeldin A. Except for the effect of monensin in Figure 2b (but not in Figure 2a), there was no correlation between the rates of cellular lysis and annexin 1 release. Annexin 1 sometimes appears as three different peptides which have been shown to be extracellular annexin 1 proteolytic fragments (Smith *et al.*, 1990; Christmas *et al.*, 1991).

Quantification of annexin 1 secretion time in monocytes

In order to determine the time required for the translated annexin 1 to be secreted, metabolic protein labelling using [^{35}S]-methionine was performed (Figure 3). This secretion was rapid since the time between annexin 1 translation and secretion was less than 15 min. It should be noted that, in agreement with our previous results, radiolabelled annexin 1 release was induced by dexamethasone.

Discussion

Our study establishes that annexin 1 is secreted. This is demonstrated in the experiment where intact rat peritoneal leukocytes released up to 50% of the total cellular annexin 1 in 30 min. Indeed, both abundance and selectivity of this release suggest that it is a genuine secretion. Such an abundant release of annexin 1 was previously reported in seminal fluids (Christmas *et al.*, 1991). Annexin 1 secretion in human blood mononuclear cells, monocytes or in rat peritoneal leukocytes is probably physiological because it is inhibited by 20 mM NH_4Cl or at 18°C and there is no apparent correlation between the rates of annexin 1 release and cellular lysis. These results support the concept that dexamethasone induces annexin 1 secretion as shown in previous studies (Goulding *et al.*, 1990; Browning *et al.*, 1990; Solito *et al.*, 1991; Peers *et al.*, 1993; Flower & Rothwell, 1994; Raynal & Pollard, 1994). It is interesting to note that other annexins were reported to be secreted with no apparent glucocorticoid inducibility except for annexin 5 in differentiated U937 cells (Pfäffle *et al.*, 1988; Christmas *et al.*, 1991; Solito *et al.*, 1991; Raynal & Pollard, 1994). Further studies remain necessary to determine to what extent secretion of annexin 1 and possibly other annexins contribute to physiological glucocorticoid action.

Some studies, on human monocytes or on leukocytes, reported that dexamethasone induces either an annexin 1 mRNA or protein synthesis or its secretion whereas others did not detect any of these events (Wallner *et al.*, 1986; Northup *et al.*, 1988; Browning *et al.*, 1990; Goulding *et al.*, 1990; Ambrose *et*

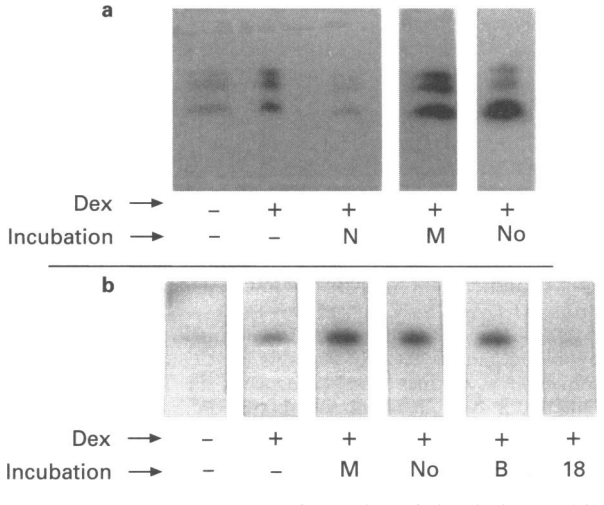

Figure 2 Western-blot analysis of the effect of chemicals or 18°C on annexin 1 release in supernatants of human adherent monocytes. Cells were incubated for 16 h (a) or 3 h (b) in the presence (+) or in the absence (–) of 10^{-6} M dexamethasone (Dex) at 37°C with either no product added (–), 20 mM NH_4Cl (N), 10 μM monensin (M), 33 μM nocodazole (No) or 0.5 μg ml^{-1} brefeldin A (B) and at 18°C (18). Equivalent volumes of supernatants were loaded.

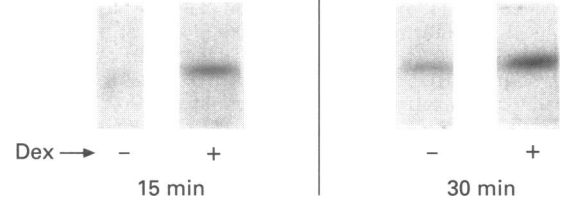

Figure 3 Detection of newly synthesized annexin 1 in human adherent monocyte supernatants. Cells were stimulated with (+) or without (–) 10^{-6} M dexamethasone (Dex) and were incubated for 15 min or 30 min in the presence of [^{35}S]-methionine (250 μCi/4.5×10^6 cells). Annexin 1 was immuno-precipitated from supernatants and detected by SDS-PAGE and autoradiography.

al., 1992; Peers *et al.*, 1993). In our study, annexin 1 secretion by both monocytes or peritoneal leukocytes in response to dexamethasone was very variable. This agrees with previous reports which relate differences in the dexamethasone response concerning annexin 1 synthesis or secretion by cells, depending on the cell type, the state of cellular activation or differentiation or on the requirement for factors in addition to glucocorticoids (Browning *et al.*, 1990; Solito *et al.*, 1991; Ambrose *et al.*, 1992; reviewed in Raynal & Pollard, 1994). This could most certainly modulate the *in vivo* occurrence of this phenomenon and make it difficult to predict in which state of differentiation/activation circulating monocytes and peritoneal leukocytes are in and, therefore, whether they will respond to glucocorticoids; indeed, we have found that annexin 1 promoter responds differently to glucocorticoids according to the type of cells and to the presence of other transcription factors (E. Solito, unpublished results).

Annexin 1 is secreted via a pathway independent of the endoplasmic reticulum-Golgi complex

The fact that monensin, nocodazole and brefeldin A do not inhibit annexin 1 secretion strongly suggests that annexin 1 is not secreted by the classical pathway (ER/Golgi) but by an alternative route. Indeed, secretion of interleukin 6 and tumour necrosis factor α (TNFα) by this classical pathway were found to be inhibited by monensin and brefeldin A in human monocytes (Rubartelli *et al.*, 1990). This is further supported by the fact that the time elapsed between annexin 1 biosynthesis and secretion, in monocytes, is shorter than 15 min and much faster than the time required for protein secretion by the classical pathway. Annexin 1, IL1-β, basic fibroblast growth factor and thioredoxin secretions share similar properties for modulation of their secretion, suggesting they could be secreted by a common secretory pathway (Rubartelli *et al.*, 1990; Newton, 1990; Rubartelli & Sitia, 1991; Mignatti *et al.*, 1992). This is consistent with the fact that all these proteins do not have any signal peptide and are synthesized in cell cytosol. Another study reported a similar inhibition of annexin 1 secretion by epidermal cells using the amine chloroquine or an incubation at 18°C (Serres *et al.*, 1994).

It is not yet known why eukaryotic organisms display this alternative secretory pathway in addition to the classical one. It was reported that many of the mammalian secreted proteins lacking a signal sequence were related to inflammation, coagulation or tissue damage (Rubartelli & Sitia, 1991). Our study shows that annexin 1 secretion can be very abundant and be rapidly processed by cells.

C.C. was recipient of fellowships from the DRET (Ministère de la Défense), the Association de la Recherche sur le Cancer and the Fondation de la Recherche Médicale.

References

AMBROSE, M.P. & HUNNINGHAKE, G.W. (1990). Corticosteroids increase lipocortin I in BAL fluid from normal individuals and patients with lung disease. *J. Appl. Physiol.*, **68**, 1668–1671.

AMBROSE, M.P., BAHNS, C.L. & HUNNINGHAKE, G.W. (1992). Lipocortin I production by human alveolar macrophages. *Am. J. Resp. Cell. Mol. Biol.*, **6**, 17–21.

BRADFORD, M. (1976). A rapid and sensitive method for the quantification of microgram of protein utilizing the principle of protein-dye binding. *Anal. Biochem.*, **72**, 248–254.

BRITIGAN, B.E., COFFMAN, T.J., ADELBERG, D.R. & COHEN, M.S. (1988). Mononuclear phagocytes have the potential for sustained hydroxylic radical production: use of spin trapping techniques to investigate mononuclear phagocyte free radical production. *J. Exp. Med.*, **168**, 2367–2372.

BROWNING, J.L., WARD, M., WALLNER, B.P. & PEPINSKY, R.B. (1990). Studies on the structural properties of lipocortin 1 and the regulation of its synthesis by steroids. In *Progress in Clinical and Biological Research*: Cytokines and Lipocortins in Inflammation and Differentiation ed. Melli, M.L. & Parente, L. Vol. 349, pp. 27–45. New York, NY: Wiley-Liss.

CHRISTMAS, P., CALLAWAY, J., FALLON, J., JONES, J. & HAIGLER, H.T. (1991). Selective secretion of annexin 1, a protein without a signal sequence, by the human prostate gland. *J. Biol. Chem.*, **266**, 2499–2507.

CIRINO, G., FLOWER, R.J., BROWNING, J.L., SINCLAIR, L.K. & PEPINSKY, R.B. (1987). Recombinant human lipocortin inhibits thromboxane release from guinea-pig isolated perfused lung. *Nature*, **328**, 270–272.

CIRINO, G., PEERS, S.H., FLOWER, R.J., BROWNING, J.L. & PEPINSKY, R.B. (1989). Human recombinant lipocortin 1 has acute local anti-inflammatory properties in the rat paw edema test. *Proc. Natl. Acad. Sci. U.S.A.*, **86**, 3428–3432.

COMÉRA, C., ROTHHUT, B. & RUSSO-MARIE, F. (1989). Identification and characterization of phospholipase A_2 inhibitory proteins in human mononuclear cells. *Eur. J. Biochem.*, **188**, 139–146.

CONTRERAS, T.J., JEMIONEK, J.F., STEVENSON, H.C., HARTWIG, V.M. & FAUCI, A.S. (1980). An improved technique for the negative selection of large numbers of human lymphocytes and monocytes by counter-flow centrifugation-elutriation. *Cell. Immunol.*, **54**, 215–218.

DEAN, R.T., JESSUP, W. & ROBERTS, C.R. (1984). Review article: effects of exogenous amines on mammalian cells with particular reference to membrane flow. *Biochem. J.*, **217**, 27–40.

FLOWER, R.J. & ROTHWELL, N.J. (1994). Lipocortin-1: cellular mechanisms and clinical relevance. *Trends Pharmacol. Sci.*, **15**, 71–76.

FRADIN, A., ROTHHUT, B., POINCELOT-CANTON, B., ERRASFA, M. & RUSSO-MARIE, F. (1988). Inhibition of eicosanoid and PAF formation by dexamethasone in rat inflammatory polymorphonuclear neutrophils may implicate lipocortin's'. *Biochim. Biophys. Acta.*, **963**, 248–257.

GOULDING, N.J., GOLDOLPHIN, J.L., SHARLAND, P.R., PEERS, S.H., SAMPSON, L., MADDISON, P.J. & FLOWER, R.J. (1990). Anti-inflammatory lipocortin 1 production by peripheral blood leukocytes in response to hydrocortisone. *Lancet*, **335**, 1416–1418.

KLAUSNER, R.D., DONALDSON, J.G. & LIPPINCOTT-SCHWARTZ, J. (1992). Brefeldin A: Insight into the control of membrane traffic and organelle structure. *J. Cell. Biol.*, **116**, 1071–1080.

LAEMMLI, U.K. (1970). Cleavage of structural proteins during the assembly to the head of bacteriophage. *Nature*, **227**, 680–685.

MARIDONNEAU-PARINI, I., ERRASFA, M. & RUSSO-MARIE, F. (1989). Inhibition of O_2-generation by dexamethasone is mimicked by lipocortin 1 in alveolar macrophages. *J. Clin. Invest.*, **83**, 1936–1940.

MIGNATTI, P., MORIMOTO, T. & RIFKIN, D.B. (1992). Basic fibroblast growth factor, a protein devoid of secretory signal sequence, is released via a pathway independent of the endoplasmic reticulum-Golgi complex. *J. Cell. Physiol.*, **151**, 81–93.

MUESH, A., HARTMAN, E., ROHDE, K., RUBARTELLI, A., SITIA, R. & RAPOPORT, T.A. (1990). A novel pathway for secretory proteins? *Trends Biol. Sci.*, **15**, 86–88.

NEWTON, R.C. (1990). The production of human interleukin-1 beta by blood monocytes. In *Progress in Clinical and Biological Research*: Cytokines and Lipocortins in Inflammation and Differentiation ed. Melli, M.L. & Parente, L. Vol. 349, pp. 217–228. New York, NY: Wiley-Liss.

NORTHUP, J.K., VALENTINE-BRAUN, K.A., JOHNSON, L.K., SEVERSON, D.L. & HOLLENBERG, M.D. (1988). Evaluation of the anti-inflammatory and phospholipase-inhibitory activity of calpactin II/lipocortin I. *J. Clin. Invest.*, **82**, 1347–1352.

PEERS, S.H., SMILIE, F., ELDERFIELD, A.J. & FLOWER, R.J. (1993). Glucocorticoid- and non-glucocorticoid induction of lipocortins (annexins) 1 and 2 in rat peritoneal leukocytes *in vivo*. *Br. J. Pharmacol.*, **108**, 66–72.

PFÄFFLE, M., RUGGIERO, F., HOFMAN, H., FERNANDEZ, M.P., SELMIN, O., YAMADA, Y., GARRONE, R. & VON DER MARK, K. (1988). Biosynthesis, secretion and extracellular localization of anchorin CII, a collagen-binding protein of the calpactin family. *EMBO J.*, **7,** 2335–2342.

RAYNAL, P. & POLLARD, H.B. (1994). Annexins: the problem of assessing the biological role for a gene family of multifunctional calcium- and phospholipid-binding proteins. *Biochim. Biophys. Acta.*, **1197,** 63–93.

RUBARTELLI, A., COZZOLINO, F., TALIO, M. & SITIA, R. (1990). A novel secretory pathway for interleukin-1β, a protein lacking a signal sequence. *EMBO J.*, **9,** 1503–1510.

RUBARTELLI, A. & SITIA, R. (1991). Interleukin-1β and thioreduxin are secreted through a novel pathway of secretion. *Biochem. Soc. Trans.*, **19,** 255–259.

SERRES, M., COMÉRA, C. & SCHMITT, D. (1994). Annexin 1 regulation in human epidermal cells. *Cell. Mol. Biol.*, **40,** 701–706.

SMITH, S.F., TETLEY, T.D., GUZ, A. & FLOWER, R.J. (1990). Detection of lipocortin 1 in human lung lavage fluid: lipocortin degradation as a possible proteolytic mechanism in the control of inflammatory mediators and inflammation. *Envir. Health Persp.*, **85,** 135–144.

SOLITO, E., RAUGEI, G., MELLI, M. & PARENTE, L. (1991). Dexamethasone induces the expression of the mRNA of lipocortin 1 and 2 and the release of lipocortin 1 and 5 in differentiated but not in undifferentiated U-937 cells. *FEBS Lett.*, **291,** 238–244.

TARTAKOFF, A.M. (1983). Perturbation of vesicular traffic with the carboxylic ionophore monensin. *Cell*, **32,** 1026–1028.

WALLNER, B.P., MATTALIANO, R.J., HESSION, C., CATE, R.L., TIZARD, R., SINCLAIR, L.K., FOELLER, C., CHOW, E.P., BROWNING, J.L., RAMACHANDRAN, K.L. & PEPINSKY, R.B. (1986). Cloning and expression of human lipocortin, a phospholipase A_2 inhibitor with potential anti-inflammatory activity. *Nature*, **320,** 77–81.

(Received November 30, 1994
Revised February 23, 1995
Accepted March 20, 1995)

British Journal of Pharmacology (1995) 115, 1048–1052 © 1995 Stockton Press All rights reserved 0007–1188/95 $12.00

Potentiation by viral respiratory infection of ovalbumin-induced guinea-pig tracheal hyperresponsiveness: role for tachykinins

A. Rudolf C. Ladenius, [1]Gert Folkerts, Henk J. van der Linde & Frans P. Nijkamp

Department of Pharmacology, Utrecht Institute for Pharmaceutical Sciences, Utrecht University, P.O. Box 80.082, 3508 TB Utrecht, The Netherlands

1 We investigated whether virus-induced airway hyperresponsiveness in guinea-pigs could be modulated by pretreatment with capsaicin and whether viral respiratory infections could potentiate ovalbumin-aerosol-induced tracheal hyperresponsiveness.

2 Animals were inoculated intratracheally with bovine parainfluenza-3 virus or control medium 7 days after treatment with capsaicin (50 mg kg^{-1}, s.c.). Four days after inoculation, tracheal contractions were measured to increasing concentrations of substance P, histamine and the cholinoceptor agonist, arecoline.

3 In tracheae from virus-infected guinea-pigs, contractions in response to substance P, histamine and arecoline were significantly enhanced ($P<0.01$) by 144%, 46% and 77%, respectively. Capsaicin pretreatment inhibited the hyperresponsiveness to substance P partly (62%) and to histamine and arecoline completely.

4 In another series of experiments animals were first sensitized with ovalbumin (20 mg kg^{-1}, i.p.). After 14 days animals were exposed to either saline or ovalbumin aerosols for 8 days. After 4 aerosol exposures (4 days) animals were inoculated with either parainfluenza-3 virus or control medium. One day after the last ovalbumin aerosol, tracheal contraction in response to increasing concentrations of substance P, histamine and arecoline was measured.

5 Tracheae from ovalbumin-aerosol-exposed control inoculated animals showed a similar degree of airway hyperresponsiveness to saline-aerosol-exposed virus-treated guinea-pigs. Virus inoculation of ovalbumin-treated animals significantly potentiated the tracheal contractions to substance P compared to either of the treatments alone. The contractions in response to histamine and arecoline were only slightly enhanced.

6 In conclusion, sensory nerves and/or tachykinins are involved in virus-induced airway hyperresponsiveness in guinea-pigs and viral respiratory infections can potentiate the increase in tracheal responsiveness to bronchoconstrictor agonists after ovalbumin exposure.

Keywords: Tracheal hyperresponsiveness; capsaicin; virus infection; ovalbumin; allergy; airway reactivity

Introduction

Characteristic features of asthma include reversible airway constriction and nonspecific airway hyperresponsiveness. Respiratory virus infections can exacerbate asthma and enhance the airway hyperresponsiveness in healthy human subjects and asthma patients (Ouellette & Reed, 1965; MacIntosh *et al.*, 1973; Empey *et al.*, 1976). The mechanisms involved in airway hyperresponsiveness remain unclear. Respiratory virus infection in guinea-pigs enhance airway smooth muscle responses to histamine, the cholinoceptor agonist, arecoline (Folkerts *et al.*, 1992; 1993a,b) and substance P (Saban *et al.*, 1987). It has been shown that viral infections decrease the activity of neutral endopeptidase, the main degradative enzyme of the tachykinins, and this action may account for the virus-induced airway hyperresponsiveness to these agents (Jacoby *et al.*, 1988, Dusser *et al.*, 1989). Histamine can release multiple tachykinins from capsaicin-sensitive sensory nerves in the lung and therefore, the histamine hyperresponsiveness could also be explained by this mechanism (Saria *et al.*, 1988). Whether, such a pathway also exists for cholinoceptor stimulation is unknown.

Repeated antigen aerosol exposure of sensitized guinea-pigs has been shown to cause a prolonged airway hyperresponsiveness (Ishida *et al.*, 1989). Previous studies have shown that depletion of neuropeptides with the neurotoxin, capsaicin, inhibits the induction of airway hyperresponsiveness after repeated aerosolized antigen in sensitized guinea-pigs (Matsuse *et al.*, 1991) and toluene diisocyanate-induced airway hyperresponsiveness (Thompson *et al.*, 1987). In addition, capsaicin aerosols, causing endogenous release of neuropeptides, could increase airway responsiveness to histamine (Umeno *et al.*, 1992) and acetylcholine and neurokinin A (Hsiue *et al.*, 1992) in guinea-pig *in vivo* acutely. Also, the intravenous administration of the tachykinin, substance P, resulted in potentiation of histamine responses in the airways (Umeno *et al.*, 1992). These studies suggest that the release of sensory neuropeptides such as tachykinins may be responsible for the induction of airway hyperresponsiveness. Thus, inhibition of neutral endopeptidase, lengthening the residence time of tachykinins in the airways may lead to increased airway responses to nonspecific agents.

The purpose of the present study was to test the hypothesis that sensory neuropeptides are important for the development of the nonspecific tracheal reactivity seen after virus infection and to investigate whether virus infection could exacerbate the tracheal hyperresponsiveness induced by repeated antigen aerosol in sensitized guinea-pigs.

Methods

Animals

Male Hartley-strain guinea-pigs (weight range 250–300 g) of SPF quality were obtained from Harlan CPB (Zeist, The Netherlands). After delivery, animals were housed in metal cages and allowed 1 week to recuperate after transport. Ani-

[1] Author for correspondence.

mals were fed normal guinea-pig chow and allowed water *ad lib*. Indicator animals were housed under identical circumstances and were regularly screened for respiratory infections by the Central Laboratory Animal Institute (Utrecht, The Netherlands). All experiments were approved by the ethics committee of Utrecht University.

Capsaicin treatment

Guinea-pigs were anaesthetized with Nembutal (30 mg kg^{-1}, i.p.). A capsaicin (12.5% solution in equal part of 95% ethanol and Tween-80, diluted to 25 mg ml^{-1} with saline) injection was given subcutaneously every hour in the following doses (in mg ml^{-1}): 0.25, 0.25, 0.5, 1.0, 3.0, 5.0, 10.0, 10.0, 20.0 for a total dose of 50 mg kg^{-1} as described previously (Ladenius & Nijkamp, 1993). Animals receiving the above mentioned solution without capsaicin will be referred to as vehicles. All animals were treated with atropine (1 mg kg^{-1}, s.c.) and mepyramine (1 mg kg^{-1}, s.c.) 30 min prior to the first capsaicin injection and atropine and mepyramine were re-administered at the same dose 4 h later. Salbutamol (10 μg kg^{-1}, s.c.) was injected 10 min before each capsaicin injection. Before each vehicle or capsaicin injection the level of anaesthesia was adjusted. After recovery from the anaesthetic animals appeared normal.

Virus inoculation

Bovine Parainfluenza 3 virus (PI-3) (kindly provided by Duphar B.V., Weesp, The Netherlands) was grown on Madin Darby Bovine Kidney cells and harvested 3–5 days (dependent on the cytopathic effects) after the initial inoculation. Accordingly, the tissue culture infective dose (TCID) of the virus suspension was determined. The virus suspension ($TCID_{50} = 10^{8.9}$ ml^{-1}) was centrifuged at 100,000 *g*, the supernatant removed and the virus-pellet resuspended in only 0.1 ml sterile saline to minimize side effects of the inoculation procedure. Growth medium was treated identically. Previous experiments have shown that PI-3 virus could be isolated from the airways of all guinea-pigs 2 days after infection (Folkerts *et al.*, 1993a).

The animals were anaesthetized with ether and placed in a supine position on a small table. The jaws were kept apart by 2 elastic bands and a needle with a bulbous tip was inserted to just behind the glottis. Then, 0.1 ml of inoculum was gently injected in the trachea, the bands were removed and the chest was gently massaged. Guinea-pigs receiving the above mentioned control solution are from now on referred to as controls. To prevent cross-infection animals were housed in separate isolators.

Sensitization and challenge

Animals were injected with ovalbumin (20 mg kg^{-1}, i.p., injection volume of 0.2 ml). After 14 days animals were exposed to either saline or 2% ovalbumin-aerosols daily for 8 consecutive days. Animals were placed under a plastic bell which was attached to the nebulizer and the aerosol started. Animals were watched closely for the appearance of respiratory signs (coughing, wheezing). As soon as animals reacted the nebulizer was turned off and the chamber cleared. Animals were observed until respiratory signs disappeared. At the end of the sensitization period *all* animals reacted upon ovalbumin exposure between breaths 5 and 20. Animals that had been exposed daily to an aerosol with saline for 30 s did not show any respiratory reaction. Aerosols were delivered with a Medix 8001 ultrasonic nebulizer which yields particles 3–5 μm in size.

Treatment protocols

In the first series of experiments animals were inoculated with either control medium or virus, 7 days after vehicle or capsaicin-treatment. Four days later experiments were performed. In the second set of experiments animals were sensitized to ovalbumin and challenged as mentioned above. After recovery from the 4th aerosol challenge, animals were inoculated with virus or control medium and 24 h after the 8th aerosol exposure, experiments were performed.

Experiments

Guinea-pigs were killed with an overdose of pentobarbitone sodium (300 mg kg^{-1}, i.p.). The trachea was removed and placed in ice-cold Krebs-bicarbonate buffer (pH = 7.4) of the following composition (mmol l^{-1}): NaCl 118.1, KCl 4.7, $CaCl_2$ 2.5, $MgSO_4$ 1.2, $NaHCO_3$ 25.0, KH_2PO_4 1.2 and glucose 8.3, gassed with 5% CO_2 and 95% O_2. Under a dissecting microscope the trachea was cleared of excess fat and connective tissue and opened by cutting the cartilaginous rings opposite the smooth muscle. Tracheae were then cut into 3 pieces of 3 rings of cartilage and each end tied with 2–0 cotton thread. Tissues were mounted in organ baths filled with Krebs (37°C) and attached to an isotonic transducer (Harvard Bioscience, Kent, UK). Througout the experiments tracheal strips were kept under a constant optimal load of 0.5 g. Using different preloads it was found that with 0.5 g the tissues demonstrated the largest contraction upon stimulation with histamine and the largest relaxation with the β-receptor agonist, salbutamol. Tissues were washed 3 times at 15 min intervals and allowed to stabilize.

When a stable tone was reached cumulative concentration-response curves to substance P, histamine, the muscarinic receptor agonist, arecoline were constructed. The 3 tissues of 3 rings each were exposed to one agent only. The isotonic transducers were connected to an analog-digital converter (Intelligent International PCI System, Burr Brown Company, Tucson, Arizona, U.S.A.) integrating the organ baths in a semi-automatic setup. This enabled continuous sampling, on-line equilibrium detection, and real-time display of the responses on a computer screen of up to 12 baths. At the end of experiments in which animals had been pretreated with either capsaicin or vehicle, all strips were exposed to capsaicin (3×10^{-7} M) to confirm depletion of tachykinins in capsaicin-pretreated animals. If the tissues did not contract after capsaicin, tissues were exposed to 30 mM KCl to ensure viability.

Chemicals

Compounds used: arecoline bromide, egg albumin (ovalbumin) (Grade V), substance P (Sigma, St. Louis, MO, U.S.A.); atropine sulphate, histamine phosphate (OPG, Utrecht, The Netherlands); mepyramine maleate (Specia, Paris, France). All chemicals used for Krebs-bicarbonate buffer were purchased from Merck. All compounds were of reagent grade or higher. Substance P, histamine and arecoline were dissolved in Krebs. Mepyramine, atropine and ovalbumin were dissolved in 0.9% saline.

Statistics

The cumulative concentration-response curves are expressed in μm contraction and presented as mean ± standard error of the mean (s.e.mean). Differences after cumulative concentration-response curves with substance P, histamine, or arecoline on isolated tissues from the medium and virus-inoculated groups were tested with a Bonferroni adjustment. The maximal contractions are expressed as percentage of the maximal contraction of the control groups. Changes between the control, virus, control-ovalbumin and virus-ovalbumin groups were first tested with ANOVA followed by a multiple range test (Student-Newman-Keuls). *P*-values < 0.05 were considered to reflect a statistically significant difference.

Results

Effects of capsaicin on virus-induced tracheal hyperresponsiveness

In the control group, concentration-response curves to substance P did not reach a clear maximal response (169.0 ± 13.6 μm, Figure 1), which is consistent with findings of Warner *et al.* (1990). The maximal contraction induced in the control group by histamine (274.0 ± 13.1 μm) was higher ($P<0.01$) than for substance P but lower ($P<0.01$) than for arecoline (371.9 ± 15.7 μm, Figure 1).

Virus infection caused a significant (Bonferroni) enhancement in the concentration-response curves to substance P, histamine and arecoline (Figure 1): the maximal responses were increased by 144% ($P<0.01$), 46% ($P<0.05$) and 77% ($P<0.01$), respectively, compared to the control groups (Figure 2a). The pD_2 values did not differ between the experimental groups after the histamine or arecoline concentration-response curves.

Capsaicin pretreatment did not influence the substance P concentration-response curve of the control group. In the virus-treated guinea-pigs the maximal contraction was increased by 53% compared to the vehicle-control group (Figure 2b) and reduced by 62% compared to virus group treated with the vehicle solution (Figure 2a). These differences did not reach the level of significance (Bonferroni). Capsaicin completely inhibited the virus-induced tracheal hyperresponsiveness to histamine and arecoline (Figure 2a and b).

Tracheal strips from vehicle-treated animals showed a small contraction when exposed to capsaicin (about 75 μm) while strips from capsaicin-pretreated ones gave no contraction but did react when exposed to KCl (results not shown).

Interactions of virus and ovalbumin-induced tracheal hyperresponsiveness

In saline-aerosol exposed control inoculated guinea-pigs the maximal tracheal contraction after a substance P concentration-response curve was 143.0 ± 11.4 μm. Virus infection and ovalbumin-aerosol exposure alone induced a similar degree of

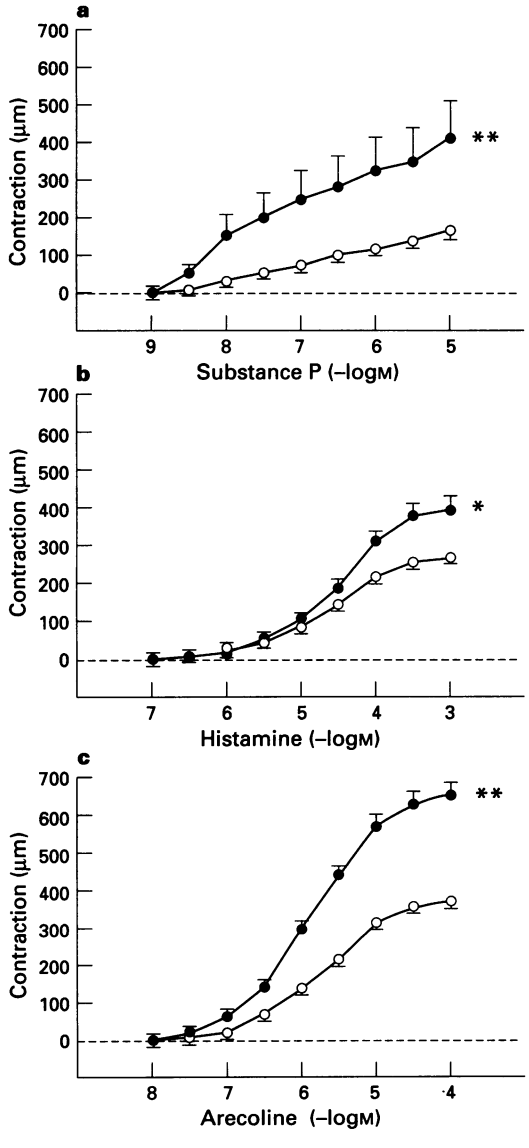

Figure 1 Concentration-response curves to (a) substance P, (b) histamine and (c) arecoline: (○) vehicle-control group; (●) vehicle-virus group. Curves were constructed 4 days after inoculation. Each data point represents the mean ± s.e.mean of 8 tracheal strips. *$P<0.05$; **$P<0.01$ (Bonferonni) compared to the control inoculated group.

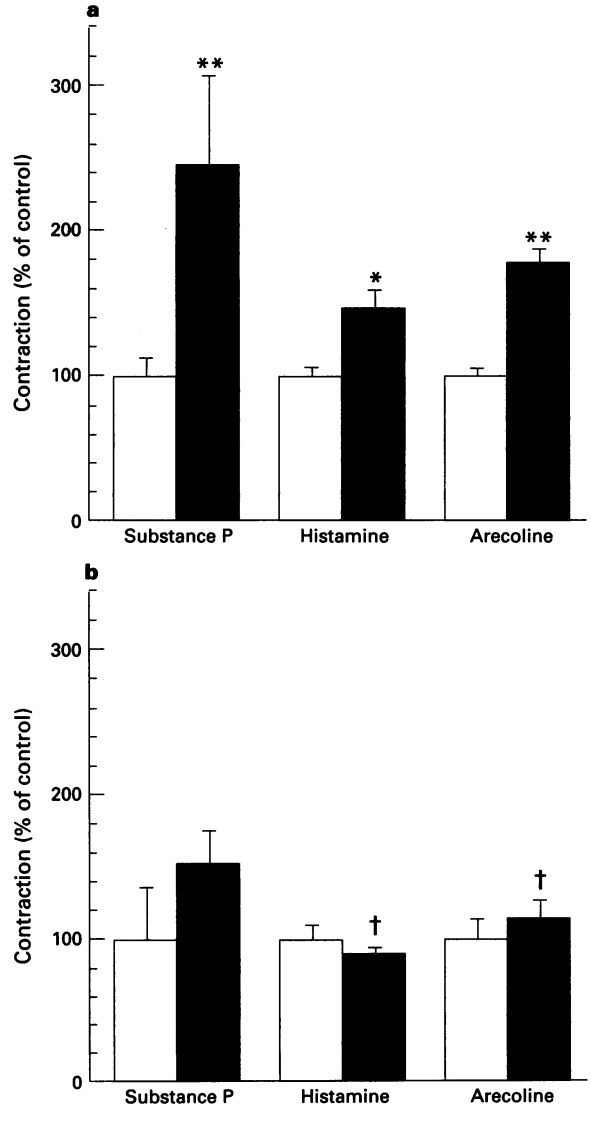

Figure 2 Maximal tracheal contractions (as % of control) in response to substance P, histamine and arecoline 4 days after inoculation with control solution (open columns) or PI-3 virus (solid columns) of animals (a) pretreated with vehicle (b) pretreated with capsaicin. *$P<0.05$; **$P<0.01$ (Bonferonni) compared to the control inoculated group. †$P<0.05$ (Bonferonni) compared with the virus inoculated groups in Figure 2a. The data are presented as mean ± s.e.mean ($n=8$).

tracheal hyperresponsiveness to substance P (Figure 3). A combination of ovalbumin-aerosol exposure and virus infection induced a tracheal hyperresponsiveness to substance P which was increased significantly compared to either treatment alone (Figure 3, $P<0.01$, Student-Neuman-Keuls).

The maximal tracheal contraction of the control group in response to histamine was 368.8 ± 38.2 μm. In virus- or ovalbumin-treated animals the maximal contractions were significantly enhanced; however, the combination had only a slight additional effect (Figure 3).

In the control group, arecoline induced a maximal contraction of 392.0 ± 32.0 μm. Pretreatment of the animals with virus or ovalbumin significantly increased the maximal responses (Figure 3). The ovalbumin-aerosol exposed guinea-pigs with or without a respiratory infection significantly enhanced the tracheal contraction compared to virus-treatment alone ($P<0.01$, Student-Neuman-Keuls). The respiratory infection in the ovalbumin-aerosol exposed animals had a small additional effect compared to ovalbumin treatment alone (Figure 3).

The pD_2 values did not differ between the experimental groups.

Discussion

In the present study it is shown that virus-induced tracheal hyperresponsiveness can be inhibited by capsaicin pretreatment. In addition, virus infection was able to potentiate responses to substance P and to a lesser extent to histamine and arecoline in ovalbumin-aerosol exposed guinea-pigs.

Airway hyperresponsiveness is a main characteristic of the pathophysiology of asthma. Although the mechanism(s) underlying the hyperresponsiveness are not clear, increasing attention has been focused on the role of the sensory innervation in the induction of airway hyperresponsiveness. In guinea-pigs respiratory virus infection has been shown to enhance airway smooth muscle responses to histamine, arecoline (Folkerts *et al.*, 1993a,b; 1995) and substance P (Saban *et al.*, 1987). The present study confirms these findings. Virus infection in guinea-pigs has been shown to cause epithelial damage (Folkerts *et al.*, 1992; 1993b). The epithelial damage could expose sensory nerve endings and cause excessive release of sensory neuropeptides (Barnes *et al.*, 1991). Several studies have now shown that endogenous release of neuropeptides or exogenously applied tachykinins can induce airway hyperresponsiveness (Umeno *et al.*, 1992; Hsiue *et al.*, 1992). Exogenously administered substance P potentiated acetylcholine-induced bronchospasm in the guinea-pig (Omini *et al.*, 1989). Tamura *et al.* (1989) reported that neurokinin A augmented methacholine responses for as long as 4 weeks in Japanese monkeys. Moreover, it has been shown that substance P antibodies can inhibit the ovalbumin-induced airway hyperresponsiveness in guinea-pigs (Ladenius *et al.*, 1991). In the present study capsaicin pretreatment depleted the sensory nerves of neuropeptides, as demonstrated by the lack of responses to exogenously applied capsaicin. Therefore, the suppression of the airway hyperresponsiveness might be due to a diminished release of sensory neuropeptides after a viral respiratory infection. This idea is supported by the finding that destruction of sensory nerves with capsaicin inhibits the induction of airway hyperresponsiveness by (a) repeated antigen inhalation, (b) toluene diisocyanate and (c) a delayed-type hypersensitivity reaction (Thompson *et al.*, 1987; Ladenius & Biggs, 1989; Matuse *et al.*, 1991; Ladenius & Nijkamp, 1993; Buckley & Nijkamp, 1994).

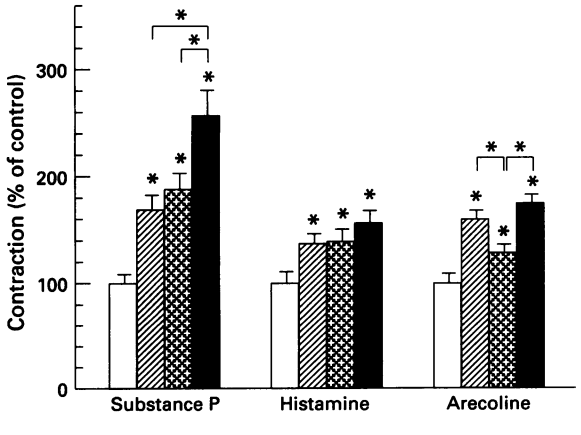

Figure 3 Maximal tracheal contractions (as % of control) in response to substance P, histamine and arecoline of guinea pigs: inoculated with control solution and exposed to a saline aerosol (open columns), inoculated with control solution and exposed to an ovalbumin-aerosol (hatched column), inoculated with PI-3 virus and exposed to a saline aerosol (cross hatched columns) or inoculated with PI-3 virus and exposed to an ovalbumin-aerosol (solid columns). *$P<0.01$ (ANOVA followed by Student-Neumann-Keuls) compared to the control inoculated group or indicated group. The data are presented as mean ± s.e.mean ($n=8$).

Part of the hyperresponsiveness to substance P was still present after capsaicin pretreatment. Interestingly, Jacoby *et al.* (1988) and Dusser *et al.* (1989) showed that the activity of the neutral endopeptidase, the main degradative enzyme for substance P, decreases in the respiratory tract after a viral infection. The increasing residence time of substance P might be responsible for the increased responsiveness in virally infected capsaicin pretreated animals.

Parainfluenza-3 virus expresses large quantities of neuraminidase on its viral coat (Scheid *et al.*, 1972). This enzyme is known to reduce the activity of neutral endopeptidase (Dusser *et al.*, 1989) but can also degrade muscarinic M_2 receptors (Fryer *et al.*, 1990). This decrease in the M_2-receptor subtype has been shown to increase bronchoconstriction induced by vagal stimulation due to a decrease in the autoinhibition of acetylcholine release. However, the decrease in M_2-receptor number can not account for an increase in tracheal reactivity to exogenously applied histamine or the muscarinic agonist, arecoline.

In ovalbumin-treated guinea-pigs PI-3 virus only moderately affected the contraction in response to histamine or arecoline. This might indicate that the pathogenesis of airway hyperresponsiveness due to viral respiratory infections or due to ovalbumin is similar. Capsaicin pretreatment inhibits both the virus-induced (this study) and the ovalbumin-induced changes in airway responsiveness (Ladenius & Biggs, 1989; Matsuse *et al.*, 1991; Ladenius & Nijkamp, 1993). Therefore, a likely explanation for the induction of the increase in tracheal responsiveness to histamine and arecoline is that the concentration of tachykinins is enhanced in the respiratory tract of both models. The possibility cannot be excluded that the shortening capacity of the smooth muscle was already maximal to these agonists after ovalbumin aerosol exposure and thus viral infection could not further increase the shortening. Maximal contraction was not achieved for substance P. Interestingly, the increased tracheal responsiveness to substance P after virus- or ovalbumin-treatment was significantly enhanced when both treatments were combined. There is growing evidence that the release of neuropeptides is increased after ovalbumin exposure (Hsiue *et al.*, 1993, Kawano *et al.*, 1993, Mosimann *et al.*, 1993). It is tempting to speculate that the enhanced tracheal responsiveness in the ovalbumin-exposed animals is due to an increased release of tachykinins which induces a non-specific airway hyperresponsiveness and that in virus-infected animals the hyperresponsiveness is due to a decreased activity of neutral endopeptidase activity. Both treatments could lead to an additional increase in airway hyperresponsiveness.

It is concluded that tachykinins contribute to the virus-induced airway hyperresponsiveness and that these neuropeptides could be involved in the enhancement of asthmatic exacerbations due to viral respiratory infections.

This work was supported by a grant from the Dutch Asthma Foundation. A.R.C.L. was supported by a grant from the Dutch Asthma Foundation. The Utrecht Institute for Pharmaceutical Sciences is part of the research schools Infection & Immunity and Groningen Utrecht Institute for Drug Exploration.

References

BARNES, P., BARANIUK, J.N. & BELVISI, M.G. (1991). Neuropeptides in the respiratory tract. Part 1. *Am. Rev. Respir. Dis.*, **144,** 1187–1198.

BUCKLEY, T.L. & NIJKAMP, F.P. (1994). Airways hyperreactivity and cellular accumulation in a delayed-type hypersensitivity reaction in the mouse. Modulation by capsaicin-sensitive nerves. *Am. J. Respir. Crit. Med.*, **149,** 400–407.

DUSSER, D.J., JACOBY, D.B., DJORKIC, T.D., RUBINSTEIN, I., BORSON, D.B. & NADEL, J.A. (1989). Virus induces airway hyperresponsiveness to tachykinins: role of neutral endopeptidase. *J. App. Physiol.*, **67,** 1504–1511.

EMPEY, D.W., LAITINEN, L.A., JACOB, S.L., GOLD, W.M. & NADEL, J.A. (1976). Mechanisms of bronchial hyperreactivity in normal subjects after respiratory tract infection. *Am. Rev. Respir. Dis.*, **113,** 131–139.

FOLKERTS, G., DE CLERCK, F., REIJNART, I., SPAN, P. & NIJKAMP, F.P. (1993a). Virus-induced airway hyperresponsiveness in the guinea-pig: possible involvement of histamine and inflammatory cells. *Br. J. Pharmacol.*, **108,** 1083–1093.

FOLKERTS, G., LINDE, VAN DER H. & NIJKAMP, F.P. (1995). Virus-induced airway hyperresponsiveness in guinea pigs is related to a deficiency in nitric oxide. *J. Clin. Invest.*, **95,** 26–30.

FOLKERTS, G., VERHEYEN, A.K.C.P., GEUENS, G.M.A., FOLKERTS, H.F. & NIJKAMP, F.P. (1993b). Virus-induced changes in airway responsiveness, morphology, and histamine levels in guinea pigs. *Am. Rev. Respir. Dis.*, **147,** 1569–1577.

FOLKERTS, G., VERHEYEN, A. & NIJKAMP, F.P. (1992). Viral infection in guinea pigs induces a sustained non-specific airway hyperresponsiveness and morphological changes of the respiratory tract. *Eur. J. Pharmacol. - Environ. Toxicol. Pharmacol. Sec.*, **228,** 121–130.

FRYER, A.D., EL-FAKAHANY, E.E. & JACOBY, D.B. (1990). Parainfluenza virus type 1 reduces the affinity of agonists for muscarinic receptors in guinea-pig lung and heart. *Eur. J. Pharmacol.*, **181,** 51–58.

HSIUE, T.-R., GARLAND, A., RAY, D.W., HERSHENSON, M.B., LEFF, A.R. & SOLWAY, J. (1992). Endogenous sensory neuropeptide release enhances nonspecific airway responsiveness in guinea pigs. *Am. Rev. Respir. Dis.*, **146,** 148–153.

HSIUE, T.-R., LEFF, A.R., GARLAND, A., HERSHENSON, M.B., RAY, D.W. & SOLWAY, J. (1993). Impaired sensory neural function after allergen-induced mediator release. *Am. Rev. Respir. Dis.*, **148,** 447–54.

ISHIDA, K., KELLY, L.J., THOMSON, R.J., BEATTIE, L.L. & SHELLENBERG, R.R. (1989). Repeated antigen challenge induces airway hyperresponsiveness with tissue eosinophilia in guinea pigs. *J. Appl. Physiol.*, **67,** 1133–1139.

JACOBY, D.B., TAMAOKI, J., BORSON, D.B. & NADEL, J.A. (1988). Influenza infection causes airway hyperresponsiveness by decreasing enkephalinase. *J. Appl. Physiol.*, **64,** 2653–2658.

KAWANO, O., KOHROGI, H., YAMAGUCHI, T., ARAKI, S. & ANDO, M. (1993). Neutral endopeptidase inhibitor potentiates allergic bronchoconstriction in guinea pigs in vivo. *J. Appl. Physiol.*, **75,** 185–190.

LADENIUS, A.R.C. & BIGGS, D.F. (1989). Capsaicin prevents the induction of airway hyperresponsiveness in a guinea-pig model of asthma. *Am. Rev. Respir. Dis.*, **139,** A232.

LADENIUS, A.R.C., CAMPBELL, J.W., SIVAPRASAD, S., SURESH, M.R. & BIGGS, D.F. (1991). Active immunization against substance P prevents the development of airway hyperresponsiveness in a guinea-pig model of asthma. *Am. Rev. Respir. Dis.*, **143,** A614.

LADENIUS, A.R.C. & NIJKAMP, F.P. (1993). Capsaicin pretreatment of guinea pigs *in vivo* prevents ovalbumin induced tracheal hyperreactivity *in vitro*. *Eur. J. Pharmacol.*, **235,** 127–131.

MACINTOSH, K., ELLIS, E.F., HOFFMAN, L.S., LYBASS, T.G., ELLER, J.J. & FULGINITI, V.A. (1973). The association of viral and bacterial respiratory infections with exacerbation of wheezing in young asthmatic children. *J. Pediatr.*, **82,** 578–90.

MATSUSE, T., THOMSON, R.J., CHEN, X.-R., SALARI, H. & SCHELLENBERG, R.R. (1991). Capsaicin inhibits airway hyperresponsiveness but not lipoxygenase activity or eosinophilia after repeated aerosolized antigen in guinea pigs. *Am. Rev. Respir. Dis.*, **144,** 368–372.

MOSIMANN, B.L., WHITE, M.V., HOHMAN, R.J., GOLDRICH, M.S., KAULBACH, H.C. & KALINER, M.A. (1993). Substance P, calcitonin gene-related peptide, and vasoactive intestinal peptide increase in nasal secretions after allergen challenge in atopic patients. *J. Allergy Clin. Immunol.*, **92,** 95–104.

OMINI, C., BRUNELLI, G., HERNANDEZ, A. & DAFFONICHIA, L. (1989). Bradykinin and substance P potentiate acetylcholine-induced bronchospasm in guinea pig. *Eur. J. Pharmacol.*, **163,** 195–197.

OUELLETTE, J.J. & REED, C.E. (1965). Increased response of asthmatic subjects after influenza vaccine. *J. Allergy*, **36,** 558–563.

SABAN, R., DICK, E.C., FISHLEDER, R.I. & BUCKNER, C.K. (1987). Enhancement by parainfluenza 3 virus infection of contractile responses to substance P and capsaicin in airway smooth muscle from the guinea pig. *Am. Rev. Respir. Dis.*, **136,** 586–591.

SARIA, A., MARTLING, C.R., YAN, Z., THEODORSSON-NORHEIM, E., GAMSE, R. & LUNDBERG, J.M. (1988). Release of multiple tachykinins from capsaicin-sensory nerves in the lung by bradykinin, histamine, dimethylphenylpiperazinum and vagal nerve stimulation. *Am. Rev. Resp. Dis.*, **137,** 1330–1335.

SCHEID, A., CALIGUIRI, L.A., COMPANS, R.W. & CHOPPIN, P.W. (1973). Isolation of paramyxovirus glycoproteins. Association of both hemagglutinating and neuraminidase activities with the larger SV5 glycoprotein. *Virology*, **50,** 640–644.

TAMURA, G., SAKAI, K., TANIGUCHI, Y., IIJIMA, H., HONMA, M., KATSUMATA, U., MARUYAMA, N., AIZAWA, T. & TAKISHIMA, T. (1989). Neurokinin A-induced bronchial hyperresponsiveness to methacholine in Japanese monkeys. *Tohoky J. Exp. Med.*, **159,** 69–73.

THOMPSON, J.E., SCYPINSKI, L.A., GORDON, T. & SHEPPARD, D. (1987). Tachykinins mediate the acute increase in airway responsiveness caused by toluene diisocyanate in guinea pigs. *Am. Rev. Respir. Dis.*, **136,** 43–49.

UMENO, E., HIROSE, T. & SISHIMA, S. (1992). Pretreatment with aerosolized capsaicin potentiates histamine-induced bronchoconstriction in guinea pigs. *Am. Rev. Respir. Dis.*, **146,** 159–162.

WARNER, E.A., KRELL, R.D. & BUCKNER, C.K. (1990). Pharmacologic studies on the differential influence of inhibitors of neutral endopeptidase on nonadrenergic, noncholinergic contractile responses of the guinea pig isolated hilar bronchus to transmural electrical stimulation and exogenously applied tachykinins. *J. Pharmacol. Exp. Ther.*, **254,** 824–830.

(Received October 17, 1994
Revised March 29, 1995
Accepted April 4, 1995)

British Journal of Pharmacology (1995) 115, 1053-1063 © 1995 Stockton Press All rights reserved 0007-1188/95 $12.00

Phosphorus-containing peptides as mixed inhibitors of endopeptidase 3.4.24.15 and 3.4.24.16: effect on neurotensin degradation *in vitro* and *in vivo*

Bruno Vincent, *Vincent Dive, **Athanasios Yiotakis, †Claire Smadja, †Raphaël Maldonado, Jean-Pierre Vincent & [1]Frédéric Checler

Institut de Pharmacologie Moléculaire et Cellulaire, UPR 411, CNRS, Université de Nice Sophia Antipolis, 660 route des Lucioles 06560 Valbonne, France; *Laboratoire Structure des protéines en solution, CEN de Saclay, Gif sur Yvette, France; **Department of Organic Chemistry, Laboratory of Organic Chemistry, University of Athens, Panepismiopolis, Zografou, Athens 15771, Greece and †Département de Chimie Organique, U266 INSERM, UA498 CNRS, UER des Sciences Pharmaceutiques et Biologiques, 4 Av. de l'Observatoire, 75006 Paris, France

1 We have examined several phosphorus-containing peptides as potential mixed inhibitors of two neurotensin-degrading zinc metallopeptidases, endopeptidase 3.4.24.15 and endopeptidase 3.4.24.16.

2 Among a series of 13 phosphonamide peptides, N-(2-(2-naphtyl)ethylphosphonyl-glycyl-prolyl-norleucine (phosphodiepryl 08) was found to inhibit potently the hydrolysis of neurotensin by purified endopeptidase 3.4.24.15 and 3.4.24.16 with an identical K_i value of 0.4 nM.

3 Phosphodiepryl 08 displayed a strong selectivity towards the two peptidases since it failed to inhibit several other zinc-containing peptidases such as endopeptidase 3.4.24.11, angiotensin-converting enzyme, aminopeptidase M, leucine aminopeptidase and carboxypeptidases A and B.

4 The protective effect of phosphodiepryl 08 on neurotensin degradation was examined *in vitro* and *in vivo* in central and peripheral bioassays.

5 Phosphodiepryl 08 virtually abolished neurotensin degradation by 4-day-old plated pure cultured neurones from mouse embryos and greatly potentiated neurotensin-induced antinociception in the mouse hot plate test.

6 In the periphery, phosphodiepryl 08 inhibited neurotensin degradation by membranes prepared from isolated longitudinal smooth muscle of guinea-pig ileum and greatly potentiated the neurotensin-induced contraction of the same longitudinal smooth muscle preparation.

7 Our study indicates that phosphodiepryl 08 behaves as a potent and selective mixed inhibitor of endopeptidase 3.4.24.15 and 3.4.24.16 and can be used as a powerful agent to prevent neurotensin degradation, *in vitro* and *in vivo*, in central and peripheral assays.

Keywords: Neurotensin; degradation; peptidases; endopeptidase 3.4.24.15; endopeptidase 3.4.24.16; phosphorus peptides; inhibitors; ileum contraction; cultured neurones; analgesia

Introduction

We previously examined the catabolic fate of the tridecapeptide neurotensin by various membrane preparations and cells of central and peripheral origin (Checler *et al.*, 1988). It appeared consistently that neurotensin was hydrolysed at its Arg^8-Arg^9 and Pro^{10}-Tyr^{11} peptidyl bonds, leading to the biologically inactive products, neurotensin (1-8) and neurotensin (1-10) (Checler *et al.*, 1988). By means of specific inhibitors, we demonstrated that endopeptidase 3.4.24.15 was responsible for the formation of neurotensin (1-8) (Checler *et al.*, 1985) while neurotensin (1-10) mainly resulted from cleavage by an unidentified peptidase (Checler *et al.*, 1983; 1984; 1985) later purified in our laboratory (Checler *et al.*, 1986b) and now called endopeptidase 3.4.24.16 (or neurolysin, Checler *et al.*, 1994). Therefore, the development of mixed inhibitors able to block potently endopeptidase 3.4.24.15 and endopeptidase 3.4.24.16 would be of considerable use for *in vitro* and *in vivo* work with neurotensin by preventing the degradation of the peptide.

Phosphonamide peptides have been shown to behave as very potent inhibitors of metallopeptidases that contain a zinc atom at their active site (Barlett & Marlowe, 1987), a physicochemical feature that is shared by both endopeptidases 3.4.24.15 and 3.4.24.16 (Pierotti *et al.*, 1990; Checler *et al.*, 1986b). Here we examine a series of phosphorus-containing peptides as potential blockers of endopeptidases 3.4.24.15 and 3.4.24.16. One of them, N-[2-(2-naphtyl)ethylphosphonyl]-Gly-Pro-norleucine (referred to as phosphodiepryl 08), inhibits both enzymes equally (K_I=0.4 nM) and displays high selectivity towards these peptidases compared to other zinc metalloexo- and endo-peptidases. In addition, we report on the ability of this agent to reduce greatly neurotensin degradation by pure cultured neurones from mouse embryos and by membranes prepared from isolated longitudinal smooth muscle of guinea-pig ileum. Finally, we examine the effect of phosphodiepryl 08 on the neurotensin-induced nociceptive response in mice after i.c.v. administration as well as on the neurotensin-induced contraction of isolated longitudinal smooth muscle from guinea-pig ileum.

Methods

Purification of endopeptidase 3.4.24.16 and endopeptidase 3.4.24.15

Rat brain endopeptidase 3.4.24.16 and endopeptidase 3.4.24.15 were purified according to procedures described previously by Barelli *et al.* (1988, 1991).

[1] Author for correspondence.

Preparation of membrane homogenates from rat brain and guinea-pig ileal longitudinal smooth muscle

Rats were decapitated, the brain immediately removed and homogenized by polytron in 5 mM Tris/HCl, pH 7.5. Protein concentrations were adjusted to 10 mg ml^{-1} in the same buffer. Longitudinal smooth muscle strips (including myenteric plexus) of about 2 cm were dissected out from the ileum of two- to three-month old guinea-pigs. Homogenization was carried out as above and protein concentrations were adjusted to 3.5 mg ml^{-1}.

Primary cultured neurones

Primary cultures of neurones were prepared from hemispheres of 14-day-old mouse embryos as previously described (Chabry *et al.*, 1990). At the beginning of the third day, cytosine arabinofuranoside (5 μM) was added to the medium for 24 h to prevent glial cell proliferation. We previously established that, in our experimental conditions, neuronal cultures appeared totally devoid of glial fibrillary acidic protein immunoreactivity, a specific astrocytic marker (Vincent *et al.*, 1994).

Degradation experiments and h.p.l.c. analysis

H.p.l.c. analysis Samples were applied on a reverse-phase C_{18} lichrosorb column (Merck) and eluted as previously described (Checler *et al.*, 1988). Absorbance was monitored at 230 nm with a detector setting of 0,05 full scale.

Neurotensin degradation by endopeptidase 3.4.24.16 and endopeptidase 3.4.24.15 Neurotensin (2 nmol, 20 μM) was incubated at 37°C with 10 μl of purified endopeptidase 3.4.24.16 or endopeptidase 3.4.24.15 in a final volume of 100 μl of 5 mM Tris/HCl pH 7.5, in the absence or in the presence of increasing concentrations of inhibitors. Incubations were acidified (10 μl of 1 M HCl) and analysed by h.p.l.c.

Neurotensin degradation by plated pure cultured neurones Monolayers of four-day-old plated neurones were washed twice with PBS buffer, pH 7.4 (mM: NaCl 140, Na_2HPO_4 8.5, KCl 2.7, KH_2PO_4 1.5). After aspiration of the buffer, neurotensin (10 nmol, 10 μM) was incubated with cells for 4 h at 37°C in a final volume of 1 ml of PBS, pH 7.4, in the absence or in the presence of various concentrations of peptidase inhibitors. At the end of the incubations, supernatants were removed, acidified (with 100 μl of 1 M HCl) and analysed by h.p.l.c. as above.

Neurotensin degradation by membranes from guinea-pig ileum longitudinal smooth muscle Neurotensin (2 nmol, 20 μM) was incubated for various times at 37°C with membrane homogenates (35 μg of protein) in a final volume of 100 μl of 5 mM Tris/HCl, pH 7.5, in the absence or in the presence of peptidase inhibitors. Incubations were then stopped by acidification (10 μl, 1 M HCl) and analysed by h.p.l.c. as above.

Carboxypeptidases A and B assays Hip-Phe and Hip-Lys (3 nmol, 30 μM) were incubated for 15 min at 37°C with 0.4 μg or 0.5 μg of purified carboxypeptidases A or B respectively, in a final volume of 100 μl of 5 mM Tris/HCl pH 7.5, in the absence or in the presence of inhibitor. Incubations were stopped and analysed by h.p.l.c. as above.

Fluorimetric assays of purified peptidases

Endopeptidase 3.4.24.16 and endopeptidase 3.4.24.15 Endopeptidase 3.4.24.16 (10 μl) was incubated with 50 μM of QFS for 1 h at 37°C, in a final volume of 100 μl of 5 mM Tris/HCl pH 7.5, in the absence or in the presence of increasing concentrations of phosphodiepryl 08. Incubations were stopped and enzymatic activities were fluorimetrically recorded as previously described (Dauch *et al.*, 1991a). Endopeptidase 3.4.24.15 was monitored with QFS as above or with 0.5 mM of Bz-Gly-Ala-Ala-Phe-pAB as the substrate (Checler, 1993).

Endopeptidase 3.4.24.11 Suc-Ala-Ala-Phe-7AMC (0.5 mM) was incubated with 25 ng of purified endopeptidase 3.4.24.11 for 10 min at 37°C in a final volume of 100 μl of 5 mM Tris/HCl pH 7.5. The 7AMC group was released from the Phe-7AMC degradation product upon exogenous aminopeptidase attack (5 μg of leucine aminopeptidase for 1 h at 37°C as described by Checler, 1993). Inhibition experiments were performed by addition of 1 μM phosphoramidon or various concentrations of phosphodiepryl 08.

Angiotensin-converting enzyme Hippuryl-His-Leu (1 mM) was incubated with 0.6 μg of purified angiotensin-converting enzyme for 10 min at 37°C in a final volume of 100 μl of 5 mM Tris/HCl pH 7.5 containing 0.3 M NaCl. Inhibition of angiotensin-converting enzyme was performed by addition of 1 μM captopril or various concentrations of phosphodiepryl 08.

Aminopeptidase M and leucine aminopeptidase Leu-7AMC (0.5 mM) was incubated for 6 min with 0.2 μg of leucine aminopeptidase or 0.5 μg of aminopeptidase M in 100 μl of 5 mM Tris/HCl pH 7.5. Inhibition studies were performed by prior incubations of the enzymes with 50 μM bestatin or increasing concentrations of phosphodiepryl 08.

Fluorimetric substrate-hydrolysing activities in whole rat brain homogenate Incubations were performed for various times at 37°C in 5 mM Tris/HCl pH 7.5 with a final concentration of 1 mg ml^{-1} of brain homogenate protein and activities were quantified as previously described (Checler, 1993). Briefly, proline endopeptidase activity was monitored by following the hydrolysis of 0.1 mM Z-Gly-Pro-7AMC and inhibition of the activity was obtained with 1 μM Z-Pro-Prolinal. Post-proline dipeptidyl aminopeptidase (DAP IV) was detected with 1 mM Gly-Pro-7AMC and inhibited by 100 μM of diprotin A. Aminopeptidase B was assayed with 0.2 mM Arg-7AMC and inhibited by 0.5 μM arphamenine B. All other activities were detected in the conditions described for assaying purified peptidases.

Hot plate test Male mice weighing 18–22 g were injected i.c.v. with 10 μl of sterile saline buffer (0.9% NaCl) or neurotensin (in saline) in the presence or in the absence of various quantities of phosphodiepryl 08. The hot plate test was derived from that described by Eddy & Leimbach (1953). The plate was maintained at a temperature of 55±0.5°C with a regulated water circulating pump. The antinociception test was assessed 15 min after i.c.v. injection and the reaction times (latency of both fore-paw licking with a cut-off time of 30 s) of mice placed in a glass cylinder (20 cm high, 16 cm diameter) surrounding the plate were determined as described (Schmidt *et al.*, 1991).

Guinea-pig ileal longitudinal smooth muscle contraction assays Female guinea-pigs (2–3 months) were used in all studies. The longitudinal smooth muscle (including the myenteric plexus) was dissected out from whole ileum according to Paton & Zar (1968) and strips 1.5–2 cm in length were set up for isometric tension recording in 3 ml organ baths containing modified Tyrode solution (mM: NaCl 136.8, KCl 2.7, $MgSO_4$ 1, NaH_2PO_4 0.4, $NaHCO_3$ 11.9, $CaCl_2$ 2.5, glucose 5.5) to which was added 100 nM neostygmine methylsulphate. The strips were allowed to equilibrate for 45 min in modified Tyrode solution (maintained at 37°C under 95% O_2 and 5% CO_2) and washed every 10 min. Peptidase inhibitors were included in organ baths before the addition of various concentrations of neurotensin.

Protein concentrations Protein concentrations were determined by the Bradford method with white egg lysozyme as the standard.

Materials

Mcc-Pro-Leu-Gly-Pro-DLys-Dnp (QFS) and diprotin A were from Novabiochem. Di-isopropylfluorophosphate-treated carboxypeptidase A, leucine aminopeptidase (microsomal, type IV), angiotensin-converting enzyme, bestatin and all the chromogenic and fluorimetric substrates were from Sigma chemicals. Carboxypeptidase B and aminopeptidase M were from Boehringer Mannheim. Neurotensin was from Neosystem. Endopeptidase 3.4.24.11 was purified and kindly provided by Dr Patrick Auberger (INSERM U 364, Faculté de Médecine, Nice, France). Arphamenine B was from Interchim. Benzyloxycarbonyl-prolyl-prolinal (Z-Pro-Prolinal) and Bz-Gly-Ala-Ala-Phe-pAB were kindly donated by Drs S. Wilk and M. Orlowski (Mount Sinai, School of Medicine, New York, U.S.A.). The synthesis of phosphorus-containing peptides has been described previously (Dive *et al.*, 1990; Yiotakis *et al.*, 1994).

Results

Effect of phosphorus-containing peptides on endopeptidases 3.4.24.15 and 3.4.24.16

Table 1 summarizes the affinities of various phosphorus-containing peptides for endopeptidase 3.4.24.15 and endopeptidase 3.4.24.16. This was assessed by means of neurotensin that was previously shown to behave as a good substrate of both peptidases. The most striking feature concerns the parallel observed between the K_i values obtained for endopeptidases 3.4.24.15 and 3.4.24.16. Indeed, there exists only a threefold factor between the K_i values determined for the inhibitors (compounds 05 and 11) that discriminate the most between the two enzymes.

As compared to phosphodiepryl 03 (compound 03), the low potency of compound 01 underlines the positive contribution of an aromatic substituent to the binding process. Interestingly, there is an optimal length (corresponding to 2 or 3 methylene groups) between this aromatic group and the phosphonamide moiety that leads to favourable interactions (compounds 03 and 04). Introduction of a substituent in the *para* position of the phenyl group (compound 05) slightly improves the K_i values for both enzymes. The fact that the addition of a naphtyl group further increases the potency of the inhibitor (compare compounds 03 and 08) probably indicates that the S_1 subsite can accomodate hydrophobic groups with distinct sizes. Compound 06 reveals that the hindrance introduced by an unsaturated double bond, drastically affects the inhibitory potency of the agent.

Replacement of the glycyl residue in the P'_1 position by an alanyl residue in the L configuration slightly improves the affinity of the compound for both peptidases (compare 03 and 07). By contrast, a D-alanyl residue in this P'_1 site strongly diminishes the affinity of the inhibitor (compare compounds 07 and 09) for both enzymes. This emphasizes the strict stereochemical requirements of the S'_1 site of these two peptidases. Introduction of an alanyl residue in P'_2 (compound 10) leads to a 24 fold reduction in K_i while such replacement in the P'_3 position (compound 11) does not modify the inhibitory potency of the molecule for endopeptidase 3.4.24.16 and only slightly increases K_i against endopeptidase 3.4.24.15.

The activity of phosphonamide and phosphinic peptides containing a pseudo amino-acid on both sides of the phosphorus moiety was also examined. The rather good potency displayed by compound 13 confirms the preference of the S_1 subsite of these peptidases for aromatic groups. Interestingly, the substitution of phosphonamide by a phosphinic group reduces the affinity of the inhibitor only by a factor of 4 and 7 for endopeptidase 3.4.24.15 and endopeptidase 3.4.24.16, respectively (compare compounds 13 and 14). This reduction is relatively slight when compared with the introduction of a phosphonate group that induces a drastic loss of affinity (compare compounds 03 and 16).

One of the best inhibitors (compound 08, referred to as phosphodiepryl 08) was thoroughly examined to establish its inhibitory potency against hydrolysis of neurotensin by purified endopeptidases 3.4.24.15 and 3.4.24.16, its selectivity towards other zinc metalloproteases and its ability to interfere with neurotensin degradation, *in vitro* and *in vivo*, in central and peripheral assays.

Effect of phosphodiepryl 08 on purified endopeptidases 3.4.24.15 and 3.4.24.16

As previously described purified endopeptidase 3.4.24.16 generates the two catabolites neurotensin (1 – 10) and neurotensin (11 – 13) (Figure 1a). The formation of both degradation products appears to be inhibited dose-dependently by phosphodiepryl 08 and was virtually abolished at a concentration of 3×10^{-8} M (Figure 1). Similarly, phosphodiepryl 08 prevents

Table 1 Inhibition of endopeptidase 3.4.24.15 and endopeptidase 3.4.24.16 by phosphorus-containing peptides

Compound	Inhibitor	K_i (nM) Endopeptidase 3.4.24.16	Endopeptidase 3.4.24.15
01	CH_3 ψ [PO_2NH]-Gly-Pro-Nle	78	150
02	ϕ CH_2 ψ [PO_2NH]-Gly-Pro-Nle	379	553
03	ϕ CH_2-CH_2 ψ [PO_2NH]-Gly-Pro-Nle	1.6	2.6
04	ϕ CH_2-CH_2-CH_2 ψ [PO_2NH]-Gly-Pro-Nle	3.4	3.9
05	pCF_3-ϕ CH_2-CH_2 ψ [PO_2NH]-Gly-Pro-Nle	0.7	2.2
06	Cin ψ [PO_2NH]-Gly-Pro-Nle	299	518
07	ϕ CH_2-CH_2 ψ [PO_2NH]-Ala-Pro-Nle	0.4	0.4
08	2-Nap CH_2-CH_2 ψ [PO_2NH]-Gly-Pro-Nle	0.4	0.4
09	ϕ CH_2-CH_2 ψ [PO_2NH]-DAla-Pro-Nle	369	251
10	ϕ CH_2-CH_2 ψ [PO_2NH]-Gly-Ala-Nle	39	40
11	ϕ CH_2-CH_2 ψ [PO_2NH]-Gly-Pro-LAla	1.4	4.2
12	ϕ CH_2-CH_2 ψ [PO_2NH]-Gly-Pro-LTyr	4.5	9.4
13	Z-(DL)Phe [PO_2NH]-Gly-Pro-Nle	5.5	8.5
14	Z-(L)Phe ψ [PO_2CH_2]-Gly-Pro-Nle	33	39
15	Z-(D)Phe ψ [PO_2CH_2]-Gly-Pro-Nle	209	323
16	ϕ CH_2-CH_2 ψ [PO_2O]-Gly-Pro-Nle	375	377

Neurotensin (2 nmol, 20 μM) was incubated with 10 μl of purified endopeptidase 3.4.24.16 or with 10 μl purified endopeptidase 3.4.24.15 for 1 h at 37°C in the presence of increasing concentrations (0.1 nM to 10 μM) of the indicated compounds. The K_i values were derived from the IC_{50} values (see Results) and are the mean of 4 independent determinations. ϕ, phenyl; Cin, cinnamoyl; 2-Nap, 2-naphtyl; Nle, norleucine, 2-aminohexanoic acid.

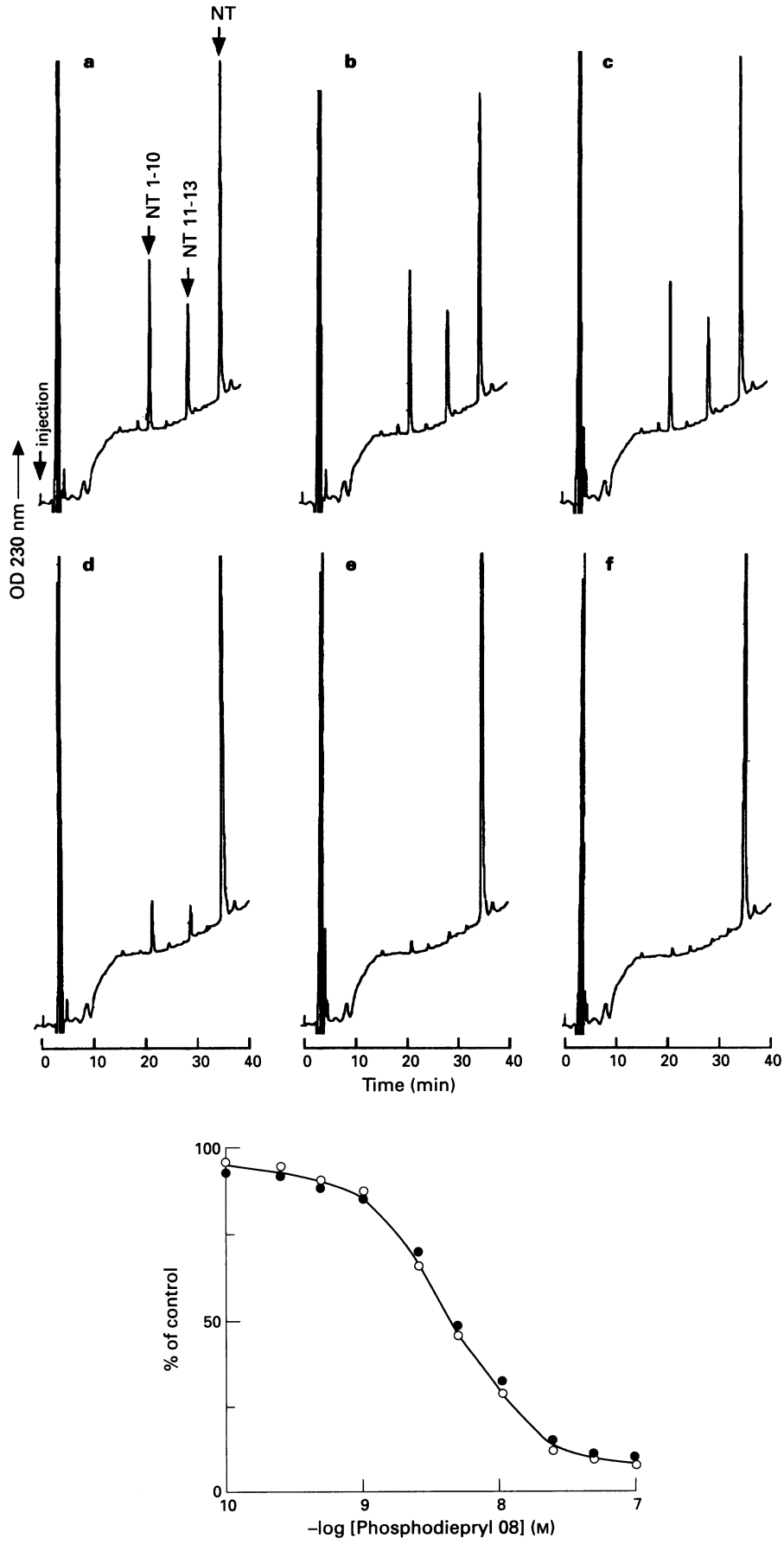

Figure 1 Effect of phosphodiepryl 08 on neurotensin hydrolysis by purified rat endopeptidase 3.4.24.16. Neurotensin (2 nmol, 20 μM) was incubated for 1 h at 37°C with 10 μl of purified endopeptidase 3.4.24.16 in 100 μl of 5 mM Tris/HCl, pH 7.5, in the absence (control, a) or in the presence of 0.1 nM (b); 1 nM (c); 10 nM (d); 100 nM (e) and 1 μM (f) phosphodiepryl 08. Incubations were acidified (10 μl, HCl 1 M) and submitted to reverse-phase h.p.l.c. as described in Methods. The curve represents the amount of neurotensin (1–10) (●) and neurotensin (11–13) (○) recovered in the presence of inhibitor and expressed as a percentage of the control value obtained in absence of phosphodiepryl 08 (a).

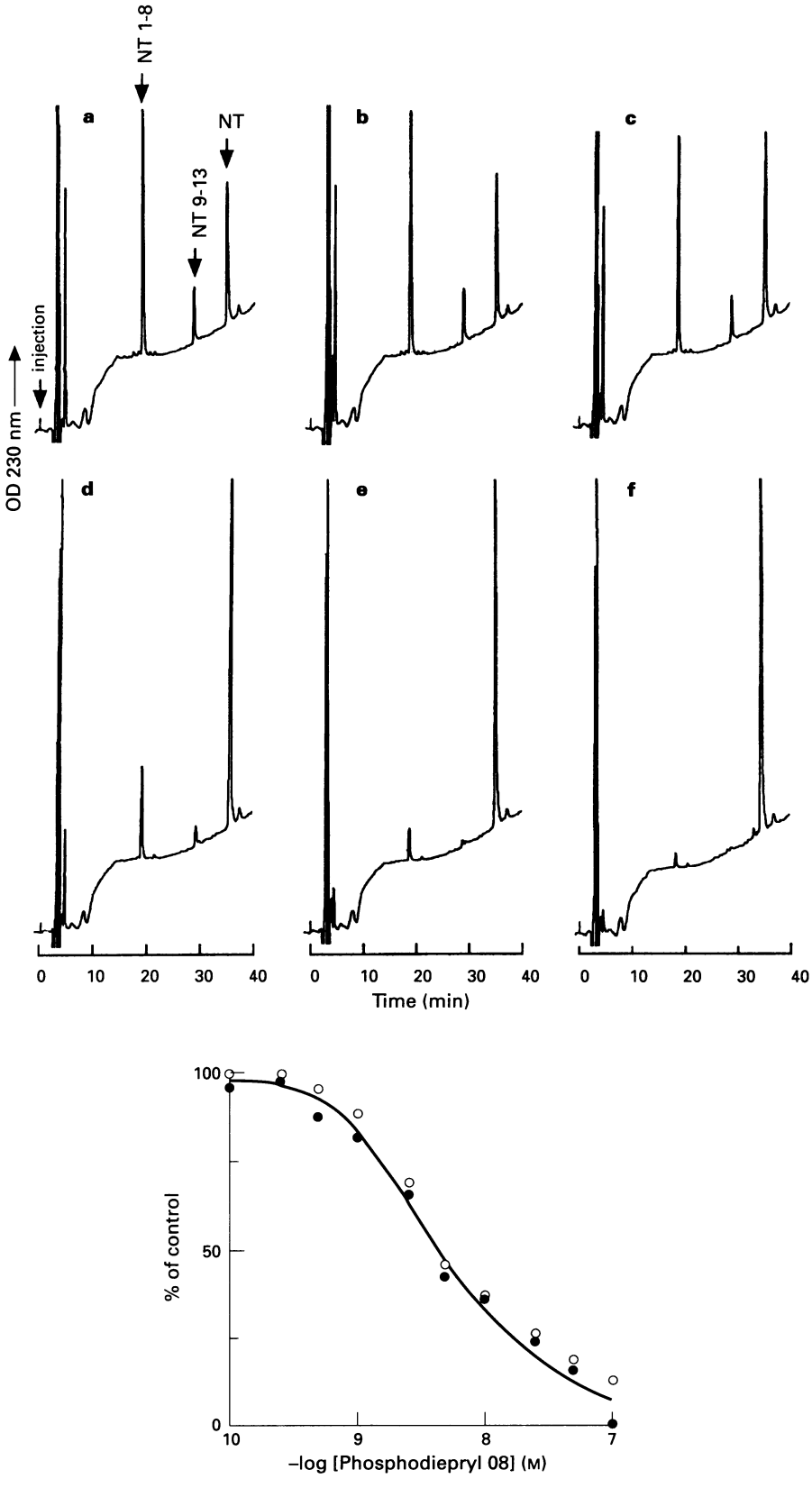

Figure 2 Effect of phosphodiepryl 08 on neurotensin hydrolysis by purified rat endopeptidase 3.4.24.15. Neurotensin (2 nmol, 20 μM) was incubated for 1 h at 37°C with 10 μl of purified endopeptidase 3.4.24.15 in 100 μl of 5 mM Tris/HCl pH 7.5 in the absence (control, a), or in the presence of 0.1 nM (b); 1 nM (c); 10 nM (d); 100 nM (e) and 1 μM (f) phosphodiepryl 08. Incubations were acidified (10 μl, HCl 1 M) and submitted to reverse-phase h.p.l.c. as described in Methods. The curve represents the amount of neurotensin (1–8) (●) and neurotensin (9–13) (○) recovered in the presence of inhibitor and expressed as the control degradation products obtained in absence of phosphodiepryl 08 (a).

the production of neurotensin (1–8) and neurotensin (9–13) (Figure 2a), the two catabolites that were generated by purified endopeptidase 3.4.24.15 (Orlowski *et al.*, 1983). The formation of these two products was diminished in parallel and was maximally inhibited at a concentration of 10^{-7} M phosphodiepryl 08 (Figure 2).

Figure 3 illustrates the effect of phosphodiepryl 08 on the hydrolysis of QFS, a quenched fluorimetric substrate of endopeptidase 3.4.24.16 (Dauch *et al.*, 1991a) and endopeptidase 3.4.24.15 (Barrett & Tisljar, 1989; Tisljar *et al.*, 1990). The curves indicate a dose-dependent and complete inhibition of the hydrolysis of the substrate. The K_i values in Table 2 were calculated according to the single relationship $IC_{50} = K_i (1 + \frac{S}{K_m})$ using K_m values of endopeptidase 3.4.24.16 for QFS and neurotensin of 25 μM and 2 μM, respectively (Dauch *et al.*, 1991a; Checler *et al.*, 1986b) and 9 μM and 2 μM for endopeptidase 24-15 (Tisljar *et al.*, 1990; Barelli *et al.*, 1991). These data indicate a K_i value of 0.4 nM for endopeptidase 3.4.24.16 whatever the substrate that was examined. The same affinity was observed for endopeptidase 3.4.24.15. Futhermore, we established that phosphodiepryl 08 inhibited the hydrolysis of Bz-Gly-Ala-Ala-Phe-pAB (a selective substrate for endopeptidase 3.4.24.15) with a virtually identical affinity (K_i = 2.2 nM, Table 2).

Selectivity of phosphodiepryl 08

We examined the putative inhibition of various purified zinc-metallopeptidases by phosphodiepryl 08. Figure 4 indicates that a concentration of 1 μM phosphodiepryl 08 did not affect endopeptidase 3.4.24.11 (neprylisin), angiotensin-converting

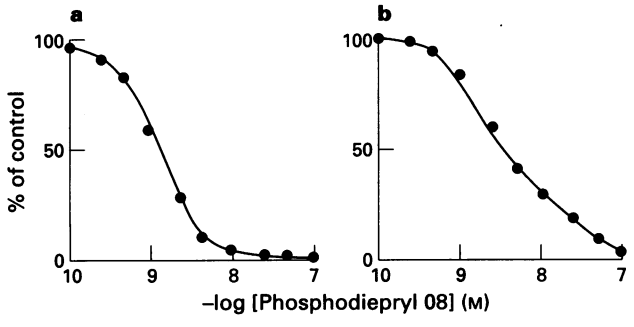

Figure 3 Effect of phosphodiepryl 08 on Mcc-Pro-Leu-Gly-Pro-DLys-Dnp (QFS) hydrolysis by purified endopeptidase 3.4.24.16 and endopeptidase 3.4.24.15. QFS (5 nmol, 50 μM) was incubated for 1 h at 37°C with 10 μl of purified endopeptidase 3.4.24.16 (a) or purified endopeptidase 3.4.24.15 (b) in 100 μl of 5 mM Tris/HCl pH 7.5 in the presence of various concentrations of phosphodiepryl 08. Incubations were stopped and fluorimetrically analysed as described in Methods. Values represent the mean of 3 independent determinations and are expressed as the percentage of activity obtained in absence of phosphodiepryl 08.

Table 2 K_i values of the inhibition of purified endopeptidase 3.4.24.15 and endopeptidase 3.4.24.16 by phosphodiepryl 08

	K_i (nM)		
Endopeptidase	*Neurotensin*	*QFS*	*Bz-Gly-Ala-Ala-Phe-pAB*
3.4.24.15	0.4	0.6	2.2
3.4.24.16	0.4	0.4	Not hydrolyzed

QFS and Bz-Gly-Ala-Ala-Phe-pAB hydrolyses were determined as described in Methods and neurotensin degradation was monitored by h.p.l.c. analysis as described in Methods. Values represent the mean of 5–8 independent determinations.

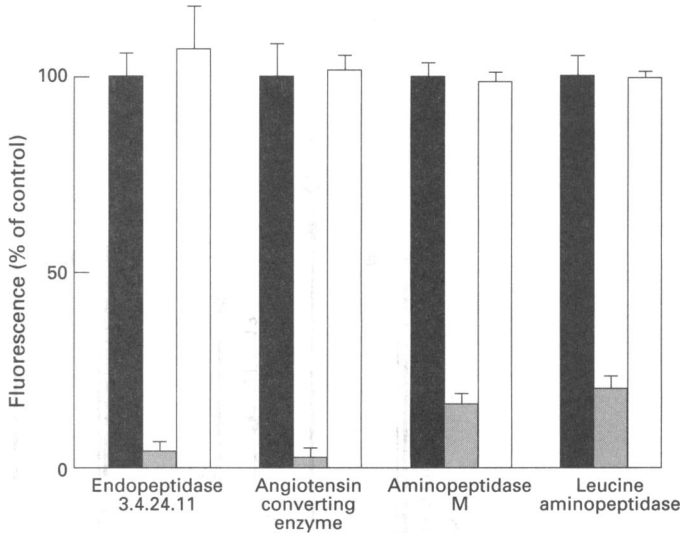

Figure 4 Effect of phosphodiepryl 08 and specific inhibitors on various purified peptidases. Activities were measured by incubating 0.5 mM Suc-Ala-Ala-Phe-7AMC (endopeptidase 3.4.24.11), 1 mM Hippuryl-His-Leu (angiotensin-converting enzyme) and 0.5 mM Leu-7AMC (aminopeptidase M and leucine aminopeptidase) under the conditions described in Methods, in the absence (solid columns) or in the presence of specific inhibitors (hatched columns) or 1 μM phosphodiepryl 08 (open columns). Incubations were stopped and activities were recorded as described in the Methods. Concentrations of inhibitors were as follows: endopeptidase 3.4.24.11, phosphoramidon 1 μM; angiotensin converting enzyme, captopril 1 μM; aminopeptidase M and leucine aminopeptidase, bestatin 50 μM. Values represent the mean ± s.e.mean of 4 independent determinations.

enzyme, leucine aminopeptidase and aminopeptidase M, the identities of which were confirmed by the sensitivity to their specific inhibitors (Figure 4). Furthermore, phosphodiepryl 08 was unable to modify the hydrolysis of Hip-Phe and Hip-Lys by carboxypeptidase A and carboxypeptidase B, respectively (Figure 5). Finally, the usefulness of phosphodiepryl 08 when employed with a crude membrane preparation from rat brain was assessed. Table 3 summarizes the effect of several specific inhibitors and phosphodiepryl 08 on the cleavage of various fluorimetric substrates by rat brain homogenates. Some of these substrates could not be considered as exclusive substrates for their pseudospecific peptidase. Indeed, the specific inhibitors of DAP IV and aminopeptidase B (i.e. diprotin A and arphamenine B, respectively) elicited only a faint or very partial inhibition of their respective peptidase. This indicated that Gly-Pro-7AMC and Arg-7AMC also behaved as substrates of additional peptidases. However, Table 3 clearly shows that these other peptidases were also unaffected by a concentration of 1 μM phosphodiepryl 08.

Effect of phosphodiepryl 08 on neurotensin degradation in the central nervous system

Two of the main neurotensin catabolites generated by plated 4-day-old pure cultured neurones are neurotensin (1–8) and neurotensin (1–10) (Figure 6a) consistent with our previous data (Checler *et al.*, 1986a; Vincent *et al.*, 1994). Phosphodiepryl 08 exerts a potent and dose-dependent inhibition of the formation of both products (Figure 6b) and potently increases the recovery of intact neurotensin. The IC_{50} observed (0.5 nM) led to the estimation of a K_i value of about 0.1 nM, in agreement with those observed with purified endopeptidases 3.4.24.15 and 3.4.24.16 (Table 2). This clearly suggests that these two peptidases mainly contribute to the inactivation of neurotensin by pure cultured neurones. In order to assess whether such conclusions also apply *in vivo* in the CNS, we examined the effect of phosphodiepryl 08 on the neurotensin-

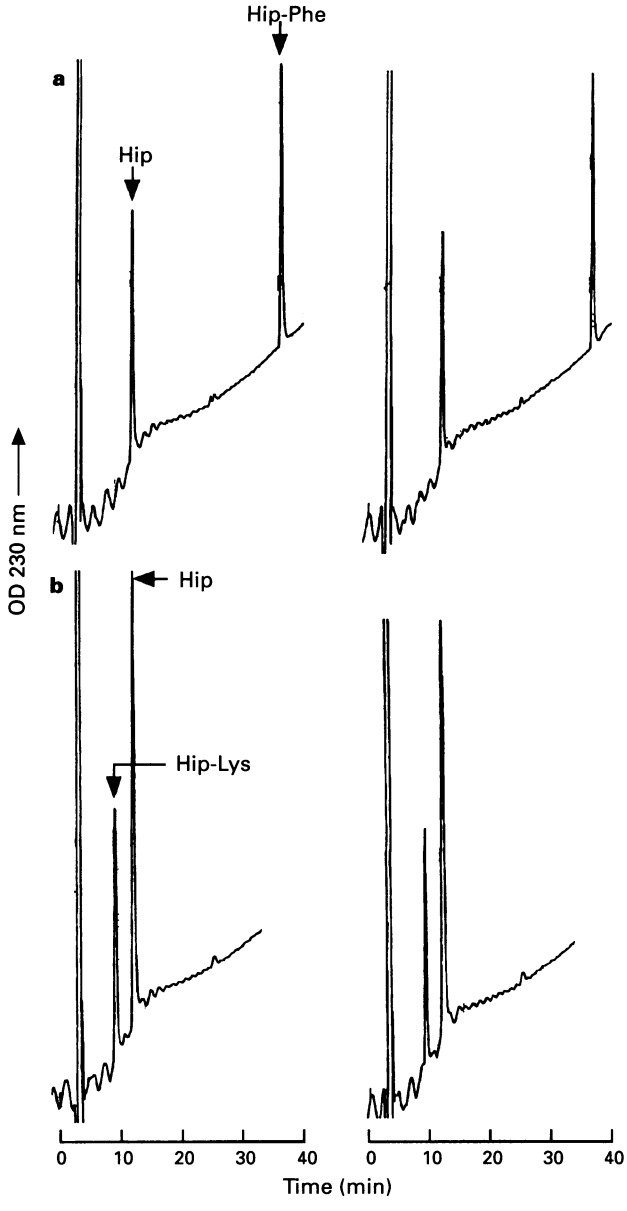

Figure 5 Effect of phosphodiepryl 08 on purified carboxypeptidase A and carboxypeptidase B. Carboxypeptidase A (0.4 μg) (a) and carboxypeptidase B (0.5 μg) (b) were incubated with Hip-Phe (3 nmol, 30 μM) and Hip-Lys (3 nmol, 30 μM), respectively, for 15 min at 37°C in a final volume of 5 mM Tris/HCl pH 7.5 in the absence (control, left panels) or in the presence of 1 μM phosphodiepryl 08 (right panels). Incubations were stopped by acidification and analysed by h.p.l.c. as described in Methods.

induced analgesic effect in mice. As shown in Figure 7, i.c.v. administration of neurotensin induced a dose-dependent antinociceptive response in the hot-plate tested mice. The administration of phosphodiepryl 08 with ineffective or submaximal doses of neurotensin greatly potentiated the antinociceptive effect of the peptide (Table 4).

Effect of phosphodiepryl 08 on peripheral neurotensin degradation

It has been shown previously that neurotensin contracts the isolated longitudinal smooth muscle from guinea-pig ileum (Kitabgi, 1982). This prejunctional effect appears to be mediated through cholinergic nerves located in the myenteric plexus that adheres to the longitudinal smooth muscle. Figure 8a illustrates the dose-dependent neurotensin-induced contraction of the longitudinal smooth muscle strip. Phosphodiepryl 08 greatly enhanced the contractile response elicited by a submaximal concentration (3 nM) of neurotensin (Figure 8b). Altogether, this seemed to indicate that endopeptidases 3.4.24.15 and 3.4.24.16 could participate in neurotensin catabolism in the gastrointestinal tract. In order to test this hypothesis further we examined the metabolic fate of neurotensin after exposure to homogenate membranes prepared from isolated longitudinal smooth muscle. Phosphodiepryl 08 slowed down the kinetics of neurotensin hydrolysis (Figure 9a) (half-lives of 13 and 47 min, in absence or in the presence of inhibitor, respectively) and virtually abolished the formation of neurotensin (1–8) and neurotensin (1–10) that corresponded to the only cleavage products identified after h.p.l.c. (Figure 9b).

Discussion

A classical strategy for the development of zinc-metalloprotease inhibitors is based on the use of the N- or C-terminal portion of the substrate to which a zinc chelating group (thiol, hydroxamate, carboalkyls) is attached in a suitable position. This approach has allowed the development of powerful and convenient molecules designed as mixed inhibitors of various metalloenzymes. Fournié-Zaluski *et al.* (1984) successfully designed a highly potent inhibitor of several enkephalin-degrading peptidases, kelatorphan, that fully prevents the degradation of exogenous enkephalins (Waksman *et al.*, 1985). Later, the same group developed the first systemically active inhibitor of endopeptidase 3.4.24.11 and aminopeptidase N, the two major peptidases that metabolize endogenous enkephalins (Noble *et al.*, 1992). This agent, designed as the prodrug RB101, produced a potent analgesic response in murine species through the elevation of extracellular levels of enkephalins (Noble *et al.*, 1992). French *et al.* (1994) also

Table 3 Effect of specific inhibitors and phosphodiepryl 08 on peptidase activities present in rat brain homogenates

		Enzyme activity	
Enzyme	*Substrate/Inhibitor*	*Specific inhibitor*	*Phospho-diepryl 08*
EC3.4.24.11	Suc-Ala-Ala-Phe-7AMC/phosphoramidon	22.2 ± 5	100 ± 4
ACE	Hip-His-Leu/Captopril	5.8 ± 1.5	93 ± 1
LAP/APM	Leu-7AMC/Bestatin	28.1 ± 2.4	87 ± 10
PE	Z-Gly-Pro-7AMC/Z-Pro-Prolinal	6.2 ± 0.8	100 ± 5
DAP IV	Gly-Pro-7AMC/Diprotin A	87 ± 0.4	100 ± 2
APB	Arg-7AMC/Arphamenine B	49 ± 3.6	96 ± 3

Activities were monitored by incubation of rat brain homogenate with the indicated substrates in the presence of phosphodiepryl 08 (1 μM) or saturating concentrations of the indicated specific inhibitors (for concentrations, see Methods). Values are expressed as a percentage of control activity obtained in absence of inhibitor and represent the mean ± s.e.mean of 4 independent determinations.

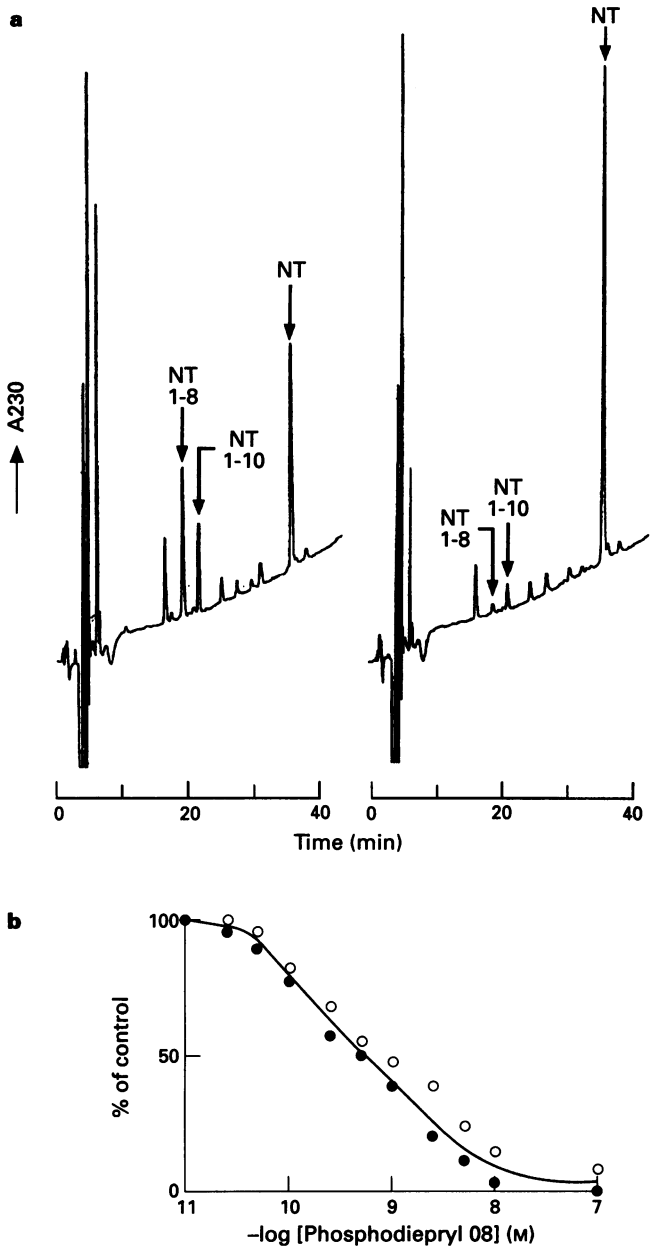

Figure 6 Effect of phosphodiepryl 08 on neurotensin hydrolysis by primary-cultured neurones. Neurotensin (10 nmol, 10 μM) was incubated with 4-day-old plated primary cultured neurones, for 4 h at 37°C, in 1 ml of PBS pH 7.4, in the absence (a, left panel), or in the presence of 10 nM phosphodiepryl 08 (a, right panel). Supernatants were then removed, acidified, (100 μl of 1 M HCl), and submitted to h.p.l.c. as described in Methods. Complete dose-response curves were established by incubating neurotensin (10 nmol, 10 μM) with the indicated increasing concentrations of phosphodiepryl 08 (b). Values are expressed as a percentage of control NT (1–8) (●) or NT (1–10) (○) recovered in absence of inhibitor and represented the mean of 4 independent determinations.

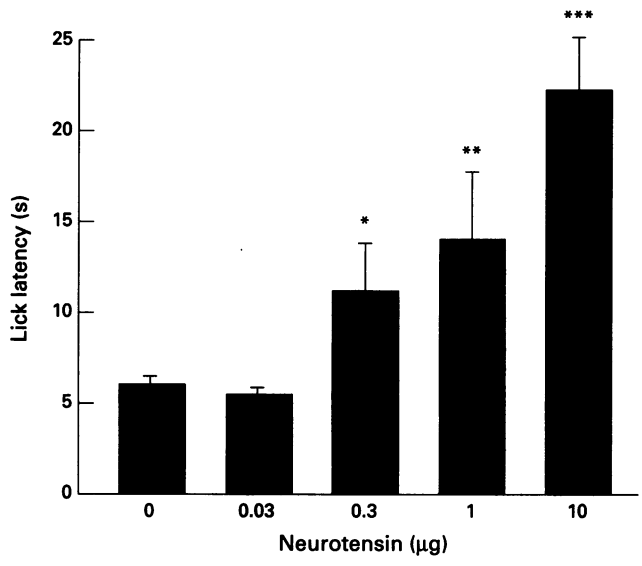

Figure 7 Neurotensin-induced antinociceptive effect on hot-plate tested mice. Fifteen min after the i.c.v. administration of saline buffer or the indicated dose of neurotensin, mice were placed on the hot plate (55°C) and the latency for the appearance of forepaw licking behaviour was determined. Columns represent the mean ± s.e.mean of results from 8 mice. $*P<0.1$ compared to the control (saline); $**P<0.05$; $***P<0.01$.

Table 4 Effect of phosphodiepryl 08 on neurotensin-induced antinociception in mice tested on the hot plate

Treatment	*Dose* (μg)	*Latency* (s)
Saline	–	5.99 ± 0.35
Phosphodiepryl 08	1	6.67 ± 1.25
Phosphodiepryl 08	3	7.50 ± 1.23
Neurotensin	0.03	5.40 ± 0.76
+ Phosphodiepryl 08	1	16.75 ± 3.34*
+ Phosphodiepryl 08	3	15.56 ± 3.71*
Neurotensin	0.3	11.27 ± 2.54
+ Phosphodiepryl 08	1	12.75 ± 2.63
+ Phosphodiepryl 08	3	18.65 ± 3.10*

Neurotensin was administered i.c.v. at the doses indicated in the absence or in the presence of various quantities of phosphodiepryl 08. Latency of appearance of forepaw licking behaviour was recorded 15 min after peptide and/or inhibitor administration. Results are given as means ± s.e.mean of 8 independent animals per group. $*P<0.05$ as compared to the same dose of neurotensin without inhibitor.

characterized a dual blocker of angiotensin-converting enzyme and endopeptidase 3.4.24.11. This agent increased the hypotensive, diuretic and natriuretic responses mediated by atrial natriuretic peptide and inhibited the hypertensive response thought to be dependent upon the conversion of angiotensin I into angiotensin II (French *et al.*, 1994).

From our previous studies, it appeared clear that potent inhibitors of the physiological degradation of neurotensin should target endopeptidases 3.4.24.16 and 3.4.24.15. Thus, we showed previously that endopeptidase 3.4.24.16 was the only peptidase that consistently participated in the metabolism of neurotensin by membrane preparations and cell cultures of central and peripheral origin (Checler *et al.*, 1988). Furthermore, we recently established that endopeptidase 3.4.24.16 was involved in the degradation of neurotensin, *in vivo*, in a model of vascularly perfused dog ileum (Barelli *et al.*, 1994). The present study indicates that endopeptidase 3.4.24.15, as well as endopeptidase 3.4.24.16, also contributed to neurotensin hydrolysis in plated pure cultured neurones. Furthermore, these two proteolytic activities appeared to contribute fully to neurotensin breakdown *in vitro* in membranes prepared from longitudinal smooth muscle of guinea-pig ileum. Therefore, the ubiquitous participation of the two enzymes in the central and peripheral degradation of neurotensin emphasizes the potential interest of developing mixed inhibitors of both activities to serve as blockers of physiological neurotensin proteolysis.

Our approach consisted in the synthesis of phosphorus-containing analogues of peptide substrates. To develop such transition-state analogues, the use of the phosphonamide

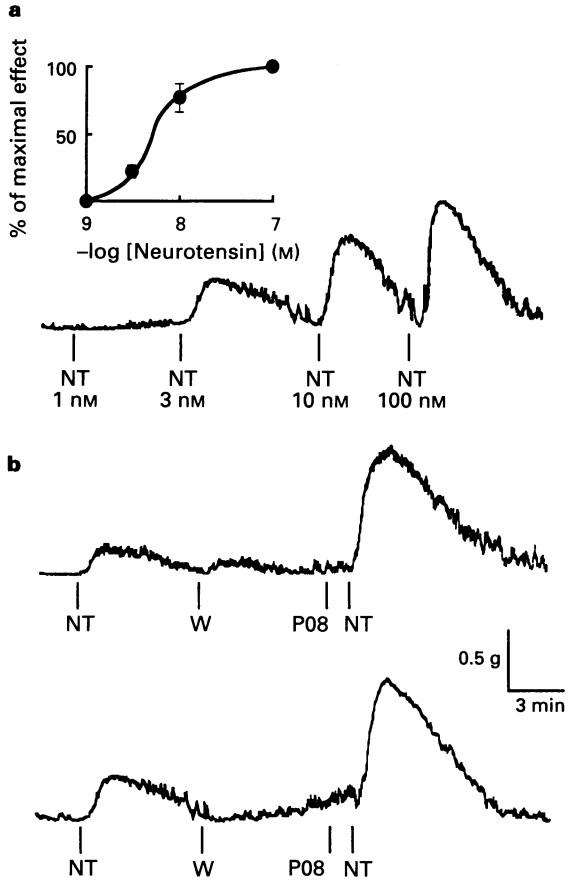

Figure 8 Effect of phosphodiepryl 08 on the neurotensin-induced contraction of isolated longitudinal smooth muscle strips from dog ileum. Preparations were allowed to equilibrate at 37°C under 95% O_2, 5% CO_2 for 45 min, in a modified Tyrode solution containing 100 nM neostigmine methylsulphate. (a) The isometric tension of the preparation was recorded in response to the indicated concentrations of neurotensin (NT). Note that between each neurotensin application, the preparation was washed out and subsequent peptide application occurred when the preparation returned to baseline level. Inset, dose-response curve of neurotensin-induced contraction. Values are expressed as a percentage of maximal contraction and represent the mean ± s.e.mean of 4 independent preparations. (b) Effect of 10 nM phosphodiepryl 08 (P08) on the contractile response elicited by 3 nM neurotensin in two separate ileal preparations.

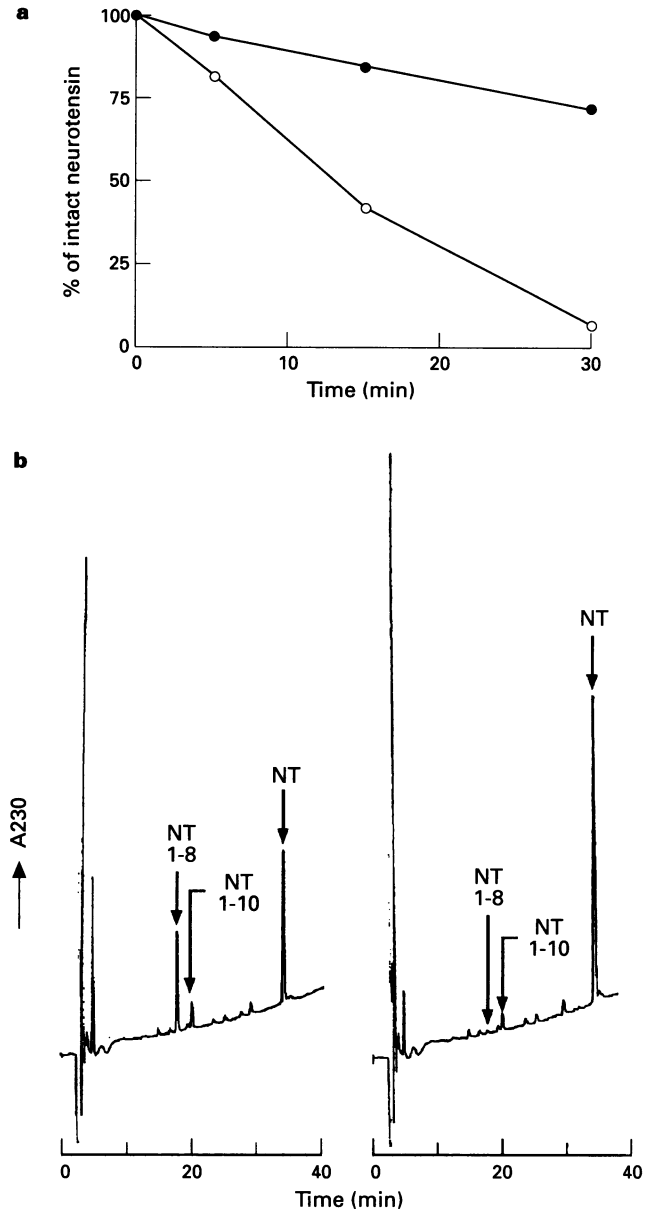

Figure 9 Effect of phosphodiepryl 08 on neurotensin hydrolysis by homogenates of guinea-pig ileal longitudinal smooth muscle. The kinetics of neurotensin hydrolysis by membrane homogenates of guinea-pig ileal longitudinal smooth muscle (a) were obtained by incubating neurotensin (2 nmol, 20 μM) at 37°C as described in Methods for various times in the absence (○) or in the presence of 10 nM phosphodiepryl 08 (●). Incubations were acidified, centrifuged (5 min, 13.00 r.p.m.), and supernatants were submitted to h.p.l.c. as described in the Methods. Intact neurotensin was quantified by comparing the remaining absorbing material with the standard amount of neurotensin incubated with preacidified membranes. Values represent the mean of 3 independent determinations. (b) Illustrates the h.p.l.c. analysis of neurotensin hydrolysis by membrane homogenates from guinea-pig ileum longitudinal smooth muscle. Neurotensin (2 nmol, 20 μM) was incubated for 15 min at 37°C with 35 μg of proteins in 100 μl of 5 mM Tris/HCl pH 7.5 in the absence (control, a) or in the presence of 10 nM phosphodiepryl 08 (b). Incubations were stopped by acidification (10 μl, 1 M HCl) and h.p.l.c. analysed as described in the Methods section.

group as a surrogate of the scissile peptide bond appeared to be the most suitable choice. Among a series of phosphorus-containing peptides, phosphodiepryl 08 behaved as a very potent mixed inhibitor ($K_i = 0.4$ nM) of endopeptidases 3.4.24.15 and 3.4.24.16. This inhibitor appears so far to be the most potent blocking agent of these two enzymes since it displays about 100 fold higher affinity than that of JMV 390-1 ($K_i = 31$ nM and 58 nM for endopeptidases 3.4.24.15 and 3.4.24.16 respectively) (Doulut *et al.*, 1993). Furthermore, JMV 390-1 also inhibits the enkephalin-degrading enzymes, endopeptidase 3.4.24.11 and aminopeptidase M *in vitro* ($K_i = 40$ and 52 nM, respectively) and *in vivo* as illustrated by the enhanced naltroxone-sensitive analgesic effect elicited by JMV 390-1 after i.c.v. administration (Doulut *et al.*, 1993). Finally, phosphodiepryl 08 is 225,000 fold more potent than the selective endopeptidase 3.4.24.16 dipeptide blocker, Pro-Ile (Dauch *et al.*, 1991b) and exhibits a 45 fold higher affinity for endopeptidase 3.4.24.15 than that observed with Cpp-Ala-Ala-Tyr-pAB, a rather selective inhibitor of this peptidase (Orlowski *et al.*, 1988).

It is important to underline the fact that phosphodiepryl 08 displays high selectivity towards endopeptidases 3.4.24.15 and 3.4.24.16. Thus, a 1 μM concentration of inhibitor (2500 fold higher than the K_i values for the two peptidases) appears unable to affect various zinc metallopeptidases including endopeptidase 24-11, angiotensin-converting enzyme, aminopeptidase M, leucine aminopeptidase and carboxypeptidases A and B.

The powerful and selective pharmacological spectrum of phosphodiepryl 08, *in vitro*, prompted us to examine whether

this agent could prevent neurotensin degradation in a peripheral bioassay as well as *in vivo*, in the central nervous system. Phosphodiepryl 08 potentiated the neurotensin-induced contraction of an isolated longitudinal smooth muscle preparation from guinea-pig ileum. Furthermore, this inhibitor increases the nociceptive response elicited by neurotensin after intracerebroventricular administration in mice. Therefore, these studies clearly established that endopeptidases 3.4.24.15 and 3.4.24.16 participate in the central and peripheral inactivation of neurotensin and suggested that phosphodiepryl 08 might be a useful tool that could ultimately permit a better understanding of the physiological role of this peptide.

It has been shown that phosphonamide bonds can easily be cleaved depending on the pH of the medium. This problem of lability can be overcome by the replacement of the phosphonamide by a phosphonate or a phosphinic group. Our study shows that the replacement by a phosphonate led to a 937 fold reduced affinity for both peptidases (compare compounds 03 and 16 in Table 1) while the introduction of a phosphinic group only diminished the potency towards the two peptidases by a 5 to 6 fold factor (compare compounds 13 and 14). These data are of importance in the context of the development of highly potent and specific inhibitors of endopeptidases 3.4.24.16 and 3.4.24.15. This should be achieved by the screening of peptide libraries containing a phosphinic moiety as a peptide bond surrogate. This work is in progress in our laboratories.

We wish to acknowledge gratefully Professor B.P. Roques (U266 INSERM, Paris) for his help in analgesia experiments. We wish to acknowledge Drs S. Wilk and M. Orlowski (Mount Sinai School of Medicine, New York) for providing us with Z-pro-prolinal, Bz-Gly-Ala-Ala-Phe-pAB and CPP-Ala-Ala-Tyr-pAB. We wish to acknowledge Dr P. Auberger (INSERM U 364, Faculté de Médecine, Nice) for providing us with purified endopeptidase 3.4.24.11. J. Kervella and F. Aguila are acknowledged for their expert secretarial and artwork assistance. This work was supported by the Centre National de la Recherche Scientifique and the Institut National de la Santé et de la Recherche Médicale.

References

BARELLI, H., FOX-THRELKELD, J.E.T., DIVE, V., DANIEL, E.E., VINCENT, J.P. & CHECLER, F. (1994). Role of endopeptidase 3.4.24.16 in the catabolism of neurotensin, *in vivo*, in the vascularly perfused dog ileum. *Br. J. Pharmacol.*, **112**, 127–132.

BARELLI, H., VINCENT, J.P. & CHECLER, F. (1988). Peripheral inactivation of neurotensin: isolation and characterization of a metallopeptidase from rat ileum. *Eur. J. Biochem.*, **175**, 481–489.

BARELLI, H., VINCENT, J.P. & CHECLER, F. (1991). Rat brain endopeptidase 24–15: specificity towards opioids, tachykinins and neurotensin-related peptides. Comparison with the neurotensin degrading metallopeptidase endopeptidase 24–16. *Neurochem. Life Sci. Adv.*, **10**, 115–124.

BARLETT, P.A. & MARLOW, C.K. (1987). Possible role for water dissociation in the slow binding of phosphorus- containing transition state analogue inhibitors of thermolysin. *Biochemistry*, **26**, 8553–8561.

BARRETT, A.J. & TISJLAR, U. (1989). The activities of 'Pz-peptidase' and 'endopeptidase 24–15' are due to a single enzyme. *Biochem. J.*, **261**, 1047–1050.

CHABRY, J., CHECLER, F., VINCENT, J.P. & MAZELLA, J. (1990). Colocalization of neurotensin receptors and of the neurotensin-degrading enzyme endopeptidase 24–16 in primary cultures of neurons. *J. Neurosci.*, **10**, 3916–3921.

CHECLER, F. (1993). Neuropeptide-degrading peptidases. In *Methods in Neurotransmitter and Neuropeptide Research*. Part 2., ed. Nagatsu, T., Parvez, H., Naoi, M. & Parvez, S. Vol. 11, pp. 375–418. Amsterdam: Elsevier Science Publishers.

CHECLER, F., BARELLI, H., DAUCH, P., DIVE, V., VINCENT, B. & VINCENT, J.P. (1995). Endopeptidase 3.4.24.16 (neurolysin): Purification and assay. In *Methods in Enzymology*, Vol. 248, pp. 593–614. San Diego, California: Academic Press.

CHECLER, F., BARELLI, H., KITABGI, P. & VINCENT, J.P. (1988). Neurotensin metabolism in various tissues from central and peripheral origins. Ubiquitous involvement of a novel neurotensin degrading metalloendopeptidase. *Biochimie*, **70**, 75–82.

CHECLER, F., DAUCH, P., BARELLI, H., DIVE, V., MASUO, Y., VINCENT, B. & VINCENT, J.P. (1994). Identification and distribution of endopeptidase EC 3.4.24.16 in the central nervous system. In *Methods in Neurosciences*, Vol. 23, pp. 363–382. London: Academic Press.

CHECLER, F., EMSON, P.C., VINCENT, J.P. & KITABGI, P. (1984). Inactivation of neurotensin by rat brain synaptic membranes. Cleavage at the Pro^{10}-Tyr^{11} bond by endopeptidase 24.11 (enkephalinase) and a peptidase distinct from proline endopeptidase. *J. Neurochem.*, **43**, 1295–1301.

CHECLER, F., MAZELLA, J., KITABGI, P. & VINCENT, J.P. (1986a). High affinity receptor sites and rapid proteolytic inactivation of neurotensin in primary cultured neurons. *J. Neurochem.*, **47**, 1742–1748.

CHECLER, F., VINCENT, J.P. & KITABGI, P. (1983). Degradation of neurotensin by rat brain synaptic membranes. Involvement of a thermolysin-like metalloendopeptidase (enkephalinase), angiotensin-converting enzyme and other unidentified peptidases. *J. Neurochem.*, **41**, 375–384.

CHECLER, F., VINCENT, J.P. & KITABGI, P. (1985). Inactivation of neurotensin by rat brain synaptic membranes partly occurs through cleavage at the Arg^8-Arg^9 peptide bond by a metalloendopeptidase. *J. Neurochem.*, **45**, 1509–1513.

CHECLER, F., VINCENT, J.P. & KITABGI, P. (1986b). Purification and characterization of a novel neurotensin degrading peptidase from rat brain synaptic membranes. *J. Biol. Chem.*, **261**, 11274–11281.

DAUCH, P., BARELLI, H., VINCENT, J.P. & CHECLER, F. (1991a). Fluorimetric assay of the neurotensin-degrading metalloendopeptidase, endopeptidase 24–16. *Biochem. J.*, **280**, 421–426.

DAUCH, P., VINCENT, J.P. & CHECLER, F. (1991b). Specific inhibition of endopeptidase 24.16 by dipeptides. *Eur. J. Biochem.*, **202**, 269–276.

DIVE, V., YIOTAKIS, A., NICOLAOU, A. & TOMA, F. (1990). Inhibition of Clostridium histolyticum chollagenases by phosphonamide peptide inhibitors. *Eur. J. Biochem.*, **191**, 685–693.

DOULUT, S., DUBUC, I., RODRIGUEZ, M., VECCHINI, F., FULCRAND, H., BARELLI, H., CHECLER, F., BOURDEI, E., AUMELAS, A., KITABGI, P., COSTENTIN, J. & MARTINEZ, J. (1993). Synthesis and analgesic effects of a new potent inhibitor of multiple neurotensin degrading enzymes. *J. Med. Chem.*, **36**, 1369–1379.

EDDY, N.B. & LEIMBACH, D. (1953). Synthetic analgesics (II): dithienylbutenyl and dithienylbutylamines. *J. Pharmacol. Exp. Ther.*, **107**, 385–393.

FOURNIÉ-ZALUSKI, M.C., CHAILLET, P., BOUBOUTOU, R., COULAUD, A., CHEROT, P., WAKSMAN, G., COSTENTIN, J. & ROQUES, B.P. (1984). Analgesic effects of kelatorphan a new highly potent inhibitor of multiple enkephalin degrading enzymes. *Eur. J. Pharmacol.*, **102**, 525–528.

FRENCH, J.F., FLYNN, G.A., GIROUX, E.L., MEHDI, S., ANDERSON, B., BEACH, D.C., KOEHL, J.R. & DAGE, R.C. (1994). Characterization of a dual inhibitor of angiotensin I converting-enzyme and neutral endopeptidase. *J. Pharmacol. Exp. Ther.*, **268**, 180–186.

KITABGI, P. (1982). Effects of neurotensin on intestinal smooth muscle: application to the study of structure-activity relationships. *Ann. N.Y. Acad. Sci.*, **400**, 37–55.

NOBLE, F., SOLEIHAC, J.M., SOROCA-LUCAS, E., TURCAUD, S., FOURNIE-ZALUSKI, M.C. & ROQUES, B.P. (1992). Inhibition of the enkephalin-metabolizing enzyme by the first systemically active mixed inhibitor prodrug RB101 induces potent analgesic responses in mice and rats. *J. Pharmacol. Exp. Ther.*, **261**, 181–190.

ORLOWSKI, M., MICHAUD, C. & CHU, T.G. (1983). A soluble metalloendopeptidase from rat brain. Purification of the enzyme and determination of specificity with synthetic and natural peptides. *Eur. J. Biochem.*, **135,** 81–88.

ORLOWSKI, M., MICHAUD, C. & MOLINEAUX, C.J. (1988). Substrate-related potent inhibitors of brain metalloendopeptidase. *Biochemistry*, **27,** 597–602.

PATON, W.D.M. & ZAR, M.A. (1968). The origin of acetylcholine release from guinea-pig intestine and longitudinal muscle strips. *J. Physiol.*, **194,** 13–33.

PIEROTTI, A., DONG, K.W., GLUCKSMAN, M.J., ORLOWSKI, M. & ROBERTS, J.L. (1990). Molecular cloning and primary structure of rat testes metalloendopeptidase EC 3.4.24.15. *Biochemistry*, **29,** 10323–10329.

SCHMIDT, C., PEYROUX, J., NOBLE, F., FOURNIE-ZALUSKI, M.C. & ROQUES, B.P. (1991). Analgesic responses elicited by endogenous enkephalins (protected by mixed peptidase inhibitors) in a variety of morphine-sensitive noxious tests. *Eur. J. Pharmacol.*, **192,** 253–262.

TISLJAR, U., KNIGHT, G. & BARRETT, A.J. (1990). An alternative quenched fluorescence substrate for Pz-peptidase. *Anal. Biochem.*, **186,** 112–115.

VINCENT, B., VINCENT, J.P. & CHECLER, F. (1994). Neurotensin and neuromedin N undergo distinct catabolic processes in astrocytes and primary cultured neurons. *Eur. J. Biochem.*, **221,** 297–306.

WAKSMAN, G., BOUBOUTOU, R., CHAILLET, P., DEVIN, J., COULAUD, A., HAMEL, E., BESSELIEVRE, R., COSTENTIN, J., FOURNIÉ-ZALUSKI, M.C. & ROQUES, B.P. (1985). Kelatorphan: a full inhibitor of enkephalin degrading enzymes. Biochemical and pharmacological properties, regional distribution of enkephalinase in rat brain by use of a tritiated derivative. *Neuropeptides*, **5,** 529–532.

YIOTAKIS, A., LECOQ, A., NICOLAOU, A., LABADIE, J. & DIVE, V. (1994). Phosphinic peptide analogues as potent inhibitors of *Corynebacterium rathayii* bacterial collagenase. *Biochem. J.*, **303,** 323–327.

(Received January 30, 1995
Revised March 7, 1995
Accepted March 22, 1995)

British Journal of Pharmacology (1995) 115, 1064–1070 © 1995 Stockton Press All rights reserved 0007–1188/95 $12.00

Interaction between a selective 5-HT_{1A} receptor antagonist and an SSRI *in vivo*: effects on 5-HT cell firing and extracellular 5-HT

[1]S.E. Gartside, V. Umbers, M. Hajós & T. Sharp

University of Oxford Department of Clinical Pharmacology, Radcliffe Infirmary, Woodstock Road, Oxford OX2 6HE

1 The acute inhibitory effect of selective 5-hydroxytryptamine (serotonin) reuptake inhibitors (SSRIs) on 5-HT neuronal activity may offset their ability to increase synaptic 5-HT in the forebrain.

2 Here, we determined the effects of the SSRI, paroxetine, and a novel selective 5-HT_{1A} receptor antagonist, WAY 100635, on 5-HT cell firing in the dorsal raphé nucleus (DRN), and on extracellular 5-HT in both the DRN and the frontal cortex (FCx). Extracellular electrophysiological recording and brain microdialysis were used in parallel experiments, in anaesthetized rats.

3 Paroxetine dose-dependently inhibited the firing of 5-HT neurones in the DRN, with a maximally effective dose of approximately 0.8 mg kg^{-1}, i.v. WAY 100635 (0.1 mg kg^{-1}, i.v.) both reversed the inhibitory effect of paroxetine and, when used as a pretreatment, caused a pronounced shift to the right of the paroxetine dose-response curve.

4 Paroxetine (0.8 mg kg^{-1}, i.v.), doubled extracellular 5-HT in the DRN, but did not alter extracellular 5-HT in the FCx. A higher dose of paroxetine (2.4 mg kg^{-1}, i.v.) did increase extracellular 5-HT in the FCx, but to a lesser extent than in the DRN. Whereas 0.8 mg kg^{-1}, i.v. paroxetine alone had no effect on extracellular 5-HT in the FCx, in rats pretreated with WAY 100635 (0.1 mg kg^{-1}), paroxetine (0.8 mg kg^{-1}, i.v.) markedly increased extracellular 5-HT in the FCx.

5 In conclusion, pretreatment with the selective 5-HT_{1A} receptor antagonist, WAY 100635, blocked the inhibitory effect of paroxetine on 5-HT neuronal activity in the DRN and, at the same time, markedly enhanced the effect of paroxetine on extracellular 5-HT in the FCx. These results may be relevant to recent clinical observations that 5-HT_{1A} receptor antagonists in combination with SSRIs have a rapid onset of antidepressant effect.

Keywords: SSRI; 5-HT_{1A} receptor antagonist; WAY 100635; microdialysis; 5-HT cell firing; dorsal raphé nucleus; frontal cortex

Introduction

It is established that selective 5-hydroxytryptamine (5-HT, serotonin) reuptake inhibitors (SSRIs) are effective in the treatment of depression. However, as with other antidepressants, several weeks of treatment with SSRIs is usually required before their therapeutic benefit becomes apparent (Åsberg *et al.*, 1986; Schatzberg *et al.*, 1987). Whilst the mechanism underlying the delay in antidepressant effect of SSRIs is not clear, there is evidence that it is only following repeated administration that SSRIs enhance 5-HT neurotransmission (Artigas *et al.*, 1994; Blier & de Montigny, 1994). Present strategies aimed at accelerating the onset of the antidepressant effect of SSRIs are focussed on shortening the time to produce this enhancement of 5-HT neurotransmission.

Although the acute administration of SSRIs might be expected to enhance the action of 5-HT on its postsynaptic receptors in the forebrain through blockade of 5-HT reuptake, it is well known that, when administered acutely, SRRIs inhibit the firing of 5-HT neurones in the midbrain raphé nuclei (Sheard *et al.*, 1972; Chaput *et al.*, 1986; Hajós *et al.*, 1995). This inhibitory effect is probably the result of a local increase in extracellular 5-HT in the raphé region and the resultant activation of somatodendritic 5-HT_{1A} autoreceptors (Rigdon & Wang, 1991). The inhibition of 5-HT cell firing induced by SSRIs would be expected to decrease 5-HT release in the forebrain. Thus, in the intact brain the acute effect of SSRIs on synaptic levels of 5-HT is likely to reflect a balance between blockade of 5-HT reuptake at the nerve terminal, and inhibition of firing of the 5-HT neurone (Fuller, 1994).

Interestingly, it has recently been reported that drugs with 5-HT_{1A} receptor antagonist properties are able to enhance the effect of SSRIs on forebrain extracellular 5-HT, as measured *in vivo* by microdialysis (Invernizzi *et al.*, 1992a; Hjorth, 1993). However, the mechanism underlying this effect has not yet been fully elucidated. In particular, it is unclear whether the doses of SSRIs used in the above studies would result in significant inhibition of 5-HT cell firing and, if so, whether the doses of 5-HT_{1A} antagonists used would block this effect. Furthermore, confirmation of the role of the 5-HT_{1A} receptor in this interaction has been precluded by the lack of availability of 5-HT_{1A} receptor antagonists which are both silent and selective.

In the present study the effects of an SSRI (paroxetine) and a putative selective 5-HT_{1A} receptor antagonist (WAY 100635) (Fletcher *et al.*, 1994) on 5-HT neuronal firing and on the extracellular 5-HT have been compared. These drugs were administered both alone and in combination. Measurements of 5-HT neuronal firing were made in the DRN. Extracellular 5-HT was measured both in the DRN itself and in the frontal cortex (FCx) which receives the majority of its 5-HT innervation from the DRN (O'Hearn & Molliver, 1984). A preliminary account of these findings has been presented to the British Pharmacological Society (Gartside *et al.*, 1995).

Methods

Animals

Male Sprague-Dawley rats (270–310 g; Harlan-Olac, Bicester, UK) were housed in groups of up to 6 under controlled conditions of temperature (21°C) and humidity (50%), in a 12 h light/dark cycle (lights on 08 h 00 min). Animals were allowed food and water *ad libitum*.

General stereotaxic surgical procedures

Rats were anaesthetized with chloral hydrate (400–500 mg kg^{-1}, i.p.) and placed in a stereotaxic frame (Kopf) with the incisor bar set at −3.3 mm. Proper surgical anaes-

[1] Author for correspondence.

thesia was maintained throughout the experiment by administration of supplementary doses of the anaesthetic. The body temperature of the animals was maintained at 36.0 ± 0.5°C by means of a homeothermic blanket with rectal probe. The skull was exposed and a burr hole drilled for the implantation of the recording electrode or microdialysis probe. A lateral tail vein was cannulated, with a 25 gauge hypodermic needle, for intravenous administration of drugs.

Electrophysiological studies

A glass capillary tube (external diameter 2.5 mm; Clarke Electromedical) was drawn out, with a pipette puller, to form a single barrelled glass microelectrode. The electrode was broken back to obtain an external tip diameter of ≈2 μm, and was then filled with a solution of 2 M NaCl with 2% Pontamine Sky Blue. Electrodes had *in vitro* impedances of 3–8 MΩ. An electrode was implanted to a depth of 4.5 mm though a burr hole drilled over the DRN (AP −7.6 mm; ML 0 mm; Paxinos & Watson, 1983) and subsequently lowered by means of a hydraulic microdriver (Kopf).

Spontaneously active presumed 5-HT neurones in the DRN, identified on the basis of their electrophysiological characteristics (see Results), were encountered between 5.0 and 6.5 mm below the dura surface. The signal was amplified (× 1000) and filtered (low frequency ⩽300 Hz; high frequency ⩾3000 Hz), and was displayed on an oscilloscope and chart recorder, and recorded on DAT tape for off-line analysis.

Extracellular recordings were made from one neurone per animal. The baseline firing activity of the neurone was recorded for at least 3 min, after which time drugs were administered intravenously. One group of animals received paroxetine, in doubling doses (initial dose 0.1 mg kg^{-1}, i.v.) at ≈2 min intervals, followed (after at least 65% inhibition had been achieved) by WAY 100635 (0.1 mg kg^{-1}, i.v.). A further group of animals received WAY 100635 (0.1 mg kg^{-1}, i.v.) and, approximately 6 min later, some of this group of animals received paroxetine in doubling doses (initial dose 0.4 mg kg^{-1}, i.v.) at ≈2 min intervals.

At the end of each experiment a small amount of Pontamine Sky Blue was iontophoretically ejected from the tip of the electrode. The brain was removed, stored in 4% paraformaldehyde, and subsequently sectioned with a vibratome. Sections were stained with cresyl violet and the position of the electrode tip determined by microscopic inspection. Only those neurones found to be located within the DRN are included in the study.

Microdialysis studies

A concentric microdialysis probe with a 3 mm tip of exposed dialysis membrane (Cordis Dow GFE9 membrane, 250 μm in diameter), was stereotaxicaly implanted in either the DRN (AP −7.5 mm; ML 2.0 mm; DV −6.3 mm, from bregma and dura surface, implanted at 18° to the vertical), or the right frontal cortex (AP +3.2 mm; ML +3.0 mm; DV −4.5 mm; Paxinos & Watson, 1983). The probe was constantly perfused at 2 μl min^{-1} with artificial cerebro-spinal fluid (aCSF) (composition (mM): NaCl 140, KCl 3, $CaCl_2$ 2.4, $MgCl_2$ 1.0, Na_2HPO_4 1.2, NaH_2PO_4 0.27, glucose 7.2, at pH 7.4). Dialysates were collected over 20 min, and were assayed immediately for 5-HT by h.p.l.c. with electrochemical detection as described elsewhere (Sharp & Zetterström, 1992).

Drugs were administered only after a stable baseline level of 5-HT had been established (typically 2–3 h post probe implantation). Two groups of animals with dialysis probes in the DRN, and 2 groups with probes in the FCx, received paroxetine (0.8 or 2.4 mg kg^{-1}, i.v.). A further 3 groups of animals, all with dialysis probes in the FCx, received vehicle injection (1 ml kg^{-1}, body weight), WAY 100635 (0.1 mg kg^{-1}, i.v.) alone, or WAY 100635 (0.1 mg kg^{-1}, i.v.), followed 10 min later by paroxetine (0.8 mg kg^{-1}, i.v.). Response to administration of drugs was determined over a 2 h period.

At the end of each experiment, the brain was removed, stored in 4% paraformaldehyde and subsequently sectioned with a freezing microtome, and the location of the microdialysis probe verified by inspection. Only experiments in which the probe was found to be correctly located in the DRN or FCx are included.

Drugs and chemicals

WAY 100635 (N-[2-[4-(2-methoxyphenyl)-1-piperazinyl]-*N*-(2-pyridinyl) cyclo-hexanecarboxamide.3HCl) and paroxetine HCl were generous gifts of Wyeth Research, Maidenhead, U.K. and SmithKline Beecham, Harlow, U.K., respectively. Chloral hydrate (Sigma) was dissolved in distilled/deionised water. WAY 100635 and paroxetine were dissolved in sterile 5% glucose solution. Chemicals used for h.p.l.c. were of analytical grade.

Data presentation and statistical analysis

For the electrophysiological studies, mean firing rate (spikes, 10 s^{-1}) were determined in periods of 60 s (pre-drug) or 30 s (post-drug). The percentage inhibition or increase quoted represents the difference between the post-drug firing rate and the pre-drug firing rate, as a percentage of the pre-drug firing rate. Individual ED_{50} values were determined by interpolation of percentage inhibition curves on a semi-log plot. Differences between groups were assessed by unpaired or single sample Student's *t* test.

Microdialysis data are presented as % of baseline ($t = 0$) values. Statistical analysis of absolute 5-HT levels was by 1- or 2-way ANOVA with *post-hoc* Tukey test. Statistical significance at the 95% level is reported.

Results

Effects of paroxetine on 5-HT cell firing in the DRN

Presumed 5-HT neurones recorded in the DRN showed the electrophysiological characteristics of immunohistologically identified 5-HT neurones (Aghajanian & VanderMaelen, 1982). Thus, they fired spontaneously and regularly, with discharge rates of between 0.4 and 2.6 spikes s^{-1}. The action potential was characterized by a large positive deflection followed by a negative or negative/positive deflection, and had a duration of around 2 ms.

Acute i.v. administration of paroxetine potently and dose-dependently inhibited the spontaneous firing of the DRN

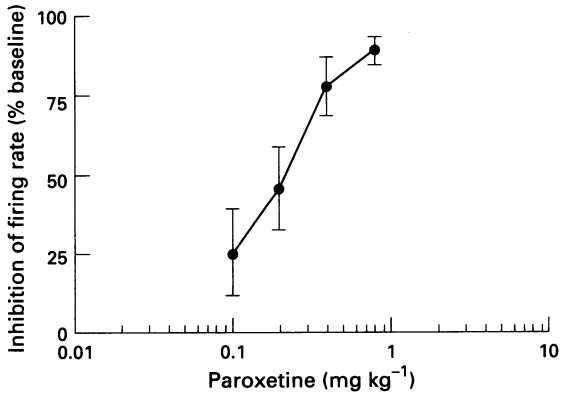

Figure 1 The relationship between increasing doses of paroxetine and changes in 5-HT cell firing in the DRN. Paroxetine was administered in cumulative doses as described in Methods. The inhibition of cell firing is expressed as a percentage of cell firing immediately before injection of the first dose of paroxetine. Each point is a mean ± s.e.mean of 7–9 determinations.

neurones (Figure 1 and Figure 2a). The mean ED_{50} calculated from individual inhibition curves for 9 cells was 0.252 ± 0.063 mg kg^{-1}, i.v. and the maximally effective dose (i.e. that dose inducing 100% inhibition) was estimated to be ≈ 0.8 mg kg^{-1}, i.v.

Effect of WAY 100635 on 5-HT cell firing in the DRN

In total, 10 presumed 5-HT neurones in the DRN were tested with a single injection of WAY 100635 (0.1 mg kg^{-1}, i.v.). In 6 of these cells, administration of WAY 100635 (0.1 mg kg^{-1}, i.v.) increased the firing rate. This effect was manifest within 120 s and persisted for at least 6 min, such that in the period 300–360 s after administration of WAY 100635, the mean firing rate in these 6 cells was 43.4 (± 10.7)% above the baseline firing rate. Three other cells showed a marked but transient inhibition of cell firing after WAY 100635, and one showed a decrease followed by an increase. Overall, in the 10 cells tested, the firing rate 300–360 s after administration of WAY 100635 was not statistically different from baseline (21.1 ± 13.3% above baseline (100%): single sample t test).

Effect of WAY 100635 and paroxetine in combination on 5-HT cell firing in the DRN

Of 9 cells inhibited by paroxetine (see above), subsequent administration of WAY 100635 (0.1 mg kg^{-1}, i.v.) almost completely reversed the effect of paroxetine in 7 (Figure 2a and b). It is of note however, that in some cases the reversal was quite short-lived and that, in these cells, further administration of WAY 100635 was apparently without effect. In the 2 cases of cells inhibited by paroxetine but not reversed by WAY 100635, it was unclear whether the cell was 'lost' before administration of the antagonist, or whether the firing remained totally inhibited even in the presence of WAY 100635.

Pretreatment with WAY 100635 (0.1 mg kg^{-1}, i.v.) caused a shift to the right of the paroxetine dose-response curve which

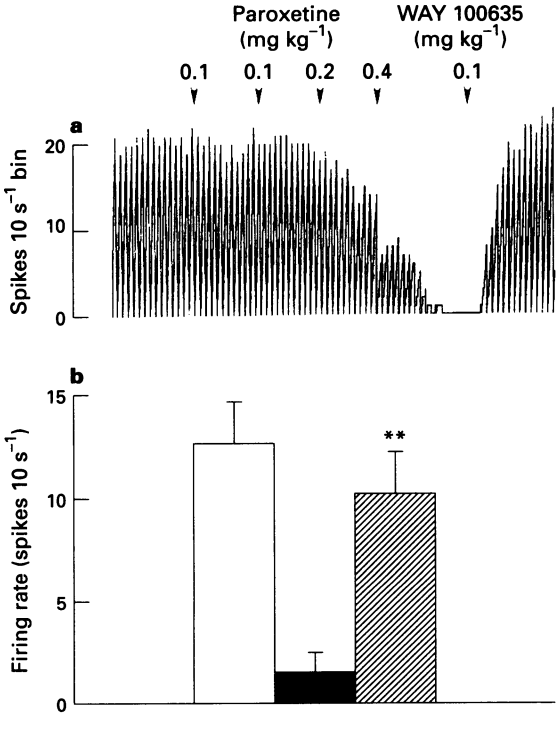

Figure 2 (a) An original rate meter recording of a single DRN cell showing inhibition of cell firing by cumulative doses of paroxetine, and reversal of the effect of paroxetine by subsequent administration of WAY 100635. Drugs were administered as indicated by the arrows. (b) Graph illustrating mean firing rates of DRN cells during 60 s periods: open column, before paroxetine; solid column, after administration of various total doses of paroxetine; and hatched column after subsequent administration of WAY 100635. **$P<0.01$ *vs* after paroxetine administration.

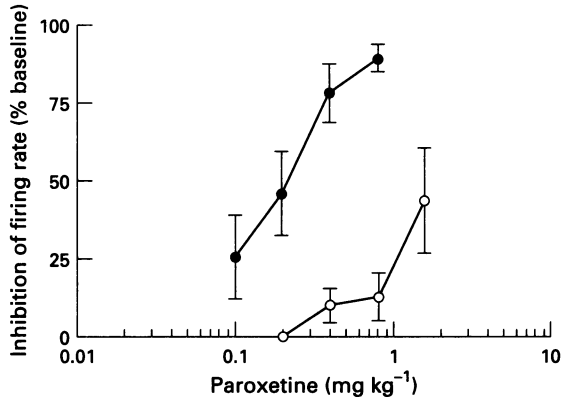

Figure 3 Mean percentage inhibition of 5-HT cells in the DRN induced by cumulative doses of paroxetine in (●) naïve rats (taken from Figure 1) and (○) rats pretreated with WAY 100635 (0.1 mg kg^{-1}, i.v.) Each point represents the mean ± s.e.mean of 5–7 determinations.

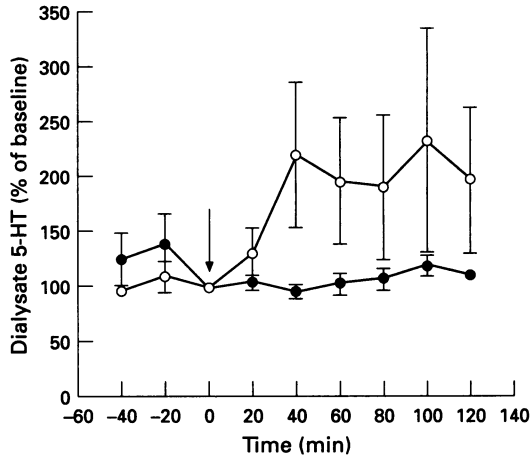

Figure 4 The effect of paroxetine (0.8 mg kg^{-1}, i.v.) on 5-HT in dialysates of (○) the DRN, and (●) the FCx. Paroxetine was given at $t=0$. Data are mean ± s.e.mean, $n=4-7$. See Results for statistical analysis.

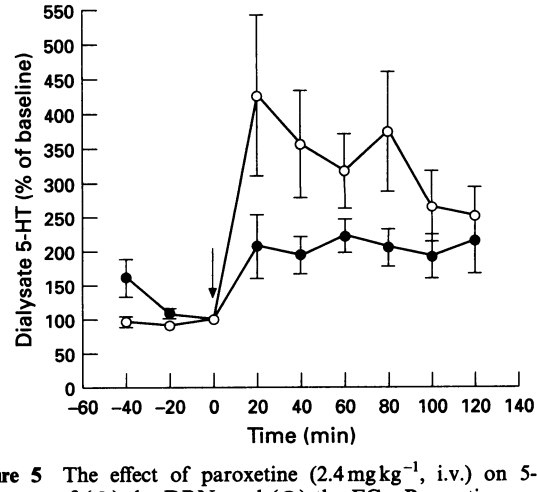

Figure 5 The effect of paroxetine (2.4 mg kg^{-1}, i.v.) on 5-HT in dialysates of (○) the DRN, and (●) the FCx. Paroxetine was given at $t=0$. Data are mean ± s.e.mean, $n=5-6$. See Results for statistical analysis.

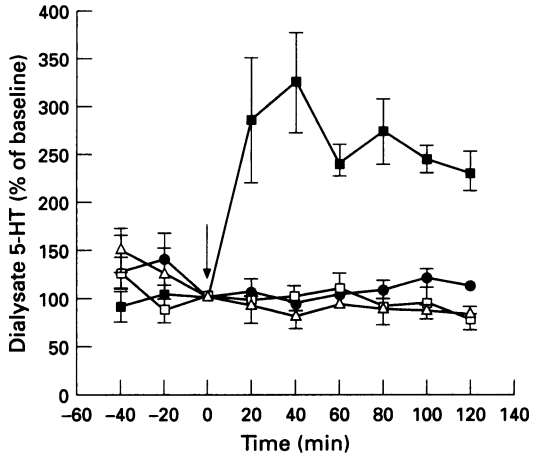

Figure 6 Time course of the effect of (△) vehicle, (□) WAY 100635 (0.1 mg kg^{-1}, i.v.), (●) paroxetine (0.8 mg kg^{-1}, i.v.) (taken from Figure 4), or (■) WAY 100635 (0.1 mg kg^{-1}, i.v.) followed by paroxetine (0.8 mg kg^{-1}, i.v.), on 5-HT in dialysates of the FCx. Paroxetine was given at $t=0$. Data are mean ± s.e.mean, $n=4-7$. See Results for statistical analysis.

was of such magnitude that it was not possible to determine an ED_{50} for paroxetine in the presence of WAY 100635 (Figure 3). However, the administration of 0.8 mg kg^{-1}, i.v. paroxetine, a dose which was maximally effective in naïve rats, caused only a small inhibition of cell firing of 12.5 ± 7.9 (7)% in animals pretreated with 0.1 mg kg^{-1}, i.v. WAY 100635.

Effect of paroxetine on extracellular 5-HT in the DRN and FCx

A dose of paroxetine (0.8 mg kg^{-1}, i.v.), which maximally suppressed firing in the DRN, increased 5-HT levels in dialysates of the DRN approximately 200% within 40 min of its administration (Figure 4). In contrast, this same dose of paroxetine (0.8 mg kg^{-1}, i.v.) did not increase 5-HT levels in dialysates of the FCx, at any time over the following 2 h.

Statistical analysis of the DRN and FCx time-course data by 2-way ANOVA showed significant main effects of brain region and time point, as well as a significant (brain region × time point) interaction ($F_{(6,42)}=3.3$; $P<0.01$). *Post-hoc* analysis revealed that 5-HT levels in dialysates of the DRN were significantly ($P<0.05$) higher than in the FCx at all time points from 20 to 80 min post-paroxetine. Basal levels of 5-HT in the DRN and FCx before injection of 0.8 mg kg^{-1} paroxetine were not significantly different (12.6 ± 3 (4) *vs* 11.2 ± 1.7 (7) fmol per sample; DRN vs FCx:NS).

A higher dose of paroxetine (2.4 mg kg^{-1}, i.v.) caused a large increase (to 400% of baseline) in 5-HT levels in dialysates of the DRN, but also an increase (to 200% of baseline) in dialysates of the FCx (Figure 5). Both responses were long-lasting (>2 h). Two-way ANOVA revealed significant main effects of brain region and time point and a significant (brain region × time point interaction) ($F_{(6,54)}=3.2$; $P<0.01$). 5-HT levels in DRN dialysates were significantly higher than those in FCx dialysates from 20 to 80 min after administration of 2.4 mg kg^{-1} paroxetine. Basal levels of 5-HT in the DRN and FCx of animals administered 2.4 mg kg^{-1} paroxetine were not significantly different (17.0 ± 4 (5) and 8.7 ± 2.0 (6) fmol per sample; DRN *vs* FCx: NS).

Effect of WAY 100635 on extracellular 5-HT in the FCx

Neither vehicle injection (1 ml kg^{-1} body weight, i.v.), nor administration of WAY 100635 (0.1 mg kg^{-1}, i.v.) alone, altered 5-HT levels in the FCx over the 2 h following the injection (Figure 6). Analysis of the time-course data by 1-way ANOVA revealed no significant effect of either treatment.

Effect of WAY 100635 and paroxetine in combination on extracellular 5-HT in the FCx

Administration of either paroxetine (0.8 mg kg^{-1}, i.v.) or WAY 100635 (0.1 mg kg^{-1}, i.v.) alone did not alter 5-HT levels in dialysates of the FCx (see above). However, in animals pretreated with WAY 100635 (0.1 mg kg^{-1}, i.v.), administration of paroxetine (0.8 mg kg^{-1}, i.v.) increased 5-HT levels in FCx dialysates to about 300% of baseline (Figure 6). Statistical analysis of the time-course by 2-way ANOVA revealed significant main effects of drug treatment and time point, and a significant interaction ($F_{(6,48)}=4.6$; $P=0.001$). 5-HT levels in the WAY 100635 pretreated group were significantly higher than in those receiving paroxetine alone at all time points between 20 and 120 min ($P<0.05$). Basal levels of 5-HT in FCx dialysates from the two groups did not differ significantly (6.8 ± 1.2 (7) *vs* 11.2 ± 1.7 (7) fmol per sample; WAY-100635 + paroxetine *vs* paroxetine: NS).

Discussion

In the intact brain the net effect of acute administration of SSRIs on synaptic levels of 5-HT will be influenced by both blockade of 5-HT reuptake at the nerve terminal, and any effect the SSRI may have on the release of 5-HT (Fuller, 1994). SSRIs, are known to inhibit the firing of DRN 5-HT neurones (Sheard *et al.*, 1972; Chaput *et al.*, 1986; Hajós *et al.*, 1995), and thus may inhibit terminal 5-HT release. Here we have investigated the inhibitory action of the SSRI, paroxetine, on 5-HT neuronal activity in the DRN. In parallel experiments, we have determined the effects of paroxetine on extracellular 5-HT in both the DRN and the FCx. Using a novel selective 5-HT$_{1A}$ receptor antagonist, WAY 100635, the consequence of preventing the inhibition of 5-HT cell firing, on extracellular 5-HT in the FCx, was determined. Measurements of 5-HT neuronal activity and extracellular 5-HT were carried out in anaesthetized rats by use of electrophysiological recording and brain microdialysis.

Effect of paroxetine on 5-HT cell firing in relation to extracellular 5-HT

Here we have shown that, in common with other SSRIs (Sheard *et al.*, 1972; Chaput *et al.*, 1986; Rigdon & Wang, 1991), paroxetine inhibits the firing of DRN neurones: a cumulative total dose of 0.8 mg kg^{-1}, i.v. causing a near total inhibition of 5-HT neuronal activity. In a recent study we observed that paroxetine also inhibited 5-HT cell firing in the median raphé nucleus (MRN) and did so at doses similar to those inhibiting firing of DRN cells (Hajós *et al.*, 1995). Since 5-HT neurones of the DRN and MRN together comprise the principle source of 5-HT innervation to the forebrain (Dahström & Fuxe, 1964; Ungerstedt, 1971), our data suggest that in the rat, paroxetine (at doses of 0.8 mg kg^{-1}, i.v. and above) causes a near total cessation of impulse flow in 5-HT neurones projecting to the forebrain.

In parallel experiments, 0.8 mg kg^{-1}, i.v. paroxetine increased extracellular 5-HT in the DRN but had no measurable effect in the FCx. A higher dose of paroxetine (2.4 mg kg^{-1}, i.v.) did increase extracellular 5-HT in the FCx, but to a lesser extent than in the DRN. In common with paroxetine, there is evidence that the SSRIs, citalopram, sertraline and fluvoxamine, also preferentially increase extracellular 5-HT in the cell body region compared to nerve terminal regions (Adell & Artigas, 1991; Bel & Artigas, 1992; Invernizzi *et al.*, 1992a,b). It has been suggested that this apparent regional selectivity may be due to 5-HT neurones responding to the increases in extracellular 5-HT in the cell body region, reducing their firing rate, so that any increase in synaptic 5-HT in the terminal region is small (Fuller, 1994). Data in the present study are consistent with this view. Thus, the dose of paroxetine which

increased extracellular 5-HT in the DRN, was that which caused a cessation of 5-HT cell firing in the DRN and, at the same time had little effect on extracellular 5-HT in the FCx. Furthermore, when this inhibition of 5-HT cell firing was blocked pharmacologically, extracellular 5-HT in the FCx increased markedly (see later).

It is perhaps surprising that paroxetine, at doses causing a near total inhibition of 5-HT neuronal activity, resulted in increased extracellular 5-HT in the DRN and the FCx. Extracellular levels of 5-HT depend principally on the rate of 5-HT release into the extracellular space, and the rate of reuptake (Fuller, 1994). When 5-HT neuronal activity is low (and hence neuronal release of 5-HT is low), it would be predicted that blockade of 5-HT reuptake would not increase extracellular 5-HT to any marked degree. In the DRN, the apparent dissociation between 5-HT cell firing and extracellular 5-HT after paroxetine might be explained on the basis of evidence that somatodendritic 5-HT release continues in the absence of 5-HT neuronal activity (Adell *et al.*, 1993). However, since the release of 5-HT from the nerve terminals is generally assumed to be dependent on 5-HT impulse flow (cf. Sharp *et al.*, 1989), our observation of a sustained increase in extracellular 5-HT in the FCx following the higher dose of paroxetine is more difficult to explain. It is possible that even at the nerve terminal a component of 5-HT release is independent of impulse flow, and that the increase in extracellular 5-HT following the higher dose of paroxetine results from a greater degree of 5-HT reuptake blockade than is achieved at the lower dose of paroxetine. Another possibility is that paroxetine at higher doses has an amphetamine-like 5-HT releasing action. Whatever the mechanism, this effect may not be unique to paroxetine in that a variety of SSRIs increase extracellular 5-HT forebrain regions when given in relatively high doses (Carboni & DiChiara, 1989; Rutter & Auerbach, 1993; Hjorth, 1993; Fuller, 1994).

A selective 5-HT$_{1A}$ receptor antagonist reverses the inhibitory effect of paroxetine on 5-HT cell firing

Here we show that the inhibition of DRN firing induced by paroxetine is prevented by the novel selective 5-HT$_{1A}$ receptor antagonist, WAY 100635 (Fletcher *et al.*, 1994). WAY 100635 (0.1 mg kg^{-1}, i.v.) both reversed the inhibitory effect of paroxetine and, when used as pretreatment, caused a pronounced shift to the right of the paroxetine dose-response curve. We have recently reported (Hajós *et al.*, 1995) that the inhibition of DRN and MRN cell-firing by paroxetine is reversed by i.v. administration of spiperone and WAY 100135, both of which have 5-HT$_{1A}$ receptor antagonist properties (Escandon *et al.*, 1994; Lanfumey *et al.*, 1994). Taken together, these findings suggest that the inhibition of raphé firing by paroxetine involves activation of 5-HT$_{1A}$ receptors. It should be noted that whilst WAY 100635 almost completely reversed the effect of paroxetine in the majority of cases, in some cells no reversal, or only a partial reversal was observed. Previously we noted that the paroxetine-induced inhibition was not reversed by spiperone or WAY 100135 in a number of cells (Hajós *et al.*, 1995). While these findings may reflect technical problems (e.g. loss of neurone during recording), the involvement of 5-HT receptors other than the 5-HT$_{1A}$ receptor might be implicated. In this respect it is relevant that, in the guinea-pig, 5-HT$_{1B/D}$ receptors have been shown to modulate 5-HT release in the DRN (Starkey & Skingle, 1994). However, a recent *in vitro* electrophysiological study suggested that 5-HT$_{1D}$ receptors have no role in the inhibition of firing of DRN 5-HT neurones by exogenous 5-HT (Craven *et al.*, 1994).

The present study does not address the site of the interaction between paroxetine and WAY 100635; however, several pieces of evidence point toward the involvement of the somatodendritic 5-HT$_{1A}$ autoreceptor in the DRN. Thus, paroxetine increases extracellular 5-HT in the DRN (this study) where 5-HT$_{1A}$ receptors, located on cell bodies and/or dendrites of 5-HT neurones (Vergé *et al.*, 1985; Sotelo *et al.*, 1990), are known to inhibit 5-HT cell firing (Sprouse & Aghajanian, 1987). Furthermore, SSRIs inhibit the firing of DRN neurones *in vitro* (Rigdon & Wang, 1991), and this effect is prevented by local application of 5-HT$_{1A}$ receptor antagonists (Jolas *et al.*, 1994).

WAY 100635 potentiates the effect of paroxetine on extracellular 5-HT in the FCx

Whereas injection of 0.8 mg kg^{-1}, i.v. paroxetine alone had no effect on extracellular 5-HT in the FCx, in rats pretreated with WAY 100635 (0.1 mg kg^{-1}, i.v.), the same dose of paroxetine induced a striking and sustained increase. A recent microdialysis study showed that pretreatment with (-)-penbutolol, or (S)-UH-301 potentiates the effects of the SSRI, citalopram, on extracellular 5-HT in the hippocampus (Hjorth, 1993). (-)-Penbutolol and (S)-UH-301 share 5-HT$_{1A}$ receptor blocking properties. When terminal 5-HT reuptake is blocked by the presence of an SSRI in the perfusion medium, systemic administration of SSRIs decreases extracellular 5-HT in the hippocampus. Using this model, Hjorth & Auerbach (1994) showed that the 5-HT$_{1A}$ receptor antagonists, pindodol and WAY 100135, block this decrease. The use of a highly selective 5-HT$_{1A}$ receptor antagonist in the present study provides further evidence that the results of the Hjorth study (1993) can indeed be attributed to 5-HT$_{1A}$ receptor blockade. That this effect of 5-HT$_{1A}$ receptor antagonists is mediated by somatodendritic 5-HT$_{1A}$ autoreceptors seems likely on the basis of evidence that injection of the non-selective 5-HT$_{1A}$ receptor antagonist methiothepin into the DRN enhanced the effect of citalopram on extracellular 5-HT in the cortex (Invernizzi *et al.*, 1992b). Importantly, our data also provide evidence of an association between the 5-HT-enhancing actions of the 5-HT$_{1A}$ receptor antagonists, and their ability to block the inhibitory effect of the SSRI on 5-HT cell-firing. Thus, in the present study WAY 100635 enhanced the effect of paroxetine on extracellular 5-HT at a dose that almost completely blocked the inhibitory effect of paroxetine on DRN firing.

Evidence that WAY 100635 is a silent 5-HT$_{1A}$ receptor antagonist

In the present study WAY 100635 (0.1 mg kg^{-1}, i.v.) alone moderately increased the firing rate (~50%) of some, but not all (6/10), DRN 5-HT neurones tested. Increases in 5-HT neuronal firing after WAY 100635 may reflect some tonic 5-HT-mediated inhibition in this population of neurones; however, the mechanism underlying the transient inhibition of firing observed in some neurones in the present study remains unclear. Two previous studies in other species (guinea-pig and cat) (Mundey *et al.*, 1994; Fornal *et al.*, 1994) have reported increased 5-HT cell firing after WAY 100635, although one other study in the rat found no increase (Fletcher *et al.*, 1994). In accord with Gurling *et al.* (1994), in the present study WAY 100635 had no effect on extracellular 5-HT in the FCx. That WAY 100635 neither consistently inhibits 5-HT cell firing nor decreases extracellular 5-HT in the forebrain confirms its lack of intrinsic activity at the 5-HT$_{1A}$ autoreceptor. Many putative selective 5-HT$_{1A}$ receptor antagonists (e.g. BMY 7378, NAN-190, MDL 73005) tested to date decrease both DRN firing and extracellular 5-HT (Sharp & Hjorth, 1990; Gartside *et al.*, 1990; Van den Hooff & Galzan, 1991; Greuel & Glaser, 1992), and as such have proved to be imperfect tools for the study of effects mediated by the 5-HT$_{1A}$ autoreceptor (for review see Fletcher *et al.*, 1993).

5-HT$_{1A}$ receptor antagonists and SSRIs in the treatment of depression

There is evidence that, although SSRIs inhibit 5-HT cell firing when given acutely, tolerance to this effect develops following long term administration, because of desensitization of the somatodendritic 5-HT$_{1A}$ autoreceptor (de Montigny *et al.*, 1990). It has been suggested that this desensitization may un-

derlie the antidepressant effect of SSRIs, since its onset coincides with the onset of the therapeutic effect (Blier & de Montigny, 1994). On this basis, the combination of a 5-HT$_{1A}$ receptor antagonist with an SSRI might, in the short term, produce a therapeutic effect equivalent to that observed after chronic administration of the SSRI alone. Interestingly, a recent open trail demonstrated that the antidepressant effect of paroxetine can be accelerated by co-administration of low doses of pindolol (Artigas *et al.*, 1994). Pindolol, like WAY 100635, has 5-HT$_{1A}$ autoreceptor antagonist properties (Sharp & Hjorth, 1990) and there is preliminary evidence that pindolol enhances the ability of an SSRI to increase extracellular 5-HT in the forebrain (Bel *et al.*, 1994). If the latter effect of pindolol underlies its antidepressant action, the present data indicate that WAY 100635 and other selective 5-HT$_{1A}$ antagonists like it, may have therapeutic use in the treatment of depression.

S.E.G. holds an MRC Training Fellowship. This work was supported by an MRC Programme grant (T.S.). We are grateful to Wyeth and SmithKline Beecham for generous gifts of drugs.

References

ADELL, A. & ARTIGAS, F. (1991). Differential effects of clomipramine given locally or systemically on extracellular 5-hydroxytryptamine in raphé nuclei and frontal cortex. *Naunyn-Schmied. Arch. Pharmacol.*, **343**, 237–244.

AGHAJANIAN, G.K. & VANDERMAELEN, C.P. (1982). Intracellular identification of central noradrenergic and serotonergic neurons by a new double labeling procedure. *J. Neurosci.*, **2**, 1786–1792.

ARTIGAS, F., PEREZ, V. & ALVAREZ, E. (1994). Pindodol induces a rapid improvement of depressed patients treated with serotonin reuptake inhibitors. *Arch. Gen. Psychiatry*, **51**, 248–251.

ÅSBERG, M., ERIKSSON, B., MATENSSON, B., TRASKMAN-BENDZ, L. & WAGNER, A. (1986). Therapeutic effects of serotonin uptake inhibitors in depression. *J. Clin. Psychiatr.*, **47**, 23–35.

BEL, N. & ARTIGAS, F. (1992). Fluvoxamine preferentially increases extracellular 5-hydroxytryptamine in the raphé nuclei: an *in vivo* microdialysis study. *Eur. J. Pharmacol.*, **229**, 101–103.

BEL, N., ROMERO, L., CELADA, P., DE MONTIGNY, C., BLIER, P. & ARTIGAS, F. (1994). Neurobiological basis for the potentiation of the antidepressant effect of 5-HT reuptake inhibitors by the 5-HT$_{1A}$ antagonist pindolol. *Proc. 6th International Conference on In Vivo Methods*, p209.

BLIER, P. & DE MONTIGNY, C. (1994). Current advances and trends in the treatment of depression. *Trends Pharmacol. Sci.*, **15**, 220–226.

CARBONI, E. & DI CHIARA, G. (1989). Serotonin release estimated by transcortical dialysis in freely-moving rats. *Neurosci.*, **32**, 637–645.

CHAPUT, Y., BLIER, P. & DE MONTIGNY, C. (1986). *In vivo* electrophysiological evidence for the regulatory role of autoreceptors on serotonergic terminals. *J. Neurosci.*, **6**, 2796–2801.

CRAVEN, R., GRAHAME-SMITH, D.G. & NEWBERRY, N. (1994). WAY-100635 and GR127935: effects on 5-hydroxytryptamine-containing neurones. *Eur. J. Pharmacol.*, **271**, R1–R3.

DAHLSTRÖM, A. & FUXE, K. (1964). Evidence for the existence of monoamine containing neurons in the central nervous system. *Acta Physiol. Scand.*, **62**, suppl 232, 1–55.

DE MONTIGNY, C., CHAPUT, Y. & BLIER, P. (1990). Modification of serotonergic neuron properties by long-term treatment with serotonin reuptake blockers. *J. Clin. Psychiatry*, **51**, Suppl B, 4–8.

ESCANDON, N.A., ZIMMERMAN, D.C. & MCCALL, R.B. (1994). Characterization of the serotonin$_{1A}$ receptor antagonist activity of WAY-100135 and spiperone. *J. Pharmacol. Exp. Ther.*, **268**, 441–447.

FLETCHER, A., BILL, D.J., CLIFFE, I.A., FORSTER, E.A., JONES, D. & REILLY, Y. (1994). A pharmacological profile of WAY-100635, a potent and selective 5-HT$_{1A}$ receptor antagonist. *Br. J. Pharmacol.*, **112**, 91P.

FLETCHER, A., CLIFFE, I.A. & DOURISH, C.T. (1993). Silent 5-HT$_{1A}$ receptor antagonists: utility as research tools and therapeutic agents. *Trends Pharmacol. Sci.*, **14**, 441–448.

FORNAL, C.A., METZLER, S.C., VEASEY, S.C., MCCREARY, A.C., DOURISH, C.T. & JACOBS, B.L. (1994). Single-unit studies in freely-moving animals provide evidence that WAY-100635, but not (S)-WAY-100135, blocks the action of endogenous serotonin at the 5-HT autoreceptor. *Br. J. Pharmacol.*, **112**, 92P.

FULLER, R.W. (1994). Minireview: Uptake inhibitors increase extracellular serotonin concentration measured by brain microdialysis. *Life Sci.*, **55**, 163–167.

GARTSIDE, S.E., COWEN, P.J. & HJORTH, S. (1990). Effects of MDL 73005EF on central pre- and postsynaptic 5-HT$_{1A}$ receptor function in the rat *in vivo*. *Eur. J. Pharmacol.*, **191**, 391–400.

GARTSIDE, S.E., UMBERS, V., HAJÓS, M. & SHARP, T. (1995). 5-HT$_{1A}$ receptor blockade prevents the inhibitory effect of paroxetine on 5-HT cell firing: relationship to changes in extracellular 5-HT. *Br. J. Pharmacol.*, **114**, 149P.

GREUEL, J.M. & GLASER, T. (1992). The putative 5-HT$_{1A}$ receptor antagonists NAN-190 and BMY 7378 are partial agonists in the rat dorsal raphé nucleus *in vivo*. *Eur. J. Pharmacol.*, **211**, 211–219.

GURLING, J., ASHWORTH-PREECE, M.A., DOURISH, C.T. & ROUTLEDGE, C. (1994). Effect of acute and chronic treatment with the selective 5-HT$_{1A}$ receptor antagonist WAY-100635 on hippocampal 5-HT release *in vivo*. *Br. J. Pharmacol.*, **112**,, 299P.

HAJÓS, M., GARTSIDE, S.E. & SHARP, T. (1995). Inhibition of median and dorsal raphé neurones by the selective 5-HT reuptake inhibitor paroxetine. *Naunyn-Schmied. Arch. Pharmacol.*, **351**, 624–629.

HJORTH, S. (1993). Serotonin 5-HT$_{1A}$ autoreceptor blockade potentiates the ability of the 5-HT reuptake inhibitor citalopram to increase nerve terminal output of 5-HT *in vivo*: a microdialysis study. *J. Neurochem.*, **60**, 776–779.

HJORTH, S. & AUERBACH, S.B. (1994). Further evidence for the importance of 5-HT autoreceptor in the action of selective serotonin reuptake inhibitors. *Eur. J. Pharmacol.*, **260**, 251–255.

INVERNIZZI, R., BELLI, S. & SAMANIN, R. (1992a). An increase of extracellular serotonin in the dorsal raphé masks the effect of sertraline in the frontal cortex. In *Monitoring Molecules in Neuroscience*. ed. Rollema, H., Westerink, B. & Drijfhout, W.J., pp. 253–255. Gröningen: University Centre for Pharmacy.

INVERNIZZI, R., BELLI, S. & SAMANIN, R. (1992b). Citalopram's ability to increase the extracellular concentrations of serotonin in the dorsal raphé prevents the drug's effect in the frontal cortex. *Brain Res.*, **584**, 322–324.

JOLAS, T., HAJ-DAHMANE, S., KIDD, E.J., LANGLOIS, X., LANFUMEY, L., FATTACCINI, C.M., VANTALON, V., LAPORTE, A.M., ADRIEN, J., GOZLAN, H. & HAMON, M. (1994). Central pre- and postsynaptic 5-HT$_{1A}$ receptors in rats treated chronically with a novel antidepressant, cericlamide. *J. Pharmacol. Exp. Ther.*, **268**, 1432–1443.

LANFUMEY, L., HAJ-DAHMANE, S. & HAMON, M. (1994). Further assessment of the antagonist properties of the novel and selective 5-HT$_{1A}$ receptor ligands (+) WAY 100135 and SDZ 216-525. *Eur. J. Pharmacol.*, **249**, 25–35.

MUNDEY, M.K., FLETCHER, A. & MARSDEN, C.A. (1994). Effect of the putative 5-HT$_{1A}$ antagonist WAY 100635 on 5-HT neuronal firing in the guinea-pig dorsal raphé nucleus. *Br. J. Pharmacol.*, **112**, 93P.

O'HEARN, E. & MOLLIVER, M.E. (1984). Organization of raphé-cortical projections in rat: a quantitative retrograde study. *Brain Res. Bull.*, **13**, 709–726.

PAXINOS, G. & WATSON, C. (1982). In *The Rat Brain in Stereotaxic Co-ordinates*. Sydney: Academic Press.

RIGDON, G.C. & WANG, C.M. (1991). Serotonin uptake blockers inhibit the firing of presumed serotonergic dorsal raphé neurons *in vitro*. *Drug Development Res.*, **22**, 135–140.

RUTTER, J.J. & AUERBACH, S.B. (1993). Acute uptake inhibition increases extracellular serotonin in the rat forebrain. *J. Pharmacol. Exp. Ther.*, **265**, 1319–1324.

SCHATZBERG, A.F., DESSAIN, E., O'NEIL, P., KATZ, D.L. & COLE, J.O. (1987). Recent studies on selective serotonergic antidepressants: trazodone, fluoxetine and fluvoxamine. *J. Clin. Psychopharmacol.*, **7**, 44S–49S.

SHARP, T. & HJORTH, S. (1990). Application of brain microdialysis to study the pharmacology of the 5-HT$_{1A}$ autoreceptor. *J. Neurosci. Methods*, **34**, 83–90.

SHARP, T., BRAMWELL, S.R., HJORTH, S. & GRAHAME-SMITH, D.G. (1989). Pharmacological characterization of 8-OH-DPAT-induced inhibition of rat hippocampal 5-HT release *in vivo* as measured by microdialysis. *Br. J. Pharmacol.*, **98**, 989–997.

SHARP, T. & ZETTERSTRÖM, T. (1992). In vivo measurement of monoamine neurotransmitter release using brain microdialysis. In *Monitoring Neuronal Activity*. ed. Stamford, J.A. pp. 147–179. Oxford: Oxford University Press.

SHEARD, M.H., ZOLOVICK, A. & AGHAJANIAN, G.K. (1972). Raphe neurons: effect of tricyclic antidepressant drugs. *Brain Res.*, **43**, 690–694.

SOTELO, C., CHOLLEY, B., EL MESTIKAWAY, S., GOZLAN, H. & HAMON, M. (1990). Direct immunocytochemical evidence of the existence of 5-HT$_{1A}$ autoreceptors on serotonergic neurons in the midbrain raphé nuclei. *Eur. J. Neurosci.*, **2**, 1144–1154.

SPROUSE, J.S. & AGHAJANIAN, G.K. (1987). Electrophysiological responses of serotoninergic dorsal raphe neurons to 5-HT$_{1A}$ and 5-HT$_{1B}$ agonists. *Synapse*, **1**, 3–9.

STARKEY, S.J. & SKINGLE, M. (1994). 5-HT$_{1D}$ as well as 5-HT$_{1A}$ autoreceptors modulate 5-HT release in the guinea pig dorsal raphé nucleus. *Neuropharmacol.*, **33**, 393–402.

UNGERSTEDT, U. (1971). Stereotaxic mapping of the monoamine pathways in the rat brain. *Acta Physiol. Scand.*, Suppl 367, 1–48.

VAN DEN HOOFF, P. & GALZAN, M. (1991). A comparison of the actions of the 5-HT$_{1A}$ ligand MDL 73005EF on rat dorsal raphé and dorsal lateral septum neurones *in vitro*. *Fundam. Clin. Pharmacol.*, **5**, 432.

VERGE, D., DAVAL, G., PATEY, A., GOZLAN, H., EL MESTIKAWY, S. & HAMON, M. (1985). Presynaptic 5-HT autoreceptors on serotonergic cell bodies and/or dendrites but not terminals are of the 5-HT$_{1A}$ subtype. *Eur. J. Pharmacol.*, **113**, 463–464.

(Received February 22, 1995
Revised April 7, 1995
Accepted April 11, 1995).

British Journal of Pharmacology (1995) 115, 1071-1079 © 1995 Stockton Press All rights reserved 0007-1188/95 $12.00

The effect of neuropeptide Y on sodium, chloride and potassium transport across the rat distal colon

D. Strabel & [1]M. Diener

Institut für Veterinär-Physiologie, Universität Zürich, Winterthurerstr. 260, CH-8057 Zürich, Switzerland

1 Neuropeptide Y (NPY; $10^{-10}-10^{-7}$ mol l^{-1}) reduced basal short-circuit current (I_{sc}) in a concentration-dependent manner in the rat distal colon but was ineffective in the proximal colon.

2 The action of NPY was dependent upon the presence of Cl^- and HCO_3^- anions and was blocked by prior treatment of the tissue with a Cl^- channel blocker. The decrease in I_{sc} was associated with an increase in mucosa-to-serosa fluxes of Na^+, Rb^+ (K^+) and Cl^-, whereas the serosa-to-mucosa flux of Cl^- was decreased.

3 The size of the inhibitory NPY effect was linearly correlated with the height of the basal I_{sc}, i.e. it inhibited 55% of basal secretory I_{sc}.

4 The action of NPY was unaffected by indomethacin and tetrodotoxin, when given alone, but was abolished, when the basal I_{sc} was decreased to values near zero by a combination of both inhibitors. This inhibition could be overcome by restoring basal I_{sc} with prostaglandin E_2, indicating that the effect of NPY is not mediated by nerves or prostaglandins, but that NPY is only effective, when anion secretion is stimulated by the spontaneous release of neurotransmitters and prostaglandins.

5 NPY inhibited the increase in I_{sc} induced by veratridine and prostaglandin E_2, but it had no effect on the I_{sc} induced by direct stimulation of the adenylate cyclase with forskolin, or on I_{sc} induced by stimulation of the Ca^{2+}-pathway with carbachol. Inhibition of the response to veratridine or prostaglandin E_2 by NPY showed the same dependence on the height of the I_{sc} just prior to addition of NPY as seen in control conditions, i.e. NPY inhibited 55% of cyclic AMP-mediated secretion.

6 These results suggest that the effect of NPY is mediated by an inhibition of cyclic AMP-stimulated secretion, which is stimulated in the rat distal colon by a continuous release of prostaglandins and neurotransmitters.

Keywords: Cl^- secretion; cyclic AMP; enteric nervous system; K^+ transport; neuropeptide Y; prostaglandins; rat colon

Introduction

Neuropeptide Y (NPY) is a 36-amino acid peptide, which was originally isolated from the brain (Tatemoto *et al.*, 1982). Like many other transmitters of the central nervous system it is also present in the gut (Furness *et al.*, 1983), where it is known to coexist with noradrenaline in sympathetic nerves and with vasoactive intestinal polypeptide (VIP) in nerves of the small intestine (Ekblad *et al.*, 1987; Cox *et al.*, 1994). At least two receptor subtypes for NPY have been identified pharmacologically, the Y_1-receptor, which is stimulated only by the intact peptide, and the Y_2-receptor, which is also stimulated by C-terminal fragments of NPY (Wahlestedt *et al.*, 1990).

NPY has been shown to exert proabsorptive and antisecretory actions in the small intestine of different species. It inhibits basal and stimulated Cl^- secretion in the rat small intestine *in vivo* (Saria & Beubler, 1985) and *in vitro* (Cox & Cuthbert, 1988; Cox *et al.*, 1988) as well as in the porcine jejunum *in vitro* (Brown *et al.*, 1990), whereas in the rabbit ileum, NPY selectively stimulates Cl^- absorption (Hubel & Renquist, 1986). Only a few studies have been performed with the colonic mucosa. In the rabbit distal colon, NPY inhibited ion secretion stimulated by VIP (Flint *et al.*, 1990), and when comparing the effect of NPY in the rat small and large intestine, only small effects of NPY on basal short-circuit current were observed in the rat descending colon (Cox *et al.*, 1988). Different mechanisms have been proposed for the action of NPY on anion transport. In rabbit (Hubel & Renquist, 1986) and pig (Brown *et al.*, 1990) small intestine, NPY was found to stimulate exclusively the absorptive, mucosa-to-serosa flux of Cl^- (J^{Cl}_{ms}), whereas in the rat small intestine both an increase in J^{Cl}_{ms} as well as a decrease in the serosa-to-mucosa flux (J^{Cl}_{ms}), i.e. a proabsorptive and an antisecretory effect of NPY have been observed (Cox *et al.*, 1988). In rabbit (Hubel & Renquist, 1986) and rat (Cox *et al.*, 1988) small intestine, the effect of NPY was unaffected by the neurotoxin, tetrodotoxin (TTX), whereas in the pig small intestine TTX abolished the response to NPY (Brown *et al.*, 1990). In contrast, in the rat small intestine, the effect of NPY was reduced by prior treatment of the tissue with the cyclo-oxygenase inhibitor, indomethacin (Cox *et al.*, 1988).

Recently, we studied the effect of another proabsorptive and antisecretory hormone, somatostatin, on ion transport in the rat distal colon. Somatostatin inhibits adenosine 3':5'-cyclic monophosphate (cyclic AMP)- and Ca^{2+}-mediated secretion (Knobloch *et al.*, 1989) and stimulates basal Cl^- absorption by stimulating J^{Cl}_{ms} (Diener & Gartmann, 1994). This latter action has been shown to be mediated by the opening of a volume-activated basolateral Cl^- channel, the activation of which can be prevented by prior addition of lipoxygenase blocker or a leukotriene D_4 receptor blocker. One aim of the present study was to investigate whether the action of NPY in the rat colon involves a similar mechanism to that of somatostatin. In the light of the published literature (see above) concerning the action of NPY in other intestinal segments, special interest was placed on a possible role of the eicosanoid and the neural system. Because no data are available about an action of proabsorptive hormones on K^+ transport, the effect of NPY on K^+ fluxes (using $^{86}Rb^+$ as a marker for K^+) was investigated and compared with two other proabsorptive hormones, somatostatin and vasopressin. The colon is a differentiated organ with well known segmental differences (see e.g. Nobles *et al.*, 1991), therefore the effect of NPY was tested in the distal and the proximal part of this organ.

[1] Author for correspondence.

Methods

Solutions

Most of the experiments were carried out in a Parsons solution containing (mmol l^{-1}): NaCl 107, KCl 4.5, $NaHCO_3$ 25, Na_2HPO_4 1.8, NaH_2PO_4 0.2, $CaCl_2$ 1.25, $MgSO_4$ 1 and glucose 12. The solution was gassed with carbogen (5% CO_2 in 95% O_2) and kept at a temperature of 37°C; pH was 7.4. When fluxes of $^{86}Rb^+$ were measured, KCl was substituted by RbCl. For the Cl^--free buffer, NaCl was replaced with Na gluconate, the Ca^{2+} concentration in this solution was elevated to 5.8 mmol l^{-1} in order to compensate the Ca^{2+}-buffering properties of gluconate (Kenyon & Gibbons, 1977). In the Na^+-free solution, NaCl was replaced by N-methyl-D-glucamine chloride. The HCO_3^--free Tyrode solution consisted of (mmol l^{-1}): NaCl 140, KCl 5.4, $CaCl_2$ 1.25, $MgSO_4$ 1, HEPES (N-(2-hydroxyethyl)piperazine-N'-2-ethansulphonic acid) 10, glucose 12; it was gassed with O_2. If in addition Cl^- was omitted from this solution, NaCl was substituted by Na gluconate and the $CaCl_2$ concentration was elevated to 10 mmol l^{-1}.

Tissue preparation

Female SIVZ-50 rats (Institut für Labortierkunde, Universität Zürich, Switzerland) with a weight of 180–220 g were used. The animals had free access to water and food until the day of the experiment. Animals were stunned by a blow on the head and killed by exsanguination (approved by the Swiss Federal Administration Bureau for Veterinary Medicine). The serosa and muscularis propria were stripped away by hand to obtain the mucosa-submucosa preparation of the distal part of the colon descendens. For comparison, some experiments were also performed with the muscle-stripped proximal colon.

Short-circuit current measurement

The tissue was fixed in a modified Ussing chamber (Andres *et al.*, 1985), bathed with a volume of 4 ml on each side of the mucosa and short-circuited by a voltage clamp (Aachen Microclamp, AC Copy Datentechnik, Aachen, Germany) with correction for fluid resistance. The exposed surface of the tissue was 1 cm^2. Short-circuit current (I_{sc}) was continuously recorded on a chart-recorder. In addition, I_{sc} and tissue conductance (Gt) were printed every min by a computer printer.

Unidirectional flux measurements

Ion flux studies were performed as previously described (Andres *et al.*, 1985). After an equilibration period of 60 min, either ^{22}Na (59 kBq) and ^{36}Cl (29 kBq), or ^{86}Rb (74 kBq) were added to one side (= labelled side) of the epithelium. After an additional 20 min (to allow isotope fluxes to reach a steady state), unidirectional ion fluxes were determined in two sequential 20 min periods, i.e. a control period and a period starting 10 min after administration of the proabsorptive hormone. From the measured unidirectional fluxes net ion fluxes were calculated. Residual ion flux, i.e. the sum of the movement of all ions other than Na^+ and Cl^-, was calculated according to: $J^R_{net} = I_{sc} - J^{Na}_{net} + J^{Cl}_{net}$. A positive J^R_{net} indicates either the absorption of a cation or the secretion of an anion.

In other experiments, Cl^- or Rb^+ accumulation on the unlabelled side was measured under control conditions in five sequential 3 min periods followed by five sequential 3 min periods starting 3 min after administration of 10^{-7} mol l^{-1} NPY to the serosal side. For these experiments 104 kBq $^{36}Cl^-$ or 120 kBq $^{86}Rb^+$, respectively, were added to the labelled side 20 min before the beginning of the flux experiment. Transport rates for Cl^- or Rb^+ were calculated separately by linear regression of isotope accumulation on the unlabelled side during the control and the NPY period. All aliquots from the labelled side were replaced by unlabelled buffer solution and appropriate correction for this replacement solution was performed.

Data evaluation

Usually, the experiments were started after an equilibration period of 1–2 h, after which the initial high I_{sc} had reached a stable plateau. The response to NPY was tested in the absence and presence of different inhibitors, which were administered to the compartment indicated in the text, stabilization of a new I_{sc} baseline was usually within 15–20 min. The baseline in I_{sc} was determined as the mean of three immediately preceding I_{sc} values, i.e. the last 3 min just before administration of NPY. In the tables, the maximal decrease in I_{sc} induced by NPY is expressed as the difference from the starting baseline (ΔI_{sc}).

Drugs

If not indicated otherwise, drugs were from Sigma, Buchs, Switzerland. Anthracene-9-carboxylic acid (Aldrich, Buchs, Switzerland), methazolamide, 5-nitro-2-(3-phenylpropylamino)-benzoate (NPPB; gift from R. Greger, Physiologisches Institut, Freiburg, Germany), and veratridine were dissolved in dimethylsulphoxide (DMSO, final maximal concentration 0.25%, v/v). Forskolin (gift from Hoechst, Frankfurt, Germany), indomethacin, nordihydroguaiaretic acid, and prostaglandin E_2 were dissolved in ethanol (final maximal concentration 0.25%, v/v). Neuropeptide Y (NPY; Peninsula, Belmont, CA, U.S.A.) was dissolved in 10 mmol l^{-1} acetic acid containing 0.1% (w/v) bovine serum albumin. Neuropeptide $Y_{(13-36)}$, somatostatin (generous gift from Curamed, Karlsruhe, Germany), vasoactive intestinal polypeptide (VIP), and vasopressin were dissolved in aqueous stock solutions containing 0.1% (w/v) bovine serum albumin. Tetrodotoxin (TTX) was dissolved in citrate buffer (5 mg mg^{-1} TTX; pH 4.3). All other drugs including SK&F 104353 (2-hydroxy-3-carboxyethylthio-3-[2-(8-phenyloctyl)phenyl] propanoic acid) (generous gift from Smith Kline & French, King of Prussia, PA, U.S.A.) were in aqueous stock solutions. Radioisotopes were obtained from NEN, Dreieich, Germany, and specific activities were 3.9 TBq g^{-1} ^{22}Na and 550 MBq g^{-1} ^{36}Cl; the initial activity of ^{86}Rb amounted to 411 GBq g^{-1}.

NPY, anthracene-9-carboxylic acid, carbachol, NPPB, prostaglandin E_2, SK&F 104353, somatostatin, tetrodotoxin, vasopressin, veratridine and VIP were added to the serosal side only, while forskolin, indomethacin, methazolamide and nordihydroguaiaretic acid were applied on both sides of the tissue.

Statistics

Results are given as means ± one standard error of the mean (s.e.mean). Standard errors for calculated values, i.e. net ion transport, were calculated by the law of error propagation. The significance of differences was tested by analysis of variances and, if indicated, by Student's paired or unpaired two-tailed t test or a U test, respectively. An F test was applied to decide which test method was to be used. Regression lines were compared by analysis of co-variances (Kenakin, 1987). The quality of regressions was checked by the squared non-linear regression coefficient (r^2).

Results

Effect of NPY on basal electrical parameters

The rat distal colon showed a baseline short-circuit current (I_{sc}) of 1.8 ± 0.1 μEq h^{-1} cm^{-2} and a baseline tissue conductance (Gt) of 10.9 ± 0.9 mS cm^{-2} ($n = 40$). NPY (administered at the serosal side) caused a concentration-dependent decrease in I_{sc} in the rat distal colon (Figure 1a) with a threshold concentration of 10^{-10} mol l^{-1} and a half-maximal effect at a

concentration of 5×10^{-9} mol l^{-1}. The response to NPY saturated at concentrations $\geqslant 5 \times 10^{-8}$ mol l^{-1} and a maximal concentration of 10^{-7} mol l^{-1} was used for all further experiments.

When all responses to NPY (10^{-7} mol l^{-1}) in the distal colon under control conditions were pooled, NPY evoked a decrease of I_{sc} of -0.9 ± 0.1 μEq h^{-1} cm^{-2} ($n=40$; $P<0.05$), which was associated with a small, insignificant decrease in Gt (-0.4 ± 0.2 mS cm^{-2}; $n=40$). In contrast, NPY did not evoke any significant change in I_{sc} in the proximal colon (Figure 1a). The response to native NPY was mimicked by the C-terminal NPY-fragment, $NPY_{(13-36)}$. Neuropeptide $Y_{(13-36)}$ (10^{-7} mol l^{-1}) caused a decrease in I_{sc} of -0.6 ± 0.1 μEq h^{-1} cm^{-2} ($n=8$; $P<0.05$), which was not significantly smaller than the response induced by native NPY.

The response to NPY was relatively transient. In general, NPY caused a maximal decrease in I_{sc} within 5–6 min, which

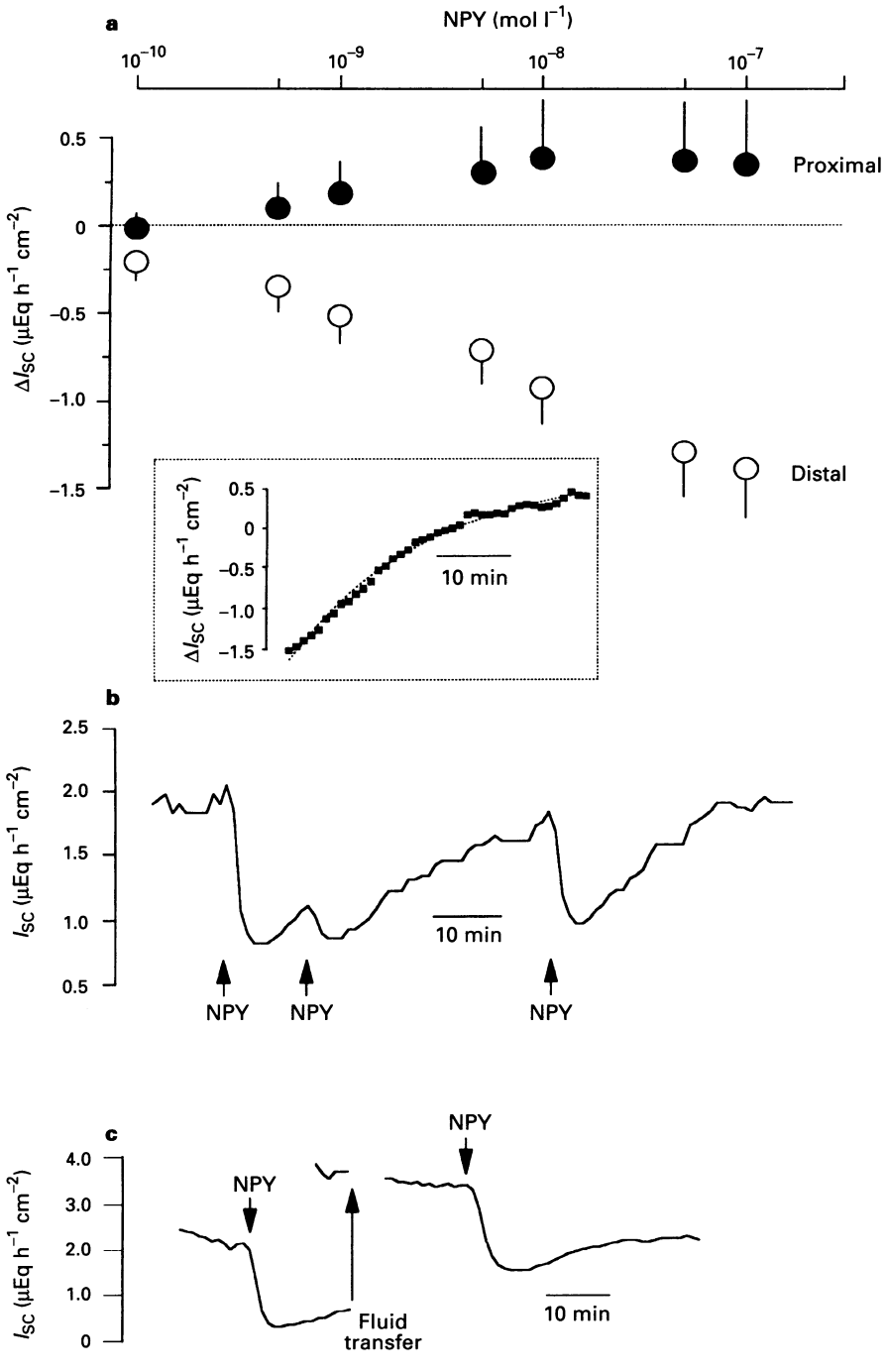

Figure 1 (a)Concentration-dependent effect of neuropeptide Y (NPY) on I_{sc} in distal (○) and proximal (●) rat colon. Values are means ± 1 s.e.mean, $n=8$. The decrease in I_{sc} induced by NPY in the distal colon was significant for all concentrations tested, whereas in the proximal colon no significant change of the I_{sc} could be evoked by the peptide. Basal I_{sc} levels were 2.6 ± 0.3 μEq h^{-1} cm^{-2} ($n=8$) in the distal and 2.1 ± 0.2 μEq h^{-1} cm^{-2} ($n=8$) in the proximal colon. (**b**) Time-course of the response to NPY (10^{-7} mol l^{-1}, administered three times without intermittent washing) in the distal colon. The experiment is representative for 6 similar experiments. The inset shows the decay in the I_{sc} response to NPY (■ = measured data points starting 8 min after NPY administration), which could be fitted ($r^2=0.992$) by a mono-exponential function (dashed line) with a half-time of 13.5 min. The data were averaged from 7 experiments. (**c**) Transfer of serosal fluid from a first tissue (lower tracing) 15 min after NPY administration (10^{-7} mol l^{-1}) to the serosal side of a second native tissue (upper tracing). The line interruption in the upper tracing is caused by omission of an artifact due to exchange of the serosal buffer. This trace is representative of 5 similar experiments.

returned to baseline within about 30 min. This decay could be adequately described ($r^2=0.992$) using a mono-exponential function with a half-time of 13.5 min ($n=7$; inset of Figure 1) suggesting that only one mechanism is responsible for the termination of the response. When NPY (10^{-7} mol l^{-1}) was administered a second time during the decay phase of a first NPY administration, the peptide induced a prompt decrease in I_{sc} (Figure 1b), which amounted to 89.6±3.0% of the first response. Even a third application of NPY, administered when the response to the first two doses had faded without an intermediate washout, induced a decrease in I_{sc}, which amounted to 63.7±6.7% of the response evoked by the first NPY application ($n=6$). In a further set of experiments, NPY (10^{-7} mol l^{-1}) was added to one group of tissues. The serosal fluid of these tissues was sucked away 15 min after peptide administration, i.e. when the I_{sc} response had started to fade. When this serosal fluid replaced the serosal fluid of a second, untreated group of tissues, no decrease in I_{sc} could be evoked (Figure 1c; $n=5$), although subsequent administration of fresh NPY showed that the preparations were sensitive to the peptide. This suggests that peptide degradation rather than receptor desensitization is responsible for the transient nature of the NPY response.

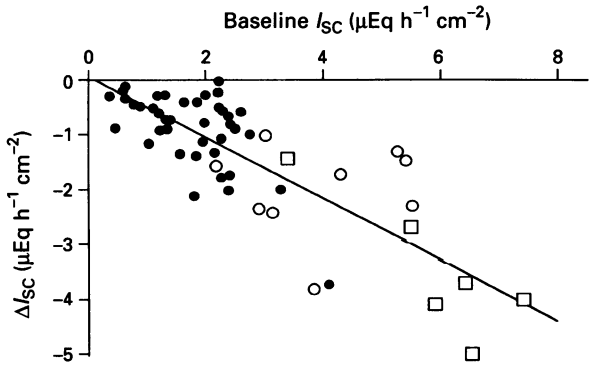

Figure 2 Dependence of neuropeptide Y (NPY) responses (10^{-7} mol l^{-1}) upon the height of the baseline I_{sc}. The effect of NPY is shown under control conditions (●), and after elevation of baseline I_{sc} with prostaglandin E_2 (10^{-6} mol l^{-1}; ○) or with veratridine (5×10^{-5} mol l^{-1}; □). The solid line gives the linear correlation pooled for all data points according to: $\Delta I_{sc}=0.07-0.56\times$ baseline ($r=0.84$; $n=56$; $P<0.05$).

The decrease in I_{sc} induced by NPY exhibited a certain degree of variability even under control conditions ranging from 0.0 μEq h^{-1} cm^{-2} to −3.7 μEq^{-1} cm^{-2} ($n=40$; ● in Figure 2). However, the decrease in I_{sc} showed a linear correlation with the baseline I_{sc} prior to addition to NPY; i.e. NPY inhibited about 55% of the spontaneous basal secretory I_{sc}.

Ionic dependence of the NPY effect

The decrease in I_{sc} caused by NPY (10^{-7} mol l^{-1}) was not dependent on the presence of Na^+ (Table 1). Omission of either Cl^- or HCO_3^- ions alone from the buffer did not diminish the response to NPY. If, however, both anions were omitted from the buffer, the effect of NPY was significantly attenuated (Table 1). The response to NPY was completely suppressed, when in addition the carbonic anhydrase blocker, methazolamide (10^{-4} mol l^{-1}) was present. Pretreatment of the mucosa with the Cl^- channel blockers, anthracene-9-carboxylic acid (10^{-3} mol l^{-1}) or NPPB (10^{-4} mol l^{-1}), also significantly reduced the response to NPY, indicating that a change in anion transport is predominantly responsible for the decrease in I_{sc}.

Measurements of unidirectional ion fluxes

The effect of NPY (10^{-7} mol l^{-1}) on unidirectional fluxes of $^{22}Na^+$ and $^{36}Cl^-$ was tested for a long time period, i.e. 20 min. Despite the results of the ion substitution experiments, which suggested a change in anion transport to be responsible for the decrease in I_{sc} induced by the peptide, no significant effect of NPY on Cl^- transport could be observed (Table 2). The only action of NPY under these conditions consisted of a significant increase in J^{Na}_{ms} from 10.9±1.3 μEq h^{-1} cm^{-2} to 12.1±1.2 μEq h^{-1} cm^{-2} ($n=9$; $P<0.05$).

In order to investigate the transient effect of NPY on anion transport in a more appropriate way, the effect of NPY on Cl^- transport was tested using a protocol developed by Cox *et al.* (1988) to investigate the effect of this peptide upon Cl^- transport in the rat jejunum. Therefore, tracer amounts of $^{36}Cl^-$ were added to one side of the epithelium and the accumulation of $^{36}Cl^-$ on the unlabelled side was measured under control conditions and in the presence of NPY (10^{-7} mol l^{-1}). Transport rates under control conditions and in the presence of NPY were calculated by linear regression, linear correlation coefficients (r) for all individual experiments were ⩾0.96.

Under control conditions, the ms-transport rate of $^{36}Cl^-$ amounted to 267±24 nmol min^{-1} cm^{-2} (Figure 3). This rate

Table 1 Baseline electrical parameters during ion replacement experiments and in the presence of inhibitors

	Baseline I_{sc} (μEq h^{-1} cm^{-2})	Δ I_{sc}	n
Control	1.8±0.1	−0.9±0.1	40
Na^+-free	2.4±0.2	−1.0±0.2	8
Cl^--free	1.8±0.2	−0.7±0.1	8
HCO_3^- -free	1.8±0.4	−0.5±0.2	8
HCO_3^- + Cl^--free	0.9±0.2	−0.2±0.1*	11
HCO_3^- /Cl^--free + methazolamide	0.6±0.2	−0.1±0.1*	9
Anthracene-9-carboxylic acid	1.4±0.2	−0.3±0.1*	8
NPPB	1.0±0.2	−0.2±0.1*	8
Nordihydroguaiaretic acid	1.6±0.3	−0.6±0.1	8
SK&F 104353	1.9±0.4	−0.6±0.2	7
Indomethacin	1.3±0.2	−0.7±0.1	6
TTX	1.3±0.5	−0.6±0.1	6
Indomethacin/TTX	0.3±0.2	−0.1±0.0*	6
Indomethacin/TTX/prostaglandin E_2	3.0±0.7	−0.9±0.1*	6

Short-circuit current levels prior to the administration of neuropeptide (NPY)(baseline) and the effect of NPY (10^{-7} mol l^{-1}; Δ I_{sc}) during control conditions, during ion replacement experiments and in the presence of anthracene-9-carboxylic acid (10^{-3} mol l^{-1}), NPPB (10^{-4} mol l^{-1}), nordihydroguaiaretic acid (10^{-5} mol l^{-1}), SK&F 104353 (5×10^{-5} mol l^{-1}), indomethacin (10^{-6} mol l^{-1}), or tetrodotoxin (10^{-6} mol l^{-1}) and the combination of indomethacin, tetrodotoxin and prostaglandin E_2 (10^{-6} mol l^{-1}). Ion replacements were applied to both sides of the tissue. The effect of NPY is given as the difference from the preceding baseline. Values are means ± 1 s.e.mean. *$P<0.05$ versus effect of NPY under control conditions.

increased to 321±28 nmol min^{-1} cm^{-2} in the presence of NPY ($n=9$; $P<0.05$). In parallel, the sm-transport of Cl^- was decreased by NPY (215±23 nmol min^{-1} cm^{-2} in the absence and 155±12 nmol min^{-1} cm^{-2} in the presence of NPY; $n=8$; $P<0.05$). This led to an increase in net Cl^- transport rate from 53±6 nmol min^{-1} cm^{-2} to 166±6 nmol min^{-1} cm^{-2} ($P<0.05$; analysis of co-variances).

Sensitivity to inhibitors

The response to NPY (10^{-7} mol l^{-1}) was neither affected by prior treatment of the mucosa with the cyclo-oxygenase inhibitor, indomethacin (10^{-6} mol l^{-1}; Table 1), nor by the neuronal toxin, tetrodotoxin (10^{-6} mol l^{-1}; Table 1), suggesting that the effect of the peptide is not mediated by prostaglandins or enteric neurones. However, prior addition of a combination of both blockers suppressed the effect of NPY; i.e. a combination of indomethacin and TTX attenuated NPY responses (Table 1). Both blockers together caused a decrease in I_{sc} from 4.0±0.4 μEq h^{-1} cm^{-2} to 0.3±0.2 μEq h^{-1} cm^{-2} ($n=6$; $P<0.05$; Table 1). In contrast, the lipoxygenase inhibitor, nordihydroguaiaretic acid (10^{-5} mol l^{-1}), and the leukotriene D_4 receptor blocker, SK&F 104353 (5×10^{-5} mol l^{-1}), which both inhibit the effect of somatostatin on basal I_{sc} (Diener & Gartmann, 1994), were without effect on the I_{sc} response induced by NPY (Table 1).

The inhibition of NPY responses by the combination of indomethacin and tetrodotoxin suggests either that the peptide effects are mediated by inhibitory prostaglandins and enteric nerves or that the spontaneous production of prostaglandins and neurotransmitters elevate the secretory state of the tissue, allowing subsequent attenuation by NPY. In order to distinguish between these possibilities, I_{sc}, which had been decreased by prior addition of indomethacin and tetrodotoxin, was elevated by prostaglandin E_2 (10^{-6} mol l^{-1}; Table 1), and subsequently NPY was applied. Under these conditions, i.e. despite the inhibition of prostaglandin production by indomethacin and the inhibition of neurotransmission by tetrodotoxin, NPY caused a decrease in I_{sc} of −0.9±0.1 μEq h^{-1} cm^{-2} ($n=6$; $P<0.05$), which was not significantly different from control responses to NPY (Table 1).

Effect of NPY on the response to secretagogues

Pretreatment of preparations with NPY (10^{-7} mol l^{-1}) did not affect the response to carbachol (5×10^{-5} mol l^{-1}), a secretagogue acting on the Ca^{2+}-pathway, nor to VIP (10^{-7} mol l^{-1}), a secretagogue acting on the cyclic AMP-pathway, nor to vera-

Table 2 Effect of neuropeptide Y (NPY) on $^{22}Na^+$ and $^{36}Cl^-$ fluxes

	J^{Na}_{ms}	J^{Na}_{sm}	J^{Na}_{net}	J^{Cl}_{ms} (μEq h^{-1} cm^{-2})	J^{Cl}_{ms}	J^{Cl}_{net}	I_{sc}	J^{R}_{net}	Gt (mS cm^{-2})
Control	10.9±1.3	4.8±0.4	6.1±1.4	16.2±1.7	9.9±0.7	6.3±1.8	1.7±0.1	1.9±2.3	11.3±0.1
NPY	12.1±1.2*	5.5±0.4	6.6±1.2	15.2±1.8	9.3±0.9	5.9±2.0	1.3±0.1*	0.6±2.3	11.5±0.9

The effect of NPY (10^{-7} mol l^{-1} at the serosal side) on mucosa-to-serosa (ms), serosa-to-mucosa (sm) and net fluxes during a 20 min flux measurement. The I_{sc} and Gt values are the means±1 s.e.mean of the complete control or NPY period, respectively, where $n=9-10$. *$P<0.05$ versus the preceding period.

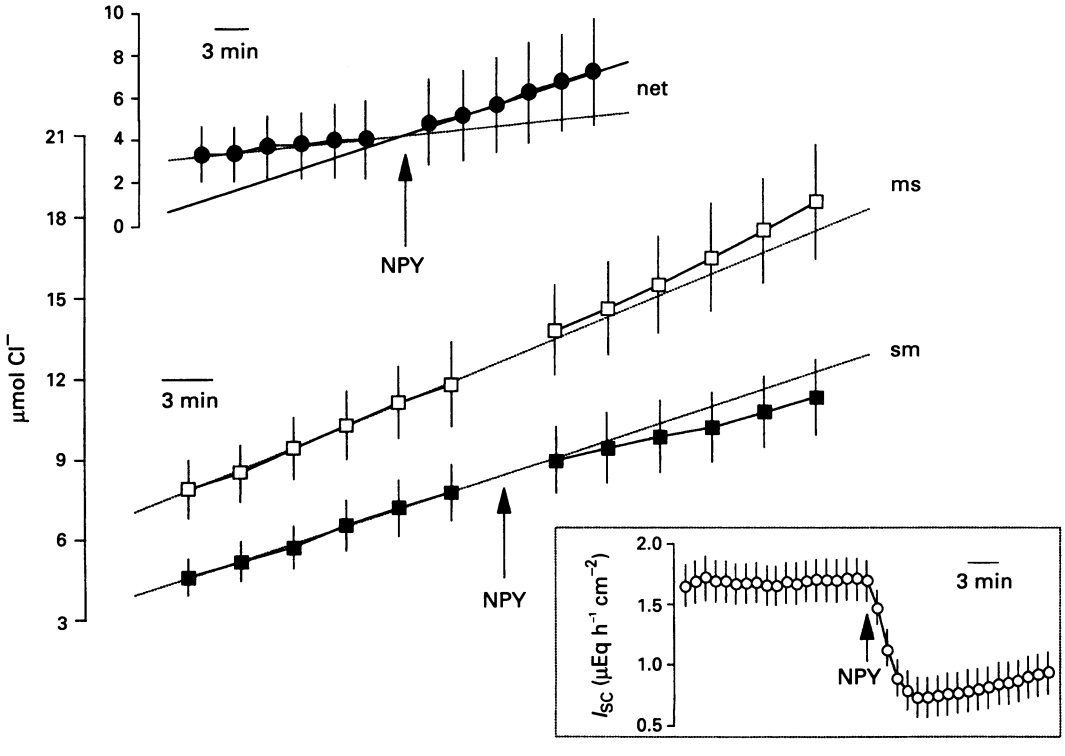

Figure 3 Effect of neuropeptide Y (NPY, 10^{-7} mol l^{-1}) upon $^{36}Cl^-$ unidirectional fluxes. Mucosa-to-serosa (ms; □), serosa-to-mucosa (sm; ■), and net (●) fluxes. The dashed lines represent the best fit line for Cl^- transport under control conditions. The inset shows the change in I_{sc} (○) induced by NPY in this series of experiments. Values are means±1s.e.mean, $n=8-9$.

Table 3 Effect of pretreatment with neuropeptide Y (NPY) on the response to secretagogues

	Distal		*Proximal*	
	Control	*+NPY*	*Control*	*+NPY*
	(μEq h^{-1} cm^{-2})			
Carbachol peak	9.5±1.2	8.7±1.7	9.0±1.2	6.3±1.2
10 min	1.9±0.5	2.5±0.7	1.9±1.1	2.3±0.5
Veratridine peak	8.2±0.7	10.5±1.2	7.0±0.9	4.9±1.4
15 min	3.6±0.5	5.1±0.6	4.1±0.6	3.2±0.6
VIP	2.8±0.4	2.9±0.3	4.4±0.3	5.0±0.7

Increase in I_{sc} induced by carbachol (5×10^{-5} mol l^{-1}), veratridine (5×10^{-5} mol l^{-1}) and vasoactive intestinal polypeptide (VIP) (10^{-7} mol l^{-1}) in the absence (control) and presence of NPY (10^{-7} mol l^{-1}) in the distal (left) and the proximal (right) rat colon. Carbachol and veratridine induced a biphasic increase in I_{sc}, which are referred to as peak and then the response 10 or 15 min after administration of the drug, respectively, For VIP, which induced a monophasic increase in I_{sc}, only the peak response is presented. Values are means±1 s.e.mean, $n=5-7$. There were no significant differences between the responses to secretagogues under control conditions and those in the presence of NPY in either colonic segment.

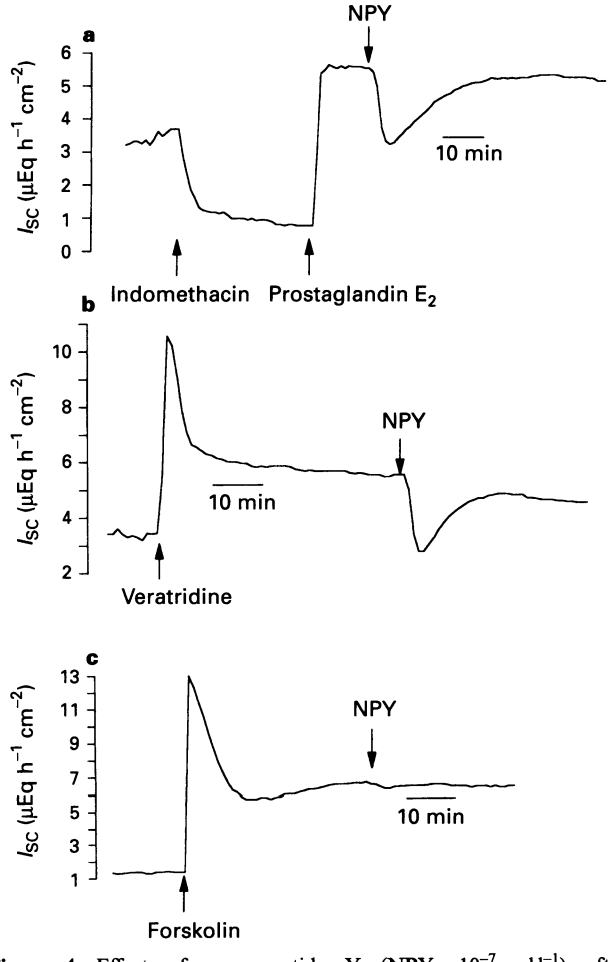

Figure 4 Effect of neuropeptide Y (NPY, 10^{-7} mol l^{-1}) after pretreatment of the mucosa with (**a**) prostaglandin E_2 (10^{-6} mol l^{-1}), (**b**) veratridine (5×10^{-5} mol l^{-1}), or (**c**) forskolin (5×10^{-6} mol l^{-1}). In the case of the prostaglandin E_2 experiments, tissues were pretreated with indomethacin (10^{-6} mol l^{-1}). Values are representative of between 6–9 experiments.

tridine (5×10^{-5} mol l^{-1}; Table 3). In order to establish whether NPY, which does not affect basal I_{sc} in the proximal colon (Figure 1a), may interfere with secretagogue-stimulated I_{sc} in the proximal colon, the experiments were repeated with this colonic segment. However, NPY proved to be completely ineffective (Table 3).

Because the missing effect of NPY pretreatment on these secretory responses might be due to the short duration of the action of the peptide, the sequence of the protocol was reversed; i.e. the respective secretagogue was administered first and NPY was added, when the I_{sc} had risen to a stable elevated plateau. Instead of VIP, which induces only a transient increase in I_{sc} in the rat colon (Knobloch *et al.*, 1989), prostaglandin E_2 was used to induce a prolonged receptor-mediated stimulation of the cyclic AMP-pathway (Diener *et al.*, 1988). Tissues were pretreated with indomethacin (10^{-6} mol l^{-1}) to enhance the sensitivity of the mucosa to exogenously applied prostaglandins (Bukhave & Rask-Madsen, 1980). Prostaglandin E_2 (10^{-6} mol l^{-1}) caused an increase in I_{sc} by 2.9±0.3 μEq h^{-1} cm^{-2} in the distal colon ($n=9$; $P<0.05$). After pretreatment with prostaglandin E_2, the response to a subsequent administration of NPY (10^{-7} mol l^{-1}) was greatly enhanced. In the presence of prostaglandin E_2, NPY induced a decrease in I_{sc} of −2.0±0.3 μEq h^{-1} cm^{-2} ($n=6$; $P<0.05$ compared with NPY response under control conditions, Figure 4a). Also pretreatment of the mucosa with the stimulating neurotoxin, veratridine, enhanced the response to NPY. Veratridine (5×10^{-5} mol l^{-1}) caused an increase in I_{sc} in the distal colon to a stable plateau of 6.4±0.7 μEq h^{-1} cm^{-2} (Figure 4b; $n=7$). Subsequent addition of NPY induced a decrease in I_{sc} of −3.8±0.5 μEq h^{-1} cm^{-2} ($n=7$; $P<0.05$), a response, which was about 4 times greater than the response to NPY under control conditions ($P<0.05$). Interestingly, the decrease in I_{sc} induced by NPY in the presence of these two secretagogues showed the same dependence on the height of the I_{sc} (○ and □ in Figure 2) as was observed for the control response to NPY (● in Figure 2) and all data could be fitted by a common regression line.

In contrast, when the cyclic AMP-pathway was stimulated by forskolin, the activator of the adenylate cyclase (Seamon & Daly, 1981), the response to NPY was unaffected. Forskolin (5×10^{-6} mol l^{-1}) induced an increase of I_{sc} of 3.2±1.0 μEq h^{-1} cm^{-2} (Figure 4c; $n=5$; $P<0.05$), and NPY administered during this plateau caused only a decrease in I_{sc} of −0.8±0.7 μEq h^{-1} cm^{-2} ($n=5$; not significantly different from the response to NPY under control conditions). Also pretreatment with the agonist of the Ca^{2+}-pathway, carbachol, did not enhance the response to NPY. Carbachol (5×10^{-5} mol l^{-1}; in the presence of TTX, 10^{-6} mol l^{-1}) caused an increase of I_{sc} to a stable plateau of 0.7±0.2 μEq h^{-1} cm^{-2} above baseline ($P<0.05$; $n=6$). Neuropeptide Y (10^{-7} mol l^{-1}), administered during this plateau (about 25–35 min after administration of carbachol), induced a decrease of I_{sc} of −0.7±0.2 μEq h^{-1} cm^{-2} ($n=6$), a response which was not significantly different from controls.

When the effect of NPY was tested in the proximal colon with the same protocol, i.e. administration of NPY (10^{-7} mol l^{-1}) during the plateau phase of the secretagogue-induced rise in I_{sc}, the peptide had no effect on the responses to veratridine, prostaglandin E_2 or carbachol ($n=5-6$ for each substance; data not shown).

Effect of NPY on K^+ transport

$^{86}Rb^+$ was used as a marker for K^+ (Foster *et al.*, 1984) in order to test, whether NPY (10^{-7} mol l^{-1}) had an effect on K^+ transport. The protocol (two consecutive periods of 3 x 5 min) was the same as that used for the determination of NPY effects on $^{36}Cl^-$ transport, i.e. transport rates under control conditions and in the presence of NPY were calculated by linear regression. Linear correlation coefficients (r) for all individual experiments were ≥ 0.93. The ms-transport rate of $^{86}Rb^+$ amounted to 7.8 ± 1.9 nmol min^{-1} cm^{-2} under control conditions (Figure 5). It increased to 9.5 ± 2.2 nmol min^{-1} cm^{-2} in the presence of NPY ($n = 10$; $P < 0.05$). In parallel, the sm-transport of $^{86}Rb^+$ decreased from 7.3 ± 0.9 nmol min^{-1} cm^{-2} to 5.8 ± 0.5 nmol min^{-1} cm^{-2} ($n = 9$); an effect which did not however reach statistical significance. The resultant was an increase in the calculated net transport rate for Rb^+ transport from 0.6 ± 0.2 nmol min^{-1} cm^{-2} to 3.8 ± 0.4 nmol min^{-1} cm^{-2} ($P < 0.05$; analysis of co-variances).

Comparison of the proabsorptive effect of NPY on K^+ transport with somatostatin and vasopressin

The effect of NPY on Rb^+ (K^+) was compared with two other proabsorptive hormones, somatostatin and vasopressin. Because both hormones exhibit a long-lasting decrease in I_{sc}, a 2 x 20 min-flux protocol was used. Somatostatin (10^{-7} mol l^{-1}) caused a long-lasting decrease in I_{sc} and Gt (Table 4). J^{Rb}_{sm} was significantly inhibited in the presence of the hormone, whereas J^{Rb}_{ms} was not altered significantly. In contrast, vasopressin (10^{-9} mol l^{-1}), which caused a decrease in I_{sc} of similar amplitude, had no significant action on J^{Rb}_{sm} or J^{Rb}_{ms} (Table 4).

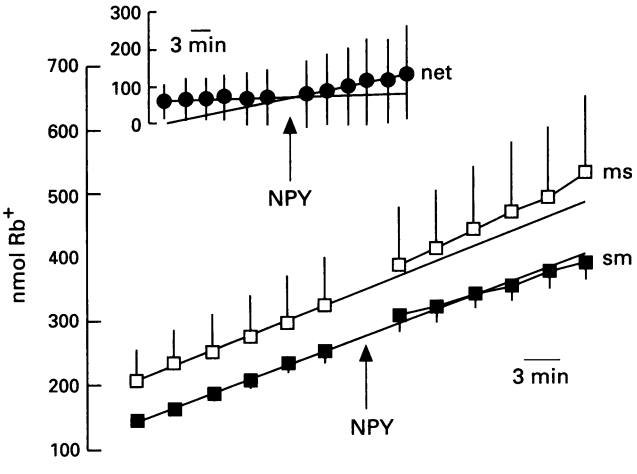

Figure 5 Effect of neuropeptide Y (NPY, 10^{-7} mol l^{-1}) upon $^{86}Rb^+$ unidirectional fluxes. Mucosa-to-serosa (ms; □), serosa-to-mucosa (sm; ■), and net (●) fluxes. The dashed lines represent the best fit line for Rb^+ transport under control conditions. Values are means ± 1 s.e.mean, $n = 9-10$.

Discussion

NPY exerts a segment-specific effect on I_{sc} in the rat colon, i.e. it inhibits basal and stimulated secretory I_{sc} in the distal colon, but is ineffective in the proximal colon. It is not clear, whether a reduced receptor number or a different receptor-effector coupling is responsible for the observed segment specificity of the NPY response. The effect of NPY in the distal colon declined with a half time of 13.5 min (Figure 1b) and the effectiveness of a second peptide addition (Figure 1b, c) suggests that peptide degradation rather than desensitization of the receptor may be responsible for the transient nature of this effect. The decrease in I_{sc} induced by NPY was dependent on the secretory state of the mucosa. The effect of NPY was higher, when basal I_{sc} was high (Figure 2) and the peptide-induced decrease in I_{sc} was about 55% of the spontaneous I_{sc}. When basal anion secretion was blocked by addition of Cl^- channel blockers such as NPPB or anthracene-9-carboxylic acid, the effect of NPY was inhibited (Table 1). Interestingly, in anion substitution studies the response to NPY could only be significantly reduced when both Cl^- and HCO_3^- anions were removed from the buffer. Responses were virtually abolished by the carbonic anhydrase blocker, methazolamide. This is probably due to the fact that the apical anion channels, which are thought to mediate cyclic AMP-sensitive Cl^- secretion e.g. outward-rectifying Cl^- channel (Reinhardt *et al.*, 1987) or cystic fibrosis transmembrane regulator Cl^- channel (Poulsen *et al.*, 1994), are also partially permeable to HCO_3^- anions. Consequently, only the simultaneous omission of both anions from the buffer reduced basal I_{sc} to low values and inhibited the action of NPY (Table 1). This decrease in I_{sc} was associated with an increase in the absorptive, i.e. J_{ms} fluxes of Na^+ and Cl^- (and K^+; see below). Whereas the effect of NPY on J^{Na}_{ms} could be demonstrated using a conventional 20 min flux period protocol, the effects of NPY on unidirectional Cl^- transport were transient and could only be shown using a short-period flux protocol; an observation made initially in the rat jejunum (Cox *et al.*, 1988). Here, J^{Cl}_{sm} was also decreased in the presence of NPY (Figure 3) and an increase in the net Cl^- transport rate from 53 ± 6 nmol min^{-1} cm^{-2} was observed (corresponding to an increase in net Cl^- transport of 6.8 ± 0.5 μ Eq h^{-1} cm^{-2}). This increase in calculated net Cl^- absorption is much larger than the observed decrease in I_{sc}, which was reduced by NPY from a mean of 1.7 ± 0.2 μEq h^{-1} cm^{-2} during the control period to 0.7 ± 0.2 μEq h^{-1} cm^{-2} and then increased slowly again (insert of Figure 3). A similar discrepancy between calculated J^{Cl}_{net} and I_{sc} has been observed in the rat jejunum (Cox *et al.*, 1988). Consequently, NPY must induce the movement of other ions which partially counteract the expected decrease in I_{sc}. In short, a significant component of NPY's effects upon Cl^- transport are a consequence of modulation of electroneutral transport.

Basal secretory I_{sc} is maintained in the rat distal colon by the spontaneous activity of submucosal neurones (Andres *et al.*, 1985) and by the spontaneous production of prostaglandins (see e.g. Diener *et al.*, 1988). Whereas indomethacin and tetrodotoxin, when given alone, did not affect the response to NPY, the combination of both abolished it (Table 1). When

Table 4 Effect of somatostatin and vasopressin on $^{86}Rb^+$ fluxes

	J^{Rb}_{ms}	J^{Rb}_{sm}	J^{RB}_{net}	I_{sc}	Gt
		(μEq h^{-1} cm^{-2})			(mS cm^{-2})
Control	0.91 ± 0.18	0.32 ± 0.05	0.59 ± 0.19	2.5 ± 0.3	8.5 ± 0.4
Somatostatin	0.84 ± 0.14	0.22 ± 0.04*	0.62 ± 0.15	0.7 ± 0.1*	7.5 ± 0.4*
Control	0.88 ± 0.18	0.38 ± 0.04	0.50 ± 0.18	2.8 ± 0.2	10.2 ± 0.5
Vasopressin	1.08 ± 0.23	0.32 ± 0.03	0.76 ± 0.23	1.5 ± 0.1*	9.4 ± 0.5*

The effect of somatostatin (10^{-7} mol l^{-1}) and vasopressin (10^{-9} mol l^{-1}) on mucosa-to-serosa (ms), serosa-to-mucosa (sm) and net fluxes during a 20 min-flux measurement. The I_{sc} and Gt values are means of the complete control or hormone period, respectively. Values are means ± 1 s.e.mean from 8–10 observations. *$P < 0.05$ versus the preceding period.

baseline I_{sc}, which had been decreased by prior addition of indomethacin and tetrodotoxin, was elevated again by prostaglandin E_2 (10^{-6} mol l^{-1}), NPY was fully effective despite the presence of indomethacin and tetrodotoxin. Because prostaglandins (Craven & DeRubertis, 1981) and many neurotransmitters of the enteric nervous system such as VIP (Prieto *et al.*, 1979) act by stimulating adenylate cyclase in the intestinal epithelium, these results suggest that the continuous release of prostaglandins and neurotransmitters leads to a stimulation of basal cyclic AMP production in the colonic mucosa and the inhibition of basal I_{sc} by NPY is caused by an attenuation of this stimulated cyclic AMP-pathway (see below). In contrast, inhibitors of the lipoxygenase pathway were without effect on NPY responses. This differs from the effect of another proabsorptive hormone, somatostatin (Diener & Gartmann, 1994) and suggests that a swelling-induced basolateral Cl^- channel, the activation of which can be prevented by nordihydroguaiaretic acid or SK&F 104353, is not involved in the NPY effect.

In addition to the inhibition of basal anion secretion, NPY also inhibited stimulated Cl^- secretion in the distal colon. This inhibition could only be shown, when NPY was applied after the secretagogues (Figure 4), but not, when the tissue was pretreated with NPY (Table 3). This apparent absence of NPY inhibition is most probably explained by the short-lasting effect of the peptide (due to the assumed rapid degradation). The effect of NPY on I_{sc} was enhanced, when the tissue was pretreated with postaglandin E_2, which stimulates adenylate cyclase by a receptor-mediated mechanism (Smith *et al.*, 1987). The same was observed with veratridine and the action of this toxin on I_{sc} in the rat distal colon is suppressed by tetrodotoxin but not significantly affected by atropine (unpublished observations) and is therefore not a muscarinic-mediated effect. In contrast, NPY had no effect on the stimulation of I_{sc} by forskolin, a direct activator of the adenylate cyclase (Figure 4). These results suggest that NPY exerts its action at a step proximal to the generation of cyclic AMP. An inhibition of the adenylate cyclase mediated by a G_i-protein has indeed been shown in several tissues e.g. rat kidney (Hackenthal *et al.*, 1987) or rat cardiac myocytes (Kassis *et al.*, 1987). A similar pattern, i.e. a pertussis toxin-sensitive inhibition of the response to receptor stimulation of the cyclic AMP-pathway via VIP, but insensitivity of the response to direct stimulation of the adenylate cyclase via forskolin has been observed for somatostatin in the rat colon (Knobloch *et al.*, 1989). It is therefore tempting to speculate that the action of NPY on rat colonic anion secretion is mediated by an inhibition of adenylate cyclase as has been demonstrated in the rabbit large intestine (Flint *et al.*, 1990). In rat cardiac myocytes isoprenaline stimulated adenylate cyclase responses were blocked by NPY but the response to forskolin was unaffected. In other tissues such as rat small intestine (Cox & Cuthbert, 1988), rabbit colon (Flint *et al.*, 1990) or porcine small intestine (Brown *et al.*, 1990) significant inhibition of the forskolin response by NPY has been observed. It is not clear, whether segment or species differences or other reasons are responsible for this discrepancy.

The effect of NPY after exogenously applied prostaglandin E_2 and following the release of endogenous neurotransmitters stimulated by veratridine, showed a dependence on the level of I_{sc} as seen with NPY effects on basal I_{sc} (Figure 2). This suggests (but does not prove) that both actions may be mediated by a common pathway, i.e. inhibition of the adenylate cyclase, e.g. mediated by a G_i-protein. In contrast, NPY had no effect upon secretion stimulated by carbachol, i.e. an agent acting via intracellular Ca^{2+}. Carbachol causes the opening of a (basolateral) K^+ conductance (Böhme *et al.*, 1991), which indirectly stimulates Cl^- secretion via apical Cl^- channels normally stimulated by cyclic AMP in this epithelium (Strabel & Diener, 1995). The absence of an effect of NPY on the carbachol response differs from that observed in the rat small intestine, where NPY also inhibits Ca^{2+}-mediated secretion (Cox & Cuthbert, 1988).

Unexpectedly, NPY also increased K^+ absorption measured using $^{86}Rb^+$ as marker for K^+. In the presence of NPY, the ms-transport rate for Rb^+ increased significantly, whereas a parallel decrease in the sm-transport did not reach statistical significance. An increase in Rb^+ absorption was also observed in the presence of another antisecretory peptide, somatostatin, although the effect of this hormone was exclusively due to an inhibition of J^{Rb}_{sm}. In contrast, vasopressin, an antisecretory peptide, which only inhibits Ca^{2+}- but not cyclic AMP-mediated secretion (Knobloch *et al.*, 1989), was without effect on unidirectional and net Rb^+ transport (Table 4). Up to now, only the opposite, i.e. a stimulation of K^+ secretion by cyclic AMP (Foster *et al.*, 1983) or agents, which increase intracellular cyclic AMP like β-receptor agonists (Smith & McCabe, 1986) or endothelin-1, which causes a release of prostaglandin E_2 (Roden *et al.*, 1992), have been shown. This suggests that transmitters of the enteric nervous system like NPY or somatostatin may be involved in the regulation of K^+ transport across the colonic wall, possibly mediated by a decrease in the intracellular cyclic AMP-concentration.

This study was supported by Schweizerischer Nationalfonds zur Förderung der wissenschaftlichen Forschung, grant 31-39310.93.

References

ANDRES, H., BOCK, R., BRIDGES, R.J., RUMMEL, W. & SCHREINER, J. (1985). Submucosal plexus and electrolyte transport across rat colonic mucosa. *J. Physiol.*, **364**, 301–312.

BÖHME, M., DIENER, M. & RUMMEL, W. (1991). Calcium- and cyclic-AMP-mediated secretory responses in isolated colonic crypts. *Pflügers Arch.*, **419**, 144–151.

BROWN, D.R., BOSTER, S.L., OVEREND, M.F., PARSONS, A.M. & TREDER, B.G. (1990). Actions of neuropeptide Y on basal, cyclic AMP-induced and neurally evoked ion transport in porcine distal jejunum. *Regul. Pept.*, **29**, 31–47.

BUKHAVE, K. & RASK-MADSEN, J. (1980). Saturation kinetics applied to in vitro effects of low prostaglandin E_2 and F_{2alpha} concentrations on ion transport across human jejunal mucosa. *Gastroenterology*, **78**, 32–42.

COX, H.M. & CUTHBERT, A.W. (1988). Neuropeptide Y antagonises secretagogue evoked chloride transport in rat jejunal epithelium. *Pflügers Arch.*, **413**, 38–42.

COX, H.M., CUTHBERT, A.W., HAKÅNSON, R. & WAHLESTEDT, C. (1988). The effect of neuropeptide Y and peptide YY on electrogenic transport in rat intestinal epithelia. *J. Physiol.*, **398**, 65–80.

COX, H., RUDOLPH, A. & GSCHMEISSNER, S. (1994). Ultrastructural co-localization of neuropeptide Y and vasoactive intestinal polypeptide in neurosecretory vesicles of submucous neurons in the rat jejunum. *Neurosci.*, **59**, 469–476.

CRAVEN, P.A. & DERUBERTIS, F.R. (1981). Stimulation of rat colonic mucosal prostaglandin synthesis by calcium and carbamylcholine: Relationship to alterations in cyclic nucleotide metabolism. *Prostaglandins*, **21**, 65–81.

DIENER, M., BRIDGES, R.J., KNOBLOCH, S.F. & RUMMEL, W. (1988). Neuronally mediated and direct effects of prostaglandins on ion transport in rat colon descendens. *Naunyn-Schmied. Arch. Pharmacol.*, **337**, 74–78.

DIENER, M. & GARTMANN, V. (1994). Effect of somatostatin on cell volume, Cl^- currents, and transepithelial Cl^- transport in rat distal colon. *Am. J. Physiol.*, **266**, G1043–G1053.

EKBLAD, E., WINTHER, C., EKMAN, R., HAKÅNSON, R. & SUNDLER, F. (1987). Projections of peptide-containing neurons in rat small intestine. *Neurosci.*, **20**, 169–188.

FLINT, J.S., BALLANTYNE, G.H., GOLDENRING, J.R., FIELDING, L.P. & MODLIN, I.M. (1990). Neuropeptide Y inhibition of vasoactive intestinal polypeptide-stimulated ion transport in the rabbit distal colon. *Arch. Surg.*, **125,** 1561–1563.

FOSTER, E.S., HAYSLETT, J.P. & BINDER, H.J. (1984). Mechanism of active potassium absorption and secretion in the rat colon. *Am. J. Physiol.*, **246,** G611–G617.

FOSTER, E.S., SANDLE, G.I., HAYSLETT, J.P. & BINDER, H.J. (1983). Cyclic adenosine monophosphate stimulates active potassium secretion in the rat colon. *Gastroenterology*, **84,** 324–330.

FURNESS, J.B., COSTA, M., EMSON, P.C., HAKÅNSON, R., MOGHIMZADEH, E., SUNDLER, F., TAYLOR, I.L. & CHANCE, R.E. (1983). Distribution, pathways and reactions to drug treatment of nerves with neuropeptide Y- and pancreatic polypeptide-like immunoreactivity in the guinea-pig digestive tract. *Cell Tissue Res.*, **234,** 71–92.

HACKENTHAL, E., AKTORIES, K., JAKOBS, K.H. & LANG, R.E. (1987). Neuropeptide Y inhibits renin release by a pertussis toxin-sensitive mechanism. *Am. J. Physiol.*, **252,** F543–F550.

HUBEL, K.A. & RENQUIST, K.S. (1986). Effect of neuropeptide Y on ion transport by the rabbit ileum. *J. Pharmacol. Exp. Ther.*, **238,** 167–169.

KASSIS, S., OLASMAA, M., TERENIUS, L. & FISHMAN, P.H. (1987). Neuropeptide Y inhibits cardiac adenylate cyclase through a pertussis toxin-sensitive G protein. *J. Biol. Chem.*, **262,** 3429–3431.

KENAKIN, T.P. (1987). *Pharmacologic Analysis of Drug-Receptor Interaction.* pp. 129–162. New York: Raven Press.

KENYON, J.L. & GIBBONS, W.R. (1977). Effect of low-chloride solutions on action potentials of sheep cardiac purkinje fibers. *J. Gen. Physiol.*, **70,** 635–660.

KNOBLOCH, S.F., DIENER, M. & RUMMEL, W. (1989). Antisecretory effects of somatostatin and vasopressin in the rat colon descendens in vitro. *Regul. Pep*, **25,** 75–85.

NOBLES, M., DIENER, M., MESTRES, P. & RUMMEL, W. (1991). Segmental heterogeneity of the rat colon in the response to activators of secretion on the cAMP-, the cGMP- and the Ca^{2+}-pathway. *Acta Physiol. Scand.*, **142,** 375–386.

POULSEN, J.H., FISCHER, H., ILLEK, B. & MACHEN, T.E. (1994). Bicarbonate conductance and pH regulatory capability of cystic fibrosis transmembrane conductance regulator. *Proc. Natl. Acad. Sci. U.S.A.*, **91,** 5340–5344.

PRIETO, J.C., LABURTHE, M. & ROSSELIN, G. (1979). Interaction of vasoactive intestinal peptide with isolated intestinal epithelial cells from rat. *Eur. J. Biochem.*, **96,** 229–237.

REINHARDT, R., BRIDGES, R.J., RUMMEL, W. & LINDEMANN, B. (1987). Properties of an anion-selective channel from rat colonic enterocyte plasma membranes reconstituted into planar phospholipid bilayers. *J. Membrane Biol.*, **95,** 47–54.

RODEN, M., PLASS, H., VIERHAPPER, H. & TURNHEIM, K. (1992). Endothelin-1 stimulates chloride and potassium secretion in rabbit descending colon. *Pflügers Arch.*, **421,** 163–167.

SARIA, A. & BEUBLER, E. (1985). Neuropeptide Y (NPY) and peptide YY (PYY) inhibit prostaglandin E_2-induced intestinal fluid and electrolyte secretion in the rat jejunum in vivo. *Eur. J. Pharmacol.*, **119,** 47–52.

SEAMON, K.B. & DALY, J.W. (1981). Forskolin: A unique diterpene activator of cyclic AMP-generating systems. *J. Cycl. Nucl. Res.*, **7,** 201–224.

SMITH, G., WARHURST, G., LEES, M. & TURNBERG, L. (1987). Evidence that PGE_2 stimulates intestinal epithelial adenylate cyclase by a receptor-mediated mechanism. *Dig. Dis. Sci.*, **32,** 71–75.

SMITH, P.L. & MCCABE, R.D. (1986). Potassium stimulation by rabbit descending colon: effects of adrenergic stimuli. *Am. J. Physiol.*, **250,** G432–G439.

STRABEL, D. & DIENER, M. (1995). Evidence against direct activation of chloride secretion by carbachol in the rat distal colon. *Eur. J. Pharmacol.*, **274,** 181–191.

TATEMOTO, K., CARLQUIST, M. & MUTT, V. (1982). Neuropeptide Y - a novel brain peptide with structural similarities to peptide YY and pancreatic peptide. *Nature*, **296,** 659–660.

WAHLESTEDT, C., GRUNDEMAR, L., HAKÅNSON, R., HEILIG, M., SHEN, G.H., ZUKOWSKA-GROJEC, Z. & REIS, D.J. (1990). Neuropeptide Y receptor subtypes, Y1 and Y2. *Ann. New York Acad. Sci.*, **611,** 7–26.

(Received November 28, 1994
Revised March 15, 1995
Accepted March 23, 1995)

British Journal of Pharmacology (1995) 115, 1080–1086 © 1995 Stockton Press All rights reserved 0007–1188/95 $12.00

Inhibition by cromoglycate and some flavonoids of nucleoside diphosphate kinase and of exocytosis from permeabilized mast cells

Matthew W. Martin, Antony J. O'Sullivan & Bastien D. Gomperts

Department of Physiology, University College London, University Street, London WC1E 6JJ

1 The anti-allergic compound, cromoglycate, is reported to possess affinity for, and to suppress the autophosphorylation of a 72kDa protein having the sequence of nucleoside diphosphate kinase (NDPK).

2 We have tested the ability of cromoglycate, and a panel of ten structurally related flavonoids of plant origin, to inhibit the NDPK reaction and the exocytotic process of permeabilized mast cells. The conditions of permeabilization (use of an isotonic medium based on sodium glutamate) were selected to ensure that NDPK activity would be an essential component in the induction of Ca^{2+}-induced exocytosis in which ATP is required for generation of GTP. For comparison, we also measured the inhibition of exocytosis induced by GTP-γ-S; this proceeds in the absence of ATP and bypasses the need for NDPK activity.

3 We found that cromoglycate does not discriminate between Ca^{2+} and GTP-γ-S-induced exocytosis and is a poor inhibitor of NDPK activity. Concentrations in the millimolar range are required for inhibition of all these functions. By comparison, many of the flavonoids are effective at concentrations in the micromolar range.

4 While we were unable to discern any systematic relationships between their ability to inhibit the three functions, two compounds, quercetin and genistein, inhibit Ca^{2+}-induced, but not GTP-γ-S-induced exocytosis. Inhibition of the late stages of the stimulus-response pathway in mast cells by these compounds is therefore likely to be due to inhibition of NDPK and the consequent failure to generate GTP.

Keywords: Mast cells; exocytosis; cromoglycate; quercetin; flavonoids; calcium; nucleoside diphosphate kinase (NDPK)

Introduction

Understanding of the mechanism and control of exocytosis, the terminal event in the stimulus-secretion pathway, has been advanced by the use of permeabilized cells (Lindau & Gomperts, 1991). By use of such preparations it is possible to control the composition of the intracellular milieu with some degree of precision, and to introduce and test the effects of normally impermeant solutes which might regulate, modulate or inhibit the exocytotic process. The present investigation concerns the mechanism of inhibition by cromoglycate and some structurally related plant flavonoids, of the exocytotic reaction of permeabilized mast cells.

Mast cells permeabilized in buffers formulated with glutamate as the major anion undergo exocytosis in response to non-hydrolysable analogues of GTP (GTP-γ-S, GppNHp etc) (Churcher & Gomperts, 1990) under conditions of very low Ca^{2+} (i.e. less than 10^{-9} M). Alternatively, exocytosis can be induced by Ca^{2+} (buffered at concentrations in the range 10^{-6}–10^{-5} M) in the absence of added guanine nucleotide. Unlike the GTP-γ-S-induced response, Ca^{2+} induced exocytosis requires provision of another nucleoside triphosphate such as ATP, UTP etc. (Lillie *et al.*, 1991). Since exocytosis due to Ca^{2+}-*plus*-ATP can be potentiated by addition of GDP at concentrations up to 100 μM (Lillie & Gomperts, 1992a), the role of the nucleoside triphosphate is likely to be that of a phosphate donor in the nucleoside diphosphate kinase (NDPK) reaction. This would allow the formation of GTP from GDP. At concentrations greater than 100 μM, GDP is inhibitory to Ca^{2+}-induced exocytosis. A guanine nucleotide thus appears to be an absolute requirement for exocytosis. Ca^{2+} must be regarded as a modulator, possibly regulating guanine nucleotide exchange on G_E, the GTP-binding protein proposed to mediate exocytosis in these cells (Lillie *et al.*, 1991).

In hepatocyte membranes, NDPK activity has been co-isolated with a GTP-binding protein, G_S, (Kimura & Shimada, 1990) and it has been suggested that it may play a role in the activation of G-proteins through its ability to generate GTP by transphosphorylation (Kimura & Johnson, 1983). We have therefore tested the ability of cromoglycate and some structurally related flavonoids as inhibitors of the NDPK reaction and also as inhibitors of exocytosis from permeabilized mast cells.

Methods

Cell preparation

Mast cells were obtained by peritoneal lavage of large (>300 g) male Sprague Dawley rats. The mast cells were isolated from contaminating cell types by centrifugation through a cushion of Percoll (Pharmacia Ltd, Milton Keynes, Bucks, UK) as previously described (Tatham & Gomperts, 1990). They were washed twice by resuspension and centrifugation.

Secretion assay

The method was as previously described (Tatham & Gomperts, 1990; Gomperts & Tatham, 1992). Cells were suspended at approximately 0.3×10^6 cells ml^{-1} in a buffered electrolyte solution which comprised L-glutamate 125 mM, PIPES 20 mM, Mg PIPES 3 mM, BSA 1 mg ml^{-1}, pH 6.8, 290 mOsm. All salts and reagents were dissolved in this buffer. Cells, streptolysin-O (permeabilising agent, 0.4 iu ml^{-1}) and other re-

[1] Author for correspondence.

agents, contained in the wells of 96-well microtitreplates were incubated for 10 min at 37°C. Incubations were carried out in 96 'V-well' microtitre plates (Greiner). After incubating the cells for 5 min at 37°C in the presence of metabolic inhibitors (antimycin A, 5 μM and 2-deoxyglucose, 6 mM, to deplete intracellular ATP) samples (about 9000 cells, in 30 μl) were added to wells previously loaded with streptolysin-O, (permeabilising agent, 0.4 iu ml^{-1} final), and either calcium buffers (EGTA, 3 mM final, to regulate Ca^{2+} in the range pCa7-pCa5) with MgATP (1 mM) or GTP-γ-S (at concentrations indicated) with Ca^{2+} buffer (EGTA 3 mM, pCa8). Final volume was 90 μl in each well. Ca^{2+} buffers were prepared as previously described (Gomperts & Tatham, 1992). After incubation at 37°C for 10 min, the reactions were quenched by addition of 100 μl of ice cold buffer and the cells were sedimented by centrifugation (5 min, 400*g*, at 4°C). Samples (50 μl) of supernatant were transferred to the equivalent wells in black plastic, opaque microtitre plates (Dynatech Microfluor) for analysis of secreted β-D-N-acetylglucosaminidase (hexosaminidase). The reactions were initiated by addition of 50 μl of a solution of 4-methylumbelliferyl N-acetyl-β-D glucosaminide (1 mM in Na citrate, 200 mM, pH 4.5, containing Triton X-100, 0.01%). After incubation at 37°C for about 4 h, the reactions were terminated by addition of 300 μl of Tris (0.2 M). Fluorescence (355–460 nm) was measured on a Fluoroskan microtitre plate reader and the readings transferred directly to a computer for manipulation using a standard spreadsheet programme. Calculation of % secretion was based on the comparison of fluorescence measured with control (no cells) and the total cell hexosaminidase content as released by Triton X-100. All secretion reactions were carried out in duplicate, and all experiments were carried out on at least 3 separate occasions.

NDPK assay

The method is based on the measurement of the rate of ADP generation following transphosphorylation from ATP to 2'-dUDP as described in Biochemica Information (Boehringer Mannheim, 1973). The rate of release of ADP is measured as the reduction in the absorbance (340 nm) due to oxidation of NADH as a consequence of reactions catalysed by pyruvate kinase and lactate dehydrogenase in the presence of appropriate substrates and cofactors. All reagents were made up in a solution comprising HEPES (160 mM), MgCl (10 mM) and KCl (10 mM), pH 7.6; 300 μl of a solution containing pyruvate kinase (1.26 iu ml^{-1} final), lactate dehydrogenase (33 iu ml^{-1} final), ATP (6.3 mM final), phosphoenolpyruvate (6.3 mM final), and NADH (1.92 mM final) were placed in wells of a flat-bottomed 96-well microtitre plate. Absorbance measurements were made at 340 nm with a Titertek Multiskan MCC/340 microtitreplate reader. Before starting the reactions, 30 μl 2'-dUDP (final concentration 0.86 mM) was added and a series of absorbance readings were taken (under manual control) to ensure the stability of the system. A range of concentrations of the test compound (10 μl) or buffer (for control) were than added and control of the instrument was transferred to the use of programme MSCAN operated by a PC. This is designed to collect readings from the microtitre plate on a time base and to transfer these as a set of 8 × 12 matrices to a computer file for subsequent analysis on a spreadsheet. Four passes were made to obtain a baseline and then the reactions were initiated by addition with mixing of 10 μl of a suspension of permeabilized mast cells prepared as described in the next paragraph. Alternatively, purified rabbit skeletal muscle NDPK (11.4 iu ml^{-1} final) was used. Measurements were made at room temperature at 15 s intervals.

To prepare mast cells for NDPK measurement, they were first treated with streptolysin-O at ice temperature. This allows the lysin to bind, but not to permeabilize the membrane, and the excess was washed away by centrifugation at 4°C. The cells become permeant as the temperature is elevated to room temperature (i.e. the condition of the enzyme assay). These cells were then used either directly in the NDPK assay to measure total cell activity, or alternatively, they were washed by centrifugation (× 2) at room temperature to remove the cytosolic component.

Presentation of data

Data illustrated in Figures 1, 2 and 3 are taken from single experiments. These are typical of many.

Materials

Nucleoside diphosphate kinase, pyruvate kinase, lactate dehydrogenase, guanosine 5'-[γ-thio]triphosphate (GTP-γ-S), phosphoenol pyruvate and ATP were all obtained from Boehringer Mannheim; 2'-deoxyuridine-5'-diphosphate (dUDP), 4-methylumbelliferyl N-acetyl-β-D-glucosaminide and NADH were obtained from Sigma; 2'-deoxythymidine 5'-diphosphate (dTDP), narigenin, phloretin and phloridzin were obtained from ICN. Samples of purified rutin (quercetin ruti-

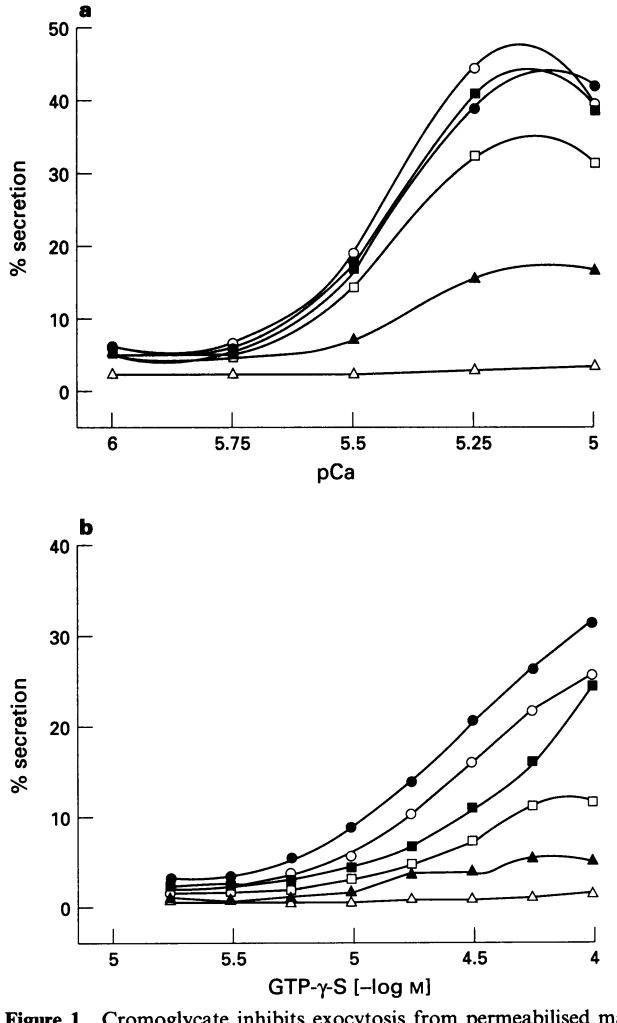

Figure 1 Cromoglycate inhibits exocytosis from permeabilised mast cells: mast cells, suspended in isotonic buffered Na glutamate and pretreated with metabolic inhibitors, were incubated with streptolysin-O, cromoglycate (at the concentrations indicated) and (a) with Ca^{2+} (buffered with EGTA (3mM) in the range pCa6–pCa5) and ATP (1 mM), or (b) with GTP-γ-S (at concentrations indicated) with Ca^{2+} buffered at pCa8. At the end of 10 min the cells were sedimented by centrifugation and the supernatant sampled for analysis of secreted hexosaminidase. Cromoglycate concentrations [$-\log_{10}$M]: (a) (●) zero; (○), 4; (■) 3.5; (□) 3; (▲) 2.5; (△) 2; (b) (●) zero; (○) 3.25; (■) 3; (□) 2.75; (▲) 2.5; (△) 2.25.

noside) and acacetin (4'-O-methyl apigenin) were kindly provided by Dr E. Wollenweber (Darmstadt, Germany). Fisetin was obtained from Aldrich. Other flavonoids were purchased from Sigma. Cromoglycate was the gift of Fisons Pharmaceuticals.

Results

Secretion measurements

Secretion was measured from mast cells permeabilized in solutions of isotonic Na glutamate. Under these conditions, exocytosis can be induced either by GTP-γ-S or by Ca^{2+}. For Ca^{2+}-induced secretion it is necessary to provide ATP which is understood to act as a donor in the NDPK reaction for the formation of GTP from GDP (Lillie & Gomperts, 1992a).

Figure 1a illustrates the results of a typical experiment in which we tested the ability of cromoglycate, applied as a range of concentrations ($10^{-4}-10^{-2}$ M) to inhibit exocytosis from permeabilized mast cells stimulated by Ca^{2+}, together with ATP. In agreement with previous work, secretion required Ca^{2+} in the range pCa6–pCa5 and achieved a maximal level of around 50% ($pCa = -\log_{10}[Ca^{2+}]$). Cromoglycate inhibited exocytosis due to the Ca^{2+}-stimulus. Suppression of exocytosis commenced at concentrations greater than $10^{-3.5}$ M and it was capable of causing total suppression at 10^{-2} M with an IC_{50} of 3.18 mM.

Cromoglycate also inhibited exocytosis stimulated by GTP-γ-S as shown in Figure 1b. In this experiment, the concentration of Ca^{2+} was suppressed to 10^{-8} M (pCa8) with EGTA (3 mM). With an IC_{50} of 3.63 mM (see Table 1), the sensitivies of Ca^{2+}-induced and GTP-γ-S-induced secretion to inhibition by cromoglycate were not significantly different ($P>0.75$).

Figure 2 illustrates the effect of the bioflavonoid quercetin on both Ca^{2+}-induced and GTP-γ-S-induced exocytosis from the permeabilized cells. As can be seen in Figure 2a, this compound inhibited secretion due to the Ca^{2+}-stimulus when applied at concentrations in excess of $10^{-5.33}$ M (~ 5 μM) with IC_{50} 54 μM. Quercetin was thus about 100 times more potent than cromoglycate. In contrast, it was without effect on GTP-γ-S-induced secretion when applied at concentrations up to 10^{-4} M (Figure 2b and Table 1).

We tested a panel of 12 structurally related plant flavonoids as possible inhibitors of Ca^{2+}-induced and GTP-γ-S-induced exocytosis. The results are summarised in Table 1 in which the compounds are listed in order of potency as inhibitors for the two systems.

For Ca^{2+}-induced secretion (measured at pCa5), potency appeared to fall into two groups. The first five compounds listed (kaempferol, fisetin, myricetin, phloretin and acacetin) all had IC_{50} below 20 μM. Quercetin, rutin (a glycoside of quercetin), narigenin, genistein and phloridzin (a glycoside of phloretin) had IC_{50}s in the range 50–100 μM. Apigenin and hesperetin are without effect at concentrations less than 100 μM (we were unable to test these two compounds at concentrations higher than this since we found that they interfered with the assay for secreted hexosaminidase). The order of inhibitory potency of Ca^{2+}-independent exocytosis induced by GTP-γ-S (100 μM) by these compounds was different. Here, phloretin, narigenin and acacetin had an IC_{50} below 20 μM with most of the compounds having IC_{50} in the range 20 μM to 60 μM. Apigenin, genistein, hesperetin, and as noted above, quercetin, were without effect on secretion induced by GTP-γ-S.

NDPK activity measurements

We measured the effect of quercetin and the panel of bioflavonoids on the activity of rabbit muscle, and mast cell NDPK. In a preliminary investigation we found that two of the compounds, genistein and myricetin were inhibitory to LDH and we were unable to test these substances as inhibitors of NDPK. An earlier report (Grisolia *et al.*, 1975) indicates inhibition of LDH and pyruvate kinase by quercetin but we were unable to substantiate this, at least in the concentration range relevant to the present work.

Figure 3 illustrates progress curves for ADP generation, catalysed by the NDPK reaction, from permeabilized mast cells. Enzyme activity was associated with both the cytosol and with insoluble structural elements of the cells. The figure illustrates the reaction for the total enzyme content and the residual component remaining after extensive washing of the permeabilised cells; this is likely to represent membrane bound activity (Kimura & Shimada, 1990). The total cell activity of NDPK varied considerably from experiment to experiment, and we have no explanation for this. Nevertheless, our data indicate that a large proportion of the NDPK was retained after washing, and must be presumed to be associated with the cell membranes.

Figure 4 illustrates the inhibition of rabbit muscle NDPK activity by quercetin. The data presented represent the average of six independent experiments in which the initial linear rate of the uninhibited reaction varied between 0.014 and 0.74 absorption units min^{-1}. In two experiments, substitution of 2'-deoxythymidine-diphosphate (2'-dTDP instead of 2'-dUDP) as the substrate for NDPK was without effect on the inhibition due to quercetin (data not shown).

Table 1 Inhibition of exocytosis from permeabilized mast cells by various flavonoids

A *Inhibition of Ca^{2+}-plus-ATP-induced exocytosis*	*Mean IC_{50} (μM)*	*s.e.mean*	n	B *Inhibition of GTP-γ-S-induced exocytosis*	*Mean IC_{50} (μM)*	*s.e.mean*	n
Kaempferol	6.7	1.8	4	Phloretin	6.6	2.2	3
Fisetin	7.4	3.6	4	Acacetin	14.6	1.1	4
Myricetin	8.4	2.2	4	Narigenin	12.5	6.6	4
Phloretin	12.6	7	3	Kaempferol	25.4	8.8	3
Acacetin	15.6	2.8	4	Myricetin	34.2	3.2	4
Quercetin	54.2	11.2	5	Fisetin	43.7	0.5	4
Rutin	65	27	3	Rutin	50.3	13	3
Narigenin	96	14	3	Phlorizin	61.4	25.6	3
Genistein	96	2.9	3	Cromoglycate	3630	1700	4
Phlorizin	103	54.8	3	Apigenin*	No effect		4
Cromoglycate	3180	240	4	Quercetin*	No effect		4
Apigenin	No effect*		4	Genistein*	No effect		3

Statistical analysis using the ANOVA test indicates that the rank orders are significant with $P<0.002$ and $P<0.02$ for Table 1A and 1B respectively.

*These compounds were tested up to a maximum concentration of 100 μM (apigenin and geniestein) and 1 mM (quercetin).

Table 2 lists the panel of flavonoids in the rank orders of their potency as inhibitors of the membrane bound, and the total NDPK activity of rat mast cells. The rank orders of inhibition of the two classes of activity are quite different and neither showed any obvious relationship to the rank orders for inhibition of either Ca^{2+} (plus ATP)-induced exocytosis or GTP-γ-S-induced exocytosis. It is worth noting that genistein, frequently applied to cells as a presumed specific inhibitor of tyrosine kinases (Mustelin *et al.*, 1990), was also an inhibitor of PK and LDH. Cromoglycate was without effect (at concentrations less than 200 μM); because of its absorbance (at 340 nm) at concentrations higher than this could not be tested.

Table 3 lists the flavonoids in their rank order of potency as inhibitors of purified rabbit muscle NDPK. Fisetin, with IC_{50} of 9.3 μM, was the most potent of the compounds tested while cromoglycate at concentrations up to 200 μM was without effect.

Discussion

The main application of cromoglycate is in the prophylactic treatment of bronchial asthma (Foreman & Pearce, 1989). Its mechanism remains poorly defined to the extent that is unknown whether its action on cells is exerted at the cell surface or at an intracellular location. A report showing that it binds and prevents the autophosphorylation of NDPK extracted from RBL-2H3 (rat basophilic leukaemia) cells (Hemmerich *et al.*, 1991; 1992) could be taken to imply an intracellular location for its activity, but its strong acid characteristic ($pK_a = \sim 2$: Cox *et al.*, 1970; Fogg & Fayad, 1978) would argue for impermeability and an action at the cell surface.

The plant flavonoids are compounds having some structural similarity to cromoglycate, most significantly the chroman moeity – two aromatic rings joined by a three carbon unit (C_6-C_3-C_6) (Goodwin & Mercer, 1983). A number of these have been shown to inhibit secretion from mast cells and neu-

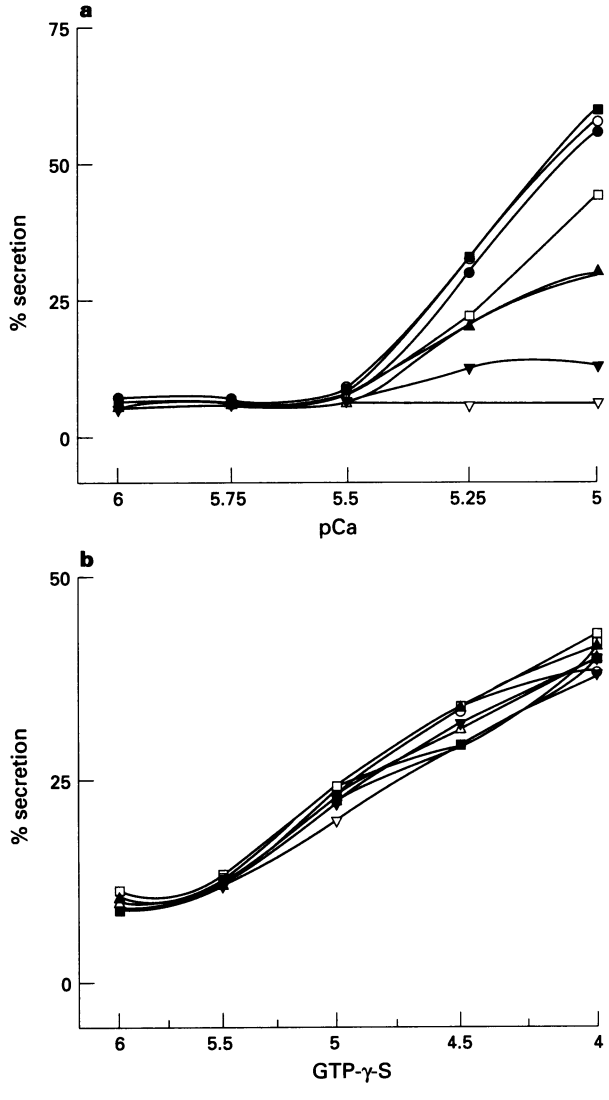

Figure 2 Quercetin inhibits exocytosis from permeabilized mast cells: mast cells, suspended in isotonic buffered Na glutamate and pretreated with metabolic inhibitors, were incubated with streptolysin-O, quercetin (at the concentrations indicated) and (a) with Ca^{2+} (buffered with EGTA (3 mM) in the range pCa6–pCa5) and ATP (1 mM), or (b) with GTP-γ-S (at concentrations indicated) with Ca^{2+} buffered at pCa8. At the end of 10 min the cells were sedimented by centrifugation and the supernatant sampled for analysis of secreted hexosaminidase. Quercetin concentrations [$-\log_{10}$M]: (●) zero; (○) 6; (■) 5.67; (□) 5.33; (▲) 4.67; (▼) 4.33; (▽) 4.

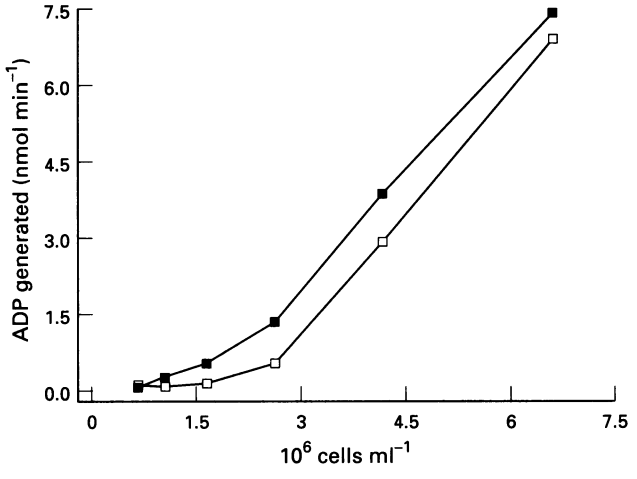

Figure 3 Nucleoside diphosphate kinase activity of unwashed and washed permeabilized mast cells: the rate of ADP generation due to the NDPK reaction of permeabilized mast cells was measured over a range of cell concentrations at room temperature using an enzyme coupled assay. The figure represents the data from a single experiment: (■) whole permeabilized cells; (□) washed permeabilized cells.

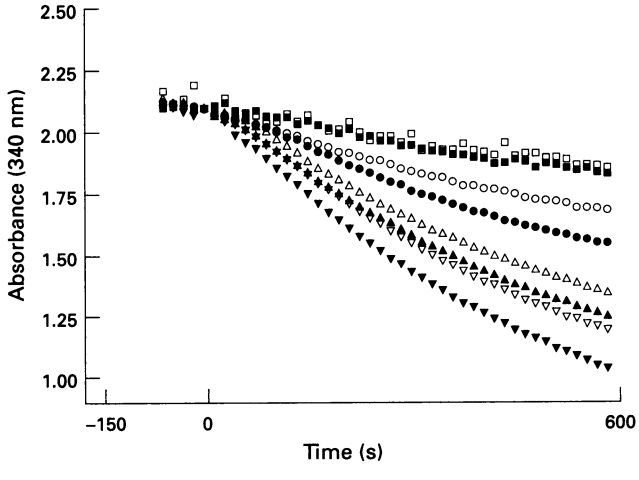

Figure 4 Quercetin inhibits nucleoside diphosphate kinase: the rate of ADP generation as a consequence of rabbit muscle NDPK activity was measured *in vitro* at room temperature using an enzyme coupled assay. The figure represents the normalized data from 6 separate experiments. Quercetin concentrations [$-\log_{10}$M]: (□) zero; (■) 6; (○) 5.67; (●) 5.33; (△) 5; (▲) 4.67; (▽) 4.33; (▼) 4.

Table 2 Inhibition of mast cell nucleoside diphosphate kinase (NDPK) by various flavonoids

	A *Total cell NDPK* Mean IC_{50} (μM)	s.e.mean	n		B *Membrane-bound NDPK* Mean IC_{50} (μM)	s.e.mean	n
Narigenin	3.89	1.87	3	Fisetin	2.83	1.74	3
Rutin	6.89	0.91	3	Quercetin	4.32	1.0	3
Phloretin	9.59	4.41	3	Rutin	6.21	2.89	3
Phlorizin	10.68	3.89	3	Narigenin	13.6	4.82	5
Fisetin	18.05	5.58	3	Morin	13.65	8.46	3
Acacetin	25.61	1.7	3	Phlorizin	16.85	7.99	3
Morin	29.62	0.85	3	Kaempferol	198.7	1.33	3
Quercetin	42.92	10.94	3	Phloretin	>200		4
Kaempferol	No effect*		4	Acacetin	>200		3
Cromoglycate	No effect*		2	Cromoglycate	No effect*		2
Hesperetin	No effect*		3	Hesperetin	No effect*		3

Statistical analysis using the ANOVA test indicates that the rank orders are significant with $P<0.005$.
*These compounds were tested up to a maximum concentration of 200 μM.

Table 3 Inhibition of purified rabbit muscle nucleoside diphosphate kinase (NDPK) by various flavonoids

	IC_{50} (μM)	s.e.mean	n
Fisetin	9.3	2.3	6
Narigenin	9.5	3.9	4
Kaempferol	10.6	2.4	4
Rutin	12.9	3.6	3
Phlorizin	13.2	2.9	5
Phloretin	14.7	2.9	6
Acacetin	20.6	4.3	6
Quercetin	28.6	5.7	6
Cromoglycate	No effect*		4

A statistical analysis using the ANOVA test indicates that the rank order is significant, with $P<0.005$.
*Cromoglycate was tested up to a maximum concentration of 200 μM.

trophils (Fewtrell & Gomperts, 1977a; Bennett *et al.*, 1981) but unlike cromoglycate which had previously been shown to affect ligand-induced secretion (Foreman *et al.*, 1975), these also block secretion due to Ca^{2+}-ionophores (Ennis *et al.*, 1981). Significantly, only the aglycone forms of quercetin and phloretin are inhibitory on intact cells but their glycosides are about equally effective when applied to permeabilized cells (Howell & Gomperts, 1987) suggesting that the flavonoids have an intracellular target for their inhibitory activity. That the actions of cromoglycate and quercetin may be related to a shared target was first suggested by the observation that quercetin is without effect on cells rendered tachyphylactic to cromoglycate (Fewtrell & Gomperts, 1977b). However, while quercetin (and the other flavonoids) clearly affect the exocytotic reaction (this paper and Howell & Gomperts, 1987), cromoglycate suppresses the extent of elevation of Ca^{2+} in antigen-stimulated mast cells, suggesting an additional target upstream of the late stages of signal transduction (White *et al.*, 1984).

In the regulation of secretion from mast cells it has been proposed that Ca^{2+} (with C_E, a Ca^{2+}-binding protein of unknown provenance) and the activating guanine nucleotide (with its associated GTP-binding protein, G_E) act in series. C_E is presumed to act as an exchange catalyst for guanine nucleotides on G_E (Lillie & Gomperts, 1992a,b; 1993). More generally, it has been suggested that the product GTP of the NDPK reaction can be channelled in a manner rendering its interaction with membrane bound G-proteins particularly favourable (Kimura & Shimada, 1988; Wieland & Jakobs, 1992). However, an earlier idea (Otero, 1990; Randazzo *et al.*, 1991) that the NDPK reaction could cause direct phosphorylation of GDP bound to G-proteins, and so set the GTPase cycle in reverse, has been dismissed (Randazzo *et al.*, 1992).

We have examined the effects of cromoglycate and a number of flavonoids in mast cells permeabilized in glutamate-based solutions and stimulated with either GTP-γ-S or Ca^{2+}. Two compounds, quercetin and genistein, are of special interest since they select between the two modes of activation. They inhibit exocytosis due to stimulation by Ca^{2+} (plus ATP) but are without effect on the response due to GTP-γ-S, and therefore probably act only to prevent a reaction linking these two stages of the secretory control pathway. The finding that secretion due to Ca^{2+}-*plus*-ATP is enhanced by GDP (Lillie & Gomperts, 1992a) (also in PC12 cells: Vu & Wagner, 1993) prompted examination of the ability of these compounds (especially quercetin and genistein) to inhibit NDPK.

We have tried to establish whether a correlation exists between the inhibitory activity of these compounds on NDPK and their ability to suppress the stimulation of exocytosis by GTP-γ-S or by Ca^{2+}-*plus*-ATP. Analysis of variance by the ANOVA test indicates that the rank orders presented in the tables (Tables 1,2,3) are significant, with $P<0.02$. Inspection of the various rank orders reveals no simple relationships between the inhibitory functions of these compounds. We have also attempted a more rigorous analysis of the rank orders using the Student Newman-Keuls test (Ostle, 1963) to compare the IC_{50} values of 9 of the flavonoids with each other. The data suggest that there is little, if any relationship between the various inhibitory functions of these compounds.

No attempt has been made here to determine the mechanism of inhibition by any of these compounds for any of the functions investigated, but it is likely that they interfere with the binding of nucleotides. Some of them are known to act as inhibitors of protein kinase C and would therefore be expected to cause inhibition of the ATP-dependent component of secretion (Churcher & Gomperts, 1990) regardless of any effects that they have on NDPK. However, not all of these known inhibitors of PKC inhibit Ca^{2+}-*plus*-ATP induced secretion. More than this, flavonoids are known inhibitors of transport ATPases including Na^+/K^+-ATPases (Kuriki & Racker, 1976; Spector *et al.*, 1980), Ca^{2+}-dependent ATPases (Fewtrell & Gomperts, 1977b; Bennett *et al.*, 1981), and the mitochondrial F_1 ATPase (Carpenedo *et al.*, 1969; Lang & Racker, 1974).

Our observations indicate that cromoglycate inhibits mast cell secretion when provided at concentrations in the millimolar range (see Table 1). Unfortunately, because of its intrinsic absorption at 340 nm we were unable to test its effect on the NDPK reaction at concentrations above 200 μM; at this concentration it was without effect. The IC_{50} for inhibition of autophosphorylation of p72 (NDPK: Hemmerich *et al.*, 1992) isolated from RBL cells is 2 mM (Hemmerich *et al.*, 1991).

In conclusion, since cromoglycate inhibits GTP-γ-S-induced secretion, which occurs in the absence of ATP and therefore with no involvement of NDPK, cromoglycate must act by a mechanism not involving this enzyme. Further, it is improbable

that cromoglycate has an intracellular site of action. In contrast, the flavonoids must penetrate the cells to exert inhibition (Howell & Gomperts, 1987). These compounds are likely to have multiple actions at different points of the stimulus-secretion pathway amongst which are steps close to the exocytotic event itself. At this level the inhibitory effect of cromoglycate must be rated as poor, requiring concentrations in the millimolar range which could never be achieved in intact cells.

Of the flavonoids, quercetin and genistein probably block the terminal stages of secretion by inhibition of NDPK. They inhibit secretion due to Ca^{2+}-*plus*-ATP but not by GTP-γ-S. However, when applied alongside the stimulus to intact cells the onset of the action of quercetin is immediate (Fewtrell & Gomperts, 1977b) and it is improbable that inhibition, e.g. of antigen-induced secretion, could be due to depletion of GTP unless its turnover rate is so rapid that the entire pool is renewed every few seconds. It is more likely that these compounds too, must have other sites of action along the stimulus-secretion pathway. The action of the flavonoid compounds is thus complex, involving a number of intracellular target sites one of which is nucleoside diphosphate kinase.

MM is an MRC research student and A.O'S is supported by the Wellcome Trust. The work was supported by grants from the Wellcome Trust and with additional help from the Vandervell Foundation and the Gower Street Secretory Mechanisms Group. We would like to thank Dr E. Wollenweber for the gift of purified flavonoids and Mr William Forde for writing the programme MSCAN.

References

BENNETT, J.P., GOMPERTS, B.D. & WOLLENWEBER, E. (1981). Inhibitory effects of natural flavonoids on secretion from mast cells and neutrophils. *Arzneimittel-forschung*, **31,** 433–437.

CARPENEDO, F., BORTIGNON, C., BRUNI, A. & SANTI, R. (1969). Effect of quercetin on membrane-linked activities. *Biochem. Pharmacol.*, **18,** 1495–1500.

CHURCHER. Y. & GOMPERTS, B.D. (1990). ATP dependent and ATP independent pathways of exocytosis revealed by interchanging glutamate and chloride as the major anion in permeabilised mast cells. *Cell Regul.*, **1,** 337–346.

COX, J.S.G., BEACH, J.E., BLAIR, A.M.J.N., CLARKE, A.J., KING, J., LEE, T.B., LOVEDAY, D.E.E., MOSS, G.F., ORR, T.S.C., RITCHIE, J.T. & SHEARD, P. (1970). Disodium cromoglycate (Intal). *Adv. Drug Res.*, **5,** 115–196.

ENNIS, M., TRUNEH, A., WHITE, J.R. & PEARCE, F.L. (1981). Inhibition of histamine secretion from mast cells. *Nature*, **289,** 186–187.

FEWTRELL, C.M.S. & GOMPERTS, B.D. (1977a). Effect of flavone inhibitors of transport ATPases on histamine secretion from rat mast cells. *Nature*, **265,** 635–636.

FEWTRELL, C.M.S. & GOMPERTS, B.D. (1977b). Quercetin: a novel inhibitor of Ca^{2+} influx and exocytosis in rat peritoneal mast cells. *Biochim. Biophys. Acta*, **469,** 52–60.

FOGG, A.G. & FAYAD, N. (1978). Differential pulse polarographic determination of disodium cromoglycate in urine. *Analyt. Chim. Acta*, **102,** 205–210.

FOREMAN, J.C., MONGAR, J.L., GOMPERTS, B.D. & GARLAND, L.G. (1975). A possible role for cyclic AMP in the regulation of histamine secretion and the action of cromoglycate. *Biochem. Pharmacol.*, **74,** 538–540.

FOREMAN, J.C. & PEARCE, F.L. (1989). Cromoglycate. In *Textbook of Immunopharmacology*. ed. Dale, M.M. & Foreman, J.C. pp. 262–274. Oxford: Blackwell Scientific.

GOMPERTS, B.D. & TATHAM, P.E.R. (1992). Regulated exocytotic secretion from permeabilized cells. In *Methods in Enzymology* ed. Rothman, J. Vol. 219, pp. 178–189. New York: Academic Press.

GOODWIN, T.W. & MERCER, E.I. (1983). *Introduction to Plant Biochemistry*. pp. 541–559. Oxford: Pergamon.

GRISOLIA, S., RUBIO, V., FEIJOO, B. & MENDELSON, J. (1975). Inhibition of lactic dehydrogenase and of pyruvate kinase by low concentrations of quercetin. *Physiol. Chem. Phys.*, **7,** 473–475.

HEMMERICH, S., SIJPKENS, D. & PECHT, I. (1991). A novel cell-permeable cromoglycate derivative inhibits type 1 Fc_ϵ receptor mediated Ca^{2+} influx and mediator secretion in rat mucosal mast cells. *Biochemistry*, **30,** 1523–1532.

HEMMERICH, S., YARDEN, Y. & PECHT, I. (1992). A cromoglycate binding protein from rat mast cells of a leukemia line is a nucleoside diphosphate kinase. *Biochemistry*, **31,** 4574–4579.

HOWELL, T.W. & GOMPERTS, B.D. (1987). Rat mast cells permeabilised with streptolysin-O secrete histamine in response to Ca^{2+} at concentrations buffered in the micromolar range. *Biochim. Biophys. Acta*, **927,** 177–183.

KIMURA, N. & JOHNSON, G.S. (1983). Increased membrane-associated nucleoside diphosphate kinase activity as a possible basis for enhanced guanine nucleotide dependent adenylate cyclase activity induced by picolinic acid treatment of simian virus 40-transformed normal rat kidney cells. *J. Biol. Chem.*, **258,** 12609–12617.

KIMURA, N. & SHIMADA, N. (1988). Direct interaction between membrane associated nucleoside diphosphate kinase and GTP-binding protein (G_S), and its regulation by hormones and guanine nucleotides. *Biochem. Biophys. Res. Commun.*, **151,** 248–256.

KIMURA, N. & SHIMADA, N. (1990). Evidence for complex formation between GTP binding protein (G_S) and membrane associated nucleoside diphosphate kinase. *Biochem. Biophys. Res. Commun.*, **168,** 99–106.

KURIKI, Y. & RACKER, E. (1976). Inhibition of (Na^+, K^+) adenosine triphosphatase and its partial reactions by quercetin. *Biochemistry*, **15,** 4951–4956.

LANG, D.R. & RACKER, E. (1974). Effects of quercetin and F_1 inhibitor on mitochondrial ATPase and energy-linked reactions in submitochondrial particles. *Biochim. Biophys. Acta*, **333,** 180–186.

LILLIE, T.H.W. & GOMPERTS, B.D. (1992a). Guanine nucleotide is essential, Ca^{2+} is a modulator, in the exocytotic reaction of permeabilised rat mast cells. *Biochem. J.*, **288,** 181–187.

LILLIE, T.H.W. & GOMPERTS, B.D. (1992b). GTP, ATP, Ca^{2+} and Mg^{2+} as effectors and modulators of exocytosis in permeabilised rat mast cells. *Phil. Trans. R. Soc. B.*, **336,** 25–34.

LILLIE, T.H.W. & GOMPERTS, B.D. (1993). A cell physiological description of G_E, a GTP-binding protein that mediates exocytosis. In *The GTPase Superfamily* ed. McCormick, F. Ciba Foundaton Symposium Vol. 176 pp. 164–184. Chichester: Wiley.

LILLIE, T.H.W., WHALLEY, T.D. & GOMPERTS, B.D. (1991). Modulation of the exocytotic reaction of permeabilised rat mast cells by ATP, other nucleotides and Mg^{2+}. *Biochim. Biophys. Acta*, **1094,** 355–363.

LINDAU, M. & GOMPERTS, B.D. (1991). Techniques and concepts in exocytosis: Focus on mast cells. *Biochim. Biophys. Acta*, **1071,** 429–471.

MUSTELIN, T., COGGESHALL, K.M., ISAKOV, N. & ALTMAN, A. (1990). T-cell antigen receptor mediated activation of phospholipase C requires tyrosine phosphorylation. *Science*, **247,** 1584–1587.

OSTLE, B. (1963). *Statistics in Research*. p. 585. Ames, Iowa: Iowa State University Press.

OTERO, A.D.S. (1990). Transphosphorylation and G protein activation. *Biochem. Pharmacol.*, **39,** 1399–1404.

RANDAZZO, P.A., NORTHUP, J.K. & KAHN, R.A. (1991). Activation of a small GTP binding protein (ARF) by nucleoside diphosphate kinase catalysed phosphorylation of bound GDP. *Science*, **254,** 850–853.

RANDAZZO, P.A., NORTHUP, J.K. & KAHN, R.A. (1992). Regulatory GTP-binding proteins (ADP-ribosylation factor, G_t and RAS) are not activated directly by nucleoside diphosphate kinase. *J. Biol. Chem.*, **267,** 18182–18189.

SPECTOR, M., O'NEAL, S. & RACKER, E. (1980). Reconstitution of the Na^+, K^+ pump of Ehrlich ascites tumor and enhancement of efficiency by quercetin. *J. Biol. Chem.*, **255,** 5504–5507.

TATHAM, P.E.R. & GOMPERTS, B.D. (1990). Cell permeabilisation. In *Peptide Hormones - A practical Approach* ed. Siddle, K. & Hutton, J.C. Vol. 2, pp. 257–269. Oxford: IRL Press.

VU, N.-D. & WAGNER, P.D. (1993). Stimulation of secretion in permeabilized PC12 cells by adenosine 5'-[γ-thio]triphosphate: Possible involvement of nucleoside diphosphate kinase. *Biochem. J.*, **296**, 169–174.

WHITE, J.R., ISHIZAKA, T., ISHIZAKA, K. & SHA'AFI, R.I. (1984). Direct demonstration of increased intracellular concentration of free calcium measured by quin-2 in stimulated rat mast cells. *Proc. Nat. Acad. Sci. U.S.A.*, **81**, 3978–3982.

WIELAND, T. & JAKOBS, K.H. (1992). Evidence for nucleoside diphosphokinase-dependent channeling of guanosine 5'-(γ-thio)-triphosphate to guanine nucleotide-binding proteins. *Mol. Pharmacol.*, **42**, 731–735.

(Received November 29, 1994
Revised March 13, 1995
Accepted March 28, 1995)

British Journal of Pharmacology (1995) 115, 1087–1095 © 1995 Stockton Press All rights reserved 0007–1188/95 $12.00

RS 39604: a potent, selective and orally active 5-HT_4 receptor antagonist

[1]S.S. Hegde, D.W. Bonhaus, L.G. Johnson, E. Leung, *R.D. Clark & R.M. Eglen

Institutes of Pharmacology and *Organic Chemistry, Syntex Discovery Research, Palo Alto, CA, 94304, U.S.A.

1 Selective antagonism of 5-HT_4 receptors may provide therapeutic benefit in certain disorders of the myocardium, alimentary and lower urinary tract. We now report on RS 39604, a novel and selective 5-HT_4 receptor antagonist and compare its pharmacological properties with those of SB 204070.

2 In guinea-pig striatal membranes, both RS 39604 and SB 204070 inhibited specific binding of [^{3}H]-GR 113808 in a concentration-dependent manner yielding pK_i estimates of 9.1 and 10.9, respectively. RS 39604 displayed a low affinity ($pK_i < 6.5$) for 5-HT_{1A}, 5-HT_{2C}, 5-HT_3, α_{1c}, D_1, D_2, M_1, M_2, AT_1, B_1 and opioid μ receptors and moderate affinity for σ_1, ($pK_i = 6.8$) and σ_2 ($pK_i = 7.8$) sites.

3 In the rat isolated oesophagus, precontracted with carbachol, RS 39604 (30–300 nM) behaved as a competitive antagonist towards 5-HT-induced relaxation ($pA_2 = 9.3$; Schild slope = 1.0). We and others have shown previously that SB 204070 behaves as an unsurmountable antagonist in this preparation ($pA_2 \sim 10.5$). In the guinea-pig isolated ileal mucosa, RS 39604 (30 nM) antagonized 5-MeOT-induced increase in short-circuit current ($pA_2 = 9.1$).

4 In anaesthetized vagotomized micropigs, RS 39604, administered by the i.v. or intraduodenal (i.duod.) route, produced dose-dependent inhibition of 5-HT-induced tachycardia ($ID_{50} = 4.7$ $\mu g\ kg^{-1}$, i.v. and 254.5 $\mu g\ kg^{-1}$, i.duod). At maximal doses of 30 $\mu g\ kg^{-1}$, i.v. and 6 $mg\ kg^{-1}$, i.duod., the inhibitory effects of RS 39604 lasted for more than 6 h. In this preparation, SB 204070 was as potent as RS 39604 by the i.v. route but was inactive by the intraduodenal route at doses up to 3 $mg\ kg^{-1}$.

5 In conscious mice, RS 39604, administered by the i.p. or p.o. route, produced dose-dependent inhibition of 5-hydroxytryptophan (5-HTP)-induced diarrhoea ($ID_{50} = 81.3$ $\mu g\ kg^{-1}$, i.p. and 1.1 $mg\ kg^{-1}$, p.o.). In this assay, SB 204070 was inactive by the oral route at doses up to 30 $mg\ kg^{-1}$.

6 In anaesthetized guinea-pigs, RS 39604 antagonized the contractile effect of 5-HT in the proximal colon by producing parallel, dextral displacement of the dose-response curve to 5-HT. The mean dose-ratios to 5-HT at 0.1 $mg\ kg^{-1}$, i.v., 1 $mg\ kg^{-1}$, i.v. and 10 $mg\ kg^{-1}$, i.duod. were 4.6, 30.7 and 10.8, respectively. SB 204070 behaved as an unsurmountable antagonist in this assay.

7 In a model of visceral pain in conscious rats, RS 39604 (0.01–1 $mg\ kg^{-1}$, i.v.) did not affect colorectal distension-induced increases in arterial pressure whereas morphine (1 $mg\ kg^{-1}$, i.v.) produced significant inhibition of the response, implying that 5-HT_4 receptors are not involved in nociception in this model.

8 The data suggest that RS 39604 is a high affinity and selective 5-HT_4 receptor antagonist that is orally active and long-lasting *in vivo*. It is concluded that RS 39604 may be the preferable probe to use for investigating the physiological and pathophysiological role of 5-HT_4 receptors *in vivo*.

Keywords: 5-HT_4 antagonist; RS 39604; SB 204070; rat oesophagus; micropig tachycardia; short-circuit current; mice diarrhoea; guinea-pig colon; visceral pain; colorectal distension

Introduction

Significant advances have been made in our understanding of the physiology and pharmacology of the 5-HT_4 receptor (see Ford & Clarke, 1993 for review). Of particular clinical significance are the findings which show that this receptor mediates several biological responses in human tissues. In human gut for example, 5-HT_4 receptors have been shown to mediate 5-HT-induced inhibition of spontaneous colonic circular muscle contractions (Tam *et al.*, 1994) and stimulation of short circuit current responses in ileal (Burleigh & Borman, 1993) and jejunal (Budhoo & Kellum, 1994) mucosa. In the lower urinary tract of man, 5-HT-induced potentiation of cholinergic transmission in the detrussor smooth muscle is also mediated by 5-HT_4 receptors (Tonini *et al.*, 1994). Furthermore, 5-HT can augment aldosterone secretion from the human adrenal cortex via activation of 5-HT_4 receptors (Lefebvre *et al.*, 1993) while agonism of 5-HT_4 receptors in the human atrium can evoke pronounced arrythmias (Kaumann & Sanders, 1994). Based on these findings and assuming a pathophysiological role of endogenous 5-HT in these tissues, it may be hypothesized that selective antagonism of 5-HT_4 receptors might be of therapeutic value notably in the treatment of irritable bowel syndrome, urinary incontinence or cardiac arrythmias.

Until recently, tropisetron (Dumuis *et al.*, 1989), DAU 6285 (Dumuis *et al.*, 1992) and SDZ 205-557 (Buchheit *et al.*, 1991) were the only compounds available that antagonized the 5-HT_4 receptor. However, these compounds, had the drawbacks of low affinity and poor preference for the 5-HT_4 receptor. Subsequently, RS 23597-190 (Eglen *et al.*, 1993) and GR 113808 (Gale *et al.*, 1994a) were identified as antagonists possessing a high affinity ($pA_2 = 7.8$ and 9.2, respectively) and selectivity (> 100 fold over other 5-HT receptors) for 5-HT_4 receptors. These two compounds, although useful as pharmacological tools, were of limited therapeutic value owing to their extremely short biological half-life (Eglen *et al.*, 1993; Gale *et al.*, 1994a). More recently, SB 204070 (Wardle *et al.*, 1994) and GR 125487 (Gale *et al.*, 1994b) were reported to antagonize the 5-HT_4 receptor with high affinity ($pK_B > 10.0$) and selectivity (> 1000 fold over other 5-HT receptors). These compounds have been used successfully to antagonize 5-HT_4 receptors *in vivo* even when administered as a single bolus intravenous dose (Banner *et al.*, 1993; Bingham *et al.*, 1993; Gale *et al.*, 1994c) although their efficacy by the oral route has not

[1] Author for correspondence.

been reported. Furthermore, GR 125487 has been found to have a long duration of action (75 and 145 min in piglet and rat, respectively) (Gale *et al.*, 1994c) although similar data for SB 204070 are lacking.

In the present study, we have assessed the pharmacological properties of RS 39604, a novel 5-HT$_4$ receptor antagonist (Figure 1), and compared it to those of SB 204070. RS 39604, in contrast to SB 204070 and GR 125487, lacks a carboxylic ester functional group (Clark *et al.*, 1994) and was designed with the intent of improving the metabolic stability of our earlier chemical leads, such as RS 23597 (Eglen *et al.*, 1993).

A preliminary account of the findings has been presented to the British Pharmacological Society, (Hegde *et al.*, 1995).

Methods

In vitro *studies*

Radioligand binding studies The affinity of compounds at 5-HT$_4$ receptors was assessed in binding studies using [^{3}H]-GR 113808 as radioligand (Grossman *et al.*, 1993). [^{3}H]-GR 113808 binding to 5-HT$_4$ receptors was measured in a synaptosomal membrane preparation of guinea-pig striatum, obtained from animals previously killed by CO_2 asphyxiation. Striata were homogenized with a hand driven glass homogenizer in a Tris (10 mM)-EDTA (5 mM) buffer (pH 7.4 at 4°C), containing 250 mM sucrose. The homogenate was filtered through a nylon mesh (160 μm pore) and then centrifuged at 1000 *g* for 15 min. The resulting pellet was suspended in a HEPES (50 mM)-EDTA (0.5 mM) buffer (pH 7.4 at 4°C) containing choline (130 mM), glucose (25 mM) and KCl (5.4 mM). The final pellet was resuspended in a Tris (25 mM) buffer (pH 7.4 at 4°C).

Binding assays were conducted in a Tris buffer (25 mM) with approximately 0.1 mg striatal protein in an assay volume of 0.5 ml at room temperature. Non-specific binding was determined with 1 μM unlabelled GR 113808. Preliminary studies have demonstrated that a 60 min incubation was sufficient for membrane binding to reach a steady state. Competition binding studies were conducted with 0.1 nM [^{3}H]-GR 113808 and varying concentrations of competing ligand. Reactions were terminated by vacuum filtration, using a Brandel cell harvester, through GF/B filters pretreated for 30 min with 0.1% polyethylenimine. Filters were then dried and the bound radioactivity determined.

The affinity of RS 39604 for a range of neurotransmitter receptors were also determined (Table 1). Details of the individual assays can be found in Wong *et al.* (1993) and references cited therein.

Rat isolated oesophageal muscularis mucosae The method used was similar to that described earlier (Baxter *et al.*, 1991). The thoracic oesophagus was isolated from male Sprague-Dawley rats (Charles River, MA, U.S.A., 200–250 g) and placed in Tyrode solution (composition, mM: NaCl 139.0, KCl 2.7, $MgCl_2$. $6H_2O$ 1.1, NaH_2PO_4 0.4, glucose 5.6, $NaHCO_3$ 11.8 and $CaCl_2$. $6H_2O$ 1.8). The outer striated muscle coat was cut longitudinally and gently peeled away to expose the inner muscularis mucosae. Tissues were then mounted vertically in 10 ml organ baths containing Tyrode solution, maintained at 37°C and gassed with 95% O_2/5% CO_2. Methysergide (1 μM) was routinely included in the Tyrode solution in order to block 5-HT$_1$ and 5-HT$_2$ receptors. In addition, cocaine (30 μM) and corticosterone (30 μM) were also included in the Tyrode solution in order to inhibit amine uptake. An initial resting tension of 1 g was applied to the preparation and readjusted to 0.5 g during the initial equilibration period of 60 min. After this period, pargyline (100 μM a monoamine oxidase inhibitor) was added to the Tyrode solution for 30 min, followed by a washout period. The tissues were then allowed to equilibrate for 30 min. Carbachol (3 μM) was added to contract the tissues. Upon establishment of a stable contraction, a cumulative concentration-effect curve to 5-HT was constructed. The tissues were then washed and equilibrated for 60 min in the presence of the appropriate concentration of the antagonist. A second concentration-effect curve to 5-HT was then constructed in the presence of the antagonist.

Short circuit current studies in guinea-pig ileal mucosa Male Hartley guinea-pigs (Charles River, MA, U.S.A., 300–350 g) were killed by CO_2 asphyxiation and a segment of distal ileum, beginning approximately 2.0 cm proximal to the ileocecal valve, was isolated. Ileal mucosal sheets were prepared and mounted in Ussing chambers (surface area of 0.6 cm^2) for the measurement of short circuit current (I_{sc}) as described previously (Cooke & Carey, 1985; Scott *et al.*, 1992). The tissues were bathed, on both sides, in 15.5 ml of Krebs-Henseleit solution (composition, in mM: NaCl 118.2, KCl 4.6, $MgSO_4$. $7H_2O$ 1.2, $NaHCO_3$ 24.8, KH_2PO_4 1.2, $CaCl_2.6H_2O$ 1.8 at 37°C and gassed with 95% O_2/5% CO_2). Glucose (10 mM) was added to the serosal solution and mannitol (10 mM) to the mucosal solution. The tissue generated potential was clamped at 0 mV using a voltage clamp amplifier (DVC 1000, World

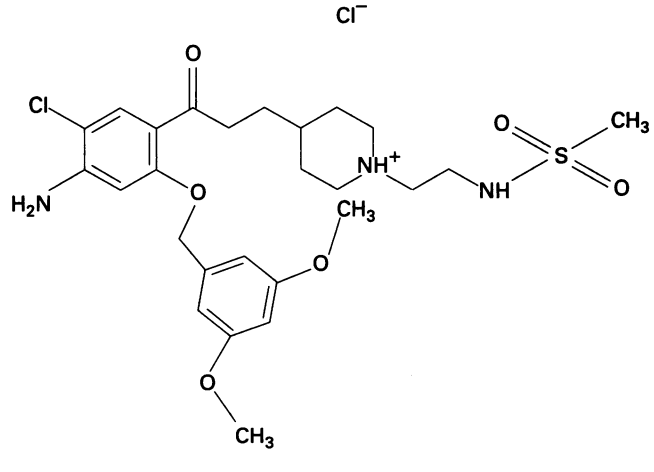

RS-39604

Figure 1 Chemical structure of RS 39604 (1-(4-amino-5-chloro-2-(3,5-dimethoxy)benzyloxyphenyl)-3-[1-((2-methylsulfonylamino)ethyl)-piperidin-4-yl]-1-propanone).

Table 1 Binding profile of RS 39604 at various receptors in radioligand binding assays

Receptor	pK_i
Adrenoceptor α_{1C}	6.4 ± 0.04
Dopamine D$_1$	< 6
Dopamine D$_2$	< 6
Muscarinic M$_1$	< 6
Muscarinic M$_2$	< 6
5-HT$_{1A}$	< 6
5-HT$_{2C}$	6.1 ± 0.05
5-HT$_3$	6.0 ± 0.2
5-HT$_4$	9.1 ± 0.1
Angiotensin AT$_1$	< 5
Bradykinin B$_1$	< 5
Opioid μ	< 6
NMDA channel	< 6
σ_1	6.8 ± 0.1
σ_2	7.8 ± 0.1

Values are means ± s.e.mean, $n = 3-4$. In all experiments the Hill coefficients were not significantly different from unity.

Precision Instruments, FL, U.S.A.). The I_{sc} required to effect a 0 mV clamp was recorded on a MacLab data acquisition system. All I_{sc} values are expressed as $\mu A\ cm^{-2}$.

Tissues were equilibrated for 60 min in the presence of vehicle or the appropriate concentration of the antagonist prior to the construction of the cumulative concentration-effect curve to 5-methoxytryptamine (5-MeOT). A single concentration-effect curve was obtained in each tissue because of agonist-induced desensitization. Adjacent tissues were used for the vehicle and drug-treatment groups. Drug additions were made to both sides of the tissue cumulatively at half log increments. Carbachol (10 μM) was added to the tissues at the end of experiments to establish tissue viability.

In vivo *studies*

5-HT-induced-tachycardia in anaesthetized micropigs The method used was modified from that described by Villalon *et al.* (1990). Yucatan micropigs of either sex (17–22 kg, S & S Farms, CA, U.S.A.) were pretreated with ketamine (approx 30 mg kg^{-1}, i.m.), anaesthetized with pentobarbitone sodium (20 mg kg^{-1}, i.v.), intubated and mechanically ventilated with room air by an animal respirator (Harvard, model 613). A femoral artery was cannulated for measurement of arterial blood pressure via a pressure transducer (Gould Statham P23ID). Dual cannulae were inserted in the ipsilateral femoral vein, one cannula for continuous infusions of supplemental anaesthetic and the second cannula for drug administration. In some experiments, a cannula was introduced into the duodenum, following a laparotomy, to allow intraduodenal administration of drugs. A limb lead II ECG electrode was monitored by subcutaneously placed electrodes and heart rate was determined by a cardiotachometer triggered by the R wave of the ECG. Following a midline ventral incision, vagus nerves were cut bilaterally. Normal body temperature was maintained with a heated water blanket. Blood gas parameters were stabilized with in a normal physiological range (pH 7.4–7.5; PCO_2 30–40, PO_2 80–100 mmHg) by adjustments of ventilatory rate, tidal volume and positive end expiratory pressure prior to the commencement of the experiment.

A dose-response curve to 5-HT (1–100 μg kg^{-1}, i.v.) was constructed for each animal to establish the ED_{50} (dose required to produce 50% of the maximal tachycardic response) for 5-HT. After obtaining three reproducible control responses to 5-HT (ED_{50} dose), each animal received (i.v. or i.d.) either vehicle or increasing cumulative doses of the antagonist with i.v. and i.d. dosing intervals of 30 and 60 min, respectively. After each dose of the antagonist or vehicle, the animal was challenged with 5-HT at 5 and 15 min for the i.v. studies and 15, 30 and 45 min for the i.duod. studies.

In a separate series of experiments, we sought to determine the duration of action of the antagonists. After obtaining three control tachycardic responses to 5-HT (ED_{50} dose), each animal was treated (i.v. or i.duod.) with either vehicle or the appropriate dose of the antagonist. For the i.v. duration study, each animal was challenged with 5-HT at 3, 10, 20 and 30 min post-dose and every 15 min thereafter for the next 330 min. For the i.d. duration study, each animal was challenged with 5-HT at 15, 30, 45 and 60 min post-dose and every 30 min thereafter for the next 420 min.

5-Hydroxytryptophan-induced diarrhoea in mice The method used was similar to that described previously (Hegde *et al.*, 1994b). Adult male Swiss-Webster mice (Harlan, San Diego, CA, U.S.A., 18–25 g) were used. The animals had free access to food and water prior to the experiments. On the day of the experiment, mice were pre-screened to exclude animals with pre-existing diarrhoea. The selected mice were randomly divided into appropriate groups. Each animal was treated intraperitoneally (i.p.) with either vehicle or the appropriate dose of antagonist. Five min later, each animal was treated with either saline or 5-hydroxytryptophan (5-HTP, 10 mg kg^{-1}, i.p.) and immediately placed in a 1 litre cup. The animals were continuously monitored for 30 min. The severity of diarrhoea was assessed using an arbitary scoring scale from 0 to 3; 0 = normal stools, 2 = swollen and/or unformed stools, 3 = severe watery diarrhoea. In a separate series of experiments, the effect of orally administered antagonist was determined. In these experiments, the animals were pre-treated with either vehicle or the appropriate dose of antagonist 10 min before 5-HTP.

In a separate series of experiments, the effect of antagonist on 16, 16, dimethyl PGE_2-induced diarrhoea was determined. Each mouse was treated with vehicle or the appropriate dose of the antagonist. Five min later, each mouse was treated with either saline or 16, 16, dimethyl PGE_2 (30 μg kg^{-1}, i.p.) and immediately placed in a 1 litre cup. The severity of diarrhoea was then scored over a 30 min observation period.

5-HT-induced contraction of the ascending colon in anaesthetized guinea-pigs The method used was similar to that described previously (Hegde *et al.*, 1994a). Male Hartley guinea-pigs (Charles River, Willmington, MA, U.S.A., 350–450 g) were used for the study. The animals were fasted, with water allowed *ad libitum* 18 h before the experiment. The animals were anaesthetized with inactin (80 mg kg^{-1}, i.p.) and the trachea was cannulated to allow artificial respiration with a ventilator (Harvard Apparatus, Model 683). The abdominal viscera were exposed and a miniature strain guage (Biomedical Dynamics, CA, U.S.A.) was sutured on the ascending colon. The strain guage, oriented to measure predominantly circular muscle tension, was connected to a signal conditioning amplifier (Measurement group, NC, U.S.A.) and a recorder (Beckman, Model 611) for measurement of tension. The left jugular vein and, in some cases, the duodenum were cannulated to allow intravenous and intraduodenal administration of drugs, respectively. Following a 1 h stabilization period, baseline tension was recorded for about 45–60 min. Each animal was treated with methysergide (3 mg kg^{-1}, i.v.) and granisetron (1 mg kg^{-1}, i.v.) in order to block 5-HT_1, 5-HT_2 and 5-HT_3 receptors. In addition, the animals were treated (i.v. or i.duod.) with either vehicle or the appropriate dose of the 5-HT_4 receptor antagonist. Sixty min later, a non-cumulative dose-effect curve to 5-HT (0.3–1000 μg kg^{-1}, i.v.) was constructed. At the end of the dose-effect curve, carbachol (100 μg kg^{-1}, i.v.) was administered to each animal.

Colorectal distension model of visceral pain in conscious rats The method used was modified from that described previously (Ness & Gebhart, 1988). Male Sprague-Dawley rats (Harlan, San Diego, CA, U.S.A., 250–300 g) were used for the study. The animals were fasted 18 h before the experiment but allowed water *ad libitum*. Each animal was anaesthetized with ether and the femoral artery and vein were cannulated for measurement of arterial pressure and drug administration, respectively. A latex balloon catheter (Viggo-Spectramed, Model SO 5325H) was introduced into the descending colon via the anus. The animals were transferred to restrainers and allowed to recover from anaesthesia (60–90 min). The arterial catheter was connected to a pressure transducer (Gould P23XL) and arterial pressure was recorded on a Beckman (Model 611) recorder. Colorectal distension was accomplished by air-inflation of the latex balloon for a period of 20 s which induced a reproducible increase in arterial pressure. After obtaining two control colorectal distension-induced pressor responses (10 min apart), each animal was treated intravenously with either vehicle or ascending cumulative doses of the antagonist. A colorectal distension-induced response was obtained 10 min after each dose of antagonist or vehicle. After the last dose, morphine (1 mg kg^{-1}, i.v.) was administered to each animal. Ten min later, another colorectal distension-induced pressor response was obtained.

Data analysis and statistical methods

Radioligand binding studies In radioligand binding studies, data from competition binding studies were analysed by fitting

to a four parameter logistic function using an iterative curve fitting program. The apparent affinities (–log K_i) of competing ligands were calculated from IC_{50} values by the Cheng-Prusoff equation (Cheng & Prusoff, 1973).

Functional isolated tissue studies In the functional studies, agonist potencies were determined by nonlinear regression using iterative curve fitting procedures (Leung *et al.*, 1992) and the relationship described by Parker & Waud (1971). The apparent affinity (pA_2) of the antagonist was determined by the method of Arunlakshana & Schild (1959), in which at least three concentrations of antagonist were used and the slope of the Schild plot determined by regression analysis. In studies where only a single concentration of the antagonist was used, the apparent affinity was calculated by the method described by Furchgott (1972).

Micropig tachycardia studies In these experiments, peak percentage inhibition of the control tachycardic response to 5-HT was determined for each antagonist. ID_{50} estimates (dose required to produce 50% of the maximal inhibition) were obtained by non-linear iterative curve fitting procedures (Leung *et al.*, 1992). In the duration studies, a repeated measures two-way analysis of variance (ANOVA) was used to determine the effects of treatment, time and their interaction. Wherever appropriate, a 2-parameter exponential model was used to determine $t_{1/2}$ (time required for the inhibitory effect to decline by 50%).

5-HTP-induced diarrhoea in mice The scorer was blind to treatments. A Mantel-Haenszel Chi-square test was used to analyse the effects of different treatments on diarrhoea score. ID_{50} estimates (dose required to produce 50% of the maximal inhibition of 5-HTP-induced diarrhoea) were calculated by non-linear regression analysis (Leung *et al.*, 1992).

5-HT-induced colonic contraction in guinea-pigs The contractile response to 5-HT in each animal was expressed as a percentage of the response to carbachol. ED_{50} (dose required to produce 50% of the maximum response) and E_{max} (maximum response) of 5-HT were estimated by nonlinear regression analysis (Leung *et al.*, 1992). Dose-ratios were calculated as the ratio of ED_{50} (antagonist)/ED_{50} (vehicle). In cases where the antagonist produced marked depression of the maximum response to 5-HT, an alternate potency estimate (ED_x) was calculated for the vehicle curve. ED_x was defined as the concentration of 5-HT required to attain a response equivalent to 50% of the maximum response of the antagonist curve. Dose-ratio was then calculated as ED_{50} (antagonist)/ED_X (vehicle).

Colorectal distension model of visceral pain in rats The change in mean arterial pressure (from pre-distension baseline) following each trial of colorectal distension were obtained. The difference between the control response and post-drug (or vehicle or morphine) response was calculated. A repeated measures two-way ANOVA was used to test the overall effects of treatment, dose and their interaction. One way ANOVA was also performed to test the effects of each dose of antagonist or morphine.

All values are either mean ± s.e.mean or mean, with 95% confidence intervals in parentheses. $P < 0.05$ was considered to be statistically signficant.

Compounds used

The following compounds were obtained from commercial sources: 5-HT, 5-MeOT, cocaine, corticosterone, pargyline, carbachol, 16, 16, dimethyl PGE_2 (Sigma Chemical Co, St. Louis, MO, U.S.A.), 5-HTP (Research Biochemicals Inc, MA, U.S.A.). Methysergide was donated by Sandoz, Basle, Switzerland. RS39604 (1-(4-amino-5-chloro-2-(3,5-dimethoxy)benzyloxyphenyl)-3-[1-((2-methylsulphonylamino)ethyl)piperidin-4-yl]-1-propanone), SB 204070 ((1-butyl-4-piperidiny)methyl-8-amino-7-chloro-1,4-benzodioxan-5-carboxylate hydrochloride) and granisetron were synthesized in the Institute of Organic Chemistry at Syntex Discovery Research.

5-HT, 5-MeOT, 5-HTP, cocaine, carbachol, pargyline and 16, 16, dimethyl PGE_2 were dissolved in either distilled water or saline. Corticosterone was dissolved in dimethyl sulphoxide (DMSO). Methysergide was dissolved in saline or ethanol. RS 39604 and SB 204070 were dissolved in either 50% ethanol (for the *in vitro* experiments) or a mixture of DMSO, ethanol and water (for the pig tachycardia experiments) or in a solution of 4.5% 2-hydroxypropyl β-cyclodextrin for the remaining experiments.

Results

In vitro *studies*

Radioligand binding studies In guinea-pig striata, RS 39604 produced concentration-dependent displacement of [^{3}H]-GR 113808 ($pK_i \pm$ s.e.mean = 9.1 ± 0.1; Hill slope ± s.e.mean = 1.1 ± 0.1). RS 39604 displayed a low affinity ($pK_i < 6.5$) for several other receptors except the σ_1 ($pK_i = 6.8$) and σ_2 site ($pK_i = 7.8$) (Table 1).

SB 204070 also produced concentration-dependent displacement of [^{3}H]-GR 113808 ($pK_i \pm$ s.e.mean = 10.9 ± 0.1; Hill slope ± s.e.mean = 1.1 ± 0.1).

Rat isolated oesophageal muscularis mucosae 5-HT produced concentration-dependent relaxation of the pre-contracted rat oesophagus with a pEC_{50} (95% confidence interval) of 8.3 (8.1–8.6) (Figure 2). RS 39604 (10–300 nM) had no effect, *per se*, on basal or carbachol-induced tone (data not shown). RS 39604 (30–300 nM) produced concentration-dependent dextral displacement of the concentration-effect curve to 5-HT without significantly altering the maximum response to 5-HT (Figure 2). Schild analysis of this data yielded a pA_2 estimate (95% confidence interval) and slope (± s.e.mean) of 9.3 (9.2–9.4) and 1.0 ± 0.2, respectively.

We and others have shown previously that, in the rat oesophagus, SB 204070 also produces concentration-dependent rightward displacement of the concentration-effect curve to 5-HT which is accompanied by a significant depression of the maximum response ($pA_2 \sim 10.5$) (Baxter *et al.*, 1994; Zeitung *et al.*, 1994).

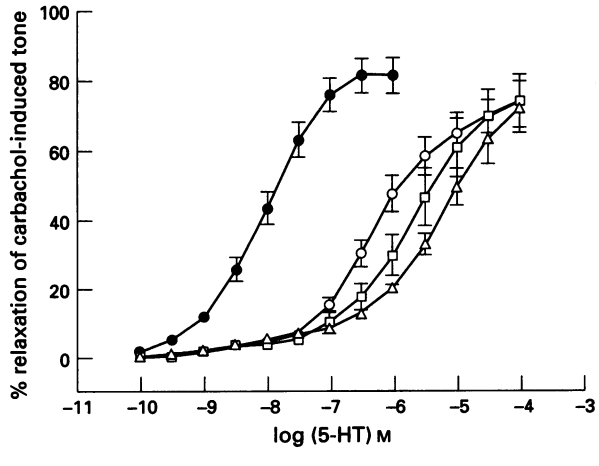

Figure 2 Effect of RS 39604 on the relaxant response to 5-HT in the rat isolated oesophagus. The concentration-effect curve to 5-HT is shown in the absence (●) and presence of RS 39604, 30 nM (○), 100 nM (□) and 300 nM (△). Results are expressed as mean ± s.e.mean, $n = 4$.

Short-circuit current studies in guinea-pig ileal mucosa We have reported, previously, that 5-HT induces a tetrodotoxin-sensitive increase in short-circuit current in this preparation (Eglen *et al.*, 1993). Furthermore, the concentration-effect curve to 5-HT is biphasic with the high potency phase being mimicked by 5-MeOT and abolished by 5-HT$_4$ antagonists such as RS 23597-190. In the present study, 5-MeOT induced a concentration-dependent rise in short-circuit current with a pEC_{50} (95% confidence interval) of 7.5 (6.9–8.0). RS 39604 (30 nM), which did not affect short-circuit current *per se*, produced a dextral shift of the concentration-effect curve to 5-MeOT without significantly altering the maximum response (Figure 3). The pA_2 estimate (95% confidence interval) of RS 39604 was calculated to be 9.1 (7.8–10.3).

In vivo *studies*

Micropig tachycardia studies Both RS 39604 and SB 204070, when administered intravenously, produced dose-dependent inhibition of 5-HT-induced tachycardia in anaesthetized micropigs (Figure 4a and b) with ID_{50} (95% confidence interval) estimates of 4.7 (3.6–6.0) and 8.0 (5.4–11.9) μg kg^{-1}, i.v., respectively. RS 39604, when administered intraduodenally, produced dose-dependent inhibition of 5-HT-induced tachycardia (Figure 4a) with an ID_{50} estimate of 246 (191–324) μg kg^{-1}, i.duod. SB 204070 had no significant inhibitory effects, when administered intraduodenally, at doses up to 3 mg kg^{-1}, i.duod. (Figure 4b). Both SB 204070 and RS 39604, when administered as escalating cumulative i.v. or i.duod. doses, did not affect baseline heart rate or arterial pressure (data not shown).

At maximal inhibitory doses of 30 μg kg^{-1}, i.v. and 6 mg kg^{-1}, i.duod., which did not affect baseline heart rate or arterial pressure *per se*, the inhibitory effects of RS 39604 toward 5-HT were statistically significant ($P < 0.05$) for more than 6 and 8 h, respectively (Figure 5). There appeared to be a temporal increase in the sensitivity of the preparation to 5-HT in animals pre-treated with vehicle. At a dose of 30 μg kg^{-1}, i.v., the $t_{1/2}$ (95% confidence interval) of RS 39604 was calculated to be 315 (278–352) min. SB 204070, when administered as a single intravenous bolus dose of 30 μg kg^{-1}, itself induced a positive chronotropic effect (increase in heart rate of approximately 25–30 beats min^{-1}) which lasted for approximately 90 min and could be partially reversed by DAU 6285 (3 mg kg^{-1}, i.v., data not shown). At 90 min post-dose, at which time baseline heart rate was re-attained, the tachycardic response to exogenous 5-HT was inhibited by approximately 35%.

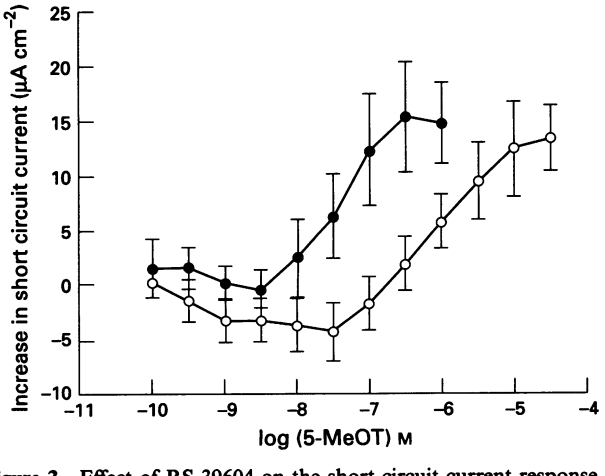

Figure 3 Effect of RS 39604 on the short-circuit current response to 5-methoxytryptamine (5-MeOT) in the guinea-pig isolated ileal mucosa. Figure shows the concentration-effect curve to 5-HT in the absence (●) and presence (○) of RS 39604 (30 nM). Results are expressed as mean ± s.e.mean, $n = 4$.

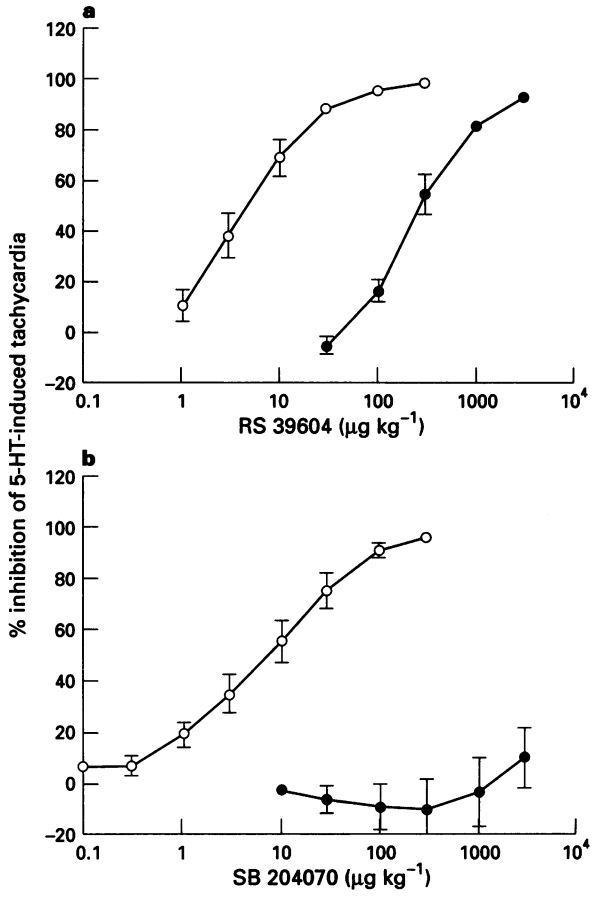

Figure 4 Effect of RS 39604 (a) and SB 204070 (b) on 5-HT-induced tachycardia in the anaesthetized micro-pig. The peak inhibitory effects of intravenously (○) or intraduodenally (●) administered antagonist are shown. The antagonists were administered as increasing cumulative doses. Results are expressed as mean ± s.e.mean, $n = 4$, and show the percentage inhibition of the control (pre-drug) tachycardic response to 5-HT.

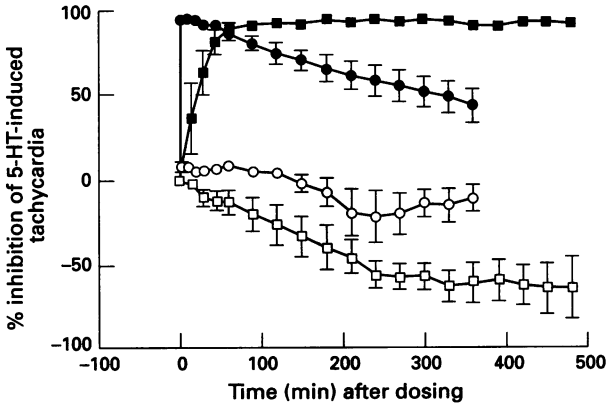

Figure 5 Time course of the effect of vehicle (open symbols) or RS 39604 (closed symbols) on 5-HT-induced tachycardia in the anaesthetized micropig. After obtaining control tachycardic responses to 5-HT, animals were pretreated at 0 min with vehicle (○) i.v., (□) i.duod. or RS 39604, 30 μg kg^{-1}, i.v. (●); 6 mg kg^{-1}, i.d. (■) after which the animals were re-challenged with 5-HT at appropriate intervals. Results are expressed as mean ± s.e.mean, $n = 4$, and show the percentage inhibition of the control (pre-drug or pre-vehicle) tachycardic response to 5-HT. The inhibitory effects of RS 39604 (i.v. and i.d.) were significantly ($P < 0.05$) different from vehicle at all time points.

5-HTP-induced diarrhoea in mice 5-HTP (10 mg kg^{-1}, i.p.) produced a significant increase in diarrhoea score (Figure 6a and 6b). RS 39604, administered i.p. or p.o., produced dose-dependent inhibition of 5-HTP-induced diarrhoea (Figure 6a and 6b). The ID_{50} (±s.e.mean) estimates were 81.3± 1.9 μg kg^{-1}, i.p. and 1.1±4.2 mg kg^{-1}, p.o. The maximal inhibitory effect of RS 39604 by the i.p. and p.o. route were 70% and 58%, respectively. RS 39604, at doses of 0.1 and 1 mg kg^{-1}, i.p., did not affect 16,16, dimethyl PGE_2-induced diarrhoea (data not shown). As reported earlier (Hegde *et al.*, 1994b), SB 204070, when administered intraperitoneally, also produced significant inhibition of 5-HTP-induced diarrhoea. The ID_{50} (±s.e.mean) and maximal inhibitory effect of SB 204070 were 0.3±0.2 μg kg^{-1}, i.p. and 36%, respectively. SB 204070, administered orally, had no inhibitory effects on 5-HTP-induced diarrhoea even at doses up to 30 mg kg^{-1} (data not shown).

5-HT-induced colonic contraction in anaesthetized guinea-pigs RS 39604 (0.1 and 1 mg kg^{-1}, i.v.) produced dose-dependent dextral displacement of the dose-effect curve to 5-HT with no significant alteration of the maximum response (Figure 7a). When administered intraduodenally at 10 mg kg^{-1}, i.p., RS 39604 also produced a significant dextral displacement of the dose-effect curve to 5-HT (data not shown). The mean dose-ratios (95% confidence interval) at 0.1 mg kg^{-1}, i.v., 1 mg kg^{-1}, i.v. and 10 mg kg^{-1}, i.d. were 4.6 (1.9–10.9), 30.7 (8.5–111.3) and 10.8 (2.6–44.4), respectively. SB 204070 (0.03 and 0.1 mg kg^{-1}, i.v.) also produced dose-dependent dextral displacement of the dose-response curve to 5-HT which was accompanied by a significant depression of the maximum response (Figure 7b). The mean dose-ratios (95% confidence interval) at 0.03 and 0.1 mg kg^{-1}, i.v. were 3.9 (1.3–12.6) and 11.2 (4.5–27.8) respectively. Both RS 39604 and SB 204070 had no effect on baseline tension *per se* (data not shown).

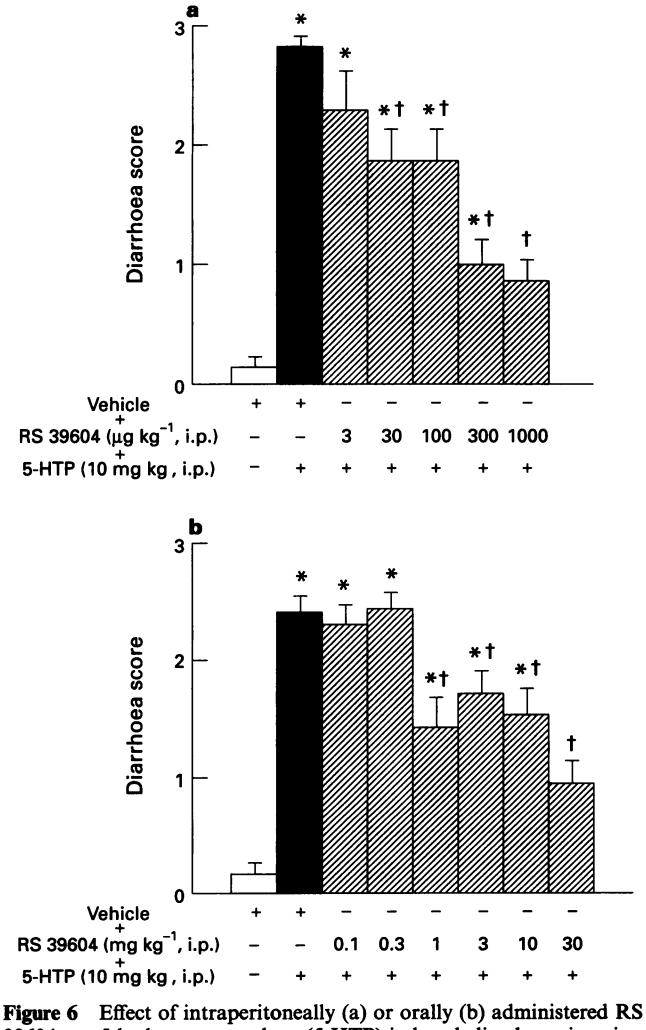

Figure 6 Effect of intraperitoneally (a) or orally (b) administered RS 39604 on 5-hydroxytryptophan (5-HTP)-induced diarrhoea in mice. Figures show the control diarrhoea score (open column), 5-HTP-induced increase in diarrhoea score (solid column) and effect of different doses of RS 39604 on 5-HTP-induced diarrhoea (hatched columns). Results are expressed as mean±s.e.mean, n=30–40. *P<0.05 vs open column; †P<0.05 vs closed column.

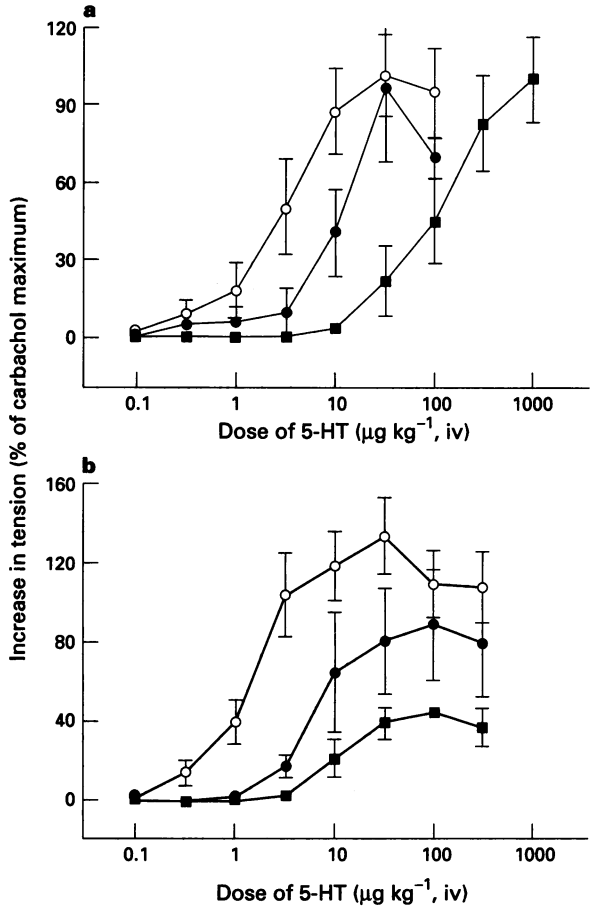

Figure 7 Effect of RS 39604 (a) and SB 204070 (b) on the contractile effects of 5-HT in the proximal colon of the anaesthetized guinea-pig: (a) shows the dose-effect curve to 5-HT in the absence (○) and presence of RS 39604, 0.1 mg kg^{-1}, i.v. (●) and 1 mg kg^{-1}, i.v. (■); (b) shows the dose-effect curve to 5-HT in the absence (○) and presence of SB 204070, 0.03 mg kg^{-1}, i.v. (●) and 0.1 mg kg^{-1}, i.v. (■). Results are expressed as mean±s.e.mean, n=5–6.

Table 2 Effect of RS 39604 and morphine on colorectal distension-induced increase in arterial pressure in rats

Treatment	*Dose* (mg kg^{-1}, i.v.)	*Change in arterial pressure* (mmHg)
Control	NA	30.6±5.3
RS 39604	0.01	31.6±5.2
	0.03	26.2±5.9
	0.1	31.0±6.4
	0.3	31.8±4.4
	1.0	29.2±5.4
Morphine	1.0	17.8±2.2*

NA=not applicable; Results are expressed as mean± s.e.mean, n=5.
*P<0.05 vs control.

Colorectal distension model of visceral pain in conscious rats In vehicle-treated rats, colorectal distension evoked reproducible increases in arterial pressure (data not shown). RS 39604 (0.01–1 mg kg^{-1}, i.v.) had no effect on colorectal distension-induced pressor responses (Table 2). In contrast, morphine (1 mg kg^{-1}, i.v.) significantly inhibited the pressor response to colorectal distension (Table 2).

Discussion

The objective of the present study was to characterize the pharmacological actions of RS 39604. The data obtained suggest that RS 39604 is a high affinity, competitive and selective 5-HT$_4$ receptor antagonist *in vitro* and, as such, is a useful addition to the existing 5-HT$_4$ receptor antagonists. More importantly, the oral activity and long duration of action of RS 39604 suggests that this compound may be the preferable pharmacological probe to use for investigating the physiological and pathophysiological significance of 5-HT$_4$ receptors *in vivo*.

In vitro *pharmacology of RS 39604*

Radioligand binding studies showed that RS 39604 binds with high affinity (pK_i = 9.1) to a single population of 5-HT$_4$ receptors in the guinea-pig striatum. This finding was confirmed in functional studies in which affinities of 9.3 and 9.1 were obtained for RS 39604 in the rat isolated oesophagus and guinea-pig ileal mucosa, respectively. In both the aforementioned preparations, RS 39604 produced parallel, dextral shifts of the concentration-effect curve to the agonist without altering the maximum response; consistent with a competitive mode of interaction. This is in contrast to SB 204070 (Wardle *et al.*, 1994; Baxter *et al.*, 1994) and GR 125487 (Gale *et al.*, 1994b), which behave as unsurmountable antagonists. The unsurmountable nature of SB 204070 has been attributed to its slow dissociation off the receptor leading to 'pseudoirreversible inhibition' (Wardle *et al.*, 1994; Baxter *et al.*, 1994). Accordingly, the lower affinity and faster off-rate of RS 39604 may enable it to attain rapid equilibrium with the agonist thereby facilitating surmountable antagonism. RS 39604 also displayed a high degree of selectivity for 5-HT$_4$ receptors as it possessed a low affinity (pK_i < 6.5) for the vast majority of other receptors studied. RS 39604 possessed moderate affinity (pK_i = 7.8) for the σ_2 site. The relevance of this finding is unclear as the functional significance of the σ_2 receptor has yet to be established (Walker *et al.*, 1990). RS 39604 thus fulfils several criteria (high affinity, selectivity and competitive) expected for an ideal antagonist and can, therefore, be considered an additional probe for further defining the 5-HT$_4$ receptor.

In vivo *pharmacology of RS 39604*

5-HT-induced tachycardia in the anaesthetized micropig is mediated exclusively by 5-HT$_4$ receptors (Villalon *et al.*, 1992). In this preparation, RS 39604, administered by the intravenous route, produced dose-dependent inhibition of 5-HT-induced tachycardia and, in this regard, was as potent as SB 204070, despite possessing a much lower affinity than the latter compound for 5-HT$_4$ receptors. This apparent discrepancy may perhaps be explained by differences in metabolic clearance of the two compounds (see below). RS 39604 was also effective when administered intraduodenally although its potency by this route was approximately 50 fold lower than that by the intravenous route. SB 204070, however, was inactive by the intraduodenal route even at doses up to 3 mg kg^{-1}, suggesting either poor absorbtion or extensive first-pass metabolism of this drug. An unexpected finding in the present study was that SB 204070, when administered intravenously as a single bolus maximal dose, evoked a positive chronotropic effect. This response to SB 204070 appears to be mediated, at least in part, by 5-HT$_4$ receptors in as much as it could be partially reversed by DAU 6285. This finding is difficult to reconcile with previous *in vitro* studies that have failed to reveal a partial agonist effect of SB 204070 even in preparations possessing a high receptor reserve of 5-HT$_4$ receptors such as the guinea-pig distal colon (Wardle *et al.*, 1994). The precise explanation for this disparity has yet to be resolved. The apparent partial agonist effect of SB 204070 precluded the accurate determination of the duration of action of this compound. When one compares equi-effective doses (30 μg kg^{-1}, i.v.) of RS 39604 and SB 204070 at 90 min post-dose (at which time the intrinsic agonist effect of SB 204070 had faded completely), the tachycardic response to 5-HT was inhibited by 80% and 35%, respectively. In a similar model, it was reported that GR 125487 had a duration of action of 75 min (Gale *et al.*, 1994c) whereas the present study has shown that RS 39604 has a duration of action of greater than 6 h. These data suggest, therefore, that the antagonistic effect of RS 39604 is more long-lasting than that of SB 204070 and GR 125487. The most likely explanation for this finding is that RS 39604, in contrast to SB 204070 and GR 125487, lacks the metabolically labile ester functionally (Clark *et al.*, 1994).

We have shown previously that 5-HTP-induced diarrhoea in mice is mediated by 5-HT$_4$ receptors as it can be antagonized by selective 5-HT$_4$ receptor antagonists such as DAU 6285, GR 113808 and SB 204070 (Hegde *et al.*, 1994b). In the present study, we showed that RS 39604, administered intraperitoneally or orally, produced significant inhibition of 5-HTP-induced diarrhoea. A non-specific effect of RS 39604 may be discounted as this compound failed to inhibit prostaglandin-induced diarrhoea. In as much as 5-HT$_4$ receptor activation stimulates electrolyte secretion in the human gut (Burleigh & Borman, 1993; Budhoo & Kellum, 1994), it is plausible that compounds, such as RS 39604, may be useful in combating the diarrhoea associated with carcinoid (Feldman, 1987) and irritable bowel syndrome (Camilleri & Prather, 1992). The p.o./i.p. potency ratio of RS 39604 was calculated to be approximately 14, suggesting only modest absorption of this compound from the gastrointestinal tract. The intraperitoneal potency of RS 39604 was approximately 25 fold lower than that reported previously for SB 204070 (Hegde *et al.*, 1994b). However, the maximal inhibition produced by RS 39604 was approximately 70% which compares with 30% for SB 204070. The precise reason for the lower maximal inhibitory effect of SB 204070 is unclear at present. The lack of activity of SB 204070 by the oral route may also be a reflection of its low oral bioavailibity in mice.

5-HT-induced contraction of the proximal colon *in vitro* (Elswood *et al.*, 1991) or *in vivo* (Hegde *et al.*, 1994a) is mediated via activation of 5-HT$_4$ receptors. Both RS 39604 and SB 204070 potently antagonized the contractile responses to 5-HT in a surmountable and unsurmountable manner, respectively, consistent with the behaviour of these compounds *in vitro*. A comparison of the dose-ratios would suggest that SB 204070 is at least 3 fold more potent than RS 39604. RS 39604 was also effective by the intraduodenal route although it was approximately 10 fold less potent.

Previous studies have shown that inhibition of colorectal distension-induced pressor response in conscious rats is a reliable predictor of visceral antinociceptive activity and response to clinically effective drugs such as morphine and clonidine (Ness & Gebhart, 1988). Furthermore, a role of 5-HT$_1$, 5-HT$_2$ and 5-HT$_3$ receptors in the modulation of visceral nociception has been demonstrated in this animal model (Danzebrink & Gebhart, 1991). The present study has shown that RS 39604, at doses up to 1 mg kg^{-1}, i.v., had no effect on colorectal distension-induced pressor responses. Although data pertaining to the penetration of RS 39604 across the blood-brain-barrier is unavailable at present, the results do not support a role of 5-HT$_4$ receptors in modulation of visceral antinociception. Such as conjecture may imply that selective 5-HT$_4$ antagonists would be ineffective in ameliorating the pain component of irritable bowel syndrome (Camilleri & Prather, 1992).

In summary, the findings of this study suggest that RS 39604 is a selective, orally active and long-acting 5-HT$_4$ receptor antagonist. Consequently, it may represent a significant improvement over some of the existing 5-HT$_4$ antagonists in assessing the physiological role of the 5-HT$_4$ receptor *in vivo*.

The authors wish to thank Sherry Hsu, Lorri Walsh, Ken Zeitung, Marc Perry, Tina Moy, Paul Ku, Sonya Wallace and Hai Ming Tang for their valuable technical assistance.

References

ARUNLAKSHANA, O. & SCHILD, H.O. (1957). Some quantitative uses of drug antagonists. *Br. J. Pharmacol. Chemother.*, **12**, 48–58.

BANNER, S.E., SMITH, M.I., BYWATER, D. & SANGER, G.J. (1993). 5-HT$_4$ receptor antagonism by SB 204070 inhibits 5-hydroxytrytophan-evoked defaecation in mice. *Br. J. Pharmacol.*, **110**, 17P.

BAXTER, G.S., CRAIG, D.A. & CLARKE, D.E. (1991). 5-Hydroxytryptamine$_4$ receptors mediate relaxation of the rat oesophageal tunica muscularis mucosae. *Naunyn Schmied. Arch. Pharmacol.*, **343**, 439–446.

BAXTER, G.S., SANGER, G.J., GASTER, L.M. & WARDLE, K.A. (1994). Tissue and agonist dependent non-surmountable antagonism by the selective 5-HT$_4$ receptor antagonist SB 204070. *Br. J. Pharmacol.*, **112**, 105P.

BINGHAM, S., KING, B.F., RUSHANT, B., SMITH, M.I. & SANGER, G.I. (1993). The 5-HT$_4$ receptor antagonist SB 204070 inhibits the contractile response to 5-HT in the dog Heidenhain pouch. *Br. J. Pharmacol.*, **110**, 16P.

BUCHHEIT, K.-H., GAMSE, R. & PFANNKUCHE, H.-J. (1991). SDZ-205-557, a selective antagonist at 5-HT$_4$ receptors in the isolated guinea-pig ileum. *Eur. J. Pharmacol.*, **200**, 373–374.

BUDHOO, M.R. & KELLUM, J.M. (1994). The 5-HT$_4$ receptor mediates 5-hydroxytryptamine-induced rise in short-circuit current in the human jejunum in vitro. *Surgery*, **116**, 396–400.

BURLEIGH, D.E. & BORMAN, R.A. (1993). Short-circuit current responses in human ileal mucosa are mediated by a 5-HT$_4$ receptor. *Eur. J. Pharmacol.*, **241**, 125–128.

CAMILLERI, M. & PRATHER, C.M. (1992). The Irritable bowel syndrome: Mechanisms and a practical approach to management. *Ann. Int. Med.*, **116**, 1001–1008.

CHENG, Y.C. & PRUSOFF, W.M. (1973). Relationship between inhibitor constant (Ki) and the concentration of inhibitor which causes 50 percent inhibition (IC_{50}) of an enzymatic reaction. *Biochem. Pharmacol.*, **92**, 881–894.

CLARK, R.D., JAHANGIR, A., LANGSTON, J.A., WEINHARDT, K.K., MILLER, A.B., LEUNG, E., BONHAUS, D.W., WONG, E.H.F. & EGLEN, R.M. (1994). Synthesis and preliminary pharmacological evaluation of 2-benzyloxy substituted aryl ketones as 5-HT$_4$ receptor antagonists. *Bioorg. Med. Chem. Lett.*, **4**, 2481–2484.

COOKE, H.J. & CAREY, H.V. (1985). Pharmacological analysis of 5-hydroxytryptamine actions on guinea-pig ileal mucosa. *Eur. J. Pharmacol.*, **111**, 329–337.

DANZEBRINK, R.M. & GEBHART, G.F. (1991). Evidence that spinal 5-HT$_1$, 5-HT$_2$ and 5-HT$_3$ receptor subtypes modulate responses to noxious colorectal distension in the rat. *Brain Res.*, **538**, 64–75.

DUMUIS, A., GOZLAN, H., SEBBEN, M., ANSANAY, H., RIZZI, C.A., TURCONI, M., MONFERINI, E., GIRALDO, E., SCHIANTARELLI, P., LADINSKY, H. & BOCKAERT, J. (1992). Characterization of a novel 5-HT$_4$ receptor antagonist of the azabicycloalkyl benzimidazolone class: DAU 6285. *Naunyn Schmied. Arch. Pharmacol.*, **345**, 264–269.

DUMUIS, A., SEBBEN, M. & BOCKAERT, J. (1989). The gastrointestinal prokinetic benzamide derivatives are agonists at the non-classical 5-HT receptor (5-HT$_4$) positively coupled to adenylate cyclase. *Naunyn Schmied. Arch. Pharmacol.*, **340**, 403–410.

EGLEN, R.M., BLEY, K., BONHAUS, D.W., CLARK, R.D., HEGDE, S.S., JOHNSON, L.G., LEUNG, E. & WONG, E.H.F. (1993). RS 23597-190: a potent and selective 5-HT$_4$ receptor antagonist. *Br. J. Pharmacol.*, **110**, 119–126.

ELSWOOD, C.J., BUNCE, K.T. & HUMPHREY, P.P.A. (1991). Identification of putative 5-HT$_4$ receptors in guinea-pig ascending colon. *Eur. J. Pharmacol.*, **196**, 149–155.

FELDMAN, J.M. (1987). Carcinoid tumours and syndrome. *Semin. Oncol.*, **14**, 237–246.

FORD, A.P.D.W. & CLARKE, D.E. (1993). The 5-HT$_4$ receptor. *Med. Res. Rev.*, **13**, 633–662.

FURCHGOTT, R.F. (1972). The classification of adrenoceptors (adrenergic receptor). An evaluation from the standpoint of receptor theory. In *Catecholamines, Handbook of Experimental Pharmacology*, Vol 33. ed. Blaschko, H. & Muscholl, E. pp. 283–335. Berlin, Heidelberg, New York: Springer.

GALE, J.D., GROSSMAN, C.J., WHITEHEAD, J.W.F., OXFORD, A.W., BUNCE, K.T. & HUMPHREY, P.P.A. (1994a). GR 113808: a novel, selective antagonist with high affinity at the 5-HT$_4$ receptor. *Br. J. Pharmacol.*, **111**, 332–338.

GALE, J.D., GROSSMAN, C.J., DARTON, J., BUNCE, K.T., WHITEHEAD, J.W.F., KNIGHT, J., PARKHOUSE, T.J., OXFORD, A.W. & HUMPHREY, P.P.A. (1994b). GR 125487: A selective and high affinity 5-HT$_4$ receptor antagonist. *Br. J. Pharmacol.*, **113**, 120P.

GALE, J.D., GREEN, A., DARTON, J., SARGENT, R.S., CLAYTON, N.M. & BUNCE, K.T. (1994c). GR 125487: a 5-HT$_4$ receptor antagonist with a long duration of action *in vivo*. *Br. J. Pharmacol.*, **113**, 119P.

GROSSMAN, C.J., KILPATRICK, G.J. & BUNCE, K.T. (1993). Development of a radioligand binding assay for 5-HT$_4$ receptors in guinea-pig and rat brain. *Br. J. Pharmacol.*, **109**, 618–624.

HEGDE, S.S., BONHAUS, D.W., LEUNG, E., WONG, E.H.F., JOHNSON, L.G., CLARK, R.D., FLIPPIN. L.A. & EGLEN, R.M. (1995). RS 39604: a potent, selective, orally active and long-lasting 5-HT$_4$ receptor antagonist. *Br. J. Pharmacol.*, (in press).

HEGDE, S.S., KU, P., LAI, K. & EGLEN, R.M. (1994a). 5-HT$_4$ receptor mediated contraction of colon in the anesthetized guinea-pig. *Br. J. Pharmacol.*, **112**, 559P.

HEGDE, S.S., MOY, T.M., PERRY, M.R., LOEB, M. & EGLEN, R.M. (1994b). Evidence for the involvement of 5-HT$_4$ receptors in 5-hydroxytryptophan-induced diarrhoea in mice. *J. Pharmacol. Exp. Ther.*, **271**, 741–747.

KAUMANN, A.J. & SANDERS, L. (1994). 5-Hydroxytryptamine causes rate-dependent arrhythmias through 5-HT$_4$ receptors in human atrium: facilitation by chronic β-adrenoceptor blockade. *Naunyn Schmied. Arch. Pharmacol.*, **349**, 331–337.

LEFEBVRE, H., CONTESSE, V., DELARUE, C., SOUBRANE, C., LEGRAND, A., KUHN, J.-M., WOLF, L.-M. & VANDRY, H. (1993). Effect of the serotonin-4 receptor agonist zacopride on aldosterone secretion from the human adrenal cortex: in vivo and in vitro studies. *J. Clin. Endocrin. Metab.*, **77**, 1662–1666.

LEUNG, E., MICHELSON, S., VILLARUBIA, C., PERKINS, L.A. & EGLEN, R.M. (1992). Analysis of concentration response relationships by seemingly unrelated non-linear regression (SUNR) technique. *J. Pharmacol. Methods*, **4**, 1209–1216.

NESS, T.J. & GEBHART, G.F. (1988). Colorectal distension as a noxious visceral stimulus: physiologic and pharmacologic characterization of pseudaffective reflexes in the rat. *Brain Res.*, **450**, 153–169.

PARKER, R.B. & WAUD, D.R. (1971). Pharmacological estimation of drug-receptor dissociation constants. Statistical evaluation. I. Agonists. *J. Pharmacol. Exp. Ther.*, **177**, 1–12.

SCOTT, C.M., BUNCE, K.T. & SPRAGGS, C.F. (1992). Investigation of the 5-hydroxytryptamine receptor mediating the 'maintained' short-circuit response in guinea-pig ileal mucosa. *Br. J. Pharmacol.*, **106**, 877–882.

TAM, F. S.-F., HILLIER, K. & BUNCE, K.T. (1994). Characterization of 5-hydroxytryptamine receptor type involved in inhibition of spontaneous activity of human isolated colonic circular muscle. *Br. J. Pharmacol.*, **113**, 143–150.

TONINI, M., MESSORI, E., FRANCESCHETTI, G.P., RIZZI, C.A., CASOLDI, A.F., COCCINI, T. & CANDURA, S.M. (1994). Characterization of the 5-HT receptor potentiating neuromuscular cholinergic transmission in strips of human isolated detrusor muscle. *Br. J. Pharmacol.*, **113**, 1–2.

VILLALON, C.M., DENBOER, M.O., HEILIGERS, J.P.C. & SAXENA, P.R. (1992). Mediation of 5-hydroxytryptamine-induced tachycardia in the pig by the 5-HT$_4$ receptor. *Br. J. Pharmacol.*, **100**, 665–667.

WALKER, J.M., BOWEN, W.D., WALKER, F.O., MATSUMOTO, R.R., DECOSTA, B. & RICE, K.C. (1990). Sigma receptors: biology and function. *Pharmacol. Rev.*, **42**, 355–402.

WARDLE, K.A., ELLIS, E.S., BAXTER, G.S., KENNETT, G.A., GASTER, L.M. & SANGER, G.J. (1994). The effects of SB 204070, a highly potent and selective 5-HT$_4$ receptor antagonist, on guinea-pig distal colon. *Br. J. Pharmacol.*, **112**, 789–794.

WONG, E.H.F., BONHAUS, D.W., WU, I., STEFANICH, E. & EGLEN, R.M. (1993). Labelling of 5-hydroxytryptamine$_3$ receptors with novel 5-HT$_3$ receptor ligand, [^{3}H]-RS 42358-197. *J. Neurochem.*, **60**, 921–930.

ZEITUNG, K.D., PERKINS, L.A., HSU, S.A.O., BONHAUS, D.W., EGLEN, R.M., WONG, E.H.F. & LEUNG, E. (1994). Comparison of GR 113808 and SB 204070 at 5-HT$_4$ receptors *in vitro*. *FASEB J.*, **8**, 533.

(Received January 23, 1995
Accepted March 28, 1995)

British Journal of Pharmacology (1995) 115, 1096-1102 © 1995 Stockton Press All rights reserved 0007-1188/95 $12.00

The *in vitro* pharmacology of ZM 241385, a potent, non-xanthine, A_{2a} selective adenosine receptor antagonist

[1]S.M. Poucher, J.R. Keddie, P. Singh, S.M. Stoggall, P.W.R. Caulkett, G. Jones & [2]M.G. Collis

Cardiovascular and Metabolism Department, ZENECA Pharmaceuticals, Mereside, Alderley Park, Macclesfield, Cheshire, SK10 4TG

1 This paper describes the *in vitro* pharmacology of ZM 241385 (4-(2-[7-amino-2-(2-furyl) [1,2,4]-triazolo[2,3-a][1,3,5]triazin-5-yl amino]ethyl) phenol), a novel non-xanthine adenosine receptor antagonist with selectivity for the A_{2a} receptor subtype.

2 ZM 241385 had high affinity for A_{2a} receptors. In rat phaeochromocytoma cell membranes, ZM 241385 displaced binding of tritiated 5'-N-ethylcarboxamidoadenosine (NECA) with a pIC_{50} of 9.52, (95% confidence limits, c.l., 9.02-10.02). In guinea-pig isolated Langendorff hearts, ZM 241385 antagonized vasodilatation of the coronary bed produced by 2-chloroadenosine (2-CADO) and 2-[*p*-(2-carboxyethyl) phenethylamino]-5'-N-ethylcarboxamidoadenosine (CGS21680) with pA_2 values of 8.57 (c.l., 8.45-8.68) and 9.02 (c.l., 8.79-9.24) respectively.

3 ZM 241385 had low potency at A_{2b} receptors and antagonized the relaxant effects of adenosine in the guinea-pig aorta with a pA_2 of 7.06, (c.l., 6.92-7.19).

4 ZM 241385 had a low affinity at A_1 receptors. In rat cerebral cortex membranes it displaced tritiated **R**-phenylisopropyladenosine (**R**-PIA) with a pIC_{50} of 5.69 (c.l., 5.57-5.81). ZM 241385 antagonized the bradycardic action of 2-CADO in guinea-pig atria with a pA_2 of 5.95 (c.l., 5.72-6.18).

5 ZM 241385 had low affinity for A_3 receptors. At cloned rat A_3 receptors expressed in chinese hamster ovary cells, it displaced iodinated aminobenzyl-5'-N-methylcarboxamido adenosine (AB-MECA) with a pIC_{50} of 3.82 (c.l., 3.67-4.06).

6 ZM 241385 had no significant additional pharmacological effects on the isolated tissues used in these studies at concentrations three orders of magnitude greater than those which block A_{2a} receptors. At 10 μM it displayed only minor inhibition of the bradycardic effects in guinea-pig atria to some concentrations of carbachol. At 10 μM, ZM 241385 had a small inhibitory effect on relaxant effects of isoprenaline in guinea-pig aortae but no effect on sodium nitrite-induced relaxation. ZM 241385 (100 μM) was without effect on phenylephrine-induced tone in guinea-pig aortae.

7 ZM 241385 (10 μM) had no inhibitory effect on rat hepatocyte phosphodiesterase types I, II, III and IV but caused a small inhibition of the calcium calmodulin-activated type I enzyme.

8 ZM 241385 is the most selective adenosine A_{2a} receptor antagonist yet described and is therefore a useful tool for characterization of responses mediated by A_2 adenosine receptors.

Keywords: Adenosine receptors: A_1 and A_2 receptors: A_2 antagonists; ZM 241385; (4-(2-[7-amino-2-(2-furyl) [1,2,4]triazolo[2,3-a][1,3,5]triazin-5-yl amino]ethyl) phenol)

Introduction

Adenosine P_1 purinoceptors were originally subdivided into A_1, which are coupled to adenylate cyclase in an inhibitory manner, and A_2, which are coupled to adenylate cyclase in a stimulatory manner (Londos & Wolff, 1977; Van Calker *et al.*, 1979; Bruns *et al.*, 1980). The A_2 receptor has been further subdivided into two classes (Daly, 1985) based upon the observations that some A_2 receptors have EC_{50} values for adenosine in the high nanomolar range and some in the micromolar range (Londos *et al.*, 1982). The high affinity A_2 receptor exists in the striatum and nucleus accumbens and their activation can be measured in broken cell adenylate cyclase assays, whereas the low affinity A_{2b} receptor exists in almost all areas of the brain and their activity can be measured by adenosine 3':5'-cyclic monophosphate (cyclic AMP) accumulation in brain slices, but not in broken cell preparations (Premont *et al.*, 1979). The high affinity, A_{2a} receptor was further characterized by [^{3}H]-5'-N-ethylcarboxamidoadenosine ([^{3}H]-NECA) binding in rat striatal membranes (Bruns *et al.*, 1986). The agonist, 2-[*p*-(2-carboxyethyl)-phenetylamino]-5'-N-ethyl-carboxamidoadenosine), CGS21680, displays higher affinity for the A_{2a} receptor than the A_{2b} (Jarvis *et al.*, 1989) and has been used widely to investigate and characterize the A_{2a} receptor subtype. More recently, an additional adenosine receptor sub-type (A_3) has been characterized (Abbracchio *et al.*, 1993; Collis & Hourani, 1994).

The search for selective adenosine receptor antagonists, which will enable a more complete understanding of the role of the various sub-types of adenosine receptor in physiological responses, has provided a significant challenge. The xanthine, PD115199 (1,3 dipropyl-8-N-[2-dimethylamino) ethyl]-*N*-methyl-4-2, 3, 6, 7-tetrahydro-2,6-dioxo) - benzenesulphonamidexanthine), although having higher affinity for the A_{2a} binding site than the A_{2b} binding site, is equipotent at A_{2a} and A_1 binding sites (Bruns *et al.*, 1987b). PD116948 (8-cyclopentyl-1-3-dipropylxanthine) has higher affinity for the A_1 receptor than for A_{2a} binding sites in rat brain studies (Bruns *et al.*, 1987a,b; Jarvis *et al.*, 1989) and clearly demonstrated A_1-selective antagonism in guinea-pig isolated tissues (Collis *et al.*, 1989). To date, the most A_{2a}-selective xanthine antagonist is 8-(3-chlorostyryl)-1,3-dipropylxanthine which in binding studies demonstrates A_{2a}:A_1 selectivity of 520 fold but only 22 fold in functional tests (Jacobson *et al.*, 1993). The compound is however, of limited utility, for functional assays due to its limited solubility (Jacobson *et al.*, 1993). A number of non-xanthine adenosine receptor antagonists have been described,

[1] Author for correspondence.
[2] Present address: Pfizer Central Research, Sandwich, Kent.

characterized primarily by binding studies. CGS15943 (5-amino-9-chloro-2-(2-furyl)-pyrazolo-[4,3-e]1,2,4-triazolo[1,5-c]quinazoline) has high affinity for the A_{2a} receptor (K_i 3 nM) but modest A_{2a}:A_1 selectivity (7 fold) (Williams *et al.*, 1987). Dionisotti *et al.* (1994) used CGS15943 as a chemical starting point for the synthesis of 5-amino-8-(4-fluorobenzyl)-2-(2-furyl)-pyrazolo-[4,3-e]1,2,4-triazolo[1.5-c]pyrimidine (8FB-PTP), which in binding assays has a K_i at A_2 receptors of 0.074 nM and 28 fold A_2:A_1 selectivity. However, in functional assays this compound loses its selectivity and is indeed modestly A_1 receptor-selective.

Therefore, based upon functional assays there are currently no A_{2a} selective, antagonists available. The following paper describes the *in vitro* pharmacology of ZM 241385 (4-(2-[7-amino-2-(2-furyl) [1,2,4]triazolo[2,3-a][1,3,5]triazin-5-yl amino]ethyl) phenol), a non-xanthine adenosine receptor antagonist. Affinity of the compound for A_{2a}, A_3 and A_1 binding sites was assessed in binding assays with membranes from a rat phaeochromocytoma (PC12) cell line (Williams *et al.*, 1986), rat cloned A_3 receptors expressed in chinese hamster ovary cell line (Olah *et al.*, 1994) and in rat cortex (Bruns *et al.*, 1987a) respectively. Evaluation of antagonism of adenosine receptor-mediated responses was further investigated in guinea-pig atria (A_1 receptor, Collis, 1983), guinea-pig Langendorff hearts (A_{2a} receptor, Ueeda *et al.*, 1991) and guinea-pig isolated aortae (A_{2b} receptor, Hargreaves *et al.*, 1991; Martin, 1992).

Methods

Ligand binding at the A_1 site in rat cerebral cortex

Alderley Park rats were killed by cervical dislocation and crude membranes from cerebral cortex were prepared by a modification of the method of Lohse *et al.* (1984). Briefly, the frontal cortex was removed and immediately homogenized in 50 mM Tris-HCl, pH 7.4. Membrane pellets were produced by a series of centrifugation and resuspension steps and finally resuspended in ice-cold buffer and stored under liquid nitrogen until required. Tritiated N^6(S-2-phenylisopropyl)adenosine (**R**-PIA, 35–60 Ci mmol^{-1}, final concentration 10 nM) binding studies were carried out in assay mixtures buffered with 50 mM Tris-HCl, pH 7.4 at room temperature. All studies were carried out in the presence of adenosine deaminase (2 u ml^{-1}) to remove endogenous adenosine.

For both the A_1 and A_{2a} binding assays the saturation isotherms were analysed with a binding analysis programme 'LIGAND' (Munson & Rodbard, 1980). The pIC_{50} was determined for all compounds.

Ligand binding at the A_{2a} site in rat PC12 cell membranes

PC12 cells were originally obtained from the Beatson Institute, Glasgow and were later maintained in the Tissue Culture Unit at ZENECA Pharmaceuticals. PC12 membranes were prepared by the same method as used for the cortex membranes, frozen and stored under liquid nitrogen until required. Binding studies were carried out by use of the same method as for the rat cortex but with tritiated NECA (50 µl, 20–40 Ci mmol^{-1}, final concentration 40 nM) instead of **R**-PIA (Hide *et al.*, 1991).

Ligand binding at the cloned rat A_3 receptor

The rat A_3 adenosine receptor was cloned and expressed into a CHO cell line as described by Zhou *et al.* (1992). Synthesis and radioligand binding of N^6-(3-[^{125}I]iodo-4-aminobenzyl-5′-N-methylcarboxamido adenosine ([^{125}I]-AB-MECA) assays for the rat A_3 receptor were undertaken as described previously (Olah *et al.*, 1994).

Adenosine A_1-receptor mediated chronotropic effects in guinea-pig atria

Dunkin Hartley guinea-pigs (male 250–400 g) were killed by cervical dislocation and their atria removed and immersed in Krebs solution. The atrial pairs were mounted in organ baths containing oxygenated Krebs solution (95% O_2/5% CO_2) at 37°C (Collis, 1983). The nucleoside transport inhibitor, dipyridamole (10 µM) was present in the Krebs solution since the agonist, 2-chloroadenosine (2-CADO) has been shown to be a substrate for the transporter (Collis & Brown, 1983; Jarvis *et al.*, 1985). Adenosine deaminase (2 u ml^{-1}) was added to remove endogenous tissue adenosine. The spontaneously beating atria were placed under a resting tension of 1 g and allowed to equilibrate for 50 min with continuous overflow. 2-CADO (range 0.01 µM–10 µM) was administered to produce a slowing of atrial rate before and after incubation of test compound for 30 min (ZM 241385, 3 µM–30 µM). The affinity of ZM 241385 (10 µM) for atrial muscarinic receptors was determined using carbachol (0.01 µM–3 µM) concentration-response curves.

Concentration-response curves to 2-CADO were plotted as % inhibition of rate against log concentration 2-CADO. Concentration-ratios were calculated from the EC_{50} concentration of 2-CADO in the absence and presence of a potential antagonist. The pA_2 values of each antagonist studied were determined by Schild plot analysis (Arunkalakshana & Schild 1959). Where the Schild plot slope was not significantly different from unity the slope gradient was constrained to one for generation of pA_2 values.

Adenosine A_{2b} receptor-mediated vasorelaxation in guinea-pig aortae

Sections (3–5 mm) of guinea-pig thoracic aorta were mounted (under 1 g resting tension) in organ baths containing oxygenated Krebs solution (95% O_2/5% CO_2) at 37°C, pre-contracted with 3 µM phenylephrine for assessment of adenosine receptor-mediated vasorelaxation responses (Collis & Brown, 1983). The nucleoside transport inhibitor, dipyridamole (10 µM) and the adenosine deaminase inhibitor erythro-9-(2-hydroxy-3-nonyl) adenine hydrochloride (EHNA, 10 µM) were present in the Krebs solution. Adenosine was added cumulatively (0.1 µM–1 mM) both before and after 30 min incubation with the test compound. The antagonists used did not affect the contractile response to phenylephrine. Additional concentrations of antagonist were investigated in fresh aortae. The specificity of ZM 241385 (10 µM) at the adenosine receptor, in this preparation, was determined by use of isoprenaline (1 nM–10 µM) and sodium nitrite (0.1 µM–1 mM) concentration-response curves before and after the adenosine antagonist.

Adenosine A_{2a}-receptor mediated vasodilatation in guinea-pig Langendorff hearts

Assessment of activity at functional A_{2a} receptors was undertaken as described by Ueeda *et al.* (1992) with some modifications. Male guinea-pigs (300–550 g) were killed and the heart rapidly removed and placed in cold, millipore-filtered modified (high potassium to arrest the contracting hearts) Krebs solution (composition in mM: NaCl 108, KCl 14.8, KH_2PO_4 1.2, $MgSO_4$ 1.2, $NaHCO_3$ 25, glucose 11, $CaCl_2$ 2.8, sodium pyruvate 2.2) i.e. equimolar substitution of KCl for NaCl. Contractions stopped within a few seconds and the heart was set up and perfused in the Langendorff mode with high potassium Krebs solution (at a temperature of 37°C and gassed with a mixture of 95% O_2/5% CO_2) at a constant flow rate of 3.5 ml min^{-1} and allowed to equilibrate for at least 20–45 min before the start of the experiment.

After equilibration, the coronary vasculature was constricted with an infusion of a near maximal dose of phenylephrine (0.3 µM) producing a coronary perfusion pressure of 55–60 mmHg which remained stable for 60 min. Concentra-

tion-response curves were then constructed to the adenosine analogues: NECA, CGS21680, 2-CADO and **R**-PIA. Antagonist potency was determined in paired Langendorff hearts. One group served as the vehicle control for responses to 2-CADO or CGS21680 whilst separate preparations were challenged with 2-CADO or CGS21680, 30 min following administration of a single concentration of antagonist.

Phosphodiesterase studies

The activity of ZM 241385 was determined against a range of phosphodiesterase enzymes from rat hepatocytes and compared with the activity of theophylline. Isolated hepatocytes were prepared from fed male Sprague Dawley rats and incubated as described by Heyworth *et al.* (1983). Cells (3–5 mg dry weight ml^{-1}) were pre-incubated at 37°C for 20 min, with constant gassing (95% O_2/5% CO_2), before use. Cyclic AMP phosphodiesterase activity was measured by a modification of the two-step procedure of Thompson & Appleman (1971). All assays were performed at 30°C in the presence of cyclic AMP (1 μM).

Compounds used

4-(2-[7-amino-2-(2-furyl) [1,2,4]triazolo[2,3-a][1,3,5]triazin-5-yl amino]ethyl) phenol (ZM 241385), 8-cyclopentyl-1-3-dipropylxanthine (PD116948), and 2-[*p*-(2-carboxyethyl)-phenetylamino]-5'-N-ethyl-carboxamidoadenosine (CGS21680) were synthesized by Dr Geraint Jones, Mr Peter Caulkett and Dr Mike Block at Zeneca Pharmaceuticals. Dipyridamole (Persantin) was obtained from Boehringer Ingelheim, Bracknell, UK. **R**-phenylisopropyladenosine (**R**-PIA), 5'-N-ethylcarboxamidoadenosine (NECA) and erythro-9-(2-hydroxy-3-nonyl) adenine hydrochloride (EHNA) were obtained from Research Biochemicals Inc. St Albans, Herts. Adenosine, 2-chloroadenosine (2-CADO), theophylline, 8-phenyltheophylline (8PT), 8-phenylsulphotheophylline (8PST), adenosine deaminase (Type IV), carbachol, isoprenaline, sodium nitrite and phenylephrine hydrochloride were all obtained from Sigma Chemical Co., Poole, Dorset. Tritiated NECA was obtained from Amersham International, Little Chalfont, Bucks. Tritiated **R**-PIA was obtained from New England Nuclear, Dreieich, Germany. ZM 241385 was made up in a stock solution at 10^{-2} M in dimethylsulphoxide (DMSO) and diluted with distilled water as required.

Results

Ligand binding at the A_1 site in rat cerebral cortex

The order of agonist affinity obtained for binding of agonist ligands in the rat cerebral cortex was **R**-PIA > NECA = 2-CADO > > CGS 21680 (Table 1), which is consistent with the binding site being of the A_1 subtype. The A_1-selective antagonist, PD116948, also displayed high affinity ($pIC_{50} = 8.34$) in this system, confirming the A_1 subtype binding site (Table 2). In contrast to PD116948, ZM 241385 displayed low affinity in competing with tritiated **R**-PIA ($pIC_{50} = 5.69$).

Ligand binding at the A_2 site in rat PC12 membranes

The order of agonist affinity obtained at the A_2 binding site in the PC12 membranes was NECA > CGS21680 > 2-CADO = **R**-PIA. This is consistent with the adenosine receptor high affinity A_{2a} binding site (Table 1). In competition studies the non-selective antagonists, 8PST and 8PT demonstrated relatively low affinity in competing with tritiated NECA from PC12 binding sites (Table 2). The A_1-selective antagonist, PD116948 ($pIC_{50} = 6.75$) was less potent than ZM 241385 ($pIC_{50} = 9.52$) which was clearly the most potent antagonist studied in this assay. In binding studies, ZM 241385 demonstrated A_{2a}:A_1 selectivity of 6,761 fold (range, 28,183–1,622).

Ligand binding at the cloned rat A_3 receptor

ZM 241385 displayed a very low affinity at the A_3 adenosine receptor cloned from rat and expressed in CHO cells with a pIC_{50} of 3.82 (c.l., 3.67–4.06, $n = 3$). The compound therefore demonstrated A_{2a}:A_3 selectivity of over 500,000 fold (range 2,218,196–91,200) in binding assays.

A_1 receptor antagonism in guinea-pig atria

The agonist potency order in the guinea-pig atria was **R**-PIA = NECA > 2-CADO > > CGS21680 (CGS21680 having a very low potency, EC_{50}, > 30,000 nM), consistent with A_1 receptor subtype (Table 1). 8PST and 8PT both demonstrated relatively low potency in the atria whereas PD116948 ($pA_2 = 8.40$) was the most potent of the xanthines at this receptor.

ZM 241385 demonstrated-concentration dependent, rightward parallel displacement of the 2-CADO concentration-response curve (Figure 1). The Schild plot slope was not different from unity (1.04); with the Schild slope constrained to 1 a pA_2 value of 5.95 (c.l., 5.72–6.18) was obtained.

A_{2b} receptor antagonism in guinea-pig aortae

The relative potency of the agonists i.e. NECA > 2-CADO > **R**-PIA confirms the presence of an A_2 receptor in the guinea-pig aorta; however, the lack of any significant activity of CGS21680 (Table 1) indicates that the A_2 receptor in this preparation is not of the A_{2a} subtype but is the A_{2b} subtype. 8PST and 8PT demonstrate low affinity in the aorta

Table 1 Comparison of the affinity and activity of selected adenosine receptor agonists in binding and functional assays

Agonists	*Rat cortex binding* IC_{50} *(nM)* ($n = 2-9$) Mean (c.l.)	*Rat PC12 binding* IC_{50} *(nM)* ($n = 2-9$) Mean (c.l.)	*G-pig atria* EC_{50} *(nM)* ($n = 4-12$) Mean (c.l.)	*G-pig aorta* EC_{30} *(nM)* ($n = 8-17$) Mean (c.l.)	*G-pig Langendorff* EC_{50} *(nM)* ($n = 4-7$) Mean (c.l.)
CGS21680	20,527 (20,520–20,534)	335 (331–339)	> 30,000	> 20,000	4.5 (3.2–7.9)
NECA	88 (55–121)	62 (61–63)	363 (190–708)	312 (255–369)	10.2 (7.9–15.8)
2-CADO	92	913	2570 (1202–5623)	3250 (2030–4470)	86.6 (65–115)
R-PIA	15.2 (12.4–17.9)	989 (983–995)	331 (95–1175)	9200 (7330–11070)	115.5 (100–158)

Mean values of potency for specific agonists are presented. Where the value has been determined three or more times the 95% confidence limit (c.l.) was calculated from the *t* value for 5% probability and the standard error of the mean value. For abbreviations, see text.

Table 2 Comparison of the affinity and activity of selected adenosine receptor agonists in binding and functional assays

Antagonists	*Rat cortex binding* pIC_{50} ($n=4$) Mean (c.l.)	*Rat PC12 binding* pIC_{50} ($n=2-6$) Mean (c.l.)	*G-pig atria* pA_2 ($n=6-15$) Mean (c.l.)	*G-pig aorta* pA_2 ($n=6-19$) Mean (c.l.)	*G-pig Langendorff* pA_2 *or* [pK_b] ($n=3-20$) Mean (c.l.)
8PST	NT	4.5	5.35 (5.14–5.55)	5.34 (5.21–5.48)	6.20 (5.99–6.42)
8PT	NT	4.5	6.30 (6.13–6.41)	6.50 (6.3–6.71)	NT
PD116948	8.34 (8.14–8.57)	6.75	8.40 (8.3–8.5))	6.69 (6.45–6.93)	[7.10] (6.96–7.15)
ZM 241385	5.69 (5.57–5.81)	9.52 (9.02–10.02)	5.95 (5.72–6.18)	7.06 (6.92–7.19)	8.57 (8.45–8.68)

All figures quoted for functional assays are pA_2 values determined by Schild plot analysis with the slope constrained to unity when not significantly different from unity. pK_b is the 'apparent' pK_b calculated as an estimate of antagonist potency when only a single concentration of antagonist was used and assumes that the antagonist behaves as a competitive antagonist with a Schild plot slope of unity. NT = not tested. For abbreviations, see text.

($pA_2 = 5.35$ and 6.03 respectively) which compares with their similar low affinity in the atria and confirms their non-selectivity at A_1 and A_2 receptors in functional models.

ZM 241385 produced rightward parallel displacements of the adenosine concentration-response curve, without any effect on the maximum response therefore showing competitive antagonism, giving a pA_2 value of 7.06 (c.l., 6.92–7.19, slope of 1.07 and constrained to unity) from the Schild Plot (Figure 2). Following ZM 241385, low concentrations of adenosine (<3 μM) resulted in a small, 20% increase in tone, likely to be due to activation of A_1 adenosine receptor subtypes (Stoggall & Shaw, 1990), before producing vasorelaxant activity.

A_{2a} receptor antagonism in guinea-pig Langendorff hearts

The potency order of agonists in lowering coronary perfusion pressure was CGS21680 > NECA > 2-CADO > **R**-PIA (Table 1). The adenosine receptor subtype involved in this response is therefore consistent with the A_{2a} sub-type.

The antagonist potencies in attenuating the effect of 2-CADO in this preparation (ZM 241385 > PD116948 > 8PST) parallel those seen in the PC12 binding studies (Table 2). 8PST ($pA_2 = 6.20$) demonstrated a relatively low affinity in all preparations whilst PD116948 demonstrated approximately a ten fold greater potency than 8PST in the Langendorff prepara-

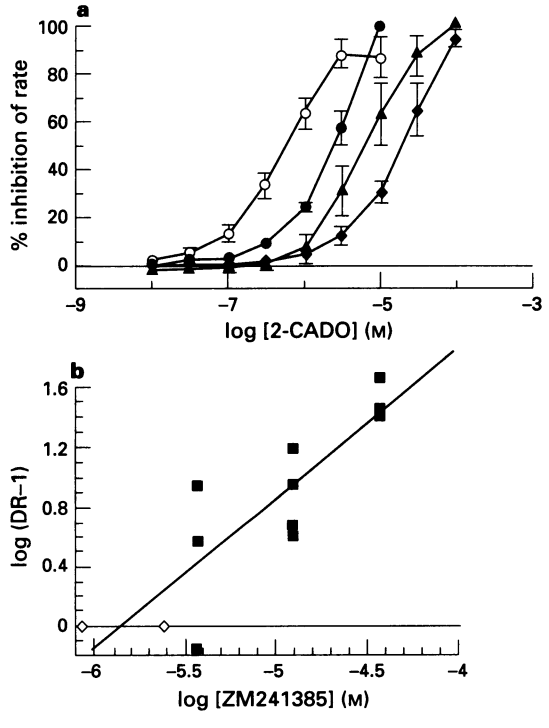

Figure 1 Effect of ZM 241385 on bradycardic effects of 2-CADO in guinea-pig isolated atria. (a) Each point represents the mean ± s.e.mean. Dose-response curve for 2-CADO in the absence (○) and presence of ZM 241385: 3×10^{-6} M (●), 10^{-5} M (▲) and 3×10^{-5} M (◆). (b) Schild regression plot for antagonism of 2-CADO-induced bradycardia in guinea-pig atria by ZM 241385 (◇ 95% confidence limits to the pA_2value).

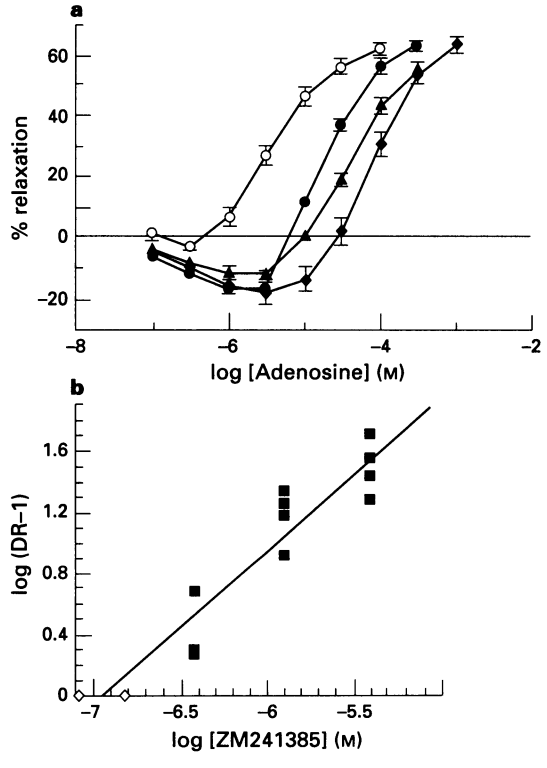

Figure 2 Effect of ZM 241385 on relaxant effects of adenosine in phenylephrine-constricted guinea-pig isolated aorta. (a) Each point represents the mean ± s.e.mean. Dose-response curve for 2-CADO in the absence (○) and presence of ZM 241385: 3×10^{-7} M (●), 10^{-6} M (▲) and 3×10^{-6} M (◆). (b) Schild regression plot for antagonism of adenosine-induced vasorelaxation in guinea-pig aorta by ZM 241385 (◇ 95% confidence limits to the pA_2value).

tion. The most potent antagonist however, was ZM 241385 which produced concentration-dependent parallel rightward shifts in the 2-CADO-mediated responses consistent with competitive antagonism ($pA_2 = 8.57$, c.l., 8.45–8.68, slope of 1.1, not different from unity, Figure 3).

ZM 241385 also showed high antagonist potency ($pA_2 = 9.02$, c.l., 8.80–9.20, slope 0.79, not different from unity) in attenuating the effects of the A_{2a} selective agonist CGS21680 in this guinea-pig Langendorff heart preparation, further demonstrating the selectivity of ZM 241385 for the A_{2a} receptor (Figure 4).

Specificity of ZM 241385

ZM 241385 (10 μM) produced a small (1.4 fold) rightward shift in the bradycardic response to the muscarinic agonist, carbachol, on guinea-pig aorta. ZM 241385 had no effect on relaxation induced by sodium nitrite, indicating lack of effect on cyclic GMP pathways at this concentration. ZM 241385 (100 μM) did not inhibit the constrictor effect of phenylephrine on guinea-pig aorta, indicating a lack of effect at α_1-adrenoceptors.

ZM 241385 (10 μM) was inactive against several rat hepatocyte cyclic AMP phosphodiesterase enzymes (Table 3); however, activity at this concentration was seen against the calcium/calmodulin activated type I phosphodiesterase. At a much higher concentration (1 mM i.e. 100,000 fold more than the pA_2 at the A_{2a} receptor) ZM 241385 inhibited a wider range of hepatocyte cyclic AMP phosphodiesterase isozymes. The effects of ZM 241385 were broadly similar to those of theophylline (Table 3).

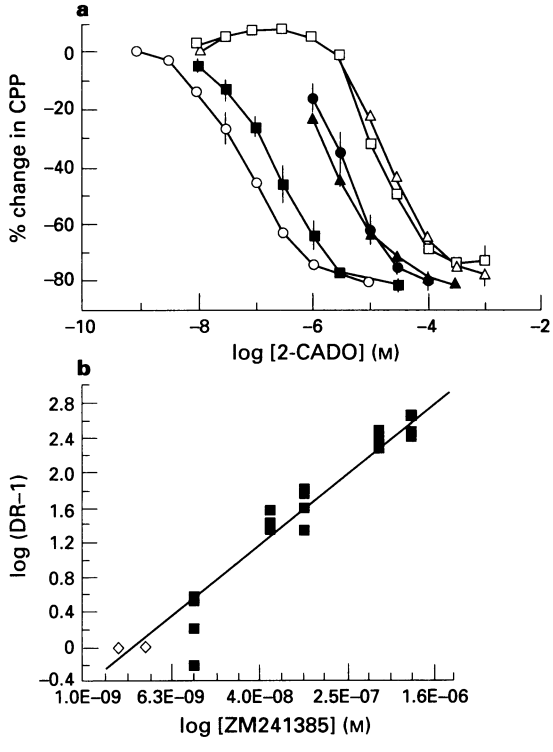

Figure 3 Effect of ZM 241385 on the vasorelaxant response of 2-CADO in phenylephrine-constricted, K^+-arrested, guinea-pig isolated Langendorff hearts. (a) Each point represents the mean ± s.e.mean, $n = 4$. Dose-response curve for 2-CADO in the absence (○) and presence of ZM 241385: 10^{-8} M (■), 5×10^{-8} M (▲), 10^{-7} M (●), 5×10^{-7} M (□) and 10^{-6} M (△). CPP = coronary perfusion pressure. (b) Schild regression plot for antagonism of 2-CADO-induced depressor response in guinea-pig Langendorff hearts by ZM 241385 (◇ 95% confidence limits to the pA_2 value).

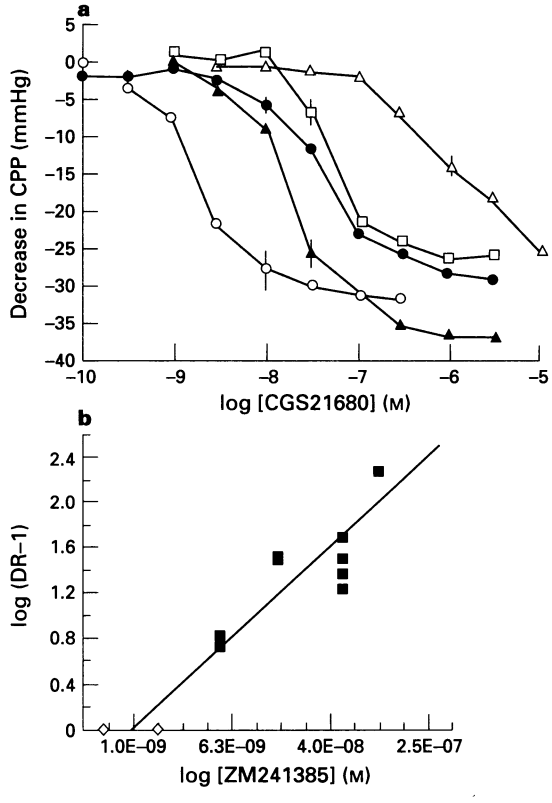

Figure 4 Effect of ZM 241385 on the vasorelaxant effects of the A_{2a}-selective agonist CGS21680 in phenylephrine-constricted, arrested, guinea-pig isolated Langendorff hearts. (a) Each point represents the mean ± s.e.mean, $n = 4$. Dose-response curve for CGS21680 in the absence (○) and presence of ZM 241385: 5×10^{-9} M (▲), 1.5×10^{-8} M (●), 5×10^{-8} M (□) and 10^{-7} M (△). CPP = coronary perfusion pressure. (b) Schild regression plot for antagonism of CGS 21680-induced depressor response in guinea-pig Langendorff hearts by ZM 241385 (◇ 95% confidence limits to the pA_2 value).

Table 3 Inhibition of hepatocyte cyclic AMP phosphodiesterases by ZM 241385 and theophylline

	Compound			
Isoform	*Theophylline* (1 mM)	*Theophylline* (10 μM)	*ZM 241385* (1 mM)	*ZM 241385* (10 μM)
IBMX-insensitive type I	NI	NI	NI	NI
Cyclic GMP-activated type II	59 ± 2	NI	47 ± 2	NI
Cyclic GMP-inhibited type III	NI	NI	NI	NI
Ca^{2+}/CaM-activated type I	30 ± 1	22 ± 2	73 ± 1	45 ± 3
Ro 1724-sensitive type IV	48 ± 2	NI	57 ± 3	NI

Results are the means (± standard error) from six determinations in three separate enzyme preparations. All assays were undertaken with a concentration of 1 μM cyclic AMP. NI, not inhibited (< 5% change in activity). For abbreviations, see text.

Discussion

The present data show that the non-xanthine, ZM 241385, is a competitive antagonist with high affinity (in the nanomolar range) at the adenosine A_{2a} receptor subtype. In addition, the compound has low affinity at the A_1 and A_3 receptor subtypes and shows 400–1000 fold selectivity for A_{2a} over A_1 receptors in isolated tissues from the guinea-pig and 6700 fold selectivity for A_{2a} over A_1 and 5000,000 fold selectivity for A_{2a} over A_3 binding sites.

In both binding and functional preparations containing A_{2a} receptors, ZM 241385 showed high affinity. Affinity of ZM 241385 in the PC12 membrane preparation was however an order of magnitude higher than when 2-CADO was used as the agonist in the guinea-pig Landendorff heart. This difference was less evident when CGS21680 was used in the guinea-pig Langendorff heart, ($pA_2 = 8.57$ with 2-CADO and 9.02 with CGS 21680). This implies a mixed population of A_{2a} and A_{2b} receptor subtypes in the guinea-pig heart, but this could not be detected by changes in the Schild plot slope (which was not different from unity for either agonist). ZM 241385 demonstrated low affinity in both A_1 preparations studied. In some studies, marked differences in affinity have been noted at A_1 receptors in ligand binding studies on cell membranes from different species (Ukena *et al.*, 1986). Although binding studies were performed only in rat membranes and functional studies were performed only in guinea-pig isolated preparations, no significant difference was noted between affinities calculated in rat and guinea-pig tissue. The lack of species difference observed for the affinity of ZM 241385 for A_1 and A_{2a} receptors suggests that it can be used to classify adenosine receptors in a number of species. Recently an A_3 receptor subtype, which induces hypotension, has been described based upon studies with N^6-2-(4-aminophenyl)ethyladenosine in pithed rats; the effect is resistant to antagonism with the xanthine, 8PST (Fozard & Carruthers, 1993). The affinity of ZM 241385 at the A_3 receptor was 500,000 fold lower than at the A_{2a} receptor subtype.

The degree of A_{2a} subtype selectivity shown by ZM 241385 exceeds that reported for other xanthine and non-xanthine adenosine receptor antagonists such as 8-(3-chlorostyryl)-1,3-dipropylxanthine, CGS15943 and 8FB-PTP. 8-(3-chlorostyryl)-1,3-dipropyl-xanthine, currently the most A_{2a}:A_1 selective antagonist described, was not tested in the current series of experiments, and therefore a direct comparison with it was not possible. In binding studies however 8-(3-chlorostyryl)-1,3-dipropyl-xanthine is reported to have a pK_i of 7.3 at A_{2a} sites on striatal membranes and A_{2a}:A_1 selectivity of 520 fold but is only 22 fold selective in functional tests (Jacobson *et al.*, 1993). In comparison, ZM 241385, was 19 times more selective than 8-(3-chlorostyryl)-1,3-dipropyl-xanthine in functional assays. In addition to its limited selectivity in functional studies, the lack of information of activity of 8-(3-chlorostyryl)-1,3-dipropyl-xanthine at A_{2b} receptor subtypes (Jacobson *et al.*, 1993) may limit the use of the compound in determining the individual A_2 adenosine receptor subtype contribution to either *in vitro* or *in vivo* functional responses. CGS 15943 has affinity for the A_{2a} receptor (K_i 3 nM) but only 7 fold A_{2a}:A_1 selectivity (Williams *et al.*, 1987). Although not assayed in all functional tests, we have found CGS 15943 to be equipotent in both atria (A_1) and aorta (A_{2b}) (pA_2 7.85, c.l., 7.59–8.10 and pA_2 7.56, c.l., 7.38–7.74 respectively, unpublished results) compared to 13 fold A_{2b}:A_1 selectivity seen with ZM 241385. Rollins *et al.* (1994) have also recently reported CGS 15943 to be 4 fold A_{2b}:A_1 selective in binding studies with cloned human receptors. In binding assays, 8FB-PTP which has a K_i at A_{2a} receptors of 0.074 nM and 28 fold A_{2a}:A_1 selectivity, loses all A_{2a} selectivity in functional assays (Dionisotti *et al.*, 1994). ZM 241385 had 30–80 fold selectivity for A_{2a} over A_{2b} receptors. ZM 241385 is not unique with respect to this selectivity as PD115199 has been reported to have a similar degree of selectivity for A_{2a} over A_{2b} receptors (Hargreaves *et al.*, 1991). PD115199 however shows little selectivity for A_{2a} relative to A_1 receptors (2.4 fold, Bruns *et al.*, 1987b).

ZM 241385 had no additional pharmacological effects at concentrations which blocked A_{2a} adenosine receptors. The minor inhibitory effects on carbachol-induced bradycardia and isoprenaline-induced aortic relaxation occurred at concentrations 3–4 orders of magnitude greater than those required to block A_{2a} receptors. A number of adenosine receptor antagonists inhibit a range of phosphodiesterases at concentrations close to those which block adenosine receptors, e.g. theophylline (Smellie *et al.*, 1979). ZM 241385 showed similar potency to theophylline as a cyclic AMP phosphodiesterase inhibitor, but because it is four orders of magnitude more potent than theophylline as an A_2 receptor antagonist (pA_2 for theophylline = 4.6) it is unlikely that phosphodiesterase inhibitory effects will complicate interpretation of its effects.

In conclusion, ZM 241385 is a novel, non-xanthine A_{2a}-selective adenosine receptor antagonist in binding studies in rat receptors and guinea-pig isolated tissue preparations. ZM 241385 is free of non-specific activity at concentrations several orders of magnitude greater than the pA_2 value for A_{2a} receptors. It is therefore, the most selective A_{2a} adenosine receptor antagonist yet described and should prove a useful tool with which to evaluate the role of A_{2a} adenosine receptors in pharmacological preparations.

We thank Laraine Redmond, Helen Musgrove and Helen Maddock for their technical assistance in undertaking the *in vitro* assays, Janet Holland and Kai Gait for technical assistance in running the binding assays, Dr Kenneth Jacobson (National Institute of Health, Bethesda, U.S.A.) for binding studies at rat A_3 receptors and Professor Miles Houslay (University of Glasgow) for assessing the compounds against hepatocyte cyclic AMP phosphodiesterases.

References

ABRACCHIO, M.P., CATTABENI, F., FREDHOLM, B.B. & WILLIAMS, M. (1993). Purinoceptor nomenclature: a status report. *Drug Dev. Res.*, **28**, 207–213.

ARUNKALAKSHANA, O. & SCHILD, H.O. (1959). Some quantitative use of drug antagonists. *Br. J. Pharmacol. Chemother.*, **14**, 48–58.

BRUNS, R.F., DALY, J.W. & SNYDER, S.H. (1980). Adenosine receptors in brain membranes: binding of N^6-cyclo-hexyl[^{3}H]adenosine and 1,3-diethyl-8-[^{3}H] phenylxanthine. *Proc Natl. Acad. Sci. U.S.A.*, **77**, 5547–5551.

BRUNS, R.F., FERGUS, J.H., BADGER, E.W., BRISTOL, J.A., SANTAY, L.A., HARTMAN, J.D., HAYS, B.J. & HUANG, C.C. (1987a). Binding of the A_1 selective adenosine antagonist 8-cyclopentyl-1,3-dipropylxanthine to rat brain membrane. *Naunyn-Schmied. Arch. Pharmacol.*, **335**, 59–63.

BRUNS, R.F., FERGUS, J.H., BADGER, E.W., BRISTOL, J.A., SANTAY, L.A., & HAYS, S.J. (1987b). PD115199: An antagonist ligand for adenosine A_2 receptors. *Naunyn-Schmied. Arch. Pharmacol.*, **335**, 64–69.

BRUNS, R.F., LU, G.H. & PUGSLEY, T.H. (1986). Characterisation of the A_2 adenosine receptor labelled by [^{3}H]NECA in striatal membranes. *Mol. Pharmacol.*, **29**, 331–346.

COLLIS, M.G. (1983). Evidence for an A_1 adenosine receptor in the guinea-pig atrium. *Br. J. Pharmacol.*, **78**, 207–212.

COLLIS, M.G. & BROWN, C.M. (1983). Adenosine relaxes the aorta by interacting with an A_2 receptor and an intracellular site. *Eur. J. Pharmacol.*, **96**, 61–69.

COLLIS, M.G. & HOURANI, S.M.O. (1994). Adenosine receptor subtypes. *Trends Pharmacol. Sci.*, **14**, 360–366.

COLLIS, M.G., STOGGALL, S.M. & MARTIN, F.M. (1989). Apparent affinity of 1,3-dipropyl-8-cyclopentylxanthine for adenosine A_1 and A_2 receptors in isolated tissues from guinea-pigs. *Br. J. Pharmacol.*, **97**, 1274–1278.

DALY, J.W. (1985). Adenosine receptors. *Adv. Cycl. Nucl. Prot. Phos. Res.*, **19**, 29–46.

DIONISOTTI, S., CONTI, A., SANDOLI, D., ZOCCHI, C., GATTA, F. & ONGINI, E. (1994). Effects of the new A_2 adenosine receptor antagonist 8FB-PTP, an 8 substituted pyrazolo-triazolo-pyrimidine, on *in vitro* functional models. *Br. J. Pharmacol.*, **112**, 659–665.

FOZARD, J.R. & CARRUTHERS, A.M. (1993). Adenosine A_3 receptors mediate hypotension in the angiotensin II-supported circulation of the pithed rat. *Br. J. Pharmacol.*, **109**, 3–5.

HARGREAVES, M.B., STOGGALL, S.M & COLLIS, M.G. (1991). Evidence that the adenosine receptor mediating relaxation in the dog lateral saphenous vein and guinea-pig aorta is of the A_{2b} subtype. *Br. J. Pharmacol.*, **102**, 198P.

HEYWORTH, B.E., WALLACE, A.V. & HOUSLAY, M. (1983). Insulin and glucagon regulate the activation of two distinct membrane bound cAMP phosphodiesterases in hepatocytes. *Biochem. J.*, **214**, 99–110.

HIDE, I., PADGETT, W.L., JACOBSON, K.A. & DALY, J.W. (1991). A_{2a} adenosine receptors from rat striatum and rat phaeochromocytoma PC12 cells: Characterisation with radioligand binding and by activation of adenylate cyclase. *Mol. Pharmacol.*, **41**, 352–359.

JACOBSON, K.A., NIKODIJEVIC, O., PADGETT, W.L., GALLO-RODRIGUEZ, C., MAILLARD, M. & DALY, J.W. (1993). 8-(3-chlorostyryl) caffeine (CSC) is a selective A_2-adenosine antagonist *in vitro* and *in vivo*. *FEBS Lett.*, **323**, 141–144.

JARVIS, S.M., MARTIN, B.W. & NG, A.S. (1985). 2-Chloroadenosine, a permeant for the nucleoside transporter. *Biochem. Pharmacol.*, **34**, 3237–3241.

JARVIS, M.F., SCHULZ, R., HUTCHINSON, A.J., DO, U.H., SILLS, M.A. & WILLIAMS, M. (1989). [^{3}H]CGS21680, a selective A_2 adenosine receptor agonist directly labels A_2 receptor in the brain. *J. Pharmacol. Exp. Ther.*, **251**, 888–893.

LOHSE, M.J., LENSCHOW, V. & SCHWABE, U. (1984). Interaction of barbiturates with adenosine receptors in rat brain. *Naunyn-Schmied. Arch. Pharmacol.*, **326**, 69–74.

LONDOS, C. & WOLFF, J. (1977). Two distinct adenosine-sensitive sites on adenylate cyclase. *Proc. Natl. Acad. Sci. U.S.A.*, **74**, 5482–5486.

LONDOS, C., WOLFF, J. & COOPER, D.M.F. (1982). Adenosine receptors and adenylate cyclase interactions. In *Regulatory Function of Adenosine*. ed. Berne, R.M., Rall, T.W. & Rubio R. pp. 17–32. Boston: Martinus Nijhoff.

MARTIN, P.L. (1992). Relative agonist potencies of C^2-substituted analogues of adenosine: evidence for adenosine A_{2b} receptors in the guinea-pig aorta. *Eur. J. Pharmacol.*, **216**, 235–242.

MUNSON, P.J. & RODBARD, D. (1980). LIGAND: a versatile computerised approach for characterisation of ligand-binding analysis. *Analyt. Biochem.*, **107**, 220–239.

OLAH, M.E., GALLO-RODRIGUEZ, C., JACOBSON, K.A. & STILES, G.L. (1994). ^{125}I-4-aminbenzyl-5'-N-methylcarboxamidoadenosine, a high affinity radioligand for the rat A_3 adenosine receptor. *Mol Pharmacol.*, **45**, 978–982.

PREMONT, J., PEREZ, G., BLANC, G., TASSIN, J.P., THIERRY, H.M., HERVE, D. & BOCKAET, J. (1979). Adenosine-sensitive adenylate cyclase in rat brain homogenates: kinetic characteristics, specificity, topographical, sub cellular, and cellular distribution. *Mol. Pharmacol.*, **16**, 790–804.

ROLLINS, P.J., TURNER, S.J., AKPOGUMA, C.I.O. & RAY, K.P. (1994). Characterisation of human adenosine type 1, 2a and 2b receptors expressed in CHO cells. *Biochem. Soc. Trans.*, **22**, 195S.

SMELLIE, F.W., DAVIS, C.W., DALY, J.W. & WELLS, J.N. (1979). Alkylxanthines: inhibition of adenosine elicited accumulation of cyclic AMP in brain slices and of brain phosphodiesterase inhibition. *Life Sci.*, **24**, 2475–2482.

STOGGALL, S.M. & SHAW, J.S. (1990). The coexistence of adenosine A_1 and A_2 receptors in guinea-pig aorta. *Eur. J. Pharmacol.*, **190**, 329–335.

THOMPSON, W.J. & APPLEMAN, M.M. (1971). Multiple cyclic nucleotide phosphodiesterase activity from rat brain. *Biochemistry*, **10**, 311–316.

UEEDA, M., THOMPSON, R.D., ARROYO, L.H. & OLSSON, R.A. (1991). 2-Alkoxyadenosines: Potent and selective agonists at the coronary artery A_2 adenosine receptor. *J. Med. Chem.*, **34**, 1334–1339.

UKENA, D., JACOBSON, K.A., PADGETT, W.L., AYALA, C., SHAMIM, M.T., KIRK, K.L., OLSSON, R. & DALY, J.W. (1986). Species differences in structure activity relationship of adenosine agonists and xanthine antagonists at brain A_1 adenosine receptors. *FEBS Lett.*, **209**, 122.

VAN CALKER, D., MULLER, M. & HAMPRECHT, B. (1979). Adenosine regulates via two different types of receptors, the accumulation of cAMP in cultured brain cells. *J. Neurochem.*, **33**, 999–1005.

WILLIAMS, M., ABREU, M. & NARONHA-BLOB, L. (1986). Adenosine (ADO) receptors in the PC12 phaeochromocytoma cell line; characterisation by radioligand binding. *Fed. Proc.*, **45**, 566.

WILLIAMS, M., FRANCIS, J., GHAI, G., BRAUNWALDER, A., PSYCHOYOS, S., STONE, G.A. & CASH, W.D. (1987). Biochemical characterisation of the triazoloquinazoline, CGS15943, a novel, non-xanthine adenosine antagonist. *J. Pharmacol. Exp. Ther.*, **241**, 415–420.

ZHOU, Q.-Y., LI, C., OLAH, M.E., JOHNSON, R.A., STILES, G.L. & CIVELLI, O. (1992). Molecular cloning and characterization of an adenosine receptor: The A3 adenosine receptor. *Proc. Natl. Acad. Sci. U.S.A.*, **89**, 7432–7436.

(Received January 23, 1995
Revised March 21, 1995
Accepted April 4, 1995)

British Journal of Pharmacology (1995) 115, 1103–1109 © 1995 Stockton Press All rights reserved 0007–1188/95 $12.00

[^{3}H]-lifarizine, a high affinity probe for inactivated sodium channels

A.C. MacKinnon, K.M. Wyatt, J.G. McGivern, R.D. Sheridan & [1]C.M. Brown

Department of Pharmacology, Syntex Research Centre, Research Avenue South, Heriot Watt University Research Park, Riccarton, Edinburgh, EH14 4AP

1 [^{3}H]-lifarizine bound saturably and reversibly to an apparently homogeneous class of high affinity sites in rat cerebrocortical membranes ($K_d = 10.7 \pm 2.9$ nM; $B_{max} = 5.10 \pm 1.43$ pmol mg^{-1} protein).

2 The binding of [^{3}H]-lifarizine was unaffected by sodium channel toxins binding to site 1 (tetrodotoxin), site 3 (α-scorpion venom) or site 5 (brevetoxin), Furthermore, lifarizine at concentrations up to 10 μM had no effect on [^{3}H]-saxitoxin (STX) binding to toxin site 1. Lifarizine displaced [^{3}H]-batrachotoxinin-A 20-α-benzoate (BTX) binding with moderate affinity (pIC_{50} 7.31 ± 0.24) indicating an interaction with toxin site 2. However, lifarizine accelerated the dissociation of [^{3}H]-BTX and decreased both the affinity and density of sites labelled by [^{3}H]-BTX, suggesting an allosteric interaction with toxin site 2.

3 The binding of [^{3}H]-lifarizine was voltage-sensitive, binding to membranes with higher affinity than to synaptosomes (pIC_{50} for cold lifarizine = 7.99 ± 0.09 in membranes and 6.68 ± 0.14 in synaptosomes). Depolarization of synaptosomes with 130 mM KCl increased the affinity of lifarizine almost 10 fold ($pIC_{50} = 7.86 \pm 0.25$). This suggests that lifarizine binds selectively to inactivated sodium channels which predominate both in the membrane preparation and in the depolarized synaptosomal preparation.

4 There was negligible [^{3}H]-lifarizine and [^{3}H]-BTX binding to solubilized sodium channels, although [^{3}H]-STX binding was retained under these conditions.

5 The potencies of a series of compounds in displacing [^{3}H]-lifarizine from rat cerebrocortical membranes correlated well with their affinities for inactivated sodium channels estimated from whole-cell voltage clamp studies in the mouse neuroblastoma cell line, N1E-115 ($r = 0.96$).

6 These results show that [^{3}H]-lifarizine is a high affinity ligand for neuronal sodium channels which potently and selectively labels a site, allosterically linked to toxin binding site 2, associated with inactivated sodium channels.

Keywords: Lifarizine; sodium channels; BTX; rat cortex; N1E-115 cells; patch-clamp; RS-87476; sodium currents; ligand binding

Introduction

Lifarizine (RS-87476) is a diphenylpiperazine analogue that is neuroprotective in a number of animal models of focal and global cerebral ischaemia (Alps *et al.*, 1990; Kucharczyk *et al.*, 1991; Brown *et al.*, 1993; 1994). Furthermore, lifarizine has shown early promise in a small-scale clinical trial designed to assess its safety and tolerance in the treatment of acute ischaemic stroke (Squire *et al.*, 1994). This neuroprotective action is thought to be mediated via an interaction of the compound with CNS voltage-gated sodium channels. Thus, lifarizine potently inhibits the neurotoxic effects of the sodium channel activator, veratridine, on rat cerebrocortical neurones in culture (May *et al.*, 1995) and exerts a potent voltage-dependent inhibition of neuronal sodium currents, an action that is mediated by a preferential interaction of lifarizine with inactivated sodium channels (McGivern *et al.*, 1995). This latter action is very similar to that produced by a number of other agents which are believed to exert their therapeutic actions via an inhibition of sodium currents. For example, local anaesthetics inhibit sodium currents by an interaction with the inactivated state of the channel (for review, see Catterall, 1987).

It has been recognised for some time that there is a good correlation between the abilities of many agents to inhibit sodium currents and their abilities to displace the sodium channel activator, [^{3}H]-batrachotoxin-A 20-α-benzoate (BTX), from its binding site (Postma & Catterall, 1984). BTX and other toxins have been used to probe sodium channel structure and function. A number of toxin binding sites have been defined for the sodium channel: tetrodotoxin (TTX) and saxitoxin (STX) bind to site 1 to inhibit sodium flux through the channel (Catterall, 1981); BTX, veratridine and aconitine bind to site 2 to induce persistent activation of the channel (Catterall, 1981; Hille *et al.*, 1987); the α-scorpion toxins and sea anemone toxins interact at site 3 to slow inactivation and potentiate the actions of toxins at site 2 (Lazdunski *et al.*, 1986); β-scorpion toxins bind to site 4 to induce a hyperpolarizing shift of the voltage-dependence of channel activation (Couraud *et al.*, 1982); the brevetoxins and the ciguatoxins bind to site 5, shift the voltage-dependence of channel activation and enhance the binding of toxins at sites 2 and 4 (Catterall & Risk, 1981; Poli *et al.*, 1986); pyrethroids and DDT act via a sixth unique site to cause persistent activation and also greatly enhance the binding of toxins to site 2 (Lombet *et al.*, 1988).

The local anaesthetic, tetracaine (Reith *et al.*, 1987), the putative local anaesthetic, PD85,639 (Thomsen *et al.*, 1993) and the anticonvulsant agent, phenytoin (Francis & Burnham, 1992), have been radiolabelled and used as probes to determine if they bind to novel sites on the voltage-gated sodium channel specific for the different therapeutic agents. Both classes of compounds allosterically interact with toxin site 2, although evidence suggests that local anaesthetic and anticonvulsant drugs do not bind to the same site on the sodium channel, as anticonvulsants (100 μM) do not compete for [^{3}H]-PD85,639 binding (Thomsen *et al.*, 1993) and local anaesthetics have very low affinity for [^{3}H]-phenytoin binding (Francis & Burnham, 1992). Recently the location of the anaesthetic receptor site in the pore of the sodium channel has been defined (Ragsdale *et*

[1] Author for correspondence.

al., 1994). In the present study we have characterized the binding of the cerebral anti-ischaemic agent, [^{3}H]-lifarizine, to rat brain sodium channels and have investigated the functional relevance of the binding site in electrophysiological experiments in voltage-clamped neuroblastoma cells.

Methods

[^{3}H]-lifarizine binding to rat cerebrocortical membranes

Male Sprague-Dawley rats (180–200 g) were decapitated and the cerebral cortex separated from other brain regions over ice. Membranes were prepared by homogenization in 25 volumes of ice-cold 50 mM Tris HCl (pH 7.4 at 25°C) with a Polytron PT 10 tissue disruptor. The homogenate was centrifuged at 48000 *g* for 15 min at 4°C. The pellet was resuspended in the same buffer and washed 3 times by resuspension and centrifugation. The final pellet was resuspended in Tris HCl buffer at an approximate protein level of 3 mg ml^{-1}, snap frozen in liquid N_2 and stored at –80°C until required. Binding assays were initiated by the addition of membrane protein (150–200 μg) to 50 mM Tris HCl (pH 7.4) containing 0.01% bovine serum albumin (BSA), 1 nM [^{3}H]-lifarizine and various concentrations of test drugs (500 μl final assay volume). Non-specific binding was determined in the presence of 1 μM lifarizine or 3 μM flunarizine. Reactions were incubated for 90 min at 25°C and bound ligand was separated from free by vacuum filtration through Whatman GF/B filters presoaked for 30 min in assay buffer containing 0.01% polyethylenimine. The filters were washed with 3 × 5 ml assay buffer and bound ligand was estimated by liquid scintillation spectrometry. Protein content was determined with protein assay kits (Pierce BSA) using BSA as the protein standard.

Initial experiments showed that [^{3}H]-lifarizine binding was linear up to 450 μg membrane protein and optimal between pH 6.0 and pH 7.8. Subsequently all assays were carried out with 150–200 μg membrane protein in 50 mM Tris HCl pH 7.4 containing 0.01% bovine serum albumin (BSA) to reduce non-specific binding. Under these conditions equilibrium was reached after 75 min with typical total binding values at 1 nM [^{3}H]-lifarizine of 2500–3000 d.p.m. and 65–70% specific binding.

[^{3}H]-BTX binding to rat cerebrocortical synaptosomes

Cerebral cortices from male Sprague-Dawley rats were roughly chopped and homogenized in a glass-Teflon hand-held homogenizer in approximately 10 volumes of ice-cold 0.32 M sucrose, 5 mM K_2HPO_4 (pH 7.4 at 4°C). The homogenate was centrifuged at 1000 *g* for 10 min, the pellet discarded and the supernatant centrifuged at 20000 *g* for 15 min. The resulting pellet was washed by resuspension in an equal volume of sucrose buffer and recentrifuged. The final pellet was suspended in a sodium-free assay buffer containing 50 mM HEPES, 5.4 mM KCl, 0.8 mM $MgSO_4$, 5.5 mM glucose and 130 mM choline chloride (pH 7.4 at 25°C). Binding assays were initiated by the addition of 150–200 μg synaptosomal protein to an assay buffer containing 1 μM TTX, 50 μg scorpion venom (*Leiurus quinquestriatus*), 5 nM [^{3}H]-BTX and various concentrations of test drugs (500 μl final volume). Non-specific binding was determined in the presence of 0.3 mM veratridine. Reactions were incubated for 90 min at 25°C and bound ligand was separated from free by vacuum filtration through GF/B filters. The filters were washed with 2 × 5 ml buffer (5 mM HEPES, 1.8 mM $CaCl_2$, 0.8 mM $MgSO_4$, 130 mM choline chloride, 0.01% BSA; pH 7.4 at 25°C) and bound ligand was estimated by liquid scintillation spectrometry.

[^{3}H]-lifarizine binding to rat cerebrocortical synaptosomes

To address the effects of depolarization on specific [^{3}H]-lifarizine binding to cerebrocortical synaptosomes, experiments were performed as described above for [^{3}H]-BTX binding to rat cortical synaptosomes or substituting KCl (130 mM) for choline chloride in the assay buffer to produce a depolarization of the preparation.

[^{3}H]-STX binding to rat cerebrocortical membranes

Cortical membranes were prepared as for the [^{3}H]-lifarizine binding assay (see above). Membrane protein (200–400 μg) was incubated with 1 nM [^{3}H]-STX in 500 μl assay buffer (50 mM Tris HCl, 0.01% BSA; pH 7.4) for 60 min at 25°C. Non-specific binding was determined in the presence of 1 μM TTX. Bound ligand was separated as described for [^{3}H]-lifarizine binding.

Solubilization and reconstitution into phospholipid vesicles

Membranes were prepared from 2 rat cortices (see above) in ice-cold 50 mM Tris HCl buffer (pH 7.4 at 25°C) containing 1 mM EGTA and the protease inhibitors, phenyl methyl sulphonyl fluoride (PMSF; 0.1 mM), iodoacetamide (1 mM), phenanthroline (1 mM) and pepstatin A (1 μM). Membrane protein (40–50 mg) was suspended in 20 ml 10 mM HEPES (pH 7.4) containing protease inhibitors, 100 mM KCl, phosphatidyl choline (0.25% w/v) and detergent (2.5% Triton X-100, 0.3% sodium cholate or 1% β-octyl glucoside). The mixture was stirred on ice for 15 min before centrifugation at 120000 *g* for 75 min at 4°C. Solubilized sodium channels were reconstituted into phosphatidylcholine: phosphatidylethanolamine (65%:35%) vesicles as previously described (Feller *et al.*, 1985).

Binding of [^{3}H]-STX, [^{3}H]-BTX or [^{3}H]-lifarizine (all at 1 nM) was carried out at 4°C for 15 min. Non-specific binding was determined with 1 μM TTX for [^{3}H]-STX binding, 0.3 mM veratridine for [^{3}H]-BTX binding and 1 μM lifarizine for [^{3}H]-lifarizine binding. Bound ligand was separated by filtration through GF/B filters which had been previously soaked overnight in 10% polyethylenimine in ice-cold solubilization buffer. Filters were washed twice with Tris HCl containing 0.01% BSA (pH 7.4 at 4°C) and bound ligand was estimated by liquid scintillation spectrometry.

Analysis of binding data

The radioligand displacement curves were analysed graphically to estimate the IC_{50} (concentration of inhibitor displacing 50% of specifically bound radioligand), using a non-linear least squares programme specially designed for the interpretation of sigmoidal concentration curves in terms of total and non-specific binding as well as inhibition constants and curve steepness. Equilibrium binding parameters (K_d and B_{max}) for [^{3}H]-lifarizine and [^{3}H]-BTX were obtained from competition experiments with various concentrations of unlabelled lifarizine and BTX (Deblasi *et al.*, 1989). Determination of dissociation kinetics was carried out at equilibrium by the addition of excess unlabelled drug or by dilution of the drug-receptor complex in 100 fold volume of assay buffer. The rate of radioligand dissociation was determined from a series of timed filtrations of the samples. The dissociation rate constant (K_{-1}) was calculated from the slope of the plot $\ln(B_t/B_0)$ *versus* time, where B_0 represents binding at time 0 (equilibrium) and B_t the binding at time t.

Electrophysiology

Voltage-dependent sodium currents were recorded from undifferentiated mouse neuroblastoma N1E-115 cells by conventional whole-cell voltage clamp techniques at room temperature (Hamill *et al.*, 1981). Cells were obtained from the European Collection of Animal Cell Cultures and used between passages 20–45. The following solutions were used to isolate sodium currents (values in mM): pipette – CsF 120, tetraethylammonium

Cl 10, NaCl 10, $CaCl_2$ 1, $MgCl_2$ 1, EGTA 11, HEPES (free acid) 10, adjusted to pH 7.3 with CsOH; extracellular – NaCl 145, KCl 3, $CaCl_2$ 1, $MgCl_2$ 1, $CdCl_2$ 0.5, HEPES (free acid) 10, D-glucose 5, adjusted to pH 7.3 with NaOH.

Cells were clamped at a holding potential of –100 mV and control sodium currents were evoked by 10 ms depolarizing steps to 0 mV. Following establishment of a stable current, cells were exposed to a single concentration of drug for 10 min. The membrane potential was then clamped to a conditioning potential of 0 mV for 20 s, after which it was returned to –100 mV and a series of test depolarizations to 0 mV were made to probe recovery from voltage-dependent block. The first test depolarization was elicited 2 s after the conditioning depolarization, with subsequent test depolarizations being evoked at a frequency of 0.2 Hz. Recovery from block followed an exponential time course which was fitted to the following function: relative $I_{Na} = 1–A.\exp(-t/\tau)$, were t is time (s), τ is the time constant of the exponential recovery (s) and A = 1–y intercept value (i.e. the extrapolated current amplitude immediately after the 20 s conditioning depolarization normalised to the pre-conditioning control current amplitude). The apparent dissociation constant (apparent K_b) of compounds for inactivated sodium channels was calculated from the following relation:

$$\text{apparent } K_b = \{(1/A)-1\}*[b] \quad (1)$$

where [b] is the concentration of drug applied. The drug concentrations used were determined empirically and were sufficient to inhibit the first post-conditioning test pulse by 50–90% (see Results for individual drug concentrations). Eq.1 was obtained by rearrangement of the logistic equation which states that $E = E_{max}* 1/(1 + K_b/[b])$, where E is the effect produced by drug b, and E_{max} is the maximum effect obtained. In the context of the present experiments, E_{max} is equal to 1 (i.e. complete inhibition of sodium current immediately after the conditioning depolarization), and E is equivalent to the term A in Eq.1. Note that Eq.1 does not incorporate a Hill coefficient, and therefore a bimolecular 1:1 reaction between the drug and its receptor on the inactivated state of the channel is assumed in the K_b estimation. This limitation arises from the use of a single concentration of drug and is explicitly acknowledged in the term 'apparent K_b'. Only those cells in which a monoexponential recovery from voltage-dependent block was observed were included in the data analysis.

Statistical analysis

Data are expressed as the mean ± s.e.mean. Significant differences ($P < 0.05$) were calculated by Student's t test.

Drugs and reagents Reagents used were of the highest analytical grade available. Lifarizine (piperazine 1-[diphenyl-methyl]-4-[(2-(4-methyl-phenyl)-5-methyl imidazol-4-yl)methyl]-trihydrochloride, KB-2796 (1-[*bis*(4-fluorophenyl) methyl]-4-(2,3,4-trimethoxybenzyl) piperazine-2HCl) and PD85,639 (α-(phenyl)-*N*-[3-(2,6-dimethyl-1-piperizinyl)-α-propyl]benzeneacetamide) were synthesized by the Recherche Syntex France or the Institute of Organic Chemistry, Syntex, Palo Alto, CA, U.S.A; [^{3}H]-lifarizine (17 Ci mmol^{-1}) was synthesized by Dr H. Parnes (Institute of Organic Chemistry, Syntex, Palo Alto, CA, U.S.A.); [^{3}H]-batrachotoxinin-A 20-α-benzoate (56 Ci mmol^{-1}; Du Pont, U.K.); [^{3}H]-saxitoxin (39 Ci mmol^{-1}; Amersham, U.K.); unlabelled batrachotoxin was kindly donated by Dr J Daly, NIH Bethesda; lidoflazine (Janssen); phenytoin sodium (Parke-Davis); dizocilpine (Research Biochemicals Inc.); brevetoxin (CalBiochem); aconitine, veratridine, lignocaine HCl, flunarizine, tetrodotoxin and scorpion venom (*Leiurus quinquestriatus*, Sigma V5251) (Sigma U.K.).

Results

[^{3}H]-lifarizine binding in rat cerebrocortical membranes

Bound [^{3}H]-lifarizine was potently displaced from cerebrocortical membranes by unlabelled lifarizine ($pIC_{50} = 7.99 \pm 0.09$, $n = 6$) with a Hill slope not significantly different from unity ($n_H = 0.87 \pm 0.08$, Student's two tailed t test). Figure 1 shows that [^{3}H]-lifarizine binding was rapidly reversed by the addition of 1 μM unlabelled lifarizine ($K_{-1} = 0.1002 \pm 0.0128$ min^{-1}; $n = 3$). Saturation studies revealed that [^{3}H]-lifarizine labelled a single class of sites in rat cerebrocortical membranes ($K_d = 10.7 \pm 2.9$ nM; $B_{max} = 5.10 \pm 1.43$ pmol mg^{-1} protein; $n = 5$; Figure 2).

Correlation of [^{3}H]-lifarizine and [^{3}H]-BTX binding

Cold lifarizine displaced [^{3}H]-BTX binding with moderate affinity (pIC_{50} 7.31 ± 0.24), suggesting an interaction with toxin site 2. Table 1 shows the affinities of a series of compounds for [^{3}H]-lifarizine binding to rat cerebrocortical membranes and [^{3}H]-BTX binding to rat cerebrocortical synaptosomes. There was a good correlation between the abilities of compounds to displace [^{3}H]-lifarizine and [^{3}H]-BTX ($r = 0.94$; Table 1 and Figure 3).

Influence of neurotoxins on [^{3}H]-lifarizine binding

Neurotoxins that interact with distinct toxin sites on the sodium channel were evaluated for their effect on [^{3}H]-lifarizine

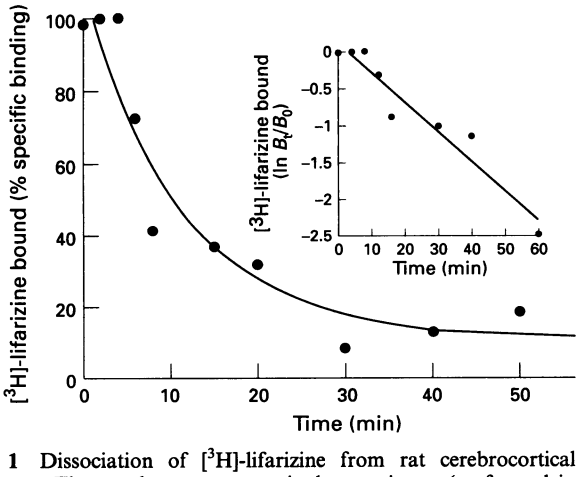

Figure 1 Dissociation of [^{3}H]-lifarizine from rat cerebrocortical membranes. The graph represents a single experiment (performed in triplicate). In this example, dissociation, initiated by the addition of 1 μM lifarizine, was rapid ($t_{1/2}$ = 6.5 min; $K_{-1} = 0.1068$ min^{-1}). Similar findings were obtained in two other experiments (see Results for mean values).

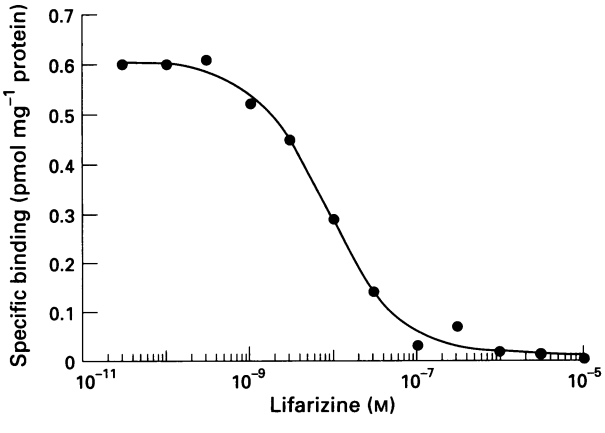

Figure 2 Saturation analysis of 1 nM [^{3}H]-lifarizine binding to rat cerebrocortical membranes. The graph represents a single experiment (performed in duplicate). The equilibrium binding constants in this example were: $K_d = 7.23$ nM and $B_{max} = 4.92$ pmol mg^{-1} protein. Similar findings were obtained in four other experiments (see Results for mean values).

Table 1 Affinity values for [^{3}H]-BTX binding to rat cerebrocortical synaptosomes and [^{3}H]-lifarizine binding to rat cerebrocortical membranes

	pIC_{50} [^{3}H]-BTX	n_H	pK_i [^{3}H]-lifarizine	n_H
Aconitine	6.29 ± 0.13	1.04 ± 0.09	5.47 ± 0.20	1.02 ± 0.09
Veratridine	5.44 ± 0.20	1.06 ± 0.12	4.67 ± 0.17	–
Phenytoin	4.69 ± 0.13	–	4.90 ± 0.12	–
Lignocaine	4.26 ± 0.21	–	4.48 ± 0.41	0.98 ± 0.09
PD85,639	6.59 ± 0.06	1.00 ± 0.11	6.43 ± 0.32	0.76 ± 0.10
Lidoflazine	7.25 ± 0.12	1.27 ± 0.25	7.52 ± 0.20	0.86 ± 0.11
Flunarizine	7.43 ± 0.21	0.99 ± 0.06	7.55 ± 0.15	0.89 ± 0.04
Lifarizine	7.31 ± 0.24	0.97 ± 0.07	8.03 ± 0.09	0.87 ± 0.08
KB-2796	7.34 ± 0.10	0.72 ± 0.15	7.70 ± 0.07	1.17 ± 0.27
Dizocilpine	5.32 ± 0.06	0.78 ± 0.09	5.31 ± 0.08	1.09 ± 0.16

Rat cerebrocortical synaptosomes ([^{3}H]-BTX) or membranes ([^{3}H]-lifarizine) were incubated with radioligand in the presence or absence of a range of concentrations of competing drug as described in Methods. The data represent the mean ± s.e.mean of at least 3 determinations performed in duplicate. The [^{3}H]-BTX affinities are presented as pIC_{50} values corrected for ligand concentration.

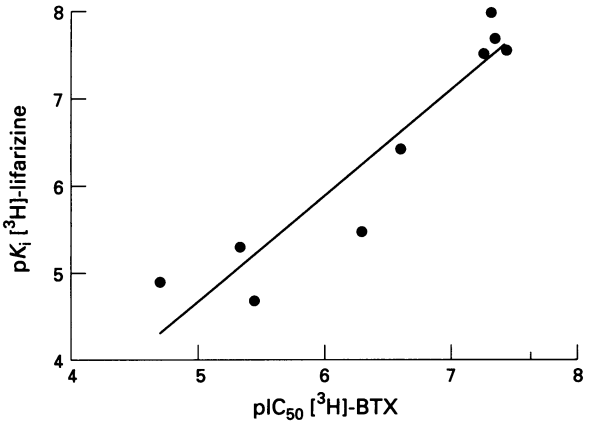

Figure 3 Correlation of binding affinity for [^{3}H]-lifarizine and [^{3}H]-BTX in rat cerebrocortical preparations. The data points are taken from Table 1. The solid line represents the line of best fit (r = 0.9, slope = 1.1).

Table 2 Effect of lifarizine on equilibrium binding of [^{3}H]-BTX to rat cerebrocortical synaptosomes

	n	K_d (nM)	B_{max} (pmol mg^{-1})
Control	8	509 ± 81	10.12 ± 1.99
Lifarizine 10 nM	3	364 ± 71	7.29 ± 0.94
30 nM	3	651 ± 293	6.13 ± 2.54
100 nM	3	856 ± 113*	4.69 ± 0.31*

Rat cerebrocortical synaptosomes were incubated with 5 nM [^{3}H]-BTX and unlabelled BTX (0.3 nM – 10 μM) in the presence or absence of lifarizine, as described in Methods. The data represent the mean ± s.e.mean of three determinations (performed in duplicate).
*P < 0.05, Student's t test.

binding (data not shown). The site 1 toxin, TTX (1 μM, n = 3), had no effect on [^{3}H]-lifarizine binding. Moreover, lifarizine, at concentrations up to 10 μM (n = 3), had no effect on [^{3}H]-STX binding to rat cerebrocortical membranes. α-Scorpion venom (up to 150 μg) and brevetoxin (10 μM) were similarly without effect on [^{3}H]-lifarizine binding. These data suggest that lifarizine does not interact with and is not influenced by toxin sites 1, 3 or 5.

Mechanism of interaction of lifarizine with the [^{3}H]-BTX binding site

The mechanism of the interaction of lifarizine with toxin site 2 was explored further by studying the effect of lifarizine on kinetic and equilibrium properties of [^{3}H]-BTX binding.

Saturation analysis of [^{3}H]-BTX binding revealed that this ligand bound to cerebrocortical synaptosomes in the presence of α-scorpion venom with K_d = 509 ± 81 nM and B_{max} = 10.12 ± 1.99 pmol mg^{-1} protein. Co-incubation with lifarizine (10, 30 or 100 nM) produced a concentration-dependent decrease in the affinity and density of sites labelled by [^{3}H]-BTX, both of which were statistically significant at 100 nM lifarizine (Table 2). These data indicated that the interaction of lifarizine with toxin site 2 is not competitive. In kinetic studies, the dissociation of [^{3}H]-BTX, initiated by an excess of the competitive inhibitor, veratridine (0.3 mM), was slow with K_{-1} = 0.00945 ± 0.00096 min^{-1} (n = 5; Figure 4). In the presence of a saturating concentration (1 μM) of lifarizine there was a small but significant increase in the dissociation rate of [^{3}H]-BTX (K_{-1} = 0.0139 ± 0.0018 min^{-1}, n = 5, P < 0.05). When [^{3}H]-BTX was dissociated by dilution of the bound ligand in 100 fold volume of incubation buffer, [^{3}H]-BTX dissociated very slowly, with less than 15% of the specific binding dissociated after 3 h (data not shown) at room temperature. Addition of lifarizine (1 μM) to the dilution buffer markedly accelerated the dissociation of [^{3}H]-BTX with more than 75% dissociated after 2 h and K_{-1} = 0.025 min^{-1} (n = 2; 0.0234 and 0.0265 min^{-1}).

Effect of depolarization

Electrophysiological experiments have demonstrated that the inhibitory effect of lifarizine on whole-cell sodium currents is markedly enhanced by membrane depolarization (McGivern *et al.*, 1995). We therefore examined the effect of KCl-induced depolarization on [^{3}H]-lifarizine binding to cerebrocortical synaptosomes. [^{3}H]-lifarizine binding to synaptosomes was of lower affinity than in membranes: pIC_{50} for unlabelled lifarizine = 7.99 ± 0.09 in membranes and 6.68 ± 0.14 in synaptosomes. However, depolarization of synaptosomes with 130 mM KCl increased the affinity of lifarizine almost 10 fold (pIC_{50} = 7.86 ± 0.25). Thus, [^{3}H]-lifarizine binding appears to be voltage-sensitive.

Solubilization and reconstitution studies

Rat cerebrocortical membranes were solubilized with Triton X-100, as described by Hartshorne & Catterall (1984). Phosphatidylcholine was included in the solubilization buffer because the presence of lipid has been found to increase greatly the stability of the α-subunit (Agnew & Raftery, 1979; Hartshorne & Catterall, 1981). Although the soluble preparation

retained [^{3}H]-STX binding, [^{3}H]-BTX and [^{3}H]-lifarizine binding were negligible under these conditions (Table 3). Solubilization of the membranes in other detergents (sodium cholate and β-octyl glucoside) also failed to produce consistently preparations retaining workable amounts of specific [^{3}H]-lifarizine and [^{3}H]-BTX binding (Table 3). When cholate-solubilized membranes were reconstituted into phosphatidylcholine: phosphatidylethanolamine vesicles, specific [^{3}H]-lifarizine binding was increased from 18±6% (n=3) to 53% (n=2; 48% and 58%).

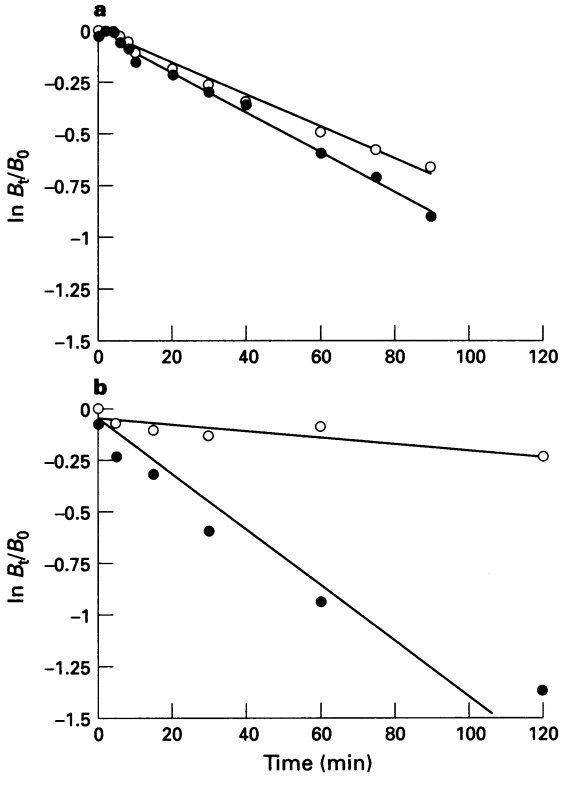

Figure 4 Dissociation of [^{3}H]-BTX from rat cerebrocortical synaptosomes. The two graphs are from separate experiments (performed in triplicate). Similar data were obtained in additional experiments (see Results from mean values). Assays were brought to equilibrium (90 min at 25°C) and dissociation was initiated either by addition of 0.3 mM veratridine (a) or by dilution of 100 fold volume of assay buffer (b). In (a), veratridine-induced dissociation was slow under control conditions (○ $t_{1/2}$=90 min and K_{-1}=0.00767 min^{-1}) but was accelerated by 1 μM lifarizine (● $t_{1/2}$=71 min and K_{-1} =0.00970 min^{-1}). In (b), dilution-induced dissociation was slow (control ○ $t_{1/2}$ >500 min) but was greatly accelerated by 1 μM lifarizine (● $t_{1/2}$=52 min and K_{-1}=0.0234 min^{-1}).

Table 3 Specific binding of [^{3}H]-STX, [^{3}H]-BTX and [^{3}H]-lifarizine to soluble rat cerebrocortical preparation

Detergent	*Ligand* [^{3}H]-STX	[^{3}H]-BTX	[^{3}H]-lifarizine
Triton X-100 (2.5%)	95±1	9±4	0
Cholate (0.3%)	76±8	31±15	18±6
β-Octyl glucoside (1%)	71±9	0	0

Binding of 1 nM ligand was determined with three different detergents at the concentrations indicated as described in Methods. The data represent the % specific binding of 1 nM ^{3}H-labelled ligand in each of the solubilized preparations and shown as the mean±s.e.mean of three determinations (performed in duplicate).

Functional relevance of the [^{3}H]-lifarizine binding site

The functional relevance of [^{3}H]-lifarizine binding was investigated by correlating the potency with which a series of compounds displaced [^{3}H]-lifarizine from rat cerebrocortical membranes with their apparent affinities for inactivated sodium channels estimated from whole-cell voltage clamp experiments in the mouse neuroblastoma cell line, N1E-115. The following compounds were included in the correlation: lifarizine (1 μM; n=4); flunarizine (1 μM; n = 4); KB-2796 (3 μM; n=3); PD85,639 (3 μM; n = 3); phenytoin (50 and 100 μM; n = 4 at each concentration); lignocaine (30, 100 and 300 μM; n = 1 at each concentration).

An example of the estimation of apparent K_b for lifarizine is illustrated in Figure 5. This shows the time-course of recovery from voltage-dependent block following a 20 s conditioning depolarization in the presence of 1 μM lifarizine. A mono-exponential fit to the data points yielded a y-intercept value of 0.145 (i.e. A = 0.855), giving an apparent K_b of 0.17 μM.

A correlation of apparent pK_b *versus* pK_i for displacement of bound [^{3}H]-lifarizine for all compounds tested is shown in

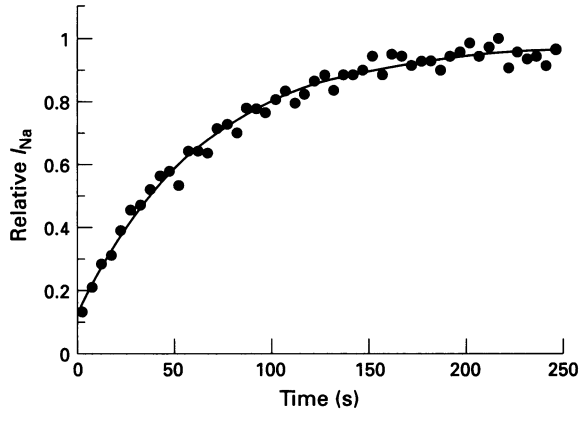

Figure 5 Recovery of sodium channels from voltage-dependent block. This graph shows recovery of sodium channels from voltage-dependent block in a single N1E-115 cell, exposed to 1 μM lifarizine. In this example, the data points are well-described by a mono-exponential function which gives an estimate for A of 0.855. The calculated apparent affinity (K_b) for the inactivated state of sodium channel is 0.17 μM.

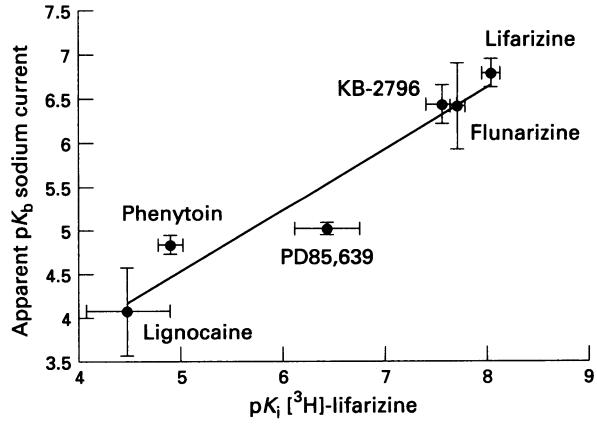

Figure 6 Correlation of apparent affinity for inactivated sodium channels with binding affinity for the [^{3}H]-lifarizine site. This graph shows the correlation of apparent affinity (pK_b) for the inactivated state of the sodium channel with affinity (pK_i) for the [^{3}H]-lifarizine site for a series of compounds (r = 0.96).

Figure 6. The correlation obtained ($r=0.96$) provides strong evidence that affinity for the [^{3}H]-lifarizine binding site is closely related to affinity for inactivated sodium channels.

Discussion

The present study demonstrates that [^{3}H]-lifarizine binds saturably and reversibly to a single class of high affinity (10.7 nM) sites on rat cerebrocortical membranes. The density of sites labelled by [^{3}H]-lifarizine was 5.1 pmol mg^{-1} protein, which is similar to the reported density of sodium channels in rat brain as determined by [^{3}H]-STX binding (4.9 pmol mg^{-1} protein; Catterall *et al.*, 1979), and to the density of sites labelled by other radioligands known to interact with the sodium channel ([^{3}H]-PD85,639: 5.2 pmol mg^{-1} protein, Thomsen *et al.*, 1993; [^{3}H]-phenytoin: 4.5 pmol mg^{-1} protein, Francis & Burnham, 1992; [^{3}H]-tetracaine: 5.2 pmol mg^{-1} protein, Reith *et al.*, 1987) and suggests a 1:1 stoichiometry for all these binding sites on the sodium channel. These results therefore provided initial circumstantial evidence that the site labelled by [^{3}H]-lifarizine is located on the sodium channel. Further support for this conclusion was provided by the finding that lifarizine displaced the site 2 sodium channel toxin, [^{3}H]-BTX, from rat cerebrocortical synaptosomes. Furthermore, there was a very good correlation between the ability of a series of compounds to displace [^{3}H]-BTX and their ability to displace [^{3}H]-lifarizine ($r=0.9$), implying that the sites labelled by the two ligands are in some way linked. However, unlike [^{3}H]-BTX binding, [^{3}H]-lifarizine binding was not influenced by α-scorpion venom or the site 5 toxin, brevetoxin both of which potentiate [^{3}H]-BTX binding, suggesting that the modes of interaction of the two radioligands with site 2 are dissimilar.

Lifarizine produced both a decrease in the affinity and the number of sites labelled by [^{3}H]-BTX. This suggests that the interaction of lifarizine with site 2 was allosteric in nature. The interaction with site 2 was probed further by examining the effect of lifarizine on the dissociation rate of [^{3}H]-BTX estimated by two methods: by initiating dissociation through addition of excess competitive agent (e.g. veratridine), or by diluting the [^{3}H]-BTX/channel complex in 100 fold volume of assay buffer. In the first method, as [^{3}H]-BTX dissociates its reassociation is prevented by the presence of excess veratridine. Any change in the dissociation rate that occurs in the presence of an additional compound (e.g. lifarizine) indicates that the compound is interacting at a site distinct from the [^{3}H]-BTX binding site. In these experiments, a saturating concentration of lifarizine (1 μM) accelerated the veratridine-induced [^{3}H]-BTX dissociation, suggesting that lifarizine interacts allosterically with toxin site 2. In the second method (diluting the [^{3}H]-BTX/channel complex at equilibrium), reassociation is also prevented since the free concentration of [^{3}H]-BTX is reduced 100 fold. With this method, lifarizine (1 μM) accelerated the dissociation of [^{3}H]-BTX, again suggesting an allosteric interaction. However, in the second method the effect of lifarizine was more marked because the control rate of [^{3}H]-BTX dissociation was much slower than in the first method. Indeed, dilution-induced [^{3}H]-BTX dissociation was negligible under control conditions. In a non-cooperative system similar dissociation rates ought to be obtained with the two experimental procedures. Negative cooperativity could be one explanation as to why the veratridine-induced dissociation of [^{3}H]-BTX was faster than the dilution-induced dissociation (in a negatively cooperative system, occupation of vacant sites by competing drug would decrease the overall affinity of the receptor population for radioligand and increase the rate of radioligand dissociation). An alternative explanation could be that veratridine does not act competitively at toxin site 2; however, there are data to suggest that it does (e.g. Catterall *et al.*, 1981). Further studies are required to elucidate which mechanism is operational here. Irrespective of which is operational, the data suggest that lifarizine acts allosterically to inhibit [^{3}H]-BTX binding. These kinetic data support the results from the equilibrium binding studies.

Solubilization of the sodium channel with Triton X-100, under the conditions described by Hartshorne & Catterall (1984), did not affect the binding of [^{3}H]-STX but abolished [^{3}H]-BTX and [^{3}H]-lifarizine binding. Subsequent attempts, with different detergents, also failed to produce a solubilized sodium channel which retained either [^{3}H]-BTX or [^{3}H]-lifarizine binding. These studies suggest that lifarizine, like BTX, requires the presence of phospholipids to maintain the channel in its native conformation. CNS sodium channels are composed of an α subunit and two β subunits (β1 and β2). The presence of the β1 subunit has been shown, in reconstitution studies, to stabilize the functional state of purified brain sodium channels in detergent solution and to be required for [^{3}H]-BTX binding (Isom *et al.*, 1994). Initial studies have shown that the binding of [^{3}H]-lifarizine was greatly increased in reconstituted sodium channel preparations and in CHO-K1 cells expressing the α and β1 subunits but not in cells expressing the α subunit only (N.P. Gillard & C.M. Brown, unpublished data). This lends further support to the idea that the channel needs to be in its native conformation for [^{3}H]-lifarizine binding to occur.

The electrophysiological experiments were undertaken in an effort to determine the functional relevance of the [^{3}H]-lifarizine binding site. Previous studies of the inhibitory effect of lifarizine on whole-cell sodium currents in N1E-115 cells have established that the inhibition is mediated by a preferential interaction of the compound with inactivated sodium channels (McGivern *et al.*, 1995). The present whole-cell voltage clamp experiments were designed to estimate the affinities of a series of sodium channel blocking agents for inactivated sodium channels in N1E-115 cells. Six compounds were examined and their apparent dissociation constants for inactivated channels ranged from 85 μM (lignocaine) to 0.17 μM (lifarizine). The apparent dissociation constants of the six compounds, as determined by an electrophysiological method, correlated remarkably well with their potencies in displacing [^{3}H]-lifarizine from rat cerebrocortical membranes ($r=0.96$), strongly suggesting that [^{3}H]-lifarizine labels a site on the channel associated with the inactivated state. This was further supported by the finding that the affinity of [^{3}H]-lifarizine in rat cerebrocortical synaptosomes under depolarized conditions (130 mM K^+, which completely depolarizes synaptosomes, e.g. Catterall *et al.*, 1981) was some 10 fold higher than under normal conditions. Indeed, the affinity of [^{3}H]-lifarizine in depolarized synaptosomes was similar to its affinity in cerebrocortical membranes. The most likely explanation for these findings is that lifarizine binds selectively to inactivated sodium channels, since these will predominate both in the membrane preparation and in the depolarized synaptosomal preparation. The lower affinity of [^{3}H]-lifarizine in non-depolarized synaptosomes may be due to a proportion, albeit unknown, of the sodium channels in this preparation being in the resting state, for which lifarizine has very low affinity (McGivern *et al.*, 1995).

Electrophysiological studies have demonstrated that lifarizine has negligible interaction with the open state of the sodium channel (McGivern *et al.*, 1995). In contrast, [^{3}H]-BTX interacts preferentially with open sodium channels (Catterall, 1980). The possibility that [^{3}H]-lifarizine and [^{3}H]-BTX interact with different states of the channel is highlighted by the abilities of α-scorpion venom and brevetoxin to enhance [^{3}H]-BTX binding by inducing an open (BTX-preferring) state of the channel, but not [^{3}H]-lifarizine binding. Inhibition of [^{3}H]-BTX binding by lifarizine may reflect a conformational change of the channel from the 'open' state, resulting in the channel being in a low affinity state for [^{3}H]-BTX. The allosteric inhibition of [^{3}H]-BTX binding may therefore be explained by an ability of lifarizine to stabilize the inactivated state of the sodium channel (as demonstrated in electrophysiological studies).

In conclusion, the present study has shown that [^{3}H]-lifarizine binds with high affinity to a site allosterically linked to toxin binding site 2 on the CNS voltage-sensitive sodium channel. Taken together, the electrophysiological and ligand binding data suggest that this site is associated with an inactivated state of the channel.

References

AGNEW, W.S. & RAFTERY, M.A. (1979). Solubilized tetrodotoxin binding component from the electroplax of *Electrophorus electricus*. Stability as a function of mixed lipid-detergent micelle composition. *Biochem.*, **18,** 1912–1919.

ALPS, B., CALDER, C., WILSON, A. & PASCAL, J.-C. (1990). Cerebral protection with a novel calcium blocker in rats. *Proc. XXth Intl. Cong. Med.* (ISIM Satellite), Stockholm, Sweden.

BROWN, C.M., CALDER, C., ALPS, B.J. & SPEDDING, M. (1993). The effect of lifarizine (RS-87476), a novel sodium and calcium channel modulator, on ischaemic dopamine depletion in the corpus striatum of the gerbil. *Br. J. Pharmacol.*, **109,** 175–177.

BROWN, C.M., SMALL, C., CALDER, C. & PATMORE, L. (1994). Neuroprotective properties of lifarizine (RS-87476) in a mouse model of focal ischaemia. *Can. J. Physiol. Pharmacol.*, **72** (Suppl. 1), 435.

CATTERALL, W.A. (1980). Neurotoxins that act on voltage-sensitive sodium channels in excitable membranes. *Annu. Rev. Pharmacol. Toxicol.*, **20,** 15–43.

CATTERALL, W.A. (1981). Localization of sodium channels in cultured neural cells. *J. Neurosci.*, **1,** 777–783.

CATTERALL, W.A. (1987). Common modes of drug action on Na^+ channels: local anesthetics, antiarrhythmics and anticonvulsants. *Trends Pharmacol. Sci.*, **8,** 57–65.

CATTERALL, W.A., MORROW, C.S., DALY, J.W. & BROWN, G.B. (1981). Binding of batrachotoxinin-A 20-α-benzoate to a receptor site associated with sodium channels in synaptic nerve ending particles. *J. Biol. Chem.*, **256,** 8922–8927.

CATTERALL, W.A., MORROW, C.S. & HARTSHORNE, R.P. (1979). Neurotoxin binding to receptor sites associated with voltage-sensitive sodium channels in intact, lysed and detergent-solubilised brain membranes. *J. Biol. Chem.*, **254,** 11379–11387.

CATTERALL, W.A. & RISK, M. (1981). Toxin T4(6) from *Ptychodiscus brevis* (formerly *Gymnodinium breve*) enhances activation of voltage-sensitive sodium channels by veratridine. *Mol. Pharmacol.*, **19,** 345–348.

COURAUD, F., JOVER, E., DUBOIS, J.M. & ROCHAT, H. (1982). Two types of scorpion receptor sites, one related to the activation, the other to the inactivation of the action potential sodium channel. *Toxicon*, **20,** 9–16.

DEBLASI, A., O'REILLY, K. & MOTULSKY, H.J. (1989). Calculating receptor number from binding experiments using same compound as radioligand and competitor. *Trends Pharmacol. Sci.*, **10,** 227–229.

FELLER, D.J., TALVENHEIMO, J.A. & CATTERALL, W.A. (1985). The sodium channel from rat brain. Reconstitution of voltage-dependent scorpion toxin binding in vesicles of defined lipid composition. *J. Biol. Chem.*, **260,** 11542–11547.

FRANCIS, J. & BURNHAM, W.M. (1992). [^{3}H]-phenytoin identifies a novel anticonvulsant-binding domain on voltage-dependent sodium channels. *Mol. Pharmacol.*, **42,** 1097–1103.

HAMILL, O.P., MARTY, A., NEHER, E., SAKMANN, B. & SIGWORTH, F.J. (1981). Improved patch-clamp techniques for high-resolution current recording from cells and cell-free membrane patches. *Pflügers Arch.*, **391,** 85–100.

HARTSHORNE, R.P. & CATTERALL, W.A. (1981). Purification of the saxitoxin receptor of the sodium channel from rat brain. *Proc. Natl. Acad. Sci. U.S.A.*, **78,** 4620–4624.

HARTSHORNE, R.P. & CATTERALL, W.A. (1984). The sodium channel from rat brain: purification and subunit composition. *J. Biol. Chem.*, **259,** 1667–1675.

HILLE, B., LEIBOWITZ, M.D., SUTRO, J.B., SCHWARZ, J.R. & HOLAN, G. (1987). State-dependent modification of sodium channels by lipid-soluble agonists. *Soc. Gen. Physiol. Series*, **41,** 109–124.

ISOM, L.L., DEJONGE, K.S. & CATTERALL, W.A. (1994). Auxiliary subunits of voltage-gated ion channels. *Neuron*, **12,** 1183–1194.

KUCHARCZYK, J., MINTOROVITCH, J., MOSELEY, M.E., ASGARI, H.S., SEVICK, R.J., DERUGIN, N. & NORMAN, D. (1991). Ischemic brain damage: reduction by sodium-calcium ion channel modulator RS-87476. *Radiology*, **179,** 221–227.

LAZDUNSKI, M., FRELIN, C., BARHANIN, J., LOMBET, A., MEIRI, H., PAURON, D., ROMEY, G., SCHMID, A., SCHWEITZ, H., VIGNE, P. & VIJVERBERG, H.P.M. (1986). Polypeptide toxins as tools to study voltage-sensitive sodium channels. *Ann. N.Y. Acad. Sci.*, **479,** 204–220.

LOMBET, A., MOURRE, C. & LAZDUNSKI, M. (1988). Interaction of insecticides of the pyrethroid family with specific binding sites on the voltage-dependent sodium channel. *Brain Res.*, **459,** 44–53.

MAY, G.R., ROWAND, W.S., MCCORMACK, J.G. & SHERIDAN, R.D. (1995). Neuroprotective profile of lifarizine (RS-87476) in rat cerebrocortical neurones in culture. *Br. J. Pharmacol.*, **114,** 1365–1370.

MCGIVERN, J.G., PATMORE, L. & SHERIDAN, R.D. (1995). Actions of the novel neuroprotective agent, lifarizine (RS-87476), on voltage-dependent sodium currents in the neuroblastoma cell line, N1E-115. *Br. J. Pharmacol.*, **114,** 1738–1744.

POLI, M.A., MENDE, T.J. & BADEN, D.G. (1986). Brevetoxins, unique activators of voltage-sensitive sodium channels, bind to specific sites in rat brain synaptosomes. *Mol. Pharmacol.*, **30,** 129–135.

POSTMA, S.W. & CATTERALL, W.A. (1984). Inhibition of binding [^{3}H]-batrachotoxinin-A 20-α-benzoate to sodium channels by local anesthetics. *Mol. Pharmacol.*, **25,** 219–227.

RAGSDALE, D.S., MCPHEE, J.C., SCHEUER, T. & CATTERALL, W.A. (1994). Molecular determinants of state-dependent block of Na^+ channels by local anesthetics. *Science*, **265,** 1724–1728.

REITH, M.E.A., KIM, S.S. & LAJTHA, A. (1987). Binding sites for [^{3}H]-tetracaine in synaptosomal sodium channel preparations from mouse brain. *Eur. J. Pharmacol.*, **143,** 171–178.

SQUIRE, I.B., LEES, K.R., PRYSE-PHILLIPS, W., KERTESZ, A. & BAMFORD, J. (1994). Efficacy and tolerability of lifarizine in acute ischaemic stroke: a pilot study. *Second Intl. Conf. on Neuroprotective Agents*, (Satellite to XIIth IUPHAR Conference, Montreal).

THOMSEN, W., HAYS, S.J., HICKS, J.L., SCHWARZ, R.D. & CATTERALL, W.A. (1993). Specific binding of the novel Na^+ channel blocker PD85,639 to the α-subunit of rat brain Na^+ channels. *Mol. Pharmacol.*, **43,** 955–964.

(Received January 13, 1995
Revised March 24, 1995
Accepted April 4, 1995)

British Journal of Pharmacology (1995) 115, 1110-1116 © 1995 Stockton Press All rights reserved 0007-1188/95 $12.00

Pharmacological profile of the novel P_{2T}-purinoceptor antagonist, FPL 67085 *in vitro* and in the anaesthetized rat *in vivo*

[1]R.G. Humphries, W. Tomlinson, J.A. Clegg, *A.H. Ingall, *N.D. Kindon & P. Leff

Departments of Pharmacology & *Medicinal Chemistry, Fisons plc, Pharmaceutical Division, Research & Development Laboratories, Bakewell Road, Loughborough, Leics LE11 0RH

1 The role of endogenous ADP in platelet aggregation *in vivo* remains unclear due to the lack of suitable P_{2T}-antagonist probes. This paper describes the potency, selectivity and specificity of the novel P_{2T}-purinoceptor antagonist, FPL 67085 (2-propylthio-D-β,γ-dichloromethylene ATP) both *in vitro* and in the anaesthetized rat *in vivo*.

2 FPL 67085 (3-30 nM) produced concentration-dependent rightward displacement of the concentration-effect (E/[A]) curve for ADP-induced aggregation of human washed platelets with no effect on ADP-independent aggregation at $\leqslant$ 10 μM.

3 Logistic fitting of ADP E/[A] data indicated that the antagonist effect of FPL 67085 did not consistently accord with simple competition: in some preparations depression of the asymptote was seen. Schild analysis of data combined from all preparations, regardless of the antagonist profile observed, gave an apparent pK_B of 8.9 (slope parameter 0.90).

4 The potency of FPL 67085 was unaffected by the P_1-purinoceptor antagonist, 8-sulphophenyltheophylline, was similar (IC_{50} 0.6-3.8 nM) in human and rat washed platelets or whole blood and, in rat blood, did not change following 2-30 min incubation at 37°C.

5 FPL 67085 was a weak ($pA_{50} \sim 4.2$) partial agonist in tissues containing P_{2X}- or P_{2Y}-purinoceptors, indicating some 30,000 fold selectivity for the P_{2T}-subtype.

6 In anaesthetized rats, intravenous infusion of FPL 67085 produced rapidly-reversible, dose-related inhibition of ADP-induced platelet aggregation measured *ex vivo* (ID_{50} 1.3 μg kg^{-1} min^{-1}) with no significant effect on haemodynamics or circulating cell counts.

7 Thus, FPL 67085 is a potent, specific and selective inhibitor of ADP-induced platelet aggregation both *in vitro* and *in vivo*. As such, it represents a novel pharmacological tool to define the role of endogenous ADP in thrombosis and the potential of P_{2T}-purinoceptor antagonists as a novel class of infusible anti-thrombotic agents for acute use in man.

Keywords: FPL 67085; P_{2T}-purinoceptor antagonist; ADP; platelet aggregation; human platelets; rat platelets; whole blood aggregation

Introduction

Platelet aggregation plays a pivotal role in normal haemostasis and in arterial thrombosis and is implicated in the pathogenesis of myocardial infarction, unstable angina and stroke and in the thrombotic complications of acute interventions such as thrombolysis and angioplasty (Fuster *et al.*, 1992). A role for adenosine diphosphate (ADP) in thrombosis and haemostasis was postulated over 20 years ago (Gaarder *et al.*, 1961). ADP-induced platelet aggregation can be demonstrated *in vitro* in platelet-rich plasma (PRP), suspensions of washed platelets and in whole blood (Born, 1962; Born & Cross, 1964; Cardinal & Flower, 1980) and *in vivo* upon intravenous (i.v.) administration of exogenous ADP to anaesthetized animals (Page *et al.*, 1982). However, the contribution of endogenous ADP to platelet aggregation *in vivo*, and hence to arterial thrombosis, has remained poorly defined. This has been due largely to the lack of potent and selective antagonists for P_{2T}-purinoceptors, the receptor which subserves the effect of ADP on platelets (Gordon, 1986). While adenosine triphosphate (ATP) is a competitive P_{2T}-purinoceptor antagonist (Macfarlane & Mills, 1975), it is, by definition, a non-selective P_2-purinoceptor ligand and is metabolically unstable. These properties limit the use of ATP in receptor classification studies *in vitro* and make it quite unsuitable as a probe for evaluating the contribution of endogenous ADP to platelet aggregation and thrombosis *in vivo*.

In a previous paper (Humphries *et al.*, 1994b), we described the pharmacology of the novel ATP analogue, FPL 66096, a potent (pK_B 8.7) P_{2T}-purinoceptor antagonist in preparations of human washed platelets with some 9000 fold selectivity for the P_{2T}-subtype compared to vascular P_{2X}- and P_{2Y}-purinoceptors *in vitro*. FPL 66096 is one of a series of novel compounds in which the anhydride link between the β and γ phosphates of ATP is replaced with a methylene link. This modification substantially reduces susceptibility of nucleotides to metabolism by ectonucleotidase enzymes (Welford *et al.*, 1986) and, therefore, makes possible investigation of the effect of selective P_{2T}-purinoceptor antagonism *in vivo* without the attendant complication of liberation of potential P_{2T}-purinoceptor agonists (the corresponding ADP-analogues). From the same series of compounds, FPL 67085 (2-propylthio-D-β,γ-dichloromethylene ATP) (Figure 1) was selected for evaluation *in vivo* and a preliminary report of our findings has been presented elsewhere (Humphries *et al.*, 1994a). In the present paper, we provide a more detailed account of the pharmacological profile of FPL 67085 both *in vitro* and *in vivo*.

Methods

Platelet aggregation in vitro

Blood sampling Blood was obtained from healthy male and female human volunteers by venepuncture or by cardiac puncture from male Sprague-Dawley rats (510-670 g, Charles

[1]Author for correspondence.

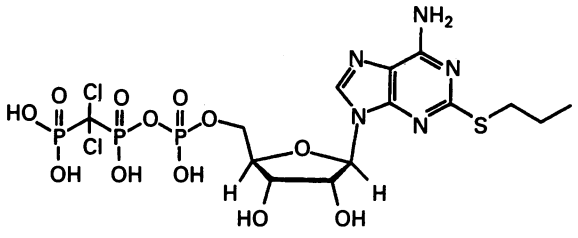

Figure 1 Chemical structure of FPL 67085.

River) anaesthetized with urethane (2 ml of 40% solution) administered intraperitoneally (i.p.). For use in washed platelet experiments, blood was anticoagulated with 1/10 volume, 3.2% trisodium citrate. For aggregation measurements in whole blood, heparin (10 u ml^{-1} final concentration) was used as anticoagulant.

Preparation of washed platelets Suspensions of human or rat washed platelets were prepared from citrated blood by differential centrifugation as described in detail by Humphries *et al.* (1994b), with prostacyclin (PGI_2, 300 ng ml^{-1}) used to stabilize platelets during the washing procedure. The final platelet pellet was resuspended initially in 10 ml (human) or 2 ml (rat) calcium-free Tyrode solution (CFT, composition (mM): NaCl 137.0, $NaHCO_3$ 11.9, NaH_2PO_4 0.4, KCl 2.7, $MgCl_2$ 1.1, D-glucose 5.6) gassed with 95% O_2/5% CO_2 and maintained at 37°C. Further CFT was added, as required, to adjust the final platelet count to 2×10^5 μl^{-1}, prior to storage at 4°C with air excluded.

To allow subsequent recovery from PGI_2-inhibition of normal function, platelets were used in aggregation studies no sooner than 2 h after final re-suspension.

Rabbit ear artery

The use of the rabbit isolated ear artery preparation for assessment of compound activity at P_{2X}-purinoceptors has been described in detail by O'Connor *et al.* (1990). Briefly, endothelium-denuded arterial rings (5 mm), obtained from male New-Zealand White rabbits (Froxfield, 2.5–3.5 kg), were mounted horizontally, under isometric conditions, on fine tungsten wire hooks in 20 ml organ baths containing modified Krebs buffer of the following composition: (mM) NaCl 117.6, NaH_2PO_4 0.9, $NaHCO_3$ 25.0, $MgSO_4$ 1.2, KCl 5.4, $CaCl_2$ 2.5, D-glucose 11.1 and indomethacin (2.8 μM). Tissues, maintained at 37°C and gassed continually with 95% O_2/5% CO_2, were subjected to an initial force of 1.0 g and allowed to equilibrate for 1 h, during which time the resting force was adjusted to achieve a final value of 0.5–1.0 g.

Guinea-pig aorta

The use of this preparation for assessment of P_{2Y}-agonist and antagonist activity has been outlined previously (Dainty *et al.*, 1992; Humphries *et al.*, 1994b). Endothelium-intact rings (3 mm) of the thoracic aorta, obtained from male Dunkin-Hartley guinea-pigs (Charles-River, 300–350 g), were mounted horizontally, under isometric conditions, on fine tungsten wire hooks in 10 ml organ baths, containing modified Krebs solution maintained under the conditions described above. Tissues were subjected to an initial force of 2 g and allowed to equilibrate for 15 min. After this time, resting force was adjusted to 2 g at 0, 3, 6 and 9 min and the bathing solution exchanged at these times. The tissues were then allowed to equilibrate for a further 15 min prior to use. As with ear artery preparations, responses were recorded as changes in force using isometric transducers (Ormed) and displayed on Advance Bryan chart recorders.

Urethane-anaesthetized rats

Male Sprague-Dawley rats (Charles River, 470–550 g) were anaesthetized with urethane (3 ml of 20% solution i.p.). Intravenous (i.v.) anaesthetic supplements (40% solution) were administered as required *via* a caudal vein cannula. Body temperature was maintained at 37 ± 0.5°C with a heating lamp. Animals were allowed to breathe spontaneously and a tracheotomy was performed to ensure a patent airway. A cannula (size: 3 French Gauge (FG)), containing heparinized saline (25 u ml^{-1}) was introduced into the left femoral artery and connected to a transducer (Gould/Statham) to record pulsatile blood pressure (BP). Care was taken to avoid systemic administration of heparin from this cannula. Mean BP and heart rate (HR) were derived electronically from the pulsatile signal and all 3 variables were recorded on a calibrated pen recorder (Devices/Lectromed). Cannulae containing non-heparinized saline were introduced into the left common carotid artery (3FG) and left jugular vein (2FG) for withdrawal of arterial blood samples and i.v. administration of compounds. Upon completion of surgery, a 30 min stabilization period was allowed before starting the experimental protocol. Animals with a BP < 50 mmHg at the end of this period were not used.

Experimental protocols

Human washed platelets Aliquots (440 μl) of platelet suspension were added to siliconized aggregation cuvettes containing 10 μl $CaCl_2$ solution (final concentration 1 mM), maintained at 37°C and stirred at 900 r.p.m. in a Biodata PAP4 aggregometer. Human fibrinogen (10 μl) was then added to give a final concentration of 0.2 mg ml^{-1} of clottable protein. Recording of aggregation was then started and baseline light transmission monitored for 20 min before addition of a single submaximal concentration of ADP (30 or 100 μM) in a volume of 10 μl. FPL 67085 (0.1–100 nM) or vehicle (saline, 30 μl) was added 15 min before ADP. The effect of the non-selective P_1-purinoceptor antagonist, 8-sulphophenyltheophylline (8-SPT, 300 μM, 20 min incubation) on the anti-aggregatory potency of FPL 67085 was also investigated. Inhibitory concentration-effect (E/[A]) curves for FPL 67085 were constructed in a time-matched manner in the absence and presence of 8-SPT, with each point obtained in duplicate. Aggregation responses were recorded as the maximum rate of increase (slope) in light transmission through the platelet suspension, following addition of ADP, using the PAP4 slope reader.

In a separate series of experiments, baseline light transmission was monitored for a shorter period (10 min) prior to addition of ADP (1–1000 μM) in a volume of 10 μl. FPL 67085 (3–30 nM) or 30 μl vehicle was added 2 min before ADP. Although only a single concentration of agonist and antagonist was added to each cuvette, use of 8-aggregometer channels enabled construction of 4, time-matched E/[A] curves for ADP-induced aggregation, with duplicate measurements for each point. Thus, in each experiment, a complete analysis of antagonism was conducted. In these experiments, aggregation responses were recorded as the maximum increase (extent) in light transmission.

P_{2T}-specificity of the anti-aggregatory effect of FPL 67085 (0.1–10 μM, 15 min incubation) was tested against responses to the thromboxane A_2-mimetic, U46619 (0.1–10 μM), rendered ADP-independent by inclusion of the non-selective P_2-purinoceptor antagonist, suramin (100 μM). E/[A] curves for U46619 were constructed as described for ADP after a 20 min monitoring of baseline light transmission. Suramin was added 1 min prior to FPL 67085 in a volume of 10 μl.

Rat washed platelets The anti-aggregatory potency of FPL 67085 (0.01–10 nM, 15 min incubation) was assessed against aggregation produced by a standard submaximal concentration of ADP (3 μM) added to aliquots of platelet suspension in micro-cuvettes. Baseline light transmission was monitored for

20 min before addition of ADP. To accommodate the use of microcuvettes, addition volumes (μl) were adjusted proportionately from those described for human washed platelets as follows: platelet suspension, 172; $CaCl_2$, 4; fibrinogen, 4; FPL 67085, 10.

Whole blood aggregation The anti-aggregatory potency of FPL 67085 was assessed against aggregation produced by a standard submaximal concentration of ADP (1 or 3 μM) in 0.5 ml samples of heparinized human or rat blood, diluted 1:1 with saline and incubated at 37°C for 2 min in a Chrono-log aggregometer. FPL 67085 (human: 0.03–10; rat: 0.3–30 nM) or vehicle (saline, 30 μl) was then added, the cuvette transferred to the impedance measuring well and the sample stirred at 900 r.p.m. for a further 2 min before addition of ADP in a volume of 20 μl. Aggregation responses were obtained in duplicate and recorded as the maximum increase in impedance (ohms) within 6 min of addition of ADP.

In a separate series of experiments, FPL 67085 was incubated with rat blood for periods of 2, 5, 10 or 30 min before 1:1 dilution of the blood sample with saline and measurement of ADP (3 μM)-induced platelet aggregation. The concentration of FPL 67085 added to undiluted blood (10–60 nM) was double that initially shown to inhibit aggregation by approximately 80% when added directly to diluted blood.

Rabbit ear artery Tissues were initially contracted with KCl (80 mM) to establish viability, followed by addition of acetylcholine (1 μM). Lack of a relaxant response to acetylcholine confirmed denudation of the endothelium. After washing, tissues were allowed to equilibrate for 45 min prior to construction of a cumulative E/[A] curve for the standard P_{2X}-agonist, D-α,β-methylene ATP (α,β-meATP, 0.03–10 μM). The tissues were then washed and, after a further 70 min equilibration period, a cumulative E/[A] curve was obtained for FPL 67085 (1–1000 μM). In control experiments, this protocol allows construction of consecutive E/[A] curves for α,β-meATP with no evidence of desensitization. Following subsequent washing, a further E/[A] curve to FPL 67085 (10–1000 μM) was obtained in the presence of α,β-meATP (30 μM) added 15 min prior to the first concentration of FPL 67085. All E/[A] curves were constructed in the presence of 8-SPT (300 μM), added 45 min before the agonist, to exclude the possible contribution of P_1-mediated effects.

Guinea-pig aorta Tissues were contracted to a stable plateau with phenylephrine (Phe, 10 μM) and the standard relaxant P_{2Y}-agonist, 2-methylthio ATP (2-MeSATP, 10 μM) added to confirm the presence of functional endothelium. After washing, tissues were again contracted with Phe (10 μM) and, when the induced tone had stabilized (at least 15 min), cumulative E/[A] curves were constructed to 2-MeSATP (1–3000 nM). After washing, and a 35 min stabilization period, tissues were again pre-contracted with Phe and an E/[A] curve constructed for FPL 67085 (0.003–10 mM), with each concentration left in contact with the tissue for at least 3 min or until any relaxant response had stabilized. To determine whether any observed relaxations were P_{2Y}-mediated, tissues were then washed and allowed to equilibrate for 35 min before pre-contraction with Phe and construction of a second curve to FPL 67085 in the presence of 2-MeSATP (10 μM). This concentration of 2-MeSATP abolishes, or produces at least a 2 orders of magnitude rightward shift and significant depression of, the 2-MeSATP E/[A] curve in this preparation. All E/[A] curves were constructed in the presence of 8-SPT (300 μM), added 35 min prior to Phe, to exclude the possible contribution of P_1-mediated effects.

Urethane-anaesthetized rats Each animal received 3 × 20 min infusions of either FPL 67085 (0.08, 0.8 and 8 μg kg^{-1} min^{-1} i.v. free acid, mol wt. 648) or vehicle (saline 0.03 ml min^{-1} i.v.). Blood samples were taken immediately prior to the first infusion, at the end of each infusion and 20 min after cessation of the final infusion, for measurement of platelet aggregation *ex vivo*. At each sampling point, 1 ml arterial blood was withdrawn into a 1 ml syringe containing 0.1 ml heparinized saline (100 u ml^{-1}). Mean BP and HR values were noted before each sample was taken. Additional samples were taken at the end of the control and final infusion periods for measurement of platelet, red blood cell (RBC) and white blood cell (WBC) counts (Technicon H1).

Immediately after sampling, ADP-induced platelet aggregation was measured in duplicate in 0.5 ml blood samples diluted 1:1 with saline and incubated at 37°C for 4 min. For the final minute of this period, cuvettes were transferred to the impedance measuring well of a Chrono-log aggregometer and the sample stirred at 900 r.p.m. ADP (3 μM) was then added in a volume of 20 μl and aggregation recorded as the maximum increase in impedance (ohms) within 6 min of addition of ADP.

Effects on ADP-induced platelet aggregation were calculated as % inhibition of the pre-infusion response. The dose of FPL 67085 producing 50% inhibition (ID_{50}) was derived by graphical interpolation.

Analysis of data

Curve fitting With the exception of data obtained for U46619 in human washed platelets, E/[A] curve data were fitted to a logistic function (i) of the form:

$$E = \frac{\alpha[A]^m}{[A_{50}]^m + [A]^m} \qquad \text{(i)}$$

in which α, $[A_{50}]$ and m are, respectively, the asymptote, location and slope parameters. $[A_{50}]$ values were assumed to be log-normally distributed and they were estimated as such and quoted as $p[A_{50}]$ ($-\log[A_{50}]$) values.

Analysis of antagonism E/[A] curve data obtained for ADP-induced platelet aggregation in the absence and presence of FPL 67085 were fitted to equation (i). Parallelism was tested by one-way analysis of variance prior to fitting of E/[A] data describing the 4 curves obtained in individual experiments to the following form of the Schild equation (Black *et al.*, 1985):

$$\log_{10}[A_{50}] = \log_{10}[A_{50}^c] + \log_{10}(1 + [B]^n/K_B) \qquad \text{(ii)}$$

where $[A_{50}^c]$ is a control $[A_{50}]$, [B] is the concentration of FPL 67085, K_B is its equilibrium dissociation constant and n is the Schild plot slope. Other parameters are as defined for equation (i). Thus, an estimate of n and K_B was obtained from each experiment.

E/[A] parameters for U46619-induced platelet aggregation were calculated from manual plots of the E/[A] data and the effect of FPL 67085 on these parameters was tested either by one-way ANOVA (α) or the non-parametric Kruskal-Wallis test ($p[A_{50}]$).

Anti-aggregatory potency Differences in pIC_{50} values obtained for FPL 67085 under different conditions (human:rat; whole blood:washed platelets; +8-SPT:-8-SPT; 2:5:10:30 min incubation) were tested by one-way ANOVA.

Urethane-anaesthetized rats Between group comparisons of control values for aggregation, BP, HR, platelet, RBC and WBC counts were made with Student's unpaired *t* test. The significance of treatment-related changes from pre-infusion values was determined by repeated measures ANOVA followed by Dunnett's multiple-comparison test where appropriate.

Data are presented as mean ± s.e. of results obtained from individual human or rat blood donors, individual tissues or from individual anaesthetized rats. All fitting procedures used either BMDP Statistical Software installed on a VAX mainframe computer, KaleidaGraph software on a Macintosh II cx computer or Fig. P software on a Compaq PC. Other statistical analyses used InStat or t-EASE software. $P < 0.05$ was taken as indicative of a statistically significant difference in all cases.

Drugs and solutions

Drugs were obtained from the following sources: U46619 (9,11-dideoxy-9α, 11α-methanoepoxy-$PGF_{2\alpha}$), indomethacin, acetylcholine bromide, phenylephrine hydrochloride, PGI_2, human fibrinogen, and the disodium salts of ADP, β,γ-meATP and α,β-meATP, Sigma Chemical Co., Poole, Dorset; 8-SPT and 2-MeSATP, Research Biochemicals Inc., St. Albans, Herts; urethane, Aldrich Chemical Co., Gillingham, Dorset; heparin sodium, Evans medical, Horsham, W. Sussex; suramin was a gift from Bayer plc, UK.

The tetrasodium salt of FPL 67085 was synthesized by N.D. Kindon, Department of Medicinal Chemistry, Fisons plc, R & D Laboratories, Loughborough, Leics., extending previously described methodology for the preparation of 2-alkylthio, β,γ-dihalomethylene analogues of ATP (Yoshikawa *et al.*, 1967; Blackburn *et al.*, 1984).

Indomethacin was dissolved in 10% w/v Na_2CO_3 at 10 mg ml^{-1} with subsequent dilutions in Krebs buffer. A working dilution of PGI_2 (0.1 mg ml^{-1}) was made in saline from a stock solution of 1 mg ml^{-1} in ethanol, no more than 1 min before use. 8-SPT was dissolved at the working concentration (5.6 mg ml^{-1}) in 6% glucose. All other drugs were dissolved in distilled water or saline.

Results

The effect of FPL 67085 on ADP-induced aggregation in human and rat washed platelets and whole blood in vitro

FPL 67085 produced concentration-dependent inhibition of ADP-induced aggregation of human and rat platelets *in vitro*. The anti-aggregatory potency of FPL 67085 (IC_{50} 0.6–3.8 nM) was similar for human and rat platelets, whether tested in suspensions of washed platelets or in whole blood and, in human washed platelets, was not affected by 8-SPT (300 μM) (Table 1).

The degree of inhibition of ADP (3 μM)-induced platelet aggregation produced by FPL 67085 (10–60 nM) did not change significantly ($P > 0.05$) when the antagonist incubation time in undiluted rat blood was increased from 2 to 30 min: 85±4 and 87±4% (mean±s.e., $n=4$), respectively.

Characterization of the anti-aggregatory effect of FPL 67085

ADP produced concentration-dependent aggregation of human washed platelets with a $p[A_{50}]$ value of 5.1±0.1 (s.e., $n=10$) and this E/[A] relationship was displaced to the right in a concentration-dependent manner by FPL 67085 (3–30 nM). In Figure 2a, curves obtained by unconstrained fitting of E/[A] data to the logistic function (i) are shown superimposed on mean (±s.e.) datum points obtained for ADP in the absence and presence of FPL 67085, from 10 replicate experiments. Statistical analysis of the E/[A] parameters (Table 2) obtained from unconstrained logistic fitting indicates that the rightward displacements produced by FPL 67085 did not differ significantly from parallelism as assessed by comparison of values of m. However, in some experiments, FPL 67085 caused an apparently concentration-dependent reduction in the maximal response, α. By the criterion of curve parallelism, therefore, the effect of FPL 67085 did not consistently accord with simple competitive antagonism. However, analysis of the rightward displacements of the E/[A] curves (using equation (ii)) indicated that the Schild plot slope criterion was met

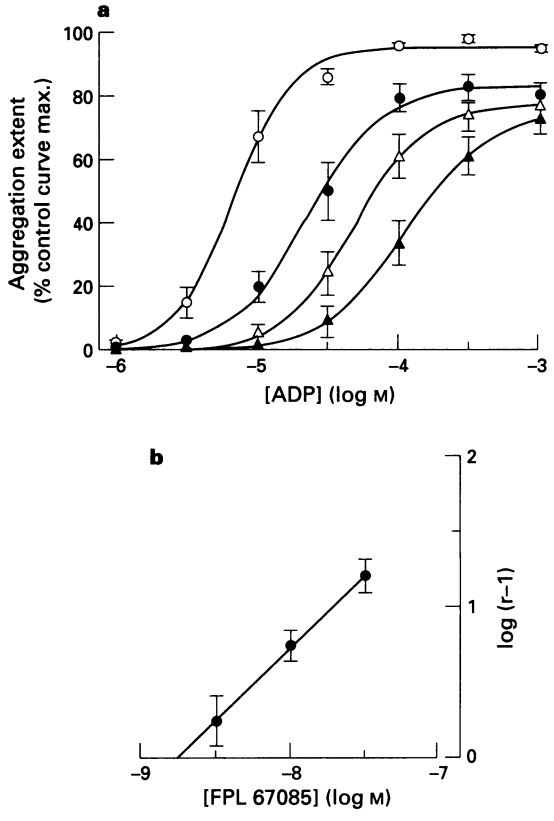

Figure 2 Analysis of antagonism by FPL 67085 of ADP-induced aggregation of human washed platelets. (a) Computer-generated lines obtained using the logistic function (i) (see text) are shown superimposed on mean datum points for E/[A] curves obtained for ADP following 2 min incubation with either FPL 67085 (● 3, △ 10 or ▲ 30 nM) or vehicle (○). Results are presented as mean responses (±s.e., $n=10$), expressed as a % of the maximum response to ADP in the control curve. (b) Corresponding Schild plot of the effect of FPL 67085 on E/[A] curves for ADP. Points show mean concentration-ratio (r) data plotted as (r-1) values (±s.e.) for 10 replicate experiments.

Table 1 The effect of FPL 67085 on ADP-induced platelet aggregation in suspensions of human and rat washed platelets and in whole blood *in vitro*

	Washed platelets		*Whole blood*
Species	*–8-SPT*	*+8-SPT*	*–8-SPT*
Human	9.05±0.12	8.60±0.09	8.89±0.22
Rat	9.21±0.11	not tested	8.42±0.24

Results are presented as mean±s.e. pIC_{50} values ($n=4$–24) for inhibition of platelet aggregation induced by a sub-maximal concentration of ADP.

Table 2 E/[A] curve parameters for ADP-induced aggregation of human washed platelets in the absence and presence of FPL 67085

[FPL 67085] (nM)	*Parameter* $p[A_{50}]$	α(%)	m
0	5.16±0.08	97±1	2.73±0.44
3	4.67±0.08**	85±4*	2.75±0.39
10	4.33±0.09**	79±5**	2.93±0.93
30	3.93±0.1**	77±5**	1.93±0.18

Values are means (±s.e.) of parameter estimates made by fitting the logistic function (i) (see text) to individual E/[A] data-sets obtained from 10 replicate experiments. *$P<0.05$ and **$P<0.01$ compared to parameter values from control E/[A] curve: ANOVA (m) followed by Bonferroni's multiple comparison test ($p[A_{50}]$); Kruskal-Wallis non-parametric ANOVA followed by Dunn's multiple comparisons test (α).

(0.90±0.06). An 'apparent pK_B' estimate (8.9±0.1, mean±s.e.) was, therefore, made from analysis of data from 10 replicate experiments. A Schild plot derived from this analysis is presented for display purposes in Figure 2b and E/[A] curves from 2 experiments representing the extremes of the effect of FPL 67085 contributing to the analysis are shown in Figure 3.

Specificity and selectivity in vitro

In human washed platelets, FPL 67085 (0.1–10 μM) had no significant effect on the position or asymptote of the E/[A] curve obtained for U46619 (0.1–10 μM) in the presence of suramin (100 μM) (Figure 4). In the standard P_{2X}-containing preparation of the rabbit isolated ear artery, FPL 67085 was an agonist with a mean p[A_{50}] of 4.2±0.2 (s.e., $n=5$). E/[A] curves did not achieve the α,β-meATP maximum (α=59±12%, mean±s.e., $n=5$) and were abolished in the presence of α,β-meATP (30 μM). In the standard P_{2Y}-containing preparation of the guinea-pig aorta, FPL 67085 was also a weak agonist (p[A_{50}]=4.2±0.1, mean±s.e., $n=4$) and E/[A] curves did not reach the same maximum as that produced by 2-MeSATP (α=73±2%, mean±s.e., $n=4$). Relaxant responses to FPL 67085 were only partially inhibited following occupation-desensitization with a high concentration of 2-MeSATP (10 μM).

The effects of i.v. infusion of FPL 67085 in urethane-anaesthetized rats

Platelet aggregation ex vivo Control aggregation responses to ADP (3 μM) in blood from saline- or FPL 67085-infused animals were not significantly different: 21.8±1.7 and 24.3±1.8 ohms, respectively (mean±s.e., $n=4$–6). The effect of i.v. infusion of FPL 67085 on aggregation measured *ex vivo* is presented graphically in Figure 5. FPL 67085 (0.08–8 μg kg^{-1} min^{-1}, i.v.) produced dose-related inhibition of ADP-induced platelet aggregation with a geometric mean ID_{50} of 1.3 μg kg^{-1} min^{-1} (range 0.7–3.6, $n=4$). Twenty minutes after cessation of infusion of the highest dose of FPL 67085, ADP-induced aggregation had returned fully to pre-infusion levels. Aggregation responses in the control, saline-infused ($n=6$), group did not change significantly throughout the experimental protocol ($P>0.05$).

Haemodynamics and cell counts BP, HR, platelet, RBC and WBC count measurements are summarized in Table 3. There was no significant difference ($P>0.05$) in baseline values between saline- and FPL 67085-infused animals. A total of 60 min infusion of FPL 67085 (20 min at each of 0.08, 0.8 and 8 μg kg^{-1} min^{-1}, i.v.) or saline (0.03 ml min^{-1}, i.v.) produced no significant change in BP, HR, platelet, RBC or WBC counts compared to corresponding pre-infusion control values ($P>0.05$).

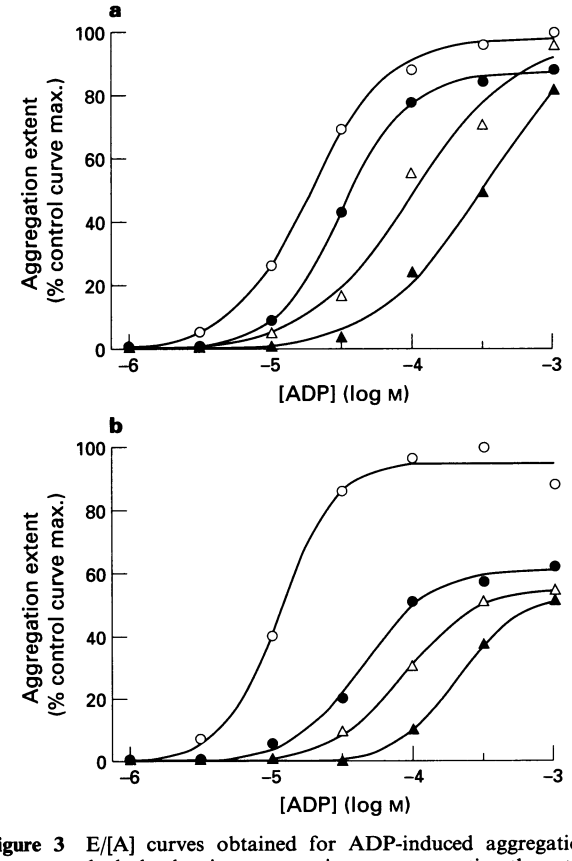

Figure 3 E/[A] curves obtained for ADP-induced aggregation of human washed platelets in two experiments representing the extremes of the effect of FPL 67085 on the ADP-asymptote: (a) no depression; (b) depression. Responses to ADP were obtained following 2 min incubation with either FPL 67085 (● 3, △ 10 or ▲ 30 nM) or vehicle (○) and are expressed as a % of the maximum response to ADP in the control curve.

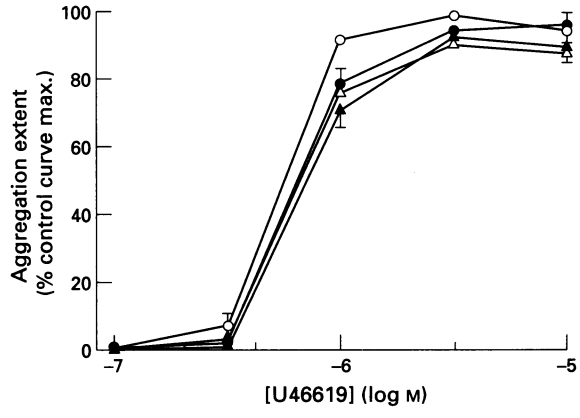

Figure 4 E/[A] curves obtained for U46619-induced aggregation of human washed platelets in the presence of suramin (100 μM). Results are presented as mean responses (±s.e., $n=4$), expressed as % of the maximum response to U46619 in the control curve. Responses were obtained following 15 min incubation with either FPL 67085 (● 0.1, △ 1 or ▲ 10 μM) or vehicle (○).

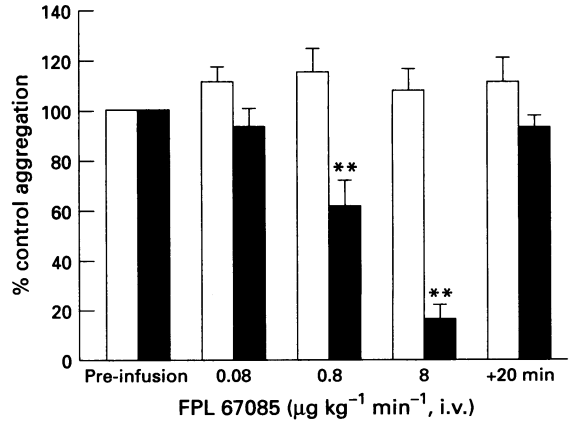

Figure 5 The effect of intravenous infusion of either FPL 67085 (0.08–8 μg kg^{-1} min^{-1}, solid columns, $n=4$) or vehicle (saline, 0.03 ml min^{-1}; open columns, $n=6$) on ADP (3 μM)-induced platelet aggregation (mean±s.e.) measured *ex vivo* in whole blood from urethane-anaesthetized rats. Blood samples were taken immediately prior to the first infusion, at the end of each infusion and 20 min after cessation of the final infusion. **$P<0.01$ compared to pre-infusion control (Dunnett's multiple-comparison test).

Table 3 The effect of intravenous infusion of FPL 67085 on blood pressure, heart rate and circulating cell counts in urethane-anaesthetized rats

	Saline		*FPL 67085*	
Variable	*Control*	*+60 min*	*Control*	*+60 min*
BP	73±4	62±5	84±10	76±5
HR	331±17	317±19	345±17	325±9
PLT	475±42	382±69	413±19	451±60
WBC	15.7±1.2	15.6±1.4	16.8±1.8	15.3±0.8
RBC	8.0±0.5	7.4±0.3	7.2±0.3	6.7±0.1

Abbreviations and units: BP: blood pressure (mmHg); HR: heart rate (beats min^{-1}); PLT: platelet count ($\times 10^3 \mu l^{-1}$); WBC: white blood cell count ($\times 10^3 \mu l^{-1}$); RBC: red blood cell count ($\times 10^6 \mu l^{-1}$). Values are means (±s.e.) before and after 3×20 min infusions of either FPL 67085 (0.08, 0.8 and 8 $\mu g kg^{-1} min^{-1}$, i.v. $n=4$) or vehicle (saline, 0.03 $ml min^{-1}$, $n=6$).

Discussion

In this study, we have demonstrated that FPL 67085 is a potent inhibitor of ADP-induced aggregation of human and rat platelets both in suspensions of washed platelets and in whole blood *in vitro*. Furthermore, we have shown that i.v. infusion of FPL 67085 results in potent and rapidly reversible inhibition of platelet aggregation *in vivo* in the anaesthetized rat.

We have shown previously that 2-propylthio-substitution on a β,γ-dihalomethylene analogue of ATP yields a compound (FPL 66096) with high affinity for the human platelet P_{2T}-purinoceptor *in vitro* (Humphries *et al.*, 1994b). In the present study, using FPL 67085, we have extended this observation to washed platelet preparations from a second species and also demonstrated that high anti-aggregatory potency is retained in whole blood from both human subjects and rats. In some experiments, antagonism of the ADP-induced aggregation of human washed platelets by FPL 67085 was non-surmountable and, under these circumstances, a pK_B should not be quoted. However, since the displacements of ADP E/[A] curves accorded with the Schild slope criterion, it may be reasonable to conclude that, whatever the curve depression was due to, it did not contribute to the rightward displacements of the E/[A] curves. Making this assumption, we estimated an 'apparent pK_B' of 8.9. It is not clear why, in some experiments in this study, the profile of FPL 67085 was fully consistent with simple competition while, in others, clear depression of the ADP asymptote was observed. Investigation of this variable behaviour of FPL 67085 is in progress. Whatever the explanation, this profile of antagonism adds further to the complexity of effects of 2-alkylthio-substituted analogues of ATP on ADP-induced platelet aggregation: FPL 66096 (2-propylthio-D-β,γ-difluoromethylene ATP) acts as an apparently competitive P_{2T}-purinoceptor antagonist (pK_B 8.7) in human washed platelets; 2-MeSATP, 2-ethylthio ATP and 2-methylthio-β,γ-methylene ATP are non-surmountable, low efficacy inhibitors of ADP-induced platelet aggregation in human PRP (Cusack & Hourani, 1982; Hourani *et al.*, 1986; Humphries *et al.*, 1994b). While differences in ionic environment and protein concentration may, in part, explain different results obtained in preparations of washed platelets and PRP, the reason for the somewhat different profiles of FPL 67085 and FPL 66096, tested under the same conditions, remains unclear. However, what is clear is the important affinity-conferring role played by the 2-propylthio substituent, a structural feature of both compounds, when compared to the other 2-alkylthio substituents mentioned above.

In common with other 2-alkylthio-substituted analogues of ATP, including FPL 66096, the anti-aggregatory effect of FPL 67085 was specific to P_{2T}-purinoceptors. Firstly, the possibility of direct or indirect agonist activity at platelet P_1-purinoceptors (A_{2a}) was excluded by use of the non-selective P_1-purinoceptor antagonist, 8-SPT. At a concentration previously shown (Humphries *et al.*, 1994b) to attenuate markedly the inhibition of aggregation produced by the P_1-purinoceptor agonist, 5'-N-ethylcarboxamidoadenosine in this system, 8-SPT had no effect on the anti-aggregatory potency of FPL 67085. Secondly, at a concentration 8,000 fold in excess of its apparent K_B, FPL 67085 had no effect on aggregation produced by the thromboxane A_2-mimetic, U46619, in the presence of suramin, a response shown previously to be ADP-independent (Humphries *et al.*, 1994b).

FPL 67085 was highly selective for the P_{2T}-purinoceptor subtype, showing no agonist or antagonist activity at P_{2X} or P_{2Y}-purinoceptors at a concentration 300 fold higher than its apparent K_B against ADP-induced aggregation of human washed platelets. Concentration-related contractions of the rabbit isolated ear artery produced by higher concentrations of FPL 67085 were prevented in the presence of a high concentration (30 μM) of α,β-meATP, implicating a P_{2X} mechanism. In preparations of the guinea-pig isolated aorta, pretreatment with 2-MeSATP did not inhibit relaxant responses to high concentrations of FPL 67085 to an extent consistent with the relaxations being wholly mediated by a P_{2Y} mechanism. It was, therefore, concluded that, in the guinea-pig aorta, relaxations produced by high concentrations of FPL 67085 involve both P_{2Y}- and an as yet undefined component, as observed previously with FPL 66096 (Humphries *et al.*, 1994b). The high affinity of FPL 67085 for the P_{2T}-purinoceptor (apparent pK_B 8.9) compared with its potency in P_{2X} and P_{2Y}-containing tissues ($p[A_{50}] \sim 4.2$), indicates that it has an approximately 4.5 orders of magnitude selectivity for the P_{2T}-purinoceptor.

In addition to experiments in human washed platelets, which would have detected activity at prostaglandin (TP, IP) or P_1 (A_{2a})-purinoceptors, the high degree of specificity of FPL 67085 has been confirmed in a wide range of functional and binding assays containing nucleotide- (P_{2U}), adenosine- (A_1, A_{2b}), catecholamine- (α_1, α_2, β_2, D_2), 5-hydroxytryptamine- (5-HT_2), angiotensin- (AT_1) and prostaglandin- (EP_2) receptors (unpublished observations).

The high potency, selectivity, and specificity of FPL 67085 for P_{2T}-purinoceptors *in vitro* made it a suitable candidate for progression to studies *in vivo*, and these features were subsequently confirmed during i.v. infusion of FPL 67085 in urethane-anaesthetized rats. In these experiments, FPL 67085 produced dose-dependent inhibition of ADP-induced platelet aggregation measured in whole blood *ex vivo*. Aggregation was inhibited by 50% at a dose of 1.3 $\mu g kg^{-1} min^{-1}$, i.v. while no effects on BP, HR or circulating cell counts were seen at $\leqslant 8 \mu g kg^{-1} min^{-1}$. The anti-aggregatory effect of infusion of FPL 67085 (8 $\mu g kg^{-1} min^{-1}$, i.v.) was fully reversed within 20 min of cessation of infusion, indicating extremely rapid metabolism or clearance in this anaesthetized rat preparation. However, when measured in rat blood *in vitro*, the effect of a concentration of FPL 67085, chosen to produce approximately 80% inhibition of ADP-induced platelet aggregation, did not change significantly when the incubation time was increased from 2 to 30 min. The stability of FPL 67085 in blood, as indicated by measurement of inhibition of platelet aggregation, contrasts with the relatively rapid breakdown of ATP in this tissue ($t_{\frac{1}{2}}$ 10 min) (Trams *et al.*, 1980). This indicates that, in rat blood over a period of 30 min, FPL 67085 is resistant to breakdown by ectonucleotidases which are present on the surface of blood cells (Pearson, 1985), confirming the reduced

susceptibility to this route of metabolism conferred by a β,γ-methylene link in the tri-phosphate chain (Welford *et al.*, 1986). Thus, the rapid offset kinetics of FPL 67085 observed *in vivo* cannot be explained by metabolic inactivation by blood components but rather must reflect an alternative metabolic process or a clearance mechanism *in vivo*.

Using FPL 67085, we have had the first opportunity to evaluate the effects of a highly potent, specific and selective P_{2T} purinoceptor antagonist *in vivo*. The pharmacodynamic and functional pharmacokinetic profile of FPL 67085 indicate that it may have clinical potential as a potent, infusible anti-platelet agent for acute use. In the present study, we have shown that i.v. infusion of this P_{2T}-purinoceptor antagonist inhibits ADP-induced platelet aggregation measured *ex vivo*. The potential of FPL 67085 and other P_{2T}-purinoceptor antagonists as novel anti-thrombotic agents will depend critically on the contribution of endogenous ADP to thrombosis *in vivo*. This question is now being addressed in animal models of thrombosis, using FPL 67085 as a probe that may also ultimately represent a suitable candidate for progression to the clinic.

References

BLACK, J.W., LEFF, P. & SHANKLEY, N.P. (1985). Further analysis of anomalous pK_B values for histamine H_2 receptor antagonists on the mouse isolated stomach assay. *Br. J. Pharmacol.*, **86**, 581–587.

BLACKBURN, G.M., KENT, D.E. & KOLKMANN, F. (1984). The synthesis and metal binding characteristics of novel, isopolar phosphonate analogues of nucleotides. *J. Chem. Soc. Perkin. Trans.*, **I**, 1119–1125.

BORN, G.V.R. (1962). Quantitative investigations into the aggregation of blood platelets. *J. Physiol.*, **162**, 67–68P.

BORN, G.V.R. & CROSS, M.J. (1964). Effects of inorganic ions and of plasma proteins on the aggregation of blood platelets by adenosine diphosphate. *J. Physiol.*, **170**, 394–414.

CARDINAL, D.C. & FLOWER, R.J. (1980). The electronic aggregometer: A novel device for assessing platelet behaviour in blood. *J. Pharmacol. Methods*, **3**, 135–158.

CUSACK, N.J. & HOURANI, S.M.O. (1982). Specific but noncompetitive inhibition by 2-alkylthio analogues of adenosine 5'-monophosphate and adenosine 5'-triphosphate of human platelet aggregation induced by adenosine 5'-diphosphate. *Br. J. Pharmacol.*, **75**, 397–400.

DAINTY, I.A., LEFF, P., MCKECHNIE, K. & O'CONNOR, S.E. (1992). Endothelium-dependent relaxations to ATP in the guinea-pig but not rat aorta are mediated predominantly through P_{2Y}-purinoceptors. *Int. J. Purine Pyrimidine Res.*, **3**, 162P.

FUSTER, V., BADIMON, L., BADIMON, J.J. & CHESEBRO, J.H. (1992). The pathogenesis of coronary artery disease and the acute coronary syndromes. *N. Engl. J. Med.*, **326**, 310–318.

GAARDER, A., JONSEN, J., LALAND, S., HELLEM, A. & OWREN, P.A. (1961). Adenosine diphosphate in red cells as a factor in the adhesiveness of human blood platelets. *Nature*, **192**, 531–532.

GORDON, J.L. (1986). Extracellular ATP: effects, sources and fate. *Biochem. J.*, **233**, 309–319.

HOURANI, S.M.O., WELFORD, L.A. & CUSACK, N.J. (1986). 2-MeS-AMP-PCP and human platelets: implications for the role of adenylate cyclase in ADP-induced aggregation? *Br. J. Pharmacol.*, **87**, 84P.

HUMPHRIES, R.G., TOMLINSON, W., CLEGG, J.A., INGALL, A.H., KINDON, N.D. & LEFF, P. (1994a). Potent and selective inhibition of ADP-induced platelet aggregation *in vitro* and *in vivo* by the novel P_{2T}-antagonist, FPL 67085. *Drug Dev. Res.*, **31**, 279.

HUMPHRIES, R.G., TOMLINSON, W., INGALL, A.H., CAGE, P.A. & LEFF, P. (1994b). FPL 66096: A novel, highly potent and selective antagonist at human platelet P_{2T}-purinoceptors. *Br. J. Pharmacol.*, **113**, 1057–1063.

MACFARLANE, D.E. & MILLS, D.C.B. (1975). The effects of ATP on platelets: evidence against the central role of released ADP in primary aggregation. *Blood*, **46**, 309–320.

O'CONNOR, S.E., WOOD, B.E. & LEFF, P. (1990). Characterization of P_{2X}-receptors in rabbit isolated ear artery. *Br. J. Pharmacol.*, **101**, 640–644.

PAGE, C.P., PAUL, W. & MORLEY, J. (1982). An *in vivo* model for studying platelet aggregation and disaggregation. *Thromb. Haemostas.*, **47**, 210–213.

PEARSON, J.D. (1985). Ectonucleotidases: measurement of activities and use of inhibitors. *Methods Pharmacol.*, **6**, 87–107.

TRAMS, E.G, KAUFMANN, H. & BURNSTOCK, G. (1980). A proposal for the role of ecto-enzymes and adenylates in traumatic shock. *J. Theor. Biol.*, **87**, 609–621.

WELFORD, L.A., CUSACK, N.J. & HOURANI, S.M.O. (1986). ATP analogues and the guinea-pig taenia coli: a comparison of the structure-activity relationships of ectonucleotidases with those of the P_2-purinoceptor. *Eur. J. Pharmacol.*, **129**, 217–224.

YOSHIKAWA, M., KATO, T. & TAKENISHI, T. (1967). A novel method for phosphorylation of nucleosides to 5'-nucleotides. *Tetrahedron Lett.*, **50**, 5065–5068.

(Received February 6, 1995
Revised March 23, 1995
Accepted April 5, 1995)

British Journal of Pharmacology (1995) 115, 1117–1125 © 1995 Stockton Press All rights reserved 0007–1188/95 $12.00

Potassium currents in human freshly isolated bronchial smooth muscle cells

[1]V.A. Snetkov, S.J. Hirst, C.H.C. Twort & J.P.T. Ward

Respiratory Research Laboratories, UMDS Smooth Muscle Group, Department of Allergy and Respiratory Medicine, UMDS, London SE1 7EH

1 K^+ currents were studied in smooth muscle cells enzymatically dissociated from human bronchi, by use of the patch-clamp technique.

2 In whole-cell recordings a depolarization-induced, 4-aminopyridine (4-AP)-sensitive current was observed in only 26 of 155 cells, and in 20 of these 26 cells its amplitude at a test potential of 0 mV was less than 100 pA.

3 In the majority of cells depolarization to –40 mV or more positive potentials induced a noisy outward current which activated within milliseconds and showed almost no inactivation even during a 5 s depolarizing voltage step. This current was insensitive to 4-AP (up to 5 mM) but was strongly inhibited in the presence of tetraethylammonium (TEA, 1 mM), charybdotoxin (ChTX, 100 nM) or iberiotoxin (IbTX, 50 nM) in the bath. The same current was also recorded by the nystatin-perforated patch technique.

4 Single channels with a conductance of about 210 pS were recorded in cell-attached patch, inside-out patch, outside-out patch and whole-cell recording configurations. Channel open state probability in inside-out patches was 0.5 at a membrane potential of 4 ± 14 mV (mean $\pm$ s.d., $n = 13$) mV even with a free Ca^{2+} concentration on the cytosolic side of the patch of less than 0.1 nM. Open state probability increased with depolarization and internal Ca^{2+} concentration. Single channels could be reversibly blocked by externally applied TEA, ChTX and IbTX.

5 In current-clamp recordings with 100 nM free Ca^{2+} in the intracellular solution both TEA and ChTX caused substantial concentration-dependent depolarization.

6 These results suggest that in human bronchial smooth muscle cells, in marked contrast to other species, the majority of the outward current induced by depolarization is not due to a delayed rectifier, but to the activity of a large conductance, ChTX-sensitive K^+ channel. The Ca^{2+}- and voltage-dependency of this channel may well allow a sufficiently high open state probability for it to play a part in the regulation of the resting membrane potential.

Keywords: Large conductance potassium channels; delayed rectifier current; 4-aminopyridine; charybdotoxin; iberiotoxin; human bronchial smooth muscle

Introduction

Previous studies of voltage-gated K^+ currents in airway smooth muscle cells (ASMC) from various species have demonstrated a delayed rectifying outward current that is independent of Ca^{2+} influx, and more sensitive to blockade by 4-aminopyridine (4-AP) than tetraethylammonium (TEA). Both whole-cell and single-channel data strongly support the hypothesis that in canine, porcine and ferret tracheal myocytes, the major outward K^+ current is a delayed rectifier (Kotlikoff, 1993). However, an outward current that is charybdotoxin (ChTX)-sensitive and activated by an increase in free cytosolic Ca^{2+} has also been reported and there is evidence that at least in some types of smooth muscle, including that of airways, large conductance, voltage- and Ca^{2+}-dependent K^+ (K_{Ca}) channels may play a role in the maintenance of membrane potential (Kannan *et al.*, 1983; Brayden & Nelson, 1992; Asano *et al.*, 1993). The presence of numerous K_{Ca} channels in canine (McCann & Welsh, 1986), porcine (Saunders & Farley, 1991), bovine (Green *et al.*, 1991) and rabbit (Kume *et al.*, 1990) ASMCs would suggest that these channels are of importance in the regulation of airway smooth muscle function, and the recent demonstration that TEA (1–10 mM) can cause a substantial depolarization in bovine tracheal ASMCs (Nara *et al.*, 1994) implies that these channels have a major influence on the membrane potential. Selective inhibition of K_{Ca} channels also influences the membrane potential in the guinea-pig trachealis, producing either regenerative action potentials (Murray *et al.*, 1991) or an increase in contractility (Suarez-Kurtz *et al.*, 1991).

The relative importance of K_{Ca} channels for outward rectification and resting potential depends on the cytosolic concentration of free Ca^{2+} ions ($[Ca^{2+}]_i$) and on channel Ca-sensitivity. It was found using both bulk fluorometric measurement (Murray & Kotlikoff, 1991) and single cell Ca^{2+} imaging (Murray *et al.*, 1993) that in human cultured airway smooth muscle cells, resting $[Ca^{2+}]_i$ is about 160 nM. Data from experiments with outside-out membrane patches from guinea-pig (Murray *et al.*, 1991) and porcine (Kume & Kotlikoff, 1991) trachealis ASMC show that at $[Ca^{2+}]_i$ of 100 nM and at a membrane potential of 0 mV, K_{Ca} channels could easily be recorded. In inside-out membrane patches from canine trachealis at more depolarized potentials, K_{Ca} channel activity was recorded at $[Ca^{2+}]_i$ of less than 0.1 nM (McCann & Welsh, 1986).

It is likely that smooth muscle tissues differ substantially in the degree to which various K^+ conductances control the resting potential and force generation. There is good evidence that in tracheal ASMC from several animal species, the membrane potential is markedly influenced by the delayed rectifier. There have, however, been very few reports on the electrical behaviour of human airway smooth muscle. Miura *et*

[1]Author for correspondence at: Division of Medicine, United Medical and Dental Schools, St Thomas' Campus, Lambeth Palace Road, London SE1 7EH.

al. (1992) have found that although charybdotoxin (ChTX) pretreatment did not affect spontaneous tone of human bronchial rings, it did influence isoprenaline- and theophylline-induced relaxation, and a brief report from Fleischmann *et al.* (1994) has suggested that a delayed rectifier is the main determinant of resting potential and basal tone in human airways. In direct contrast we have found that in human cultured bronchial smooth muscle cells there was little evidence for any substantive current due to a delayed rectifier. Instead, the major outward current in the presence of physiological intracellular Ca^{2+} was due to ChTX-sensitive K_{Ca} channels (Snetkov *et al.*, 1994). Cells in culture may alter their phenotype, however, and we have therefore investigated ion currents underlying the electrical behaviour of smooth muscle cells freshly isolated from human bronchi obtained following elective surgery.

Methods

Freshly dissociated cells

Human bronchial tissue was obtained from 17 patients of either sex (mean age 63 years, range 36–84 years) following pneumonectomy or lobectomy. Small pieces (2 by 5 mm) of epithelium-denuded smooth muscle from 3rd or 4th generation bronchi were dissected from the cartilage and kept for 30 min in Ca^{2+}-free physiological salt solution (PSS; see below for composition) at 36°C to facilitate relaxation. Tissue was then incubated for 40 min at 36°C in Ca^{2+}-free PSS containing 2 mg ml^{-1} collagenase (Worthington Type I), 2 mg ml^{-1} papain, 5 mg ml^{-1} bovine serum albumin and 20 μM dithiothreitol. Tissue was washed with fresh Ca^{2+}-free PSS and, after 20 min, cells were collected after gentle trituration with a wide-bore flame-polished Pasteur pipette. Five to ten minutes before use, a drop of the cell suspension was placed on a cleaned glass coverslip. This procedure resulted in mixture of long, relaxed cells and cells at different extents of contraction, but no difference was found between data obtained from relaxed and contracted cells. An alternative protocol where collagenase was used together with elastase and soybean trypsin inhibitor was equally successful.

Recording and analysis

Single cells were studied by standard patch-clamp techniques (Hamill *et al.*, 1981) using an Axopatch-1C amplifier (Axon Instruments, U.S.A.). The experiments were carried out at room temperature (20–21°C). The bath (≈ 0.5 ml) was continuously perfused (1–5 ml min^{-1}) with normal PSS during whole-cell experiments, or internal KCl solution during recording from inside-out patches (for solutions see below). When the perforated patch technique was used (Horn & Marty, 1988) in order to minimize changes to the intracellular environment, the pipette solution contained 150 μg ml^{-1} nystatin. A relatively low access resistance (< 30 MOhms) was achieved approximately 15 min after establishing the cell-attached configuration, and decreased further during the course of the experiment. Voltage pulse and ramp commands were generated by software (PATCH v.5, Cambridge Electronic Design, Cambridge, U.K.) to obtain current-voltage ($I-V$) curves. For the ramp protocol the holding potential was maintained at –70 mV, and 1 s voltage ramps from –100 mV to +100 mV were applied every 15 s. For the pulse protocol the holding potential was –80 mV, and 50 ms hyperpolarizing and depolarizing pulses were applied every 10 s. When 5 s pulses were used to study time-dependent inactivation, the inter-pulse interval was increased to 1 min. Current-voltage curves were plotted using current values measured at the end of the 50 ms voltage pulses, or at the respective points of the voltage ramps. Current responses were normalised, when appropriate, to cell size in terms of cell capacitance, which was measured using the built-in circuit of the Axopatch-1C amplifier. Preliminary experiments on a variety of smooth muscle cells that contained substantial delayed rectifier current (freshly isolated from rat pulmonary artery or bronchi, or rabbit trachealis) demonstrated that, during the protocols used in our experiments, there was no significant inactivation of voltage-gated currents.

Drugs used were added to the perfusing solution, and the responses were obtained and averaged from the same cell before, during and after drug application. Any second drug was applied only if the response was restored completely following washout. Recording in the presence of a drug was started following full equilibration, but at least 5 min were allowed if the drug used had no apparent effect.

Single channel currents were filtered at 1 kHz (–3 dB, low pass 80 dB/dec, Bessel type) and digitised with a 5 kHz sampling frequency using a CED 1401 interface (Cambridge Electronic Design, Cambridge, U.K.). The open state probabilities were calculated using PATCH v.5 software, and their voltage-dependence was fitted to the Boltzmann equation using SigmaPlot v.5 software (Jandel Scientific, Inc., U.S.A.). Current-clamp records were sampled at 5 Hz using a custom sampling programme for the CED 1401 interface.

Solutions and reagents

The solution used as internal in whole-cell recording, and both as external and internal in inside-out configuration, contained (mM): KCl 140, $MgCl_2$ 2, ethylene glycol-*bis*-(β-aminoethyl ether)-*N,N,N',N'*-tetraacetic acid (EGTA) 5, *N*-2-hydroxyethyl-piperazine-*N'*-2-ethanesulphonic acid (HEPES) 10, adjusted to pH 7.2 with KOH. Free Ca^{2+} concentration was calculated as described by Fabiato (1988). The bath solution for whole-cell recording (PSS) contained (in mM): NaCl 135, KCl 5, $MgCl_2$ 2, $CaCl_2$ 2, glucose 11, HEPES 10, adjusted to pH 7.4 with NaOH. All solutions were filtered before use (0.22 μm; Millipore, U.S.A.). Charybdotoxin and iberiotoxin were obtained from Peninsula Laboratories, U.S.A., and type I collagenase from Worthington Biochemical Corporation, U.S.A. All other reagents were purchased from Sigma Chemical Company (Poole, Dorset).

The results are expressed as mean ± s.d. when appropriate, and n values refer to the number of cells investigated. Differences between means were tested for significance by Student's t test or analysis of variance as appropriate, and a P value of less than 0.05 was regarded as significant.

This study was approved by the Ethics Committee of the West Lambeth Health Authority.

Results

Whole-cell currents

4-Aminopyridine (4-AP)-sensitive outward current In only 26 of 155 cells did depolarization to –40 mV and more positive potentials result in an outwardly rectifying current that possessed a 4-AP-sensitive component. The 4-AP-sensitive current amplitude distribution in these cells showed a wide range (10–400 pA at 0 mV, mean 94 ± 133 pA, $n = 26$), but with a strong skew towards lower amplitudes, such that in the majority of cells showing this current (20 of 26) the current was less than 100 pA at 0 mV, with 17 cells having currents less than 50 pA. In the few cells where current amplitude was large enough for analysis, (> 100 pA, 6 of 26), the time course of activation was best fitted by second-order exponentials (n^2 kinetics), and was faster at more positive potentials (Figure 1a). Ramp-generated current-voltage relationships in these cells revealed a characteristic 'shoulder' between –20 and +20 mV (Figure 1b and 1c).

Experiments were performed to determine the sensitivity of this current to various K^+ channel blocking agents. The depolarization-induced outward current in these cells was only slightly reduced by 1 mM tetraethylammonium (TEA) (Figure

1b), but was markedly reduced by 2 mM 4-AP (Figures 1b,c). 100 nM ChTX was not effective against this current. Neither the Ca^{2+}-buffering capacity of the intracellular solution, nor the removal of Ca^{2+} from the external solution had any effect on the outward current. In the 6 cells where this current had sufficient amplitude for proper analysis it could be identified as a delayed rectifier on the basis of outward rectification, delayed activation, 4-AP sensitivity and resistance to TEA and ChTX. It is important to note that in the same experimental conditions a large voltage-gated delayed rectifier current could be found in all smooth muscle cells isolated from rat trachealis and bronchi, and rabbit trachealis (unpublished observations). The small amplitude and rare occurrence of this current in human bronchial cells made more detailed study impossible. However, we cannot exclude the possibility that a 4-AP-sensitive current with an amplitude of less than 50 pA was concealed by the relatively large and noisy 4-AP-resistant component seen in the majority of cells studied (see below).

4-AP-resistant outward current In contrast, in the vast majority of cells (129 of 155) depolarization from a holding potential of –80 mV resulted in a noisy, 4-AP- (5 mM) resistant, outward current. The amplitude varied between cells and was dependent on the $[Ca^{2+}]_i$ and was much larger than that of the 4-AP-sensitive current, with a mean value of 560 ± 124 pA ($n = 74$) at 0 mV with $[Ca^{2+}]_i$ less than 0.1 nM. The time-course of activation was best fitted by a first-order exponential (Figure 2a). The current was not sensitive to 4-AP (up to 5 mM), but was substantially reduced by 100 nM ChTX in the bath solution (Figure 2b). TEA (1 mM) and iberiotoxin (50 nM, IbTX) were also very effective inhibitors (Figure 2c). It should be noted that while the effect of ChTX was fast and reversible, that of IbTX developed more slowly, and full recovery was not achieved even after 20 min washout (not shown). The effects of these K^+ channel inhibitors on the current-voltage relationships are summarized in Figure 3. Apamin (1 μM), a blocker of small-conductance Ca^{2+}-dependent K^+ channels ($n = 3$), and glibenclamide (1 μM), a blocker of ATP-dependent K^+ channels ($n = 3$), were without effect upon whole-cell currents under the conditions of the present study. None of the above results was affected by the addition of 2 mM ATP and/or 0.2 mM GTP to the internal solution. The TEA-, ChTX- and IbTX-sensitive current did not show steady-state inactivation (Figure 4a), and did not decrease substantially even during a 5 s depolarization (Figure 4b).

The membrane potential at which a measurable outward

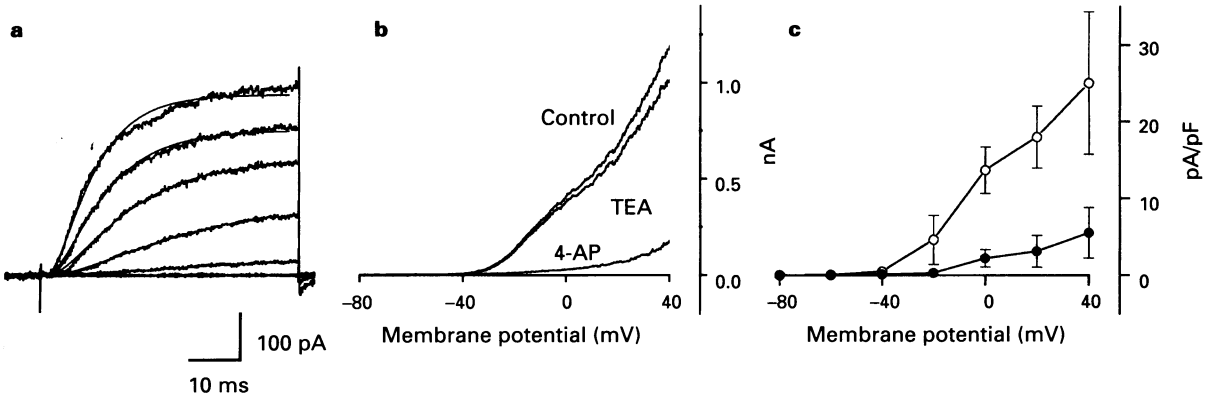

Figure 1 (a) Delayed rectifier whole-cell currents induced in a single freshly dispersed human bronchial smooth muscle cell by 50 ms depolarizing voltage steps from a holding potential of –80 mV to –100, –50, –40, –30, –20, –10 and 0 mV. Thin lines represent fit by second-order exponentials. (b) Current-voltage relationships obtained from a single cell using 1 s voltage ramps from –100 to +50 mV prior to drug application (Control), in the presence of 2 mM 4-aminopyridine (4-AP) and then 1 mM tetraethylammonium (TEA) after complete 4-AP washout. (c) Mean ramp-generated current-voltage relationships (at 20 mV intervals, normalised for cell capacitance) from cells possessing significant (see text) delayed rectifier current in the absence (○) and presence (●) of 2 mM 4-AP. Mean ± s.d., $n = 6$ cells. Internal KCl solution in all figures contained less than 0.1 nM free $[Ca^{2+}]$.

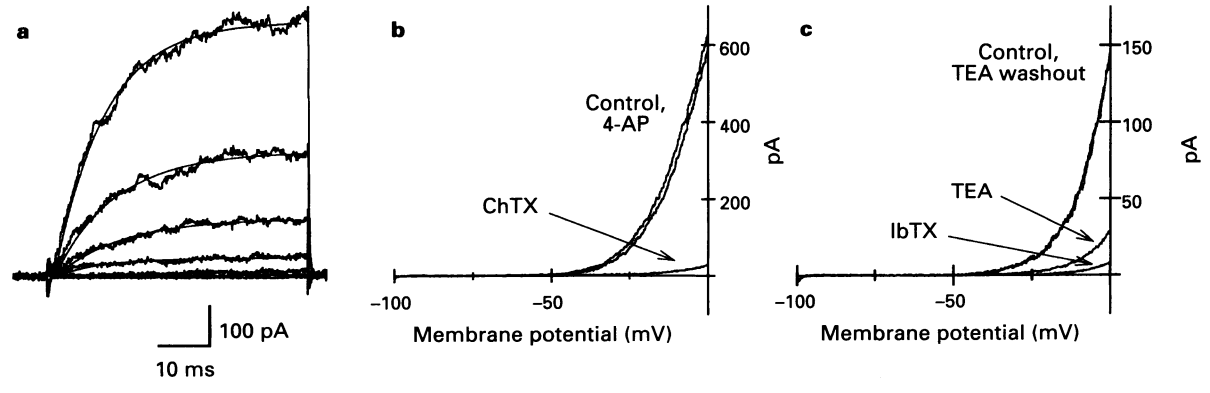

Figure 2 (a) 4-aminopyridine (4-AP)-resistant whole-cell currents induced in a single freshly dispersed human bronchial smooth muscle cell by 50 ms depolarizing voltage steps from a holding potential of –80 mV to –100, –50, –40, –30, –20, –10 and 0 mV. Thin lines represent fit by first-order exponentials. (b) Current-voltage relationships obtained from a single cell using 1 s voltage ramps from –100 mV to 0 mV prior to drug application (Control), in the presence of 5 mM 4-AP and then 100 nM charybdotoxin (ChTX) after complete 4-AP washout. (c) Current-voltage relationships obtained from a single cell using 1 s voltage ramps from –100 mV to 0 mV prior to drug application (control), in the presence of 1 mM tetraethylammonium (TEA) and then 50 nM iberiotoxin (IbTX) after complete TEA washout. Internal KCl solution in all figures contained less than 0.1 nM free $[Ca^{2+}]$.

current could be recorded varied somewhat between cells, being typically in the range –40 to –20 mV with a $[Ca^{2+}]_i$ < 0.1 nM. However, when $[Ca^{2+}]_i$ was increased to 100 nM the activation threshold shifted towards more negative potentials and the current amplitude was strongly increased (Figure 5a). In a few cells (14 out of 155) a measurable outward current was observed only after depolarization to + 50 mV or more positive with a $[Ca^{2+}]_i$ < 0.1 nM.

In 7 cells from 3 patients where whole-cell recording was performed by use of the nystatin permeabilized patch technique, depolarization to –40 mV and more positive potentials elicited an outward current that was sensitive to TEA and ChTX, but was not affected by 4-AP. This current showed characteristics similar to that observed in the majority of cells using conventional whole-cell techniques. In the course of the experiment the whole-cell current was initially recorded in perforated patch configuration with an $[Ca^{2+}]_i$ in the pipette solution of 100 nM. After patch disruption by additional suction, a current could be recorded in the conventional whole-cell configuration for long periods, as previously reported by Zhou & Neher (1993). After cell dialysis the current changed only slightly, which implies that resting $[Ca^{2+}]_i$ in the freshly dispersed cells is close to 100 nM (data not shown).

Single channel currents

Single channel recording revealed at least 4 types of single channel in freshly isolated human bronchial cells with con-

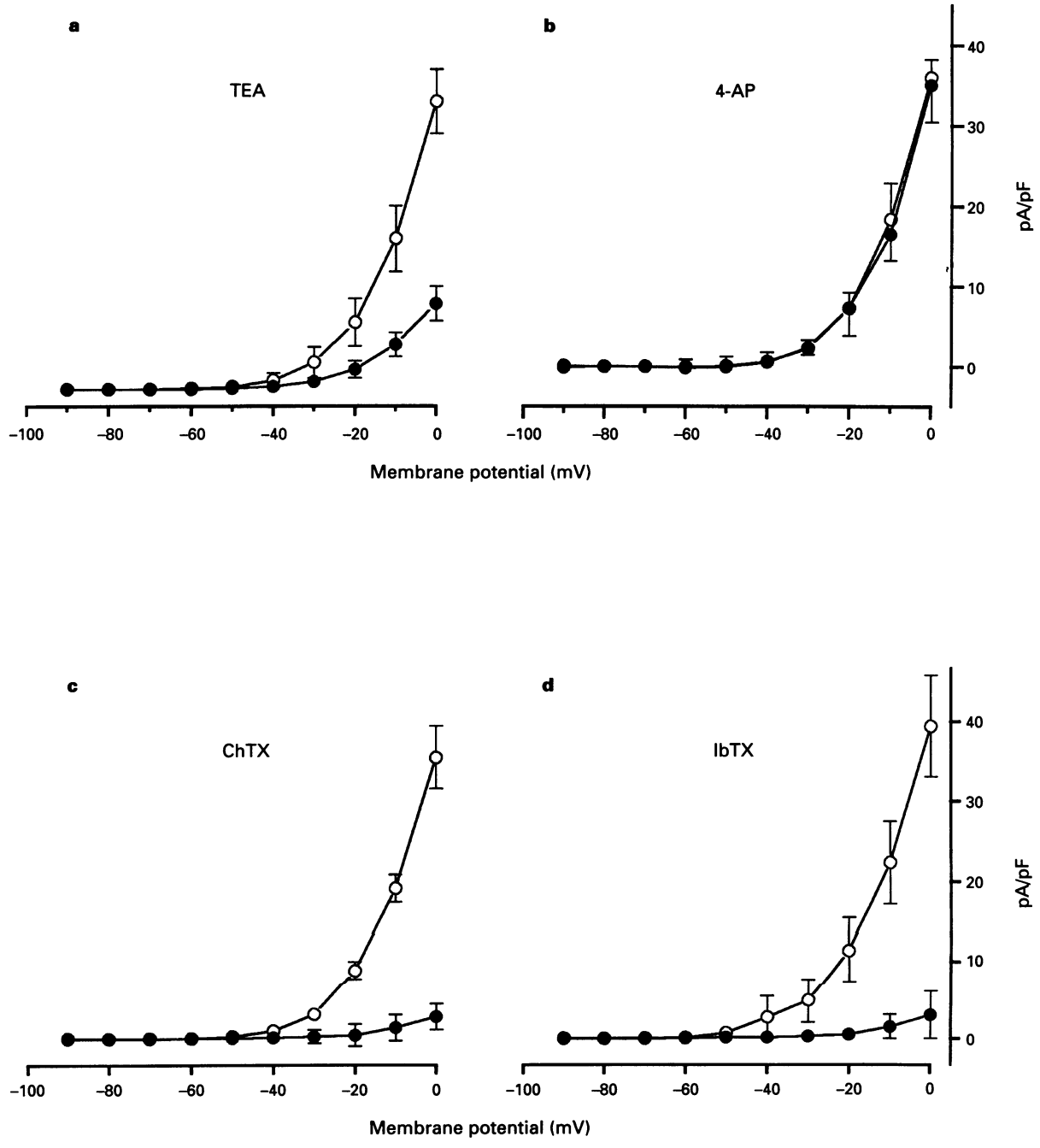

Figure 3 Mean ramp-generated current-voltage relationships (at 10 mV intervals; normalised for cell capacitance) in the absence (○) and presence (●) of various K^+ channel blockers: (a) 1 mM tetraethylammonium (TEA, $n=34$); (b) 5 mM 4-aminopyridine (4-AP, $n=12$); (c) 100 nM charybdotoxin (ChTX, $n=14$); (d) 50 nM iberiotoxin (IbTX, $n=5$). Means ± s.d. Internal KCl solution in all figures contained less than 0.1 nM free $[Ca^{2+}]$.

ductances of around 210, 130, 80 and 20 pS. The most abundant single channels had a conductance of 214±26 pS ($n=34$) with 140 mM KCl solution in the pipette, and 177±23 pS ($n=7$) with external NaCl solution in the pipette, and these were recorded in all cell-attached patches even at hyperpolarizing pipette potentials (Figure 6). Each patch contained up to 6 large conductance channels when pipettes with a resistance of 2–5 MOhm were used. However, with pipettes of 10–15 MOhm it was possible to obtain patches containing only one channel. It should be noted that the large channel currents, recorded from the cell-attached patches, were often distorted by the high input resistance of the cell. Channels with the same conductance (209±14 pS, $n=13$) were also recorded in inside-out patches with symmetrical 140 mM KCl across the membrane. Again, these channels could be recorded easily even at negative membrane potentials (e.g. –80 mV) and with $[Ca^{2+}]_i$ less than 0.1 nM. The voltage-dependence of the open state probability at 0 Ca^{2+} and 5 mM EGTA on the cytosolic side ($[Ca^{2+}]_i$ less than 0.1 nM) was suitably fitted by the Boltzmann equation, giving a mean V_{50} of 4±14 mV ($n=13$). The open state probability was increased further when cytosolic $[Ca^{2+}]_i$ was increased (Figure 5b), with a corresponding shift in the voltage-dependency (Figure 5c).

Channels were not sensitive to 10 mM TEA applied to the cytosolic side, while Ba^{2+} (1 mM) strongly increased the open state probability at negative membrane potentials, and de-

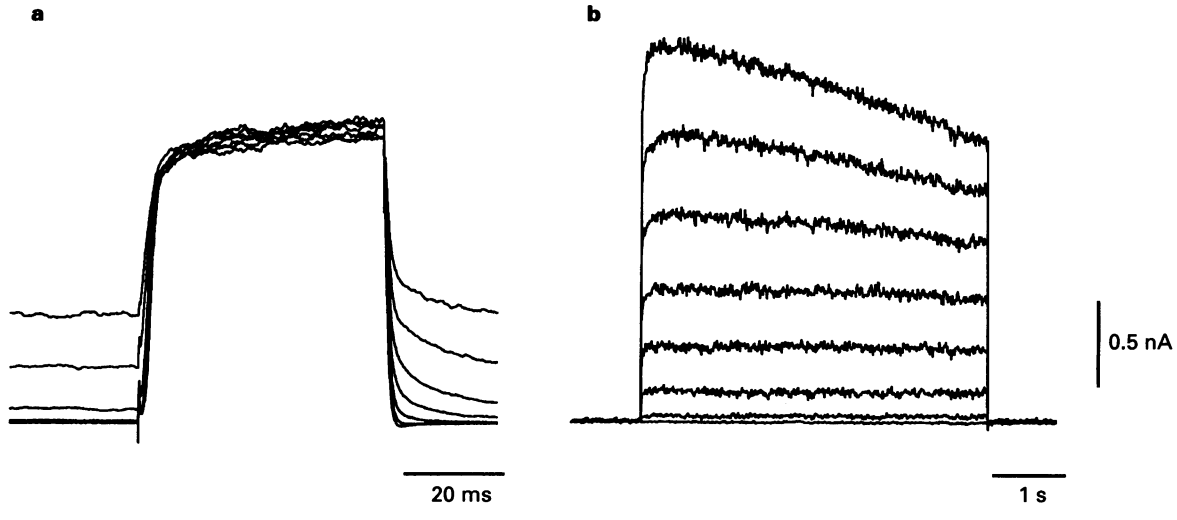

Figure 4 (a) The family of whole-cell currents induced by 50 ms depolarizing pulses to +80 mV from holding potentials of –90, –70, –50, –30, –10, +10 and +30 mV. (b) The family of whole-cell currents induced by 5 s depolarizing pulses to –40, –20, 0 +20, +40, +60, +80 and +100 mV from holding potential of –70 mV. All data obtained from the same cell; less than 0.1 nM free internal $[Ca^{2+}]$.

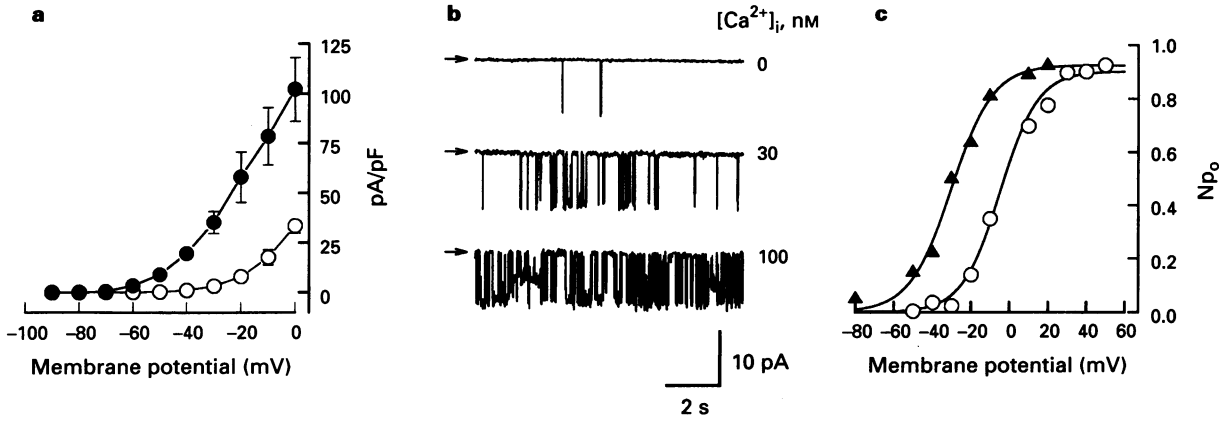

Figure 5 (a) Mean ramp-generated current-voltage relationships (at 10 mV intervals; normalized for cell capacitance) with $[Ca^{2+}]_i$ < 0.1 nM (○; $n=34$) and 100 nM (●, $n=11$); mean±s.d. (b) Large conductance single channel currents recorded from an inside-out patch containing only one channel, at nominally 0 (< 0.1 nM), 30 and 100 nM $[Ca^{2+}]_i$. Symmetrical 140 mM KCl, membrane potential –40 mV. Arrows indicate closed state and all figures follow the normal convention that a downward deflection represents an inward current. (c) Voltage-dependence of the open state probability of large conductance channels recorded from the same patch as (b) with $[Ca^{2+}]_i$ < 0.1 nM (○) and 30 nM $[Ca^{2+}]_i$ (▲). Curves fitted by the Boltzmann equation:

$$\frac{Np_o}{Np_{omax}} = 1 + \exp\left(\frac{V_{50}-V}{k}\right)$$

where Np_o is open state probability with N channels in patch at potential V, Np_{omax} is maximum open state probability for N channels in patch, and k is the slope constant. The half-maximal activation potential V_{50} was calculated as –5 mV and –30 mV for nominally 0 and 30 nM $[Ca^{2+}]_i$ respectively. Experiments performed with symmetrical 140 mM KCl.

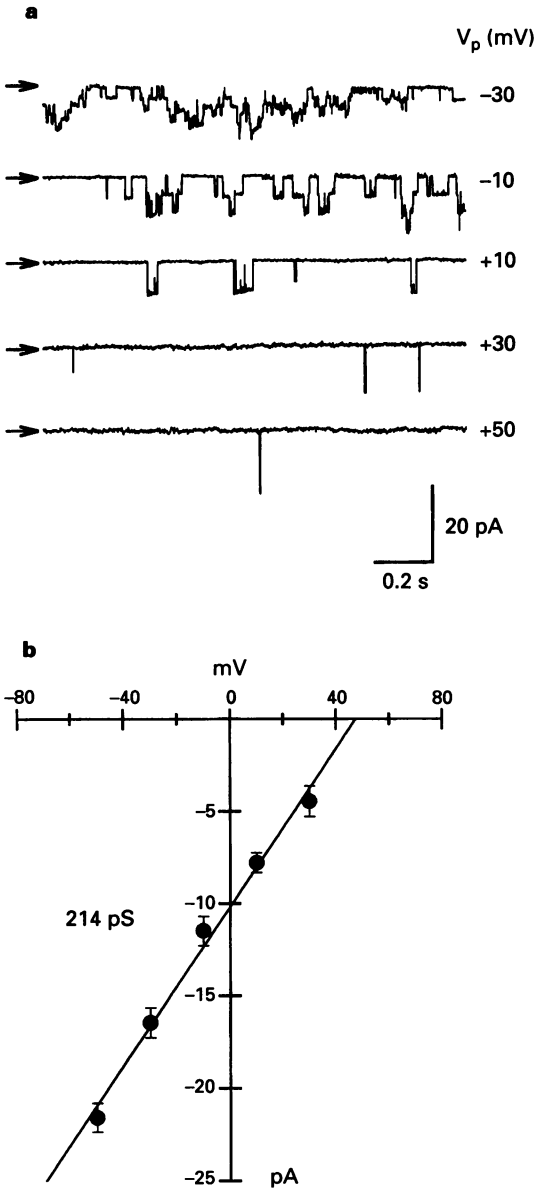

Figure 6 (a) Single channels recorded in cell-attached patch with KCl solution in the recording pipette; bath contained external NaCl solution. Numbers represent pipette potential (V_p) in mV; thus positive potentials refer to hyperpolarization above cell resting potential. Arrows indicate closed state. (b) Mean current-voltage relationship; the straight line corresponds to a slope conductance of 214±26 pS. Mean±s.d., $n=14$ cells.

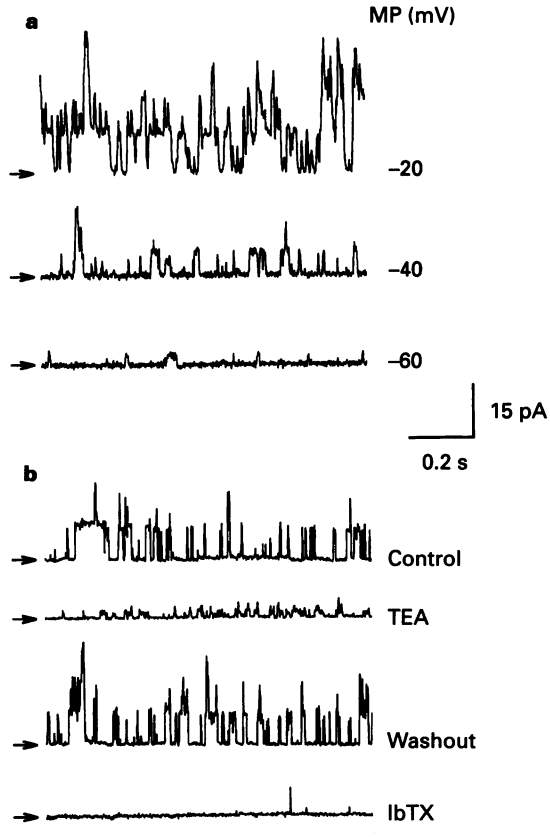

Figure 7 Single channels recorded in whole-cell configuration. Cell input resistance > 20 GOhm. Normal NaCl external solution, and less than 0.1 nM $[Ca^{2+}]_i$ in the internal KCl solution. (a) Voltage-dependence of single channel activity. Numbers indicate membrane potential (MP) in mV. (b) Effects of tetraethylammonium (TEA, 1 mM) and iberiotoxin (IbTX, 50 nM) on single channels recorded in whole-cell configuration. MP, -20 mV. Arrows indicate closed state.

creased it at positive potentials (data not shown). Channels recorded from outside-out patches were sensitive to externally applied TEA (1 mM), which induced strong flickering block of the open channel. External application of ChTX (100 nM) or IbTX (50 nM) resulted in a strong decrease of opening state probability without affecting the amplitude of the single channel current.

The same large conductance single channels were also observed in whole-cell configuration when small cells with an input resistance higher than 20 GOhm were used. In such records rare openings were observed even at a membrane potential of -60 mV and $[Ca^{2+}]_i$ less than 0.1 nM. Depolarization strongly enhanced single channel activity (Figure 7a), resulting in a substantial outward current at potentials positive to -40 mV. As with the corresponding macroscopic current, these single channels could be blocked by externally applied TEA or IbTX (Figure 7b). This observation implies that not only the depolarization-induced whole-cell current, but also the resting membrane potential of human bronchial ASMCs could be influenced by the activity of K_{Ca} channels.

We therefore performed current-clamp recordings to examine the role of K_{Ca} channels in the maintenance of the membrane potential. In current-clamp recordings using an intracellular solution with a low $[Ca^{2+}]_i$ (< 0.1 nM), cells displayed a membrane potential of -41±9 mV ($n=6$) which fluctuated strongly, presumably due to stochastic activity of large conductance channels. Application of 1 mM or 5 mM TEA caused depolarizations of 11±1 mV (1 mM; $n=3$), and 17±3 mV (5 mM; $n=3$), whereas 4-AP (5 mM) had no appreciable effect on membrane potential. In the presence of a more physiological $[Ca^{2+}]_i$ (100 nM) the resting membrane potential was significantly more negative at -58±7 mV ($n=11$; $P<0.01$), and application of TEA again depolarized the cells by 1.23±3.5 mV (1 mM; $n=7$) and 23.5±2.5 mV (5 mM; $n=6$); ChTX also induced a substantial depolarization (Figure 8a). The effect of 4-AP under these conditions was variable; 5 mM 4-AP induced in some cells no response, but in others a rather slowly developing depolarization which was not always reversible (Figure 8b). The mean depolarization induced by 5 mM 4-AP under these conditions was 12.5±11.5 mV, ($n=6$). It should be noted that voltage-clamp experiments on the same cells, performed immediately before going into current clamp, showed as in the majority of other cells used in this study that most of the voltage activated outward current was sensitive to TEA, with only a small component, if any, sensitive to 4-AP.

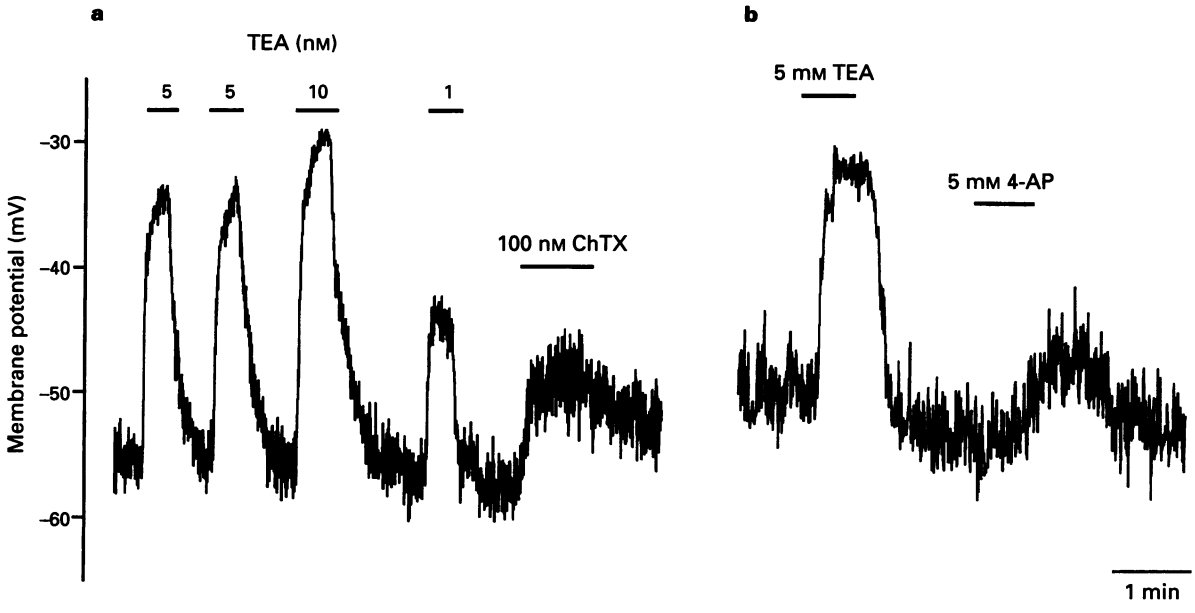

Figure 8 (a) Typical depolarization induced by tetraethylammonium (TEA, 1, 5, 10 mM) and charybdotoxin (ChTX, 100 nM) recorded under whole-cell current-clamp conditions. (b) Effects of TEA (5 mM) and 4-aminopyridine (4-AP, 5 mM) on membrane potential in another cell. Internal solution: 140 mM KCl, $[Ca^{2+}]_i$ = 100 nM. Horizontal bars represent time and duration of application of drug.

Discussion

The ASMC membrane is richly endowed with high-conductance Ca^{2+}-dependent K^+ channels and there is a corresponding macroscopic current which is activated under specific conditions. McCann & Welsh (1986) suggested that such channels may play a major role in determining the outward rectification of ASMC, and Muraki *et al.* (1990) also found a relatively large Ca^{2+}-dependent, TEA-sensitive component of total current in canine tracheal ASMCs. On the other hand, Kotlikoff and co-authors have reported that in freshly dispersed ASMC from several animal species, including dogs, the major voltage-dependent outward current is a 4-AP-sensitive delayed rectifier, and have suggested that the Ca^{2+}-dependent K^+ current may only be important in agonist-induced responses (e.g. Kotlikoff, 1993; Fleischmann *et al.*, 1993).

In contrast, we have found in the present study of freshly dispersed human bronchial smooth muscle cells that a 4-AP-sensitive delayed rectifier was measurable only in a small proportion of cells, and was relatively small. In the majority of cells the major outward current differed substantially from the delayed rectifier previously described for ASMCs in other species, in that: (i) it had first order activation kinetics; (ii) it was sensitive to IbTX, ChTX and TEA but not to 4-AP; and (iii) it did not demonstrate strong steady-state or time-dependent inactivation. These results are consistent with those we have previously reported for human bronchial smooth muscle cells in culture (Snetkov *et al.*, 1994). It should be noted that under identical recording conditions we have found a substantial delayed rectifier current with an amplitude of several hundred pA in ASMCs dispersed from rat, rabbit and bovine airway smooth muscle (Snetkov *et al.*, 1994; and unpublished observations), suggesting that this may be a true species variation. Although ChTX was initially regarded as a specific blocker of the large conductance Ca^{2+}-dependent K^+ channels (Miller *et al.*, 1985), it has recently been shown that some cloned, voltage-gated K^+ channels are also very sensitive to ChTX (Stühmer *et al.*, 1989; Grissmer *et al.*, 1994). As we have shown, however, the major current observed in these cells was also sensitive to IbTX, an agent which does not affect voltage-gated channels (Galvez *et al.*, 1990; Giangiacomo *et al.*, 1993).

Single channel recording revealed the existence of a large conductance K^+ channel which shared the properties of large conductance Ca^{2+}-dependent K^+ channels that have previously been observed in many tissues. These generally have a conductance between 140–250 pS, are sensitive to TEA applied from the extracellular but not cytosolic side, and show a voltage-dependent effect of Ba^{2+} such as that described in smooth muscle cells from canine and bovine trachealis (McCann & Welsh, 1986; Green *et al.*, 1991). The effect of Ba^{2+} in increasing P_o at negative potentials may reflect an ability to substitute for Ca^{2+} in terms of channel activation (Green *et al.*, 1991). The only atypical feature of the large conductance K^+ channels observed in this study seems to be the unusually negative half-activation potential (V_{50} = 4 mV) at an extremely low cytosolic Ca^{2+} concentration. Indeed, Kume *et al.* (1990) found that Ca^{2+}-dependent channels from rabbit trachea only started to open at 0 mV with a cytosolic Ca^{2+} of 0.25–0.4 μM. Murray *et al.* (1991) recorded activity in outside-out patches from guinea-pig trachealis with 100 nM Ca^{2+} on the cytosolic side at a membrane potential between 0 and +60 mV, whereas McCann & Welsh (1986) found a very low open state probability in inside-out patches from canine trachealis at 0.01 μM Ca^{2+} even at +40 mV, although occasional openings could be recorded at +60 mV even when the Ca^{2+}-free cytosolic solution, contained 10 mM EGTA. It is notable that, in our studies on randomly growing human cultured bronchial smooth muscle cells, the large conductance K^+ channels showed a similar sensitivity to Ca^{2+} to those reported in these latter studies, and differed sharply from freshly isolated cells (Snetkov *et al.*, 1994).

The apparently high sensitivity to Ca^{2+} found in these freshly isolated cells could reflect several factors reported elsewhere. For example Sansom & Stockand (1994) have demonstrated two isoforms of K_{Ca} channels isolated from bovine mesenteric artery smooth muscle cells and studied in lipid bilayers. These had the same conductance, but very different V_{50} values of –33 mV and +41 mV at a $[Ca^{2+}]_i$ of 1 μM (Sansom & Stockand, 1994). It is interesting to note that this difference is not dissimilar to that between the V_{50} of K_{Ca} channels found in the present study of freshly isolated human bronchial cells (4 mV), and the V_{50} of channels from cultured cells (+120 mV) that we have reported recently (Snetkov *et al.*, 1994).

It has also been shown that K_{Ca} channel activity in ASMCs

is regulated independently through both phosphorylation-dependent, cyclic AMP-dependent protein kinase-mediated, and membrane-delimited, G_s-protein mediated pathways (Kume *et al.*, 1994). Activation of any of those mechanisms shifts the relationship between voltage and open state probability by several tens of millivolts towards the physiological range of membrane potential. In addition, in cerebral artery smooth muscle cells, a cyclic GMP-dependent protein kinase, in the presence of cyclic GMP and ATP, increases K_{Ca} channel activity approximately eight fold (Robertson *et al.*, 1993). These data indicate that phosphorylation of the channel or of an associated regulatory protein causes a substantial leftward shift in the activation curve. It is therefore possible that the phosphorylation state of K_{Ca} channels in freshly dispersed human ASMCs may differ from that in other species.

On the other hand large conductance Ca^{2+}-independent K^+ channels have been reported in smooth muscle cells from bovine (Green *et al.*, 1991) and porcine (Saunders & Farley, 1991) trachealis, and from rat tail artery (Furspan & Webb, 1990). The channels observed in our study differed in several respects from the apparent Ca^{2+}-independent large conductance channels described in bovine tracheal ASMC by Green *et al.* (1991), which were sensitive to cytosolic TEA, activated at more positive potentials, and were observed exclusively in inside-out patches. Our results strongly suggest that in the large majority of cells the depolarization-induced outward current was due to the activity of large conductance, Ca^{2+}-sensitive K^+ channels, which were present at high density. The role of these channels in the generation of the whole-cell current could be seen particularly well during recordings from very small cells containing small numbers of channels (Figure 7).

Our current-clamp studies clearly demonstrate that the resting membrane potential in these bronchial smooth muscle cells is strongly influenced by intracellular [Ca^{2+}], and that both TEA and ChTX can cause a substantial depolarization. This is fairly good evidence that the K_{Ca} channels that we have described have an important role in the maintenance of resting membrane potential in this tissue. In contrast 4-AP had a less profound effect on membrane potential, which was not observed in all cells, or when intracellular [Ca^{2+}] was low. This might indicate the presence of a small number of delayed rectifier channels, which were not discernible in the voltage clamp experiments. Alternatively 4-AP may affect other conductances such as the K_{ATP} channel, which is known to be blocked by 4-AP (Beech & Bolton, 1989), or have another non-specific effect. Further studies are required to clarify these actions of 4-AP.

One possible source of variation between these experiments and previous studies on ASMCs may derive from the origin of the tissue. In this report all tissue was derived from bronchial sections, whereas most previous work has been performed on trachealis. However in preliminary experiments we have found that tracheal and bronchial smooth muscle cells of the rat were similar in their electrophysiology, and like many other species (excluding man) both exhibited a delayed rectifier as the major outward K^+ current (unpublished observations). Moreover we have recently obtained human trachealis from a single subject, and our preliminary studies suggest that cells from this tissue show identical responses to those described above for human bronchial smooth muscle cells (unpublished observations). We feel that our results are therefore likely to be related to a true species variation, rather than to the origin of the tissue within the airways.

In conclusion, these results suggest that in contrast to most other species, the major outward current in human bronchial smooth muscle is not due to a delayed rectifier, but to a large conductance ChTX-sensitive K^+ channel. The Ca^{2+}- and voltage-dependency of this current may well allow a sufficiently high open state probability for it to play a part in the regulation of the resting membrane potential, and hence airway excitability.

Supported by the Wellcome Trust, grant numbers 035721 (V.A.S.) and 039419 (S.J.H.).

References

ASANO, M., MASUZAWA-ITO, K. & MATSUDA, T. (1993). Charybdotoxin-sensitive K^+ channels regulate the myogenic tone in the resting state of arteries from spontaneously hypertensive rats. *Br. J. Pharmacol.*, **108**, 214–222.

BEECH, D.J. & BOLTON, T.B. (1989). Properties of the cromakalim-induced potassium conductance in smooth muscle cells isolated from the rabbit portal vein. *Br. J. Pharmacol.*, **98**, 851–864.

BRAYDEN, J.E. & NELSON, M.T. (1992). Regulation of arterial tone by activation of calcium-dependent potassium channels. *Science*, **256**, 532–535.

FABIATO, A. (1988). Computer program for calculating total from specified free or free from specified total ionic concentrations in aqueous solutions containing multiple metals and ligands. *Methods Enzymol.*, **157**, 378–417.

FLEISCHMANN, B.K., HAY, D.W.P. & KOTLIKOFF, M.I. (1994). Control of basal tone by delayed rectifier potassium channels in human airways. *Am. J. Resp. Crit. Care Med.*, **149**, A1080.

FLEISCHMANN, B.K., WASHABAU, R.J. & KOTLIKOFF, M.I. (1993). Control of resting membrane potential by delayed rectifier potassium currents in ferret airway smooth muscle cells. *J. Physiol.*, **469**, 625–638.

FURSPAN, P.B. & WEBB, R.C. (1990). Potassium channels and vascular reactivity in genetically hypertensive rats. *Hypertension*, **15**, 687–691.

GALVEZ, A., GIMENEZ-GALLEGO, G., REUBEN, J.P., ROY-CONTANCIN, L., FEIGENBAUM, P. & GARCIA, M.L. (1990). Purification and characterization of a unique, potent, peptidyl probe for the high conductance calcium-activated potassium channel from venom of the scorpion, *Buthus tamulus*. *J. Biol. Chem.*, **265**, 11083–11090.

GIANGIACOMO, K.M., SUGG, E.E., GARCIA-CALVO, M., LEONARD, R.J., MCMANUS, O.B. & GARCIA, M.L. (1993). Synthetic charybdotoxin-iberiotoxin chimeric peptides define toxin binding sites on calcium-activated and voltage-dependent potassium channels. *Biochemistry*, **32**, 2363–2370.

GREEN, K.A., FOSTER, R.W. & SMALL, R.C. (1991). A patch-clamp study of K^+-channel activity in bovine isolated tracheal smooth muscle cells. *Br. J. Pharmacol.*, **102**, 871–878.

GRISSMER, S., NGUYEN, A.N., AIYAR, J., HANSON, D.C., MATHER, R.J., GUTMAN, G.A., KARMILOWICZ, M.J., AUPERIN, D.D. & CHANDY, K.G. (1994). Pharmacological characterization of five cloned voltage-gated K^+ channels, types Kv1.1, 1.2, 1.3, 1.5 and 3.1, stably expressed in mammalian cell lines. *Mol. Pharmacol.*, **45**, 1227–34.

HAMILL, O.P., MARTY, A., NEHER, E., SAKMANN, B. & SIGWORTH, F.J. (1981). Improved patch-clamp techniques for high-resolution current recording from cells and cell-free membrane patches. *Pflügers Arch.*, **391**, 85–100.

HORN, R. & MARTY, A. (1988). Muscarinic activation of ionic currents measured by a new whole-cell recording method. *J. Gen. Physiol.*, **92**, 145–159.

KANNAN, M.S., JAGER, L.P., DANIEL, E.E. & GARFIELD, R.E. (1983). Effects of 4-aminopyridine and tetraethylammonium chloride on the electrical activity and cable properties of canine tracheal smooth muscle. *J. Pharmacol. Exp. Ther.*, **227**, 706–715.

KOTLIKOFF, M.I. (1993). Potassium channels in airway smooth muscle: a tale of two channels. *Pharmacol. Ther.*, **58**, 1–12.

KUME, H., HALL, I.P., WASHABAU, R.J., TAKAGI, K. & KOTLIKOFF, M.I. (1994). β-Adrenergic agonists regulate K_{Ca} channels in airway smooth muscle by cAMP-dependent and -independent mechanisms. *J. Clin. Invest.*, **93,** 371–379.

KUME, H. & KOTLIKOFF, M.I. (1991). Muscarinic inhibition of single K_{Ca} channels in smooth muscle cells by a pertussis-sensitive G protein. *Am. J. Physiol.*, **261,** C1204–C1209.

KUME, H., TAKAGI, K, SATAKE, T., TOKUNO, H. & TOMITA, T. (1990). Effects of intracellular pH on calcium-activated potassium channels in rabbit tracheal smooth muscle. *J. Physiol.*, **424,** 445–457.

MCCANN, J.D. & WELSH, M.J. (1986). Calcium-activated potassium channels in canine airway muscle. *J. Physiol.*, **372,** 113–127.

MILLER, C., MOCZYDLOWSKI, E., LATORRE, R. & PHILLIPS, M. (1985). Charybdotoxin, a protein inhibitor of single Ca^{2+}-activated K^+ channels from mammalian skeletal muscle. *Nature*, **313,** 316–318.

MIURA, M., BELVISI, M.G., STRETTON, C.D., YACOUB, M.H. & BARNES, P.J. (1992). Role of potassium channels in bronchodilator responses in human airways. *Am. Rev. Resp. Dis.*, **146,** 132–136.

MURAKI, K., IMAIZUMI, Y., KOJIMA, T., KAWAI, T. & WATANABE, M. (1990). Effects of tetraethylammonium and 4-aminopyridine on outward currents and excitability in canine tracheal smooth muscle cells. *Br. J. Pharmacol.*, **100,** 507–515.

MURRAY, R.K., BERRY, J.L., COOK, S.J., FOSTER, R.W., GREEN, K.A. & SMALL, R.C. (1991). Guinea-pig isolated trachealis: the effect of charybdotoxin on mechanical activity, membrane potential changes and the activity of plasmalemmal K^+-channels. *Br. J. Pharmacol.*, **103,** 1814–1818.

MURRAY, R.K., FLEISCHMANN, B.K. & KOTLIKOFF, M.I. (1993). Receptor-activated Ca influx in human airway smooth muscle – use of Ca imaging and perforated patch-clamp techniques. *Am. J. Physiol.*, **264,** C485–C490.

MURRAY, R.K. & KOTLIKOFF, M.I. (1991). Receptor-activated calcium influx in human airway smooth muscle cells. *J. Physiol.*, **435,** 123–144.

NARA, M., SASAKI, T., SHIMURA, S., IROKAWA, T., NAGAKI, M., MIURA, M. & SHIRATO, K. (1994). Endothelin-1 opens a receptor-operated K^+ channel in bovine tracheal smooth muscle cell to modulate its responsiveness to histamine. *Am. J. Resp. Crit. Care Med.*, **149,** A1080.

ROBERTSON, B.E., SCHUBERT, R., HESCHELER, J. & NELSON, M.T. (1993). cGMP-dependent protein kinase activates Ca-activated K channels in cerebral artery smooth muscle cells. *Am. J. Physiol.*, **265,** C299–C303.

SANSOM, S.C. & STOCKAND, J.D. (1994). Differential Ca^{2+} sensitivities of BK(Ca) isochannels in bovine mesenteric vascular smooth muscle. *Am. J. Physiol.*, **266,** C1182–C1189.

SAUNDERS, H.M. & FARLEY, J.M. (1991). Spontaneous transient outward currents and Ca^{++}-activated K^+ channels in swine tracheal smooth muscle cells. *J. Pharmacol. Exp. Ther.*, **257,** 1114–1120.

SNETKOV, V.A., HIRST, S.J., TWORT, C.H.C. & WARD, J.P.T. (1994). Potassium currents in human bronchial and rabbit tracheal smooth muscle cells in culture. *Am. J. Resp. Crit. Care Med.*, **149,** A1082.

STÜHMER, W., RUPPERSBERG, J.P., SCHRÖTER, K.H., SAKMANN, B., STOCKER, M., GIESE, K.P., PERSCHKE, A., BAUMANN, A. & PONGS, O. (1989). Molecular basis of functional diversity of voltage-gated potassium channels in mammalian brain. *EMBO J.*, **8,** 3235–44.

SUAREZ-KURTZ, G., GARCIA, M.L. & KACZOROWSKI, G.J. (1991). Effects of charybdotoxin and iberiotoxin on the spontaneous motility and tonus of different guinea pig smooth muscle tissues. *J. Pharmacol. Exp. Ther.*, **259,** 439–443.

ZHOU, Z. & NEHER, E. (1993). Mobile and immobile calcium buffers in bovine adrenal chromaffin cells. *J. Physiol.*, **469,** 247–274.

(Received February 13, 1995
Revised April 3, 1995
Accepted April 5, 1995)

British Journal of Pharmacology

VOLUME 115 (6) JULY 1995

SPECIAL REPORT

D.R. Collins, R.G. Pertwee & S.N. Davies. Prevention by the cannabinoid antagonist, SR141716A, of cannabinoid-mediated blockade of long-term potentiation in the rat hippocampal slice **869**

PAPERS

V. Bauer, V.V. Rekalov, I. Juránek, D. Gergel & P. Bohov. Effect of illuminated nifedipine, a potent antioxidant, on intestinal and vascular smooth muscles **871**

M. Bushfield, M. Metcalfe & A.M. Naylor. Activation of the micturition reflex by NK_2 receptor stimulation in the anaesthetized guinea-pig **875**

K. Masuda, T. Kamimura, K. Watanabe, T. Suga, M. Kanesaki, A. Takeuchi, A. Imaizumi & Y. Suzuki. Pharmacological activity of the C-terminal and N-terminal domains of secretory leukoprotease inhibitor *in vitro* **883**

J. Petersson, P.M. Zygmunt, L. Brandt & E.D. Högestätt. Substance P-induced relaxation and hyperpolarization in human cerebral arteries **889**

J. Pintor & M.T. Miras-Portugal. A novel receptor for diadenosine polyphosphates coupled to calcium increase in rat midbrain synaptosomes **895**

D. Godin, F. Rioux, F. Marceau & G. Drapeau. Mode of action of thrombin in the rabbit aorta **903**

A.M. Hosie, H.A. Baylis, S.D. Buckingham & D.B. Sattelle. Actions of the insecticide fipronil, on dieldrin-sensitive and resistant GABA receptors of *Drosophila melanogaster* **909**

A Lindén, S. Yoshihara, B. Chan & J.A. Nadel. Inhibition of bronchoconstriction by pituitary adenylate cyclase activating polypeptide (PACAP 1-27) in guinea-pigs *in vivo* **913**

K. Miura, T. Ebara, M. Okumura, T. Matsuura, S. Kim, T. Yukimura & H. Iwao. Attenuation of adrenomedullin-induced renal vasodilatation by N^G-nitro L-arginine but not glibenclamide **917**

P.B. Osborne & J.T. Williams. Characterization of acute homologous desensitization of μ-opioid receptor-induced currents in locus coeruleus neurones **925**

A.J. Kaumann, J.A. Lynham & A.M. Brown. Labelling with [^{125}I]-SB 207710 of a small 5-HT_4 receptor population in piglet right atrium: functional relevance **933**

H. Sipma, A. den Hertog & A. Nelemans. Ca^{2+}-dependent and -independent mechanism of cyclic-AMP reduction: mediation by bradykinin B_2 receptors **937**

J.P. Hannon, H.J. Pfannkuche & J.R. Fozard. A role for mast cells in adenosine A_3 receptor-mediated hypotension in the rat **945**

S. Adodra & T.G. Hales. Potentiation, activation and blockade of $GABA_A$ receptors of clonal murine hypothalamic GT1-7 neurones by propofol **953**

N.J. Welsh, N.P. Shankley & J.W. Black. Application of a model to explore interspecies differences in acetylcholine M-receptor-stimulated gastric acid secretion **961**

V. Lischke, R. Busse & M. Hecker. Selective inhibition by barbiturates of the synthesis of endothelium-derived hyperpolarizing factor in the rabbit carotid artery **969**

W. Feniuk, J. Dimech, E.M. Jarvie & P.P.A. Humphrey. Further evidence from functional studies for somatostatin receptor heterogeneity in guinea-pig isolated ileum, vas deferens and right atrium **975**

B.A. Kenny, D.H. Chalmers, P.C. Philpott & A.M. Naylor. Characterization of an α_{1D}-adrenoceptor mediating the contractile response of rat aorta to noradrenaline **981**

M. Fukao, Y. Hattori, M. Kanno, I. Sakuma & A. Kitabatake. Thapsigargin- and cyclopiazonic acid-induced endothelium-dependent hyperpolarization in rat mesenteric artery **987**

K.B. Mian & W. Martin. Differential sensitivity of basal and acetylcholine-stimulated activity of nitric oxide to destruction by superoxide anion in rat aorta **993**

H. Azuma, J. Sato, H. Hamasaki, A. Sugimoto, E. Isotani & S. Obayashi. Accumulation of endogenous inhibitors for nitric oxide synthesis and decreased content of L-arginine in regenerated endothelial cells **1001**

M.J. Cumberbatch, B.A. Chizh & P.M. Headley. Modulation of excitatory amino acid responses by tachykinins and selective tachykinin receptor agonists in the rat spinal cord **1005**

B.A. Chizh, M.J. Cumberbatch, P.J. Birch & P. M. Headley. Endogenous modulation of excitatory amino acid responsiveness by tachykinin NK_1 and NK_2 receptors in the rat spinal cord **1013**

P.K.E. Zygmunt, P.M. Zygmunt, E.D. Högestätt & K-E. Andersson. NANC neurotransmission in lamina propria of the rabbit urethra: regulation by different subsets of calcium channels **1020**

G. Edwards, J. Schneider, A. Niederste-Hollenberg, Th. Noack & A.H. Weston. Effects of BRL55834 in rat portal vein and bovine trachea: evidence for the induction of a glibenclamide-resistant, ATP-sensitive potassium current **1027**

STOCKTON

S. Sabry, F. Mondon, M. Levy, F. Ferré & A.T. Dinh-Xuan. Endothelial modulation of vasoconstrictor responses to endothelin-1 in human placental stem villi small arteries **1038**

C. Coméra & F. Russo-Marie. Glucocorticoid-induced annexin 1 secretion by monocytes and peritoneal leukocytes **1043**

A.R.C. Ladenius, G. Folkerts, H.J. van der Linde & F.P. Nijkamp. Potentiation by viral respiratory infection of ovalbumin-induced guinea-pig tracheal hyperresponsiveness: role for tachykinins **1048**

B. Vincent, V. Dive, A. Yiotakis, C. Smadja, R. Maldonado, J-P. Vincent & F. Checler. Phosphorus-containing peptides as mixed inhibitors of endopeptidase 3.4.24.15 and 3.4.24.16: effect on neurotensin degradation *in vitro* and *in vivo* **1053**

S.E. Gartside, V. Umbers, M. Hajos & T. Sharp. Interaction between a selective 5-HT_{1A} receptor antagonist and an SSRI *in vivo*: effects on 5-HT cell firing and extracellular 5-HT **1064**

D. Strabel & M. Diener. The effect of neuropeptide Y on sodium, chloride and potassium transport across the rat distal colon **1071**

M.W. Martin, A.J. O'Sullivan & B.D. Gomperts. Inhibition by cromoglycate and some flavonoids of nucleoside diphosphate kinase and of exocytosis from permeabilized mast cells **1080**

S.S. Hegde, D.W. Bonhaus, L.G. Johnson, E. Leung, R.D. Clark & R.M. Eglen. RS 39604: a potent, selective and orally active 5-HT_4 receptor antagonist **1087**

S.M. Poucher, J.R. Keddie, P. Singh, S.M. Stoggall, P.W.R. Caulkett, G. Jones & M.G. Collis. The *in vitro* pharmacology of ZM 241385, a potent, non-xanthine, A_{2a} selective adenosine receptor antagonist **1096**

A.C. MacKinnon, K.M. Wyatt, J.G. McGivern, R.D. Sheridan & C.M. Brown. [^{3}H]-lifarizine, a high affinity probe for inactivated sodium channels **1103**

R.G. Humphries, W. Tomlinson, J.A. Clegg, A.H. Ingall, N.D. Kindon & P. Leff. Pharmacological profile of the novel P_{2T}-purinoceptor antagonist, FPL 67085 *in vitro* and in the anaesthetized rat *in vivo* **1110**

V.A. Snetkov, S.J. Hirst, C.H.C. Twort & J.P.T. Ward. Potassium currents in human freshly isolated bronchial smooth muscle cells **1117**

The *British Journal of Pharmacology* is published by Stockton Press, a division of Macmillan Press Ltd. It is the official publication of the British Pharmacological Society.

Scope The *British Journal of Pharmacology* is published twice a month. It welcomes contribution in all fields of experimental pharmacology including neuroscience, biochemical, cellular and molecular pharmacology. The Board of Editors represents a wide range of expertise and ensures that well-presented work is published as promptly as possible, consistent with maintaining the overall quality of the journal.

This journal is covered by Current Contents, Excerpta Medica, BIOSIS, CABS and Index Medicus.

Editorial Manuscripts (plus two copies) and all editorial correspondence should be sent to: The Editorial Office, British Journal of Pharmacology, St George's Hospital Medical School, Cranmer Terrace, London SW17 0RE, UK. Tel: +44 (0)181 767 6765; Fax: +44 (0)181 767 5645.

Advertisements Enquiries concerning advertisements should be addressed to: Michael Rowley, Hasler House, High Street, Great Dunmow, Essex CM6 1AP, UK. Tel: +44 (0)1371 874613; Fax: +44 (0)1371 872273.

Publisher All business correspondence, supplement enquiries and reprint requests should be addressed to British Journal of Pharmacology, Stockton Press, Houndmills, Basingstoke, Hampshire RG21 2XS, UK. Tel: +44 (0)1256 29242; Fax: +44 (0)1256 810526. Publisher: Marija Vukovojac. Production Controller: Karen Stuart.

Subscriptions – EU/Rest of World Subscription price per annum (3 volumes, 24 issues) £620, rest of world £820 (Airmail), £685 (Surface mail) or equivalent in any other currency. Orders must be accompanied by remittance. Cheques should be made payable to Macmillan Magazines and sent to: The Subscription Department Macmillan Press Ltd, Houndmills, Basingstoke, Hampshire RG21 2XS, UK. Where appropriate, subscribers may make payments into UK Post Office Giro Account No. 519 2455. Full details must accompany the payment. Subscribers from EC territories should add sales tax at the local rate.

Subscriptions – USA USA subscribers call toll free 1-800-221-2123 or send check/money order/credit card details to: Stockton Press, 49, West 24th Street, New York, NY 10010; Tel: 212 627 5757, Fax: 212 627 9256. USA annual subscription rates: $1230 Airmail; $1030 Surface (Institutional/Corporate); $225 (Individual making personal payment).

British Journal of Pharmacology (ISSN 0007–1188) is published twice a month by Macmillan Press Ltd, c/o Mercury Airfreight International Ltd, 2323 Randolph Avenue, Avenel, NJ 07001, USA. Subscription price for institutions is $1030 per annum (surface). 2nd class postage is paid at Rahway NJ. Postmaster: send address corrections to Macmillan Press Ltd, c/o Mercury Airfreight International Ltd, 2323 Randolph Avenue, Avenel NJ 07001.

Reprints of any article in this journal are available from Stockton Press, Houndmills, Basingstoke, Hampshire RG21 2XS, UK.
Tel: +44 (0)1256 29242; Fax: +44 (0)1256 810526.

Copyright © 1995 Stockton Press
ISSN 0007–1188

All rights of reproduction are reserved in respect of all papers, articles, illustrations, etc., published in this journal in all countries of the world.

All material published in this journal is protected by copyright, which covers exclusive rights to reproduce and distribute the material. No material published in this journal may be reproduced or stored on microfilm or in electronic, optical or magnetic form without the written authorisation of the Publisher.

Authorisation to photocopy items for internal or personal use of specific clients, is granted by Stockton Press for libraries and other users registered with the Copyright Clearance Center (CCC) Transaction Reporting Service, provided that the base fee of $12.00 per copy is paid directly to CCC, 21 Congress St., Salem, MA 01970, USA. 0007–1188/95 $12.00 + $0.00.

Apart from any fair dealing for the purposes of research or private study, or criticism or review, as permitted under the Copyright, Designs and Patent Act 1988, this publication may be reproduced, stored or transmitted, in any form or by any means, only with the prior permission in writing of the publishers, or in the case of reprographic reproduction, in accordance with the terms of licences issued by the Copyright Licensing Agency.

BRITISH JOURNAL OF PHARMACOLOGY

The *British Journal of Pharmacology* welcomes contributions in all fields of experimental pharmacology including neuroscience, biochemical, cellular and molecular pharmacology. The Board of Editors represents a wide range of expertise and ensures that well-presented work is published as promptly as possible, consistent with maintaining the overall quality of the journal.

Edited for the British Pharmacological Society by

A.T. Birmingham
(Chairman)

R.W. Horton **W.A. Large**
(Secretaries)

Editorial Board

P.I. Aaronson *London*
J.A. Angus *Melbourne, Australia*
G.W. Bennett *Nottingham*
T.P. Blackburn *Harlow*
N.G. Bowery *London*
W.C. Bowman *Glasgow*
S.D. Brain *London*
K.D. Butler *Horsham*
M. Caulfield *London*
R. Chess-Williams *Sheffield*
T. Cocks *Melbourne, Australia*
S.J. Coker *Liverpool*
R.A. Coleman *Ware*
Helen M. Cox *London*
A.J. Cross *London*
V. Crunelli *Cardiff*
T.C. Cunnane *Oxford*
F. Cunningham *London*
A. Dickenson *London*
J.R. Docherty *Dublin*
A. Dray *London*
L. Edvinsson *Lund, Sweden*
G. Edwards *Manchester*
J.M. Edwardson *Cambridge*
R.M. Eglen *Palo Alto, USA*
P.C. Emson *Cambridge*
A.C. Foster *San Diego, USA*
J.R. Fozard *Basle, Switzerland*
Allison D. Fryer *Baltimore, USA*
J.P. Gallagher *Galveston, USA*
Sheila M. Gardiner *Nottingham*
C.J. Garland *Bristol*
A. Gibson *London*
M.A. Giembycz *London*
W.R. Giles *Calgary, Canada*
R.G. Goldie *Perth, Australia*
R.J. Griffiths *Connecticut, USA*
R.W. Gristwood *Cambridge*
Judith M. Hall *London*
D.W.P. Hay *Philadelphia, USA*
P.G. Hellewell *London*
P.E. Hicks *Edinburgh*
S.J. Hill *Nottingham*
K. Hillier *Southampton*
S.M.O. Hourani *Guildford*
J.C. Hunter *Palo Alto, USA*
E.J. Johns *Birmingham*
R.S.G. Jones *Oxford*
C.C. Jordan *Ware*
P.A.T. Kelly *Edinburgh*
D.A. Kendall *Nottingham*
C. Kennedy *Glasgow*
P. Leff *Loughborough*
A.T. McKnight *Cambridge*
C.A. Maggi *Florence, Italy*
Janice M. Marshall *Birmingham*
G. Martin *Beckenham*
W. Martin *Glasgow*
A. Mathie *London*
D.N. Middlemiss *Harlow*
P.K. Moore *London*
C.D. Nicholson *Oss, The Netherlands*
H. Osswald *Tübingen, Germany*
F.L. Pearce *London*
J.D. Pearson *London*
A.G. Renwick *Southampton*
P.J. Roberts *Bristol*
G.J. Sanger *Harlow*
W.C. Sessa *Connecticut, USA*
P. Sneddon *Glasgow*
K. Starke *Freiburg, Germany*
R.J. Summers *Melbourne, Australia*
P.V. Taberner *Bristol*
J. Tamargo *Madrid, Spain*
C. Thiemermann *London*
M.D. Tricklebank *Basle, Switzerland*
T.J. Verbeuren *Suresnes, France*
R.R. Vollmer *Pittsburgh, USA*
K.J. Watling *Boston, USA*
A.H. Weston *Manchester*
J. Westwick *Bath*
Eileen Winslow *Riom, France*
E.H.F. Wong Milan, Italy
B. Woodward *Bath*

Corresponding Editors

P.R. Adams *Stony Brook, U.S.A.*
C. Bell *Dublin*
F.E. Bloom *La Jolla, U.S.A.*
A.L.A. Boura *Newcastle, Australia*
N.J. Dun *Toledo, U.S.A.*
R.F. Furchgott *New York, U.S.A.*
T. Godfraind *Brussels, Belgium*
S.Z. Langer *Paris, France*
R.J. Miller *Chicago, U.S.A.*
R.C. Murphy *Denver, U.S.A.*
E. Muscholl *Mainz, Germany*
R.A. North *Geneva, Switzerland*
M. Otsuka *Tokyo, Japan*
M.J. Rand *Melbourne, Australia*
S. Rosell *Södertalje, Sweden*
P. Seeman *Toronto, Canada*
L. Szekeres *Szeged, Hungary*
B. Uvnas *Stockholm, Sweden*
P.A. Van Zwieten *Amsterdam, Netherlands*
V.M. Varagič *Belgrade, Yugoslavia*
G. Velo *Verona, Italy*
Wang Zhen Gang *Beijing, China*
M.B.H. Youdim *Haifa, Israel*

Submission of manuscripts: Manuscripts (two copies) should be sent to The Editorial Office, British Journal of Pharmacology, St. George's Hospital Medical School, Cranmer Terrace, London SW17 0RE.

Authors should consult the Instructions to Authors and the Nomenclature Guidelines for Authors in Vol. **114,** 245–255. These Instructions and Guidelines also appear with the journal Index for Volumes **111–113,** 1994. A checklist of the essential requirements is summarised in each issue of the journal, or as the last page of the issue.

Whilst every effort is made by the publishers and editorial committee to see that no inaccurate or misleading data, opinion or statement appears in this Journal, they and the *British Pharmacological Society* wish to make it clear that the data and opinions appearing in the articles and advertisements herein are the responsibility of the contributor or advertiser concerned. Accordingly, the *British Pharmacological Society*, the publishers and the editorial committee and their respective employees, officers and agents accept no liability whatsoever for the consequences of any such inaccurate or misleading data, opinion or statement.

S. Sabry, F. Mondon, M. Levy, F. Ferré & A.T. Dinh-Xuan. Endothelial modulation of vasoconstrictor responses to endothelin-1 in human placental stem villi small arteries **1038**

C. Coméra & F. Russo-Marie. Glucocorticoid-induced annexin 1 secretion by monocytes and peritoneal leukocytes **1043**

A.R.C. Ladenius, G. Folkerts, H.J. van der Linde & F.P. Nijkamp. Potentiation by viral respiratory infection of ovalbumin-induced guinea-pig tracheal hyperresponsiveness: role for tachykinins **1048**

B. Vincent, V. Dive, A. Yiotakis, C. Smadja, R. Maldonado, J-P. Vincent & F. Checler. Phosphorus-containing peptides as mixed inhibitors of endopeptidase 3.4.24.15 and 3.4.24.16: effect on neurotensin degradation *in vitro* and *in vivo* **1053**

S.E. Gartside, V. Umbers, M. Hajos & T. Sharp. Interaction between a selective 5-HT_{1A} receptor antagonist and an SSRI *in vivo*: effects on 5-HT cell firing and extracellular 5-HT **1064**

D. Strabel & M. Diener. The effect of neuropeptide Y on sodium, chloride and potassium transport across the rat distal colon **1071**

M.W. Martin, A.J. O'Sullivan & B.D. Gomperts. Inhibition by cromoglycate and some flavonoids of nucleoside diphosphate kinase and of exocytosis from permeabilized mast cells **1080**

S.S. Hegde, D.W. Bonhaus, L.G. Johnson, E. Leung, R.D. Clark & R.M. Eglen. RS 39604: a potent, selective and orally active 5-HT_4 receptor antagonist **1087**

S.M. Poucher, J.R. Keddie, P. Singh, S.M. Stoggall, P.W.R. Caulkett, G. Jones & M.G. Collis. The *in vitro* pharmacology of ZM 241385, a potent, non-xanthine, A_{2a} selective adenosine receptor antagonist **1096**

A.C. MacKinnon, K.M. Wyatt, J.G. McGivern, R.D. Sheridan & C.M. Brown. [^{3}H]-lifarizine, a high affinity probe for inactivated sodium channels **1103**

R.G. Humphries, W. Tomlinson, J.A. Clegg, A.H. Ingall, N.D. Kindon & P. Leff. Pharmacological profile of the novel P_{2T}-purinoceptor antagonist, FPL 67085 *in vitro* and in the anaesthetized rat *in vivo* **1110**

V.A. Snetkov, S.J. Hirst, C.H.C. Twort & J.P.T. Ward. Potassium currents in human freshly isolated bronchial smooth muscle cells **1117**

The *British Journal of Pharmacology* is published by Stockton Press, a division of Macmillan Press Ltd. It is the official publication of the British Pharmacological Society.

Scope The *British Journal of Pharmacology* is published twice a month. It welcomes contribution in all fields of experimental pharmacology including neuroscience, biochemical, cellular and molecular pharmacology. The Board of Editors represents a wide range of expertise and ensures that well-presented work is published as promptly as possible, consistent with maintaining the overall quality of the journal.

This journal is covered by Current Contents, Excerpta Medica, BIOSIS, CABS and Index Medicus.

Editorial Manuscripts (plus two copies) and all editorial correspondence should be sent to: The Editorial Office, British Journal of Pharmacology, St George's Hospital Medical School, Cranmer Terrace, London SW17 0RE, UK. Tel: +44 (0)181 767 6765; Fax: +44 (0)181 767 5645.

Advertisements Enquiries concerning advertisements should be addressed to: Michael Rowley, Hasler House, High Street, Great Dunmow, Essex CM6 1AP, UK. Tel: +44 (0)1371 874613; Fax: +44 (0)1371 872273.

Publisher All business correspondence, supplement enquiries and reprint requests should be addressed to British Journal of Pharmacology, Stockton Press, Houndmills, Basingstoke, Hampshire RG21 2XS, UK. Tel: +44 (0)1256 29242; Fax: +44 (0)1256 810526. Publisher: Marija Vukovojac. Production Controller: Karen Stuart.

Subscriptions – EU/Rest of World Subscription price per annum (3 volumes, 24 issues) £620, rest of world £820 (Airmail), £685 (Surface mail) or equivalent in any other currency. Orders must be accompanied by remittance. Cheques should be made payable to Macmillan Magazines and sent to: The Subscription Department Macmillan Press Ltd, Houndmills, Basingstoke, Hampshire RG21 2XS, UK. Where appropriate, subscribers may make payments into UK Post Office Giro Account No. 519 2455. Full details must accompany the payment. Subscribers from EC territories should add sales tax at the local rate.

Subscriptions – USA USA subscribers call toll free 1-800-221-2123 or send check/money order/credit card details to: Stockton Press, 49, West 24th Street, New York, NY 10010; Tel: 212 627 5757, Fax: 212 627 9256. USA annual subscription rates: $1230 Airmail; $1030 Surface (Institutional/Corporate); $225 (Individual making personal payment).

British Journal of Pharmacology (ISSN 0007–1188) is published twice a month by Macmillan Press Ltd, c/o Mercury Airfreight International Ltd, 2323 Randolph Avenue, Avenel, NJ 07001, USA. Subscription price for institutions is $1030 per annum (surface). 2nd class postage is paid at Rahway NJ. Postmaster: send address corrections to Macmillan Press Ltd, c/o Mercury Airfreight International Ltd, 2323 Randolph Avenue, Avenel NJ 07001.

Reprints of any article in this journal are available from Stockton Press, Houndmills, Basingstoke, Hampshire RG21 2XS, UK.
Tel: +44 (0)1256 29242; Fax: +44 (0)1256 810526.

Copyright © 1995 Stockton Press
ISSN 0007–1188

All rights of reproduction are reserved in respect of all papers, articles, illustrations, etc., published in this journal in all countries of the world.

All material published in this journal is protected by copyright, which covers exclusive rights to reproduce and distribute the material. No material published in this journal may be reproduced or stored on microfilm or in electronic, optical or magnetic form without the written authorisation of the Publisher.

Authorisation to photocopy items for internal or personal use of specific clients, is granted by Stockton Press for libraries and other users registered with the Copyright Clearance Center (CCC) Transaction Reporting Service, provided that the base fee of $12.00 per copy is paid directly to CCC, 21 Congress St., Salem, MA 01970, USA. 0007–1188/95 $12.00 + $0.00.

Apart from any fair dealing for the purposes of research or private study, or criticism or review, as permitted under the Copyright, Designs and Patent Act 1988, this publication may be reproduced, stored or transmitted, in any form or by any means, only with the prior permission in writing of the publishers, or in the case of reprographic reproduction, in accordance with the terms of licences issued by the Copyright Licensing Agency.

PREPARATION OF MANUSCRIPTS

Authors are strongly recommended to read the full *Instructions to Authors* and *Nomenclature Guidelines for Authors* (*Br. J. Pharmacol.* 1995, **114,** 245–255) before submitting a manuscript for publication in the *British Journal of Pharmacology*. The manuscript and cover letter should be checked against the following list before mailing.

The original and one copy of the manuscript must be supplied. Manuscripts must be typed in double-line spacing on one side of A4 paper, in type not smaller than 12 characters per inch or 10 point. Both copies to include Tables and a set of labelled Figures. One set of Figures without numbers or letters is also to be included. The text to be arranged in the following subsections:

1. **Title**—To have no more than 150 characters on a separate page, which should also include a Short Title (50 characters maximum) and the name and address of the author for correspondence.
2. **Summary**—To be arranged in numbered paragraphs (Full Papers) or a single paragraph (Special Reports).
   —to include aims, principal results and conclusions.
   —to include Key words (10 maximum) at end of summary.
3. **Introduction**—To contain concise statements of the problem and the aims of the investigation.
4. **Methods**—To have brief but adequate account of the procedures; *full names of drugs* (*including those referred to by manufacturer's code*), sources of drugs and statistical tests to be stated.
5. **Results**—To have no repetition of data in Figures, Tables and text.
6. **Discussion**—Findings and conclusions to be placed in context of other relevant work.
   NB Simple repetition of results and unwarranted speculation are not acceptable.
7. **Acknowledgements**—Sources of support. Sources of drugs not widely available commercially.
8. **References**—All references in the text to be included in the Reference List and *vice versa*. References in alphabetical order with complete citations; Journals publishing 'in press' papers identified.
   References to manuscripts submitted to other journals but not yet accepted are not allowed.
9. **Tables**—Each on a separate page and prepared in accordance with current requirements of the Journal.
10. **Figures**—Both labelled and non-labelled Figures to be prepared in accordance with current requirements of the Journal (see *Instructions to Authors*, 1994, **114,** 245–251) and provided with Figure Number and Authors' names on back (*in pencil*).
    —each legend to be typed on a separate page and carrying keys to symbols.
    —keys to symbols and histograms must not appear on the figures themselves, but in the respective legends.
    —'box style' figures are not in keeping with the Journal style; line drawings etc must have only left-hand and bottom axes.
11. **Manuscripts**—To be accompanied by a declaration signed by each author that
    (a) results are original
    (b) approval of all persons concerned has been given to submit manuscripts for consideration (see also 12b)
    (c) the same material is neither 'in press' (i.e. is in proof or has definitely been accepted for publication) nor under consideration elsewhere. Furthermore it will not be submitted or published elsewhere before a decision has been reached by the Editorial Board of the *British Journal of Pharmacology* and will not be submitted elsewhere if accepted by the *British Journal of Pharmacology*.
    (d) Copyright assignment is included.
12. **Cover letter**—To state clearly
    (a) Corresponding author's full postal address, telephone, telex or Fax number
    (b) where appropriate, that *either* ethical approval has been given for investigation *or* Company or Institutional permission to publish work has been received.
13. **Reminder**—Packaging to be sufficiently robust to protect Figures and to withstand mailing.

Failure to comply with *Instructions to Authors* may lead to substantial delays in processing, review and publication and may even jeopardize acceptance of the manuscript.

NOMENCLATURE

Authors are reminded that accepted receptor and associated terminology is laid out in *Nomenclature Guidelines for Authors*, as published in the *British Journal of Pharmacology, Br. J. Pharmacol.*, 1995, **114,** 253–255.

SPECIAL REPORTS

The purpose of *Special Reports* is to provide rapid publication for **new** and **important** results which the Editorial Board considers are likely to be of special pharmacological significance. *Special Reports* will have publication priority over all other material and so authors are asked to consider carefully the status of their work before submission.

In order to speed publication there is normally no revision allowed beyond very minor typographical or grammatical corrections. If significant revision is required, the Board may either invite rapid re-submission or, more probably, propose that it be re-written as a Full Paper and be re-submitted for consideration. In order to reduce delays, proofs of *Special Reports* will be sent to authors but **essential corrections must reach the Production Office within 48 hours of receipt**. Authors should ensure that their submitted material conforms exactly to the following requirements.

Special Reports should normally occupy no more than two printed pages of the Journal; two illustrations (Figures or Tables, with legends) are permitted. As a guideline, with type face of 12 pitch and double-line spacing, a page of A4 paper could contain about 400 words. The absolute maximum length of the *Special Report* is 1700 words. For each Figure or Table, please deduct 200 words. The manuscript should comprise a Title page with key words (maximum of 10), a Summary consisting of a single short paragraph, followed by Introduction, Methods, Results, Discussion and References (maximum of 10). In all other respects, the requirements are the same as for Full Papers (see current 'Instructions to Authors').

BRITISH JOURNAL OF PHARMACOLOGY VOLUME 115(6) 1995

SPECIAL REPORT

D.R. Collins, R.G. Pertwee & S.N. Davies. Prevention by the cannabinoid antagonist, SR141716A, of cannabinoid-mediated blockade of long-term potentiation in the rat hippocampal slice **869**

PAPERS

V. Bauer, V.V. Rekalov, I. Juránek, D. Gergel & P. Bohov. Effect of illuminated nifedipine, a potent antioxidant, on intestinal and vascular smooth muscles **871**

M. Bushfield, M. Metcalfe & A.M. Naylor. Activation of the micturition reflex by NK_2 receptor stimulation in the anaesthetized guinea-pig **875**

K. Masuda, T. Kamimura, K. Watanabe, T. Suga, M. Kanesaki, A. Takeuchi, A. Imaizumi & Y. Suzuki. Pharmacological activity of the C-terminal and N-terminal domains of secretory leukoprotease inhibitor *in vitro* **883**

J. Petersson, P.M. Zygmunt, L. Brandt & E.D. Högestätt. Substance P-induced relaxation and hyperpolarization in human cerebral arteries **889**

J. Pintor & M.T. Miras-Portugal. A novel receptor for diadenosine polyphosphates coupled to calcium increase in rat midbrain synaptosomes **895**

D. Godin, F. Rioux, F. Marceau & G. Drapeau. Mode of action of thrombin in the rabbit aorta **903**

A.M. Hosie, H.A. Baylis, S.D. Buckingham & D.B. Sattelle. Actions of the insecticide fipronil, on dieldrin-sensitive and resistant GABA receptors of *Drosophila melanogaster* **909**

A Lindén, S. Yoshihara, B. Chan & J.A. Nadel. Inhibition of bronchoconstriction by pituitary adenylate cyclase activating polypeptide (PACAP 1-27) in guinea-pigs *in vivo* **913**

K. Miura, T. Ebara, M. Okumura, T. Matsuura, S. Kim, T. Yukimura & H. Iwao. Attenuation of adrenomedullin-induced renal vasodilatation by N^G-nitro L-arginine but not glibenclamide **917**

P.B. Osborne & J.T. Williams. Characterization of acute homologous desensitization of μ-opioid receptor-induced currents in locus coeruleus neurones **925**

A.J. Kaumann, J.A. Lynham & A.M. Brown. Labelling with [^{125}I]-SB 207710 of a small 5-HT_4 receptor population in piglet right atrium: functional relevance **933**

H. Sipma, A. den Hertog & A. Nelemans. Ca^{2+}-dependent and -independent mechanism of cyclic-AMP reduction: mediation by bradykinin B_2 receptors **937**

J.P. Hannon, H.J. Pfannkuche & J.R. Fozard. A role for mast cells in adenosine A_3 receptor-mediated hypotension in the rat **945**

S. Adodra & T.G. Hales. Potentiation, activation and blockade of $GABA_A$ receptors of clonal murine hypothalamic GT1-7 neurones by propofol **953**

N.J. Welsh, N.P. Shankley & J.W. Black. Application of a model to explore interspecies differences in acetylcholine M-receptor-stimulated gastric acid secretion **961**

V. Lischke, R. Busse & M. Hecker. Selective inhibition by barbiturates of the synthesis of endothelium-derived hyperpolarizing factor in the rabbit carotid artery **969**

W. Feniuk, J. Dimech, E.M. Jarvie & P.P.A. Humphrey. Further evidence from functional studies for somatostatin receptor heterogeneity in guinea-pig isolated ileum, vas deferens and right atrium **975**

B.A. Kenny, D.H. Chalmers, P.C. Philpott & A.M. Naylor. Characterization of an α_{1D}-adrenoceptor mediating the contractile response of rat aorta to noradrenaline **981**

M. Fukao, Y. Hattori, M. Kanno, I. Sakuma & A. Kitabatake. Thapsigargin- and cyclopiazonic acid-induced endothelium-dependent hyperpolarization in rat mesenteric artery **987**

K.B. Mian & W. Martin. Differential sensitivity of basal and acetylcholine-stimulated activity of nitric oxide to destruction by superoxide anion in rat aorta **993**

H. Azuma, J. Sato, H. Hamasaki, A. Sugimoto, E. Isotani & S. Obayashi. Accumulation of endogenous inhibitors for nitric oxide synthesis and decreased content of L-arginine in regenerated endothelial cells **1001**

M.J. Cumberbatch, B.A. Chizh & P.M. Headley. Modulation of excitatory amino acid responses by tachykinins and selective tachykinin receptor agonists in the rat spinal cord **1005**

B.A. Chizh, M.J. Cumberbatch, P.J. Birch & P. M. Headley. Endogenous modulation of excitatory amino acid responsiveness by tachykinin NK_1 and NK_2 receptors in the rat spinal cord **1013**

P.K.E. Zygmunt, P.M. Zygmunt, E.D. Högestätt & K-E. Andersson. NANC neurotransmission in lamina propria of the rabbit urethra: regulation by different subsets of calcium channels **1020**

G. Edwards, J. Schneider, A. Niederste-Hollenberg, Th. Noack & A.H. Weston. Effects of BRL55834 in rat portal vein and bovine trachea: evidence for the induction of a glibenclamide-resistant, ATP-sensitive potassium current **1027**

S. Sabry, F. Mondon, M. Levy, F. Ferré & A.T. Dinh-Xuan. Endothelial modulation of vasoconstrictor responses to endothelin-1 in human placental stem villi small arteries **1038**

C. Coméra & F. Russo-Marie. Glucocorticoid-induced annexin 1 secretion by monocytes and peritoneal leukocytes **1043**

A.R.C. Ladenius, G. Folkerts, H.J. van der Linde & F.P. Nijkamp. Potentiation by viral respiratory infection of ovalbumin-induced guinea-pig tracheal hyperresponsiveness: role for tachykinins **1048**

B. Vincent, V. Dive, A. Yiotakis, C. Smadja, R. Maldonado, J-P. Vincent & F. Checler. Phosphorus-containing peptides as mixed inhibitors of endopeptidase 3.4.24.15 and 3.4.24.16: effect on neurotensin degradation *in vitro* and *in vivo* **1053**

S.E. Gartside, V. Umbers, M. Hajos & T. Sharp. Interaction between a selective 5-HT_{1A} receptor antagonist and an SSRI *in vivo*: effects on 5-HT cell firing and extracellular 5-HT **1064**

D. Strabel & M. Diener. The effect of neuropeptide Y on sodium, chloride and potassium transport across the rat distal colon **1071**

M.W. Martin, A.J. O'Sullivan & B.D. Gomperts. Inhibition by cromoglycate and some flavonoids of nucleoside diphosphate kinase and of exocytosis from permeabilized mast cells **1080**

S.S. Hegde, D.W. Bonhaus, L.G. Johnson, E. Leung, R.D. Clark & R.M. Eglen. RS 39604: a potent, selective and orally active 5-HT_4 receptor antagonist **1087**

S.M. Poucher, J.R. Keddie, P. Singh, S.M. Stoggall, P.W.R. Caulkett, G. Jones & M.G. Collis. The *in vitro* pharmacology of ZM 241385, a potent, non-xanthine, A_{2a} selective adenosine receptor antagonist **1096**

A.C. MacKinnon, K.M. Wyatt, J.G. McGivern, R.D. Sheridan & C.M. Brown. [^{3}H]-lifarizine, a high affinity probe for inactivated sodium channels **1103**

R.G. Humphries, W. Tomlinson, J.A. Clegg, A.H. Ingall, N.D. Kindon & P. Leff. Pharmacological profile of the novel P_{2T}-purinoceptor antagonist, FPL 67085 *in vitro* and in the anaesthetized rat *in vivo* **1110**

V.A. Snetkov, S.J. Hirst, C.H.C. Twort & J.P.T. Ward. Potassium currents in human freshly isolated bronchial smooth muscle cells **1117**

STOCKTON

Typeset by Elite Typesetting Techniques, Eastleigh, Hants
and printed in Great Britain by Unwin Brothers Ltd., The Gresham Press, Old Woking, Surrey